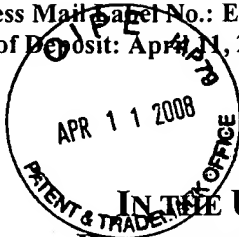


Express Mail Label No.: EV869898868US  
Date of Deposit: April 11, 2008

Attorney Docket No.: 25619-501



**COPY**

**IN THE UNITED STATES PATENT AND TRADEMARK OFFICE  
BEFORE THE BOARD OF PATENT APPEALS AND INTERFERENCES**

In Re Application of:  
Shoenfeld *et al.*

Confirmation No.: 1174

Application Serial No. 09/806,400

Group Art Unit: 1644

Filing Date: March 30, 2001

Examiner: Ronald Schwadron

Title: COMPOSITIONS FOR THE PREVENTION AND/OR TREATMENT OF ATHEROSCLEROSIS

**Mail Stop: Appeal Brief - Patents**  
Commissioner for Patents  
P.O. Box 1450  
Alexandria, VA 22313-1450

**APPEAL BRIEF**

Applicants file this Appeal Brief, in triplicate, pursuant to 37 C.F.R. § 41.37, in support of their Notice of Appeal, dated May 25, 2007. A Petition for a One-Month Extension of Time and the required fee are filed herewith. With extension, this Appeal Brief is due on or before Monday, August 27, 2007. A check in the amount of \$250.00 is enclosed to cover the fee for filing a brief in support of an appeal required under 37 C.F.R. § 41.20(b)(2). Applicants do not believe any additional fees are due. However, the Commissioner is authorized to charge any additional fees that may be due, or to credit any overpayment, to Deposit Account No. 50-0311, Reference 25619-501.

**REAL PARTY IN INTEREST**

The real party in interest is Vascular Biogenics, Ltd, the assignee of the application from all inventors.

**RELATED APPEALS AND INTERFERENCES**

There are no related appeals and interferences for this matter.

**STATUS OF CLAIMS**

Claims 1-27 are cancelled. Claim 28 is pending and is the subject of this appeal.

## STATUS OF AMENDMENTS

No claim amendments were submitted after final rejection.

## SUMMARY OF THE CLAIMED SUBJECT MATTER

The sole independent claim on appeal is claim 28, which recites the following.

A method for treatment of atherosclerosis in a subject (claim 14 as originally filed) comprising:

- administering a therapeutically effective amount of an enteric coated tablet or granule composition (page 14, line 1 - page 15, line 4) comprising
- isolated human oxidized low density lipoprotein and a pharmaceutically acceptable carrier for oral administration (page 15, line 30 - page 16, line 11).

## GROUND OF REJECTION TO BE REVIEWED ON APPEAL

The rejection of claim 28 under 35 U.S.C. § 112, first paragraph, as failing to comply with the enablement requirement. It is the Examiner's position that claim 28 is not enabled for treating humans and inducing oral tolerance.

## ARGUMENT

Applicants appeal the Examiner's enablement rejection of claim 28 under 35 U.S.C. § 112, first paragraph, as failing to comply with the enablement requirement.

The Examiner states that the specification does not disclose how to use the claimed method to treat or prevent atherosclerosis in humans *in vivo* using an oral tolerance inducing amount of oxidized LDL. The Examiner further states that it is unpredictable whether human disease can be treated via inducing oral tolerance to a disease antigen. *See*, Final Office Action at pages 2-6. In support of the rejection, the Examiner recites *In re Wands*, 858 F.2d 731, 737 (Fed. Cir. 1988) factors (5), (7), (3) and (2) against claim 28 at pages 3-4 of the Final Office Action.

### State of the Prior Art (Wands Factor 5) and Predictability or Unpredictability of the Art (Wands Factor 7)

The Examiner states that regarding *Wands* factors (5) and (7), there is a high unpredictability in the art. Specifically, the Examiner cites Spack et al. *Expert Opin. On Invest. Drugs*, 6:1715-1727, 1997 ("Spack") and McKown et al., *Arthritis and Rheum.* 42:1204-1208, 1999 ("McKown") to show that it is unpredictable whether human disease can be treated via the induction of oral tolerance to a disease antigen. *See*, Final Office Action at pages 4-5.

Applicants submit that pending claim 28 does not recite or require the induction of oral tolerance



as stated by the Examiner. In fact, claim 28 is not directed to the induction of oral tolerance at all; rather, claim 28 is directed to a method of treating atherosclerosis by administering a therapeutically effective amount of an enteric coated tablet or granule composition comprising isolated human oxidized LDL and a pharmaceutically acceptable carrier for oral administration. As such, the Examiner's arguments regarding the unpredictability of disease treatment via inducing oral tolerance to a disease antigen, including the discussion of McKown and Spack is misplaced and improper.

Applicants have previously argued in the December 7, 2005 Amendment and Response, August 31, 2006 Amendment and Response and the In-Person-Interview conducted on November 15, 2005 that the claims are directed to treating atherosclerosis and do not recite or require the induction of oral tolerance. However, the Examiner has stated that although the claims are not directed to a specific mechanism of action, the disclosure indicates that the claimed method works via oral tolerance and that the disclosure is sufficient to maintain the enablement rejection under 35 U.S.C. §112, first paragraph. *See*, Final Office Action at page 5 and the Office Action mailed March 3, 2006 at page 7.

The Examiner's assertion is incorrect. It is well recognized under U.S. law, that it is not a requirement of patentability that an inventor correctly set forth, or even know, how or why the invention works. *Newman v. Quigg*, 877 F.2d 1575, 1581 (Fed. Cir. 1989). It is axiomatic that an inventor need not comprehend the scientific principles on which the practical effectiveness of his invention rests, nor is the inventor's theory or belief as to how the invention works a necessary element in the specification to satisfy the enablement requirement. *Fromson v. Advance Offset Plate, Inc.*, 720 F.2d 1565, 1570 (Fed. Cir. 1983). A patent applicant need only teach how to achieve the claimed result, even if the theory of operation is not correctly explained or even understood. *In re Isaacs*, 347 F.2d 887, 892, 146 USPQ 193, 197 (C.C.P.A. 1965). Applicants submit that the instant application discloses a method of treating atherosclerosis by administering a therapeutically effective amount of an enteric coated tablet or granule composition comprising isolated human oxidized LDL and a pharmaceutically acceptable carrier for oral administration and thus satisfies the how-to-use requirement of 35 U.S.C. §112, first paragraph, irrespective of whether the claimed method works via oral tolerance or another unidentified mechanism.

#### The Presence or Absence of Working Examples (*Wands* Factor 3)

The Examiner states that regarding *Wands* factor (3), while the specification provides an example in a mouse model, there were copious amounts of mouse research that suggested that while oral tolerance could be used to treat multiple sclerosis and rheumatoid arthritis in such models, said diseases were not successfully treated in humans using oral tolerance. The Examiner again cites McKown and Spack to support this assertion. *See*, Final Office Action at pages 4-5.

As described *supra*, claim 28 is not directed to the induction of oral tolerance and is not directed to the treatment of multiple sclerosis or rheumatoid arthritis and the citation of Spack and McKown is not relevant to the currently recited invention. The instant invention and the additional data generated using the teachings of the specification and reported in the December 7, 2005 Harats § 1.132 Declaration, attached hereto in the Evidence Appendix, readily demonstrate to one of ordinary skill in the art how to make and use the present invention to treat atherosclerosis by oral administration of isolated human oxidized LDL.

Specifically, the instant specification and the additional data supplied in the December 7, 2005 Harats § 1.132 Declaration provides a working example that demonstrates the successful treatment of atherosclerosis in an LDL-receptor deficient mouse by oral administration of isolated human oxidized LDL. *See*, Specification at, *e.g.*, page 15, lines 20-29; and page 18, line 18 to page 19, line 31. It is well recognized in the art that the LDL-receptor deficient mouse is the preferred animal model to evaluate the effects of pharmacologic agents on atherosclerosis. LDL-receptor deficient mice, under appropriate conditions, develop complex atherosclerotic lesions and provide practical atherosclerotic mouse models and are the most utilized model to study lipids and atherosclerosis. *See*, August 31, 2006 Harats § 1.132 Declaration at ¶ 5-6 attached hereto in the Evidence Appendix.

Specifically, the use of animal models (*i.e.* murine models) to evaluate the effects of pharmacologic agents on atherosclerosis was well recognized in the art when the instant application was filed (*See, e.g.*, Bocan, *Curr. Pharm. Des.* 4(1):37-52, 1998); and, the LDL-receptor deficient mouse was recognized in the art as a preferred model of atherosclerosis at the time of the instant application. (*See, e.g.*, Ishibashi et al., *J Clin Invest.* 92:883-893, 1993; Lichtman et al., *Arterioscler. Thromb. Vasc. Biol.* 19(8):1938-44, 1999; Maron, R. et al., *FASEB J.* 14:A1199-(Abstr.), 2000). Moreover, mice having targeted inactivation of the apolipoprotein E (ApoE) gene and of the LDL-receptor gene, under appropriate conditions, develop complex atherosclerotic lesions and provide practical atherosclerotic mouse models and are the most utilized model to study lipids and atherosclerosis. *See*, December 7, 2005 Harats § 1.132 Declaration at ¶ 6.

To further support the rejection, the Examiner cites Wouters et al. *Clin. Chem. Lab. Med.* 43(5): 470-479, 2005 (“Wouters”) and states that Wouters discloses that the LDL-receptor mouse displays cholesterol metabolic pathways not found in humans and as a consequence “this route can serve as a backup mechanism for lipoprotein clearance in LDL-receptor mice, yielding unforeseen side effects.” *See*, Final Office Action at page 6. Although the LDL-receptor deficient mouse is not the optimal model for genetic human familial hypercholesterolemia, it is one of the most predictable models for human atherosclerosis and the likelihood of new molecules to work as anti-atherosclerosis drugs in humans is

high (*See, e.g., Babaei et al., Cardiovasc Res.* 48(1):158-67, 2000; *Burleigh et al., Biochem Pharmacol.* 70(3):334-42, 2005; *Chen et al., Circulation.* 106(1):20-3, 2002; *Collins et al., Arterioscler Thromb Vasc Biol.* 21(3):365-71, 2001; *Cyrus et al., Circulation.* 107(4):521-3, 2003; *Elhage et al., Am J Pathol.* 167(1):267-74, 2005; *Li et al., J Clin Invest.* 106(4):523-31, 2000; *Napoli et al., Proc Natl Acad Sci U S A.* 99(19):12467-70, 2002). Human atherosclerotic plaques are infiltrated with lymphocytes and display an inflammatory phenotype that includes expression of pro-inflammatory cytokines. In this sense the LDL-receptor deficient mice have plaques similar to those of humans containing a significant number of lymphocytes (*See, e.g., Roselaar et al., Arterioscler Thromb Vasc Biol.* 16(8):1013-8, 1996). Moreover, therapeutic strategies that apply for atheroprotection in humans are similarly successful in LDL receptor deficient mice and may not be so in ApoE knockout mice (*See, e.g., Wang et al., Atherosclerosis.* 162(1):23-31, 2002). These findings indicate that plaques developing in LDL receptor deficient mice may be more relevant to human atherosclerosis than other non-human models and thus, it is one of the most widely employed models for drug development in the field of atherosclerosis. *See, December 7, 2005 Harats § 1.132 Declaration at ¶ 6.*

The Amount of Direction or Guidance Presented (*Wands* Factor 2)

The Examiner states that regarding *Wands* factor (2), there is no disclosure in the specification as to what doses would be used to induce the functional parameters recited in the claim which are related to properties of the oral tolerance induction mechanism. *See, Final Office Action at pages 4-6.*

Once again, as described in detail *supra*, claim 28 is not directed to the induction of oral tolerance but rather are directed to a method of treating atherosclerosis by oral administration of an enteric coated tablet or granule composition comprising isolated human oxidized LDL and a pharmaceutically acceptable carrier

Applicants have provided working examples that demonstrate the successful treatment of atherosclerosis by oral administration isolated human oxidized LDL in an LDL-receptor deficient mouse and the LDL-receptor deficient mouse is the most art-recognized model of the biochemical and morphological effects of atherosclerosis. Further, the working examples provide a range of concentrations of the composition to treat atherosclerosis (*See, e.g., page 18, lines 27-29; page 19, lines 18-19*). Applicants assert that one of ordinary skill in the art, using the teachings of the instant invention, would be able to determine the corresponding doses useful in other species, including humans, without undue experimentation. The specification need not disclose what is well known in the art. *Genentech, Inc. v. Novo Nordisk A/S*, 108 F.3d 1361, 1366 (Fed. Cir. 1997) citing *Hybritech Inc. v. Monoclonal Antibodies, Inc.*, 802 F.2d 1367, 1385, 231 U.S.P.Q. (BNA) 81, 94 (Fed. Cir. 1986). *See, December 7,*

2005 Harats § 1.132 Declaration at ¶ 7-8.

### Argument Conclusion

As described *supra*, Applicants have provided several working examples, both in the specification and additional data confirming the results described in the specification, and demonstrated successful treatment of atherosclerosis by oral administration of isolated human oxidized LDL. Therefore, Applicants assert that one of ordinary skill in the art, using the teachings of the instant invention would be able to readily determine how to make and use the present invention and respectfully request that the Board reverse the Examiner's rejection of claim 28 under 35 U.S.C. § 112, first paragraph.

### **CLAIMS APPENDIX**

A claims appendix listing the pending claim on appeal is attached to the end of this paper.

### **EVIDENCE APPENDIX**

An evidence appendix including the Declaration of Dror Harats under 37 C.F.R. §1.132 filed with Applicants December 7, 2005 Amendment and Response is attached to this paper. This §1.132 Declaration was entered into the record and considered by the Examiner in the Office Action mailed on March 3, 2006.

The evidence appendix attached to this paper also includes the Declaration of Dror Harats under 37 C.F.R. §1.132 filed with Applicants August 31, 2006 Amendment and Response. This §1.132 Declaration was entered into the record and considered by the Examiner in the Final Office Action mailed on November 29, 2006.

The evidence appendix attached to this paper also includes the following references submitted December 7, 2005 in a Supplemental Information Disclosure Statement and entered into the record by the Examiner in the non-final Office Action mailed March 3, 2006:

- Bocan, *Curr. Pharm. Des.* 4(1):37-52, 1998;
- Ishibashi et al., *J Clin Invest.* 92:883-893, 1993;
- Lichtman et al., *Arterioscler. Thromb. Vasc. Biol.* 19(8):1938-44, 1999;
- Maron, R. et al., *FASEB J.* 14:A1199-(Abstr.), 2000;
- Babaei et al., *Cardiovasc Res.* 48(1):158-67, 2000;
- Burleigh et al., *Biochem Pharmacol.* 70(3):334-42, 2005;
- Chen et al., *Circulation.* 106(1):20-3, 2002;

- Collins *et al.*, *Arterioscler Thromb Vasc Biol.* 21(3):365-71, 2001;
- Cyrus *et al.*, *Circulation.* 107(4):521-3, 2003;
- Elhage *et al.*, *Am J Pathol.* 167(1):267-74, 2005;
- Li *et al.*, *J Clin Invest.* 106(4):523-31, 2000;
- Napoli *et al.*, *Proc Natl Acad Sci U S A.* 99(19):12467-70, 2002;
- Roselaar *et al.*, *Arterioscler Thromb Vasc Biol.* 16(8):1013-8, 1996; and
- Wang *et al.*, *Atherosclerosis.* 162(1): 23-31, 2002.

These Declarations under §1.132 and these references are relied upon by Applicants in this appeal.

#### RELATED PROCEEDINGS APPENDIX

A related proceedings appendix, indicating that there are no related proceedings, is attached to the end of this paper.

Respectfully submitted,



Ivor R. Elrifi, Reg. No. 39,529  
Matthew Pavao, Reg. No. 50,572  
Attorneys for Applicants  
c/o MINTZ LEVIN  
Tel.: (617) 542-6000  
Fax: (617) 542-2241  
**Customer No.: 30623**

Dated: April 11, 2008

**APPENDIX  
CLAIMS ON APPEAL**

Claim 28 (Previously Presented) A method for treatment of atherosclerosis in a subject, comprising administering a therapeutically effective amount of an enteric coated tablet or granule composition comprising isolated human oxidized low density lipoprotein and a pharmaceutically acceptable carrier for oral administration.

**APPENDIX  
RELATED PROCEEDINGS**

None

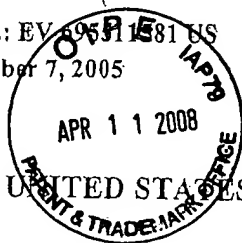
ACTIVE 4298212v.1

## EVIDENCE APPENDIX

Express Mail Label No.: EV 460368575US

Date of Deposit: December 7, 2005

Attorney Docket No. 25619-501 (Formerly 01/21885)



## IN THE UNITED STATES PATENT AND TRADEMARK OFFICE

APPLICANTS: Schoenfeld *et al.*  
SERIAL NUMBER: 09/806,400  
FILING DATE: March 30, 2001  
FOR: COMPOSITIONS FOR THE PREVENTION AND/OR TREATMENT OF  
ATHEROSCLEROSIS

EXAMINER: Ronald Schwadron  
ART UNIT: 1644

Mail Stop RCE  
Commissioner for Patents  
P.O. Box 1450  
Alexandria, VA 22313-1450

## DECLARATION OF DROR HARATS UNDER 37 C.F.R. §1.132

I, Dror Harats, of 71 Mendes Street, 53 765 Ramat Gan, Israel, declare and state that:

1. I am a coinventor, together with Yahuda Shoenfeld and Jacob George, in the above-referenced patent application.
2. I received an M.D. degree from the Hebrew University Hadassah Medical School, Jerusalem, Israel. I worked as a post-doctoral fellow at the University of California at San Francisco from 1991-1994.
3. I am presently employed as the head of the "Institute of Lipids and Atherosclerosis" at the Sheba Medical Center in Tel-Hashomer, Israel. I am an Associate Professor of Medicine at the Sackler School of Medicine, Tel-Aviv University, Tel-Aviv, Israel. I also serve as the Secretary of the Israeli Society for Research, Prevention and Treatment of Atheroclerosis, and drafted the Guidelines for Prevention of Cardiovascular Diseases in Israel, and am a member in good standing of the European Taskforce for Prevention and Treatment of Atherosclerosis and Cardiovascular Diseases.
4. My research focuses on atherosclerosis. Since the beginning of my career, I have published over 80 scientific articles in highly regarded journals and books, and have presented my achievements at many international scientific conferences.



5. I have reviewed the Final Office Action dated July 22, 2005. I understand that Claims 14, 18-20 and 26 are rejected under 35 U.S.C. §112, first paragraph, as failing to comply with the enablement requirement. I appreciate the Examiner's time discussing my invention at the November 2005 interview. In response to that rejection, as discussed at the interview with the Examiner, the claims have now been amended to recite a method of treating atherosclerosis by oral administration of an enteric coated composition comprising isolated copper-oxidized LDL or isolated human copper-oxidized LDL.
6. The specification provides an example in a mouse model (as described in the Specification at, *e.g.*, page 15, lines 20-29; and page 18, line 18 to page 19, line 31). I believe that the LDLR deficient mice used in the studies disclosed in the present application is the preferred, art-recognized model for atherosclerosis, for the reasons outlined below.

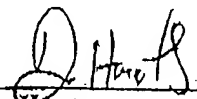
Specifically, mice having targeted inactivation of the apolipoprotein E (ApoE) gene and of the LDLR gene, under appropriate conditions, develop complex atherosclerotic lesions and provide practical atherosclerotic mouse models and are the most utilized model to study lipids and atherosclerosis. ApoE is critical in lipoprotein trafficking (clearance of chylomicrons, VLDL, and HDL). Thus mice lacking apoE have plasma cholesterol levels that are 4 to 5 times normal and develop atherosclerotic lesions spontaneously, even when fed a normal diet. The lesions resemble human lesions and progress over time from an initial fatty streak to a complex lesion with a fibrous cap. Mice lacking the LDLR have less overt disease, with a modest 2 times normal plasma cholesterol level when maintained on a normal diet, and they develop atherosclerosis only slowly. However, in response to a high-fat, high-cholesterol diet, LDLR-deficient mice exhibit massive elevations in plasma cholesterol and rapidly develop atherosclerotic lesions throughout the aorta.

The predictable development of atherosclerotic lesions and plaques and their resemblance to human atherosclerotic lesions and plaques along with other more general advantages of mice, such as their small size, short generation time, and relative ease to care, have made the mouse a most valid, effective and practical model for the study of atherosclerosis.

Although the LDL-receptor deficient mouse isn't the optimal model for genetic human familial hypercholesterolemia, it is one of the most predictable models for human atherosclerosis and the likelihood of new molecules to work as anti-atherosclerosis drugs in humans is high. Human atherosclerotic plaques are infiltrated with lymphocytes and display an inflammatory phenotype that includes expression of pro-inflammatory cytokines. In this sense the LDL-receptor deficient mice have plaques similar to those of humans containing a significant number of lymphocytes. Moreover, therapeutic strategies that apply for atheroprotection in humans are similarly successful in LDL receptor deficient mice and may not be so in ApoE knockout mice. These findings indicate that plaques developing in LDL receptor deficient mice may be more relevant to human atherosclerosis than other non-human models and is one of the most widely employed models for drug development in the field of atherosclerosis.

7. I believe that the present invention provides a range of concentrations of the composition to treat atherosclerosis (*See, e.g.*, page 18, lines 27-29; page 19, lines 18-19) in the art-preferred model (LDLR deficient mice) for studying the biochemical and morphologic effects of atherosclerosis and that one of ordinary skill in the art, using the teachings of the instant invention, would be able to readily determine the corresponding doses useful in humans, without undue experimentation.
8. We prepared and orally administered various dosages of isolated copper-oxidized LDL to mice according to the teachings of the instant specification and evaluated the aortic sinus lesion area in the aorta. As shown in Figure 1 appended hereto, oral administration of isolated copper-oxidized LDL decreases the aortic sinus lesion area by 45% as compared to non treated mice at several tested dosages per mouse (10 $\mu$ g, 100 $\mu$ g or 1000 $\mu$ g). Further, as shown in Figure 2 appended hereto, when mice were orally administered isolated copper-oxidized LDL at varying mg/kg body weight dosages (0.35mg/kg, 3.5mg/kg or 35mg/kg) results showed decreases in the aortic sinus lesion area similar to results shown in Figure 1. These results show that a skilled artisan can, as a matter of routine, readily determine the appropriate therapeutically effective dose in humans.

9. I also understand that claims 14, 19, 27 and 28 are rejected under 35 U.S.C. §103(a) as being unpatentable over Sima et al., 11<sup>th</sup> *Int. Symp on Atherosclerosis*, page 227, October 1997 ("Sima") and Hansson et al., 11<sup>th</sup> *Symp on Atherosclerosis*, page 289, October 1997 ("Hansson") in view of U.S. Patent No. 6,541,011 to Punnonen ("Punnonen").
10. As described at the interview, neither of Sima and Hansson suggest any desirability or incentive to orally administer an enteric coated composition comprising isolated copper-oxidized LDL to treat atherosclerosis. In contrast, those references clearly teach that OxLDL contributes to the development of atherosclerosis (*i.e.*, OxLDL is pro-atherosclerotic) -- teaching away from the claimed invention. Additionally, OxLDL is ingested on a daily basis as part of a routine diet and OxLDL is degraded in the gut following ingestion. For this reason, at the time the application was filed, one of ordinary skill in the art would not be motivated to combine Sima and Hansson with Punnonen with a reasonable expectation of success. The results described in the specification demonstrate that the composition of the claimed invention (enteric coated composition comprising isolated copper-oxidized LDL and a pharmaceutically acceptable carrier for oral administration) displays the unexpected ability to treat atherosclerosis.
11. I further declare that all statements made herein of our own knowledge are true and that all statements made on information and belief are believed to be true; and further that these statements were made with the knowledge that willful false statements and the like so made are punishable by fine or imprisonment, or both, under 18 U.S.C. § 1001 and that willful false statements may jeopardize the validity of this application and any patent issuing therefrom.

  
\_\_\_\_\_  
Dror Harats

Signed this 4 day of December, 2005  
Encl:  
Appendix I



# Appendix 1

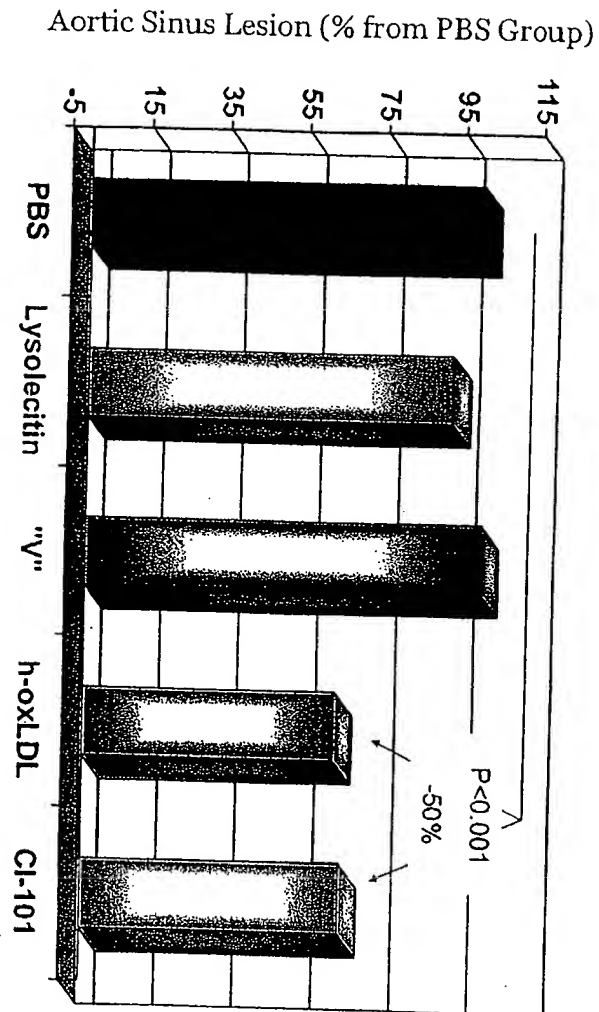


Figure 1.

Express Mail Label No.: EV 45175122

Date of Deposit: August 31, 2006

Attorney Docket No. 25619-501

## IN THE UNITED STATES PATENT AND TRADEMARK OFFICE

APPLICANTS: Schoenfeld *et al.*  
SERIAL NUMBER: 09/806,400 EXAMINER: Ronald Schwadron  
FILING DATE: March 30, 2001 ART UNIT: 1644  
FOR: COMPOSITIONS FOR THE PREVENTION AND/OR TREATMENT OF  
ATHEROSCLEROSIS

Mail Stop Amendment  
Commissioner for Patents  
P.O. Box 1450  
Alexandria, VA 22313-1450

## DECLARATION OF DROR HARATS UNDER 37 C.F.R. §1.132

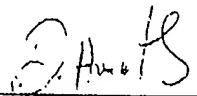
I, Dror Harats, of 71 Mendes Street, 53 765 Ramat Gan, Israel, declare and state that:

1. I am a coinventor, together with Yehuda Shoenfeld and Jacob George, in the above-referenced patent application.
2. I received an M.D. degree from the Hebrew University Hadassah Medical School, Jerusalem, Israel. I worked as a post-doctoral fellow at the University of California at San Francisco from 1991-1994.
3. I am presently employed as the head of the "Institute of Lipids and Atherosclerosis" at the Sheba Medical Center in Tel-Hashomer, Israel. I am an Associate Professor of Medicine at the Sackler School of Medicine, Tel-Aviv University, Tel-Aviv, Israel. I also serve as the Secretary of the Israeli Society for Research, Prevention and Treatment of Atherosclerosis, and drafted the Guidelines for Prevention of Cardiovascular Diseases in Israel, and am a member in good standing of the European Taskforce for Prevention and Treatment of Atherosclerosis and Cardiovascular Diseases.
4. My research focuses on atherosclerosis. Since the beginning of my career, I have published over 80 scientific articles in highly regarded journals and books, and have presented my achievements at many international scientific conferences.

5. I have reviewed the Office Action dated March 3, 2006. I understand that Claims 14 and 28 are rejected under 35 U.S.C. § 112, first paragraph, as failing to comply with the enablement requirement. The Examiner asserts that the specification does not disclose how to use the claimed method to treat or prevent atherosclerosis in humans *in vivo* using an oral tolerance inducing amount of oxidized LDL. The pending claim is not directed to the induction of oral tolerance, rather, it is directed to a method of treating atherosclerosis by oral administration of an enteric coated tablet or granule composition comprising isolated human oxidized LDL.
6. The specification provides an example in a mouse model (as described in the Specification at, e.g., page 15, lines 20-29; and page 18, line 18 to page 19, line 31). I assert that the LDLR deficient mice used in the studies disclosed in the present application, as well as the more recent studies, provided in the previous declaration, is a preferred, art-recognized model for atherosclerosis, as described in my previous declarations and supported by the state of the art.

Specifically, it is well recognized in the art that the LDLR deficient mouse is one of the preferred animal model to evaluate the effects of pharmacologic agents on atherosclerosis. LDLR deficient mice, under appropriate conditions, develop complex atherosclerotic lesions and provide practical atherosclerotic mouse models and are the most utilized model to study lipids and atherosclerosis.

7. I further declare that all statements made herein of our own knowledge are true and that all statements made on information and belief are believed to be true; and further that these statements were made with the knowledge that willful false statements and the like so made are punishable by fine or imprisonment, or both, under 18 U.S.C. § 1001 and that willful false statements may jeopardize the validity of this application and any patent issuing therefrom.

  
\_\_\_\_\_  
Dror Harats

Signed this 28 day of August, 2006



## Blockade of endothelin receptors markedly reduces atherosclerosis in LDL receptor deficient mice: role of endothelin in macrophage foam cell formation

Saeid Babaei<sup>a,b</sup>, Pierre Picard, Amir Ravandi<sup>a</sup>, Juan Carlos Monge<sup>a</sup>, Tony C. Lee<sup>a</sup>,  
Peter Cernacek<sup>c</sup>, Duncan J. Stewart<sup>a,b,\*</sup>

<sup>a</sup>Division of Cardiology, Terrence Donnelly Heart Center, St. Michael's Hospital, 30 Bond Street, Toronto, Ontario, Canada, M5B 1W8

<sup>b</sup>Departments of Medicine and of Laboratory Medicine and Pathobiology, University of Toronto, Toronto, Ontario, Canada

<sup>c</sup>Montreal Heart Institute, Department of Laboratory Medicine, Montreal, Quebec, Canada

Received 19 January 2000; accepted 7 June 2000

### Abstract

**Objective:** We evaluated the direct effects of long-term blockade of ET<sub>A</sub> and ET<sub>B</sub> receptors using a mixed endothelin (ET) receptor antagonist, LU224332, in the low density lipoprotein receptor (LDL-R) knockout mouse model of atherosclerosis. **Methods:** Four groups of LDL-R deficient mice were studied: control mice fed normal chow (group I); mice fed a high cholesterol (HC, 1.25%) diet alone (group II), HC fed animals treated with LU224332 (group III); and mice fed normal chow treated with the LU compound (group IV). All treatments were continued for 8 weeks at which time the animals were sacrificed and the aortae were removed and stained with oil red O. Atherosclerotic area (AA) was determined by quantitative morphometry and normalized relative to total aortic area (TA). **Results:** Cholesterol feeding resulted in a marked increase in total plasma cholesterol (~15 fold) and widespread aortic atherosclerosis (AA/TA: group I: 0.013±0.007; group II: 0.33±0.11;  $P<0.001$ ). Atherosclerotic lesions were characterized by immunohistochemistry as consisting mainly of macrophages which also showed high levels of ET-1 expression. Treatment with ET antagonist significantly reduced the development of atherosclerosis (AA/TA: group III: 0.19±0.07,  $P<0.01$  vs. group II), without altering plasma cholesterol levels and blood pressure. The direct effect of LU224332 on macrophage activation and foam-cell formation was determined in vitro using a human macrophage cell line, THP-1. Treatment of the THP-1 cells with LU224332 significantly reduced cholesterol ester and triacylglycerol accumulation and foam-cell formation on exposure to oxidized LDL ( $P<0.01$  and  $P<0.05$ , respectively). **Conclusion:** We conclude that a nonselective ET receptor antagonist substantially inhibited the development of atherosclerosis in a genetic model of hyperlipidemia, possibly by inhibiting macrophage foam-cell formation, suggesting a role for these agents in the treatment and prevention of atherosclerotic vascular disease. © 2000 Elsevier Science B.V. All rights reserved.

**Keywords:** Atherosclerosis; Cholesterol; Endothelins; Macrophages; Receptors

### 1. Introduction

Spontaneous mutations in the low-density lipoprotein receptor (LDL-R) gene result in severe hypercholesterolemia and atherosclerosis in Watanabe rabbits and rhesus monkeys [1], and represents the genetic basis of familial hypercholesterolemia in humans [2]. Ishibashi et al. [3] have

produced LDL-R deficient mice by targeted disruption of this gene. On high cholesterol feeding these animals exhibited marked elevations in serum cholesterol-rich lipoprotein particles including very low density lipoprotein (VLDL), intermediate density lipoprotein (IDL) and LDL, associated with massive xanthomatosis and atherosclerosis in a manner similar to patients with familial hypercholesterolemia [3].

Endothelial cells normally protect against many of the

\*Corresponding author. Tel.: +1-416-864-5724; fax: +1-416-864-5419.

E-mail address: stewartd@smh.toronto.on.ca (D.J. Stewart).

Time for primary review 22 days.

initiating events in atherosclerosis by the production of vasodilator, antithrombotic and antiproliferative factors [4] such as nitric oxide (NO), which prevents adhesion of blood elements to the endothelium including platelets and monocytes, and inhibits migration and proliferation of medial smooth muscle cells (SMCs) [5,6]. Indeed, reduced endothelium-dependent dilation and decreased bioavailability of NO is an early feature of hyperlipidemia both in experimental models [4,7] and patients [8,9], which can be improved by administration of exogenous L-arginine, the substrate for NO generation by NO synthase (NOS) [10]. Endothelial dysfunction is characterized not only by reduced release of vasodilator autacoids such as NO, but also by increased production of vasoconstrictor factors including endothelin-1 (ET-1) [11]. ET-1 is a 21-amino-acid peptide which, in addition to its powerful vasoconstrictor and hypertensive actions [12], has a number of other biological activities which are likely important in chronic vascular disorders. These include stimulation of cellular proliferation [13], synthesis of matrix proteins [14], and chemotactic effects on monocytes [15,16]. Several indirect lines of evidence support a role for ET-1 in the development of atherosclerosis [17]. OxLDL results in increased ET-1 expression in cultured endothelial cells [18] and circulating ET-1 levels are elevated in patients with atherosclerosis [19]. More relevant, perhaps, are the observations of increased ET-1 expression in human atherosclerotic lesions [20,21], associated with complications of atherosclerosis [22].

ET-1 transduces its biological effects through an interaction with two specific receptors.  $ET_A$  is selective for ET-1 and is found predominantly on target cells, such as vascular SMCs [23], and mediates the vasoconstrictor [24] and pro-proliferative actions of ET-1 [25]. In contrast, in the vessel wall  $ET_B$  is found mostly on the endothelial cell, and mediates the release of NO and prostacyclin [26], which serves to counteract the direct effects of ET-1 on the underlying SMCs. However,  $ET_B$  can also be found to a variable degree on SMCs [27,28] and has been described as the predominant receptor of a human monocyte/macrophage cell line [29,30].

The use of selective  $ET_A$  receptor blockers has been recently shown to reduce atherosclerosis [31,32] and improve endothelium-dependent vasodilation [32,33], possibly by unmasking  $ET_B$ -mediated NO production in response to endogenous ET-1. Whether the use of a mixed  $ET_A$  and  $ET_B$  antagonist, which would not be expected to increase vascular endothelial cell NO release, would produce a similar benefit is not certain. We hypothesized that a non-selective ET receptor blocker would reduce atherosclerosis in the LDL-R deficient mouse model by direct actions on SMCs and/or macrophages, inhibiting the proatherogenic response to increased endogenous vascular ET-1 production. We now report that LU224332, a mixed  $ET_A$  and  $ET_B$  antagonist, substantially reduced atherosclerosis in cholesterol-fed LDL-R deficient mice, and also

inhibited the uptake of OxLDL by macrophages in vitro. These data provide strong evidence for a direct role of ET-1 in atherogenesis.

## 2. Methods

### 2.1. Experimental protocol

LDL-R deficient mice in the C57BL/6J background were purchased from Jackson Laboratory. Sixty male LDL-R deficient mice were entered into the study at 22 weeks of age and were maintained on a 12-h-dark–12-h-light cycle with unrestricted access to food and water for the entire length of the experimental protocol. The use and care of LDL-R deficient mice was in accordance with the Canadian Council of Animal Care guidelines and was approved by the Animal Care and Ethics Committee of St. Michael's Hospital. Animals were assigned to four experimental groups (15 mice/group) as follows: (I) control (normal diet, no treatment); (II) high cholesterol (HC) diet without pharmacological intervention; (III) HC diet with ET antagonist treatment and (IV) ET antagonist treatment in mice receiving normal diet. All mice received their specific treatment for a period of 8 weeks before being sacrificed. The ET antagonist treatment groups received LU224332 (10 mg/kg/day) in their drinking water. This compound (a generous gift of Dr. M. Kirchengast from Knoll, Ludwigshafen, Germany) has previously been shown to exhibit equal affinity for the  $ET_A$  and  $ET_B$  receptors ( $ET_A$ : 3.5 and  $ET_B$ : 7.2 nmol/l; ratio: 2.1) [34]. To insure appropriate dosage of the ET antagonist, water intake was monitored at regular intervals and the drug dilution was adjusted accordingly. No difference in food intake, drinking patterns, or body weight was noted between animals from each group (Table 1). The HC diet consisted of 1.25% cholesterol, 7.5% (w/w) cocoa butter, 7.5% casein and 0.5% (w/w) sodium cholate. This chow preparation was shown in previous reports to promote atherogenesis [3]. After 8 weeks of treatment, mice were sacrificed and perfusion fixed with 10% formalin. The aorta were then dissected from the aortic valve to the iliac bifurcation and further fixed in 10% formalin overnight at 4°C.

Table 1  
Feeding behavior and body weight variations\*

	Group I	Group II	Group III	Group IV
Food intake (g/day)	2.4±0.3	2.0±0.5	2.1±0.6	2.4±0.6
Water intake (ml/day)	3.3±1.5	3.8±2.1	3.5±1.8	3.2±1.6
Body weight (g)	28.7±2.7	29.6±3.1	30.1±2.0	27.5±1.9

\* Values shown are mean±S.D. No difference was noted between any experimental groups for food intake, water intake or body weight measurements by the end of the experimental protocol when subjected to one-way ANOVA with post hoc student *t*-test.



## 2.2. Quantification of xanthomatosis

The degree of xanthomatosis was graded according to the following scale: facial lesions: 0=none; 1=mild (snout only); 2=moderate (snout and eye lids); 3=severe (marked lesions); and limb swelling: 0=none; 1=mild/moderate (front paws only); and 2=severe (all four limbs). Addition of facial lesion and limb swelling grades represented the semiquantitative score.

## 2.3. Morphometry and immunohistochemistry

Aortae from each experimental group were opened longitudinally and stained with oil red O and a computer-assisted video imaging system was used to assess the extent of the atherosclerosis area (C-imaging analysis). For immunohistochemistry, the aortae of four animals from each group were divided into three regions: aortic arch, thoracic and abdominal aorta. Paraffin sections (5  $\mu$ m) were cut from each region and endogenous peroxidase activity was quenched by 3%  $H_2O_2$  in methanol for 20 min; nonspecific antibody binding was blocked with 10% goat serum in PBS for 30 min, and adjacent sections from each group were immunostained using the following antibodies: a polyclonal rabbit ET-1 antibody (Peninsula Labs., Belmont, CA, USA) at 1:150 dilution overnight at 4°C, and secondary reaction with goat anti-rabbit biotinylated antibody (1:250 dilution, Vector Labs. Burlingame, USA) for 45 min at room temperature (RT); a polyclonal rat antibody to the mouse monocyte/macrophage marker MOMA-2 (Serotec, Kidlington, Oxford, UK) at 1:100 dilution overnight at 4°C, and secondary reaction with biotinylated rabbit anti-rat IgG (1:250 dilution, Vector Laboratories) for 45 min at RT; a monoclonal mouse antibody to smooth muscle  $\alpha$ -actin (Boehringer Mannheim) at 1:100 dilution for 60 min at RT and secondary reaction with biotinylated anti-mouse IgG (1:150 dilution, Vector Laboratories) for 30 min at RT. Following incubation with the secondary antibodies, the sections were treated with streptavidin–biotin–peroxidase complexes (Vectastain ABC kit, Vector Labs.) for 30 min at RT. Diaminobenzadine was used as the peroxidase substrate and hematoxylin as the nuclear counterstain. Negative control slides were prepared by substituting preimmune serums for the primary antibody.

## 2.4. Cholesterol measurements

Blood was extracted by cardiac ventricular puncture in five animals in groups I, II and IV, and six for group III at the time of sacrifice and centrifuged at 1500 rpm for 10 min for plasma separation and collection. Total cholesterol was measured with an enzymatic cholesterol assay in a colorimetric procedure on a Technicon RA1000 (Bayer, Tarrytown, NY, USA).

## 2.5. Blood pressure measurements

In a separate experimental series, fifteen animals (five control; five HC-fed and five treated with the LU compound) were anaesthetized with an intraperitoneal injection of a mixture of xylazine (5 mg/kg, Bayer) and ketamine (50 mg/kg, Wyeth-Ayerst Canada) after 2 weeks of the representative treatments. A catheter constructed of stretched PE200 tubing (Becton Dickinson) was filled with 50 U/ml heparin in saline and was inserted into the right common carotid artery. Pulsatile blood pressure was measured using a CDXIII pressure transducer (COBE Canada) and recorded on the Biopac MP100 data acquisition system with ACKNOWLEDGE software (Biopac Systems). Animals were allowed to stabilize for 20 min after the onset of anesthesia, and then mean arterial pressure was registered continuously for 10 min and mean values were determined.

## 2.6. LU224332 concentrations in mouse plasma

Plasma levels of LU224332 were measured with a radioreceptor assay as previously described [35]. Briefly, 0.1 ml of plasma obtained from cardiac puncture-blood samples from animals receiving ( $n=7$ ) or not receiving ( $n=6$ ) the LU compound was mixed with 1 ml of methanol, thoroughly vortexed, and centrifuged for 15 min at 2800 g. The supernatant was evaporated under a stream of air. The dry residue was reconstituted in 150  $\mu$ l of the binding buffer. The reaction was carried out at RT in a total volume of 200  $\mu$ l; 50  $\mu$ l of the radioligand ( $^{125}$ I-ET1,  $\approx 10\,000$  cpm per tube) was mixed with 50  $\mu$ l of the sample. The reaction was started by addition of 100  $\mu$ l of porcine aortic membranes (5–7  $\mu$ g protein/tube). It was terminated after 3 h by addition of 1 ml of ice-cold 5 g/l BSA in PBS, pH 7.4, followed immediately by a rapid centrifugation (3 min at 13 000 g). The supernatant was carefully aspirated, and the radioactivity of pellets was counted in an automated gamma-counter. The standard curves, constructed with 18.75 to 1200 nM of LU224332 added to normal rat plasma were linear within this range.

## 2.7. Cell culture

THP-1 monocyte/macrophage cell line was obtained from the American Type Tissue Culture Collection (TIB 202) and were propagated in RPMI 1640 with 10% FCS, penicillin/streptomycin (100 U/ml) at 37°C, 5%  $CO_2$ . Cells were plated at a density of  $1 \times 10^6$  cells/ml in 10% FCS medium containing phorbol myristate acetate ( $10^{-7}$  M) for 72 h to induce differentiation into macrophages, and washed extensively with serum-free RPMI medium prior to incubation with or without lipoproteins as indicated for each experiment. In all experiments, cell viability exceeded 90% as determined by trypan blue exclusion.

### 2.8. Lipoprotein isolation and oxidation

LDL (1.019–1.069 g/ml) was obtained by density gradient ultracentrifugation [36] from plasma of fasted normolipidemic individuals. LDL (2 mg protein/ml) was subsequently dialyzed against 0.1 M phosphate buffer, pH 7.4, containing 0.1 mM EDTA for 24 h (three buffer changes). LDL samples were sterilized by passing through a 0.22- $\mu$ m filter (Millipore, Milford, MA, USA), kept at 4°C, and used within 1 week. Lipoprotein concentration was determined by the method of Lowry et al. [37] and expressed as mg/ml. Oxidation of LDL (5 mg protein/5 ml) was performed by dialysis against 5  $\mu$ M  $\text{CuSO}_4 \cdot 5\text{H}_2\text{O}$  in 0.1 M phosphate buffer, pH 7.4, for 12 h at 37°C in the dark.

### 2.9. Cellular cholesterol and triacylglycerol accumulation

THP-1 cells were incubated for 24 h with 100  $\mu$ g/ml native or oxidized LDL (OxLDL) in the presence or absence of  $10^{-7}$  M LU224332. After incubation the cells were washed once with ice cold PBS containing 0.4% BSA and twice with PBS alone. Cells were scraped from the culture flask into PBS and sonicated. The cellular lipids were extracted with chloroform–methanol (2:1, v/v). The lipid extract was digested with phospholipase C (*Clostridium welchii*; Sigma) as previously described [38]. The reaction mixture was extracted with chloroform–methanol (2:1, v/v) containing 100  $\mu$ g tridecanoylglycerol as internal standard. The lipid extracts were then reacted for 30 min at 20°C with Sylon BFT (Sigma) plus one part dry pyridine. This procedure converts the free fatty acids into silyl esters and the free sterols, diacylglycerols and ceramides into silyl ethers, leaving the cholesteryl esters and triacylglycerols unmodified. The free cholesterol, cholesterol esters and triacylglycerols were quantified using a non-polar capillary column as previously described [39].

### 2.10. Data analysis

Statistical differences between groups were evaluated using the one-way ANOVA test with post hoc student *t*-test where appropriate. For semiquantitative scoring of xanthoma, the statistical difference between groups was evaluated using the Mann–Whitney test. Data are presented as mean  $\pm$  S.D. unless otherwise indicated. A value of  $P < 0.05$  was considered significant.

## 3. Results

Cholesterol-fed animals accumulated foam-cells along the inner curvature of the aortic arch and throughout the descending aortae, leading to the formation of fibro-fatty plaques at 8 weeks of treatment (Fig. 1b, d and f).

Histological examination revealed that the atherosclerotic plaques contained a necrotic core with cholesterol crystals covered by a thin fibrous cap. Occasional SMCs could be identified in the plaque area and fibrous cap by immunostaining with an antibody against  $\alpha$ -actin (Fig. 1b), however,  $\alpha$ -actin positive cells were mostly restricted to the medial layer of the aortae (Fig. 1a and b). Immunostaining with monocyte/macrophage specific antibody (MOMA-2) showed little or no staining in animals receiving normal chow (Fig. 1c), whereas the majority of cells within the intimal lesion of HC fed animals were MOMA-2 positive (Fig. 1d). In animals receiving normal chow, ET-1 staining was restricted to endothelial cells (Fig. 1e), whereas ET-1 was predominantly located to macrophage rich intimal aortic lesions of HC treated animals, consistent with previous reports [15,21] (Fig. 1f).

The degree of xanthomatosis, derived using a semiquantitative grading system, is presented in Fig. 2A. In LDL-R knockout mice fed a normal chow for 8 weeks (Fig. 2, group I), no xanthomatous lesions were observed. In contrast, in the cholesterol-fed LDL-R deficient mice (group II) xanthomatous lesions of the face, ventral surface of the trunk and swelling of the extremities began to appear at 6 weeks and were present in all animals by 8 weeks [xanthomatosis score (XS) of  $4.0 \pm 0.6$  (median  $\pm$  S.D.) Fig. 2]. In the cholesterol-fed LDL-R deficient mice treated with ET antagonist (group III), significantly fewer xanthomatous lesions were apparent in at 8 weeks [XS:  $1.5 \pm 0.5$  (median  $\pm$  S.D.) Fig. 2]. LDL-R deficient mice fed 1.25% cholesterol were severely hyperlipidemic with mean plasma cholesterol levels 15-fold higher than normal chow-fed animals (group I:  $4.8 \pm 0.6$  mM vs. group II:  $65.6 \pm 6.5$  mM;  $P < 0.001$ ). Treatment of cholesterol-fed LDL-R deficient mice with the ET antagonist did not alter plasma lipid levels (group III:  $66.6 \pm 5.1$  mM) (Fig. 2B). As well, arterial blood pressure was not significantly different in animals fed normal or HC diets ( $78 \pm 7$  and  $78 \pm 3$  mmHg, respectively), either with or without treatment with the ET antagonist for 15 days ( $74 \pm 7$  and  $78 \pm 3$  mmHg, respectively) (five animals in each group). These results are consistent with previous reports using endothelin antagonist in mice [32] and other normotensive animal models [40]. Treatment with LU224332 (10 mg/kg/day for 2 weeks) resulted in measurable plasma levels of the ET antagonist ( $708 \pm 357$  nmol/l), which was well in excess of the  $K_i$  for both ET receptors (see Methods).

The extent of aortic lipid deposition was visualised by oil red O staining (Fig. 3A) and quantified by computer assisted morphometry (Fig. 3B). Extensive atherosclerosis was seen in the HC diet group (group II), whereas only minimal lipid deposition was found in animals receiving normal mouse chow mainly at the bifurcations of great vessels (group I). LU224332 treatment (group III) significantly reduced the extent of atherosclerotic involvement in the aortae by almost 45% (Fig. 3B,  $P < 0.01$ ).

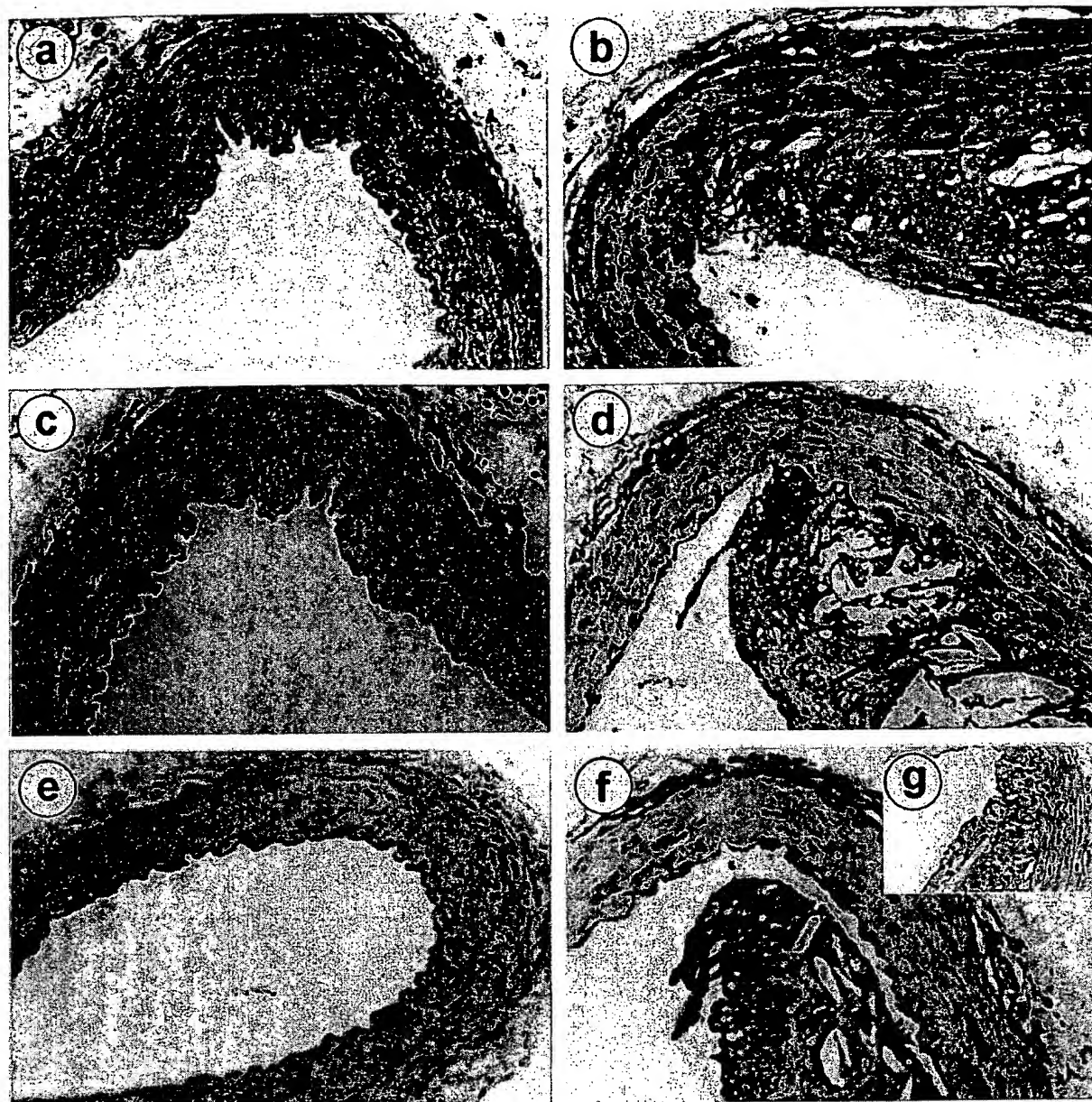
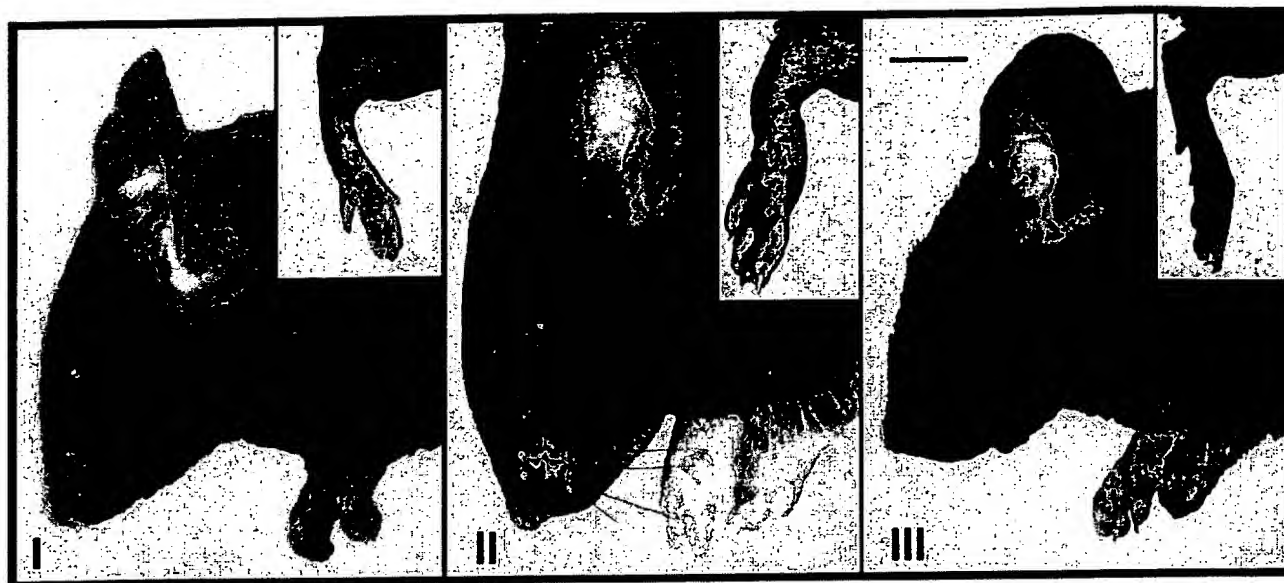


Fig. 1. Photomicrographs show representative sections of thoracic aorta from LDL-R deficient mice fed normal chow (groups I: a, c and e) or a high cholesterol diet (group II: b, d, f and g). Immunostaining for SMCs using an  $\alpha$ -actin antibody revealed a similar pattern of staining in both normal chow (a) and high cholesterol (b) fed animals, largely restricted to the medial layer of the vessels with only partial staining in the atherosclerotic lesion. In contrast, immunostaining with MOMA-2 revealed an absence of macrophages in normal chow fed animals (c) with a very dense accumulation of macrophages in the lesions of high cholesterol fed animals (d). Immunostaining for ET-1 on sequential sections revealed expression of this peptide limited to endothelial cells of normal chow-fed animals (e), with marked ET-1 staining in the HC animals (f) predominantly located to the intimal macrophage rich lesions. Negative control slides were prepared by substituting preimmune rabbit serum for the primary antibody in a section from group II (g).

In order to study the direct effect of endothelin receptor blockade on macrophage lipid accumulation, THP-1 human macrophages were incubated with 100  $\mu$ g/ml of native LDL (nLDL) or Ox LDL, in the presence or absence of LU224332 ( $10^{-7}$  M). After 24 h, cellular cholesteryl ester (CE) and triacylglycerol (TG) were quantified as described in Methods. Treatment of cells with Ox LDL

resulted in 3-fold increase in CE and TG levels compared to nLDL alone ( $P < 0.01$  and  $P < 0.05$ , respectively; Fig. 4A). The addition of LU224332 completely prevented macrophage CE and reduced TG deposition induced by Ox LDL ( $P < 0.01$  and  $P < 0.05$ , respectively; Fig. 4B), reducing macrophage lipid accumulation to levels not different from nLDL alone.

A



B

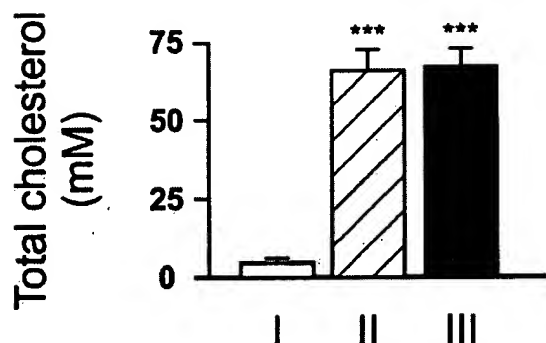


Fig. 2. Animals on regular chow diet, (group I), did not develop xanthomas. In contrast, mice fed high cholesterol (HC) diet alone, group II, developed facial xanthomatous lesions and marked swelling of the paws by the end of the experimental protocol. The LDL-R deficient mice receiving supplemental endothelin antagonist (LU224332) together with HC diet, (group III), showed much reduced facial xanthomatous and minimal swelling of the extremities (A). The mean xanthomatosis score for experimental groups II and III are presented in the results section. Average total plasma cholesterol values (mM) in groups I, II and III are shown in (B).

#### 4. Discussion

The results of the present study demonstrate an important anti-atherosclerotic effect of a non-selective ET receptor antagonist in a model of homozygous familial hypercholesterolemia, the LDL receptor (LDL-R) deficient mouse. In addition to preventing atherosclerosis, treatment with the ET antagonist significantly reduced xanthoma formation without affecting total cholesterol levels or arterial pressure. These results support the hypothesis that the ET system contributes directly to the pathogenesis of atherosclerosis and that ET blockers may have therapeutic utility in the treatment of this vascular disorder.

In the vessel wall, the  $ET_A$  receptor is located primarily on SMCs, whereas the  $ET_B$  subtype is found mainly on the endothelial layer, infiltrating macrophages [29] and to a variable extent SMCs [28]. Although  $ET_A$  may mediate many of the effects of ET-1 that are likely relevant to atherosclerosis, the presence of the  $ET_B$  receptors on macrophages and its up regulation on SMCs of vascular lesions [27], suggest that this receptor subtype may contribute importantly to the pathogenesis of atherosclerosis as well. In fact, a recent report has suggested that accumulation of foamy macrophages and T lymphocytes in the fibrous plaque may modulate the switching of ET receptor subtypes from  $ET_A$  to  $ET_B$  in SMCs [41].

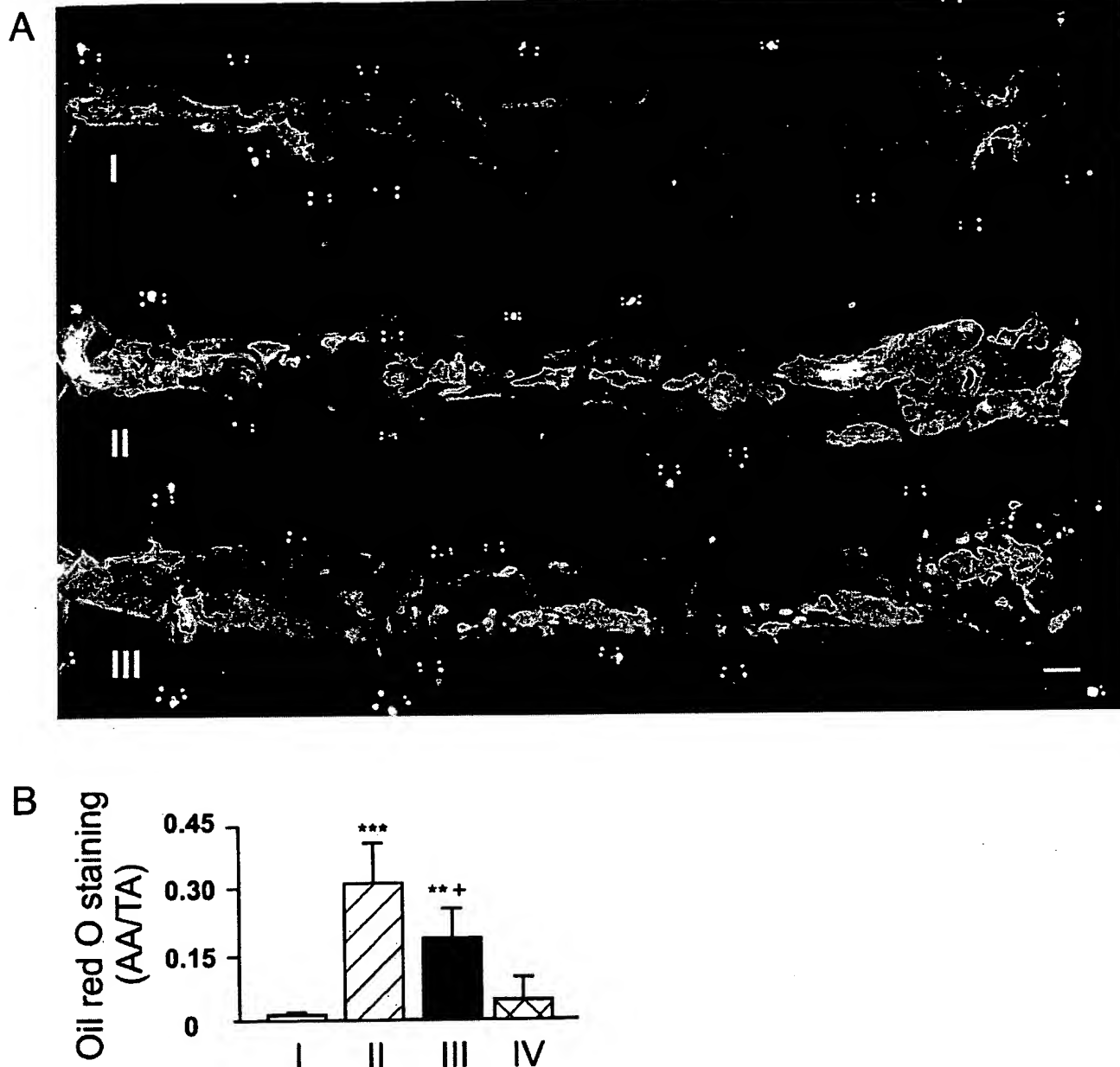


Fig. 3. Representative oil red O staining on the full length luminal surface of aortas from LDL-R deficient mice. Extensive lipid deposition could be seen in the HC diet group (group II), while only minimal lipid deposition was found in animals receiving normal mouse chow (group I). Aortas from LU224332 treated animals (group III) showed reduced aortic atherosclerosis (A). Mean values for atherosclerotic area relative to total aortic luminal surface are shown in panel B ( $n=6$ , group I;  $n=9$ , group II and III;  $n=5$ , group IV). Asterisks indicate statistical difference versus group I using the one-way ANOVA with post-hoc Student *t*-test (\*\*,  $P<0.01$ ; \*\*\*,  $P<0.001$ ). The plus sign indicates a statistical difference versus group II using the one-way ANOVA with post-hoc Student *t*-test (+,  $P<0.01$ ).

Cultured rat peritoneal macrophages have been described to express nearly exclusively  $ET_B$  receptors [42] whereas both  $ET_A$  and  $ET_B$  receptors have been demonstrated by in situ hybridization on macrophages in the early inflammatory intimal lesion of hyperlipidemic hamsters [31].

In contrast, stimulation of  $ET_B$  receptors on the endothelial cells releases vasodilators, such as NO, which may protect against atherosclerosis [43]. Kowala et al. [31] previously reported that an  $ET_A$  selective antagonist re-

duced fatty-streak formation in a hamster model of early atherosclerosis. However, to some extent this effect might have been due to a lipid lowering action of certain  $ET$  antagonists [31,44]. Recently, Barton et al. [32] reported that another  $ET_A$  selective antagonist reduced atherosclerosis in the apoE-deficient mouse model of atherosclerosis, further supporting an important role for ET-1 in this disease. This was associated with a marked improvement in endothelium-dependent dilation and increased nitrate/

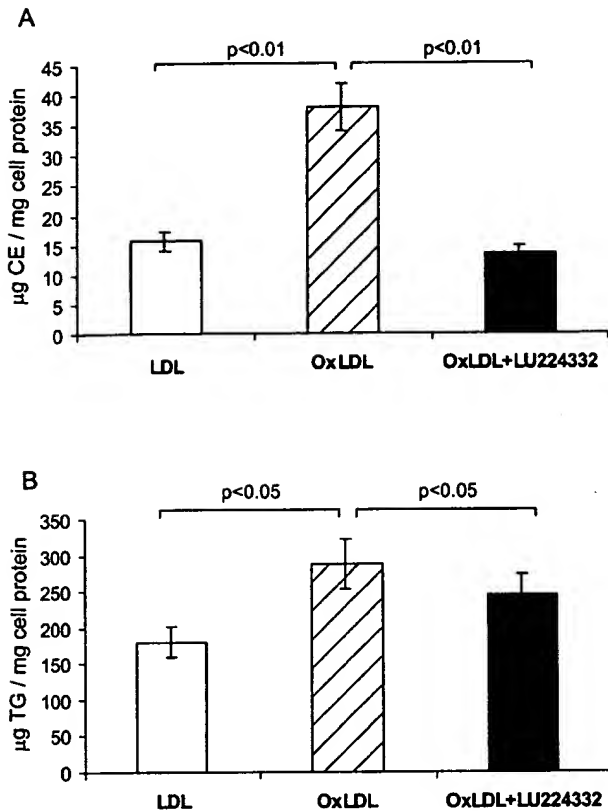


Fig. 4. Mean values  $\pm$  S.D. ( $n=4$ ) for cellular cholesterol ester (CE; A) and triacylglycerol (TG; B) accumulation in THP-1 cell line in presence of nLDL or OxLDL with or without LU224332 for 24 h. LU224332 prevented CE and TG uptake induced by OxLDL ( $P<0.01$  and  $P<0.05$ , respectively).

nitrite levels in the blood [32], likely as a result of selective  $ET_A$  blockade which spares the endothelial  $ET_B$  receptor. Therefore, it is possible that an increase in endothelial NO production may have contributed indirectly to the anti-atherogenic effects of  $ET_A$  blockade in these studies. It is well established that other strategies to increase endothelial NO release, i.e. L-arginine supplementation [45,46], and angiotensin converting enzyme inhibition [47,48] reduce atherosclerosis in a variety of animal models. In the present study a balanced  $ET_A$  and  $ET_B$  receptor antagonist was used, which would not be expected to favorably alter the balance of endothelial versus smooth muscle ET receptor activation. Indeed, it could be argued that blockade of endothelial  $ET_B$  receptor with this compound would be counterproductive and could reduce the overall beneficial effect of the ET antagonist in atherosclerotic models. Nonetheless, a marked reduction in atherosclerosis and xanthomatosis was seen with LU224332 in the absence of any changes in plasma lipids, which may be ascribed to direct effects of ET-1 on the cellular events leading to the initiating and/or progression of atherosclerosis. However, we cannot exclude the possibility that mixed ET blockade may have resulted in

improvement in endothelial function by an indirect mechanism. Increased NO production has been previously reported with both selective and non-selective ET antagonists in the rat Langerdorff heart model [49], possibly due to increased coronary flow and therefore intimal shear forces [49].

In addition to its potent vasoconstrictor effects, ET-1 has a number of biological activities, which might contribute directly to the morphological changes characteristic of atherosclerosis. Endothelin-1 is a co-mitogen for vascular SMCs [13], and can act in concert with other well-characterized growth factors, such as PDGF, which are believed to initiate and maintain cell proliferation in the atheromatous [17]. ET-1 is also a powerful stimulus for secretion of collagen [14] and other matrix components which represent a major constituent of the atherosclerotic lesion. Therefore the inhibition of ET-1 action on atheromatous SMCs may be critical in the anti-atherosclerotic effects of LU224332. As well, ET-1 may also contribute to the recruitment of monocytes into the developing intimal lesion either directly [15] or indirectly by increasing MCP-1 [16]. Macrophages play a key role in the pathogenesis of atherosclerosis [30]. The marked up-regulation of expression of ET-1 in macrophages seen in this and other studies also suggest that this peptide may contribute to chronic inflammatory changes in this disease.

ET-1 has been shown to increase the release of inflammatory cytokines from macrophages [50,51]. In turn, cytokines such as  $TNF\alpha$ , IL-1 and IL-6 have been shown to increase ET-1 production by macrophages [52]. Thus ET-1 may serve to amplify and sustain macrophage activation in the developing atheromatous [51]. Interruption of this positive feedback pathway is a potential mechanism by which ET receptor antagonists may reduce the progression of atherosclerosis in addition to its effects on SMC proliferation and matrix secretion. In support of this, a marked decrease in xanthomas formation, a non-vascular lesion which is dependent on macrophage activation [3] was also observed in LDL-R deficient mice treated with the ET antagonist. Further evidence in favor of a direct effect of ET-1 on macrophage foam-cell formation was provided by in vitro studies using the human THP-1 monocyte-macrophage cell line. These cells differentiate into macrophages on exposure to phorbol ester, in which state they have previously been characterized to express predominantly the  $ET_B$  receptor [29]. The ability of the LU224332 compound to largely prevent cholesterol ester and triacylglycerol accumulation in these cells on exposure to Ox LDL is consistent with a crucial role for endogenous ET-1 in macrophage activation and foam-cell formation.

In summary, nonselective inhibition of ET receptors with LU224332 reduced atherosclerosis and xanthomatosis independently of any change in lipid levels. Prominent ET-1 expression in macrophage-rich atherosclerotic lesions observed in vivo, together with the ability of the ET receptor antagonist to directly reduce macrophage lipid



accumulation in vitro, point to a role for ET-1 in foam-cell formation. Thus, antagonism of the ET system may provide a new pharmacological approach to reduce the vessel wall response to chronic injury induced by hyperlipidemia, and thereby inhibit intimal lesion formation and progression of atherosclerosis.

## Acknowledgements

This work was supported by the Medical Research Council of Canada (MRC MT11620). DJS is the Dexter H.C. Man Chair of Cardiology of the University of Toronto. SB is supported by a Fellowship from the KM Hunter/Medical Research Council of Canada. TCL is supported by a studentship from the Canadian Hypertension Society/Pfizer Canada Inc./MRC. We are grateful to Dr. Phil Connelly for assisting us in the measurements of plasma cholesterol levels and for his helpful comments and advice. Also we would like to thank Dr. M. Kirchengast from Knoll company for his generous gift of the LU224332 compound.

## References

- [1] Brown MS, Goldstein JL. Lipoprotein receptors in the liver. Control signals for plasma cholesterol traffic. *J Clin Invest* 1983;72(3):743–747.
- [2] Goldstein JL, Dana SE, Brunschede GY, Brown MS. Genetic heterogeneity in familial hypercholesterolemia: evidence for two different mutations affecting functions of low-density lipoprotein receptor. *Proc Natl Acad Sci USA* 1975;72(3):1092–1096.
- [3] Ishibashi S, Goldstein JL, Brown MS, Herz J, Burns DK. Massive xanthomatosis and atherosclerosis in cholesterol-fed low density lipoprotein receptor-negative mice. *J Clin Invest* 1994;93(5):1885–1893.
- [4] Dusting GJ, Fennessy P, Yin ZL, Gurevich V. Nitric oxide in atherosclerosis: vascular protector or villain? *Clin Exp Pharmacol Physiol Suppl* 1998;25:S34–S41.
- [5] Wever RM, Luscher TF, Cosentino F, Rabelink TJ. Atherosclerosis and the two faces of endothelial nitric oxide synthase. *Circulation* 1998;97(1):108–112.
- [6] Toutouzas PC, Tousoulis D, Davies GJ. Nitric oxide synthesis in atherosclerosis. *Eur Heart J* 1998;19(10):1504–1511.
- [7] Maxwell AJ, Tsao PS, Cooke JP. Modulation of the nitric oxide synthase pathway in atherosclerosis. *Exp Physiol* 1998;83(5):573–584.
- [8] Bult H. Nitric oxide and atherosclerosis: possible implications for therapy. *Mol Med Today* 1996;2(12):510–518.
- [9] John S, Schlaich M, Langenfeld M et al. Increased bioavailability of nitric oxide after lipid-lowering therapy in hypercholesterolemic patients: a randomized, placebo-controlled, double-blind study. *Circulation* 1998;98(3):211–216.
- [10] Thorne S, Mullen MJ, Clarkson P, Donald AE, Deanfield JE. Early endothelial dysfunction in adults at risk from atherosclerosis: different responses to L-arginine. *J Am Coll Cardiol* 1998;32(1):110–116.
- [11] Yanagisawa M, Kurihara H, Kimura S et al. A novel potent vasoconstrictor peptide produced by vascular endothelial cells. *Nature* 1988;332(6163):411–415.
- [12] Eglen RM, Michel AD, Sharif NA, Swank SR, Whiting RL. The pharmacological properties of the peptide, endothelin. *Br J Pharmacol* 1989;97(4):1297–1307.
- [13] Assender JW, Irenius E, Fredholm BB. Endothelin-1 causes a prolonged protein kinase C activation and acts as a co-mitogen in vascular smooth muscle cells. *Acta Physiol Scand* 1996;157(4):451–460.
- [14] Rizvi MA, Katwa L, Spadone DP, Myers PR. The effects of endothelin-1 on collagen type I and type III synthesis in cultured porcine coronary artery vascular smooth muscle cells. *J Mol Cell Cardiol* 1996;28(2):243–252.
- [15] Achmad TH, Rao GS. Chemotaxis of human blood monocytes toward endothelin-1 and the influence of calcium channel blockers. *Biochem Biophys Res Commun* 1992;189(2):994–1000.
- [16] Helset E, Sildnes T, Konopski ZS. Endothelin-1 stimulates monocytes in vitro to release chemotactic activity identified as interleukin-8 and monocyte chemotactic protein-1. *Mediators Inflamm* 1994;3:155–160.
- [17] Kowala MC. The role of endothelin in the pathogenesis of atherosclerosis. *Adv Pharmacol* 1997;37:299–318.
- [18] He Y, Kwan WC, Steinbrecher UP. Effects of oxidized low density lipoprotein on endothelin secretion by cultured endothelial cells and macrophages. *Atherosclerosis* 1996;119(1):107–118.
- [19] Lerman A, Edwards BS, Hallett JW, Heublein DM, Sandberg SM, Burnett Jr. JC. Circulating and tissue endothelin immunoreactivity in advanced atherosclerosis. *New Engl J Med* 1991;325(14):997–1001.
- [20] Jones GT, van Rij AM, Solomon C, Thomson IA, Packer SG. Endothelin-1 is increased overlying atherosclerotic plaques in human arteries. *Atherosclerosis* 1996;124(1):25–35.
- [21] Zeiher AM, Goebel H, Schachinger V, Ihling C. Tissue endothelin-1 immunoreactivity in the active coronary atherosclerotic plaque. A clue to the mechanism of increased vasoreactivity of the culprit lesion in unstable angina. *Circulation* 1995;91(4):941–947.
- [22] Lerman A, Webster MW, Chesebro JH et al. Circulating and tissue endothelin immunoreactivity in hypercholesterolemic pigs. *Circulation* 1993;88(6):2923–2928.
- [23] Bacon CR, Davenport AP. Endothelin receptors in human coronary artery and aorta. *Br J Pharmacol* 1996;117(5):986–992.
- [24] Kohan DE. Endothelins in the normal and diseased kidney. *Am J Kidney Dis* 1997;29(1):2–26.
- [25] Kanse SM, Wijelath E, Kanthou C, Newman P, Kakkar VV. The proliferative responsiveness of human vascular smooth muscle cells to endothelin correlates with endothelin receptor density. *Lab Invest* 1995;72(3):376–382.
- [26] Vane JR, Anggard EE, Botting RM. Regulatory functions of the vascular endothelium. *New Engl J Med* 1990;323(1):27–36.
- [27] Azuma H, Hamasaki H, Sato J, Isotani E, Obayashi S, Matsubara O. Different localization of ET<sub>A</sub> and ET<sub>B</sub> receptors in the hyperplastic vascular wall. *J Cardiovasc Pharmacol* 1995;25(5):802–809.
- [28] Sumner MJ, Cannon TR, Munding JW, White DG, Watts IS. Endothelin ET<sub>A</sub> and ET<sub>B</sub> receptors mediate vascular smooth muscle contraction. *Br J Pharmacol* 1992;107(3):858–860.
- [29] Magazine HI, Andersen TT, Bruner CA, Malik AB. Vascular contractile potency of endothelin-1 is increased in the presence of monocytes or macrophages. *Am J Physiol* 1994;266(4 Pt 2):H1620–H1625.
- [30] Murakami T, Yamada N. Modification of macrophage function and effects on atherosclerosis. *Curr Opin Lipidol* 1996;7(5):320–323.
- [31] Kowala MC, Rose PM, Stein PD et al. Selective blockade of the endothelin subtype A receptor decreases early atherosclerosis in hamsters fed cholesterol. *Am J Pathol* 1995;146(4):819–826.
- [32] Barton M, Haudenschield CC, d'Uscio LV, Shaw S, Munter K, Luscher TF. Endothelin E.T.A. receptor blockade restores NO-mediated endothelial function and inhibits atherosclerosis in apolipoprotein E-deficient mice. *Proc Natl Acad Sci USA* 1998;95(24):14367–14372.
- [33] Best PJ, McKenna CJ, Hasdai D, Holmes Jr. DR, Lerman A.

- Chronic endothelin receptor antagonism preserves coronary endothelial function in experimental hypercholesterolemia. *Circulation* 1999;99(13):1747–1752.
- [34] Raschack M, Gock S, Unger L et al. LU302 872 and its racemate (LU224332) show balanced endothelin-A/B receptor affinity, high oral activity, and inhibit human prostate tissue contractions. *J Cardiovasc Pharmacol* 1998;31(Suppl 1):S241–S244.
- [35] Cernacek P, Franchi L, Dupuis J, Rouleau JL, Levy M. Radioreceptor assay of an endothelin A receptor antagonist in plasma and urine. *Clin Chem* 1998;44(8 Pt 1):1666–1673.
- [36] Havel RJ, Eder HA, Bragdon JH. The distribution and chemical composition of ultracentrifugally separated lipoproteins in human serum. *J Clin Invest* 1955;34:1345–1353.
- [37] Lowry OH, Rosebrough NJ, Farr AL, Randall RJ. Protein measurement with the Folin phenol reagent. *J Biol Chem* 1951;193:265–275.
- [38] Kuksis A, Myher JJ, Geher K et al. Comparative determination of plasma phospholipids by automated gas–liquid chromatographic and manual colorimetric phosphorus methods. *J Chromatogr* 1980;182(1):1–26.
- [39] Ravandi A, Kuksis A, Shaikh NA. Glycated phosphatidylethanolamine promotes macrophage uptake of low density lipoprotein and accumulation of cholesteryl esters and triacylglycerols. *J Biol Chem* 1999;274(23):16494–16500.
- [40] Moreau P. Endothelin in hypertension: a role for receptor antagonists? *Cardiovasc Res* 1998;39(3):534–542.
- [41] Iwasa S, Fan J, Shimokama T, Nagata M, Watanabe T. Increased immunoreactivity of endothelin-1 and endothelin B receptor in human atherosclerotic lesions. A possible role in atherogenesis. *Atherosclerosis* 1999;146(1):93–100.
- [42] Sakurai-Yamashita Y, Yamashita K, Yoshida A et al. Rat peritoneal macrophages express endothelin ET(B) but not endothelin ET(A) receptors. *Eur J Pharmacol* 1997;338(2):199–203.
- [43] Aji W, Ravalli S, Szabolcs M et al. L-Arginine prevents xanthoma development and inhibits atherosclerosis in LDL receptor knockout mice. *Circulation* 1997;95(2):430–437.
- [44] Iwasa S, Fan J, Miyauchi T, Watanabe T. Non-selective endothelin receptor antagonist, SB209670, reduces diet-induced hypercholesterolemia and atherosclerosis in apolipoprotein E-deficient mice. *Circulation* 1999;100(18):1–474, Abstract.
- [45] Jeremy RW, McCarron H, Sullivan D. Effects of dietary L-arginine on atherosclerosis and endothelium-dependent vasodilatation in the hypercholesterolemic rabbit. Response according to treatment duration, anatomic site, and sex. *Circulation* 1996;94(3):498–506.
- [46] Cooke JP, Andon NA, Girerd XJ, Hirsch AT, Creager MA. Arginine restores cholinergic relaxation of hypercholesterolemic rabbit thoracic aorta. *Circulation* 1991;83(3):1057–1062.
- [47] Dusting GJ, Hyland R, Hickey H, Makdissi M. Angiotensin-converting enzyme inhibitors reduce neointimal thickening and maintain endothelial nitric oxide function in rabbit carotid arteries. *Am J Cardiol* 1995;76(15):24E–27E.
- [48] Luscher TF, Wenzel RR, Moreau P, Takase H. Vascular protective effects of ACE inhibitors and calcium antagonists: theoretical basis for a combination therapy in hypertension and other cardiovascular diseases. *Cardiovasc Drugs Ther* 1995;9(3):509–523.
- [49] Goodwin AT, Amrani M, Gray CC, Jayakumar J, Yacoub MH. Role of endogenous endothelin in the regulation of basal coronary tone in the rat. *J Physiol* 1998;511(2):549–557.
- [50] Ruetten H, Thiernemann C. Endothelin-1 stimulates the biosynthesis of tumour necrosis factor in macrophages: ET-receptors, signal transduction and inhibition by dexamethasone. *J Physiol Pharmacol* 1997;48(4):675–688.
- [51] Speciale L, Roda K, Saresella M, Taramelli D, Ferrante P. Different endothelins stimulate cytokine production by peritoneal macrophages and microglial cell line. *Immunology* 1998;93(1):109–114.
- [52] Kahaleh MB, Fan PS. Effect of cytokines on the production of endothelin by endothelial cells. *Clin Exp Rheumatol* 1997;15(2):163–167.



# Animal Models of Atherosclerosis and Interpretation of Drug Intervention Studies

Thomas M.A. Bocan

Department of Vascular and Cardiac Diseases, Parke-Davis Pharmaceutical Research, Division of Warner Lambert Company, 2800 Plymouth Road, Ann Arbor, MI 48105, USA

**Abstract:** Atherosclerosis has often been defined as a multifactorial disease; however, a common risk factor associated with accelerated vascular disease in man or animals is an elevated plasma cholesterol level. Even though there is no one perfect animal model that completely replicates the stages of human atherosclerosis, cholesterol feeding and mechanical endothelial injury are two common features shared by most models of atherosclerosis. The models may differ with respect to degree of dietary cholesterol supplementation, length of hypercholesterolemia, dietary regimen and type, duration and degree of mechanical endothelial injury. With the advent of genetic engineering, transgenic mouse models have supplemented the classical dietary cholesterol induced disease models such as the cholesterol-fed hamster, rabbit, pig and monkey. The desire to limit the progression of atherosclerosis has spawned numerous drug intervention studies. Biochemical as well as morphologic and morphometric changes in the extent, structure and composition of atherosclerotic lesions following drug intervention have become major endpoints of *in vivo* drug intervention studies. Interpretations of alterations in vascular pathology following drug administration are often confounded by associated changes in plasma lipids and lipoproteins, limitation of the animal models and additional properties of compounds unrelated to their primary mode of action. Thus, the current review will summarize the pathology of atherosclerosis, describe various animal models of vascular disease and provide a critical review of the methods utilized and conclusions drawn when evaluating pharmacologic agents in animals.



## Introduction

Atherosclerosis has often been defined as a multifactorial disease. In addition, hypercholesterolemia has become a widely accepted risk factor for premature development of coronary artery disease. Classical thinking argued that development of clinically significant atherosclerotic lesions was associated with two major processes. One is fibrocellular proliferation, which adds to intimal bulk and eventually leads to chronic ischemic syndromes via gradual constriction of the arterial lumen. The second process involves the combination of cellular necrosis and lipid deposition within the arterial intima. Enlargement of a lipid-rich core tends to erode the fibrous cap [1], eventuating in plaque rupture, exposure of circulating blood to highly thrombogenic material and sudden ischemic episodes such as myocardial infarction [2,3]. Considering our classical understanding of atherosclerosis progression, the current article will review the histologic landmarks of the various stages of atherosclerosis and also provide a dynamic understanding of how the stages might be interrelated. A comparison of various hypercholesterolemia-induced animal models of atherosclerosis will be made with a focus on their advantages and limitations when used to evaluate novel antiatherosclerotic drugs. Finally, the antiatherosclerotic activity of inhibitors of acyl-coenzyme A:cholesterol O-acyltransferase (ACAT) Fig. (1) (1-14), 3-hydroxy-3-methylglutaryl coenzyme A (HMG-CoA reductase) Fig. (2) (15-18), 15-lipoxygenase (15-LO) and lipoprotein oxidation (anti-oxidants) Fig. (3) (19-22) will be discussed; however, an emphasis will be on describing how the models can discern the compound's *direct* from *indirect* antiatherosclerotic activity.

## Pathology of Atherosclerosis

Atherosclerosis is a focal disease that has been shown to develop in a distinct pattern in both man and animals [4,5]. As depicted in Fig. (4), atherosclerotic lesion development can be divided into six histologically distinct stages or lesion types and five dynamic phases [6,7]. The formation of an intimal cushion at distinct sites within the arterial tree appears to precede the development of atherosclerosis and may be considered a normal aging process. Smooth muscle cells (SMC) migrate from the media, proliferate in the intima and secrete extracellular matrix. Extracellular lipid accumulation that is primarily of lipoprotein origin [8] decorates the secreted collagen, elastin and proteoglycans of the developing intima. Oxidation of the insudant lipoproteins [9] appears to set up a chemotactic gradient and stimulate endothelial cells to upregulate adhesion molecules, i.e., vascular cell adhesion molecule-1 (VCAM-1) [10], responsible for the recruitment of monocyte-macrophages. Monocyte-macrophages are a hallmark of Type I to III lesions and are both a culprit cell responsible for promoting lesion development and a potential point of therapeutic intervention. The major difference in Type I to III lesions lies in the relative amounts of monocyte-macrophage foam cells, SMC, extracellular matrix and lipid and the gross extent of these lesions on the arterial surface. These lesions have classically been termed fatty dots, fatty streaks or fibrolipid lesions to denote their relative extent and degree of fibrosis. Therefore, progression from the innocuous intimal cushion to the Type III lesion that may occur over the first 20 to 30 years of life can be characterized as Phase 1.

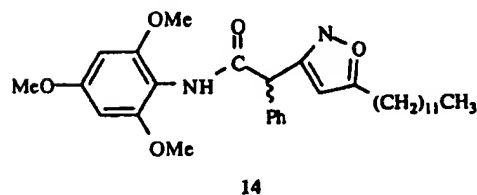
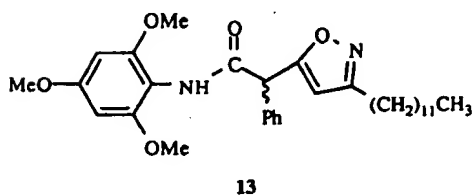
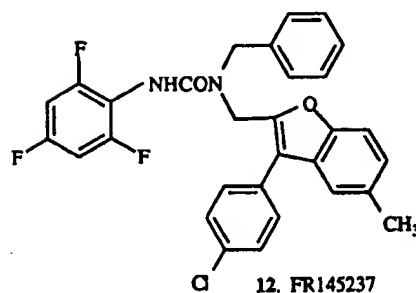
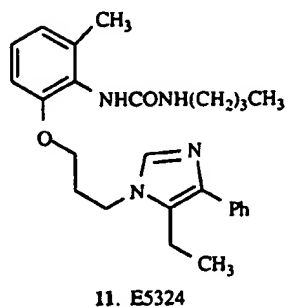
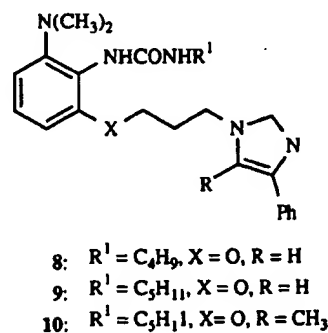
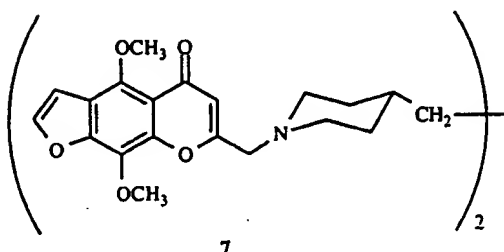
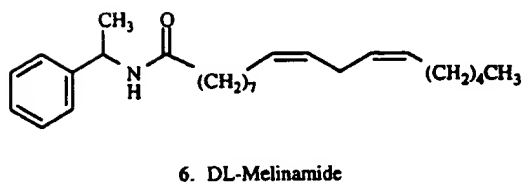
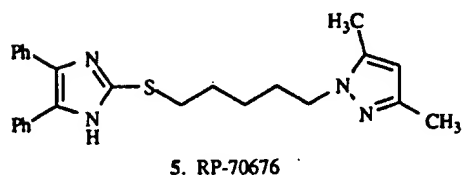
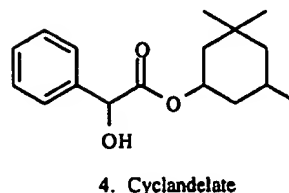
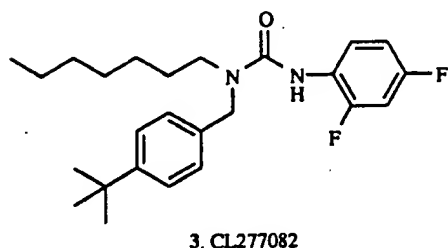
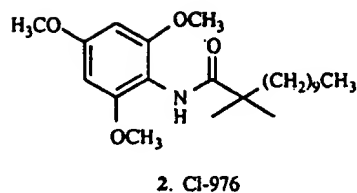
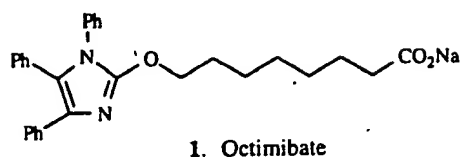


Fig. (1). ACAT inhibitors.

Enlargement of the extracellular lipid pool and formation of a deep intimal lipid-rich necrotic core is a distinguishing characteristic of the Type IV lesion. Type IV lesions can be described as a transitional lesion with many potential fates.

Episodic plaque fissures, microthrombi formation and expansion of the fibrous cap overlying the necrotic core can lead to the formation of the potentially more stable Type V lesions (Phase 2). Type V lesions that are often referred to as fibrous plaques

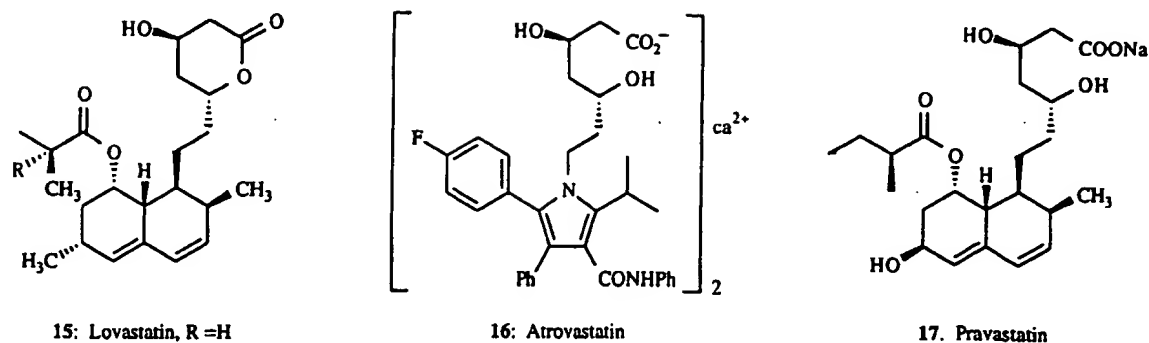


Fig. (2). HMG-CoA reductase inhibitors.

have a developed fibrous cap, deep-intimal necrosis and a lipid-rich necrotic core composed of cholesterol clefts, calcium deposits and evidence of neovascularization. Continued fibrosis of a Type V lesion could silently occlude the arterial lumen (Phase 5). Rupture of the fibrous cap of a Type IV lesion can also generate a mural thrombus that is rapidly recanalized and retracted into the arterial wall to form a Type V lesion (Phase 3). A marked rupture (Phase 4) of the fibrous cap, generation of an occlusive thrombus, myocardial infarction and sudden death is a final fate of the Type IV lesion and for the purpose of classification has been denoted as a Type VI complicated plaque.

In summary, atherosclerotic lesion progression in man involves episodes of SMC proliferation, extracellular matrix deposition and remodeling, lipid infiltration, endothelial cell-monocyte interactions, monocyte migration into the intima, monocyte-macrophage foam cell formation, necrotic lipid-rich core formation, calcium deposition, neovascularization, mural microthrombi and occlusive acute thrombosis. Some of the cell-derived factors that may contribute to atherosclerotic lesion development have previously been reviewed [11].

### Animal Models of Atherosclerosis

Given the complexity of atherosclerotic lesion development in man, the challenge exists to develop animal models that closely mimic the human disease. One must accept, however, that there is no one perfect animal model that completely replicates the stages of human atherosclerosis but that the models are useful in studying specific pathologic processes

associated with the disease. Irrespective of species, there are several common features shared by most models of atherosclerosis. Firstly, induction of vascular lesions in most animal models is dependent upon development of a plasma hypercholesterolemia. Plasma cholesterol elevations can either be induced by dietary supplementation with cholesterol, hepatic overproduction of lipoproteins or genetic mutation of receptors and/or receptor ligands responsible for lipoprotein clearance. Secondly, to accelerate development of atherosclerotic lesions in hypercholesterolemic animals various forms of acute or chronic endothelial damage have been employed. The animal models differ with respect to degree of dietary cholesterol supplementation, length of hypercholesterolemia, dietary regimen and type, duration and degree of mechanical endothelial injury. Thus, this section will describe the various rabbit, hamster, pig, monkey and transgenic mouse models of atherosclerosis with respect to the different experimental protocols utilized to induce atherosclerotic lesions, the stage of atherosclerotic lesion development being replicated and advantages or disadvantages of the model for drug intervention studies.

### Rabbits

The cholesterol-fed rabbit has been extensively used as a model of atherosclerosis since the identification by Anitschkow [12] in 1913 that short-term cholesterol feeding results in formation of foamy lesions within the aorta. Historically, supplementation of commercial rabbit chow with 1 to 3%

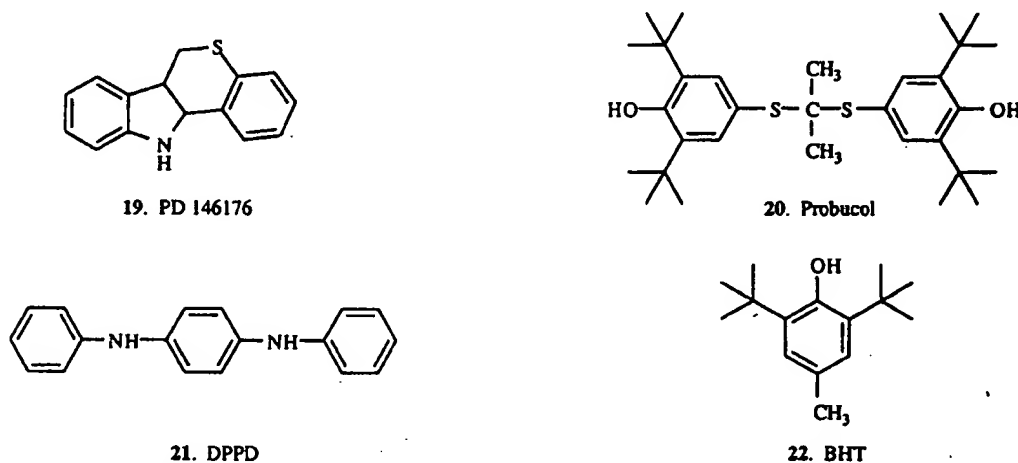


Fig. (3). Antioxidants and 15-LO inhibitors.

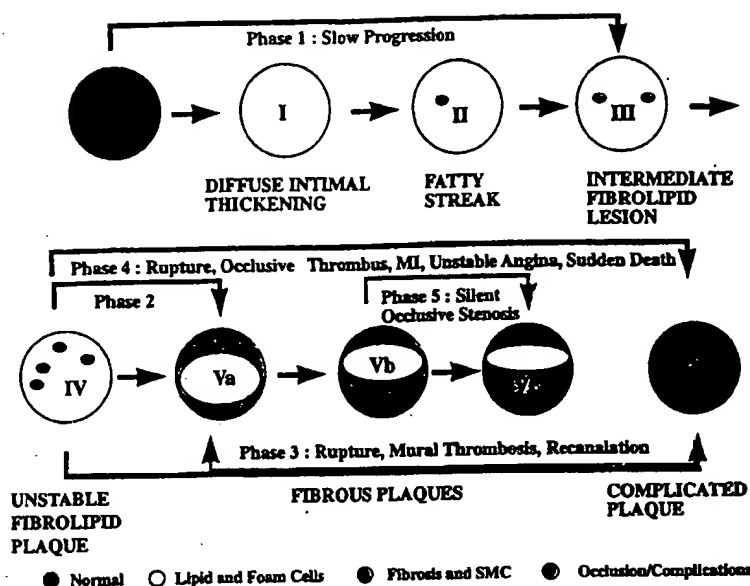


Fig. (4). Schematic representation of atherosclerotic lesion progression (adapted from references [6, 7]).

cholesterol and 4 to 8% fat [13] for 6 to 8 weeks has resulted in marked elevations in plasma cholesterol, i.e., 1000 to 3000 mg/dl, cholesteryl ester accumulation in hepatic and peripheral tissues [14,15] and development of aortic macrophage foam cell enriched lesions. Development of atherosclerosis in the coronaries is limited to the small intramyocardial vessels and not the larger epicardial vessels as has been found in man [16]. The rabbit atherosclerotic lesions were reminiscent in cellular composition to Type I to III human lesions. Krichevsky and colleagues have performed numerous cholesterol feeding experiments in which they maintained the cholesterol supplementation constant, i.e., 2%, and altered the type of dietary fat to further refine the role of cholesterol metabolism in atherosclerosis progression. A notable finding was that upon addition of 6% peanut oil or 6% coconut oil to a 2% cholesterol diet two histologically distinct atherosclerotic lesions developed [17,18]. Peanut oil supplementation produced aortic lesions that contained relatively little lipid but abundant smooth muscle cell proliferation and collagen deposition. In contrast, addition of 6% coconut oil to the diet resulted in lesions with demonstrable intracellular lipid and intimal proliferation; however, less collagen and elastin were evident. Although elevated plasma cholesterol levels induce atherosclerotic lesions and dietary fat composition may affect the cellular composition of the lesion in rabbits, prolonged hypercholesterolemia results in exponential cholesterol enrichment of many peripheral organs [19].

The marked cholesteryl ester enrichment of peripheral organs such as the liver and spleen may be problematic when evaluating pharmacologic agents. Liver metabolism of compounds may be compromised or enhanced in animals fed a high cholesterol diet and the resulting plasma levels may be either an underestimate or overestimate of the actual efficacious drug levels. Feeding a 2% cholesterol diet results in marked plasma total cholesterol levels and cholesteryl ester enriched beta-VLDL as the primary plasma lipoprotein [20]. Given the pro-atherogenic nature of beta-VLDL [21], the direct antiatherosclerotic activity of compounds with mechanisms

unrelated to cholesterol lowering may be masked due to the profound effect of beta-VLDL on monocyte-macrophage cholesteryl ester enrichment. We have noted that while compounds like ACAT inhibitors Fig. (1) (1-14) which prevent the accumulation of cholesteryl esters are antiatherosclerotic under such conditions, the 15-LO inhibitor, PD146176 Fig (3) (19), lacks activity because its mechanism of action may be related to oxidation of lipoproteins or pre-macrophage events such as monocyte adherence and transmigration.

Rabbit models of atherosclerosis have been developed which limit the amount of dietary cholesterol supplementation [22]; however, such models are time consuming and for that reason may have limited utility for screening antiatherosclerotic agents. Wilson and colleagues [22] fed rabbits an agar-gel diet containing 19% butter and 1% corn oil for up to 5 years. Plasma total cholesterol levels were approximately 300 mg/dl and over the course of 5 years atherosclerotic lesions representing Type I to V lesions were noted. Advanced atherosclerosis can also be induced in a shorter time frame by intermittent feeding of a 1% cholesterol, 5% cottonseed oil diet for 2 months followed by 6 months of a chow diet and 2 additional months of the cholesterol diet [23,24]. While plasma cholesterol levels fluctuated with dietary cholesterol supplementation, the five stages of atherosclerosis were present in both aorta and coronary arteries. Protracted feeding of a low cholesterol diet or intermittent feeding of high and low cholesterol diets produced histologically similar atherosclerotic lesions. Given the disparate plasma total cholesterol levels, these data suggest that the lipoprotein profile may play an important role in the rate at which atherosclerotic lesions develop. Feeding studies have indicated that beta-VLDL was the primary lipoprotein in rabbits fed a cholesterol diet while LDL-like particles predominated in animals fed a semisynthetic casein-enriched diet [25]. Morphologic and morphometric analysis of rabbits fed either a 0.125% to 0.5% cholesterol or casein-enriched diet for 6 months revealed that atherosclerotic lesions developed in both models; however, the nature and extent of lesions varied [25, 26]. At comparable plasma cholesterol levels, the cholesterol-fed

rabbits had approximately twice the extent of aortic atherosclerosis relative to the casein-fed animals and Type IV-V lesions predominated. In the casein-fed rabbits, 30% of the aorta contained atherosclerotic lesions that ranged in appearance from fatty dots to fibrous plaques with a necrotic lipid-rich core [25,26]. These data indicate that under a similar time frame and plasma cholesterol level the type of dietary supplementation can affect the quantity and type of atherosclerotic lesion that develops primarily by altering the major cholesterol carrying lipoprotein, i.e., beta-VLDL or LDL.

Genetic models of atherosclerosis, namely, the homozygote Watanabe Heritable Hyperlipidemic rabbit (WHHL) which lacks functional LDL receptors, have also been compared to cholesterol-fed rabbit models [27,28]. Like the casein-fed rabbits, plasma cholesterol was primarily distributed in LDL. In WHHL rabbits, leukocyte margination, subendothelial accumulation of isolated lipid-filled macrophages, accumulation of SMC and formation of fatty streaks occurred over the first 4 weeks of life [27]. A similar sequence of lesion formation was noted in New Zealand White rabbits fed a 0.1% to 0.2% cholesterol diet. Expansion of the lipid-filled monocyte-macrophage rich lesions, i.e., Type I-III fatty streaks, occurred during the first 6 months in both types of rabbits while complex Type V fibrous plaque lesions were noted in the WHHL and cholesterol-fed rabbits by 13 months of age [28-30]. An enrichment of cholesteryl ester, primarily cholesteryl oleate, was noted in the aorta of both animals over the course of 13 months and such a finding was consistent with the morphologic data noted above [31]. Despite the different lipoprotein distribution, one must conclude that the development of atherosclerosis in WHHL and cholesterol-fed rabbit is very similar and occurs within a similar time frame. One might propose that the WHHL rabbits may be useful to assess agents which lower plasma cholesterol by altering lipoprotein production since these animals lack functional LDL receptors. Cholesterol-fed models are less expensive and time consuming and may be manipulated by altering the level of cholesterol intake to assess the significance of graded degrees of hypercholesterolemia on cellular processes associated with lesion formation, e.g., monocyte adherence, margination and foam cell formation.

Thus far in the discussion of rabbits as models of atherosclerosis it is apparent that human-like atherosclerotic lesions can be induced by elevating plasma cholesterol levels through continuous or intermittent feeding of a cholesterol diet, a casein-enriched diet or by deleting functional LDL receptors as in the WHHL rabbit. It is also quite obvious that in such models a great deal of time is required to induce atherosclerotic lesions comparable to man, i.e., 6 months to 5 years.

Hypercholesterolemia and mechanical denudation of the endothelium in various vascular regions of the rabbit have been utilized to develop shorter-term models of atherosclerosis with a high degree of predictability as to the location and type of atherosclerotic lesion. Acute mechanical injury of the arterial vessel wall can be achieved using a variety of methods. A balloon embolectomy catheter [32] can denude the vessel and distend the media while gentle denudation can be achieved by drawing a nylon filament over the surface of the vessel [33, 34]. Moderate injury and denudation occur following cutting of the internal elastic lamina with a metal or diamond tipped catheter [35]. Chronic endothelial damage has been shown to promote

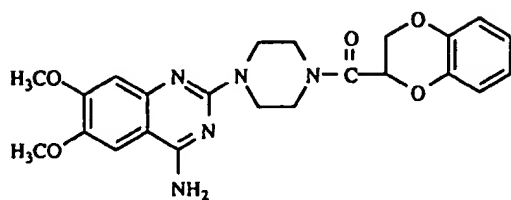
thrombosis at the catheter tip and formation of fibrous lesions [36, 37]. We have used a combination of chronic endothelial injury using a surgically implanted sterile nylon monofilament and dietary cholesterol supplementation [38, 39]. Combination of hypercholesterolemia and endothelial injury has allowed one to develop a model of atherosclerosis that is reproducible, has a high incidence of lesion formation and a predictable lesion site and type. The character of the atherosclerotic lesion is dependent upon the degree, length and type of hypercholesterolemia induced.

In summary, hypercholesterolemic rabbits are valuable models and the most widely used model for the evaluation of pharmacologic agents. Five types of human-like atherosclerotic lesions can be induced in the rabbit; however, the model is limited in that evidence of the complicated ruptured fibrous plaques cannot be found. Rabbits are also valuable for atherosclerosis research because unlike other models, atherosclerotic lesions progress even after removal of dietary cholesterol supplementation [23,40]. Evaluation of the direct antiatherosclerotic properties of hypocholesterolemic agents requires normalization of plasma cholesterol levels by diet prior to drug administration. Since rabbit atherosclerotic lesions will become more complex following cholesterol removal, agents which act by directly altering cellular processes such as ACAT inhibitors that limit macrophage accumulation can be discerned and their effect on lesion progression/regression can be monitored.

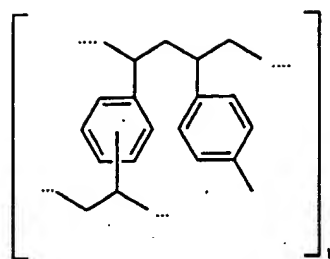
### Hamster

Another model of atherosclerosis that has received recent attention is the hypercholesterolemic hamster. Male hamsters fed a 3% cholesterol, 15% butterfat diet for up to a month had elevated plasma cholesterol levels and the presence of Type I fatty dots and fatty streaks within the aortic arch [41]. Within 3 to 4 months of the very high cholesterol/fat diet, expansion of the fatty streaks into the thoracic aorta around sites of intercostal ostia was noted [41]. By 10 months of cholesterol supplementation when plasma cholesterol levels were 17-times normal, advanced Type V lesions were observed in the aortic arch of the hamster but their extent was quite limited, i.e., 30% of the cross-sectional vessel surface. Feeding hamsters a 0.2% cholesterol, 10% coconut oil for 10 weeks [42] or 0.05% cholesterol, 10% coconut oil for 8 weeks [43] resulted in the accumulation of monocyte-macrophages within the aorta arch. Thus, short-term feeding of a cholesterol and either coconut oil or butterfat diet to hamsters is a model of subendothelial monocyte-macrophage foam cell formation. Atherosclerotic lesions can be found predictably within the inner curvature of the aortic arch and can be identified by staining with the lipid dye, Oil Red O. Such a model is useful due to its size for the acute evaluation of agents that may interfere with the early stages of lesion formation, e.g., monocyte adherence, transmigration and foam cell formation.

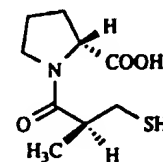
The hypercholesterolemic hamster has been used for the evaluation of numerous pharmacologic agents with varying mechanisms of action. Doxazosin Fig. (5) (23), an alpha-1 adrenergic inhibitor, and cholestyramine Fig. (5) (24) decreased the extent of Oil Red O-positive macrophage foam cells; however, one could not discern that this was a direct effect on the arterial wall because plasma cholesterol levels were



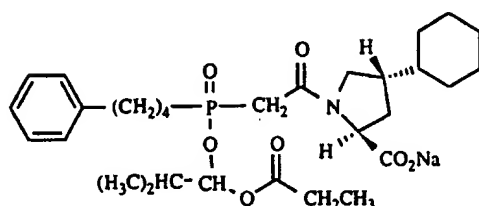
### 23. Doxazosin



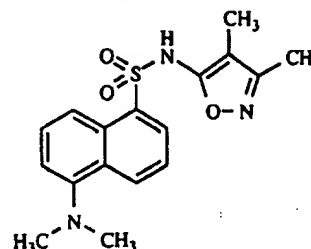
## 24. Cholestyramine



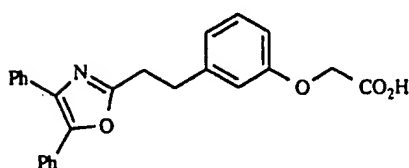
## 25. Captopril



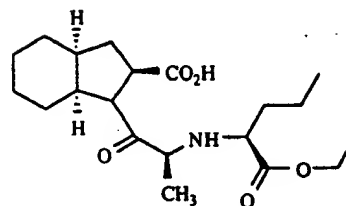
## 26. Fosinopril



**27. BMS-182874**



28. BMY-42393



## 29. Perindopril

**Fig. (5).** Broad group of compounds reported to possess antiatherosclerotic activities.

reduced by both groups and doxazosin (23) lowered blood pressure [43]. Higher doses of doxazosin (23) did not have any greater lipid lowering effect but a more marked reduction in macrophage foam cell area was noted and such data is suggestive that the compound may have a direct effect on monocyte-macrophage accumulation [42]. The HMG-CoA reductase inhibitor, lovastatin Fig. (2) (15), also was shown to reduce macrophage accumulation but again the changes were associated with a decrease in plasma cholesterol levels [44]. Inhibitors of angiotensin converting enzyme such as captopril Fig. (5) (25) without lowering plasma cholesterol and fosinopril Fig. (5) (26) by lowering LDL cholesterol, reduced aortic arch macrophage accumulation [45]. An additional study with captopril (25) and fosinopril (26) aimed at assessing the ability of these compounds to regress hamster atherosclerotic lesions was performed [46]. Both compounds were reported to reduce macrophage accumulation and thereby induce regression; however, while a group of animals was necropsied at 4 weeks to establish the degree of atherosclerosis prior to intervention only the drug treated animals were followed for an additional 6 weeks. A control designed to assess the effect of plasma cholesterol lowering or continued cholesterol feeding without intervention was not included. The ACAT inhibitor, octimibate [47] Fig. (1) (1), and endothelial subtype A receptor antagonist, BMS-182874 [48] Fig. (5) (27), both of which lowered plasma cholesterol, and the prostacyclin agonist, BMY42393 [47] Fig. (5) (28) in the absence of cholesterol lowering, have been

shown to limit macrophage accumulation in the hypercholesterolemic hamster. Thus, the hypercholesterolemic hamster has proven to be a useful model for the assessment of compounds; however, the changes in plasma cholesterol and blood pressure confound the interpretation of the atherosclerotic data and limit one's ability to ascribe the activity to a direct effect of the compounds.

## Swine

Swine are a non-rodent model of atherosclerosis in which atherosclerotic lesions have been found to develop spontaneously [49]. The pathogenesis of lesion development in pigs has been shown to closely parallel the stages of lesion formation as seen in man [50-52]. In addition, atherosclerotic lesion development can be exacerbated by combination of hypercholesterolemia and endothelial injury [53-56]. A strain of pigs with mutant apolipoprotein B alleles has been identified and these animals have been shown to be hypercholesterolemic due to defective lipoprotein clearance and prone to premature development of atherosclerosis [57-60]. Unlike the rabbit and hamster where lesions predominate in the aorta, atherosclerotic lesions have been observed in cerebral [61] and coronary [62] vessels of the pig. Thus, swine are a useful model for the evaluation of atherosclerosis from the perspective that lesions develop spontaneously, their circulatory system and localization of lesions are similar to man and the lesions are



responsive to dietary intervention by exhibiting regression after prolonged periods [63,64].

Despite their similarity to man with respect to atherosclerosis development, swine are not widely used for the evaluation of antiatherosclerotic agents. We have reported that the ACAT inhibitor, CI-976 Fig. (1) (2), blunted the progression of diet- and injury-induced atherosclerotic lesions in Yucatan miniature pigs potentially by inhibiting arterial ACAT and by lowering plasma VLDL-cholesterol levels [65]. The ACE inhibitor, perindopril Fig. (5) (29), was evaluated in hypercholesterolemic miniature pigs and noted to limit the development and monocyte-macrophage enrichment of aortic lesion; however, mean arterial blood pressure (MABP) was reduced in the animals [66]. Such reductions in MABP like the decrease in VLDL-cholesterol levels confound the interpretation of the data and limit one's ability to ascertain whether the compounds had a direct effect on lesion development. The limited a priori knowledge of a compound's effect on plasma cholesterol or blood pressure and the animal's inherent size are major disadvantages of using pigs for assessment of a compound's direct antiatherosclerotic potential. Miniature swine weigh approximately 12 kg at 4 months of age and in our studies feeding pigs a 2% cholesterol, 16% fat diet resulted in a doubling of their body weight within 4 months of diet initiation. Therefore, although swine are excellent models of atherosclerosis that mimic the human disease from the perspective of lesion pathology, such a model may be limited to evaluation of the antiatherosclerotic potential of compounds during their drug development stages rather than discovery phases.

## Monkeys

Non-human primates have often been portrayed as ideal models of human atherosclerosis due to their close phylogenetic association to man. The morphologic characterization of atherosclerotic lesion progression and regression has been performed in cynomolgous (*Macaca fascicularis*) [67-69], rhesus (*Macaca mulatta*) [70], cebus (*Cebus albifrons*) [71], squirrel (*Saimiri sciureus*) [71] and pigtail (*Macaca nemestrina*) [72-75] monkeys. The pathology of atherosclerotic lesion development in various monkey species has been shown to be quite similar to man. Spontaneous development of atherosclerotic lesions is rare in non-human primates; however, like in the animals noted above cholesterol feeding has been shown to promote the development of atherosclerosis in the monkey. Experimentally induced advanced atherosclerosis in monkeys requires approximately 3 years and addition of dietary cholesterol supplementation to produce plasma cholesterol levels of between 350 and 500 mg/dl. The localization of atherosclerotic lesions was similar to man in that lesions were present in the coronary arteries, abdominal aorta and iliac arteries. Plasma cholesterol levels of 200-400 mg/dl have been noted to produce advanced Type V fibrous plaques in *Macaca nemestrina* after 3.5 years of diet [72,73]. A retrospective evaluation of cebus and squirrel monkeys administered a normal diet without cholesterol supplementation and ranging in age from 12 to 20 years highlighted the difference in susceptibility to atherosclerosis and lesion character [71]. The older squirrel monkeys were found to have advanced Type IV-V atherosclerotic lesions containing lipid enrichment and a necrotic lipid core in the abdominal aorta

while lesions from older cebus monkeys were characterized as

diffuse intimal thickening without lipid accumulation [71]. Thus, it is apparent from evaluation of monkey models of atherosclerosis that lesions of comparable character to man, swine and in some cases rabbits can be achieved; however, a combination of a lower plasma cholesterol level and a longer period of time is required for lesion progression.

Few studies have been performed in monkeys using either dietary or pharmacologic intervention to promote lesion regression. After a 30 month lesion induction phase, switching cynomolgous monkeys to a chow diet initially, i.e., 6 months, results in a reduction in monocyte-macrophages and cholesteryl esters; however, intimal necrosis and free cholesterol monohydrate remain [67]. Within 12 months, the atherosclerotic lesions tended to resolve to an intimal scar with a lipid composition similar to normal vessels except for the presence of cholesterol crystals [67]. The bile acid sequestrant, cholestyramine Fig. (5) (24), the antioxidant, probucol Fig. (3) (20), either alone or upon coadministration was shown to promote atherosclerosis lesion regression in the rhesus monkeys [76] presumably due to lowering plasma cholesterol levels. Therefore, although atherosclerotic lesion development appears to mimic human disease progression, the utility of using these animals for drug discovery is limited by their availability and potential variability due to their underlying differences in age and degree of atherosclerosis progression. In addition, given the time frames required for lesion development in the monkey, rabbits fed a low cholesterol diet may be a viable substitute as shown by Wilson and colleagues [22].

## Transgenic Mice

Due to advances in molecular biology and the realization that mice, in general, are normally resistant to the development of atherosclerosis [77], genetically engineered mice have been developed which are predisposed to hypercholesterolemia-induced disease. Two well-characterized transgenic mouse models of atherosclerosis are the apolipoprotein E (apoE)-deficient mouse [78-80] and the low density lipoprotein (LDL) receptor-negative mouse [81,82]. ApoE is a major component of plasma lipoproteins that has a high affinity for LDL receptors and chylomicron remnant receptors [83,84] and may be important in facilitating reverse-cholesterol transport from peripheral tissues. The apoE-deficient mice have been shown to be hypercholesterolemic, i.e., 400 to 700 mg/dl at 5 to 55 weeks of age, while maintained on a chow diet [79]. Atherosclerotic lesions develop naturally over the time frame of 11 to 64 weeks within the aortic sinus and exhibit a similar histologic appearance as Type I to V lesions. Monocyte-macrophage foam cells predominate either as individual cells or clusters in the early stages of lesion development, i.e., less than 28 weeks, while fibrosis, intimal necrosis, acellular, necrotic lipid-rich cores with evidence of cholesterol clefts can be found after 32 weeks of age [79]. A similar histologic pattern can be seen in apoE-deficient mice fed a Western-type diet, i.e., 0.15% cholesterol; however, the timecourse of lesion development is shorter and the extent of atherosclerosis is greater [80]. Cholesterol-fed apoE-deficient mice have plasma cholesterol levels of 1000 to 4400 mg/dl over 6 to 40 weeks of age. Evidence of Type IV-V complex fibrous plaques can be seen as

early as 15 weeks and the lesions are not only present in the aortic sinus but also associated with the bifurcations of such major branch vessels as the common carotids, celiac, mesenteric, renal and iliac arteries [80].

The LDL receptor-negative transgenic mouse has also been developed [81,82]. Unlike the apoE-deficient mice, atherosclerotic lesions do not occur naturally during the timeframes currently studied, i.e., 6 months [82]. Dietary supplementation with 0.15% cholesterol results in plasma cholesterol levels of 900 to 1000 mg/dl over 6 months and the development of atherosclerotic lesions within the aortic sinus. The morphologic appearance and extent of atherosclerosis in the LDL receptor-negative mouse is similar to comparably fed apoE-deficient mice; however, plasma cholesterol levels are half that noted for the apoE-deficient mice and there is greater variability in the latter mouse model [82]. Thus, both the apoE and LDL receptor-deficient mice are viable small animal models for the evaluation of atherosclerotic lesion progression.

The utility of apoE and LDL receptor-deficient mice for the evaluation of antiatherosclerotic agents has yet to be determined. Few studies have been reported which utilize these mice in drug intervention studies. The antioxidant, N,N'-diphenyl 1,4-phenylenediamine (DPPD) Fig. (3) (21) has been evaluated in apoE-deficient mice fed along with a 0.15% cholesterol diet for 6 months and was found to reduce the extent of aortic atherosclerosis by 36%, i.e., control - 22%; DPPD (21) - 14% lesion coverage [85]. In contrast, probucol Fig. (3) (20), another antioxidant with hypolipidemic properties, accelerated the development of atherosclerosis in apoE-deficient mice irrespective of whether the compound was administered in a chow or cholesterol containing diet and despite lowering plasma cholesterol level [86]. Such paradoxical observations raise an important issue relating to interpretation of the results of drug intervention studies in genetically derived mouse models. One must question the appropriateness of the model for testing the specific compound of interest. For instance, unlike the LDL receptor-negative mouse that is a model of a naturally occurring abnormality, i.e., familial hypercholesterolemia, apoE-deficient mice possess a specific genetic deletion of an apolipoprotein that may be necessary for reverse-cholesterol transport. One can argue that if a compound's antiatherosclerotic activity is mediated through apoE metabolism such a mouse model would be inappropriate for assessing the compound's activity.

Numerous other transgenic mouse models have been developed. A few transgenic mouse models of potential relevance to atherosclerosis from the perspective of lipoprotein metabolism are the human apolipoprotein B [87], apolipoprotein (a) [88], Lp(a) [89,90] and cholesteryl ester transfer protein (CETP) [91] transgenic models. In addition, one might predict that site specific deletions or overexpression of pro-atherosclerotic molecules such as adhesion molecules, growth factors, cytokines or integrins, for example, would be useful models for the assessment of direct acting antiatherosclerotic agents. A caveat to such an approach is exemplified by the comparison of the apoE- and LDL receptor-deficient mice. Both genetic defects resulted in a similar atherosclerotic lesion pathology and required some degree of hypercholesterolemia. Therefore, temporal evaluations of lesion development in the presence and absence of pharmacologic agents may be more informative in assessing whether the specific gene product/defect exacerbates disease progression and

whether pathologic redundancies limit the efficacy of the specific pharmacologic entity.

## Pharmacologic Intervention Studies

### ACAT

Acyl-CoA:cholesterol O-acyltransferase (ACAT) is the primary enzyme responsible for the esterification of cholesterol in all mammalian cells, but under conditions of excessive cholesterol accumulation in the vascular wall, ACAT may be responsible for the generation of the hallmark of atherosclerosis, namely, the monocyte-macrophage foam cell. Since ACAT and cholesterol esterification may be considered a pro-atherogenic event, we and others have hypothesized that inhibition of arterial wall ACAT may prevent the formation of the macrophage-enriched fatty streak and the development of the clinically significant fibrous plaque. In addition, given the observations that monocyte-macrophages are localized to the potentially friable shoulder regions of atherosclerotic lesions and in association with matrix degrading enzymes, one might speculate that by limiting the accumulation of monocyte-macrophages through inhibition of ACAT one would promote the development of a stable plaque morphology.

Several inhibitors of ACAT have been evaluated in animals and they have been found to be antiatherosclerotic by measuring changes in lesion extent and/or cholesteryl ester enrichment. Schaffer and coworkers [92] reported that administration of CL277082 Fig. (1) (3) to rabbits for 16 weeks after a 10-week lesion induction phase resulted in a 49% reduction in aortic cholesteryl ester content. Cyclandelate Fig. (1) (4), a relatively weak inhibitor ( $IC_{50} = 80$  (M) with an unknown mechanism of inhibition [93] was shown to blunt the increase in aortic total cholesterol content when given to rabbits in a low-cholesterol chow diet after a lesion induction phase [94]. A more specific and potent inhibitor of ACAT, namely, RP-70676 Fig. (1) (5), administered in a similar manner as cyclandelate (4), was reported to decrease aortic free and esterified cholesterol content by 27 to 42% [95]. In addition, melinamide [96,97] Fig. (1) (6) and the furobenzochrome Fig. (1) (7) reported by Gammill et al. [98] were shown to prevent lesion formation in cholesterol-fed rabbits. Kimura and colleagues have also reported that a series of phenylureas Fig. (1) (8, 9, 10) limited the progression of aortic atherosclerotic lesions in the rabbit [99,100]. Other potent and systemically bioavailable inhibitors of ACAT, namely, E5324 [101] Fig. (1)(11) and FR145237 [102] Fig. (1)(12), significantly inhibited the progression and cholesterol enrichment of aortic atherosclerosis in rabbits. CI-976 Fig. (1)(2), a potent, systemically bioavailable inhibitor of ACAT was evaluated in hypercholesterolemic Yucatan micropigs and was noted to prevent the formation of atherosclerotic lesions [65]. Despite achieving plasma CI-976 (2) levels of 9 to 52 times the  $IC_{50}$  for inhibition of ACAT in mouse peritoneal macrophages, an accepted *in vitro* model of foam cell formation, one was left to conclude in this model that the antiatherosclerotic activity of the compound may be related to reductions in plasma VLDL-cholesterol since the antiatherosclerotic activity was highly correlated with plasma VLDL-cholesterol levels. Therefore, given the fact that in each of the studies cited above plasma total cholesterol levels were reduced in the animal models to the same extent or greater than



animals switched to a chow, low cholesterol diet, classification of these compounds as direct acting antiatherosclerotic agents is difficult.

Direct inhibition of arterial wall ACAT with a potent, systemically bioavailable agent although much harder to discern both preclinically and clinically may provide a greater vascular benefit than can be achieved by plasma cholesterol lowering alone. The ACAT inhibitor, CI-976 Fig. (1)(2), a fatty acid amide, was evaluated in a cholesterol-fed rabbit model of atherosclerosis at a dose that was bioavailable but did not lower plasma total cholesterol [39]. CI-976 (2) prevented the accumulation of monocyte-macrophages within a preestablished fibrofoamy lesion, attenuated the development of thoracic aortic fatty streak-like lesions and decreased the cholesteryl ester enrichment of the developed lesions. We have also reported that two isoxazoles Fig. (1)(13, 14) which were bioavailable based on a bioassay designed to assess plasma ACAT inhibitory bioequivalents limited the development of thoracic aortic foamy lesions but were inactive in the more fibroproliferative femoral lesions of the rabbit [103]. Others have also reported that in Watanabe heritable hyperlipidemic (WHHL) rabbits, a model of familial hypercholesterolemia lacking the LDL receptor, E5324 [104] Fig. (1)(11) and FR145237 [102] Fig. (1)(12) can limit the development of atherosclerotic lesions in the thoracic and coronary arteries in the absence of plasma cholesterol lowering. Kogushi et al. [104] have also shown that E5324 (11) markedly reduced aortic ACAT activity; however, such a decrease may be related to the reduction in lesion and macrophage extent and not a representation of direct arterial wall ACAT inhibition. Considering the data with CI-976 (2), E5324 (11) and FR145237 (12), one can conclude that ACAT inhibition has the potential to limit atherosclerosis progression by specifically affecting vascular monocyte-macrophage accumulation. However, it is also quite apparent from the various studies cited above that the experimental protocols can be quite varied.

The animal experimental protocols can be classified into several major categories. Firstly, compounds were administered either at the initiation of dietary cholesterol supplementation and the animals were necropsied after 2 to 4 months of treatment. These studies are often termed progression studies in that the effect of the compound on monocyte-macrophage accumulation or generation of Type I to Type III lesions is being studied. However, the hypocholesterolemic activity of the compounds limits the assessment of direct antiatherosclerotic activity. Secondly, compounds were given after a degree of hypercholesterolemia and atherosclerotic lesion development has been established. In most cases, animals were fed a cholesterol diet for 8 to 10 weeks and administered the various compounds either in the same cholesterol diet or a chow diet for an additional 6 to 8 weeks. Such studies can assess whether compounds can limit the further progression of a preestablished lesion and/or promote lesion regression. The ability to study lesion regression is often lost because few studies randomize animals based on their plasma total cholesterol and necropsy a group prior to drug intervention in order to assess the type, extent and composition of the lesions. Under these regression paradigms the antiatherosclerotic activity of the compound is best assessed when compared to either a group of animals switched to a chow diet or administered a cholesterol absorption inhibitor such as cholestyramine Fig. (5)(24) in order to match the degree of cholesterol lowering. Despite the extended period

of hypercholesterolemia such rabbit models are still representative of early fibrofoamy lesions (Type I-III) and not a reflection of the more advanced Type IV-V fibrous plaques. Thirdly, WHHL rabbits that appear refractory to plasma cholesterol lowering caused by ACAT inhibition can be used to assess a compound's antiatherosclerotic activity. The WHHL may be a very good model for the assessment of ACAT inhibitors in that plasma total and lipoprotein cholesterol levels remain relatively constant following treatment and more advanced atherosclerotic fibrous plaque lesions may develop in the long-term. Fourthly, as reported for CI-976 (2), a combination of chronic endothelial injury and cholesterol feeding in either a progression or regression paradigm can allow one to not only assess the development and regression of atherosclerotic lesions but also determine whether the compounds have an effect on the cellular composition of a defined, well-characterized lesion with a greater than 99% incidence of occurrence. Finally, models of more advanced atherosclerosis can also be developed and used to assess whether ACAT inhibitors can limit the formation or promote the more rapid development of advanced fibrous plaques. Rabbits exposed to chronic endothelial injury within one week of study initiation and sequentially fed a cholesterol, fat diet for 9 weeks, a fat only diet for 6 weeks and various compounds for 8 additional weeks has allowed us to develop advanced fibrous plaques in the rabbit within 23 weeks and to further address the benefit of ACAT inhibitors. Therefore, numerous models have been developed specifically for testing the direct antiatherosclerotic activity of ACAT inhibitors; however, our conclusions ascribing the activity of the compound to direct inhibition of arterial ACAT is still based on circumstantial evidence.

Numerous in vitro, biochemical and pharmacokinetic studies have been performed in order to relate plasma drug levels with the compound's  $IC_{50}$  for macrophage ACAT inhibition. The basis for claiming that an ACAT inhibitor is directly antiatherosclerotic appears to be rooted in the concept that if plasma drug levels are maintained above the  $IC_{50}$  for inhibition of macrophage ACAT and plasma total and lipoprotein cholesterol levels are unchanged then the compound has direct antiatherosclerotic properties. One assumes that the compound at steady state will partition into the various atherosclerotic lesions and inhibit macrophage ACAT. Direct measurement of arterial wall ACAT and vessel drug levels have been performed [104]. Given the observations that ACAT inhibitors limit arterial wall macrophage enrichment, i.e., a source of arterial ACAT, one must be cautious in interpreting a reduction in arterial wall ACAT activity as evidence for direct ACAT inhibition. A more plausible explanation is that there is a decrease in the amount of ACAT enzyme due to a reduction in macrophage accumulation. Standardization of atherosclerotic lesion size and cellular composition prior to acute administration of the ACAT inhibitor and assessment of ACAT activity may provide more definitive proof of direct arterial wall ACAT inhibition. However, an absence of ACAT inhibition may be misleading in that during the microsome isolation procedures compounds may be diluted out of the sample. Quantification of vessel drug levels is not only problematic and their accuracy can be questioned for the same reasons as noted above for the measurement of ACAT activity but also drug extraction efficiency and metabolism become an issue. Although still circumstantial another marker of arterial ACAT inhibition is the cholesteryl ester content of the vessel wall under comparable

levels of plasma total cholesterol exposure and atherosclerotic lesion/macrophage extents.

### HMG-CoA Reductase Inhibitors

3-hydroxy-3-methylglutaryl coenzyme A reductase (HMG-CoA reductase), in addition to being the rate limiting enzyme in the cholesterol biosynthetic pathway, is involved in the regulation of receptors for LDL-cholesterol [105]. In experimental animals [106], and patients with heterozygous familial hypercholesterolemia [107] inhibition of hepatic HMG-CoA reductase leads to an increased number of LDL receptors on the cell surface, which ultimately results in an enhanced clearance of plasma LDL and a reduction in plasma total cholesterol levels. However, in nonfamilial hypercholesterolemic and familial combined hyperlipidemic patients, HMG-CoA reductase inhibitors lower plasma cholesterol by inhibiting lipoprotein production [108]. Reductions in plasma total cholesterol of over 30% and in LDL-cholesterol of 40% have been observed in clinical trials with various doses of atorvastatin [109] Fig. (2)(16), lovastatin [110] Fig. (2)(15), pravastatin [111] Fig. (2)(17), and simvastatin [112] Fig. (2)(18). In addition, the recent Scandinavian Simvastatin Survival Study (4S) [113] has shown that lowering plasma cholesterol by 35% with diet and simvastatin (18) significantly reduces the risk of mortality by 30%, coronary heart disease mortality by 42%, and incidence of nonfatal myocardial infarction by 37%. The West of Scotland Study (WOSCOPS) has demonstrated that lowering plasma LDL-cholesterol by 26% with diet and pravastatin (17) significantly reduced the risk of mortality from definite coronary events by 31% [114]. Thus, the data in man indicate that inhibitors of HMG-CoA reductase by reducing plasma cholesterol may limit the development of atherosclerosis and reduce the risk of mortality.

Several animal studies have also shown that lovastatin (15) and pravastatin (17) can attenuate atherosclerotic lesion development when plasma total and LDL-cholesterol are reduced [115-118], and that atorvastatin (16) can limit lesion development independent of changes in plasma cholesterol [119]. Due to the potent hypolipidemic activity of HMG-CoA reductase inhibitors, the assessment of these compound's direct antiatherosclerotic potential in preclinical models of atherosclerosis is difficult. However, comparison of compounds with a similar plasma total cholesterol exposure may allow one to assess whether an agent has any inherent antiatherosclerotic properties. For instance, we reported that in a cholesterol-fed rabbit model of lesion progression, lovastatin (15), pravastatin (17) and atorvastatin (16) reduced plasma total cholesterol exposure over the course of the experiment by 37% to 43% [119]. Given the linear relationship between plasma cholesterol and atherosclerosis extent noted previously [120], one might expect that the degree and composition of the atherosclerotic lesions would be similar amongst the three treatment groups. Despite equal plasma cholesterol levels, pravastatin (17) and lovastatin (15) had no effect on thoracic aortic lesion extent or iliac-femoral cross-sectional lesion area. In contrast, atorvastatin (16) reduced the thoracic aortic lesion extent from 44% to 19% and iliac-femoral lesion area by 67%. Thus, we concluded that atorvastatin can directly limit atherosclerosis lesion progression.

Evaluation of the various HMG-CoA reductase inhibitors in a rabbit model of atherosclerosis lesion progression highlights the power of the experimental design in formulating an interpretation of the data. Given the fact that plasma cholesterol levels were reduced, an analysis of a subset of compounds with the same cholesterol exposure allowed one to assess their relative antiatherosclerotic activity and also ascribe the activity to a direct effect on the lesion. Establishment of the effect of lipid-lowering on atherosclerosis development is an important factor when assessing compound efficacy. Addition of control treatments such as cholestyramine Fig. (5)(24), a non-absorbable resin, or diets containing graded cholesterol contents are methods for assessing the antiatherosclerotic activity of a compound at defined plasma cholesterol levels. Reductions in lesion size, extent or composition above that predicted for a given plasma cholesterol level may indicate that the compound is directly altering a pro-atherogenic event.

Comparison of biochemical, morphologic and morphometric results may allow one to establish the consistency of the effect and to identify potential mechanisms for the observed antiatherosclerotic activity. For instance [119], not only did atorvastatin Fig. (2)(16) decrease the extent of thoracic aortic atherosclerosis but also reduced the cholesteryl ester content of the thoracic aorta, a secondary marker that is reflective of the lesion extent and composition, i.e., lipid, monocyte-macrophage enrichment. Examination of the histopathology of the atherosclerotic lesions and morphometric changes following treatment allowed one to discern potential mechanisms responsible for the observed antiatherosclerotic activity. For example, pravastatin Fig. (2)(17) had no effect on lesion or monocyte-macrophage area while atorvastatin Fig. (2)(16) reduced both parameters. One might conclude from these data that pravastatin (17) lacked sufficient plasma drug levels or did not penetrate the arterial wall and that atorvastatin (16) by directly limiting lesion size through inhibition of smooth muscle cell migration and proliferation indirectly reduced macrophage accumulation. The later hypothesis is consistent with observations made by others which indicate that HMG-CoA reductase inhibitors in tissue culture limit SMC proliferation [121-123] and migration [124] by interfering with isoprenoid synthesis [125].

Therefore, by controlling for the degree of plasma cholesterol lowering and combining multiple efficacy parameters, one might not only be able to discriminate the direct antiatherosclerotic activity of a compound from that due to plasma cholesterol lowering but also by evaluating the structure of the atherosclerotic lesions identify potential mechanisms which can be tested in vitro or in appropriate animal models.

### Anti-Oxidants and 15-Lipoxygenase Inhibitors

Steinberg and colleagues [126] have reported that oxidatively modified LDL may be important in the progression of atherosclerosis due to the observations that oxidized LDL is cytotoxic, chemotactic and chemostatic. Oxidative modification of insudant plasma lipoproteins is presumably an extracellular event [126] and the resulting oxidized lipoproteins have been implicated in the regulation of chemokines [127] and pro-atherogenic adhesion molecules [128]. Both apolipoprotein B [129-132], the major protein in LDL, and lipid peroxides have been localized to atherosclerotic lesions [133]. Oxidatively

modified LDL or such oxidation products as malondialdehyde-conjugated LDL or 4-hydroxynonenal-conjugated LDL have been localized to WHHL rabbits [134-136]. Thus, one can conclude that oxidation of lipoproteins may be important in the development of atherosclerosis and that general antioxidants may be antiatherosclerotic in both man and models of atherosclerosis.

Several studies investigating the antiatherosclerotic activity of general antioxidants have been performed in New Zealand white rabbits [137-140], WHHL rabbits [141,142], pigs [143] and monkeys [76] under a variety of experimental conditions. In cholesterol-fed rabbits, butylated hydroxytoluene (BHT) Fig. (3)(22), vitamins E plus C, vitamins E plus A and probucol Fig. (3)(20) limited the development of thoracic aortic lesions [137-140, 144-146]. Probuco (20) has been shown by numerous individuals to reduce the extent, cholesterol enrichment and cross-sectional lesion size of atherosclerotic lesions in WHHL rabbits [141,142], balloon-injured normocholesterolemic pigs [143] and hypercholesterolemic monkeys [76]. Close examination of the lesion histopathology revealed that probucol (20) reduced the extent of atherosclerosis by decreasing the abundance of monocyte-macrophages within the lesion [146]. Mechanistic studies in rabbits fed cholesterol for a short time period, i.e., 5 wks, indicated that probucol (20) can limit the adhesion of monocytes to the endothelial cell surface. The single study in coronary artery balloon-injured pigs also indicated that probucol (20) can limit the development of primarily fibroproliferative lesions through presumably affecting SMC migration and proliferation [143]. Thus, one can conclude that antioxidants and specifically, probucol (20), can limit the development and cellular composition of atherosclerotic lesions in various animal models of atherosclerosis irrespective of whether the compound was administered to animals with or without pre-established lesions.

In most of the studies noted above, plasma cholesterol lowering was minimal so attempts to identify surrogate markers of vascular efficacy of the various antioxidants were made. Resistance of lipoproteins to oxidation was a major surrogate marker used by most investigators [141,142]. Measurements of vascular reactivity were also made [147,148]. In hypercholesterolemic rabbits, probucol (20) treatment preserved endothelial function and vascular rings upon exposure to acetylcholine in organ culture were shown to relax normally [147]. The improved vascular responsiveness is quite remarkable and one can conclude that antioxidants may improve vascular function; however, while in both studies plasma total cholesterol levels were relatively constant among the control and probucol-treated (20) groups, one study [148] reported that the cholesterol content of vessels from the drug-treated group was reduced. Since atherosclerosis is comprised of multiple stages and drugs such as probucol (20) can alter the type as well as cellular and lipid composition of the atherosclerotic lesions, correlation of pathology with functional changes is important in the assessment of drug efficacy. Experimental protocols can be designed to assess the inherent activity of compounds to promote vasorelaxation. Given the observation that some agents lower plasma or vascular cholesterol levels, administration of agents to normocholesterolemic animals or atherosclerotic animals where plasma cholesterol levels are normalized by diet may allow one to assess whether the compound has a direct effect on vascular relaxation either in the presence or absence of underlying disease.

Based on the pathology data and the localization of epitopes of oxidized LDL within the arterial wall, one can suggest that general antioxidants may be useful antiatherosclerotic agents. However, specific inhibitors of the oxidation process may allow one to target a specific pro-atherogenic process and to better characterize the compound's activity in models of atherosclerosis. A new enzyme specific target, namely arachidonate 15-lipoxygenase (15-LO), has emerged [149]. Arachidonate 15-lipoxygenase is a lipid-peroxidizing enzyme that is also present in atherosclerotic lesions. Investigators have found the 15-LO gene [150], stereospecific products of the 15-LO enzyme [151] and coincident localization of 15-LO mRNA, protein and epitopes of oxidized LDL within macrophage-rich areas of atherosclerotic lesions [149]. We have identified a specific inhibitor of 15-LO, namely, PD146176 Fig. (3)(19), and have evaluated the compound in several models of atherosclerosis [152,153].

Evaluation of PD146176 (19) in the hypercholesterolemic rabbit under three specific experimental paradigms has allowed us to conclude that in the absence of lowering plasma total and lipoprotein cholesterol levels PD146176 (19) can attenuate the development of diet induced atherosclerotic lesions through specific inhibition of monocyte-macrophage accumulation. In addition, PD146176 (19) can limit the development and macrophage enrichment of pre-established atherosclerotic lesions. PD146176 (19) administered to rabbits coincident with a cholesterol diet reduced the gross extent of foamy lesions (Type I-III lesions) within and cholesterol enrichment of the thoracic and abdominal aorta [152]. PD146176 (19) administered to rabbits coincident with a cholesterol diet and induction of a chronic endothelial injury not only reduced the progression of foamy thoracic lesions but also specifically limited the accumulation of monocyte-macrophages within a fibrofoamy iliac-femoral lesion without affecting the overall lesion size [153]. PD146176 (19) administered after establishment of fibrofoamy Type IV lesions through a combination of chronic endothelial injury and dietary cholesterol supplementation reduced the extent, cross-sectional area and monocyte-macrophage content of the more advanced Type V fibrous plaque [153]. In all three studies, assessment of plasma total and lipoprotein levels, vascular lipid content and histologic evidence for the presence of 15-LO in the lesions were necessary to corroborate the findings and maintain the implication that 15-LO was involved. Thus, these data highlight the antiatherosclerotic potential of a specific 15-LO inhibitor.

The brief summary of the antiatherosclerotic effects of PD146176 (19) can also be used to exemplify the power of the animal models of atherosclerosis. The simplest model, a rabbit fed a 0.25% cholesterol, 3% peanut, 3% coconut oil diet illustrated that the compound can prevent the formation of cholesteryl ester enriched Type III foamy atherosclerotic lesions. One might propose that evaluation of rabbits fed cholesterol for shorter periods of time would allow one to assess whether the observed antiatherosclerotic activity was due to reduced monocyte adherence. In the second rabbit model, induction of a fibrofoamy lesion by chronic endothelial injury allowed one to build upon the first observation and suggest that the compound specifically limited monocyte-macrophage accumulation because the absolute lesion cross-sectional area was unchanged. In the most complex model, one was able to assess whether PD146176 (19) could limit the progression of the disease to a fibrous plaque or promote regression of a

preestablished fibrofoamy lesion. In addition, one can obtain such mechanistic information as to the involvement of 15-LO in advanced atherosclerosis and whether further monocyte-macrophage enrichment can be blunted.

## Conclusions

Atherosclerotic lesion development can be divided into six histologically distinct stages and five dynamic phases. Specifically, atherosclerotic lesion progression in man involves episodes of SMC proliferation, extracellular matrix deposition and remodeling, lipid infiltration, endothelial cell-monocyte interactions, monocyte migration into the intima, monocyte-macrophage foam cell formation, necrotic lipid-rich core formation, calcium deposition, neovascularization, mural microthrombi and occlusive acute thrombosis. Given the complexity of atherosclerotic lesion development in man, the challenge exists to develop animal models that closely mimic the human disease. One must accept, however, that there is no one perfect animal model that completely replicates the stages of human atherosclerosis but that the models are useful in studying specific pathologic processes associated with the disease. Hypercholesterolemic rabbits either with or without endothelial injury are valuable models and the most widely used model for the evaluation of pharmacologic agents. Five types of human-like atherosclerotic lesions can be induced in the rabbit; however, the model is limited in that evidence of the plaque rupture cannot be found. Hypercholesterolemic hamsters are a model of an early pro-atherogenic event, namely, subendothelial monocyte-macrophage foam cell formation. Swine are a useful model for the evaluation of atherosclerosis from the perspective that lesions develop spontaneously, their circulatory system and localization of lesions are similar to man and the lesions are responsive to dietary intervention by exhibiting regression after prolonged periods. Non-human primates have often been portrayed as ideal models of human atherosclerosis due to their close phylogenetic association to man; however, lesions of comparable character to man can be induced more efficiently and over shorter time periods in swine and in some cases rabbits through a combination of hypercholesterolemia and endothelial injury. Numerous transgenic mouse models have been developed in recent years. A common finding among the various mouse models of atherosclerosis is that a similar atherosclerotic lesion pathology develops and all require some degree of hypercholesterolemia. Therefore, temporal evaluations of lesion development in the presence and absence of pharmacologic agents may be more informative in assessing whether the specific gene product/defect exacerbates disease progression and whether pathologic redundancies limit the efficacy of the specific pharmacologic entity. Based on evaluation of the various animal models and pharmacologic agents, one can conclude that: (1) each animal model provides insight into specific aspects of the disease process; (2) a hypercholesterolemic state is required in all models for the development of atherosclerosis; (3) discrimination of the *direct* antiatherosclerotic activity of a compound from its *indirect* activity requires one to limit the number of confounding factors, e.g., hypocholesterolemic and antihypertensive effect; (4) combination of biochemical, morphologic and morphometric measures allows one to both validate the antiatherosclerotic effect and define potential mechanisms; (5) reducing monocyte-macrophage involvement irrespective of mechanism or animal

model effectively limits the development of atherosclerotic lesions.

## Abbreviations

ACAT	=	Acyl-coenzyme A:cholesterol O-acyltransferase
HMG-CoA reductase	=	3-Hydroxy-3-methylglutaryl coenzyme A
15-LO	=	15-Lipoxygenase
SMC	=	Smooth muscle cells
VCAM-1	=	Vascular cell adhesion molecule-1
VLDL	=	Very low density lipoproteins
LDL	=	Low density lipoproteins
WHHL	=	Watanabe heritable hyperlipidemic rabbit
ACE	=	Angiotensin converting enzyme
MABP	=	Mean arterial blood pressure
ApoE	=	Apolipoprotein E
CETP	=	Cholesteryl ester transfer protein
4S	=	Scandinavian Simvastatin Survival Study
WOSCOP	=	The West of Scotland Study

## Acknowledgement

I would like to thank Dr. D. Robert Sliskovic for his kind invitation to write this article and for his help in preparation of the figures depicting chemical structures of the compounds cited in the manuscript.

## References

- [1] Tracy, R.E. *Lab. Invest.*, 1979, 41, 546.
- [2] Constantinides, P. J. *Ultrastruct. Res.*, 1966, 6, 1.
- [3] Ridolfi, R.L.; Hutchins, G.M. *Am. Heart J.*, 1977, 93, 468.
- [4] Cornhill, J.F.; Herderick, E.E.; Stry, H.C. *Monogr. Atheroscler.*, 1990, 15, 13.
- [5] Cornhill, J.F.; Barrett, W.A.; Herderick, E.E.; Mahley, R.W.; Fry, D.L. *Arterioscler.*, 1985, 5, 415.
- [6] Stry, H.C.; Chandler, A.B.; Glagov, S.; Guyton, J.R.; Insull, W. Jr.; Rosenfeld, M.E.; Schaffer, S.A.; Schwartz, C.J.; Wagner, W.D.; Wissler, R.W. *Circ.*, 1994, 89, 2462.
- [7] Fuster, V. *Circ.*, 1994, 90, 2126.
- [8] Smith, E.B.; Evans, P.H.; Downham, M.D. *J. Atheroscler. Res.*, 1967, 7, 171.
- [9] Kume, N.; Cybulsky, M.I.; Gimbrone, M.A. *J. Clin. Invest.*, 1992, 90, 1138.
- [10] Cybulsky, M.I.; Gimbrone, M.A. *Science*, 1991, 252, 788.

- [11] Krause, B.R.; Sliskovic, D.R.; Bocan, T.M.A. *Exp. Opin. Invest. Drugs*, 1995, 4, 353.
- [12] Anitschkow, N. *Beitr. Pathol. Anat. Allgem. Pathol.*, 1913, 56, 379.
- [13] Jokinen, M.P.; Clarkson, T.B.; Prichard, R.W. *Exp. Mol. Pathol.*, 1985, 42, 1.
- [14] Prior, J.T.; Kurtz, D.M.; Ziegler, D.D. *Arch. Pathol.*, 1961, 71, 672.
- [15] Kroon, P.A.; Thompson; Chao, Y. *Atherosclerosis*, 1985, 56, 323.
- [16] Prior, J.T.; Kurtz, D.M.; Ziegler, D.D. *Arch. Pathol.*, 1961, 71, 82.
- [17] Kritchevsky, D.; Tepper, S.A.; Vesselinovitch, D.; Wissler, R.W. *Atherosclerosis*, 1971, 14, 53.
- [18] Kritchevsky, D.; Tepper, S.A.; Kim, H.K.; Story, J.A.; Vesselinovitch, D.; Wissler, R.W. *Exp. Molec. Pathol.*, 1976, 24, 375.
- [19] Ho, K.J.; Pang, L.C.; Taylor, C.B. *Atherosclerosis*, 1974, 19, 561.
- [20] Ross, A.C.; Minick, C.R.; Zilversmit, D.B. *Atherosclerosis*, 1978, 29, 301.
- [21] Mahley, R.W.; Innerarity, T.L.; Rall, S.C. Jr; Weisgraber, K.H. *Ann. NY Acad. Sci.*, 1985, 454, 209.
- [22] Wilson, R.B.; Miller, R.A.; Middleton, C.C.; Kinden, D. *Arterioscler.*, 1982, 2, 228.
- [23] Constantinides, P.; Booth, J.; Carlson, G. *Arch. Pathol.*, 1960, 70, 712.
- [24] Constantinides, P. *J. Atherosclerosis Res.*, 1961, 1, 374.
- [25] Daley, S.J.; Herderick, E.E.; Cornhill, F.; Rogers, K.A. *Arterioscler. Thromb.*, 1994, 14, 95.
- [26] Daley, S.J.; Klemp, K.F.; Guyton, J.R.; Rogers, K.A. *Arterioscler. Thromb.*, 1994, 14, 105.
- [27] Rosenfeld, M.E.; Tsukada, T.; Gown, A.M.; Ross, R. *Arterioscler.*, 1987, 7, 9.
- [28] Rosenfeld, M.E.; Tsukada, T.; Chait, A.; Bierman, E.L.; Gown, A.M.; Ross, R. *Arterioscler.*, 1987, 7, 24.
- [29] Tsukada, T.; Rosenfeld, M.; Ross, R.; Gown, A.M. *Arterioscler.*, 1986, 6, 601.
- [30] Shiomi, M.; Ito, T.; Tsukada, T.; Yata, T.; Ueda, M. *Arterioscler. Thromb.*, 1994, 14, 931.
- [31] Rosenfeld, M.E.; Chait, A.; Bierman, E.L.; King, W.; Goodwin, P.; Walden, C.E.; Ross, R. *Arterioscler.*, 1988, 8, 338.
- [32] Stadius, M.L.; Rowan, R.; Fleishhauer, J.F.; Kernoff, R.; Billingham, M.; Gown, A.M. *Arterioscler. Thromb.*, 1992, 12, 1267.
- [33] Reidy, M.A.; Harker, L.A.; Schwartz, S. *Fed. Proc.*, 1983, 42, 771.
- [34] Reidy, M.A.; Yoshida, K.; Harker, L.A.; Schwartz, S.M. *Arterioscler.*, 1986, 6, 305.
- [35] Bjorkerud, S.; Bondjers, G. *Atherosclerosis*, 1971, 13, 355.
- [36] Moore, S. *Lab. Invest.*, 1973, 29, 478.
- [37] Moore, S.; Friedman, R.J.; Singal, D.P.; Gaudie, J.; Blajchman, M.A.; Roberts, R.S. *Thrombos. Haemostasis (Stuttgart)*, 1976, 35, 70.
- [38] Bocan, T.M.A.; Bak Mueller, S.; Uhlendorf, P.D.; Ferguson, E.; Newton, R.S. *Expt. Molec. Pathol.*, 1991, 54, 201.
- [39] Bocan, T.M.A.; Bak Mueller, S.; Uhlendorf, P.D.; Newton, R.S.; Krause, B.R. *Arterioscler. Thromb.*, 1991, 11, 1830.
- [40] Friedman, M.; Byers, S.O. *Am. J. Pathol.*, 1963, 43, 349.
- [41] Nistor, A.; Bulla, A.; Filip, D.A.; Radu, A. *Atherosclerosis*, 1987, 68, 159.
- [42] Foxall, T.L.; Shwaery, G.T.; Stucchi, A.F.; Nicolosi, R.J.; Wong, S.S. *Am. J. Pathol.*, 1992, 140, 1357.
- [43] Kowala, M.C.; Nunnari, J.J.; Durham, S.K.; Nicolosi, R.J. *Atherosclerosis*, 1991, 91, 35.
- [44] Otto, J.; Ordovas, J.M.; Smith, D.; van Dongen, D.; Nicolosi, R.J.; Schaefer, E.J. *Atherosclerosis*, 1995, 114, 19.
- [45] Kowala, M.C.; Grove, R.I.; Aberg, G. *Atherosclerosis*, 1994, 108, 61.
- [46] Kowala, M.C.; Recce, R.; Beyer, S.; Aberg, G. *J. Cardiovascular Pharm.*, 1995, 25, 179.
- [47] Kowala, M.C.; Mazzucco, C.E.; Hartl, K.S.; Seiler, S.M.; Warr, G.A.; Abid, S.; Grove, R.I. *Arterioscler. Thromb.*, 1993, 13, 435.
- [48] Kowala, M.C.; Rose, P.M.; Stein, P.D.; Goller, N.; Recce, R.; Beyer, S.; Valentine, M.; Barton, D.; Durham, S.K. *Am. J. Pathol.*, 1995, 146, 819.
- [49] Gotlieb, H.; Lalich, J.J. *Am. J. Pathol.*, 1954, 30, 851.
- [50] Moreland, A.F.; Clarkson, T.B.; Lofland, H.B. *Arch. Pathol.*, 1963, 76, 99.
- [51] French, J.E.; Jennings, M.A.; Florey, H.W. *Ann. N Y Acad. Sci.*, 1965, 127, 780.
- [52] Reitman, J.S.; Mahley, R.W.; Fry, D.L. *Atherosclerosis*, 1982, 43, 119.
- [53] Nam, S.C.; Lee, W.M.; Jarmolych, J.; Lee, K.T.; Thomas, W.A. *Exp. Molec. Pathol.*, 1973, 18, 369.
- [54] Lee, W.M.; Lee K.T. *Exp. Molec. Pathol.*, 1975, 23, 491.
- [55] Fritz, K.E.; Daoud, A.S.; Augustyn, J.M.; Jarmolych, J. *Exp. Molec. Pathol.*, 1980, 32, 61.
- [56] Dov Gal, D.V.M.; Rongione, A.J.; Slovenkai, G.A.; DeJesus, S.T.; Lucas, A.; Fields, C.D.; Isner, J.M. *Am. Heart J.*, 1990, 119, 291.
- [57] Rapacz, J.; Hasler-Rapacz, J.; Taylor, K.M.; Checovich, W.J.; Attie, A.D. *Science*, 1986, 234, 1573.
- [58] Lowe, S.W.; Checovich, W.J.; Rapacz, J.; Attie, A.D. *J. Biol. Chem.*, 1988, 263, 15467.
- [59] Checovich, W.J.; Fitch, W.L.; Krauss, R.M.; Smith, M.P.; Rapacz, J.; Smith, C.L.; Attie, A.D. *Biochem.*, 1988, 27, 1934.
- [60] Prescott, M.F.; McBride, C.H.; Hasler-Rapacz, L.; Von-Linden, J.; Rapacz, J. *Am. J. Pathol.*, 1991, 139.



- [61] Detweiler, D.K.; Ratcliffe, H.L.; Luginbuhl, H. *Ann. N. Y. Acad. Sci.*, 1968, 149, 868.
- [62] Reddick, R.L.; Read, M.S.; Brinkhous, K.M.; Bellinger, D.; Nichols, T.; Griggs, T.R. *Arterioscler.*, 1990, 10, 541.
- [63] Daoud, A.S.; Jarmolych, J.; Augustyn J.M.; Fritz, K.E.; Singh, J.K.; Lee, K.T. *Arch. Pathol. Lab. Med.*, 1976, 100, 372.
- [64] Fritz, K.E.; Augustyn, J.M.; Jarmolych, J.; Daoud, A.S.; Lee, K.T. *Arch. Pathol. Lab. Med.*, 1976, 100, 380.
- [65] Bocan, T.M.A.; Bak Mueller, S.; Uhlendorf, P.D.; QuenbyBrown, E.; Mazur, M.J.; Black, A.E. *Atherosclerosis*, 1993, 99, 175.
- [66] Charpiot, P.; Rolland, P.H.; Friggi, A.; Piquet, P.; Scalbert, E.; Bodard, H.; Barlatier, A.; Latrille, V.; Tranier, P.; Mercier, C.; Luccioni, R.; Calaf, R.; Garcon, D. *Arterioscler. Thromb.*, 1993, 13, 1125.
- [67] Small, D.M.; Bond, M.G.; Waugh, D.; Prack, M.; Sawyer, J.K. *J. Clin. Invest.*, 1984, 73, 1590.
- [68] Stary, H.C.; Malinow, M.R. *Atherosclerosis*, 1982, 43, 151.
- [69] Kramsch, D.M.; Hollander, W. *Expt. Molec. Pathol.*, 1968, 9, 1.
- [70] DePalma, R.G.; Klein, L.; Bellon, E.M.; Koletsky, S. *Arch. Surg.*, 1980, 115, 1268.
- [71] Hoover, G.A.; Nicolosi, R.J.; Camp, R.R.; Hayes, K.C. *Arterioscler.*, 1982, 2, 252.
- [72] Masuda, J.; Ross, R. *Arterioscler.*, 1990, 10, 164.
- [73] Masuda, J.; Ross, R. *Arterioscler.*, 1990, 10, 178.
- [74] Faggiotto, A.; Ross, R.; Harker, L. *Arterioscler.*, 1984, 4, 323.
- [75] Faggiotto, A.; Ross, R. *Arterioscler.*, 1984, 4, 341.
- [76] Wissler, R.W.; Vesselinovitch, D. *Appl. Pathol.*, 1983, 1, 89.
- [77] Paigen, B.; Ishida, B.Y.; Verstuyft, J.; Winters, R.B.; Albee, D. *Arterioscler.*, 1990, 10, 316.
- [78] Plump, A.S.; Smith, J.D.; Hayek, T.; Aalto-Setälä, K.; Walsh, A.; Verstuyft, J.G.; Rubin, E.M.; Breslow, J.L. *Cell*, 1992, 71, 343.
- [79] Reddick, R.L.; Zhang, S.H.; Maeda, N. *Arterioscler. Thromb.*, 1994, 14, 141.
- [80] Nakashima, Y.; Plump, A.S.; Raines, E.W.; Breslow, J.L.; Ross, R. *Arterioscler. Thromb.*, 1994, 14, 133.
- [81] Ishibashi, S.; Goldstein, J.L.; Brown, M.S.; Herz, J.; Burns, D.K. *J. Clin. Invest.*, 1994, 93, 1885.
- [82] Tangirala, R.K.; Rubin, E.M.; Palinski, W. *J. Lipid Res.*, 1995, 36, 2320.
- [83] Mahley, R.W. *Science*, 1988, 240, 622.
- [84] Brown, M.S.; Goldstein, J.L. *Science*, 1986, 232, 4.
- [85] Tangirala, R.K.; Casanada, F.; Miller, E.; Witzum, J.L.; Steinberg, D.; Palinski, W. *Arterioscler. Thromb. Vasc. Biol.*, 1995, 15, 1625.
- [86] Zhang, S.H.; Reddick, R.L.; Avdievich, E.; Surles, L.K.; Jones, R.G.; Reynolds, J.B.; Quarfordt, S.H.; Maeda, N. *J. Clin. Invest.*, 1997, 99, 2858.
- [87] Purcell-Huynh, D.A.; Farese, R.V., Jr.; Johnson, D.F.; Flynn, L.M.; Pierotti, V.; Newland, D.L.; Linton, M.F.; Sanan, D.A.; Young, S.G. *J. Clin. Invest.*, 1995, 95, 2246.
- [88] Lawn, R.M.; Wade, D.P.; Hammer, R.E.; Chiesa, G.; Verstuyft, J.G.; Rubin, E.M. *Nature*, 1992, 360, 670.
- [89] Mancini, F.P.; Newland, D.L.; Mooser, V.; Murata, J.; Marcovina, S.; Young, S.G.; Hammer, R.E.; Sanan, D.A.; Hobbs, H.H. *Arterioscler. Thromb. Vasc. Biol.*, 1995, 15, 1911.
- [90] Callow, M.J.; Verstuyft, J.; Tangirala, R.; Palinski, W.; Rubin, E.M. *J. Clin. Invest.*, 1995, 96, 1639.
- [91] Maruti, K.R.; Castle, C.K.; Boyle, T.P.; Lin, A.H.; Murray, R.W.; Melchior, G.W. *Nature*, 1993, 364, 73.
- [92] Schaffer, S.A.; Bloom, J.D.; DeVries, V.G.; Dutia, M.; Katocs, A.S. Jr.; Largis, E. In *Atherosclerosis VII*; Fidge, N.H.; Nestel, P.J., Eds; Elsevier Science Publishers B.V.: Amsterdam, 1986, pp 633-636.
- [93] Heffron, F.; Middleton, B.; White, D.A. *Biochem. Pharm.*, 1990, 39, 575.
- [94] Middleton, B.; Middleton, A.; White, D.A.; Bell, G.D. *Atherosclerosis*, 1984, 171, 171.
- [95] Ashton, M.J.; Bridge, A.W.; Bush, R.C.; Dron, D.I.; Harris, N.V.; Jones, G.D.; Lythgoe, D.J.; Riddell, D.; Smith, C. *Bioorg. Med. Chem. Lett.* 1992, 2, 375.
- [96] Fukushima, H.; Aono, S.; Nakamura, Y.; Endo, M.; Imai, T. *J. Atheroscler. Res.*, 1969, 10, 403.
- [97] Fukushima, H.; Toki, K.; Nakatani, H. *J. Atheroscler. Res.*, 1969, 9, 57.
- [98] Gammill, R.B.; Bell, F.P.; Bell, L.T.; Bisaha, S.N.; Wilson, G.J. *J. Med. Chem.* 1990, 33, 2686.
- [99] Kimura, T.; Takase, Y.; Hayashi, K.; Tanaka, H.; Ohtsuka, I.; Sacki, T.; Kogushi, M.; Yamada, T.; Fujimori, T.; Saitou, I.; Akasaka, K. *J. Med. Chem.*, 1993, 36, 1630.
- [100] Kimura, T.; Watanabe, N.; Matsui, M.; Hayashi, K.; Tanaka, H.; Ohtsuka, I.; Sacki, T.; Kogushi, M.; Kobayashi, H.; Akasaka, K.; Yamagishi, Y.; Saitou, I.; Yamatsu, I. *J. Med. Chem.*, 1993, 36, 1641.
- [101] Tanaka, H.; Ohtsuka, I.; Kogushi, M.; Kimura, T.; Fujimori, T.; Sacki, T.; Hayashi, K.; Kobayashi, H.; Yamada, T.; Hiyoshi, H.; Saito, I. *Atherosclerosis*, 1994, 107, 187.
- [102] Matsuo, M.; Ito, F.; Konto, A.; Aketa, M.; Tomoi, M.; Shimomura, K. *Biochim. Biophys. Acta*, 1995, 1259, 254.
- [103] White, A.D.; Purchase II, C.F.; Picard, J.A.; Anderson, M.K.; Bak Mueller, S.; Bocan, T.M.A.; Bousley, R.F.; Hamelehle, K.L.; Krause, B.R.; Lee, P.; Stanfield, R.L.; Reindel, J.F. *J. Med. Chem.*, 1996, 39, 3908.
- [104] Kogushi, M.; Tanaka, H.; Ohtsuka, I.; Yamada, T.; Kobayashi, H.; Sacki, T.; Takada, M.; Hiyoshi, H.; Yanagimachi, M.; Kimura, T.; Yoshitake, S.; Saito, I. *Atherosclerosis*, 1996, 124, 203.
- [105] Brown, M.S.; Goldstein, J.L. *Science*, 1986, 232, 34.

- [106] Kovanen, P.T.; Bilheimer, D.W.; Goldstein, J.L.; Jaramillo, J.J.; Brown, M.S. *Proc. Natl. Acad. Sci. USA*, 1981, 78, 1194.
- [107] Bilheimer, D.W.; Grundy, S.M.; Brown, M.S.; Goldstein, J.L. *Proc. Natl. Acad. Sci. USA*, 1983, 80, 4124.
- [108] Arad, Y.; Ramakrishnan, R.; Ginsberg, H.N. *Metabolism*, 1992, 41, 487.
- [109] Nawrocki, J.W.; Weiss, S.R.; Davidson, M.H.; Sprecher, D.L.; Schwartz, S.S.; Lupien, P.J.; Jones, P.H.; Haber, H.E.; Black, D.M. *Arterioscl. Thromb. Vasc. Biol.*, 1995, 15, 678.
- [110] Walker, J.F. *Drugs*, 1988, 36, 83.
- [111] McTavish, D.; Sorkin, E.M. *Drugs*, 1991, 42, 65.
- [112] Todd, P.A.; Goa, K.L. *Drugs*, 1990, 40, 583.
- [113] *Lancet*, 1994, 344, 1383.
- [114] Shepherd, J.; Cobbe, S.M.; Ford, I.; Isles, C.G.; Lorimer, A.R.; MacFarlane, P.W.; McKillop, J.H.; Packard, C.J. *N. Engl. J. Med.*, 1995, 333, 1301.
- [115] Kritchevsky, D.; Tepper, S.A.; Klurfeld, D.M. *Pharm. Res. Comm.*, 1981, 13, 921.
- [116] Kobayashi, M.; Ishida, F.; Takahashi, T.; Taguchi, K.; Watanabe, K.; Ohmura, I.; Kamei, T. *Jpn. J. Pharmacol.* 1989, 49, 125.
- [117] Zhu, B.Q.; Sievers, R.E.; Sun, Y.P.; Isenberg, W.M.; Parmley, W.W. *J. Cardiovas. Pharm.*, 1992, 19, 246.
- [118] Shiomi, M.; Ito, T.; Watanabe, Y.; Tsujita, Y.; Kuroda, M.; Arai, M.; Fukami, M.; Fukushima, J.; Tamura, A. *Atherosclerosis* 1990, 83, 69.
- [119] Bocan, T.M.A.; Mazur, M.J.; BakMueller, S.; QuenbyBrown, E.; Sliskovic, D.R.; O'Brien, P.M.; Creswell, M.W.; Lee, H.; Uhlendorf, P.D.; Roth, B.D.; Newton, R.S. *Atherosclerosis*, 1994, 111, 127.
- [120] Bocan, T.M.A.; BakMueller, S.; Mazur, M.J.; Uhlendorf, P.D.; QuenbyBrown, E.; Kieft, K.A. *Atherosclerosis*, 1993, 102, 9.
- [121] Corsini, A.; Mazzotti, M.; Raiteri, M.; Soma, M.; Fumagalli, R.; Paoletti, R. *XI Intl. Symp. Drugs Affecting Lipid Metabolism*, 1992, 7.
- [122] Corsini, A.; Raiteri, M.; Soma, M.; Fumagalli, R.; Paoletti, R. *Pharmacol. Res.*, 1991, 23, 173.
- [123] Falke, P.; Mattiasson, I.; Stavenow, L.; Hood, B. *Pharm. Toxicol.*, 1989, 64, 173.
- [124] Hidaka, Y.; Tomoyo, E.; Yonemoto, M.; Kamei, T. *Atherosclerosis*, 1992, 95, 87.
- [125] Corsini, A.; Bernini, F.; Quarato, P.; Donetti, E.; Bellosa, S.; Fumagalli, R.; Paoletti, R.; Soma, V.M. *Cardiology*, 1996, 87, 458.
- [126] Steinberg, D.; Parthasarathy, S.; Carew, T.E.; Khoo, J.C.; Witztum, J.L. *New Engl. J. Med.*, 1989, 320, 915.
- [127] Rajavashisth, T.B.; Andalibi, A.A.; Territo, M.C.; Berliner, J.A.; Navab, M.; Fogelman, A.M.; Lusis, A.J. *Nature*, 1990, 344, 254.
- [128] Kume, N.; Cybulsky, M.I.; Gimbrone, M.A. *J. Clin. Invest.*, 1992, 90, 1138.
- [129] Kao, C.Y.; Wissler, R.W. *Exp. Molec. Pathol.*, 1965, 4, 465.
- [130] Knieriem, H.J.; Kao, C.Y.; Wissler, R.W. *Arch. Pathol. Lab. Med.*, 1967, 84, 118.
- [131] Yomantas, S.; Elner, V.M.; Schaffner, T.; Wissler, R.W. *Arch. Pathol. Lab. Med.*, 1984, 108, 374.
- [132] Bocan, T.M.A.; Brown, S.A.; Guyton, J.R. *Arterioscler.*, 1988, 8, 499.
- [133] Glavind, J.; Hartmann, S.; Clemmeson, J.; Jessan, K.E.; Dam, H. *Acta Pathol. Microbiol. Scand.*, 1952, 3-, 1.
- [134] Boyd, H.C.; Gown, A.M.; Wolfbauer, G.; Chait, A. *Am. J. Pathol.*, 1989, 135, 815.
- [135] Haberland, M.E.; Fong, D.; Cheng, L. *Science*, 1988, 241, 215.
- [136] Palinski, W.; Rosenfeld, M.E.; Yla-Herttuala, S.; Gurtner, G.C.; Socher, S.S.; Butler, S.W.; Parthasarathy, S.; Carew, T.E.; Steinberg, D.; Witztum, J.L. *Proc. Natl. Acad. Sci. USA*, 1989, 86, 1372.
- [137] Daugherty, A.; Zweifel, B.S.; Schonfeld, G. *Br. J. Pharmacol.*, 1989, 98, 612.
- [138] Tawara, K.; Ishihara, M.; Ogawa, H.; Tomikawa, M. *Jpn. J. Pharmacol.*, 1986, 41, 211.
- [139] Stein, Y.; Stein, O.; Delplanque, B.; Fesmire, J.D.; Lee, D.M.; Alaupovic, P. *Atherosclerosis*, 1989, 75, 145.
- [140] Carew, T.E.; Schwenke, D.C.; Steinberg, D. *Proc. Natl. Acad. Sci. USA*, 1987, 84, 7725.
- [141] Daugherty, A.; Zweifel, B.S.; Schonfeld, G. *Br. J. Pharmacol.*, 1991, 103, 1013.
- [142] Kita, T.; Nagano, Y.; Yokode, M.; Ishii, K.; Kume, N.; Ooshima, A.; Kawai, C. *Proc. Natl. Acad. Sci. USA*, 1987, 84, 5928.
- [143] Schneider, J.E.; Berk, B.C.; Gravanis, M.B.; Santoian, E.C.; Cipolla, G.D.; Tarazona, N.; Lassegue, B.; King, S.B., 3<sup>rd</sup> *Circ.*, 1993, 88, 628.
- [144] Bjorkhem, I.; Henriksson-Freyschuss, A.; Breuer, O.; Diczfaluzy, U.; Berglund, L.; Henriksson, P. *Arterioscler. Thromb.*, 1991, 11, 15.
- [145] Brattsand, R. *Atherosclerosis*, 1975, 22, 47.
- [146] Bocan, T.M.A.; BakMueller, S.; QuenbyBrown, E.; Uhlendorf, P.D.; Mazur, M.J.; Newton, R.S. *Expt. Molec. Pathol.*, 1992, 57, 70.
- [147] Keaney, J.F., Jr.; Xu, A.; Cunningham, D.; Jackson, T.; Frei, B.; Vita, J.A. *J. Clin. Invest.*, 1995, 95, 2520.
- [148] Del Rio, M.; Chulia, T.; Ruiz, E.; Tejerina, T. *Br. J. Pharmacol.*, 1996, 118, 1639.
- [149] Yla-Herttuala, S.; Rosenfeld, M.E.; Parthasarathy, S.; Glass, C.K.; Sigal, E.; Witztum, J.L.; Steinberg, D. *Proc. Natl. Acad. Sci. USA*, 1990, 87, 6959.
- [150] Yla-Herttuala, S. *Herz*, 1992, 17, 270.
- [151] Kuhn, H.; Belkner, J.; Zula, S.; Fahrenklemp, T.; Wohlfeil, S. *J. Exp. Med.*, 1994, 179, 1903.

- [152] Sendobry, S.M.; Cornicelli, J.A.; Welch, K.; Bocan, T.; Tait, B.; Trivedi, B.K.; Colbry, N.; Dyer, R.D.; Feinmark, S.J.; Daugherty, A. *Br. J. Pharmacol.*, 1997, 120, 1199.
- [153] Bocan, T.M.A.; Rosebury, W.S.; BakMueller, S.; Kuchera, S.; Welch, K.; Daugherty, A.; Cornicelli, J.A. *Atherosclerosis*, 1997, in press.





## Inhibition of cyclooxygenase with indomethacin phenethylamide reduces atherosclerosis in apoE-null mice

Michael E. Burleigh<sup>d,1</sup>, Vladimir R. Babaev<sup>a,1</sup>, Mayur B. Patel<sup>b</sup>, Brenda C. Crews<sup>b</sup>,  
Rory P. Remmel<sup>c</sup>, Jason D. Morrow<sup>a,d</sup>, John A. Oates<sup>a,d</sup>, Lawrence J. Marnett<sup>b</sup>,  
Sergio Fazio<sup>a,c</sup>, MacRae F. Linton<sup>a,d,\*</sup>

<sup>a</sup> Department of Medicine, Division Cardiovascular Medicine, Vanderbilt University School of Medicine,  
383 Preston Research Building, Nashville, TN 37232-6300, USA

<sup>b</sup> Department of Biochemistry, Vanderbilt University Medical Center, Nashville, TN 37232-6300, USA

<sup>c</sup> Department of Pathology, Vanderbilt University Medical Center, Nashville, TN 37232-6300, USA

<sup>d</sup> Department of Pharmacology, Vanderbilt University Medical Center, Nashville, TN 37232-6300, USA

<sup>e</sup> Department of Medicinal Chemistry, College of Pharmacy, University of Minnesota, Minneapolis, MN 55455, USA

Received 7 December 2004; accepted 14 April 2005

### Abstract

Non-selective inhibition of cyclooxygenase (COX) has been reported to reduce atherosclerosis in both rabbit and murine models. In contrast, selective inhibition of COX-2 has been shown to suppress early atherosclerosis in LDL-receptor null mice but not more advanced lesions in apoE deficient (apoE<sup>-/-</sup>) mice. We investigated the efficacy of the novel COX inhibitor indomethacin phenethylamide (INDO-PA) on the development of different stages of atherosclerotic lesion formation in female apoE<sup>-/-</sup> mice. INDO-PA, which is highly selective for COX-2 in vitro, reduced platelet thromboxane production by 61% in vivo, indicating partial inhibition of COX-1 in vivo. Treatment of female apoE<sup>-/-</sup> mice with 5 mg/kg INDO-PA significantly reduced early to intermediate aortic atherosclerotic lesion formation (44 and 53%, respectively) in both the aortic sinus and aorta en face compared to controls. Interestingly, there was no difference in the extent of atherosclerosis in the proximal aorta in apoE<sup>-/-</sup> mice treated from 11 to 21 weeks of age with INDO-PA, yet there was a striking (76%) reduction in lesion size by en face analysis in these mice. These studies demonstrate the ability of non-selective COX inhibition with INDO-PA to reduce early to intermediate atherosclerotic lesion formation in apoE<sup>-/-</sup> mice, supporting a role for anti-inflammatory approaches in the prevention of atherosclerosis.

© 2005 Elsevier Inc. All rights reserved.

**Keywords:** Atherosclerosis; Prostaglandins; Cyclooxygenase; COX inhibition; ApoE<sup>-/-</sup> mice; Aorta

### 1. Introduction

Atherosclerosis has features of an inflammatory disease and is the leading cause of death in industrialized nations [1]. Cyclooxygenase (COX) plays a key role as an inflammatory mediator in virtually all diseases involving inflammation [2]. COX exists as two isoforms, which are coded for by two separate genes [2,3]. COX-1 is found in most tissues and mediates normal physiology requiring prostaglandin production. COX-2 is induced rapidly at sites of inflammation and is expressed in atherosclerotic lesions of

humans [4,5], and mice [6] by macrophages, smooth muscle cells and endothelial cells.

Eicosanoids produced by COX-1 and COX-2 have been ascribed a variety of functions in the promotion of cardiovascular health and disease. The beneficial effect of low dose aspirin in reducing cardiovascular events has been largely attributed to inhibition of platelet thromboxane production, a COX-1 mediated process [7]. In contrast, COX-2 has been proposed to play both beneficial and deleterious roles in cardiovascular health [8–11]. Recent evidence from the Adenomatous Polyp Prevention on Vioxx (APPROVe) trial indicating that selective COX-2 inhibition with rofecoxib results in increased cardiovascular events after 18 months compared to placebo has resulted in removal of rofecoxib from the market ([www.vioxx.com](http://www.vioxx.com)). Yet studies in animal

\* Corresponding author. Tel.: +1 615 936 1656; fax: +1 615 936 1872.  
E-mail address: [macrae.linton@vanderbilt.edu](mailto:macrae.linton@vanderbilt.edu) (M.F. Linton).

<sup>1</sup> These authors have contributed equally to this work.

models and humans support roles for COX-2 in promoting endothelial dysfunction [12], early atherosclerotic lesion formation [6] and plaque instability [13,14]. The dramatic removal of rofecoxib from the market highlights our need for a better understanding of the roles of COX-1 and COX-2 in atherosclerosis, plaque rupture, and cardiovascular events.

Non-selective inhibition of COX has been reported to reduce atherosclerosis both in cholesterol fed rabbit models [15] and genetically altered murine models of atherosclerosis [6,16]. Belton et al. have reported that selective inhibition of COX-1 attenuates atherosclerosis in apoE deficient mice [9]. However, reports on the impact of selective COX-2 inhibition on the development of atherosclerosis in murine models have been mixed with decreased, increased or unchanged atherosclerotic lesion area [6,16–19]. The divergence in the results may be the consequence of differences in experimental design, including efficacy and selectivity of the inhibitors, gender of the mice and stage of atherosclerotic lesions.

A new class of COX-2 selective inhibitors has been developed by derivatization of the conventional non-steroidal anti-inflammatory drugs (NSAIDs) indomethacin, resulting in >1100 times more selectivity for COX-2 than COX-1 when tested *in vitro* [20]. In the current studies, we examined the impact of this novel amide derivative of indomethacin, designated INDO-PA, on the development of different stages of atherosclerosis in apoE<sup>-/-</sup> mice. Interestingly, INDO-PA was found to produce a 61% reduction in platelet thromboxane, indicating partial inhibition of COX-1 *in vivo*. Treatment of apoE<sup>-/-</sup> mice with INDO-PA dramatically reduced aortic prostaglandin levels and early and intermediate aortic atherosclerotic lesion formation. These studies demonstrate the ability of non-selective COX inhibition with INDO-PA to reduce early and intermediate atherosclerotic lesion formation in apoE<sup>-/-</sup> mice, supporting the efficacy of anti-inflammatory approaches in the prevention of atherosclerosis.

## 2. Methods

### 2.1. Animal procedures

Female apoE<sup>-/-</sup> mice were at the 10th backcross into the C57BL/6 background and originally purchased from Jackson Laboratories (Bar Harbor, ME). Mice were maintained on a rodent chow diet containing 4.5% fat (PMI No. 5010, St. Louis, MO) and autoclaved acidified (pH 2.8) water. Animal care and experimental procedures were carried out in accordance with the regulations and under the approval of Vanderbilt University's Animal Care Committee.

### 2.2. COX inhibition

The dose of INDO-PA used in our study was chosen based on oral dosing in acute studies of carageenan-

induced footpad edema plethysmometry in rats in which the oral ED<sub>50</sub> for this assay in rats is 1.5 mg/kg [20]. Treatment of apoE<sup>-/-</sup> mice with 5 mg/kg INDO-PA intraperitoneal (IP; 3.33-fold over ED<sub>50</sub> in rats) was well-tolerated and did not produce any gastric ulceration and toxicity even at a dose of 30 mg/kg of INDO-PA (data not shown). In contrast, apoE<sup>-/-</sup> mice were able to tolerate daily doses of 2.5-mg/kg indomethacin by the IP route but higher doses (3 mg/kg) of it resulted in gastrointestinal hemorrhage with 100% mortality by 1 week (data not shown). Drugs were administered daily based on the body weight by IP injection (100  $\mu$ l) in a sterile mixture of 1% DMSO, 5% ethanol, 5% Tween-80 and 89% PBS

### 2.3. Serum cholesterol and triglyceride analysis

Mice were fasted for 4 h and blood was collected under isoflurane anesthesia. Serum was separated by centrifugation and lipoprotein integrity was preserved by using 1 mM phenylmethylsulfonyl fluoride (Sigma). The concentration of total cholesterol and triglycerides was determined using Sigma kits adapted for 96-well plate assay as described [21].

### 2.4. Platelet thromboxane level measurement

Nine-week-old apoE<sup>-/-</sup> mice were given vehicle ( $n = 10$ ) or 5 mg/kg INDO-PA ( $n = 9$ ) for 1 week. Ninety minutes after the final injection, blood samples were collected in the presence of 25 units of heparin sodium (Sigma) and 1.25  $\mu$ l 10  $\mu$ M A23187 Ca<sup>++</sup> ionophore (Calbiochem). Blood was placed in a 37 °C water bath for 30 min. Plasma was isolated by centrifugation at 1100 rpm for 10 min at 4 °C. Platelet thromboxane A<sub>2</sub> metabolite, thromboxane B<sub>2</sub> (TxB<sub>2</sub>) was quantified by gas chromatography/mass spectrometry (GC/MS) as described [22].

### 2.5. Aortic prostaglandin levels analysis

Seven-week-old apoE<sup>-/-</sup> mice were given daily vehicle ( $n = 4$ ) or 5 mg/kg INDO-PA ( $n = 5$ ) for 9 weeks. Ninety minutes after the last dose administration, mice were sacrificed by cervical dislocation. Aortas were dissected free of adjacent adventitial tissue and snap-frozen in liquid nitrogen. Prostacyclin metabolite 6-keto PGF<sub>1 $\alpha$</sub>  and PGE<sub>2</sub> were purified as described and quantified by GC/MS by the Eicosanoid Analysis Core at Vanderbilt University [23].

### 2.6. Analysis of Aortic Lesions

ApoE<sup>-/-</sup> mice were sacrificed and flushed with PBS through the left ventricle. The aorta was dissected and pinned out in an *en face* preparation as described previously [24]. In the first experiment, a subset of the distal aortas ( $n = 3$ ) in each group were snap-frozen in liquid nitrogen for prostaglandin determinations. The heart with

the proximal aorta was embedded in OCT and snap-frozen in liquid nitrogen. Fifteen alternate cryosections of 10- $\mu$ m thickness were collected from the proximal aorta starting from the beginning of the aortic sinus and extending 300  $\mu$ m distally as described [25]. The sections were stained with Oil-Red-O and lesion area was quantified using a Kontron computer system [24].

## 2.7. Data analysis

Data are expressed as mean  $\pm$  S.E.M. Total serum cholesterol, triglycerides, PGE<sub>2</sub>, 6-keto PGF<sub>1 $\alpha$</sub> , TxB<sub>2</sub> and aortic lesion areas between the groups were determined using the SigmaStat V.2 Software (SPSS Inc., Chicago, IL) by Student's *t*-test and the Mann–Whitney rank sum test, respectively.

## 3. Results

### 3.1. INDO-PA inhibits platelet thromboxane production in apoE<sup>-/-</sup> mice

INDO-PA has been reported to be a highly selective COX-2 inhibitor in vitro [20]. The structures of indomethacin and the amide derivative used in the treatments, INDO-PA, are shown in panels A and B of Fig. 1.

To test the COX-2 selectivity of INDO-PA, we measured platelet thromboxane production in apoE<sup>-/-</sup> deficient mice (Fig. 1C). Surprisingly, INDO-PA inhibited platelet thromboxane A<sub>2</sub> metabolite TxB<sub>2</sub> production by 61% compared to vehicle (25.7  $\pm$  3.0 ng/ml versus 65.9  $\pm$  2.4 ng/ml, respectively; *p* = 0.001). Thus, in contrast to its behavior in vitro, INDO-PA significantly inhibited COX-1 expression in apoE<sup>-/-</sup> mice in vivo.

### 3.2. INDO-PA does not affect plasma lipid levels in apoE<sup>-/-</sup> mice

To examine the impact of treatment with INDO-PA on lipid metabolism and atherosclerosis, three independent studies were designed to allow the development of fatty streak, intermediate and advanced atherosclerotic lesions in female apoE<sup>-/-</sup> mice. These mice were treated for different periods: from ages 7 to 16 weeks, from 9 to 18 weeks and from 11 to 21 weeks. However, serum lipids remained unchanged throughout the course of treatment in all three studies (Tables 1–3).

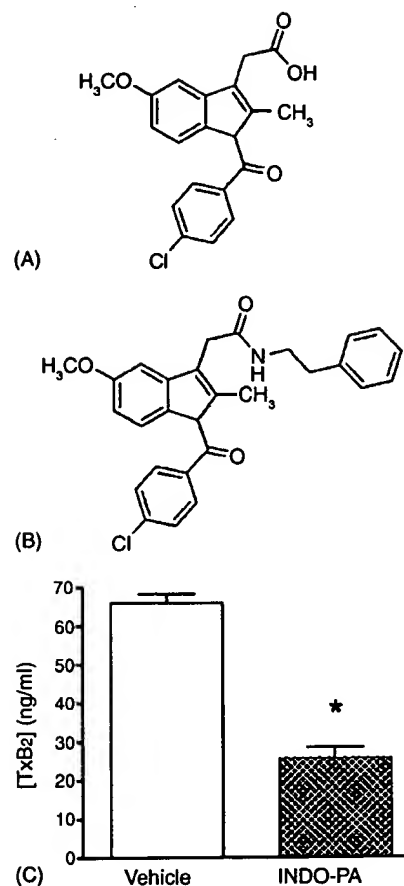


Fig. 1. Inhibition of Ca<sup>2+</sup> ionophore stimulated platelet thromboxane production: (A) chemical structure of indomethacin, (B) chemical structure of indomethacin amide derivative INDO-PA and (C) ApoE<sup>-/-</sup> mice were given vehicle (clear bar) or INDO-PA (hatched bar) for a week. Blood was collected and stimulated using A23187 Ca<sup>2+</sup> ionophore. Platelet production of the thromboxane metabolite TxB<sub>2</sub> was analyzed by GC/MS.

### 3.3. INDO-PA reduces atherosclerosis in apoE<sup>-/-</sup> mice

Treatment of 7-week-old apoE<sup>-/-</sup> mice with INDO-PA for 16 weeks significantly reduced atherosclerotic lesion formation in the proximal aorta by 44% (29620  $\pm$  4148  $\mu$ m<sup>2</sup> versus 52525  $\pm$  6007  $\mu$ m<sup>2</sup>; *p* = 0.013) and by 47% in the en face analysis of the aortas (0.43  $\pm$  0.04% versus 0.81  $\pm$  0.08%; *p* = 0.033) compared to mice treated with vehicle, respectively (Fig. 2A and B). Representative Oil-Red-O stained sections from the proximal aorta of mice treated with vehicle (Fig. 3A) or INDO-PA (Fig. 3B) indicate fatty streak lesions consisting predominantly of foam cells.

Table 1  
Serum lipid levels in apoE<sup>-/-</sup> mice treated with vehicle or INDO-PA from 7 to 16 weeks of age

Animal group	Baseline		6 weeks		10 weeks	
	Chol.	Trigl.	Chol.	Trig.	Chol.	Trig.
Vehicle ( <i>n</i> = 10)	320 $\pm$ 13	55 $\pm$ 3	276 $\pm$ 10	62 $\pm$ 2	311 $\pm$ 9	69 $\pm$ 5
INDO-PA ( <i>n</i> = 10)	333 $\pm$ 16	54 $\pm$ 6	260 $\pm$ 6	69 $\pm$ 3	322 $\pm$ 6	72 $\pm$ 4

Values are in mg/dl (mean  $\pm$  S.E.M.). The number of animals in each group is indicated by *n*.

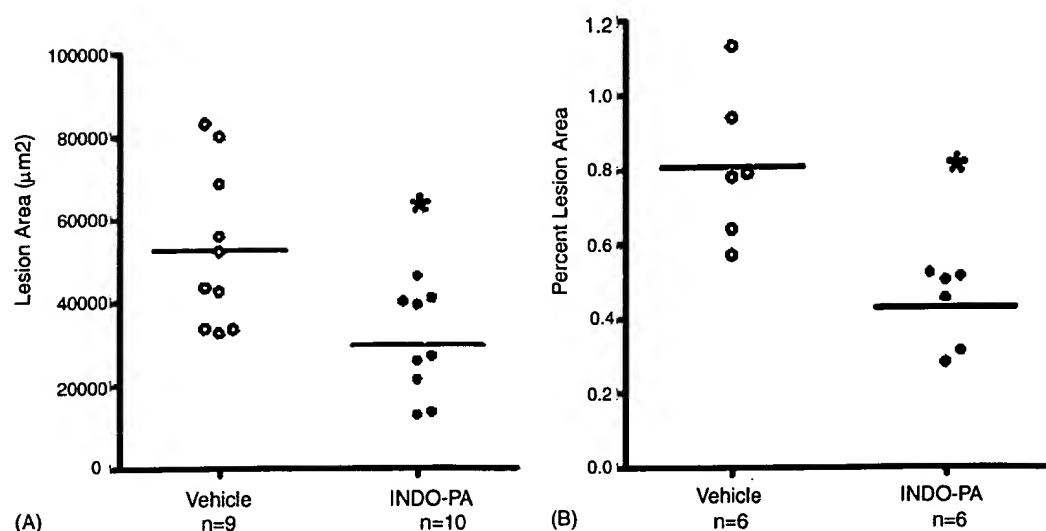


Fig. 2. Reduced atherosclerosis in apoE<sup>-/-</sup> mice treated with INDO-PA from 7 to 16 weeks of age. (A) The extent of atherosclerotic lesions in female apoE<sup>-/-</sup> after treatment with vehicle (open circles) or INDO-PA (filled circles) was quantified using Oil-Red-O stained sections. Values are in µm<sup>2</sup> with horizontal bar representing the mean of each group. (B) En face preparation of whole aortas were stained with Sudan IV and analyzed by a video imaging system. Data are represented as the percent of lesion area for each mouse and the horizontal bar represents the mean for each group.

Table 2  
Serum lipid levels in apoE<sup>-/-</sup> mice treated with vehicle or INDO-PA from 9 to 19 weeks of age

Animal group	2 weeks		9 weeks	
	Chol.	Trig.	Chol.	Trig.
Vehicle (n = 13)	352 ± 24	101 ± 8	396 ± 30	72 ± 5
INDO-PA (n = 10)	343 ± 9	110 ± 5	408 ± 27	89 ± 6

Values are in mg/dl (mean ± S.E.M.). The number of animals in each group is indicated by *n*.

To examine the impact of INDO-PA on the production of two aortic prostaglandins, PGE<sub>2</sub> and PGI<sub>2</sub>, apoE<sup>-/-</sup> mice were treated with INDO-PA or vehicle for 9 weeks. As shown in Fig. 4, INDO-PA inhibited production of PGE<sub>2</sub> by 88% compared to vehicle (5.13 ± 1.01 ng/mg versus 43.79 ± 14.31 ng/mg tissue, respectively; *p* = 0.001). INDO-PA also inhibited production of the PGI<sub>2</sub> metabolite by 87% compared to vehicle (29.13 ± 9.21 ng/mg versus 229.22 ± 61.98 ng/mg tissue, respectively; *p* = 0.002).

In the next study, INDO-PA treatment of 9-week-old apoE<sup>-/-</sup> mice for 9 weeks significantly reduced atherosclerosis by 53% in the proximal aorta (60997 ± 12280 µm<sup>2</sup> versus 129808 ± 18926 µm<sup>2</sup>; *p* = 0.023; Fig. 5A) and by 64% in the en face analysis of the aorta (0.40 ± 0.05% versus 1.12 ± 0.22%; *p* = 0.021; Fig. 5B) compared to the vehicle treatment group. The atherosclerotic lesions in these mice consisted of both fatty streaks and intermediate

lesions in the proximal aorta in the vehicle group (Fig. 3C) and INDO-PA treated group (Fig. 3D).

In contrast, treatment of 11-week-old apoE<sup>-/-</sup> mice with INDO-PA for 10 weeks produced only a trend for a 19% (*p* = 0.38) reduction in the extent of atherosclerosis in the proximal aorta that did not achieve statistical significance compared to mice treated with vehicle (Fig. 6A). The atherosclerotic lesions in the proximal aortas of these mice were intermediate to advanced in stage both in the vehicle-treated (Fig. 3E) and INDO-PA-treated mice (Fig. 3F) with evidence of connective tissue. Interestingly, there was a dramatic 76% reduction (Fig. 6B) in the en face analysis of the extent of aortic atherosclerosis in the apoE<sup>-/-</sup> mice treated with INDO-PA compared to the vehicle-treated group (0.61 ± 0.18% versus 2.5 ± 0.39%, respectively; *p* = 0.022).

#### 4. Discussion

We examined the impact of a novel amide derivative of indomethacin, INDO-PA, on the development of atherosclerosis in female apoE<sup>-/-</sup> mice. Although INDO-PA is highly selective for COX-2 enzyme in vitro [20], we have found that INDO-PA inhibits platelet thromboxane in vivo. Treatment of apoE<sup>-/-</sup> mice with INDO-PA dramatically reduced early to intermediate atherosclerotic

Table 3  
Serum lipid levels in apoE<sup>-/-</sup> mice treated with vehicle or INDO-PA from 11 to 21 weeks of age

Animal group	Baseline		2 weeks		9 weeks	
	Chol.	Trig.	Chol.	Trig.	Chol.	Trig.
Vehicle (n = 9)	292 ± 9	64 ± 3	242 ± 15	98 ± 6	271 ± 18	89 ± 3
INDO-PA (n = 9)	282 ± 16	58 ± 5	257 ± 23	99 ± 9	306 ± 29	96 ± 4

Values are in mg/dl (mean ± S.E.M.). The number of animals in each group is indicated by *n*.

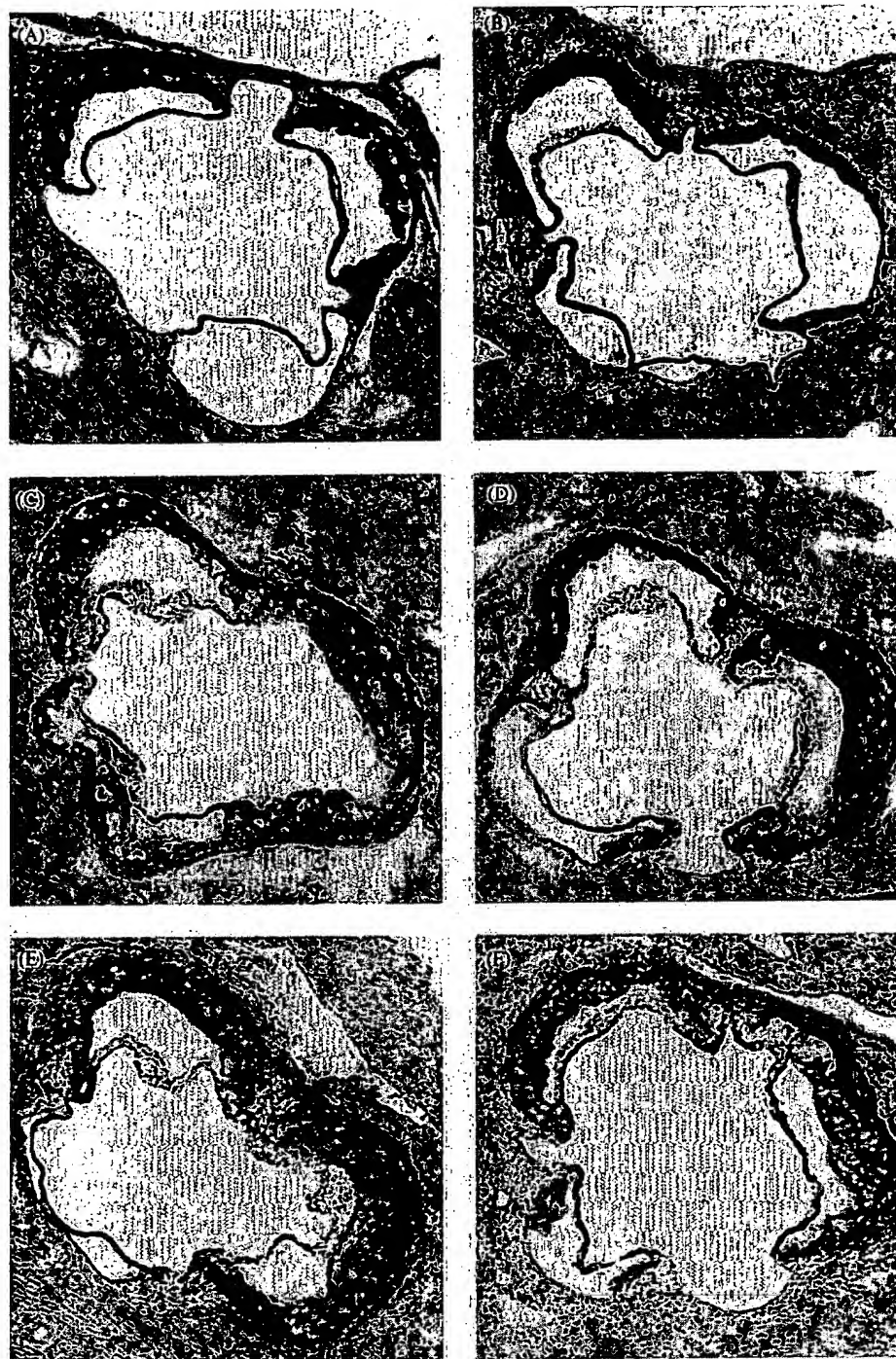


Fig. 3. Representative Oil-Red-O stained aortic root sections from groups treated with vehicle and INDO-PA. (A and B) Early stage atherosclerotic lesions in apoE<sup>-/-</sup> mice treated with vehicle (A) and INDO-PA (B) from 7 to 16 weeks of age. (C and D). Intermediate stage atherosclerotic lesions in apoE<sup>-/-</sup> mice treated with vehicle (C) and INDO-PA (D) from 9 to 18 weeks of age. (E and F) Advanced stage atherosclerotic lesions in apoE<sup>-/-</sup> mice treated with vehicle (E) and INDO-PA (F) from 7 to 16 weeks of age.

lesion formation. In addition, INDO-PA inhibited PGE<sub>2</sub> and PGI<sub>2</sub> metabolite production in the aorta by 88 and 87%, respectively, demonstrating efficacy of the INDO-PA in inhibiting prostaglandins in the artery wall *in vivo*. Thus, non-selective inhibition of COX with INDO-PA reduces the development of atherosclerosis in apoE<sup>-/-</sup> mice, supporting the potential for COX inhibition and

anti-inflammatory approaches in the prevention of atherosclerosis.

Treatment with 5 mg/kg INDO-PA (3.33-fold over ED<sub>50</sub> for oral dosing in rats [20]) was well-tolerated and did not produce gastric ulceration in apoE<sup>-/-</sup> mice. In these mice at steady state of INDO-PA, we observed a significant but incomplete (61%) inhibition of platelet thromboxane pro-

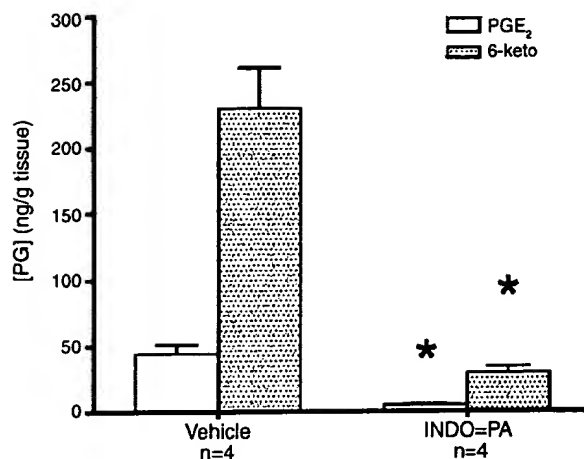


Fig. 4. Inhibition of prostaglandin production in aortic tissue of apoE<sup>-/-</sup> mice. ApoE<sup>-/-</sup> mice were given vehicle or INDO-PA beginning at 7 weeks of age for 9 weeks. Aortas were analyzed by GC/MS for PGE<sub>2</sub> and PGI<sub>2</sub> metabolite 6-keto-PGF<sub>1α</sub>.

duction indicating partial inhibition of platelet COX-1. Further studies in rats have verified that a small percentage of INDO-PA (5–10%) is converted into indomethacin *in vivo* (R.P. Remmel and L.J. Marnett, unpublished results). Although these data indicate that INDO-PA is only partially selective, previous data demonstrating that >90% inhibition of platelet thromboxane is required to inhibit platelet aggregation [26,27] suggests that inhibition of thromboxane-mediated-platelet aggregation is unlikely to have contributed significantly to the reduction in atherosclerosis. Three decades ago, non-selective inhibition of COX was reported to reduce atherosclerosis in cholesterol fed rabbits [15]. We and others have shown that non-selective inhibition of COX with indomethacin associated with 90–95% reductions in platelet thromboxane reduces

early and intermediate atherosclerotic lesions in LDLR<sup>-/-</sup> mice fed a western diet [6,16]. In contrast, Egan et al. have recently reported that treatment of 6-week-old western diet fed apoBec-1/LDLR DKO mice with indomethacin for 13 weeks was associated with only a 70% reduction in platelet thromboxane and caused a 12.9% reduction in complex atherosclerotic lesions [28]. Thus, differences in these studies include the mouse model used, the extent of atherosclerosis and the efficacy of the indomethacin. Data with regard to the impact of aspirin on murine models have been conflicting, with a study by Cayatte et al. showing no effect [29] and studies in high-fat diet fed apoE<sup>-/-</sup> [30] and LDLR<sup>-/-</sup> mice [31] demonstrating significant reductions in lesion formation. However, Cayatte et al. reported that a thromboxane receptor antagonist, which inhibited serum thromboxane activity by only 39%, reduced atherosclerosis in apoE<sup>-/-</sup> mice [29]. The authors interpreted these results as indicating that eicosanoids other than thromboxane are involved in promoting atherosclerosis. Recently, Belton et al. have reported that selective inhibition of COX-1, which reduced urinary 2,3-dinor-TxB<sub>2</sub>, by around 50% reduced atherosclerotic lesion formation in apoE deficient mice [9]. Thus, it is possible that inhibition of thromboxane may have contributed to the reduction in atherosclerosis seen with INDO-PA by partially offsetting potentially negative effects of reducing prostacyclin. However, it is also possible that reductions of other eicosanoids due to inhibition of COX-1 and/or COX-2 may have contributed to the reduction in atherosclerosis.

Reports on the impact of selective COX-2 inhibition on the development of atherosclerosis in murine models have been mixed indicating decreased, increased or unchanged atherosclerotic lesion area [6,16–19]. The differences in results of these studies may be explained by variability in

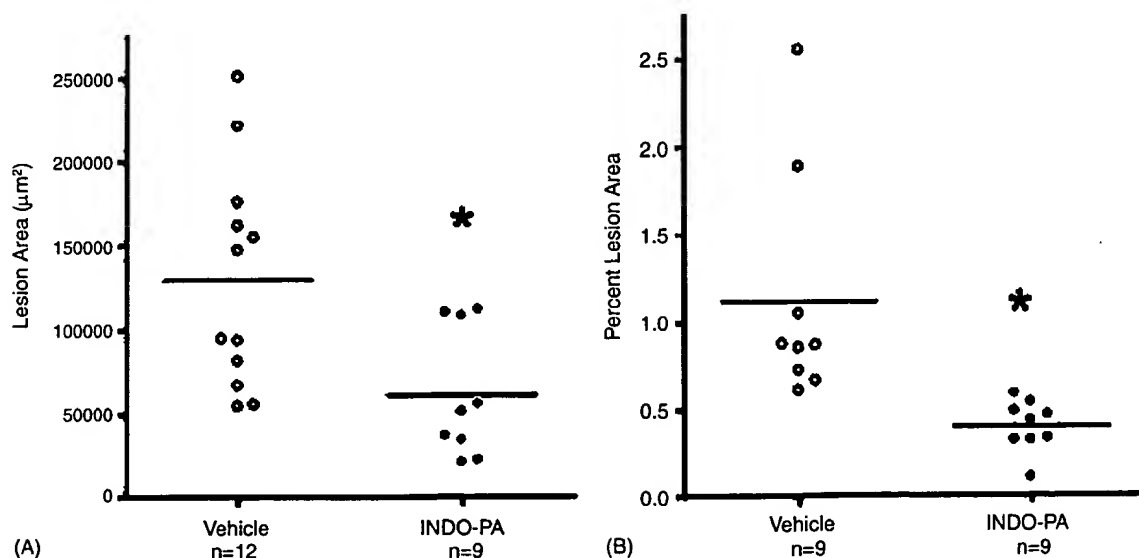


Fig. 5. Reduced atherosclerosis in apoE<sup>-/-</sup> mice treated with INDO-PA from 9 to 18 weeks of age. (A) The extent of atherosclerotic lesions in the proximal aorta of apoE<sup>-/-</sup> mice after treatment with vehicle (open circles) or INDO-PA (filled circles) was quantified using Oil-Red-O stained sections. (B) En face preparation of whole aortas were stained with Sudan IV and analyzed by a video imaging system. Data are represented as the percent of lesion area for each mouse and the horizontal bar represents the mean for each group.

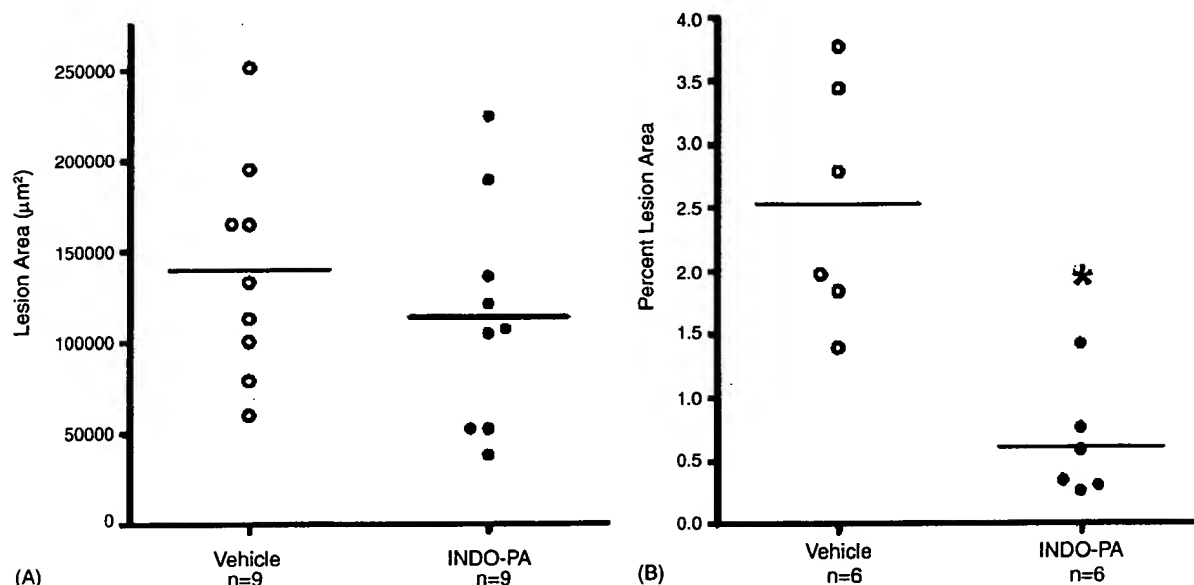


Fig. 6. Impact of INDO-PA treatment on atherosclerosis in apoE<sup>-/-</sup> mice from 11 to 21 weeks of age. (A) The extent of atherosclerotic lesions in the proximal aorta of apoE<sup>-/-</sup> after treatment with vehicle (open circles) or INDO-PA (filled circles) was quantified using Oil-Red-O stained sections from 300 µm of the proximal aorta. (B) En face preparation of whole aortas were stained with Sudan IV and analyzed by a video imaging system.

experimental design, including efficacy and selectivity of the inhibitors, gender of the mice and atherosclerotic lesion stage. We have previously reported that rofecoxib reduces early atherosclerotic lesion formation in LDLR<sup>-/-</sup> mice [6]. Consistent with our results, Krul et al. have presented data that treatment of apoE<sup>-/-</sup> mice with a selective COX-2 inhibitor, celecoxib, results in a significant reduction in aortic atherosclerosis [32]. Using bone marrow transplantation studies, we have demonstrated that macrophage COX-2 expression promotes early atherosclerotic lesion formation in LDLR<sup>-/-</sup> mice [6], providing genetic evidence consistent with COX-2 inhibition reducing early atherosclerotic lesion formation. In contrast, the ability of selective inhibition of COX-2 to impact atherogenesis appears to be limited in the setting of advanced atherosclerotic lesions [9,17,18], perhaps due to LXR-mediated downregulation of COX-2 in macrophage-derived foam cells [33] and the inhibition of anti-proliferative effects of COX-2 expression in smooth muscle cells [34]. Thus, the impact of COX-2 on atherosclerosis is complex and may vary according to the cell type and lesion stage.

Our current results demonstrate that non-selective inhibition of COX with INDO-PA reduces the formation of early and intermediate atherosclerotic lesions in female apoE<sup>-/-</sup> mice. Interestingly, we saw a non-significant trend for a reduction of atherosclerosis in the proximal aortas of apoE<sup>-/-</sup> mice with advanced stage lesions, whereas the extent of atherosclerosis in the en face aortas was dramatically reduced by 76%. In murine models, atherosclerosis develops first in the proximal aorta and then progresses distally [24,25]. These results are reminiscent of the findings that treatment with the selective COX-2 inhibitor, nimesulide, produced a non-significant trend for a reduction in atherosclerosis in

LDLR<sup>-/-</sup> mice with intermediate stage lesions, whereas treatment with indomethacin produced a significant reduction in atherosclerosis [16]. Although INDO-PA partially inhibits COX-1, we believe that it is acting largely as a COX-2 inhibitor, given the relatively low rate of conversion to indomethacin in vivo, the incomplete inhibition of platelet COX-1, and the much improved safety profile of INDO-PA compared to indomethacin. These results suggest that as the disease progresses from intermediate to advanced lesion stage, COX-2 inhibition appears to have less of an effect on modulating progression of atherosclerosis. Interestingly, INDO-PA virtually eliminated the progression of atherosclerosis in the en face aortas, as can be seen by the similar lesion burdens in all three treatment groups.

Although atherosclerosis is the pathological substrate underlying heart attack and stroke, plaque rupture and thrombosis are responsible for precipitating acute cardiovascular events. Mounting evidence supports the critical involvement of eicosanoids in the processes of plaque rupture and thrombosis. Inhibition of COX-1 mediated production of platelet thromboxane by aspirin reduces the risk for myocardial infarction and stroke [7]. In contrast, rofecoxib, a highly selective COX-2 inhibitor, has recently been taken off the market due to evidence from the APPROVe trial demonstrating increased cardiovascular events after 18 months ([www.vioxx.com](http://www.vioxx.com)). The mechanism responsible for the increased cardiovascular events in patients on rofecoxib remains to be elucidated. Concerns have been raised that COX-2 inhibition may promote cardiovascular events by inhibiting prostacyclin and promoting a prothrombotic state [11]. However, the impact of a prothrombotic state might be expected to cause an increase in cardiovascular events sooner than the



18 months seen in the APPROVe trial, suggesting that other mechanisms may be responsible.

Although three published studies have reported an increase in cardiovascular events in patients taking rofecoxib, principally at doses >25 mg a day [10,35,36], other studies found no evidence for increased risk of cardiovascular events with rofecoxib [37,38] or celecoxib [39]. Several important questions remain to be answered. Is the increase in cardiovascular events seen with rofecoxib a class effect that pertains to all other COX-2 inhibitors? Does the presence of COX-1 inhibition in addition to COX-2 inhibition, as seen with non-selective COX inhibitors, eliminate this risk of increased cardiovascular events due to chronic COX-2 inhibition alone? Recently, Pfizer has announced an increase in cardiovascular events associated with valdecoxib in patients in two small studies of patients undergoing coronary artery bypass grafting [19], and no increase in cardiovascular events based on clinical trial database of nearly 8000 patients treated with valdecoxib for durations ranging from 6 to 52 weeks ([http://www.pfizer.com/are/news\\_releases/2004pr/mn\\_2004\\_1015.html](http://www.pfizer.com/are/news_releases/2004pr/mn_2004_1015.html)). Although our current studies do not address the issues of plaque rupture and thrombosis, our results support the ability of non-selective COX inhibition to reduce atherosclerosis. Thus, non-selective inhibition of COX has the potential to favorably impact atherosclerosis, plaque rupture and thrombosis. A better understanding of the complex roles of COX-1 and COX-2 in atherogenesis and plaque stability may lead to new therapeutic approaches to the prevention of cardiovascular disease.

## Acknowledgements

The authors are thankful to Lei Ding and Youmin Zhang for excellent technical expertise. This work was supported by National Institutes of Health grants HL65405, HL53989, HL 57986, DK59637 (Lipid, Lipoprotein and Atherosclerosis Core of the Vanderbilt Mouse Metabolic Phenotyping Centers). M.E.B. is supported by American Heart Association grant (0215110B). V.R.B. is supported by American Heart Association grant (0160160B).

## References

- [1] Ross R. Atherosclerosis—an inflammatory disease. *New Eng J Med* 1999;340:115–26.
- [2] DuBois R, Abramson S, Crofford L, Gupta RA, Simon L, Van De Putte L, et al. Cyclooxygenase in biology and disease. *FASEB J* 1998;12:1063–73.
- [3] Vane JR, Bakhle YS, Botting RM. Cyclooxygenase 1 and 2. *Ann Rev Pharmacol Toxicol* 1998;38:97–120.
- [4] Baker CS, Hall RJ, Evans TJ, Pomerance A, Macloof J, Creminon C, et al. Cyclooxygenase-2 is widely expressed in atherosclerotic lesions affecting native and transplanted human coronary arteries and colocalizes with inducible nitric oxide synthase and nitrotyrosine particularly in macrophages. *Arterioscler Thromb Vasc Biol* 1999;19(3):646–55.
- [5] Schonbeck U, Sukhova GK, Graber P, Coulter S, Libby P. Augmented expression of cyclooxygenase-2 in human atherosclerotic lesions. *Am J Pathol* 1999;155:1281–91.
- [6] Burleigh ME, Babaev VR, Oates JA, Harris RC, Gautam S, Riendeau D, et al. Cyclooxygenase-2 promotes early atherosclerotic lesion formation in LDL receptor-deficient mice. *Circulation* 2002;105: 1816–23.
- [7] Hennekens CH, Dyken ML, Fuster V. Aspirin as a therapeutic agent in cardiovascular disease: a statement for healthcare professionals from the American Heart Association. *Circulation* 1997;96:2751–3.
- [8] Cheng Y, Austin SC, Rocca B, Koller BH, Coffman TM, Grosser T, et al. Role of prostacyclin in the cardiovascular response to thromboxane A<sub>2</sub>. *Science* 2002;296(5567):539–41.
- [9] Belton OA, Duffy A, Toomey S, Fitzgerald DJ. Cyclooxygenase isoforms and platelet vessel wall interactions in the apolipoprotein E knockout mouse model of atherosclerosis. *Circulation* 2003;108: 3017–23.
- [10] Bombardier C, Laine L, Reicin A, Shapiro D, Burgos-Vargas R, Davis B, et al., VIGOR Study Group. Comparison of upper gastrointestinal toxicity of rofecoxib and naproxen in patients with rheumatoid arthritis. *New Eng J Med* 2000;343:1520–8.
- [11] Mukherjee D, Nissen SE, Topol EJ. Risk of cardiovascular events associated with selective COX-2 inhibitors. *J Am Med Assoc* 2001;286:954–9.
- [12] Chenevard R, Hurlimann D, Bechir M, Enseleit F, Spieker L, Hermann M, et al. Selective COX-2 inhibition improves endothelial function in coronary artery disease. *Circulation* 2003;107(3):405–9.
- [13] Cipollone F, Prontera C, Pini B, Marini M, Fazia M, De Cesare D, et al. Overexpression of functionally coupled cyclooxygenase-2 and prostaglandin E synthase in symptomatic atherosclerotic plaques as a basis of prostaglandin E<sub>2</sub>-dependent plaque instability. *Circulation* 2001;104(8):921–7.
- [14] Cipollone F, Toniato E, Martinotti S, Fazia M, Lezzi A, Cuccurullo C, et al. Identification of new elements of plaque stability study G, a polymorphism in the cyclooxygenase 2 gene as an inherited protective factor against myocardial infarction and stroke. *J Am Med Assoc* 2004;291:2221–8.
- [15] Bailey JM, Butler J. Anti-inflammatory drugs in experimental atherosclerosis. I. Relative potencies for inhibiting plaque formation. *Atherosclerosis* 1973;17(3):515–22.
- [16] Pratico D, Tillmann C, Zhang ZB, Li H, FitzGerald GA. Acceleration of atherogenesis by COX-1-dependent prostanoid formation in low density lipoprotein receptor knockout mice. *Proc Natl Acad Sci USA* 2001;98:3358–63.
- [17] Olesen M, Kwong E, Mezli A, Kontny F, Seljelot I, Arnesen H, et al. No effect of cyclooxygenase inhibition on plaque size in atherosclerosis-prone mice. *Scand Cardiovasc J* 2002;36:362–7.
- [18] Bea F, Blessing E, Bennett BJ, Kuo CC, Campbell LA, Kreuzer J, et al. Chronic inhibition of cyclooxygenase-2 does not alter plaque composition in a mouse model of advanced unstable atherosclerosis. *Cardiovasc Res* 2003;60:198–204.
- [19] Rott D, Zhu J, Burnett MS, Zhou YF, Zalles-Ganley A, Ogunmakina J, et al. Effects of MF-tricyclic, a selective cyclooxygenase-2 inhibitor, on atherosclerosis progression and susceptibility to cytomegalovirus replication in apolipoprotein-E knockout mice. *J Am Coll Cardiol* 2003;41:1812–9.
- [20] Kalgutkar AS, Crews BC, Rowlinson SW, Marnett AB, Kozak KR, Remmel RP, et al. Biochemically based design of cyclooxygenase-2 (COX-2) inhibitors: facile conversion of nonsteroidal antiinflammatory drugs to potent and highly selective COX-2 inhibitors. *Proc Natl Acad Sci USA* 2000;97(2):925–30.
- [21] Linton MF, Atkinson JB, Fazio S. Prevention of atherosclerosis in apoE deficient mice by bone marrow transplantation. *Science* 1995;267:1034–7.



- [22] Marnett LJ, Wright TL, Crews BC, Tannenbaum SR, Morrow JD. Regulation of prostaglandin biosynthesis by nitric oxide is revealed by targeted deletion of inducible nitric-oxide synthase. *J Biol Chem* 2000;275:13427–30.
- [23] Reese J, Paria BC, Brown N, Zhao X, Morrow JD, Dey SK. Coordinated regulation of fetal and maternal prostaglandins directs successful birth and postnatal adaptation in the mouse. *Proc Natl Acad Sci USA* 2000;97(17):9759–64.
- [24] Babaev VR, Patel MB, Semenkovich CF, Fazio S, Linton MF. Macrophage lipoprotein lipase promotes foam cell formation and atherosclerosis in low density lipoprotein receptor-deficient mice. *J Biol Chem* 2000;275:26293–9.
- [25] Paigen B, Holmes P, Mitchell D, Albee D. Comparison of atherosclerotic lesions and HDL-lipid levels in male, females, and testosterone-treated female mice from strains C57BL/6, BALB/c and C3H. *Atherosclerosis* 1987;68:215–21.
- [26] Czervionke RL, Hoak JC, Fry GL. Effect of aspirin on thrombin-induced adherence of platelets to cultured cells from the blood vessel wall. *J Clin Invest* 1978;62(4):847–56.
- [27] FitzGerald GA, Oates JA, Hawiger J, Maas RL, Roberts 2nd LJ, Lawson JA, et al. Endogenous biosynthesis of prostacyclin and thromboxane and platelet function during chronic administration of aspirin in man. *J Clin Invest* 1983;71(3):676–88.
- [28] Egan KM, Wang M, Lucitt MB, Zukas AM, Pure E, Lawson JA, et al. Cyclooxygenases, thromboxane, and atherosclerosis: plaque destabilization by cyclooxygenase-2 inhibition combined with thromboxane receptor antagonism. *Circulation* 2005;111(3):334–42.
- [29] Cayatte AJ, Du Y, Oliver-Krasinski J, Lavielle G, Verbeuren TJ, Cohen RA. The thromboxane receptor antagonist S18886 but not aspirin inhibits atherogenesis in apo E-deficient mice: evidence that eicosanoids other than thromboxane contribute to atherosclerosis. *Arterioscler Thromb Vasc Biol* 2000;20:1724–8.
- [30] Paul A, Calleja L, Camps J, Osada J, Vilella E, Ferre N, et al. The continuous administration of aspirin attenuates atherosclerosis in apolipoprotein E-deficient mice. *Life Sci* 2000;68(4):457–65.
- [31] Cyrus T, Sung S, Zhao L, Funk CD, Tang S, Pratico D. Effect of low-dose aspirin on vascular inflammation, plaque stability, and atherogenesis in low-density lipoprotein receptor-deficient mice. *Circulation* 2002;106(10):1282–7.
- [32] Krul ES, Napawan N, Butteiger DT, Hayes K, Krause L, Freidrich GE, et al. Atherosclerosis is reduced in cholesterol-fed apoE<sup>-/-</sup> mice administered an ASBT inhibitor or a selective COX-2 inhibitor. *Arterioscler Thromb Vasc Biol* 2002;22:P409.
- [33] Joseph SB, Castrillo A, Laffitte BA, Mangelsdorf DJ, Tontonoz P. Reciprocal regulation of inflammation and lipid metabolism by liver X receptors. *Nat Med* 2003;9:213–9.
- [34] Kothapalli D, Fuki I, Ali K, Stewart S, Zhao L, Yahil R, et al. Antimitogenic effects of HDL and APOE mediated by Cox-2-dependent IP activation. *J Clin Invest* 2004;113(4):609–18.
- [35] Ray WA, Stein CM, Daugherty JR, Hall K, Arbogast PG, Griffin MR. COX-2 selective non-steroidal anti-inflammatory drugs and risk of serious coronary heart disease. *Lancet* 2002;360:1071–3.
- [36] Solomon D, Schneeweiss S, Glynn R, Kiyota Y, Levin R, Mogun H, et al. Relationship between selective cyclooxygenase-2 inhibitors and acute myocardial infarction in older adults. *Circulation* 2004;109:2068–73.
- [37] Konstam MA, Weir MR, Reicin A, Shapiro D, Sperling RS, Barr E, et al. Cardiovascular thrombotic events in controlled, clinical trials of rofecoxib. *Circulation* 2001;104:2280–8.
- [38] Reicin AS, Shapiro D, Sperling RS, Barr E, Yu Q. Comparison of cardiovascular thrombotic events in patients with osteoarthritis treated with rofecoxib versus nonselective nonsteroidal anti-inflammatory drugs (ibuprofen, diclofenac, and nabumetone). *Am J Cardiol* 2002;89:204–9.
- [39] Silverstein F, Faich G, Goldstein J, Simon L, Pincus T, Whelton A, et al. Gastrointestinal toxicity with celecoxib vs nonsteroidal anti-inflammatory drugs for osteoarthritis and rheumatoid arthritis: the CLASS study. A randomized controlled trial. Celecoxib Long-term Arthritis Safety Study. *J Am Med Assoc* 2000;284:1247–55.

# Simvastatin Reduces Neointimal Thickening in Low-Density Lipoprotein Receptor-Deficient Mice After Experimental Angioplasty Without Changing Plasma Lipids

Zhiping Chen, MS; Tatsuya Fukutomi, MD; Alexandre C. Zago, MD; Raila Ehlers, MD; Patricia A. Detmers, PhD; Samuel D. Wright, PhD; Campbell Rogers, MD; Daniel I. Simon, MD

**Background**—Statins exert antiinflammatory and antiproliferative actions independent of cholesterol lowering. To determine whether these actions might affect neointimal formation, we investigated the effect of simvastatin on the response to experimental angioplasty in LDL receptor-deficient (LDLR<sup>-/-</sup>) mice, a model of hypercholesterolemia in which changes in plasma lipids are not observed in response to simvastatin.

**Methods and Results**—Carotid artery dilation (2.5 atm) and complete endothelial denudation were performed in male C57BL/6J LDLR<sup>-/-</sup> mice treated with low-dose (2 mg/kg) or high-dose (20 mg/kg) simvastatin or vehicle subcutaneously 72 hours before and then daily after injury. After 7 and 28 days, intimal and medial sizes were measured and the intima to media area ratio (I:M) was calculated. Total plasma cholesterol and triglyceride levels were similar in simvastatin- and vehicle-treated mice. Intimal thickening and I:M were reduced significantly by low- and high-dose simvastatin compared with vehicle alone. Simvastatin treatment was associated with reduced cellular proliferation (BrdU), leukocyte accumulation (CD45), and platelet-derived growth factor-induced phosphorylation of the survival factor Akt and increased apoptosis after injury.

**Conclusions**—Simvastatin modulates vascular repair after injury in the absence of lipid-lowering effects. Although the mechanisms are not yet established, additional research may lead to new understanding of the actions of statins and novel therapeutic interventions for preventing restenosis. (*Circulation*. 2002;106:20-23.)

**Key Words:** restenosis ■ statins ■ inflammation ■ apoptosis

Statins inhibit the enzyme 3-hydroxy-3-methylglutaryl coenzyme A (HMG-CoA) reductase, the first committed step of sterol synthesis, and lower plasma cholesterol levels. In large clinical trials, statins have been shown to reduce coronary events in primary or secondary prevention settings.<sup>1</sup> Effects on clinical and angiographic restenosis after coronary intervention, however, have not been conclusively demonstrated. Several clinical studies have failed to demonstrate a link between statin therapy and the risk of restenosis after balloon angioplasty,<sup>2</sup> whereas more recent studies suggest that statins may reduce restenosis after stenting.<sup>3</sup>

Statins are known to have broad effects in addition to lowering plasma cholesterol. The product of HMG-CoA reductase, mevalonate, is an important precursor for many isoprenoids, thereby endowing statins with the ability to directly alter cellular events other than cholesterol synthesis. For example, the isoprenoids farnesylpyrophosphate and geranylgeranylpyrophosphate play important roles in signal transduction in cellular migration, proliferation, and survival via their attachment to critical signaling proteins, such as Ras and Rho.<sup>4</sup>

We used a hyperlipidemic model, the LDLR<sup>-/-</sup> mouse, to test the antiinflammatory and antiproliferative actions of simvastatin on neointimal thickening after experimental angioplasty in an atherosclerotic background. An essential feature of the chosen model is that simvastatin does not affect plasma lipid levels in mice, allowing the study of effects of simvastatin distinct from cholesterol lowering.

## Methods

### Carotid Injury

Male LDLR<sup>-/-</sup> C57BL/6J mice (Jackson Laboratories, Bar Harbor, Me), maintained on a high-fat (20.1%) diet containing 1.25% cholesterol for 12 weeks after weaning, underwent unilateral carotid artery dilation (2.5 atm) and complete endothelial denudation.<sup>5</sup> Animal care and procedures were reviewed and approved by Harvard Medical School Standing Committee on Animals and performed in accordance with the guidelines of the American Association for Accreditation of Laboratory Animal Care and the National Institutes of Health.

### Simvastatin Treatment

Treatments were via subcutaneous injection 72 hours before and daily after injury. LDLR<sup>-/-</sup> mice were divided into 3 treatment

Received March 29, 2002; revision received May 8, 2002; accepted May 9, 2002.

From the Cardiovascular Division (Z.C., T.F., A.C.Z., R.E., C.R., D.I.S.), Brigham and Women's Hospital, Boston, Mass; Harvard-MIT Division of Health Sciences and Technology (C.R.), Cambridge, Mass; and Merck Research Laboratories (P.A.D., S.D.W.), Rahway, NJ.

Correspondence to Daniel I. Simon, MD, Cardiovascular Division, Brigham and Women's Hospital, 75 Francis St, Tower 3, Boston, MA 02115. E-mail dsimon@rics.bwh.harvard.edu

© 2002 American Heart Association, Inc.

*Circulation* is available at <http://www.circulationaha.org>

DOI: 10.1161/01.CIR.0000022843.76104.01

**Quantitative Morphometry and Immunohistochemical Analysis of Mouse Carotid Arteries After Injury**

	Simvastatin			ANOVA	P	
	Vehicle	Low	High		Vehicle vs Low	Vehicle vs High
Cholesterol, 21 d, mg/dL	856±89	922±167	1130±279	0.074	NS	NS
Triglyceride, 21 d, mg/dL	216±36	234±43	223±44	0.751	NS	NS
Intimal area, mm <sup>2</sup>						
7 d	0.010±0.004	0.006±0.004	0.006±0.004	0.320	NS	NS
28 d	0.047±0.023	0.021±0.013	0.019±0.015	0.004	0.011	0.012
Medial area, mm <sup>2</sup>						
28 d	0.078±0.015	0.063±0.014	0.074±0.031	0.299	NS	NS
I:M, 28 d	0.64±0.37	0.32±0.17	0.24±0.15	0.008	0.036	0.012
EEL, mm <sup>2</sup>						
7 d	0.104±0.013	0.113±0.035	0.103±0.014	0.778	NS	NS
28 d	0.223±0.032	0.191±0.040	0.192±0.053	0.184	NS	NS
BrdU+ cells, %						
Media, 7 d	19.2±2.8	12.0±5.8	11.0±4.5	0.299	NS	NS
Intima, 28 d	4.6±1.8	1.7±0.5	1.9±0.8	0.0184	0.042	0.050
CD45+ cells, %						
Intima, 7 d	59.2±11.9	44.2±5.2	39.1±12.8	0.0429	0.047	0.049
Intima, 28 d	34.4±3.6	24.3±2.2	20.9±8.0	0.0120	0.026	0.025
TUNEL+ cells, %						
Intima, 7 d	3.5±1.1	6.9±3.3	9.2±4.2	0.0872	0.193	0.039
Media, 7 d	2.5±0.4	4.2±0.3	5.8±1.0	0.0002	0.002	0.001

groups: PBS vehicle (control group) or 2 mg/kg (low-dose) or 20 mg/kg (high-dose) alkaline-hydrolyzed simvastatin.<sup>6</sup>

**Lipid Analysis**

Blood was collected via retro-orbital puncture into heparin-coated capillary tubes. Plasma cholesterol and triglyceride measurements were performed as reported.<sup>7</sup>

**Tissue Harvesting and Analysis**

Carotid arteries were harvested and processed for quantitative morphometry 7 days (control, n=5; low-dose, n=5; high-dose, n=4) or 28 days (control, n=9; low-dose, n=10; high-dose, n=7) after vascular injury.<sup>5</sup> Standard avidin-biotin procedures for mouse leukocytes (CD45) and macrophages (Mac-3) (PharMingen, San Diego, Calif), BrdU (DAKO, Carpinteria, Calif), and smooth muscle cell (SMC)  $\alpha$ -actin (DAKO) were used for immunohistochemistry. Apoptotic cells were detected by the TUNEL method using Apo Tag (Intergen). Immunostained sections were quantified as the number of immunostained-positive cells per total number of nuclei.

**Ex Vivo Akt Signaling Assay**

Aortas were harvested from all animals, opened longitudinally, and incubated with 30 ng/mL platelet-derived growth factor (PDGF)-BB (R&D Systems, Minneapolis, Minn) for 15 minutes at 37°C. Aortic lysates were prepared<sup>8</sup> and then subjected to Western analysis using antibodies to Akt and Phospho-Akt (Ser473) (Cell Signaling Technology, Beverly, Mass).

**Data Analysis**

All data are presented as mean±SD. Statistical comparisons of the principal end points were performed using one-way ANOVA to determine a difference in mean values between the 3 groups, followed by *t* tests for the 3 pair-wise comparisons when the ANOVA false-positive rate was <5%. For ANOVA with a false-

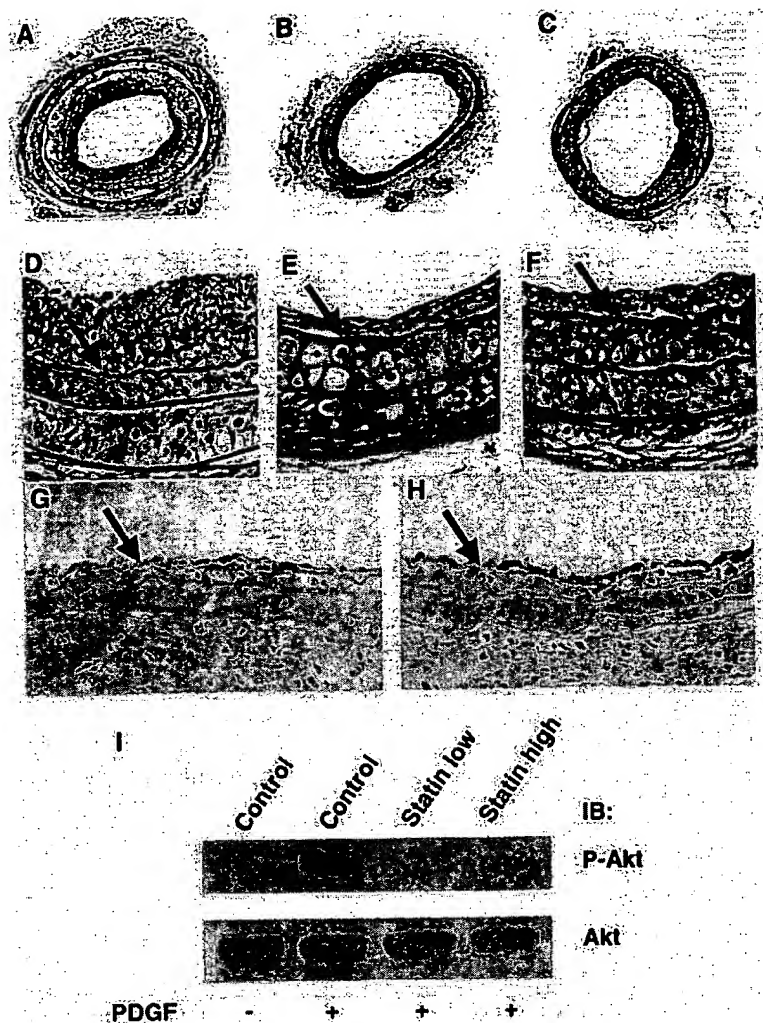
positive rate of >5%, the pair-wise comparisons were reported to be statistically nonsignificant (NS). For the primary study end point of intimal area 28 days after injury, a Bonferroni corrective for 3 pair-wise comparisons was applied, in which the *t* test *P*<0.0167 was used to signify a false-positive rate of 5%.

**Results****Simvastatin Does Not Alter Plasma Lipids in LDLR<sup>-/-</sup> Mice**

We sought evidence that simvastatin modulates vascular repair independent of cholesterol lowering. To determine whether plasma cholesterol is unresponsive to simvastatin in LDLR<sup>-/-</sup> mice, as it is in normal<sup>9</sup> and apoE-deficient<sup>7</sup> mice, we dosed LDLR<sup>-/-</sup> animals with 2 mg/kg simvastatin, 20 mg/kg simvastatin, or vehicle control and measured plasma lipid levels. Simvastatin did not alter plasma cholesterol or triglyceride levels in LDLR<sup>-/-</sup> mice at either of the 2 doses tested (Table).

**Simvastatin Decreases Neointimal Thickening, Cellular Proliferation, and Leukocyte Accumulation After Carotid Injury**

Carotid artery dilation and complete endothelial denudation were performed in LDLR<sup>-/-</sup> mice treated with 2 or 20 mg/kg simvastatin or vehicle subcutaneously 72 hours before and then daily after injury until euthanasia. In mice receiving vehicle, intimal thickening began by 7 days after injury and progressed significantly between 7 days (0.010±0.004 mm<sup>2</sup>) and 28 days (0.047±0.023 mm<sup>2</sup>). Low- and high-dose simvastatin reduced intimal thickening at 28 days by 55%



Photomicrographs of mouse carotid arteries after injury (A through H). VerHoeff elastin stain 28 days after injury: vehicle (A); low-dose simvastatin (B); high-dose simvastatin (original magnification  $\times 38$ ) (C); vehicle (D); low-dose simvastatin (E); and high-dose simvastatin ( $\times 150$ ) (F). Neointima separates the internal elastic lamina (arrows) from the lumen. Apoptotic (TUNEL-positive) cells 7 days after injury: vehicle (G); high-dose simvastatin ( $\times 150$ ) (H). Simvastatin and Akt signaling (I). Aortae were harvested from mice treated with simvastatin or vehicle and incubated with PDGF-BB. Aortic lysates were immunoblotted sequentially using antibodies to Akt and Phospho-Akt (Ser473).

( $P=0.012$ ) and 60% ( $P=0.011$ ), respectively (Figure, panels A through F, Table). Medial area was unaffected by simvastatin treatment. I:M at 28 days in control mice was  $0.64 \pm 0.37$  and was reduced 50% by low-dose ( $P=0.036$ ) and 62% by high-dose ( $P=0.012$ ) simvastatin. Intimal and medial thickening were accompanied by progressive vessel enlargement (ie, positive remodeling), as determined by external elastic lamina area measurements over time, which was comparable in vehicle- and simvastatin-treated mice.

We assessed cellular proliferation by quantifying incorporation of BrdU. Substantial proliferation was observed 7 days after injury in control vessels (19.2% of medial cells), and proliferation was still evident at 28 days (4.6% of intimal cells). Low- and high-dose simvastatin reduced medial proliferation at 7 days by 38% and 43%, respectively, and intimal proliferation at 28 days by 63% ( $P=0.042$ ) and 59% ( $P=0.050$ ) (Table).

Immunohistochemistry was performed to identify the cellular components of the neointima 28 days after injury. In vehicle-treated animals, 48% of cells were SMCs ( $\alpha$ -actin-positive) and 34% were monocytes or macrophages (CD45- and Mac3-positive). Altered leukocyte accumulation within vessels was observed in simvastatin-treated mice. Inflammatory cells (CD45-positive) invading the intima were reduced

by 25% to 34% ( $P<0.05$ ) at 7 days and 29% to 39% ( $P<0.03$ ) at 28 days in simvastatin-treated compared with control mice.

### Simvastatin Increases Apoptosis

Because statins prevent isoprenylation of Rho proteins and their translocation to the membrane fraction, and because there is increasing evidence that Rho activates signals that regulate apoptosis,<sup>10</sup> we investigated the effects of simvastatin on apoptosis after injury. Low- and high-dose simvastatin significantly increased the number of apoptotic (TUNEL-positive) cells in the intima (by 197% and 263%, respectively) and media (168% and 232%, respectively) at 7 days compared with control (Table, Figure, panels G and H).

To identify a biochemical correlate of simvastatin action promoting apoptosis, we examined signaling of the survival factor, Akt, in arteries from mice treated with simvastatin. Injured carotid arteries are completely devoid of endothelium and lined with a platelet monolayer.<sup>5</sup> Therefore, we examined PDGF-induced phosphorylation and activation of Akt by Western blot analysis of aortic samples from mice treated with low- and high-dose simvastatin or vehicle for 7 days. PDGF-induced phosphorylation of Akt was impaired in the aortae of simvastatin-treated mice (Figure, panel I).

## Discussion

Our study provides definitive in vivo evidence that simvastatin inhibits neointimal thickening in a cholesterol-independent manner accompanied by reduced vascular inflammation and proliferation and increased apoptosis. These results establish a role for statins in inhibiting neointimal formation after experimental angioplasty in a setting in which simvastatin did not alter plasma lipids.

Restenosis is a complex cascade of wound-healing responses to vascular injury, characterized by thrombosis, inflammation, cellular proliferation/migration, and extracellular matrix deposition. Increasing evidence suggests that antiinflammatory<sup>7</sup> and antiproliferative<sup>11</sup> effects of statins play important roles in attenuating atherosclerosis,<sup>1,7</sup> transplant vasculopathy,<sup>12</sup> and restenosis.<sup>3</sup> Statins inhibit the synthesis of isoprenoid intermediates that are important lipid attachments for signaling proteins, including Ras and the Rho family of small GTP-binding proteins (eg, Rho, Rac, and Cdc42).<sup>4</sup> Rho is implicated in various biological functions relevant to vascular injury, including cellular migration, proliferation, and survival.<sup>10,13</sup> Statins attenuate vascular SMC proliferation in vitro by decreasing Rho geranylgeranylation and membrane localization and inhibiting Cdk activity.<sup>11</sup>

We provide biochemical evidence that PDGF-induced phosphorylation of Akt is inhibited in aortic tissue from simvastatin-treated mice. Akt functions as an antiapoptotic protein, protecting against cell death induced by growth factor withdrawal or ischemia-reperfusion injury.<sup>14</sup> The effects of statins on Akt signaling seem to be tissue-specific. Statins rapidly activate Akt signaling in endothelial cells, enhance phosphorylation of endothelial NO synthase, and inhibit apoptosis.<sup>15</sup> In contrast, statins impair Akt activation in SMCs,<sup>16</sup> leading to diminished SMC proliferation and induction of apoptosis via effects on phosphatidylinositol-3 kinase or Rho.<sup>11</sup> These divergent actions of statins on Akt activation in endothelial cells and SMCs may act in synchrony to diminish neointimal thickening after denuding injury.

Prior clinical trials of statins after balloon angioplasty have failed to show a reduction in restenosis,<sup>2</sup> likely because of the predominant role of vascular remodeling rather than neointimal thickening in this setting.<sup>17</sup> However, recent studies of statin use after stenting, with minimal remodeling and profound neointimal thickening,<sup>17</sup> have suggested benefit.<sup>3</sup>

Our results support the hypothesis that simvastatin has antiinflammatory, antiproliferative, and proapoptotic actions relevant to preventing restenosis. Although mechanisms are not yet established, additional research may lead to new

understanding of the actions of statins, additional impetus for broad statin use after vascular intervention independent of lipid profile, and novel therapies for preventing restenosis.

## Acknowledgments

This research was supported by National Institutes of Health Grants R01 HL57506 (to Dr Simon), R01 DK55656 (to Dr Simon), and K08 HL03104 (to Dr Rogers) and a Merck Medical School Grant (to Dr Simon).

## References

1. Bucher HC, Griffith LE, Guyatt GH. Systematic review on the risk and benefit of different cholesterol-lowering interventions. *Arterioscler Thromb Vasc Biol.* 1999;19:187-195.
2. Weintraub WS, Boccuzzi SJ, Klein JL, et al. Lack of effect of lovastatin on restenosis after coronary angioplasty: Lovastatin Restenosis Trial Study Group. *N Engl J Med.* 1994;331:1331-1337.
3. Walter DH, Schachinger V, Elsner M, et al. Effect of statin therapy on restenosis after coronary stent implantation. *Am J Cardiol.* 2000;85:962-968.
4. Casey PJ. Protein lipidation in cell signaling. *Science.* 1995;268:221-225.
5. Simon DI, Chen Z, Seifert P, et al. Decreased neointimal formation in Mac-1<sup>-/-</sup> mice reveals a role for inflammation in vascular repair after angioplasty. *J Clin Invest.* 2000;105:293-300.
6. Endres M, Laufs U, Huang Z, et al. Stroke protection by 3-hydroxy-3-methylglutaryl (HMG)-CoA reductase inhibitors mediated by endothelial nitric oxide synthase. *Proc Natl Acad Sci U S A.* 1998;95:8880-8885.
7. Sparrow CP, Burton CA, Hernandez M, et al. Simvastatin has anti-inflammatory and antiatherosclerotic activities independent of plasma cholesterol lowering. *Arterioscler Thromb Vasc Biol.* 2001;21:115-121.
8. DiChiara MR, Kiely JM, Gimbrone MA Jr, et al. Inhibition of E-selectin gene expression by transforming growth factor  $\beta$  in endothelial cells involves coactivator integration of Smad and nuclear factor  $\kappa$ B-mediated signals. *J Exp Med.* 2000;192:695-704.
9. Endo A, Tsujita Y, Kuroda M, et al. Effects of ML-236B on cholesterol metabolism in mice and rats: lack of hypocholesterolemic activity in normal animals. *Biochim Biophys Acta.* 1979;575:266-276.
10. van Nieuw Amerongen GP, van Hinsbergh VW. Cytoskeletal effects of rho-like small guanine nucleotide-binding proteins in the vascular system. *Arterioscler Thromb Vasc Biol.* 2001;21:300-311.
11. Laufs U, Marra D, Node K, et al. 3-Hydroxy-3-methylglutaryl-CoA reductase inhibitors attenuate vascular smooth muscle cell proliferation by preventing rho GTPase-induced down-regulation of p27Kip1. *J Biol Chem.* 1999;274:21926-21931.
12. Kobashigawa JA, Katznelson S, Laks H, et al. Effect of pravastatin on outcomes after cardiac transplantation. *N Engl J Med.* 1995;333:621-627.
13. Shibata R, Kai H, Seki Y, et al. Role of Rho-Associated kinase in neointimal formation after vascular injury. *Circulation.* 2001;103:284-289.
14. Fujio Y, Nguyen T, Wencker D, et al. Akt promotes survival of cardiomyocytes in vitro and protects against ischemia-reperfusion injury in mouse heart. *Circulation.* 2000;101:660-667.
15. Kureishi Y, Luo Z, Shiojima I, et al. The HMG-CoA reductase inhibitor simvastatin activates the protein kinase Akt and promotes angiogenesis in normocholesterolemic animals. *Nat Med.* 2000;6:1004-1010.
16. Weiss RH, Ramirez A, Joo A. Short-term pravastatin mediates growth inhibition and apoptosis, independently of Ras, via the signaling proteins p27Kip1 and p13 kinase. *J Am Soc Nephrol.* 1999;10:1880-1890.
17. Hoffmann R, Mintz GS, Dussaillant GR, et al. Patterns and mechanisms of in-stent restenosis: a serial intravascular ultrasound study. *Circulation.* 1996;94:1247-1254.

## Atherosclerosis and Lipoproteins

### Troglitazone Inhibits Formation of Early Atherosclerotic Lesions in Diabetic and Nondiabetic Low Density Lipoprotein Receptor-Deficient Mice

Alan R. Collins, Woerner P. Meehan, Ulrich Kintscher, Simon Jackson, Shu Wakino, Grace Noh, Wulf Palinski, Willa A. Hsueh, Ronald E. Law

**Abstract**—Peroxisome proliferator-activated receptor- $\gamma$  (PPAR $\gamma$ ) is a ligand-activated nuclear receptor expressed in all of the major cell types found in atherosclerotic lesions: monocytes/macrophages, endothelial cells, and smooth muscle cells. In vitro, PPAR $\gamma$  ligands inhibit cell proliferation and migration, 2 processes critical for vascular lesion formation. In contrast to these putative antiatherogenic activities, PPAR $\gamma$  has been shown in vitro to upregulate the CD36 scavenger receptor, which could promote foam cell formation. Thus, it is unclear what impact PPAR $\gamma$  activation will have on the development and progression of atherosclerosis. This issue is important because thiazolidinediones, which are ligands for PPAR $\gamma$ , have recently been approved for the treatment of type 2 diabetes, a state of accelerated atherosclerosis. We report herein that the PPAR $\gamma$  ligand, troglitazone, inhibited lesion formation in male low density lipoprotein receptor-deficient mice fed either a high-fat diet, which also induces type 2 diabetes, or a high-fructose diet. Troglitazone decreased the accumulation of macrophages in intimal xanthomas, consistent with our in vitro observation that troglitazone and another thiazolidinedione, rosiglitazone, inhibited monocyte chemoattractant protein-1-directed transendothelial migration of monocytes. Although troglitazone had some beneficial effects on metabolic risk factors (in particular, a reduction of insulin levels in the diabetic model), none of the systemic cardiovascular risk factors was consistently improved in either model. These observations suggest that the inhibition of early atherosclerotic lesion formation by troglitazone may result, at least in part, from direct effects of PPAR $\gamma$  activation in the artery wall. (*Arterioscler Thromb Vasc Biol.* 2001;21:365-371.)

**Key Words:** atherosclerosis ■ diabetes mellitus ■ pharmacology

Peroxisome proliferator-activated receptor- $\gamma$  (PPAR $\gamma$ ), a nuclear receptor, is expressed in all major cell types participating in vascular injury: endothelial cells (ECs), macrophages, and vascular smooth muscle cells (VSMCs).<sup>1-6</sup> Activation of this receptor in vitro inhibits inflammatory processes, including cytokine production and expression of NO synthase.<sup>2</sup> In early clinical investigations, ligands of PPAR $\gamma$ , such as thiazolidinediones (TZDs), have also been reported to improve endothelium-dependent vasodilation, suggesting that PPAR $\gamma$  activation enhances NO production and protects against vascular injury.<sup>7,8</sup> Activation of PPAR $\gamma$  also inhibits 2 other processes critical for vascular lesion formation, cell proliferation, and migration.<sup>3,5,6,9,10</sup> In vivo, 2 TZDs, troglitazone (TRO) and pioglitazone, significantly reduced arterial neointimal hyperplasia after endothelial injury in rats.<sup>11-13</sup> In such balloon-catheterized arteries, neointima formation essentially reflects increased migration and proliferation of VSMCs, a major contributor to the growth of

See page 295

atherosclerotic lesions. TRO also inhibited neointima formation in stents placed in the coronary arteries of patients with type 2 diabetes.<sup>14</sup>

We and others have recently demonstrated that PPAR $\gamma$  activation by TZDs and 15-deoxy- $\Delta^{12,14}$ -prostaglandin J<sub>2</sub> inhibits EC expression of vascular cell adhesion molecule-1, which mediates monocyte adherence to the endothelial surface.<sup>4,15</sup> Because inflammation, dysregulated growth, and migration of monocytes and VSMCs play an important role in the development of atherosclerosis, we hypothesized that PPAR $\gamma$  activation in cells of the vasculature would inhibit the atherosclerotic process. On the other hand, TZDs also stimulate conversion of macrophages into foam cells; therefore, ligand-dependent activation of PPAR $\gamma$  has been postulated to promote atherosclerosis.<sup>16</sup>

Received August 10, 2000; revision accepted December 1, 2000.

From the Division of Endocrinology, Diabetes, and Hypertension (A.R.C., W.P.M., U.K., S.J., S.W., G.N., W.A.H., R.E.L.), Department of Medicine, UCLA School of Medicine, Los Angeles, Calif; the Molecular Biology Institute (W.A.H., R.E.L.), Los Angeles, Calif; the Department of Medicine/Cardiology (U.K.), Virchow-Klinikum, Humboldt University, and the German Heart Institute (U.K.), Berlin, Germany; and the Department of Medicine (W.P.), UCSD, La Jolla, Calif.

Correspondence to Ronald E. Law, PhD, University of California, Los Angeles, Division of Endocrinology, Diabetes, and Hypertension, 900 Veteran Ave, Suite 24-130, Box 957073, Los Angeles, CA 90095. E-mail rlaw@mednet.ucla.edu

© 2001 American Heart Association, Inc.

*Arterioscler Thromb Vasc Biol.* is available at <http://www.atvbaha.org>

The impact of TZDs on atherosclerosis is a critical issue. TZDs improve insulin-mediated glucose uptake and are used extensively in the treatment of insulin resistance and type 2 diabetes mellitus.<sup>17</sup> Coronary artery disease mortality is increased 2- to 4-fold in type 2 diabetes.<sup>18</sup> Atherosclerosis is the major cause of demise in people with diabetes; therefore, it is important to determine the action of any antidiabetic drug on the atherosclerotic process.

To determine whether PPAR $\gamma$  activation has proatherogenic or antiatherogenic effects, we administered TRO to male LDL receptor-deficient (LDLR<sup>-/-</sup>) mice fed either a high-fat or a high-fructose atherogenic diet. Both models develop substantial hypercholesterolemia and macrophage-laden lesions, designated intimal xanthomata, which do not normally progress to mature atherosclerotic plaques.<sup>19</sup> In addition, the high-fat diet induces hyperglycemia and hyperinsulinemia in the LDLR<sup>-/-</sup> mouse, making it also a model of type 2 diabetes.<sup>20,21</sup> In contrast, fructose does not increase glucose or insulin in this model<sup>21</sup> and, therefore, was useful because the effects of TZDs on atherosclerosis could be studied in the absence of improvements in insulin action.

## Methods

### Transendothelial Monocyte Migration

THP-1 cells ( $5 \times 10^4$ ), a human monocytic leukemia cell line, were added to a human aortic EC monolayer covering a gelatin-coated 8- $\mu$ m porous membrane and incubated for 30 minutes at 37°C to facilitate their attachment. Cells were then pretreated with the indicated ligands or vehicle (dimethyl sulfoxide) for 30 minutes at 37°C. Migration was induced by the addition of monocyte chemoattractant protein-1 (MCP-1, 50 ng/mL) to the lower compartment. After 90 minutes, nonmigrating THP-1 cells and human aortic ECs were removed with a cotton tip, and the membranes were fixed and stained with the Quik-Diff Stain Set (DADE, Miami, Fla) to identify migrated cells. The number of migrated cells was determined per  $\times 320$  high-power field. Experiments were performed in duplicate and were repeated at least 3 times.

### Western Blots

Western immunoblots were performed as previously described.<sup>10</sup> Membranes were incubated with rabbit polyclonal antibodies (1:1000 dilution, New England Biolabs) that recognize either (1) total extracellular signal-regulated kinase (ERK) or (2) ERK phosphorylated on threonine 202 and tyrosine 204.

### Animals and Diets

Male LDLR<sup>-/-</sup> mice were obtained (C57BL/6J-Ldlr<sup>tm1J</sup>, stock No. 002207, Jackson Laboratory, Bar Harbor, Me) and were group-housed under a 12-hour light and 12-hour dark regimen. All animal protocols were approved by the UCLA Animal Research Committee and complied with all federal, state, and institutional regulations. At 3 months of age, the mice were randomly assigned to 1 of 5 dietary regimens: (1) chow (Harlan Teklad 8604), (2) high-fat complex carbohydrate (Research Diets), (3) high-fat complex carbohydrate with 4 g TRO/kg of food, (4) high fructose (Research Diets), or (5) high fructose with 4 g TRO/kg of food. The high-fat diet consisted of 21% fat, 20% protein, 50% carbohydrate, and 0.15% cholesterol. Our high-fat diet differed from those commonly used to study atherogenesis in LDLR<sup>-/-</sup> mice in that the majority of the nonfat energy came from complex carbohydrate sources instead of sucrose. The high-fructose diet contained 4% fat, 16% protein, 71% fructose, and 0.15% cholesterol. Sources of fat in the diets were corn oil (1% in all diets) and anhydrous milk fat (3% in the fructose diets and 20% in the high fat diets). Mice and feed were weighed weekly, and the rate of consumption of drug was computed. The mice were fed for a period of 12 weeks.

### Metabolic Measurements

Blood samples from the retro-orbital sinus were obtained from the mice before the beginning of treatment and every month thereafter and from the abdominal vena cava at euthanasia. Mice were fasted overnight before the collection of the blood samples. Plasma glucose was measured by glucose oxidase reaction (Beckman Glucose Analyzer 2, Beckman Instruments). Plasma lipids were measured by the UCLA Lipid Analysis Laboratory. Plasma insulin was determined by ELISA. Blood pressures were obtained by using an indirect tail-cuff method with a controlled temperature chamber (IITC, Inc) by a technician blinded to the treatment groups.

### Vessel Preparation and Image Analysis

Mice were euthanized and perfused with 7.5% sucrose in 4% paraformaldehyde. Aortas were dissected out, split longitudinally, pinned flat in a dissection pan, and stained with Sudan IV to detect lipids and determine lesion area. Images were captured by use of a Sony 3-CCD video camera and analyzed by a single technician who was blinded to the study protocol and used ImagePro image analysis software. The extent of lesion formation is expressed as the percentage of the total aortic surface area covered by lesions.

### Cross Sections: Determination of Intimal Macrophage Content

The largest lesions from the aortic arch were excised and embedded in paraffin. The avidin-biotin-peroxidase complex technique for immunostaining was used. Macrophages were stained by using monoclonal antibody to CD68 (titer 1:100, KP1 clone, M0814, Dako Corp). Nonimmune serum was used as a control. Primary antibody incubations were performed in 1% BSA/2% goat serum containing PBS for 60 minutes. Biotinylated rabbit anti-mouse (Dako) was applied; incubation with a streptavidin-peroxidase complex followed. Peroxidase activity was detected with the use of diaminobenzidine tetrahydrochloride as a chromogen. Slides were then counterstained with hematoxylin. Images of the stained sections were analyzed by using the software described above. After tracing the intimal area to be measured with a cursor, 5 pixels of color, which defined the anti-CD68 stain, were sampled by the operator. The area encompassed by the pixels, which was not contiguous, in the color range for anti-CD68 was then computed automatically by the software. This approach has been successfully used by Shi et al<sup>22</sup> to quantify lesional macrophages in a mouse model of transplant arteriosclerosis.

### Statistical Analysis

Statistical analysis was performed by using 2-factorial ANOVA with Student-Newman-Keuls to determine the differences between individual group means.

## Results

### TRO Inhibits Monocyte Migration

VSMC migration and proliferation play an important atherogenic role in the progression of fatty streaks toward more advanced atherosclerotic lesions, such as transitional lesions and classical atheromas. We have previously shown that PPAR $\gamma$  ligands inhibit ERK mitogen-activated protein kinase (MAPK)-dependent migration of VSMCs.<sup>10,11</sup> However, in the earliest stages of atherosclerotic lesions, recruitment of adherent monocytes through their migration into the subendothelium and their phenotypic transformation to macrophages and foam cells play a far greater role than VSMCs in humans and in murine models.<sup>23</sup>

To investigate whether TRO-mediated PPAR $\gamma$  activation affects monocyte recruitment and to further explore its mechanism, we carried out a series of *in vitro* experiments before our *in vivo* studies. MCP-1 is an important *in vivo* migration factor promoting the subendothelial accumulation of monocytes. TRO inhibited MCP-1-directed transmigration



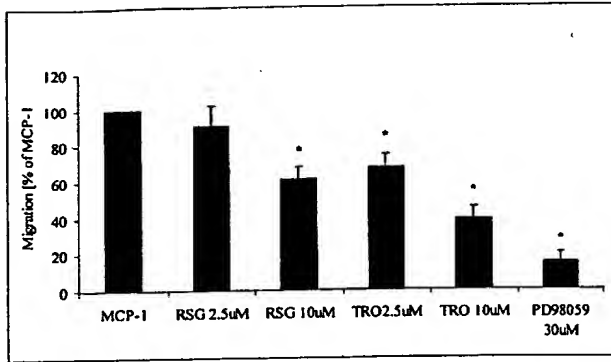


**Figure 1.** PPAR $\gamma$  ligands inhibit MCP-1-directed transendothelial migration of monocytes. Migration of THP-1 monocytes through ECs was determined by using a modified Boyden chamber assay as described in Methods. The number of migrating cells was quantified by microscopy with the use of high-power fields. Results represent 3 independent experiments performed in duplicate. \* $P < 0.05$  vs MCP-1 alone.

tion of THP-1 monocytes by  $32.7 \pm 6.5\%$  at  $2.5 \mu\text{mol/L}$  and by  $61.4 \pm 6.7\%$  at  $10 \mu\text{mol/L}$  (Figure 1). TRO contains a vitamin E moiety that may confer an antioxidant activity that can inhibit monocyte recruitment and endothelial expression of adhesion molecules. However, rosiglitazone (RSG), another PPAR $\gamma$  ligand that lacks antioxidant activity, also inhibited monocyte transmigration, albeit with a lesser potency than TRO (Figure 1). Inhibition of monocyte transmigration by TRO, therefore, is likely to be mediated at least in part through PPAR $\gamma$ .

MCP-1 rapidly induced ERK activation, reaching a peak at 5 minutes, which was blocked by PD98059, an inhibitor of MAPK ERK kinase (MEK, an upstream kinase), which phosphorylates and activates ERK (Figure 2). PD98059 attenuated MCP-1-directed transmigration by  $84.8 \pm 4.8\%$ . In combination, these data suggest that activation of PPAR $\gamma$  in monocytes may inhibit their migration by interfering with ERK-MAPK signaling, although the precise mechanism remains to be determined.

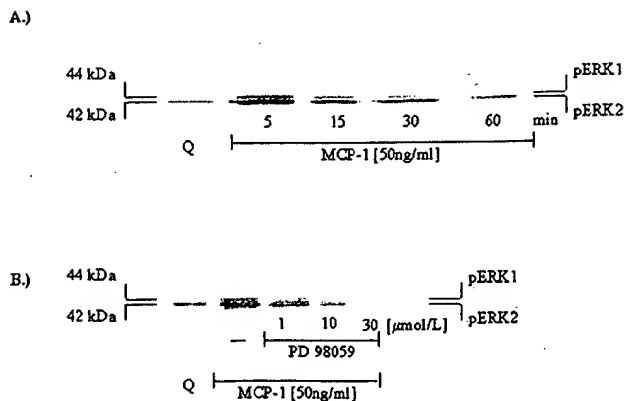


**Figure 2.** MCP-1 activates the ERK-MAPK pathway in THP-1 human monocytes. A, Quiescent (Q) THP-1 cells were stimulated with MCP-1 (50 ng/mL) for 5 minutes. Whole-cell protein extracts were immunoblotted with a phosphospecific ERK1 (pERK1)/ERK2 (pERK2) MAPK antibody. A representative blot of 3 different experiments is shown. B, Conditions were the same as in panel A except that cells were treated with MEK inhibitor PD98059 (1 to  $30 \mu\text{mol/L}$ ) or vehicle (dimethyl sulfoxide, -) before and during stimulation with MCP-1 (50 ng/mL). A representative blot of 3 different experiments is shown.

### TRO Inhibits Intimal Macrophage Accumulation and Lesion Formation in Male LDLR $^{-/-}$ Mice

LDLR $^{-/-}$  mice that were fed a regular chow diet develop few lesions across the surface of the aorta. Male 3-month-old LDLR $^{-/-}$  mice were placed on either a high-fat or high-fructose diet to induce atherosclerosis. LDLR $^{-/-}$  males were used in the present study because they develop hyperglycemia and become diabetic on a high-fat diet but remain normoglycemic when fed a high-fructose diet. Moreover, males develop twice the level of surface lesions as do females,<sup>24</sup> and their use obviates the potentially confounding influence of the vascular protection in females afforded by estrogen. Comparison of the impact of TRO on atherogenesis in these 2 dietary models was undertaken to distinguish any activity of PPAR $\gamma$  to normalize metabolic abnormalities accompanying diabetes that contribute to high-fat-induced xanthomata formation from any direct effects on the vasculature. To assess the impact of TRO on aortic lesions, 1 high-fat diet group and 1 high-fructose diet group received TRO at 400 mg/kg body wt per day from drugs pelleted into the atherogenic diets. This dose of TRO was chosen because we previously demonstrated its efficacy in inhibiting intimal hyperplasia in rats after balloon injury.<sup>11</sup>

The en face method, which makes use of computer-assisted analysis of color images of Sudan IV-stained lipid-containing material in the entire aorta, was used to determine the percentage of surface area affected by lesions.<sup>24</sup> Male LDLR $^{-/-}$  mice on normal chow for 3 months had  $<0.20\%$  lesions (Figure 3A). The high-fat diet increased the amount of surface lesions after 3 months to  $3.90 \pm 0.16\%$  ( $n=8$ , Figure 3B). TRO inhibited the high-fat-induced lesions by 30% ( $2.76 \pm 0.36\%$  of the aortic surface,  $n=8$ ,  $P < 0.02$ ; Figure 3C). Similar to Merat et al,<sup>21</sup> we noted that the high-fructose diet was more atherogenic than the high-fat diet, causing  $8.42 \pm 0.94\%$  lesions ( $n=17$ , Figure 3D). TRO reduced lesions in fructose-fed LDLR $^{-/-}$  males by 42% ( $4.90 \pm 0.65\%$ ,  $n=14$ ,  $P < 0.01$ ; Figure 3E). Quantitative results are summarized in Figure 4.

TRO-treated male LDLR $^{-/-}$  mice fed either the high-fat or high-fructose diet for 3 months developed lesions that contained substantially fewer CD68-staining macrophages (Figure 5A through 5D). Lesions induced by a high-fat diet contained  $39.1 \pm 6.8\%$  macrophages (percent of cross-sectional intimal area) compared with  $13.3 \pm 4.9\%$  ( $P < 0.01$ ) in mice administered TRO (Figure 5E). Similar results were obtained for males fed the high-fructose diet, where TRO decreased macrophage accumulation from  $40.4 \pm 3.5\%$  to  $17.1 \pm 1.7\%$  ( $P < 0.01$ , Figure 5E). The lesions in the TRO-fed animals tended to be smaller in volume than those in males not fed TRO. The relative macrophage content in the larger lesions (not treated with TRO) exceeded the content in the smaller lesions (treated with TRO) by 140% to 200%. The reduction in macrophage accumulation in the lesions of TRO-treated animals is unlikely to be the result of their being an earlier lesion stage, because the relative macrophage content is known to be greatest in the smaller (ie, early-stage) lesions.

### Effect of TRO on Metabolic Parameters

All metabolic measurements determined on blood samples drawn before treatment were similar in all groups (Tables 1



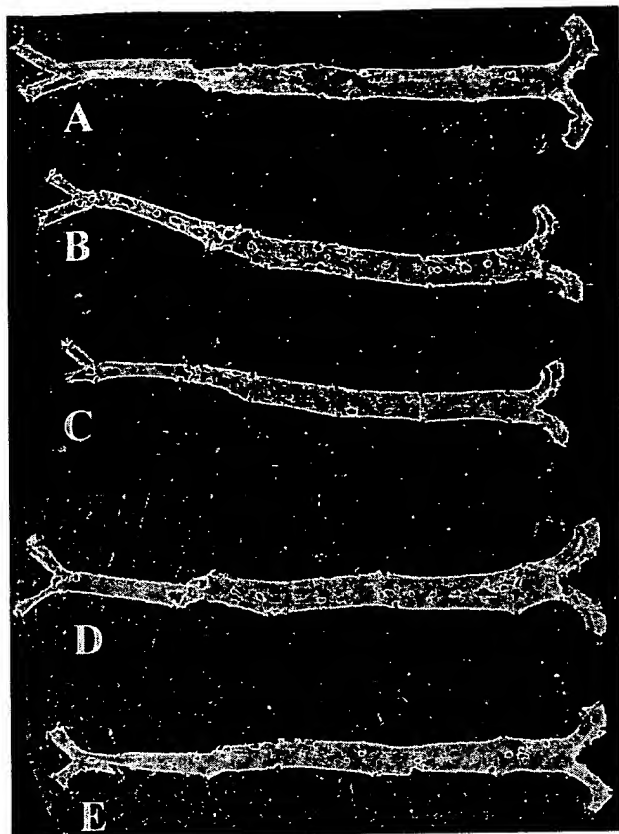


**Figure 3.** TRO attenuates atherosclerosis in male  $LDLR^{-/-}$  mice. The aorta is stained by Sudan IV to detect the lipids present in lesions. A, Chow diet. B, High-fat diet. C, High-fat diet and TRO. D, High-fructose diet. E, High-fructose diet and TRO.

and 2). In accordance with previous studies on male  $LDLR^{-/-}$  mice, we found that a high-fat diet induced diabetes<sup>20,21</sup> (Table 1). Glucose levels progressively increased throughout

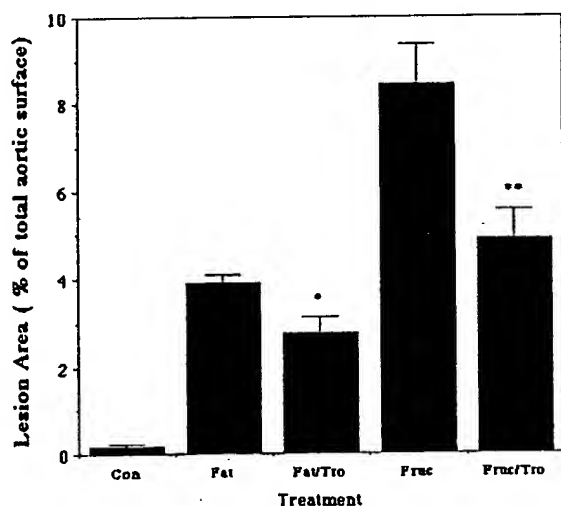


**Figure 4.** Quantification of the antiatherogenic activity of TRO in male  $LDLR^{-/-}$  mice. Mean atherosclerotic surface lesion areas were determined in mice fed a normal chow, high-fat, or high-fructose diet in the absence or presence of TRO for 3 months. Image analysis and quantification of the percentage of the total aortic area staining for Sudan IV were performed by using computer-assisted image analysis. TRO produced a significant decrease in mice fed a high-fat (30% decrease,  $*P<0.05$ ) and high-fructose (42% decrease,  $**P<0.05$ ) diet.

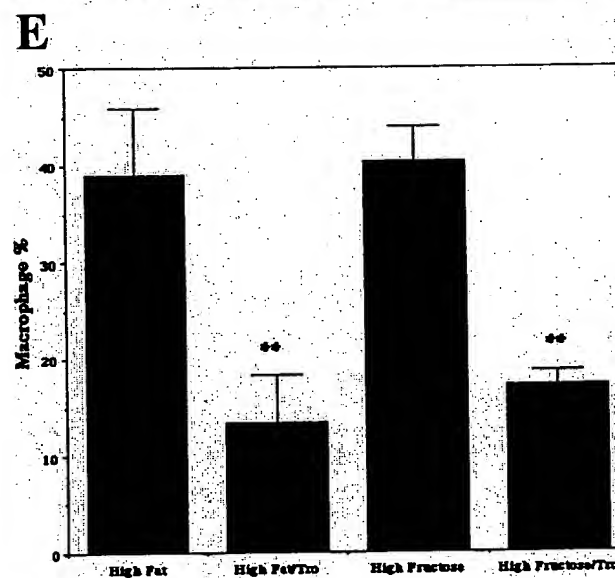
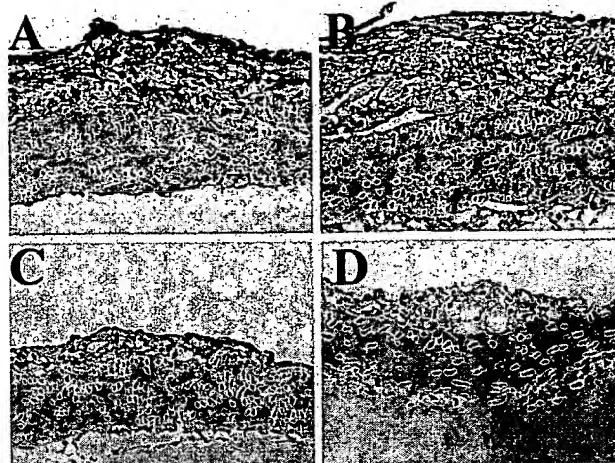


**Figure 5.** TRO inhibits accumulation of lesional macrophages. Sections from the aortic arch were immunostained by using antibody against CD68 to detect macrophages. Quantification of the percentage of the intimal area staining ( $**P<0.05$ ) for CD68 was performed by computer-assisted image analysis. A, High-fat diet ( $n=6$ ). B, High-fat diet and TRO ( $n=6$ ). C, High-fructose diet ( $n=6$ ). D, High-fructose diet and TRO ( $n=6$ ). E, Quantification of the macrophage content.

the study, reaching a maximum of 285 mg/dL at 3 months compared with 148 mg/dL for mice on normal chow. The fat-fed males were also hyperinsulinemic ( $1198 \pm 149$  versus  $664 \pm 113$  pg/mL on normal chow), consistent with the development of early-stage type II diabetes. Although TRO did not decrease hyperglycemia in high-fat-fed male mice, TRO administration completely normalized their plasma insulin levels. In marked contrast, mice on a high-fructose diet had normal fasting plasma glucose and insulin levels, which were not altered by TRO.

$LDLR^{-/-}$  males developed severe hypercholesterolemia on either the high-fat or high-fructose diet, achieving levels 3- to 4-fold greater than those in animals maintained on regular chow (Table 2). TRO lowered total plasma cholesterol by 27% in males on the high-fructose diet but had no effect on the high-fat-fed mice. Triglycerides were elevated in the high-fat-fed males but not in the high-fructose group; TRO

TABLE 1. Plasma Glucose and Insulin Levels and Final Body Weights

	Chow Diet	High-Fat Diet	High-Fat Diet/TRO	High-Fructose Diet	High-Fructose Diet/TRO
Glucose, mg/dL					
Start	158.7±14.63	173.2±12.12	169.4±7.98	137.8±11.53	148.5±27.67
1 mo	148.9±6.60	190.5±10.92	155.1±9.13*	121.2±6.44	114.8±4.55
2 mo	144.8±10.96	201.1±9.09	189.6±27.37	128.6±13.09	121.89±17.32
3 mo	148.5±14.87	284.8±25.00	268.9±13.90	152.3±15.80	181.9±23.47
Insulin, pg/mL					
3 mo	664.7±113.62	1198.7±149.81	691.2±109.14†	304.4±47.49	278.7±37.9
Body weight, g					
	27.3±0.56	42.5±0.66	37.0±0.89†	25.9±0.37	24.2±0.34

Values are mean±SEM.

\* $P<0.05$  vs high-fat; † $P<0.01$  vs high-fat diet.

did not alter triglycerides in either model. HDL cholesterol (HDL) decreased with both of the diets, compared with normal chow, as frequently reported.<sup>3</sup> TRO further lowered the HDL in the high-fat-fed males but increased it in the high-fructose-fed group. Plasma free fatty acid levels increased in males on the high-fat diet but not in those on the high-fructose diet; TRO decreased free fatty acid levels in both models.

### Discussion

The most significant finding of the present study is that TRO inhibited lesion formation in a type 2 diabetic mouse model and a nondiabetic LDLR<sup>-/-</sup> mouse model of intimal xanthomata. Mice fed the high-fat diet developed extensive hypercholesterolemia that was not affected by TRO. These mice also gained substantial weight and showed an

increase in circulating free fatty acid levels, which probably contributed to their insulin resistance, hyperinsulinemia, and fasting hyperglycemia.<sup>25</sup> The increase in triglycerides and decrease in HDL are consistent with insulin resistance. TRO decreased circulating insulin but did not affect glucose in this model. The same has been reported in humans with type 2 diabetes, of whom 20% treated with TRO showed no improvement in glucose control, but all demonstrated improved insulin sensitivity.<sup>26</sup> In contrast to the response in humans, TRO did not alter triglycerides and further decreased HDL. Mice fed the high-fructose diet also developed severe hypercholesterolemia but did not gain weight or develop hyperinsulinemia or elevations in free fatty acids or triglycerides. In this model, TRO decreased the free fatty acids, increased HDL, and decreased total cholesterol.

TABLE 2. Plasma Lipid Levels

	Chow Diet	High-Fat Diet	High-Fat Diet/TRO	High-Fructose Diet	High-Fructose Diet/TRO
Total Cholesterol, mg/dL					
Start	292.2±14.63	277.7±5.77	278.8±9.24	321.8±20.87	328.0±18.32
1 mo	316.0±11.51	583.3±72.18	541.9±62.22	489.1±24.58	360.8±21.37†
2 mo	315.8±10.26	1307.0±110.11	1173.0±122.11	1052.3±33.78	816.7±25.02‡
3 mo/final	317.9±17.79	1341.9±52.14	1313.63±28.83	1167.7±46.17	862.1±23.70‡
HDL, mg/dL					
Start	110.6±4.51	111.2±1.87	109.9±3.07	121.2±2.59	113.5±8.39
1 mo	111.2±3.19	108.2±1.93	108.9±2.65	104.2±3.08	106.6±4.58
2 mo	112.1±4.06	94.4±3.52	98.2±12.66	100.4±3.56	105.3±4.76
3 mo	112.4±5.00	104.8±7.84	81.8±6.86*	90.1±4.48	108.4±5.10†
Free fatty acids, mg/dL					
Start	67.1±2.82	63.5±1.82	58.2±2.67	91.0±6.96	82.5±4.38
1 mo	69.4±2.97	70.4±2.11	66.6±2.67	66.9±4.90	71.2±3.75
2 mo	65.7±2.87	88.6±7.32	74.2±4.19	68.7±3.67	65.8±3.57
3 mo	61.7±3.68	72.5±2.42	57.1±2.07*	61.7±1.52	53.1±2.81†
Triglycerides, mg/dL					
Start	122.0±4.43	109.1±5.32	101.1±5.72	84.8±5.09	111.83±16.00
1 mo	126.0±11.1	124.3±7.00	113.6±7.48	85.8±4.98	94.0±6.47
2 mo	86.9±4.98	156.6±30.55	191.8±64.47	81.2±5.98	79.8±6.47
3 mo	71.6±6.92	141.8±7.84	159.1±19.79	75.3±6.89	69.0±4.85

Values are mean±SEM.

\* $P<0.01$  vs high-fat diet; † $P<0.05$  vs high-fructose diet, and ‡ $P<0.001$  vs high-fructose diet.

Despite the difference in metabolic responses between the diabetic and nondiabetic animals, both hypercholesterolemic models responded to TRO with decreased lesion formation. These results suggest that TRO has direct vascular effects, separate from its metabolic effects, that decrease the atherosclerotic process. Alternatively, the antiatherogenic effects of TRO in the 2 different models might involve the collection of distinct metabolic processes. For example, hemodynamic effects of TRO related to its reported activity to lower blood pressure in animal models and in humans could also impact pathophysiological processes in high-fat- and high-fructose-fed LDLR<sup>-/-</sup> mice.<sup>27-30</sup> All major cell types contributing to this vascular lesion formation express PPAR $\gamma$ , which provides a mechanism for the direct effect of thiazolidinedione ligands in the vessel wall.<sup>3,5,6,9</sup> Data from *in vitro* experiments had suggested mechanisms by which activation of PPAR $\gamma$  could either accelerate or attenuate the atherosclerotic process.<sup>2-6,9,10,16</sup> The present study provides conclusive evidence that ligand-induced PPAR $\gamma$  activation by TRO reduces intimal xanthomata in murine models.

TRO had several systemic effects that may have contributed to its attenuation of intimal xanthomata. In the diabetic high-fat-fed mouse, TRO lowered insulin and glucose levels and decreased HDLC (which is thought to promote atherogenesis). In the fructose-fed model, TRO decreased total cholesterol and increased HDLC. Our finding that TRO was more potent in suppressing lesion formation in the fructose-fed model compared with the high-fat-fed mice could be due to the observed 27% reduction in total cholesterol. A common effect of TRO in the high-fat-fed and high-fructose-fed LDLR<sup>-/-</sup> models is its suppression of circulating free fatty acid levels. However, increased circulating free fatty acids have not been shown to be an independent risk factor for atherosclerosis.

Inflammation in the vascular wall has clearly emerged as a major culprit in the development of atherosclerosis.<sup>31</sup> Damage to the endothelium and the subsequent recruitment and transendothelial migration of monocytes constitute critical early cellular responses during atherogenesis.<sup>31</sup> Transmigration of monocytes into the subendothelial space is strongly stimulated by the chemokine MCP-1, which is expressed and secreted by ECs and VSMCs. The essential role of MCP-1 in atherogenesis is underscored by a recent study demonstrating that crossing MCP-1-deficient mice into LDLR<sup>-/-</sup> mice attenuated lesion formation by >80%.<sup>32</sup> Our group and others have shown that TRO and other PPAR $\gamma$  ligands inhibit growth factor-directed ERK-MAPK-dependent VSMC migration.<sup>5,10,11</sup> Cell migration requires *de novo* gene transcription that is consistent with PPAR $\gamma$  acting in the nucleus to inhibit this process.<sup>10</sup> In particular, activation of PPAR $\gamma$  can inhibit ERK-MAPK signaling to the nucleus.<sup>11,33</sup> Because MCP-1-directed migration of monocytes is ERK-MAPK dependent, interference with this pathway by TRO could contribute to the observed reduction in intimal xanthomata and lesional macrophages in treated LDLR<sup>-/-</sup> mice.

TRO and another PPAR $\gamma$  ligand, RSG, which does not contain an  $\alpha$ -tocopherol moiety, inhibited MCP-1-directed migration of human monocytes *in vitro*. TRO also consistently decreased intimal macrophage accumulation in the diabetic and nondiabetic mice. These findings support the concept that inhibition of monocyte attachment and migration

in the vessel by TRO may be one of the mechanisms contributing to the reduction of atherogenesis. Although it cannot be ruled out that the reduction of intimal monocytes in part reflected the reduced lesion size induced by TRO treatment, this is unlikely to be the sole explanation, because the relative intimal monocyte/macrophage content is known to be greatest in the early stages (smaller lesions) of atherosclerosis. In any case, the antiatherosclerotic activity of TRO-induced PPAR $\gamma$  activation clearly prevailed over its hypothesized promotion of foam cell formation via increased expression of the scavenger receptor CD36.<sup>16</sup>

Unlike other PPAR $\gamma$  ligands, TRO has an  $\alpha$ -tocopherol (vitamin E) moiety that theoretically could contribute to its antiatherogenic activity through antioxidant effects.<sup>34</sup> Vitamin E has been shown to suppress atherosclerosis in the apoE knockout model, which develops advanced atherosclerotic lesions.<sup>35,36</sup> Whether the dose of vitamin E provided by TRO in the present study is enough to impact lesion formation is doubtful. At 400 mg/kg TRO per day, LDLR<sup>-/-</sup> mice received the equivalent of 8 IU of vitamin E, a dose much lower than that reported to affect atherosclerosis or to significantly protect LDL against oxidation.<sup>35-38</sup> Another line of evidence for the assumption that the effect of TRO on lesion formation was not, to a significant degree, dependent on antioxidant effects is provided by a parallel study demonstrating that 2 other PPAR $\gamma$  ligands, RSG and GW7845, which do not contain the  $\alpha$ -tocopherol moiety, inhibited atherogenesis in the aortic root of male LDLR<sup>-/-</sup> mice fed a high-fat, cholesterol-enriched diet.<sup>39</sup> In addition, the recent Heart Outcomes Prevention Evaluation (HOPE) clinical trial in humans did not show an effect of vitamin E on coronary artery disease events or mortality.<sup>40</sup>

In summary, given the absence of consistent major metabolic changes present in diabetic and nondiabetic mice, it is likely that TRO at least in part decreases early atherosclerotic lesion formation through direct vascular effects. In human subjects with diabetes, who have a high risk for coronary disease, TRO improves insulin resistance and other proatherogenic metabolic parameters, which may improve cardiovascular risk. It is possible that some of the vascular effects observed in our murine models may also be present in humans. Although Li et al<sup>39</sup> and our data demonstrate that PPAR $\gamma$  ligands suppress early atherosclerotic lesions, intimal xanthomata do not inexorably progress to more advanced atherosclerotic plaques; in fact, they often regress.<sup>19</sup> Therefore, determining the effects of PPAR $\gamma$  ligands on more advanced atherosclerotic lesions may prove to be a stronger predictor of their potential clinical benefit. Nonetheless, the present results indicate that an investigation of potential antiatherogenic effects of PPAR $\gamma$  ligands is strongly warranted.

### Acknowledgments

This work was supported by National Institutes of Health grant HL-58328 to Willa A. Hsueh. Shu Wakino was supported by a Mary K. Iacocca Fellowship in Diabetes. Ulrich Kintscher was supported by a Gonda (Goldschneid) Fellowship in Diabetes.

### References

1. Ricote M, Huang J, Fajas L, Li A, Welch J, Najib J, Witztum JL, Auwerx J, Palinski W, Glass CK. Expression of the peroxisome proliferator-activated receptor gamma (PPARgamma) in human atherosclerosis and

- regulation in macrophages by colony stimulating factors and oxidized low density lipoprotein. *Proc Natl Acad Sci U S A*. 1998;95:7614-7619.
2. Ricote M, Li AC, Willson TM, Kelly CJ, Glass CK. The peroxisome proliferator-activated receptor- $\gamma$  is a negative regulator of macrophage activation. *Nature*. 1998;391:79-82.
  3. Xin X, Yang S, Kowalski J, Gerritsen ME. Peroxisome proliferator-activated receptor  $\gamma$  ligands are potent inhibitors of angiogenesis in vitro and in vivo. *J Biol Chem*. 1999;274:9116-9121.
  4. Jackson SM, Parhami F, Xi XP, Berliner JA, Hsueh WA, Law RE, Demer LL. Peroxisome proliferator-activated receptor activators target human endothelial cells to inhibit leukocyte-endothelial cell interaction. *Arterioscler Thromb Vasc Biol*. 1999;19:2094-2104.
  5. Marx N, Schonbeck U, Lazar MA, Libby P, Plutzky J. Peroxisome proliferator-activated receptor  $\gamma$  activators inhibit gene expression and migration in human vascular smooth muscle cells. *Circ Res*. 1998;83:1097-1103.
  6. Law RE, Goetze S, Xi XP, Jackson S, Kawano Y, Demer L, Fishbein MC, Meehan WP, Hsueh WA. Expression and function of PPAR $\gamma$  in rat and human vascular smooth muscle cells. *Circulation*. 2000;101:1311-1318.
  7. Tack CJ, Ong MK, Lutterman JA, Smits P. Insulin-induced vasodilatation and endothelial function in obesity/insulin resistance: effects of troglitazone. *Diabetologia*. 1998;41:569-576.
  8. Murakami T, Mizuno S, Ohsato K, Moriuchi I, Arai Y, Nio Y, Kaku B, Takahashi Y, Ohnaka M. Effects of troglitazone on frequency of coronary vasospastic-induced angina pectoris in patients with diabetes mellitus. *Am J Cardiol*. 1999;84:92-94. A8. Abstract.
  9. Tanaka T, Itoh H, Do KK, Fukunaga Y, Arai H, Hosoda K. Activation of PPAR $\gamma$  inhibits macrophage proliferation and migration: possible therapeutic effectiveness of thiazolidinediones on diabetic vascular complications. *Diabetes*. 1999;48(suppl 1):A30. Abstract.
  10. Goetze S, Xi XP, Kawano H, Gotlibowski T, Fleck E, Hsueh WA, Law RE. PPAR  $\gamma$ -ligands inhibit migration mediated by multiple chemoattractants in vascular smooth muscle cells. *J Cardiovasc Pharmacol*. 1999;33:798-806.
  11. Law RE, Meehan WP, Xi XP, Graf K, Wuthrich DA, Coats W, Faxon D, Hsueh WA. Troglitazone inhibits vascular smooth muscle cell growth and intimal hyperplasia. *J Clin Invest*. 1996;98:1897-1905.
  12. Igarashi M, Takeda Y, Ishibashi N, Takahashi K, Mori S, Tominaga M, Saito Y. Pioglitazone reduces smooth muscle cell density of rat carotid arterial intima induced by balloon catheterization. *Horm Metab Res*. 1997;29:444-449.
  13. Yoshimoto T, Naruse M, Shizume H, Naruse K, Tanabe A, Tanaka M, Tago K, Irie K, Muraki T, Demura H, et al. Vascular-protective effects of insulin sensitizing agent pioglitazone in neointimal thickening and hypertensive vascular hypertrophy. *Atherosclerosis*. 1999;145:333-340.
  14. Takagi T, Akasaka T, Yamamoto A, Honda Y, Hozumi T, Morioka S, Yoshida K. Troglitazone reduces neointimal tissue proliferation after coronary stent implantation in patients with non-insulin dependent diabetes mellitus: a serial intravascular ultrasound study. *J Am Coll Cardiol*. 2000;36:1529-1535.
  15. Pasceri V, Wu HD, Willerson JT, Yeh ET. Modulation of vascular inflammation in vitro and in vivo by peroxisome proliferator-activated receptor- $\gamma$  activators. *Circulation*. 2000;101:235-238.
  16. Tontonoz P, Nagy L, Alvarez JG, Thomazy VA, Evans RM. PPAR $\gamma$  promotes monocyte/macrophage differentiation and uptake of oxidized LDL. *Cell*. 1998;93:241-252.
  17. Saltiel AR, Olefsky JM. Thiazolidinediones in the treatment of insulin resistance and type II diabetes. *Diabetes*. 1996;45:1661-1669.
  18. Savage PJ. Cardiovascular complications of diabetes mellitus: what we know and what we need to know about their prevention. *Ann Intern Med*. 1996;124:123-126.
  19. Virmani R, Kolodgie FD, Burke AP, Farb A, Schwartz SM. Lessons from sudden coronary death: a comprehensive morphological classification scheme for atherosclerotic lesions. *Arterioscler Thromb Vasc Biol*. 2000;20:1262-1275.
  20. Towler DA, Bidder M, Latifi T, Coleman T, Semenkovich CF. Diet-induced diabetes activates an osteogenic gene regulatory program in the aortas of low density lipoprotein receptor-deficient mice. *J Biol Chem*. 1998;273:30427-30434.
  21. Merat S, Casanada F, Sutphin M, Palinski W, Reaven PD. Western-type diets induce insulin resistance and hyperinsulinemia in LDL receptor-deficient mice but do not increase aortic atherosclerosis compared with normoinsulinemic mice in which similar plasma cholesterol levels are achieved by a fructose-rich diet. *Arterioscler Thromb Vasc Biol*. 1999;19:1223-1230.
  22. Shi C, Lee WS, Russell ME, Zhang D, Fletcher DL, Newell JB, Haber E. Hypercholesterolemia exacerbates transplant arteriosclerosis via increased neointimal smooth muscle cell accumulation: studies in apolipoprotein E knockout mice. *Circulation*. 1997;96:2722-2728.
  23. Nakashima Y, Plump AS, Raines EW, Breslow JL, Ross R. ApoE-deficient mice develop lesions of all phases of atherosclerosis throughout the arterial tree. *Arterioscler Thromb*. 1994;14:133-140.
  24. Tangirala RK, Rubin EM, Palinski W. Quantitation of atherosclerosis in murine models: correlation between lesions in the aortic origin and in the entire aorta, and differences in the extent of lesions between sexes in LDL receptor-deficient and apolipoprotein E-deficient mice. *J Lipid Res*. 1995;36:2320-2328.
  25. Kelley DE, Goodpaster B, Wing RR, Simoneau JA. Skeletal muscle fatty acid metabolism in association with insulin resistance, obesity, and weight loss. *Am J Physiol*. 1999;277:E1130-E1141.
  26. Suter SL, Nolan JJ, Wallace P, Gumbiner B, Olefsky JM. Metabolic effects of new oral hypoglycemic agent CS-045 in NIDDM subjects. *Diabetes Care*. 1992;15:193-203.
  27. Fujiwara K, Hayashi K, Matsuda H, Kubota E, Honda M, Ozawa Y, Saruta T. Altered pressure-natriuresis in obese Zucker rats. *Hypertension*. 1999;33:1470-1475.
  28. Sung BH, Izzo JL Jr, Dandona P, Wilson MF. Vasodilatory effects of troglitazone improve blood pressure at rest and during mental stress in type 2 diabetes mellitus. *Hypertension*. 1999;34:83-88.
  29. Kawai T, Takei I, Oguma Y, Ohashi N, Tokui M, Oguchi S, Katsukawa F, Hirose H, Shimada A, Watanabe K, et al. Effects of troglitazone on fat distribution in the treatment of male type 2 diabetes. *Metabolism*. 1999;48:1102-1107.
  30. Chen S, Noguchi Y, Izumida T, Tatebe J, Katayama S. A comparison of the hypotensive and hypoglycaemic actions of an angiotensin converting enzyme inhibitor, an AT1a antagonist and troglitazone. *J Hypertens*. 1996;14:1325-1330.
  31. Ross R. Atherosclerosis is an inflammatory disease. *Am Heart J*. 1999;138:S419-S420.
  32. Gu L, Okada Y, Clinton SK, Gerard C, Sukhova GK, Libby P, Rollins BJ. Absence of monocyte chemoattractant protein-1 reduces atherosclerosis in low density lipoprotein receptor-deficient mice. *Mol Cell*. 1998;2:275-281.
  33. Goetze S, Xi XP, Graf K, Fleck E, Hsueh WA, Law RE. Troglitazone inhibits angiotensin II-induced extracellular signal-regulated kinase 1/2 nuclear translocation and activation in vascular smooth muscle cells. *FEBS Lett*. 1999;452:277-282.
  34. Inoue I, Katayama S, Takahashi K, Negishi K, Miyazaki T, Sonoda M, Komoda T. Troglitazone has a scavenging effect on reactive oxygen species. *Biochem Biophys Res Commun*. 1997;235:113-116.
  35. Shaish A, George J, Gilburd B, Keren P, Levkovitz H, Harats D. Dietary beta-carotene and alpha-tocopherol combination does not inhibit atherogenesis in an apoE-deficient mouse model. *Arterioscler Thromb Vasc Biol*. 1999;19:1470-1475.
  36. Pratico D, Tangirala RK, Rader DJ, Rokach J, FitzGerald GA. Vitamin E suppresses isoprostane generation in vivo and reduces atherosclerosis in apoE-deficient mice. *Nat Med*. 1998;4:1189-1192.
  37. Crawford RS, Kirk EA, Rosenfeld ME, LeBoeuf RC, Chait A. Dietary antioxidants inhibit development of fatty streak lesions in the LDL receptor-deficient mouse. *Arterioscler Thromb Vasc Biol*. 1998;18:1506-1513.
  38. Bird DA, Tangirala RK, Fruebis J, Steinberg D, Witztum JL, Palinski W. Effect of probucol on LDL oxidation and atherosclerosis in LDL receptor-deficient mice. *J Lipid Res*. 1998;39:1079-1090.
  39. Li AC, Brown KK, Silvestre MJ, Willson TM, Palinski W, Glass CK. Peroxisome proliferator-activated receptor  $\gamma$  ligands inhibit development of atherosclerosis in LDL receptor-deficient mice. *J Clin Invest*. 2000;106:523-531.
  40. Yusuf S, Dagenais G, Pogue J, Bosch J, Sleight P. Vitamin E supplementation and cardiovascular events in high-risk patients: the Heart Outcomes Prevention Evaluation Study Investigators. *N Engl J Med*. 2000;342:154-160.

## Vitamin E Reduces Progression of Atherosclerosis in Low-Density Lipoprotein Receptor-Deficient Mice With Established Vascular Lesions

Tillmann Cyrus, MD; Yuemang Yao, BSc; Joshua Rokach, PhD;  
Lina X. Tang, MD; Domenico Praticò, MD

**Background**—A growing body of evidence from animal studies supports the hypothesis that oxidative stress-mediated mechanisms play a central role in early atherogenesis. In contrast, clinical trials with antioxidant vitamins have not produced consistent results in humans with established atherosclerosis.

**Methods and Results**—Low-density lipoprotein receptor-deficient mice (LDLR KO) were fed a high-fat diet for 3 months to induce atheroma. At this time, 1 group of mice was euthanized for examination of atherosclerosis, and 2 other groups were randomized to receive high-fat diet either alone or supplemented with vitamin E for 3 additional months. At the end of the study, LDLR KO on a vitamin E-supplemented fat diet had decreased 8,12-iso-isoprostane (iP)<sub>F<sub>2a</sub></sub>-VI and monocyte chemoattractant protein-1 levels, but increased nitric oxide levels compared with mice on placebo. No difference in lipid levels was observed between the 2 groups. Compared with baseline, placebo group had progression of atherosclerosis. In contrast, vitamin E-treated animals showed a significant reduction in progression of atherosclerosis.

**Conclusions**—These results demonstrate that in LDLR KO, vitamin E supplementation reduces progression of established atherosclerosis by suppressing oxidative and inflammatory reactions and increasing nitric oxide levels. (*Circulation*. 2003;107:521-523.)

**Key Words:** atherosclerosis ■ antioxidants ■ lipids ■ inflammation ■ nitric oxide

Atherogenesis is a chronic disease influenced by multiple genetic and environmental factors that involves a complex interplay between blood components and the artery wall and is characterized by oxidative and inflammatory reactions.<sup>1</sup> Consistent data indicate that oxidative processes are of functional importance in animal models of atherogenesis.<sup>2</sup> Epidemiological studies support these findings, indicating an inverse relationship between antioxidant vitamin intake and cardiovascular disease.<sup>3</sup> Several clinical trials, however, have shown conflicting results as to whether or not antioxidant vitamins reduce atherosclerosis progression and cardiovascular events.<sup>4</sup> Furthermore, in healthy subjects, vitamin E supplementation did not reduce the progression of the carotid artery intima-media thickness over a 3-year period.<sup>5</sup>

Several considerations can be made to explain these conflicting results, among them the endogenous antioxidant status of the study participants before enrollment and the timing of the intervention relative to the atherosclerotic process. It is plausible that in mice, vitamin E is effective because it is typically given at an early stage of the disease. In contrast, in humans, it has little or no effect because it is

administered when atherosclerotic lesions are already established.

Most animal studies have focused their attention on the effect of antioxidants on the formation of fatty streaks, the earliest cellular lesion of atherosclerosis. In contrast, the possible contribution of oxidative stress to the progression of atherosclerosis has been poorly investigated. Previously, we have shown that vitamin E suppresses in vivo lipid peroxidation and induces a significant reduction of early atherogenesis in different mouse models of atherosclerosis.<sup>6,7</sup> The present study was designed to test the hypothesis that chronic attenuation of oxidative stress by vitamin E would have an impact on established atherosclerosis in low-density lipoprotein-receptor deficient (LDLR KO) mice.

### Methods

#### Animal Experimental Protocol

All procedures were approved by the Institutional Committee. LDLR KO mice (n=42, Jackson Laboratories, Bar Harbor, Me) were allowed to age to 12 months and were then fed a high-fat diet (normal chow supplemented with 0.15% cholesterol and 20% butter fat) for a total of 12 weeks prior baseline analysis. At this time-point blood was drawn, plasma cholesterol was quantitated, and mice were

Received November 8, 2002; revision received December 11, 2002; accepted December 12, 2002.

From the Center for Experimental Therapeutics and Department of Pharmacology, University of Pennsylvania, School of Medicine, Philadelphia, Pa; and The Claude Pepper Institute and Department of Chemistry (J.R.), Florida Institute of Technology, Melbourne, Fla.

Correspondence to Domenico Praticò, MD, University of Pennsylvania, Biomedical Research Building 2/3, Room 812, 421, Curie Blvd, Philadelphia, PA 19104. E-mail domenico@spirit.gcr.upenn.edu

© 2003 American Heart Association, Inc.

*Circulation* is available at <http://www.circulationaha.org>

DOI: 10.1161/01.CIR.0000055186.40785.C4

divided in 3 groups of 14 animals each, with mean cholesterol levels that were not significantly different. One group of animals was killed immediately for analysis of atherosclerosis (baseline group). The remaining mice were randomized to receive high-fat diet alone or supplemented with vitamin E (2 I.U/g diet) for 3 additional months. Blood samples were obtained from mice at baseline and then at monthly intervals until the end of the study.

### Biochemical Analyses

Plasma cholesterol and triglyceride levels were measured enzymatically and vitamin E levels were assayed by high-performance liquid chromatography as previously described.<sup>6,7</sup> Total plasma NO metabolites were evaluated with measurements of nitrite+nitrate by a colorimetric assay (Assay Design). Plasma 8,12-*iso*-iPF<sub>2a</sub>-VI levels were measured by gas chromatography/mass spectrometry, as previously described.<sup>7,9</sup> Levels of soluble intercellular adhesion molecules-1 (s-ICAM1) and monocyte chemoattractant protein-1 (MCP-1) were measured by ELISA kits (Endogen, Inc and R&D System).<sup>7,9</sup>

### Preparation of Mouse Aortas and Quantitation of Atherosclerosis

After the final blood collection, mice were euthanized and the aortic tree was perfused for 10 minutes with ice-cold PBS containing 20  $\mu$ mol/L BHT and 2 mmol/L EDTA (pH 7.4) as previously described.<sup>7,9</sup> After removal of the surrounding adventitial fat tissue, the aorta was opened longitudinally, fixed in formal-sucrose, and stained with Sudan IV. The extent of atherosclerosis was determined using the en face method, in a blinded fashion as previously described.<sup>6,7</sup>

### Histology and Immunohistochemistry

Briefly, serial frozen sections of the aortic root of the proximal aorta, starting at the sinus, were examined. Immunostaining for macrophage content was performed as previously described.<sup>7,9</sup> Briefly, a Mab to mouse macrophages (MOMA-2; Accurate Chemicals), and a Mab anti-human smooth muscle  $\alpha$ -actin (Sigma Chemical Co) for smooth muscle cells were used. Antibody reactivity was detected using a Nova red substrate kit (SK-4800, Vector Laboratory). Cross sections were counterstained with hematoxylin. As control, no primary antibody was added to the same sections. Images of immunostained sections were captured and analyzed in a blinded fashion as previously described.<sup>7,9</sup>

### Statistical Analysis

Results were expressed as mean $\pm$ SEM. Data were analyzed by ANOVA and subsequently by Student's unpaired 2-tailed *t* test, as indicated. Probability values less than 0.05 were considered as significant.

## Results

### Vitamin E Effects on Plasma Lipids

Compared with baseline group, mice from the placebo group showed a further significant increase in both plasma cholesterol and triglycerides. This increase was also evident in LDLR KO mice receiving the high-fat diet supplemented with vitamin E (Table). No significant difference in lipid levels was found between mice on vitamin E or high-fat diet alone. Compliance with vitamin E dietary regimen was demonstrated by a significant increase in its circulating levels in mice on vitamin E-enriched diet (Table). Elevation of plasma vitamin E levels was also evident when the values were normalized for cholesterol (data not shown).

### Vitamin E Effects on Oxidative and Inflammatory Processes

Plasma levels of 8,12-*iso*-iPF<sub>2a</sub>-VI, a major F<sub>2</sub>-isoprostane and a specific marker of lipid peroxidation,<sup>8</sup> were further

### Characteristics of the 3 Groups of Mice

	Baseline	High-Fat Diet	
		Placebo	Vitamin E
Cholesterol, mg/dL	800 $\pm$ 50	1150 $\pm$ 100†	1115 $\pm$ 85
Triglycerides, mg/dL	450 $\pm$ 45	710 $\pm$ 60†	680 $\pm$ 70
Vitamin E, $\mu$ M	20 $\pm$ 2	16 $\pm$ 1.8†	52 $\pm$ 2.2*
8,12- <i>iso</i> -iPF <sub>2a</sub> -VI, pg/mL	750 $\pm$ 60	1100 $\pm$ 55†	630 $\pm$ 50
sICAM-1, ng/ml	11 $\pm$ 1.5	14 $\pm$ 2	10 $\pm$ 2*
MCP-1, ng/ml	200 $\pm$ 15	245 $\pm$ 21	180 $\pm$ 16*
Nox, $\mu$ M	30 $\pm$ 3.2	18 $\pm$ 2.6†	48 $\pm$ 2.4*

Each group includes 14 mice. Results are expressed as mean $\pm$ SEM.

\**P*<0.05 vs placebo; †*P*<0.05 vs baseline.

elevated in LDLR KO mice kept on a high-fat diet alone when compared with the baseline group. In contrast, vitamin E significantly reduced these levels to values that were similar to the ones observed in mice at baseline (Table). At the end of the study, mice on the high-fat diet alone had a further increase in s-ICAM-1 and MCP-1 circulating levels, whereas vitamin E significantly reduced them (Table). Because impaired NO synthesis has been described in hypercholesterolemia,<sup>10</sup> we examined the effect of vitamin E supplementation on NO metabolite (NOx) levels. Compared with baseline, plasma NOx levels were further reduced in mice on a high-fat diet alone. In contrast, vitamin E supplementation preserved higher plasma NOx levels compared with both baseline and the placebo group (Table).

### Vitamin E Effects on Preexisting Atherosclerotic Lesions

The Sudan IV-stained aorta preparations of the LDLR KO mice on the high-fat diet for 3 months showed atherosclerotic lesions mainly localized in the sinus and arch portions, covering 11.2 $\pm$ 1.4% of the entire vessel (Figure 1). The aortas from mice receiving a high-fat diet for 3 additional months demonstrated further progression of atherosclerosis, which involved the thoracic and abdominal portions of the aorta. In contrast, this area was significantly reduced in LDLR KO mice on high-fat diet supplemented with vitamin E (Figure 1). No significant difference was observed with the baseline group (Figure 1).

Immunohistochemical analyses of aortic root sections showed no difference in the percentage area occupied by

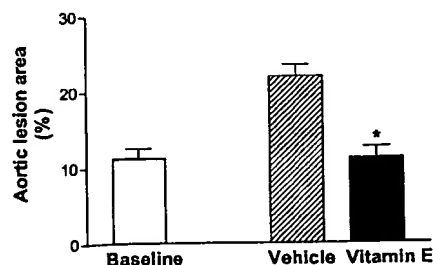


**Figure 1.** Percentage of total aortic atherosclerotic lesion areas in LDLR KO mice fed a high-fat diet for 3 months (baseline), and those fed a high-fat diet alone or with vitamin E for 12 additional weeks (n=14 per group). \**P*<0.01 versus placebo.



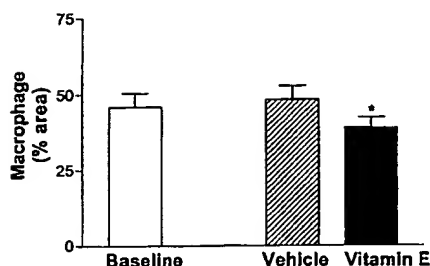


**Figure 2.** Percentage area of aortic root atherosclerotic lesions occupied by macrophages in LDLR KO mice fed high-fat diet for 3 months (baseline), and those fed a high-fat diet alone or with vitamin E for 12 additional weeks ( $n=8$  per group).  $*P<0.01$  versus placebo.

macrophages between baseline and placebo group after normalized to total lesion area. However, this area was significantly reduced in mice receiving vitamin E compared with placebo (Figure 2). Finally, no difference in smooth muscle cell content was observed among the 3 groups (data not shown).

### Discussion

In the current study, we demonstrated for the first time that chronic supplementation of vitamin E retards the progression of established atherosclerotic lesions in LDLR KO mice on a high-fat diet by decreasing oxidative and inflammatory reactions and increasing NO levels.

Lipid peroxidation, in particular oxidative modification of LDL in vivo, is thought to play a functional role in atherogenesis.<sup>2</sup> Evidence consistent with this hypothesis includes the presence of oxidized lipids in atherosclerotic lesions and the reduction of murine atherosclerosis by structurally distinct antioxidants.<sup>11–13</sup> Several trials have shown, however, that antioxidants do not reduce the risk of fatal or non-fatal infarction in an unselected population with established atherosclerosis.<sup>4</sup> These conflicting results do not necessarily mean that the oxidative hypothesis of atherosclerosis is incorrect. It is possible that the animal intervention studies deal primarily with early lesions, whereas clinical trials deal with established ones. We have previously shown that in vivo lipid peroxidation is increased in the apolipoprotein E-deficient mice and LDLR KO mice, and that its inhibition by vitamin E coincides with a reduction in atherosclerosis.<sup>6,7</sup> It is plausible that in humans antioxidants have little or no effect because they are given when lesions are already established. To test this hypothesis, LDLR KO mice initially kept on a high-fat diet for 3 months were subsequently randomized to either receive a high-fat diet supplemented with vitamin E or stay on the high-fat diet alone for 12 additional weeks. We found that vitamin E reduced progression of atherosclerosis without affecting lipid levels by suppressing oxidative stress. These results support the concept that vitamin E is effective in LDLR KO mice whether it is given at the early phase of atherogenesis or after the disease is established.

Atherosclerosis is associated with oxidative stress, which is characterized by a reduction of endogenous antioxidants and NO levels.<sup>14,15</sup> We confirmed these data by showing that vitamin E restores and increases these levels. Reactive oxygen species can interact with NO and produce peroxynitrate, which in turn can further sustain oxidative injury to the endothelium. By restoring the endogenous antioxidant status, vitamin E increases NO levels and limits peroxynitrate formation, which could then act as additional antiatherogenic mechanisms by reducing vascular inflammation. Indeed, our present findings demonstrate that by reducing oxidative stress, vitamin E improves indices of inflammation and endothelial function, which are critically involved in the progression of atherosclerosis.

In interpreting our results, we must consider an important limitation of this study; no animal model mimics perfectly human atherosclerosis. Despite this fact, our study supports the hypothesis that the discrepancies between animal studies and clinical trials with vitamin E cannot be explained by the timing of the intervention, ie, early versus established lesions.

### Acknowledgments

This work was supported by a grant from the American Heart Association (030211N) to Dr Praticò.

### References

- Glass CK, Witztum JL. Atherosclerosis: the road ahead. *Cell*. 2001;104:503–516.
- Witztum JL, Steinberg D. The oxidative modification hypothesis of atherosclerosis: does it hold for humans. *Trends Cardiovasc Med*. 2001;11:93–102.
- Rimm EB, Stampfer MJ, Ascherio A, et al. Vitamin E consumption and the risk of coronary heart disease in men. *N Engl J Med*. 1993;328:1450–1456.
- Praticò D. Vitamin E: murine studies versus clinical trials. *Ital Heart J*. 2001;2:878–881.
- Hodis HN, Mack WJ, LaBree L, et al. Alpha-tocopherol supplementation in healthy individuals reduces low-density lipoprotein oxidation but not atherosclerosis. *Circulation*. 2002;106:1453–1459.
- Praticò D, Tangirala RK, Rader DJ, et al. Vitamin E suppresses isoprostane generation in vivo and reduces atherosclerosis in ApoE-deficient mice. *Nat Med*. 1998;4:1189–1192.
- Cyrus T, Tang LX, Rokach J, et al. Lipid peroxidation and platelet activation in murine atherosclerosis. *Circulation*. 2001;104:1940–1945.
- Praticò D, Lawson JA, Rokach J, et al. The isoprostanes in biology and medicine. *Trends Endocr Metab*. 2001;12:243–247.
- Praticò D, Cyrus T, Zhang Z, et al. Acceleration of atherogenesis by COX-1-dependent prostanoid formation in low-density lipoprotein receptor deficient mice. *Proc Natl Acad Sci U S A*. 2001;98:3358–3363.
- Ishikawa I, Sugawara D, Wang X, et al. Heme oxygenase-1 inhibits atherosclerotic lesion formation in LDL-receptor knockout mice. *Circ Res*. 2001;88:506–512.
- Witztum JL, Berliner JA. Oxidized phospholipids and isoprostanes in atherosclerosis. *Curr Opin Lipidol*. 1998;9:441–448.
- Tangirala RK, Casanada F, Miller E, et al. Effect of the anti-oxidant N,N'-diphenyl 1,4-phenylenediamine (DPPD) on atherosclerosis in apoE-deficient mice. *Arterioscler Thromb Vasc Biol*. 1994;15:1625–1630.
- Cynshi O, Kawabe Y, Suzuki T, et al. Antiatherogenic effects of the antioxidant BO-653 in three different animal models. *Proc Natl Acad Sci U S A*. 1998;95:10123–10128.
- Praticò D. Lipid peroxidation in mouse models of atherosclerosis. *Trends Cardiovasc Med*. 2001;11:112–116.
- Oemar B, Tschudi MR, Godoy N, et al. Reduced endothelial synthase expression and production in human atherosclerosis. *Circulation*. 1998;97:2494–2498.

Vascular Biology, Atherosclerosis and Endothelium Biology

# The Atheroprotective Effect of 17 $\beta$ -Estradiol Depends on Complex Interactions in Adaptive Immunity

Rima Elhage,\* Pierre Gourdy,\* Jacek Jawien,<sup>†</sup>  
Laurent Bouchet,\* Caroine Castano,\*  
Catherine Fievet,<sup>‡</sup> Göran K. Hansson,<sup>†</sup>  
Jean-François Arnal,\* and Francis Bayard\*

From INSERM U589,\* IFR31, Institut L. Bugnard, Toulouse, France; INSERM U545 Institut Pasteur,<sup>‡</sup> Lille, France; and the Center for Molecular Medicine and Department of Medicine,<sup>†</sup> Karolinska Institute, Stockholm, Sweden

**Estradiol prevents fatty streak formation in chow-fed atherosclerosis-prone apolipoprotein E (ApoE)-deficient mice. We previously reported that fatty streak development of immunodeficient ApoE<sup>-/-</sup>/recombination activating gene 2 (RAG-2<sup>-/-</sup>) double-deficient mice was insensitive to estradiol. In the present work, we demonstrate that the reconstitution of ApoE<sup>-/-</sup>/RAG-2<sup>-/-</sup> with bone marrow from immunocompetent ApoE<sup>-/-</sup>/RAG-2<sup>+/+</sup> mice restores the protective effect of estradiol on fatty streak constitution. We extended this demonstration to the model of low-density lipoprotein receptor-deficient mice, establishing the obligatory role of mature lymphocytes in this process. We then investigated whether the protective effect of estradiol was mediated by a specific lymphocyte subpopulation by studying the hormonal effect on fatty streak constitution in recently developed models of ApoE<sup>-/-</sup> mice deficient in selective T-lymphocyte subsets (either TCR $\alpha\beta$ <sup>+</sup>, CD4<sup>+</sup>, CD8<sup>+</sup>, or TCR $\gamma\delta$ <sup>+</sup> lymphocytes) or B lymphocytes. In all these specifically immunodeficient mice, estradiol administration to ovariectomized mice conferred protection as in immunocompetent ApoE<sup>-/-</sup> mice, clearly demonstrating that no single lymphocyte subpopulation was specifically required for this effect. These results point to additional lymphocyte-dependent mechanisms such as modulating the interactions among lymphocytes and between lymphocytes and endothelial and/or antigen-presenting cells. (*Am J Pathol* 2005, 167:267-274)**

Fuller understanding of the mechanism of atherosclerosis prevention by estrogens is urgently needed.<sup>1</sup> Two controlled prospective and randomized studies did not demonstrate a beneficial effect of hormone replacement therapy whether in secondary<sup>2</sup> or in primary prevention.<sup>3</sup> In contrast to these clinical data, estrogen hormones have been shown to decrease macrophage-derived foam-cell infiltration in different animal species including atherosclerosis-prone apolipoprotein E-deficient (ApoE<sup>-/-</sup>) mice<sup>4,5</sup> although the mechanisms of this effect have remained obscure.

Recent cumulative evidence have suggested that both innate and adaptive immune responses modulate the rate of lesion progression.<sup>6-8</sup> Indeed, several studies have confirmed the importance of T lymphocytes present in early lesions of atherosclerosis.<sup>9-12</sup> Furthermore, previous observations have demonstrated the particular role for specific T-lymphocyte subsets. For example, Zhou and colleagues<sup>13</sup> showed that CD4<sup>+</sup> T cells aggravate the atherosclerotic process.

In this context, we previously reported that ApoE<sup>-/-</sup> mice with homozygous disruption at the recombination activating gene 2 (RAG-2<sup>-/-</sup>) loci presented a reduced level of atherosclerotic lesions that were insensitive to estradiol (E2).<sup>14</sup> In the present studies, we first demonstrated that the reconstitution of ApoE<sup>-/-</sup>/RAG-2<sup>-/-</sup> with bone marrow from immunocompetent ApoE<sup>-/-</sup>/RAG-

Supported in part by INSERM, the Ministère de la Recherche et de la Technologie (Université Paul Sabatier), Action Concertée Incitative 2001 and 2003, Association pour la Recherche contre le Cancer, MSD, Theramex Laboratories, European Vascular Genomics Network (grant no.503254), Fondation de France, the Conseil Régional Midi-Pyrénées, and the French Society of Atherosclerosis (to R.E.).

Accepted for publication February 10, 2005.

Supplemental material for this article appears on <http://ajp.amjpathol.org>.

Present address of J.J.: Department of Pharmacology, Jagiellonian University School of Medicine, Grzegorzeczka 16, PL 31-531 Krakow, Poland.

Address reprint requests to F. Bayard, INSERM U589, IFR31, Institut L. Bugnard, BP 84225, 31432 Toulouse Cédex 4, France. E-mail: bayard@toulouse.inserm.fr.



$2^{+}/^{+}$  mice restores the protective effect of E2 on fatty streak constitution and extended this demonstration to the model of low-density lipoprotein receptor (LDLR)-deficient mice. We then hypothesized that E2 could target a specific lymphocyte subset to exert its protective effect on fatty streak constitution. To solve this question, we compared the effect of E2 in immunocompetent ApoE $^{-/-}$  mice and in models of ApoE $^{-/-}$  mice deficient in specific lymphocyte subsets developed in our laboratory. We observed that no T- or B-lymphocyte subpopulation specifically mediated the protective effect of E2, pointing to additional lymphocyte-dependent mechanisms.

## Materials and Methods

### Animals

The specific pathogen-free conditions of animal care and regular chow diet feeding as well as the production of ApoE- and RAG-2-deficient mice (ApoE $^{-/-}$ /RAG-2 $^{-/-}$ ) have been described previously.<sup>14,15</sup> The ApoE $^{-/-}$ /RAG-2 $^{-/-}$  mice had been backcrossed into a C57BL/6 background for six generations.

Low-density lipoprotein receptor-deficient (LDLR $^{-/-}$ ) mice were purchased from Charles River (L'arbrès, France). RAG-2-deficient (RAG-2 $^{-/-}$ ) mice were purchased from CDTA (Orléans, France). Both strains had been backcrossed into a C57BL/6 background for more than 10 generations. Female LDLR $^{-/-}$  mice were crossed with male RAG-2 $^{-/-}$  mice in our animal facility to obtain LDLR and RAG-2 double-deficient mice (LDLR $^{-/-}$ /RAG-2 $^{-/-}$ ). RAG-2 and LDLR gene disruptions were assessed by polymerase chain reaction genotyping as previously described.<sup>16,17</sup> The production of the double-deficient models is reported elsewhere.<sup>12</sup> Briefly, TCR $\beta$ -deficient (TCR $\beta$  $^{-/-}$ ), CD4-deficient (CD4 $^{-/-}$ ), CD8-deficient (CD8 $^{-/-}$ ), TCR $\delta$ -deficient (TCR $\delta$  $^{-/-}$ ) male mice were crossed with female ApoE $^{-/-}$  mice. B-lymphocyte-deficient mice were obtained similarly by crossing  $\mu$ mt-deficient<sup>18</sup> B $^{-/-}$  male mice with female ApoE $^{-/-}$  mice. Heterozygous ApoE $^{-/-}$ /TCR $\beta$  $^{+/-}$ , ApoE $^{-/-}$ /CD4 $^{+/-}$ , ApoE $^{-/-}$ /CD8 $^{+/-}$ , ApoE $^{-/-}$ /TCR $\delta$  $^{+/-}$ , ApoE $^{-/-}$ /B $^{+/-}$  populations were generated and used as the parental genotypes. The offspring of these heterozygous strains, TCR $\beta$  $^{+/-}$ , CD4 $^{+/-}$ , CD8 $^{+/-}$ , TCR $\delta$  $^{+/-}$ , B $^{+/-}$  and TCR $\beta$  $^{-/-}$ , CD4 $^{-/-}$ , CD8 $^{-/-}$ , TCR $\delta$  $^{-/-}$ , B $^{-/-}$  served as the subjects of our studies. Confirmation of gene disruption was screened by polymerase chain reaction genotyping and phenotyping of blood lymphocytes or splenocytes by flow cytometry.<sup>12</sup> All strains had been backcrossed into a C57BL/6 background for more than 10 generations.

Only female animals were used in the present studies. As shown in Figure 1, mice were ovariectomized at 5 weeks of age and, 1 week later, were administered with either 60-day time-release placebo or 0.1 mg of estradiol-17 $\beta$  pellets (Innovative Research of America, Sarasota, FL) implanted subcutaneously into the back of the animals, using a sterile trochar and forceps. New pellets were reimplanted 7 weeks later. The dose of 0.1 mg of E2, releasing 80  $\mu$ g/kg/day, had previously been defined

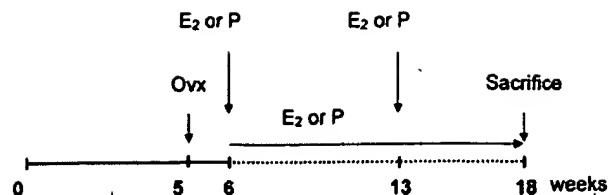


**Figure 1.** Protocol to study fatty streak formation in immunocompetent or immunodeficient ApoE-deficient mice. OvX, ovariectomy; E2, estradiol-17 $\beta$  pellet; P, placebo pellet.

as adequate for a maximal effect on fatty streak constitution in female mice.<sup>15</sup> ApoE $^{-/-}$  mice were maintained under chow diet throughout the experiments, whereas LDLR $^{-/-}$  mice were switched to a high-fat diet (15% fat, 1.25% cholesterol, no cholate, TD96335; Harlan Teklad, WI) at 5 weeks of age. After E2 or placebo treatment for 12 weeks, all mice were sacrificed with an overdose of ketalar after a 16-hour fast. Blood was collected by orbital puncture for serum lipid analysis.<sup>15</sup> Uterus was weighted to assess the efficacy of E2 treatment. All experimental procedures were performed in accordance with the recommendations of the European Accreditation of Laboratory Animal Care Institute.

### Bone Marrow Transplantation

As shown in Figure 2, ApoE $^{-/-}$ /RAG-2 $^{-/-}$  and LDLR $^{-/-}$ /RAG-2 $^{-/-}$  mice were ovariectomized at 5 weeks of age and received a sublethal dose of whole-body irradiation (400 rads) 1 week later. The day after irradiation, donor ApoE $^{-/-}$  or ApoE $^{-/-}$ /RAG-2 $^{-/-}$ , C57BL/6 or RAG-2 $^{-/-}$  mice were killed, and their femurs and tibias removed aseptically. Marrow cavities were flushed, and single-cell

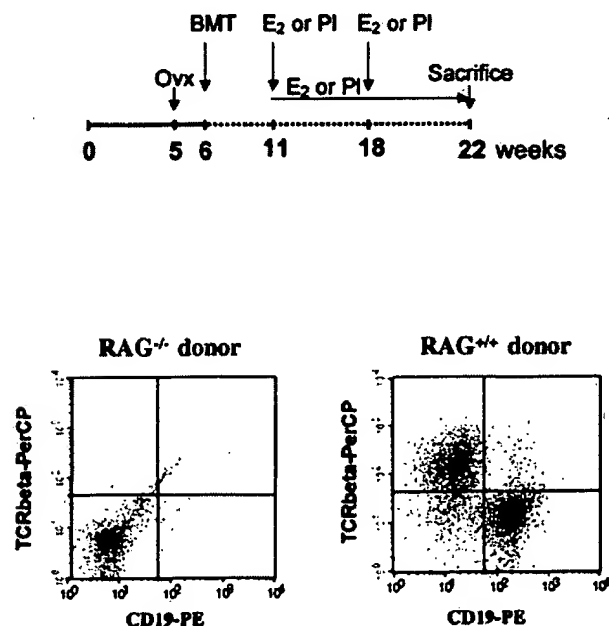


**Figure 2.** Protocol of bone marrow transplantation (BMT) and flow cytometry analysis of spleen lymphocyte repopulation of ApoE $^{-/-}$ /RAG-2 $^{-/-}$  mice transplanted using bone marrow from ApoE $^{-/-}$ /RAG-2 $^{-/-}$  or ApoE $^{-/-}$ /RAG-2 $^{+/+}$  donor mice. Splenocytes were co-labeled with anti-TCR $\beta$ -PerCP/anti-CD19-PE-conjugated antibodies.

**Table 1.** Body Weight, Total Cholesterol, and Aortic Root Lesion Area in Placebo (PI)- or Estradiol-17 $\beta$  (E<sub>2</sub>)-Treated Ovariectomized ApoE<sup>-/-</sup>/RAG<sup>-/-</sup> Female Mice after Bone Marrow Transplantation from ApoE<sup>-/-</sup>/RAG<sup>-/-</sup> or ApoE<sup>-/-</sup>/RAG<sup>+/+</sup> Donors

Donor genotype	Treatment	Body weight (g)	Total cholesterol (g/L)	Lesion area ( $\mu\text{m}^2$ )
ApoE <sup>-/-</sup> /RAG <sup>+/+</sup>	PI	25.3 $\pm$ 0.7	5.9 $\pm$ 0.4	66662 $\pm$ 5838
	E <sub>2</sub>	23.5 $\pm$ 0.6	4.8 $\pm$ 0.4	34919 $\pm$ 6532*
ApoE <sup>-/-</sup> /RAG <sup>-/-</sup>	PI	26.8 $\pm$ 1.7	5.4 $\pm$ 0.4	33451 $\pm$ 5816†
	E <sub>2</sub>	24.3 $\pm$ 0.3	4.4 $\pm$ 0.7	41844 $\pm$ 5294

Results are means  $\pm$  SEM ( $n = 7$ ).

\* $P < 0.05$  versus the corresponding PI-treated mice.

† $P < 0.05$  versus ApoE<sup>-/-</sup>/RAG<sup>+/+</sup>-transplanted PI-treated mice.

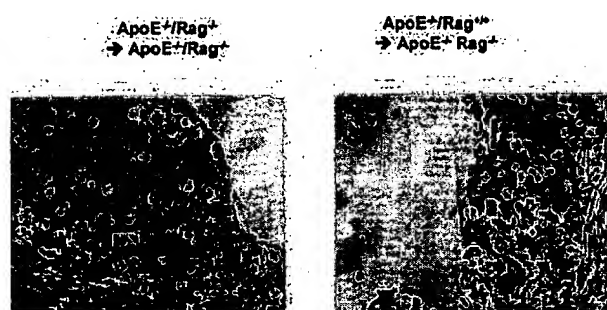


**Figure 3.** Immunohistochemical analysis of representative lesions from individual ApoE<sup>-/-</sup>/RAG-2<sup>-/-</sup> transplanted using bone marrow from ApoE<sup>-/-</sup>/RAG-2<sup>+/+</sup> or ApoE<sup>-/-</sup>/RAG-2<sup>-/-</sup> donor mice using anti-CD3 antibodies.

suspensions were prepared. The irradiated recipients received  $15 \times 10^6$  bone marrow cells in 0.2 ml of phosphate-buffered saline by tail vein injection. One week before and 4 weeks after the bone marrow transplantation, Bactrim (sulfamethoxazole 200 mg/ml, trimethoprim 48 mg/ml) was added to drinking water. After 5 additional weeks, all transplanted mice were implanted subcutaneously with placebo or E<sub>2</sub> pellets and LDLr<sup>-/-</sup>/RAG-2<sup>-/-</sup> mice were switched to the high-fat diet to induce atherosclerotic lesion formation. Mice were sacrificed 11 weeks later (at 22 weeks of age). Blood and tissues were collected as described above.

### Tissue Preparation and Lesion Analysis

The circulatory system was perfused with 0.9% NaCl by cardiac intraventricular canalization. The heart and ascending aorta were removed and kept frozen. Surface lesion area was measured by computer-assisted image quantification in the aortic root, by a trained observer blinded to the genotype and treatment of the mice, as previously described<sup>15</sup> but using a Leica image analyzer.

The rest of the entire aortic tree was removed and cleaned of adventitia, split longitudinally to the iliac bifurcation, and pinned flat on a dissection pan for analysis by *en face* preparation. Images were captured using a Sony-3CCD video camera and fraction covered by lesions evaluated as a percentage of the total aortic area.

### Immunohistochemistry

Cryostat sections from the proximal aorta were fixed in acetone, air-dried, and reacted with a primary rat monoclonal anti-mouse macrophage (clone MOMA-2 from Serotec, Oxford, UK) used at a 1:50 dilution or a primary goat polyclonal anti-CD3 (clone M-20 from Santa Cruz Biotechnology, Santa Cruz, CA) used at a 1:100 dilution. Then, sections were incubated with corresponding preadsorbed secondary biotinylated antibodies (Vector Laboratories, Burlingame, CA): binding of rat monoclonal anti-macrophage was revealed using biotinylated rabbit anti-rat IgG and binding of goat polyclonal anti-CD3 was revealed using biotinylated horse anti-goat IgG. The binding of the biotinylated antibodies was visualized with an avidin DH-biotinylated peroxidase complex (Vectastain ABC kit, Vector Laboratories) and AEC peroxidase substrate kit (Vector Laboratories). Counterstaining was performed using Mayer's hemalun. Macrophage and T-cell quantification was determined by scoring samples from at least four sections per animal. A minimum of three animals was analyzed per group. Two investigators who were blinded to the sample identity performed analysis.

### Analysis of Plasma Lipids and Lipoproteins

Serum cholesterol concentrations were determined by an enzymatic assay adapted to microtiter plates using com-

**Table 2.** Body Weight, Total Cholesterol, and Aortic Root Lesion Area in Placebo (PI)- or Estradiol-17 $\beta$  (E<sub>2</sub>)-Treated Ovariectomized LDLr<sup>-/-</sup>/RAG<sup>-/-</sup> Female Mice after Bone Marrow Transplantation from RAG<sup>-/-</sup> or C57BL/6 Mice

Donor genotype	Treatment	Body weight (g)	Total cholesterol (g/L)	Lesion area ( $\mu\text{m}^2$ /section)
C57BL/6	PI	28.1 $\pm$ 1.2	9.3 $\pm$ 0.8	84480 $\pm$ 9185
	E <sub>2</sub>	24.9 $\pm$ 0.7*	6.4 $\pm$ 0.7*	35333 $\pm$ 8317*
RAG <sup>-/-</sup>	PI	27.1 $\pm$ 0.6	11.1 $\pm$ 0.6	35900 $\pm$ 5600†
	E <sub>2</sub>	24.0 $\pm$ 0.5*	9.9 $\pm$ 0.5	42800 $\pm$ 6600

The animals had been on HFD for 12 weeks. Results are means  $\pm$  SEM ( $n \geq 7$ ).

\* $P < 0.05$  versus C57BL/6-transplanted PI-treated mice.

† $P < 0.05$  versus the corresponding PI-treated mice.

**Table 3.** Body Weight, Total Cholesterol, and Lesion Area of Ovariectomized Placebo (PI)- or Estradiol-17 $\beta$  (E<sub>2</sub>)-Treated Immunocompetent ApoE<sup>-/-</sup> Control and Immunodeficient ApoE<sup>-/-</sup>/TCR $\delta$ <sup>-/-</sup>, CD4<sup>-/-</sup>, CD8<sup>-/-</sup>, TCR $\delta$ <sup>-/-</sup> or B<sup>-/-</sup> Female Mice

Genotype	Body weight (g)			Total cholesterol (g/L)
	NC	PI	E2	NC
ApoE <sup>-/-</sup>	22.0 $\pm$ 0.5	28.7 $\pm$ 1.5	22.9 $\pm$ 0.5*	3.4 $\pm$ 0.1
ApoE <sup>-/-</sup> /TCR $\delta$ <sup>-/-</sup>	21.0 $\pm$ 0.5	20.9 $\pm$ 0.6†	21.5 $\pm$ 0.5	3.0 $\pm$ 0.2
ApoE <sup>-/-</sup> /CD4 <sup>-/-</sup>	19.5 $\pm$ 0.4	21.9 $\pm$ 1.2†	21.9 $\pm$ 0.6	3.0 $\pm$ 0.2
ApoE <sup>-/-</sup> /CD8 <sup>-/-</sup>	21.5 $\pm$ 0.5	23.5 $\pm$ 0.8†	22.9 $\pm$ 0.5	3.1 $\pm$ 0.2
ApoE <sup>-/-</sup> /TCR $\delta$ <sup>-/-</sup>	20.1 $\pm$ 0.4	27.6 $\pm$ 1.4	21.9 $\pm$ 0.1*	2.9 $\pm$ 0.1
ApoE <sup>-/-</sup> /B <sup>-/-</sup>	—	26.8 $\pm$ 0.9	24.3 $\pm$ 0.4*	—

Data of intact corresponding mice (NC) have been published previously<sup>12</sup> and are indicated in italics for comparison. Results are means  $\pm$  SEM ( $n \geq 8$ ).

\* $P < 0.05$  versus corresponding C (placebo-treated) mice.

† $P < 0.05$  versus corresponding immunocompetent mice.

(table continues)

mercially available reagents (Roche Molecular Biochemicals, Germany). Lipoprotein cholesterol profiles were obtained by Fast Protein liquid chromatography as previously described.<sup>19</sup>

### Statistical Analysis

The results are expressed as means  $\pm$  SEM. For each parameter (body weight, total cholesterol, lesion area), the effects of genotype were studied by comparing each immunodeficient group with its corresponding immunocompetent group of mice. The effect of E2 treatment was studied comparing placebo- and E2-treated mice in selective immunodeficient or in immunocompetent mice. A one-factor analysis of variance was used (Bonferroni/Dunn's test);  $P < 0.05$  was considered as significant. Statistical analyses were performed using the Statview statistical software (Abacus Concepts, Inc., Berkeley, CA). When appropriate, an unpaired *t*-test was also performed.

## Results

### Immunocompetent Bone Marrow Transplantation Restored Both the Level of Lesions and E2 Sensitivity in ApoE<sup>-/-</sup>/RAG-2<sup>-/-</sup> and LDLr<sup>-/-</sup>/RAG-2<sup>-/-</sup> Mice

To explore the role of lymphocytes in fatty streak constitution and E2 prevention, ApoE<sup>-/-</sup>/RAG-2<sup>-/-</sup> ovariectomized female mice received bone marrow transplantation from ApoE<sup>-/-</sup>/RAG-2<sup>-/-</sup> (ApoE<sup>-/-</sup>/RAG-2<sup>-/-</sup>  $\rightarrow$  ApoE<sup>-/-</sup>/RAG-2<sup>-/-</sup>) or from ApoE<sup>-/-</sup>/RAG-2<sup>+/+</sup> (ApoE<sup>-/-</sup>/RAG-2<sup>+/+</sup>  $\rightarrow$  ApoE<sup>-/-</sup>/RAG-2<sup>-/-</sup>) mice (Figure 2), and then were treated with placebo or E2 pellets. Sixteen weeks after bone marrow transplantation, ApoE<sup>-/-</sup>/RAG-2<sup>+/+</sup>  $\rightarrow$  ApoE<sup>-/-</sup>/RAG-2<sup>-/-</sup> placebo-treated mice presented a significantly higher level of fatty streaks when compared with ApoE<sup>-/-</sup>/RAG-2<sup>-/-</sup>  $\rightarrow$  ApoE<sup>-/-</sup>/RAG-2<sup>-/-</sup> placebo-treated mice (Table 1). Immunohistochemical analysis showed the presence of CD3-reactive cells in lesions obtained from ApoE<sup>-/-</sup>/RAG-2<sup>+/+</sup>  $\rightarrow$  ApoE<sup>-/-</sup>/RAG-2<sup>-/-</sup> mice but not in lesions obtained from ApoE<sup>-/-</sup>/RAG-2<sup>-/-</sup>  $\rightarrow$  ApoE<sup>-/-</sup>/

RAG-2<sup>-/-</sup> mice, irrespective of placebo or E2 treatment (Figure 3 and data not shown). Importantly, although E2 was still ineffective in ApoE<sup>-/-</sup>/RAG-2<sup>-/-</sup>  $\rightarrow$  ApoE<sup>-/-</sup>/RAG-2<sup>-/-</sup> mice, the protective effect of the hormone was restored in ApoE<sup>-/-</sup>/RAG-2<sup>+/+</sup>  $\rightarrow$  ApoE<sup>-/-</sup>/RAG-2<sup>-/-</sup> mice (Table 1).

Because ApoE-deficiency could be involved in these observations and because the RAG-2-deficient mice used were not fully backcrossed into the C57/BL6 background, similar experiments were performed in the LDLr-deficient mice. We first confirmed that E2 significantly decreased body weight (26.1  $\pm$  0.6 g versus 23.6  $\pm$  0.5 g,  $P < 0.05$ ), serum cholesterol (11.1  $\pm$  0.4 g/L versus 7.9  $\pm$  0.7 g/L,  $P < 0.01$ ), and fatty streak deposit (119,400  $\pm$  7400  $\mu$ m<sup>2</sup>/section versus 41,400  $\pm$  5400  $\mu$ m<sup>2</sup>/section for placebo- and E2-treated mice, respectively;  $n = 9$ ,  $P < 0.01$ ) in immunocompetent LDLr<sup>-/-</sup> mice on a 12-week high-fat diet in agreement with a previous report.<sup>20</sup> The effect on fatty streak was abolished in LDLr<sup>-/-</sup>/RAG-2<sup>-/-</sup> mice (42,000  $\pm$  13,100  $\mu$ m<sup>2</sup>/section versus 40,300  $\pm$  11,300  $\mu$ m<sup>2</sup>/section, respectively;  $n = 8$ ) whereas the effect on body weight (24.4  $\pm$  1.3 g/L versus 22.9  $\pm$  0.9 g/L,  $P < 0.05$ ) and serum cholesterol (9.9  $\pm$  0.4 g/L versus 7.4  $\pm$  0.7 g/L,  $P < 0.01$ ) persisted. Bone marrow graft experiments were also performed in this last model of ovariectomized female LDLr<sup>-/-</sup>/RAG-2<sup>-/-</sup> mice. As shown in Table 2, Placebo-treated LDLr<sup>-/-</sup>/RAG-2<sup>-/-</sup> mice that had received C57BL/6 bone marrow, presented a significantly higher level of fatty streaks when compared with those that had received RAG-2<sup>-/-</sup> bone marrow. Again, although E2 remained ineffective in RAG-2<sup>-/-</sup>  $\rightarrow$  LDLr<sup>-/-</sup>/RAG-2<sup>-/-</sup> mice, the protective effect of the hormone was restored in C57BL/6  $\rightarrow$  LDLr<sup>-/-</sup>/RAG-2<sup>-/-</sup> mice (Table 2).

### Effect of E2 Treatment on Body Weight and Serum Lipids in Immunocompetent and Selectively Immunodeficient ApoE<sup>-/-</sup> Mice

We then asked whether the protective effect of E2 could be mediated by a specific T-lymphocyte subset or B lymphocytes, considering the hormonal effect in selec-

Table 3. Continued

Total cholesterol (g/L)		Lesion area ( $\mu\text{m}^2/\text{section}$ )		
PI	E2	NC	PI	E2
5.6 $\pm$ 0.3	3.1 $\pm$ 0.2*	73,214 $\pm$ 2963	113,465 $\pm$ 5288	36,299 $\pm$ 1979*
4.4 $\pm$ 0.2†	3.1 $\pm$ 0.2*	37,048 $\pm$ 4749	65,053 $\pm$ 7753†	37,104 $\pm$ 4418*
5.8 $\pm$ 0.5	2.7 $\pm$ 0.2*	77,745 $\pm$ 12,629	114,835 $\pm$ 21,656	42,541 $\pm$ 5431*
5.6 $\pm$ 0.4	3.2 $\pm$ 0.1*	76,909 $\pm$ 4722	110,537 $\pm$ 16,142	47,782 $\pm$ 11,285*
5.6 $\pm$ 0.3	2.8 $\pm$ 0.2*	57,589 $\pm$ 3737	101,557 $\pm$ 8125	27,730 $\pm$ 3637*
4.6 $\pm$ 0.2†	2.6 $\pm$ 0.3*	—	93,432 $\pm$ 11,183	38,348 $\pm$ 5752*

tively immunodeficient ApoE<sup>-/-</sup> female mice. The statistical analysis presented in Table 3 refers to comparisons of each group of immunodeficient mice with its corresponding immunocompetent group. Data from a group of 10 ApoE<sup>-/-</sup> female mice are given for comparison (Table 3, line 1).

Uterine weight was <20 mg in ovariectomized mice and increased to 172  $\pm$  13 mg on average with E2 treatment, showing that the level of E2 stimulation was similar in all genotypes. Body weight decreased, reflecting mainly adipose tissue reduction, in immunocompetent ApoE<sup>-/-</sup> control and in immunodeficient ApoE<sup>-/-</sup>/TCR $\delta$ <sup>-/-</sup> and ApoE<sup>-/-</sup>/B<sup>-/-</sup> mice under E2 treatment. In the immunodeficient ApoE<sup>-/-</sup>/TCR $\beta$ <sup>-/-</sup>, ApoE<sup>-/-</sup>/CD4<sup>-/-</sup>, and ApoE<sup>-/-</sup>/CD8<sup>-/-</sup> mice, body weight was lower in placebo-treated mice when compared to their immunocompetent littermates and was not influenced by E2, suggesting a role for TCR $\alpha\beta$ <sup>+</sup> T lymphocytes in weight regulation. Total serum cholesterol was lower in ovariectomized ApoE<sup>-/-</sup>/TCR $\beta$ <sup>-/-</sup> and ApoE<sup>-/-</sup>/B<sup>-/-</sup> when compared with their respective immunocompetent littermates and decreased under E2 treatment in all strains. Fast performance liquid chromatography showed that the E2-induced decrease concerned the very low-density lipoprotein, intermediary/low-density lipoprotein, and high-density lipoprotein fractions (see Supplemental Figure A at <http://ajp.amjpathol.org>) in agreement with our previous report.<sup>15</sup>

#### Effect of E2 Treatment on Lesion Area in Immunocompetent and Selectively Immunodeficient ApoE<sup>-/-</sup> Mice

At the level of the aortic root, the lesion area of ovariectomized immunodeficient mice given placebo did not differ significantly from the corresponding immunocompetent mice except for the ApoE<sup>-/-</sup>/TCR $\beta$ <sup>-/-</sup> mice, which presented a decreased level of lesions (Table 3). E2 treatment induced a significant decrease of fatty streak development in all groups of mice, including the ApoE<sup>-/-</sup>/TCR $\beta$ <sup>-/-</sup> strain. To further analyze the influence of serum cholesterol on the lesion formation, we sought to analyze subgroups of mice with comparable serum cholesterol levels. Such subgroups could be selected among

the whole series of immunocompetent mice that serve as control for the immunodeficient groups (ie, a total of 50 PI-treated and 50 E2-treated mice) with cholesterolemia arbitrarily encompassed between 4 and 6 g/L. In these subgroups of ovariectomized placebo ( $n = 19$ )- and E2 ( $n = 12$ )-treated mice, with similar serum cholesterol (5.0  $\pm$  0.1 g/L and 4.9  $\pm$  0.1 g/L, respectively;  $P = 0.67$ ), lesion area still dramatically differed (109,824  $\pm$  4304  $\mu\text{m}^2/\text{section}$  and 35,722  $\pm$  4206  $\mu\text{m}^2/\text{section}$ ,  $P < 0.001$ ), strongly suggesting that the E2-induced decrease of serum cholesterol is not the main factor preventing fatty streak formation.

Histo- as well as immunohistochemical analysis showed that, under E2 treatment, residual lesions were essentially fatty streaks containing lipid-laden macrophages, with few characteristics of advanced lesions such as fibrous caps and were substantially less complex than lesions in ovariectomized ApoE<sup>-/-</sup> control mice (not shown). Remarkably, T lymphocytes were still detectable at a comparable density (2  $\pm$  1%) in these residual lesions (Figure 4). Similar observations were made in all of the series of specifically immunodeficient mice including the ApoE<sup>-/-</sup>/TCR $\beta$ <sup>-/-</sup> (Figure 4).

In the rest of the aorta, lesions were identifiable by *en face* analysis at predilection sites including the aortic arch and the orifices of the brachiocephalic, left subclavian, common carotid, and intercostal arteries. However, the level was low (<3.0% of the total aortic area) except in the ApoE<sup>-/-</sup>/CD4<sup>-/-</sup> group of mice (13.5  $\pm$  3.0%,  $n = 3$ ). In this last group, lesions were observed at the predilection sites and also at the orifice of the large abdominal arteries, in particular the celiac trunk and renal arteries. E2 induced a spectacular (more than fivefold)



Figure 4. Anti-CD3 immunolabeling of representative lesions from ovariectomized ApoE<sup>-/-</sup>, ApoE<sup>-/-</sup>/TCR $\beta$ <sup>-/-</sup>, and ApoE<sup>-/-</sup>/TCR $\delta$ <sup>-/-</sup> mice after 3 months of treatment with E2 pellets.

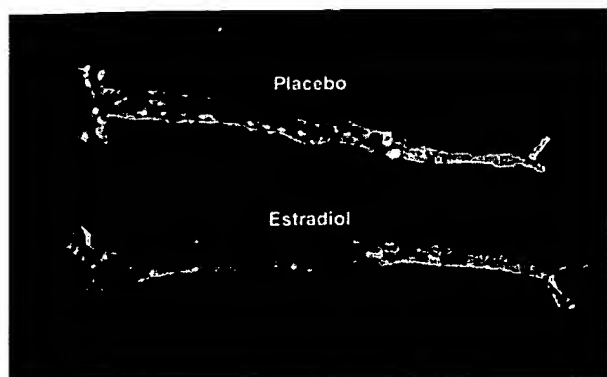


**Figure 5.** Representative *en face* aorta preparations from placebo- and E2-treated ovariectomized ApoE<sup>-/-</sup>/CD4<sup>-/-</sup> mice.

protective effect at these different sites, especially in the ApoE<sup>-/-</sup>/CD4<sup>-/-</sup> group (<3.0%, *n* = 3; Figure 5).

## Discussion

The present results definitely demonstrate that, in the C57BL/6 mouse strain, mature lymphocytes are required for the preventive effect of E2 on the atheromatous process irrespective of the model of genetically-induced hypercholesterolemia, namely ApoE<sup>-/-</sup> and LDLr<sup>-/-</sup> mice. Indeed, after bone marrow transplantation from immunocompetent donors into immunodeficient mice, lymphocytes were recovered in the lesions and a significant increase in the level of these lesions could be demonstrated. Most importantly, E2 activity was restored after bone marrow transplantation from immunocompetent donors, while E2 was still inactive after bone marrow transplantation from immunodeficient donors to the immunodeficient recipients.

Like our data obtained in intact nonovariectomized mice,<sup>12</sup> the measurement of lesion area in placebo-treated ovariectomized mice show a similar level of lesions in immunocompetent and immunodeficient mice, except in the ApoE<sup>-/-</sup>/TCRβ<sup>-/-</sup> mice, supporting the deleterious role of αβ T lymphocytes in the atheromatous process. Noteworthy, considering our previous<sup>12</sup> and present data, a protective effect of endogenous ovarian estrogens could be demonstrated in all strains because ovariectomized mice developed a higher level of lesions than intact mice. This observation is in accordance with a previous report.<sup>21</sup> Moreover, E2 treatment, administered at a dose previously defined as adequate for a maximal effect,<sup>15</sup> induced a significant decrease in lesion size in all groups of mice (Table 3). Except in ApoE<sup>-/-</sup>/TCRβ<sup>-/-</sup> mice, the residual lesion level was lower than that measured in intact female mice.<sup>12</sup> In addition, *en face* analysis showed that the effect of E2 was not restricted to the aortic sinus. Interestingly, E2 exerted a stronger preventive effect of lesion development in the thoracic and abdominal sites than at the level of the aortic sinus, particularly in ApoE<sup>-/-</sup>/CD4<sup>-/-</sup> mice (Figure 5). Although the selective immune deficiency may generate compensatory expansion of other lymphocyte subsets, such as ApoE<sup>-/-</sup>/CD4<sup>-/-</sup> mice presenting with a greater number

of CD8<sup>+</sup> and double-negative CD4-CD8 cells than ApoE<sup>-/-</sup> mice,<sup>12,22</sup> we demonstrate here that E2 was active in all strains, suggesting that no single T-lymphocyte subpopulation directly mediated the protective effect. This included the populations of regulatory T cells able to control the expansion and differentiation of activated T cells<sup>23,24</sup> and the TCRγδ<sup>+</sup> T cells. E2 has been recently claimed to induce one of these regulatory T-lymphocyte subpopulations<sup>25,26</sup> suggesting that it could play a key role in the suppression of harmful immune responses. Our data do not support such a hypothesis in the atherosclerotic process. Finally, the protective effect was also maintained in B-lymphocyte-deficient mice. This excluded a protective role mediated by immunoglobulins that are known to increase under E2 stimulation<sup>27</sup> and have been suggested to prevent atherosclerosis.<sup>27-30</sup>

Interestingly, E2 administration significantly decreased serum cholesterol levels in nearly all conditions analyzed in the present work. However, although serum cholesterol level remains a key determinant of atherosclerosis, several lines of evidence support the fact that the protective effect of E2 occurs mainly at the level of the arterial wall. First, although E2 decreased serum cholesterol levels in immunodeficient LDLr<sup>-/-</sup>/RAG-2<sup>-/-</sup> mice (the present work) as well as ApoE<sup>-/-</sup>/RAG-2<sup>-/-</sup> mice<sup>14</sup> to a similar extent than in immunocompetent mice, it was completely inactive on lesion area. Second, although the maximal decrease of serum cholesterol was obtained with endogenous E2 (Table 3), the maximal decrease in lesion area required higher E2 doses, in line with previous reports.<sup>15,21</sup> Third, in subgroups of ovariectomized placebo- or E2-treated ApoE<sup>-/-</sup> mice arbitrarily selected for similar serum cholesterol levels, fatty streak area was threefold lower in the latter group. Indeed, using cholesterol-clamped rabbits, Holm and colleagues<sup>31</sup> had previously demonstrated a plasma lipid-independent anti-atherogenic effect of estrogen, in line with Adams and co-workers,<sup>32</sup> who suggested, as early as 1990, a similar conclusion in surgically postmenopausal monkeys.

Altogether, these series of observation points to one (or more) additional lymphocyte-dependent mechanism(s) involved in the protective effect of E2. E2 is a negative regulator of lymphopoiesis, that selectively depletes functional precursors of B and T cells.<sup>33</sup> It also inactivates the intrathymic T-cell differentiation pathway and induces thymocyte apoptosis.<sup>34</sup> Indeed, we observed a remarkable 80% thymic atrophy (85.2 ± 7.5 mg versus 14.1 ± 1.8 mg) and 50% decrease of circulating lymphocytes in our E2-treated ApoE<sup>-/-</sup> mice (6804 ± 568 per μl versus 3520 ± 215 per μl; *P* < 0.001). However, in agreement with Hodgkin and colleagues,<sup>35</sup> T lymphocytes were still detectable in the residual lesions (Figure 3), showing that, despite their decrease in blood, lymphocytes could still reach and infiltrate the remaining lesions.

The protective effect could also be mediated through the modulation of the interactions between lymphocytes and other cell populations, such as endothelial and/or antigen-presenting cells, leading to a local control of the intimal immune process. First, Shi and colleagues<sup>36,37</sup> recently provided strong evidence for the crucial role of

endothelial cells rather than hematopoietic cells as determinants of atherosclerosis susceptibility in C57BL/6 mice. Second, decreased proinflammatory<sup>38–40</sup> or increased anti-inflammatory cytokine<sup>41,42</sup> production resulting from the local interaction between lymphocytes and antigen-presenting cells could explain the protective effect of E2. Indeed, it has recently been reported that estrogens repress Th1 activity and T-cell production of the key inflammatory cytokine tumor necrosis factor- $\alpha$  in bone<sup>43</sup> but we reported the opposite effect in antigen-specific CD4<sup>+</sup> or NKT cell response.<sup>44,45</sup> Further work will be necessary to precisely define the mechanisms of these interactions.

In conclusion, we have demonstrated that lymphocytes are instrumental in the protective effect of E2 but that no single lymphocyte subpopulation is specifically required for this effect. These data point to additional lymphocyte-dependent mechanisms such as modulating the interactions among lymphocytes and between lymphocytes and endothelial and/or antigen-presenting cells.

### Acknowledgments

We thank Mrs. M.J. Fouque, P. Guillou, and M. Larribe for technical and secretarial assistance.

### References

- Waters DD, Gordon D, Rossouw JE, Cannon III RO, Collins P, Herrington DM, Hsia J, Langer R, Mosca L, Ouyang P, Sopko G, Stefanick ML: Women's ischemic syndrome evaluation: current status and future research directions: report of the National Heart, Lung and Blood Institute Workshop: October 2–4, 2002: section 4: lessons from hormone replacement trials. *Circulation* 2004, 109:e53–e55
- Hulley S, Grady D, Bush T, Furberg C, Herrington D, Riggs B, Vittinghoff E: Randomized trial of estrogen plus progestin for secondary prevention of coronary heart disease in postmenopausal women. Heart and Estrogen/Progestin Replacement Study (HERS) Research Group. *JAMA* 1998, 280:605–613
- Rossouw JE, Anderson GL, Prentice RL, LaCroix AZ, Kooperberg C, Stefanick ML, Jackson RD, Beresford SA, Howard BV, Johnson KC, Kotchen JM, Ockene J: Risks and benefits of estrogen plus progestin in healthy postmenopausal women: principal results from the Women's Health Initiative randomized controlled trial. *JAMA* 2002, 288:321–333
- Arnall JF, Gourdy P, Elhage R, Garmy-Susini B, Delmas E, Bouchet L, Castano C, Barreira Y, Couloumiers JC, Prats H, Prats AC, Bayard F: Estrogens and atherosclerosis. *Eur J Endocrinol* 2004, 150:113–117
- Hodgins JB, Maeda N: Minireview: estrogen and mouse models of atherosclerosis. *Endocrinology* 2002, 143:4495–4501
- Ross R: Atherosclerosis—an inflammatory disease. *N Engl J Med* 1999, 340:115–125
- Hansson GK, Libby P, Schonbeck U, Yan ZQ: Innate and adaptive immunity in the pathogenesis of atherosclerosis. *Circ Res* 2002, 91:281–291
- Binder CJ, Chang MK, Shaw PX, Miller YI, Hartvigsen K, Dewan A, Witztum JL: Innate and acquired immunity in atherogenesis. *Nat Med* 2002, 8:1218–1226
- Roselaar SE, Kakkannathu PX, Daugherty A: Lymphocyte populations in atherosclerotic lesions of apoE<sup>−/−</sup> and LDL receptor<sup>−/−</sup> mice. Decreasing density with disease progression. *Arterioscler Thromb Vasc Biol* 1996, 16:1013–1018
- Song L, Leung C, Schindler C: Lymphocytes are important in early atherosclerosis. *J Clin Invest* 2001, 108:251–259
- Reardon CA, Blachowicz L, White T, Cabana V, Wang Y, Lukens J, Bluestone J, Getz GS: Effect of immune deficiency on lipoproteins and atherosclerosis in male apolipoprotein E-deficient mice. *Arterioscler Thromb Vasc Biol* 2001, 21:1011–1016
- Elhage R, Gourdy P, Bouchet L, Jawien J, Fouque M-J, Fiévet C, Huc X, Barreira Y, Couloumiers J-C, Arnall J-F, Bayard F: Deleting TCR $\alpha$  or CD4<sup>+</sup> T lymphocytes leads to opposite effects on site-specific atherosclerosis in female apolipoprotein E-deficient mice. *Am J Pathol* 2004, 165:2013–2019
- Zhou X, Nicoletti A, Elhage R, Hansson GK: Transfer of CD4(+) T cells aggravates atherosclerosis in immunodeficient apolipoprotein E knockout mice. *Circulation* 2000, 102:2919–2922
- Elhage R, Clamens S, Reardon-Alulis C, Getz GS, Fievet C, Maret A, Arnall JF, Bayard F: Loss of atheroprotective effect of estradiol in immunodeficient mice. *Endocrinology* 2000, 141:462–465
- Elhage R, Arnall JF, Pierragi M-T, Duverger N, Fiévet C, Faye JC, Bayard F: Estradiol-17 $\beta$  prevents fatty streak formation in apolipoprotein E-deficient mice. *Arterioscler Thromb Vasc Biol* 1997, 17:2679–2684
- Ishibashi S, Goldstein JL, Brown MS, Herz J, Burns DK: Massive xanthomatosis and atherosclerosis in cholesterol-fed low density lipoprotein receptor-negative mice. *J Clin Invest* 1994, 93:1885–1893
- Shinkai Y, Rathbun G, Lam KP, Oltz EM, Stewart V, Mendelsohn M, Charron J, Datta M, Young F, Stall AM, Alt FW: RAG-2-deficient mice lack mature lymphocytes owing to inability to initiate V(D)J rearrangement. *Cell* 1992, 68:855–867
- Kitamura D, Roes J, Kuhn R, Rajewsky K: A B cell-deficient mouse by targeted disruption of the membrane exon of the immunoglobulin mu chain gene. *Nature* 1991, 350:423–426
- Duez H, Chao YS, Hernandez M, Torpieri G, Poulain P, Mundt S, Mallat Z, Teissier E, Burton CA, Tedgui A, Fruchart JC, Fievet C, Wright SD, Staels B: Reduction of atherosclerosis by the peroxisome proliferator-activated receptor alpha agonist fenofibrate in mice. *J Biol Chem* 2002, 277:48051–48057
- Marsh MM, Walker VR, Curtiss LK, Banka CL: Protection against atherosclerosis by estrogen is independent of plasma cholesterol levels in LDL receptor-deficient mice. *J Lipid Res* 1999, 40:893–900
- Bourassa P-A, Milos PM, Gaynor BJ, Breslow JL, Aiello RJ: Estrogen reduces atherosclerotic lesion development in apolipoprotein E-deficient mice. *Proc Natl Acad Sci USA* 1996, 93:10022–10027
- Shedlock DJ, Whitmire JK, Tan J, MacDonald AS, Ahmed R, Shen H: Role of CD4 T cell help and costimulation in CD8 T cell responses during *Listeria monocytogenes* infection. *J Immunol* 2003, 170:2053–2063
- Shevach EM, McHugh RS, Piccirilli CA, Thornton AM: Control of T-cell activation by CD4<sup>+</sup> CD25<sup>+</sup> suppressor T cells. *Immunol Rev* 2001, 182:58–67
- Roncarolo MG, Bacchetta R, Bordignon C, Narula S, Levings MK: Type 1 T regulatory cells. *Immunol Rev* 2001, 182:68–79
- Matejuk A, Bakke AC, Hopke C, Dwyer J, Vandenbark AA, Offner H: Estrogen treatment induces a novel population of regulatory cells, which suppresses experimental autoimmune encephalomyelitis. *J Neurosci Res* 2004, 77:119–126
- Polanczyk MJ, Carson BD, Subramanian S, Afentoulis M, Vandenbark AA, Ziegler SF, Offner H: Cutting edge: estrogen drives expansion of the CD4<sup>+</sup>CD25<sup>+</sup> regulatory T cell compartment. *J Immunol* 2004, 173:2227–2230
- Caligiuri G, Nicoletti A, Poirier B, Hansson GK: Protective immunity against atherosclerosis carried by B cells of hypercholesterolemic mice. *J Clin Invest* 2002, 109:745–753
- Verthelyi DI, Ahmed SA: Estrogen increases the number of plasma cells and enhances their autoantibody production in nonautoimmune C57BL/6 mice. *Cell Immunol* 1998, 189:125–134
- Horkko S, Bird DA, Miller E, Itabe H, Leitinger N, Subbanagounder G, Berliner JA, Friedman P, Dennis EA, Curtiss LK, Palinski W, Witztum JL: Monoclonal autoantibodies specific for oxidized phospholipids or oxidized phospholipid-protein adducts inhibit macrophage uptake of oxidized low-density lipoproteins. *J Clin Invest* 1999, 103:117–128
- Major AS, Fazio S, Linton MF: B-lymphocyte deficiency increases atherosclerosis in LDL receptor-null mice. *Arterioscler Thromb Vasc Biol* 2002, 22:1892–1898
- Holm P, Korsgaard N, Shalmi M, Andersen HL, Hougaard P, Skouby SO, Stender S: Significant reduction of the antiatherogenic effect of estrogen by long-term inhibition of nitric oxide synthesis in cholesterol-clamped rabbits. *J Clin Invest* 1997, 100:821–828

32. Adams MR, Kaplan JR, Manuck SB, Koritnik DR, Parks JS, Wolfe MS, Clarkson TB: Inhibition of coronary artery atherosclerosis by 17-beta estradiol in ovariectomized monkeys. Lack of an effect of added progesterone. *Arteriosclerosis* 1990, 10:1051-1057
33. Medina KL, Garrett KP, Thompson LF, Rossi MI, Payne KJ, Kincade PW: Identification of very early lymphoid precursors in bone marrow and their regulation by estrogen. *Nat Immunol* 2001, 2:718-724
34. Okasha SA, Ryu S, Do Y, McKallip RJ, Nagarkatti M, Nagarkatti PS: Evidence for estradiol-induced apoptosis and dysregulated T cell maturation in the thymus. *Toxicology* 2001, 163:49-62
35. Hodgins JB, Kregel JH, Reddick RL, Korach KS, Smithies O, Maeda N: Estrogen receptor alpha is a major mediator of 17beta-estradiol's atheroprotective effects on lesion size in ApoE<sup>-/-</sup> mice. *J Clin Invest* 2001, 107:333-340
36. Shi W, Haberland ME, Jien ML, Shih DM, Lusis AJ: Endothelial responses to oxidized lipoproteins determine genetic susceptibility to atherosclerosis in mice. *Circulation* 2000, 102:75-81
37. Shi W, Wang NJ, Shih DM, Sun VZ, Wang X, Lusis AJ: Determinants of atherosclerosis susceptibility in the C3H and C57BL/6 mouse model: evidence for involvement of endothelial cells but not blood cells or cholesterol metabolism. *Circ Res* 2000, 86:1078-1084
38. Gupta S, Pablo AM, Jiang X, Wang N, Tall AR, Schindler C: IFN-gamma potentiates atherosclerosis in ApoE knock-out mice. *J Clin Invest* 1997, 99:2752-2761
39. Lee TS, Yen HC, Pan CC, Chau LY: The role of interleukin 12 in the development of atherosclerosis in ApoE-deficient mice. *Arterioscler Thromb Vasc Biol* 1999, 19:734-742
40. Elhage R, Jawien J, Rudling M, Ljunggren HG, Takeda K, Akira S, Bayard F, Hansson GK: Reduced atherosclerosis in interleukin-18 deficient apolipoprotein E-knockout mice. *Cardiovasc Res* 2003, 59:234-240
41. Mailat Z, Besnard S, Duriez M, Deleuze V, Emmanuel F, Bureau MF, Soubrier F, Esposito B, Duez H, Fievet C, Staels B, Duverger N, Scherman D, Tedgui A: Protective role of interleukin-10 in atherosclerosis. *Circ Res* 1999, 85:e17-e24
42. Robertson AKL, Rudling M, Zhou X, Gorelik L, Flavell RA, Hansson GK: Disruption of TGF-(beta) signaling in T cells accelerates atherosclerosis. *J Clin Invest* 2003, 112:1342-1350
43. Cenci S, Toraldo G, Weitzmann MN, Roggia C, Gao Y, Qian WP, Sierra O, Pacifici R: Estrogen deficiency induces bone loss by increasing T cell proliferation and lifespan through IFN-gamma-induced class II transactivator. *Proc Natl Acad Sci USA* 2003, 100:10405-10410
44. Maret A, Coudert JD, Garidou L, Foucras G, Gourdy P, Krust A, Dupont S, Chambon P, Druet P, Bayard F, Guery JC: Estradiol enhances primary antigen-specific CD4 T cell responses and Th1 development in vivo. Essential role of estrogen receptor alpha expression in hematopoietic cells. *Eur J Immunol* 2003, 33:512-521
45. Gourdy P, Araujo LM, Zhu R, Garmy-Susini B, Diem S, Laurell H, Leite-De-Moraes M, Dy M, Arnal JF, Bayard F, Herbelin A: Relevance of sexual dimorphism to regulatory T cells: estradiol promotes IFN-gamma production by invariant natural killer T cells. *Blood* 2005, 105:2415-2420



## Hypercholesterolemia in Low Density Lipoprotein Receptor Knockout Mice and its Reversal by Adenovirus-mediated Gene Delivery

Shun Ishibashi,\* Michael S. Brown,\* Joseph L. Goldstein,\* Robert D. Gerard,† Robert E. Hammer,\*\* and Joachim Herz\*  
Departments of \*Molecular Genetics and †Biochemistry and ‡Howard Hughes Medical Institute, University of Texas Southwestern Medical Center at Dallas, Dallas, Texas 75235

### Abstract

We employed homologous recombination in embryonic stem cells to produce mice lacking functional LDL receptor genes. Homozygous male and female mice lacking LDL receptors (*LDLR*<sup>-/-</sup> mice) were viable and fertile. Total plasma cholesterol levels were twofold higher than those of wild-type littermates, owing to a seven- to ninefold increase in intermediate density lipoproteins (IDL) and LDL without a significant change in HDL. Plasma triglyceride levels were normal. The half-lives for intravenously administered <sup>125</sup>I-VLDL and <sup>125</sup>I-LDL were prolonged by 30-fold and 2.5-fold, respectively, but the clearance of <sup>125</sup>I-HDL was normal in the *LDLR*<sup>-/-</sup> mice. Unlike wild-type mice, *LDLR*<sup>-/-</sup> mice responded to moderate amounts of dietary cholesterol (0.2% cholesterol/10% coconut oil) with a major increase in the cholesterol content of IDL and LDL particles. The elevated IDL/LDL level of *LDLR*<sup>-/-</sup> mice was reduced to normal 4 d after the intravenous injection of a recombinant replication-defective adenovirus encoding the human LDL receptor driven by the cytomegalovirus promoter. The virus restored expression of LDL receptor protein in the liver and increased the clearance of <sup>125</sup>I-VLDL. We conclude that the LDL receptor is responsible in part for the low levels of VLDL, IDL, and LDL in wild-type mice and that adenovirus-encoded LDL receptors can acutely reverse the hypercholesterolemic effects of LDL receptor deficiency. (*J. Clin. Invest.* 1993. 92:883-893.) Key words: homologous recombination • lipoprotein metabolism • very low density lipoprotein • gene therapy • liver receptors

### Introduction

The LDL receptor removes cholesterol-rich intermediate density lipoproteins (IDL)<sup>1</sup> and LDL from plasma and thereby regulates the plasma cholesterol level (1). The lipoproteins that

bind to the LDL receptor are derived from triglyceride-rich VLDL, which are secreted by the liver. In the circulation some of the triglycerides of VLDL are removed by lipoprotein lipase, and the resultant IDL particle is cleared rapidly into the liver, owing to its content of apolipoprotein E (apo E), a high affinity ligand for the LDL receptor. Some IDL particles escape hepatic uptake and are converted to LDL in a reaction that leads to the loss of apo E. The sole remaining protein, apo B-100, binds to LDL receptors with relatively low affinity, thus causing LDL particles to circulate for relatively prolonged periods (2).

Triglyceride-depleted, cholesterol-rich remnants of intestinal chylomicrons are taken into the liver by the LDL receptor and by a genetically distinct molecule designated the chylomicron remnant receptor (3, 4). The latter receptor recognizes apo E when it is present on chylomicron remnant particles together with apo B-48, a truncated version of apo B-100 that is produced in the intestine (3). Circumstantial evidence suggests that the chylomicron remnant receptor is the same as the LDL receptor-related protein/ $\alpha_2$ -macroglobulin receptor (LRP) (4). The action of this receptor may be facilitated by the preliminary binding of the chylomicron remnants to cell-associated glycosaminoglycans in hepatic sinusoids (5).

Genetic defects in the LDL receptor produce hypercholesterolemia in humans with familial hypercholesterolemia (FH) (6), Watanabe-heritable hyperlipidemic (WHHL) rabbits (7), and rhesus monkeys (8). Humans and rabbits with two defective LDL receptor genes (FH and WHHL homozygotes) have massively elevated levels of IDL and LDL, and they develop fulminant atherosclerosis at an early age. Tracer studies with <sup>125</sup>I-labeled lipoproteins revealed a retarded clearance of IDL and LDL, and an increased conversion of IDL to LDL in humans (9) and rabbits (10) with LDL receptor deficiency.

Evidence from one human pedigree (11) and from monozygotic/dizygotic twin pair correlations (12) indicates that other genes can influence the degree of hypercholesterolemia in subjects with LDL receptor deficiency. These genes are likely to influence cholesterol levels even in people with normal LDL receptors. Identification of these genes has not been possible in human linkage studies, nor in breeding experiments with WHHL rabbits. Linkage studies would be facilitated by the availability of an inbred mouse strain with LDL receptor deficiency. The consequences of LDL receptor deficiency in mice are difficult to predict because mice, like rats, have a fundamental difference in LDL metabolism when compared with other species that have been studied (13). In mice and rats a substantial fraction of the VLDL secreted from liver contains apo B-48 instead of apo B-100 (14-16). Remnants derived from the apo B-48 containing particles are cleared into the liver and are not converted to LDL (17). Some of this clearance may be mediated by the chylomicron remnant receptor. For this reason, LDL receptor deficiency in mice would not be predicted to raise the plasma LDL level as profoundly as it does in WHHL rabbits.

Received for publication 1 April 1993.

1. Abbreviations used in this paper: AdCMV-Luc, recombinant adenovirus containing luciferase cDNA; AdCMV-LDLR, recombinant adenovirus containing human LDL receptor cDNA; CMV, cytomegalovirus; ES, embryonic stem cells; FH, familial hypercholesterolemia; FPLC, fast performance liquid chromatography; IDL, intermediate density lipoproteins; LRP, LDL receptor-related protein/ $\alpha_2$ -macroglobulin receptor; *LDLR*<sup>-/-</sup> and *LDLR*<sup>+/-</sup>, mice homozygous and heterozygous, respectively, for LDL receptor gene disruption; pfu, plaque-forming units; WHHL, Watanabe-heritable hyperlipidemic rabbits.

J. Clin. Invest.

© The American Society for Clinical Investigation, Inc.  
0021-9738/93/08/0883/11 \$2.00  
Volume 92, August 1993, 883-893



Mice deficient in LDL receptors might also aid in the development of gene therapy techniques designed to enhance the expression of hepatic LDL receptors. Using homozygous WHHL rabbits as a model, Chowdhury et al. (18) infected autologous hepatocytes *ex vivo* with a recombinant retrovirus carrying an expressible cDNA copy of the rabbit LDL receptor under control of the chicken  $\beta$ -actin promoter. After infusion of these transduced hepatocytes into the spleen, LDL receptor expression was visualized in 2–4% of liver cells. Although functional studies of  $^{125}\text{I}$ -LDL turnover were not performed, these workers observed a fall of  $\sim 30\%$  in the level of total plasma cholesterol, which did not occur in animals injected with hepatocytes transduced with a control retrovirus encoding an irrelevant protein. With this technique the expression of LDL receptors persisted for 2–4 mo. Although the 30% reduction in plasma cholesterol was statistically significant, the level remained quite elevated (above 500 mg/dl) when compared with normal rabbits, ( $< 100$  mg/dl), presumably owing to the expression of LDL receptors in only a small percentage of hepatocytes. Similar results were obtained in transient experiments following the intravenous injection of a plasmid containing the LDL receptor cDNA complexed to an asialo-orosomucoid/poly-L-lysine conjugate (19).

In mice, gene manipulation has produced significant effects on LDL receptor expression. Several years ago Hofmann et al. (20) and Yokode et al. (21) produced transgenic mice that overexpressed hepatic LDL receptors encoded by the human LDL receptor gene driven by the metallothionein or transferrin promoter. They showed that these receptors enhanced the clearance of radiolabeled LDL from plasma of normal mice. Yokode et al. (22) then demonstrated that these mice were resistant to the cholesterol-elevating effects of a high cholesterol diet.

Recently, Herz and Gerard (23) developed a recombinant replication-defective adenovirus vector containing an expressible cDNA copy of the human LDL receptor driven by the cytomegalovirus (CMV) promoter. 4 d after its intravenous injection, this virus elicited the expression of high levels of human LDL receptors in more than 90% of mouse hepatocytes, and this enhanced markedly the uptake of  $^{125}\text{I}$ -LDL by the liver. The use of adenovirus vectors was based on the observations of Stratford-Perricaudet et al. (24), who injected recombinant adenoviruses encoding ornithine transcarbamylase into neonatal mice homozygous for a defect in this gene. The recombinant adenovirus produced a level of enzyme activity in liver sufficient to eliminate the pathologic manifestations of the disease, and expression apparently persisted for 1 yr.

The current studies were conducted in order to learn the consequences of LDL receptor deficiency in mice and to learn whether adenovirus vectors will acutely reverse these consequences. For these purposes, we have used the techniques of homologous recombination in cultured embryonic stem (ES) cells (25–27) to produce mice that lack functional LDL receptors. We show that these mice develop a marked elevation in plasma IDL and LDL levels when compared with control mice and that this elevation can be eliminated acutely by the intravenous administration of a recombinant adenovirus encoding the human LDL receptor.

## Methods

**General methods.** Unless otherwise indicated, DNA manipulations were performed by standard techniques (28). Immunoblot (29) and

ligand blot analyses (30) were performed as described in the indicated references. Cholesterol and triglycerides were determined enzymatically with assay kits obtained from Boehringer Mannheim (Biochemicals, Indianapolis, IN) and Sigma Chemical Co. (St. Louis, MO), respectively. The normal mouse diet (Teklad 4% Mouse/Rat Diet 7001 from Harlan Teklad Premier Laboratory Diets, Madison, WI) contained 4% (wt/wt) animal fat with  $< 0.04\%$  (wt/wt) cholesterol. Mouse VLDL ( $d < 1.006$  g/ml), LDL ( $d 1.025$ – $1.50$  g/ml), and HDL ( $d 1.063$ – $1.215$  g/ml) were isolated by sequential ultracentrifugation (31) from pooled plasma obtained from *LDLR*<sup>-/-</sup> mice that had been fasted overnight. Rabbit VLDL ( $d < 1.006$  g/ml) was isolated by the same procedure from plasma obtained from fasted WHHL rabbits. Lipoproteins were radiolabeled with  $^{125}\text{I}$  by the iodine monochloride method (31). A 0.2% cholesterol/10% coconut oil diet was prepared by supplementing the normal mouse diet with 0.2% (wt/wt) cholesterol dissolved in a final concentration of 10% (vol/wt) coconut oil.

**Cloning of mouse LDL receptor cDNA.** Mouse LDL receptor cDNA was amplified by PCR from mouse liver first strand cDNA using poly(A)<sup>+</sup> RNA and the following primers:

Primer A, 5'-ATTCTAGAGGGTGAAGTGGTGTGAG-3' (exon 14);

Primer B, 5'-ATAATTCACCTGACCATCTGTCTCGAGGGGTAG-3' (exon 18);

Primer C, 5'-AAATG(T/C)ATC(T/G)(T/C)C(T/A)GCAAGTGGGTCTG(C/T)GA(T/C)GGCAG-3' (exon 2);

Primer D 5'-CTGCTCCTCATTCCCTCTGCCAGCCA-3' (exon 16).

Amplification with primers A and B yielded a cDNA fragment corresponding to exons 14–18. cDNA spanning exons 2–16 was amplified with primers C and D. Primers A, B, and C were designed and based on the conservation of the LDL receptor coding sequence between human, rabbit, hamster, rat, and cow (32, 33). Primer D was designed and based on the mouse exon 16 cDNA sequence contained in the amplification product obtained with primers A and B. Amplification products were blunt-end cloned into pGEM3Zf(+) (Promega Corp., Madison, WI) and sequenced.

**Construction of gene replacement vector.** Southern blot analysis of mouse C57B1/6 genomic DNA with an exon 2–16 cDNA probe revealed a 16-kb BamHI fragment. This fragment was enriched by sucrose density ultracentrifugation and cloned into the  $\lambda$ Dash II vector (Stratagene Corp., La Jolla, CA), and recombinant phages containing the fragment were isolated by plaque screening. After subcloning into pGEM3Zf(+), the *Pol2sneobpA* expression cassette (34) was inserted into a unique SalI site in exon 4 (Fig. 1). This *neo* expression cassette was flanked by 12 kb of LDL receptor genomic sequences including exons 1 to 4. The short arm of the targeting vector contained a 1.2-kb SalI-SacI fragment with sequences of exon 4 and intron 4. The SalI sites were destroyed during the cloning. Two copies of the herpes simplex thymidine kinase gene (35) were inserted in tandem at the 3' end of the short arm of the targeting vector (Fig. 1).

**ES cell culture.** Mouse ES cells (AB-1, kindly provided by A. Bradley, Baylor College of Medicine, Houston) were cultured on leukemia inhibitory factor-producing STO feeder cells as described (36). Approximately  $2 \times 10^7$  cells were electroporated with linearized targeting vector (25  $\mu\text{g}/\text{ml}$ , 275 V, 330  $\mu\text{F}$ ) in an electroporator (GIBCO Bethesda Research Laboratories) and seeded onto irradiated feeder layers (10,000 rad). After selection with 190  $\mu\text{g}/\text{ml}$  G418 and 0.25  $\mu\text{M}$  1-[2-deoxy, 2-fluoro- $\beta$ -D-arabinofuranosyl]-5-iodouracil (FlAU; Bristol-Myers Co., New York, NY) recombinant clones were identified by PCR as described (34) using Primers E and F (Primer E, located in 3'-untranslated region of *neo* cassette, 5'-GATTGGGAAGACAATAGCAGGCATGC-3'; Primer F, located in intron 4, 5'-GGCAAGATGGCTCAGCAAGCAAAGGC-3'). Homologous recombination was verified by Southern blot analysis after BamHI digestion and probing with a genomic DNA fragment located 3' of the targeting construct (Fig. 1). Nine independent stem cell clones containing a disrupted LDL receptor allele were injected into C57B1/6 blastocysts (27), yielding a total of 17 chimeric males whose coat color (agouti) indi-

cated a contribution of stem cells ranging from 30 to 100%. Of the 17 chimeric males, 15 were fertile, and 13 gave offspring that carried the disrupted LDL receptor allele. Five of these males exclusively transmitted the stem cell-derived genome through the germline. All experiments were performed with the F2 or F3 generation descendants, which were hybrids between the C57B1/6J and 129Sv strains.

**Plasma lipoprotein analysis.** Blood was sampled from the retro-orbital plexus into tubes containing EDTA (Microvette CB 1000 capillary tubes; Sarstedt, Inc., Newton, NC). Pooled mouse plasma (0.6 ml from 3 to 5 mice) was ultracentrifuged at  $d = 1.215$  g/ml, and the resulting lipoprotein fraction ( $d < 1.215$  g/ml) was subjected to fast performance liquid chromatography (FPLC) gel filtration on a Superose 6 (Sigma Chemical Co.) column as previously described (22). For apoprotein analysis, peak fractions were pooled, precipitated with trichloroacetic acid, washed with acetone, and subjected to electrophoresis on 3–15% SDS polyacrylamide gels as described (22). Gels were calibrated with Rainbow high molecular weight markers (Amersham Corp., Arlington Heights, IL) and stained with Coomassie blue.

**Preparation of recombinant adenoviruses.** Recombinant replication-deficient adenoviruses containing the firefly luciferase cDNA (AdCMV-Luc) and the human LDL receptor cDNA (AdCMV-LDLR) driven by the cytomegalovirus promoter/enhancer were prepared as previously described (23). Briefly, virus particles for injection into animals were grown on human embryonic kidney 293 cells and purified by cesium chloride density gradient centrifugation. Particles were further purified by gel filtration on a Sepharose CL-4B (Pharmacia LKB Biotechnology, Piscataway, NJ) column equilibrated with 10 mM Tris-HCl, 137 mM NaCl, 5 mM KCl, 1 mM MgCl<sub>2</sub> at pH 7.4. BSA was added at a final concentration of 1 mg/ml, after which each virus preparation was stored in multiple aliquots at  $-70^{\circ}\text{C}$ . Viruses were titered on 293 cells; the titer ranged between  $10^{10}$  and  $10^{11}$  plaque-forming units (pfu) per ml.

For administration to mice, each recombinant adenovirus was injected as a single dose ( $2 \times 10^9$  pfu in 200  $\mu\text{l}$ ) into the external jugular vein of a nonfasted animal that had been anesthetized with sodium pentobarbital as previously described (23).

**Immunohistochemistry.** Mice were killed 4 d after injection of recombinant virus, the liver was removed, and a sector extending from the surface of the liver to the portal area was immediately frozen (without fixation) in OCT Compound 4583 (Miles Laboratories, Inc., Elkhart, IN) at  $-196^{\circ}\text{C}$  and stored at  $-70^{\circ}\text{C}$  until cutting. For immunohistochemistry, sections of 6  $\mu\text{m}$  were cut on a Leitz Cryostat (E. Leitz, Inc., Rockleigh, NJ) at  $-20^{\circ}\text{C}$  and mounted onto polylysine-coated slides. Before immunostaining, tissue sections were fixed in 100% (vol/vol) methanol at  $-20^{\circ}\text{C}$  for 30 s followed by two washes in PBS. All incubations were performed at  $20^{\circ}\text{C}$ . Samples were blocked by incubation for 20 min with 50 mM Tris-HCl, 80 mM NaCl, 2 mM CaCl<sub>2</sub> at pH 8 containing 10% (vol/vol) fetal calf serum. Sections were then incubated for 1 h with 20  $\mu\text{g}/\text{ml}$  of polyclonal rabbit IgG directed against the bovine LDL receptor (37) followed by three 5-min washes with PBS. Bound primary antibody was detected by incubation for 45 min with the indicated concentrations of FITC-labeled goat anti-rabbit IgG (GIBCO Bethesda Research Laboratories, Gaithersburg, MD). Slides were washed again three times in PBS, rinsed once briefly in water, and mounted under a coverslip with DABCO (90% vol/vol glycerol, 50 mM Tris-HCl at pH 9, 25% (wt/vol) 1,4-diazadicyclo-[2.2.2]-octane).

## Results

To disrupt the LDL receptor gene in murine ES cells, we constructed a gene targeting vector of the replacement type (35) as described in Methods. The targeting vector and the expected genomic structure of the disrupted locus are shown in Fig. 1. The *neo* cassette was inserted into exon 4 of the LDL receptor gene. The disrupted locus is predicted to encode a nonfunctional protein that is truncated within the ligand binding do-

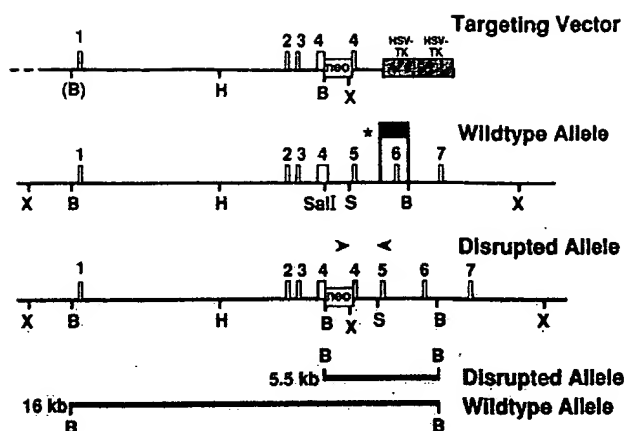


**Figure 1.** Strategy for targeted disruption of the LDL receptor locus in the mouse genome. A targeting vector of the replacement type was constructed as described in Methods. The *neo* gene is driven by the murine RNA polymerase II promoter and followed by the 3'-untranslated region of the bovine growth hormone gene containing the polyadenylation signal (34). The transcriptional direction of the *neo* gene is parallel to that of the LDL receptor. Two copies of the herpes simplex virus thymidine kinase gene (HSV-TK) (reference 35) flank the 3' homology segment. In the event of homologous recombination, the disrupted allele will have acquired additional sites for the restriction endonucleases *Bam*HI (B) and *Xba*I (X). The expected *Bam*HI digestion pattern resulting from a targeting event is shown at the bottom. The DNA probe used for Southern blotting (denoted by the asterisk and the heavy bracket) is a 1.7-kb *Bgl*II-*Bam*HI genomic fragment containing exon 6 and flanking intron sequences. The positions of the two oligonucleotides used for PCR diagnosis of homologous recombination are indicated by the arrows (oligo 1: 3' end of *neo* cassette; oligo 2: downstream of *Sac*I site in intron 4). B, *Bam*HI; H, *Hind*III; X, *Xba*I; S, *Sac*I.

main of the receptor. This receptor fragment should not bind LDL, and it should not remain associated with the cell membrane since it lacks the membrane spanning segment.

ES cells were electroporated with the linearized targeting vector and subjected to positive and negative selection using standard procedures (36). Homologous recombination events were detected by PCR and verified by digestion of genomic ES cell DNA with *Bam*HI. The presence of a diagnostic 5.5-kb *Bam*HI fragment in addition to the wild-type 16-kb fragment is indicative of gene targeting when the Southern blot is probed with a genomic DNA fragment located outside of the targeting vector (indicated by the asterisk in Fig. 1). The frequency of homologous recombination was very high. Approximately 50% of clones that were resistant to both G418 and FIAU exhibited homologous recombination.

Recombinant stem cell clones injected into C57B1/6 blastocysts (27) gave rise to chimeric animals with a stem cell-derived coat color contribution that ranged from 30 to 100%. Several male chimeras derived from independently targeted stem cell clones efficiently transmitted the stem cell-derived genome through the germ line. Offspring heterozygous for the disrupted LDL receptor allele were diagnosed by Southern blotting. When heterozygous animals were mated to each other, their offspring included animals that were wild-type (+/+), heterozygous (+/-), and homozygous (-/-) for the disrupted LDL receptor allele. Fig. 2 shows a representative

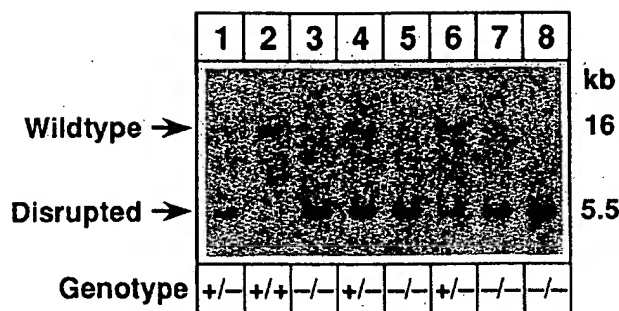


**Figure 2.** Genotypes of offspring from matings of *LDLR*<sup>+/-</sup> mice. Male and female mice heterozygous for the disrupted LDL receptor allele (+/-) were mated, and tail DNA from the offspring was analyzed by Southern blotting using a genomic DNA fragment located outside of the targeting construct (denoted by the asterisk in Fig. 1). The genotypes of one litter containing mice that are wild-type (+/+), heterozygous (+/-), or homozygous (-/-) for the disrupted LDL receptor allele are shown. The wild-type allele is represented by a band at 16 kb, while the disrupted allele creates a band at 5.5 kb when genomic DNA is digested with *Bam*HI (see Fig. 1).

genomic Southern blot that reveals the diagnostic bands for the wild-type and disrupted LDL receptor gene. Of 177 offspring from 28 heterozygous matings, the three genotypes were produced in the ratio of 47:93:37 (Table I), which is consistent with the expected Mendelian ratio of 1:2:1. Homozygous male and female animals were fertile and produced normal-sized litters when mated to each other.

To confirm the inability of the disrupted gene to produce full-length LDL receptors, we prepared liver membranes from wild-type, heterozygous, and homozygous animals. Proteins were solubilized with detergent, and 50  $\mu$ g of each sample were analyzed by SDS gel electrophoresis and immunoblotting with a polyclonal antibody that detects the mouse LDL receptor. As shown in Fig. 3 A, normal LDL receptor protein was readily detected by the antibody in wild-type (+/+, lanes 1 and 4) and in heterozygous animals (+/-, lane 2), but was undetectable in animals that were homozygous for the LDL receptor defect (-/-, lane 3). An abnormal band (marked by an asterisk) was present in liver membranes prepared from heterozygous (lane

**Table I. Plasma Cholesterol Concentrations in Offspring from 28 Matings between *LDLR*<sup>+/-</sup> Mice**

Sex	Total Plasma Cholesterol Level (mg/dl)		
	+/+	+/-	-/-
Male	119 $\pm$ 4 (n = 19)	158 $\pm$ 4 (n = 39)	228 $\pm$ 9 (n = 16)
Female	100 $\pm$ 4* (n = 28)	138 $\pm$ 4* (n = 54)	239 $\pm$ 8 (n = 21)

Total plasma cholesterol concentrations were measured from the indicated number (n) of male and female mice (nonfasting) that were wild-type (+/+), heterozygous (+/-), or homozygous (-/-) for a disrupted LDL receptor allele. The 177 mice arose from 28 litters born to crosses between heterozygous males and females. Genotype was determined by Southern blot analysis. Nonfasting blood samples were obtained between 46 and 56 d of age (mean age, 52 d).

\* Sex difference, *P* = 0.01 (unpaired *t* test).

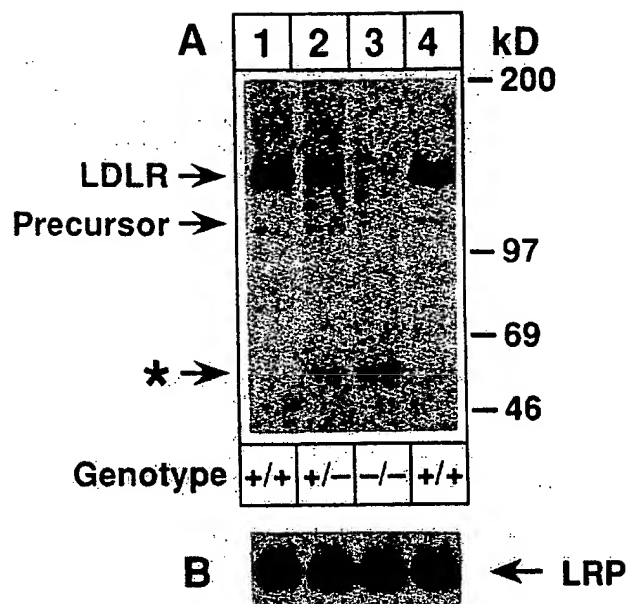


**Figure 3.** Immunoblot analysis of LDL receptors in liver membranes from mice carrying the disrupted LDL receptor allele. Liver membranes from mice that were wild-type (+/+, lanes 1 and 4), heterozygous (+/-, lane 2), or homozygous (-/-, lane 3) for the disrupted LDL receptor allele were solubilized with Triton X-100 as previously described (51). An aliquot of each sample (50  $\mu$ g protein) was subjected to 6.5% SDS-PAGE under nonreducing conditions, and the proteins were transferred to nitrocellulose filters for immunoblot analysis (A) and ligand blot analysis (B). The filter in A was incubated with 5  $\mu$ g/ml rabbit anti-LDL receptor IgG (37), and bound IgG was detected by an immunoperoxidase procedure using the ECL kit (Amersham). The positions of migration of the mature LDL receptor (LDLR) and its precursor are indicated. The immunoreactive protein marked by the asterisk (\*) represents the truncated form of the LDL receptor caused by insertion of the *neo* cassette into exon 4. The filter in B was incubated with 1  $\mu$ g/ml <sup>125</sup>I-labeled recombinant 39-kD fusion protein (10<sup>6</sup> cpm/ml), which binds to LRP (30). After incubation and washing, the filters in A and B were exposed to Kodak XAR-5 film for 1 min and 6 h, respectively. Gels were calibrated with high molecular weight markers.

2) and homozygous (lane 3) animals, but was absent in wild-type liver membranes (lanes 1 and 4). This latter protein presumably represents the truncated product made from the disrupted allele. Fig. 3 B shows that expression of the LRP/ $\alpha$ <sub>2</sub>M receptor was not affected by the disruption of the LDL receptor as shown by ligand blotting of an equivalent filter probed with an <sup>125</sup>I-labeled 39-kD fusion protein that binds to this receptor (30).

Mice heterozygous or homozygous for the disrupted LDL receptor allele have elevated plasma cholesterol levels when compared with their wild-type litter mates. Table I shows total plasma cholesterol levels of mice from 28 litters derived from the mating of heterozygous animals and fed a normal chow diet. The mean age of the animals at the time of measurement was 52 d. Total (nonfasting) plasma cholesterol values are ~ 35% elevated in heterozygotes and about two times higher in *LDLR*<sup>-/-</sup> mice when compared to wild-type litter mates. In animals of wild-type or heterozygous genotype, females had a lower total plasma cholesterol level than males. This difference was absent in the *LDLR*<sup>-/-</sup> mice. There was no significant

difference in plasma triglyceride concentration among animals of the three genotypes (8–10 animals per group) whose average nonfasting values on a normal chow diet ranged from 119 to 133 mg/dl (data not shown).

To learn which lipoprotein fraction was affected by the loss of functional LDL receptors in the mouse, we used FPLC to determine the lipoprotein cholesterol profiles of male and female mice of the three different genotypes fed a normal chow diet (Fig. 4 A–C). Plasma of wild-type mice contained very little cholesterol in the IDL/LDL fraction. A small but definite increase in this fraction was observed in heterozygous mice of either sex. Animals homozygous for the LDL receptor defect showed a marked increase almost exclusively in the IDL/LDL fraction with a small increase in VLDL. For all genotypes, the HDL-cholesterol level was slightly higher in male mice as compared with female mice, but there was no dramatic effect of LDL receptor gene disruption.

To estimate the relative elevation of IDL/LDL from the data of Fig. 4 A–C, we added up the total cholesterol content of each column fraction within the IDL/LDL peak and then expressed the data relative to the levels observed in wild-type mice of the same sex. These data revealed that the IDL/LDL cholesterol was elevated about twofold in *LDLR*<sup>+/-</sup> mice of either sex and 7.4- to 9-fold in male and female *LDLR*<sup>-/-</sup> mice, respectively. The HDL-cholesterol was elevated only modestly (~1.3-fold) in the *LDLR*<sup>-/-</sup> mice.

Fig. 4 D–F shows comparisons of the lipoprotein cholesterol profiles of male mice of the different genotypes fed either a normal chow diet with or without 0.2% cholesterol/10% coconut oil. Wild-type mice showed only a small difference in lipoprotein profile in response to the cholesterol-enriched diet. Heterozygous mice responded with a small, but distinct elevation in IDL/LDL cholesterol. In the *LDLR*<sup>-/-</sup> mice the cholesterol content of the IDL/LDL fraction rose about threefold. The mean total plasma cholesterol levels for the three genotypes before (fasted) and after (nonfasted) cholesterol feeding were as follows: +/+, 146 and 149 mg/dl; +/-, 188 and 196 mg/dl; and -/-, 293 and 425 mg/dl, respectively.

The apoproteins of the various fractions in Fig. 4 D–F were analyzed by SDS polyacrylamide gel electrophoresis and Coomassie blue staining (Fig. 5). On the normal chow diet, the heterozygous mice showed a distinct elevation in apo B-100 and apo E in the IDL/LDL fraction. The IDL/LDL fraction from *LDLR*<sup>-/-</sup> mice had a much more marked increase of these two apoproteins as well as of apo B-48. The 0.2% cholesterol/10% coconut oil diet elicited a pronounced increase in apo B-100, apo B-48, and apo E in the IDL/LDL fraction of the *LDLR*<sup>-/-</sup> mice. A small increase in the apo E of VLDL and HDL was also apparent in the cholesterol-fed mice (homozygotes > heterozygotes > wild-type).

To evaluate the functional effect of the LDL receptor deficiency, we compared the ability of *LDLR*<sup>-/-</sup> mice and wild-

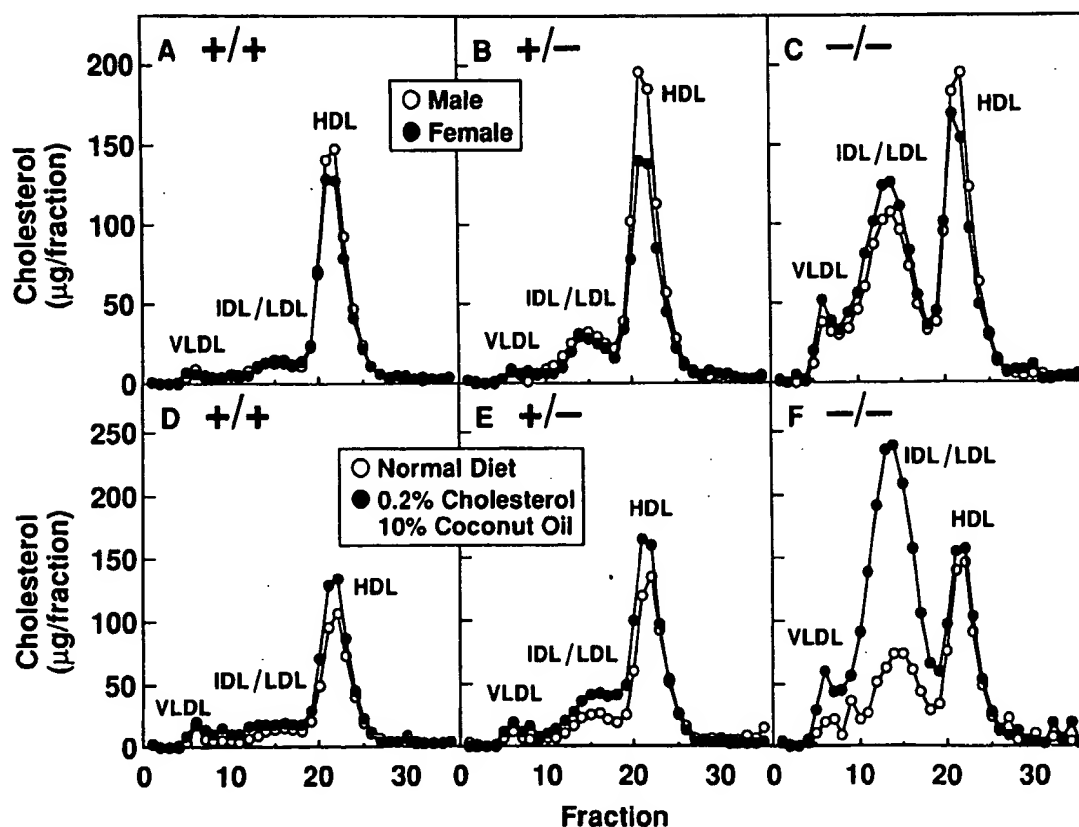
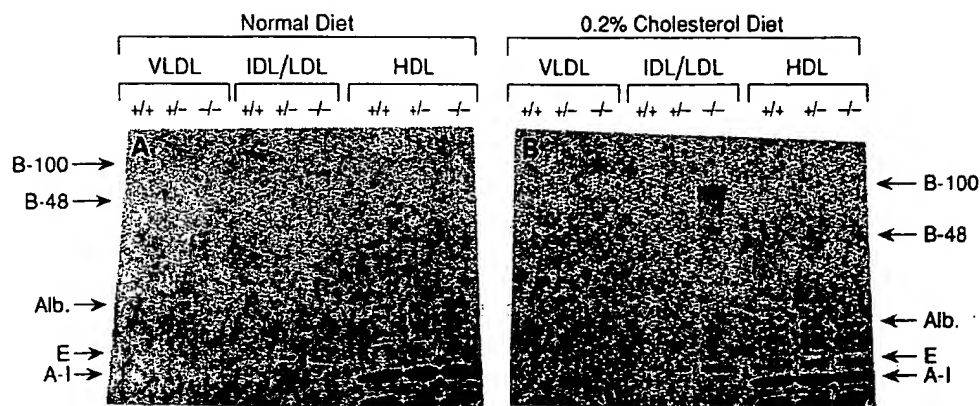


Figure 4. FPLC profiles of mouse plasma lipoproteins from wild-type (+/+) and mutant mice carrying the disrupted LDL receptor allele in heterozygous (+/-) and homozygous (-/-) forms. Mice with the indicated genotype ( $n = 10$  for each sex in A–C and  $n = 5$  males in D–F) were fed a normal diet in A–C or the indicated diet in D–F for 7 wk. The pooled plasma from each group (collected from 12-h fasted animals in A–C and from nonfasted animals in D–F) was subjected to gel filtration on FPLC, and the cholesterol content of each fraction was measured as described in Methods. The mice were 8–9 wk of age in A–C and 16–17 wk in D–F.



**Figure 5.** SDS-gel electrophoresis of lipoprotein fractions from wild-type and mutant mice fed different diets. Male mice ( $n = 5$  per group) that were wild-type (+/+), heterozygous (+/-) or homozygous (-/-) for the disrupted LDL receptor allele were fed either a normal diet (A) or a diet containing 0.2% cholesterol and 10% coconut oil (B) as described in the legend to Fig. 4. The apoproteins from the VLDL, IDL/LDL, and HDL containing fractions in Fig.

4 (equivalent to 70  $\mu$ l of plasma) were subjected to electrophoresis on 3–15% SDS gradient gels. Proteins were stained with Coomassie blue. The positions of migration of apo B-100, apo B-48, albumin (Alb.), apo E, and apo A-I are indicated.

type mice to clear  $^{125}$ I-labeled lipoproteins from the circulation (Fig. 6). For this purpose, we isolated three lipoprotein fractions (VLDL, LDL, and HDL) by ultracentrifugation of pooled plasma of 50  $LDLR^{-/-}$  mice. After radiolabeling with  $^{125}$ I, each lipoprotein was injected into the external jugular vein of three wild-type (+/+) and three homozygous (-/-) animals. Blood was obtained at the indicated intervals, and the radioactivity was expressed relative to the radioactivity at 2 min after injection of the label. As shown in Fig. 6 A, wild-type mice (open circles) clear  $^{125}$ I-VLDL much more efficiently than  $LDLR^{-/-}$  animals (closed circles). In the wild-type ani-

mals 50% of the radioactivity had been eliminated within 10 min, and this was prolonged to 5 h in the  $LDLR^{-/-}$  mice. The clearance of  $^{125}$ I-LDL was also retarded in the  $LDLR^{-/-}$  animals (half-time for disappearance, 5 h in the  $LDLR^{-/-}$  mice vs. 2 h in the wild-type animals) (Fig. 6 B). The clearance of  $^{125}$ I-HDL (half-time of 5.5 h) was not affected by the receptor deficiency (Fig. 6 C).

In order to determine whether adenovirus-mediated gene transfer of the human LDL receptor can reverse the abnormalities caused by the knockout of the LDL receptor, we injected  $2 \times 10^9$  pfu of recombinant virus containing either the luciferase cDNA (AdCMV-Luc) or the LDL receptor cDNA (AdCMV-LDLR) into  $LDLR^{-/-}$  mice. This dose has been found previously to cause expression of the foreign gene in the majority of hepatocytes (23). 4 d after administration of the recombinant viruses, liver membrane proteins were prepared from the individual animals and separated by SDS gel electrophoresis (Fig. 7). Lane 1 shows an immunoblot of a wild-type mouse liver,

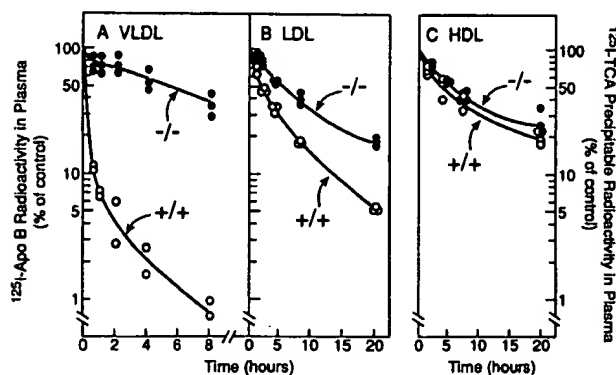


**Figure 6.** Disappearance of  $^{125}$ I-labeled lipoproteins from the circulation in wild-type (o) and  $LDLR^{-/-}$  (●) mice. For each graph, 3 wild-type and 3  $LDLR^{-/-}$  male mice, 20–24 wk of age that had been fasted for 12 h, were anesthetized with sodium pentobarbital (60 mg/kg). Each mouse received an intravenous bolus via the external jugular vein of 0.25 ml of 0.15 M NaCl containing bovine serum albumin (2 mg/ml) and one of the following  $^{125}$ I-labeled mouse lipoproteins: 15  $\mu$ g protein of  $^{125}$ I-VLDL (2,500 cpm/ng protein), 15  $\mu$ g protein of  $^{125}$ I-LDL (1,110 cpm/ng protein), or 15  $\mu$ g protein of  $^{125}$ I-HDL (491 cpm/ng protein). Blood was collected at the indicated time by retro-orbital puncture. In A and B, the plasma content of  $^{125}$ I-labeled apo B was measured by isopropanol precipitation followed by gamma counting (10, 52). In C, the plasma content of trichloroacetic acid-precipitable  $^{125}$ I-radioactivity was measured. The "100% of control" represents the average value for plasma  $^{125}$ I-radioactivity in the wild-type and mutant mice at 2 min after injection. One wild-type animal in A died ~30 min after the intravenous injection.

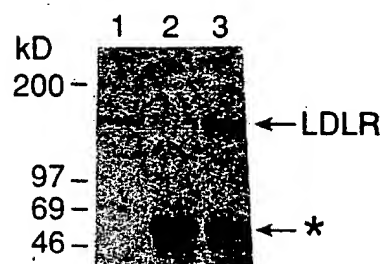


**Figure 7.** Immunoblot analysis of LDL receptors in liver membranes from  $LDLR^{-/-}$  mice 4 d after injection of recombinant adenovirus expressing the human LDL receptor cDNA. Male mice homozygous for the disrupted LDL receptor allele, 17 wk of age, were injected intra-

venously with  $2 \times 10^9$  pfu of adenovirus containing either the luciferase cDNA (lane 2) or the human LDL receptor cDNA (lane 3) as described in Methods. 4 d after administration of the virus, the animals were killed, and liver membranes were prepared from single mice, subjected to SDS gel electrophoresis under reducing conditions (5% [vol/vol] 2-mercaptoethanol), and transferred to filters for immunoblot analysis with a rabbit anti-LDL receptor IgG as described in the legend to Fig. 3. Lane 1 contains liver membrane proteins from a wild-type mouse not injected with recombinant adenovirus. The position of migration of the mature LDL receptor (LDLR) is indicated by the arrow. The immunoreactive protein marked by the asterisk (\*) represents the truncated form of the LDL receptor caused by insertion of the *neo* cassette into exon 4.

revealing the normal mouse LDL receptor. As expected, no intact LDL receptor protein is detectable by immunoblotting in the liver of an *LDLR*<sup>-/-</sup> mouse injected with the luciferase-containing control virus (lane 2). In contrast, injection of AdCMV-LDLR led to high-level expression of the intact receptor in the liver of an *LDLR*<sup>-/-</sup> mouse (lane 3).

Fig. 8 shows an immunohistochemical analysis of LDL receptor expression in the livers of *LDLR*<sup>-/-</sup> mice 4 d after injection of AdCMV-Luc (A) or AdCMV-LDLR (B). In animals injected with the luciferase-containing virus, there were no detectable LDL receptors (A). In the mice injected with AdCMV-LDLR the majority of cells showed positive immunofluorescence (B). The enhanced magnification in C shows that the virally encoded receptor was expressed in a polarized fashion on the blood-sinusoidal surface of the hepatocyte, as is the human LDL receptor in transgenic mice (21).

To test the function of the adenovirus-encoded receptor, we measured the clearance of <sup>125</sup>I-labeled VLDL (Fig. 9). For this experiment we used VLDL isolated from WHHL rabbits, which are deficient in functional LDL receptors. In preliminary experiments we found that <sup>125</sup>I-labeled VLDL from WHHL rabbits is cleared from the circulation of normal mice approximately as rapidly as <sup>125</sup>I-labeled mouse VLDL, and the rabbit lipoprotein is much easier to obtain. *LDLR*<sup>-/-</sup> mice that received recombinant adenovirus encoding the human LDL receptor cleared the <sup>125</sup>I-labeled rabbit VLDL from their plasma at a rapid rate (Fig. 9). In contrast, mice that had received the luciferase-containing virus cleared the <sup>125</sup>I-VLDL at a rate that was similar to that of uninjected animals (compare with Fig. 6 A).

We next sought to determine whether the adenovirus-encoded receptors could normalize the lipoprotein profile of *LDLR*<sup>-/-</sup> mice. For this purpose we injected the control virus (AdCMV-Luc) or the LDL receptor-containing virus (AdCMV-LDLR) into *LDLR*<sup>-/-</sup> male mice (3 animals per group). 4 d after injection the animals were exsanguinated, the pooled plasma of each group was subjected to FPLC gel filtration, and the cholesterol content of the fractions was plotted (Fig. 10). The lipoprotein profile of the mice that had been injected with the luciferase-containing virus closely resembled the profile of uninjected animals (compare with Fig. 4). In the group that had received the LDL receptor-containing virus, the IDL/LDL peak disappeared, and there was a slight increase in VLDL-cholesterol.

## Discussion

The current results demonstrate that elimination of functional LDL receptor genes by homologous recombination profoundly elevates IDL and LDL levels in mice and that these abnormalities can be reversed postnatally by adenovirus-mediated transfer of a gene encoding the LDL receptor. The experiments establish a new animal model by which to explore genetic and environmental factors that interact with LDL receptors to control cholesterol levels. They also provide a new model system in which to study somatic cell gene therapy targeted at the liver.

The most profound functional change observed in the current study was the marked reduction in the clearance rate of <sup>125</sup>I-labeled VLDL from plasma in the homozygous *LDLR*<sup>-/-</sup> mice. The time required for clearance of 50% of the injected lipoprotein rose from 10 min to 300 min, a 30-fold change. These data indicate that the LDL receptor is responsible for

most of the rapid clearance of VLDL remnants and IDL from plasma of mice. The exact proportion cleared by the LDL receptor may be overestimated in these studies because the labeled VLDL was prepared from LDL receptor-deficient animals, i.e., *LDLR*<sup>-/-</sup> mice or homozygous WHHL rabbits. Although these particles float in the VLDL density range ( $d < 1.006$  g/ml), they are likely to represent partially metabolized VLDL particles that have overaccumulated in the donor animals because of the LDL receptor deficiency. Any VLDL particle that is rapidly cleared from plasma in the receptor-deficient animals would be underrepresented in the sample that is used for labeling. This would include large apo E-rich VLDL particles containing either apo B-48 or apo B-100, which may be cleared in part by the chylomicron remnant receptor (38). This problem of underrepresentation of rapidly cleared particles is a problem with all lipoprotein clearance studies (see Discussion in reference 38). Despite these limitations, the data indicate clearly that the VLDL fraction of mice contains a substantial number of particles that are normally cleared by the LDL receptor, presumably owing to their content of apo E. In LDL receptor deficiency states, these particles remain in plasma for long periods and are presumably converted to LDL. Although such conversion was not studied in the current study, it was previously demonstrated in WHHL rabbits (10, 39).

Striking parallels exist between the findings in the current study of *LDLR*<sup>-/-</sup> mice and previous studies of lipoprotein clearance in homozygous WHHL rabbits (10, 39) and FH homozygotes (9). In all three species the most profound abnormality involves the clearance of VLDL remnants and IDL. In WHHL rabbits, the half-time for VLDL clearance was extended from 12 to 480 min (10), a result that parallels the 10 to 300 min change in the current study. In a study of <sup>125</sup>I-VLDL turnover in FH homozygotes, Soutar et al. (9) observed a sevenfold decrease in the clearance of <sup>125</sup>I-IDL derived from <sup>125</sup>I-VLDL (fractional turnover rate 0.48/h in normal subjects vs. 0.064/h in FH homozygotes). Using a more complex kinetic analysis, James et al. (43) also found a decreased clearance of VLDL remnants and IDL. This indicates that a major function of the LDL receptor in all three species is the clearance of remnant particles derived from VLDL, thereby preventing their conversion into LDL.

The relative decline in LDL clearance observed in LDL receptor-deficient mice (2.5-fold) also correlates well with observations in WHHL rabbits. Yamada et al. (39) observed a reduction of 2-fold, Pittman et al. (40) 2.6-fold, and Spady et al. (41) 3.5-fold. In FH homozygotes the reduction in LDL clearance is also about threefold (42, 43). These data indicate that about 60% of LDL particles are normally cleared by the LDL receptor in mice. The residual clearance of LDL observed in the absence of LDL receptors is likely to be mediated by another receptor with a lower affinity for LDL. Like the LDL receptor, this alternate receptor functions primarily in the liver (40).

The absolute level of plasma LDL-cholesterol in the *LDLR*<sup>-/-</sup> mice is much lower than that observed in WHHL rabbits or FH homozygotes. Although we did not measure LDL-cholesterol quantitatively, it is apparent from the FPLC profiles that the IDL/LDL peak contains ~ 50% of the total cholesterol in the plasma of the *LDLR*<sup>-/-</sup> mice, which would indicate an IDL/LDL-cholesterol level of ~ 130 mg/dl. This contrasts with LDL-cholesterol levels above 450 mg/dl in WHHL rabbits (10, 44) and FH homozygotes (2). This differ-



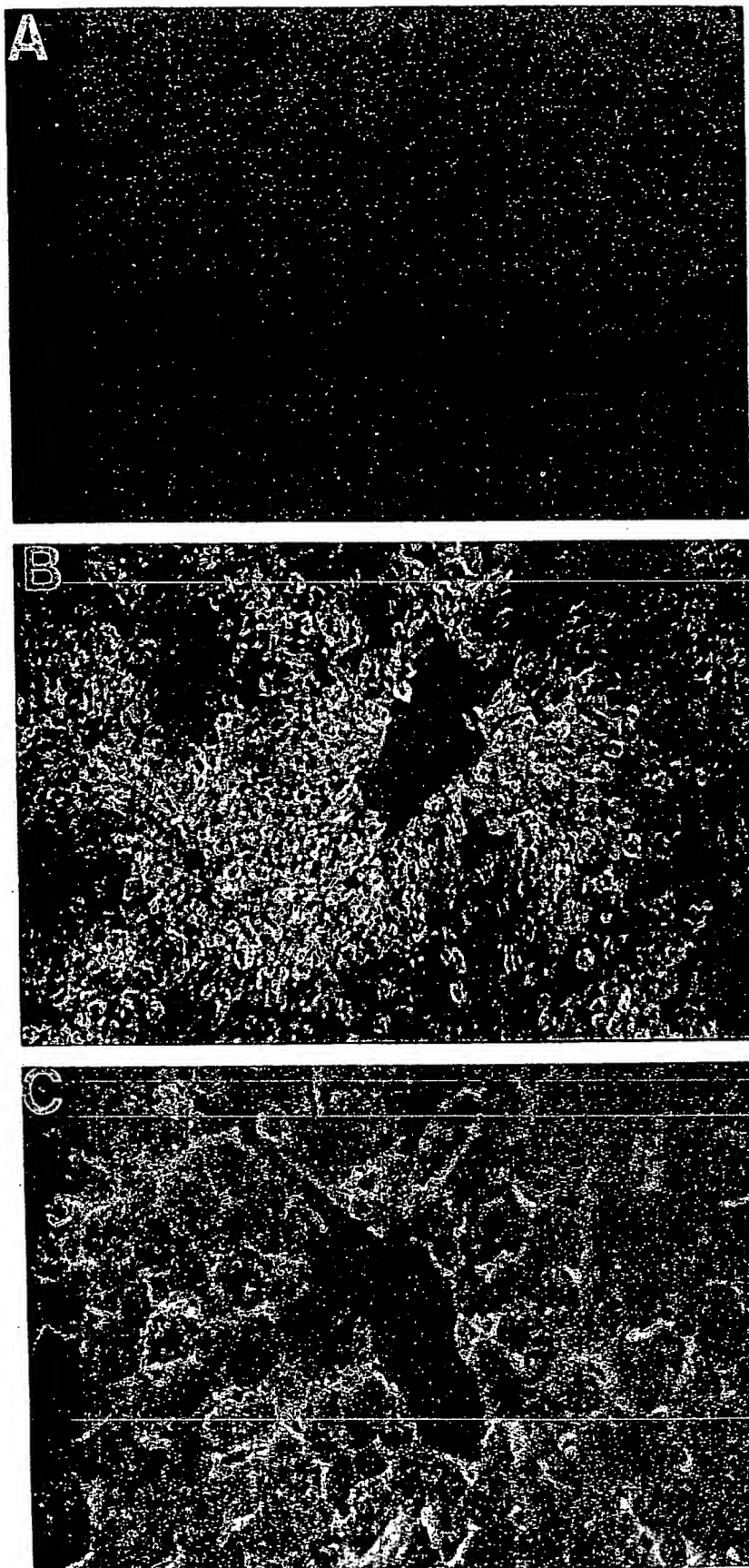


**Figure 8.** Immunohistochemical staining of LDL receptors in the liver of an *LDLR*<sup>-/-</sup> mouse after treatment with recombinant adenovirus expressing the human LDL receptor cDNA. Male mice homozygous for the disrupted LDL receptor allele, 18 wk of age, were injected intravenously with  $2 \times 10^9$  pfu of either AdCMV-Luciferase (*A*) or AdCMV-LDLR (*B* and *C*) as described in Methods. Four days after administration of the virus, the livers were removed for immunohistochemistry. Frozen sections were incubated with 20  $\mu$ g/ml of rabbit polyclonal anti-LDL receptor antibody, and bound IgG was detected with 5  $\mu$ g/ml FITC-labeled goat anti-rabbit IgG as described in Methods. Magnification, *A* and *B*,  $\times 25$ ; *C*,  $\times 100$ .

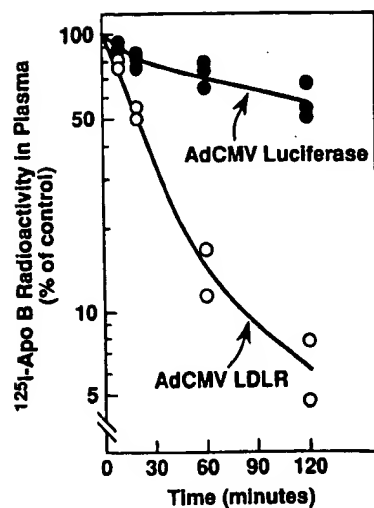


**Figure 9.** Disappearance of  $^{125}\text{I}$ -VLDL from the circulation of  $\text{LDLR}^{-/-}$  mice after treatment with recombinant adenovirus expressing the human LDL receptor cDNA. Three male mice homozygous for the disrupted LDL receptor allele, 19 wk of age, were injected intravenously with  $2 \times 10^9$  pfu of either AdCMV-LDLR (○) or AdCMV-Luciferase (●). 4 d after administration of the virus, the animals (nonfasted) were injected with 15

$\mu\text{g}$  protein of  $^{125}\text{I}$ -labeled VLDL (308 cpm/ $\mu\text{g}$  protein) isolated from WHHL rabbits. Blood was collected at the indicated time by retro-orbital puncture, and the plasma content of  $^{125}\text{I}$ -labeled apo B was measured by isopropanol precipitation (10, 52). The "100% of control" represents the average value for plasma  $^{125}\text{I}$ -radioactivity 1 min after injection. One animal injected with AdCMV-LDLR died  $\sim 10$  min after injection of the  $^{125}\text{I}$ -VLDL.

ence might be explained by the production of VLDL containing apo B-48 in livers of mice, but not rabbits or humans. About 70% of the apo B mRNA in the livers of adult mice encodes the apo B-48 isoform (14). Remnants derived from apo B-48 containing VLDL might be cleared relatively rapidly by the livers of the  $\text{LDLR}^{-/-}$  mice, owing to the ability of the

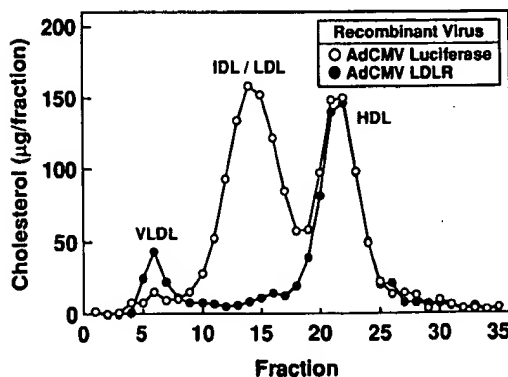


**Figure 10.** FPLC profiles of plasma lipoproteins from  $\text{LDLR}^{-/-}$  mice after treatment with recombinant adenovirus expressing the human LDL receptor cDNA. Three male mice homozygous for the LDL receptor disrupted allele, 17 wk of age, were injected with  $2 \times 10^9$  pfu of adenovirus containing either the luciferase cDNA (○) or the human LDL receptor cDNA (●). 4 d after administration of the virus, blood was collected from the animals (nonfasted), and the plasma from the three animals in each group was pooled and subjected to gel filtration on FPLC. The cholesterol content of each fraction was determined as described in Methods. The mean total plasma cholesterol levels in the two groups of mice were 279 mg/dl (○) and 139 mg/dl (●).

apo E/apo B-48 particles to bind to chylomicron remnant receptors, thereby leading to lower levels of LDL.

The hypothesized role of apo E/apo B-48 particles is supported by a comparison of the current data with those of Zhang et al. (45) and Plump et al. (46), who eliminated the gene for apo E in mice using a similar homologous recombination technique. Apo E $^{-/-}$  mice had total plasma cholesterol levels of 400–500 mg/dl, nearly all of which was contained in particles with the size of VLDL and VLDL remnants. The level of apo B-48 in plasma was also markedly elevated (45). The severity of this abnormality in comparison with the effects of LDL receptor deficiency supports the notion that apo E binds to two receptors, the LDL receptor and the chylomicron remnant receptor. Knockout of apo E therefore has a more profound effect on lipoprotein clearance than knockout of the LDL receptor in mice.

In humans the opposite is true, i.e., LDL receptor deficiency raises the total plasma cholesterol more than does apo E deficiency. Receptor-negative FH homozygotes have total plasma cholesterol levels of 700–1,000 mg/dl (2), whereas individuals with an absence of apo E have plasma cholesterol levels of 443 to 614 mg/dl (47). This is likely due, in part, to the fact that human livers do not produce apo B-48 and that apo E accelerates the removal of apo B-100 containing VLDL remnants primarily by binding to only one receptor, namely, the LDL receptor.

LDL receptors are believed to constitute an important defense against the cholesterol-elevating effect of dietary cholesterol (1). In rabbits (48) and hamsters (49), dietary cholesterol elevates plasma LDL-cholesterol levels in part by suppressing LDL receptors. In the current study, LDL receptor-deficient mice responded to the 0.2% cholesterol/10% coconut oil diet with a rise in plasma LDL-cholesterol that was much greater than was observed in wild-type mice. There was also a definite increase in the amounts of apo B-100 and apo E in plasma, particularly in the IDL/LDL fraction (Fig. 5). Thus, when LDL receptors are already absent as a result of genetic elimination, mice become hyperresponsive to dietary cholesterol.

The current experiments with recombinant adenovirus demonstrate that this vector can restore LDL receptor expression within 4 d in an LDL receptor-deficient mouse. However, many technical problems would have to be overcome before such therapy could be considered for humans. First, it is unknown whether or not the expression of adenovirus-encoded genes in liver will persist for long periods. The genome of the defective virus does not replicate, nor does it integrate into the genome at any appreciable frequency. On the other hand, Stratford-Perricaudet et al. (24) did note persistent expression for a year after injection of the virus into neonatal animals lacking ornithine transcarbamylase activity. Second, adenovirus-encoded proteins are likely to be the targets of immune reactions. Mice are known to develop an immune response to adenoviral proteins (50), which might hamper its use for long periods in these animals. Nearly all humans are expected to possess antibodies against adenovirus, and these might prevent use of this vector in people. Despite these reservations about human applicability, the adenovirus vector is a useful experimental tool to change the expression of genes acutely in the liver. In the current studies, we used it to reveal the type of result to be expected when more applicable long-term gene delivery methods have been developed.



## Acknowledgments

We thank Phil Soriano for expert advice and help. Scott Clark, Lucy Lundquist, Wen-Ling Niu, and Sadeq Hassan provided excellent technical assistance.

This work was supported by National Institutes of Health grants HL-20948 and HL-17669, and by grants from the Moss Heart Foundation and the Perot Family Foundation. S. Ishibashi is the recipient of a postdoctoral fellowship from the Sasakawa Health Science Foundation, Tokyo, Japan. R. D. Gerard is an Established Investigator of the American Heart Association. J. Herz is supported by the Syntex Scholar Program and is a Lucille P. Markey Scholar.

*Note added in proof.* The LDL receptor-deficient mice described in this paper will become available in September 1993 from Jackson Laboratories, 600 Main Street, Bar Harbor, ME 04609.

## References

1. Brown, M. S., and J. L. Goldstein. 1986. A receptor-mediated pathway for cholesterol homeostasis. *Science (Wash. DC)*. 232:34-47.
2. Goldstein, J. L., and M. S. Brown. 1989. Familial hypercholesterolemia. In *The Metabolic Basis of Inherited Disease*. C. R. Scriver, A. L. Beaudet, W. S. Sly, and D. Valle, editors. McGraw-Hill Publishing Co., New York, 1215-1250.
3. Mahley, R. W. 1988. Apolipoprotein E: Cholesterol transport protein with expanding role in cell biology. *Science (Wash. DC)*. 240:622-630.
4. Brown, M. S., J. Herz, R. C. Kowal, and J. L. Goldstein. 1991. The low-density lipoprotein receptor-related protein: double agent or decoy? *Curr. Opin. in Lipidol.* 2:65-72.
5. Ji, Z.-S., W. J. Brecht, D. Miranda, M. M. Hussain, T. L. Innerarity, and R. W. Mahley. 1993. Role of heparan sulfate proteoglycans in the binding and uptake of apolipoprotein E-enriched remnant lipoproteins by cultured cells. *J. Biol. Chem.* 268:10160-10167.
6. Hobbs, H. H., M. S. Brown, and J. L. Goldstein. 1992. Molecular genetics of the LDL receptor gene in familial hypercholesterolemia. *Hum. Mutat.* 1:445-466.
7. Watanabe, Y., T. Ito, and M. Shiomi. 1985. The effect of selective breeding on the development of coronary atherosclerosis in WHHL rabbits. An animal model for familial hypercholesterolemia. *Atherosclerosis*. 56:71-97.
8. Scanu, A. M., A. Khalil, L. Neven, M. Tidore, G. Dawson, D. Pfaffinger, E. Jackson, K. D. Carey, H. C. McGill, and G. M. Fless. 1988. Genetically determined hypercholesterolemia in a rhesus monkey family due to a deficiency of the LDL receptor. *J. Lipid Res.* 29:1671-1681.
9. Soutar, A. K., N. B. Myant, and G. R. Thompson. 1982. The metabolism of very low density and intermediate density lipoproteins in patients with familial hypercholesterolemia. *Atherosclerosis*. 43:217-231.
10. Kita, T., M. S. Brown, D. W. Bilheimer, and J. L. Goldstein. 1982. Delayed clearance of very low density and intermediate density lipoproteins with enhanced conversion to low density lipoprotein in WHHL rabbits. *Proc. Natl. Acad. Sci. USA*. 79:5693-5697.
11. Hobbs, H. H., E. Leitersdorf, C. C. Leffert, D. R. Cryer, M. S. Brown, and J. L. Goldstein. 1989. Evidence for a dominant gene that suppresses hypercholesterolemia in a family with defective low density lipoprotein receptors. *J. Clin. Invest.* 84:656-664.
12. Lamon-Fava, S., D. Jimenez, J. C. Christian, R. R. Fabsitz, T. Reed, D. Carmelli, W. P. Castelli, J. M. Ordovas, P. W. F. Wilson, and E. J. Schaefer. 1991. The NHLBI twin study: heritability of apolipoprotein A-I, B, and low density lipoprotein subclasses and concordance for lipoprotein(a). *Atherosclerosis*. 91:97-106.
13. Spady, D. K., L. A. Woollett, and J. M. Dietschy. 1993. Regulation of plasma LDL-cholesterol levels by dietary cholesterol and fatty acids. *Annu. Rev. Nutr.* 13:355-381.
14. Higuchi, K., K. Kitagawa, K. Kogishi, and T. Takeda. 1992. Developmental and age-related changes in apolipoprotein B mRNA editing in mice. *J. Lipid Res.* 33:1753-1764.
15. Scott, J. 1989. The molecular and cell biology of apolipoprotein-B. *Mol. Biol. Med.* 6:65-80.
16. Chan, L. 1992. Apolipoprotein B, the major protein component of triglyceride-rich and low density lipoproteins. *J. Biol. Chem.* 267:25621-25624.
17. Van't Hooft, F. M., D. A. Hardman, J. P. Kane, and R. J. Havel. 1982. Apolipoprotein B (B-48) of rat chylomicrons is not a precursor of the apolipoprotein of low density lipoproteins. *Proc. Natl. Acad. Sci. USA*. 79:179-182.
18. Chowdhury, J. R., M. Grossman, S. Gupta, N. R. Chowdhury, J. R. Baker, Jr., and J. M. Wilson. 1991. Long-term improvement of hypercholesterolemia after *ex vivo* gene therapy in LDLR-deficient rabbits. *Science (Wash. DC)*. 254:1802-1805.
19. Wilson, J. M., M. Grossman, C. H. Wu, N. R. Chowdhury, G. Y. Wu, and J. R. Chowdhury. 1992. Hepatocyte-directed gene transfer *in vivo* leads to transient improvement of hypercholesterolemia in low density lipoprotein receptor-deficient rabbits. *J. Biol. Chem.* 267:963-967.
20. Hofmann, S. L., D. W. Russell, M. S. Brown, J. L. Goldstein, and R. E. Hammer. 1988. Overexpression of low density lipoprotein (LDL) receptor eliminates LDL from plasma in transgenic mice. *Science (Wash. DC)*. 239:1277-1281.
21. Pathak, R. K., M. Yokode, R. E. Hammer, S. L. Hofmann, M. S. Brown, J. L. Goldstein, and R. G. W. Anderson. 1990. Tissue-specific sorting of the human LDL receptor in polarized epithelia of transgenic mice. *J. Cell Biol.* 111:347-359.
22. Yokode, M., R. E. Hammer, S. Ishibashi, M. S. Brown, and J. L. Goldstein. 1990. Diet-induced hypercholesterolemia in mice: Prevention by overexpression of LDL receptors. *Science (Wash. DC)*. 250:1273-1275.
23. Herz, J., and R. D. Gerard. 1993. Adenovirus-mediated low density lipoprotein receptor gene transfer accelerates cholesterol clearance in normal mice. *Proc. Natl. Acad. Sci. USA*. 90:2812-2816.
24. Stratford-Perricaudet, L. D., M. Levrero, J.-F. Chasse, M. Perricaudet, and P. Briand. 1990. Evaluation of the transfer and expression in mice of an enzyme-encoding gene using a human adenovirus vector. *Hum. Gene Ther.* 1:241-256.
25. Capecchi, M. R. 1989. Altering the genome by homologous recombination. *Science (Wash. DC)*. 244:1288-1292.
26. Smithies, O. 1991. Altering genes in animals and humans. In *Etiology of Human Disease at the DNA Level*. J. Lindsten and U. Pettersson, editors. Raven Press, New York. 221-259.
27. Bradley, A. 1987. Production and analysis of chimaeric mice. In *Teratocarcinomas and Embryonic Stem Cells: A Practical Approach*. E. J. Robertson, editor. IRL Press, Oxford, UK/Washington, DC. 113-151.
28. Sambrook, J., E. F. Fritsch, and T. Maniatis. 1989. *Molecular cloning: A Laboratory Manual*. Cold Spring Harbor Laboratory Press, Cold Spring Harbor, New York.
29. Yokode, M., R. K. Pathak, R. E. Hammer, M. S. Brown, J. L. Goldstein, and R. G. W. Anderson. 1992. Cytoplasmic sequence required for basolateral targeting of LDL receptor in livers of transgenic mice. *J. Cell Biol.* 117:39-46.
30. Willnow, T. F., J. L. Goldstein, K. Orth, M. S. Brown, and J. Herz. 1992. Low density lipoprotein receptor-related protein (LRP) and gp330 bind similar ligands, including plasminogen activator-inhibitor complexes and lactoferrin, an inhibitor of chylomicron remnant clearance. *J. Biol. Chem.* 267:26172-26180.
31. Goldstein, J. L., S. K. Basu, and M. S. Brown. 1983. Receptor-mediated endocytosis of LDL in cultured cells. *Methods Enzymol.* 98:241-260.
32. Yamamoto, T., C. G. Davis, M. S. Brown, W. J. Schneider, M. L. Casey, J. L. Goldstein, and D. W. Russell. 1984. The human LDL receptor: A cysteine-rich protein with multiple Alu sequences in its mRNA. *Cell*. 39:27-38.
33. Mehta, K. D., W.-J. Chen, J. L. Goldstein, and M. S. Brown. 1991. The low density lipoprotein receptor in *Xenopus laevis*. I. Five domains that resemble the human receptor. *J. Biol. Chem.* 266:10406-10414.
34. Soriano, P., C. Montgomery, R. Geske, and A. Bradley. 1991. Targeted disruption of the *c-src* proto-oncogene leads to osteopetrosis in mice. *Cell*. 64:693-702.
35. Mansour, S. L., K. R. Thomas, and M. R. Capecchi. 1988. Disruption of the proto-oncogene *int-2* in mouse embryo-derived stem cells: a general strategy for targeting mutations to non-selectable genes. *Nature (Lond.)*. 336:348-352.
36. McMahon, A. P., and A. Bradley. 1990. The *Wnt-1* (*int-1*) proto-oncogene is required for development of a large region of the mouse brain. *Cell*. 62:1073-1085.
37. Russell, D. W., W. J. Schneider, T. Yamamoto, K. L. Luskey, M. S. Brown, and J. L. Goldstein. 1984. Domain map of the LDL receptor: sequence homology with the epidermal growth factor precursor. *Cell*. 37:577-585.
38. Yamada, N., D. M. Shames, K. Takahashi, and R. J. Havel. 1988. Metabolism of apolipoprotein B-100 in large very low density lipoproteins of blood plasma. *J. Clin. Invest.* 82:2106-2113.
39. Yamada, N., D. M. Shames, and R. J. Havel. 1987. Effect of LDL receptor deficiency on the metabolism of apolipoprotein B-100 in blood plasma: kinetic studies in normal and Watanabe heritable hyperlipidemic rabbits. *J. Clin. Invest.* 80:507-515.
40. Pittman, R. C., T. E. Carew, A. D. Attie, J. L. Witztum, Y. Watanabe, and D. Steinberg. 1982. Receptor-dependent and receptor-independent degradation of low density lipoprotein in normal rabbits and in receptor-deficient mutant rabbits. *J. Biol. Chem.* 257:7994-8000.
41. Spady, D. K., M. Huettinger, D. W. Bilheimer, and J. M. Dietschy. 1987. Role of receptor-independent low density lipoprotein transport in the maintenance of tissue cholesterol balance in the normal and WHHL rabbit. *J. Lipid Res.* 28:32-41.
42. Bilheimer, D. W., N. J. Stone, and S. M. Grundy. 1979. Metabolic studies in familial hypercholesterolemia: evidence for a gene-dosage effect *in vivo*. *J. Clin. Invest.* 64:524-533.
43. James, R. W., B. Martin, D. Pometta, J. C. Fruchart, P. Duriez, P. Fuchois, J. P. Farriaux, A. Tacquet, T. Demant, R. J. Clegg, A. Munro, M. F. Oliver

- et al. 1989. Apolipoprotein B metabolism in homozygous familial hypercholesterolemia. *J. Lipid Res.* 30:159-169.
44. Havel, R. J., T. Kita, L. Kotite, J. P. Kane, R. L. Hamilton, J. L. Goldstein, and M. S. Brown. 1982. Concentration and composition of lipoproteins in blood plasma of WHHL rabbits. *Arteriosclerosis*. 3:467-474.
45. Zhang, S. H., R. L. Reddick, J. A. Piedrahita, and N. Maeda. 1992. Spontaneous hypercholesterolemia and arterial lesions in mice lacking apolipoprotein E. *Science (Wash. DC)*. 258:468-471.
46. Plump, A. S., J. D. Smith, T. Hayek, K. Aalto-Setälä, A. Walsh, J. G. Verstuyft, E. M. Rubin, and J. L. Breslow. 1992. Severe hypercholesterolemia and atherosclerosis in apolipoprotein E deficient mice created by homologous recombination in ES cells. *Cell*. 71:343-353.
47. Schaefer, E. J., R. E. Gregg, G. Ghiselli, T. M. Forte, J. M. Ordovas, L. A. Zech, and H. B. Brewer, Jr. 1986. Familial apolipoprotein E deficiency. *J. Clin. Invest.* 78:1206-1219.
48. Kovanen, P. T., M. S. Brown, S. K. Basu, D. W. Bilheimer, and J. L. Goldstein. 1981. Saturation and suppression of hepatic lipoprotein receptors: a mechanism for the hypercholesterolemia of cholesterol-fed rabbits. *Proc. Natl. Acad. Sci. USA*. 78:1396-1400.
49. Spady, D. K., and J. M. Dietschy. 1988. Interaction of dietary cholesterol and triglycerides in the regulation of hepatic low density lipoprotein transport in the hamster. *J. Clin. Invest.* 81:300-309.
50. Ginsberg, H. S., L. L. Moldawer, P. B. Schgal, M. Redington, P. L. Kilian, R. M. Chanock, and G. A. Prince. 1991. A mouse model for investigating the molecular pathogenesis of adenovirus pneumonia. *Proc. Natl. Acad. Sci. USA*. 88:1651-1655.
51. Kowal, R. C., J. Herz, J. L. Goldstein, V. Esser, and M. S. Brown. 1989. Low density lipoprotein receptor-related protein mediates uptake of cholesteryl esters derived from apoprotein E-enriched lipoproteins. *Proc. Natl. Acad. Sci. USA*. 86:5810-5814.
52. Holmquist, L., K. Carlson, and L. A. Carlson. 1978. Comparison between the use of isopropanol and tetramethylurea for the solubilisation and quantitation of human serum very low density apolipoproteins. *Anal. Biochem.* 88:457-460.

# Peroxisome proliferator-activated receptor $\gamma$ ligands inhibit development of atherosclerosis in LDL receptor-deficient mice

Andrew C. Li,<sup>1</sup> Kathleen K. Brown,<sup>2</sup> Mercedes J. Silvestre,<sup>3</sup>  
Timothy M. Willson,<sup>4</sup> Wulf Palinski,<sup>3</sup> and Christopher K. Glass<sup>1,3</sup>

<sup>1</sup>Department of Cellular and Molecular Medicine, University of California, San Diego, La Jolla, California, USA

<sup>2</sup>Department of Metabolic Diseases, Glaxo Wellcome Research and Development, Research Triangle Park, North Carolina, USA

<sup>3</sup>Department of Medicine, University of California, San Diego, La Jolla, California, USA

<sup>4</sup>Department of Medicinal Chemistry, Glaxo Wellcome Research and Development, Research Triangle Park, North Carolina, USA

Address correspondence to: Andrew C. Li, Department of Cellular and Molecular Medicine, University of California, San Diego, 9500 Gilman Drive, La Jolla, California 92093-0651, USA.  
Phone: (858) 534-7559; Fax: (858) 534-8549; E-mail: acli@ucsd.edu.

The Palinski and Glass laboratories contributed equally to this work.

Received for publication May 18, 2000, and accepted in revised form July 5, 2000.

The peroxisome proliferator-activated receptor  $\gamma$  (PPAR $\gamma$ ) is a nuclear receptor that regulates fat-cell development and glucose homeostasis and is the molecular target of a class of insulin-sensitizing agents used for the management of type 2 diabetes mellitus. PPAR $\gamma$  is highly expressed in macrophage foam cells of atherosclerotic lesions and has been demonstrated in cultured macrophages to both positively and negatively regulate genes implicated in the development of atherosclerosis. We report here that the PPAR $\gamma$ -specific agonists rosiglitazone and GW7845 strongly inhibited the development of atherosclerosis in LDL receptor-deficient male mice, despite increased expression of the CD36 scavenger receptor in the arterial wall. The antiatherogenic effect in male mice was correlated with improved insulin sensitivity and decreased tissue expression of TNF- $\alpha$  and gelatinase B, indicating both systemic and local actions of PPAR $\gamma$ . These findings suggest that PPAR $\gamma$  agonists may exert antiatherogenic effects in diabetic patients and provide impetus for efforts to develop PPAR $\gamma$  ligands that separate proatherogenic activities from antidiabetic and antiatherogenic activities.

*J. Clin. Invest.* 106:523-531 (2000).

## Introduction

Complications of atherosclerosis are the leading cause of death in Western societies and have an extremely high incidence in individuals with type 2 diabetes mellitus (1, 2). Atherosclerosis is initiated by the accumulation of plasma LDL in the arterial wall, its oxidation, and the recruitment of circulating monocytes (3, 4). Once monocytes in the arterial intima have undergone phenotypic transformation to macrophages, they take up oxidized LDL (oxLDL) via several scavenger receptors that include scavenger receptor A (SR-A), CD36, and macrophage mannose receptor (5-7). This results in massive cholesterol accumulation and formation of foam cells. Interactions between oxLDL, macrophages, smooth muscle cells infiltrated from the arterial media, and T cells recruited from the circulation result in a chronic inflammatory condition that is thought to influence the further evolution of early atherosclerotic lesions toward more advanced, clinically relevant lesions (8). Interactions between arterial cells are mediated by an array of cytokines and adhesion molecules (9), and increasing experimental evidence suggests that many of these factors promote atherogenesis. For example, hypercholesterolemic mice in which the gene encoding

macrophage chemotactic protein 1 (MCP-1) has been disrupted are resistant to the development of atherosclerosis (10, 11). In analogy, disruption of the *SR-A* and *CD36* genes results in a significant reduction of hypercholesterolemia-induced atherosclerosis in mice (12, 13). These observations suggest that interventions directed at altering the genetic responses of vascular cells to proatherogenic stimuli, such as hypercholesterolemia, may be beneficial.

Several regulatory pathways have been identified that control the expression of potentially atherogenic genes. These include NF- $\kappa$ B, a transcription factor involved in the regulation of many proinflammatory factors and adhesion molecules, such as TNF- $\alpha$  and gelatinase B (14, 15). Recent studies have also documented the expression of the peroxisome proliferator-activated receptor  $\gamma$  (PPAR $\gamma$ ) in macrophage foam cells, endothelial cells, and smooth muscle cells of human and murine atherosclerotic lesions (16-20). PPAR $\gamma$  is a member of the nuclear receptor superfamily of ligand-dependent transcription factors that both positively and negatively regulate gene expression in response to the binding of a number of fatty acid metabolites, including oxidized linoleic acid (9- and 13-HODE) and

15 deoxy  $\Delta^{2,14}$  prostaglandin  $J_2$  (21–23). PPAR $\gamma$  is expressed in many other tissues and is particularly highly expressed in fat. PPAR $\gamma$  promotes adipocyte differentiation in vitro and has recently been shown to be essential for the development of adipose tissue in vivo (24–26). PPAR $\gamma$  also appears to play a critical role in glucose homeostasis, because it is the molecular target of a class of insulin-sensitizing drugs referred to as thiazolidinediones (TZDs) (27).

The biological roles of PPAR $\gamma$  in the macrophage and its effects on atherosclerosis are uncertain. PPAR $\gamma$ -specific ligands have been shown to inhibit the expression of a number of proinflammatory genes, including TNF- $\alpha$ , IL-1 $\beta$ , iNOS, and gelatinase B (28, 29). These findings suggested that PPAR $\gamma$  functions as a negative regulator of macrophage activation and that synthetic PPAR $\gamma$  ligands might exert anti-inflammatory and antiatherogenic effects. Consistent with this, PPAR $\gamma$  ligands have recently been shown to inhibit inflammatory bowel disease in a rodent model (30). However, PPAR $\gamma$  has also been shown to stimulate transcription of the CD36 gene (19, 21). In conjunction with the finding that PPAR $\gamma$  can be activated by 9- and 13-HODE present in oxLDL, a “PPAR $\gamma$  cycle” has been proposed in which oxLDL lipids would induce the activity of PPAR $\gamma$ , leading to increased expression of CD36, which in turn would increase the uptake of oxLDL. This cycle would thus promote foam-cell formation and atherosclerosis.

Resolving the question of whether PPAR $\gamma$  agonists promote or inhibit atherosclerosis is of clinical importance because many patients with type 2 diabetes, who are at high risk of developing atherosclerosis and its complications, are currently using PPAR $\gamma$  agonists for the control of hyperglycemia. To determine whether the activation of PPAR $\gamma$  promotes or inhibits the development of atherosclerosis in an animal model, we administered two structurally distinct PPAR $\gamma$ -specific ligands to LDL receptor-deficient (LDLR $^{-/-}$ ) mice fed a Western-style diet and measured their effects on lipid and glucose metabolism, extent of atherosclerosis, and expression of potential target genes in the artery wall. Both PPAR $\gamma$ -specific ligands exerted potent antiatherogenic effects in male mice despite upregulation of CD36 mRNA. Antiatherogenic effects correlated with improved insulin sensitivity and inhibition of TNF- $\alpha$  and gelatinase B expression.

## Methods

**Animals and diet.** A breeding colony was generated from the tenth-generation homozygous LDLR $^{-/-}$  mice in a C57BL/6 background (The Jackson Laboratories, Bar Harbor, Maine, USA). In three separate experiments, three groups of both males and females were matched for age (8 to 12 weeks), plasma cholesterol, and glucose levels before feeding. Four animals were housed per cage and in a facility with an 11-hour light cycle (light, 7 am to 6 pm). All three groups were fed a Western-style diet consisting of 0.01% added cholesterol and 21% milk fat

(TD98338; Harlan-Teklad, Madison, Wisconsin, USA), which induced extensive atherosclerosis in the aortic origin, but not in the descending aorta at 10 weeks. In addition to the diet, one group received rosiglitazone and another group received GW7845. The animals were fed 3–4 g food/mouse/day with a drug delivery of 20 mg/kg of body weight/day. New batches of food/drug were prepared weekly and stored at 4°C. The amount of food given and the food left remaining were weighed daily. The animals were weighed every 2 weeks, and the drug dosages were adjusted accordingly. To induce extensive atherosclerosis in the aorta, in a separate experiment male mice were fed a diet containing 1.25% cholesterol and 21% milk fat (TD96121; Harlan-Teklad) for 4 months. Two weeks before sacrifice, the animals were divided into three groups. A control group received the diet treated only with the solvent, the second group received the diet together with rosiglitazone (20 mg/kg/day), and the third group received the diet and GW7845 (20 mg/kg/day). All animals had ad libitum access to water. The animal experiments were performed according to NIH guidelines and were approved by UCSD's Animal Subjects Committee.

**Glucose, insulin, and lipid levels.** Retro-orbital bleeds were performed before the start of the studies and every 4 weeks thereafter until the animals were sacrificed at 10 weeks. The animals were bled, nonfasted, at 10 am and blood was drawn up in EDTA-coated microcapillary tubes. Plasma was isolated from whole blood and glucose levels were determined, using a Precision QID glucometer (MediSense Inc., Bedford, Massachusetts, USA). Insulin levels were determined using a competitive radioimmunoassay (Linco Research Inc., St. Charles, Missouri, USA). Plasma cholesterol and triglyceride levels were measured by enzymatic methods using an automated bichromatic analyzer (Abbot Diagnostics, Dallas, Texas, USA). To determine the lipoprotein profiles, remaining terminal plasma samples were pooled according to the animals' respective groups, and the cholesterol content of lipoprotein fractions in plasma was determined by FPLC. One hundred milliliters of the pooled plasma was loaded onto a Superose 6B column, and 250  $\mu$ L of sample fractions were collected and analyzed for cholesterol.

**Oral glucose tolerance test.** Two weeks before the mice were sacrificed, oral glucose tolerance tests were performed. Animals were fasted for 4 hours. Animals were gavaged with glucose (0.75 mg/g body weight) using 20% glucose. Blood samples (25  $\mu$ L) were taken at 0, 15, 30, 60, and 90 minutes. Glucose levels were determined in whole blood and insulin levels in plasma.

**Hemoglobin A $_{1c}$ , nonesterified fatty acid, HDL $_c$ , and drug levels.** Whole blood and plasma were sent to Glaxo Wellcome Research Institute (Research Triangle Park, North Carolina, USA) for analysis for HbA $_{1c}$ , HDL $_c$ , and nonesterified fatty acid (NEFA) levels. The plasma was isolated immediately and quickly frozen in liquid nitrogen to prevent the breakdown of NEFA. Drug levels were determined by mass spectrometry.

**Tissue preparation and morphometric analysis of atherosclerotic lesions.** The heart was perfused from its apex with cold PBS treated with diethylpyrocarbonate (DEPC). The heart, containing the aortic origin, was carefully dissected. The upper half of the heart was placed in a fixative containing 4% paraformaldehyde, 5% sucrose in PBS, pH 7.4, and fixed overnight, followed by alcohol dehydration and paraffin embedding. For morphometric determination of atherosclerosis, serial 9- $\mu$ m-thick sections were cut from the apex toward the base of the heart. Sections containing the aortic origin, totaling 180  $\mu$ m in length, were stained with a modified van Gieson's elastin stain to enhance the contrast between the atherosclerotic intima and the surrounding tissue (31). Analysis was performed on every other section ( $n = 8-10$  per mouse). Thus, a total length of 180  $\mu$ m of the aortic origin was examined. Quantification of atherosclerosis was performed using computer-assisted image analysis, as described previously (32). All morphometry was performed by the same investigator blinded to the tissue identity.

**RNA isolation from aortic valves and aortas.** The upper half of the hearts, containing the aortic valves and the aortas, extending from the root to the second intercostal region and up to the carotids, were weighed and flash frozen in liquid nitrogen and stored at  $-80^{\circ}\text{C}$ . Isolation of total RNA was performed using RNeasy kit (QIAGEN Inc., Valencia, California, USA) according to the manufacturer's protocol. Total RNA was treated with deoxyribonuclease I (QIAGEN Inc.) for 20 minutes at room temperature to remove contaminating genomic DNA. The amount of RNA was determined by spectrophotometry, and 200 ng of RNA was loaded onto a 1.5% agarose gel to determine its quality before analysis.

**RT-PCR-based quantitative gene expression analysis.** Real-time detection of PCR was performed at the Center for Aids Research Genomics Core of the Veterans Medical Research Foundation in La Jolla, California, USA. Using the Perkin-Elmer ABI Prism 7700 and Sequence Detection System software (Perkin-Elmer, Foster City, California, USA), the differential displays of mRNAs for TNF- $\alpha$ , MCP-1, VCAM-1, gelatinase B, macrosialin, CD36, and SR-A were determined. Briefly, 1  $\mu$ g of total RNA was used to generate cDNA using an oligo dT oligodeoxynucleotide primer (T<sub>12-18</sub>) following the protocol for Omniscript (QIAGEN Inc.). The following primers and probes were made: TNF- $\alpha$ : 5'CGGAGTC-CGGGCAGGT 3' (forward), 5' GCTGGGTAGAGAATG-GATGAACA 3' (reverse), 5' ACTTTGGAGTCATTGCTCT-GTGAAGGG AATG 3' (probe); MCP-1: 5' CAGCCAGATGCAGTTAACGC 3' (forward), 5' GCC-TACTCATTGGGATCATCTTG 3' (reverse), 5' CCACT-CACCTGCTGCTACTCATTACCA 3' (probe); VCAM-1: 5' TGC GAGTACCAATTGTTCTCAT 3' (forward), 5' CATGGTCAGAACGGACTTGGA 3' (reverse), 5' ACCCA-GATAGACAGCCCACTAAACGCGAA 3' (probe); gelatinase B: 5' TCACCTTACCCGCGTGTA 3' (forward), 5' GTGCTCCGCGACACCAA 3' (reverse), 5' ACCCGAAGCG-

GACATTGTCATCCAG 3' (probe); macrosialin: 5' CAAG-GTCCAGGGAGG TTGTG 3' (forward), 5' CCAAAG-GTAAGCTGTCCATAAGGA 3' (reverse), 5' CGGTACC-CATCCCCACCTGTCTCTCTC 3' (probe); CD36: 5' TCCAGCCAATGCCTTTGC 3' (forward), 5' TGGAGAT-TACTTTTCAGTGCAGAA 3' (reverse), 5' TCACCCCTCCA-GAATCCAGACAACCA 3' (probe); SR-A: 5' CATGAACGA-GAGGATGCTGACT 3' (forward), 5' GGAAGGGATGCTGTCATTGAA 3' (reverse), 5' CAGTTCAGAATCCGTGAAATTTGACGCAC 3' (probe); and GAPDH: 5' CCACCCATGGCAAATTC 3' (forward), 5' TGGGATTCCATTGATGACAAG 3' (reverse), 5' TGGCACCGTCAAGGCTGAGAACG 3' (probe). Equal amounts of cDNA were used in triplicate and amplified with the Taqman Master Mix provided by Perkin-Elmer. Amplification efficiencies were validated and normalized against GAPDH and nanograms of product were calculated using the standard curve method for quantitation against cDNA that was reverse transcribed from isolated aortas of LDLR<sup>-/-</sup> mice fed a 1.25% cholesterol and 21% milk-fat diet for 4 months. Total RNA that was not reverse transcribed was also analyzed to determine genomic DNA contamination.

**Statistical analysis.** Groups were compared by ANOVA and unpaired *t* tests using the StatView analysis program (SAS Institute Inc., Cary, North Carolina, USA). Data are expressed as the mean plus or minus SEM.

## Results

Intervention studies were performed in LDLR<sup>-/-</sup> mice fed a Western-style diet for 10 weeks, starting at age 8-12 weeks. To reduce the possibility that effects of a single PPAR $\gamma$  ligand on atherosclerosis resulted from PPAR $\gamma$ -independent mechanisms, two distinct PPAR $\gamma$  agonists were used: rosiglitazone and GW7845. Rosiglitazone is a member of the TDZ class of insulin sensitizers that was developed using rodent models of type 2 diabetes. It has an effective concentration of 50% (EC<sub>50</sub>) for murine PPAR $\gamma$  of 76 nM (33). GW7845 is a member of the tyrosine-based class of insulin sensitizers that was developed using human PPAR $\gamma$  as a molecular target. It has an EC<sub>50</sub> for murine PPAR $\gamma$  of 1.2 nM (33). Both drugs are highly specific for PPAR $\gamma$ , with EC<sub>50</sub> for PPAR $\alpha$  and PPAR $\delta$  in excess of 10  $\mu$ M (33). We initially performed a pilot study using a calculated dose of 20 mg rosiglitazone/kg/day to establish appropriate dietary cholesterol content and extent of atherosclerosis. Rosiglitazone exerted a significant antiatherogenic effect in male mice in this study, but not in female mice (data not shown). However, because the 1.25% added dietary cholesterol resulted in serum cholesterol levels in excess of 2,000 mg/dL, a potential protective effect in females could have been overwhelmed. Two subsequent intervention studies were therefore carried out in which the added cholesterol was reduced to 0.01%. Each experiment resulted in the same pattern of responses to dietary and drug treatments, and the data from the two studies were pooled to increase statistical power.

**Table 1**  
Average weights, cholesterol, triglyceride, and HDL<sub>c</sub> levels

	Weight g	Total Cholesterol mg/dL	Triglycerides mg/dL	HDL <sub>c</sub> mg/dL		Weight g	Total Cholesterol mg/dL	Triglycerides mg/dL	HDL <sub>c</sub> mg/dL
<b>Males</b>					<b>Females</b>				
<b>Control (n = 10)</b>					<b>Control (n = 10)</b>				
T = 0 weeks	24.4 ± 0.8	258 ± 11	128 ± 17		T = 0 weeks	19.0 ± 0.7	235 ± 12	37 ± 12	
T = 4 weeks	36.7 ± 1.2	1258 ± 143	1150 ± 195		T = 4 weeks	24.1 ± 1.9	1053 ± 97	576 ± 258	
T = 8 weeks	38.9 ± 1.3	1552 ± 83	1279 ± 170		T = 8 weeks	27.2 ± 1.3	1211 ± 68	621 ± 207	
T = 10 weeks	42.5 ± 1.4	1549 ± 89	1226 ± 153	127 ± 5	T = 10 weeks	28.4 ± 1.7	1240 ± 109	722 ± 241	115 ± 4
<b>Ro (n = 12)</b>					<b>Ro (n = 10)</b>				
T = 0 weeks	26.1 ± 0.9	245 ± 10	121 ± 20		T = 0 weeks	20.4 ± 0.5	242 ± 6	47 ± 11	
T = 4 weeks	36.7 ± 1.3	1258 ± 103	1150 ± 265		T = 4 weeks	23.7 ± 1.1	1027 ± 6	624 ± 24	
T = 8 weeks	38.6 ± 1.4	1371 ± 72	1366 ± 134		T = 8 weeks	27.6 ± 1.1	1395 ± 81	1000 ± 107	
T = 10 weeks	40.4 ± 1.3	1440 ± 69	1541 ± 126	115 ± 4 <sup>A</sup>	T = 10 weeks	29.7 ± 1.3	1513 ± 55 <sup>A</sup>	1251 ± 69 <sup>B</sup>	96 ± 3 <sup>B</sup>
<b>GW7845 (n = 10)</b>					<b>GW7845 (n = 7)</b>				
T = 0 weeks	26.3 ± 0.9	249 ± 9	116 ± 22		T = 0 weeks	20.0 ± 0.8	232 ± 11	48 ± 12	
T = 4 weeks	33.5 ± 3.5	1275 ± 168	1406 ± 276		T = 4 weeks	25.0 ± 1.1	1139 ± 82	927 ± 145	
T = 8 weeks	39.9 ± 1.0	1533 ± 81	1790 ± 184		T = 8 weeks	28.6 ± 1.2	1395 ± 90	1049 ± 131	
T = 10 weeks	41.7 ± 2.2	1626 ± 109	1507 ± 200	123 ± 3	T = 10 weeks	28.5 ± 1.4	1449 ± 136	1228 ± 157 <sup>B</sup>	104 ± 4 <sup>A</sup>

Data are expressed as the mean ± SEM; n represents the number of mice per group. Values were determined in plasma samples from nonfasting animals. Ro, rosiglitazone. <sup>A</sup>P < 0.05 and <sup>B</sup>P < 0.005, drug treatment group vs. control group.

At a dose of 20 mg/kg/day, rosiglitazone plasma levels averaged 6.4 plus or minus 0.06 µg/mL in male mice and 5.1 plus or minus 0.69 µg/mL in female mice at 10 weeks. GW7845 levels averaged 3.2 plus or minus 0.39 µg/mL in male mice and 3.2 plus or minus 0.46 µg/mL in female mice after 10 weeks of treatment. These serum levels are sufficient to exert inhibitory effects on proinflammatory gene expression in vitro (29). All animals appeared healthy throughout the study. Serum aspartate aminotransferase and alkaline phosphatase levels were used to assess potential liver toxicity and were not altered at the end of the study (data not shown). Histologic analysis of the bone marrow indi-

cated a significant increase in percentage of marrow fat, and marked extramedullary hematopoiesis was observed in both male and female mice (data not shown). There were no significant changes in complete blood counts or hemoglobin. Data for body weight, total cholesterol, triglycerides, and HDL<sub>c</sub> at specific time points are presented in Table 1. The body weights in all groups increased during the intervention period, but the relative weight gain in males was greater than that in females. The Western diet resulted in a marked increase in total cholesterol within 1 month; the total cholesterol then remained constant at approximately 1,500 mg/dL in males. There was a slight increase in

**Table 2**  
Average glucose, insulin, HbA<sub>1c</sub>, NEFA levels

	Glucose mg/dL	Insulin ng/mL	Hb A <sub>1c</sub> %	NEFA mEq/L		Glucose mg/dL	Insulin ng/mL	Hb A <sub>1c</sub> %	NEFA mEq/L
<b>Males</b>					<b>Females</b>				
<b>Control (n = 10)</b>					<b>Control (n = 10)</b>				
T = 0 weeks	307 ± 20	1.12 ± 0.17	5.50 ± 0.16		T = 0 weeks	267 ± 11	0.55 ± 0.04	5.57 ± 0.15	
T = 4 weeks	211 ± 24	1.38 ± 0.25	5.62 ± 0.11		T = 4 weeks	299 ± 14	1.48 ± 0.18	5.39 ± 0.05	
T = 8 weeks	245 ± 14	4.18 ± 0.41	5.29 ± 0.07		T = 8 weeks	273 ± 21	1.95 ± 0.49	4.96 ± 0.10	
T = 10 weeks	344 ± 22	4.24 ± 0.30	5.31 ± 0.13	0.60 ± 0.06	T = 10 weeks	347 ± 16	1.44 ± 0.30	5.11 ± 0.16	0.64 ± 0.06
<b>Ro (n = 12)</b>					<b>Ro (n = 10)</b>				
T = 0 weeks	282 ± 13	0.95 ± 0.08	5.46 ± 0.11		T = 0 weeks	250 ± 8	0.63 ± 0.13	5.39 ± 0.15	
T = 4 weeks	211 ± 11	1.38 ± 0.11	5.62 ± 0.11		T = 4 weeks	210 ± 10	0.75 ± 0.05	5.78 ± 0.03	
T = 8 weeks	207 ± 8	2.03 ± 0.44	5.08 ± 0.13		T = 8 weeks	216 ± 10	1.91 ± 0.53	4.94 ± 0.09	
T = 10 weeks	315 ± 10	1.45 ± 0.33 <sup>B</sup>	4.91 ± 0.12 <sup>A</sup>	0.65 ± 0.04	T = 10 weeks	312 ± 11	0.93 ± 0.33	4.87 ± 0.07	0.85 ± 0.11
<b>GW7845 (n = 10)</b>					<b>GW7845 (n = 7)</b>				
T = 0 weeks	317 ± 8	1.01 ± 0.18	5.78 ± 0.06		T = 0 weeks	261 ± 14	0.94 ± 0.13	5.20 ± 0.16	
T = 4 weeks	211 ± 13	1.54 ± 0.49	5.76 ± 0.11		T = 4 weeks	225 ± 16	1.07 ± 0.15	5.47 ± 0.12	
T = 8 weeks	204 ± 14	2.01 ± 0.32	5.32 ± 0.09		T = 8 weeks	190 ± 6	1.75 ± 0.59	4.75 ± 0.07	
T = 10 weeks	311 ± 13	1.65 ± 0.36 <sup>B</sup>	4.81 ± 0.16 <sup>A</sup>	0.63 ± 0.05	T = 10 weeks	311 ± 13	1.29 ± 0.37	4.80 ± 0.16	0.81 ± 0.08

Data are expressed as the mean ± SEM; n represents the number of mice per group. Values were determined in plasma samples from nonfasting animals. Ro, rosiglitazone. <sup>A</sup>P < 0.05 and <sup>B</sup>P < 0.005, drug treatment group vs. control group.

cholesterol levels of treated females, but this effect only reached statistical significance ( $P = 0.05$ ) in the rosiglitazone treatment group after 10 weeks. Triglycerides were significantly increased and HDL<sub>c</sub> levels were decreased in female mice treated with rosiglitazone or GW7845. A decrease in HDL<sub>c</sub> levels was seen in male mice treated with rosiglitazone only.

**PPAR $\gamma$  ligands inhibit the development of atherosclerosis in male mice.** Atherosclerosis at the aortic origin was determined by computer-assisted image analysis as described previously (32). Male and female control animals exhibited similar levels of atherosclerosis. Lesions were observed underneath most of the valve leaflets, with some lesions exhibiting areas of central necrosis (Figure 1a). Macroscopically detectable lesions were generally absent from the thoracic or abdominal aorta (data not shown). Markedly fewer and smaller lesions were found in male mice that were treated with either rosiglitazone or GW7845, with quantitative analysis indicating a 60 to 80% reduction in lesion area (Figure 1b). In contrast, the extent of atherosclerosis in female mice treated with either rosiglitazone or GW7845 was not statistically different from that in control mice, confirming the findings of the initial pilot study.

**Metabolic effects of PPAR $\gamma$  ligands.** To investigate possible mechanisms accounting for antiatherogenic effects of PPAR $\gamma$  ligands in male mice and lack of these effects in female mice, lipoprotein levels were evaluated in control and treatment groups. Fast-performance liquid chromatography (FPLC) analysis of pooled terminal serum samples indicated that GW7845 and rosiglitazone had no effect on the lipoprotein profile in male mice (Figure 2a). In contrast, in female mice the VLDL, IDL, and LDL fractions were increased and the HDL fraction decreased in both the rosiglitazone and GW7845 treatment groups (Figure 2b).

Effects of PPAR $\gamma$  ligands on serum glucose, insulin, HbA<sub>1c</sub>, and NEFA levels are presented in Table 2. The Western diet itself did not significantly alter glucose, HbA<sub>1c</sub>, or NEFA levels, but insulin levels rose in both male and female mice. Rosiglitazone and GW7845 treatment resulted in a significant decrease in insulin levels in male mice but had no significant effect on insulin levels in female mice (Table 2). HbA<sub>1c</sub> decreased in males treated with rosiglitazone and GW7845.

To further investigate the effects of rosiglitazone and GW7845 on glucose homeostasis, the response to an oral glucose challenge was assessed in LDLR<sup>-/-</sup> mice fed the Western diet for 8 weeks. LDLR<sup>-/-</sup> mice fed a nor-

mal chow diet were used as additional control groups. Mice were fasted for 4 hours before being given an oral glucose load of 0.75 mg/g. Blood samples were taken at 0, 15, 30, 60, and 90 minutes for measurement of glucose and insulin levels. In male mice, the Western diet had relatively little effect on glucose levels in response to the oral glucose challenge (Figure 3a). In female mice, after glucose administration, the Western diet resulted in modest elevations in glucose that were normalized by treatment with either rosiglitazone or GW7845 (Figure 3b). Striking differences in the insulin responses to oral glucose challenge were noted between

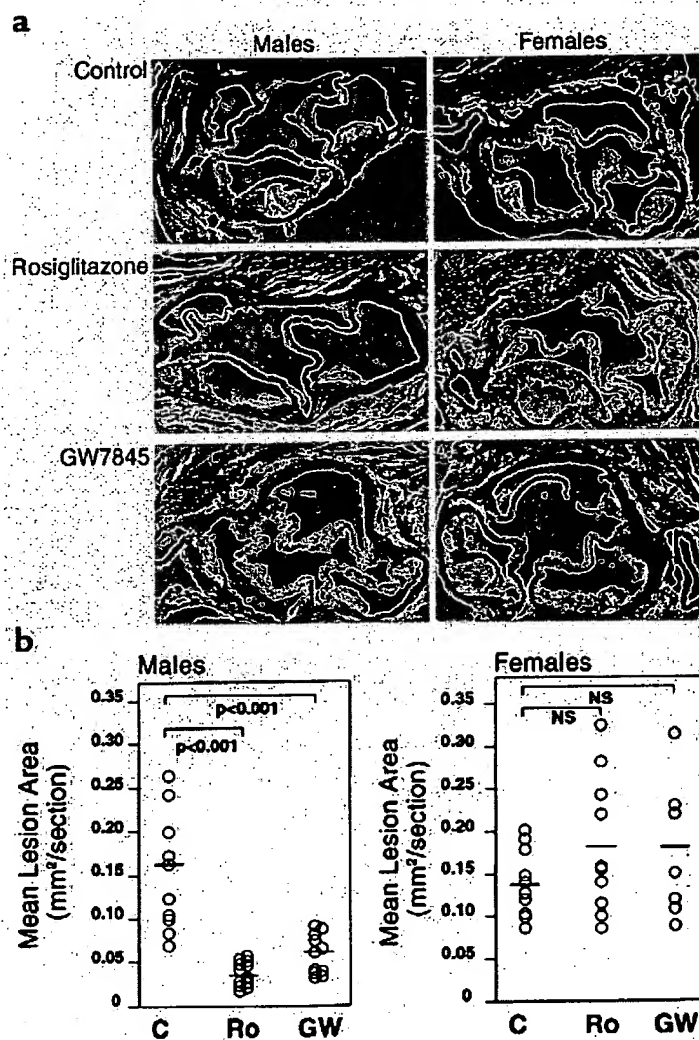


**Figure 1** Atherosclerosis in LDLR<sup>-/-</sup> mice fed a high-fat, cholesterol-enriched Western diet for 10 weeks. (a) Sections through the aortic root at the levels of the aortic valves were stained for elastin to highlight the medial boundaries of atherosclerotic lesions. (b) Quantitative analysis of lesion areas in control mice (C), mice treated with rosiglitazone (Ro), and mice treated with GW7845 (GW). For male mice, means ± SEM were: C, 0.161 ± 0.067 mm<sup>2</sup>/section (n = 10); Ro, 0.037 ± 0.014 mm<sup>2</sup>/section (n = 12); GW, 0.063 ± 0.027 mm<sup>2</sup>/section (n = 10). For female mice, means ± SEM were: C, 0.131 ± 0.035 mm<sup>2</sup>/section (n = 10); Ro, 0.183 ± 0.088 mm<sup>2</sup>/section (n = 10); GW, 0.181 ± 0.0091 mm<sup>2</sup>/section (n = 10). NS, not statistically significant.



male and female mice treated with rosiglitazone and GW7845. The Western diet resulted in increased fasting insulin levels in both male and female mice (Figure 3, c and d), compared with the chow-fed controls. Treatment with rosiglitazone or GW7845 resulted in normalization of the fasting insulin levels and the insulin response to glucose challenge in male mice, but not in female mice (Figure 3, c and d), consistent with changes in insulin levels observed in the intervention studies (Table 2).

**Effects of PPAR $\gamma$  ligands on gene expression.** To investigate potential effects of PPAR $\gamma$  ligands on patterns of gene expression within the arterial wall, RNA analysis was performed in LDLR $^{-/-}$  mice fed a Western diet for 10 weeks in the absence or presence of rosiglitazone or GW7845 as described for the intervention studies. RNA was isolated from the base of the heart containing the aortic origin affected by atherosclerosis and analyzed for TNF- $\alpha$ , MCP-1, VCAM-1, and gelatinase B mRNA levels, using quantitative real-time PCR. TNF- $\alpha$  and

gelatinase B mRNA levels were significantly lower in male mice treated with rosiglitazone or GW7845 (Figure 4). Decreases in TNF- $\alpha$  and gelatinase B were smaller in female mice and did not reach statistical significance in the case of gelatinase B. Levels of VCAM-1 and MCP-1, which are thought to be involved in monocyte adhesion to the vessel wall and migration into the lesion, respectively (34), did not change significantly among the groups (Figure 4). Reductions in TNF- $\alpha$  and gelatinase B mRNA levels were also observed in RNA prepared from the apex of the heart, suggesting general effects of the PPAR $\gamma$  ligands (data not shown). Differences in the responses of TNF- $\alpha$  and gelatinase B genes to PPAR $\gamma$  ligand between male and female mice were not likely due to differences in PPAR $\gamma$  expression, because PPAR $\gamma$  mRNA levels were approximately two times higher in female tissues (data not shown).

Because there were significant differences in lesion size in male controls and animals treated with solvent, rosiglitazone, or GW7845, we also investigated whether PPAR $\gamma$  ligands altered levels of gene expression in the artery wall under conditions of equivalent degrees of atherosclerosis. LDLR $^{-/-}$  male mice were fed a 1.25% cholesterol and 21% milk-fat diet for 16 weeks to induce significant atherosclerosis in the aortic arch. Mice were then treated with rosiglitazone, GW7845, or control solvent for 2 weeks while maintaining the high-fat, high-cholesterol diet. Aortas were dissected and weighed to confirm comparable levels of atherosclerosis (35). As an additional control group, mRNA was isolated from aortas of normocholesterolemic animals. The aortas from each group were pooled, and mRNA was isolated for analysis of macrophage-specific membrane glycoprotein that serves as a marker of tissue macrophages (36). Macrophage expression was low in normal aortas and markedly increased in atherosclerotic aortas, as expected. Macrophage levels were not significantly altered by 2 weeks of treatment with rosiglitazone or GW7845, consistent with our observation that PPAR $\gamma$  ligands do not alter macrophage expression in peritoneal macrophages (data not shown) and reflecting comparable levels of atherosclerosis in these three groups. SR-A and MCP-1 mRNA levels were also elevated in atherosclerotic aortas, as expected. Surprisingly, the mRNA levels for VCAM-1 remained unchanged. In contrast to previous findings in cell-culture models (29, 37), mRNA levels for these genes were not decreased by treatment with PPAR $\gamma$  ligands. However, treatment with rosiglitazone or GW7845 significantly increased CD36 expression and inhibited TNF- $\alpha$  expression, indicating actions of PPAR $\gamma$  on gene expression in the artery wall. The effects on CD36 expression were tissue specific, because no increase in CD36 expression was observed in cardiac tissue of mice treated with rosiglitazone or GW7845 (data not shown).

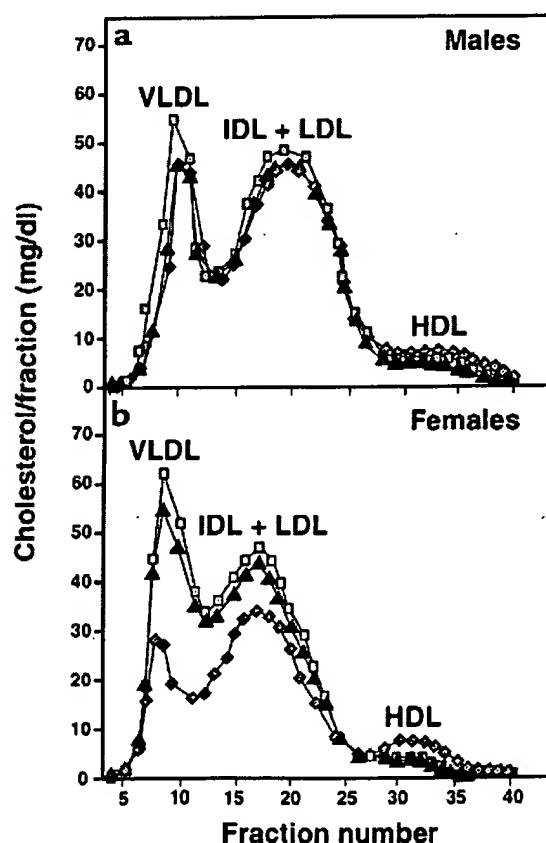
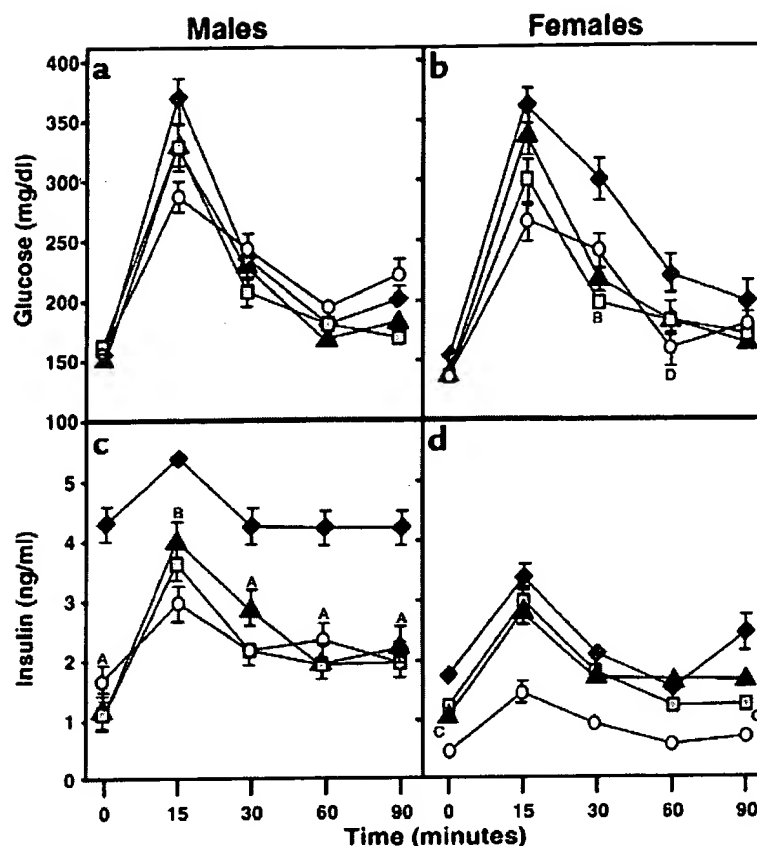


**Figure 2**

Size distribution of lipoprotein particles in LDLR $^{-/-}$  mice fed a high-fat, cholesterol-enriched diet and treated with solvent (control; diamonds), rosiglitazone (squares), or GW7845 (triangles) for 10 weeks. Plasma was pooled from four mice from each treatment group and fractionated by FPLC. Mean cholesterol content in each fraction was determined in duplicate.

**Figure 3**

Glucose and insulin responses to an oral glucose challenge in LDLR<sup>-/-</sup> mice fed the normal chow (circles); high-fat, cholesterol-enriched diet and solvent (control; diamonds); rosiglitazone (squares); or GW7845 (triangles). Blood glucose and plasma insulin levels were determined at base line (after a 4-hour fast) and 15, 30, 60, and 90 minutes after oral administration of 0.75 mg glucose/g body weight. Samples were taken from eight animals per group. Data are expressed as the mean  $\pm$  SEM. <sup>A</sup>*P* < 0.0001, <sup>B</sup>*P* < 0.002, <sup>C</sup>*P* < 0.015, and <sup>D</sup>*P* < 0.04, drug treatment group vs. control group.



## Discussion

The present studies demonstrate that PPAR $\gamma$  ligands significantly inhibit the development of atherosclerosis in LDLR<sup>-/-</sup> male mice fed a Western-style diet. These mice, in addition to being hypercholesterolemic, were obese, hypertriglyceridemic, and insulin resistant. They thus exhibit clinical features of many human diabetic patients who are candidates for treatment with PPAR $\gamma$  ligands. Rosiglitazone and GW7845 reduced the extent of atherosclerosis despite a significant increase in the expression of CD36 in the vessel wall. These observations suggest that the potential of PPAR $\gamma$  ligands to promote the development of foam cells by upregulation of CD36 is overcome by other systemic and local actions. Several mechanisms could potentially account for the net antiatherosclerotic effects of rosiglitazone and GW7845. A number of proinflammatory cytokines, including TNF- $\alpha$ , IL-1 $\alpha$ , and IL-1 $\beta$ , have been suggested to promote the development of atherosclerosis (38). Systemic reductions in the circulating levels of these cytokines or reductions in their expression within cells of the artery wall could potentially underlie at least some of the antiatherosclerotic effects of rosiglitazone and GW7845. Although previous studies have suggested effects of PPAR $\gamma$  ligands on MCP-1 expression in macrophages and smooth muscle cells and VCAM-1 expression in endothelial cells (18, 39–41), we did not observe significant alter-

ations in VCAM-1 or MCP-1 expression in mice treated with PPAR $\gamma$  agonists. This may reflect the cellular heterogeneity of the aortic origin and vessel wall from which RNA was isolated for analysis. The antiatherogenic effects of rosiglitazone and GW7845 in male mice also correlated with improved insulin sensitivity. However, to date, no experimental evidence for a direct influence of insulin resistance on atherosclerosis has been provided in humans or murine models (42). Further investigation will be required to establish the major mechanisms underlying the therapeutic effects of PPAR $\gamma$  ligands in this model system.

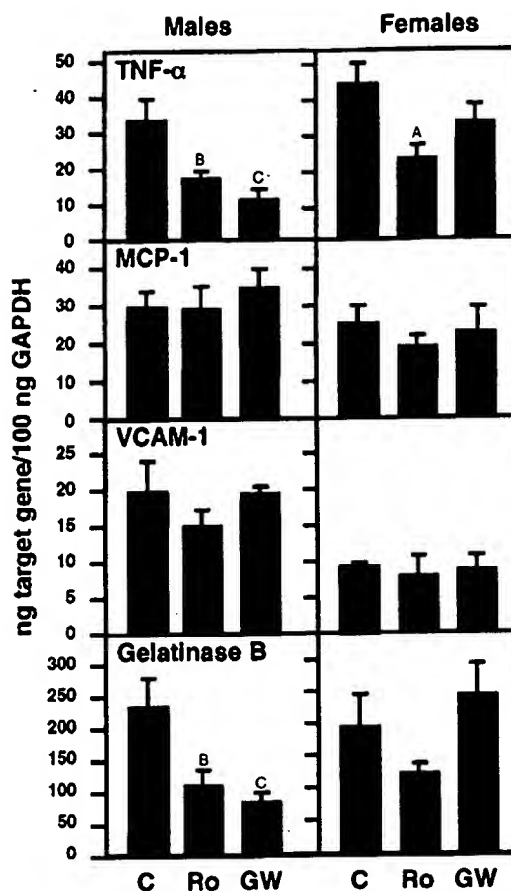
Intriguingly, female mice did not exhibit a reduction in atherosclerosis in response to PPAR $\gamma$ -specific ligands. This lack of a response was not due to altered drug levels or differences in levels of PPAR $\gamma$  expression in the artery wall. Rosiglitazone and GW7845 were less effective in correcting hyperinsulinemia in female mice and did not influence the expression of gelatinase B or TNF- $\alpha$  in tissues. In contrast to male mice, PPAR $\gamma$  ligands altered the lipoprotein size distribution in female mice, reducing HDL levels and skewing the profile to larger particles. Reductions in HDL levels could potentially account for lack of effect of rosiglitazone and GW7845 on the extent of atherosclerosis, but the lack of effect on gelatinase B and TNF- $\alpha$  levels suggest gender-specific differences in the responses to

**Figure 4**

Expression of TNF- $\alpha$ , MCP-1, VCAM-1, and gelatinase B mRNA in the aortic root. The mRNA levels were quantitated using real-time RT-PCR. Six to seven samples per group were analyzed. C, control; Ro, rosiglitazone; GW, GW7845. Data are expressed as mean  $\pm$  SEM. <sup>A</sup> $P < 0.05$ , <sup>B</sup> $P < 0.01$ , and <sup>C</sup> $P < 0.001$ , drug treatment groups vs. cholesterol group.

PPAR $\gamma$  ligands. The basis for these differences is unclear, but they are likely to relate to influences of estrogens and progestins. Consistent with this, preliminary studies of ovariectomized female mice indicate metabolic responses to rosiglitazone and GW7845 that are much more similar to male mice. Studies of the efficacy of TZDs as insulin sensitizers in human diabetic patients have not revealed any significant gender-specific differences, but most female patients enrolled in these studies are postmenopausal.

In concert, these studies provide clear evidence that activation of PPAR $\gamma$  inhibits the development of atherosclerosis in a murine model. These effects were observed using relatively high doses of PPAR $\gamma$  ligands that also induced adipogenesis in bone marrow and secondary extramedullary hematopoiesis. Extending this proof of principle to human populations will require clinical investigation in diabetic and nondiabetic patients. Because the PPAR $\gamma$  agonists used in these studies exerted both potentially antiatherogenic (e.g., down-regulation of TNF- $\alpha$ ) and potentially proatherogenic (e.g., upregulation of CD36) effects on patterns of gene expression in the artery wall, the development of novel PPAR $\gamma$  ligands that dissociate proatherogenic activities from antidiabetic and antiatherogenic activities would be highly desirable. Recent successes in the development of selective estrogen receptor modulators (43) suggest that such goals are attainable.

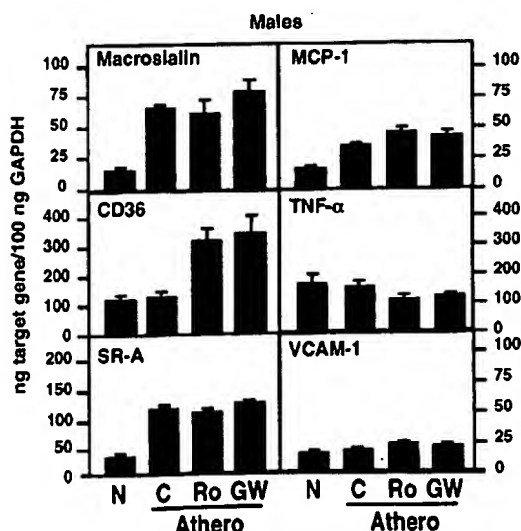


#### Acknowledgments

We wish to thank Florencia Casanada, Jennifer Patterson, and Joseph Juliano for isolating the aortas and determining the plasma cholesterol and triglycerides; Jane Binz and Jennifer Becker for HbA<sub>1c</sub>, NEFA, and HDL<sub>c</sub> analysis; Harry Marr for drug level determination; Jacques Corbeil and Christine Plotkin at the

**Figure 5**

Expression of macrophage markers, CD36, SR-A, MCP-1, TNF- $\alpha$ , and VCAM-1 mRNA in the aorta. Male LDLR<sup>-/-</sup> mice were fed either a normal chow diet (N) or a high-cholesterol diet for 4 months to induce the development of atherosclerosis (Athero). Animals fed the high-cholesterol diet were then treated with either solvent control, rosiglitazone, or GW7845 for 2 weeks. The mRNA levels were quantitated using real-time RT-PCR. Data represent pooled aortas with an average weight of  $3.86 \pm 0.16$  mg/aorta for normal chow (N) ( $n = 11$ );  $5.75 \pm 0.67$  mg/aorta for high cholesterol (C) ( $n = 6$ );  $5.67 \pm 0.56$  mg/aorta for high cholesterol/rosiglitazone (Ro) ( $n = 6$ ); and  $5.80 \pm 0.70$  mg/aorta for high cholesterol/GW7845 (GW) ( $n = 6$ ). Data are in triplicates and expressed as mean  $\pm$  SEM.



Center for AIDS Research Genomics Core, Veterans Medical Research Foundation for advice and performing the RT-PCR quantification analysis; and Tanya Schneiderman and Amy Johnson for their assistance in preparing the manuscript. This work was supported by NIH Specialized Center of Research (SCOR) on Molecular Medicine and Atherosclerosis grant (HL-56989) and a grant from the Glaxo Wellcome Research Institute. A.C. Li is supported by a Mentored-Clinical Scientist Development Award (HL-03625). C.K. Glass is an Established Investigator of the American Heart Association.

- Kannel, W., and McGee, D. 1979. Diabetes and cardiovascular disease: the Framingham study. *JAMA*. 241:2035-2038.
- Uusitupa, M., Niskanen, L., and Siitonen, O. 1990. 5-year incidence of atherosclerotic vascular disease in relation to general risk factors, insulin levels, and abnormalities in lipoprotein composition in non-insulin-dependent diabetic and nondiabetic subjects. *Circulation*. 82:27-36.
- Steinberg, D., Parthasarathy, S., Carew, T.E., Khoo, J.C., and Witztum, J.L. 1989. Beyond cholesterol. Modifications of low-density lipoprotein that increase its atherogenicity. *N. Engl. J. Med.* 320:915-924.
- Napoli, C., et al. 1997. Fatty streak formation occurs in human fetal aortas and is greatly enhanced by maternal hypercholesterolemia. Intimal accumulation of low density lipoprotein and its oxidation precede monocyte recruitment into early atherosclerotic lesions. *J. Clin. Invest.* 100:2680-2690.
- Kodama, T., Reddy, P., Kishimoto, C., and Krieger, M. 1988. Purification and characterization of a bovine acetyl low density lipoprotein receptor. *Proc. Natl. Acad. Sci. USA*. 85:9238-9242.
- Endemann, G., et al. 1993. CD36 is a receptor for oxidized low density lipoprotein. *J. Biol. Chem.* 268:11811-11816.
- Ramprasad, M.P., Terpstra, V., Kondratenko, N., Quehenberger, O., and Steinberg, D. 1996. Cell surface expression of mouse macrophage and human CD68 and their role as macrophage receptors for oxidized low density lipoprotein. *Proc. Natl. Acad. Sci. USA*. 93:14833-14838.
- Ross, R. 1986. The pathogenesis of atherosclerosis. *N. Engl. J. Med.* 314:488-500.
- Ross, R. 1999. Atherosclerosis: an inflammatory disease. *N. Engl. J. Med.* 340:115-126.
- Boring, L., Gosling, J., Cleary, M., and Charo, I.F. 1998. Decreased lesion formation in CCR2<sup>-/-</sup> mice reveals a role for chemokines in the initiation of atherosclerosis. *Nature*. 394:894-897.
- Gosling, J., et al. 1999. MCP-1 deficiency reduces susceptibility to atherosclerosis in mice that overexpress human apolipoprotein B. *J. Clin. Invest.* 103:773-778.
- Suzuki, H., et al. 1997. A role for macrophage scavenger receptors in atherosclerosis and susceptibility to infection. *Nature*. 386:292-296.
- Febbraio, M., et al. 2000. Targeted disruption of the class B scavenger receptor CD36 protects against atherosclerotic lesion development in mice. *J. Clin. Invest.* 105:1049-1056.
- Barnes, P.J., and Karin, M. 1997. Nuclear factor-kappaB: a pivotal transcription factor in chronic inflammatory diseases. *N. Engl. J. Med.* 336:1066-1071.
- Sato, H., Kita, M., and Seiki, M. 1993. v-Src activates the expression of 92-kDa type IV collagenase gene through the AP-1 site and the GT box homologous to retinoblastoma control elements. A mechanism regulating gene expression independent of that by inflammatory cytokines. *J. Biol. Chem.* 268:23460-23468.
- Ricote, M., et al. 1998. Expression of the peroxisome proliferator-activated receptor  $\gamma$  (PPAR $\gamma$ ) in human atherosclerosis and regulation in macrophages by colony stimulating factors and oxidized low density lipoprotein. *Proc. Natl. Acad. Sci. USA*. 95:7614-7619.
- Marx, N., Sukhova, G., Murphy, C., Libby, P., and Plutzky, J. 1998. Macrophages in human atheroma contain PPAR $\gamma$ : differentiation-dependent peroxisome proliferator-activated receptor gamma expression and reduction of MMP-9 activity through PPAR $\gamma$  activation in mononuclear phagocytes *in vitro*. *Am. J. Pathol.* 153:17-23.
- Jackson, S.M., et al. 1999. Peroxisome proliferator-activated receptor activators target human endothelial cells to inhibit leukocyte-endothelial cell interaction. *Arterioscler. Thromb. Vasc. Biol.* 19:2094-2104.
- Tontonoz, P., Nagy, L., Alvarez, J.G.A., Thomazy, V.A., and Evans, R.M. 1998. PPAR $\gamma$  promotes monocyte/macrophage differentiation and uptake of oxidized LDL. *Cell*. 93:241-252.
- Pasceri, V., Wu, H.D., Willerson, J.T., and Yeh, E.T. 2000. Modulation of vascular inflammation *in vitro* and *in vivo* by peroxisome proliferator-activated receptor-gamma activators. *Circulation*. 101:235-238.
- Nagy, L., Tontonoz, P., Alvarez, J.G.A., Chen, H., and Evans, R.M. 1998. Oxidized LDL regulates macrophage gene expression through ligand activation of PPAR-gamma. *Cell*. 93:229-240.
- Forman, B.M., et al. 1995. 15-Deoxy- $\Delta^{12,14}$ -prostaglandin J<sub>2</sub> is a ligand for the adipocyte determination factor PPAR $\gamma$ . *Cell*. 83:803-812.
- Kliwer, S.A., et al. 1997. Fatty acids and eicosanoids regulate gene expression through direct interactions with peroxisome proliferator-activated receptors  $\alpha$  and  $\gamma$ . *Proc. Natl. Acad. Sci. USA*. 94:4318-4323.
- Barak, Y., et al. 1999. PPAR $\gamma$  is required for placental, cardiac, and adipose tissue development. *Mol. Cell*. 4:585-595.
- Kubota, N., et al. 1999. PPAR $\gamma$  mediates high-fat diet-induced adipocyte hypertrophy and insulin resistance. *Mol. Cell*. 4:597-609.
- Rosen, E.D., et al. 1999. PPAR $\gamma$  is required for the differentiation of adipose tissue *in vivo* and *in vitro*. *Mol. Cell*. 4:611-617.
- Nolan, J.J., Ludvik, B., Beersden, P., Joyce, M., and Olefsky, J. 1994. Improvement in glucose tolerance and insulin resistance in obese subjects treated with troglitazone. *N. Engl. J. Med.* 331:1188-1193.
- Jiang, C., Ting, A.T., and Seed, B. 1998. PPAR-gamma agonists inhibit production of monocyte inflammatory cytokines. *Nature*. 391:82-86.
- Ricote, M., Li, A.C., Willson, T.M., Kelly, C.J., and Glass, C.K. 1998. The peroxisome proliferator-activated receptor- $\gamma$  is a negative regulator of macrophage activation. *Nature*. 391:79-82.
- Su, C.G., et al. 1999. A novel therapy for colitis utilizing PPAR- $\gamma$  ligands to inhibit the epithelial inflammatory response. *J. Clin. Invest.* 104:383-389.
- Sheehan, D.C., and Hrapchak, B.B. 1980. *Theory and practice of histotechnology*. C.V. Mosby Co., St. Louis, Missouri, USA. 481 pp.
- Tangirala, R.K., Rubin, E.M., and Palinski, W. 1995. Quantitation of atherosclerosis in murine models: correlation between lesions in the aortic origin and in the entire aorta, and differences in the extent of lesions between sexes in LDL receptor-deficient and apolipoprotein E-deficient mice. *J. Lipid Res.* 36:1-9.
- Willson, T., Brown, P., Sternbach, D., and Henke, B. 2000. The PPARs: from orphan receptors to drug discovery. *J. Med. Chem.* 43:527-550.
- Fruebis, J., Gonzales, V., Silvestre, M., and Palinski, W. 1997. Effect of probucol treatment on gene expression of VCAM-1, MCP-1 and M-CSF in the aortic wall of LDL receptor-deficient rabbits during early atherogenesis. *Arterioscler. Thromb. Vasc. Biol.* 17:1289-1302.
- Tsimikas, S., Shortall, B.P., Witztum, J.L., and Palinski, W. 2000. *In vivo* uptake of radiolabeled MDA2, an oxidation-specific monoclonal antibody, provides an accurate measure of atherosclerotic lesions rich in oxidized LDL and is highly sensitive to their regression. *Arterioscler. Thromb. Vasc. Biol.* 20:689-697.
- Holness, C.L., and Simmons, D.L. 1993. Molecular cloning of CD68, a human macrophage marker related to lysosomal glycoproteins. *Blood*. 81:1607-1613.
- Goetze, S., et al. 1999. PPAR gamma-ligands inhibit migration mediated by multiple chemoattractants in vascular smooth muscle cells. *J. Cardiovasc. Pharmacol.* 33:798-806.
- Libby, P., Sukhova, G., Lee, R.T., and Galis, Z.S. 1995. Cytokines regulate vascular functions related to stability of the atherosclerotic plaque. *J. Cardiovasc. Pharmacol.* 25(Suppl. 2):S9-S12.
- Murao, K., et al. 1999. Thiazolidinedione inhibits the production of monocyte chemoattractant protein-1 in cytokine-treated human vascular endothelial cells. *FEBS Lett.* 454:27-30.
- Law, R.E., et al. 1996. Troglitazone inhibits vascular smooth muscle cell growth and intimal hyperplasia. *J. Clin. Invest.* 98:1897-1905.
- Staels, B., et al. 1998. Activation of human aortic smooth-muscle cells is inhibited by PPAR $\alpha$  but not by PPAR $\gamma$  activators. *Nature*. 393:790-793.
- Merat, S., Casanada, F., Sutphin, M., Palinski, W., and Reaven, P.D. 1999. Western-type diets induce insulin resistance and hyperinsulinemia in LDL receptor-deficient mice but do not increase aortic atherosclerosis compared with normoinsulinemic mice in which similar plasma cholesterol levels are achieved by a fructose-rich diet. *Arterioscler. Thromb. Vasc. Biol.* 19:1223-1230.
- Roe, E.B., Chiu, K.M., and Arnaud, C.D. 2000. Selective estrogen receptor modulators and postmenopausal health. *Adv. Intern. Med.* 45:257-278.

# Hyperlipidemia and Atherosclerotic Lesion Development in LDL Receptor-Deficient Mice Fed Defined Semipurified Diets With and Without Cholate

Andrew H. Lichtman, Steven K. Clinton, Kaeko Iiyama, Philip W. Connelly,  
Peter Libby, Myron I. Cybulsky

**Abstract**—Past studies of atherosclerosis in mice have used chow-based diets supplemented with cholesterol, lipid, and sodium cholate to overcome species resistance to lesion formation. Similar diets have been routinely used in studies with LDL receptor-deficient (LDLR<sup>-/-</sup>) mice. The nonphysiological nature and potential toxicity of cholate-containing diets have led to speculation that atherogenesis in these mice may not accurately reflect the human disease process. We have designed a semipurified AIN-76A-based diet that can be fed in powdered, pelleted, or liquid form and manipulated for the precise evaluation of diet-genetic interactions in murine atherosclerosis. LDLR<sup>-/-</sup> mice were randomly assigned among 4 diets (n=6/diet) as follows: 1, control, 10% kcal lipid; 2, high fat (40% kcal), moderate cholesterol (0.5% by weight); 3, high fat, high cholesterol (1.25% by weight); and 4, high fat, high cholesterol, and 0.5% (wt/wt) sodium cholate. Fasting serum cholesterol was increased in all cholesterol-supplemented mice compared with controls after 6 or 12 weeks of feeding ( $P<0.01$ ). The total area of oil red O-stained atherosclerotic lesions was determined from digitally scanned photographs. In contrast to the control group, all mice in cholesterol-supplemented dietary groups 2 to 4 had lesions involving 7.01% to 12.79% area of the thoracic and abdominal aorta at 12 weeks ( $P<0.002$ , for each group versus control). The distribution pattern of atherosclerotic lesions was highly reproducible and comparable. The histological features of lesions in mice fed cholate-free or cholate-containing diets were similar. This study shows that sodium cholate is not necessary for the formation of atherosclerosis in LDLR<sup>-/-</sup> mice and that precisely defined semipurified diets are a valuable tool for the examination of diet-gene interactions. (*Arterioscler Thromb Vasc Biol.* 1999;19:1938-1944.)

**Key Words:** atherosclerosis ■ LDL receptor ■ dietary lipids ■ cholesterol ■ mice

The development of murine models defective in genes controlling lipid metabolism and lipoprotein expression provides an opportunity to understand better the complex interactions between diet and genetics in atherosclerosis. In the last several years, embryonic stem cell and transgenic technologies have been used to alter the expression levels of various genes affecting lipoprotein metabolism and have led to the development of murine knockout and transgenic models of atherogenesis. The ApoE knockout (ApoE<sup>-/-</sup>),<sup>1,2</sup> LDL receptor knockout (LDLR<sup>-/-</sup>),<sup>3</sup> and human ApoB transgenic mice<sup>4,5</sup> develop lesions throughout the arterial tree. Their distribution pattern and morphological features share many similarities with human atherosclerosis, suggesting that similar pathogenic mechanisms may be involved.<sup>6,7</sup> ApoE<sup>-/-</sup> mice develop hypercholesterolemia and atherosclerotic lesions spontaneously, and this can be accelerated by feeding a

Western-type diet.<sup>1,6</sup> In contrast, LDLR<sup>-/-</sup> mice fed a chow diet have only a 2-fold elevation in plasma cholesterol compared with control mice and do not develop significant lesions in the first 6 months of life.<sup>3</sup> When fed a diet consisting of 1.25% cholesterol, 7.5% cocoa butter, 7.5% casein, and 0.5% cholic acid, these mice develop marked hypercholesterolemia and lesions throughout the aorta within 3 to 4 months.<sup>8</sup> Because hypercholesterolemia and lesion formation in LDLR<sup>-/-</sup> mice are readily enhanced by a diet supplemented with fat, cholesterol, and cholate, these mice provide a unique opportunity for evaluation of early events in atherogenesis.

Before the development of atherosclerosis-prone gene-targeted mutant mice, many studies were performed with normal mice fed chow-based diets supplemented with varying amounts of saturated fats, cholesterol, and cholate to

Received September 22, 1998; revision accepted January 11, 1999.

From the Vascular Research Division (A.H.L.), Department of Pathology, and the Vascular Medicine and Atherosclerosis Unit (P.L.), Cardiovascular Division, Department of Medicine, Brigham and Women's Hospital, Harvard Medical School, Boston, Mass; the Arthur G. James Cancer Hospital and Research Institute (S.K.C.), Ohio State University, Columbus, Ohio; and the Department of Laboratory Medicine and Pathobiology (K.I., M.I.C.), University of Toronto, Toronto Hospital Research Centre, and the Departments of Laboratory Medicine and Pathobiology, Medicine, and Biochemistry (P.W.C.), University of Toronto, St Michael's Hospital, Toronto, Ontario, Canada.

Correspondence to Andrew H. Lichtman, MD, PhD, Department of Pathology, Brigham and Women's Hospital, 221 Longwood Avenue, Boston, MA 02115. E-mail alichtman@rics.bwh.harvard.edu

© 1999 American Heart Association, Inc.

*Arterioscler Thromb Vasc Biol.* is available at <http://www.atvbaha.org>

induce atheromatous lesions. In particular, C57BL/6 mice are susceptible to dietary intervention and develop foam cell-rich lesions in the aortic root, but not advanced atheromas.<sup>9-13</sup> Dietary cholate was required to achieve significant hypercholesterolemia, presumably by interfering with hepatobiliary excretion of cholesterol. Most published studies of atherosclerosis in the LDLR<sup>-/-</sup> mice have relied on similar diets supplemented with cholate, cholesterol, and lipid that were used in the earlier C57BL/6 mouse studies. This has led to criticisms of the LDLR<sup>-/-</sup> mouse model based on the speculation that toxic metabolic effects of cholate may modify the pathogenesis of vascular disease in ways not relevant to human atherosclerosis. For example, cholate may cause hepatic steatosis that can progress to cirrhosis accompanied by several host metabolic, physiological, and hormonal changes that can potentially interfere with the interpretation of studies focusing on the histopathological and molecular events during atherogenesis. Recent data from our group and others indicate that cholate is not necessary and that a diet supplemented with cholesterol and saturated fat is sufficient for aortic lesion development in LDLR<sup>-/-</sup> mice.<sup>14,15</sup>

From a nutritional perspective, the dilution of a chow diet with purified lipids, such as hydrogenated coconut oil, increases the caloric density of the diet and reduces the ratio of essential nutrients to dietary energy, thereby potentially contributing to marginal nutrient intake in mice consuming the atherogenic diet. Chow diets do not take advantage of the accumulated knowledge concerning nutritional requirements of mice and the experience of many investigators using precisely controlled semipurified or purified diets for studies of chronic disease processes in rodents.<sup>16-19</sup> Chow diets are formulated from natural ingredients to satisfy the minimal nutrient requirements for growth and reproduction but they differ individual nutrients over time, seasonally, in different geographic locations and between companies in the sources of ingredients included in the final product.<sup>20</sup> Furthermore, many man-made and natural toxins are detected in chow diets, such as aflatoxins, nitrosamines, pesticides, herbicides, and heavy metals.<sup>20-22</sup> Chow diets contain a variety of natural substances from grains, fruits, and vegetables that may modify lipid metabolism and atherogenesis, including a diverse array of soluble and insoluble fiber sources and a multitude of biologically active phytochemicals such as carotenoids and flavonoids. For example, the latter constituents may exert antioxidant actions that could influence atherogenesis and confound experiments.

We propose that investigators of atherogenesis using the many new transgenic and gene knockout models should consider using precisely defined semipurified diets in their studies. This approach adds very little to the overall costs of *in vivo* investigations and can help improve the quality of data obtained and the comparison of results among laboratories over time. Furthermore, the use of semipurified diets in murine studies provides a method for precise control of dietary and nutritional factors, allowing for a meaningful evaluation of specific nutritional interventions that may be relevant to human disease processes. We therefore designed and tested several semipurified diet formulations in a study of atherogenesis in LDLR<sup>-/-</sup> mice.

## Methods

### Mice

Male LDLR<sup>-/-</sup> mice (homozygous) from a mixed C57BL/6J×129Sv background (50% C57BL/6J:50% 129Sv) were purchased from Jackson Laboratories and maintained in the Longwood Medical Research Center facility in accordance with guidelines of the Committee on Animals of the Harvard Medical School and those prepared by the Committee on Care and Use of Laboratory Animals of the Institute of Laboratory Resources, National Research Council [DHEW publication No. (NIH) FS-23]. At 8 to 12 weeks of age, mice that reached a weight of 21 to 22 g were randomly assigned to 1 of 4 diets (see below) fed *ad libitum* for 12 weeks. For experiments that included analyses of body weight, total plasma cholesterol and triglycerides, and atherosclerotic lesion formation in the aorta, groups consisted of 6 mice. Additional male LDLR<sup>-/-</sup> mice were fed identical diets and killed to obtain plasma for lipoprotein analysis, liver function tests, and tissues for histology.

### Diets

Four diets were used in this study. Each diet was a modification of the AIN-76A semipurified diet for mice and rats<sup>18,19</sup> and prepared by Dr Edward A. Ulman at Research Diets, Inc, according to our formulations (Table 1). The diets provide adequate concentrations of all known essential nutrients for the mouse. The carbohydrate component was altered from the original AIN-76A formulation by including expanded maltose dextrin, which allows the lipid concentration to vary from the range of 10% to 40% of total energy (≈5% to 20% by weight) without a problem of "settling out." Furthermore, the carbohydrate modifications allow a diet to be fed as a powder, a liquid formulation, or processed into pellets (used in this study). The 4 experimental diet groups include diet 1 group (Research Diet D12102), control (10% kcal lipid); diet 2 group (Research Diet D12107), high fat (40% kcal lipid), moderate cholesterol (0.5% by weight); diet 3 group (Research Diet D12108), high fat, high cholesterol (1.25% by weight); and diet 4 group (Research Diet D12109), high fat, high cholesterol, and sodium cholate (0.5% by weight). The addition of lipid to the baseline diet formulation is achieved by substituting fat (9 kcal/g of metabolizable energy) for carbohydrate (4 kcal/g of metabolizable energy) based on an equal amount of energy (kcal) rather than an equal weight (g). This approach is necessary to maintain a constant ratio of all other nutrients in the diet to energy. This technique of diet formulation avoids the problem of reduced nutrient content of the high-fat diets prepared by the dilution technique (ie, chow diluted with fat) or when fat is substituted for carbohydrate on the basis of weight.

### Cholesterol Measurements and Liver Function Tests

Serum samples were collected for lipid analysis after overnight fasting. At 0 (initiation of the study), 6 and 12 weeks, blood was obtained from individual mice by tail-vein nicking and total serum cholesterol and triglyceride levels were determined by colorimetric assays (Sigma Chemical Co). Blood was obtained from the retroorbital plexus for analysis of plasma lipoproteins by fast protein liquid chromatography gel-filtration chromatography after 12 weeks of diet. Samples were anticoagulated with EDTA (3 mmol/L or 0.1% final) and sodium azide 0.02% was added as a preservative. To obtain a plasma volume of at least 250  $\mu$ L, plasma was pooled from several mice within each group. Erythrocytes and leukocytes were removed by low-speed (400g, 10 minutes, 4°C) and platelets by high-speed (3000g, 5 minutes, 4°C) centrifugations. Plasma was stored at 4°C for <2 days. Plasma was subjected to fast protein liquid chromatography gel-filtration chromatography by using a Superose 6HR 10/30 column (Pharmacia Biotech) as was previously described.<sup>23</sup> Filtered plasma (200  $\mu$ L) was loaded on the column and was eluted with 2 mmol/L sodium phosphate, 0.14 mol/L NaCl, 5 mmol/L Na<sub>2</sub>EDTA, 0.02% NaN<sub>3</sub>, pH 7.4, at a constant flow rate of 0.5 mL/min. Fractions (0.5 mL) were collected and total cholesterol, triglycerides, free cholesterol, and choline-containing phospholipids were measured on a Technicon RA1000 (Bayer Corp). Triglycerides were corrected for free glycerol by using a triglyceride blank reagent (Bayer Corp). The cholesterol and triglyceride assays were standard-

TABLE 1. Formulation for the Diets Used in This Study and Their Macronutrient Contents as Percentages of Total Energy

	Diet 1 (10% kcal fat, 0% cholesterol§§, 0% cholate§§)		Diet 2 (40% kcal fat, 0.5% cholesterol, 0% cholate)		Diet 3 (40% kcal fat, 1.25% cholesterol, 0% cholate)		Diet 4 (40% kcal fat, 1.25% cholesterol, 0.5% cholate)	
Ingredient	Grams	kcal	Grams	kcal	Grams	kcal	Grams	kcal
Formulation								
Casein†	200.0	800	200.0	800	200.0	800	200.0	800
Cystine	3.0	12	3.0	12	3.0	12	3.0	12
Soy oil‡	25.0	225	25.0	225	25.0	225	25.0	225
Cocoa butter§	20.0	180	155.0	1395	155.0	1395	155.0	1395
Corn Starch	375.0	1500	212.0	848	212.0	848	212.0	848
Malto-dextrin	125.0	500	71.0	284	71.0	284	71.0	284
Sucrose	200.0	800	113.0	452	113.0	452	113.0	452
Cellulose¶	50.0	0	50.0	0	50.0	0	50.0	0
Mineral Mix#	10.0	0	10.0	0	10.0	0	10.0	0
Dicalcium phosphate#	13.0	0	13.0	0	13.0	0	13.0	0
Calcium carbonate#	5.5	0	5.5	0	5.5	0	5.5	0
Potassium citrate, monohydrate#	16.5	0	16.5	0	16.5	0	16.5	0
Vitamin mix**	10.0	40	10.0	40	10.0	40	10.0	40
Choline††	2.0	0	2.0	0	2.0	0	2.0	0
Cholesterol	0	0	4.5	0	11.25	0	11.25	0
Cholate	0	0	0	0	0	0	4.5	0
Total grams or kcal*	1055.0	4057	890.6	4056	897.35	4056	901.85	4056
	% kcal		% kcal		% kcal		% kcal	
Macronutrient content								
Protein	20		20		20		20	
Carbohydrate	70		40		40		40	
Lipid	10		40		40		40	
kcal/g in diet*	3.8		4.5		4.5		4.5	

\*Calculations based on estimated metabolizable energy of 4 kcal/g (16.7 kJ/g) of protein and carbohydrate and 9 kcal/g (37.7 kJ/g) of lipid. The concentrations of minerals, vitamins, and fiber were adjusted to maintain a constant ratio to energy.

†Alcohol extracted casein, 99% protein.

‡Soy oil provides a minimal supply of essential fatty acids.

§We have selected cocoa butter for this study, because it is a saturated fat but has no cholesterol.

||Malto-dextrin 10 is a component of the carbohydrate fraction that assists in maintaining the lipid fraction equally dispersed throughout the diet during shipping, storage, and feeding.

¶BW200 cellulose.

#AIN-76A mineral mixtures with the calcium and phosphate removed. Dicalcium phosphate, calcium carbonate, and potassium citrate, monohydrate are replaced, to increase phosphate and potassium relative to the original formulation.

\*\*AIN-76A vitamin mixture.

††Choline provided as choline bitartrate.

§§Cholesterol and cholate (which do not contribute to total energy) are expressed as percent w/w.

ized with the National Heart Lung and Blood Institutes—Center for Disease Control Lipid Standardization program. Reagents for free cholesterol and choline-containing phospholipid measurements were purchased from Boehringer Mannheim (Germany) and external standards were not available for these assays.

Liver function tests were performed on serum samples by the Tufts Veterinary Diagnostic Laboratory, using an automated analyzer. These tests included serum lactate dehydrogenase (LDH), serum glutamic-oxaloacetic transaminase (SGOT), serum glutamic-pyruvate transaminase (SGPT), and serum bilirubin.

### Tissue Sampling and Analyses

The surface area of aorta occupied by atherosclerotic lesions was quantified by en face oil red O staining, using an approach modified from Palinski et al.<sup>24</sup> Mice were killed, after 12 weeks of diet, by ether inhalation. A catheter was inserted into the left ventricle and

the arterial tree was perfused with PBS (25 mL), then 10% buffered formaldehyde (40 mL, pH 7.4) at a pressure of 100 mm Hg. The entire aorta attached to the heart was dissected and placed overnight in formaldehyde. Using a stereomicroscope, the adventitial fat was dissected and the aorta was stained with oil red O as described by Nunnari et al.<sup>25</sup> After staining, the remaining adventitial fat was easily detected and was removed. The aorta was opened longitudinally, pinned en face on a black silicone-covered dish, and photographed while immersed in PBS. Slides were scanned into a Macintosh computer and the percent surface area occupied by oil red O-stained lesions was determined by using image analysis software (NIH Image). The aortic arch (1 mm above the aortic valve cusps to 2 mm below the ostium of the right subclavian artery), the descending thoracic aorta (extending to 1 mm above the ostium of the celiac artery), the abdominal aorta (including the bifurcation and 0.5 mm of the iliac arteries), and the total aorta were evaluated. After photography, portions of aorta that contained lesions were cross-sectioned



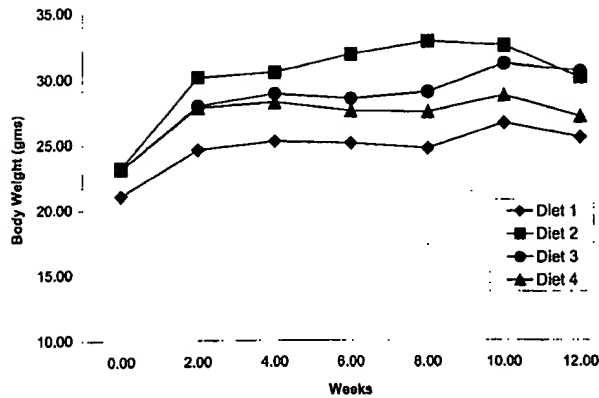


**Figure 1.** Body weights of LDLR<sup>-/-</sup> mice fed diets varying in fat, cholesterol, and cholate content. Mice were fed the diets described in Table 1 and were weighed every 2 weeks for 12 weeks. The data represent the mean weights for the 6 mice in each group at each time point.

and embedded in paraffin. Histological sections were prepared and stained with hematoxylin and eosin.

Liver slices, obtained from each animal at the time it was killed, were fixed in formalin, paraffin-embedded, and histological sections were stained with hematoxylin and eosin.

### Statistical Analysis

Food intake, body weight, and serum lipids were initially analyzed by ANOVA<sup>26</sup> followed by Fisher's PLSD<sup>26</sup> to calculate pairwise comparisons among treatment groups by using Statview 4.5 (Abacus Concepts, Inc).

## Results

### Body Weight

The mean body weight of mice fed each of the 4 diets for 12 weeks is shown in Figure 1. Mice fed the high-fat+0.5% cholesterol diet (diet 2) showed increased body weight ( $P<0.02$ ) compared with controls (diet 1) during weeks 2 through 10. This is a common observation in studies where rodents are provided a high-fat diet, which is more palatable, resulting in a slightly greater intake of diet (kcal). However, we did not attempt to measure food intake in this study, because mice were not individually housed and they typically waste significant amounts of food when provided ad libitum. Additional effort is necessary to accurately quantitate the amount of food consumed in murine studies. Those fed a high-fat diet with higher concentrations of cholesterol or supplemented with cholate did not exhibit a weight gain that was significantly different from controls.

### Lipid Analyses

The analyses of total serum cholesterol and triglyceride levels at 0, 6, and 12 weeks are shown in Table 2. A significant effect of diet on serum cholesterol was observed at 6 weeks ( $P<0.0009$ , ANOVA). Pairwise comparisons show that mice fed diet 1 (control diet) have significantly lower serum cholesterol than those fed the high-fat diets supplemented with 0.5% cholesterol (diet 2;  $P<0.02$ , PLSD), 1.25% cholesterol (diet 3;  $P<0.02$ , PLSD), or 1.25% cholesterol and cholate (diet 4;  $P<0.0001$ , PLSD). A statistically significant difference was not found between diet groups 2 and 3. However, the addition of cholate (diet 4) increased serum cholesterol compared with diets 1, 2, and 3 ( $P<0.009$ , for all comparisons; PLSD).

**TABLE 2.** Plasma Cholesterol and Triglycerides at Different Time Points

Diet	Cholesterol (mg/dL)		
	Week 0 (Baseline)	Week 6	Week 12
1 (10% fat)	104±18	97±21	124±49
2 (40% fat; 0.5% cholesterol)	133±51	327±56*	328±111
3 (40% fat; 1.25% cholesterol)	130±37	331±46*	597±131*
4 (40% fat; 1.25% cholesterol; 0.5% cholate)	129±59	598±71*†‡	761±208*†
Diet	Triglycerides (mg/dL)		
	Week 0 (Baseline)	Week 6	Week 12
1 (10% fat)	52±7	50±6	63±19
2 (40% fat; 0.5% cholesterol)	40±10	85±14	110±37
3 (40% fat; 1.25% cholesterol)	50±11	58±8	141±34
4 (40% fat; 1.25% cholesterol; 0.5% cholate)	41±10	74±10	80±37

Data represent mean±SEM values for nonfasting plasma cholesterol and triglycerides.

\* $P<0.02$  compared with diet group 1.

† $P<0.02$  compared with diet group 2.

‡ $P<0.02$  compared with diet group 3.

Similar results were observed at 12 weeks, although variation in serum cholesterol was greater ( $P<0.005$ , ANOVA). Pairwise comparisons at 12 weeks show that mice fed diet 1 (control diet) have lower serum cholesterol than those fed the high-fat diets supplemented with 0.5% cholesterol (diet 2;  $P<0.15$ , PLSD), 1.25% cholesterol (diet 3;  $P<0.007$ , PLSD), or 1.25% cholesterol and cholate (diet 4;  $P<0.001$ , PLSD). The addition of cholate (diet 4) increased serum cholesterol compared with those fed supplemental cholesterol without cholate ( $P<0.007$  versus diet 2 and  $P=0.31$  versus diet 3, both PLSD). Diets did not have any significant effect on serum triglyceride levels at 6 or 12 weeks.

The analysis of plasma lipoproteins by fast protein liquid chromatography gel-filtration chromatography after 12 weeks of diet is summarized in Figure 2. The extent of lipids recovered in Superose fractions was relatively uniform and comparable in all dietary groups. Percent recovery ranged from 83% to 87% for total cholesterol, 90% to 94% for choline-containing phospholipids, and 68% to 120% for triglycerides. The data revealed that elevated total cholesterol in dietary groups 2 through 4 was the result of increased VLDL and IDL/LDL lipoproteins (Figure 2). Levels of HDL lipoproteins varied inversely with VLDL and IDL/LDL. For each lipoprotein class, levels of free cholesterol and choline-containing phospholipids were as expected, and in different dietary groups their ratios were comparable. These ratios typically were between 1 and 2 for VLDL and IDL/LDL and  $<0.6$  for HDL (data not shown). There was no evidence for significant levels of lipoprotein X and HDL-E particles.

### Development of Atherosclerotic Lesions in the Aorta

En face oil red O staining revealed minimal atherosclerotic lesion formation in mice fed diet 1 (control diet) for 12 weeks. In contrast, lesions were readily detected in each of the groups fed cholesterol-containing diets (Figure 3 and

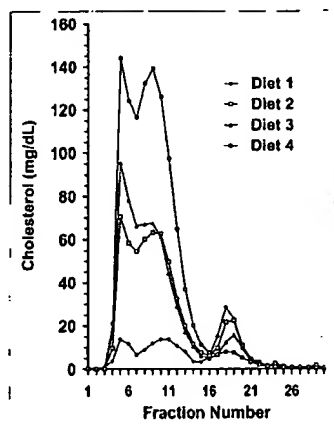


**Figure 2.** Plasma cholesterol profiles of LDLR<sup>-/-</sup> mice fed diets varying in fat, cholesterol, and cholate content. Mice were fed the diets described in Table 1 for 12 weeks, when blood samples were obtained from each dietary group and plasma was pooled. Plasma was subjected to fast protein liquid chromatography gel-filtration chromatography as described in Methods. Lipoproteins were measured in each fraction and the total cholesterol levels are plotted.

Table 3). The percent surface area of the entire aorta involved by lesions was significantly greater in mice fed diets 2, 3, and 4, compared with controls (diet 1), as well as in mice fed diet 4 compared with group 2. The interpretation was similar

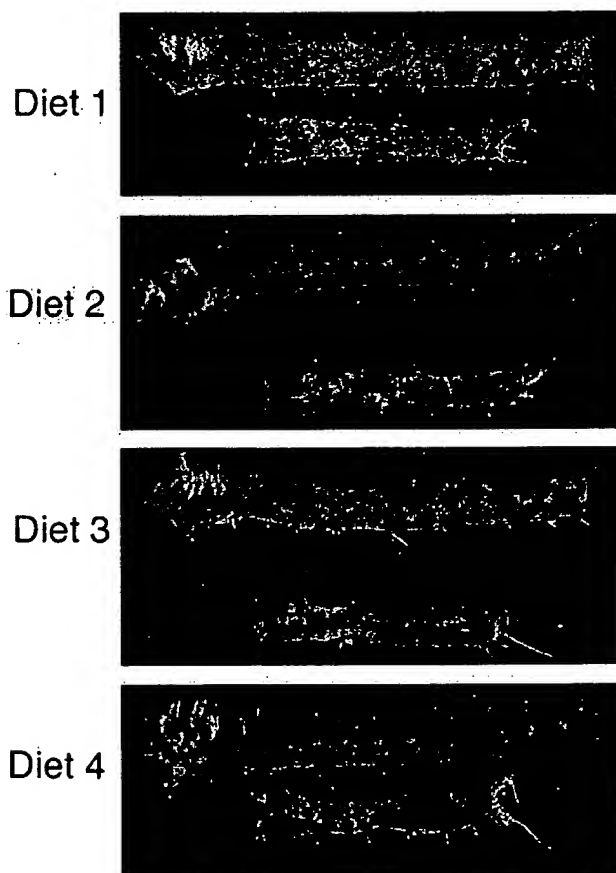


**Figure 3.** Oil red O-stained atherosclerotic lesions in aortas of LDLR<sup>-/-</sup> mice fed diets varying in fat, cholesterol, and cholate content. Mice were killed after being fed defined diets described in Table 1 for 12 weeks. Aortas were prepared and stained with oil red O as described in Methods. One representative aorta from a total of 6 in each of the 4 dietary groups is shown.

when the arch, thoracic, and abdominal regions were evaluated individually (Table 3). The anatomic distribution of atherosclerotic lesions was identical in dietary groups 2, 3, and 4 (Figure 3). Lesion-predisposed sites included the aortic root, the lesser curvature of the arch, and near the orifice of the brachiocephalic, intercostal, celiac, superior mesenteric, and renal arteries.

Histological examination revealed a similar morphology and cellularity in atheromas from each of the groups fed cholesterol-containing diets (Figure 4). The lesions had characteristic intimal thickening with foam cells, and apparent smooth muscle cell infiltration.

### Liver Function Tests and Histology

To determine if consumption of a cholate-containing diet for 12 weeks led to liver damage, serum liver enzyme levels and liver-derived products were measured and histological sections of liver were evaluated. The liver function test results were comparable between all dietary groups, suggesting that the liver parenchyma and biliary system were not seriously damaged after 12 weeks of feeding. Of particular interest, mice in group 4 (fed 1.25% cholesterol with cholate) did not have a significant elevation in serum bilirubin, alkaline phosphatase,  $\gamma$ -glutamyltransferase (GGT), alanine aminotransferase (ALT), or aspartate aminotransferase (AST), or decrease in albumin when compared with group 3 (also fed 1.25% cholesterol, but without cholate) (data not shown). Hematoxylin and eosin sections of liver revealed substantial steatosis in dietary groups 3 and 4, with greater fatty changes observed in the cholate-supplemented group. There was no histological evidence of hepatocyte necrosis, apoptosis, inflammation, fibrosis, or cirrhosis at the time point examined. However, all cholate-fed mice had stones in the gallbladder, whereas none were observed in mice fed cholate-free diets.

### Discussion

This study demonstrates that nutritionally defined semipurified diets are appropriate for the study of diet-genetic interactions in murine atherosclerosis. They offer several advantages compared with the commonly used chow-based diets, including reproducibility and uniformity of content, and the ability to precisely alter composition. Dietary lipid saturation and concentration are frequently the focus of hypotheses in experimental atherogenesis as a consequence of the enormous body of clinical and epidemiological data suggesting their importance in vascular disease. A semipurified diet allows the investigator to alter lipid concentration by substitution for an equivalent amount of energy from carbohydrate, to maintain a constant ratio of all other nutrients to energy in the control and high-fat diets. This is impossible to achieve when adding fat by dilution to a chow diet. The dilution technique confuses the interpretation of results. Indeed many investigators using diets prepared by dilution of chow with fat are seemingly unaware of the fact that mice consuming an identical amount of energy from the high-fat diet are also exposed to a significantly lower amount of all components of the chow, such as protein, all vitamins and minerals, and biologically active but nonnutrient factors such as fiber and phytochemicals, including those with antioxidant properties. The role of specific vitamin and mineral deficiencies or excess can be precisely examined by using semipurified diets

TABLE 3. Atherosclerotic Lesion Formation in Mouse Aortas After 12 Weeks of Diet

Dietary Group (n=6)	Percentages of Aortic Surface Area Involved by Oil Red O-Stained Lesions			
	Total	Arch	Thoracic	Abdominal
1 (control)	0.16±0.32	0.10±0.19	0.08±0.17	0.67±0.94
2 (0.5% cholesterol)	7.02±3.97‡	24.96±12.09§	2.80±2.35*	5.45±4.17*
3 (1.25% cholesterol)	8.27±3.59§	31.66±11.93§	3.57±3.50*	4.10±2.90*
4 (1.25% cholesterol+cholate)	12.79±4.80§	34.62±15.24§	10.30±3.63§	5.69±5.15*

\*P&lt;0.05; ‡P&lt;0.003; §P&lt;0.001, compared with group 1.

||P&lt;0.05, compared with group 2.

because their contents can be individually manipulated in the AIN vitamin and mineral formulations.<sup>18,19</sup> The use of standardized formulations will allow investigators to compare data derived from different laboratories without the concern that unquantifiable differences in the chow diets used contributed to the reported results.

The semipurified formulation can be provided as a liquid or in powdered form. The liquid diet allows the investigator to obtain more precise estimates of intake because mice typically disperse much of a solid diet in a cage. Liquid diets also facilitate studies of the effects of alcohol intake and are ideal for macrophage colony-stimulating factor-deficient mice, which exhibit osteopetrosis and have no teeth, making it impossible to consume a pelleted diet.<sup>27-29</sup>

The effects of dietary cholate on atherosclerosis susceptibility in genetically engineered mice should be reevaluated based on our results. Mice are very resistant to the development of atheromatous lesions in the arterial tree. Historically, investigators interested in genetic differences between murine strains in susceptibility to fatty streak formation devised diets

composed of chow diluted with saturated fat and supplemented with cholesterol and cholate.<sup>10</sup> This diet led to the discovery that the C57BL/6 strain was more susceptible to the formation of fatty streaks in the aortic root.<sup>9</sup> Although this dietary approach lacks many characteristics desired by experimental nutritionists, many investigators have subsequently used it in newer models of atherosclerosis developed with transgenic and gene-deletion technology. However, the potential hepatotoxic effects of cholate<sup>11,30,31</sup> have raised concerns that LDLR<sup>-/-</sup> mice fed such diets are not useful for modeling human disease.<sup>32</sup> Our study clearly shows that cholate is not required for the development of atherosclerotic lesions throughout the aorta in the LDLR<sup>-/-</sup> strain, and therefore cholate is unnecessary as a dietary additive in studies of atherogenesis in these mice. Subsequent experiments demonstrated a rapid onset of lesion formation, in that most mice fed diet 3 for 4 weeks had early lesions in the lesser curvature of the aortic arch (data not shown). Compared with mice fed diet 3 (high fat, 1.25% cholesterol), the inclusion of cholate (0.5%, wt/wt) in diet 4 caused a further increase in plasma lipids and a trend toward a greater area of the aortic surface involved by atheromatous lesions. This trend was not statistically significant because of high inter-animal variability. Cholate-fed mice also developed gallstones over the 12 weeks of investigation. It is our opinion that dietary cholate is unnecessary and perhaps a liability in studies of atherogenesis in the LDLR<sup>-/-</sup> mouse.

Traditionally, cholesterol supplements of ≥1% have been used in murine and rabbit studies to enhance hyperlipidemia and the rate of lesion formation, thereby shortening the duration of studies. Diets high in cholesterol and fat may cause time- and dose-dependent hepatotoxicity, therefore lowering cholesterol concentration, may be advantageous. Our study begins to address this issue. We demonstrated that the lesion area after 12 weeks of consuming 0.5% cholesterol (diet 2) was essentially indistinguishable from mice fed cholesterol at 1.25% (diet 3). At 12 weeks of feeding, there was a trend toward higher serum cholesterol and triglycerides in diet group 3. Perhaps this would lead to accelerated lesion progression and differences in lesion area would become significant in studies of longer duration. Cholesterol levels <0.5% can induce lesions in LDLR<sup>-/-</sup> mice. Palinski et al<sup>14</sup> fed LDLR<sup>-/-</sup> mice for 6 months with a diet containing 21% fat and 0.15% cholesterol (without cholate) and observed extensive atherosclerotic lesion formation throughout the aorta. In evaluating aortas of retired LDLR<sup>-/-</sup> breeders >1 year of age, we observed lesions in the aortic arch in most (unpublished data, 1998). This indicates that LDLR<sup>-/-</sup>

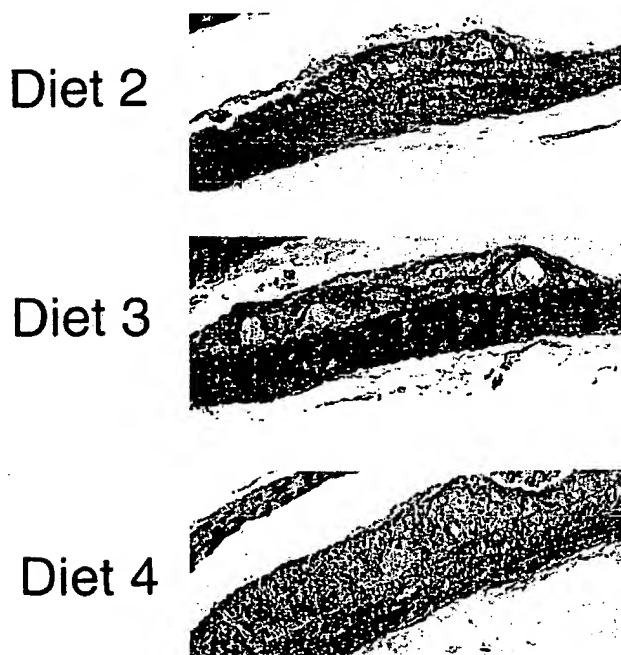


Figure 4. Histological appearance of aortic atherosclerotic lesions in LDLR<sup>-/-</sup> mice fed diets varying in fat, cholesterol, and cholate content. Hematoxylin and eosin-stained sections of formalin-fixed lesions from the aortas described in Figure 3 are shown.

mice can develop lesions spontaneously even when fed a regular laboratory chow; however, their rate of formation is very slow, as lesions generally are not found in mice <6 months old.

The existing literature on newer models of murine atherogenesis does not allow investigators to evaluate the role of dietary lipid concentration or the source of the lipid on lesion formation. In our study, the lipid content of diet 1 (control diet) was 10% of total energy (4.3% by weight), whereas in diets 2, 3, and 4 it was 40% (20% by weight). We included soy oil at 5.5% of total energy to ensure that a supply of essential fatty acids was constant in all diets. We then manipulated cocoa butter as the variable lipid. We recommend that future investigators maintain a constant baseline supply of essential fatty acids in the diet unless they are particularly interested in this as a variable. It is possible that investigators manipulating the fat source could naively prepare or purchase a saturated fat-enriched diet deficient in essential fatty acids, which could complicate the interpretation of murine studies. Furthermore, essential fatty acid deficiency is not observed in humans except in situations of several metabolic or gastrointestinal diseases. Humans consuming diets rich in saturated fat and cholesterol easily achieve adequate intake of essential fatty acids. Therefore, murine models will more closely mimic human dietary patterns if essential fatty acid intake is adequate.

### Acknowledgments

This work was supported by NIH grant 1 P50 HL56985 (A.H.L., P.L.), NIH grant RO1 CA 72482-01A1 (S.K.C.), Heart and Stroke Foundation of Ontario grant T-3032 (P.W.C.), and Heart and Stroke Foundation of Ontario grant T-3588 and an Established Investigatorship from the American Heart Association (M.I.C.).

### References

- Plump AS, Smith JD, Hayek T, Aalto-Setälä K, Walsh A, Verstuyft JG, Rubin EM, Breslow JL. Severe hypercholesterolemia and atherosclerosis in apolipoprotein E-deficient mice created by homologous recombination in ES cells. *Cell*. 1992;71:343-353.
- Zhang SH, Reddick RL, Piedrahita JA, Maeda N. Spontaneous hypercholesterolemia and arterial lesions in mice lacking apolipoprotein E. *Science*. 1992;258:468-471.
- Ishibashi S, Brown MS, Goldstein JL, Gerard RD, Hammer RE, Herz J. Hypercholesterolemia in low density lipoprotein receptor knockout mice and its reversal by adenovirus-mediated gene delivery. *J Clin Invest*. 1993;92:883-893.
- Callow MJ, Stoltzfus LJ, Lawn RM, Rubin EM. Expression of human apolipoprotein B and assembly of lipoprotein(a) in transgenic mice. *Proc Natl Acad Sci U S A*. 1994;91:2130-2134.
- McCormick SP, Linton MF, Hobbs HH, Taylor S, Curtiss LK, Young SG. Expression of human apolipoprotein B90 in transgenic mice: demonstration that apolipoprotein B90 lacks the structural requirements to form lipoprotein. *J Biol Chem*. 1994;269:24284-24289.
- Nakashima Y, Plump AS, Raines EW, Breslow JL, Ross R. ApoE-deficient mice develop lesions of all phases of atherosclerosis throughout the arterial tree. *Arterioscler Thromb*. 1994;14:133-140.
- Reddick RL, Zhang SH, Maeda N. Atherosclerosis in mice lacking apo E: evaluation of lesion development and progression. *Arterioscler Thromb*. 1994;14:141-147.
- Ishibashi S, Goldstein JL, Brown MS, Herz J, Burns DK. Massive xanthomatosis and atherosclerosis in cholesterol-fed low density lipoprotein receptor-negative mice. *J Clin Invest*. 1994;93:1885-1893.
- Paigen B, Morrow A, Brandon C, Mitchell D, Holmes P. Variation in susceptibility to atherosclerosis among inbred strains of mice. *Atherosclerosis*. 1985;57:65-73.
- Paigen B, Morrow A, Holmes PA, Mitchell D, Williams RA. Quantitative assessment of atherosclerotic lesions in mice. *Atherosclerosis*. 1987;68:231-240.
- Nishina PM, Verstuyft J, Paigen B. Synthetic low and high fat diets for the study of atherosclerosis in the mouse. *J Lipid Res*. 1990;31:859-869.
- Vesselinovitch D, Wissler RW. Experimental production of atherosclerosis in mice. 2. Effects of atherogenic and high-fat diets on vascular changes in chronically and acutely irradiated mice. *J Atheroscler Res*. 1968;8:497-523.
- Vesselinovitch D, Wissler RW, Doull J. Experimental production of atherosclerosis in mice. 1. Effect of various synthetic diets and radiation on survival time, food consumption and body weight in mice. *J Atheroscler Res*. 1968;8:483-495.
- Palinski W, Tangirala RK, Miller E, Young SG, Witztum JL. Increased autoantibody titers against epitopes of oxidized LDL in LDL receptor-deficient mice with increased atherosclerosis. *Arterioscler Thromb Vasc Biol*. 1995;15:1569-1576.
- Lichtman AH, Clinton SK, Iiyama K, Henault L, Libby P, Cybulsky MI. Comparative effects of precisely defined semipurified diets supplemented with lipid, cholesterol, and sodium cholate on serum lipids and aortic atherosclerosis in LDL receptor-deficient (LDLR<sup>-/-</sup>) mice. *FASEB J*. 1997;11:A154. Abstract.
- Reeves PG, Nielsen FH, Fahey GC Jr. AIN-93 purified diets for laboratory rodents: final report of the American Institute of Nutrition ad hoc writing committee on the reformulation of the AIN-76A rodent diet. *J Nutr*. 1993;123:1939-1951.
- Rao GN. Rodent diets for carcinogenesis studies. *J Nutr*. 1988;118:929-931.
- American Institute of Nutrition. AIN report of the AIN ad hoc committee on standards for nutritional studies. *J Nutr*. 1977;107:1340-1348.
- American Institute of Nutrition. AIN second report of the ad hoc committee on standards for nutritional studies. *J Nutr*. 1980;110:1726.
- Rao GN, Knapka JJ. Contaminant and nutrient concentrations of natural ingredient rat and mouse diet used in chemical toxicology studies. *Fundam Appl Toxicol*. 1987;9:329-338.
- Oller WL, Kendall DC, Greenman DL. Variability of selected nutrients and contaminants monitored in rodent diets: a 6-year study. *J Toxicol Environ Health*. 1989;27:47-56.
- Fowler GG. Toxicology of nisin. *Food Cosmet Toxicol*. 1973;11:351-352.
- van Gent T, van Tol A. Automated gel permeation chromatography of plasma lipoproteins by preparative fast protein liquid chromatography. *J Chromatogr*. 1990;525:433-441.
- Palinski W, Ord VA, Plump AS, Breslow JL, Steinberg D, Witztum JL. ApoE-deficient mice are a model of lipoprotein oxidation in atherosclerosis: demonstration of oxidation-specific epitopes in lesions and high titers of autoantibodies to malondialdehyde-lysine in serum. *Arterioscler Thromb*. 1994;14:605-616.
- Nunnari JJ, Zand T, Joris I, Majno G. Quantitation of oil red O staining of the aorta in hypercholesterolemic rats. *Exp Mol Pathol*. 1989;51:1-8.
- Steel RGD, Torrie JH. *Principals and Procedures of Statistics*. New York, NY: McGraw-Hill Book Co, Inc; 1980.
- Clinton SK, Underwood R, Hayes L, Sherman ML, Kufe DW, Libby P. Macrophage colony-stimulating factor gene expression in vascular cells and in experimental and human atherosclerosis. *Am J Pathol*. 1992;140:301-316.
- Qiao JH, Tripathi J, Mishra NK, Cai Y, Tripathi S, Wang XP, Imes S, Fishbein MC, Clinton SK, Libby P, Lusis AJ, Rajavashisth TB. Role of macrophage colony-stimulating factor in atherosclerosis: studies of osteopetrotic mice. *Am J Pathol*. 1997;150:1687-1699.
- Kodama H, Yamasaki A, Nose M, Niida S, Ohgami Y, Abe M, Kumegawa M, Suda T. Congenital osteoclast deficiency in osteopetrotic (op/op) mice is cured by injections of macrophage colony-stimulating factor. *J Exp Med*. 1991;173:269-272.
- Nishina PM, Wang J, Toyofuku W, Kuypers FA, Ishida BY, Paigen B. Atherosclerosis and plasma and liver lipids in nine inbred strains of mice. *Lipids*. 1993;28:599-605.
- Delzenne NM, Calderon PB, Taper HS, Roberfroid MB. Comparative hepatotoxicity of cholic acid, deoxycholic acid and lithocholic acid in the rat: in vivo and in vitro studies. *Toxicol Lett*. 1992;61:291-304.
- Breslow JL. Mouse models of atherosclerosis. *Science*. 1996;272:685-688.

## Evidence Appendix

183.9

# **MUCOSAL ADMINISTRATION OF HSP 65 DECREASES ATHEROSCLEROSIS AND INFLAMMATION IN THE AORTIC ARCH OF LDL RECEPTOR DEFICIENT MICE**

R. Maron, G.K. Sukhova, A.M. Faria, E. Hoffman, F. Mach, P. Libby, and H.L. Weiner. Center for Neurologic Diseases and Vascular Medicine and Atherosclerosis Unit, Brigham and Women's Hospital, Harvard Medical School, Boston, MA.

Increasing evidence supports the involvement of inflammation and immunity in atherogenesis, as well as the role of autoimmunity to heat shock proteins in the progression of atherosclerosis. Mucosal administration of autoantigens decreases organ specific inflammation and disease in animal models (diabetes, arthritis and EAE) and is being tested in human clinical trials. We examined the effect of nasal or oral administration of HSP65 on atherosclerotic lesion formation in mice lacking the receptor for low-density lipoprotein maintained on a high cholesterol diet. Animals were nasally treated with 0.8ug HSP 65 three times every second day or orally treated with 8 ug HSP 65 on 5 consecutive days. A high cholesterol diet was started after the last treatment and mice were mucosally treated once/week for 8 weeks at which time pathologic analysis was performed. In nasally treated animals, we found a reduction in macrophage-positive area in the aortic arch (3.44% vs. 13.03% in controls,  $p = 0.006$ ) as well as a reduced number of T-cells ( $p = 0.02$ ). There was also a decrease in the size of atherosclerotic plaques. A similar trend was observed in orally treated animals but was not significant. Mice nasally treated with HSP also gained significantly less weight than fed or control treated mice. Our results suggest that nasal treatment with HSP reduces the inflammatory process associated with atherosclerosis and may provide a new treatment approach.

183.11

# **Phase I Clinical Trial of Orally Delivered Hepatitis B Surface Antigen Expressed in Potato Tubers.**

<sup>1</sup>Yasmin Thanavala, <sup>1</sup>Adrienne Scott, <sup>1</sup>Srabani Pal, <sup>1</sup>Martin Mahoney and <sup>2</sup>Charles Arntzen. <sup>1</sup>Roswell Park Cancer Institute, Buffalo, NY; <sup>2</sup>Boyce Thompson Institute for Plant Research, Ithaca, NY.

A randomized, doubleblind, placebo-controlled phase I clinical trial has been completed at Roswell Park Cancer Institute to evaluate the safety, tolerability and immunogenicity of orally delivered HBsAg expressed as a protein in transgenic potato tubers. Forty-five healthy healthcare workers with a history of known positive anti-HBc

183.7

**CHOLERA TOXIN B SUBUNIT AS MUCOSAL CARRIER-DELIVERY SYSTEM FOR SPECIFIC IMMUNOTHERAPY.**C. Czerniksky<sup>1</sup>, F. Anjuere<sup>2</sup>, C. Rask<sup>3</sup>, J. Holmgren<sup>2</sup>. <sup>1</sup>INSERM Unit 364, Nice, France; <sup>2</sup>Dept of Medical Microbiology, University of Göteborg, Sweden.

Over the past few years attention has been devoted to the development of effective formulations that could prevent or halt untoward immune responses, such as those underlying autoimmune disorders, allergic reactions, and by and large chronic inflammation. Studies initiated in this laboratory have documented the efficiency of cholera B subunit as a powerful mucosal immunomodulating and carrier-delivery system agents for optimal induction of immune tolerance in various preclinical models of autoimmune diseases. More recently, this system has proven to be especially effective for suppressing type I allergic responses and also for suppressing Th2-driven immunopathological responses to persistent infectious microorganisms. The mechanisms of action of this system and in particular the role of mucosal dendritic cells in the induction of such form of suppression is currently under study. These studies will be presented and their implications will be discussed. (supported by INSERM, Swedish Medical Research Council, European Communities EC Biotech IV NovoNordisk, Triotol)

183.9

**MUCOSAL ADMINISTRATION OF HSP 65 DECREASES ATHEROSCLEROSIS AND INFLAMMATION IN THE AORTIC ARCH OF LDL RECEPTOR DEFICIENT MICE**

R. Marm, G.K. Sathorn, A.M. Par, E. Hoffman, E. Mach, P. Libby, and H.L. Weiner. Center for Neurologic Diseases and Vascular Medicine and Atherosclerosis Unit, Brigham and Women's Hospital, Harvard Medical School, Boston, MA.

Increasing evidence supports the involvement of inflammation and immunity in atherogenesis, as well as the role of autoimmunity to heat shock proteins in the progression of atherosclerosis. Mucosal administration of autoantigens decreases organ specific inflammation and disease in animal models (diabetes, arthritis and EAE) and is being tested in human clinical trials. We examined the effect of nasal or oral administration of HSP65 on atherosclerotic lesion formation in mice lacking the receptor for low-density lipoprotein maintained on a high cholesterol diet. Animals were nasally treated with 0.8ug HSP 65 three times every second day or orally treated with 8 ug HSP 65 on 5 consecutive days. A high cholesterol diet was started after the last treatment and mice were mucosally treated once/week for 8 weeks at which time pathologic analysis was performed. In nasally treated animals, we found a reduction in macrophage-positive area in the aortic arch (3.44% vs. 13.03% in controls,  $p = 0.006$ ) as well as a reduced number of T-cells ( $p = 0.03$ ). There was also a decrease in the size of atherosclerotic plaques. A similar trend was observed in orally treated animals but was not significant. Mice nasally treated with HSP also gained significantly less weight than fed or control treated mice. Our results suggest that nasal treatment with HSP reduces the inflammatory process associated with atherosclerosis and may provide a new treatment approach.

183.11

**Phase I Clinical Trial of Orally Delivered Hepatitis B Surface Antigen Expressed in Potato Tubers.**Y. Yanina Thanasias, I. Adrienne Scott, I. Graham Pal, Martin Mahoney and Charles Armstrong. <sup>1</sup>Roswell Park Cancer Institute, Buffalo, NY; <sup>2</sup>Boyer Thompson Institute for Plant Research, Ithaca, NY.

A randomized, double-blind, placebo-controlled phase I clinical trial has been completed at Roswell Park Cancer Institute to evaluate the safety, tolerability and immunogenicity of orally delivered HBsAg expressed as a protein in transgenic potatoes. Forty-five healthy healthcare workers with a history of known positive response to a primary series of recombinant hepatitis B vaccine (meeting all inclusion criteria and none of the exclusion criteria) were recruited for the trial. The 45 volunteers were randomized into one of three groups. Each group ate either vaccinated or placebo potato at defined intervals. Study subjects were randomized by use of a centrally generated block randomization list. This list was provided to the study pharmacist who was unblinded to study group assignments. All other study personnel and the study subjects remained blinded through the completion of the study. Subjects had baseline chemistry, hematology and anti-HBs antibody determinations performed before their first dose of vaccine and at predetermined intervals throughout the trial. As a phase I study, this was primarily an assessment of the relative safety and immunogenicity of transgenic HBsAg expressing potatoes.

183.8

**MYELIN-SPECIFIC TOLERANCE ATTENUATES DISEASE SEVERITY IN A VIRALLY INDUCED MODEL OF MULTIPLE SCLEROSIS.** Katherine L. Neville, Lou Matis, and Stephen D. Miller. Northwestern University Medical School, Chicago, IL, 60611, and <sup>2</sup>Alexion Pharmaceuticals, New Haven, CT, 06511.

Theiler's Murine Encephalomyelitis Virus-Induced Demyelinating Disease (TMEV-IDO) is a relevant model for the autoimmune disease multiple sclerosis (MS). Approximately 30 days after intracerebral inoculation of SJL mice with TMEV, clinical disease signs arise, characterized by spastic paralysis, chronic disease progression, and mononuclear cell infiltrate into the CNS. While initial demyelination in TMEV-IDO is mediated by virus-specific CD4+ T cells, reactivity to myelin epitopes can be detected in TMEV infected mice 55 days post infection, demonstrating autoimmune specificity in this virally induced disease. Administration of the fusion protein MP4, a fusion of myelin proteins MSP and PLP, to TMEV infected SJL mice 40 days post infection attenuates disease severity in MP4 treated animals compared to controls, and also decreases DTH reactivity to myelin peptides, indicating anti-myelin responses are centrally involved in the chronic progressive nature of TMEV-induced paralysis. Additionally, T cells isolated from the spinal cords of TMEV infected animals proliferate and secrete IFN $\gamma$  in response to PLP139-181 peptide stimulation *in vitro*. Both isolation of myelin specific cells from the CNS of TMEV infected animals, and myelin specific tolerance in TMEV-IDO indicate anti-myelin T cell responses contribute to disease severity in this virally induced model of MS, and support the idea of antigen specific tolerance as an effective treatment of ongoing autoimmune disease. (Supported by NIH grant NS23349)

183.10

**HIGH DOSE -ANTIGEN FEEDING INDUCES CD4 T CELLS WITH SUPPRESSOR ACTIVITY IN THE LIVER.**

T. WATANABE, Y. WAKATSUKI, M. YOSHIDA, T. ITOH, T. ICHII, T. CHIBA, and T. KITA. Dept. of Clinical and Bio-Regulatory Science, Kyoto Univ. Grad. Sch. of Med., Kyoto 606-8507, Japan.

Oral feeding of low or high dose-antigens (Ag) induces Ag-specific immuno-suppression in subsequent systemic challenge with the same Ag. Since a part of Ag fed at high dose should reach to the liver as an immunogenic form, we examined the possibility that Ag-specific T cells are activated by high dose-Ag feeding. OVA-TCR transgenic mice were fed 100 mg or 1mg of OVA, or PBS every other day for five times and then CD4 T cells were purified from Peyer's patch, spleen, and liver. Only intrasplenic CD4 T cells (IHLs) from high dose Ag-fed mice suppressed both Ag-specific DTH and antibody responses when adoptively transferred to naive Balb/c mice. Upon Ag-stimulation *in vitro*, the secretion of IL-10, TGF- $\beta$ , and especially IL-4 by IHLs from Ag-fed mice were increased in an Ag-dose dependent manner. In contrast, IL-2 secretion and proliferative responses by these T cells were decreased. In addition, these IHLs from Ag-fed mice inhibited Ag-specific proliferation of naive splenic CD4 T cells. FACS analysis revealed decrease in the population of Ag-specific CD4 T cells in the liver by Ag-feeding, associated with the up-regulation of FasL expression, suggesting that clonal deletion was induced in the liver. Naive splenic CD4 T cells cultured with OVA presented by liver-derived APCs showed a similar profile of cytokine production to that of IHLs. Taken together, these data suggest that high dose-Ag feeding induces CD4 T cells with suppressor activity in the liver. Not only clonal deletion but also active suppression is considered to be induced in the liver after high dose-Ag feeding.

183.12

**ORAL IMMUNIZATION BY FOOD IS LESS EFFECTIVE THAN INTRAGASTRIC IMMUNIZATION**

T.G.M. Lasterdager and L.A.Th. Hilgers. (SPON: W.J.A. Boersma). DLO-Institute for Animal Science and Health, P.O.Box 65, 8200 AB, Lelystad, The Netherlands

The feasibility of edible vaccines was studied by oral immunization of mice with chicken ovalbumin (OVA) mixed with standard food. Other mice were immunized with a similar dose of OVA via intragastric immunization. Intragastric immunization elicited 20-fold higher numbers of anti-OVA IgA and 34-fold higher numbers of anti-OVA IgG producing cells in the lamina propria of the gut than food immunization. Furthermore, intragastric immunization elicited a 20-fold higher anti-OVA IgG response in serum and a 2-fold higher anti-OVA IgA response in faeces than food immunization. The addition of the *Vibrio cholerae* toxin to food did not enhance the immune response. Possible explanations for the differences between these immunization routes will be discussed. We concluded that intragastric immunization is merely limited indicative for the effectiveness of edible vaccines.



# Chronic treatment with nitric oxide-releasing aspirin reduces plasma low-density lipoprotein oxidation and oxidative stress, arterial oxidation-specific epitopes, and atherogenesis in hypercholesterolemic mice

Claudio Napoli<sup>1,2\*</sup>, Eric Ackah<sup>3</sup>, Filomena de Nigris<sup>4\*</sup>, Piero Del Soldato<sup>5</sup>, Francesco P. D'Armiento<sup>6\*</sup>, Ettore Crimi<sup>1</sup>, Mario Condorelli<sup>1\*</sup>, and William C. Sessa<sup>5</sup>

<sup>1</sup>Departments of Medicine and Human Pathology, School of Medicine, Federico II University of Naples, 80131 Naples, Italy; <sup>2</sup>Department of Medicine-0682, University of California at San Diego, La Jolla, CA 92093; <sup>3</sup>Department of Pharmacology and Molecular Cardiology Program, Boyer Center for Molecular Medicine, Yale University School of Medicine, New Haven, CT 06536; <sup>4</sup>NicOx, 06906 Sophia Antipolis, France; and <sup>5</sup>Department of Anesthesiology, University of Novara, 28100 Novara, Italy

Edited by Louis J. Ignarro, University of California, Los Angeles School of Medicine, Los Angeles, CA, and approved July 8, 2002 (received for review April 23, 2002)

The effects of chronic treatment with nitric oxide-containing aspirin (NO-aspirin, NCX-4016) in comparison with regular aspirin or placebo on the development of a chronic disease such as atherosclerosis were investigated in hypercholesterolemic low-density lipoprotein (LDL)-receptor-deficient mice. Male mice were assigned randomly to receive in a volume of 10 ml/kg either placebo ( $n = 10$ ), 30 mg/kg/day NO-aspirin ( $n = 10$ ), or 18 mg/kg/day of regular aspirin ( $n = 10$ ). After 12 weeks of treatment, the computer-assisted imaging analysis revealed that NO-aspirin reduced the aortic cumulative lesion area by  $39.8 \pm 12.3\%$  compared with that of the placebo ( $P < 0.001$ ). Regular aspirin did not reduce significantly aortic lesions ( $-5.1 \pm 2.3\%$ ) compared with the placebo ( $P = 0.867$ , not significant (NS)). Furthermore, NO-aspirin reduced significantly plasma LDL oxidation compared with aspirin and placebo, as shown by the significant reduction of malondialdehyde content ( $P < 0.001$ ) as well as by the prolongation of lag-time ( $P < 0.01$ ). Similarly, systemic oxidative stress, measured by plasma isoprostanes, was significantly reduced by treatment with NCX-4016 ( $P < 0.05$ ). More importantly, mice treated with NO-aspirin revealed by immunohistochemical analysis of aortic serial sections a significant decrease in the intimal presence of oxidation-specific epitopes of oxLDL (E06 monoclonal antibody,  $P < 0.01$ ), and macrophages-derived foam cells (F4/80 monoclonal antibody,  $P < 0.05$ ), compared with placebo or aspirin. These data indicate that enhanced NO release by chronic treatment with the NO-containing aspirin has antiatherosclerotic and antioxidant effects in the arterial wall of hypercholesterolemic mice.

atherosclerosis | LDL-receptor-deficient mice

Endothelial dysfunction has been shown in the presence of atherosclerosis (ref. 1 and reviewed in refs. 2–4). Several lines of evidence indicate that restoring nitric oxide (NO)-mediated signaling pathways in atherosclerotic arteries may decrease the disease (2–4). The essential findings are that the biochemical properties of NO allow its exploitation as both a cell signaling molecule through its interaction with redox centers in heme proteins and a rapid reaction with other biologically relevant radical species. The direct reaction of NO with radicals can have, at least in part, antioxidant effects. In arterial cells, the antioxidant properties of NO can be greatly amplified by the activation of signal transduction pathways that lead to the increased synthesis of endogenous antioxidants or down-regulate responses to pro-inflammatory stimuli. Studies in humans and in animal models have shown that low-density lipoprotein (LDL) oxidation may play a pivotal role in the pathogenesis of atherosclerosis (reviewed in refs. 5, 6). Recent data indicate that LDL oxidation may promote *per se* activation of several signaling

pathways and transcription factors in human coronary arteries (7–9). Several of these pathways are reduced by concomitant administration of vitamin E (7, 9). Thus, compounds with antioxidant properties may reduce downstream effects induced by LDL oxidation in the arterial wall, and this phenomenon could retard the progression of atherosclerosis.

In preliminary experiments, we evaluated the antioxidant properties *in vitro* of several nitro-compounds and found that some of these agents had antioxidant properties. In this study, we used male LDL-receptor-deficient mice (10, 11) to address the effects of a NO-containing aspirin derivative (NCX-4016) on the development of a chronic disease such as atherosclerosis and on plasma LDL oxidation and systemic oxidative stress. NO-releasing aspirin (NCX-4016) is a drug well characterized *in vitro* and *in vivo* (reviewed in ref. 12). Hypercholesterolemic mice develop hypercholesterolemia on a cholesterol mouse chow diet (10, 13) and extensive atherosclerosis, with lesions progressing from lipid-laden fatty streaks to advanced lesions (10, 11, 13–15). By using this model, we investigated the chronic effects of treatment with NO-aspirin or regular aspirin on aortic lesion development, plasma LDL oxidation, and oxidative stress, as well as oxidation-specific epitopes of LDL in the arterial wall.

## Materials and Methods

**Drugs and Experimental Protocol.** The experiments conformed to the Guide for the Care and Use of Laboratory Animals (National Institutes of Health Publication No. 85–23, revised 1996) and the Guidelines of the American Heart Association. The experiments described here were carried out on male LDL-receptor-deficient mice of 18 weeks on high-cholesterol and cholate-free diet (21% by weight fat, 0.15% by weight cholesterol, and 19.5% by weight casein; no. 8137, Teklad, Madison, WI). LDL-receptor-deficient mice crossed with C57BL/6J mice for 10 generations, develop only “moderately” elevated plasma cholesterol levels (250–300 mg/dl) when fed regular mouse chow (10, 11). However, high cholesterol levels are easily achieved by enriched-cholesterol diets that induce extensive atherosclerosis throughout the arterial tree (10, 11). We selected only male mice to avoid gender-related differences (10). Mice were assigned randomly to be treated for 12 weeks with 30 mg/kg day of NCX-4016 (a generous gift from NicOx;  $n = 10$ , 30-mg compound contains 18 mg of aspirin) or 18 mg/kg/day

This paper was submitted directly (Track II) to the PNAS office.

Abbreviation: LDL, low-density lipoprotein.

\*To whom reprint requests should be addressed. E-mail: claudnap@tin.it or cnapoli@ucsd.edu.



of aspirin (Sigma;  $n = 10$ ), or placebo (saline vehicle) given by gavage. These drug doses were chosen on the basis of previous studies *in vivo* (12, 16, 17) and did not affect blood pressure in mice measured by tail cuff ( $P = \text{NS}$ , not shown). At the end of the study, mice were killed with a lethal dose of sodium pentobarbital and *in situ* fixation of the aorta at physiologic pressure [100 mmHg (1 mmHg = 33 Pa)] was performed with PBS/paraformaldehyde (4%, 0.1 mol/liter, pH 7.3) for histology and normal saline for immunohistochemistry (see below).

**Plasma Determination and LDL Oxidation.** Blood was collected at the time of killing into Eppendorf tubes with 1 mM  $\text{Na}_2\text{EDTA}$ . Plasma cholesterol was determined enzymatically (18, 19). LDL particles ( $d = 1.006 - 1.063$  g/ml) were isolated from 2 ml of pooled plasma from two animals of each group by sequential-density ultracentrifugation (18, 19). The protein content of LDL was measured by the method of Lowry (20). Susceptibility of LDL to *in vitro* oxidation was induced by 1  $\mu\text{M}$  copper sulfate at 37°C for 12 h, as described (18, 19, 21). At the end of the incubation, the formation of thiobarbituric acid reactive substances was determined by the thiobarbituric acid method, as described (18, 19, 21). Lag-time was determined by monitoring the changes measured at 234 nm in the absorbance and observed at room temperature (23°C) every 10 min for a period of 4 h (19, 21). Measurement of the isoprostane 8-epi-PGF<sub>2</sub> purified from plasma samples was made by using a commercially available immunoassay (Cayman Chemical, Ann Arbor, MI) according to the manufacturer's instructions.

**Morphometric Assessment of Lesions and Immunohistochemistry of Lesion Components.** The aorta was dissected, cleaned of adherent fat and fascia, cut open, washed thoroughly with cold sterile PBS containing 2 mM EDTA, placed in ice-cold PBS containing 50  $\mu\text{M}$  butylated hydroxytoluene, 0.001% aprotinin, 50 mM EDTA, and 0.008% chloramphenicol, and equilibrated with nitrogen (10, 11, 22, 23). Each arterial segment then was divided into two parts. One of these was immersed in cysteine prodrug 2-oxothiazolidine-4-carboxylate (5 mM)-containing medium (Dako, Milan) and flash frozen in liquid nitrogen; 7- $\mu\text{m}$ -thick sections were taken and prepared with a cryotome for computer-assisted morphometric determination of lipid-rich lesions (30 cryosections from arteries were stained with oil red-O and counterstained with hematoxylin), as described in detail (10, 11, 16, 22, 23). The second part of each arterial segment was fixed in buffered 10% formalin and paraffin embedded; 12–15 serial sections (5- $\mu\text{m}$  thickness) were prepared for immunohistochemistry (10, 11, 16, 22, 23). Duplicate serial sections of the fixed and paraffin-embedded arterial segments were immunostained with E06, murine monoclonal antibody against oxidation-specific-lipids and oxidized phospholipid epitopes of ox-LDL, and F4/80, a monoclonal antibody against mouse monocyte/macrophages-derived foam cells (10, 11, 16, 22, 23). Antibodies were used at a dilution of 1:500. Epitopes recognized by the primary antibody were detected by an avidin-biotin-peroxidase computer-assisted method (10, 11, 16, 22, 23).

**Statistical Analysis.** Results are expressed as mean  $\pm$  SEM. Evaluation of the atherogenesis and the immunohistochemistry were performed in a blinded way regarding the treatment given to mice. A Student's *t* test was used to compare differences among groups. Statistical significance was defined as  $P < 0.05$ .

## Results

**Lipid Profile.** Plasma cholesterol levels were similar among groups of LDL-receptor-deficient mice ( $724 \pm 68$  mg/dl,  $746 \pm 72$  and  $738 \pm 57$  in placebo, NCX-4016 and aspirin-treated groups, respectively;  $P = \text{NS}$  for all comparisons). Similarly, plasma triglyceride levels were comparable in all three groups of mice

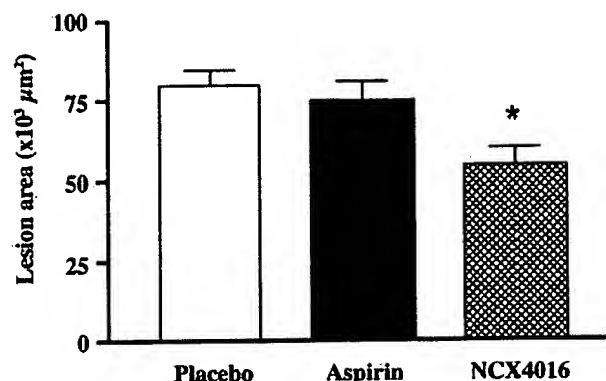


**Fig. 1.** Effects of various treatments on atherosclerotic lesion area in male LDL-receptor-deficient mice after 12 weeks of treatment with placebo, regular aspirin (18 mg/kg), or equimolar doses of nitric oxide-releasing aspirin (NCX-4016, 30 mg/kg). Mean lesion area of oil-red O-stained sections was calculated by computer-assisted imaging analysis. Results are expressed as the mean  $\pm$  SEM of the aortic lesions of 10 animals from each group. \*,  $P < 0.01$  vs. placebo-treated mice.

( $165 \pm 22$  mg/dl,  $172 \pm 32$ , and  $170 \pm 28$  in placebo, NCX-4016, and aspirin-treated groups, respectively;  $P = \text{NS}$  for all comparisons).

**Evaluation of Atherogenesis.** Computer-assisted imaging analysis revealed that 30 mg/kg of NCX-4016 reduced the aortic cumulative lesion area by  $39.8 \pm 12.3\%$  compared with that of the placebo ( $P < 0.001$ ). In another set of experiments ( $n = 5$ ), 30 mg/kg of NCX-4016 reduced the aortic cumulative lesion area by  $24.1 \pm 10.8\%$  ( $P = 0.589$ , NS). The equimolar dose of aspirin (18 mg/kg) did not reduce significantly aortic lesions ( $-5.1 \pm 2.3\%$ ) compared with the placebo ( $P = 0.867$ , NS; Fig. 1). Fig. 2 shows some examples of high magnifications of oil-red O-stained aorta of a placebo-treated mouse (A) and NCX-4016-treated mouse (B). The reduction of the atherosclerotic lesions was coupled with a marked decrease in the thickness of lesions (oil-red O staining) of a NCX-4016-treated mouse in comparison to the placebo-treated mouse (C).

**Immunohistochemistry.** Mice treated with 30 mg/kg/day of NCX-4016 revealed a significant decrease of intimal macrophages-derived foam cells ( $-28.3 \pm 10.2\%$  of F4/80-positive arterial sections,  $P < 0.05$  vs. placebo-treated group) and oxidation-specific epitopes of oxidized LDL by ( $-35.8 \pm 11.9\%$  of E06-positive arterial section,  $P < 0.01$  vs. placebo-treated group; Fig. 3). Thus, NCX-4016 significantly reduced the expression of oxidation-specific epitopes and macrophage accumulation in the arterial wall compared with that of the placebo-treated group as well as aspirin-treated group.

**Effect of Different Treatments on Plasma LDL Oxidizability and Oxidative Stress.** Treatment with 30 mg/kg/day of NCX-4016 reduced significantly plasma LDL oxidation and systemic oxidative stress compared with both placebo and, to a lesser extent, aspirin (Table 1). This reduction of plasma LDL oxidation was shown by significant reduction of LDL malondialdehyde content of around 40% ( $P < 0.001$  vs. placebo;  $P < 0.04$  vs. aspirin), as well as by the prolongation of lag-time of oxidizability of around 20% ( $P < 0.01$  vs. placebo;  $P < 0.05$  vs. aspirin). In the same group of mice above ( $n = 5$ ) treated with 10 mg/kg of NCX-4016, the compound reduced LDL malondialdehyde content to  $19.3 \pm 4.0$  nmol/mg of protein ( $P < 0.05$  vs. placebo;  $P = \text{NS}$  vs. aspirin) and LDL lag-time reached  $120 \pm 33$  min ( $P = \text{NS}$  vs.

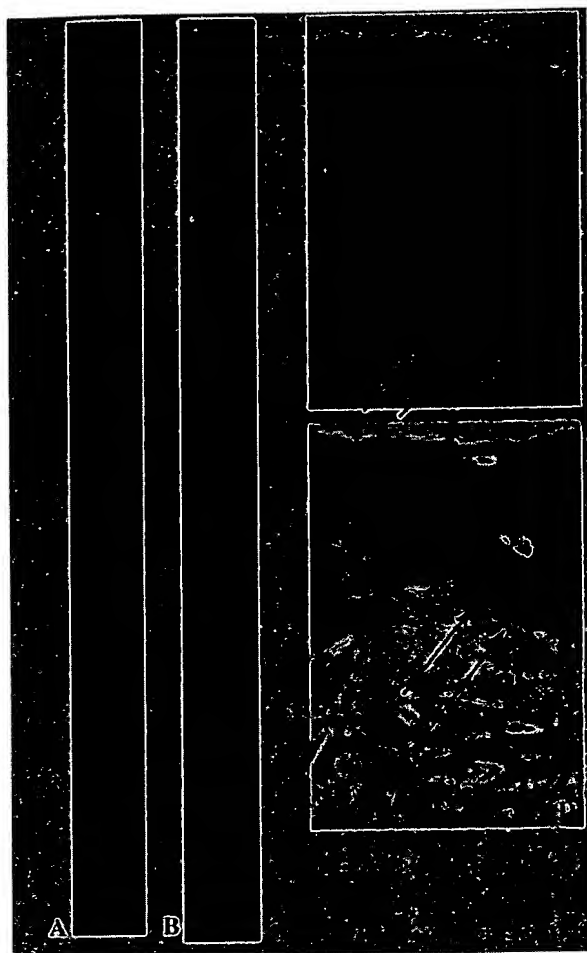


Fig. 2. High-magnifications ( $\times 25$ ) of oil-red O-stained thoracic aorta of placebo-treated mouse (A), placebo-treated mouse (B), and nitric oxide-releasing aspirin-treated mouse (30 mg/kg). Sustained reduction of the thickness of lesions of nitric oxide-releasing aspirin-treated mouse (D) in comparison to the placebo-treated mouse (C) (both  $\times 320$  magnification). Arrows indicate the degree of staining in relation to the intima.

placebo and aspirin). Similarly, plasma isoprostanes were reduced significantly by treatment with NCX-4016 (Table 1).

## Discussion

Our article demonstrates that chronic delivery of NO achieved with the NO-releasing aspirin significantly attenuates the devel-

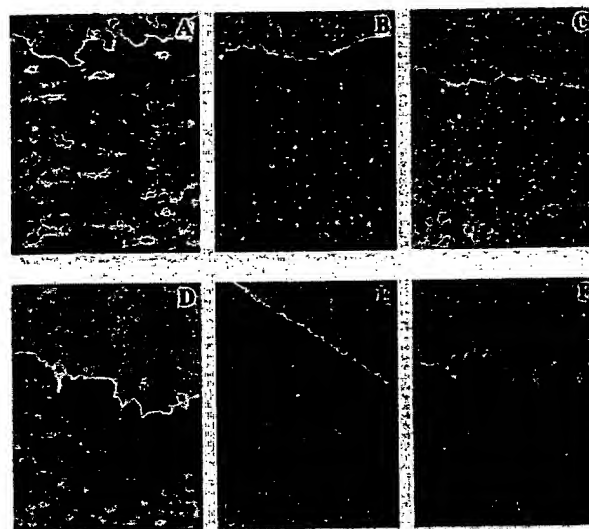


Fig. 3. Treatment with (C) 30 mg/kg nitric oxide-releasing aspirin (NCX-4016) was more effective than (B) 18 mg/kg of regular aspirin or (A) placebo in reducing oxidation-specific epitopes in E06-positive sections ( $\times 275$ ). Indeed, placebo-treated animals had a diffuse staining for oxidation-specific epitopes (A). This staining was partially reduced and increased in the subendothelial space in aspirin-treated mice (B). Nitric oxide-releasing aspirin reduced the overall immunostaining throughout the serial section (C). Similarly, macrophage accumulation was reduced in F4/80 positive sections in nitric oxide-releasing aspirin-treated animals (F) when compared with regular aspirin-treated (E) or placebo-treated (D) LDL-receptor-deficient mice ( $\times 275$ ). The negative immunostaining (brown) in C and F appears in blue.

opment of a chronic disease such as atherosclerosis in hypercholesterolemic LDL receptor-deficient mice without affecting plasma cholesterol levels. The enhancement of the NO pathway may play an important role in antiatherogenic effect of NO-releasing aspirin (reviewed in ref. 4). This study also demonstrates that in parallel to the attenuation of atherosclerosis, NO-aspirin reduced the susceptibility *ex vivo* of plasma LDL to oxidative modification and systemic oxidative stress measured by plasma isoprostanes. Isoprostane levels are a well recognized indicator of oxidative stress in animal models and in humans (24). Antioxidant protection could be related to the scavenging activity of free radicals by NO-containing aspirin both in plasma and in the arterial wall. Superoxide anion and NO are known to react rapidly to form the stable peroxynitrite anion, and peroxynitrite decomposition generates a strong oxidant with reactivity similar to hydroxyl radical (25). However, the causal role of peroxynitrite in atherogenesis is not established. Nevertheless, the properties of NO-releasing aspirin can also affect multiple

Table 1. Parameters of susceptibility to *ex vivo* peroxidation of LDL and systemic oxidative stress in LDL-receptor-deficient mice treated with nitric oxide-releasing aspirin (NCX-4016) or regular aspirin

	LDL lag-time, min	LDL MDA, nmol/mg prot	Plasma isoprostane 8-epi-PGF <sub>2</sub> , pg/ml
Placebo-treated LDL-receptor-deficient mice (n = 10)	112 $\pm$ 22	24.5 $\pm$ 4.2	143 $\pm$ 37 (n = 6)
NCX-4016-treated LDL-receptor-deficient mice (n = 10)	131 $\pm$ 18*	14.3 $\pm$ 2.4**	119 $\pm$ 21*** (n = 6)
Aspirin-treated LDL-receptor-deficient mice (n = 10)	115 $\pm$ 15	22.3 $\pm$ 4.7	128 $\pm$ 38 (n = 6)

LDL-receptor-deficient mice treated with NCX-4016 (30 mg/kg/day), and aspirin (18 mg/kg/day); MDA, malondialdehyde at 12 h after exposure of LDL to 1  $\mu$ M copper sulphate (n = 10 for each group). Lag-time represents an index of LDL oxidizability; increased values of lag-time reflect increased resistance of LDL to oxidative modification (n = 10 for each group, see also refs. 19 and 21). In a subset of animals (n = 6), plasma isoprostane levels (8-epi PGF<sub>2</sub>) were measured. \*,  $P < 0.05$  or \*\*,  $P < 0.01$  vs. placebo or aspirin-treated mice; \*\*\*,  $P < 0.05$  vs. placebo-treated mice by ANOVA followed by t test and Bonferroni's correction. See text for further details.

radical species generated in the arterial wall. An increasing number of compounds releasing NO or modulating the NO pathway are now available (reviewed in ref. 26). Further studies should evaluate whether these newly developed compounds, clinically used drugs, or other NO-donors could be helpful in retarding atherosclerotic lesion formation and its clinical sequelae.

Oxidative modification of LDL plays a crucial role in human early atherosclerotic lesions (22, 23, 27) leading to atherosclerosis-related diseases (5, 6). Some studies (28) also demonstrated the important role of inhibition of LDL oxidation on the attenuation of atherosclerosis in hypercholesterolemic mice. In the present study, we showed that NCX-4016 reduced formation in the arterial wall of oxidation-specific epitopes of oxidized LDL. Thus, NCX-4016 has a potent antioxidant effect also in the atherosclerotic lesions of mice probably by means of scavenging of the radical-induced oxidation of LDL also in the arterial wall. Oxidized LDL may induce apoptosis in human coronary cells (7, 8). This phenomenon may favor the development of unstable atherosclerotic lesions (7, 8). However, apoptosis in macrophages also may reduce a potential source of mediators which can contribute to destabilizing the plaque (e.g., metalloproteinases and MCP-1). Nevertheless, the reduction of oxidative stress *in vivo* could also attenuate the degree of unstable atheroma. In another experimental setting, we showed recently that NCX-4016 reduced restenosis after arterial injury and macrophage deposition in hypercholesterolemic mice (16) and in aged rats (17), perhaps, at least in part, through its antioxidant effects. These properties may be particularly useful when applied to hypercholesterolemic or elderly patients. Obviously, the chronic development of atherosclerosis is a completely different pathophysiological condition from restenosis after arterial injury. Indeed, restenotic inflammatory lesions already appear after 14 days from the arterial injury. In the present study, we have also shown that the antiatherogenic effect was coupled to

the reduction of macrophage-derived foam cells at the site of lesions. This beneficial effect may contribute to the reduction of lesion progression observed in hypercholesterolemic mice, and it is also consistent with the inhibition of macrophage-dependent LDL oxidation by *in vitro* NO donors (26, 29).

The findings of the present study are in agreement with an important role of NO in the development of atherosclerosis in hypercholesterolemic mice. Accordingly, the role of endogenous NO in the progression of atherosclerosis in apolipoprotein E-knockout mice was recently investigated by using N(omega)-nitro-L-arginine methyl ester (L-NAME), an inhibitor of nitric oxide synthase (NOS) or with the NOS substrate L-arginine for 8 weeks (30). L-NAME treatment resulted in a significant inhibition of NO-mediated vascular responses and a significant increase in the atherosclerotic plaque area in the aorta of these mice. In contrast, L-arginine treatment had no influence on endothelial function and did not alter lesion size. The acceleration in lesion size concomitant to the severely impaired NO-mediated responses indicates that lack of endogenous NO (4, 31) is an important progression factor of atherosclerosis in the apolipoprotein E-knockout mouse.

We conclude that enhanced NO release by chronic treatment with NO-containing aspirin attenuates the development of a chronic disease such as atherosclerosis in hypercholesterolemic mice. Although the natural history of the atherosclerotic disease is different between rodents and humans, these data should be considered a further piece of evidence supporting the key role of NO in atherogenesis. Inhibition of oxidation-sensitive mechanisms by NO-aspirin, and possible other NO-related anti-inflammatory effects (reviewed in ref. 32), both in plasma and in atherosclerotic lesions, together with reduced macrophage accumulation, may have an important role in contributing to this antiatherogenic effect.

This work was supported by National Institutes of Health Grants HL57665, HL41371, and HL64793, and by Italian Institutes of Health Grant ISNIH.99.56980.

- Ludmer, P. L., Selwyn, A. P., Shook, T. L., Wayne, R. R., Mudge, G. H., Alexander, R. W. & Ganz, P. (1986) *N. Engl. J. Med.* 315, 1046–1051.
- Ignarro, L. J., Cirino, G., Casini, A. & Napoli, C. (1999) *J. Cardiovasc. Pharmacol.* 34, 876–884.
- Drexler, H. (1999) *Cardiovasc. Res.* 43, 572–579.
- Napoli, C. & Ignarro, L. J. (2001) *Nitric Oxide* 5, 88–97.
- Witztum, J. L. & Steinberg, D. (1991) *J. Clin. Invest.* 88, 1785–1791.
- Steinberg, D. (1997) *J. Biol. Chem.* 272, 20963–20966.
- de Nigris, F., Maida, I., Palumbo, G., Anania, V. & Napoli, C. (2000) *Biochem. Pharmacol.* 59, 1477–1487.
- Napoli, C., Quehenberger, O., de Nigris, F., Abete, P., Glass, C. K. & Palinski, W. (2000) *FASEB J.* 14, 1996–2007.
- de Nigris, F., Youssef, T., Ciafrè, S., Franconi, F., Anania, V., Condorelli, G., Palinski, W. & Napoli, C. (2000) *Circulation* 102, 2111–2117.
- Palinski, W., Napoli, C. & Reaven, P. D. (2000) *Harvard Series*, eds Simon, D. I. & Rogers, C. (Humana, Totowa, NJ), pp. 149–174.
- Napoli, C., de Nigris, F., Welch, J. S., Calara, F. B., Stuart, R., Glass, C. K. & Palinski, W. (2002) *Circulation* 105, 1360–1367.
- Del Soldato, P., Sorrentino, R. & Pinto, A. (1999) *Trends Pharmacol. Sci.* 8, 319–323.
- Zhang, S. H., Reddick, R. L., Piedrahita, J. & Maeda, N. (1992) *Science* 258, 468–471.
- Nakashima, Y., Plump, A. S., Raines, E. W., Breslow, J. L. & Ross, R. (1994) *Arterioscler. Thromb.* 14, 133–139.
- Reddick, R. L., Zhang, S. H. & Maeda, N. (1994) *Arterioscler. Thromb.* 14, 141–148.
- Napoli, C., Cirino, G., Del Soldato, P., Sorrentino, R., Sica, V., Condorelli, M., Pinto, A. & Ignarro, L. J. (2001) *Proc. Natl. Acad. Sci. USA* 98, 2860–2864.
- Napoli, C., Aldini, G., Wallace, J. L., de Nigris, F., Maffei, R., Abete, P., Bonaduce, D., Condorelli, G., Rengo, F., Sica, V., et al. (2002) *Proc. Natl. Acad. Sci. USA* 99, 1689–1694.
- Napoli, C., Chiariello, M., Palumbo, G. & Ambrosio, G. (1996) *Cardiovasc. Drugs Ther.* 10, 417–424.
- Napoli, C., Mancini, F. P., Corso, G., Malorni, A., Crescenzi, E., Postiglione, A. & Palumbo, G. (1997) *J. Biochem.* 121, 1096–1101.
- Lowry, O. H., Rosebrough, N. J. & Farr, L. (1951) *J. Biol. Chem.* 193, 265–275.
- Napoli, C., Postiglione, A., Triggiani, M., Corso, G., Palumbo, G., Carbone, V., Rocco, A., Ambrosio, G., Montefusco, S., Malorni, A., et al. (1995) *Atherosclerosis* 11, 263–275.
- Napoli, C., D'Armiento, F. P., Mancini, F. P., Palumbo, G., Witztum, J. L. & Palinski, W. (1997) *J. Clin. Invest.* 100, 2680–2690.
- Napoli, C., Witztum, J. L., de Nigris, F., D'Armiento, F. P. & Palinski, W. (1999) *Circulation* 99, 2003–2010.
- Witztum, J. L. & Berliner, J. A. (1998) *Curr. Opin. Lipidol.* 9, 441–448.
- Beckman, J. S., Beckman, T. W., Chen, J., Marshall, P. A. & Freeman, B. A. (1990) *Proc. Natl. Acad. Sci. USA* 87, 1620–1624.
- Ignarro, L. J., Napoli, C. & Loscalzo, J. (2002) *Circ. Res.* 90, 21–28.
- Napoli, C., Glass, C. K., Witztum, J. L., D'Armiento, F. P., Deutch, R. & Palinski, W. (1999) *Lancet* 354, 1234–1241.
- Aviram, M., Maor, I., Keidar, S., Hayek, T., Oiknine, J., Bar-El, Y., Adler, Z., Kertzman, V. & Milo, S. (1995) *Biochem. Biophys. Res. Commun.* 216, 501–513.
- Hogg, N., Struck, A., Goss, S. P. A., Santanam, N., Joseph, J., Parthasarathy, S. & Kalyanaraman, B. (1995) *J. Lipid Res.* 36, 1756–1762.
- Kausar, K., da Cunha, V., Fitch, R., Mallari, C. & Rubanyi, G. M. (2000) *Am. J. Physiol.* 278, H1679–H1685.
- Rudic, R. D. & Sessa, W. C. (1999) *Am. J. Hum. Genet.* 64, 673–677.
- Wallace, J. L., Ignarro, L. J. & Fiorucci, S. (2002) *Nat. Rev. Drug Discovery* 1, 375–382.

Evidence Appendix

(*Arteriosclerosis, Thrombosis, and Vascular Biology*. 1996;16:1013.)  
© 1996 American Heart Association, Inc.

Articles

## Lymphocyte Populations in Atherosclerotic Lesions of ApoE -/- and LDL Receptor -/- Mice

### Decreasing Density With Disease Progression

Simon E. Roselaar; Paul X. Kakkanathu; Alan Daugherty

the Departments of Medicine (S.E.R., P.X.K., A.D.) and Biochemistry and Molecular Biophysics (A.D.), Washington University School of Medicine, St Louis, Mo.

Correspondence to Alan Daugherty, Box 8086, Cardiovascular Division, Washington University School of Medicine, St Louis, MO 63110. E-mail doco@imgate.wustl.edu.

### Abstract

Lymphocytes are prominent components of human atherosclerotic lesions, but their presence in murine models of disease has not been confirmed. Lymphocyte subpopulations have been identified in apoE -/- and LDL receptor -/- mice fed a cholesterol-enriched diet for up to 3 months. ApoE -/- mice had higher serum cholesterol concentrations than did LDL receptor -/- mice during most of the feeding period, primarily due to large increases in VLDL concentrations. Total area of atherosclerotic lesions was greater at all times in apoE -/- than LDL receptor -/- mice (lesion area after 3 months on cholesterol-enriched diet: apoE -/-,  $993 \pm 193$  and LDL receptor -/-,  $560 \pm 131 \mu\text{m}^2 \times 10^3$ , mean  $\pm$  SEM,  $n=6$  in each group). Lesions in apoE -/- mice contained larger macrophage-rich necrotic cores and more calcification than did those in LDL receptor -/- mice. Immunocytochemical analyses of tissue sections of ascending aortas performed with monoclonal antibodies to T and B lymphocytes and macrophages revealed that T lymphocytes immunoreactive for Thy 1.2, CD5, CD4, and CD8 were observed in lesions from both strains, but no B lymphocytes were detected. The density of Thy 1.2<sup>+</sup> T lymphocytes in lesions was greatest at 1 month (apoE -/-,  $98 \pm 23$  and LDL receptor -/-,  $201 \pm 40$  lymphocytes/mm<sup>2</sup>,  $n=6$  in each group), decreasing in apoE -/- mice to  $12 \pm 3$  and in LDL receptor -/- mice to  $51 \pm 20$  lymphocytes/mm<sup>2</sup> at 3 months. The presence of T lymphocytes in murine atherosclerotic lesions makes these animals potentially useful for studying the involvement of the immune system in atherogenesis.

**Key Words:** atherosclerosis • murine model • T lymphocytes • immunohistochemistry

Cellular processes that occur during human atherogenesis may be examined by using animal

### This Article

- ▶ [Abstract FREE](#)
- ▶ [Alert me when this article is cited](#)
- ▶ [Alert me if a correction is posted](#)
- ▶ [Citation Map](#)

### Services

- ▶ [Email this article to a friend](#)
- ▶ [Similar articles in this journal](#)
- ▶ [Similar articles in PubMed](#)
- ▶ [Alert me to new issues of the journal](#)
- ▶ [Download to citation manager](#)
- ▶ [Cited by other online articles](#)
- ▶ [Request Permissions](#)

### Google Scholar

- ▶ [Articles by Roselaar, S. E.](#)
- ▶ [Articles by Daugherty, A.](#)
- ▶ [Articles citing this Article](#)

### PubMed

- ▶ [PubMed Citation](#)
- ▶ [Articles by Roselaar, S. E.](#)
- ▶ [Articles by Daugherty, A.](#)

models of atherosclerosis that simulate human disease. The PDAY study<sup>1</sup> established similarities in the evolution of atherosclerotic disease in humans and Watanabe heritable hyperlipidemic rabbits, cholesterol-fed rabbits,<sup>2 3</sup> and rhesus monkeys.<sup>4 5</sup> In addition, initial studies with cholesterol-fed C57BL/6J mice have led to the increasing use of mice in the study of events in atherogenesis.<sup>6</sup> More recently, genetically modified mice deficient in either apoE<sup>7</sup> or LDL receptors<sup>8</sup> have become available. ApoE-deficient mice are grossly hypercholesterolemic and spontaneously develop atherosclerosis that has the morphological characteristics of human disease<sup>9 10 11</sup>; disease development is accelerated by feeding these mice cholesterol-enriched diets.<sup>12 13</sup> LDL receptor deficiency in mice produces only a mild increase in plasma cholesterol concentrations but imparts an increased responsiveness to cholesterol-enriched diets, leading to pronounced atherosclerotic lesion development.<sup>14</sup>

Atherosclerotic lesions are mostly made up of macrophages and smooth muscle cells, but there is increasing recognition of the presence of T lymphocytes.<sup>15 16 17 18</sup> Both CD4<sup>+</sup> and CD8<sup>+</sup> T lymphocytes are present at all stages of development of human lesions.<sup>19 20</sup> These T lymphocytes are activated, as judged from the presence of activation markers<sup>21</sup> and expression of MHC class II antigens on adjacent smooth muscle cells.<sup>22</sup> Expression of MHC class II is induced by the T lymphocyte-derived cytokine interferon gamma, which is detectable in lesions.<sup>23 24</sup> T lymphocytes in atherosclerotic lesions are polyclonal in origin.<sup>25</sup> The full spectrum of antigens against which T lymphocytes are directed has not been elucidated, but it is known that oxidized LDL activates a small subset.<sup>26</sup> B lymphocytes are also found in human atherosclerotic lesions.<sup>15 27</sup>

The role of the immune system in atherogenesis is controversial. Lesions that develop in cholesterol-fed rabbits contain T lymphocytes that may be active participants in lesion formation since immunosuppression results in enhancement of the atherogenic process.<sup>28</sup> The severity of atherosclerotic lesions is also increased in immune-suppressed<sup>29</sup> and MHC class I-deficient C57BL/6J mice<sup>30</sup> fed a cholesterol-enriched diet. However, in contrast to lesions in hypercholesterolemic rabbits, lymphocytes have not been detected in murine atherosclerotic lesions.<sup>31</sup> Studies to define the role of the immune system in atherogenesis require an animal model in which T lymphocytes are present in lesions, as they are in human disease. We therefore used monoclonal antibodies to evaluate whether lymphocytes are present in atherosclerotic lesions of cholesterol-fed apoE  $-/-$  and LDL receptor  $-/-$  mice. Immunostaining for Thy 1.2, CD5, CD4, and CD8 was positive in atherosclerotic lesions in both strains of mice, although the density of T lymphocytes in each strain differed markedly. The presence of lymphocytes in atherosclerotic lesions of these mice makes them valuable for the study of the role of the immune system in atherogenesis.

## Methods

### Animals

LDL receptor  $-/-$  and apoE  $-/-$  mice (8 female and 10 male in each group) were obtained from Jackson Laboratories. Both strains of mice were originally generated as C57BL/6JxC129 hybrids,

and mice used in this study were backcrossed six generations into a C57BL/6J background. Mice were housed in specific pathogen-free rooms and fed a normal mouse laboratory diet (Ralston Purina) until they were 6 weeks of age, after which they were fed a diet containing 1.25% cholesterol, 0.5% cholic acid, and 15% fat (Harlan Teklad, catalogue No. 88051) for up to 3 months. All procedures were approved by the Washington University Animal Studies Committee.

### **Removal of Aortas and Blood Samples**

Six mice of each strain were selected after 1, 2, and 3 months on a high-cholesterol diet. Nonfasting animals were anesthetized by metaphane inhalation (Pitman-Moore), bled retro-orbitally, and killed by cervical dislocation. Hearts were removed en bloc and placed in ice-cold Ringer's lactate, washed free of blood, and embedded and frozen in optimal cutting temperature compound (Tissue Tek). Sections of aorta (10  $\mu$ m) were cut on a cryostat<sup>6</sup> and placed on Probe-on-Plus microscope slides (Fisher Scientific). Serum was separated from whole blood by centrifugation and stored at 4°C.

### **Serum Cholesterol Concentrations and Lipoprotein Cholesterol Distribution**

Serum concentrations of total cholesterol were measured by using an enzyme-based colorimetric assay (Wako Chemical Co). Lipoprotein cholesterol distributions were determined by fast-performance liquid chromatography of pooled serum samples from all six mice in each group after 3 months of feeding.<sup>32</sup>

### **Histology and Immunocytochemistry**

Frozen sections were fixed in acetone for 5 minutes. Macrophages were detected with anti-mouse monoclonal antibody MOMA-2 (rat IgG<sub>2b</sub>, Serotec). All lymphocyte antibodies were initially screened for their ability to stain cells in splenic tissue (positive control). T lymphocytes were immunostained with monoclonal antibodies to murine CD5 (clone 57-7.3, rat IgG<sub>2a</sub>K, Life Technologies), Thy 1.2 (clone 30-H12, rat IgG<sub>2b</sub>, Collaborative Biomedical Products, and clone AT83A, rat IgM, Dr Osami Kanagawa, Washington University), CD8 (clone YTS 105.18, rat IgG<sub>2a</sub>, Serotec), and CD4 (clone GK1.5, rat IgG, Dr Osami Kanagawa). Tissue sections were blocked with nonimmune rabbit serum. The secondary antibody was an affinity-purified, mouse serum-adsorbed, biotinylated rabbit anti-rat IgG (BA 4001, Vector Laboratories).

Immunocytochemical analysis was performed by using a Fisher MicroProbe system and Vectastain Elite ABC kits (Vector). Negative controls were obtained with isotype-matched irrelevant antibodies or no primary antibody. Immunoreactivity was visualized by using 3-amino 9-ethyl carbazole (Biomed Corp), which forms a red precipitate. Accumulation of neutral lipid in lesions was visualized by staining with oil red O. Tissue sections were counterstained with aqueous hematoxylin (Biomed).

### **Quantification of Lesion Areas and Numbers of T Lymphocytes**

Consecutive 10- $\mu$ m-thick aortic cross sections were cut, beginning at the most proximal part of the aortic sinus.<sup>6</sup> Sections were placed consecutively on each of eight separate slides, after which

the ninth section was placed on the first slide, next to the first section, continuing for 48 sections. A single slide, upon which were six aortic cross sections from each mouse, was analyzed for lesion dimensions and for any given stain or immunostain. Total atherosclerotic lesion area and numbers of Thy 1.2<sup>+</sup> lymphocytes were quantified by using an image-analysis system consisting of a Nikon Optiphot-2 microscope attached to a Javelin JE3462 high-resolution camera and a personal computer equipped with a Coreco-Oculus OC-TCX frame grabber and high-resolution monitor. Computerized color-image analysis was performed by using Image-Pro Plus software (Media Cybernetics). The area of each lesion in all six cross sections in every mouse was recorded, as was the total number of T lymphocytes determined by immunostaining for Thy 1.2. For each mouse studied, total atherosclerotic lesion area was calculated as the sum of the areas of all lesions in all six aortic cross sections on one slide. Thy 1.2-immunopositive lymphocytes were counted per section, and T-lymphocyte density was expressed as the number of lymphocytes per square millimeter of atherosclerotic lesion area.

### Statistics

Differences in serum cholesterol concentrations, atherosclerotic lesion areas, and T-lymphocyte numbers were compared either by two-tailed Student's *t* test, or, if data failed to meet the requirements for use of this parametric test, by the Mann-Whitney rank-sum test. Data analyses were performed by using SigmaStat for Windows (Jandel Scientific).

### Results

All animals tolerated the cholesterol-enriched diet without overt adverse affects. Total serum cholesterol concentrations before commencing the diet and at 1 and 2 months were higher in apoE  $-/-$  than LDL receptor  $-/-$  mice, but they did not differ significantly at 3 months (Fig 1). Analyses of lipoprotein cholesterol distribution by size-exclusion fast-performance liquid chromatography demonstrated that regardless of diet, apoE  $-/-$  mice carried the major fraction of cholesterol in VLDL, while LDL receptor  $-/-$  mice carried cholesterol predominantly in an LDL-sized fraction. <sup>8 9 10 11</sup>

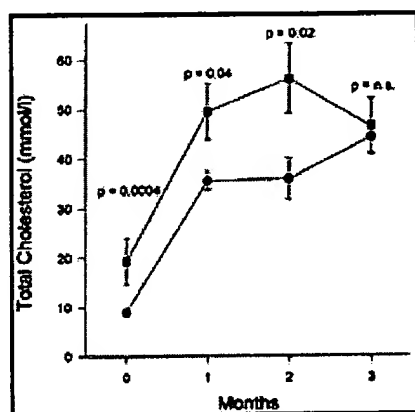


**Figure 1.** Line graph shows total serum cholesterol concentrations in apoE  $-/-$  and LDL receptor  $-/-$  mice. Cholesterol concentrations were measured by using enzymatic assays as described in "Methods." Points indicate means of six observations; bars, SEM; ■, apoE  $-/-$  mice; and ○, LDL receptor  $-/-$  mice.

[View larger version \(16K\):](#)  
[\[in this window\]](#)



[\[in a new window\]](#)

Atherosclerotic lesions were characterized after 1, 2, and 3 months of cholesterol feeding for size, macrophage content, and lymphocyte number and distribution. The two strains of mice had atherosclerotic lesions with markedly different cellular architectures and areas. At all times, aortic atherosclerotic lesions of apoE  $-/-$  mice were larger than those in LDL receptor  $-/-$  mice (Fig 2<sup>□</sup>). Lesions from the two types of mice were of similar cellular composition after 1 month of cholesterol feeding, composed predominantly of macrophages. By 3 months, lesions in apoE  $-/-$  mice had large cores of necrotic macrophages, a feature less abundant in LDL receptor  $-/-$  mice. Chondrocytes and early bone formation were readily discernible in all apoE  $-/-$  mice examined at 3 months, but in only one of six LDL receptor  $-/-$  mice. Bands of smooth muscle cells and extracellular matrix were present in apoE  $-/-$  but not LDL receptor  $-/-$  mice after 3 months (Fig 3<sup>□</sup>).

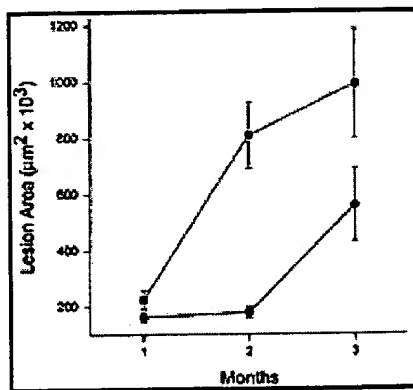
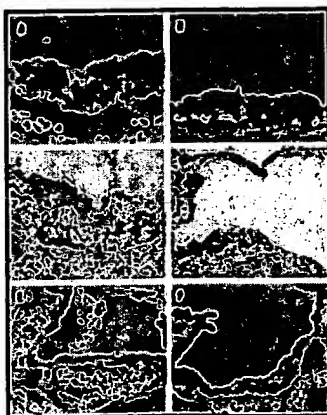


**Figure 2.** Line graph shows area of atherosclerotic lesions in apoE  $-/-$  and LDL receptor  $-/-$  mice after 1, 2, and 3 months on a cholesterol-enriched diet. Points indicate means of six observations; bars, SEM; ■, apoE  $-/-$  mice; and •, LDL receptor  $-/-$  mice.

[View larger version \(13K\):](#)

[\[in this window\]](#)

[\[in a new window\]](#)



[View larger version \(115K\):](#)

**Figure 3.** Photomicrographs show presence of macrophages and lipid deposits in murine atherosclerotic lesions. Aortic sections were immunostained for macrophages as described in "Methods." Macrophages were immunostained with MOMA-2 after 1 month of cholesterol feeding in (A) apoE  $-/-$  and (B) LDL receptor  $-/-$  mice. At 1 month the two animal strains had lesions with similar morphological characteristics. After 3 months of cholesterol feeding, differences were observed in MOMA-2-immunostained macrophages: apoE  $-/-$  mice had necrotic macrophage core regions and macrophage accumulation under the endothelium separated by bands of nonstaining cells and matrix (C). In contrast, lesions from LDL receptor  $-/-$  mice immunostained uniformly for macrophages, and necrotic cores were uncommon (D).

[\[in this window\]](#)  
[\[in a new window\]](#)

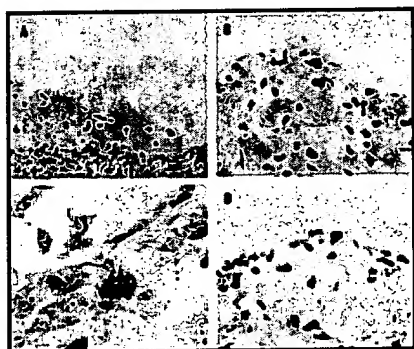
Staining for neutral lipids with oil red O was patchy in apoE  $-/-$  mice after 3 months of cholesterol feeding (E) but relatively uniform in LDL receptor  $-/-$  mice (F) (original magnification  $\times 100$  [A and B],  $\times 40$  [C through F]).

T lymphocytes were detected by using antibodies to Thy 1.2, CD5, CD4, and CD8 (Table 1). Thy 1.2 and CD5 antigens are pan-T-cell markers, although CD5 is also present on a subset of B lymphocytes in serosal cavities. Immunostaining for Thy 1.2 and CD5 was observed in lesions from both strains. Furthermore, the distribution and number of cells exhibiting positive immunostaining was similar with both Thy 1.2 antibodies (Fig 4A) and the CD5 antibody (Fig 4B). Several monoclonal antibodies directed against T-lymphocyte antigen CD4 and an antibody to the B-lymphocyte marker CD45R were used to identify the subsets of lymphocytes present in mouse atherosclerotic lesions (Table 1). No B lymphocytes were observed in lesions, although the CD45R antibody produced excellent immunostaining of splenic tissue that was used as a control. Because only one of the anti-CD4 antibodies (GK1.5) resulted in appreciable splenic immunostaining, it was used to demonstrate the presence of CD4<sup>+</sup> cells in atherosclerotic lesions (Fig 4C). In splenic tissue, CD4 immunostaining was less intense on positive cells than was Thy 1.2, CD5, and CD8 immunostaining. CD8<sup>+</sup> cells were detected in the lesions of both strains (Fig 4D). The relatively low intensity of CD4<sup>+</sup> subset immunostaining indicated that formal quantification may result in a misleading underestimate of cell numbers. Therefore, because robust immunostaining of T-lymphocyte subsets was not as consistently achieved as for Thy 1.2 antigen, no quantitative assessment of these subtypes was performed.

**View this table:** Table 1. Primary Antibodies Used to Detect Lymphocytes in

[\[in this window\]](#) Atherosclerotic Lesions

[\[in a new window\]](#)



**View larger version (135K):**

[\[in this window\]](#)

[\[in a new window\]](#)

**Figure 4.** Photomicrographs. A, T lymphocytes positive for Thy 1.2 in shoulder region of a lesion from an LDL receptor  $-/-$  mouse fed a cholesterol-enriched diet for 1 month. B, T lymphocytes positive for CD5 in an apo E  $-/-$  mouse fed a cholesterol-enriched diet for 3 months. C, T lymphocytes positive for CD4 in a lesion from an LDL receptor  $-/-$  mouse after 1 month of cholesterol feeding. D, T lymphocytes positive for CD8 in an atherosclerotic lesion from an LDL receptor  $-/-$  mouse fed a cholesterol-enriched diet for 2 months (original magnification  $\times 200$  [A and B],  $\times 1000$  [C],  $\times 400$  [D]).

T lymphocytes, as determined by Thy 1.2 immunoreactivity, were present in atherosclerotic lesions at all intervals. The density of Thy 1.2<sup>+</sup> T lymphocytes was greatest after only 1 month of cholesterol feeding in both strains of mice (Fig 5). At the intervals studied beyond 1 month, there was a significant reduction in lesion T-lymphocyte density, which was particularly sparse after 3 months in apoE -/- mice. At all intervals, lesions of LDL receptor -/- mice contained a greater density of Thy 1.2<sup>+</sup> cells than did lesions of apoE -/- mice. In neither strain of mice was there a specific region in atherosclerotic lesions that preferentially accumulated T lymphocytes, as has been discerned in the human disease.<sup>15</sup> The distribution of lymphocytes was patchy, with small foci of cells generally located beneath the endothelium and few cells near the media or in the lipid core. No T lymphocytes were detected in the media.

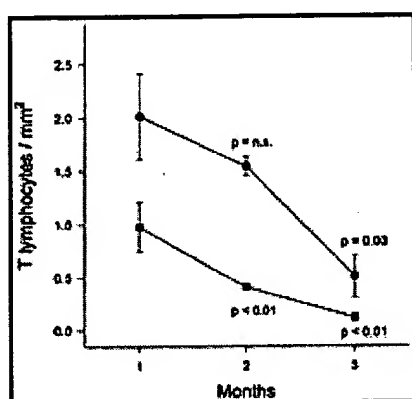


**Figure 5.** Line graph shows T-lymphocyte density of Thy 1.2<sup>+</sup> cells in both strains of mice at 1, 2, and 3 months. Points indicate means of six observations; bars, SEM; ■, apoE -/- mice; and •, LDL receptor -/- mice. Statistical significance at 2 and 3 months (as determined by Mann-Whitney rank-sum test) is stated relative to the density at 1 month for each strain.

[View larger version \(13K\):](#)

[\[in this window\]](#)

[\[in a new window\]](#)

## Discussion

We observed striking differences in the dimensions and morphological characteristics of lesions in apoE -/- and LDL receptor -/- mice. Our observations of atherosclerotic lesions from apoE -/- mice are similar to earlier ones.<sup>10 11 12 13</sup> Compared with LDL receptor -/- mice, lesions in apoE -/- mice were larger at all intervals studied and had a markedly increased number of chondrocytes and bands of smooth muscle cells. ApoE -/- mice had significantly increased concentrations of total serum cholesterol at most intervals, with most being in a VLDL fraction. Cholesterol-enriched VLDL has been demonstrated to promote cholesterol esterification in macrophages,<sup>33 34 35</sup> which may be a factor in the formation of lesions of disparate morphology in apoE -/- and LDL receptor -/- mice, although this has not been proven.

The principal finding of this study is that Thy 1.2<sup>+</sup>, CD5<sup>+</sup>, CD4<sup>+</sup>, and CD8<sup>+</sup> T lymphocytes are present in atherosclerotic lesions in cholesterol-fed apoE -/- and LDL receptor -/- mice. Thy 1.2 is a 112-amino acid glycoprotein present in varying amounts on the surface of neural and lymphoid cells, with expression depending on the state of differentiation.<sup>36</sup> In mice, Thy 1.2 is found on

mature T lymphocytes. CD5 is a monomeric 67-kD glycoprotein on all mature T lymphocytes, with higher expression on CD4 $^{+}$  than CD8 $^{+}$  cells.<sup>37</sup> CD5 also occurs on the B1a subset of B lymphocytes found in serosal cavities. CD5 functions as a tyrosine kinase substrate in association with the T-cell receptor  $\zeta$  chain/CD3 and protein tyrosine kinases p56<sup>lck</sup> and p59<sup>fyn</sup> in T lymphocytes and may also act as an independent signaling molecule.<sup>38</sup>

Previous immunohistochemical analyses of atherosclerotic lesions in several strains of mice, including the apoE  $-/-$  strain, have shown an absence of T lymphocytes.<sup>31</sup> A possible explanation for this apparent contradiction is the interval at which lesions were studied. In the present study, lymphocyte density decreased with lesion maturity; particularly in apoE  $-/-$  mice, this cell type was sparse after 3 months of cholesterol feeding. The fact that Qiao et al<sup>31</sup> studied lesions after cholesterol feeding of a longer duration than in the present study may explain the lack of detectable lymphocytes. In addition, in our study, several of the anti-CD4 antibodies tested resulted in weak and diffuse immunostaining of splenic tissue (Table 2). Therefore, the difference between this and previous reports with regard to detection of lymphocytes might be partly attributed to differences in the affinity of antibodies used in immunohistochemical testing. However, while lymphocytes have not been reported in atherosclerotic lesions, CD4 $^{+}$ , CD8 $^{+}$ , and CD23 $^{+}$  (B lymphocytes) have been demonstrated in aortic fatty streaks of vasculitis-prone MRL/*lpr* mice.<sup>39</sup>

In both apoE  $-/-$  and LDL receptor  $-/-$  mice, the density of T lymphocytes in lesions decreased as lesions matured. Signals responsible for recruitment of lymphocytes have not been defined, although one proposed mediator is the lysophospholipid formed by the oxidation of LDL.<sup>40 41</sup> Early lymphocytic recruitment to atherosclerotic lesions occurred, but further development of lesions ensued without a proportional increase in T lymphocytes. The early recruitment of lymphocytes to atherosclerotic lesions has also been observed in cholesterol-fed rabbits<sup>42 43</sup> and rats.<sup>44</sup> Lymphocyte residence time and trafficking within atherosclerotic lesions have not been defined but may be important parameters. Introduction of exogenous lymphocytes distinguishable on the basis of a genetically incorporated marker may assist in understanding the biology of lymphocytes within atherosclerotic lesions.

ApoE has been proposed as an endogenous regulator of the immune system, since it inhibits both monocyte<sup>45</sup> and T lymphocyte<sup>46</sup> proliferation. ApoE also inhibits interleukin-2-dependent T-cell proliferation, possibly by preventing transition from the G1<sub>A</sub> phase of the cell cycle.<sup>47</sup> ApoE synthesis by macrophages varies according to the state of cell differentiation<sup>48</sup> and may be inhibited by interferon gamma<sup>49</sup> and stimulated by increasing intracellular cholesterol concentrations.<sup>50</sup> However, since apoE  $-/-$  mice develop severe atherosclerosis and inhibition of T lymphocytes enhances development of atherosclerosis,<sup>28 29 30</sup> the physiological significance of the inhibitory effect of apoE on T lymphocytes in atherosclerotic lesions remains to be determined.

T lymphocytes are present in atherosclerotic lesions in apoE  $-/-$  and LDL receptor  $-/-$  mice,

making both strains useful for the study of immunologic factors affecting the development of atherosclerosis. In addition, we observed differences in morphological characteristics of lesions that could be due to altered lipoprotein metabolism or immunologic factors, both of which are likely to be targets of pharmacological intervention in the modulation of atherosclerotic disease.

## Acknowledgments

Simon E. Roselaar is a fellow of the American Heart Association, Missouri Affiliate. Alan Daugherty is an Established Investigator of the American Heart Association. We are grateful to Drs Jeffrey E. Saffitz and Osami Kanagawa for advice on histology and providing antibodies, to Dustie Delfel-Butteiger for technical assistance, to Beth Engeszer, Sandy Sendobry, and Debra Rateri for editorial assistance, and to Kelly Hall for secretarial assistance.

Received October 4, 1995; revision received February 22, 1996; **References**

1. Wissler RW and the PDAY Investigators. New insights into the pathogenesis of atherosclerosis as revealed by PDAY. *Atherosclerosis*. 1994;108(suppl):S3-S20.
2. Rosenfeld ME, Tsukada T, Gown AM, Ross R. Fatty streak initiation in Watanabe heritable hyperlipidemic and comparably hypercholesterolemic fat-fed rabbits. *Arteriosclerosis*. 1987;7:9-23.[[Abstract](#)]
3. Rosenfeld ME, Tsukada T, Chait A, Bierman EL, Gown AM, Ross R. Fatty streak expansion and maturation in Watanabe heritable hyperlipidemic and comparably hypercholesterolemic fat-fed rabbits. *Arteriosclerosis*. 1987;7:24-34.[[Abstract](#)]
4. Faggiotto A, Ross R, Harker L. Studies of hypercholesterolemia in the nonhuman primate, I: changes that lead to fatty streak formation. *Arteriosclerosis*. 1984;4:323-340.[[Abstract](#)]
5. Faggiotto A, Ross R. Studies of hypercholesterolemia in the nonhuman primate, II: fatty streak conversion to fibrous plaque. *Arteriosclerosis*. 1984;4:341-356.[[Abstract](#)]
6. Paigen B, Morrow A, Holmes PA, Mitchell D, Williams RA. Quantitative assessment of atherosclerotic lesions in mice. *Atherosclerosis*. 1987;68:231-240.[[Medline](#)] [[Order article via Infotrieve](#)]
7. Piedrahita JA, Zhang SH, Hagaman JR, Oliver PM, Maeda N. Generation of mice carrying a mutant apolipoprotein E gene inactivated by gene targeting in embryonic stem cells. *Proc Natl Acad Sci U S A*. 1992;89:4471-4475.[[Abstract/Free Full Text](#)]
8. Ishibashi S, Brown MS, Goldstein JL, Gerard RD, Hammer RE, Herz J. Hypercholesterolemia in low density lipoprotein receptor knockout mice and its reversal by adenovirus-mediated gene delivery. *J Clin Invest*. 1993;92:883-893.[[Medline](#)] [[Order article via Infotrieve](#)]
9. Zhang SH, Reddick RL, Piedrahita JA, Maeda N. Spontaneous hypercholesterolemia and arterial lesions in mice lacking apolipoprotein E. *Science*. 1992;258:468-471.[[Medline](#)] [[Order article via Infotrieve](#)]
10. Plump AS, Smith JD, Hayek T, Aalto-Setälä K, Walsh A, Verstuyft JG, Rubin EM, Breslow JL. Severe hypercholesterolemia and atherosclerosis in apolipoprotein-E-deficient mice created by homologous recombination in ES cells. *Cell*. 1992;71:343-353.[[Medline](#)] [[Order article via Infotrieve](#)]
11. Zhang SH, Reddick RL, Burkey B, Maeda N. Diet-induced atherosclerosis in mice heterozygous and homozygous for apolipoprotein E gene disruption. *J Clin Invest*. 1994;94:937-945.[[Medline](#)] [[Order article via Infotrieve](#)]
12. Nakashima Y, Plump AS, Raines EW, Breslow JL, Ross R. ApoE-deficient mice develop lesions in all phases of atherosclerosis throughout the arterial tree. *Arterioscler Thromb*.

- 1994;14:133-140.[Abstract]
13. Reddick RL, Zhang SH, Maeda N. Atherosclerosis in mice lacking apo E. *Arterioscler Thromb*. 1994;14:141-147.[Abstract]
14. Ishibashi S, Goldstein JL, Brown MS, Herz J, Burns DK. Massive xanthomatosis and atherosclerosis in cholesterol-fed low density lipoprotein receptor-negative mice. *J Clin Invest*. 1994;93:1885-1893.[Medline] [Order article via Infotrieve]
15. Jonasson L, Holm J, Skalli OO, Bondjers B, Hansson GK. Regional accumulation of T cells, macrophages, and smooth muscle cells in human atherosclerotic plaques. *Arteriosclerosis*. 1986;6:131-138.[Abstract]
16. Emeson EE, Robertson AA. T lymphocytes in aortic and coronary intimas: their potential role in atherogenesis. *Am J Pathol*. 1988;130:369-376.[Abstract]
17. Hansson GK, Jonasson L, Lojsthe B, Stemme S, Kocher O, Gabbiani G. Localization of T lymphocytes and macrophages in fibrous and complicated human atherosclerotic plaques. *Atherosclerosis*. 1988;72:135-141.[Medline] [Order article via Infotrieve]
18. Katsuda S, Boyd HC, Fligner C, Ross R, Gown AM. Human atherosclerosis, III: immunocytochemical analysis of the cell composition of lesions of young adults. *Am J Pathol*. 1992;140:907-914.[Abstract]
19. Xu Q, Oberhuber G, Gruschwitz M, Wick G. Immunology of atherosclerosis: cellular composition and major histocompatibility complex class II antigen expression in aortic intima, fatty streaks and atherosclerotic plaques in young and aged human specimens. *Clin Immunol Immunopathol*. 1990;56:344-359.[Medline] [Order article via Infotrieve]
20. Munro JM, Van der Walt JD, Munro CS, Chalmers JAC, Cox EL. An immunohistochemical analysis of human aortic fatty streaks. *Hum Pathol*. 1987;18:375-380.[Medline] [Order article via Infotrieve]
21. Stemme S, Holm J, Hansson GK. T lymphocytes in human atherosclerotic plaques are memory cells expressing CD45RO and integrin VLA-1. *Arterioscler Thromb*. 1992;12:206-211.[Abstract]
22. Hansson GK, Jonasson L, Holm J, Claesson-Welsh L. Class II MHC antigen expression in the atherosclerotic plaque: smooth muscle cells express HLA-DR, HLA-DQ and the invariant gamma chain. *Clin Exp Immunol*. 1986;64:261-268.[Medline] [Order article via Infotrieve]
23. Hansson GK, Holm J, Jonasson L. Detection of activated T lymphocytes in the human atherosclerotic plaque. *Am J Pathol*. 1989;135:169-175.[Abstract]
24. Geng YJ, Holm J, Nygren S, Bruzelius M, Stemme S, Hansson GK. Expression of the macrophage scavenger receptor in atheroma: relationship to immune activation and the T-cell cytokine interferon- $\gamma$ . *Arterioscler Thromb Vasc Biol*. 1995;15:1995-2002. [Abstract/Free Full Text]
25. Stemme S, Rymo L, Hansson GK. Polyclonal origin of T lymphocytes in human atherosclerotic plaques. *Lab Invest*. 1991;65:654-660.[Medline] [Order article via Infotrieve]
26. Stemme S, Faber B, Holm J, Wiklund O, Witztum JL, Hansson GK. T lymphocytes from human atherosclerotic plaques recognize oxidized low density lipoprotein. *Proc Natl Acad Sci U S A*. 1995;92:3893-3897.[Abstract/Free Full Text]
27. Sohma Y, Sasano H, Shiga R, Saeki S, Suzuki T, Nagura H, Masato N, Yamamoto T. Accumulation of plasma cells in atherosclerotic lesions of Watanabe heritable hyperlipidemic rabbits. *Proc Natl Acad Sci U S A*. 1995;92:4937-4941. [Abstract/Free Full Text]
28. Roselaar SE, Schonfeld G, Daugherty A. Enhanced development of atherosclerosis in cholesterol-fed rabbits by suppression of cell-mediated immunity. *J Clin Invest*. 1995;96:1389-1394.[Medline] [Order article via Infotrieve]
29. Emeson EE, Shen ML. Accelerated atherosclerosis in hyperlipidemic C57BL/6 mice

- treated with cyclosporin A. *Am J Pathol.* 1993;142:1906-1915.[Abstract]
30. Fyfe AJ, Qiao JH, Lusis AJ. Immune deficient mice develop typical atherosclerotic fatty streaks when fed an atherogenic diet. *J Clin Invest.* 1994;94:2516-2520.[Medline] [Order article via Infotrieve]
31. Qiao JH, Xie PZ, Fishbein MC, Kreuser J, Drake TA, Demer LL, Lusis AJ. Pathology of atheromatous lesions in inbred and genetically engineered mice. *Arterioscler Thromb.* 1994;14:1480-1487.[Abstract]
32. Daugherty A, Rateri DL. Heterogeneity of very low density lipoprotein fractions: factors influencing the ability of specific subfractions to modulate cholesterol metabolism in macrophages in vitro. *Coron Artery Dis.* 1991;2:775-787.
33. Goldstein JL, Ho YK, Brown MS. Cholesteryl ester accumulation in macrophages resulting from receptor-mediated uptake and degradation of hypercholesterolemic canine  $\beta$ -very low density lipoproteins. *J Biol Chem.* 1980;255:1839-1848.[Abstract/Free Full Text]
34. Mahley RW, Innerarity TL, Brown MS, Ho YK, Goldstein JL. Cholesteryl ester synthesis in macrophages: stimulation by  $\beta$ -very low density lipoproteins from cholesterol-fed animals of several species. *J Lipid Res.* 1980;21:970-980.[Abstract]
35. Daugherty A, Oida K, Sobel BE, Schonfeld G. Dependence of metabolic and structural heterogeneity of cholesterol ester-rich very low density lipoproteins on the duration of cholesterol feeding in rabbits. *J Clin Invest.* 1988;82:562-570.[Medline] [Order article via Infotrieve]
36. Giguère V, Isobe KI, Grosfeld F. Structure of the murine Thy-1 gene. *EMBO J.* 1985;4:2017-2024.[Abstract]
37. Ledbetter JA, Rouse RV, Micklem HS, Herzenberg LA. T cell subsets defined by expression of Lyt-1,2,3 and Thy-1 antigens: two-parameter immunofluorescence and cytotoxicity analysis with monoclonal antibodies modifies current views. *J Exp Med.* 1980;152:280-295.[Abstract/Free Full Text]
38. Tarakhovsky A, Müller W, Rajewsky K. Lymphocyte populations and immune responses in CD5-deficient mice. *Eur J Immunol.* 1994;24:1678-1684.[Medline] [Order article via Infotrieve]
39. Qiao JH, Castellani LW, Fishbein MC, Lusis AJ. Immune complex-mediated vasculitis increases coronary artery lipid accumulation in autoimmune-prone MRL mice. *Arterioscler Thromb.* 1993;13:932-943.[Abstract]
40. McMurray HF, Parthasarathy S, Steinberg D. Oxidatively modified low density lipoprotein is a chemoattractant for human T-lymphocytes. *J Clin Invest.* 1993;92:1004-1008.[Medline] [Order article via Infotrieve]
41. Daugherty A, Roselaar SE. Lipoprotein oxidation as a mediator of atherogenesis: insights from pharmacological studies. *Cardiovasc Res.* 1995;29:297-311.[Medline] [Order article via Infotrieve]
42. Hansson GK, Seifert PS, Olsson G, Bondjers G. Immunohistochemical detection of macrophages and T lymphocytes in atherosclerotic lesions of cholesterol-fed rabbits. *Arterioscler Thromb.* 1991;11:745-750.[Abstract]
43. Drew AF, Tipping PG. T helper cell infiltration and foam cell proliferation are early events in the development of atherosclerosis in cholesterol-fed rabbits. *Arterioscler Thromb Vasc Biol.* 1995;15:1563-1568.[Abstract/Free Full Text]
44. Haraoka S, Shimokama T, Watanabe T. Participation of T lymphocytes in atherogenesis: sequential and quantitative observation of aortic lesions of rats with diet-induced hypercholesterolaemia using en face double immunostaining. *Virchows Arch.* 1995;426:307-315.[Medline] [Order article via Infotrieve]
45. Okano Y, Macy M, Cardin AD, Harmony JAK. Suppression of lymphocyte activation by plasma lipoproteins: modulation by cell number and type. *Exp Cell Biol.* 1985;53:199-212.[Medline] [Order article via Infotrieve]



46. Pepe MG, Curtiss LK. Apolipoprotein E is a biologically active constituent of the normal immunoregulatory lipoprotein, LDL-In. *J Immunol.* 1986;136:3716-3723.  
[\[Abstract/Free Full Text\]](#)
47. Mistry MJ, Clay MA, Kelly ME, Steiner MA, Harmony JAK. Apolipoprotein E restricts interleukin-dependent T lymphocyte proliferation at the G1<sub>A</sub>/G1<sub>B</sub> boundary. *Cell Immunol.* 1995;160:14-23.  
[\[Medline\]](#) [\[Order article via Infotrieve\]](#)
48. Werb Z, Chin JR. Onset of apoprotein E secretion during differentiation of mouse bone marrow-derived mononuclear phagocytes. *J Cell Biol.* 1983;97:1113-1118.  
[\[Abstract\]](#)
49. Brand K, Mackman N, Curtiss LK. Interferon- $\gamma$  inhibits macrophage apolipoprotein E production by posttranslational mechanisms. *J Clin Invest.* 1993;91:2031-2039.  
[\[Medline\]](#) [\[Order article via Infotrieve\]](#)
50. Mazzone T, Gump H, Diller P, Getz GS. Macrophage free cholesterol content regulates apolipoprotein E synthesis. *J Biol Chem.* 1987;262:11657-11662.  
[\[Abstract/Free Full Text\]](#)

## Anti-atherosclerotic effect of simvastatin depends on the presence of apolipoprotein E

Yi-Xin (Jim) Wang <sup>a,\*</sup>, Baby Martin-McNulty <sup>a</sup>, Ling-Yuh Huw <sup>b</sup>, Valdeci da Cunha <sup>a</sup>, Joe Post <sup>a</sup>, Josephine Hinchman <sup>a</sup>, Ronald Vergona <sup>a</sup>, Mark E. Sullivan <sup>a</sup>, William Dole <sup>b</sup>, Katalin Kauser <sup>b</sup>

<sup>a</sup> Department of Pharmacology, Berlex Biosciences, P.O. Box 4099, 15049 San Pablo Avenue 15049 San Pablo Avenue, Richmond, CA 94804-0099, USA

<sup>b</sup> Department of Cardiovascular Research, Berlex Biosciences, PO Box Richmond, CA 94804, USA

Received 19 June 2001; received in revised form 19 July 2001; accepted 2 August 2001

### Abstract

Low density lipoprotein receptor deficient (LDLR-KO) and apolipoprotein E deficient (apo E-KO) mice both develop hyperlipidemia and atherosclerosis by different mechanisms. The aim of the present study was to compare the effects of simvastatin on cholesterol levels, endothelial dysfunction, and aortic lesions in these two models of experimental atherosclerosis. Male LDLR-KO mice fed a high cholesterol (HC; 1%) diet developed atherosclerosis at 8 months of age with hypercholesterolemia. The addition of simvastatin (300 mg/kg daily) to the HC diet for 2 more months lowered total cholesterol levels by ~57% and reduced aortic plaque area by ~15% compared with the LDLR-KO mice continued on HC diet alone,  $P < 0.05$ . Simvastatin treatment also improved acetylcholine (ACh)-induced endothelium-dependent vasorelaxation in isolated aortic rings, which was associated with an increase in NOS-3 expression by ~88% in the aorta measured by real time polymerase chain reaction (PCR),  $P < 0.05$ . In contrast, in age-matched male apo E-KO mice fed a normal diet, the same treatment of simvastatin elevated serum total cholesterol by ~35%, increased aortic plaque area by ~15%, and had no effect on endothelial function. These results suggest that the therapeutic effects of simvastatin may depend on the presence of a functional apolipoprotein E. © 2002 Elsevier Science Ireland Ltd. All rights reserved.

**Keywords:** HMG-CoA reductase inhibitor; Atherosclerotic plaque; Cholesterol; Endothelial dysfunction; NOS-3; Apo E-knockout; LDLR-knockout; Mouse

### 1. Introduction

Hypercholesterolemia is a major risk factor for development of atherosclerotic vascular disease [1]. Hydroxy-methylglutaryl-coenzyme A (HMG CoA) reductase inhibitors (statins) lower cholesterol and reduce cardiovascular morbidity and mortality in patients with atherosclerosis [2–4]. A growing data base suggests that the beneficial actions of statins may be due to direct effects on the vascular wall in addition to lipid lowering. Moreover, atherosclerosis is often

accompanied by endothelial dysfunction due to impaired endothelial nitric oxide (NO) production [5–8]. Statins have been shown to restore endothelial function by restoring NO-mediated vasodilation in hyperlipidemic rabbits [9] and in patients with coronary artery disease [10,11]. This improvement in endothelial function contributes to the cardiovascular benefits achieved by statin treatment.

Low density lipoprotein receptor deficient (LDLR-KO) and apolipoprotein E deficient (apo E-KO) mice have been used to study mechanisms of atherogenesis [12,13]. It has been shown that simvastatin lowers lipid levels in LDLR-KO [14], but not in apo E-KO [15] mice. The present study was to compare the effect of simvastatin on atherosclerosis development be-

\* Corresponding author. Tel.: +1-510-669-4489; fax: +1-510-669-4247.

E-mail address: jim\_wang@berlex.com (Y.-X.J. Wang).

tween the two animal models of atherosclerosis. In addition, the effects of simvastatin on endothelial function and endothelial nitric oxide synthase (NOS-3) were also examined.

## 2. Methods

### 2.1. Animals and experimental design

Two-month-old male LDLR-KO mice (Jackson Laboratories, Bar Harbor, ME) were fed a high cholesterol (HC; 1%) diet for 8 months. At 10 months of age the animals developed moderate atherosclerotic lesions in the aorta ( $35 \pm 3\%$ ) accompanied by hypercholesterolemia ( $591 \pm 75$  mg/dl). They were then randomly divided into three groups, control group; continued on a HC diet; simvastatin group; fed a HC diet supplemented with 0.15% simvastatin (HC + SIM); and regular diet (RD) group, withdrawn from the HC diet and fed a regular chow diet. The above treatments were continued for 2 months.

Apo E-KO mice spontaneously develop hypercholesterolemia and atherosclerosis without the need for a cholesterol supplementation. For the present studies, 10-month-old male apo E-KO mice (Jackson Laboratories, Bar Harbor, ME) were used. One group of mice were fed a grain-based rodent diet (Bio-Serv, NJ) as controls and the other was on the same diet supplemented with 0.15% simvastatin for 1–3 months. The daily dose of simvastatin in both LDLR-KO and apo E mice was approximately 300 mg/kg, which has been shown to effectively reduce cholesterol by 37% in LDLR-KO mice [14].

At the end of the treatment period, all animals were fasted overnight and euthanized. Blood samples were collected via cardiac puncture at the time of death. Total serum cholesterol, triglycerides and high density lipoprotein (HDL) levels were determined enzymatically (performed by IDEXX, West Sacramento, CA). LDL values were calculated from total cholesterol and HDL levels. The aortae were isolated for measurements of atherosclerotic lesion area, vascular reactivity, and NOS-3 mRNA expression.

### 2.2. Measurement of atherosclerotic plaque

The aortae were isolated, cleaned from the adherent connective tissue, fixed with 10% formalin, cut open longitudinally and pinned on black wax-coated petri dishes as previously described in detail [5]. Atherosclerotic plaque area is visible without staining. The images of the open luminal surface of the aortae were recorded at a resolution of  $512 \times 512$  using a

RGB 3-chip CCD digital camera (Sony) mounted on a dissecting microscope (Nikon SMZ-2T) attached to a computer in 24 bit true image format. The images were analyzed using C-Simple software (C. Imaging 1208, Compix, Mars, PA). Atherosclerotic plaque area was quantified and expressed as a percentage of total luminal surface area of the aorta.

### 2.3. Assessment of vascular reactivity

The thoracic aortae were dissected, cleaned from the adherent connective tissue, and placed in a HEPES-buffered solution containing (in mM), 140 NaCl; 4.5 KCl; 1.0  $\text{MgCl}_2$ ; 5.5 glucose; 1.5  $\text{CaCl}_2$ ; and 10 HEPES at pH 7.4 and 20 °C. The aortae were cut into four rings and were placed in organ-bath chambers containing 15 ml of Krebs solution with the following composition (in mM), 118 NaCl; 24.9  $\text{NaHCO}_3$ ; 4.7 KCl; 1.18  $\text{KH}_2\text{PO}_4$ ; 1.66  $\text{MgSO}_4$ ; 5.55 glucose; 2.0 Na-pyruvate; and 2.0  $\text{CaCl}_2$ . The solution was continually bubbled with a 5%  $\text{CO}_2$  and 95%  $\text{O}_2$  gas mixture and maintained at pH 7.4 and 37 °C. Vessels were pre-treated with indomethacin ( $10^{-5}$  M) for 30 min to inhibit cyclooxygenase mediated vascular effects and pre-contracted with KCl (40 mM), and washed with Krebs solution. Aortic rings were then stretched to 500 mg tension and allowed to equilibrate for 2 h prior to initiation of the experimental protocol. Tension measurements were recorded using Grass force-transducers connected to a data acquisition system (MP100 WS, Biopac, Goleta, CA). Data were digitized on-line at a rate of 1 sample per s and subsequently analyzed using Acknowledge software. Concentration response curves to U46619 (9,11-dideoxy-9 $\alpha$ , 11 $\alpha$ -methanoepoxy prostaglandin  $F_{25}$ ), a thromboxane receptor agonist, were then generated. The calculated concentration of U46619 that produced 80% of the maximal contractile response ( $\text{EC}_{80}$ ) was 20 nM. Endothelium-mediated relaxation was measured as the response to acetylcholine (ACh; 0.01 nM–10  $\mu\text{M}$ ) in rings pre-contracted with U-46619 (30 nM). In the LDLR-KO mice, endothelium-independent aortic ring relaxation was also measured as the response to sodium nitroprusside (SNP, 0.001–1  $\mu\text{M}$ ).

### 2.4. Measurement of NOS-3 mRNA

The isolated aortae were homogenized in 600  $\mu\text{l}$  RLT buffer (Qiagen) using disposable generator probes (Omni International). Total RNA was then isolated using a RNeasy kit with DNase I digestion (Qiagen). Relative abundance of NOS-3 and internal control GAPDH were measured by real-time quantitative polymerase chain reaction (PCR) performed on an ABI PRISM 7700 Sequence Detector (PE Biosys-

tems). One-step reverse transcriptase (RT)-PCR amplification of NOS-3 was carried out in a 50  $\mu$ l reaction mixture consisting of 1  $\times$  TaqMan buffer A with the following composition (mM), 5.5  $\text{MgCl}_2$ ; 0.3 dATP; 0.3 dCTP; 0.3  $\mu$ M dGTP; 0.3 dUTP; 0.025 U/ $\mu$ l AmpliTaq Gold DNA polymerase, 0.025 U/ $\mu$ l RNase inhibitor, 0.025 U/ $\mu$ l multiscribe RT, 200 nM of each primer, and 100 nM probe. Thermal cycle conditions were 48  $^{\circ}\text{C}$  for 30 min and 95  $^{\circ}\text{C}$  for 10 min followed by 40 cycles at 95  $^{\circ}\text{C}$  for 15 s and 60  $^{\circ}\text{C}$  for 1 min. Primers and the probe for NOS-3 were, upper primer, 5'-CGTCATCGGCGTGCT-3' (nt 3436–3450), lower primer, 5'-ACCTCCTGGGT-GCGC-3' (nt 3510–3496), and the probe, 5'-6FAM-CGGGATCAGCAACGCTACCA-TAMRA-3' (nt 3452–3471). Primers and TaqMan probe for rodent GAPDH were purchased from PE Biosystems (P/N 4308313). Hundred nanomol of each primer and 200 mM of the probe were used in the reaction. The expressions of NOS-3 and GAPDH were calculated against a standard curve with serial dilution of total RNA from murine hemangioendothelioma (EOMA) cells [16]. The experiment was repeated twice in triplicate for each sample. Values presented here are the ratio of NOS-3/GAPDH.

### 2.5. Statistics

All results are presented as the mean  $\pm$  S.E.M. for the number of animals ( $n$ ) indicated. Multiple comparisons of mean values were performed by analysis of variance (ANOVA) followed by a subsequent Student–Newman–Keuls test for repeated measures. Differences were considered to be statistically significant when the  $P$  value was  $<0.05$ . The statistical analysis was performed using Statistica software (STATSOFT, Tulsa, OK).

## 3. Results

### 3.1. Effects of simvastatin in LDLR-KO mice

LDLR-KO mice fed a HC diet for 10 months had hypercholesterolemia and developed atherosclerotic lesions in the aorta (Fig. 1). Treatment with simvastatin (HC + SIM) decreased serum LDL cholesterol with no significant effects on HDL cholesterol or triglycerides levels (Table 1). As a result, the ratio of HDL/LDL was significantly higher in the HC + SIM compared with the HC group (Table 1). Simvastatin also reduced atherosclerotic lesion area by  $\sim 15\%$ , compared with that in the HC group (Fig. 1). Mice given the regression diet for 2 months showed similar changes in lipid profiles and atherosclerotic lesions as were seen following simvastatin treatment (Table 1

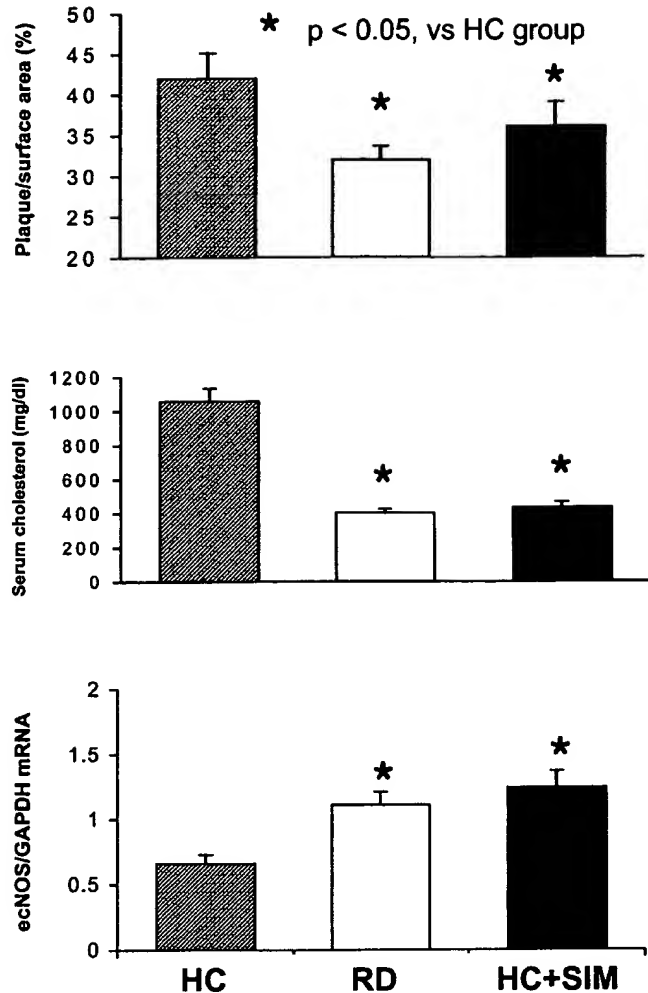


Fig. 1. Aortic atherosclerotic lesion area (top,  $n=8$  per group), total serum cholesterol levels (middle,  $n=11$  per group), and NOS-3 mRNA expression in the aorta (bottom,  $n=3$  per group) of the LDLR-KO mice fed a HC diet without or with (HC + SIM) the supplementation of simvastatin (300 mg/kg, daily), or withdrawn from a HC diet and fed a RD, for 2 months.

and Fig. 1). Combining the data from all three groups, aortic atherosclerotic lesion area was positively correlated to total serum cholesterol levels and negatively correlated to the ratio of HDL/LDL (Fig. 2).

Table 1  
Effects of simvastatin and diet on serum lipid profile (mg/dl) in LDLR-KO mice ( $n=11$  per group)

	HC	RD	HC+SIM
LDL	917 $\pm$ 80	256 $\pm$ 19**	322 $\pm$ 27**
HDL	98 $\pm$ 6	102 $\pm$ 8	77 $\pm$ 6
HDL/LDL	0.12 $\pm$ 0.01	0.38 $\pm$ 0.04**	0.24 $\pm$ 0.03**
Triglyceride	213 $\pm$ 16	226 $\pm$ 19	175 $\pm$ 21

\*,  $P, 0.05$ ; \*\*,  $P<0.01$ ; vs. HC.

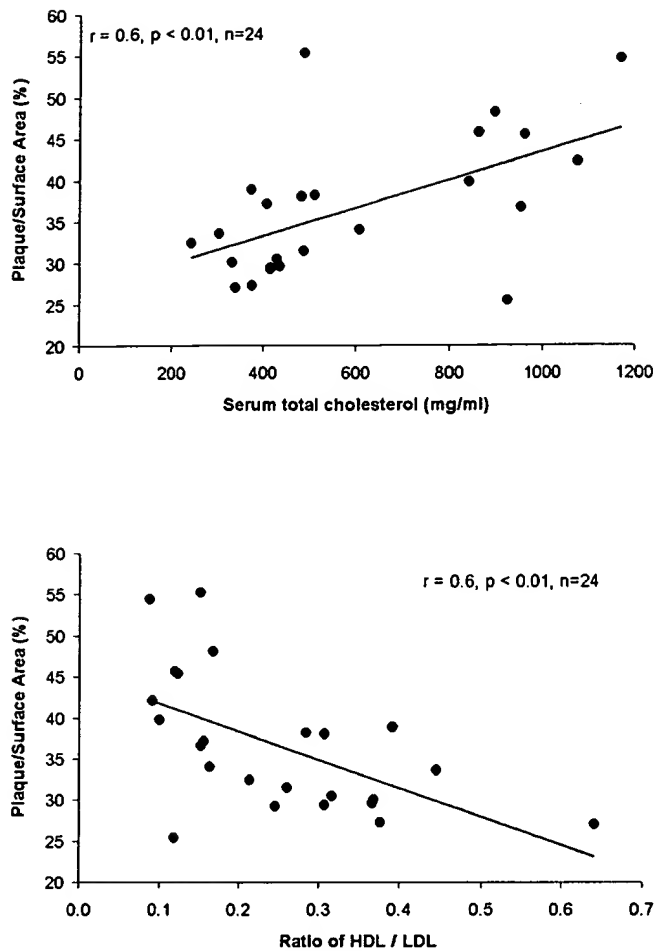


Fig. 2. The aortic atherosclerotic lesion area was positively correlated to the total circulating cholesterol levels (top) and negatively correlated to the ratio of HDL/LDL in the LDLR-KO mice. The data included all three groups of the mice fed a HC diet without or with (HC + SIM) the supplementation of simvastatin (300 mg/kg, daily), or withdrawn from a HC diet and fed a RD, for 2 months.

ACh-induced endothelial NO-mediated aortic relaxation was significantly greater in both the HC + SIM and RD groups than that in the HC group (Fig. 3A). Thus, the maximum responses were significantly greater in both the HC + SIM and RD groups than that in the HC group (Table 2). Endothelium-independent relaxation to SNP did not significantly differ among the three groups (Fig. 3B and Table 3). The expression of NOS-3 mRNA was significantly higher in both the HC + SIM and RD groups than the expression levels in the HC group (Fig. 1).

### 3.2. Effects of simvastatin in apo E-KO mice

Age-matched apo E-KO mice fed a RD had hypercholesterolemia and developed atherosclerotic lesions in the aorta, which tended to increase over time (Fig. 4). Serum total and LDL cholesterol levels were higher and HDL cholesterol levels lower in the simvastatin than in the control group (Fig. 4 and Table 3). As a result of these changes, the ratio of HDL/LDL was significantly lower in the simvastatin than the control group. Triglyceride levels were not significantly different between the two groups. Aortic lesion area was greater in the simvastatin than control group (Fig. 4). Combining the data from both groups at all time points, aortic atherosclerotic lesion area was positively correlated to total serum cholesterol levels and negatively correlated to the ratio of HDL/LDL (Fig. 5).

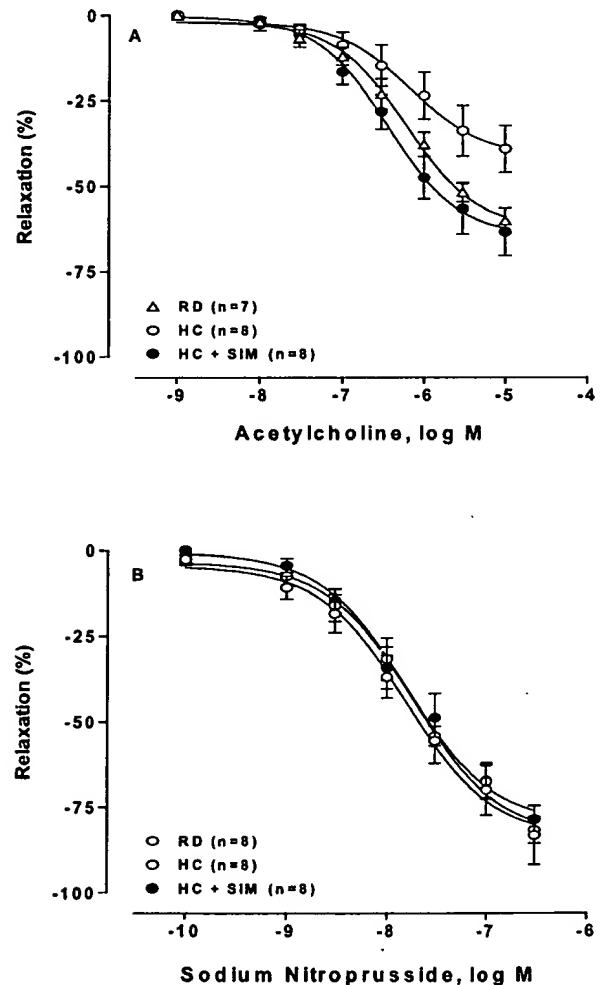


Fig. 3. Concentration-response curves of ACh (A) or SNP (B) induced relaxation in the aortic rings isolated from LDLR-KO mice fed a HC diet without or with (HC + SIM) the supplementation of simvastatin (300 mg/kg, daily), or withdrawn from a HC diet and fed a RD, for 2 months.

Table 2

Sensitivity (log EC<sub>50</sub>, pD<sub>2</sub>) and maximal response (*E*<sub>max</sub>) to ACh and SNP in isolated aortae from LDLR-KO mice fed a RD, HC diet without or with simvastatin (HC+SIM)

Groups	N	ACh		SNP	
		pD <sub>2</sub>	<i>E</i> <sub>max</sub> (%)	pD <sub>2</sub>	<i>E</i> <sub>max</sub> (%)
HC	8	6.17 ± 0.20	39.2 ± 6.8 <sup>a</sup>	7.74 ± 0.18	81.8 ± 3.8
RD	7	6.2 ± 0.16	60.2 ± 3.6	7.8 ± 0.21	83.3 ± 8.5
HC+SIM	8	6.45 ± 0.11	63.4 ± 6.9	7.79 ± 0.22	78.8 ± 4.2

<sup>a</sup> *P* < 0.05 vs. RD group.

ACh-induced relaxation of the aortae isolated from apo E-KO mice were not significantly different between the simvastatin and control groups at both the 2 and 3 months time points (Fig. 6 and Table 4).

#### 4. Discussion

The major findings of the present study are that simvastatin has opposite effects on serum lipids and atherosclerosis in two different genetic mouse model of atherosclerosis. In the LDLR-KO mice, simvastatin decreased serum cholesterol levels and aortic lesion area. These changes were associated with an improvement in endothelial NO-dependent vasorelaxation and an increased NOS-3 mRNA expression. In contrast, in the apo E-KO mice, the same treatment with simvastatin increased serum cholesterol levels and aortic lesion area, with no changes in endothelial NO-mediated vasorelaxation.

Table 3

Effects of simvastatin on serum lipid profiles (mg/dl) in apo E-KO mice (*n* = 7–12 per group)

Treatment (month)	Vehicle	Simvastatin
<b>LDL**</b>		
1	463 ± 55	630 ± 41
2	474 ± 42	727 ± 39
3	462 ± 46	605 ± 42
<b>HDL*</b>		
1	70 ± 6	59 ± 4
2	88 ± 10	51 ± 6
3	100 ± 5	48 ± 6
<b>HDL/LDL*</b>		
1	0.16 ± 0.01	0.10 ± 0.01
2	0.19 ± 0.02	0.07 ± 0.01
3	0.26 ± 0.05	0.08 ± 0.01
<b>Triglycerides</b>		
1	193 ± 32	198 ± 48
2	173 ± 19	141 ± 7
3	158 ± 21	109 ± 8

<sup>\*</sup>, *P* < 0.05; <sup>\*\*</sup>, *P* < 0.01 between two groups.

These data indicate that an intact functional apolipoprotein E may be essential for the lipid lowering, anti-atherosclerosis and other therapeutic benefits of simvastatin.

#### 4.1. Effects of simvastatin on hypercholesterolemia

In the present study, simvastatin at a daily dose of 300 mg/kg significantly reduced total cholesterol by

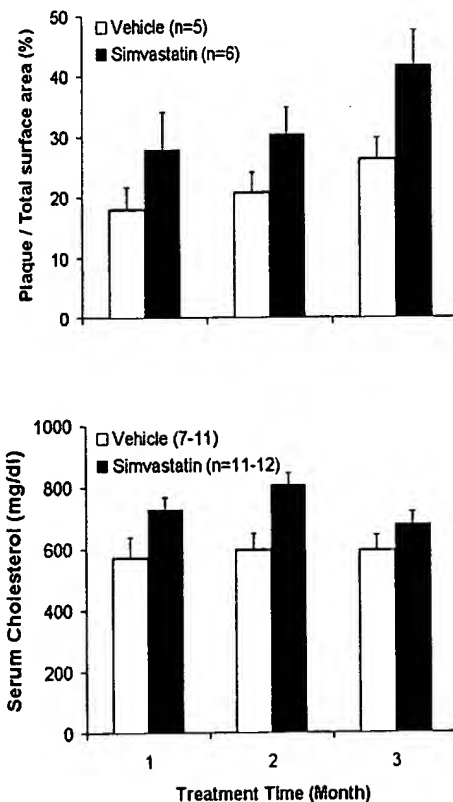


Fig. 4. Atherosclerotic lesion area in the aorta (top) and total serum cholesterol levels (bottom) of the apo E-KO mice treated with simvastatin (300 mg/kg, daily) or vehicle for 1–3 months. *P* < 0.05 between the simvastatin and vehicle treatment group for both the plaque area and total serum cholesterol levels.

57% in LDLR-KO mice fed a HC diet. This result is consistent with a previous report by Bisgaier et al., who reported that at the same daily dose, simvastatin reduced total circulating cholesterol by 37% in LDLR-KO mice [14]. The magnitude of cholesterol lowering by simvastatin was also similar to that observed in untreated LDLR-KO mice fed a regression diet for 2 months. In contrast, the same dose of simvastatin resulted in a 27% increase in serum cholesterol in apo E-KO mice. This finding is consistent with that of Quarfordt et al., who also reported that lovastatin (50 mg/kg daily) increased circulating cholesterol by 70% in apo E-KO mice, but not in wild-type controls [15]. These results suggest that the lipid lowering effect of statins may depend on the presence of intact apolipoprotein E, which functions to transport circulating cholesterol into cells, particularly hepatocytes and acts as an important mediator

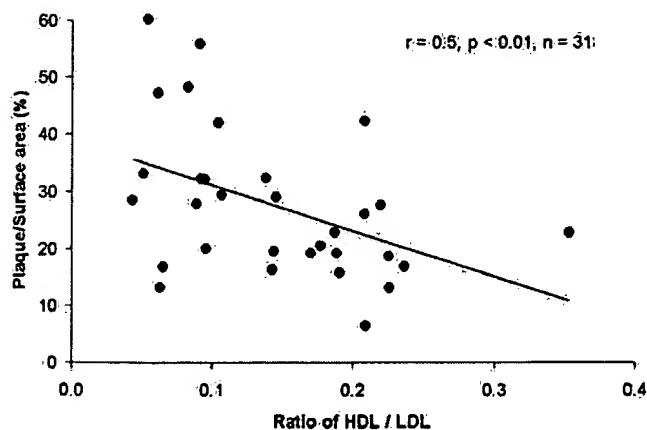
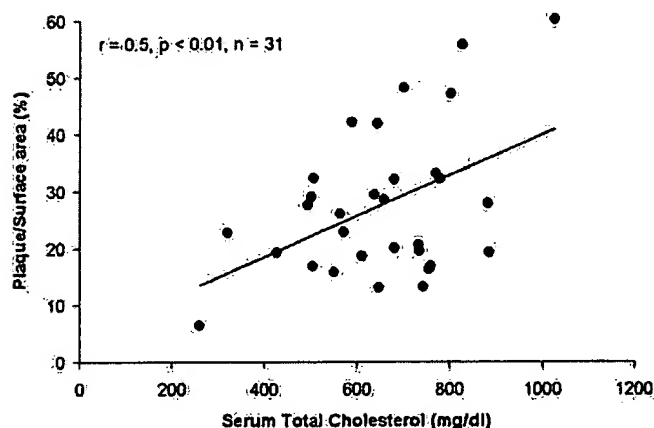


Fig. 5. The aortic atherosclerotic lesion area was positively correlated to the total circulating cholesterol levels (top) and negatively correlated to the ratio of HDL/LDL in the apo E-KO mice. The data included all groups of mice treated with simvastatin (300 mg/kg, daily) or vehicle for 1–3 months.

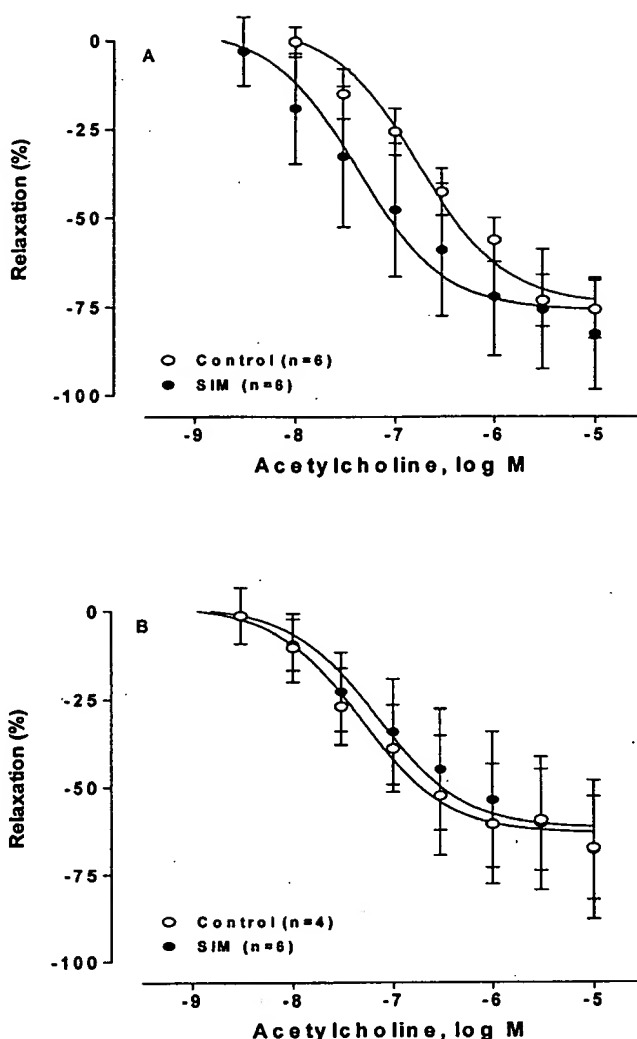


Fig. 6. Concentration–response curves of ACh-induced relaxation of the aortic rings isolated from apo E-KO mice treated with simvastatin (300 mg/kg per day) or vehicle for 2 (top) and 3 (bottom) months.

for hepatic metabolic clearance of circulating cholesterol [12]. In the absence of the apolipoprotein E, hepatic clearance and metabolism of cholesterol are reduced, resulting in hypercholesterolemia [12,13,17]. Impairment of hepatic cholesterol transport may also result in up-regulation of cholesterol synthesis [18]. Indeed, lovastatin has been reported to increase the expression of HMG CoA reductase mRNA [19] and protein [20], thereby increasing cholesterol synthesis [15] in apo E-KO mice, but not in wild-type controls. This may explain the paradoxical elevation of cholesterol in simvastatin-treated apo E-KO mice.

#### 4.2. Effects of simvastatin on atherosclerosis

Accompanied by its lipid lowering effect, simvastatin significantly reduced aortic atherosclerotic



Table 4

Sensitivity (log EC<sub>50</sub>, pD<sub>2</sub>) and maximal response ( $E_{\max}$ ) to ACh and SNP in isolated aortae from apo E-KO mice treated without (control) or with simvastatin for 2 or 3 months

Groups	Duration					
	Two months			Three months		
	<i>N</i>	pD <sub>2</sub>	$E_{\max}$ (%)	<i>N</i>	pD <sub>2</sub>	$E_{\max}$ (%)
Control	6	6.75 ± 0.27	75.8 ± 8.2	4	7.31 ± 0.20	67.5 ± 14.7
Simvastatin	6	7.37 ± 0.34	82.6 ± 15.7	6	7.15 ± 0.32	68.0 ± 19.8

plaque area in LDLR-KO mice. In contrast, simvastatin accelerated atherosclerosis that accompanied an elevation of serum cholesterol levels in apo E-KO mice. Hypercholesterolemia is an important risk factor leading to atherosclerosis. Animals with hypercholesterolemia, resulting from either a HC diet [21–23] or from inherited defects in lipid metabolism [5–7], develop atherosclerotic plaques in the vascular wall. Therefore, the reduction in atherosclerotic lesions by simvastatin in LDLR-KO mice can be explained by its lipid lowering effect, since similar reduction in serum cholesterol and aortic lesion area were observed in untreated mice fed a RD. On the other hand, the increase in atherosclerosis by simvastatin in apo E-KO mice could be explained by elevated serum lipids. This is consistent with a previous report that feeding a HC diet to apo E-KO mice further exacerbated hypercholesterolemia and accelerated lesion development [24]. HDL is known to be involved in reversing cholesterol transport from the vascular wall [25,26]. Therefore, elevation of HDL/LDL ratio by simvastatin in LDLR-KO mice could also contribute to its anti-atherosclerotic effect. Likewise, reduction of HDL/LDL ratio by simvastatin in apo E-KO mice could contribute to acceleration of atherosclerosis. The fact that aortic lesions correlated positively to the total serum cholesterol levels and negatively to the HDL/LDL ratio in both the LDLR-KO and apo E-KO mice support the above view.

#### 4.3. Effect of simvastatin on endothelial function

Endothelial dysfunction, characterized by reduced NO-dependent vascular relaxation, is an early marker of atherosclerosis [27]. Endothelial function is impaired in a number of experimental models of atherosclerosis, including hyperlipidemic rabbits [9] and apo E-KO mice [5], as well as in patients with atherosclerosis [8]. Statins have been shown to reverse endothelial dysfunction in hyperlipidemic rabbits [9] and in humans [10,11]. This effect of statins has been attributed to stabilization of NOS-3 mRNA leading

to the increase in NOS-3 expression [28,29]. Indeed, in the present study, simvastatin treatment significantly increased the expression of NOS-3 mRNA in the aorta of LDLR-KO mice. This was associated with enhanced ACh-induced endothelial NO dependent vasorelaxation. Although there is strong evidence that direct effect on NOS-3 expression is the underlying mechanism for the improvement in endothelial function, the present study was not designed to determine the mechanism of action of simvastatin on NOS-3 and can not differentiate direct effects on the vascular wall from secondary effects due to changes in serum lipids. In apo E-KO mice, on the other hand, the potential direct beneficial effect of simvastatin on endothelial function could be masked or compromised by increased cholesterol levels and atherosclerosis. This may explain the lack of significant effect of simvastatin treatment on ACh-induced NO-dependent aortic ring relaxation in the apo E-KO mice.

During the preparation of this manuscript, Sparrow et al. published a paper demonstrating both anti-inflammatory and anti-atherosclerotic activities of simvastatin in apo E-KO mice [30]. In that study, simvastatin had no significant effect on circulating cholesterol levels. The apo E-KO mice were fed a HC diet, which resulted in a very high circulating cholesterol levels (~1000 mg/dl) and severe atherosclerosis in the aorta. The apo E-KO mice in the present study were fed a RD, resulting in moderate hyperlipidemia with serum cholesterol levels at ~500 mg/dl and a less severe atherosclerosis. These differences in the diet and circulating lipid levels, as well as the severity of atherosclerosis, may contribute, at least in part, to the different results.

In summary, the present study demonstrates that in LDLR-KO mice, treatment with simvastatin for 2 months significantly decreased serum cholesterol levels, improved endothelial function, and reduced atherosclerosis. In contrast, in apo E-KO mice, the same treatment of simvastatin elevated serum cholesterol levels and increased atherosclerosis with no effect on endothelial function. Thus, the beneficial

effects of statins may depend on the presence of functional apolipoprotein E. It has to be pointed out that the mechanisms involved in atherosclerosis induction in these animal models are different. In LDLR-KO mice, it is diet-induced, while in apo E-KO mice, it is primarily due to 'genetics'. This difference may also explain the different effects observed regarding endothelial function. Thus, whether the current findings can be applied to human, as they are less dependent on apo E for the catabolism of LDL, is a new pharmacogenetic topic that needs to be further studied.

### Acknowledgements

The authors would like to thank the Animal Care Group under the direction of William Lillis for proper care and feeding the animals over the duration of these studies. We also would like to thank Merck & Co., Inc. for kindly providing simvastatin. During the period of these experiments, Valdeci da Cunha, as a visiting scientist at Berlex Biosciences from Federal University of Espirito Santo, Brazil, was supported by CAPES (0680/98-2).

### References

- [1] Anderson KM, Castelli WP, Levy D. Cholesterol and mortality. Thirty years of follow-up from the Framingham study. *J Am Med Assoc* 1987;257:2176–80.
- [2] Jones P, Kafonek S, Laurora I, Hunninghake D. Comparative dose efficacy study of atorvastatin versus simvastatin, pravastatin, lovastatin, and fluvastatin in patients with hypercholesterolemia (the CURVES study; see comments). *Am J Cardiol* 1998;81:582–7 [published erratum appears in *Am J Cardiol* 1998;82(1):128].
- [3] Dart A, Jerums G, Nicholson G, d'Emden M, Hamilton-Craig I, Tallis G, Best J, West M, Sullivan D, Bracs P, Black D. A multicenter, double-blind, 1-year study comparing safety and efficacy of atorvastatin versus simvastatin in patients with hypercholesterolemia (see comments). *Am J Cardiol* 1997;80:39–44.
- [4] Bertolini S, Bon GB, Campbell LM, Farnier M, Langan J, Mahla G, Pauciullo P, Sirtori C, Egros F, Fayyad R, Nawrocki JW. Efficacy and safety of atorvastatin compared to pravastatin in patients with hypercholesterolemia. *Atherosclerosis* 1997;130:191–7.
- [5] Wang YX, Halks-Miller M, Vergona R, Sullivan ME, Fitch R, Mallari C, Martin-McNulty B, da Cunha V, Freay A, Rubanyi GM, Kauser K. Increased aortic stiffness assessed by pulse wave velocity in apolipoprotein E-deficient mice. *Am J Physiol Heart Circ Physiol* 2000;278:H428–34.
- [6] Rosenfeld ME, Tsukada T, Gown AM, Ross R. Fatty streak initiation in Watanabe Heritable Hyperlipemic and comparably hypercholesterolemic fat-fed rabbits. *Arteriosclerosis* 1987;7:9–23.
- [7] Rosenfeld ME, Tsukada T, Chait A, Bierman EL, Gown AM, Ross R. Fatty streak expansion and maturation in Watanabe Heritable Hyperlipemic and comparably hypercholesterolemic fat-fed rabbits. *Arteriosclerosis* 1987;7:24–34.
- [8] Anderson TJ, Gerhard MD, Meredith IT, Charbonneau F, Delagrangue D, Creager MA, Selwyn AP, Ganz P. Systemic nature of endothelial dysfunction in atherosclerosis. *Am J Cardiol* 1995;75:71B–4B.
- [9] Senaratne MP, Thomson AB, Kappagoda CT. Lovastatin prevents the impairment of endothelium dependent relaxation and inhibits accumulation of cholesterol in the aorta in experimental atherosclerosis in rabbits. *Cardiovasc Res* 1991;25:568–78.
- [10] Anderson TJ, Meredith IT, Yeung AC, Frei B, Selwyn AP, Ganz P. The effect of cholesterol-lowering and antioxidant therapy on endothelium-dependent coronary vasomotion (see comments). *New Engl J Med* 1995;332:488–93.
- [11] Treasure CB, Klein JL, Weintraub WS, Talley JD, Stillabower ME, Kosinski AS, Zhang J, Bocuzzi SJ, Cedarholm JC, Alexander RW. Beneficial effects of cholesterol-lowering therapy on the coronary endothelium in patients with coronary artery disease (see comments). *New Engl J Med* 1995;332:481–7.
- [12] Breslow JL. Mouse models of atherosclerosis. *Science* 1996;272:685–8.
- [13] Zhang SH, Reddick RL, Piedrahita JA, Maeda N. Spontaneous hypercholesterolemia and arterial lesions in mice lacking apolipoprotein E. *Science* 1992;258:468–71.
- [14] Bisgaier CL, Essenburg AD, Auerbach BJ, Pape ME, Sekerke CS, Gee A, Wolle S, Newton RS. Attenuation of plasma low density lipoprotein cholesterol by select 3-hydroxy-3-methylglutaryl coenzyme A reductase inhibitors in mice devoid of low density lipoprotein receptors. *J Lipid Res* 1997;38:2502–15.
- [15] Quarfordt SH, Oswald B, Landis B, Xu HS, Zhang SH, Maeda N. In vivo cholesterol kinetics in apolipoprotein E-deficient and control mice. *J Lipid Res* 1995;36:1227–35.
- [16] Obeso J, Weber J, Auerbach R. A hemangioendothelioma-derived cell line: its use as a model for the study of endothelial cell biology. *Lab Invest* 1990;63:259–69.
- [17] Ghiselli G, Schaefer EJ, Gascon P, Breser HB Jr. Type III hyperlipoproteinemia associated with apolipoprotein E deficiency. *Science* 1981;214:1239–41.
- [18] Siperstein MD, Guest JM. Studies on the homeostatic control of cholesterol synthesis. *J Clin Invest* 1959;38:1043–4.
- [19] Pitman WA, Osgood DP, Smith D, Schaefer EJ, Ordovas JM. The effects of diet and lovastatin on regression of fatty streak lesions and on hepatic and intestinal mRNA levels for the LDL receptor and HMG CoA reductase in F1B hamsters. *Atherosclerosis* 1998;138:43–52.
- [20] Bilhartz LE, Spady DK, Dietschy JM. Inappropriate hepatic cholesterol synthesis expands the cellular pool of sterol available for recruitment by bile acids in the rat. *J Clin Invest* 1989;84:1181–7.
- [21] Nascimento CA, Kauser K, Rubanyi GM. Effect of 17 $\beta$ -estradiol in hypercholesterolemic rabbits with severe endothelial dysfunction. *Am J Physiol* 1999;276:H1788–94.
- [22] Masuda J, Ross R. Atherogenesis during low level hypercholesterolemia in the nonhuman primate. II. Fatty streak conversion to fibrous plaque. *Arteriosclerosis* 1990;10:178–87.
- [23] Masuda J, Ross R. Atherogenesis during low level hypercholesterolemia in the nonhuman primate. I. Fatty streak formation. *Arteriosclerosis* 1990;10:164–77.
- [24] van Ree JH, van den Broek WJ, Dahlmans VE, Groot PH, Vidgeon-Hart M, Frants RR, Wieringa B, Havekes LM, Hofker MH. Diet-induced hypercholesterolemia and atherosclerosis in heterozygous apolipoprotein E-deficient mice. *Atherosclerosis* 1994;111:25–37.
- [25] Kannel WB, Wilson PW. Efficacy of lipid profiles in prediction of coronary disease. *Am Heart J* 1992;124:768–74.
- [26] Badimon JJ, Badimon L, Fuster V. Regression of atherosclerotic lesions by high density lipoprotein plasma fraction in the cholesterol-fed rabbit. *J Clin Invest* 1990;85:1234–41.

- [27] Harrison DG. From isolated vessels to the catheterization laboratory. Studies of endothelial function in the coronary circulation of humans. *Circulation* 1989;80:703–6.
- [28] Laufs U, La Fata V, Plutzky J, Liao JK. Upregulation of endothelial nitric oxide synthase by HMG CoA reductase inhibitors. *Circulation* 1998;97:1129–35.
- [29] Laufs U, Liao JK. Post-transcriptional regulation of endothelial nitric oxide synthase mRNA stability by Rho GTPase. *J Biol Chem* 1998;273:24266–71.
- [30] Sparrow CP, Burton CA, Hernandez M, Mundt S, Hassing H, Patel S, Rosa R, Hermanowski-Vosatka A, Wang PR, Zhang D, Peterson L, Detmers PA, Chao YS, Wright SD. Simvastatin has anti-inflammatory and anti-atherosclerotic activities independent of plasma cholesterol lowering. *Arterioscler Thromb Vasc Biol* 2001;21:115–21.



## Blockade of endothelin receptors markedly reduces atherosclerosis in LDL receptor deficient mice: role of endothelin in macrophage foam cell formation

Saeid Babaei<sup>a,b</sup>, Pierre Picard, Amir Ravandi<sup>a</sup>, Juan Carlos Monge<sup>a</sup>, Tony C. Lee<sup>a</sup>,  
Peter Cernacek<sup>c</sup>, Duncan J. Stewart<sup>a,b,\*</sup>

<sup>a</sup>Division of Cardiology, Terrence Donnelly Heart Center, St. Michael's Hospital, 30 Bond Street, Toronto, Ontario, Canada, M5B 1W8

<sup>b</sup>Departments of Medicine and of Laboratory Medicine and Pathobiology, University of Toronto, Toronto, Ontario, Canada

<sup>c</sup>Montreal Heart Institute, Department of Laboratory Medicine, Montreal, Quebec, Canada

Received 19 January 2000; accepted 7 June 2000

### Abstract

**Objective:** We evaluated the direct effects of long-term blockade of ET<sub>A</sub> and ET<sub>B</sub> receptors using a mixed endothelin (ET) receptor antagonist, LU224332, in the low density lipoprotein receptor (LDL-R) knockout mouse model of atherosclerosis. **Methods:** Four groups of LDL-R deficient mice were studied: control mice fed normal chow (group I); mice fed a high cholesterol (HC, 1.25%) diet alone (group II), HC fed animals treated with LU224332 (group III); and mice fed normal chow treated with the LU compound (group IV). All treatments were continued for 8 weeks at which time the animals were sacrificed and the aortae were removed and stained with oil red O. Atherosclerotic area (AA) was determined by quantitative morphometry and normalized relative to total aortic area (TA). **Results:** Cholesterol feeding resulted in a marked increased in total plasma cholesterol (~15 fold) and widespread aortic atherosclerosis (AA/TA: group I: 0.013±0.007; group II: 0.33±0.11;  $P<0.001$ ). Atherosclerotic lesions were characterized by immunohistochemistry as consisting mainly of macrophages which also showed high levels of ET-1 expression. Treatment with ET antagonist significantly reduced the development of atherosclerosis (AA/TA: group III: 0.19±0.07,  $P<0.01$  vs. group II), without altering plasma cholesterol levels and blood pressure. The direct effect of LU224332 on macrophage activation and foam-cell formation was determined in vitro using a human macrophage cell line, THP-1. Treatment of the THP-1 cells with LU224332 significantly reduced cholesterol ester and triacylglycerol accumulation and foam-cell formation on exposure to oxidized LDL ( $P<0.01$  and  $P<0.05$ , respectively). **Conclusion:** We conclude that a nonselective ET receptor antagonist substantially inhibited the development of atherosclerosis in a genetic model of hyperlipidemia, possibly by inhibiting macrophage foam-cell formation, suggesting a role for these agents in the treatment and prevention of atherosclerotic vascular disease. © 2000 Elsevier Science B.V. All rights reserved.

**Keywords:** Atherosclerosis; Cholesterol; Endothelins; Macrophages; Receptors

### 1. Introduction

Spontaneous mutations in the low-density lipoprotein receptor (LDL-R) gene result in severe hypercholesteremia and atherosclerosis in Watanabe rabbits and rhesus monkeys [1], and represents the genetic basis of familial hypercholesteremia in humans [2]. Ishibashi et al. [3] have

produced LDL-R deficient mice by targeted disruption of this gene. On high cholesterol feeding these animals exhibited marked elevations in serum cholesterol-rich lipoprotein particles including very low density lipoprotein (VLDL), intermediate density lipoprotein (IDL) and LDL, associated with massive xanthomatosis and atherosclerosis in a manner similar to patients with familial hypercholesterolemia [3].

Endothelial cells normally protect against many of the

\*Corresponding author. Tel.: +1-416-864-5724; fax: +1-416-864-5419.

E-mail address: stewartd@smh.toronto.on.ca (D.J. Stewart).

Time for primary review 22 days.

initiating events in atherosclerosis by the production of vasodilator, antithrombotic and antiproliferative factors [4] such as nitric oxide (NO), which prevents adhesion of blood elements to the endothelium including platelets and monocytes, and inhibits migration and proliferation of medial smooth muscle cells (SMCs) [5,6]. Indeed, reduced endothelium-dependent dilation and decreased bioavailability of NO is an early feature of hyperlipidemia both in experimental models [4,7] and patients [8,9], which can be improved by administration of exogenous L-arginine, the substrate for NO generation by NO synthase (NOS) [10]. Endothelial dysfunction is characterized not only by reduced release of vasodilator autacoids such as NO, but also by increased production of vasoconstrictor factors including endothelin-1 (ET-1) [11]. ET-1 is a 21-amino-acid peptide which, in addition to its powerful vasoconstrictor and hypertensive actions [12], has a number of other biological activities which are likely important in chronic vascular disorders. These include stimulation of cellular proliferation [13], synthesis of matrix proteins [14], and chemotactic effects on monocytes [15,16]. Several indirect lines of evidence support a role for ET-1 in the development of atherosclerosis [17]. OxLDL results in increased ET-1 expression in cultured endothelial cells [18] and circulating ET-1 levels are elevated in patients with atherosclerosis [19]. More relevant, perhaps, are the observations of increased ET-1 expression in human atherosclerotic lesions [20,21], associated with complications of atherosclerosis [22].

ET-1 transduces its biological effects through an interaction with two specific receptors. ET<sub>A</sub> is selective for ET-1 and is found predominantly on target cells, such as vascular SMCs [23], and mediates the vasoconstrictor [24] and pro-proliferative actions of ET-1 [25]. In contrast, in the vessel wall ET<sub>B</sub> is found mostly on the endothelial cell, and mediates the release of NO and prostacyclin [26], which serves to counteract the direct effects of ET-1 on the underlying SMCs. However, ET<sub>B</sub> can also be found to a variable degree on SMCs [27,28] and has been described as the predominant receptor of a human monocyte/macrophage cell line [29,30].

The use of selective ET<sub>A</sub> receptor blockers has been recently shown to reduce atherosclerosis [31,32] and improve endothelium-dependent vasodilation [32,33], possibly by unmasking ET<sub>B</sub>-mediated NO production in response to endogenous ET-1. Whether the use of a mixed ET<sub>A</sub> and ET<sub>B</sub> antagonist, which would not be expected to increase vascular endothelial cell NO release, would produce a similar benefit is not certain. We hypothesized that a non-selective ET receptor blocker would reduce atherosclerosis in the LDL-R deficient mouse model by direct actions on SMCs and/or macrophages, inhibiting the proatherogenic response to increased endogenous vascular ET-1 production. We now report that LU224332, a mixed ET<sub>A</sub> and ET<sub>B</sub> antagonist, substantially reduced atherosclerosis in cholesterol-fed LDL-R deficient mice, and also

inhibited the uptake of OxLDL by macrophages *in vitro*. These data provide strong evidence for a direct role of ET-1 in atherogenesis.

## 2. Methods

### 2.1. Experimental protocol

LDL-R deficient mice in the C57BL/6J background were purchased from Jackson Laboratory. Sixty male LDL-R deficient mice were entered into the study at 22 weeks of age and were maintained on a 12-h-dark–12-h-light cycle with unrestricted access to food and water for the entire length of the experimental protocol. The use and care of LDL-R deficient mice was in accordance with the Canadian Council of Animal Care guidelines and was approved by the Animal Care and Ethics Committee of St. Michael's Hospital. Animals were assigned to four experimental groups (15 mice/group) as follows: (I) control (normal diet, no treatment); (II) high cholesterol (HC) diet without pharmacological intervention; (III) HC diet with ET antagonist treatment and (IV) ET antagonist treatment in mice receiving normal diet. All mice received their specific treatment for a period of 8 weeks before being sacrificed. The ET antagonist treatment groups received LU224332 (10 mg/kg/day) in their drinking water. This compound (a generous gift of Dr. M. Kircheggast from Knoll, Ludwigshafen, Germany) has previously been shown to exhibit equal affinity for the ET<sub>A</sub> and ET<sub>B</sub> receptors (ET<sub>A</sub>: 3.5 and ET<sub>B</sub>: 7.2 nmol/l; ratio: 2.1) [34]. To insure appropriate dosage of the ET antagonist, water intake was monitored at regular intervals and the drug dilution was adjusted accordingly. No difference in food intake, drinking patterns, or body weight was noted between animals from each group (Table 1). The HC diet consisted of 1.25% cholesterol, 7.5% (w/w) cocoa butter, 7.5% casein and 0.5% (w/w) sodium cholate. This chow preparation was shown in previous reports to promote atherogenesis [3]. After 8 weeks of treatment, mice were sacrificed and perfusion fixed with 10% formalin. The aorta were then dissected from the aortic valve to the iliac bifurcation and further fixed in 10% formalin overnight at 4°C.

Table 1  
Feeding behavior and body weight variations\*

	Group I	Group II	Group III	Group IV
Food intake (g/day)	2.4±0.3	2.0±0.5	2.1±0.6	2.4±0.6
Water intake (ml/day)	3.3±1.5	3.8±2.1	3.5±1.8	3.2±1.6
Body weight (g)	28.7±2.7	29.6±3.1	30.1±2.0	27.5±1.9

\* Values shown are mean±S.D. No difference was noted between any experimental groups for food intake, water intake or body weight measurements by the end of the experimental protocol when subjected to one-way ANOVA with post hoc student *t*-test.

## 2.2. Quantification of xanthomatosis

The degree of xanthomatosis was graded according to the following scale: facial lesions: 0=none; 1=mild (snout only); 2=moderate (snout and eye lids); 3=severe (marked lesions); and limb swelling: 0=none; 1=mild/moderate (front paws only); and 2=severe (all four limbs). Addition of facial lesion and limb swelling grades represented the semiquantitative score.

## 2.3. Morphometry and immunohistochemistry

Aortae from each experimental group were opened longitudinally and stained with oil red O and a computer-assisted video imaging system was used to assess the extent of the atherosclerosis area (C-imaging analysis). For immunohistochemistry, the aortae of four animals from each group were divided into three regions: aortic arch, thoracic and abdominal aorta. Paraffin sections (5  $\mu$ m) were cut from each region and endogenous peroxidase activity was quenched by 3%  $H_2O_2$  in methanol for 20 min; nonspecific antibody binding was blocked with 10% goat serum in PBS for 30 min, and adjacent sections from each group were immunostained using the following antibodies: a polyclonal rabbit ET-1 antibody (Peninsula Labs., Belmont, CA, USA) at 1:150 dilution overnight at 4°C, and secondary reaction with goat anti-rabbit biotinylated antibody (1:250 dilution, Vector Labs. Burlingame, USA) for 45 min at room temperature (RT); a polyclonal rat antibody to the mouse monocyte/macrophage marker MOMA-2 (Serotec, Kidlington, Oxford, UK) at 1:100 dilution overnight at 4°C, and secondary reaction with biotinylated rabbit anti-rat IgG (1:250 dilution, Vector Laboratories) for 45 min at RT; a monoclonal mouse antibody to smooth muscle  $\alpha$ -actin (Boehringer Mannheim) at 1:100 dilution for 60 min at RT and secondary reaction with biotinylated anti-mouse IgG (1:150 dilution, Vector Laboratories) for 30 min at RT. Following incubation with the secondary antibodies, the sections were treated with streptavidin–biotin–peroxidase complexes (Vectastain ABC kit, Vector Labs.) for 30 min at RT. Diaminobenzadine was used as the peroxidase substrate and hematoxylin as the nuclear counterstain. Negative control slides were prepared by substituting preimmune serums for the primary antibody.

## 2.4. Cholesterol measurements

Blood was extracted by cardiac ventricular puncture in five animals in groups I, II and IV, and six for group III at the time of sacrifice and centrifuged at 1500 rpm for 10 min for plasma separation and collection. Total cholesterol was measured with an enzymatic cholesterol assay in a colorimetric procedure on a Technicon RA1000 (Bayer, Tarrytown, NY, USA).

## 2.5. Blood pressure measurements

In a separate experimental series, fifteen animals (five control; five HC-fed and five treated with the LU compound) were anaesthetized with an intraperitoneal injection of a mixture of xylazine (5 mg/kg, Bayer) and ketamine (50 mg/kg, Wyeth-Ayerst Canada) after 2 weeks of the representative treatments. A catheter constructed of stretched PE200 tubing (Becton Dickinson) was filled with 50 U/ml heparin in saline and was inserted into the right common carotid artery. Pulsatile blood pressure was measured using a CDXIII pressure transducer (COBE Canada) and recorded on the Biopac MP100 data acquisition system with ACKNOWLEDGE software (Biopac Systems). Animals were allowed to stabilize for 20 min after the onset of anesthesia, and then mean arterial pressure was registered continuously for 10 min and mean values were determined.

## 2.6. LU224332 concentrations in mouse plasma

Plasma levels of LU224332 were measured with a radioreceptor assay as previously described [35]. Briefly, 0.1 ml of plasma obtained from cardiac puncture-blood samples from animals receiving ( $n=7$ ) or not receiving ( $n=6$ ) the LU compound was mixed with 1 ml of methanol, thoroughly vortexed, and centrifuged for 15 min at 2800 g. The supernatant was evaporated under a stream of air. The dry residue was reconstituted in 150  $\mu$ l of the binding buffer. The reaction was carried out at RT in a total volume of 200  $\mu$ l; 50  $\mu$ l of the radioligand ( $^{125}$ I-ET1,  $\approx 10\,000$  cpm per tube) was mixed with 50  $\mu$ l of the sample. The reaction was started by addition of 100  $\mu$ l of porcine aortic membranes (5–7  $\mu$ g protein/tube). It was terminated after 3 h by addition of 1 ml of ice-cold 5 g/l BSA in PBS, pH 7.4, followed immediately by a rapid centrifugation (3 min at 13 000 g). The supernatant was carefully aspirated, and the radioactivity of pellets was counted in an automated gamma-counter. The standard curves, constructed with 18.75 to 1200 nM of LU224332 added to normal rat plasma were linear within this range.

## 2.7. Cell culture

THP-1 monocyte/macrophage cell line was obtained from the American Type Tissue Culture Collection (TIB 202) and were propagated in RPMI 1640 with 10% FCS, penicillin/streptomycin (100 U/ml) at 37°C, 5%  $CO_2$ . Cells were plated at a density of  $1 \times 10^6$  cells/ml in 10% FCS medium containing phorbol myristate acetate ( $10^{-7}$  M) for 72 h to induce differentiation into macrophages, and washed extensively with serum-free RPMI medium prior to incubation with or without lipoproteins as indicated for each experiment. In all experiments, cell viability exceeded 90% as determined by trypan blue exclusion.

### 2.8. Lipoprotein isolation and oxidation

LDL (1.019–1.069 g/ml) was obtained by density gradient ultracentrifugation [36] from plasma of fasted normolipidemic individuals. LDL (2 mg protein/ml) was subsequently dialyzed against 0.1 M phosphate buffer, pH 7.4, containing 0.1 mM EDTA for 24 h (three buffer changes). LDL samples were sterilized by passing through an 0.22- $\mu$ m filter (Millipore, Milford, MA, USA), kept at 4°C, and used within 1 week. Lipoprotein concentration was determined by the method of Lowry et al. [37] and expressed as mg/ml. Oxidation of LDL (5 mg protein/5 ml) was performed by dialysis against 5  $\mu$ M  $\text{CuSO}_4 \cdot 5\text{H}_2\text{O}$  in 0.1 M phosphate buffer, pH 7.4, for 12 h at 37°C in the dark.

### 2.9. Cellular cholesterol and triacylglycerol accumulation

THP-1 cells were incubated for 24 h with 100  $\mu$ g/ml native or oxidized LDL (OxLDL) in the presence or absence of  $10^{-7}$  M LU224332. After incubation the cells were washed once with ice cold PBS containing 0.4% BSA and twice with PBS alone. Cells were scraped from the culture flask into PBS and sonicated. The cellular lipids were extracted with chloroform–methanol (2:1, v/v). The lipid extract was digested with phospholipase C (*Clostridium welchii*; Sigma) as previously described [38]. The reaction mixture was extracted with chloroform–methanol (2:1, v/v) containing 100  $\mu$ g tridecanoylglycerol as internal standard. The lipid extracts were then reacted for 30 min at 20°C with Sylon BFT (Sigma) plus one part dry pyridine. This procedure converts the free fatty acids into silyl esters and the free sterols, diacylglycerols and ceramides into silyl ethers, leaving the cholesteryl esters and triacylglycerols unmodified. The free cholesterol, cholesterol esters and triacylglycerols were quantified using a non-polar capillary column as previously described [39].

### 2.10. Data analysis

Statistical differences between groups were evaluated using the one-way ANOVA test with post hoc student *t*-test where appropriate. For semiquantitative scoring of xanthoma, the statistical difference between groups was evaluated using the Mann–Whitney test. Data are presented as mean  $\pm$  S.D. unless otherwise indicated. A value of  $P < 0.05$  was considered significant.

## 3. Results

Cholesterol-fed animals accumulated foam-cells along the inner curvature of the aortic arch and throughout the descending aortae, leading to the formation of fibro-fatty plaques at 8 weeks of treatment (Fig. 1b, d and f).

Histological examination revealed that the atherosclerotic plaques contained a necrotic core with cholesterol crystals covered by a thin fibrous cap. Occasional SMCs could be identified in the plaque area and fibrous cap by immunostaining with an antibody against  $\alpha$ -actin (Fig. 1b), however,  $\alpha$ -actin positive cells were mostly restricted to the medial layer of the aortae (Fig. 1a and b). Immunostaining with monocyte/macrophage specific antibody (MOMA-2) showed little or no staining in animals receiving normal chow (Fig. 1c), whereas the majority of cells within the intimal lesion of HC fed animals were MOMA-2 positive (Fig. 1d). In animals receiving normal chow, ET-1 staining was restricted to endothelial cells (Fig. 1e), whereas ET-1 was predominantly located to macrophage rich intimal aortic lesions of HC treated animals, consistent with previous reports [15,21] (Fig. 1f).

The degree of xanthomatosis, derived using a semiquantitative grading system, is presented in Fig. 2A. In LDL-R knockout mice fed a normal chow for 8 weeks (Fig. 2, group I), no xanthomatous lesions were observed. In contrast, in the cholesterol-fed LDL-R deficient mice (group II) xanthomatous lesions of the face, ventral surface of the trunk and swelling of the extremities began to appear at 6 weeks and were present in all animals by 8 weeks [xanthomatosis score (XS) of  $4.0 \pm 0.6$  (median  $\pm$  S.D.) Fig. 2]. In the cholesterol-fed LDL-R deficient mice treated with ET antagonist (group III), significantly fewer xanthomatous lesions were apparent in at 8 weeks [XS:  $1.5 \pm 0.5$  (median  $\pm$  S.D.) Fig. 2]. LDL-R deficient mice fed 1.25% cholesterol were severely hyperlipidemic with mean plasma cholesterol levels 15-fold higher than normal chow-fed animals (group I:  $4.8 \pm 0.6$  mM vs. group II:  $65.6 \pm 6.5$  mM;  $P < 0.001$ ). Treatment of cholesterol-fed LDL-R deficient mice with the ET antagonist did not alter plasma lipid levels (group III:  $66.6 \pm 5.1$  mM) (Fig. 2B). As well, arterial blood pressure was not significantly different in animals fed normal or HC diets ( $78 \pm 7$  and  $78 \pm 3$  mmHg, respectively), either with or without treatment with the ET antagonist for 15 days ( $74 \pm 7$  and  $78 \pm 3$  mmHg, respectively) (five animals in each group). These results are consistent with previous reports using endothelin antagonist in mice [32] and other normotensive animal models [40]. Treatment with LU224332 (10 mg/kg/day for 2 weeks) resulted in measurable plasma levels of the ET antagonist ( $708 \pm 357$  nmol/l), which was well in excess of the  $K_i$  for both ET receptors (see Methods).

The extent of aortic lipid deposition was visualised by oil red O staining (Fig. 3A) and quantified by computer assisted morphometry (Fig. 3B). Extensive atherosclerosis was seen in the HC diet group (group II), whereas only minimal lipid deposition was found in animals receiving normal mouse chow mainly at the bifurcations of great vessels (group I). LU224332 treatment (group III) significantly reduced the extent of atherosclerotic involvement in the aortae by almost 45% (Fig. 3B,  $P < 0.01$ ).



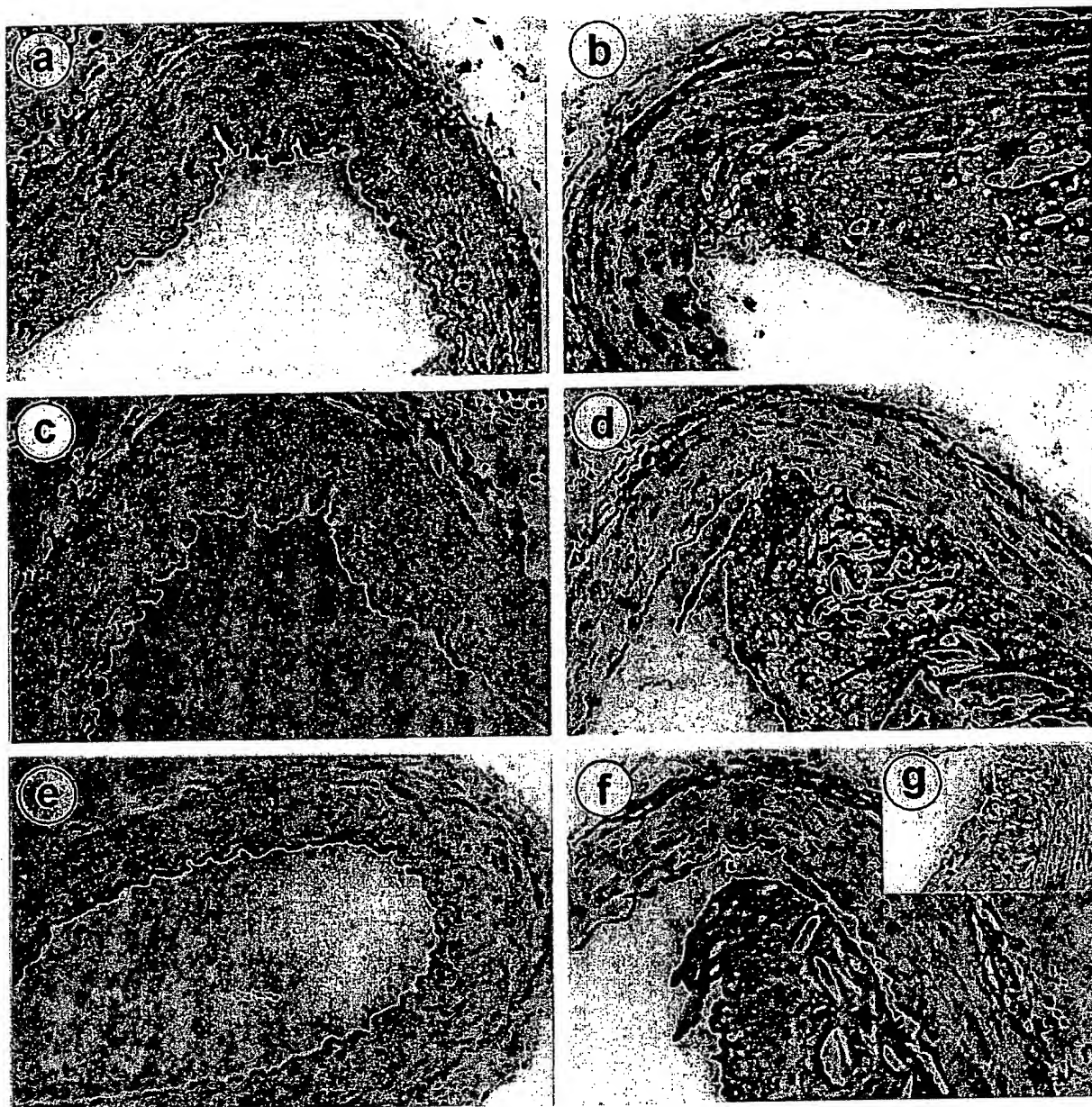
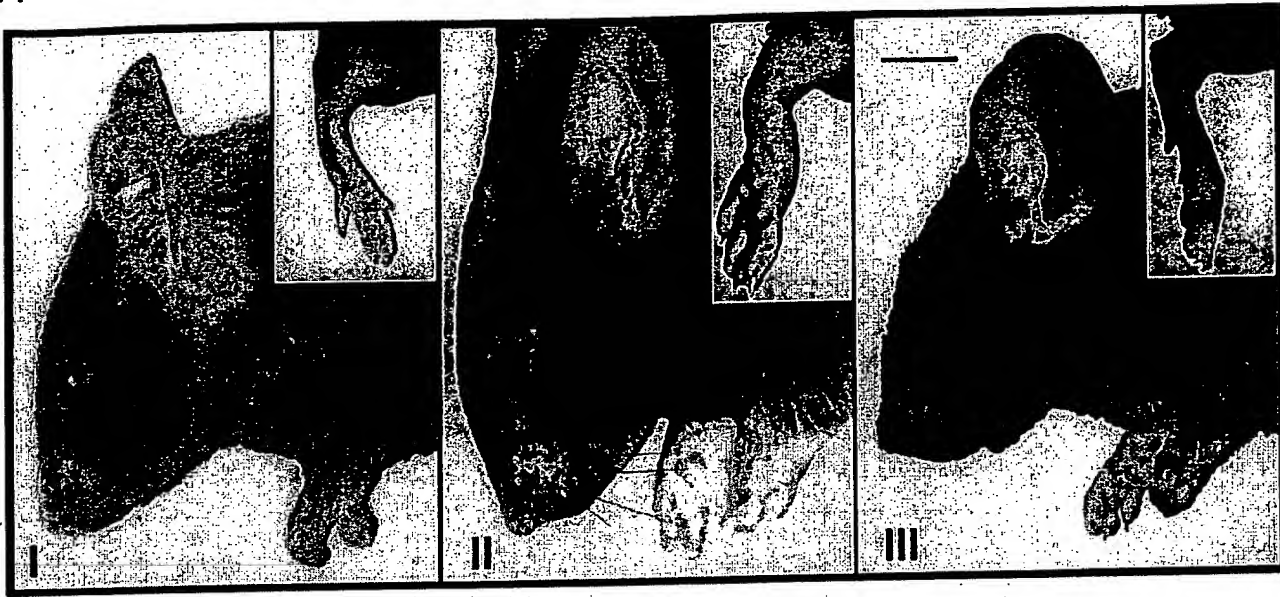


Fig. 1. Photomicrographs show representative sections of thoracic aorta from LDL-R deficient mice fed normal chow (groups I: a, c and e) or a high cholesterol diet (group II: b, d, f and g). Immunostaining for SMCs using an  $\alpha$ -actin antibody revealed a similar pattern of staining in both normal chow (a) and high cholesterol (b) fed animals, largely restricted to the medial layer of the vessels with only partial staining in the atherosclerotic lesion. In contrast, immunostaining with MOMA-2 revealed an absence of macrophages in normal chow fed animals (c) with a very dense accumulation of macrophages in the lesions of high cholesterol fed animals (d). Immunostaining for ET-1 on sequential sections revealed expression of this peptide limited to endothelial cells of normal chow-fed animals (e), with marked ET-1 staining in the HC animals (f) predominantly located to the intimal macrophage rich lesions. Negative control slides were prepared by substituting preimmune rabbit serum for the primary antibody in a section from group II (g).

In order to study the direct effect of endothelin receptor blockade on macrophage lipid accumulation, THP-1 human macrophages were incubated with 100  $\mu$ g/ml of native LDL (nLDL) or Ox LDL, in the presence or absence of LU224332 ( $10^{-7}$  M). After 24 h, cellular cholesteryl ester (CE) and triacylglycerol (TG) were quantified as described in Methods. Treatment of cells with Ox LDL

resulted in 3-fold increase in CE and TG levels compared to nLDL alone ( $P < 0.01$  and  $P < 0.05$ , respectively; Fig. 4A). The addition of LU224332 completely prevented macrophage CE and reduced TG deposition induced by Ox LDL ( $P < 0.01$  and  $P < 0.05$ , respectively; Fig. 4B), reducing macrophage lipid accumulation to levels not different from nLDL alone.

A



B

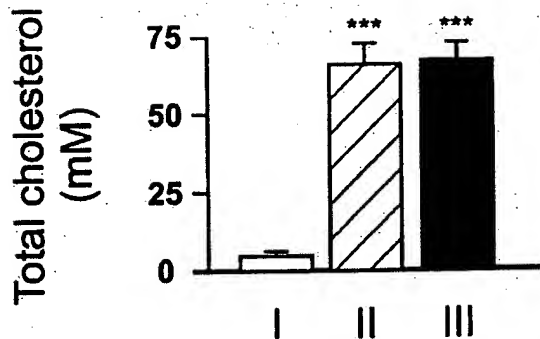


Fig. 2. Animals on regular chow diet, (group I), did not develop xanthomas. In contrast, mice fed high cholesterol (HC) diet alone, group II, developed facial xanthomatous lesions and marked swelling of the paws by the end of the experimental protocol. The LDL-R deficient mice receiving supplemental endothelin antagonist (LU224332) together with HC diet, (group III), showed much reduced facial xanthomatous and minimal swelling of the extremities (A). The mean xanthomatosis score for experimental groups II and III are presented in the results section. Average total plasma cholesterol values (mM) in groups I, II and III are shown in (B).

#### 4. Discussion

The results of the present study demonstrate an important anti-atherosclerotic effect of a non-selective ET receptor antagonist in a model of homozygous familial hypercholesterolemia, the LDL receptor (LDL-R) deficient mouse. In addition to preventing atherosclerosis, treatment with the ET antagonist significantly reduced xanthoma formation without affecting total cholesterol levels or arterial pressure. These results support the hypothesis that the ET system contributes directly to the pathogenesis of atherosclerosis and that ET blockers may have therapeutic utility in the treatment of this vascular disorder.

In the vessel wall, the  $ET_A$  receptor is located primarily on SMCs, whereas the  $ET_B$  subtype is found mainly on the endothelial layer, infiltrating macrophages [29] and to a variable extent SMCs [28]. Although  $ET_A$  may mediate many of the effects of ET-1 that are likely relevant to atherosclerosis, the presence of the  $ET_B$  receptors on macrophages and its up regulation on SMCs of vascular lesions [27], suggest that this receptor subtype may contribute importantly to the pathogenesis of atherosclerosis as well. In fact, a recent report has suggested that accumulation of foamy macrophages and T lymphocytes in the fibrous plaque may modulate the switching of ET receptor subtypes from  $ET_A$  to  $ET_B$  in SMCs [41].

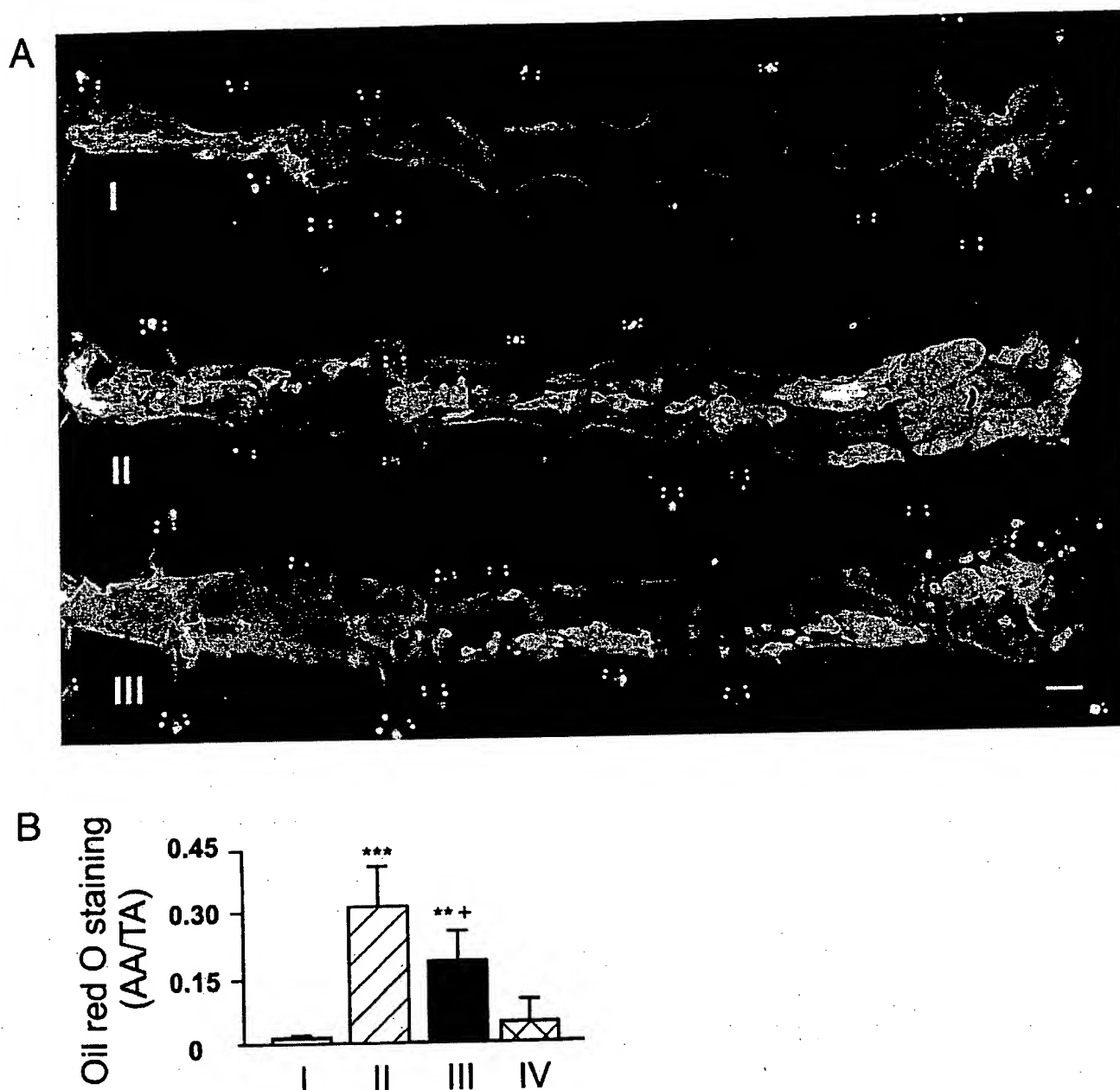


Fig. 3. Representative oil red O staining on the full length luminal surface of aortas from LDL-R deficient mice. Extensive lipid deposition could be seen in the HC diet group (group II), while only minimal lipid deposition was found in animals receiving normal mouse chow (group I). Aortas from LU224332 treated animals (group III) showed reduced aortic atherosclerosis (A). Mean values for atherosclerotic area relative to total aortic luminal surface are shown in panel B ( $n=6$ , group I;  $n=9$ , group II and III;  $n=5$ , group IV). Asterisks indicate statistical difference versus group I using the one-way ANOVA with post-hoc Student *t*-test (\*\*,  $P<0.01$ ; \*\*\*,  $P<0.001$ ). The plus sign indicates a statistical difference versus group II using the one-way ANOVA with post-hoc Student *t*-test (+,  $P<0.01$ ).

Cultured rat peritoneal macrophages have been described to express nearly exclusively  $ET_B$  receptors [42] whereas both  $ET_A$  and  $ET_B$  receptors have been demonstrated by *in situ* hybridization on macrophages in the early inflammatory intimal lesion of hyperlipidemic hamsters [31].

In contrast, stimulation of  $ET_B$  receptors on the endothelial cells releases vasodilators, such as NO, which may protect against atherosclerosis [43]. Kowala et al. [31] previously reported that an  $ET_A$  selective antagonist re-

duced fatty-streak formation in a hamster model of early atherosclerosis. However, to some extent this effect might have been due to a lipid lowering action of certain ET antagonists [31,44]. Recently, Barton et al. [32] reported that another  $ET_A$  selective antagonist reduced atherosclerosis in the apoE-deficient mouse model of atherosclerosis, further supporting an important role for ET-1 in this disease. This was associated with a marked improvement in endothelium-dependent dilation and increased nitrate/

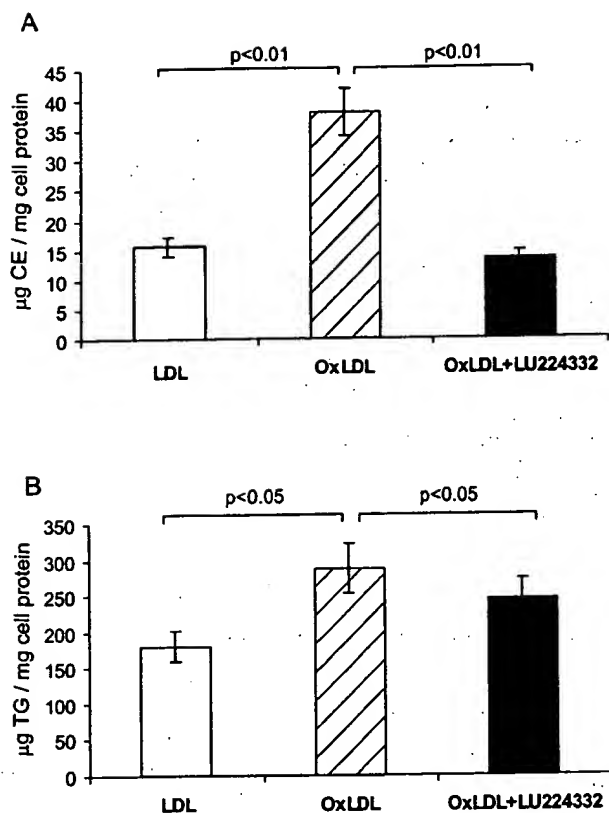


Fig. 4. Mean values  $\pm$  S.D. ( $n=4$ ) for cellular cholesterol ester (CE; A) and triacylglycerol (TG; B) accumulation in THP-1 cell line in presence of nLDL or OxLDL with or without LU224332 for 24 h. LU224332 prevented CE and TG uptake induced by OxLDL ( $P<0.01$  and  $P<0.05$ , respectively).

nitrite levels in the blood [32], likely as a result of selective  $ET_A$  blockade which spares the endothelial  $ET_B$  receptor. Therefore, it is possible that an increase in endothelial NO production may have contributed indirectly to the anti-atherogenic effects of  $ET_A$  blockade in these studies. It is well established that other strategies to increase endothelial NO release, i.e. L-arginine supplementation [45,46], and angiotensin converting enzyme inhibition [47,48] reduce atherosclerosis in a variety of animal models. In the present study a balanced  $ET_A$  and  $ET_B$  receptor antagonist was used, which would not be expected to favorably alter the balance of endothelial versus smooth muscle ET receptor activation. Indeed, it could be argued that blockade of endothelial  $ET_B$  receptor with this compound would be counterproductive and could reduce the overall beneficial effect of the ET antagonist in atherosclerotic models. Nonetheless, a marked reduction in atherosclerosis and xanthomatosis was seen with LU224332 in the absence of any changes in plasma lipids, which may be ascribed to direct effects of ET-1 on the cellular events leading to the initiating and/or progression of atherosclerosis. However, we cannot exclude the possibility that mixed ET blockade may have resulted in

improvement in endothelial function by an indirect mechanism. Increased NO production has been previously reported with both selective and non-selective ET antagonists in the rat Langerdorff heart model [49], possibly due to increased coronary flow and therefore intimal shear forces [49].

In addition to its potent vasoconstrictor effects, ET-1 has a number of biological activities, which might contribute directly to the morphological changes characteristic of atherosclerosis. Endothelin-1 is a co-mitogen for vascular SMCs [13], and can act in concert with other well-characterized growth factors, such as PDGF, which are believed to initiate and maintain cell proliferation in the atheromatous [17]. ET-1 is also a powerful stimulus for secretion of collagen [14] and other matrix components which represent a major constituent of the atherosclerotic lesion. Therefore the inhibition of ET-1 action on atheromatous SMCs may be critical in the anti-atherosclerotic effects of LU224332. As well, ET-1 may also contribute to the recruitment of monocytes into the developing intimal lesion either directly [15] or indirectly by increasing MCP-1 [16]. Macrophages play a key role in the pathogenesis of atherosclerosis [30]. The marked up-regulation of expression of ET-1 in macrophages seen in this and other studies also suggest that this peptide may contribute to chronic inflammatory changes in this disease.

ET-1 has been shown to increase the release of inflammatory cytokines from macrophages [50,51]. In turn, cytokines such as  $TNF\alpha$ , IL-1 and IL-6 have been shown to increase ET-1 production by macrophages [52]. Thus ET-1 may serve to amplify and sustain macrophage activation in the developing atheromatous [51]. Interruption of this positive feedback pathway is a potential mechanism by which ET receptor antagonists may reduce the progression of atherosclerosis in addition to its effects on SMC proliferation and matrix secretion. In support of this, a marked decrease in xanthomas formation, a non-vascular lesion which is dependent on macrophage activation [3] was also observed in LDL-R deficient mice treated with the ET antagonist. Further evidence in favor of a direct effect of ET-1 on macrophage foam-cell formation was provided by in vitro studies using the human THP-1 monocyte-macrophage cell line. These cells differentiate into macrophages on exposure to phorbol ester, in which state they have previously been characterized to express predominantly the  $ET_B$  receptor [29]. The ability of the LU224332 compound to largely prevent cholesterol ester and triacylglycerol accumulation in these cells on exposure to Ox LDL is consistent with a crucial role for endogenous ET-1 in macrophage activation and foam-cell formation.

In summary, nonselective inhibition of ET receptors with LU224332 reduced atherosclerosis and xanthomatosis independently of any change in lipid levels. Prominent ET-1 expression in macrophage-rich atherosclerotic lesions observed in vivo, together with the ability of the ET receptor antagonist to directly reduce macrophage lipid

accumulation in vitro, point to a role for ET-1 in foam-cell formation. Thus, antagonism of the ET system may provide a new pharmacological approach to reduce the vessel wall response to chronic injury induced by hyperlipidemia, and thereby inhibit intimal lesion formation and progression of atherosclerosis.

## Acknowledgements

This work was supported by the Medical Research Council of Canada (MRC MT11620). DJS is the Dexter H.C. Man Chair of Cardiology of the University of Toronto. SB is supported by a Fellowship from the KM Hunter/Medical Research Council of Canada. TCL is supported by a studentship from the Canadian Hypertension Society/Pfizer Canada Inc./MRC. We are grateful to Dr. Phil Connelly for assisting us in the measurements of plasma cholesterol levels and for his helpful comments and advice. Also we would like to thank Dr. M. Kirchengast from Knoll company for his generous gift of the LU224332 compound.

## References

- [1] Brown MS, Goldstein JL. Lipoprotein receptors in the liver. Control signals for plasma cholesterol traffic. *J Clin Invest* 1983;72(3):743–747.
- [2] Goldstein JL, Dana SE, Brunschede GY, Brown MS. Genetic heterogeneity in familial hypercholesterolemia: evidence for two different mutations affecting functions of low-density lipoprotein receptor. *Proc Natl Acad Sci USA* 1975;72(3):1092–1096.
- [3] Ishibashi S, Goldstein JL, Brown MS, Herz J, Burns DK. Massive xanthomatosis and atherosclerosis in cholesterol-fed low density lipoprotein receptor-negative mice. *J Clin Invest* 1994;93(5):1885–1893.
- [4] Dusting GJ, Fennessy P, Yin ZL, Gurevich V. Nitric oxide in atherosclerosis: vascular protector or villain? *Clin Exp Pharmacol Physiol Suppl* 1998;25:S34–S41.
- [5] Wever RM, Luscher TF, Cosentino F, Rabelink TJ. Atherosclerosis and the two faces of endothelial nitric oxide synthase. *Circulation* 1998;97(1):108–112.
- [6] Toutouzas PC, Tousoulis D, Davies GJ. Nitric oxide synthesis in atherosclerosis. *Eur Heart J* 1998;19(10):1504–1511.
- [7] Maxwell AJ, Tsao PS, Cooke JP. Modulation of the nitric oxide synthase pathway in atherosclerosis. *Exp Physiol* 1998;83(5):573–584.
- [8] Bult H. Nitric oxide and atherosclerosis: possible implications for therapy. *Mol Med Today* 1996;2(12):510–518.
- [9] John S, Schlaich M, Langenfeld M et al. Increased bioavailability of nitric oxide after lipid-lowering therapy in hypercholesterolemic patients: a randomized, placebo-controlled, double-blind study. *Circulation* 1998;98(3):211–216.
- [10] Thorne S, Mullen MJ, Clarkson P, Donald AE, Deanfield JE. Early endothelial dysfunction in adults at risk from atherosclerosis: different responses to L-arginine. *J Am Coll Cardiol* 1998;32(1):110–116.
- [11] Yanagisawa M, Kurihara H, Kimura S et al. A novel potent vasoconstrictor peptide produced by vascular endothelial cells. *Nature* 1988;332(6163):411–415.
- [12] Eglen RM, Michel AD, Sharif NA, Swank SR, Whiting RL. The pharmacological properties of the peptide, endothelin. *Br J Pharmacol* 1989;97(4):1297–1307.
- [13] Assender JW, Irenius E, Fredholm BB. Endothelin-1 causes a prolonged protein kinase C activation and acts as a co-mitogen in vascular smooth muscle cells. *Acta Physiol Scand* 1996;157(4):451–460.
- [14] Rizvi MA, Katwa L, Spadone DP, Myers PR. The effects of endothelin-1 on collagen type I and type III synthesis in cultured porcine coronary artery vascular smooth muscle cells. *J Mol Cell Cardiol* 1996;28(2):243–252.
- [15] Achmad TH, Rao GS. Chemotaxis of human blood monocytes toward endothelin-1 and the influence of calcium channel blockers. *Biochem Biophys Res Commun* 1992;189(2):994–1000.
- [16] Helset E, Sildnes T, Konopski ZS. Endothelin-1 stimulates monocytes in vitro to release chemotactic activity identified as interleukin-8 and monocyte chemotactic protein-1. *Mediators Inflamm* 1994;3:155–160.
- [17] Kowala MC. The role of endothelin in the pathogenesis of atherosclerosis. *Adv Pharmacol* 1997;37:299–318.
- [18] He Y, Kwan WC, Steinbrecher UP. Effects of oxidized low density lipoprotein on endothelin secretion by cultured endothelial cells and macrophages. *Atherosclerosis* 1996;119(1):107–118.
- [19] Lerman A, Edwards BS, Hallett JW, Heublein DM, Sandberg SM, Burnett Jr. JC. Circulating and tissue endothelin immunoreactivity in advanced atherosclerosis. *New Engl J Med* 1991;325(14):997–1001.
- [20] Jones GT, van Rij AM, Solomon C, Thomson IA, Packer SG. Endothelin-1 is increased overlying atherosclerotic plaques in human arteries. *Atherosclerosis* 1996;124(1):25–35.
- [21] Zeiher AM, Goebel H, Schachinger V, Ihling C. Tissue endothelin-1 immunoreactivity in the active coronary atherosclerotic plaque. A clue to the mechanism of increased vasoreactivity of the culprit lesion in unstable angina. *Circulation* 1995;91(4):941–947.
- [22] Lerman A, Webster MW, Chesebro JH et al. Circulating and tissue endothelin immunoreactivity in hypercholesterolemic pigs. *Circulation* 1993;88(6):2923–2928.
- [23] Bacon CR, Davenport AP. Endothelin receptors in human coronary artery and aorta. *Br J Pharmacol* 1996;117(5):986–992.
- [24] Kohan DE. Endothelins in the normal and diseased kidney. *Am J Kidney Dis* 1997;29(1):2–26.
- [25] Kanse SM, Wijelath E, Kanthou C, Newman P, Kakkar VV. The proliferative responsiveness of human vascular smooth muscle cells to endothelin correlates with endothelin receptor density. *Lab Invest* 1995;72(3):376–382.
- [26] Vane JR, Anggard EE, Botting RM. Regulatory functions of the vascular endothelium. *New Engl J Med* 1990;323(1):27–36.
- [27] Azuma H, Hamasaki H, Sato J, Isotani E, Obayashi S, Matsubara O. Different localization of ET<sub>A</sub> and ET<sub>B</sub> receptors in the hyperplastic vascular wall. *J Cardiovasc Pharmacol* 1995;25(5):802–809.
- [28] Sumner MJ, Cannon TR, Mundin JW, White DG, Watts IS. Endothelin ET<sub>A</sub> and ET<sub>B</sub> receptors mediate vascular smooth muscle contraction. *Br J Pharmacol* 1992;107(3):858–860.
- [29] Magazine HI, Andersen TT, Bruner CA, Malik AB. Vascular contractile potency of endothelin-1 is increased in the presence of monocytes or macrophages. *Am J Physiol* 1994;266(4 Pt 2):H1620–H1625.
- [30] Murakami T, Yamada N. Modification of macrophage function and effects on atherosclerosis. *Curr Opin Lipidol* 1996;7(5):320–323.
- [31] Kowala MC, Rose PM, Stein PD et al. Selective blockade of the endothelin subtype A receptor decreases early atherosclerosis in hamsters fed cholesterol. *Am J Pathol* 1995;146(4):819–826.
- [32] Barton M, Haudenschild CC, d'Uscio LV, Shaw S, Munter K, Luscher TF. Endothelin E.T.A. receptor blockade restores NO-mediated endothelial function and inhibits atherosclerosis in apolipoprotein E-deficient mice. *Proc Natl Acad Sci USA* 1998;95(24):14367–14372.
- [33] Best PJ, McKenna CJ, Hasdai D, Holmes Jr. DR, Lerman A.

- Chronic endothelin receptor antagonism preserves coronary endothelial function in experimental hypercholesterolemia. *Circulation* 1999;99(13):1747–1752.
- [34] Raschack M, Gock S, Unger L et al. LU302 872 and its racemate (LU224332) show balanced endothelin-A/B receptor affinity, high oral activity, and inhibit human prostate tissue contractions. *J Cardiovasc Pharmacol* 1998;31(Suppl 1):S241–S244.
- [35] Cernacek P, Franchi L, Dupuis J, Rouleau JL, Levy M. Radioreceptor assay of an endothelin A receptor antagonist in plasma and urine. *Clin Chem* 1998;44(8 Pt 1):1666–1673.
- [36] Havel RJ, Eder HA, Bragdon JH. The distribution and chemical composition of ultracentrifugally separated lipoproteins in human serum. *J Clin Invest* 1955;34:1345–1353.
- [37] Lowry OH, Rosebrough NJ, Farr AL, Randall RJ. Protein measurement with the Folin phenol reagent. *J Biol Chem* 1951;193:265–275.
- [38] Kuksis A, Myher JJ, Geher K et al. Comparative determination of plasma phospholipids by automated gas–liquid chromatographic and manual colorimetric phosphorus methods. *J Chromatogr* 1980;182(1):1–26.
- [39] Ravandi A, Kuksis A, Shaikh NA. Glycated phosphatidylethanolamine promotes macrophage uptake of low density lipoprotein and accumulation of cholesteryl esters and triacylglycerols. *J Biol Chem* 1999;274(23):16494–16500.
- [40] Moreau P. Endothelin in hypertension: a role for receptor antagonists? *Cardiovasc Res* 1998;39(3):534–542.
- [41] Iwasa S, Fan J, Shimokama T, Nagata M, Watanabe T. Increased immunoreactivity of endothelin-1 and endothelin B receptor in human atherosclerotic lesions. A possible role in atherogenesis. *Atherosclerosis* 1999;146(1):93–100.
- [42] Sakurai-Yamashita Y, Yamashita K, Yoshida A et al. Rat peritoneal macrophages express endothelin ET(B) but not endothelin ET(A) receptors. *Eur J Pharmacol* 1997;338(2):199–203.
- [43] Aji W, Ravalli S, Szabolcs M et al. L-Arginine prevents xanthoma development and inhibits atherosclerosis in LDL receptor knockout mice. *Circulation* 1997;95(2):430–437.
- [44] Iwasa S, Fan J, Miyauchi T, Watanabe T. Non-selective endothelin receptor antagonist, SB209670, reduces diet-induced hypercholesterolemia and atherosclerosis in apolipoprotein E-deficient mice. *Circulation* 1999;100(18):I–474, Abstract.
- [45] Jeremy RW, McCarron H, Sullivan D. Effects of dietary L-arginine on atherosclerosis and endothelium-dependent vasodilatation in the hypercholesterolemic rabbit. Response according to treatment duration, anatomic site, and sex. *Circulation* 1996;94(3):498–506.
- [46] Cooke JP, Andon NA, Girerd XJ, Hirsch AT, Creager MA. Arginine restores cholinergic relaxation of hypercholesterolemic rabbit thoracic aorta. *Circulation* 1991;83(3):1057–1062.
- [47] Dusting GJ, Hyland R, Hickey H, Makdissi M. Angiotensin-converting enzyme inhibitors reduce neointimal thickening and maintain endothelial nitric oxide function in rabbit carotid arteries. *Am J Cardiol* 1995;76(15):24E–27E.
- [48] Luscher TF, Wenzel RR, Moreau P, Takase H. Vascular protective effects of ACE inhibitors and calcium antagonists: theoretical basis for a combination therapy in hypertension and other cardiovascular diseases. *Cardiovasc Drugs Ther* 1995;9(3):509–523.
- [49] Goodwin AT, Amrani M, Gray CC, Jayakumar J, Yacoub MH. Role of endogenous endothelin in the regulation of basal coronary tone in the rat. *J Physiol* 1998;511(2):549–557.
- [50] Ruetten H, Thiemermann C. Endothelin-1 stimulates the biosynthesis of tumour necrosis factor in macrophages: ET-receptors, signal transduction and inhibition by dexamethasone. *J Physiol Pharmacol* 1997;48(4):675–688.
- [51] Speciale L, Roda K, Saresella M, Taramelli D, Ferrante P. Different endothelins stimulate cytokine production by peritoneal macrophages and microglial cell line. *Immunology* 1998;93(1):109–114.
- [52] Kahaleh MB, Fan PS. Effect of cytokines on the production of endothelin by endothelial cells. *Clin Exp Rheumatol* 1997;15(2):163–167.



# Animal Models of Atherosclerosis and Interpretation of Drug Intervention Studies

Thomas M.A. Bocan

Department of Vascular and Cardiac Diseases, Parke-Davis Pharmaceutical Research, Division of Warner Lambert Company, 2800 Plymouth Road, Ann Arbor, MI 48105, USA

**Abstract:** Atherosclerosis has often been defined as a multifactorial disease; however, a common risk factor associated with accelerated vascular disease in man or animals is an elevated plasma cholesterol level. Even though there is no one perfect animal model that completely replicates the stages of human atherosclerosis, cholesterol feeding and mechanical endothelial injury are two common features shared by most models of atherosclerosis. The models may differ with respect to degree of dietary cholesterol supplementation, length of hypercholesterolemia, dietary regimen and type, duration and degree of mechanical endothelial injury. With the advent of genetic engineering, transgenic mouse models have supplemented the classical dietary cholesterol induced disease models such as the cholesterol-fed hamster, rabbit, pig and monkey. The desire to limit the progression of atherosclerosis has spawned numerous drug intervention studies. Biochemical as well as morphologic and morphometric changes in the extent, structure and composition of atherosclerotic lesions following drug intervention have become major endpoints of *in vivo* drug intervention studies. Interpretations of alterations in vascular pathology following drug administration are often confounded by associated changes in plasma lipids and lipoproteins, limitation of the animal models and additional properties of compounds unrelated to their primary mode of action. Thus, the current review will summarize the pathology of atherosclerosis, describe various animal models of vascular disease and provide a critical review of the methods utilized and conclusions drawn when evaluating pharmacologic agents in animals.



## Introduction

Atherosclerosis has often been defined as a multifactorial disease. In addition, hypercholesterolemia has become a widely accepted risk factor for premature development of coronary artery disease. Classical thinking argued that development of clinically significant atherosclerotic lesions was associated with two major processes. One is fibrocellular proliferation, which adds to intimal bulk and eventually leads to chronic ischemic syndromes via gradual constriction of the arterial lumen. The second process involves the combination of cellular necrosis and lipid deposition within the arterial intima. Enlargement of a lipid-rich core tends to erode the fibrous cap [1], eventuating in plaque rupture, exposure of circulating blood to highly thrombogenic material and sudden ischemic episodes such as myocardial infarction [2,3]. Considering our classical understanding of atherosclerosis progression, the current article will review the histologic landmarks of the various stages of atherosclerosis and also provide a dynamic understanding of how the stages might be interrelated. A comparison of various hypercholesterolemia-induced animal models of atherosclerosis will be made with a focus on their advantages and limitations when used to evaluate novel antiatherosclerotic drugs. Finally, the antiatherosclerotic activity of inhibitors of acyl-coenzyme A:cholesterol O-acyltransferase (ACAT) Fig. (1) (1-14), 3-hydroxy-3-methylglutaryl coenzyme A (HMG-CoA reductase) Fig. (2) (15-18), 15-lipoxygenase (15-LO) and lipoprotein oxidation (anti-oxidants) Fig. (3) (19-22) will be discussed; however, an emphasis will be on describing how the models can discern the compound's *direct* from *indirect* antiatherosclerotic activity.

## Pathology of Atherosclerosis

Atherosclerosis is a focal disease that has been shown to develop in a distinct pattern in both man and animals [4,5]. As depicted in Fig. (4), atherosclerotic lesion development can be divided into six histologically distinct stages or lesion types and five dynamic phases [6,7]. The formation of an intimal cushion at distinct sites within the arterial tree appears to precede the development of atherosclerosis and may be considered a normal aging process. Smooth muscle cells (SMC) migrate from the media, proliferate in the intima and secrete extracellular matrix. Extracellular lipid accumulation that is primarily of lipoprotein origin [8] decorates the secreted collagen, elastin and proteoglycans of the developing intima. Oxidation of the insudant lipoproteins [9] appears to set up a chemotactic gradient and stimulate endothelial cells to upregulate adhesion molecules, i.e., vascular cell adhesion molecule-1 (VCAM-1) [10], responsible for the recruitment of monocyte-macrophages. Monocyte-macrophages are a hallmark of Type I to III lesions and are both a culprit cell responsible for promoting lesion development and a potential point of therapeutic intervention. The major difference in Type I to III lesions lies in the relative amounts of monocyte-macrophage foam cells, SMC, extracellular matrix and lipid and the gross extent of these lesions on the arterial surface. These lesions have classically been termed fatty dots, fatty streaks or fibrolipid lesions to denote their relative extent and degree of fibrosis. Therefore, progression from the innocuous intimal cushion to the Type III lesion that may occur over the first 20 to 30 years of life can be characterized as Phase 1.





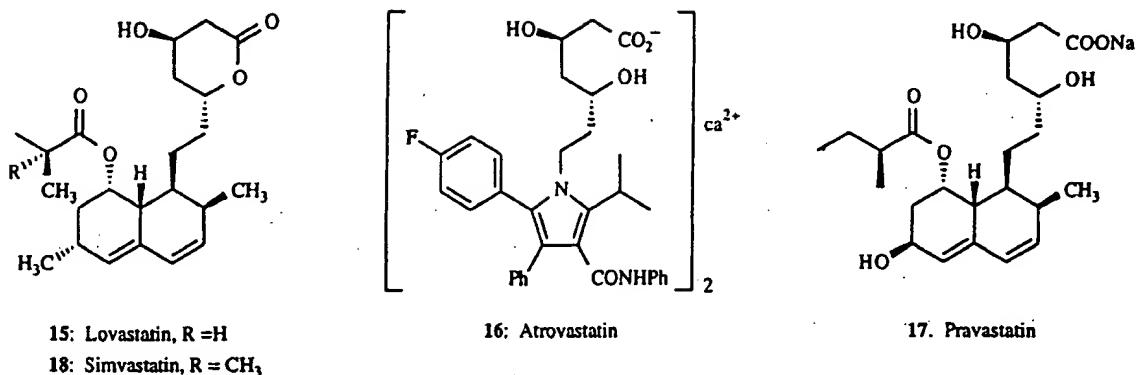


Fig. (2). HMG-CoA reductase inhibitors.

have a developed fibrous cap, deep-intimal necrosis and a lipid-rich necrotic core composed of cholesterol clefts, calcium deposits and evidence of neovascularization. Continued fibrosis of a Type V lesion could silently occlude the arterial lumen (Phase 5). Rupture of the fibrous cap of a Type IV lesion can also generate a mural thrombus that is rapidly recanalated and retracted into the arterial wall to form a Type V lesion (Phase 3). A marked rupture (Phase 4) of the fibrous cap, generation of an occlusive thrombus, myocardial infarction and sudden death is a final fate of the Type IV lesion and for the purpose of classification has been denoted as a Type VI complicated plaque.

In summary, atherosclerotic lesion progression in man involves episodes of SMC proliferation, extracellular matrix deposition and remodeling, lipid infiltration, endothelial cell-monocyte interactions, monocyte migration into the intima, monocyte-macrophage foam cell formation, necrotic lipid-rich core formation, calcium deposition, neovascularization, mural microthrombi and occlusive acute thrombosis. Some of the cell-derived factors that may contribute to atherosclerotic lesion development have previously been reviewed [11].

### Animal Models of Atherosclerosis

Given the complexity of atherosclerotic lesion development in man, the challenge exists to develop animal models that closely mimic the human disease. One must accept, however, that there is no one perfect animal model that completely replicates the stages of human atherosclerosis but that the models are useful in studying specific pathologic processes

associated with the disease. Irrespective of species, there are several common features shared by most models of atherosclerosis. Firstly, induction of vascular lesions in most animal models is dependent upon development of a plasma hypercholesterolemia. Plasma cholesterol elevations can either be induced by dietary supplementation with cholesterol, hepatic overproduction of lipoproteins or genetic mutation of receptors and/or receptor ligands responsible for lipoprotein clearance. Secondly, to accelerate development of atherosclerotic lesions in hypercholesterolemic animals various forms of acute or chronic endothelial damage have been employed. The animal models differ with respect to degree of dietary cholesterol supplementation, length of hypercholesterolemia, dietary regimen and type, duration and degree of mechanical endothelial injury. Thus, this section will describe the various rabbit, hamster, pig, monkey and transgenic mouse models of atherosclerosis with respect to the different experimental protocols utilized to induce atherosclerotic lesions, the stage of atherosclerotic lesion development being replicated and advantages or disadvantages of the model for drug intervention studies.

### Rabbits

The cholesterol-fed rabbit has been extensively used as a model of atherosclerosis since the identification by Anitschkow [12] in 1913 that short-term cholesterol feeding results in formation of foamy lesions within the aorta. Historically, supplementation of commercial rabbit chow with 1 to 3%

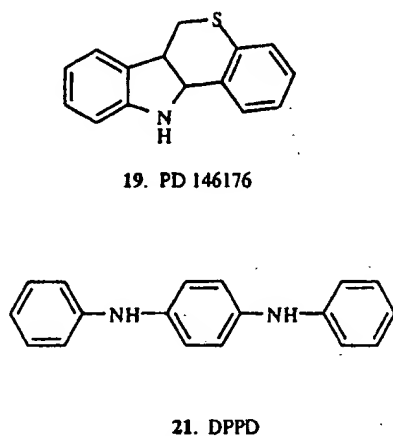
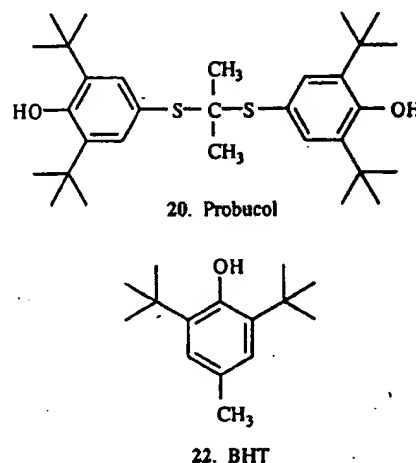


Fig. (3). Antioxidants and 15-LO inhibitors.



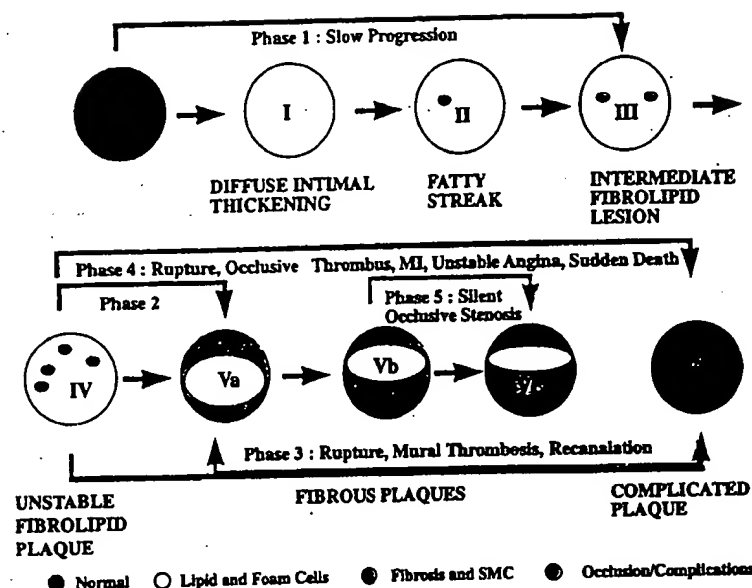


Fig. (4). Schematic representation of atherosclerotic lesion progression (adapted from references [6, 7]).

cholesterol and 4 to 8% fat [13] for 6 to 8 weeks has resulted in marked elevations in plasma cholesterol, i.e., 1000 to 3000 mg/dl, cholesteryl ester accumulation in hepatic and peripheral tissues [14,15] and development of aortic macrophage foam cell enriched lesions. Development of atherosclerosis in the coronaries is limited to the small intramyocardial vessels and not the larger epicardial vessels as has been found in man [16]. The rabbit atherosclerotic lesions were reminiscent in cellular composition to Type I to III human lesions. Kritchewsky and colleagues have performed numerous cholesterol feeding experiments in which they maintained the cholesterol supplementation constant, i.e., 2%, and altered the type of dietary fat to further refine the role of cholesterol metabolism in atherosclerosis progression. A notable finding was that upon addition of 6% peanut oil or 6% coconut oil to a 2% cholesterol diet two histologically distinct atherosclerotic lesions developed [17,18]. Peanut oil supplementation produced aortic lesions that contained relatively little lipid but abundant smooth muscle cell proliferation and collagen deposition. In contrast, addition of 6% coconut oil to the diet resulted in lesions with demonstrable intracellular lipid and intimal proliferation; however, less collagen and elastin were evident. Although elevated plasma cholesterol levels induce atherosclerotic lesions and dietary fat composition may affect the cellular composition of the lesion in rabbits, prolonged hypercholesterolemia results in exponential cholesterol enrichment of many peripheral organs [19].

The marked cholesteryl ester enrichment of peripheral organs such as the liver and spleen may be problematic when evaluating pharmacologic agents. Liver metabolism of compounds may be compromised or enhanced in animals fed a high cholesterol diet and the resulting plasma levels may be either an underestimate or overestimate of the actual efficacious drug levels. Feeding a 2% cholesterol diet results in marked plasma total cholesterol levels and cholesteryl ester enriched beta-VLDL as the primary plasma lipoprotein [20]. Given the pro-atherogenic nature of beta-VLDL [21], the direct antiatherosclerotic activity of compounds with mechanisms

unrelated to cholesterol lowering may be masked due to the profound effect of beta-VLDL on monocyte-macrophage cholesteryl ester enrichment. We have noted that while compounds like ACAT inhibitors Fig. (1) (1-14) which prevent the accumulation of cholesteryl esters are antiatherosclerotic under such conditions, the 15-LO inhibitor, PD146176 Fig (3) (19), lacks activity because its mechanism of action may be related to oxidation of lipoproteins or pre-macrophage events such as monocyte adherence and transmigration.

Rabbit models of atherosclerosis have been developed which limit the amount of dietary cholesterol supplementation [22]; however, such models are time consuming and for that reason may have limited utility for screening antiatherosclerotic agents. Wilson and colleagues [22] fed rabbits an agar-gel diet containing 19% butter and 1% corn oil for up to 5 years. Plasma total cholesterol levels were approximately 300 mg/dl and over the course of 5 years atherosclerotic lesions representing Type I to V lesions were noted. Advanced atherosclerosis can also be induced in a shorter time frame by intermittent feeding of a 1% cholesterol, 5% cottonseed oil diet for 2 months followed by 6 months of a chow diet and 2 additional months of the cholesterol diet [23,24]. While plasma cholesterol levels fluctuated with dietary cholesterol supplementation, the five stages of atherosclerosis were present in both aorta and coronary arteries. Protracted feeding of a low cholesterol diet or intermittent feeding of high and low cholesterol diets produced histologically similar atherosclerotic lesions. Given the disparate plasma total cholesterol levels, these data suggest that the lipoprotein profile may play an important role in the rate at which atherosclerotic lesions develop. Feeding studies have indicated that beta-VLDL was the primary lipoprotein in rabbits fed a cholesterol diet while LDL-like particles predominated in animals fed a semisynthetic casein-enriched diet [25]. Morphologic and morphometric analysis of rabbits fed either a 0.125% to 0.5% cholesterol or casein-enriched diet for 6 months revealed that atherosclerotic lesions developed in both models; however, the nature and extent of lesions varied [25, 26]. At comparable plasma cholesterol levels, the cholesterol-fed

rabbits had approximately twice the extent of aortic atherosclerosis relative to the casein-fed animals and Type IV-V lesions predominated. In the casein-fed rabbits, 30% of the aorta contained atherosclerotic lesions that ranged in appearance from fatty dots to fibrous plaques with a necrotic lipid-rich core [25,26]. These data indicate that under a similar time frame and plasma cholesterol level the type of dietary supplementation can affect the quantity and type of atherosclerotic lesion that develops primarily by altering the major cholesterol carrying lipoprotein, i.e., beta-VLDL or LDL.

Genetic models of atherosclerosis, namely, the homozygote Watanabe Heritable Hyperlipidemic rabbit (WHHL) which lacks functional LDL receptors, have also been compared to cholesterol-fed rabbit models [27,28]. Like the casein-fed rabbits, plasma cholesterol was primarily distributed in LDL. In WHHL rabbits, leukocyte margination, subendothelial accumulation of isolated lipid-filled macrophages, accumulation of SMC and formation of fatty streaks occurred over the first 4 weeks of life [27]. A similar sequence of lesion formation was noted in New Zealand White rabbits fed a 0.1% to 0.2% cholesterol diet. Expansion of the lipid-filled monocyte-macrophage rich lesions, i.e., Type I-III fatty streaks, occurred during the first 6 months in both types of rabbits while complex Type V fibrous plaque lesions were noted in the WHHL and cholesterol-fed rabbits by 13 months of age [28-30]. An enrichment of cholesteryl ester, primarily cholesteryl oleate, was noted in the aorta of both animals over the course of 13 months and such a finding was consistent with the morphologic data noted above [31]. Despite the different lipoprotein distribution, one must conclude that the development of atherosclerosis in WHHL and cholesterol-fed rabbit is very similar and occurs within a similar time frame. One might propose that the WHHL rabbits may be useful to assess agents which lower plasma cholesterol by altering lipoprotein production since these animals lack functional LDL receptors. Cholesterol-fed models are less expensive and time consuming and may be manipulated by altering the level of cholesterol intake to assess the significance of graded degrees of hypercholesterolemia on cellular processes associated with lesion formation, e.g., monocyte adherence, margination and foam cell formation.

Thus far in the discussion of rabbits as models of atherosclerosis it is apparent that human-like atherosclerotic lesions can be induced by elevating plasma cholesterol levels through continuous or intermittent feeding of a cholesterol diet, a casein-enriched diet or by deleting functional LDL receptors as in the WHHL rabbit. It is also quite obvious that in such models a great deal of time is required to induce atherosclerotic lesions comparable to man, i.e., 6 months to 5 years.

Hypercholesterolemia and mechanical denudation of the endothelium in various vascular regions of the rabbit have been utilized to develop shorter-term models of atherosclerosis with a high degree of predictability as to the location and type of atherosclerotic lesion. Acute mechanical injury of the arterial vessel wall can be achieved using a variety of methods. A balloon embolectomy catheter [32] can denude the vessel and distend the media while gentle denudation can be achieved by drawing a nylon filament over the surface of the vessel [33, 34]. Moderate injury and denudation occur following cutting of the internal elastic lamina with a metal or diamond tipped catheter [35]. Chronic endothelial damage has been shown to promote

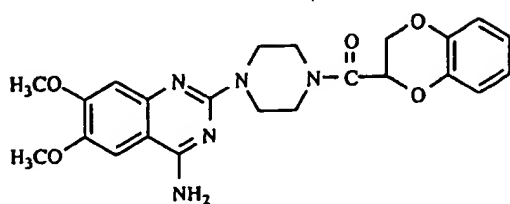
thrombosis at the catheter tip and formation of fibrous lesions [36, 37]. We have used a combination of chronic endothelial injury using a surgically implanted sterile nylon monofilament and dietary cholesterol supplementation [38, 39]. Combination of hypercholesterolemia and endothelial injury has allowed one to develop a model of atherosclerosis that is reproducible, has a high incidence of lesion formation and a predictable lesion site and type. The character of the atherosclerotic lesion is dependent upon the degree, length and type of hypercholesterolemia induced.

In summary, hypercholesterolemic rabbits are valuable models and the most widely used model for the evaluation of pharmacologic agents. Five types of human-like atherosclerotic lesions can be induced in the rabbit; however, the model is limited in that evidence of the complicated ruptured fibrous plaques cannot be found. Rabbits are also valuable for atherosclerosis research because unlike other models, atherosclerotic lesions progress even after removal of dietary cholesterol supplementation [23,40]. Evaluation of the direct antiatherosclerotic properties of hypocholesterolemic agents requires normalization of plasma cholesterol levels by diet prior to drug administration. Since rabbit atherosclerotic lesions will become more complex following cholesterol removal, agents which act by directly altering cellular processes such as ACAT inhibitors that limit macrophage accumulation can be discerned and their effect on lesion progression/regression can be monitored.

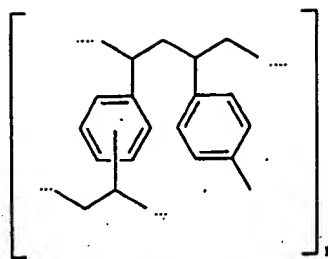
## Hamster

Another model of atherosclerosis that has received recent attention is the hypercholesterolemic hamster. Male hamsters fed a 3% cholesterol, 15% butterfat diet for up to a month had elevated plasma cholesterol levels and the presence of Type I fatty dots and fatty streaks within the aortic arch [41]. Within 3 to 4 months of the very high cholesterol/fat diet, expansion of the fatty streaks into the thoracic aorta around sites of intercostal ostia was noted [41]. By 10 months of cholesterol supplementation when plasma cholesterol levels were 17-times normal, advance Type V lesions were observed in the aortic arch of the hamster but their extent was quite limited, i.e., 30% of the cross-sectional vessel surface. Feeding hamsters a 0.2% cholesterol, 10% coconut oil for 10 weeks [42] or 0.05% cholesterol, 10% coconut oil for 8 weeks [43] resulted in the accumulation of monocyte-macrophages within the aorta arch. Thus, short-term feeding of a cholesterol and either coconut oil or butterfat diet to hamsters is a model of subendothelial monocyte-macrophage foam cell formation. Atherosclerotic lesions can be found predictably within the inner curvature of the aortic arch and can be identified by staining with the lipid dye, Oil Red O. Such a model is useful due to its size for the acute evaluation of agents that may interfere with the early stages of lesion formation, e.g., monocyte adherence, transmigration and foam cell formation.

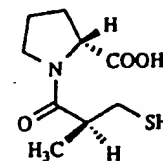
The hypercholesterolemic hamster has been used for the evaluation of numerous pharmacologic agents with varying mechanisms of action. Doxazosin Fig. (5) (23), an alpha-1 adrenergic inhibitor, and cholestyramine Fig. (5) (24) decreased the extent of Oil Red O-positive macrophage foam cells; however, one could not discern that this was a direct effect on the arterial wall because plasma cholesterol levels were



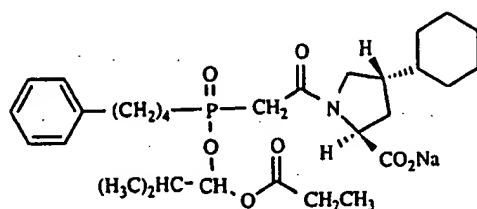
23. Doxazosin



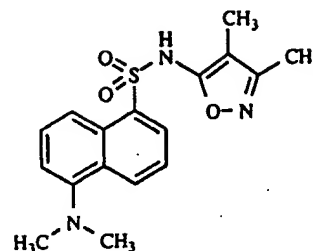
24. Cholestyramine



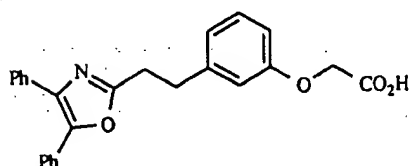
25. Captopril



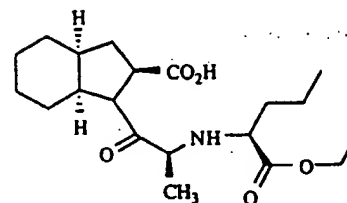
26. Fosinopril



27. BMS-182874



28. BMY-42393



29. Perindopril

Fig. (5). Broad group of compounds reported to possess antiatherosclerotic activities.

reduced by both groups and doxazosin (23) lowered blood pressure [43]. Higher doses of doxazosin (23) did not have any greater lipid lowering effect but a more marked reduction in macrophage foam cell area was noted and such data is suggestive that the compound may have a direct effect on monocyte-macrophage accumulation [42]. The HMG-CoA reductase inhibitor, lovastatin Fig. (2) (15), also was shown to reduce macrophage accumulation but again the changes were associated with a decrease in plasma cholesterol levels [44]. Inhibitors of angiotensin converting enzyme such as captopril Fig. (5) (25) without lowering plasma cholesterol and fosinopril Fig. (5) (26) by lowering LDL cholesterol, reduced aortic arch macrophage accumulation [45]. An additional study with captopril (25) and fosinopril (26) aimed at assessing the ability of these compounds to regress hamster atherosclerotic lesions was performed [46]. Both compounds were reported to reduce macrophage accumulation and thereby induce regression; however, while a group of animals was necropsied at 4 weeks to establish the degree of atherosclerosis prior to intervention only the drug treated animals were followed for an additional 6 weeks. A control designed to assess the effect of plasma cholesterol lowering or continued cholesterol feeding without intervention was not included. The ACAT inhibitor, octimibe [47] Fig. (1) (1), and endothelial subtype A receptor antagonist, BMS-182874 [48] Fig. (5) (27), both of which lowered plasma cholesterol, and the prostacyclin agonist, BMY42393 [47] Fig. (5) (28) in the absence of cholesterol lowering, have been

shown to limit macrophage accumulation in the hypercholesterolemic hamster. Thus, the hypercholesterolemic hamster has proven to be a useful model for the assessment of compounds; however, the changes in plasma cholesterol and blood pressure confound the interpretation of the antiatherosclerotic data and limit one's ability to ascribe the activity to a direct effect of the compounds.

## Swine

Swine are a non-rodent model of atherosclerosis in which atherosclerotic lesions have been found to develop spontaneously [49]. The pathogenesis of lesion development in pigs has been shown to closely parallel the stages of lesion formation as seen in man [50-52]. In addition, atherosclerotic lesion development can be exacerbated by combination of hypercholesterolemia and endothelial injury [53-56]. A strain of pigs with mutant apolipoprotein B alleles has been identified and these animals have been shown to be hypercholesterolemic due to defective lipoprotein clearance and prone to premature development of atherosclerosis [57-60]. Unlike the rabbit and hamster where lesions predominate in the aorta, atherosclerotic lesions have been observed in cerebral [61] and coronary [62] vessels of the pig. Thus, swine are a useful model for the evaluation of atherosclerosis from the perspective that lesions develop spontaneously, their circulatory system and localization of lesions are similar to man and the lesions are

responsive to dietary intervention by exhibiting regression after prolonged periods [63,64].

Despite their similarity to man with respect to atherosclerosis development, swine are not widely used for the evaluation of antiatherosclerotic agents. We have reported that the ACAT inhibitor, CI-976 Fig. (1) (2), blunted the progression of diet- and injury-induced atherosclerotic lesions in Yucatan miniature pigs potentially by inhibiting arterial ACAT and by lowering plasma VLDL-cholesterol levels [65]. The ACE inhibitor, perindopril Fig. (5) (29), was evaluated in hypercholesterolemic miniature pigs and noted to limit the development and monocyte-macrophage enrichment of aortic lesion; however, mean arterial blood pressure (MABP) was reduced in the animals [66]. Such reductions in MABP like the decrease in VLDL-cholesterol levels confound the interpretation of the data and limit one's ability to ascertain whether the compounds had a direct effect on lesion development. The limited a priori knowledge of a compound's effect on plasma cholesterol or blood pressure and the animal's inherent size are major disadvantages of using pigs for assessment of a compound's direct antiatherosclerotic potential. Miniature swine weigh approximately 12 kg at 4 months of age and in our studies feeding pigs a 2% cholesterol, 16% fat diet resulted in a doubling of their body weight within 4 months of diet initiation. Therefore, although swine are excellent models of atherosclerosis that mimic the human disease from the perspective of lesion pathology, such a model may be limited to evaluation of the antiatherosclerotic potential of compounds during their drug development stages rather than discovery phases.

## Monkeys

Non-human primates have often been portrayed as ideal models of human atherosclerosis due to their close phylogenetic association to man. The morphologic characterization of atherosclerotic lesion progression and regression has been performed in cynomolgous (*Macaca fascicularis*) [67-69], rhesus (*Macaca mulatta*) [70], cebus (*Cebus albifrons*) [71], squirrel (*Saimiri sciureus*) [71] and pigtail (*Macaca nemestrina*) [72-75] monkeys. The pathology of atherosclerotic lesion development in various monkey species has been shown to be quite similar to man. Spontaneous development of atherosclerotic lesions is rare in non-human primates; however, like in the animals noted above cholesterol feeding has been shown to promote the development of atherosclerosis in the monkey. Experimentally induced advanced atherosclerosis in monkeys requires approximately 3 years and addition of dietary cholesterol supplementation to produce plasma cholesterol levels of between 350 and 500 mg/dl. The localization of atherosclerotic lesions was similar to man in that lesions were present in the coronary arteries, abdominal aorta and iliac arteries. Plasma cholesterol levels of 200-400 mg/dl have been noted to produce advanced Type V fibrous plaques in *Macaca nemestrina* after 3.5 years of diet [72,73]. A retrospective evaluation of cebus and squirrel monkeys administered a normal diet without cholesterol supplementation and ranging in age from 12 to 20 years highlighted the difference in susceptibility to atherosclerosis and lesion character [71]. The older squirrel monkeys were found to have advanced Type IV-V atherosclerotic lesions containing lipid enrichment and a necrotic lipid core in the abdominal aorta

while lesions from older cebus monkeys were characterized as

diffuse intimal thickening without lipid accumulation [71]. Thus, it is apparent from evaluation of monkey models of atherosclerosis that lesions of comparable character to man, swine and in some cases rabbits can be achieved; however, a combination of a lower plasma cholesterol level and a longer period of time is required for lesion progression.

Few studies have been performed in monkeys using either dietary or pharmacologic intervention to promote lesion regression. After a 30 month lesion induction phase, switching cynomolgous monkeys to a chow diet initially, i.e., 6 months, results in a reduction in monocyte-macrophages and cholesteryl esters; however, intimal necrosis and free cholesterol monohydrate remain [67]. Within 12 months, the atherosclerotic lesions tended to resolve to an intimal scar with a lipid composition similar to normal vessels except for the presence of cholesterol crystals [67]. The bile acid sequestrant, cholestyramine Fig. (5) (24), the antioxidant, probucol Fig. (3) (20), either alone or upon coadministration was shown to promote atherosclerosis lesion regression in the rhesus monkeys [76] presumably due to lowering plasma cholesterol levels. Therefore, although atherosclerotic lesion development appears to mimic human disease progression, the utility of using these animals for drug discovery is limited by their availability and potential variability due to their underlying differences in age and degree of atherosclerosis progression. In addition, given the time frames required for lesion development in the monkey, rabbits fed a low cholesterol diet may be a viable substitute as shown by Wilson and colleagues [22].

## Transgenic Mice

Due to advances in molecular biology and the realization that mice, in general, are normally resistant to the development of atherosclerosis [77], genetically engineered mice have been developed which are predisposed to hypercholesterolemia-induced disease. Two well-characterized transgenic mouse models of atherosclerosis are the apolipoprotein E (apoE)-deficient mouse [78-80] and the low density lipoprotein (LDL) receptor-negative mouse [81,82]. ApoE is a major component of plasma lipoproteins that has a high affinity for LDL receptors and chylomicron remnant receptors [83,84] and may be important in facilitating reverse-cholesterol transport from peripheral tissues. The apoE-deficient mice have been shown to be hypercholesterolemic, i.e., 400 to 700 mg/dl at 5 to 55 weeks of age, while maintained on a chow diet [79]. Atherosclerotic lesions develop naturally over the time frame of 11 to 64 weeks within the aortic sinus and exhibit a similar histologic appearance as Type I to V lesions. Monocyte-macrophage foam cells predominate either as individual cells or clusters in the early stages of lesion development, i.e., less than 28 weeks, while fibrosis, intimal necrosis, acellular, necrotic lipid-rich cores with evidence of cholesterol clefts can be found after 32 weeks of age [79]. A similar histologic pattern can be seen in apoE-deficient mice fed a Western-type diet, i.e., 0.15% cholesterol; however, the timecourse of lesion development is shorter and the extent of atherosclerosis is greater [80]. Cholesterol-fed apoE-deficient mice have plasma cholesterol levels of 1000 to 4400 mg/dl over 6 to 40 weeks of age. Evidence of Type IV-V complex fibrous plaques can be seen as



early as 15 weeks and the lesions are not only present in the aortic sinus but also associated with the bifurcations of such major branch vessels as the common carotids, celiac, mesenteric, renal and iliac arteries [80].

The LDL receptor-negative transgenic mouse has also been developed [81,82]. Unlike the apoE-deficient mice, atherosclerotic lesions do not occur naturally during the timeframes currently studied, i.e., 6 months [82]. Dietary supplementation with 0.15% cholesterol results in plasma cholesterol levels of 900 to 1000 mg/dl over 6 months and the development of atherosclerotic lesions within the aortic sinus. The morphologic appearance and extent of atherosclerosis in the LDL receptor-negative mouse is similar to comparably fed apoE-deficient mice; however, plasma cholesterol levels are half that noted for the apoE-deficient mice and there is greater variability in the latter mouse model [82]. Thus, both the apoE and LDL receptor-deficient mice are viable small animal models for the evaluation of atherosclerotic lesion progression.

The utility of apoE and LDL receptor-deficient mice for the evaluation of antiatherosclerotic agents has yet to be determined. Few studies have been reported which utilize these mice in drug intervention studies. The antioxidant, N,N'-diphenyl 1,4-phenylenediamine (DPPD) Fig. (3) (21) has been evaluated in apoE-deficient mice fed along with a 0.15% cholesterol diet for 6 months and was found to reduce the extent of aortic atherosclerosis by 36%, i.e., control - 22%; DPPD (21) - 14% lesion coverage [85]. In contrast, probucol Fig. (3) (20), another antioxidant with hypolipidemic properties, accelerated the development of atherosclerosis in apoE-deficient mice irrespective of whether the compound was administered in a chow or cholesterol containing diet and despite lowering plasma cholesterol level [86]. Such paradoxical observations raise an important issue relating to interpretation of the results of drug intervention studies in genetically derived mouse models. One must question the appropriateness of the model for testing the specific compound of interest. For instance, unlike the LDL receptor-negative mouse that is a model of a naturally occurring abnormality, i.e., familial hypercholesterolemia, apoE-deficient mice possess a specific genetic deletion of an apolipoprotein that may be necessary for reverse-cholesterol transport. One can argue that if a compound's antiatherosclerotic activity is mediated through apoE metabolism such a mouse model would be inappropriate for assessing the compound's activity.

Numerous other transgenic mouse models have been developed. A few transgenic mouse models of potential relevance to atherosclerosis from the perspective of lipoprotein metabolism are the human apolipoprotein B [87], apolipoprotein (a) [88], Lp(a) [89,90] and cholesteryl ester transfer protein (CETP) [91] transgenic models. In addition, one might predict that site specific deletions or overexpression of pro-atherosclerotic molecules such as adhesion molecules, growth factors, cytokines or integrins, for example, would be useful models for the assessment of direct acting antiatherosclerotic agents. A caveat to such an approach is exemplified by the comparison of the apoE- and LDL receptor-deficient mice. Both genetic defects resulted in a similar atherosclerotic lesion pathology and required some degree of hypercholesterolemia. Therefore, temporal evaluations of lesion development in the presence and absence of pharmacologic agents may be more informative in assessing whether the specific gene product/defect exacerbates disease progression and

whether pathologic redundancies limit the efficacy of the specific pharmacologic entity.

## Pharmacologic Intervention Studies

### ACAT

Acyl-CoA:cholesterol O-acyltransferase (ACAT) is the primary enzyme responsible for the esterification of cholesterol in all mammalian cells, but under conditions of excessive cholesterol accumulation in the vascular wall, ACAT may be responsible for the generation of the hallmark of atherosclerosis, namely, the monocyte-macrophage foam cell. Since ACAT and cholesterol esterification may be considered a pro-atherogenic event, we and others have hypothesized that inhibition of arterial wall ACAT may prevent the formation of the macrophage-enriched fatty streak and the development of the clinically significant fibrous plaque. In addition, given the observations that monocyte-macrophages are localized to the potentially friable shoulder regions of atherosclerotic lesions and in association with matrix degrading enzymes, one might speculate that by limiting the accumulation of monocyte-macrophages through inhibition of ACAT one would promote the development of a stable plaque morphology.

Several inhibitors of ACAT have been evaluated in animals and they have been found to be antiatherosclerotic by measuring changes in lesion extent and/or cholesteryl ester enrichment. Schaffer and coworkers [92] reported that administration of CL277082 Fig. (1) (3) to rabbits for 16 weeks after a 10-week lesion induction phase resulted in a 49% reduction in aortic cholesteryl ester content. Cyclandalate Fig. (1) (4), a relatively weak inhibitor ( $IC_{50} = 80$  (M) with an unknown mechanism of inhibition [93] was shown to blunt the increase in aortic total cholesterol content when given to rabbits in a low-cholesterol chow diet after a lesion induction phase [94]. A more specific and potent inhibitor of ACAT, namely, RP-70676 Fig. (1) (5), administered in a similar manner as cyclandalate (4), was reported to decrease aortic free and esterified cholesterol content by 27 to 42% [95]. In addition, melinamide [96,97] Fig. (1) (6) and the furobenzochromene Fig. (1) (7) reported by Gammill et al. [98] were shown to prevent lesion formation in cholesterol-fed rabbits. Kimura and colleagues have also reported that a series of phenylureas Fig. (1) (8, 9, 10) limited the progression of aortic atherosclerotic lesions in the rabbit [99,100]. Other potent and systemically bioavailable inhibitors of ACAT, namely, E5324 [101] Fig. (1)(11) and FR145237 [102] Fig. (1)(12), significantly inhibited the progression and cholesterol enrichment of aortic atherosclerosis in rabbits. CI-976 Fig. (1)(2), a potent, systemically bioavailable inhibitor of ACAT was evaluated in hypercholesterolemic Yucatan micropigs and was noted to prevent the formation of atherosclerotic lesions [65]. Despite achieving plasma CI-976 (2) levels of 9 to 52 times the  $IC_{50}$  for inhibition of ACAT in mouse peritoneal macrophages, an accepted *in vitro* model of foam cell formation, one was left to conclude in this model that the antiatherosclerotic activity of the compound may be related to reductions in plasma VLDL-cholesterol since the antiatherosclerotic activity was highly correlated with plasma VLDL-cholesterol levels. Therefore, given the fact that in each of the studies cited above plasma total cholesterol levels were reduced in the animal models to the same extent or greater than



animals switched to a chow, low cholesterol diet, classification of these compounds as direct acting antiatherosclerotic agents is difficult.

Direct inhibition of arterial wall ACAT with a potent, systemically bioavailable agent although much harder to discern both preclinically and clinically may provide a greater vascular benefit than can be achieved by plasma cholesterol lowering alone. The ACAT inhibitor, CI-976 Fig. (1)(2), a fatty acid amide, was evaluated in a cholesterol-fed rabbit model of atherosclerosis at a dose that was bioavailable but did not lower plasma total cholesterol [39]. CI-976 (2) prevented the accumulation of monocyte-macrophages within a preestablished fibrofoamy lesion, attenuated the development of thoracic aortic fatty streak-like lesions and decreased the cholesteryl ester enrichment of the developed lesions. We have also reported that two isoxazoles Fig. (1)(13, 14) which were bioavailable based on a bioassay designed to assess plasma ACAT inhibitory bioequivalents limited the development of thoracic aortic foamy lesions but were inactive in the more fibroproliferative femoral lesions of the rabbit [103]. Others have also reported that in Watanabe heritable hyperlipidemic (WHHL) rabbits, a model of familial hypercholesterolemia lacking the LDL receptor, E5324 [104] Fig. (1)(11) and FR145237 [102] Fig. (1)(12) can limit the development of atherosclerotic lesions in the thoracic and coronary arteries in the absence of plasma cholesterol lowering. Kogushi et al. [104] have also shown that E5324 (11) markedly reduced aortic ACAT activity; however, such a decrease may be related to the reduction in lesion and macrophage extent and not a representation of direct arterial wall ACAT inhibition. Considering the data with CI-976 (2), E5324 (11) and FR145237 (12), one can conclude that ACAT inhibition has the potential to limit atherosclerosis progression by specifically affecting vascular monocyte-macrophage accumulation. However, it is also quite apparent from the various studies cited above that the experimental protocols can be quite varied.

The animal experimental protocols can be classified into several major categories. Firstly, compounds were administered either at the initiation of dietary cholesterol supplementation and the animals were necropsied after 2 to 4 months of treatment. These studies are often termed progression studies in that the effect of the compound on monocyte-macrophage accumulation or generation of Type I to Type III lesions is being studied. However, the hypocholesterolemic activity of the compounds limits the assessment of direct antiatherosclerotic activity. Secondly, compounds were given after a degree of hypercholesterolemia and atherosclerotic lesion development has been established. In most cases, animals were fed a cholesterol diet for 8 to 10 weeks and administered the various compounds either in the same cholesterol diet or a chow diet for an additional 6 to 8 weeks. Such studies can assess whether compounds can limit the further progression of a preestablished lesion and/or promote lesion regression. The ability to study lesion regression is often lost because few studies randomize animals based on their plasma total cholesterol and necropsy a group prior to drug intervention in order to assess the type, extent and composition of the lesions. Under these regression paradigms the antiatherosclerotic activity of the compound is best assessed when compared to either a group of animals switched to a chow diet or administered a cholesterol absorption inhibitor such as cholestyramine Fig. (5)(24) in order to match the degree of cholesterol lowering. Despite the extended period

of hypercholesterolemia such rabbit models are still representative of early fibrofoamy lesions (Type I-III) and not a reflection of the more advanced Type IV-V fibrous plaques. Thirdly, WHHL rabbits that appear refractory to plasma cholesterol lowering caused by ACAT inhibition can be used to assess a compound's antiatherosclerotic activity. The WHHL may be a very good model for the assessment of ACAT inhibitors in that plasma total and lipoprotein cholesterol levels remain relatively constant following treatment and more advanced atherosclerotic fibrous plaque lesions may develop in the long-term. Fourthly, as reported for CI-976 (2), a combination of chronic endothelial injury and cholesterol feeding in either a progression or regression paradigm can allow one to not only assess the development and regression of atherosclerotic lesions but also determine whether the compounds have an effect on the cellular composition of a defined, well-characterized lesion with a greater than 99% incidence of occurrence. Finally, models of more advanced atherosclerosis can also be developed and used to assess whether ACAT inhibitors can limit the formation or promote the more rapid development of advanced fibrous plaques. Rabbits exposed to chronic endothelial injury within one week of study initiation and sequentially fed a cholesterol, fat diet for 9 weeks, a fat only diet for 6 weeks and various compounds for 8 additional weeks has allowed us to develop advanced fibrous plaques in the rabbit within 23 weeks and to further address the benefit of ACAT inhibitors. Therefore, numerous models have been developed specifically for testing the direct antiatherosclerotic activity of ACAT inhibitors; however, our conclusions ascribing the activity of the compound to direct inhibition of arterial ACAT is still based on circumstantial evidence.

Numerous *in vitro*, biochemical and pharmacokinetic studies have been performed in order to relate plasma drug levels with the compound's  $IC_{50}$  for macrophage ACAT inhibition. The basis for claiming that an ACAT inhibitor is directly antiatherosclerotic appears to be rooted in the concept that if plasma drug levels are maintained above the  $IC_{50}$  for inhibition of macrophage ACAT and plasma total and lipoprotein cholesterol levels are unchanged then the compound has direct antiatherosclerotic properties. One assumes that the compound at steady state will partition into the various atherosclerotic lesions and inhibit macrophage ACAT. Direct measurement of arterial wall ACAT and vessel drug levels have been performed [104]. Given the observations that ACAT inhibitors limit arterial wall macrophage enrichment, i.e., a source of arterial ACAT, one must be cautious in interpreting a reduction in arterial wall ACAT activity as evidence for direct ACAT inhibition. A more plausible explanation is that there is a decrease in the amount of ACAT enzyme due to a reduction in macrophage accumulation. Standardization of atherosclerotic lesion size and cellular composition prior to acute administration of the ACAT inhibitor and assessment of ACAT activity may provide more definitive proof of direct arterial wall ACAT inhibition. However, an absence of ACAT inhibition may be misleading in that during the microsome isolation procedures compounds may be diluted out of the sample. Quantification of vessel drug levels is not only problematic and their accuracy can be questioned for the same reasons as noted above for the measurement of ACAT activity but also drug extraction efficiency and metabolism become an issue. Although still circumstantial another marker of arterial ACAT inhibition is the cholesteryl ester content of the vessel wall under comparable

levels of plasma total cholesterol exposure and atherosclerotic lesion/macrophage extents.

### HMG-CoA Reductase Inhibitors

3-hydroxy-3-methylglutaryl coenzyme A reductase (HMG-CoA reductase), in addition to being the rate limiting enzyme in the cholesterol biosynthetic pathway, is involved in the regulation of receptors for LDL-cholesterol [105]. In experimental animals [106], and patients with heterozygous familial hypercholesterolemia [107] inhibition of hepatic HMG-CoA reductase leads to an increased number of LDL receptors on the cell surface, which ultimately results in an enhanced clearance of plasma LDL and a reduction in plasma total cholesterol levels. However, in nonfamilial hypercholesterolemic and familial combined hyperlipidemic patients, HMG-CoA reductase inhibitors lower plasma cholesterol by inhibiting lipoprotein production [108]. Reductions in plasma total cholesterol of over 30% and in LDL-cholesterol of 40% have been observed in clinical trials with various doses of atorvastatin [109] Fig. (2)(16), lovastatin [110] Fig. (2)(15), pravastatin [111] Fig. (2)(17), and simvastatin [112] Fig. (2)(18). In addition, the recent Scandinavian Simvastatin Survival Study (4S) [113] has shown that lowering plasma cholesterol by 35% with diet and simvastatin (18) significantly reduces the risk of mortality by 30%, coronary heart disease mortality by 42%, and incidence of nonfatal myocardial infarction by 37%. The West of Scotland Study (WOSCOPS) has demonstrated that lowering plasma LDL-cholesterol by 26% with diet and pravastatin (17) significantly reduced the risk of mortality from definite coronary events by 31% [114]. Thus, the data in man indicate that inhibitors of HMG-CoA reductase by reducing plasma cholesterol may limit the development of atherosclerosis and reduce the risk of mortality.

Several animal studies have also shown that lovastatin (15) and pravastatin (17) can attenuate atherosclerotic lesion development when plasma total and LDL-cholesterol are reduced [115-118], and that atorvastatin (16) can limit lesion development independent of changes in plasma cholesterol [119]. Due to the potent hypolipidemic activity of HMG-CoA reductase inhibitors, the assessment of these compound's direct antiatherosclerotic potential in preclinical models of atherosclerosis is difficult. However, comparison of compounds with a similar plasma total cholesterol exposure may allow one to assess whether an agent has any inherent antiatherosclerotic properties. For instance, we reported that in a cholesterol-fed rabbit model of lesion progression, lovastatin (15), pravastatin (17) and atorvastatin (16) reduced plasma total cholesterol exposure over the course of the experiment by 37% to 43% [119]. Given the linear relationship between plasma cholesterol and atherosclerosis extent noted previously [120], one might expect that the degree and composition of the atherosclerotic lesions would be similar amongst the three treatment groups. Despite equal plasma cholesterol levels, pravastatin (17) and lovastatin (15) had no effect on thoracic aortic lesion extent or iliac-femoral cross-sectional lesion area. In contrast, atorvastatin (16) reduced the thoracic aortic lesion extent from 44% to 19% and iliac-femoral lesion area by 67%. Thus, we concluded that atorvastatin can directly limit atherosclerosis lesion progression.

Evaluation of the various HMG-CoA reductase inhibitors in a rabbit model of atherosclerosis lesion progression highlights the power of the experimental design in formulating an interpretation of the data. Given the fact that plasma cholesterol levels were reduced, an analysis of a subset of compounds with the same cholesterol exposure allowed one to assess their relative antiatherosclerotic activity and also ascribe the activity to a direct effect on the lesion. Establishment of the effect of lipid-lowering on atherosclerosis development is an important factor when assessing compound efficacy. Addition of control treatments such as cholestyramine Fig. (5)(24), a non-absorbable resin, or diets containing graded cholesterol contents are methods for assessing the antiatherosclerotic activity of a compound at defined plasma cholesterol levels. Reductions in lesion size, extent or composition above that predicted for a given plasma cholesterol level may indicate that the compound is directly altering a pro-atherogenic event.

Comparison of biochemical, morphologic and morphometric results may allow one to establish the consistency of the effect and to identify potential mechanisms for the observed antiatherosclerotic activity. For instance [119], not only did atorvastatin Fig. (2)(16) decrease the extent of thoracic aortic atherosclerosis but also reduced the cholesteryl ester content of the thoracic aorta, a secondary marker that is reflective of the lesion extent and composition, i.e., lipid, monocyte-macrophage enrichment. Examination of the histopathology of the atherosclerotic lesions and morphometric changes following treatment allowed one to discern potential mechanisms responsible for the observed antiatherosclerotic activity. For example, pravastatin Fig. (2)(17) had no effect on lesion or monocyte-macrophage area while atorvastatin Fig. (2)(16) reduced both parameters. One might conclude from these data that pravastatin (17) lacked sufficient plasma drug levels or did not penetrate the arterial wall and that atorvastatin (16) by directly limiting lesion size through inhibition of smooth muscle cell migration and proliferation indirectly reduced macrophage accumulation. The later hypothesis is consistent with observations made by others which indicate that HMG-CoA reductase inhibitors in tissue culture limit SMC proliferation [121-123] and migration [124] by interfering with isoprenoid synthesis [125].

Therefore, by controlling for the degree of plasma cholesterol lowering and combining multiple efficacy parameters, one might not only be able to discriminate the direct antiatherosclerotic activity of a compound from that due to plasma cholesterol lowering but also by evaluating the structure of the atherosclerotic lesions identify potential mechanisms which can be tested in vitro or in appropriate animal models.

### Anti-Oxidants and 15-Lipoxygenase Inhibitors

Steinberg and colleagues [126] have reported that oxidatively modified LDL may be important in the progression of atherosclerosis due to the observations that oxidized LDL is cytotoxic, chemotactic and chemostatic. Oxidative modification of insudant plasma lipoproteins is presumably an extracellular event [126] and the resulting oxidized lipoproteins have been implicated in the regulation of chemokines [127] and pro-atherogenic adhesion molecules [128]. Both apolipoprotein B [129-132], the major protein in LDL, and lipid peroxides have been localized to atherosclerotic lesions [133]. Oxidatively

modified LDL or such oxidation products as malondialdehyde-conjugated LDL or 4-hydroxynonenal-conjugated LDL have been localized to WHHL rabbits [134-136]. Thus, one can conclude that oxidation of lipoproteins may be important in the development of atherosclerosis and that general antioxidants may be antiatherosclerotic in both man and models of atherosclerosis.

Several studies investigating the antiatherosclerotic activity of general antioxidants have been performed in New Zealand white rabbits [137-140], WHHL rabbits [141,142], pigs [143] and monkeys [76] under a variety of experimental conditions. In cholesterol-fed rabbits, butylated hydroxytoluene (BHT) Fig. (3)(22), vitamins E plus C, vitamins E plus A and probucol Fig. (3)(20) limited the development of thoracic aortic lesions [137-140, 144-146]. Probuco (20) has been shown by numerous individuals to reduce the extent, cholesterol enrichment and cross-sectional lesion size of atherosclerotic lesions in WHHL rabbits [141,142], balloon-injured normocholesterolemic pigs [143] and hypercholesterolemic monkeys [76]. Close examination of the lesion histopathology revealed that probucol (20) reduced the extent of atherosclerosis by decreasing the abundance of monocyte-macrophages within the lesion [146]. Mechanistic studies in rabbits fed cholesterol for a short time period, i.e., 5 wks, indicated that probucol (20) can limit the adhesion of monocytes to the endothelial cell surface. The single study in coronary artery balloon-injured pigs also indicated that probucol (20) can limit the development of primarily fibroproliferative lesions through presumably affecting SMC migration and proliferation [143]. Thus, one can conclude that antioxidants and specifically, probucol (20), can limit the development and cellular composition of atherosclerotic lesions in various animal models of atherosclerosis irrespective of whether the compound was administered to animals with or without pre-established lesions.

In most of the studies noted above, plasma cholesterol lowering was minimal so attempts to identify surrogate markers of vascular efficacy of the various antioxidants were made. Resistance of lipoproteins to oxidation was a major surrogate marker used by most investigators [141,142]. Measurements of vascular reactivity were also made [147,148]. In hypercholesterolemic rabbits, probucol (20) treatment preserved endothelial function and vascular rings upon exposure to acetylcholine in organ culture were shown to relax normally [147]. The improved vascular responsiveness is quite remarkable and one can conclude that antioxidants may improve vascular function; however, while in both studies plasma total cholesterol levels were relatively constant among the control and probucol-treated (20) groups, one study [148] reported that the cholesterol content of vessels from the drug-treated group was reduced. Since atherosclerosis is comprised of multiple stages and drugs such as probucol (20) can alter the type as well as cellular and lipid composition of the atherosclerotic lesions, correlation of pathology with functional changes is important in the assessment of drug efficacy. Experimental protocols can be designed to assess the inherent activity of compounds to promote vasorelaxation. Given the observation that some agents lower plasma or vascular cholesterol levels, administration of agents to normocholesterolemic animals or atherosclerotic animals where plasma cholesterol levels are normalized by diet may allow one to assess whether the compound has a direct effect on vascular relaxation either in the presence or absence of underlying disease.

Based on the pathology data and the localization of epitopes of oxidized LDL within the arterial wall, one can suggest that general antioxidants may be useful antiatherosclerotic agents. However, specific inhibitors of the oxidation process may allow one to target a specific pro-atherogenic process and to better characterize the compound's activity in models of atherosclerosis. A new enzyme specific target, namely arachidonate 15-lipoxygenase (15-LO), has emerged [149]. Arachidonate 15-lipoxygenase is a lipid-peroxidizing enzyme that is also present in atherosclerotic lesions. Investigators have found the 15-LO gene [150], stereospecific products of the 15-LO enzyme [151] and coincident localization of 15-LO mRNA, protein and epitopes of oxidized LDL within macrophage-rich areas of atherosclerotic lesions [149]. We have identified a specific inhibitor of 15-LO, namely, PD146176 Fig. (3)(19), and have evaluated the compound in several models of atherosclerosis [152,153].

Evaluation of PD146176 (19) in the hypercholesterolemic rabbit under three specific experimental paradigms has allowed us to conclude that in the absence of lowering plasma total and lipoprotein cholesterol levels PD146176 (19) can attenuate the development of diet induced atherosclerotic lesions through specific inhibition of monocyte-macrophage accumulation. In addition, PD146176 (19) can limit the development and macrophage enrichment of pre-established atherosclerotic lesions. PD146176 (19) administered to rabbits coincident with a cholesterol diet reduced the gross extent of foamy lesions (Type I-III lesions) within and cholesterol enrichment of the thoracic and abdominal aorta [152]. PD146176 (19) administered to rabbits coincident with a cholesterol diet and induction of a chronic endothelial injury not only reduced the progression of foamy thoracic lesions but also specifically limited the accumulation of monocyte-macrophages within a fibrofoamy iliac-femoral lesion without affecting the overall lesion size [153]. PD146176 (19) administered after establishment of fibrofoamy Type IV lesions through a combination of chronic endothelial injury and dietary cholesterol supplementation reduced the extent, cross-sectional area and monocyte-macrophage content of the more advanced Type V fibrous plaque [153]. In all three studies, assessment of plasma total and lipoprotein levels, vascular lipid content and histologic evidence for the presence of 15-LO in the lesions were necessary to corroborate the findings and maintain the implication that 15-LO was involved. Thus, these data highlight the antiatherosclerotic potential of a specific 15-LO inhibitor.

The brief summary of the antiatherosclerotic effects of PD146176 (19) can also be used to exemplify the power of the animal models of atherosclerosis. The simplest model, a rabbit fed a 0.25% cholesterol, 3% peanut, 3% coconut oil diet illustrated that the compound can prevent the formation of cholesteryl ester enriched Type III foamy atherosclerotic lesions. One might propose that evaluation of rabbits fed cholesterol for shorter periods of time would allow one to assess whether the observed antiatherosclerotic activity was due to reduced monocyte adherence. In the second rabbit model, induction of a fibrofoamy lesion by chronic endothelial injury allowed one to build upon the first observation and suggest that the compound specifically limited monocyte-macrophage accumulation because the absolute lesion cross-sectional area was unchanged. In the most complex model, one was able to assess whether PD146176 (19) could limit the progression of the disease to a fibrous plaque or promote regression of a

preestablished fibrofoamy lesion. In addition, one can obtain such mechanistic information as to the involvement of 15-LO in advanced atherosclerosis and whether further monocyte-macrophage enrichment can be blunted.

## Conclusions

Atherosclerotic lesion development can be divided into six histologically distinct stages and five dynamic phases. Specifically, atherosclerotic lesion progression in man involves episodes of SMC proliferation, extracellular matrix deposition and remodeling, lipid infiltration, endothelial cell-monocyte interactions, monocyte migration into the intima, monocyte-macrophage foam cell formation, necrotic lipid-rich core formation, calcium deposition, neovascularization, mural microthrombi and occlusive acute thrombosis. Given the complexity of atherosclerotic lesion development in man, the challenge exists to develop animal models that closely mimic the human disease. One must accept, however, that there is no one perfect animal model that completely replicates the stages of human atherosclerosis but that the models are useful in studying specific pathologic processes associated with the disease. Hypercholesterolemic rabbits either with or without endothelial injury are valuable models and the most widely used model for the evaluation of pharmacologic agents. Five types of human-like atherosclerotic lesions can be induced in the rabbit; however, the model is limited in that evidence of the plaque rupture cannot be found. Hypercholesterolemic hamsters are a model of an early pro-atherogenic event, namely, subendothelial monocyte-macrophage foam cell formation. Swine are a useful model for the evaluation of atherosclerosis from the perspective that lesions develop spontaneously, their circulatory system and localization of lesions are similar to man and the lesions are responsive to dietary intervention by exhibiting regression after prolonged periods. Non-human primates have often been portrayed as ideal models of human atherosclerosis due to their close phylogenetic association to man; however, lesions of comparable character to man can be induced more efficiently and over shorter time periods in swine and in some cases rabbits through a combination of hypercholesterolemia and endothelial injury. Numerous transgenic mouse models have been developed in recent years. A common finding among the various mouse models of atherosclerosis is that a similar atherosclerotic lesion pathology develops and all require some degree of hypercholesterolemia. Therefore, temporal evaluations of lesion development in the presence and absence of pharmacologic agents may be more informative in assessing whether the specific gene product/defect exacerbates disease progression and whether pathologic redundancies limit the efficacy of the specific pharmacologic entity. Based on evaluation of the various animal models and pharmacologic agents, one can conclude that: (1) each animal model provides insight into specific aspects of the disease process; (2) a hypercholesterolemic state is required in all models for the development of atherosclerosis; (3) discrimination of the *direct* antiatherosclerotic activity of a compound from its *indirect* activity requires one to limit the number of confounding factors, e.g., hypocholesterolemic and antihypertensive effect; (4) combination of biochemical, morphologic and morphometric measures allows one to both validate the antiatherosclerotic effect and define potential mechanisms; (5) reducing monocyte-macrophage involvement irrespective of mechanism or animal

model effectively limits the development of atherosclerotic lesions.

## Abbreviations

ACAT	=	Acyl-coenzyme A:cholesterol O-acyltransferase
HMG-CoA reductase	=	3-Hydroxy-3-methylglutaryl coenzyme A
15-LO	=	15-Lipoxygenase
SMC	=	Smooth muscle cells
VCAM-1	=	Vascular cell adhesion molecule-1
VLDL	=	Very low density lipoproteins
LDL	=	Low density lipoproteins
WHHL	=	Watanabe heritable hyperlipidemic rabbit
ACE	=	Angiotensin converting enzyme
MABP	=	Mean arterial blood pressure
ApoE	=	Apolipoprotein E
CETP	=	Cholesteryl ester transfer protein
4S	=	Scandinavian Simvastatin Survival Study
WOSCOP	=	The West of Scotland Study

## Acknowledgement

I would like to thank Dr. D. Robert Sliskovic for his kind invitation to write this article and for his help in preparation of the figures depicting chemical structures of the compounds cited in the manuscript.

## References

- [1] Tracy, R.E. *Lab. Invest.*, 1979, 41, 546.
- [2] Constantinides, P. J. *Ultrastruct. Res.*, 1966, 6, 1.
- [3] Ridolfi, R.L.; Hutchins, G.M. *Am. Heart J.*, 1977, 93, 468.
- [4] Cornhill, J.F.; Herderick, E.E.; Stary, H.C. *Monogr. Atheroscler.*, 1990, 15, 13.
- [5] Cornhill, J.F.; Barrett, W.A.; Herderick, E.E.; Mahley, R.W.; Fry, D.L. *Arterioscler.*, 1985, 5, 415.
- [6] Stary, H.C.; Chandler, A.B.; Glagov, S.; Guyton, J.R.; Insull, W. Jr.; Rosenfeld, M.E.; Schaffer, S.A.; Schwartz, C.J.; Wagner, W.D.; Wissler, R.W. *Circ.*, 1994, 89, 2462.
- [7] Fuster, V. *Circ.*, 1994, 90, 2126.
- [8] Smith, E.B.; Evans, P.H.; Downham, M.D. *J. Atheroscler. Res.*, 1967, 7, 171.
- [9] Kume, N.; Cybulsky, M.I.; Gimbrone, M.A. *J. Clin. Invest.*, 1992, 90, 1138.
- [10] Cybulsky, M.I.; Gimbrone, M.A. *Science*, 1991, 252, 788.

- [11] Krause, B.R.; Sliskovic, D.R.; Bocan, T.M.A. *Exp. Opin. Invest. Drugs*, 1995, 4, 353.
- [12] Anitschkow, N. *Beitr. Pathol. Anat. Allgem. Pathol.*, 1913, 56, 379.
- [13] Jokinen, M.P.; Clarkson, T.B.; Prichard, R.W. *Exp. Mol. Pathol.*, 1985, 42, 1.
- [14] Prior, J.T.; Kurtz, D.M.; Ziegler, D.D. *Arch. Pathol.*, 1961, 71, 672.
- [15] Kroon, P.A.; Thompson; Chao, Y. *Atherosclerosis*, 1985, 56, 323.
- [16] Prior, J.T.; Kurtz, D.M.; Ziegler, D.D. *Arch. Pathol.*, 1961, 71, 82.
- [17] Kritchevsky, D.; Tepper, S.A.; Vesselinovitch, D.; Wissler, R.W. *Atherosclerosis*, 1971, 14, 53.
- [18] Kritchevsky, D.; Tepper, S.A.; Kim, H.K.; Story, J.A.; Vesselinovitch, D.; Wissler, R.W. *Exp. Molec. Pathol.*, 1976, 24, 375.
- [19] Ho, K.J.; Pang, L.C.; Taylor, C.B. *Atherosclerosis*, 1974, 19, 561.
- [20] Ross, A.C.; Minick, C.R.; Zilversmit, D.B. *Atherosclerosis*, 1978, 29, 301.
- [21] Mahley, R.W.; Innerarity, T.L.; Rall, S.C. Jr; Weisgraber, K.H. *Ann. NY Acad. Sci.*, 1985, 454, 209.
- [22] Wilson, R.B.; Miller, R.A.; Middleton, C.C.; Kinden, D. *Arterioscler.*, 1982, 2, 228.
- [23] Constantinides, P.; Booth, J.; Carlson, G. *Arch. Pathol.*, 1960, 70, 712.
- [24] Constantinides, P. *J. Atherosclerosis Res.*, 1961, 1, 374.
- [25] Daley, S.J.; Herderick, E.E.; Cornhill, F.; Rogers, K.A. *Arterioscler. Thromb.*, 1994, 14, 95.
- [26] Daley, S.J.; Klemp, K.F.; Guyton, J.R.; Rogers, K.A. *Arterioscler. Thromb.*, 1994, 14, 105.
- [27] Rosenfeld, M.E.; Tsukada, T.; Gown, A.M.; Ross, R. *Arterioscler.*, 1987, 7, 9.
- [28] Rosenfeld, M.E.; Tsukada, T.; Chait, A.; Bierman, E.L.; Gown, A.M.; Ross, R. *Arterioscler.*, 1987, 7, 24.
- [29] Tsukada, T.; Rosenfeld, M.; Ross, R.; Gown, A.M. *Arterioscler.*, 1986, 6, 601.
- [30] Shiomi, M.; Ito, T.; Tsukada, T.; Yata, T.; Ueda, M. *Arterioscler. Thromb.*, 1994, 14, 931.
- [31] Rosenfeld, M.E.; Chait, A.; Bierman, E.L.; King, W.; Goodwin, P.; Walden, C.E.; Ross, R. *Arterioscler.*, 1988, 8, 338.
- [32] Stadius, M.L.; Rowan, R.; Fleishhauer, J.F.; Kernoff, R.; Billingham, M.; Gown, A.M. *Arterioscler. Thromb.*, 1992, 12, 1267.
- [33] Reidy, M.A.; Harker, L.A.; Schwartz, S. *Fed. Proc.*, 1983, 42, 771.
- [34] Reidy, M.A.; Yoshida, K.; Harker, L.A.; Schwartz, S.M. *Arterioscler.*, 1986, 6, 305.
- [35] Bjorkerud, S.; Bondjers, G. *Atherosclerosis*, 1971, 13, 355.
- [36] Moore, S. *Lab. Invest.*, 1973, 29, 478.
- [37] Moore, S.; Friedman, R.J.; Singal, D.P.; Gaudie, J.; Blajchman, M.A.; Roberts, R.S. *Thrombos. Haemostasis (Stuttgart)*, 1976, 35, 70.
- [38] Bocan, T.M.A.; Bak Mueller, S.; Uhlendorf, P.D.; Ferguson, E.; Newton, R.S. *Exp. Molec. Pathol.*, 1991, 54, 201.
- [39] Bocan, T.M.A.; Bak Mueller, S.; Uhlendorf, P.D.; Newton, R.S.; Krause, B.R. *Arterioscler. Thromb.*, 1991, 11, 1830.
- [40] Friedman, M.; Byers, S.O. *Am. J. Pathol.*, 1963, 43, 349.
- [41] Nistor, A.; Bulla, A.; Filip, D.A.; Radu, A. *Atherosclerosis*, 1987, 68, 159.
- [42] Foxall, T.L.; Shwaery, G.T.; Stucchi, A.F.; Nicolosi, R.J.; Wong, S.S. *Am. J. Pathol.*, 1992, 140, 1357.
- [43] Kowala, M.C.; Nunnari, J.J.; Durham, S.K.; Nicolosi, R.J. *Atherosclerosis*, 1991, 91, 35.
- [44] Otto, J.; Ordovas, J.M.; Smith, D.; van Dongen, D.; Nicolosi, R.J.; Schaefer, E.J. *Atherosclerosis*, 1995, 114, 19.
- [45] Kowala, M.C.; Grove, R.I.; Aberg, G. *Atherosclerosis*, 1994, 108, 61.
- [46] Kowala, M.C.; Recce, R.; Beyer, S.; Aberg, G. *J. Cardiovascular Pharm.*, 1995, 25, 179.
- [47] Kowala, M.C.; Mazzucco, C.E.; Hartl, K.S.; Seiler, S.M.; Warr, G.A.; Abid, S.; Grove, R.I. *Arterioscler. Thromb.*, 1993, 13, 435.
- [48] Kowala, M.C.; Rose, P.M.; Stein, P.D.; Goller, N.; Recce, R.; Beyer, S.; Valentine, M.; Barton, D.; Durham, S.K. *Am. J. Pathol.*, 1995, 146, 819.
- [49] Gottlieb, H.; Lalich, J.J. *Am. J. Pathol.*, 1954, 30, 851.
- [50] Moreland, A.F.; Clarkson, T.B.; Lofland, H.B. *Arch. Pathol.*, 1963, 76, 99.
- [51] French, J.E.; Jennings, M.A.; Florey, H.W. *Ann. N.Y. Acad. Sci.*, 1965, 127, 780.
- [52] Reitman, J.S.; Mahley, R.W.; Fry, D.L. *Atherosclerosis*, 1982, 43, 119.
- [53] Nam, S.C.; Lee, W.M.; Jarmolych, J.; Lee, K.T.; Thomas, W.A. *Exp. Molec. Pathol.*, 1973, 18, 369.
- [54] Lee, W.M.; Lee, K.T. *Exp. Molec. Pathol.*, 1975, 23, 491.
- [55] Fritz, K.E.; Daoud, A.S.; Augustyn, J.M.; Jarmolych, J. *Exp. Molec. Pathol.*, 1980, 32, 61.
- [56] Dov Gal, D.V.M.; Rongione, A.J.; Slovenkai, G.A.; DeJesus, S.T.; Lucas, A.; Fields, C.D.; Isner, J.M. *Am. Heart J.*, 1990, 119, 291.
- [57] Rapacz, J.; Hasler-Rapacz, J.; Taylor, K.M.; Checovich, W.J.; Attie, A.D. *Science*, 1986, 234, 1573.
- [58] Lowe, S.W.; Checovich, W.J.; Rapacz, J.; Attie, A.D. *J. Biol. Chem.*, 1988, 263, 15467.
- [59] Checovich, W.J.; Fitch, W.L.; Krauss, R.M.; Smith, M.P.; Rapacz, J.; Smith, C.L.; Attie, A.D. *Biochem.*, 1988, 27, 1934.
- [60] Prescott, M.F.; McBride, C.H.; Hasler-Rapacz, L.; Von-Linden, J.; Rapacz, J. *Am. J. Pathol.*, 1991, 139.



- [61] Detweiler, D.K.; Ratcliffe, H.L.; Luginbuhl, H. *Ann. N. Y. Acad. Sci.*, 1968, 149, 868.
- [62] Reddick, R.L.; Read, M.S.; Brinkhous, K.M.; Bellinger, D.; Nichols, T.; Griggs, T.R. *Arterioscler.*, 1990, 10, 541.
- [63] Daoud, A.S.; Jarmolych, J.; Augustyn J.M.; Fritz, K.E.; Singh, J.K.; Lee, K.T. *Arch. Pathol. Lab. Med.*, 1976, 100, 372.
- [64] Fritz, K.E.; Augustyn, J.M.; Jarmolych, J.; Daoud, A.S.; Lee, K.T. *Arch. Pathol. Lab. Med.*, 1976, 100, 380.
- [65] Bocan, T.M.A.; Bak Mueller, S.; Uhlendorf, P.D.; QuenbyBrown, E.; Mazur, M.J.; Black, A.E. *Atherosclerosis*, 1993, 99, 175.
- [66] Charpiot, P.; Rolland, P.H.; Friggi, A.; Piquet, P.; Scalbert, E.; Bodard, H.; Barlatier, A.; Latrille, V.; Tranier, P.; Mercier, C.; Luccioni, R.; Calaf, R.; Garcon, D. *Arterioscler. Thromb.*, 1993, 13, 1125.
- [67] Small, D.M.; Bond, M.G.; Waugh, D.; Prack, M.; Sawyer, J.K. *J. Clin. Invest.*, 1984, 73, 1590.
- [68] Stary, H.C.; Malinow, M.R. *Atherosclerosis*, 1982, 43, 151.
- [69] Kramsch, D.M.; Hollander, W. *Expt. Molec. Pathol.*, 1968, 9, 1.
- [70] DePalma, R.G.; Klein, L.; Bellon, E.M.; Koletsky, S. *Arch. Surg.*, 1980, 115, 1268.
- [71] Hoover, G.A.; Nicolosi, R.J.; Camp, R.R.; Hayes, K.C. *Arterioscler.*, 1982, 2, 252.
- [72] Masuda, J.; Ross, R. *Arterioscler.*, 1990, 10, 164.
- [73] Masuda, J.; Ross, R. *Arterioscler.*, 1990, 10, 178.
- [74] Faggiotto, A.; Ross, R.; Harker, L. *Arterioscler.*, 1984, 4, 323.
- [75] Faggiotto, A.; Ross, R. *Arterioscler.*, 1984, 4, 341.
- [76] Wissler, R.W.; Vesselinovitch, D. *Appl. Pathol.*, 1983, 1, 89.
- [77] Paigen, B.; Ishida, B.Y.; Verstuyft, J.; Winters, R.B.; Albee, D. *Arterioscler.*, 1990, 10, 316.
- [78] Plump, A.S.; Smith, J.D.; Hayek, T.; Aalto-Setälä, K.; Walsh, A.; Verstuyft, J.G.; Rubin, E.M.; Breslow, J.L. *Cell*, 1992, 71, 343.
- [79] Reddick, R.L.; Zhang, S.H.; Maeda, N. *Arterioscler. Thromb.*, 1994, 14, 141.
- [80] Nakashima, Y.; Plump, A.S.; Raines, E.W.; Breslow, J.L.; Ross, R. *Arterioscler. Thromb.*, 1994, 14, 133.
- [81] Ishibashi, S.; Goldstein, J.L.; Brown, M.S.; Herz, J.; Burns, D.K. *J. Clin. Invest.*, 1994, 93, 1885.
- [82] Tangirala, R.K.; Rubin, E.M.; Palinski, W. *J. Lipid Res.*, 1995, 36, 2320.
- [83] Mahley, R.W. *Science*, 1988, 240, 622.
- [84] Brown, M.S.; Goldstein, J.L. *Science*, 1986, 232, 4.
- [85] Tangirala, R.K.; Casanada, F.; Miller, E.; Witzum, J.L.; Steinberg, D.; Palinski, W. *Arterioscler. Thromb. Vasc. Biol.*, 1995, 15, 1625.
- [86] Zhang, S.H.; Reddick, R.L.; Avdievich, E.; Surles, L.K.; Jones, R.G.; Reynolds, J.B.; Quarfordt, S.H.; Maeda, N. *J. Clin. Invest.*, 1997, 99, 2858.
- [87] Purcell-Huynh, D.A.; Farese, R.V., Jr.; Johnson, D.F.; Flyna, L.M.; Pierotti, V.; Newland, D.L.; Linton, M.F.; Sanan, D.A.; Young, S.G. *J. Clin. Invest.*, 1995, 95, 2246.
- [88] Lawn, R.M.; Wade, D.P.; Hammer, R.E.; Chiesa, G.; Verstuyft, J.G.; Rubin, E.M. *Nature*, 1992, 360, 670.
- [89] Mancini, F.P.; Newland, D.L.; Mooser, V.; Murata, J.; Marcovina, S.; Young, S.G.; Hammer, R.E.; Sanan, D.A.; Hobbs, H.H. *Arterioscler. Thromb. Vasc. Biol.*, 1995, 15, 1911.
- [90] Callow, M.J.; Verstuyft, J.; Tangirala, R.; Palinski, W.; Rubin, E.M. *J. Clin. Invest.*, 1995, 96, 1639.
- [91] Marotti, K.R.; Castle, C.K.; Boyle, T.P.; Lin, A.H.; Murray, R.W.; Melchior, G.W. *Nature*, 1993, 364, 73.
- [92] Schaffer, S.A.; Bloom, J.D.; DeVries, V.G.; Dutia, M.; Katocs, A.S. Jr.; Largis, E. In *Atherosclerosis VII*; Fidge, N.H.; Nestel, P.J., Eds; Elsevier Science Publishers B.V.: Amsterdam, 1986, pp 633-636.
- [93] Heffron, F.; Middleton, B.; White, D.A. *Biochem. Pharm.*, 1990, 39, 575.
- [94] Middleton, B.; Middleton, A.; White, D.A.; Bell, G.D. *Atherosclerosis*, 1984, 171, 171.
- [95] Ashton, M.J.; Bridge, A.W.; Bush, R.C.; Dron, D.I.; Harris, N.V.; Jones, G.D.; Lythgoe, D.J.; Riddell, D.; Smith, C. *Bioorg. Med. Chem. Lett.* 1992, 2, 375.
- [96] Fukushima, H.; Aono, S.; Nakamura, Y.; Endo, M.; Imai, T. *J. Atheroscler. Res.*, 1969, 10, 403.
- [97] Fukushima, H.; Toki, K.; Nakatani, H. *J. Atheroscler. Res.*, 1969, 9, 57.
- [98] Gammill, R.B.; Bell, F.P.; Bell, L.T.; Bisaha, S.N.; Wilson, G.J. *J. Med. Chem.* 1990, 33, 2686.
- [99] Kimura, T.; Takase, Y.; Hayashi, K.; Tanaka, H.; Ohtsuka, I.; Saeki, T.; Kogushi, M.; Yamada, T.; Fujimori, T.; Saitou, I.; Akasaka, K. *J. Med. Chem.*, 1993, 36, 1630.
- [100] Kimura, T.; Watanabe, N.; Matsui, M.; Hayashi, K.; Tanaka, H.; Ohtsuka, I.; Saeki, T.; Kogushi, M.; Kabayashi, H.; Akasaka, K.; Yamagishi, Y.; Saitou, I.; Yamatsu, I. *J. Med. Chem.*, 1993, 36, 1641.
- [101] Tanaka, H.; Ohtsuka, I.; Kogushi, M.; Kimura, T.; Fujimori, T.; Saeki, T.; Hayashi, K.; Kobayashi, H.; Yamada, T.; Hiyoshi, H.; Saito, I. *Atherosclerosis*, 1994, 107, 187.
- [102] Matsuo, M.; Ito, F.; Konto, A.; Aketa, M.; Tomoi, M.; Shimomura, K. *Biochim. Biophys. Acta*, 1995, 1259, 254.
- [103] White, A.D.; Purchase II, C.F.; Picard, J.A.; Anderson, M.K.; Bak Mueller, S.; Bocan, T.M.A.; Bousley, R.F.; Hamelchle, K.L.; Krause, B.R.; Lee, P.; Stanfield, R.L.; Reindel, J.F. *J. Med. Chem.*, 1996, 39, 3908.
- [104] Kogushi, M.; Tanaka, H.; Ohtsuka, I.; Yamada, T.; Kobayashi, H.; Saeki, T.; Takada, M.; Hiyoshi, H.; Yanagimachi, M.; Kimura, T.; Yoshitake, S.; Saito, I. *Atherosclerosis*, 1996, 124, 203.
- [105] Brown, M.S.; Goldstein, J.L. *Science*, 1986, 232, 34.

- [106] Kovanen, P.T.; Bilheimer, D.W.; Goldstein, J.L.; Jaramillo, J.J.; Brown, M.S. *Proc. Natl. Acad. Sci. USA*, 1981, 78, 1194.
- [107] Bilheimer, D.W.; Grundy, S.M.; Brown, M.S.; Goldstein, J.L. *Proc. Natl. Acad. Sci. USA*, 1983, 80, 4124.
- [108] Arad, Y.; Ramakrishnan, R.; Ginsberg, H.N. *Metabolism*, 1992, 41, 487.
- [109] Nawrocki, J.W.; Weiss, S.R.; Davidson, M.H.; Sprecher, D.L.; Schwartz, S.S.; Lupien, P.J.; Jones, P.H.; Haber, H.E.; Black, D.M. *Arterioscl. Thromb. Vasc. Biol.*, 1995, 15, 678.
- [110] Walker, J.F. *Drugs*, 1988, 36, 83.
- [111] McTavish, D.; Sorkin, E.M. *Drugs*, 1991, 42, 65.
- [112] Todd, P.A.; Goa, K.L. *Drugs*, 1990, 40, 583.
- [113] *Lancet*, 1994, 344, 1383.
- [114] Shepherd, J.; Cobbe, S.M.; Ford, I.; Isles, C.G.; Lorimer, A.R.; MacFarlane, P.W.; McKillop, J.H.; Packard, C.J. *N. Engl. J. Med.*, 1995, 333, 1301.
- [115] Kritchevsky, D.; Tepper, S.A.; Klurfeld, D.M. *Pharm. Res. Comm.*, 1981, 13, 921.
- [116] Kobayashi, M.; Ishida, F.; Takahashi, T.; Taguchi, K.; Watanabe, K.; Ohmura, I.; Kamei, T. *Jpn. J. Pharmacol.* 1989, 49, 125.
- [117] Zhu, B.Q.; Sievers, R.E.; Sun, Y.P.; Isenberg, W.M.; Parmley, W.W. *J. Cardiovas. Pharm.*, 1992, 19, 246.
- [118] Shiomi, M.; Ito, T.; Watanabe, Y.; Tsujita, Y.; Kuroda, M.; Arai, M.; Fukami, M.; Fukushima, J.; Tamura, A. *Atherosclerosis* 1990, 83, 69.
- [119] Bocan, T.M.A.; Mazur, M.J.; BakMueller, S.; QuenbyBrown, E.; Sliskovic, D.R.; O'Brien, P.M.; Creswell, M.W.; Lee, H.; Uhlendorf, P.D.; Roth, B.D.; Newton, R.S. *Atherosclerosis*, 1994, 111, 127.
- [120] Bocan, T.M.A.; BakMueller, S.; Mazur, M.J.; Uhlendorf, P.D.; QuenbyBrown, E.; Kieft, K.A. *Atherosclerosis*, 1993, 102, 9.
- [121] Corsini, A.; Mazzotti, M.; Raiteri, M.; Soma, M.; Fumagalli, R.; Paoletti, R. *XI Intl. Symp. Drugs Affecting Lipid Metabolism*, 1992, 7.
- [122] Corsini, A.; Raiteri, M.; Soma, M.; Fumagalli, R.; Paoletti, R. *Pharmacol. Res.*, 1991, 23, 173.
- [123] Falke, P.; Mattiasson, I.; Stavenow, L.; Hood, B. *Pharm. Toxicol.*, 1989, 64, 173.
- [124] Hidaka, Y.; Tomoyo, E.; Yonemoto, M.; Kamei, T. *Atherosclerosis*, 1992, 95, 87.
- [125] Corsini, A.; Bernini, F.; Quarato, P.; Donetti, E.; Bellosa, S.; Fumagalli, R.; Paoletti, R.; Soma, V.M. *Cardiology*, 1996, 87, 458.
- [126] Steinberg, D.; Parthasarathy, S.; Carew, T.E.; Khoo, J.C.; Witztum, J.L. *New Engl. J. Med.*, 1989, 320, 915.
- [127] Rajavashisth, T.B.; Andalibi, A.A.; Territo, M.C.; Berliner, J.A.; Navab, M.; Fogelman, A.M.; Lusis, A.J. *Nature*, 1990, 344, 254.
- [128] Kume, N.; Cybulsky, M.I.; Gimbrone, M.A. *J. Clin. Invest.*, 1992, 90, 1138.
- [129] Kao, C.Y.; Wissler, R.W. *Exp. Molec. Pathol.*, 1965, 4, 465.
- [130] Knieriem, H.J.; Kao, C.Y.; Wissler, R.W. *Arch. Pathol. Lab. Med.*, 1967, 84, 118.
- [131] Yomantas, S.; Elner, V.M.; Schaffner, T.; Wissler, R.W. *Arch. Pathol. Lab. Med.*, 1984, 108, 374.
- [132] Bocan, T.M.A.; Brown, S.A.; Guyton, J.R. *Arterioscler.*, 1988, 8, 499.
- [133] Glavind, J.; Hartmann, S.; Clemmeson, J.; Jessen, K.E.; Dam, H. *Acta Pathol. Microbiol. Scand.*, 1952, 3-, 1.
- [134] Boyd, H.C.; Gown, A.M.; Wolfbauer, G.; Chait, A. *Am. J. Pathol.*, 1989, 135, 815.
- [135] Haberland, M.E.; Fong, D.; Cheng, L. *Science*, 1988, 241, 215.
- [136] Palinski, W.; Rosenfeld, M.E.; Yla-Herttuala, S.; Gurtner, G.C.; Socher, S.S.; Butler, S.W.; Parthasarathy, S.; Carew, T.E.; Steinberg, D.; Witztum, J.L. *Proc. Natl. Acad. Sci. USA*, 1989, 86, 1372.
- [137] Daugherty, A.; Zweifel, B.S.; Schonfeld, G. *Br. J. Pharmacol.*, 1989, 98, 612.
- [138] Tawara, K.; Ishihara, M.; Ogawa, H.; Tomikawa, M. *Jpn. J. Pharmacol.*, 1986, 41, 211.
- [139] Stein, Y.; Stein, O.; Delplanque, B.; Fesmire, J.D.; Lee, D.M.; Alaupovic, P. *Atherosclerosis*, 1989, 75, 145.
- [140] Carew, T.E.; Schwenke, D.C.; Steinberg, D. *Proc. Natl. Acad. Sci. USA*, 1987, 84, 7725.
- [141] Daugherty, A.; Zweifel, B.S.; Schonfeld, G. *Br. J. Pharmacol.*, 1991, 103, 1013.
- [142] Kita, T.; Nagano, Y.; Yokode, M.; Ishii, K.; Kume, N.; Ooshima, A.; Kawai, C. *Proc. Natl. Acad. Sci. USA*, 1987, 84, 5928.
- [143] Schneider, J.E.; Berk, B.C.; Gravanis, M.B.; Santoian, E.C.; Cipolla, G.D.; Tarazona, N.; Lassegue, B.; King, S.B., 3<sup>rd</sup> *Circ.*, 1993, 88, 628.
- [144] Bjorkhem, I.; Henriksson-Freyschuss, A.; Breuer, O.; Diczfalusy, U.; Berglund, L.; Henriksson, P. *Arterioscler. Thromb.*, 1991, 11, 15.
- [145] Brattsand, R. *Atherosclerosis*, 1975, 22, 47.
- [146] Bocan, T.M.A.; BakMueller, S.; QuenbyBrown, E.; Uhlendorf, P.D.; Mazur, M.J.; Newton, R.S. *Expt. Molec. Pathol.*, 1992, 57, 70.
- [147] Keaney, J.F., Jr.; Xu, A.; Cunningham, D.; Jackson, T.; Frei, B.; Vita, J.A. *J. Clin. Invest.*, 1995, 95, 2520.
- [148] Del Rio, M.; Chulia, T.; Ruiz, E.; Tejerina, T. *Br. J. Pharmacol.*, 1996, 118, 1639.
- [149] Yla-Herttuala, S.; Rosenfeld, M.E.; Parthasarathy, S.; Glass, C.K.; Sigal, E.; Witztum, J.L.; Steinberg, D. *Proc. Natl. Acad. Sci. USA*, 1990, 87, 6959.
- [150] Yla-Herttuala, S. *Herz*, 1992, 17, 270.
- [151] Kuhn, H.; Belkner, J.; Zalaa, S.; Fahrenklemp, T.; Wohlfeil, S. *J. Exp. Med.*, 1994, 179, 1903.



- [152] Sendobry, S.M.; Comicelli, J.A.; Welch, K.; Bocan, T.; Tait, B.; Trivedi, B.K.; Colbry, N.; Dyer, R.D.; Feinmark, S.J.; Daugherty, A. *Br. J. Pharmacol.*, 1997, 120, 1199.
- [153] Bocan, T.M.A.; Rosebury, W.S.; BakMueller, S.; Kuchera, S.; Welch, K.; Daugherty, A.; Comicelli, J.A. *Atherosclerosis*, 1997, in press.



## Inhibition of cyclooxygenase with indomethacin phenethylamide reduces atherosclerosis in apoE-null mice

Michael E. Burleigh<sup>d,1</sup>, Vladimir R. Babaev<sup>a,1</sup>, Mayur B. Patel<sup>b</sup>, Brenda C. Crews<sup>b</sup>,  
Rory P. Remmel<sup>c</sup>, Jason D. Morrow<sup>a,d</sup>, John A. Oates<sup>a,d</sup>, Lawrence J. Marnett<sup>b</sup>,  
Sergio Fazio<sup>a,c</sup>, MacRae F. Linton<sup>a,d,\*</sup>

<sup>a</sup> Department of Medicine, Division Cardiovascular Medicine, Vanderbilt University School of Medicine,  
383 Preston Research Building, Nashville, TN 37232-6300, USA

<sup>b</sup> Department of Biochemistry, Vanderbilt University Medical Center, Nashville, TN 37232-6300, USA

<sup>c</sup> Department of Pathology, Vanderbilt University Medical Center, Nashville, TN 37232-6300, USA

<sup>d</sup> Department of Pharmacology, Vanderbilt University Medical Center, Nashville, TN 37232-6300, USA

<sup>e</sup> Department of Medicinal Chemistry, College of Pharmacy, University of Minnesota, Minneapolis, MN 55455, USA

Received 7 December 2004; accepted 14 April 2005

### Abstract

Non-selective inhibition of cyclooxygenase (COX) has been reported to reduce atherosclerosis in both rabbit and murine models. In contrast, selective inhibition of COX-2 has been shown to suppress early atherosclerosis in LDL-receptor null mice but not more advanced lesions in apoE deficient (apoE<sup>-/-</sup>) mice. We investigated the efficacy of the novel COX inhibitor indomethacin phenethylamide (INDO-PA) on the development of different stages of atherosclerotic lesion formation in female apoE<sup>-/-</sup> mice. INDO-PA, which is highly selective for COX-2 in vitro, reduced platelet thromboxane production by 61% in vivo, indicating partial inhibition of COX-1 in vivo. Treatment of female apoE<sup>-/-</sup> mice with 5 mg/kg INDO-PA significantly reduced early to intermediate aortic atherosclerotic lesion formation (44 and 53%, respectively) in both the aortic sinus and aorta en face compared to controls. Interestingly, there was no difference in the extent of atherosclerosis in the proximal aorta in apoE<sup>-/-</sup> mice treated from 11 to 21 weeks of age with INDO-PA, yet there was a striking (76%) reduction in lesion size by en face analysis in these mice. These studies demonstrate the ability of non-selective COX inhibition with INDO-PA to reduce early to intermediate atherosclerotic lesion formation in apoE<sup>-/-</sup> mice, supporting a role for anti-inflammatory approaches in the prevention of atherosclerosis.

© 2005 Elsevier Inc. All rights reserved.

**Keywords:** Atherosclerosis; Prostaglandins; Cyclooxygenase; COX inhibition; ApoE<sup>-/-</sup> mice; Aorta

### 1. Introduction

Atherosclerosis has features of an inflammatory disease and is the leading cause of death in industrialized nations [1]. Cyclooxygenase (COX) plays a key role as an inflammatory mediator in virtually all diseases involving inflammation [2]. COX exists as two isoforms, which are coded for by two separate genes [2,3]. COX-1 is found in most tissues and mediates normal physiology requiring prostaglandin production. COX-2 is induced rapidly at sites of inflammation and is expressed in atherosclerotic lesions of

humans [4,5], and mice [6] by macrophages, smooth muscle cells and endothelial cells.

Eicosanoids produced by COX-1 and COX-2 have been ascribed a variety of functions in the promotion of cardiovascular health and disease. The beneficial effect of low dose aspirin in reducing cardiovascular events has been largely attributed to inhibition of platelet thromboxane production, a COX-1 mediated process [7]. In contrast, COX-2 has been proposed to play both beneficial and deleterious roles in cardiovascular health [8–11]. Recent evidence from the Adenomatous Polyp Prevention on Vioxx (APPROVe) trial indicating that selective COX-2 inhibition with rofecoxib results in increased cardiovascular events after 18 months compared to placebo has resulted in removal of rofecoxib from the market ([www.vioxx.com](http://www.vioxx.com)). Yet studies in animal

\* Corresponding author. Tel.: +1 615 936 1656; fax: +1 615 936 1872.

E-mail address: [macrae.linton@vanderbilt.edu](mailto:macrae.linton@vanderbilt.edu) (M.F. Linton).

<sup>1</sup> These authors have contributed equally to this work.

models and humans support roles for COX-2 in promoting endothelial dysfunction [12], early atherosclerotic lesion formation [6] and plaque instability [13,14]. The dramatic removal of rofecoxib from the market highlights our need for a better understanding of the roles of COX-1 and COX-2 in atherosclerosis, plaque rupture, and cardiovascular events.

Non-selective inhibition of COX has been reported to reduce atherosclerosis both in cholesterol fed rabbit models [15] and genetically altered murine models of atherosclerosis [6,16]. Belton et al. have reported that selective inhibition of COX-1 attenuates atherosclerosis in apoE deficient mice [9]. However, reports on the impact of selective COX-2 inhibition on the development of atherosclerosis in murine models have been mixed with decreased, increased or unchanged atherosclerotic lesion area [6,16–19]. The divergence in the results may be the consequence of differences in experimental design, including efficacy and selectivity of the inhibitors, gender of the mice and stage of atherosclerotic lesions.

A new class of COX-2 selective inhibitors has been developed by derivatization of the conventional non-steroidal anti-inflammatory drugs (NSAIDs) indomethacin, resulting in >1100 times more selectivity for COX-2 than COX-1 when tested *in vitro* [20]. In the current studies, we examined the impact of this novel amide derivative of indomethacin, designated INDO-PA, on the development of different stages of atherosclerosis in apoE<sup>-/-</sup> mice. Interestingly, INDO-PA was found to produce a 61% reduction in platelet thromboxane, indicating partial inhibition of COX-1 *in vivo*. Treatment of apoE<sup>-/-</sup> mice with INDO-PA dramatically reduced aortic prostaglandin levels and early and intermediate aortic atherosclerotic lesion formation. These studies demonstrate the ability of non-selective COX inhibition with INDO-PA to reduce early and intermediate atherosclerotic lesion formation in apoE<sup>-/-</sup> mice, supporting the efficacy of anti-inflammatory approaches in the prevention of atherosclerosis.

## 2. Methods

### 2.1. Animal procedures

Female apoE<sup>-/-</sup> mice were at the 10th backcross into the C57BL/6 background and originally purchased from Jackson Laboratories (Bar Harbor, ME). Mice were maintained on a rodent chow diet containing 4.5% fat (PMI No. 5010, St. Louis, MO) and autoclaved acidified (pH 2.8) water. Animal care and experimental procedures were carried out in accordance with the regulations and under the approval of Vanderbilt University's Animal Care Committee.

### 2.2. COX inhibition

The dose of INDO-PA used in our study was chosen based on oral dosing in acute studies of carageenan-

induced footpad edema plethysmometry in rats in which the oral ED<sub>50</sub> for this assay in rats is 1.5 mg/kg [20]. Treatment of apoE<sup>-/-</sup> mice with 5 mg/kg INDO-PA intraperitoneal (IP; 3.33-fold over ED<sub>50</sub> in rats) was well-tolerated and did not produce any gastric ulceration and toxicity even at a dose of 30 mg/kg of INDO-PA (data not shown). In contrast, apoE<sup>-/-</sup> mice were able to tolerate daily doses of 2.5-mg/kg indomethacin by the IP route but higher doses (3 mg/kg) of it resulted in gastrointestinal hemorrhage with 100% mortality by 1 week (data not shown). Drugs were administered daily based on the body weight by IP injection (100  $\mu$ l) in a sterile mixture of 1% DMSO, 5% ethanol, 5% Tween-80 and 89% PBS.

### 2.3. Serum cholesterol and triglyceride analysis

Mice were fasted for 4 h and blood was collected under isoflurane anesthesia. Serum was separated by centrifugation and lipoprotein integrity was preserved by using 1 mM phenylmethylsulfonyl fluoride (Sigma). The concentration of total cholesterol and triglycerides was determined using Sigma kits adapted for 96-well plate assay as described [21].

### 2.4. Platelet thromboxane level measurement

Nine-week-old apoE<sup>-/-</sup> mice were given vehicle ( $n = 10$ ) or 5 mg/kg INDO-PA ( $n = 9$ ) for 1 week. Ninety minutes after the final injection, blood samples were collected in the presence of 25 units of heparin sodium (Sigma) and 1.25  $\mu$ l 10  $\mu$ M A23187 Ca<sup>++</sup> ionophore (Calbiochem). Blood was placed in a 37 °C water bath for 30 min. Plasma was isolated by centrifugation at 1100 rpm for 10 min at 4 °C. Platelet thromboxane A<sub>2</sub> metabolite, thromboxane B<sub>2</sub> (TxB<sub>2</sub>) was quantified by gas chromatography/mass spectrometry (GC/MS) as described [22].

### 2.5. Aortic prostaglandin levels analysis

Seven-week-old apoE<sup>-/-</sup> mice were given daily vehicle ( $n = 4$ ) or 5 mg/kg INDO-PA ( $n = 5$ ) for 9 weeks. Ninety minutes after the last dose administration, mice were sacrificed by cervical dislocation. Aortas were dissected free of adjacent adventitial tissue and snap-frozen in liquid nitrogen. Prostacyclin metabolite 6-keto PGF<sub>1 $\alpha$</sub>  and PGE<sub>2</sub> were purified as described and quantified by GC/MS by the Eicosanoid Analysis Core at Vanderbilt University [23].

### 2.6. Analysis of Aortic Lesions

ApoE<sup>-/-</sup> mice were sacrificed and flushed with PBS through the left ventricle. The aorta was dissected and pinned out in an *en face* preparation as described previously [24]. In the first experiment, a subset of the distal aortas ( $n = 3$ ) in each group were snap-frozen in liquid nitrogen for prostaglandin determinations. The heart with

the proximal aorta was embedded in OCT and snap-frozen in liquid nitrogen. Fifteen alternate cryosections of 10- $\mu$ m thickness were collected from the proximal aorta starting from the beginning of the aortic sinus and extending 300  $\mu$ m distally as described [25]. The sections were stained with Oil-Red-O and lesion area was quantified using a Kontron computer system [24].

### 2.7. Data analysis

Data are expressed as mean  $\pm$  S.E.M. Total serum cholesterol, triglycerides, PGE<sub>2</sub>, 6-keto PGF<sub>1 $\alpha$</sub> , TxB<sub>2</sub> and aortic lesion areas between the groups were determined using the SigmaStat V.2 Software (SPSS Inc., Chicago, IL) by Student's *t*-test and the Mann–Whitney rank sum test, respectively.

## 3. Results

### 3.1. INDO-PA inhibits platelet thromboxane production in apoE<sup>-/-</sup> mice

INDO-PA has been reported to be a highly selective COX-2 inhibitor in vitro [20]. The structures of indomethacin and the amide derivative used in the treatments, INDO-PA, are shown in panels A and B of Fig. 1.

To test the COX-2 selectivity of INDO-PA, we measured platelet thromboxane production in apoE<sup>-/-</sup> deficient mice (Fig. 1C). Surprisingly, INDO-PA inhibited platelet thromboxane A<sub>2</sub> metabolite TxB<sub>2</sub> production by 61% compared to vehicle ( $25.7 \pm 3.0$  ng/ml versus  $65.9 \pm 2.4$  ng/ml, respectively;  $p = 0.001$ ). Thus, in contrast to its behavior in vitro, INDO-PA significantly inhibited COX-1 expression in apoE<sup>-/-</sup> mice in vivo.

### 3.2. INDO-PA does not affect plasma lipid levels in apoE<sup>-/-</sup> mice

To examine the impact of treatment with INDO-PA on lipid metabolism and atherosclerosis, three independent studies were designed to allow the development of fatty streak, intermediate and advanced atherosclerotic lesions in female apoE<sup>-/-</sup> mice. These mice were treated for different periods: from ages 7 to 16 weeks, from 9 to 18 weeks and from 11 to 21 weeks. However, serum lipids remained unchanged throughout the course of treatment in all three studies (Tables 1–3).

Table 1

Serum lipid levels in apoE<sup>-/-</sup> mice treated with vehicle or INDO-PA from 7 to 16 weeks of age

Animal group	Baseline		6 weeks		10 weeks	
	Chol.	Trigl.	Chol.	Trig.	Chol.	Trig.
Vehicle ( $n = 10$ )	$320 \pm 13$	$55 \pm 3$	$276 \pm 10$	$62 \pm 2$	$311 \pm 9$	$69 \pm 5$
INDO-PA ( $n = 10$ )	$333 \pm 16$	$54 \pm 6$	$260 \pm 6$	$69 \pm 3$	$322 \pm 6$	$72 \pm 4$

Values are in mg/dl (mean  $\pm$  S.E.M.). The number of animals in each group is indicated by *n*.

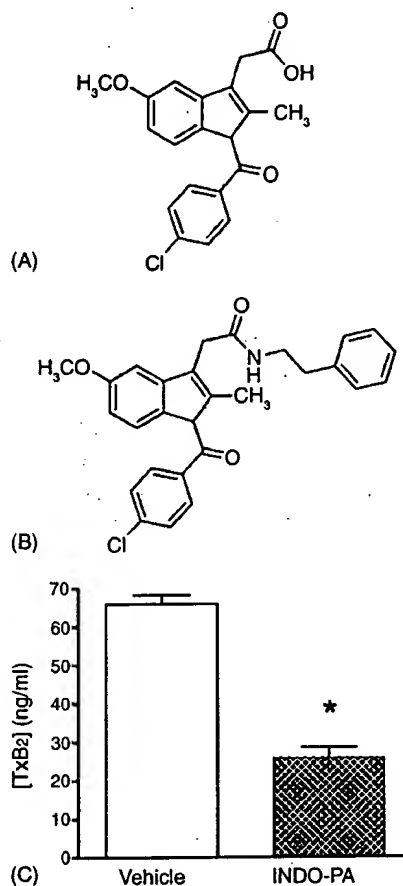


Fig. 1. Inhibition of Ca<sup>2+</sup> ionophore stimulated platelet thromboxane production: (A) chemical structure of indomethacin, (B) chemical structure of indomethacin amide derivative INDO-PA and (C) ApoE<sup>-/-</sup> mice were given vehicle (clear bar) or INDO-PA (hatched bar) for a week. Blood was collected and stimulated using A23187 Ca<sup>2+</sup> ionophore. Platelet production of the thromboxane metabolite TxB<sub>2</sub> was analyzed by GC/MS.

### 3.3. INDO-PA reduces atherosclerosis in apoE<sup>-/-</sup> mice

Treatment of 7-week-old apoE<sup>-/-</sup> mice with INDO-PA for 16 weeks significantly reduced atherosclerotic lesion formation in the proximal aorta by 44% ( $29620 \pm 4148$   $\mu$ m<sup>2</sup> versus  $52525 \pm 6007$   $\mu$ m<sup>2</sup>;  $p = 0.013$ ) and by 47% in the en face analysis of the aortas ( $0.43 \pm 0.04\%$  versus  $0.81 \pm 0.08\%$ ;  $p = 0.033$ ) compared to mice treated with vehicle, respectively (Fig. 2A and B). Representative Oil-Red-O stained sections from the proximal aorta of mice treated with vehicle (Fig. 3A) or INDO-PA (Fig. 3B) indicate fatty streak lesions consisting predominantly of foam cells.

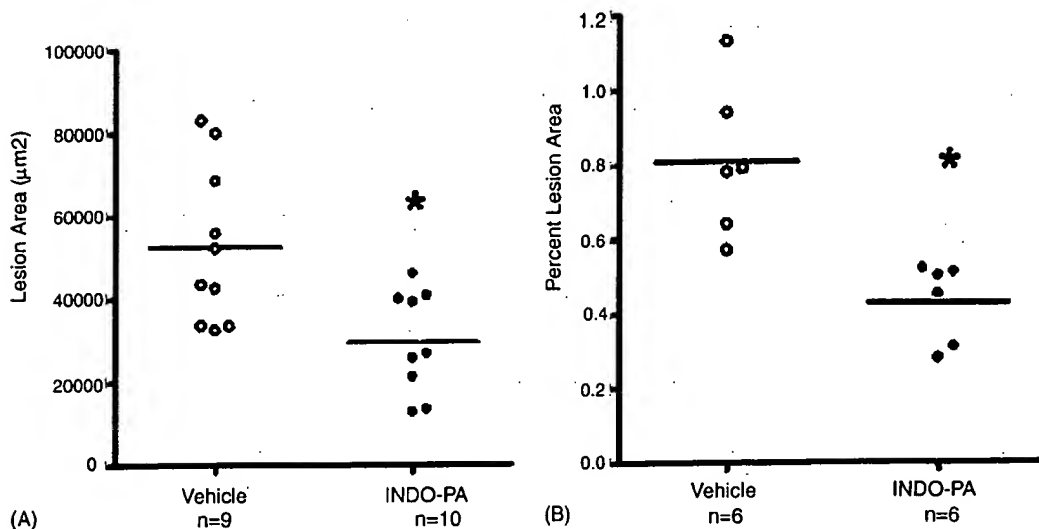


Fig. 2. Reduced atherosclerosis in apoE<sup>-/-</sup> mice treated with INDO-PA from 7 to 16 weeks of age. (A) The extent of atherosclerotic lesions in female apoE<sup>-/-</sup> after treatment with vehicle (open circles) or INDO-PA (filled circles) was quantified using Oil-Red-O stained sections. Values are in µm<sup>2</sup> with horizontal bar representing the mean of each group. (B) En face preparation of whole aortas were stained with Sudan IV and analyzed by a video imaging system. Data are represented as the percent of lesion area for each mouse and the horizontal bar represents the mean for each group.

Table 2  
Serum lipid levels in apoE<sup>-/-</sup> mice treated with vehicle or INDO-PA from 9 to 19 weeks of age

Animal group	2 weeks		9 weeks	
	Chol.	Trig.	Chol.	Trig.
Vehicle (n = 13)	352 ± 24	101 ± 8	396 ± 30	72 ± 5
INDO-PA (n = 10)	343 ± 9	110 ± 5	408 ± 27	89 ± 6

Values are in mg/dl (mean ± S.E.M.). The number of animals in each group is indicated by n.

To examine the impact of INDO-PA on the production of two aortic prostaglandins, PGE<sub>2</sub> and PGI<sub>2</sub>, apoE<sup>-/-</sup> mice were treated with INDO-PA or vehicle for 9 weeks. As shown in Fig. 4, INDO-PA inhibited production of PGE<sub>2</sub> by 88% compared to vehicle (5.13 ± 1.01 ng/mg versus 43.79 ± 14.31 ng/mg tissue, respectively; *p* = 0.001). INDO-PA also inhibited production of the PGI<sub>2</sub> metabolite by 87% compared to vehicle (29.13 ± 9.21 ng/mg versus 229.22 ± 61.98 ng/mg tissue, respectively; *p* = 0.002).

In the next study, INDO-PA treatment of 9-week-old apoE<sup>-/-</sup> mice for 9 weeks significantly reduced atherosclerosis by 53% in the proximal aorta (60997 ± 12280 µm<sup>2</sup> versus 129808 ± 18926 µm<sup>2</sup>; *p* = 0.023; Fig. 5A) and by 64% in the en face analysis of the aorta (0.40 ± 0.05% versus 1.12 ± 0.22%; *p* = 0.021; Fig. 5B) compared to the vehicle treatment group. The atherosclerotic lesions in these mice consisted of both fatty streaks and intermediate

lesions in the proximal aorta in the vehicle group (Fig. 3C) and INDO-PA treated group (Fig. 3D).

In contrast, treatment of 11-week-old apoE<sup>-/-</sup> mice with INDO-PA for 10 weeks produced only a trend for a 19% (*p* = 0.38) reduction in the extent of atherosclerosis in the proximal aorta that did not achieve statistical significance compared to mice treated with vehicle (Fig. 6A). The atherosclerotic lesions in the proximal aortas of these mice were intermediate to advanced in stage both in the vehicle-treated (Fig. 3E) and INDO-PA-treated mice (Fig. 3F) with evidence of connective tissue. Interestingly, there was a dramatic 76% reduction (Fig. 6B) in the en face analysis of the extent of aortic atherosclerosis in the apoE<sup>-/-</sup> mice treated with INDO-PA compared to the vehicle-treated group (0.61 ± 0.18% versus 2.5 ± 0.39%, respectively; *p* = 0.022).

#### 4. Discussion

We examined the impact of a novel amide derivative of indomethacin, INDO-PA, on the development of atherosclerosis in female apoE<sup>-/-</sup> mice. Although INDO-PA is highly selective for COX-2 enzyme in vitro [20], we have found that INDO-PA inhibits platelet thromboxane in vivo. Treatment of apoE<sup>-/-</sup> mice with INDO-PA dramatically reduced early to intermediate atherosclerotic

Table 3  
Serum lipid levels in apoE<sup>-/-</sup> mice treated with vehicle or INDO-PA from 11 to 21 weeks of age

Animal group	Baseline		2 weeks		9 weeks	
	Chol.	Trig.	Chol.	Trig.	Chol.	Trig.
Vehicle (n = 9)	292 ± 9	64 ± 3	242 ± 15	98 ± 6	271 ± 18	89 ± 3
INDO-PA (n = 9)	282 ± 16	58 ± 5	257 ± 23	99 ± 9	306 ± 29	96 ± 4

Values are in mg/dl (mean ± S.E.M.). The number of animals in each group is indicated by n.

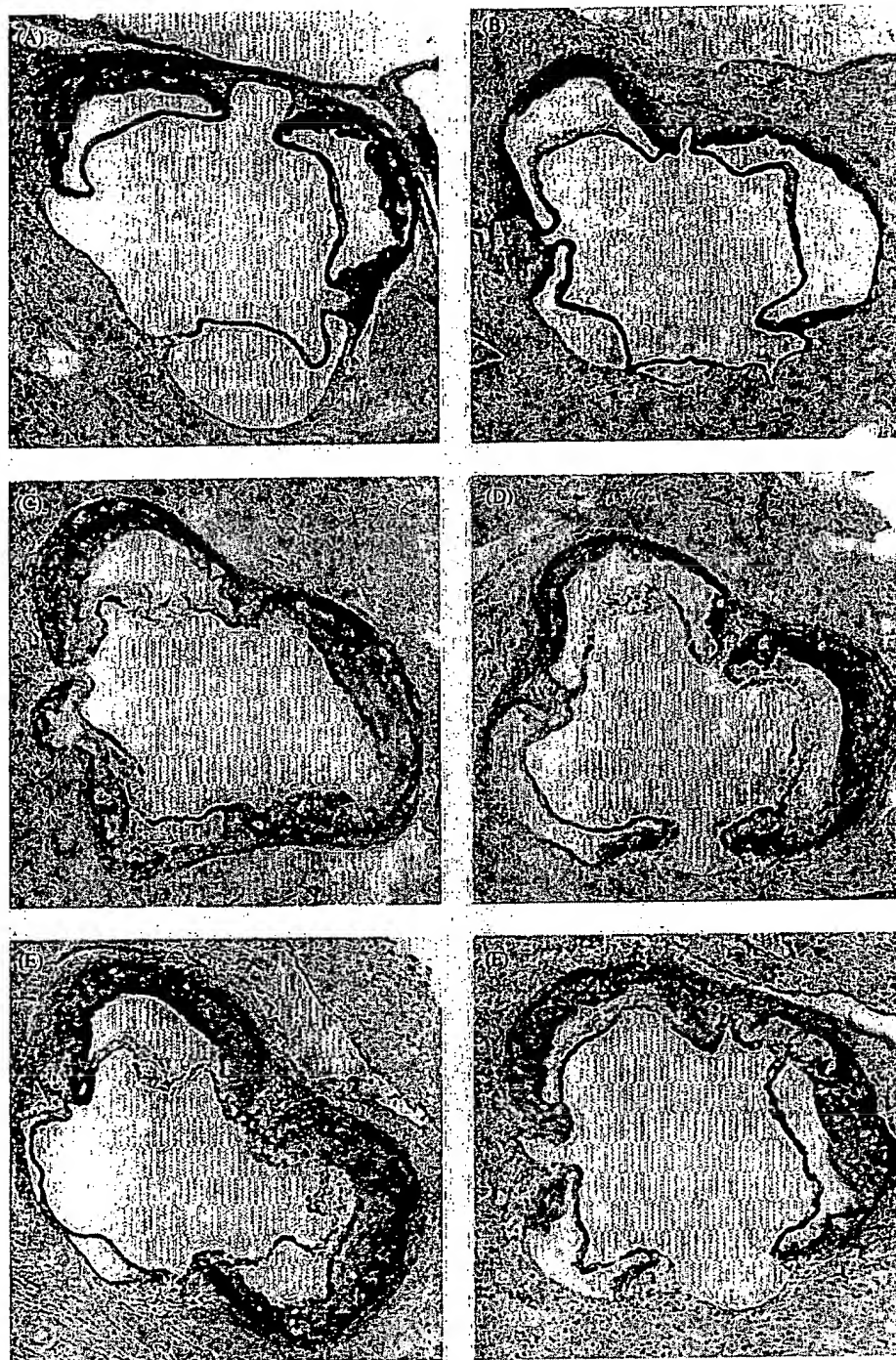


Fig. 3. Representative Oil-Red-O stained aortic root sections from groups treated with vehicle and INDO-PA. (A and B) Early stage atherosclerotic lesions in apoE<sup>-/-</sup> mice treated with vehicle (A) and INDO-PA (B) from 7 to 16 weeks of age. (C and D) Intermediate stage atherosclerotic lesions in apoE<sup>-/-</sup> mice treated with vehicle (C) and INDO-PA (D) from 9 to 18 weeks of age. (E and F) Advanced stage atherosclerotic lesions in apoE<sup>-/-</sup> mice treated with vehicle (E) and INDO-PA (F) from 7 to 16 weeks of age.

lesion formation. In addition, INDO-PA inhibited PGE<sub>2</sub> and PGI<sub>2</sub> metabolite production in the aorta by 88 and 87%, respectively, demonstrating efficacy of the INDO-PA in inhibiting prostaglandins in the artery wall *in vivo*. Thus, non-selective inhibition of COX with INDO-PA reduces the development of atherosclerosis in apoE<sup>-/-</sup> mice, supporting the potential for COX inhibition and

anti-inflammatory approaches in the prevention of atherosclerosis.

Treatment with 5 mg/kg INDO-PA (3.33-fold over ED<sub>50</sub> for oral dosing in rats [20]) was well-tolerated and did not produce gastric ulceration in apoE<sup>-/-</sup> mice. In these mice at steady state of INDO-PA, we observed a significant but incomplete (61%) inhibition of platelet thromboxane pro-

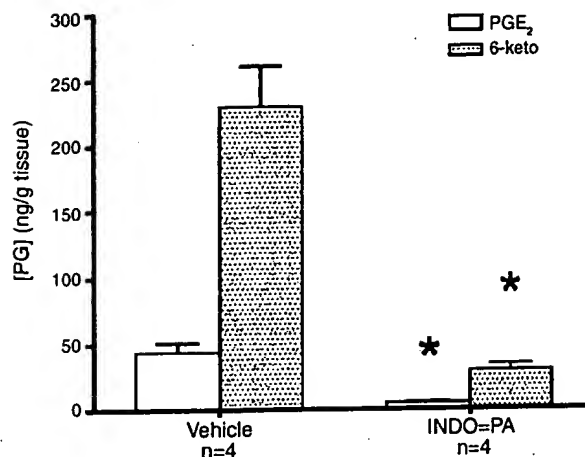


Fig. 4. Inhibition of prostaglandin production in aortic tissue of apoE<sup>-/-</sup> mice. ApoE<sup>-/-</sup> mice were given vehicle or INDO-PA beginning at 7 weeks of age for 9 weeks. Aortas were analyzed by GC/MS for PGE<sub>2</sub> and PGI<sub>2</sub> metabolite 6-keto-PGF<sub>1α</sub>.

duction indicating partial inhibition of platelet COX-1. Further studies in rats have verified that a small percentage of INDO-PA (5–10%) is converted into indomethacin in vivo (R.P. Remmel and L.J. Marnett, unpublished results). Although these data indicate that INDO-PA is only partially selective, previous data demonstrating that >90% inhibition of platelet thromboxane is required to inhibit platelet aggregation [26,27] suggests that inhibition of thromboxane-mediated-platelet aggregation is unlikely to have contributed significantly to the reduction in atherosclerosis. Three decades ago, non-selective inhibition of COX was reported to reduce atherosclerosis in cholesterol fed rabbits [15]. We and others have shown that non-selective inhibition of COX with indomethacin associated with 90–95% reductions in platelet thromboxane reduces

early and intermediate atherosclerotic lesions in LDLR<sup>-/-</sup> mice fed a western diet [6,16]. In contrast, Egan et al. have recently reported that treatment of 6-week-old western diet fed apoBec-1/LDLR DKO mice with indomethacin for 13 weeks was associated with only a 70% reduction in platelet thromboxane and caused a 12.9% reduction in complex atherosclerotic lesions [28]. Thus, differences in these studies include the mouse model used, the extent of atherosclerosis and the efficacy of the indomethacin. Data with regard to the impact of aspirin on murine models have been conflicting, with a study by Cayatte et al. showing no effect [29] and studies in high-fat diet fed apoE<sup>-/-</sup> [30] and LDLR<sup>-/-</sup> mice [31] demonstrating significant reductions in lesion formation. However, Cayatte et al. reported that a thromboxane receptor antagonist, which inhibited serum thromboxane activity by only 39%, reduced atherosclerosis in apoE<sup>-/-</sup> mice [29]. The authors interpreted these results as indicating that eicosanoids other than thromboxane are involved in promoting atherosclerosis. Recently, Belton et al. have reported that selective inhibition of COX-1, which reduced urinary 2,3-dinor-TxB<sub>2</sub>, by around 50% reduced atherosclerotic lesion formation in apoE deficient mice [9]. Thus, it is possible that inhibition of thromboxane may have contributed to the reduction in atherosclerosis seen with INDO-PA by partially offsetting potentially negative effects of reducing prostacyclin. However, it is also possible that reductions of other eicosanoids due to inhibition of COX-1 and/or COX-2 may have contributed to the reduction in atherosclerosis.

Reports on the impact of selective COX-2 inhibition on the development of atherosclerosis in murine models have been mixed indicating decreased, increased or unchanged atherosclerotic lesion area [6,16–19]. The differences in results of these studies may be explained by variability in

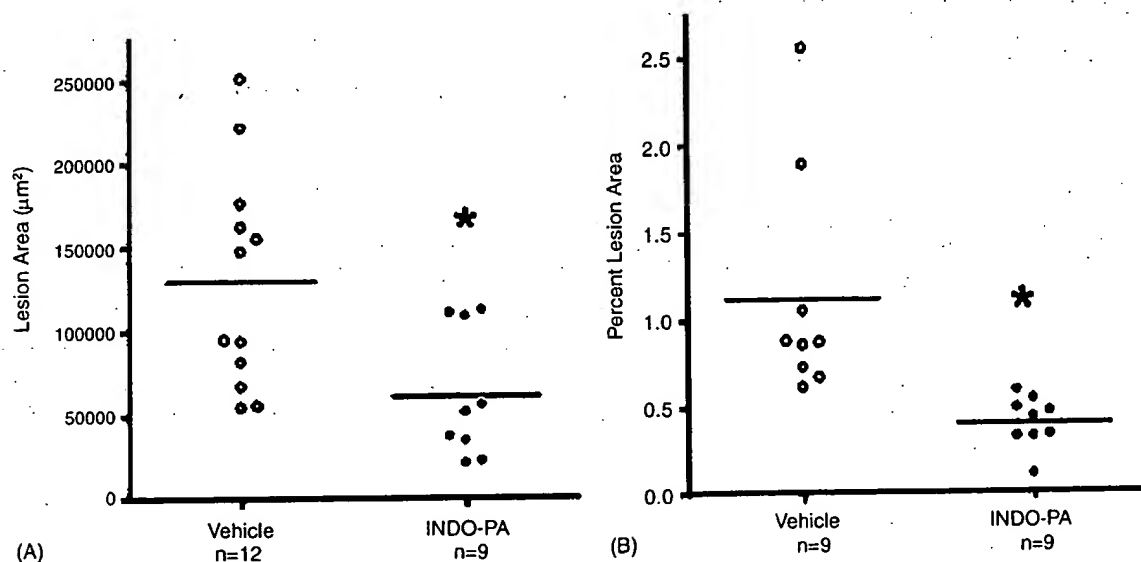


Fig. 5. Reduced atherosclerosis in apoE<sup>-/-</sup> mice treated with INDO-PA from 9 to 18 weeks of age. (A) The extent of atherosclerotic lesions in the proximal aorta of apoE<sup>-/-</sup> mice after treatment with vehicle (open circles) or INDO-PA (filled circles) was quantified using Oil-Red-O stained sections. (B) En face preparation of whole aortas were stained with Sudan IV and analyzed by a video imaging system. Data are represented as the percent of lesion area for each mouse and the horizontal bar represents the mean for each group.



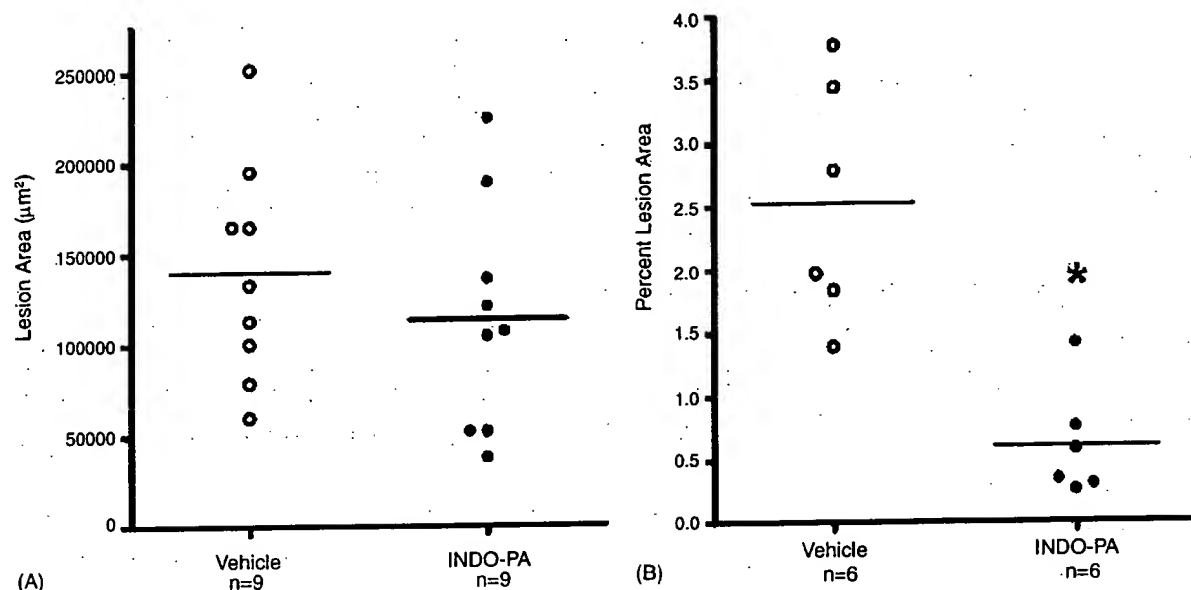


Fig. 6. Impact of INDO-PA treatment on atherosclerosis in apoE<sup>-/-</sup> mice from 11 to 21 weeks of age. (A) The extent of atherosclerotic lesions in the proximal aorta of apoE<sup>-/-</sup> after treatment with vehicle (open circles) or INDO-PA (filled circles) was quantified using Oil-Red-O stained sections from 300 µm of the proximal aorta. (B) En face preparation of whole aortas were stained with Sudan IV and analyzed by a video imaging system.

experimental design, including efficacy and selectivity of the inhibitors, gender of the mice and atherosclerotic lesion stage. We have previously reported that rofecoxib reduces early atherosclerotic lesion formation in LDLR<sup>-/-</sup> mice [6]. Consistent with our results, Krul et al. have presented data that treatment of apoE<sup>-/-</sup> mice with a selective COX-2 inhibitor, celecoxib, results in a significant reduction in aortic atherosclerosis [32]. Using bone marrow transplantation studies, we have demonstrated that macrophage COX-2 expression promotes early atherosclerotic lesion formation in LDLR<sup>-/-</sup> mice [6], providing genetic evidence consistent with COX-2 inhibition reducing early atherosclerotic lesion formation. In contrast, the ability of selective inhibition of COX-2 to impact atherogenesis appears to be limited in the setting of advanced atherosclerotic lesions [9,17,18], perhaps due to LXR-mediated downregulation of COX-2 in macrophage-derived foam cells [33] and the inhibition of anti-proliferative effects of COX-2 expression in smooth muscle cells [34]. Thus, the impact of COX-2 on atherosclerosis is complex and may vary according to the cell type and lesion stage.

Our current results demonstrate that non-selective inhibition of COX with INDO-PA reduces the formation of early and intermediate atherosclerotic lesions in female apoE<sup>-/-</sup> mice. Interestingly, we saw a non-significant trend for a reduction of atherosclerosis in the proximal aortas of apoE<sup>-/-</sup> mice with advanced stage lesions, whereas the extent of atherosclerosis in the en face aortas was dramatically reduced by 76%. In murine models, atherosclerosis develops first in the proximal aorta and then progresses distally [24,25]. These results are reminiscent of the findings that treatment with the selective COX-2 inhibitor, nimesulide, produced a non-significant trend for a reduction in atherosclerosis in

LDLR<sup>-/-</sup> mice with intermediate stage lesions, whereas treatment with indomethacin produced a significant reduction in atherosclerosis [16]. Although INDO-PA partially inhibits COX-1, we believe that it is acting largely as a COX-2 inhibitor, given the relatively low rate of conversion to indomethacin in vivo, the incomplete inhibition of platelet COX-1, and the much improved safety profile of INDO-PA compared to indomethacin. These results suggest that as the disease progresses from intermediate to advanced lesion stage, COX-2 inhibition appears to have less of an effect on modulating progression of atherosclerosis. Interestingly, INDO-PA virtually eliminated the progression of atherosclerosis in the en face aortas, as can be seen by the similar lesion burdens in all three treatment groups.

Although atherosclerosis is the pathological substrate underlying heart attack and stroke, plaque rupture and thrombosis are responsible for precipitating acute cardiovascular events. Mounting evidence supports the critical involvement of eicosanoids in the processes of plaque rupture and thrombosis. Inhibition of COX-1 mediated production of platelet thromboxane by aspirin reduces the risk for myocardial infarction and stroke [7]. In contrast, rofecoxib, a highly selective COX-2 inhibitor, has recently been taken off the market due to evidence from the APPROVe trial demonstrating increased cardiovascular events after 18 months ([www.viox.com](http://www.viox.com)). The mechanism responsible for the increased cardiovascular events in patients on rofecoxib remains to be elucidated. Concerns have been raised that COX-2 inhibition may promote cardiovascular events by inhibiting prostacyclin and promoting a prothrombotic state [11]. However, the impact of a prothrombotic state might be expected to cause an increase in cardiovascular events sooner than the

18 months seen in the APPROVe trial, suggesting that other mechanisms may be responsible.

Although three published studies have reported an increase in cardiovascular events in patients taking rofecoxib, principally at doses >25 mg a day [10,35,36], other studies found no evidence for increased risk of cardiovascular events with rofecoxib [37,38] or celecoxib [39]. Several important questions remain to be answered. Is the increase in cardiovascular events seen with rofecoxib a class effect that pertains to all other COX-2 inhibitors? Does the presence of COX-1 inhibition in addition to COX-2 inhibition, as seen with non-selective COX inhibitors, eliminate this risk of increased cardiovascular events due to chronic COX-2 inhibition alone? Recently, Pfizer has announced an increase in cardiovascular events associated with valdecoxib in patients in two small studies of patients undergoing coronary artery bypass grafting [19], and no increase in cardiovascular events based on clinical trial database of nearly 8000 patients treated with valdecoxib for durations ranging from 6 to 52 weeks ([http://www.pfizer.com/are/news\\_releases/2004pr/mn\\_2004\\_1015.html](http://www.pfizer.com/are/news_releases/2004pr/mn_2004_1015.html)). Although our current studies do not address the issues of plaque rupture and thrombosis, our results support the ability of non-selective COX inhibition to reduce atherosclerosis. Thus, non-selective inhibition of COX has the potential to favorably impact atherosclerosis, plaque rupture and thrombosis. A better understanding of the complex roles of COX-1 and COX-2 in atherogenesis and plaque stability may lead to new therapeutic approaches to the prevention of cardiovascular disease.

## Acknowledgements

The authors are thankful to Lei Ding and Youmin Zhang for excellent technical expertise. This work was supported by National Institutes of Health grants HL65405, HL53989, HL 57986, DK59637 (Lipid, Lipoprotein and Atherosclerosis Core of the Vanderbilt Mouse Metabolic Phenotyping Centers). M.E.B. is supported by American Heart Association grant (0215110B). V.R.B. is supported by American Heart Association grant (0160160B).

## References

- [1] Ross R. Atherosclerosis—an inflammatory disease. *New Eng J Med* 1999;340:115–26.
- [2] DuBois R, Abramson S, Crofford L, Gupta RA, Simon L, Van De Putte L, et al. Cyclooxygenase in biology and disease. *FASEB J* 1998;12:1063–73.
- [3] Vane JR, Bakhle YS, Botting RM. Cyclooxygenase 1 and 2. *Ann Rev Pharmacol Toxicol* 1998;38:97–120.
- [4] Baker CS, Hall RJ, Evans TJ, Pomerance A, MacIouf J, Creminon C, et al. Cyclooxygenase-2 is widely expressed in atherosclerotic lesions affecting native and transplanted human coronary arteries and colocalizes with inducible nitric oxide synthase and nitrotyrosine particularly in macrophages. *Arterioscler Thromb Vasc Biol* 1999;19(3):646–55.
- [5] Schonbeck U, Sukhova GK, Graber P, Coulter S, Libby P. Augmented expression of cyclooxygenase-2 in human atherosclerotic lesions. *Am J Pathol* 1999;155:1281–91.
- [6] Burleigh ME, Babaev VR, Oates JA, Harris RC, Gautam S, Riendeau D, et al. Cyclooxygenase-2 promotes early atherosclerotic lesion formation in LDL receptor-deficient mice. *Circulation* 2002;105: 1816–23.
- [7] Hennekens CH, Dyken ML, Fuster V. Aspirin as a therapeutic agent in cardiovascular disease: a statement for healthcare professionals from the American Heart Association. *Circulation* 1997;96:2751–3.
- [8] Cheng Y, Austin SC, Rocca B, Koller BH, Coffman TM, Grosser T, et al. Role of prostacyclin in the cardiovascular response to thromboxane A<sub>2</sub>. *Science* 2002;296(5567):539–41.
- [9] Belton OA, Duffy A, Toomey S, Fitzgerald DJ. Cyclooxygenase isoforms and platelet vessel wall interactions in the apolipoprotein E knockout mouse model of atherosclerosis. *Circulation* 2003;108: 3017–23.
- [10] Bombardier C, Laine L, Reicin A, Shapiro D, Burgos-Vargas R, Davis B, et al. VIGOR Study Group. Comparison of upper gastrointestinal toxicity of rofecoxib and naproxen in patients with rheumatoid arthritis. *New Eng J Med* 2000;343:1520–8.
- [11] Mukherjee D, Nissen SE, Topol EJ. Risk of cardiovascular events associated with selective COX-2 inhibitors. *J Am Med Assoc* 2001;286:954–9.
- [12] Chenevard R, Hurlimann D, Bechir M, Enseleit F, Spieker L, Hermann M, et al. Selective COX-2 inhibition improves endothelial function in coronary artery disease. *Circulation* 2003;107(3):405–9.
- [13] Cipollone F, Prontera C, Pini B, Marini M, Fazio M, De Cesare D, et al. Overexpression of functionally coupled cyclooxygenase-2 and prostaglandin E synthase in symptomatic atherosclerotic plaques as a basis of prostaglandin E<sub>2</sub>-dependent plaque instability. *Circulation* 2001;104(8):921–7.
- [14] Cipollone F, Toniato E, Martinotti S, Fazio M, Lezzi A, Cuccurullo C, et al. Identification of new elements of plaque stability study G, a polymorphism in the cyclooxygenase 2 gene as an inherited protective factor against myocardial infarction and stroke. *J Am Med Assoc* 2004;291:2221–8.
- [15] Bailey JM, Butler J. Anti-inflammatory drugs in experimental atherosclerosis. I. Relative potencies for inhibiting plaque formation. *Atherosclerosis* 1973;17(3):515–22.
- [16] Pratico D, Tillmann C, Zhang ZB, Li H, FitzGerald GA. Acceleration of atherogenesis by COX-1-dependent prostanoid formation in low density lipoprotein receptor knockout mice. *Proc Natl Acad Sci USA* 2001;98:3358–63.
- [17] Olesen M, Kwong E, Meztli A, Kontny F, Seljeflot I, Arnesen H, et al. No effect of cyclooxygenase inhibition on plaque size in atherosclerosis-prone mice. *Scand Cardiovasc J* 2002;36:362–7.
- [18] Bea F, Blessing E, Bennett BJ, Kuo CC, Campbell LA, Kreuzer J, et al. Chronic inhibition of cyclooxygenase-2 does not alter plaque composition in a mouse model of advanced unstable atherosclerosis. *Cardiovasc Res* 2003;60:198–204.
- [19] Rott D, Zhu J, Burnett MS, Zhou YF, Zalles-Ganley A, Ogunmakinwa J, et al. Effects of MF-tricyclic, a selective cyclooxygenase-2 inhibitor, on atherosclerosis progression and susceptibility to cytomegalovirus replication in apolipoprotein-E knockout mice. *J Am Coll Cardiol* 2003;41:1812–9.
- [20] Kalgutkar AS, Crews BC, Rowlinson SW, Marnett AB, Kozak KR, Remmel RP, et al. Biochemically based design of cyclooxygenase-2 (COX-2) inhibitors: facile conversion of nonsteroidal antiinflammatory drugs to potent and highly selective COX-2 inhibitors. *Proc Natl Acad Sci USA* 2000;97(2):925–30.
- [21] Linton MF, Atkinson JB, Fazio S. Prevention of atherosclerosis in apoE deficient mice by bone marrow transplantation. *Science* 1995;267:1034–7.

- [22] Marnett LJ, Wright TL, Crews BC, Tannenbaum SR, Morrow JD. Regulation of prostaglandin biosynthesis by nitric oxide is revealed by targeted deletion of inducible nitric-oxide synthase. *J Biol Chem* 2000;275:13427–30.
- [23] Reese J, Paria BC, Brown N, Zhao X, Morrow JD, Dey SK. Coordinated regulation of fetal and maternal prostaglandins directs successful birth and postnatal adaptation in the mouse. *Proc Natl Acad Sci USA* 2000;97(17):9759–64.
- [24] Babaev VR, Patel MB, Semenkovich CF, Fazio S, Linton MF. Macrophage lipoprotein lipase promotes foam cell formation and atherosclerosis in low density lipoprotein receptor-deficient mice. *J Biol Chem* 2000;275:26293–9.
- [25] Paigen B, Holmes P, Mitchell D, Albee D. Comparison of atherosclerotic lesions and HDL-lipid levels in male, females, and testosterone-treated female mice from strains C57BL/6, BALB/c and C3H. *Atherosclerosis* 1987;68:215–21.
- [26] Czervionke RL, Hoak JC, Fry GL. Effect of aspirin on thrombin-induced adherence of platelets to cultured cells from the blood vessel wall. *J Clin Invest* 1978;62(4):847–56.
- [27] FitzGerald GA, Oates JA, Hawiger J, Maas RL, Roberts 2nd LJ, Lawson JA, et al. Endogenous biosynthesis of prostacyclin and thromboxane and platelet function during chronic administration of aspirin in man. *J Clin Invest* 1983;71(3):676–88.
- [28] Egan KM, Wang M, Lucitt MB, Zukas AM, Pure E, Lawson JA, et al. Cyclooxygenases, thromboxane, and atherosclerosis: plaque destabilization by cyclooxygenase-2 inhibition combined with thromboxane receptor antagonism. *Circulation* 2005;111(3):334–42.
- [29] Cayatte AJ, Du Y, Oliver-Krasinski J, Lavielle G, Verbeuren TJ, Cohen RA. The thromboxane receptor antagonist S18886 but not aspirin inhibits atherogenesis in apo E-deficient mice: evidence that eicosanoids other than thromboxane contribute to atherosclerosis. *Arterioscler Thromb Vasc Biol* 2000;20:1724–8.
- [30] Paul A, Calleja L, Camps J, Osada J, Vilella E, Ferre N, et al. The continuous administration of aspirin attenuates atherosclerosis in apolipoprotein E-deficient mice. *Life Sci* 2000;68(4):457–65.
- [31] Cyrus T, Sung S, Zhao L, Funk CD, Tang S, Pratico D. Effect of low-dose aspirin on vascular inflammation, plaque stability, and atherogenesis in low-density lipoprotein receptor-deficient mice. *Circulation* 2002;106(10):1282–7.
- [32] Krul ES, Napawan N, Butteiger DT, Hayes K, Krause L, Freidrich GE, et al. Atherosclerosis is reduced in cholesterol-fed apoE<sup>−/−</sup> mice administered an ASBT inhibitor or a selective COX-2 inhibitor. *Arterioscler Thromb Vasc Biol* 2002;22:P409.
- [33] Joseph SB, Castrillo A, Laffitte BA, Mangelsdorf DJ, Tontonoz P. Reciprocal regulation of inflammation and lipid metabolism by liver X receptors. *Nat Med* 2003;9:213–9.
- [34] Kothapalli D, Fuki I, Ali K, Stewart S, Zhao L, Yahil R, et al. Antimitogenic effects of HDL and APOE mediated by Cox-2-dependent IP activation. *J Clin Invest* 2004;113(4):609–18.
- [35] Ray WA, Stein CM, Daugherty JR, Hall K, Arbogast PG, Griffin MR. COX-2 selective non-steroidal anti-inflammatory drugs and risk of serious coronary heart disease. *Lancet* 2002;360:1071–3.
- [36] Solomon D, Schneeweiss S, Glynn R, Kiyota Y, Levin R, Mogun H, et al. Relationship between selective cyclooxygenase-2 inhibitors and acute myocardial infarction in older adults. *Circulation* 2004;109:2068–73.
- [37] Konstam MA, Weir MR, Reicin A, Shapiro D, Sperling RS, Barr E, et al. Cardiovascular thrombotic events in controlled, clinical trials of rofecoxib. *Circulation* 2001;104:2280–8.
- [38] Reicin AS, Shapiro D, Sperling RS, Barr E, Yu Q. Comparison of cardiovascular thrombotic events in patients with osteoarthritis treated with rofecoxib versus nonselective nonsteroidal anti-inflammatory drugs (ibuprofen, diclofenac, and nabumetone). *Am J Cardiol* 2002;89:204–9.
- [39] Silverstein F, Faich G, Goldstein J, Simon L, Pincus T, Whelton A, et al. Gastrointestinal toxicity with celecoxib vs nonsteroidal anti-inflammatory drugs for osteoarthritis and rheumatoid arthritis: the CLASS study. A randomized controlled trial. Celecoxib Long-term Arthritis Safety Study. *J Am Med Assoc* 2000;284:1247–55.

# Simvastatin Reduces Neointimal Thickening in Low-Density Lipoprotein Receptor-Deficient Mice After Experimental Angioplasty Without Changing Plasma Lipids

Zhiping Chen, MS; Tatsuya Fukutomi, MD; Alexandre C. Zago, MD; Raila Ehlers, MD; Patricia A. Detmers, PhD; Samuel D. Wright, PhD; Campbell Rogers, MD; Daniel I. Simon, MD

**Background**—Statins exert antiinflammatory and antiproliferative actions independent of cholesterol lowering. To determine whether these actions might affect neointimal formation, we investigated the effect of simvastatin on the response to experimental angioplasty in LDL receptor-deficient (LDLR<sup>-/-</sup>) mice, a model of hypercholesterolemia in which changes in plasma lipids are not observed in response to simvastatin.

**Methods and Results**—Carotid artery dilation (2.5 atm) and complete endothelial denudation were performed in male C57BL/6J LDLR<sup>-/-</sup> mice treated with low-dose (2 mg/kg) or high-dose (20 mg/kg) simvastatin or vehicle subcutaneously 72 hours before and then daily after injury. After 7 and 28 days, intimal and medial sizes were measured and the intima to media area ratio (I:M) was calculated. Total plasma cholesterol and triglyceride levels were similar in simvastatin- and vehicle-treated mice. Intimal thickening and I:M were reduced significantly by low- and high-dose simvastatin compared with vehicle alone. Simvastatin treatment was associated with reduced cellular proliferation (BrdU), leukocyte accumulation (CD45), and platelet-derived growth factor-induced phosphorylation of the survival factor Akt and increased apoptosis after injury.

**Conclusions**—Simvastatin modulates vascular repair after injury in the absence of lipid-lowering effects. Although the mechanisms are not yet established, additional research may lead to new understanding of the actions of statins and novel therapeutic interventions for preventing restenosis. (*Circulation*. 2002;106:20-23.)

**Key Words:** restenosis ■ statins ■ inflammation ■ apoptosis

Statins inhibit the enzyme 3-hydroxy-3-methylglutaryl coenzyme A (HMG-CoA) reductase, the first committed step of sterol synthesis, and lower plasma cholesterol levels. In large clinical trials, statins have been shown to reduce coronary events in primary or secondary prevention settings.<sup>1</sup> Effects on clinical and angiographic restenosis after coronary intervention, however, have not been conclusively demonstrated. Several clinical studies have failed to demonstrate a link between statin therapy and the risk of restenosis after balloon angioplasty,<sup>2</sup> whereas more recent studies suggest that statins may reduce restenosis after stenting.<sup>3</sup>

Statins are known to have broad effects in addition to lowering plasma cholesterol. The product of HMG-CoA reductase, mevalonate, is an important precursor for many isoprenoids, thereby endowing statins with the ability to directly alter cellular events other than cholesterol synthesis. For example, the isoprenoids farnesylpyrophosphate and geranylgeranylpyrophosphate play important roles in signal transduction in cellular migration, proliferation, and survival via their attachment to critical signaling proteins, such as Ras and Rho.<sup>4</sup>

We used a hyperlipidemic model, the LDLR<sup>-/-</sup> mouse, to test the antiinflammatory and antiproliferative actions of simvastatin on neointimal thickening after experimental angioplasty in an atherosclerotic background. An essential feature of the chosen model is that simvastatin does not affect plasma lipid levels in mice, allowing the study of effects of simvastatin distinct from cholesterol lowering.

## Methods

### Carotid Injury

Male LDLR<sup>-/-</sup> C57BL/6J mice (Jackson Laboratories, Bar Harbor, Me), maintained on a high-fat (20.1%) diet containing 1.25% cholesterol for 12 weeks after weaning, underwent unilateral carotid artery dilation (2.5 atm) and complete endothelial denudation.<sup>5</sup> Animal care and procedures were reviewed and approved by Harvard Medical School Standing Committee on Animals and performed in accordance with the guidelines of the American Association for Accreditation of Laboratory Animal Care and the National Institutes of Health.

### Simvastatin Treatment

Treatments were via subcutaneous injection 72 hours before and daily after injury. LDLR<sup>-/-</sup> mice were divided into 3 treatment

Received March 29, 2002; revision received May 8, 2002; accepted May 9, 2002.

From the Cardiovascular Division (Z.C., T.F., A.C.Z., R.E., C.R., D.I.S.), Brigham and Women's Hospital, Boston, Mass; Harvard-MIT Division of Health Sciences and Technology (C.R.), Cambridge, Mass; and Merck Research Laboratories (P.A.D., S.D.W.), Rahway, NJ.

Correspondence to Daniel I. Simon, MD, Cardiovascular Division, Brigham and Women's Hospital, 75 Francis St, Tower 3, Boston, MA 02115. E-mail dsimon@rics.bwh.harvard.edu

© 2002 American Heart Association, Inc.

*Circulation* is available at <http://www.circulationaha.org>

DOI: 10.1161/01.CIR.0000022843.76104.01

## Quantitative Morphometry and Immunohistochemical Analysis of Mouse Carotid Arteries After Injury

	Simvastatin			ANOVA	P	
	Vehicle	Low	High		Vehicle vs Low	Vehicle vs High
Cholesterol, 21 d, mg/dL	856±89	922±167	1130±279	0.074	NS	NS
Triglyceride, 21 d, mg/dL	216±36	234±43	223±44	0.751	NS	NS
Intimal area, mm <sup>2</sup>						
7 d	0.010±0.004	0.006±0.004	0.006±0.004	0.320	NS	NS
28 d	0.047±0.023	0.021±0.013	0.019±0.015	0.004	0.011	0.012
Medial area, mm <sup>2</sup>						
28 d	0.078±0.015	0.063±0.014	0.074±0.031	0.299	NS	NS
I:M, 28 d	0.64±0.37	0.32±0.17	0.24±0.15	0.008	0.036	0.012
EEL, mm <sup>2</sup>						
7 d	0.104±0.013	0.113±0.035	0.103±0.014	0.778	NS	NS
28 d	0.223±0.032	0.191±0.040	0.192±0.053	0.184	NS	NS
BrdU+ cells, %						
Media, 7 d	19.2±2.8	12.0±5.8	11.0±4.5	0.299	NS	NS
Intima, 28 d	4.6±1.8	1.7±0.5	1.9±0.8	0.0184	0.042	0.050
CD45+ cells, %						
Intima, 7 d	59.2±11.9	44.2±5.2	39.1±12.8	0.0429	0.047	0.049
Intima, 28 d	34.4±3.6	24.3±2.2	20.9±8.0	0.0120	0.026	0.025
TUNEL+ cells, %						
Intima, 7 d	3.5±1.1	6.9±3.3	9.2±4.2	0.0872	0.193	0.039
Media, 7 d	2.5±0.4	4.2±0.3	5.8±1.0	0.0002	0.002	0.001

groups: PBS vehicle (control group) or 2 mg/kg (low-dose) or 20 mg/kg (high-dose) alkaline-hydrolyzed simvastatin.<sup>6</sup>

### Lipid Analysis

Blood was collected via retro-orbital puncture into heparin-coated capillary tubes. Plasma cholesterol and triglyceride measurements were performed as reported.<sup>7</sup>

### Tissue Harvesting and Analysis

Carotid arteries were harvested and processed for quantitative morphometry 7 days (control, n=5; low-dose, n=5; high-dose, n=4) or 28 days (control, n=9; low-dose, n=10; high-dose, n=7) after vascular injury.<sup>8</sup> Standard avidin-biotin procedures for mouse leukocytes (CD45) and macrophages (Mac-3) (PharMingen, San Diego, Calif), BrdU (DAKO, Carpinteria, Calif), and smooth muscle cell (SMC)  $\alpha$ -actin (DAKO) were used for immunohistochemistry. Apoptotic cells were detected by the TUNEL method using Apo Tag (Intergen). Immunostained sections were quantified as the number of immunostained-positive cells per total number of nuclei.

### Ex Vivo Akt Signaling Assay

Aortas were harvested from all animals, opened longitudinally, and incubated with 30 ng/mL platelet-derived growth factor (PDGF)-BB (R&D Systems, Minneapolis, Minn) for 15 minutes at 37°C. Aortic lysates were prepared<sup>9</sup> and then subjected to Western analysis using antibodies to Akt and Phospho-Akt (Ser473) (Cell Signaling Technology, Beverly, Mass).

### Data Analysis

All data are presented as mean±SD. Statistical comparisons of the principal end points were performed using one-way ANOVA to determine a difference in mean values between the 3 groups, followed by *t* tests for the 3 pair-wise comparisons when the ANOVA false-positive rate was <5%. For ANOVA with a false-

positive rate of >5%, the pair-wise comparisons were reported to be statistically nonsignificant (NS). For the primary study end point of intimal area 28 days after injury, a Bonferroni corrective for 3 pair-wise comparisons was applied, in which the *t* test *P*<0.0167 was used to signify a false-positive rate of 5%.

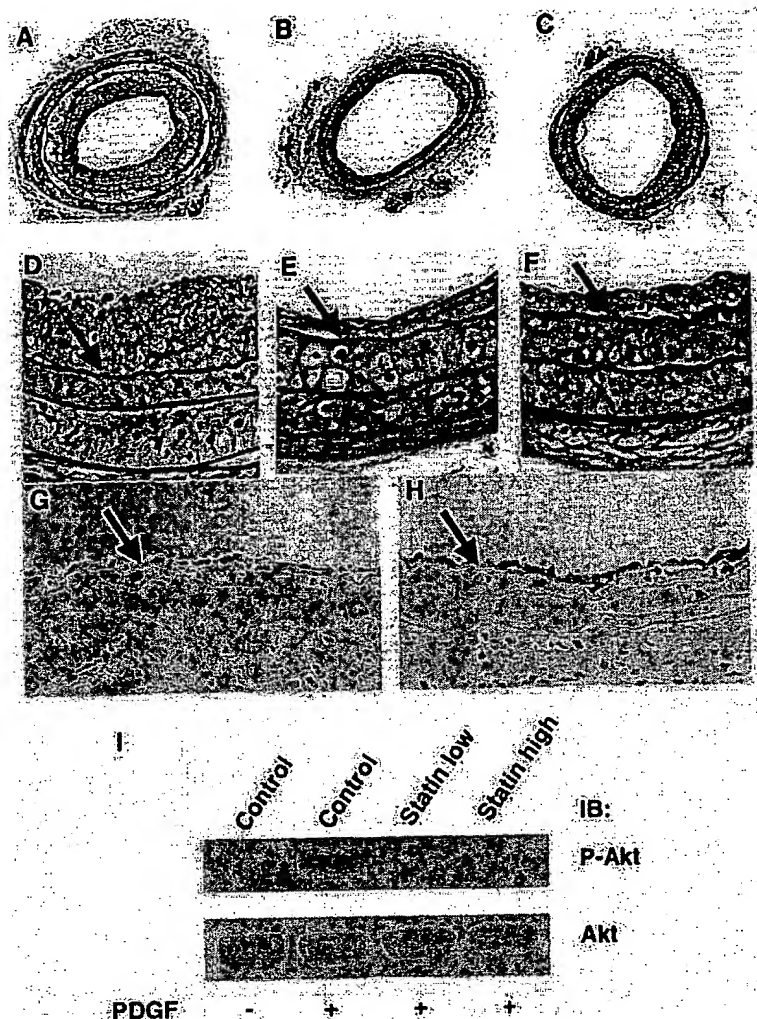
## Results

### Simvastatin Does Not Alter Plasma Lipids in LDLR<sup>-/-</sup> Mice

We sought evidence that simvastatin modulates vascular repair independent of cholesterol lowering. To determine whether plasma cholesterol is unresponsive to simvastatin in LDLR<sup>-/-</sup> mice, as it is in normal<sup>9</sup> and apoE-deficient<sup>7</sup> mice, we dosed LDLR<sup>-/-</sup> animals with 2 mg/kg simvastatin, 20 mg/kg simvastatin, or vehicle control and measured plasma lipid levels. Simvastatin did not alter plasma cholesterol or triglyceride levels in LDLR<sup>-/-</sup> mice at either of the 2 doses tested (Table).

### Simvastatin Decreases Neointimal Thickening, Cellular Proliferation, and Leukocyte Accumulation After Carotid Injury

Carotid artery dilation and complete endothelial denudation were performed in LDLR<sup>-/-</sup> mice treated with 2 or 20 mg/kg simvastatin or vehicle subcutaneously 72 hours before and then daily after injury until euthanasia. In mice receiving vehicle, intimal thickening began by 7 days after injury and progressed significantly between 7 days (0.010±0.004 mm<sup>2</sup>) and 28 days (0.047±0.023 mm<sup>2</sup>). Low- and high-dose simvastatin reduced intimal thickening at 28 days by 55%



Photomicrographs of mouse carotid arteries after injury (A through H). VerHoeff elastin stain 28 days after injury: vehicle (A); low-dose simvastatin (B); high-dose simvastatin (original magnification  $\times 38$ ) (C); vehicle (D); low-dose simvastatin (E); and high-dose simvastatin ( $\times 150$ ) (F). Neointima separates the internal elastic lamina (arrows) from the lumen. Apoptotic (TUNEL-positive) cells 7 days after injury: vehicle (G); high-dose simvastatin ( $\times 150$ ) (H). Simvastatin and Akt signaling (I). Aortae were harvested from mice treated with simvastatin or vehicle and incubated with PDGF-BB. Aortic lysates were immunoblotted sequentially using antibodies to Akt and Phospho-Akt (Ser473).

( $P=0.012$ ) and 60% ( $P=0.011$ ), respectively (Figure, panels A through F, Table). Medial area was unaffected by simvastatin treatment. I:M at 28 days in control mice was  $0.64 \pm 0.37$  and was reduced 50% by low-dose ( $P=0.036$ ) and 62% by high-dose ( $P=0.012$ ) simvastatin. Intimal and medial thickening were accompanied by progressive vessel enlargement (ie, positive remodeling), as determined by external elastic lamina area measurements over time, which was comparable in vehicle- and simvastatin-treated mice.

We assessed cellular proliferation by quantifying incorporation of BrdU. Substantial proliferation was observed 7 days after injury in control vessels (19.2% of medial cells), and proliferation was still evident at 28 days (4.6% of intimal cells). Low- and high-dose simvastatin reduced medial proliferation at 7 days by 38% and 43%, respectively, and intimal proliferation at 28 days by 63% ( $P=0.042$ ) and 59% ( $P=0.050$ ) (Table).

Immunohistochemistry was performed to identify the cellular components of the neointima 28 days after injury. In vehicle-treated animals, 48% of cells were SMCs ( $\alpha$ -actin-positive) and 34% were monocytes or macrophages (CD45- and Mac3-positive). Altered leukocyte accumulation within vessels was observed in simvastatin-treated mice. Inflammatory cells (CD45-positive) invading the intima were reduced

by 25% to 34% ( $P<0.05$ ) at 7 days and 29% to 39% ( $P<0.03$ ) at 28 days in simvastatin-treated compared with control mice.

### Simvastatin Increases Apoptosis

Because statins prevent isoprenylation of Rho proteins and their translocation to the membrane fraction, and because there is increasing evidence that Rho activates signals that regulate apoptosis,<sup>10</sup> we investigated the effects of simvastatin on apoptosis after injury. Low- and high-dose simvastatin significantly increased the number of apoptotic (TUNEL-positive) cells in the intima (by 197% and 263%, respectively) and media (168% and 232%, respectively) at 7 days compared with control (Table, Figure, panels G and H).

To identify a biochemical correlate of simvastatin action promoting apoptosis, we examined signaling of the survival factor, Akt, in arteries from mice treated with simvastatin. Injured carotid arteries are completely devoid of endothelium and lined with a platelet monolayer.<sup>5</sup> Therefore, we examined PDGF-induced phosphorylation and activation of Akt by Western blot analysis of aortic samples from mice treated with low- and high-dose simvastatin or vehicle for 7 days. PDGF-induced phosphorylation of Akt was impaired in the aortae of simvastatin-treated mice (Figure, panel I).

## Discussion

Our study provides definitive in vivo evidence that simvastatin inhibits neointimal thickening in a cholesterol-independent manner accompanied by reduced vascular inflammation and proliferation and increased apoptosis. These results establish a role for statins in inhibiting neointimal formation after experimental angioplasty in a setting in which simvastatin did not alter plasma lipids.

Restenosis is a complex cascade of wound-healing responses to vascular injury, characterized by thrombosis, inflammation, cellular proliferation/migration, and extracellular matrix deposition. Increasing evidence suggests that antiinflammatory<sup>7</sup> and antiproliferative<sup>11</sup> effects of statins play important roles in attenuating atherosclerosis,<sup>1,7</sup> transplant vasculopathy,<sup>12</sup> and restenosis.<sup>3</sup> Statins inhibit the synthesis of isoprenoid intermediates that are important lipid attachments for signaling proteins, including Ras and the Rho family of small GTP-binding proteins (eg, Rho, Rac, and Cdc42).<sup>4</sup> Rho is implicated in various biological functions relevant to vascular injury, including cellular migration, proliferation, and survival.<sup>10,13</sup> Statins attenuate vascular SMC proliferation in vitro by decreasing Rho geranylgeranylation and membrane localization and inhibiting Cdk activity.<sup>11</sup>

We provide biochemical evidence that PDGF-induced phosphorylation of Akt is inhibited in aortic tissue from simvastatin-treated mice. Akt functions as an antiapoptotic protein, protecting against cell death induced by growth factor withdrawal or ischemia-reperfusion injury.<sup>14</sup> The effects of statins on Akt signaling seem to be tissue-specific. Statins rapidly activate Akt signaling in endothelial cells, enhance phosphorylation of endothelial NO synthase, and inhibit apoptosis.<sup>15</sup> In contrast, statins impair Akt activation in SMCs,<sup>16</sup> leading to diminished SMC proliferation and induction of apoptosis via effects on phosphatidylinositol-3 kinase or Rho.<sup>11</sup> These divergent actions of statins on Akt activation in endothelial cells and SMCs may act in synchrony to diminish neointimal thickening after denuding injury.

Prior clinical trials of statins after balloon angioplasty have failed to show a reduction in restenosis,<sup>2</sup> likely because of the predominant role of vascular remodeling rather than neointimal thickening in this setting.<sup>17</sup> However, recent studies of statin use after stenting, with minimal remodeling and profound neointimal thickening,<sup>17</sup> have suggested benefit.<sup>3</sup>

Our results support the hypothesis that simvastatin has antiinflammatory, antiproliferative, and proapoptotic actions relevant to preventing restenosis. Although mechanisms are not yet established, additional research may lead to new

understanding of the actions of statins, additional impetus for broad statin use after vascular intervention independent of lipid profile, and novel therapies for preventing restenosis.

## Acknowledgments

This research was supported by National Institutes of Health Grants R01 HL57506 (to Dr Simon), R01 DK55656 (to Dr Simon), and K08 HL03104 (to Dr Rogers) and a Merck Medical School Grant (to Dr Simon).

## References

1. Bucher HC, Griffith LE, Guyatt GH. Systematic review on the risk and benefit of different cholesterol-lowering interventions. *Arterioscler Thromb Vasc Biol.* 1999;19:187-195.
2. Weintraub WS, Boccuzzi SJ, Klein JL, et al. Lack of effect of lovastatin on restenosis after coronary angioplasty: Lovastatin Restenosis Trial Study Group. *N Engl J Med.* 1994;331:1331-1337.
3. Walter DH, Schachinger V, Elsner M, et al. Effect of statin therapy on restenosis after coronary stent implantation. *Am J Cardiol.* 2000;85:962-968.
4. Casey PJ. Protein lipidation in cell signaling. *Science.* 1995;268:221-225.
5. Simon DI, Chen Z, Seifert P, et al. Decreased neointimal formation in Mac-1<sup>-/-</sup> mice reveals a role for inflammation in vascular repair after angioplasty. *J Clin Invest.* 2000;105:293-300.
6. Endres M, Laufs U, Huang Z, et al. Stroke protection by 3-hydroxy-3-methylglutaryl (HMG)-CoA reductase inhibitors mediated by endothelial nitric oxide synthase. *Proc Natl Acad Sci U S A.* 1998;95:8880-8885.
7. Sparrow CP, Burton CA, Hernandez M, et al. Simvastatin has anti-inflammatory and antiatherosclerotic activities independent of plasma cholesterol lowering. *Arterioscler Thromb Vasc Biol.* 2001;21:115-121.
8. DiChiara MR, Kiely JM, Gimbrone MA Jr, et al. Inhibition of E-selectin gene expression by transforming growth factor  $\beta$  in endothelial cells involves coactivator integration of Smad and nuclear factor  $\kappa$ B-mediated signals. *J Exp Med.* 2000;192:695-704.
9. Endo A, Tsujita Y, Kuroda M, et al. Effects of ML-236B on cholesterol metabolism in mice and rats: lack of hypocholesterolemic activity in normal animals. *Biochim Biophys Acta.* 1979;575:266-276.
10. van Nieuw Amerongen GP, van Hinsbergh VW. Cytoskeletal effects of rho-like small guanine nucleotide-binding proteins in the vascular system. *Arterioscler Thromb Vasc Biol.* 2001;21:300-311.
11. Laufs U, Marra D, Node K, et al. 3-Hydroxy-3-methylglutaryl-CoA reductase inhibitors attenuate vascular smooth muscle cell proliferation by preventing rho GTPase-induced down-regulation of p27Kip1. *J Biol Chem.* 1999;274:21926-21931.
12. Kobashigawa JA, Katznelson S, Laks H, et al. Effect of pravastatin on outcomes after cardiac transplantation. *N Engl J Med.* 1995;333:621-627.
13. Shibata R, Kai H, Seki Y, et al. Role of Rho-Associated kinase in neointima formation after vascular injury. *Circulation.* 2001;103:284-289.
14. Fujio Y, Nguyen T, Wencker D, et al. Akt promotes survival of cardiomyocytes in vitro and protects against ischemia-reperfusion injury in mouse heart. *Circulation.* 2000;101:660-667.
15. Kureishi Y, Luo Z, Shiojima I, et al. The HMG-CoA reductase inhibitor simvastatin activates the protein kinase Akt and promotes angiogenesis in normocholesterolemic animals. *Nat Med.* 2000;6:1004-1010.
16. Weiss RH, Ramirez A, Joo A. Short-term pravastatin mediates growth inhibition and apoptosis, independently of Ras, via the signaling proteins p27Kip1 and p13 kinase. *J Am Soc Nephrol.* 1999;10:1880-1890.
17. Hoffmann R, Mintz GS, Dussaillant GR, et al. Patterns and mechanisms of in-stent restenosis: a serial intravascular ultrasound study. *Circulation.* 1996;94:1247-1254.



# Atherosclerosis and Lipoproteins

## Troglitazone Inhibits Formation of Early Atherosclerotic Lesions in Diabetic and Nondiabetic Low Density Lipoprotein Receptor-Deficient Mice

Alan R. Collins, Woerner P. Meehan, Ulrich Kintscher, Simon Jackson, Shu Wakino, Grace Noh, Wulf Palinski, Willa A. Hsueh, Ronald E. Law

**Abstract**—Peroxisome proliferator-activated receptor- $\gamma$  (PPAR $\gamma$ ) is a ligand-activated nuclear receptor expressed in all of the major cell types found in atherosclerotic lesions: monocytes/macrophages, endothelial cells, and smooth muscle cells. In vitro, PPAR $\gamma$  ligands inhibit cell proliferation and migration, 2 processes critical for vascular lesion formation. In contrast to these putative antiatherogenic activities, PPAR $\gamma$  has been shown in vitro to upregulate the CD36 scavenger receptor, which could promote foam cell formation. Thus, it is unclear what impact PPAR $\gamma$  activation will have on the development and progression of atherosclerosis. This issue is important because thiazolidinediones, which are ligands for PPAR $\gamma$ , have recently been approved for the treatment of type 2 diabetes, a state of accelerated atherosclerosis. We report herein that the PPAR $\gamma$  ligand, troglitazone, inhibited lesion formation in male low density lipoprotein receptor-deficient mice fed either a high-fat diet, which also induces type 2 diabetes, or a high-fructose diet. Troglitazone decreased the accumulation of macrophages in intimal xanthomas, consistent with our in vitro observation that troglitazone and another thiazolidinedione, rosiglitazone, inhibited monocyte chemoattractant protein-1-directed transendothelial migration of monocytes. Although troglitazone had some beneficial effects on metabolic risk factors (in particular, a reduction of insulin levels in the diabetic model), none of the systemic cardiovascular risk factors was consistently improved in either model. These observations suggest that the inhibition of early atherosclerotic lesion formation by troglitazone may result, at least in part, from direct effects of PPAR $\gamma$  activation in the artery wall. (*Arterioscler Thromb Vasc Biol.* 2001;21:365-371.)

**Key Words:** atherosclerosis ■ diabetes mellitus ■ pharmacology

Peroxisome proliferator-activated receptor- $\gamma$  (PPAR $\gamma$ ), a nuclear receptor, is expressed in all major cell types participating in vascular injury: endothelial cells (ECs), macrophages, and vascular smooth muscle cells (VSMCs).<sup>1-6</sup> Activation of this receptor in vitro inhibits inflammatory processes, including cytokine production and expression of NO synthase.<sup>2</sup> In early clinical investigations, ligands of PPAR $\gamma$ , such as thiazolidinediones (TZDs), have also been reported to improve endothelium-dependent vasodilation, suggesting that PPAR $\gamma$  activation enhances NO production and protects against vascular injury.<sup>7,8</sup> Activation of PPAR $\gamma$  also inhibits 2 other processes critical for vascular lesion formation, cell proliferation, and migration.<sup>3,5,9,10</sup> In vivo, 2 TZDs, troglitazone (TRO) and pioglitazone, significantly reduced arterial neointimal hyperplasia after endothelial injury in rats.<sup>11-13</sup> In such balloon-catheterized arteries, neointima formation essentially reflects increased migration and proliferation of VSMCs, a major contributor to the growth of

See page 295

atherosclerotic lesions. TRO also inhibited neointima formation in stents placed in the coronary arteries of patients with type 2 diabetes.<sup>14</sup>

We and others have recently demonstrated that PPAR $\gamma$  activation by TZDs and 15-deoxy- $\Delta^{12,14}$ -prostaglandin J<sub>2</sub> inhibits EC expression of vascular cell adhesion molecule-1, which mediates monocyte adherence to the endothelial surface.<sup>4,15</sup> Because inflammation, dysregulated growth, and migration of monocytes and VSMCs play an important role in the development of atherosclerosis, we hypothesized that PPAR $\gamma$  activation in cells of the vasculature would inhibit the atherosclerotic process. On the other hand, TZDs also stimulate conversion of macrophages into foam cells; therefore, ligand-dependent activation of PPAR $\gamma$  has been postulated to promote atherosclerosis.<sup>16</sup>

Received August 10, 2000; revision accepted December 1, 2000.

From the Division of Endocrinology, Diabetes, and Hypertension (A.R.C., W.P.M., U.K., S.J., S.W., G.N., W.A.H., R.E.L.), Department of Medicine, UCLA School of Medicine, Los Angeles, Calif; the Molecular Biology Institute (W.A.H., R.E.L.), Los Angeles, Calif; the Department of Medicine/Cardiology (U.K.), Virchow-Klinikum, Humboldt University, and the German Heart Institute (U.K.), Berlin, Germany; and the Department of Medicine (W.P.), UCSD, La Jolla, Calif.

Correspondence to Ronald E. Law, PhD, University of California, Los Angeles, Division of Endocrinology, Diabetes, and Hypertension, 900 Veteran Ave, Suite 24-130, Box 957073, Los Angeles, CA 90095. E-mail rlaw@mednet.ucla.edu

© 2001 American Heart Association, Inc.

*Arterioscler Thromb Vasc Biol.* is available at <http://www.atvbaha.org>

The impact of TZDs on atherosclerosis is a critical issue. TZDs improve insulin-mediated glucose uptake and are used extensively in the treatment of insulin resistance and type 2 diabetes mellitus.<sup>17</sup> Coronary artery disease mortality is increased 2- to 4-fold in type 2 diabetes.<sup>18</sup> Atherosclerosis is the major cause of demise in people with diabetes; therefore, it is important to determine the action of any antidiabetic drug on the atherosclerotic process.

To determine whether PPAR $\gamma$  activation has proatherogenic or antiatherogenic effects, we administered TRO to male LDL receptor-deficient (LDLR<sup>-/-</sup>) mice fed either a high-fat or a high-fructose atherogenic diet. Both models develop substantial hypercholesterolemia and macrophage-laden lesions, designated intimal xanthomata, which do not normally progress to mature atherosclerotic plaques.<sup>19</sup> In addition, the high-fat diet induces hyperglycemia and hyperinsulinemia in the LDLR<sup>-/-</sup> mouse, making it also a model of type 2 diabetes.<sup>20,21</sup> In contrast, fructose does not increase glucose or insulin in this model<sup>21</sup> and, therefore, was useful because the effects of TZDs on atherosclerosis could be studied in the absence of improvements in insulin action.

## Methods

### Transendothelial Monocyte Migration

THP-1 cells ( $5 \times 10^4$ ), a human monocytic leukemia cell line, were added to a human aortic EC monolayer covering a gelatin-coated 8- $\mu$ m porous membrane and incubated for 30 minutes at 37°C to facilitate their attachment. Cells were then pretreated with the indicated ligands or vehicle (dimethyl sulfoxide) for 30 minutes at 37°C. Migration was induced by the addition of monocyte chemoattractant protein-1 (MCP-1, 50 ng/mL) to the lower compartment. After 90 minutes, nonmigrating THP-1 cells and human aortic ECs were removed with a cotton tip, and the membranes were fixed and stained with the Quik-Diff Stain Set (DADE, Miami, Fla) to identify migrated cells. The number of migrated cells was determined per  $\times 320$  high-power field. Experiments were performed in duplicate and were repeated at least 3 times.

### Western Blots

Western immunoblots were performed as previously described.<sup>10</sup> Membranes were incubated with rabbit polyclonal antibodies (1:1000 dilution, New England Biolabs) that recognize either (1) total extracellular signal-regulated kinase (ERK) or (2) ERK phosphorylated on threonine 202 and tyrosine 204.

### Animals and Diets

Male LDLR<sup>-/-</sup> mice were obtained (C57BL/6J-Ldlr<sup>tm1J</sup>, stock No. 002207, Jackson Laboratory, Bar Harbor, Me) and were group-housed under a 12-hour light and 12-hour dark regimen. All animal protocols were approved by the UCLA Animal Research Committee and complied with all federal, state, and institutional regulations. At 3 months of age, the mice were randomly assigned to 1 of 5 dietary regimens: (1) chow (Harlan Teklad 8604), (2) high-fat complex carbohydrate (Research Diets), (3) high-fat complex carbohydrate with 4 g TRO/kg of food, (4) high fructose (Research Diets), or (5) high fructose with 4 g TRO/kg of food. The high-fat diet consisted of 21% fat, 20% protein, 50% carbohydrate, and 0.15% cholesterol. Our high-fat diet differed from those commonly used to study atherogenesis in LDLR<sup>-/-</sup> mice in that the majority of the nonfat energy came from complex carbohydrate sources instead of sucrose. The high-fructose diet contained 4% fat, 16% protein, 71% fructose, and 0.15% cholesterol. Sources of fat in the diets were corn oil (1% in all diets) and anhydrous milk fat (3% in the fructose diets and 20% in the high fat diets). Mice and feed were weighed weekly, and the rate of consumption of drug was computed. The mice were fed for a period of 12 weeks.

### Metabolic Measurements

Blood samples from the retro-orbital sinus were obtained from the mice before the beginning of treatment and every month thereafter and from the abdominal vena cava at euthanasia. Mice were fasted overnight before the collection of the blood samples. Plasma glucose was measured by glucose oxidase reaction (Beckman Glucose Analyzer 2, Beckman Instruments). Plasma lipids were measured by the UCLA Lipid Analysis Laboratory. Plasma insulin was determined by ELISA. Blood pressures were obtained by using an indirect tail-cuff method with a controlled temperature chamber (IITC, Inc) by a technician blinded to the treatment groups.

### Vessel Preparation and Image Analysis

Mice were euthanized and perfused with 7.5% sucrose in 4% paraformaldehyde. Aortas were dissected out, split longitudinally, pinned flat in a dissection pan, and stained with Sudan IV to detect lipids and determine lesion area. Images were captured by use of a Sony 3-CCD video camera and analyzed by a single technician who was blinded to the study protocol and used ImagePro image analysis software. The extent of lesion formation is expressed as the percentage of the total aortic surface area covered by lesions.

### Cross Sections: Determination of Intimal Macrophage Content

The largest lesions from the aortic arch were excised and embedded in paraffin. The avidin-biotin-peroxidase complex technique for immunostaining was used. Macrophages were stained by using monoclonal antibody to CD68 (titer 1:100, KP1 clone, M0814, Dako Corp). Nonimmune serum was used as a control. Primary antibody incubations were performed in 1% BSA/2% goat serum containing PBS for 60 minutes. Biotinylated rabbit anti-mouse (Dako) was applied; incubation with a streptavidin-peroxidase complex followed. Peroxidase activity was detected with the use of diaminobenzidine tetrahydrochloride as a chromogen. Slides were then counterstained with hematoxylin. Images of the stained sections were analyzed by using the software described above. After tracing the intimal area to be measured with a cursor, 5 pixels of color, which defined the anti-CD68 stain, were sampled by the operator. The area encompassed by the pixels, which was not contiguous, in the color range for anti-CD68 was then computed automatically by the software. This approach has been successfully used by Shi et al<sup>22</sup> to quantify lesional macrophages in a mouse model of transplant arteriosclerosis.

### Statistical Analysis

Statistical analysis was performed by using 2-factorial ANOVA with Student-Newman-Keuls to determine the differences between individual group means.

## Results

### TRO Inhibits Monocyte Migration

VSMC migration and proliferation play an important atherogenic role in the progression of fatty streaks toward more advanced atherosclerotic lesions, such as transitional lesions and classical atheromas. We have previously shown that PPAR $\gamma$  ligands inhibit ERK mitogen-activated protein kinase (MAPK)-dependent migration of VSMCs.<sup>10,11</sup> However, in the earliest stages of atherosclerotic lesions, recruitment of adherent monocytes through their migration into the subendothelium and their phenotypic transformation to macrophages and foam cells play a far greater role than VSMCs in humans and in murine models.<sup>23</sup>

To investigate whether TRO-mediated PPAR $\gamma$  activation affects monocyte recruitment and to further explore its mechanism, we carried out a series of in vitro experiments before our in vivo studies. MCP-1 is an important in vivo migration factor promoting the subendothelial accumulation of monocytes. TRO inhibited MCP-1-directed transmigration

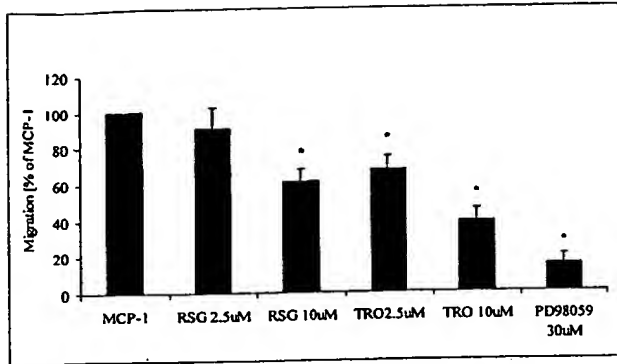


**Figure 1.** PPAR $\gamma$  ligands inhibit MCP-1-directed transendothelial migration of monocytes. Migration of THP-1 monocytes through ECs was determined by using a modified Boyden chamber assay as described in Methods. The number of migrating cells was quantified by microscopy with the use of high-power fields. Results represent 3 independent experiments performed in duplicate. \* $P < 0.05$  vs MCP-1 alone.

tion of THP-1 monocytes by  $32.7 \pm 6.5\%$  at  $2.5 \mu\text{mol/L}$  and by  $61.4 \pm 6.7\%$  at  $10 \mu\text{mol/L}$  (Figure 1). TRO contains a vitamin E moiety that may confer an antioxidant activity that can inhibit monocyte recruitment and endothelial expression of adhesion molecules. However, rosiglitazone (RSG), another PPAR $\gamma$  ligand that lacks antioxidant activity, also inhibited monocyte transmigration, albeit with a lesser potency than TRO (Figure 1). Inhibition of monocyte transmigration by TRO, therefore, is likely to be mediated at least in part through PPAR $\gamma$ .

MCP-1 rapidly induced ERK activation, reaching a peak at 5 minutes, which was blocked by PD98059, an inhibitor of MAPK ERK kinase (MEK, an upstream kinase), which phosphorylates and activates ERK (Figure 2). PD98059 attenuated MCP-1-directed transmigration by  $84.8 \pm 4.8\%$ . In combination, these data suggest that activation of PPAR $\gamma$  in monocytes may inhibit their migration by interfering with ERK-MAPK signaling, although the precise mechanism remains to be determined.

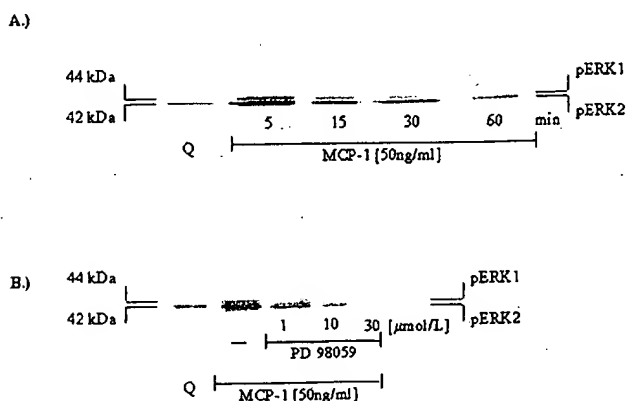


**Figure 2.** MCP-1 activates the ERK-MAPK pathway in THP-1 human monocytes. A, Quiescent (Q) THP-1 cells were stimulated with MCP-1 (50 ng/mL) for 5 minutes. Whole-cell protein extracts were immunoblotted with a phosphospecific ERK1 (pERK1)/ERK2 (pERK2) MAPK antibody. A representative blot of 3 different experiments is shown. B, Conditions were the same as in panel A except that cells were treated with MEK inhibitor PD98059 (1 to  $30 \mu\text{mol/L}$ ) or vehicle (dimethyl sulfoxide, -) before and during stimulation with MCP-1 (50 ng/mL). A representative blot of 3 different experiments is shown.

## TRO Inhibits Intimal Macrophage Accumulation and Lesion Formation in Male LDLR $^{-/-}$ Mice

LDLR $^{-/-}$  mice that were fed a regular chow diet develop few lesions across the surface of the aorta. Male 3-month-old LDLR $^{-/-}$  mice were placed on either a high-fat or high-fructose diet to induce atherosclerosis. LDLR $^{-/-}$  males were used in the present study because they develop hyperglycemia and become diabetic on a high-fat diet but remain normoglycemic when fed a high-fructose diet. Moreover, males develop twice the level of surface lesions as do females,<sup>24</sup> and their use obviates the potentially confounding influence of the vascular protection in females afforded by estrogen. Comparison of the impact of TRO on atherogenesis in these 2 dietary models was undertaken to distinguish any activity of PPAR $\gamma$  to normalize metabolic abnormalities accompanying diabetes that contribute to high-fat-induced xanthomata formation from any direct effects on the vasculature. To assess the impact of TRO on aortic lesions, 1 high-fat diet group and 1 high-fructose diet group received TRO at 400 mg/kg body wt per day from drugs pelleted into the atherogenic diets. This dose of TRO was chosen because we previously demonstrated its efficacy in inhibiting intimal hyperplasia in rats after balloon injury.<sup>11</sup>

The en face method, which makes use of computer-assisted analysis of color images of Sudan IV-stained lipid-containing material in the entire aorta, was used to determine the percentage of surface area affected by lesions.<sup>24</sup> Male LDLR $^{-/-}$  mice on normal chow for 3 months had  $<0.20\%$  lesions (Figure 3A). The high-fat diet increased the amount of surface lesions after 3 months to  $3.90 \pm 0.16\%$  ( $n=8$ , Figure 3B). TRO inhibited the high-fat-induced lesions by 30% ( $2.76 \pm 0.36\%$  of the aortic surface,  $n=8$ ,  $P < 0.02$ ; Figure 3C). Similar to Merat et al,<sup>21</sup> we noted that the high-fructose diet was more atherogenic than the high-fat diet, causing  $8.42 \pm 0.94\%$  lesions ( $n=17$ , Figure 3D). TRO reduced lesions in fructose-fed LDLR $^{-/-}$  males by 42% ( $4.90 \pm 0.65\%$ ,  $n=14$ ,  $P < 0.01$ ; Figure 3E). Quantitative results are summarized in Figure 4.

TRO-treated male LDLR $^{-/-}$  mice fed either the high-fat or high-fructose diet for 3 months developed lesions that contained substantially fewer CD68-staining macrophages (Figure 5A through 5D). Lesions induced by a high-fat diet contained  $39.1 \pm 6.8\%$  macrophages (percent of cross-sectional intimal area) compared with  $13.3 \pm 4.9\%$  ( $P < 0.01$ ) in mice administered TRO (Figure 5E). Similar results were obtained for males fed the high-fructose diet, where TRO decreased macrophage accumulation from  $40.4 \pm 3.5\%$  to  $17.1 \pm 1.7\%$  ( $P < 0.01$ , Figure 5E). The lesions in the TRO-fed animals tended to be smaller in volume than those in males not fed TRO. The relative macrophage content in the larger lesions (not treated with TRO) exceeded the content in the smaller lesions (treated with TRO) by 140% to 200%. The reduction in macrophage accumulation in the lesions of TRO-treated animals is unlikely to be the result of their being an earlier lesion stage, because the relative macrophage content is known to be greatest in the smaller (ie, early-stage) lesions.

## Effect of TRO on Metabolic Parameters

All metabolic measurements determined on blood samples drawn before treatment were similar in all groups (Tables 1

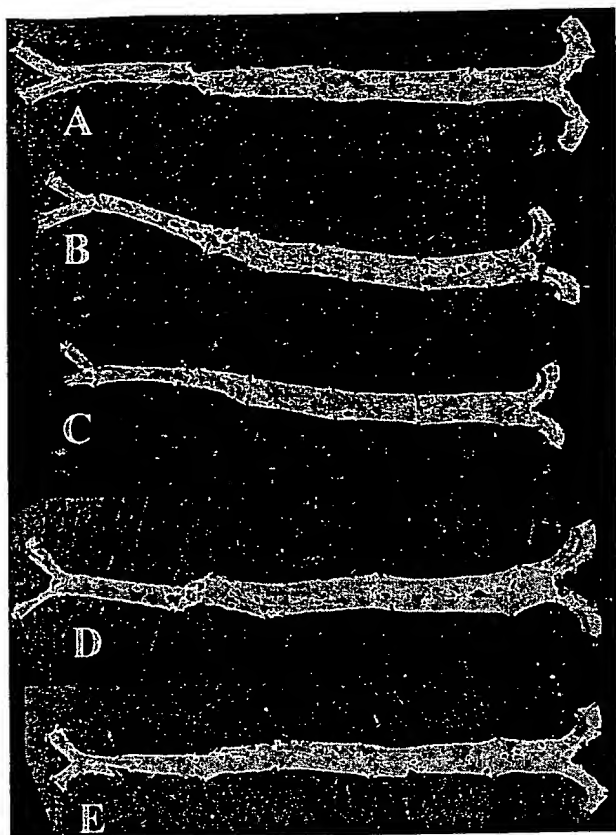


**Figure 3.** TRO attenuates atherosclerosis in male  $LDLR^{-/-}$  mice. The aorta is stained by Sudan IV to detect the lipids present in lesions. A, Chow diet. B, High-fat diet. C, High-fat diet and TRO. D, High-fructose diet. E, High-fructose diet and TRO.

and 2). In accordance with previous studies on male  $LDLR^{-/-}$  mice, we found that a high-fat diet induced diabetes<sup>20,21</sup> (Table 1). Glucose levels progressively increased throughout

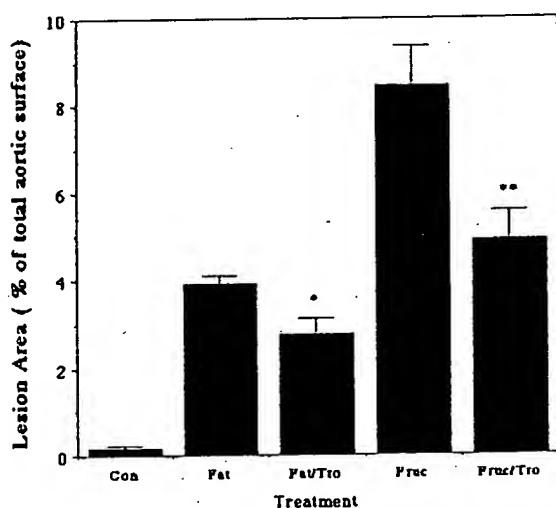


**Figure 4.** Quantification of the antiatherogenic activity of TRO in male  $LDLR^{-/-}$  mice. Mean atherosclerotic surface lesion areas were determined in mice fed a normal chow, high-fat, or high-fructose diet in the absence or presence of TRO for 3 months. Image analysis and quantification of the percentage of the total aortic area staining for Sudan IV were performed by using computer-assisted image analysis. TRO produced a significant decrease in mice fed a high-fat (30% decrease,  $*P<0.05$ ) and high-fructose (42% decrease,  $**P<0.05$ ) diet.

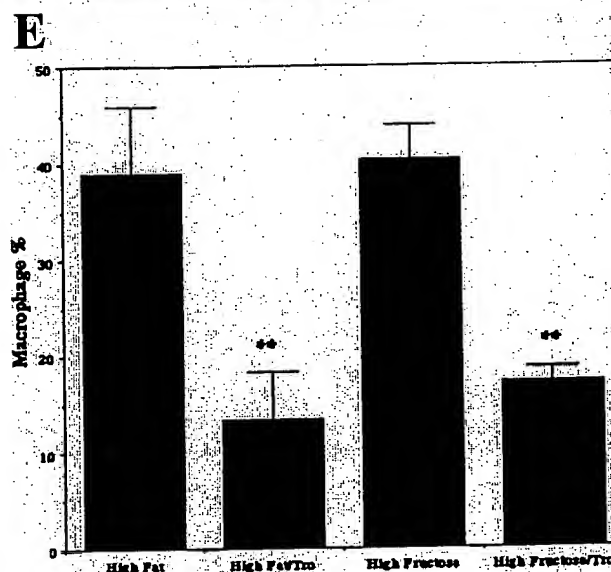
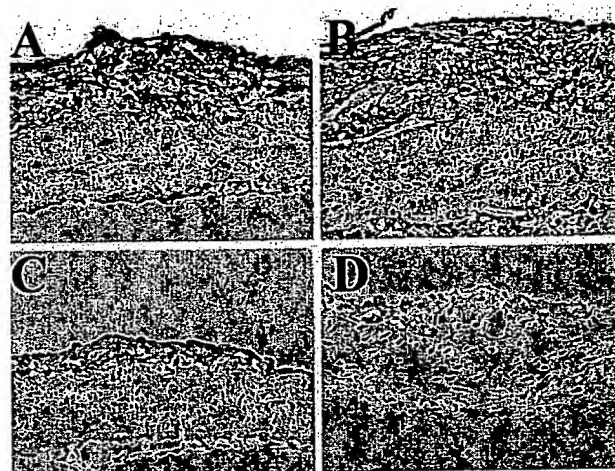


**Figure 5.** TRO inhibits accumulation of lesional macrophages. Sections from the aortic arch were immunostained by using antibody against CD68 to detect macrophages. Quantification of the percentage of the intimal area staining ( $**P<0.05$ ) for CD68 was performed by computer-assisted image analysis. A, High-fat diet ( $n=6$ ). B, High-fat diet and TRO ( $n=6$ ). C, High-fructose diet ( $n=6$ ). D, High-fructose diet and TRO ( $n=6$ ). E, Quantification of the macrophage content.

the study, reaching a maximum of 285 mg/dL at 3 months compared with 148 mg/dL for mice on normal chow. The fat-fed males were also hyperinsulinemic ( $1198 \pm 149$  versus  $664 \pm 113$  pg/mL on normal chow), consistent with the development of early-stage type II diabetes. Although TRO did not decrease hyperglycemia in high-fat-fed male mice, TRO administration completely normalized their plasma insulin levels. In marked contrast, mice on a high-fructose diet had normal fasting plasma glucose and insulin levels, which were not altered by TRO.

$LDLR^{-/-}$  males developed severe hypercholesterolemia on either the high-fat or high-fructose diet, achieving levels 3- to 4-fold greater than those in animals maintained on regular chow (Table 2). TRO lowered total plasma cholesterol by 27% in males on the high-fructose diet but had no effect on the high-fat-fed mice. Triglycerides were elevated in the high-fat-fed males but not in the high-fructose group; TRO

TABLE 1. Plasma Glucose and Insulin Levels and Final Body Weights

	Chow Diet	High-Fat Diet	High-Fat Diet/TRO	High-Fructose Diet	High-Fructose Diet/TRO
Glucose, mg/dL					
Start	158.7±14.63	173.2±12.12	169.4±7.98	137.8±11.53	148.5±27.67
1 mo	148.9±6.60	190.5±10.92	155.1±9.13*	121.2±6.44	114.8±4.55
2 mo	144.8±10.96	201.1±9.09	189.6±27.37	128.6±13.09	121.89±17.32
3 mo	148.5±14.87	284.8±25.00	268.9±13.90	152.3±15.80	181.9±23.47
Insulin, pg/mL					
3 mo	664.7±113.62	1198.7±149.81	691.2±109.14†	304.4±47.49	278.7±37.9
Body weight, g	27.3±0.56	42.5±0.66	37.0±0.89†	25.9±0.37	24.2±0.34

Values are mean±SEM.

\* $P<0.05$  vs high-fat; † $P<0.01$  vs high-fat diet.

did not alter triglycerides in either model. HDL cholesterol (HDL-C) decreased with both of the diets, compared with normal chow, as frequently reported.<sup>3</sup> TRO further lowered the HDL-C in the high-fat-fed males but increased it in the high-fructose-fed group. Plasma free fatty acid levels increased in males on the high-fat diet but not in those on the high-fructose diet; TRO decreased free fatty acid levels in both models.

### Discussion

The most significant finding of the present study is that TRO inhibited lesion formation in a type 2 diabetic mouse model and a nondiabetic LDLR<sup>-/-</sup> mouse model of intimal xanthomata. Mice fed the high-fat diet developed extensive hypercholesterolemia that was not affected by TRO. These mice also gained substantial weight and showed an

increase in circulating free fatty acid levels, which probably contributed to their insulin resistance, hyperinsulinemia, and fasting hyperglycemia.<sup>25</sup> The increase in triglycerides and decrease in HDL-C are consistent with insulin resistance. TRO decreased circulating insulin but did not affect glucose in this model. The same has been reported in humans with type 2 diabetes, of whom 20% treated with TRO showed no improvement in glucose control, but all demonstrated improved insulin sensitivity.<sup>26</sup> In contrast to the response in humans, TRO did not alter triglycerides and further decreased HDL-C. Mice fed the high-fructose diet also developed severe hypercholesterolemia but did not gain weight or develop hyperinsulinemia or elevations in free fatty acids or triglycerides. In this model, TRO decreased the free fatty acids, increased HDL-C, and decreased total cholesterol.

TABLE 2. Plasma Lipid Levels

	Chow Diet	High-Fat Diet	High-Fat Diet/TRO	High-Fructose Diet	High-Fructose Diet/TRO
Total Cholesterol, mg/dL					
Start	292.2±14.63	277.7±5.77	278.8±9.24	321.8±20.87	328.0±18.32
1 mo	316.0±11.51	583.3±72.18	541.9±62.22	489.1±24.58	360.8±21.37†
2 mo	315.8±10.26	1307.0±110.11	1173.0±122.11	1052.3±33.78	816.7±25.02‡
3 mo/final	317.9±17.79	1341.9±52.14	1313.63±28.83	1167.7±46.17	862.1±23.70‡
HDL-C, mg/dL					
Start	110.6±4.51	111.2±1.87	109.9±3.07	121.2±2.59	113.5±8.39
1 mo	111.2±3.19	108.2±1.93	108.9±2.65	104.2±3.08	106.6±4.58
2 mo	112.1±4.06	94.4±3.52	98.2±12.66	100.4±3.56	105.3±4.76
3 mo	112.4±5.00	104.8±7.84	81.8±6.86*	90.1±4.48	108.4±5.10†
Free fatty acids, mg/dL					
Start	67.1±2.82	63.5±1.82	58.2±2.67	91.0±6.96	82.5±4.38
1 mo	69.4±2.97	70.4±2.11	66.6±2.67	66.9±4.90	71.2±3.75
2 mo	65.7±2.87	88.6±7.32	74.2±4.19	68.7±3.67	65.8±3.57
3 mo	61.7±3.68	72.5±2.42	57.1±2.07*	61.7±1.52	53.1±2.81†
Triglycerides, mg/dL					
Start	122.0±4.43	109.1±5.32	101.1±5.72	84.8±5.09	111.83±16.00
1 mo	126.0±11.1	124.3±7.00	113.6±7.48	85.8±4.98	94.0±6.47
2 mo	86.9±4.98	156.6±30.55	191.8±64.47	81.2±5.98	79.8±6.47
3 mo	71.6±6.92	141.8±7.84	159.1±19.79	75.3±6.89	69.0±4.85

Values are mean±SEM.

\* $P<0.01$  vs high-fat diet; † $P<0.05$  vs high-fructose diet, and ‡ $P<0.001$  vs high-fructose diet.

Despite the difference in metabolic responses between the diabetic and nondiabetic animals, both hypercholesterolemic models responded to TRO with decreased lesion formation. These results suggest that TRO has direct vascular effects, separate from its metabolic effects, that decrease the atherosclerotic process. Alternatively, the antiatherogenic effects of TRO in the 2 different models might involve the collection of distinct metabolic processes. For example, hemodynamic effects of TRO related to its reported activity to lower blood pressure in animal models and in humans could also impact pathophysiological processes in high-fat- and high-fructose-fed LDLR<sup>-/-</sup> mice.<sup>27-30</sup> All major cell types contributing to this vascular lesion formation express PPAR $\gamma$ , which provides a mechanism for the direct effect of thiazolidinedione ligands in the vessel wall.<sup>3,5,6,9</sup> Data from *in vitro* experiments had suggested mechanisms by which activation of PPAR $\gamma$  could either accelerate or attenuate the atherosclerotic process.<sup>2-6,9,10,16</sup> The present study provides conclusive evidence that ligand-induced PPAR $\gamma$  activation by TRO reduces intimal xanthomata in murine models.

TRO had several systemic effects that may have contributed to its attenuation of intimal xanthomata. In the diabetic high-fat-fed mouse, TRO lowered insulin and glucose levels and decreased HDLC (which is thought to promote atherogenesis). In the fructose-fed model, TRO decreased total cholesterol and increased HDLC. Our finding that TRO was more potent in suppressing lesion formation in the fructose-fed model compared with the high-fat-fed mice could be due to the observed 27% reduction in total cholesterol. A common effect of TRO in the high-fat-fed and high-fructose-fed LDLR<sup>-/-</sup> models is its suppression of circulating free fatty acid levels. However, increased circulating free fatty acids have not been shown to be an independent risk factor for atherosclerosis.

Inflammation in the vascular wall has clearly emerged as a major culprit in the development of atherosclerosis.<sup>31</sup> Damage to the endothelium and the subsequent recruitment and transendothelial migration of monocytes constitute critical early cellular responses during atherogenesis.<sup>31</sup> Transmigration of monocytes into the subendothelial space is strongly stimulated by the chemokine MCP-1, which is expressed and secreted by ECs and VSMCs. The essential role of MCP-1 in atherogenesis is underscored by a recent study demonstrating that crossing MCP-1-deficient mice into LDLR<sup>-/-</sup> mice attenuated lesion formation by >80%.<sup>32</sup> Our group and others have shown that TRO and other PPAR $\gamma$  ligands inhibit growth factor-directed ERK-MAPK-dependent VSMC migration.<sup>5,10,11</sup> Cell migration requires *de novo* gene transcription that is consistent with PPAR $\gamma$  acting in the nucleus to inhibit this process.<sup>10</sup> In particular, activation of PPAR $\gamma$  can inhibit ERK-MAPK signaling to the nucleus.<sup>11,33</sup> Because MCP-1-directed migration of monocytes is ERK-MAPK dependent, interference with this pathway by TRO could contribute to the observed reduction in intimal xanthomata and lesional macrophages in treated LDLR<sup>-/-</sup> mice.

TRO and another PPAR $\gamma$  ligand, RSG, which does not contain an  $\alpha$ -tocopherol moiety, inhibited MCP-1-directed migration of human monocytes *in vitro*. TRO also consistently decreased intimal macrophage accumulation in the diabetic and nondiabetic mice. These findings support the concept that inhibition of monocyte attachment and migration

in the vessel by TRO may be one of the mechanisms contributing to the reduction of atherogenesis. Although it cannot be ruled out that the reduction of intimal monocytes in part reflected the reduced lesion size induced by TRO treatment, this is unlikely to be the sole explanation, because the relative intimal monocyte/macrophage content is known to be greatest in the early stages (smaller lesions) of atherosclerosis. In any case, the antiatherosclerotic activity of TRO-induced PPAR $\gamma$  activation clearly prevailed over its hypothesized promotion of foam cell formation via increased expression of the scavenger receptor CD36.<sup>16</sup>

Unlike other PPAR $\gamma$  ligands, TRO has an  $\alpha$ -tocopherol (vitamin E) moiety that theoretically could contribute to its antiatherogenic activity through antioxidant effects.<sup>34</sup> Vitamin E has been shown to suppress atherosclerosis in the apoE knockout model, which develops advanced atherosclerotic lesions.<sup>35,36</sup> Whether the dose of vitamin E provided by TRO in the present study is enough to impact lesion formation is doubtful. At 400 mg/kg TRO per day, LDLR<sup>-/-</sup> mice received the equivalent of 8 IU of vitamin E, a dose much lower than that reported to affect atherosclerosis or to significantly protect LDL against oxidation.<sup>35-38</sup> Another line of evidence for the assumption that the effect of TRO on lesion formation was not, to a significant degree, dependent on antioxidant effects is provided by a parallel study demonstrating that 2 other PPAR $\gamma$  ligands, RSG and GW7845, which do not contain the  $\alpha$ -tocopherol moiety, inhibited atherogenesis in the aortic root of male LDLR<sup>-/-</sup> mice fed a high-fat, cholesterol-enriched diet.<sup>39</sup> In addition, the recent Heart Outcomes Prevention Evaluation (HOPE) clinical trial in humans did not show an effect of vitamin E on coronary artery disease events or mortality.<sup>40</sup>

In summary, given the absence of consistent major metabolic changes present in diabetic and nondiabetic mice, it is likely that TRO at least in part decreases early atherosclerotic lesion formation through direct vascular effects. In human subjects with diabetes, who have a high risk for coronary disease, TRO improves insulin resistance and other proatherogenic metabolic parameters, which may improve cardiovascular risk. It is possible that some of the vascular effects observed in our murine models may also be present in humans. Although Li et al<sup>39</sup> and our data demonstrate that PPAR $\gamma$  ligands suppress early atherosclerotic lesions, intimal xanthomata do not inexorably progress to more advanced atherosclerotic plaques; in fact, they often regress.<sup>19</sup> Therefore, determining the effects of PPAR $\gamma$  ligands on more advanced atherosclerotic lesions may prove to be a stronger predictor of their potential clinical benefit. Nonetheless, the present results indicate that an investigation of potential antiatherogenic effects of PPAR $\gamma$  ligands is strongly warranted.

### Acknowledgments

This work was supported by National Institutes of Health grant HL-58328 to Willa A. Hsueh. Shu Wakino was supported by a Mary K. Iacocca Fellowship in Diabetes. Ulrich Kintscher was supported by a Gonda (Goldschmeid) Fellowship in Diabetes.

### References

1. Ricote M, Huang J, Fajas L, Li A, Welch J, Najib J, Witztum JL, Auwerx J, Palinski W, Glass CK. Expression of the peroxisome proliferator-activated receptor gamma (PPARgamma) in human atherosclerosis and



- regulation in macrophages by colony stimulating factors and oxidized low density lipoprotein. *Proc Natl Acad Sci U S A*. 1998;95:7614-7619.
2. Ricote M, Li AC, Willson TM, Kelly CJ, Glass CK. The peroxisome proliferator-activated receptor- $\gamma$  is a negative regulator of macrophage activation. *Nature*. 1998;391:79-82.
  3. Xin X, Yang S, Kowalski J, Gerritsen ME. Peroxisome proliferator-activated receptor  $\gamma$  ligands are potent inhibitors of angiogenesis in vitro and in vivo. *J Biol Chem*. 1999;274:9116-9121.
  4. Jackson SM, Parhami F, Xi XP, Berliner JA, Hsueh WA, Law RE, Demer LL. Peroxisome proliferator-activated receptor activators target human endothelial cells to inhibit leukocyte-endothelial cell interaction. *Arterioscler Thromb Vasc Biol*. 1999;19:2094-2104.
  5. Marx N, Schonbeck U, Lazar MA, Libby P, Plutzky J. Peroxisome proliferator-activated receptor  $\gamma$  activators inhibit gene expression and migration in human vascular smooth muscle cells. *Circ Res*. 1998;83:1097-1103.
  6. Law RE, Goetze S, Xi XP, Jackson S, Kawano Y, Demer L, Fishbein MC, Meehan WP, Hsueh WA. Expression and function of PPAR $\gamma$  in rat and human vascular smooth muscle cells. *Circulation*. 2000;101:1311-1318.
  7. Tack CJ, Ong MK, Lutterman JA, Smits P. Insulin-induced vasodilatation and endothelial function in obesity/insulin resistance: effects of troglitazone. *Diabetologia*. 1998;41:569-576.
  8. Murakami T, Mizuno S, Ohsato K, Moriuchi I, Arai Y, Nio Y, Kaku B, Takahashi Y, Ohnaka M. Effects of troglitazone on frequency of coronary vasospastic-induced angina pectoris in patients with diabetes mellitus. *Am J Cardiol*. 1999;84:92-94. A8. Abstract.
  9. Tanaka T, Itoh H, Do KK, Fukunaga Y, Arai H, Hosoda K. Activation of PPAR $\gamma$  inhibits macrophage proliferation and migration: possible therapeutic effectiveness of thiazolidinediones on diabetic vascular complications. *Diabetes*. 1999;48(suppl 1):A30. Abstract.
  10. Goetze S, Xi XP, Kawano H, Gotlibowski T, Fleck E, Hsueh WA, Law RE. PPAR  $\gamma$ -ligands inhibit migration mediated by multiple chemoattractants in vascular smooth muscle cells. *J Cardiovasc Pharmacol*. 1999;33:798-806.
  11. Law RE, Meehan WP, Xi XP, Graf K, Wuthrich DA, Coats W, Faxon D, Hsueh WA. Troglitazone inhibits vascular smooth muscle cell growth and intimal hyperplasia. *J Clin Invest*. 1996;98:1897-1905.
  12. Igarashi M, Takeda Y, Ishibashi N, Takahashi K, Mori S, Tominaga M, Saito Y. Pioglitazone reduces smooth muscle cell density of rat carotid arterial intima induced by balloon catheterization. *Horm Metab Res*. 1997;29:444-449.
  13. Yoshimoto T, Naruse M, Shizume H, Naruse K, Tanabe A, Tanaka M, Tago K, Irie K, Muraki T, Demura H, et al. Vascular-protective effects of insulin sensitizing agent pioglitazone in neointimal thickening and hypertensive vascular hypertrophy. *Atherosclerosis*. 1999;145:333-340.
  14. Takagi T, Akasaka T, Yamamuro A, Honda Y, Hozumi T, Morioka S, Yoshida K. Troglitazone reduces neointimal tissue proliferation after coronary stent implantation in patients with non-insulin dependent diabetes mellitus: a serial intravascular ultrasound study. *J Am Coll Cardiol*. 2000;36:1529-1535.
  15. Pasceri V, Wu HD, Willerson JT, Yeh ET. Modulation of vascular inflammation in vitro and in vivo by peroxisome proliferator-activated receptor- $\gamma$  activators. *Circulation*. 2000;101:235-238.
  16. Tontonoz P, Nagy L, Alvarez JG, Thomazy VA, Evans RM. PPAR $\gamma$  promotes monocyte/macrophage differentiation and uptake of oxidized LDL. *Cell*. 1998;93:241-252.
  17. Saltiel AR, Olefsky JM. Thiazolidinediones in the treatment of insulin resistance and type II diabetes. *Diabetes*. 1996;45:1661-1669.
  18. Savage PJ. Cardiovascular complications of diabetes mellitus: what we know and what we need to know about their prevention. *Ann Intern Med*. 1996;124:123-126.
  19. Virmani R, Kolodgie FD, Burke AP, Farb A, Schwartz SM. Lessons from sudden coronary death: a comprehensive morphological classification scheme for atherosclerotic lesions. *Arterioscler Thromb Vasc Biol*. 2000;20:1262-1275.
  20. Towler DA, Bidder M, Latifi T, Coleman T, Semenkovich CF. Diet-induced diabetes activates an osteogenic gene regulatory program in the aortas of low density lipoprotein receptor-deficient mice. *J Biol Chem*. 1998;273:30427-30434.
  21. Merat S, Casanada F, Sutphin M, Palinski W, Reaven PD. Western-type diets induce insulin resistance and hyperinsulinemia in LDL receptor-deficient mice but do not increase aortic atherosclerosis compared with normoinsulinemic mice in which similar plasma cholesterol levels are achieved by a fructose-rich diet. *Arterioscler Thromb Vasc Biol*. 1999;19:1223-1230.
  22. Shi C, Lee WS, Russell ME, Zhang D, Fletcher DL, Newell JB, Haber E. Hypercholesterolemia exacerbates transplant arteriosclerosis via increased neointimal smooth muscle cell accumulation: studies in apolipoprotein E knockout mice. *Circulation*. 1997;96:2722-2728.
  23. Nakashima Y, Plump AS, Raines EW, Breslow JL, Ross R. ApoE-deficient mice develop lesions of all phases of atherosclerosis throughout the arterial tree. *Arterioscler Thromb*. 1994;14:133-140.
  24. Tangirala RK, Rubin EM, Palinski W. Quantitation of atherosclerosis in murine models: correlation between lesions in the aortic origin and in the entire aorta, and differences in the extent of lesions between sexes in LDL receptor-deficient and apolipoprotein E-deficient mice. *J Lipid Res*. 1995;36:2320-2328.
  25. Kelley DE, Goodpaster B, Wing RR, Simoneau JA. Skeletal muscle fatty acid metabolism in association with insulin resistance, obesity, and weight loss. *Am J Physiol*. 1999;277:E1130-E1141.
  26. Suter SL, Nolan JJ, Wallace P, Gumbiner B, Olefsky JM. Metabolic effects of new oral hypoglycemic agent CS-045 in NIDDM subjects. *Diabetes Care*. 1992;15:193-203.
  27. Fujiwara K, Hayashi K, Matsuda H, Kubota E, Honda M, Ozawa Y, Saruta T. Altered pressure-natriuresis in obese Zucker rats. *Hypertension*. 1999;33:1470-1475.
  28. Sung BH, Izzo JL Jr, Dandona P, Wilson MF. Vasodilatory effects of troglitazone improve blood pressure at rest and during mental stress in type 2 diabetes mellitus. *Hypertension*. 1999;34:83-88.
  29. Kawai T, Takei I, Oguma Y, Ohashi N, Tokui M, Oguchi S, Katsukawa F, Hirose H, Shimada A, Watanabe K, et al. Effects of troglitazone on fat distribution in the treatment of male type 2 diabetes. *Metabolism*. 1999;48:1102-1107.
  30. Chen S, Noguchi Y, Izumida T, Tatebe J, Katayama S. A comparison of the hypotensive and hypoglycaemic actions of an angiotensin converting enzyme inhibitor, an AT1a antagonist and troglitazone. *J Hypertens*. 1996;14:1325-1330.
  31. Ross R. Atherosclerosis is an inflammatory disease. *Am Heart J*. 1999;138:S419-S420.
  32. Gu L, Okada Y, Clinton SK, Gerard C, Sukhova GK, Libby P, Rollins BJ. Absence of monocyte chemoattractant protein-1 reduces atherosclerosis in low density lipoprotein receptor-deficient mice. *Mol Cell*. 1998;2:275-281.
  33. Goetze S, Xi XP, Graf K, Fleck E, Hsueh WA, Law RE. Troglitazone inhibits angiotensin II-induced extracellular signal-regulated kinase 1/2 nuclear translocation and activation in vascular smooth muscle cells. *FEBS Lett*. 1999;452:277-282.
  34. Inoue I, Katayama S, Takahashi K, Negishi K, Miyazaki T, Sonoda M, Komoda T. Troglitazone has a scavenging effect on reactive oxygen species. *Biochem Biophys Res Commun*. 1997;235:113-116.
  35. Shaish A, George J, Gilburd B, Keren P, Levkovitz H, Harats D. Dietary beta-carotene and alpha-tocopherol combination does not inhibit atherogenesis in an apoE-deficient mouse model. *Arterioscler Thromb Vasc Biol*. 1999;19:1470-1475.
  36. Pratico D, Tangirala RK, Rader DJ, Rokach J, FitzGerald GA. Vitamin E suppresses isoprostane generation in vivo and reduces atherosclerosis in apoE-deficient mice. *Nat Med*. 1998;4:1189-1192.
  37. Crawford RS, Kirk EA, Rosenfeld ME, LeBoeuf RC, Chait A. Dietary antioxidants inhibit development of fatty streak lesions in the LDL receptor-deficient mouse. *Arterioscler Thromb Vasc Biol*. 1998;18:1506-1513.
  38. Bird DA, Tangirala RK, Fruebis J, Steinberg D, Witztum JL, Palinski W. Effect of probucol on LDL oxidation and atherosclerosis in LDL receptor-deficient mice. *J Lipid Res*. 1998;39:1079-1090.
  39. Li AC, Brown KK, Silvestre MJ, Willson TM, Palinski W, Glass CK. Peroxisome proliferator-activated receptor  $\gamma$  ligands inhibit development of atherosclerosis in LDL receptor-deficient mice. *J Clin Invest*. 2000;106:523-531.
  40. Yusuf S, Dagenais G, Pogue J, Bosch J, Sleight P. Vitamin E supplementation and cardiovascular events in high-risk patients: the Heart Outcomes Prevention Evaluation Study Investigators. *N Engl J Med*. 2000;342:154-160.



# Vitamin E Reduces Progression of Atherosclerosis in Low-Density Lipoprotein Receptor-Deficient Mice With Established Vascular Lesions

Tillmann Cyrus, MD; Yuemang Yao, BSc; Joshua Rokach, PhD;  
Lina X. Tang, MD; Domenico Praticò, MD

**Background**—A growing body of evidence from animal studies supports the hypothesis that oxidative stress-mediated mechanisms play a central role in early atherogenesis. In contrast, clinical trials with antioxidant vitamins have not produced consistent results in humans with established atherosclerosis.

**Methods and Results**—Low-density lipoprotein receptor-deficient mice (LDLR KO) were fed a high-fat diet for 3 months to induce atheroma. At this time, 1 group of mice was euthanized for examination of atherosclerosis, and 2 other groups were randomized to receive high-fat diet either alone or supplemented with vitamin E for 3 additional months. At the end of the study, LDLR KO on a vitamin E-supplemented fat diet had decreased 8,12-*iso*-isoprostane (iP)<sub>F<sub>2α</sub></sub>-VI and monocyte chemoattractant protein-1 levels, but increased nitric oxide levels compared with mice on placebo. No difference in lipid levels was observed between the 2 groups. Compared with baseline, placebo group had progression of atherosclerosis. In contrast, vitamin E-treated animals showed a significant reduction in progression of atherosclerosis.

**Conclusions**—These results demonstrate that in LDLR KO, vitamin E supplementation reduces progression of established atherosclerosis by suppressing oxidative and inflammatory reactions and increasing nitric oxide levels. (*Circulation*. 2003;107:521-523.)

**Key Words:** atherosclerosis ■ antioxidants ■ lipids ■ inflammation ■ nitric oxide

Atherogenesis is a chronic disease influenced by multiple genetic and environmental factors that involves a complex interplay between blood components and the artery wall and is characterized by oxidative and inflammatory reactions.<sup>1</sup> Consistent data indicate that oxidative processes are of functional importance in animal models of atherogenesis.<sup>2</sup> Epidemiological studies support these findings, indicating an inverse relationship between antioxidant vitamin intake and cardiovascular disease.<sup>3</sup> Several clinical trials, however, have shown conflicting results as to whether or not antioxidant vitamins reduce atherosclerosis progression and cardiovascular events.<sup>4</sup> Furthermore, in healthy subjects, vitamin E supplementation did not reduce the progression of the carotid artery intima-media thickness over a 3-year period.<sup>5</sup>

Several considerations can be made to explain these conflicting results, among them the endogenous antioxidant status of the study participants before enrollment and the timing of the intervention relative to the atherosclerotic process. It is plausible that in mice, vitamin E is effective because it is typically given at an early stage of the disease. In contrast, in humans, it has little or no effect because it is

administered when atherosclerotic lesions are already established.

Most animal studies have focused their attention on the effect of antioxidants on the formation of fatty streaks, the earliest cellular lesion of atherosclerosis. In contrast, the possible contribution of oxidative stress to the progression of atherosclerosis has been poorly investigated. Previously, we have shown that vitamin E suppresses *in vivo* lipid peroxidation and induces a significant reduction of early atherogenesis in different mouse models of atherosclerosis.<sup>6,7</sup> The present study was designed to test the hypothesis that chronic attenuation of oxidative stress by vitamin E would have an impact on established atherosclerosis in low-density lipoprotein-receptor deficient (LDLR KO) mice.

## Methods

### Animal Experimental Protocol

All procedures were approved by the Institutional Committee. LDLR KO mice (n=42, Jackson Laboratories, Bar Harbor, Me) were allowed to age to 12 months and were then fed a high-fat diet (normal chow supplemented with 0.15% cholesterol and 20% butter fat) for a total of 12 weeks prior baseline analysis. At this time-point blood was drawn, plasma cholesterol was quantitated, and mice were

Received November 8, 2002; revision received December 11, 2002; accepted December 12, 2002.  
From the Center for Experimental Therapeutics and Department of Pharmacology, University of Pennsylvania, School of Medicine, Philadelphia, Pa; and The Claude Pepper Institute and Department of Chemistry (J.R.), Florida Institute of Technology, Melbourne, Fla.  
Correspondence to Domenico Praticò, MD, University of Pennsylvania, Biomedical Research Building 2/3, Room 812, 421, Curie Blvd, Philadelphia, PA 19104. E-mail domenico@spirit.gcr.upenn.edu  
© 2003 American Heart Association, Inc.

*Circulation* is available at <http://www.circulationaha.org>

DOI: 10.1161/01.CIR.0000055186.40785.C4

divided in 3 groups of 14 animals each, with mean cholesterol levels that were not significantly different. One group of animals was killed immediately for analysis of atherosclerosis (baseline group). The remaining mice were randomized to receive high-fat diet alone or supplemented with vitamin E (2 I.U/g diet) for 3 additional months. Blood samples were obtained from mice at baseline and then at monthly intervals until the end of the study.

### Biochemical Analyses

Plasma cholesterol and triglyceride levels were measured enzymatically and vitamin E levels were assayed by high-performance liquid chromatography as previously described.<sup>6,7</sup> Total plasma NO metabolites were evaluated with measurements of nitrite+nitrate by a colorimetric assay (Assay Design). Plasma 8,12-*iso*-iPF<sub>2</sub><sub>a</sub>-VI levels were measured by gas chromatography/mass spectrometry, as previously described.<sup>7,8</sup> Levels of soluble intercellular adhesion molecules-1 (s-ICAM1) and monocyte chemoattractant protein-1 (MCP-1) were measured by ELISA kits (Endogen, Inc and R&D System).<sup>7,9</sup>

### Preparation of Mouse Aortas and Quantitation of Atherosclerosis

After the final blood collection, mice were euthanized and the aortic tree was perfused for 10 minutes with ice-cold PBS containing 20  $\mu$ mol/L BHT and 2 mmol/L EDTA (pH 7.4) as previously described.<sup>7,9</sup> After removal of the surrounding adventitial fat tissue, the aorta was opened longitudinally, fixed in formal-sucrose, and stained with Sudan IV. The extent of atherosclerosis was determined using the en face method, in a blinded fashion as previously described.<sup>6,7</sup>

### Histology and Immunohistochemistry

Briefly, serial frozen sections of the aortic root of the proximal aorta, starting at the sinus, were examined. Immunostaining for macrophage content was performed as previously described.<sup>7,9</sup> Briefly, a Mab to mouse macrophages (MOMA-2; Accurate Chemicals), and a Mab anti-human smooth muscle  $\alpha$ -actin (Sigma Chemical Co) for smooth muscle cells were used. Antibody reactivity was detected using a Nova red substrate kit (SK-4800, Vector Laboratory). Cross sections were counterstained with hematoxylin. As control, no primary antibody was added to the same sections. Images of immunostained sections were captured and analyzed in a blinded fashion as previously described.<sup>7,9</sup>

### Statistical Analysis

Results were expressed as mean $\pm$ SEM. Data were analyzed by ANOVA and subsequently by Student's unpaired 2-tailed *t* test, as indicated. Probability values less than 0.05 were considered as significant.

## Results

### Vitamin E Effects on Plasma Lipids

Compared with baseline group, mice from the placebo group showed a further significant increase in both plasma cholesterol and triglycerides. This increase was also evident in LDLR KO mice receiving the high-fat diet supplemented with vitamin E (Table). No significant difference in lipid levels was found between mice on vitamin E or high-fat diet alone. Compliance with vitamin E dietary regimen was demonstrated by a significant increase in its circulating levels in mice on vitamin E-enriched diet (Table). Elevation of plasma vitamin E levels was also evident when the values were normalized for cholesterol (data not shown).

### Vitamin E Effects on Oxidative and Inflammatory Processes

Plasma levels of 8,12-*iso*-iPF<sub>2</sub><sub>a</sub>-VI, a major F<sub>2</sub>-isoprostane and a specific marker of lipid peroxidation,<sup>8</sup> were further

### Characteristics of the 3 Groups of Mice

	Baseline	High-Fat Diet	
		Placebo	Vitamin E
Cholesterol, mg/dL	800 $\pm$ 50	1150 $\pm$ 100†	1115 $\pm$ 85
Triglycerides, mg/dL	450 $\pm$ 45	710 $\pm$ 60†	680 $\pm$ 70
Vitamin E, $\mu$ M	20 $\pm$ 2	16 $\pm$ 1.8†	52 $\pm$ 2.2*
8,12- <i>iso</i> -iPF <sub>2</sub> <sub>a</sub> -VI, pg/mL	750 $\pm$ 60	1100 $\pm$ 55†	630 $\pm$ 50
sICAM-1, ng/ml	11 $\pm$ 1.5	14 $\pm$ 2	10 $\pm$ 2*
MCP-1, ng/ml	200 $\pm$ 15	245 $\pm$ 21	180 $\pm$ 16*
Nox, $\mu$ M	30 $\pm$ 3.2	18 $\pm$ 2.6†	48 $\pm$ 2.4*

Each group includes 14 mice. Results are expressed as mean $\pm$ SEM.

\**P*<0.05 vs placebo; †*P*<0.05 vs baseline.

elevated in LDLR KO mice kept on a high-fat diet alone when compared with the baseline group. In contrast, vitamin E significantly reduced these levels to values that were similar to the ones observed in mice at baseline (Table). At the end of the study, mice on the high-fat diet alone had a further increase in s-ICAM-1 and MCP-1 circulating levels, whereas vitamin E significantly reduced them (Table). Because impaired NO synthesis has been described in hypercholesterolemia,<sup>10</sup> we examined the effect of vitamin E supplementation on NO metabolite (NOx) levels. Compared with baseline, plasma NOx levels were further reduced in mice on a high-fat diet alone. In contrast, vitamin E supplementation preserved higher plasma NOx levels compared with both baseline and the placebo group (Table).

### Vitamin E Effects on Preexisting Atherosclerotic Lesions

The Sudan IV-stained aorta preparations of the LDLR KO mice on the high-fat diet for 3 months showed atherosclerotic lesions mainly localized in the sinus and arch portions, covering 11.2 $\pm$ 1.4% of the entire vessel (Figure 1). The aortas from mice receiving a high-fat diet for 3 additional months demonstrated further progression of atherosclerosis, which involved the thoracic and abdominal portions of the aorta. In contrast, this area was significantly reduced in LDLR KO mice on high-fat diet supplemented with vitamin E (Figure 1). No significant difference was observed with the baseline group (Figure 1).

Immunohistochemical analyses of aortic root sections showed no difference in the percentage area occupied by

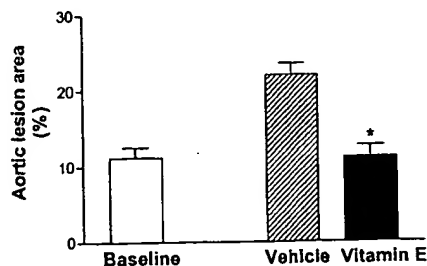


**Figure 1.** Percentage of total aortic atherosclerotic lesion areas in LDLR KO mice fed a high-fat diet for 3 months (baseline), and those fed a high-fat diet alone or with vitamin E for 12 additional weeks (*n*=14 per group). \**P*<0.01 versus placebo.

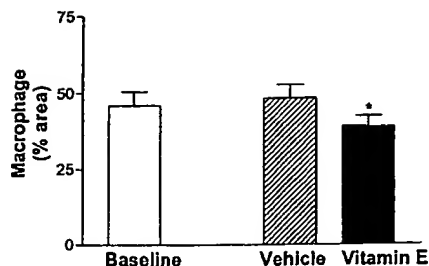


**Figure 2.** Percentage area of aortic root atherosclerotic lesions occupied by macrophages in LDLR KO mice fed high-fat diet for 3 months (baseline), and those fed a high-fat diet alone or with vitamin E for 12 additional weeks ( $n=8$  per group). \* $P<0.01$  versus placebo.

macrophages between baseline and placebo group after normalized to total lesion area. However, this area was significantly reduced in mice receiving vitamin E compared with placebo (Figure 2). Finally, no difference in smooth muscle cell content was observed among the 3 groups (data not shown).

### Discussion

In the current study, we demonstrated for the first time that chronic supplementation of vitamin E retards the progression of established atherosclerotic lesions in LDLR KO mice on a high-fat diet by decreasing oxidative and inflammatory reactions and increasing NO levels.

Lipid peroxidation, in particular oxidative modification of LDL in vivo, is thought to play a functional role in atherogenesis.<sup>2</sup> Evidence consistent with this hypothesis includes the presence of oxidized lipids in atherosclerotic lesions and the reduction of murine atherosclerosis by structurally distinct antioxidants.<sup>11–13</sup> Several trials have shown, however, that antioxidants do not reduce the risk of fatal or non-fatal infarction in an unselected population with established atherosclerosis.<sup>4</sup> These conflicting results do not necessarily mean that the oxidative hypothesis of atherosclerosis is incorrect. It is possible that the animal intervention studies deal primarily with early lesions, whereas clinical trials deal with established ones. We have previously shown that in vivo lipid peroxidation is increased in the apolipoprotein E-deficient mice and LDLR KO mice, and that its inhibition by vitamin E coincides with a reduction in atherosclerosis.<sup>6,7</sup> It is plausible that in humans antioxidants have little or no effect because they are given when lesions are already established. To test this hypothesis, LDLR KO mice initially kept on a high-fat diet for 3 months were subsequently randomized to either receive a high-fat diet supplemented with vitamin E or stay on the high-fat diet alone for 12 additional weeks. We found that vitamin E reduced progression of atherosclerosis without affecting lipid levels by suppressing oxidative stress. These results support the concept that vitamin E is effective in LDLR KO mice whether it is given at the early phase of atherogenesis or after the disease is established.

Atherosclerosis is associated with oxidative stress, which is characterized by a reduction of endogenous antioxidants and NO levels.<sup>14,15</sup> We confirmed these data by showing that vitamin E restores and increases these levels. Reactive oxygen species can interact with NO and produce peroxynitrate, which in turn can further sustain oxidative injury to the endothelium. By restoring the endogenous antioxidant status, vitamin E increases NO levels and limits peroxynitrate formation, which could then act as additional antiatherogenic mechanisms by reducing vascular inflammation. Indeed, our present findings demonstrate that by reducing oxidative stress, vitamin E improves indices of inflammation and endothelial function, which are critically involved in the progression of atherosclerosis.

In interpreting our results, we must consider an important limitation of this study; no animal model mimics perfectly human atherosclerosis. Despite this fact, our study supports the hypothesis that the discrepancies between animal studies and clinical trials with vitamin E cannot be explained by the timing of the intervention, ie, early versus established lesions.

### Acknowledgments

This work was supported by a grant from the American Heart Association (030211N) to Dr Praticò.

### References

- Glass CK, Witztum JL. Atherosclerosis: the road ahead. *Cell*. 2001;104:503–516.
- Witztum JL, Steinberg D. The oxidative modification hypothesis of atherosclerosis: does it hold for humans. *Trends Cardiovasc Med*. 2001;11:93–102.
- Rimm EB, Stampfer MJ, Ascherio A, et al. Vitamin E consumption and the risk of coronary heart disease in men. *N Engl J Med*. 1993;328:1450–1456.
- Praticò D. Vitamin E: murine studies versus clinical trials. *Ital Heart J*. 2001;2:878–881.
- Hodis HN, Mack WJ, LaBree L, et al. Alpha-tocopherol supplementation in healthy individuals reduces low-density lipoprotein oxidation but not atherosclerosis. *Circulation*. 2002;106:1453–1459.
- Praticò D, Tangirala RK, Rader DJ, et al. Vitamin E suppresses isoprostane generation in vivo and reduces atherosclerosis in Apo-E-deficient mice. *Nat Med*. 1998;4:1189–1192.
- Cyrus T, Tang LX, Rokach J, et al. Lipid peroxidation and platelet activation in murine atherosclerosis. *Circulation*. 2001;104:1940–1945.
- Praticò D, Lawson JA, Rokach J, et al. The isoprostanes in biology and medicine. *Trends Endocr Metab*. 2001;12:243–247.
- Praticò D, Cyrus T, Zhang Z, et al. Acceleration of atherogenesis by COX-1-dependent prostanoid formation in low-density lipoprotein receptor deficient mice. *Proc Natl Acad Sci U S A*. 2001;98:3358–3363.
- Ishikawa I, Sugawara D, Wang X, et al. Heme oxygenase-1 inhibits atherosclerotic lesion formation in LDL-receptor knockout mice. *Circ Res*. 2001;88:506–512.
- Witztum JL, Berliner JA. Oxidized phospholipids and isoprostanes in atherosclerosis. *Curr Opin Lipidol*. 1998;9:441–448.
- Tangirala RK, Casanada F, Miller E, et al. Effect of the anti-oxidant N,N'-diphenyl 1,4-phenylenediamine (DPPD) on atherosclerosis in apoE-deficient mice. *Arterioscler Thromb Vasc Biol*. 1994;15:1625–1630.
- Cynshi O, Kawabe Y, Suzuki T, et al. Antiatherogenic effects of the antioxidant BO-653 in three different animal models. *Proc Natl Acad Sci U S A*. 1998;95:10123–10128.
- Praticò D. Lipid peroxidation in mouse models of atherosclerosis. *Trends Cardiovasc Med*. 2001;11:112–116.
- Oemar B, Tschudi MR, Godoy N, et al. Reduced endothelial synthase expression and production in human atherosclerosis. *Circulation*. 1998;97:2494–2498.

*Vascular Biology, Atherosclerosis and Endothelium Biology*

# The Atheroprotective Effect of 17 $\beta$ -Estradiol Depends on Complex Interactions in Adaptive Immunity

Rima Elhage,\* Pierre Gourdy,\* Jacek Jawien,<sup>†</sup>  
Laurent Bouchet,\* Caroline Castano,\*  
Catherine Fievet,<sup>‡</sup> Göran K. Hansson,<sup>†</sup>  
Jean-François Arnal,\* and Francis Bayard\*

From INSERM U589,\* IFR31, Institut L. Bugnard, Toulouse, France; INSERM U545 Institut Pasteur,<sup>‡</sup> Lille, France; and the Center for Molecular Medicine and Department of Medicine,<sup>†</sup> Karolinska Institute, Stockholm, Sweden

**Estradiol prevents fatty streak formation in chow-fed atherosclerosis-prone apolipoprotein E (ApoE)-deficient mice. We previously reported that fatty streak development of immunodeficient ApoE<sup>-/-</sup>/recombination activating gene 2 (RAG-2<sup>-/-</sup>) double-deficient mice was insensitive to estradiol. In the present work, we demonstrate that the reconstitution of ApoE<sup>-/-</sup>/RAG-2<sup>-/-</sup> with bone marrow from immunocompetent ApoE<sup>-/-</sup>/RAG-2<sup>+/+</sup> mice restores the protective effect of estradiol on fatty streak constitution. We extended this demonstration to the model of low-density lipoprotein receptor-deficient mice, establishing the obligatory role of mature lymphocytes in this process. We then investigated whether the protective effect of estradiol was mediated by a specific lymphocyte subpopulation by studying the hormonal effect on fatty streak constitution in recently developed models of ApoE<sup>-/-</sup> mice deficient in selective T-lymphocyte subsets (either TCR $\alpha\beta$ <sup>+</sup>, CD4<sup>+</sup>, CD8<sup>+</sup>, or TCR $\gamma\delta$ <sup>+</sup> lymphocytes) or B lymphocytes. In all these specifically immunodeficient mice, estradiol administration to ovariectomized mice conferred protection as in immunocompetent ApoE<sup>-/-</sup> mice, clearly demonstrating that no single lymphocyte subpopulation was specifically required for this effect. These results point to additional lymphocyte-dependent mechanisms such as modulating the interactions among lymphocytes and between lymphocytes and endothelial and/or antigen-presenting cells. (*Am J Pathol* 2005, 167:267–274)**

Fuller understanding of the mechanism of atherosclerosis prevention by estrogens is urgently needed.<sup>1</sup> Two controlled prospective and randomized studies did not demonstrate a beneficial effect of hormone replacement therapy whether in secondary<sup>2</sup> or in primary prevention.<sup>3</sup> In contrast to these clinical data, estrogen hormones have been shown to decrease macrophage-derived foam-cell infiltration in different animal species including atherosclerosis-prone apolipoprotein E-deficient (ApoE<sup>-/-</sup>) mice<sup>4,5</sup> although the mechanisms of this effect have remained obscure.

Recent cumulative evidence have suggested that both innate and adaptive immune responses modulate the rate of lesion progression.<sup>6–8</sup> Indeed, several studies have confirmed the importance of T lymphocytes present in early lesions of atherosclerosis.<sup>9–12</sup> Furthermore, previous observations have demonstrated the particular role for specific T-lymphocyte subsets. For example, Zhou and colleagues<sup>13</sup> showed that CD4<sup>+</sup> T cells aggravate the atherosclerotic process.

In this context, we previously reported that ApoE<sup>-/-</sup> mice with homozygous disruption at the recombination activating gene 2 (RAG-2<sup>-/-</sup>) loci presented a reduced level of atherosclerotic lesions that were insensitive to estradiol (E2).<sup>14</sup> In the present studies, we first demonstrated that the reconstitution of ApoE<sup>-/-</sup>/RAG-2<sup>-/-</sup> with bone marrow from immunocompetent ApoE<sup>-/-</sup>/RAG-

Supported in part by INSERM, the Ministère de la Recherche et de la Technologie (Université Paul Sabatier), Action Concertée Incitative 2001 and 2003, Association pour la Recherche contre le Cancer, MSD, Theramex Laboratories, European Vascular Genomics Network (grant no.503254), Fondation de France, the Conseil Régional Midi-Pyrénées, and the French Society of Atherosclerosis (to R.E.).

Accepted for publication February 10, 2005.

Supplemental material for this article appears on <http://ajp.amj-pathol.org>.

Present address of J.J.: Department of Pharmacology, Jagiellonian University School of Medicine, Grzegorzeczka 16, PL 31-531 Krakow, Poland.

Address reprint requests to F. Bayard, INSERM U589, IFR31, Institut L. Bugnard, BP 84225, 31432 Toulouse Cédex 4, France. E-mail: bayard@toulouse.inserm.fr.

2<sup>+/+</sup> mice restores the protective effect of E2 on fatty streak constitution and extended this demonstration to the model of low-density lipoprotein receptor (LDLR)-deficient mice. We then hypothesized that E2 could target a specific lymphocyte subset to exert its protective effect on fatty streak constitution. To solve this question, we compared the effect of E2 in immunocompetent ApoE<sup>-/-</sup> mice and in models of ApoE<sup>-/-</sup> mice deficient in specific lymphocyte subsets developed in our laboratory. We observed that no T- or B-lymphocyte subpopulation specifically mediated the protective effect of E2, pointing to additional lymphocyte-dependent mechanisms.

## Materials and Methods

### Animals

The specific pathogen-free conditions of animal care and regular chow diet feeding as well as the production of ApoE- and RAG-2-deficient mice (ApoE<sup>-/-</sup>/RAG-2<sup>-/-</sup>) have been described previously.<sup>14,15</sup> The ApoE<sup>-/-</sup>/RAG-2<sup>-/-</sup> mice had been backcrossed into a C57BL/6 background for six generations.

Low-density lipoprotein receptor-deficient (LDLR<sup>-/-</sup>) mice were purchased from Charles River (L'Arbresle, France). RAG-2-deficient (RAG-2<sup>-/-</sup>) mice were purchased from CDTA (Orléans, France). Both strains had been backcrossed into a C57BL/6 background for more than 10 generations. Female LDLR<sup>-/-</sup> mice were crossed with male RAG-2<sup>-/-</sup> mice in our animal facility to obtain LDLR and RAG-2 double-deficient mice (LDLR<sup>-/-</sup>/RAG-2<sup>-/-</sup>). RAG-2 and LDLR gene disruptions were assessed by polymerase chain reaction genotyping as previously described.<sup>16,17</sup> The production of the double-deficient models is reported elsewhere.<sup>12</sup> Briefly, TCR $\beta$ -deficient (TCR $\beta$ <sup>-/-</sup>), CD4-deficient (CD4<sup>-/-</sup>), CD8-deficient (CD8<sup>-/-</sup>), TCR $\delta$ -deficient (TCR $\delta$ <sup>-/-</sup>) male mice were crossed with female ApoE<sup>-/-</sup> mice. B-lymphocyte-deficient mice were obtained similarly by crossing  $\mu$ mt-deficient<sup>18</sup> B<sup>-/-</sup> male mice with female ApoE<sup>-/-</sup> mice. Heterozygous ApoE<sup>-/-</sup>/TCR $\beta$ <sup>+/-</sup>, ApoE<sup>-/-</sup>/CD4<sup>+/-</sup>, ApoE<sup>-/-</sup>/CD8<sup>+/-</sup>, ApoE<sup>-/-</sup>/TCR $\delta$ <sup>+/-</sup>, ApoE<sup>-/-</sup>/B<sup>+/-</sup> populations were generated and used as the parental genotypes. The offspring of these heterozygous strains, TCR $\beta$ <sup>+/+</sup>, CD4<sup>+/+</sup>, CD8<sup>+/+</sup>, TCR $\delta$ <sup>+/+</sup>, B<sup>+/+</sup> and TCR $\beta$ <sup>-/-</sup>, CD4<sup>-/-</sup>, CD8<sup>-/-</sup>, TCR $\delta$ <sup>-/-</sup>, B<sup>-/-</sup> served as the subjects of our studies. Confirmation of gene disruption was screened by polymerase chain reaction genotyping and phenotyping of blood lymphocytes or splenocytes by flow cytometry.<sup>12</sup> All strains had been backcrossed into a C57BL/6 background for more than 10 generations.

Only female animals were used in the present studies. As shown in Figure 1, mice were ovariectomized at 5 weeks of age and, 1 week later, were administered with either 60-day time-release placebo or 0.1 mg of estradiol-17 $\beta$  pellets (Innovative Research of America, Sarasota, FL) implanted subcutaneously into the back of the animals, using a sterile trochar and forceps. New pellets were reimplanted 7 weeks later. The dose of 0.1 mg of E2, releasing 80  $\mu$ g/kg/day, had previously been defined

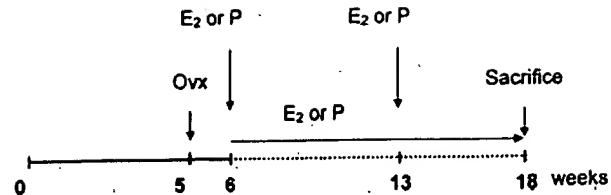


Figure 1. Protocol to study fatty streak formation in immunocompetent or immunodeficient ApoE-deficient mice. Ovx, ovariectomy; E2, estradiol-17 $\beta$  pellet; PI, placebo pellet.

as adequate for a maximal effect on fatty streak constitution in female mice.<sup>15</sup> ApoE<sup>-/-</sup> mice were maintained under chow diet throughout the experiments, whereas LDLR<sup>-/-</sup> mice were switched to a high-fat diet (15% fat, 1.25% cholesterol, no cholate, TD96335; Harlan Teklad, WI) at 5 weeks of age. After E2 or placebo treatment for 12 weeks, all mice were sacrificed with an overdose of ketalar after a 16-hour fast. Blood was collected by orbital puncture for serum lipid analysis.<sup>15</sup> Uterus was weighted to assess the efficacy of E2 treatment. All experimental procedures were performed in accordance with the recommendations of the European Accreditation of Laboratory Animal Care Institute.

### Bone Marrow Transplantation

As shown in Figure 2, ApoE<sup>-/-</sup>/RAG-2<sup>-/-</sup> and LDLR<sup>-/-</sup>/RAG-2<sup>-/-</sup> mice were ovariectomized at 5 weeks of age and received a sublethal dose of whole-body irradiation (400 rads) 1 week later. The day after irradiation, donor ApoE<sup>-/-</sup> or ApoE<sup>-/-</sup>/RAG-2<sup>-/-</sup>, C57BL/6 or RAG-2<sup>-/-</sup> mice were killed, and their femurs and tibias removed aseptically. Marrow cavities were flushed, and single-cell

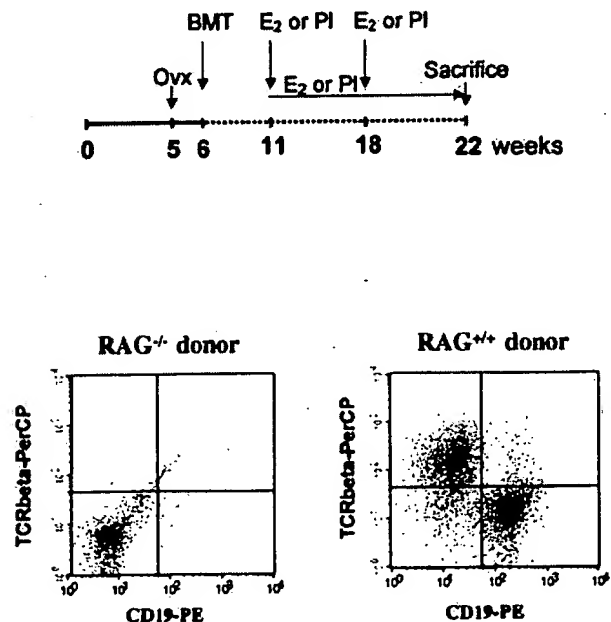


Figure 2. Protocol of bone marrow transplantation (BMT) and flow cytometry analysis of spleen lymphocyte repopulation of ApoE<sup>-/-</sup>/RAG-2<sup>-/-</sup> mice transplanted using bone marrow from ApoE<sup>-/-</sup>/RAG-2<sup>-/-</sup> or ApoE<sup>-/-</sup>/RAG-2<sup>+/+</sup> donor mice. Splenocytes were co-labeled with anti-TCR $\beta$ -PerCP/anti-CD19-PE-conjugated antibodies.

**Table 1.** Body Weight, Total Cholesterol, and Aortic Root Lesion Area in Placebo (PI)- or Estradiol-17 $\beta$  (E<sub>2</sub>)-Treated Ovariectomized ApoE<sup>-/-</sup>/RAG<sup>-/-</sup> Female Mice after Bone Marrow Transplantation from ApoE<sup>-/-</sup>/RAG<sup>-/-</sup> or ApoE<sup>-/-</sup>/RAG<sup>+/+</sup> Donors

Donor genotype	Treatment	Body weight (g)	Total cholesterol (g/L)	Lesion area ( $\mu\text{m}^2$ )
ApoE <sup>-/-</sup> /RAG <sup>+/+</sup>	PI	25.3 $\pm$ 0.7	5.9 $\pm$ 0.4	66662 $\pm$ 5838
	E <sub>2</sub>	23.5 $\pm$ 0.6	4.8 $\pm$ 0.4	34919 $\pm$ 6532*
ApoE <sup>-/-</sup> /RAG <sup>-/-</sup>	PI	26.8 $\pm$ 1.7	5.4 $\pm$ 0.4	33451 $\pm$ 5816†
	E <sub>2</sub>	24.3 $\pm$ 0.3	4.4 $\pm$ 0.7	41844 $\pm$ 5294

Results are means  $\pm$  SEM (n = 7).

\*P < 0.05 versus the corresponding PI-treated mice.

†P < 0.05 versus ApoE<sup>-/-</sup>/RAG<sup>+/+</sup>-transplanted PI-treated mice.

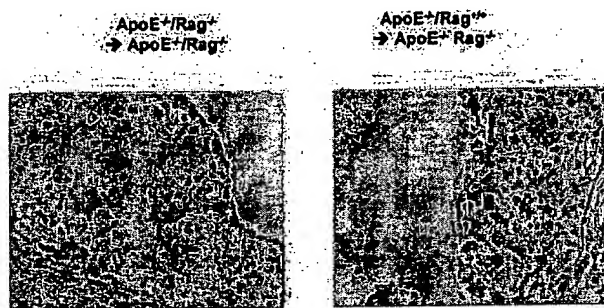


**Figure 3.** Immunohistochemical analysis of representative lesions from individual ApoE<sup>-/-</sup>/RAG-2<sup>-/-</sup> transplanted using bone marrow from ApoE<sup>-/-</sup>/RAG-2<sup>+/+</sup> or ApoE<sup>-/-</sup>/RAG-2<sup>-/-</sup> donor mice using anti-CD3 antibodies.

suspensions were prepared. The irradiated recipients received  $15 \times 10^6$  bone marrow cells in 0.2 ml of phosphate-buffered saline by tail vein injection. One week before and 4 weeks after the bone marrow transplantation, Bactrim (sulfamethoxazole 200 mg/ml, trimethoprim 48 mg/ml) was added to drinking water. After 5 additional weeks, all transplanted mice were implanted subcutaneously with placebo or E<sub>2</sub> pellets and LDLr<sup>-/-</sup>/RAG-2<sup>-/-</sup> mice were switched to the high-fat diet to induce atherosclerotic lesion formation. Mice were sacrificed 11 weeks later (at 22 weeks of age). Blood and tissues were collected as described above.

### Tissue Preparation and Lesion Analysis

The circulatory system was perfused with 0.9% NaCl by cardiac intraventricular canalization. The heart and ascending aorta were removed and kept frozen. Surface lesion area was measured by computer-assisted image quantification in the aortic root, by a trained observer blinded to the genotype and treatment of the mice, as previously described<sup>15</sup> but using a Leica image analyzer.

The rest of the entire aortic tree was removed and cleaned of adventitia, split longitudinally to the iliac bifurcation, and pinned flat on a dissection pan for analysis by *en face* preparation. Images were captured using a Sony-3CCD video camera and fraction covered by lesions evaluated as a percentage of the total aortic area.

### Immunohistochemistry

Cryostat sections from the proximal aorta were fixed in acetone, air-dried, and reacted with a primary rat monoclonal anti-mouse macrophage (clone MOMA-2 from Serotec, Oxford, UK) used at a 1:50 dilution or a primary goat polyclonal anti-CD3 (clone M-20 from Santa Cruz Biotechnology, Santa Cruz, CA) used at a 1:100 dilution. Then, sections were incubated with corresponding preadsorbed secondary biotinylated antibodies (Vector Laboratories, Burlingame, CA): binding of rat monoclonal anti-macrophage was revealed using biotinylated rabbit anti-rat IgG and binding of goat polyclonal anti-CD3 was revealed using biotinylated horse anti-goat IgG. The binding of the biotinylated antibodies was visualized with an avidin DH-biotinylated peroxidase complex (Vectastain ABC kit, Vector Laboratories) and AEC peroxidase substrate kit (Vector Laboratories). Counterstaining was performed using Mayer's hemalum. Macrophage and T-cell quantification was determined by scoring samples from at least four sections per animal. A minimum of three animals was analyzed per group. Two investigators who were blinded to the sample identity performed analysis.

### Analysis of Plasma Lipids and Lipoproteins

Serum cholesterol concentrations were determined by an enzymatic assay adapted to microtiter plates using com-

**Table 2.** Body Weight, Total Cholesterol, and Aortic Root Lesion Area in Placebo (PI)- or Estradiol-17 $\beta$  (E<sub>2</sub>)-Treated Ovariectomized LDLr<sup>-/-</sup>/RAG<sup>-/-</sup> Female Mice after Bone Marrow Transplantation from RAG<sup>-/-</sup> or C57BL/6 Mice

Donor genotype	Treatment	Body weight (g)	Total cholesterol (g/L)	Lesion area ( $\mu\text{m}^2$ /section)
C57BL/6	PI	28.1 $\pm$ 1.2	9.3 $\pm$ 0.8	84480 $\pm$ 9185
	E <sub>2</sub>	24.9 $\pm$ 0.7*	6.4 $\pm$ 0.7*	35333 $\pm$ 8317*
RAG <sup>-/-</sup>	PI	27.1 $\pm$ 0.6	11.1 $\pm$ 0.6	35900 $\pm$ 5600†
	E <sub>2</sub>	24.0 $\pm$ 0.5*	9.9 $\pm$ 0.5	42800 $\pm$ 6600

The animals had been on HFD for 12 weeks. Results are means  $\pm$  SEM (n  $\geq$  7).

\*P < 0.05 versus C57BL/6-transplanted PI-treated mice.

†P < 0.05 versus the corresponding PI-treated mice.

**Table 3.** Body Weight, Total Cholesterol, and Lesion Area of Ovariectomized Placebo (PI)- or Estradiol-17 $\beta$  (E<sub>2</sub>)-Treated Immunocompetent ApoE<sup>-/-</sup> Control and Immunodeficient ApoE<sup>-/-</sup>/TCR $\delta$ <sup>-/-</sup>, CD4<sup>-/-</sup>, CD8<sup>-/-</sup>, TCR $\delta$ <sup>-/-</sup> or B<sup>-/-</sup> Female Mice

Genotype	Body weight (g)			Total cholesterol (g/L)
	NC	PI	E2	NC
ApoE <sup>-/-</sup>	22.0 $\pm$ 0.5	28.7 $\pm$ 1.5	22.9 $\pm$ 0.5*	3.4 $\pm$ 0.1
ApoE <sup>-/-</sup> /TCR $\delta$ <sup>-/-</sup>	21.0 $\pm$ 0.5	20.9 $\pm$ 0.6†	21.5 $\pm$ 0.5	3.0 $\pm$ 0.2
ApoE <sup>-/-</sup> /CD4 <sup>-/-</sup>	19.5 $\pm$ 0.4	21.9 $\pm$ 1.2†	21.9 $\pm$ 0.6	3.0 $\pm$ 0.2
ApoE <sup>-/-</sup> /CD8 <sup>-/-</sup>	21.5 $\pm$ 0.5	23.5 $\pm$ 0.8†	22.9 $\pm$ 0.5	3.1 $\pm$ 0.2
ApoE <sup>-/-</sup> /TCR $\delta$ <sup>-/-</sup>	20.1 $\pm$ 0.4	27.6 $\pm$ 1.4	21.9 $\pm$ 0.1*	2.9 $\pm$ 0.1
ApoE <sup>-/-</sup> /B <sup>-/-</sup>	—	26.8 $\pm$ 0.9	24.3 $\pm$ 0.4*	—

Data of intact corresponding mice (NC) have been published previously<sup>12</sup> and are indicated in italics for comparison. Results are means  $\pm$  SEM ( $n \geq 8$ ).

\* $P < 0.05$  versus corresponding C (placebo-treated) mice.

† $P < 0.05$  versus corresponding immunocompetent mice.

(table continues)

mercially available reagents (Roche Molecular Biochemicals, Germany). Lipoprotein cholesterol profiles were obtained by Fast Protein liquid chromatography as previously described.<sup>19</sup>

### Statistical Analysis

The results are expressed as means  $\pm$  SEM. For each parameter (body weight, total cholesterol, lesion area), the effects of genotype were studied by comparing each immunodeficient group with its corresponding immunocompetent group of mice. The effect of E2 treatment was studied comparing placebo- and E2-treated mice in selective immunodeficient or in immunocompetent mice. A one-factor analysis of variance was used (Bonferroni/Dunn's test);  $P < 0.05$  was considered as significant. Statistical analyses were performed using the Statview statistical software (Abacus Concepts, Inc., Berkeley, CA). When appropriate, an unpaired t-test was also performed.

## Results

### Immunocompetent Bone Marrow Transplantation Restored Both the Level of Lesions and E2 Sensitivity in ApoE<sup>-/-</sup>/RAG-2<sup>-/-</sup> and LDLr<sup>-/-</sup>/RAG-2<sup>-/-</sup> Mice

To explore the role of lymphocytes in fatty streak constitution and E2 prevention, ApoE<sup>-/-</sup>/RAG-2<sup>-/-</sup> ovariectomized female mice received bone marrow transplantation from ApoE<sup>-/-</sup>/RAG-2<sup>-/-</sup> (ApoE<sup>-/-</sup>/RAG-2<sup>-/-</sup>  $\rightarrow$  ApoE<sup>-/-</sup>/RAG-2<sup>-/-</sup>) or from ApoE<sup>-/-</sup>/RAG-2<sup>+/+</sup> (ApoE<sup>-/-</sup>/RAG-2<sup>+/+</sup>  $\rightarrow$  ApoE<sup>-/-</sup>/RAG-2<sup>-/-</sup>) mice (Figure 2), and then were treated with placebo or E2 pellets. Sixteen weeks after bone marrow transplantation, ApoE<sup>-/-</sup>/RAG-2<sup>+/+</sup>  $\rightarrow$  ApoE<sup>-/-</sup>/RAG-2<sup>-/-</sup> placebo-treated mice presented a significantly higher level of fatty streaks when compared with ApoE<sup>-/-</sup>/RAG-2<sup>-/-</sup>  $\rightarrow$  ApoE<sup>-/-</sup>/RAG-2<sup>-/-</sup> placebo-treated mice (Table 1). Immunohistochemical analysis showed the presence of CD3-reactive cells in lesions obtained from ApoE<sup>-/-</sup>/RAG-2<sup>+/+</sup>  $\rightarrow$  ApoE<sup>-/-</sup>/RAG-2<sup>-/-</sup> mice but not in lesions obtained from ApoE<sup>-/-</sup>/RAG-2<sup>-/-</sup>  $\rightarrow$  ApoE<sup>-/-</sup>/

RAG-2<sup>-/-</sup> mice, irrespective of placebo or E2 treatment (Figure 3 and data not shown). Importantly, although E2 was still ineffective in ApoE<sup>-/-</sup>/RAG-2<sup>-/-</sup>  $\rightarrow$  ApoE<sup>-/-</sup>/RAG-2<sup>-/-</sup> mice, the protective effect of the hormone was restored in ApoE<sup>-/-</sup>/RAG-2<sup>+/+</sup>  $\rightarrow$  ApoE<sup>-/-</sup>/RAG-2<sup>-/-</sup> mice (Table 1).

Because ApoE-deficiency could be involved in these observations and because the RAG-2-deficient mice used were not fully backcrossed into the C57/BL6 background, similar experiments were performed in the LDLr-deficient mice. We first confirmed that E2 significantly decreased body weight (26.1  $\pm$  0.6 g versus 23.6  $\pm$  0.5 g,  $P < 0.05$ ), serum cholesterol (11.1  $\pm$  0.4 g/L versus 7.9  $\pm$  0.7 g/L,  $P < 0.01$ ), and fatty streak deposit (119,400  $\pm$  7400  $\mu$ m<sup>2</sup>/section versus 41,400  $\pm$  5400  $\mu$ m<sup>2</sup>/section for placebo- and E2-treated mice, respectively;  $n = 9$ ,  $P < 0.01$ ) in immunocompetent LDLr<sup>-/-</sup> mice on a 12-week high-fat diet in agreement with a previous report.<sup>20</sup> The effect on fatty streak was abolished in LDLr<sup>-/-</sup>/RAG-2<sup>-/-</sup> mice (42,000  $\pm$  13,100  $\mu$ m<sup>2</sup>/section versus 40,300  $\pm$  11,300  $\mu$ m<sup>2</sup>/section, respectively;  $n = 8$ ) whereas the effect on body weight (24.4  $\pm$  1.3 g/L versus 22.9  $\pm$  0.9 g/L,  $P < 0.05$ ) and serum cholesterol (9.9  $\pm$  0.4 g/L versus 7.4  $\pm$  0.7 g/L,  $P < 0.01$ ) persisted. Bone marrow graft experiments were also performed in this last model of ovariectomized female LDLr<sup>-/-</sup>/RAG-2<sup>-/-</sup> mice. As shown in Table 2, Placebo-treated LDLr<sup>-/-</sup>/RAG-2<sup>-/-</sup> mice that had received C57BL/6 bone marrow, presented a significantly higher level of fatty streaks when compared with those that had received RAG-2<sup>-/-</sup> bone marrow. Again, although E2 remained ineffective in RAG-2<sup>-/-</sup>  $\rightarrow$  LDLr<sup>-/-</sup>/RAG-2<sup>-/-</sup> mice, the protective effect of the hormone was restored in C57BL/6  $\rightarrow$  LDLr<sup>-/-</sup>/RAG-2<sup>-/-</sup> mice (Table 2).

### Effect of E2 Treatment on Body Weight and Serum Lipids in Immunocompetent and Selectively Immunodeficient ApoE<sup>-/-</sup> Mice

We then asked whether the protective effect of E2 could be mediated by a specific T-lymphocyte subset or B lymphocytes, considering the hormonal effect in selec-



Table 3. Continued

Total cholesterol (g/L)		Lesion area ( $\mu\text{m}^2/\text{section}$ )		
PI	E2	NC	PI	E2
5.6 $\pm$ 0.3	3.1 $\pm$ 0.2*	73,214 $\pm$ 2963	113,465 $\pm$ 5288	36,299 $\pm$ 1979*
4.4 $\pm$ 0.2†	3.1 $\pm$ 0.2*	37,048 $\pm$ 4749	65,053 $\pm$ 7753†	37,104 $\pm$ 4418*
5.8 $\pm$ 0.5	2.7 $\pm$ 0.2*	77,745 $\pm$ 12,629	114,835 $\pm$ 21,656	42,541 $\pm$ 5431*
5.6 $\pm$ 0.4	3.2 $\pm$ 0.1*	76,909 $\pm$ 4722	110,537 $\pm$ 16,142	47,782 $\pm$ 11,285*
5.6 $\pm$ 0.3	2.8 $\pm$ 0.2*	57,589 $\pm$ 3737	101,557 $\pm$ 8125	27,730 $\pm$ 3637*
4.6 $\pm$ 0.2†	2.6 $\pm$ 0.3*	—	93,432 $\pm$ 11,183	38,348 $\pm$ 5752*

tively immunodeficient ApoE<sup>-/-</sup> female mice. The statistical analysis presented in Table 3 refers to comparisons of each group of immunodeficient mice with its corresponding immunocompetent group. Data from a group of 10 ApoE<sup>-/-</sup> female mice are given for comparison (Table 3, line 1).

Uterine weight was <20 mg in ovariectomized mice and increased to 172  $\pm$  13 mg on average with E2 treatment, showing that the level of E2 stimulation was similar in all genotypes. Body weight decreased, reflecting mainly adipose tissue reduction, in immunocompetent ApoE<sup>-/-</sup> control and in immunodeficient ApoE<sup>-/-</sup>/TCR $\delta$ <sup>-/-</sup> and ApoE<sup>-/-</sup>/B<sup>-/-</sup> mice under E2 treatment. In the immunodeficient ApoE<sup>-/-</sup>/TCR $\beta$ <sup>-/-</sup>, ApoE<sup>-/-</sup>/CD4<sup>-/-</sup>, and ApoE<sup>-/-</sup>/CD8<sup>-/-</sup> mice, body weight was lower in placebo-treated mice when compared to their immunocompetent littermates and was not influenced by E2, suggesting a role for TCR $\alpha\beta$ <sup>+</sup> T lymphocytes in weight regulation. Total serum cholesterol was lower in ovariectomized ApoE<sup>-/-</sup>/TCR $\beta$ <sup>-/-</sup> and ApoE<sup>-/-</sup>/B<sup>-/-</sup> when compared with their respective immunocompetent littermates and decreased under E2 treatment in all strains. Fast performance liquid chromatography showed that the E2-induced decrease concerned the very low-density lipoprotein, intermediary/low-density lipoprotein, and high-density lipoprotein fractions (see Supplemental Figure A at <http://ajp.amjpathol.org>) in agreement with our previous report.<sup>15</sup>

#### Effect of E2 Treatment on Lesion Area in Immunocompetent and Selectively Immunodeficient ApoE<sup>-/-</sup> Mice

At the level of the aortic root, the lesion area of ovariectomized immunodeficient mice given placebo did not differ significantly from the corresponding immunocompetent mice except for the ApoE<sup>-/-</sup>/TCR $\beta$ <sup>-/-</sup> mice, which presented a decreased level of lesions (Table 3). E2 treatment induced a significant decrease of fatty streak development in all groups of mice, including the ApoE<sup>-/-</sup>/TCR $\beta$ <sup>-/-</sup> strain. To further analyze the influence of serum cholesterol on the lesion formation, we sought to analyze subgroups of mice with comparable serum cholesterol levels. Such subgroups could be selected among

the whole series of immunocompetent mice that serve as control for the immunodeficient groups (ie, a total of 50 PI-treated and 50 E2-treated mice) with cholesterolemia arbitrarily encompassed between 4 and 6 g/L. In these subgroups of ovariectomized placebo ( $n = 19$ )- and E2 ( $n = 12$ )-treated mice, with similar serum cholesterol (5.0  $\pm$  0.1 g/L and 4.9  $\pm$  0.1 g/L, respectively;  $P = 0.67$ ), lesion area still dramatically differed (109,824  $\pm$  4304  $\mu\text{m}^2/\text{section}$  and 35,722  $\pm$  4206  $\mu\text{m}^2/\text{section}$ ,  $P < 0.001$ ), strongly suggesting that the E2-induced decrease of serum cholesterol is not the main factor preventing fatty streak formation.

Histo- as well as immunohistochemical analysis showed that, under E2 treatment, residual lesions were essentially fatty streaks containing lipid-laden macrophages, with few characteristics of advanced lesions such as fibrous caps and were substantially less complex than lesions in ovariectomized ApoE<sup>-/-</sup> control mice (not shown). Remarkably, T lymphocytes were still detectable at a comparable density (2  $\pm$  1%) in these residual lesions (Figure 4). Similar observations were made in all of the series of specifically immunodeficient mice including the ApoE<sup>-/-</sup>/TCR $\beta$ <sup>-/-</sup> (Figure 4).

In the rest of the aorta, lesions were identifiable by *en face* analysis at predilection sites including the aortic arch and the orifices of the brachiocephalic, left subclavian, common carotid, and intercostal arteries. However, the level was low (<3.0% of the total aortic area) except in the ApoE<sup>-/-</sup>/CD4<sup>-/-</sup> group of mice (13.5  $\pm$  3.0%,  $n = 3$ ). In this last group, lesions were observed at the predilection sites and also at the orifice of the large abdominal arteries, in particular the celiac trunk and renal arteries. E2 induced a spectacular (more than fivefold)



Figure 4. Anti-CD3 immunolabeling of representative lesions from ovariectomized ApoE<sup>-/-</sup>, ApoE<sup>-/-</sup>/TCR $\beta$ <sup>-/-</sup>, and ApoE<sup>-/-</sup>/TCR $\delta$ <sup>-/-</sup> mice after 3 months of treatment with E2 pellets.

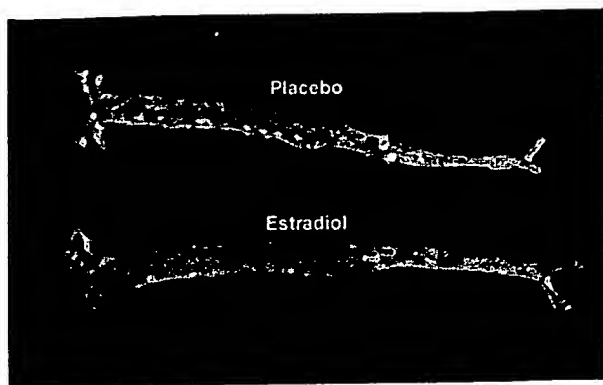


**Figure 5.** Representative *en face* aorta preparations from placebo- and E2-treated ovariectomized ApoE<sup>-/-</sup>/CD4<sup>-/-</sup> mice.

protective effect at these different sites, especially in the ApoE<sup>-/-</sup>/CD4<sup>-/-</sup> group (<3.0%, *n* = 3; Figure 5).

## Discussion

The present results definitely demonstrate that, in the C57BL/6 mouse strain, mature lymphocytes are required for the preventive effect of E2 on the atheromatous process irrespective of the model of genetically-induced hypercholesterolemia, namely ApoE<sup>-/-</sup> and LDLr<sup>-/-</sup> mice. Indeed, after bone marrow transplantation from immunocompetent donors into immunodeficient mice, lymphocytes were recovered in the lesions and a significant increase in the level of these lesions could be demonstrated. Most importantly, E2 activity was restored after bone marrow transplantation from immunocompetent donors, while E2 was still inactive after bone marrow transplantation from immunodeficient donors to the immunodeficient recipients.

Like our data obtained in intact nonovariectomized mice,<sup>12</sup> the measurement of lesion area in placebo-treated ovariectomized mice show a similar level of lesions in immunocompetent and immunodeficient mice, except in the ApoE<sup>-/-</sup>/TCRβ<sup>-/-</sup> mice, supporting the deleterious role of αβ T lymphocytes in the atheromatous process. Noteworthy, considering our previous<sup>12</sup> and present data, a protective effect of endogenous ovarian estrogens could be demonstrated in all strains because ovariectomized mice developed a higher level of lesions than intact mice. This observation is in accordance with a previous report.<sup>21</sup> Moreover, E2 treatment, administered at a dose previously defined as adequate for a maximal effect,<sup>15</sup> induced a significant decrease in lesion size in all groups of mice (Table 3). Except in ApoE<sup>-/-</sup>/TCRβ<sup>-/-</sup> mice, the residual lesion level was lower than that measured in intact female mice.<sup>12</sup> In addition, *en face* analysis showed that the effect of E2 was not restricted to the aortic sinus. Interestingly, E2 exerted a stronger preventive effect of lesion development in the thoracic and abdominal sites than at the level of the aortic sinus, particularly in ApoE<sup>-/-</sup>/CD4<sup>-/-</sup> mice (Figure 5). Although the selective immune deficiency may generate compensatory expansion of other lymphocyte subsets, such as ApoE<sup>-/-</sup>/CD4<sup>-/-</sup> mice presenting with a greater number

of CD8<sup>+</sup> and double-negative CD4-CD8 cells than ApoE<sup>-/-</sup> mice,<sup>12,22</sup> we demonstrate here that E2 was active in all strains, suggesting that no single T-lymphocyte subpopulation directly mediated the protective effect. This included the populations of regulatory T cells able to control the expansion and differentiation of activated T cells<sup>23,24</sup> and the TCRγδ<sup>+</sup> T cells. E2 has been recently claimed to induce one of these regulatory T-lymphocyte subpopulations<sup>25,26</sup> suggesting that it could play a key role in the suppression of harmful immune responses. Our data do not support such a hypothesis in the atherosclerotic process. Finally, the protective effect was also maintained in B-lymphocyte-deficient mice. This excluded a protective role mediated by immunoglobulins that are known to increase under E2 stimulation<sup>27</sup> and have been suggested to prevent atherosclerosis.<sup>27-30</sup>

Interestingly, E2 administration significantly decreased serum cholesterol levels in nearly all conditions analyzed in the present work. However, although serum cholesterol level remains a key determinant of atherosclerosis, several lines of evidence support the fact that the protective effect of E2 occurs mainly at the level of the arterial wall. First, although E2 decreased serum cholesterol levels in immunodeficient LDLr<sup>-/-</sup>/RAG-2<sup>-/-</sup> mice (the present work) as well as ApoE<sup>-/-</sup>/RAG-2<sup>-/-</sup> mice<sup>14</sup> to a similar extent than in immunocompetent mice, it was completely inactive on lesion area. Second, although the maximal decrease of serum cholesterol was obtained with endogenous E2 (Table 3), the maximal decrease in lesion area required higher E2 doses, in line with previous reports.<sup>15,21</sup> Third, in subgroups of ovariectomized placebo- or E2-treated ApoE<sup>-/-</sup> mice arbitrarily selected for similar serum cholesterol levels, fatty streak area was threefold lower in the latter group. Indeed, using cholesterol-clamped rabbits, Holm and colleagues<sup>31</sup> had previously demonstrated a plasma lipid-independent anti-atherogenic effect of estrogen, in line with Adams and co-workers,<sup>32</sup> who suggested, as early as 1990, a similar conclusion in surgically postmenopausal monkeys.

Altogether, these series of observation points to one (or more) additional lymphocyte-dependent mechanism(s) involved in the protective effect of E2. E2 is a negative regulator of lymphopoiesis, that selectively depletes functional precursors of B and T cells.<sup>33</sup> It also inactivates the intrathymic T-cell differentiation pathway and induces thymocyte apoptosis.<sup>34</sup> Indeed, we observed a remarkable 80% thymic atrophy (85.2 ± 7.5 mg versus 14.1 ± 1.8 mg) and 50% decrease of circulating lymphocytes in our E2-treated ApoE<sup>-/-</sup> mice (6804 ± 568 per μl versus 3520 ± 215 per μl; *P* < 0.001). However, in agreement with Hodgkin and colleagues,<sup>35</sup> T lymphocytes were still detectable in the residual lesions (Figure 3), showing that, despite their decrease in blood, lymphocytes could still reach and infiltrate the remaining lesions.

The protective effect could also be mediated through the modulation of the interactions between lymphocytes and other cell populations, such as endothelial and/or antigen-presenting cells, leading to a local control of the intimal immune process. First, Shi and colleagues<sup>36,37</sup> recently provided strong evidence for the crucial role of

endothelial cells rather than hematopoietic cells as determinants of atherosclerosis susceptibility in C57BL/6 mice. Second, decreased proinflammatory<sup>38–40</sup> or increased anti-inflammatory cytokine<sup>41,42</sup> production resulting from the local interaction between lymphocytes and antigen-presenting cells could explain the protective effect of E2. Indeed, it has recently been reported that estrogens repress Th1 activity and T-cell production of the key inflammatory cytokine tumor necrosis factor- $\alpha$  in bone<sup>43</sup> but we reported the opposite effect in antigen-specific CD4<sup>+</sup> or NKT cell response.<sup>44,45</sup> Further work will be necessary to precisely define the mechanisms of these interactions.

In conclusion, we have demonstrated that lymphocytes are instrumental in the protective effect of E2 but that no single lymphocyte subpopulation is specifically required for this effect. These data point to additional lymphocyte-dependent mechanisms such as modulating the interactions among lymphocytes and between lymphocytes and endothelial and/or antigen-presenting cells.

## Acknowledgments

We thank Mrs. M.J. Fouque, P. Guillou, and M. Larribe for technical and secretarial assistance.

## References

- Waters DD, Gordon D, Rossouw JE, Cannon III RO, Collins P, Herrington DM, Hsia J, Langer R, Mosca L, Ouyang P, Sopko G, Stefanick ML: Women's ischemic syndrome evaluation: current status and future research directions: report of the National Heart, Lung and Blood Institute Workshop: October 2–4, 2002: section 4: lessons from hormone replacement trials. *Circulation* 2004, 109:e53–e55
- Hulley S, Grady D, Bush T, Furberg C, Herrington D, Riggs B, Vittinghoff E: Randomized trial of estrogen plus progestin for secondary prevention of coronary heart disease in postmenopausal women. Heart and Estrogen/Progestin Replacement Study (HERS) Research Group. *JAMA* 1998, 280:605–613
- Rossouw JE, Anderson GL, Prentice RL, LaCroix AZ, Kooperberg C, Stefanick ML, Jackson RD, Beresford SA, Howard BV, Johnson KC, Kotchen JM, Ockene J: Risks and benefits of estrogen plus progestin in healthy postmenopausal women: principal results from the Women's Health Initiative randomized controlled trial. *JAMA* 2002, 288:321–333
- Arnal JF, Gourdy P, Elhage R, Garmy-Susini B, Delmas E, Bouchet L, Castano C, Barreira Y, Couloumiers JC, Prats H, Prats AC, Bayard F: Estrogens and atherosclerosis. *Eur J Endocrinol* 2004, 150:113–117
- Hodgin JB, Maeda N: Minireview: estrogen and mouse models of atherosclerosis. *Endocrinology* 2002, 143:4495–4501
- Ross R: Atherosclerosis—an inflammatory disease. *N Engl J Med* 1999, 340:115–125
- Hansson GK, Libby P, Schonbeck U, Yan ZQ: Innate and adaptive immunity in the pathogenesis of atherosclerosis. *Circ Res* 2002, 91:281–291
- Binder CJ, Chang MK, Shaw PX, Miller YI, Hartvigsen K, Dewan A, Witztum JL: Innate and acquired immunity in atherogenesis. *Nat Med* 2002, 8:1218–1226
- Roselaar SE, Kakkannathu PX, Daugherty A: Lymphocyte populations in atherosclerotic lesions of apoE<sup>−/−</sup> and LDL receptor<sup>−/−</sup> mice. Decreasing density with disease progression. *Arterioscler Thromb Vasc Biol* 1996, 16:1013–1018
- Song L, Leung C, Schindler C: Lymphocytes are important in early atherosclerosis. *J Clin Invest* 2001, 108:251–259
- Reardon CA, Blachowicz L, White T, Cabana V, Wang Y, Lukens J, Bluestone J, Getz GS: Effect of immune deficiency on lipoproteins and atherosclerosis in male apolipoprotein E-deficient mice. *Arterioscler Thromb Vasc Biol* 2001, 21:1011–1016
- Elhage R, Gourdy P, Bouchet L, Jawien J, Fouque M-J, Fiévet C, Huc X, Barreira Y, Couloumiers J-C, Arnal J-F, Bayard F: Deleting TCR $\alpha$  or CD4<sup>+</sup> T lymphocytes leads to opposite effects on site-specific atherosclerosis in female apolipoprotein E-deficient mice. *Am J Pathol* 2004, 165:2013–2019
- Zhou X, Nicoletti A, Elhage R, Hansson GK: Transfer of CD4(+) T cells aggravates atherosclerosis in immunodeficient apolipoprotein E knockout mice. *Circulation* 2000, 102:2919–2922
- Elhage R, Clamens S, Reardon-Alulis C, Getz GS, Fievet C, Maret A, Arnal JF, Bayard F: Loss of atheroprotective effect of estradiol in immunodeficient mice. *Endocrinology* 2000, 141:462–465
- Elhage R, Arnal JF, Pierraggi M-T, Duverger N, Fiévet C, Faye JC, Bayard F: Estradiol-17 $\beta$  prevents fatty streak formation in apolipoprotein E-deficient mice. *Arterioscler Thromb Vasc Biol* 1997, 17:2679–2684
- Ishibashi S, Goldstein JL, Brown MS, Herz J, Burns DK: Massive xanthomatosis and atherosclerosis in cholesterol-fed low density lipoprotein receptor-negative mice. *J Clin Invest* 1994, 93:1885–1893
- Shinkai Y, Rathbun G, Lam KP, Oltz EM, Stewart V, Mendelsohn M, Charron J, Datta M, Young F, Stall AM, Alt FW: RAG-2-deficient mice lack mature lymphocytes owing to inability to initiate V(D)J rearrangement. *Cell* 1992, 68:855–867
- Kitamura D, Roes J, Kuhn R, Rajewsky K: A B cell-deficient mouse by targeted disruption of the membrane exon of the immunoglobulin mu chain gene. *Nature* 1991, 350:423–426
- Duez H, Chao YS, Hernandez M, Torpier G, Poulain P, Mundt S, Mallat Z, Teissier E, Burton CA, Tedgui A, Fruchart JC, Fievet C, Wright SD, Staels B: Reduction of atherosclerosis by the peroxisome proliferator-activated receptor  $\alpha$  agonist fenofibrate in mice. *J Biol Chem* 2002, 277:48051–48057
- Marsh MM, Walker VR, Curtiss LK, Banka CL: Protection against atherosclerosis by estrogen is independent of plasma cholesterol levels in LDL receptor-deficient mice. *J Lipid Res* 1999, 40:893–900
- Bourassa P-A, Milos PM, Gaynor BJ, Breslow JL, Aiello RJ: Estrogen reduces atherosclerotic lesion development in apolipoprotein E-deficient mice. *Proc Natl Acad Sci USA* 1996, 93:10022–10027
- Shedlock DJ, Whitmire JK, Tan J, MacDonald AS, Ahmed R, Shen H: Role of CD4 T cell help and costimulation in CD8 T cell responses during *Listeria monocytogenes* infection. *J Immunol* 2003, 170:2053–2063
- Shevach EM, McHugh RS, Piccirillo CA, Thornton AM: Control of T-cell activation by CD4<sup>+</sup> CD25<sup>+</sup> suppressor T cells. *Immunol Rev* 2001, 182:58–67
- Roncarolo MG, Bacchetta R, Bordignon C, Narula S, Levings MK: Type 1 T regulatory cells. *Immunol Rev* 2001, 182:68–79
- Matejuk A, Bakke AC, Hopke C, Dwyer J, Vandenbark AA, Offner H: Estrogen treatment induces a novel population of regulatory cells, which suppresses experimental autoimmune encephalomyelitis. *J Neurosci Res* 2004, 77:119–126
- Polanczyk MJ, Carson BD, Subramanian S, Afentoulis M, Vandenbark AA, Ziegler SF, Offner H: Cutting edge: estrogen drives expansion of the CD4<sup>+</sup>CD25<sup>+</sup> regulatory T cell compartment. *J Immunol* 2004, 173:2227–2230
- Caligiuri G, Nicoletti A, Poirier B, Hansson GK: Protective immunity against atherosclerosis carried by B cells of hypercholesterolemic mice. *J Clin Invest* 2002, 109:745–753
- Verthelyi DI, Ahmed SA: Estrogen increases the number of plasma cells and enhances their autoantibody production in nonautoimmune C57BL/6 mice. *Cell Immunol* 1998, 189:125–134
- Horkko S, Bird DA, Miller E, Itabe H, Leitinger N, Subbanagounder G, Berliner JA, Friedman P, Dennis EA, Curtiss LK, Palinski W, Witztum JL: Monoclonal autoantibodies specific for oxidized phospholipids or oxidized phospholipid-protein adducts inhibit macrophage uptake of oxidized low-density lipoproteins. *J Clin Invest* 1999, 103:117–128
- Major AS, Fazio S, Linton MF: B-lymphocyte deficiency increases atherosclerosis in LDL receptor-null mice. *Arterioscler Thromb Vasc Biol* 2002, 22:1892–1898
- Holm P, Korsgaard N, Shalmi M, Andersen HL, Hougaard P, Skouby SO, Stender S: Significant reduction of the antiatherogenic effect of estrogen by long-term inhibition of nitric oxide synthesis in cholesterol-clamped rabbits. *J Clin Invest* 1997, 100:821–828

32. Adams MR, Kaplan JR, Manuck SB, Koritnik DR, Parks JS, Wolfe MS, Clarkson TB: Inhibition of coronary artery atherosclerosis by 17-beta estradiol in ovariectomized monkeys. Lack of an effect of added progesterone. *Arteriosclerosis* 1990, 10:1051-1057
33. Medina KL, Garrett KP, Thompson LF, Rossi MI, Payne KJ, Kincade PW: Identification of very early lymphoid precursors in bone marrow and their regulation by estrogen. *Nat Immunol* 2001, 2:718-724
34. Okasha SA, Ryu S, Do Y, McKallip RJ, Nagarkatti M, Nagarkatti PS: Evidence for estradiol-induced apoptosis and dysregulated T cell maturation in the thymus. *Toxicology* 2001, 163:49-62
35. Hodgins JB, Kregge JH, Reddick RL, Korach KS, Smithies O, Maeda N: Estrogen receptor alpha is a major mediator of 17beta-estradiol's atheroprotective effects on lesion size in ApoE<sup>-/-</sup> mice. *J Clin Invest* 2001, 107:333-340
36. Shi W, Haberland ME, Jien ML, Shih DM, Lusis AJ: Endothelial responses to oxidized lipoproteins determine genetic susceptibility to atherosclerosis in mice. *Circulation* 2000, 102:75-81
37. Shi W, Wang NJ, Shih DM, Sun VZ, Wang X, Lusis AJ: Determinants of atherosclerosis susceptibility in the C3H and C57BL/6 mouse model: evidence for involvement of endothelial cells but not blood cells or cholesterol metabolism. *Circ Res* 2000, 86:1078-1084
38. Gupta S, Pablo AM, Jiang X, Wang N, Tall AR, Schindler C: IFN-gamma potentiates atherosclerosis in ApoE knock-out mice. *J Clin Invest* 1997, 99:2752-2761
39. Lee TS, Yen HC, Pan CC, Chau LY: The role of interleukin 12 in the development of atherosclerosis in ApoE-deficient mice. *Arterioscler Thromb Vasc Biol* 1999, 19:734-742
40. Elhage R, Jawien J, Rudling M, Ljunggren HG, Takeda K, Akira S, Bayard F, Hansson GK: Reduced atherosclerosis in interleukin-18 deficient apolipoprotein E-knockout mice. *Cardiovasc Res* 2003, 59:234-240
41. Mallat Z, Besnard S, Duriez M, Deleuze V, Emmanuel F, Bureau MF, Soubrier F, Esposito B, Duez H, Fievet C, Staels B, Duverger N, Scherman D, Tedgui A: Protective role of interleukin-10 in atherosclerosis. *Circ Res* 1999, 85:e17-e24
42. Robertson AKL, Rudling M, Zhou X, Gorelik L, Flavell RA, Hansson GK: Disruption of TGF-(beta) signaling in T cells accelerates atherosclerosis. *J Clin Invest* 2003, 112:1342-1350
43. Cenci S, Toraldo G, Weitzmann MN, Roggia C, Gao Y, Qian WP, Sierra O, Pacifici R: Estrogen deficiency induces bone loss by increasing T cell proliferation and lifespan through IFN-gamma-induced class II transactivator. *Proc Natl Acad Sci USA* 2003, 100:10405-10410
44. Maret A, Coudert JD, Garidou L, Foucras G, Gourdy P, Krust A, Dupont S, Chambon P, Druet P, Bayard F, Guery JC: Estradiol enhances primary antigen-specific CD4 T cell responses and Th1 development in vivo. Essential role of estrogen receptor alpha expression in hematopoietic cells. *Eur J Immunol* 2003, 33:512-521
45. Gourdy P, Araujo LM, Zhu R, Garay-Susini B, Diem S, Laurell H, Leite-De-Moraes M, Dy M, Arnal JF, Bayard F, Herbelin A: Relevance of sexual dimorphism to regulatory T cells: estradiol promotes IFN-gamma production by invariant natural killer T cells. *Blood* 2005, 105:2415-2420

## Hypercholesterolemia in Low Density Lipoprotein Receptor Knockout Mice and its Reversal by Adenovirus-mediated Gene Delivery

Shun Ishibashi,\* Michael S. Brown,\* Joseph L. Goldstein,\* Robert D. Gerard,\* Robert E. Hammer,\*\* and Joachim Herz\*  
Departments of \*Molecular Genetics and †Biochemistry and ‡Howard Hughes Medical Institute, University of Texas Southwestern Medical Center at Dallas, Dallas, Texas 75235

### Abstract

We employed homologous recombination in embryonic stem cells to produce mice lacking functional LDL receptor genes. Homozygous male and female mice lacking LDL receptors (*LDLR*<sup>-/-</sup> mice) were viable and fertile. Total plasma cholesterol levels were twofold higher than those of wild-type littermates, owing to a seven- to ninefold increase in intermediate density lipoproteins (IDL) and LDL without a significant change in HDL. Plasma triglyceride levels were normal. The half-lives for intravenously administered <sup>125</sup>I-VLDL and <sup>125</sup>I-LDL were prolonged by 30-fold and 2.5-fold, respectively, but the clearance of <sup>125</sup>I-HDL was normal in the *LDLR*<sup>-/-</sup> mice. Unlike wild-type mice, *LDLR*<sup>-/-</sup> mice responded to moderate amounts of dietary cholesterol (0.2% cholesterol/10% coconut oil) with a major increase in the cholesterol content of IDL and LDL particles. The elevated IDL/LDL level of *LDLR*<sup>-/-</sup> mice was reduced to normal 4 d after the intravenous injection of a recombinant replication-defective adenovirus encoding the human LDL receptor driven by the cytomegalovirus promoter. The virus restored expression of LDL receptor protein in the liver and increased the clearance of <sup>125</sup>I-VLDL. We conclude that the LDL receptor is responsible in part for the low levels of VLDL, IDL, and LDL in wild-type mice and that adenovirus-encoded LDL receptors can acutely reverse the hypercholesterolemic effects of LDL receptor deficiency. (*J. Clin. Invest.* 1993. 92:883-893.) Key words: homologous recombination • lipoprotein metabolism • very low density lipoprotein • gene therapy • liver receptors

### Introduction

The LDL receptor removes cholesterol-rich intermediate density lipoproteins (IDL)<sup>1</sup> and LDL from plasma and thereby regulates the plasma cholesterol level (1). The lipoproteins that

bind to the LDL receptor are derived from triglyceride-rich VLDL, which are secreted by the liver. In the circulation some of the triglycerides of VLDL are removed by lipoprotein lipase, and the resultant IDL particle is cleared rapidly into the liver, owing to its content of apolipoprotein E (apo E), a high affinity ligand for the LDL receptor. Some IDL particles escape hepatic uptake and are converted to LDL in a reaction that leads to the loss of apo E. The sole remaining protein, apo B-100, binds to LDL receptors with relatively low affinity, thus causing LDL particles to circulate for relatively prolonged periods (2).

Triglyceride-depleted, cholesterol-rich remnants of intestinal chylomicrons are taken into the liver by the LDL receptor and by a genetically distinct molecule designated the chylomicron remnant receptor (3, 4). The latter receptor recognizes apo E when it is present on chylomicron remnant particles together with apo B-48, a truncated version of apo B-100 that is produced in the intestine (3). Circumstantial evidence suggests that the chylomicron remnant receptor is the same as the LDL receptor-related protein/ $\alpha_2$ -macroglobulin receptor (LRP) (4). The action of this receptor may be facilitated by the preliminary binding of the chylomicron remnants to cell-associated glycosaminoglycans in hepatic sinusoids (5).

Genetic defects in the LDL receptor produce hypercholesterolemia in humans with familial hypercholesterolemia (FH) (6), Watanabe-heritable hyperlipidemic (WHHL) rabbits (7), and rhesus monkeys (8). Humans and rabbits with two defective LDL receptor genes (FH and WHHL homozygotes) have massively elevated levels of IDL and LDL, and they develop fulminant atherosclerosis at an early age. Tracer studies with <sup>125</sup>I-labeled lipoproteins revealed a retarded clearance of IDL and LDL, and an increased conversion of IDL to LDL in humans (9) and rabbits (10) with LDL receptor deficiency.

Evidence from one human pedigree (11) and from monozygotic/dizygotic twin pair correlations (12) indicates that other genes can influence the degree of hypercholesterolemia in subjects with LDL receptor deficiency. These genes are likely to influence cholesterol levels even in people with normal LDL receptors. Identification of these genes has not been possible in human linkage studies, nor in breeding experiments with WHHL rabbits. Linkage studies would be facilitated by the availability of an inbred mouse strain with LDL receptor deficiency. The consequences of LDL receptor deficiency in mice are difficult to predict because mice, like rats, have a fundamental difference in LDL metabolism when compared with other species that have been studied (13). In mice and rats a substantial fraction of the VLDL secreted from liver contains apo B-48 instead of apo B-100 (14-16). Remnants derived from the apo B-48 containing particles are cleared into the liver and are not converted to LDL (17). Some of this clearance may be mediated by the chylomicron remnant receptor. For this reason, LDL receptor deficiency in mice would not be predicted to raise the plasma LDL level as profoundly as it does in WHHL rabbits.

Received for publication 1 April 1993.

1. Abbreviations used in this paper: AdCMV-Luc, recombinant adenovirus containing luciferase cDNA; AdCMV-LDLR, recombinant adenovirus containing human LDL receptor cDNA; CMV, cytomegalovirus; ES, embryonic stem cells; FH, familial hypercholesterolemia; FPLC, fast performance liquid chromatography; IDL, intermediate density lipoproteins; LRP, LDL receptor-related protein/ $\alpha_2$ -macroglobulin receptor; *LDLR*<sup>-/-</sup> and *LDLR*<sup>+/-</sup>, mice homozygous and heterozygous, respectively, for LDL receptor gene disruption; pfu, plaque-forming units; WHHL, Watanabe-heritable hyperlipidemic rabbits.

*J. Clin. Invest.*

© The American Society for Clinical Investigation, Inc.

0021-9738/93/08/0883/11 \$2.00

Volume 92, August 1993, 883-893

Mice deficient in LDL receptors might also aid in the development of gene therapy techniques designed to enhance the expression of hepatic LDL receptors. Using homozygous WHHL rabbits as a model, Chowdhury et al. (18) infected autologous hepatocytes *ex vivo* with a recombinant retrovirus carrying an expressible cDNA copy of the rabbit LDL receptor under control of the chicken  $\beta$ -actin promoter. After infusion of these transduced hepatocytes into the spleen, LDL receptor expression was visualized in 2–4% of liver cells. Although functional studies of  $^{125}$ I-LDL turnover were not performed, these workers observed a fall of  $\sim 30\%$  in the level of total plasma cholesterol, which did not occur in animals injected with hepatocytes transduced with a control retrovirus encoding an irrelevant protein. With this technique the expression of LDL receptors persisted for 2–4 mo. Although the 30% reduction in plasma cholesterol was statistically significant, the level remained quite elevated (above 500 mg/dl) when compared with normal rabbits, ( $< 100$  mg/dl), presumably owing to the expression of LDL receptors in only a small percentage of hepatocytes. Similar results were obtained in transient experiments following the intravenous injection of a plasmid containing the LDL receptor cDNA complexed to an asialo-orosomucoid/poly-L-lysine conjugate (19).

In mice, gene manipulation has produced significant effects on LDL receptor expression. Several years ago Hofmann et al. (20) and Yokode et al. (21) produced transgenic mice that overexpressed hepatic LDL receptors encoded by the human LDL receptor gene driven by the metallothionein or transferrin promoter. They showed that these receptors enhanced the clearance of radiolabeled LDL from plasma of normal mice. Yokode et al. (22) then demonstrated that these mice were resistant to the cholesterol-elevating effects of a high cholesterol diet.

Recently, Herz and Gerard (23) developed a recombinant replication-defective adenovirus vector containing an expressible cDNA copy of the human LDL receptor driven by the cytomegalovirus (CMV) promoter. 4 d after its intravenous injection, this virus elicited the expression of high levels of human LDL receptors in more than 90% of mouse hepatocytes, and this enhanced markedly the uptake of  $^{125}$ I-LDL by the liver. The use of adenovirus vectors was based on the observations of Stratford-Perricaudet et al. (24), who injected recombinant adenoviruses encoding ornithine transcarbamylase into neonatal mice homozygous for a defect in this gene. The recombinant adenovirus produced a level of enzyme activity in liver sufficient to eliminate the pathologic manifestations of the disease, and expression apparently persisted for 1 yr.

The current studies were conducted in order to learn the consequences of LDL receptor deficiency in mice and to learn whether adenovirus vectors will acutely reverse these consequences. For these purposes, we have used the techniques of homologous recombination in cultured embryonic stem (ES) cells (25–27) to produce mice that lack functional LDL receptors. We show that these mice develop a marked elevation in plasma IDL and LDL levels when compared with control mice and that this elevation can be eliminated acutely by the intravenous administration of a recombinant adenovirus encoding the human LDL receptor.

## Methods

**General methods.** Unless otherwise indicated, DNA manipulations were performed by standard techniques (28). Immunoblot (29) and

ligand blot analyses (30) were performed as described in the indicated references. Cholesterol and triglycerides were determined enzymatically with assay kits obtained from Boehringer Mannheim (Biochemicals, Indianapolis, IN) and Sigma Chemical Co. (St. Louis, MO), respectively. The normal mouse diet (Teklad 4% Mouse/Rat Diet 7001 from Harlan Teklad Premier Laboratory Diets, Madison, WI) contained 4% (wt/wt) animal fat with  $< 0.04\%$  (wt/wt) cholesterol. Mouse VLDL ( $d < 1.006$  g/ml), LDL ( $d 1.025$ – $1.50$  g/ml), and HDL ( $d 1.063$ – $1.215$  g/ml) were isolated by sequential ultracentrifugation (31) from pooled plasma obtained from *LDLR*<sup>-/-</sup> mice that had been fasted overnight. Rabbit VLDL ( $d < 1.006$  g/ml) was isolated by the same procedure from plasma obtained from fasted WHHL rabbits. Lipoproteins were radiolabeled with  $^{125}$ I by the iodine monochloride method (31). A 0.2% cholesterol/10% coconut oil diet was prepared by supplementing the normal mouse diet with 0.2% (wt/wt) cholesterol dissolved in a final concentration of 10% (vol/wt) coconut oil.

**Cloning of mouse LDL receptor cDNA.** Mouse LDL receptor cDNA was amplified by PCR from mouse liver first strand cDNA using poly(A)<sup>+</sup> RNA and the following primers:

Primer A, 5'-ATTCTAGAGGGTGAAGTGGTGTGAG-3' (exon 14);

Primer B, 5'-ATAATTCAGTACCATCTGTCTCGAGGGGTAG-3' (exon 18);

Primer C, 5'-AAATG(T/C)ATC(T/G)(T/C)C(T/A)GCAAGTGGGTCTG(C/T)GA(T/C)GGCAG-3' (exon 2);

Primer D 5'-CTGCTCCTCATTCCTCTGCCAGCCA-3' (exon 16).

Amplification with primers A and B yielded a cDNA fragment corresponding to exons 14–18. cDNA spanning exons 2–16 was amplified with primers C and D. Primers A, B, and C were designed and based on the conservation of the LDL receptor coding sequence between human, rabbit, hamster, rat, and cow (32, 33). Primer D was designed and based on the mouse exon 16 cDNA sequence contained in the amplification product obtained with primers A and B. Amplification products were blunt-end cloned into pGEM3Zf(+) (Promega Corp., Madison, WI) and sequenced.

**Construction of gene replacement vector.** Southern blot analysis of mouse C57B1/6 genomic DNA with an exon 2–16 cDNA probe revealed a 16-kb BamHI fragment. This fragment was enriched by sucrose density ultracentrifugation and cloned into the  $\lambda$ Dash II vector (Stratagene Corp., La Jolla, CA), and recombinant phages containing the fragment were isolated by plaque screening. After subcloning into pGEM3Zf(+), the *Pol2sneobpA* expression cassette (34) was inserted into a unique *Sal*I site in exon 4 (Fig. 1). This *neo* expression cassette was flanked by 12 kb of LDL receptor genomic sequences including exons 1 to 4. The short arm of the targeting vector contained a 1.2-kb *Sal*I–*Sac*I fragment with sequences of exon 4 and intron 4. The *Sal*I sites were destroyed during the cloning. Two copies of the herpes simplex thymidine kinase gene (35) were inserted in tandem at the 3' end of the short arm of the targeting vector (Fig. 1).

**ES cell culture.** Mouse ES cells (AB-1, kindly provided by A. Bradley, Baylor College of Medicine, Houston) were cultured on leukemia inhibitory factor-producing STO feeder cells as described (36). Approximately  $2 \times 10^7$  cells were electroporated with linearized targeting vector (25  $\mu$ g/ml, 275 V, 330  $\mu$ F) in an electroporator (GIBCO Bethesda Research Laboratories) and seeded onto irradiated feeder layers (10,000 rad). After selection with 190  $\mu$ g/ml G418 and 0.25  $\mu$ M 1-[2-deoxy, 2-fluoro- $\beta$ -D-arabinofuranosyl]-5-iodouracil (FIAU; Bristol-Myers Co., New York, NY) recombinant clones were identified by PCR as described (34) using Primers E and F (Primer E, located in 3'-untranslated region of *neo* cassette, 5'-GATTGGGAAGACAATAGCAGGCATGC-3'; Primer F, located in intron 4, 5'-GGCAAGATGGCTCAGCAAGCAAAGGC-3'). Homologous recombination was verified by Southern blot analysis after *Bam*HI digestion and probing with a genomic DNA fragment located 3' of the targeting construct (Fig. 1). Nine independent stem cell clones containing a disrupted LDL receptor allele were injected into C57B1/6 blastocysts (27), yielding a total of 17 chimeric males whose coat color (agouti) indi-



cated a contribution of stem cells ranging from 30 to 100%. Of the 17 chimeric males, 15 were fertile, and 13 gave offspring that carried the disrupted LDL receptor allele. Five of these males exclusively transmitted the stem cell-derived genome through the germline. All experiments were performed with the F2 or F3 generation descendants, which were hybrids between the C57B1/6J and 129Sv strains.

**Plasma lipoprotein analysis.** Blood was sampled from the retro-orbital plexus into tubes containing EDTA (Microvette CB 1000 capillary tubes; Sarstedt, Inc., Newton, NC). Pooled mouse plasma (0.6 ml from 3 to 5 mice) was ultracentrifuged at  $d = 1.215$  g/ml, and the resulting lipoprotein fraction ( $d < 1.215$  g/ml) was subjected to fast performance liquid chromatography (FPLC) gel filtration on a Superose 6 (Sigma Chemical Co.) column as previously described (22). For apoprotein analysis, peak fractions were pooled, precipitated with trichloroacetic acid, washed with acetone, and subjected to electrophoresis on 3–15% SDS polyacrylamide gels as described (22). Gels were calibrated with Rainbow high molecular weight markers (Amersham Corp., Arlington Heights, IL) and stained with Coomassie blue.

**Preparation of recombinant adenoviruses.** Recombinant replication-deficient adenoviruses containing the firefly luciferase cDNA (AdCMV-Luc) and the human LDL receptor cDNA (AdCMV-LDLR) driven by the cytomegalovirus promoter/enhancer were prepared as previously described (23). Briefly, virus particles for injection into animals were grown on human embryonic kidney 293 cells and purified by cesium chloride density gradient centrifugation. Particles were further purified by gel filtration on a Sepharose CL-4B (Pharmacia LKB Biotechnology, Piscataway, NJ) column equilibrated with 10 mM Tris-HCl, 137 mM NaCl, 5 mM KCl, 1 mM MgCl<sub>2</sub> at pH 7.4. BSA was added at a final concentration of 1 mg/ml, after which each virus preparation was stored in multiple aliquots at  $-70^{\circ}\text{C}$ . Viruses were titered on 293 cells; the titer ranged between  $10^{10}$  and  $10^{11}$  plaque-forming units (pfu) per ml.

For administration to mice, each recombinant adenovirus was injected as a single dose ( $2 \times 10^9$  pfu in 200  $\mu\text{l}$ ) into the external jugular vein of a nonfasted animal that had been anesthetized with sodium pentobarbital as previously described (23).

**Immunohistochemistry.** Mice were killed 4 d after injection of recombinant virus, the liver was removed, and a sector extending from the surface of the liver to the portal area was immediately frozen (without fixation) in OCT Compound 4583 (Miles Laboratories, Inc., Elkhart, IN) at  $-196^{\circ}\text{C}$  and stored at  $-70^{\circ}\text{C}$  until cutting. For immunohistochemistry, sections of 6  $\mu\text{m}$  were cut on a Leitz Cryostat (E. Leitz, Inc., Rockleigh, NJ) at  $-20^{\circ}\text{C}$  and mounted onto polylysine-coated slides. Before immunostaining, tissue sections were fixed in 100% (vol/vol) methanol at  $-20^{\circ}\text{C}$  for 30 s followed by two washes in PBS. All incubations were performed at  $20^{\circ}\text{C}$ . Samples were blocked by incubation for 20 min with 50 mM Tris-HCl, 80 mM NaCl, 2 mM CaCl<sub>2</sub> at pH 8 containing 10% (vol/vol) fetal calf serum. Sections were then incubated for 1 h with 20  $\mu\text{g}/\text{ml}$  of polyclonal rabbit IgG directed against the bovine LDL receptor (37) followed by three 5-min washes with PBS. Bound primary antibody was detected by incubation for 45 min with the indicated concentrations of FITC-labeled goat anti-rabbit IgG (GIBCO Bethesda Research Laboratories, Gaithersburg, MD). Slides were washed again three times in PBS, rinsed once briefly in water, and mounted under a coverslip with DABCO (90% vol/vol glycerol, 50 mM Tris-HCl at pH 9, 25% (wt/vol) 1,4-diazabicyclo-[2.2.2]-octane).

## Results

To disrupt the LDL receptor gene in murine ES cells, we constructed a gene targeting vector of the replacement type (35) as described in Methods. The targeting vector and the expected genomic structure of the disrupted locus are shown in Fig. 1. The *neo* cassette was inserted into exon 4 of the LDL receptor gene. The disrupted locus is predicted to encode a nonfunctional protein that is truncated within the ligand binding do-

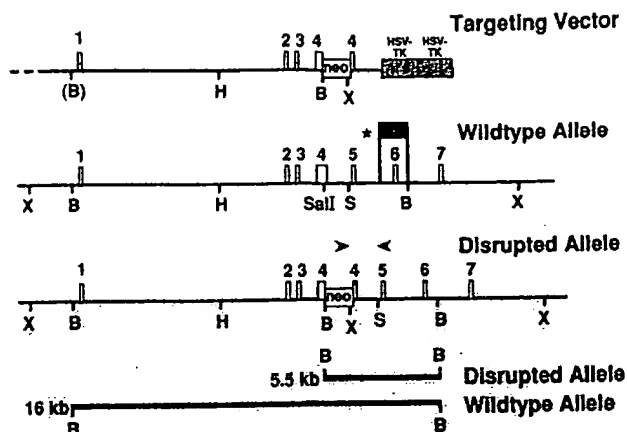


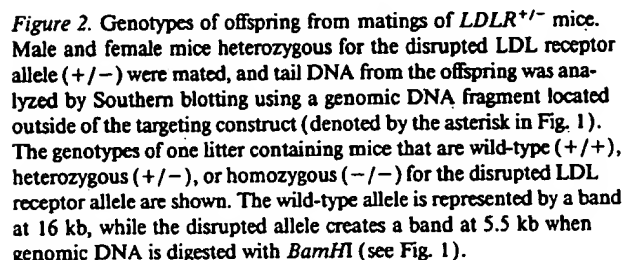
**Figure 1.** Strategy for targeted disruption of the LDL receptor locus in the mouse genome. A targeting vector of the replacement type was constructed as described in Methods. The *neo* gene is driven by the murine RNA polymerase II promoter and followed by the 3'-untranslated region of the bovine growth hormone gene containing the polyadenylation signal (34). The transcriptional direction of the *neo* gene is parallel to that of the LDL receptor. Two copies of the herpes simplex virus thymidine kinase gene (HSV-TK) (reference 35) flank the 3' homology segment. In the event of homologous recombination, the disrupted allele will have acquired additional sites for the restriction endonucleases *Bam*HI (B) and *Xba*I (X). The expected *Bam*HI digestion pattern resulting from a targeting event is shown at the bottom. The DNA probe used for Southern blotting (denoted by the asterisk and the heavy bracket) is a 1.7-kb *Bgl*II-*Bam*HI genomic fragment containing exon 6 and flanking intron sequences. The positions of the two oligonucleotides used for PCR diagnosis of homologous recombination are indicated by the arrows (oligo 1: 3' end of *neo* cassette; oligo 2: downstream of *Sac*I site in intron 4). B, *Bam*HI; H, *Hind*III; X, *Xba*I; S, *Sac*I.

main of the receptor. This receptor fragment should not bind LDL, and it should not remain associated with the cell membrane since it lacks the membrane spanning segment.

ES cells were electroporated with the linearized targeting vector and subjected to positive and negative selection using standard procedures (36). Homologous recombination events were detected by PCR and verified by digestion of genomic ES cell DNA with *Bam*HI. The presence of a diagnostic 5.5-kb *Bam*HI fragment in addition to the wild-type 16-kb fragment is indicative of gene targeting when the Southern blot is probed with a genomic DNA fragment located outside of the targeting vector (indicated by the asterisk in Fig. 1). The frequency of homologous recombination was very high. Approximately 50% of clones that were resistant to both G418 and FIAU exhibited homologous recombination.

Recombinant stem cell clones injected into C57B1/6 blastocysts (27) gave rise to chimeric animals with a stem cell-derived coat color contribution that ranged from 30 to 100%. Several male chimeras derived from independently targeted stem cell clones efficiently transmitted the stem cell-derived genome through the germ line. Offspring heterozygous for the disrupted LDL receptor allele were diagnosed by Southern blotting. When heterozygous animals were mated to each other, their offspring included animals that were wild-type (+/+), heterozygous (+/-), and homozygous (-/-) for the disrupted LDL receptor allele. Fig. 2 shows a representative

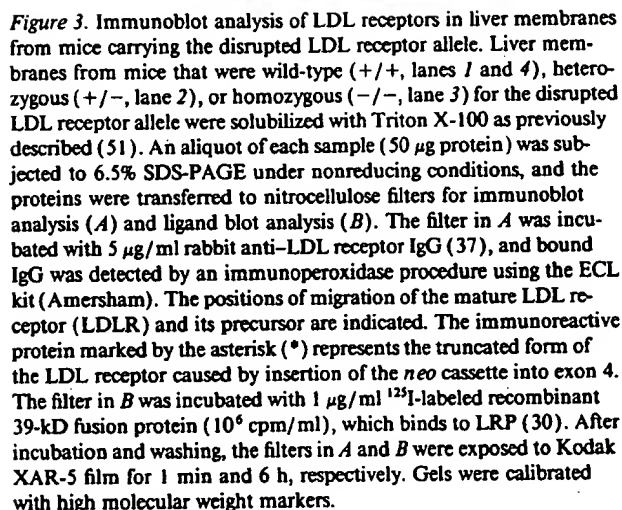




To confirm the inability of the disrupted gene to produce full-length LDL receptors, we prepared liver membranes from wild-type, heterozygous, and homozygous animals. Proteins were solubilized with detergent, and 50  $\mu$ g of each sample were analyzed by SDS gel electrophoresis and immunoblotting with a polyclonal antibody that detects the mouse LDL receptor. As shown in Fig. 3 A, normal LDL receptor protein was readily detected by the antibody in wild-type (+/+ , lanes 1 and 4) and in heterozygous animals (+/- , lane 2), but was undetectable in animals that were homozygous for the LDL receptor defect (-/- , lane 3). An abnormal band (marked by an asterisk) was present in liver membranes prepared from heterozygous (lane

Sex	Total Plasma Cholesterol Level (mg/dl)		
	+/+	+/-	-/-
Male	119±4 (n = 19)	158±4 (n = 39)	228±9 (n = 16)
Female	100±4* (n = 28)	138±4* (n = 54)	239±8 (n = 21)

\* Sex difference,  $P = 0.01$  (unpaired  $t$  test).



Mice heterozygous or homozygous for the disrupted LDL receptor allele have elevated plasma cholesterol levels when compared with their wild-type litter mates. Table I shows total plasma cholesterol levels of mice from 28 litters derived from the mating of heterozygous animals and fed a normal chow diet. The mean age of the animals at the time of measurement was 52 d. Total (nonfasting) plasma cholesterol values are ~ 35% elevated in heterozygotes and about two times higher in *LDLR*<sup>-/-</sup> mice when compared to wild-type litter mates. In animals of wild-type or heterozygous genotype, females had a lower total plasma cholesterol level than males. This difference was absent in the *LDLR*<sup>-/-</sup> mice. There was no significant

difference in plasma triglyceride concentration among animals of the three genotypes (8–10 animals per group) whose average nonfasting values on a normal chow diet ranged from 119 to 133 mg/dl (data not shown).

To learn which lipoprotein fraction was affected by the loss of functional LDL receptors in the mouse, we used FPLC to determine the lipoprotein cholesterol profiles of male and female mice of the three different genotypes fed a normal chow diet (Fig. 4 A–C). Plasma of wild-type mice contained very little cholesterol in the IDL/LDL fraction. A small but definite increase in this fraction was observed in heterozygous mice of either sex. Animals homozygous for the LDL receptor defect showed a marked increase almost exclusively in the IDL/LDL fraction with a small increase in VLDL. For all genotypes, the HDL-cholesterol level was slightly higher in male mice as compared with female mice, but there was no dramatic effect of LDL receptor gene disruption.

To estimate the relative elevation of IDL/LDL from the data of Fig. 4 A–C, we added up the total cholesterol content of each column fraction within the IDL/LDL peak and then expressed the data relative to the levels observed in wild-type mice of the same sex. These data revealed that the IDL/LDL cholesterol was elevated about twofold in  $LDLR^{+/-}$  mice of either sex and 7.4- to 9-fold in male and female  $LDLR^{-/-}$  mice, respectively. The HDL-cholesterol was elevated only modestly (~ 1.3-fold) in the  $LDLR^{-/-}$  mice.

Fig. 4 D–F shows comparisons of the lipoprotein cholesterol profiles of male mice of the different genotypes fed either a normal chow diet with or without 0.2% cholesterol/10% coconut oil. Wild-type mice showed only a small difference in lipoprotein profile in response to the cholesterol-enriched diet. Heterozygous mice responded with a small, but distinct elevation in IDL/LDL cholesterol. In the  $LDLR^{-/-}$  mice the cholesterol content of the IDL/LDL fraction rose about threefold. The mean total plasma cholesterol levels for the three genotypes before (fasted) and after (nonfasted) cholesterol feeding were as follows:  $+/+$ , 146 and 149 mg/dl;  $+/-$ , 188 and 196 mg/dl; and  $-/-$ , 293 and 425 mg/dl, respectively.

The apoproteins of the various fractions in Fig. 4 D–F were analyzed by SDS polyacrylamide gel electrophoresis and Coomassie blue staining (Fig. 5). On the normal chow diet, the heterozygous mice showed a distinct elevation in apo B-100 and apo E in the IDL/LDL fraction. The IDL/LDL fraction from  $LDLR^{-/-}$  mice had a much more marked increase of these two apoproteins as well as of apo B-48. The 0.2% cholesterol/10% coconut oil diet elicited a pronounced increase in apo B-100, apo B-48, and apo E in the IDL/LDL fraction of the  $LDLR^{-/-}$  mice. A small increase in the apo E of VLDL and HDL was also apparent in the cholesterol-fed mice (homozygotes > heterozygotes > wild-type).

To evaluate the functional effect of the LDL receptor deficiency, we compared the ability of  $LDLR^{-/-}$  mice and wild-

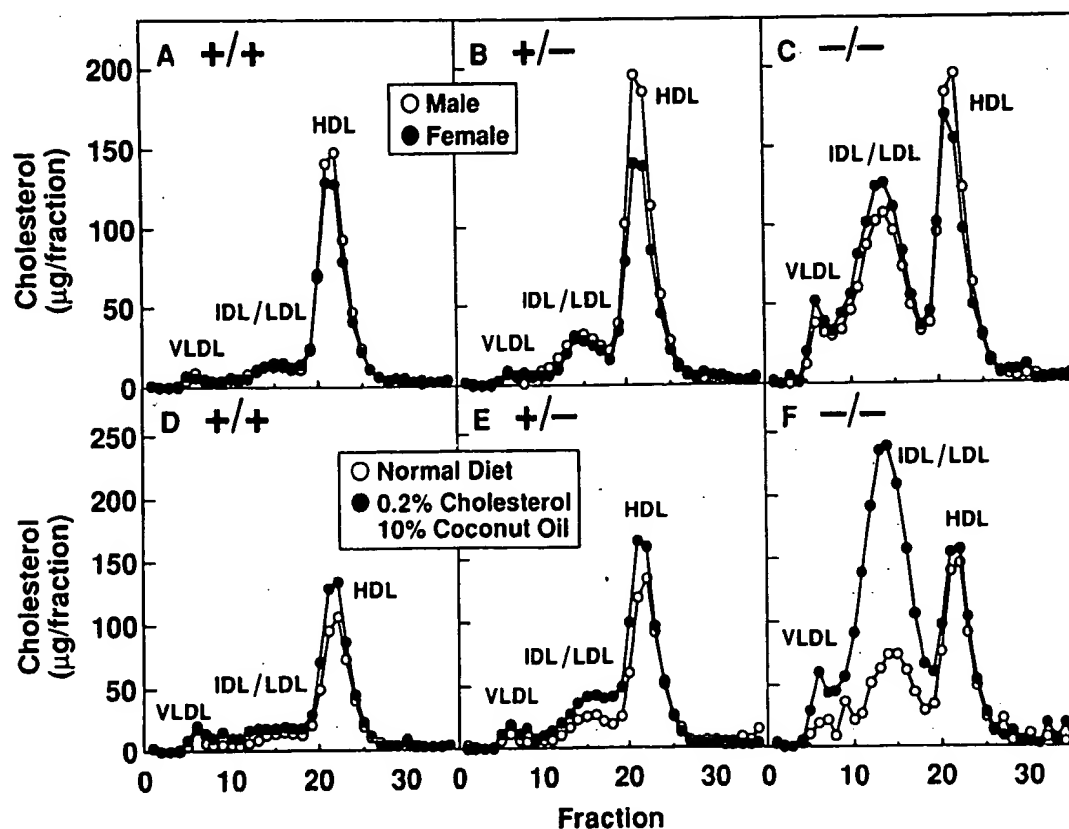


Figure 4. FPLC profiles of mouse plasma lipoproteins from wild-type ( $+/+$ ) and mutant mice carrying the disrupted LDL receptor allele in heterozygous ( $+/-$ ) and homozygous ( $-/-$ ) forms. Mice with the indicated genotype ( $n = 10$  for each sex in A–C and  $n = 5$  males in D–F) were fed a normal diet in A–C or the indicated diet in D–F for 7 wk. The pooled plasma from each group (collected from 12-h fasted animals in A–C and from nonfasted animals in D–F) was subjected to gel filtration on FPLC, and the cholesterol content of each fraction was measured as described in Methods. The mice were 8–9 wk of age in A–C and 16–17 wk in D–F.

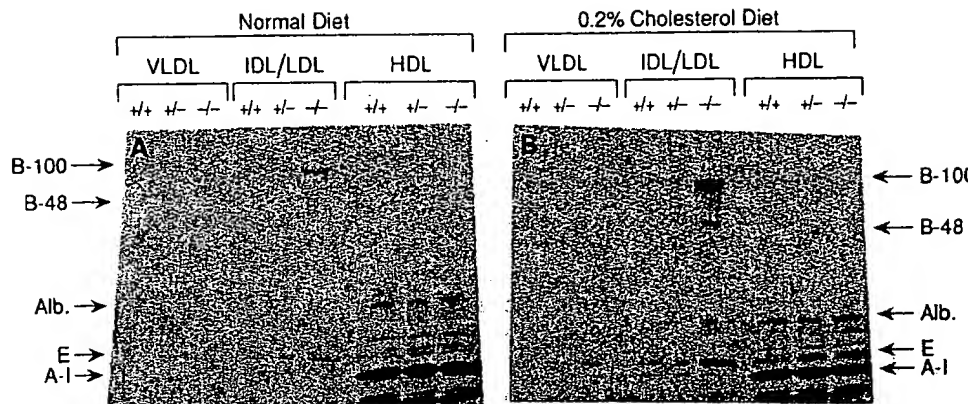


Figure 5. SDS-gel electrophoresis of lipoprotein fractions from wild-type and mutant mice fed different diets. Male mice ( $n = 5$  per group) that were wild-type (+/+), heterozygous (+/-) or homozygous (-/-) for the disrupted LDL receptor allele were fed either a normal diet (A) or a diet containing 0.2% cholesterol and 10% coconut oil (B) as described in the legend to Fig. 4. The apoproteins from the VLDL, IDL/LDL, and HDL containing fractions in Fig.

4 (equivalent to 70  $\mu$ l of plasma) were subjected to electrophoresis on 3–15% SDS gradient gels. Proteins were stained with Coomassie blue. The positions of migration of apo B-100, apo B-48, albumin (Alb.), apo E, and apo A-I are indicated.

type mice to clear  $^{125}$ I-labeled lipoproteins from the circulation (Fig. 6). For this purpose, we isolated three lipoprotein fractions (VLDL, LDL, and HDL) by ultracentrifugation of pooled plasma of 50  $LDLR^{-/-}$  mice. After radiolabeling with  $^{125}$ I, each lipoprotein was injected into the external jugular vein of three wild-type (+/+) and three homozygous (-/-) animals. Blood was obtained at the indicated intervals, and the radioactivity was expressed relative to the radioactivity at 2 min after injection of the label. As shown in Fig. 6A, wild-type mice (open circles) clear  $^{125}$ I-VLDL much more efficiently than  $LDLR^{-/-}$  animals (closed circles). In the wild-type ani-

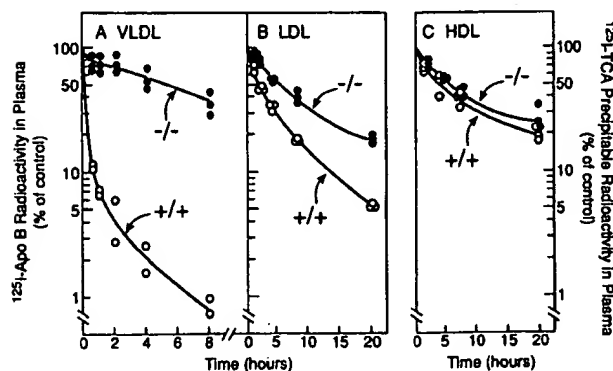


Figure 6. Disappearance of  $^{125}$ I-labeled lipoproteins from the circulation in wild-type (o) and  $LDLR^{-/-}$  (•) mice. For each graph, 3 wild-type and 3  $LDLR^{-/-}$  male mice, 20–24 wk of age that had been fasted for 12 h, were anesthetized with sodium pentobarbital (60 mg/kg). Each mouse received an intravenous bolus via the external jugular vein of 0.25 ml of 0.15 M NaCl containing bovine serum albumin (2 mg/ml) and one of the following  $^{125}$ I-labeled mouse lipoproteins: 15  $\mu$ g protein of  $^{125}$ I-VLDL (2,500 cpm/ng protein), 15  $\mu$ g protein of  $^{125}$ I-LDL (1,110 cpm/ng protein), or 15  $\mu$ g protein of  $^{125}$ I-HDL (491 cpm/ng protein). Blood was collected at the indicated time by retro-orbital puncture. In A and B, the plasma content of  $^{125}$ I-labeled apo B was measured by isopropanol precipitation followed by gamma counting (10, 52). In C, the plasma content of trichloroacetic acid-precipitable  $^{125}$ I-radioactivity was measured. The “100% of control” represents the average value for plasma  $^{125}$ I-radioactivity in the wild-type and mutant mice at 2 min after injection. One wild-type animal in A died ~ 30 min after the intravenous injection.

mals 50% of the radioactivity had been eliminated within 10 min, and this was prolonged to 5 h in the  $LDLR^{-/-}$  mice. The clearance of  $^{125}$ I-LDL was also retarded in the  $LDLR^{-/-}$  animals (half-time for disappearance, 5 h in the  $LDLR^{-/-}$  mice vs. 2 h in the wild-type animals) (Fig. 6B). The clearance of  $^{125}$ I-HDL (half-time of 5.5 h) was not affected by the receptor deficiency (Fig. 6C).

In order to determine whether adenovirus-mediated gene transfer of the human LDL receptor can reverse the abnormalities caused by the knockout of the LDL receptor, we injected  $2 \times 10^9$  pfu of recombinant virus containing either the luciferase cDNA (AdCMV-Luc) or the LDL receptor cDNA (AdCMV-LDLR) into  $LDLR^{-/-}$  mice. This dose has been found previously to cause expression of the foreign gene in the majority of hepatocytes (23). 4 d after administration of the recombinant viruses, liver membrane proteins were prepared from the individual animals and separated by SDS gel electrophoresis (Fig. 7). Lane 1 shows an immunoblot of a wild-type mouse liver,

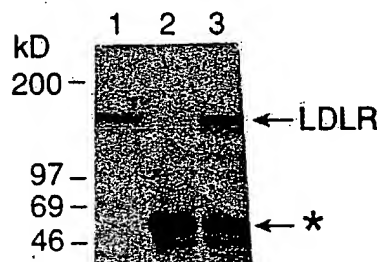


Figure 7. Immunoblot analysis of LDL receptors in liver membranes from  $LDLR^{-/-}$  mice 4 d after injection of recombinant adenovirus expressing the human LDL receptor cDNA. Male mice homozygous for the disrupted LDL receptor allele, 17 wk of age, were injected intra-

venously with  $2 \times 10^9$  pfu of adenovirus containing either the luciferase cDNA (lane 2) or the human LDL receptor cDNA (lane 3) as described in Methods. 4 d after administration of the virus, the animals were killed, and liver membranes were prepared from single mice, subjected to SDS gel electrophoresis under reducing conditions (5% [vol/vol] 2-mercaptoethanol), and transferred to filters for immunoblot analysis with a rabbit anti-LDL receptor IgG as described in the legend to Fig. 3. Lane 1 contains liver membrane proteins from a wild-type mouse not injected with recombinant adenovirus. The position of migration of the mature LDL receptor (LDLR) is indicated by the arrow. The immunoreactive protein marked by the asterisk (\*) represents the truncated form of the LDL receptor caused by insertion of the *neo* cassette into exon 4.

revealing the normal mouse LDL receptor. As expected, no intact LDL receptor protein is detectable by immunoblotting in the liver of an *LDLR*<sup>-/-</sup> mouse injected with the luciferase-containing control virus (lane 2). In contrast, injection of AdCMV-LDLR led to high-level expression of the intact receptor in the liver of an *LDLR*<sup>-/-</sup> mouse (lane 3).

Fig. 8 shows an immunohistochemical analysis of LDL receptor expression in the livers of *LDLR*<sup>-/-</sup> mice 4 d after injection of AdCMV-Luc (A) or AdCMV-LDLR (B). In animals injected with the luciferase-containing virus, there were no detectable LDL receptors (A). In the mice injected with AdCMV-LDLR the majority of cells showed positive immunofluorescence (B). The enhanced magnification in C shows that the virally encoded receptor was expressed in a polarized fashion on the blood-sinusoidal surface of the hepatocyte, as is the human LDL receptor in transgenic mice (21).

To test the function of the adenovirus-encoded receptor, we measured the clearance of <sup>125</sup>I-labeled VLDL (Fig. 9). For this experiment we used VLDL isolated from WHHL rabbits, which are deficient in functional LDL receptors. In preliminary experiments we found that <sup>125</sup>I-labeled VLDL from WHHL rabbits is cleared from the circulation of normal mice approximately as rapidly as <sup>125</sup>I-labeled mouse VLDL, and the rabbit lipoprotein is much easier to obtain. *LDLR*<sup>-/-</sup> mice that received recombinant adenovirus encoding the human LDL receptor cleared the <sup>125</sup>I-labeled rabbit VLDL from their plasma at a rapid rate (Fig. 9). In contrast, mice that had received the luciferase-containing virus cleared the <sup>125</sup>I-VLDL at a rate that was similar to that of uninjected animals (compare with Fig. 6A).

We next sought to determine whether the adenovirus-encoded receptors could normalize the lipoprotein profile of *LDLR*<sup>-/-</sup> mice. For this purpose we injected the control virus (AdCMV-Luc) or the LDL receptor-containing virus (AdCMV-LDLR) into *LDLR*<sup>-/-</sup> male mice (3 animals per group). 4 d after injection the animals were exsanguinated, the pooled plasma of each group was subjected to FPLC gel filtration, and the cholesterol content of the fractions was plotted (Fig. 10). The lipoprotein profile of the mice that had been injected with the luciferase-containing virus closely resembled the profile of uninjected animals (compare with Fig. 4). In the group that had received the LDL receptor-containing virus, the IDL/LDL peak disappeared, and there was a slight increase in VLDL-cholesterol.

## Discussion

The current results demonstrate that elimination of functional LDL receptor genes by homologous recombination profoundly elevates IDL and LDL levels in mice and that these abnormalities can be reversed postnatally by adenovirus-mediated transfer of a gene encoding the LDL receptor. The experiments establish a new animal model by which to explore genetic and environmental factors that interact with LDL receptors to control cholesterol levels. They also provide a new model system in which to study somatic cell gene therapy targeted at the liver.

The most profound functional change observed in the current study was the marked reduction in the clearance rate of <sup>125</sup>I-labeled VLDL from plasma in the homozygous *LDLR*<sup>-/-</sup> mice. The time required for clearance of 50% of the injected lipoprotein rose from 10 min to 300 min, a 30-fold change. These data indicate that the LDL receptor is responsible for

most of the rapid clearance of VLDL remnants and IDL from plasma of mice. The exact proportion cleared by the LDL receptor may be overestimated in these studies because the labeled VLDL was prepared from LDL receptor-deficient animals, i.e., *LDLR*<sup>-/-</sup> mice or homozygous WHHL rabbits. Although these particles float in the VLDL density range ( $d < 1.006$  g/ml), they are likely to represent partially metabolized VLDL particles that have overaccumulated in the donor animals because of the LDL receptor deficiency. Any VLDL particle that is rapidly cleared from plasma in the receptor-deficient animals would be underrepresented in the sample that is used for labeling. This would include large apo E-rich VLDL particles containing either apo B-48 or apo B-100, which may be cleared in part by the chylomicron remnant receptor (38). This problem of underrepresentation of rapidly cleared particles is a problem with all lipoprotein clearance studies (see Discussion in reference 38). Despite these limitations, the data indicate clearly that the VLDL fraction of mice contains a substantial number of particles that are normally cleared by the LDL receptor, presumably owing to their content of apo E. In LDL receptor deficiency states, these particles remain in plasma for long periods and are presumably converted to LDL. Although such conversion was not studied in the current study, it was previously demonstrated in WHHL rabbits (10, 39).

Striking parallels exist between the findings in the current study of *LDLR*<sup>-/-</sup> mice and previous studies of lipoprotein clearance in homozygous WHHL rabbits (10, 39) and FH homozygotes (9). In all three species the most profound abnormality involves the clearance of VLDL remnants and IDL. In WHHL rabbits, the half-time for VLDL clearance was extended from 12 to 480 min (10), a result that parallels the 10 to 300 min change in the current study. In a study of <sup>125</sup>I-VLDL turnover in FH homozygotes, Soutar et al. (9) observed a sevenfold decrease in the clearance of <sup>125</sup>I-IDL derived from <sup>125</sup>I-VLDL (fractional turnover rate 0.48/h in normal subjects vs. 0.064/h in FH homozygotes). Using a more complex kinetic analysis, James et al. (43) also found a decreased clearance of VLDL remnants and IDL. This indicates that a major function of the LDL receptor in all three species is the clearance of remnant particles derived from VLDL, thereby preventing their conversion into LDL.

The relative decline in LDL clearance observed in LDL receptor-deficient mice (2.5-fold) also correlates well with observations in WHHL rabbits. Yamada et al. (39) observed a reduction of 2-fold, Pittman et al. (40) 2.6-fold, and Spady et al. (41) 3.5-fold. In FH homozygotes the reduction in LDL clearance is also about threefold (42, 43). These data indicate that about 60% of LDL particles are normally cleared by the LDL receptor in mice. The residual clearance of LDL observed in the absence of LDL receptors is likely to be mediated by another receptor with a lower affinity for LDL. Like the LDL receptor, this alternate receptor functions primarily in the liver (40).

The absolute level of plasma LDL-cholesterol in the *LDLR*<sup>-/-</sup> mice is much lower than that observed in WHHL rabbits or FH homozygotes. Although we did not measure LDL-cholesterol quantitatively, it is apparent from the FPLC profiles that the IDL/LDL peak contains ~ 50% of the total cholesterol in the plasma of the *LDLR*<sup>-/-</sup> mice, which would indicate an IDL/LDL-cholesterol level of ~ 130 mg/dl. This contrasts with LDL-cholesterol levels above 450 mg/dl in WHHL rabbits (10, 44) and FH homozygotes (2). This differ-

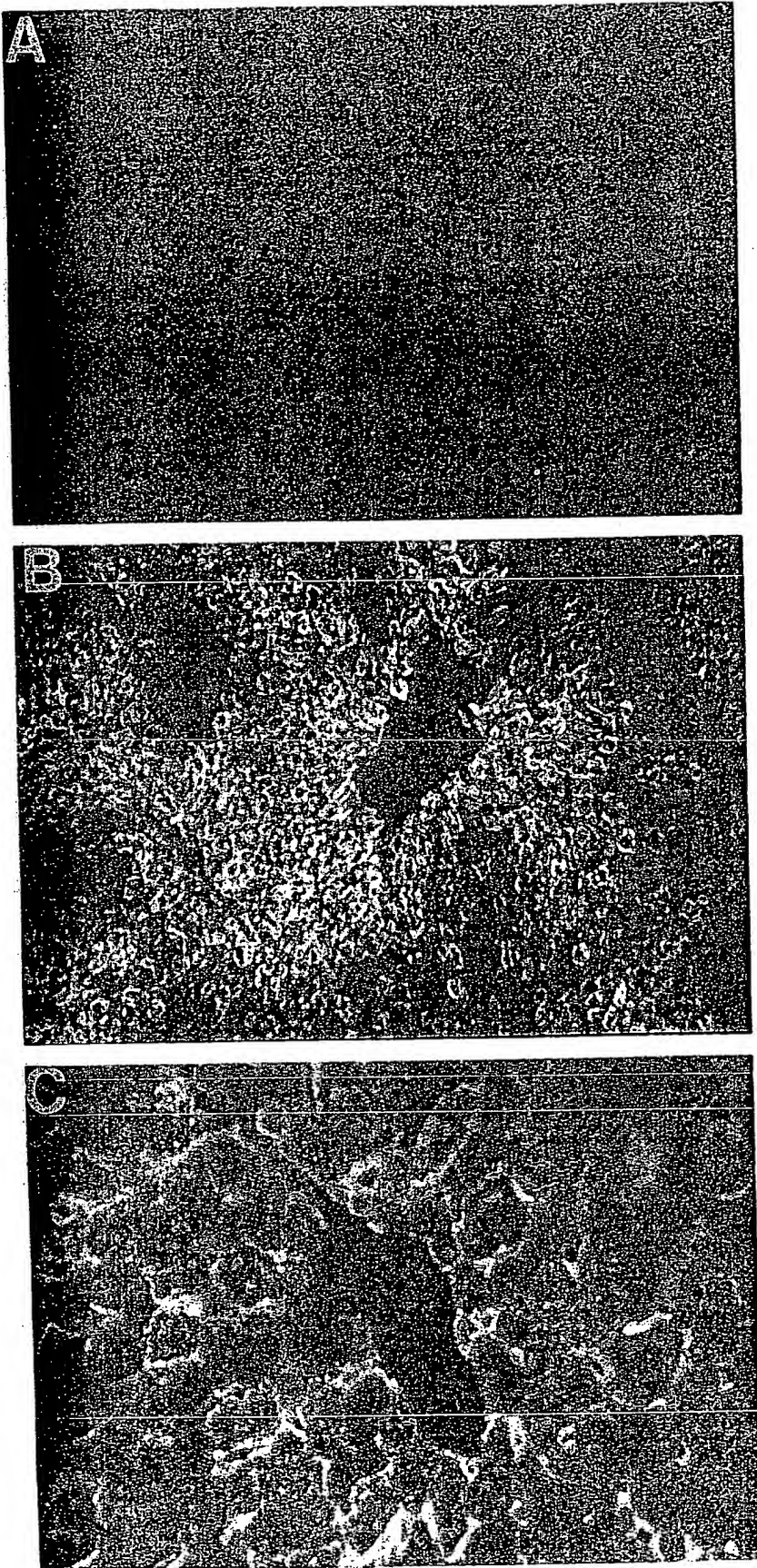


**Figure 8.** Immunohistochemical staining of LDL receptors in the liver of an *LDLR*<sup>-/-</sup> mouse after treatment with recombinant adenovirus expressing the human LDL receptor cDNA. Male mice homozygous for the disrupted LDL receptor allele, 18 wk of age, were injected intravenously with  $2 \times 10^9$  pfu of either AdCMV-Luciferase (*A*) or AdCMV-LDLR (*B* and *C*) as described in Methods. Four days after administration of the virus, the livers were removed for immunohistochemistry. Frozen sections were incubated with 20  $\mu$ g/ml of rabbit polyclonal anti-LDL receptor antibody, and bound IgG was detected with 5  $\mu$ g/ml FITC-labeled goat anti-rabbit IgG as described in Methods. Magnification, *A* and *B*,  $\times 25$ ; *C*,  $\times 100$ .



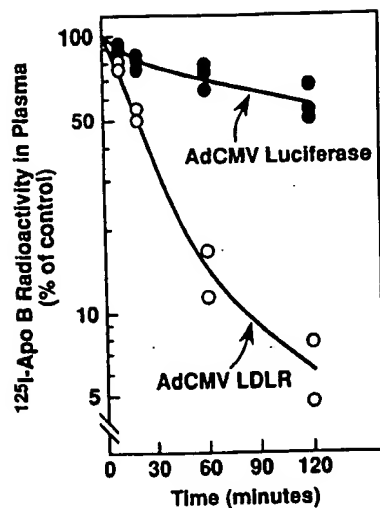


**Figure 9.** Disappearance of  $^{125}\text{I}$ -VLDL from the circulation of  $\text{LDLR}^{-/-}$  mice after treatment with recombinant adenovirus expressing the human LDL receptor cDNA. Three male mice homozygous for the disrupted LDL receptor allele, 19 wk of age, were injected intravenously with  $2 \times 10^9$  pfu of either AdCMV-LDLR (○) or AdCMV-Luciferase (●). 4 d after administration of the virus, the animals (nonfasted) were injected with 15

$\mu\text{g}$  protein of  $^{125}\text{I}$ -labeled VLDL (308 cpm/ng protein) isolated from WHHL rabbits. Blood was collected at the indicated time by retro-orbital puncture, and the plasma content of  $^{125}\text{I}$ -labeled apo B was measured by isopropanol precipitation (10, 52). The "100% of control" represents the average value for plasma  $^{125}\text{I}$ -radioactivity 1 min after injection. One animal injected with AdCMV-LDLR died  $\sim 10$  min after injection of the  $^{125}\text{I}$ -VLDL.

ence might be explained by the production of VLDL containing apo B-48 in livers of mice, but not rabbits or humans. About 70% of the apo B mRNA in the livers of adult mice encodes the apo B-48 isoform (14). Remnants derived from apo B-48 containing VLDL might be cleared relatively rapidly by the livers of the  $\text{LDLR}^{-/-}$  mice, owing to the ability of the

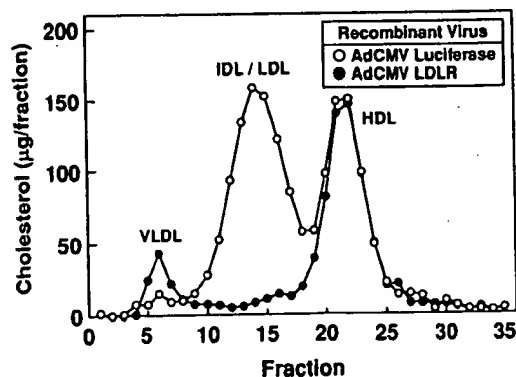


**Figure 10.** FPLC profiles of plasma lipoproteins from  $\text{LDLR}^{-/-}$  mice after treatment with recombinant adenovirus expressing the human LDL receptor cDNA. Three male mice homozygous for the LDL receptor disrupted allele, 17 wk of age, were injected with  $2 \times 10^9$  pfu of adenovirus containing either the luciferase cDNA (○) or the human LDL receptor cDNA (●). 4 d after administration of the virus, blood was collected from the animals (nonfasted), and the plasma from the three animals in each group was pooled and subjected to gel filtration on FPLC. The cholesterol content of each fraction was determined as described in Methods. The mean total plasma cholesterol levels in the two groups of mice were 279 mg/dl (○) and 139 mg/dl (●).

apo E/apo B-48 particles to bind to chylomicron remnant receptors, thereby leading to lower levels of LDL.

The hypothesized role of apo E/apo B-48 particles is supported by a comparison of the current data with those of Zhang et al. (45) and Plump et al. (46), who eliminated the gene for apo E in mice using a similar homologous recombination technique. Apo E $^{-/-}$  mice had total plasma cholesterol levels of 400–500 mg/dl, nearly all of which was contained in particles with the size of VLDL and VLDL remnants. The level of apo B-48 in plasma was also markedly elevated (45). The severity of this abnormality in comparison with the effects of LDL receptor deficiency supports the notion that apo E binds to two receptors, the LDL receptor and the chylomicron remnant receptor. Knockout of apo E therefore has a more profound effect on lipoprotein clearance than knockout of the LDL receptor in mice.

In humans the opposite is true, i.e., LDL receptor deficiency raises the total plasma cholesterol more than does apo E deficiency. Receptor-negative FH homozygotes have total plasma cholesterol levels of 700–1,000 mg/dl (2), whereas individuals with an absence of apo E have plasma cholesterol levels of 443 to 614 mg/dl (47). This is likely due, in part, to the fact that human livers do not produce apo B-48 and that apo E accelerates the removal of apo B-100 containing VLDL remnants primarily by binding to only one receptor, namely, the LDL receptor.

LDL receptors are believed to constitute an important defense against the cholesterol-elevating effect of dietary cholesterol (1). In rabbits (48) and hamsters (49), dietary cholesterol elevates plasma LDL-cholesterol levels in part by suppressing LDL receptors. In the current study, LDL receptor-deficient mice responded to the 0.2% cholesterol/10% coconut oil diet with a rise in plasma LDL-cholesterol that was much greater than was observed in wild-type mice. There was also a definite increase in the amounts of apo B-100 and apo E in plasma, particularly in the IDL/LDL fraction (Fig. 5). Thus, when LDL receptors are already absent as a result of genetic elimination, mice become hyperresponsive to dietary cholesterol.

The current experiments with recombinant adenovirus demonstrate that this vector can restore LDL receptor expression within 4 d in an LDL receptor-deficient mouse. However, many technical problems would have to be overcome before such therapy could be considered for humans. First, it is unknown whether or not the expression of adenovirus-encoded genes in liver will persist for long periods. The genome of the defective virus does not replicate, nor does it integrate into the genome at any appreciable frequency. On the other hand, Stratford-Perricaudet et al. (24) did note persistent expression for a year after injection of the virus into neonatal animals lacking ornithine transcarbamylase activity. Second, adenovirus-encoded proteins are likely to be the targets of immune reactions. Mice are known to develop an immune response to adenoviral proteins (50), which might hamper its use for long periods in these animals. Nearly all humans are expected to possess antibodies against adenovirus, and these might prevent use of this vector in people. Despite these reservations about human applicability, the adenovirus vector is a useful experimental tool to change the expression of genes acutely in the liver. In the current studies, we used it to reveal the type of result to be expected when more applicable long-term gene delivery methods have been developed.

## Acknowledgments

We thank Phil Soriano for expert advice and help. Scott Clark, Lucy Lundquist, Wen-Ling Niu, and Sadeq Hassan provided excellent technical assistance.

This work was supported by National Institutes of Health grants HL-20948 and HL-17669, and by grants from the Moss Heart Foundation and the Perot Family Foundation. S. Ishibashi is the recipient of a postdoctoral fellowship from the Sasakawa Health Science Foundation, Tokyo, Japan. R. D. Gerard is an Established Investigator of the American Heart Association. J. Herz is supported by the Syntex Scholar Program and is a Lucille P. Markey Scholar.

*Note added in proof.* The LDL receptor-deficient mice described in this paper will become available in September 1993 from Jackson Laboratories, 600 Main Street, Bar Harbor, ME 04609.

## References

1. Brown, M. S., and J. L. Goldstein. 1986. A receptor-mediated pathway for cholesterol homeostasis. *Science (Wash. DC)*. 232:34-47.
2. Goldstein, J. L., and M. S. Brown. 1989. Familial hypercholesterolemia. In *The Metabolic Basis of Inherited Disease*. C. R. Scriver, A. L. Beaudet, W. S. Sly, and D. Valle, editors. McGraw-Hill Publishing Co., New York, 1215-1250.
3. Mahley, R. W. 1988. Apolipoprotein E: Cholesterol transport protein with expanding role in cell biology. *Science (Wash. DC)*. 240:622-630.
4. Brown, M. S., J. Herz, R. C. Kowal, and J. L. Goldstein. 1991. The low-density lipoprotein receptor-related protein: double agent or decoy? *Curr. Opin. in Lipidol.* 2:65-72.
5. Ji, Z.-S., W. J. Brecht, D. Miranda, M. M. Hussain, T. L. Innerarity, and R. W. Mahley. 1993. Role of heparan sulfate proteoglycans in the binding and uptake of apolipoprotein E-enriched remnant lipoproteins by cultured cells. *J. Biol. Chem.* 268:10160-10167.
6. Hobbs, H. H., M. S. Brown, and J. L. Goldstein. 1992. Molecular genetics of the LDL receptor gene in familial hypercholesterolemia. *Hum. Mutat.* 1:445-466.
7. Watanabe, Y., T. Ito, and M. Shiomi. 1985. The effect of selective breeding on the development of coronary atherosclerosis in WHHL rabbits. An animal model for familial hypercholesterolemia. *Atherosclerosis*. 56:71-97.
8. Scanu, A. M., A. Khalil, L. Neven, M. Tidore, G. Dawson, D. Pfaffinger, E. Jackson, K. D. Carey, H. C. McGill, and G. M. Fless. 1988. Genetically determined hypercholesterolemia in a rhesus monkey family due to a deficiency of the LDL receptor. *J. Lipid Res.* 29:1671-1681.
9. Soutar, A. K., N. B. Myant, and G. R. Thompson. 1982. The metabolism of very low density and intermediate density lipoproteins in patients with familial hypercholesterolaemia. *Atherosclerosis*. 43:217-231.
10. Kita, T., M. S. Brown, D. W. Bilheimer, and J. L. Goldstein. 1982. Delayed clearance of very low density and intermediate density lipoproteins with enhanced conversion to low density lipoprotein in WHHL rabbits. *Proc. Natl. Acad. Sci. USA*. 79:5693-5697.
11. Hobbs, H. H., E. Leitersdorf, C. C. Leffert, D. R. Cryer, M. S. Brown, and J. L. Goldstein. 1989. Evidence for a dominant gene that suppresses hypercholesterolemia in a family with defective low density lipoprotein receptors. *J. Clin. Invest.* 84:656-664.
12. Lamou-Fava, S., D. Jimenez, J. C. Christian, R. R. Fabsitz, T. Reed, D. Carmelli, W. P. Castelli, J. M. Ordovas, P. W. F. Wilson, and E. J. Schaefer. 1991. The NHLBI twin study: heritability of apolipoprotein A-I, B, and low density lipoprotein subclasses and concordance for lipoprotein(a). *Atherosclerosis*. 91:97-106.
13. Spady, D. K., L. A. Woollett, and J. M. Dietschy. 1993. Regulation of plasma LDL-cholesterol levels by dietary cholesterol and fatty acids. *Annu. Rev. Nutr.* 13:355-381.
14. Higuchi, K., K. Kitagawa, K. Kogishi, and T. Takeda. 1992. Developmental and age-related changes in apolipoprotein B mRNA editing in mice. *J. Lipid Res.* 33:1753-1764.
15. Scott, J. 1989. The molecular and cell biology of apolipoprotein-B. *Mol. Biol. Med.* 6:65-80.
16. Chan, L. 1992. Apolipoprotein B, the major protein component of triglyceride-rich and low density lipoproteins. *J. Biol. Chem.* 267:25621-25624.
17. Van't Hooft, F. M., D. A. Hardman, J. P. Kane, and R. J. Havel. 1982. Apolipoprotein B (B-48) of rat chylomicrons is not a precursor of the apolipoprotein of low density lipoproteins. *Proc. Natl. Acad. Sci. USA*. 79:179-182.
18. Chowdhury, J. R., M. Grossman, S. Gupta, N. R. Chowdhury, J. R. Baker, Jr., and J. M. Wilson. 1991. Long-term improvement of hypercholesterolemia after *ex vivo* gene therapy in LDLR-deficient rabbits. *Science (Wash. DC)*. 254:1802-1805.
19. Wilson, J. M., M. Grossman, C. H. Wu, N. R. Chowdhury, G. Y. Wu, and J. R. Chowdhury. 1992. Hepatocyte-directed gene transfer *in vivo* leads to transient improvement of hypercholesterolemia in low density lipoprotein receptor-deficient rabbits. *J. Biol. Chem.* 267:963-967.
20. Hofmann, S. L., D. W. Russell, M. S. Brown, J. L. Goldstein, and R. E. Hammer. 1988. Overexpression of low density lipoprotein (LDL) receptor eliminates LDL from plasma in transgenic mice. *Science (Wash. DC)*. 239:1277-1281.
21. Pathak, R. K., M. Yokode, R. E. Hammer, S. L. Hofmann, M. S. Brown, J. L. Goldstein, and R. G. W. Anderson. 1990. Tissue-specific sorting of the human LDL receptor in polarized epithelia of transgenic mice. *J. Cell Biol.* 111:347-359.
22. Yokode, M., R. E. Hammer, S. Ishibashi, M. S. Brown, and J. L. Goldstein. 1990. Diet-induced hypercholesterolemia in mice: Prevention by overexpression of LDL receptors. *Science (Wash. DC)*. 250:1273-1275.
23. Herz, J., and R. D. Gerard. 1993. Adenovirus-mediated low density lipoprotein receptor gene transfer accelerates cholesterol clearance in normal mice. *Proc. Natl. Acad. Sci. USA*. 90:2812-2816.
24. Stratford-Perricaudet, L. D., M. Leverro, J.-F. Chasse, M. Perricaudet, and P. Briand. 1990. Evaluation of the transfer and expression in mice of an enzyme-encoding gene using a human adenovirus vector. *Hum. Gene Ther.* 1:241-256.
25. Capecchi, M. R. 1989. Altering the genome by homologous recombination. *Science (Wash. DC)*. 244:1288-1292.
26. Smithies, O. 1991. Altering genes in animals and humans. In *Etiology of Human Disease at the DNA Level*. J. Lindsten and U. Pettersson, editors. Raven Press, New York. 221-259.
27. Bradley, A. 1987. Production and analysis of chimaeric mice. In *Teratocarcinomas and Embryonic Stem Cells: A Practical Approach*. E. J. Robertson, editor. IRL Press, Oxford, UK/Washington, DC. 113-151.
28. Sambrook, J., E. F. Fritsch, and T. Maniatis. 1989. *Molecular cloning: A Laboratory Manual*. Cold Spring Harbor Laboratory Press, Cold Spring Harbor, New York.
29. Yokode, M., R. K. Pathak, R. E. Hammer, M. S. Brown, J. L. Goldstein, and R. G. W. Anderson. 1992. Cytoplasmic sequence required for basolateral targeting of LDL receptor in livers of transgenic mice. *J. Cell Biol.* 117:39-46.
30. Willnow, T. F., J. L. Goldstein, K. Orth, M. S. Brown, and J. Herz. 1992. Low density lipoprotein receptor-related protein (LRP) and gp330 bind similar ligands, including plasminogen activator-inhibitor complexes and lactoferrin, an inhibitor of chylomicron remnant clearance. *J. Biol. Chem.* 267:26172-26180.
31. Goldstein, J. L., S. K. Basu, and M. S. Brown. 1983. Receptor-mediated endocytosis of LDL in cultured cells. *Methods Enzymol.* 98:241-260.
32. Yamamoto, T., C. G. Davis, M. S. Brown, W. J. Schneider, M. L. Casey, J. L. Goldstein, and D. W. Russell. 1984. The human LDL receptor: A cysteine-rich protein with multiple Alu sequences in its mRNA. *Cell*. 39:27-38.
33. Mehta, K. D., W.-J. Chen, J. L. Goldstein, and M. S. Brown. 1991. The low density lipoprotein receptor in *Xenopus laevis*. I. Five domains that resemble the human receptor. *J. Biol. Chem.* 266:10406-10414.
34. Soriano, P., C. Montgomery, R. Geske, and A. Bradley. 1991. Targeted disruption of the *c-src* proto-oncogene leads to osteopetrosis in mice. *Cell*. 64:693-702.
35. Mansour, S. L., K. R. Thomas, and M. R. Capecchi. 1988. Disruption of the proto-oncogene *int-2* in mouse embryo-derived stem cells: a general strategy for targeting mutations to non-selectable genes. *Nature (Lond.)*. 336:348-352.
36. McMahon, A. P., and A. Bradley. 1990. The *Wnt-1 (int-1)* proto-oncogene is required for development of a large region of the mouse brain. *Cell*. 62:1073-1085.
37. Russell, D. W., W. J. Schneider, T. Yamamoto, K. L. Luskey, M. S. Brown, and J. L. Goldstein. 1984. Domain map of the LDL receptor: sequence homology with the epidermal growth factor precursor. *Cell*. 37:577-585.
38. Yamada, N., D. M. Shames, K. Takahashi, and R. J. Havel. 1988. Metabolism of apolipoprotein B-100 in large very low density lipoproteins of blood plasma. *J. Clin. Invest.* 82:2106-2113.
39. Yamada, N., D. M. Shames, and R. J. Havel. 1987. Effect of LDL receptor deficiency on the metabolism of apolipoprotein B-100 in blood plasma: kinetic studies in normal and Watanabe heritable hyperlipidemic rabbits. *J. Clin. Invest.* 80:507-515.
40. Pittman, R. C., T. E. Carew, A. D. Attie, J. L. Witztum, Y. Watanabe, and D. Steinberg. 1982. Receptor-dependent and receptor-independent degradation of low density lipoprotein in normal rabbits and in receptor-deficient mutant rabbits. *J. Biol. Chem.* 257:7994-8000.
41. Spady, D. K., M. Huettinger, D. W. Bilheimer, and J. M. Dietschy. 1987. Role of receptor-independent low density lipoprotein transport in the maintenance of tissue cholesterol balance in the normal and WHHL rabbit. *J. Lipid Res.* 28:32-41.
42. Bilheimer, D. W., N. J. Stone, and S. M. Grundy. 1979. Metabolic studies in familial hypercholesterolemia: evidence for a gene-dosage effect *in vivo*. *J. Clin. Invest.* 64:524-533.
43. James, R. W., B. Martin, D. Pometta, J. C. Fruchart, P. Duriez, P. Fuchs, J. P. Farriaux, A. Tacquet, T. Demant, R. J. Clegg, A. Munro, M. F. Oliver



et al. 1989. Apolipoprotein B metabolism in homozygous familial hypercholesterolemia. *J. Lipid Res.* 30:159-169.

44. Havel, R. J., T. Kita, L. Kotite, J. P. Kane, R. L. Hamilton, J. L. Goldstein, and M. S. Brown. 1982. Concentration and composition of lipoproteins in blood plasma of WHHL rabbits. *Arteriosclerosis*. 3:467-474.

45. Zhang, S. H., R. L. Reddick, J. A. Piedrahita, and N. Maeda. 1992. Spontaneous hypercholesterolemia and arterial lesions in mice lacking apolipoprotein E. *Science (Wash. DC)*. 258:468-471.

46. Plump, A. S., J. D. Smith, T. Hayek, K. Aalto-Setälä, A. Walsh, J. G. Verstuyft, E. M. Rubin, and J. L. Breslow. 1992. Severe hypercholesterolemia and atherosclerosis in apolipoprotein E deficient mice created by homologous recombination in ES cells. *Cell*. 71:343-353.

47. Schaefer, E. J., R. E. Gregg, G. Ghiselli, T. M. Forte, J. M. Ordovas, L. A. Zech, and H. B. Brewer, Jr. 1986. Familial apolipoprotein E deficiency. *J. Clin. Invest.* 78:1206-1219.

48. Kovanen, P. T., M. S. Brown, S. K. Basu, D. W. Bilheimer, and J. L. Goldstein. 1981. Saturation and suppression of hepatic lipoprotein receptors: a

mechanism for the hypercholesterolemia of cholesterol-fed rabbits. *Proc. Natl. Acad. Sci. USA*. 78:1396-1400.

49. Spady, D. K., and J. M. Dietschy. 1988. Interaction of dietary cholesterol and triglycerides in the regulation of hepatic low density lipoprotein transport in the hamster. *J. Clin. Invest.* 81:300-309.

50. Ginsberg, H. S., L. L. Moldawer, P. B. Sehgal, M. Redington, P. L. Kilian, R. M. Chanock, and G. A. Prince. 1991. A mouse model for investigating the molecular pathogenesis of adenovirus pneumonia. *Proc. Natl. Acad. Sci. USA*. 88:1651-1655.

51. Kowal, R. C., J. Herz, J. L. Goldstein, V. Esser, and M. S. Brown. 1989. Low density lipoprotein receptor-related protein mediates uptake of cholesteryl esters derived from apoprotein E-enriched lipoproteins. *Proc. Natl. Acad. Sci. USA*. 86:5810-5814.

52. Holmquist, L., K. Carlson, and L. A. Carlson. 1978. Comparison between the use of isopropanol and tetramethylurea for the solubilisation and quantitation of human serum very low density apolipoproteins. *Anal. Biochem.* 88:457-460.

# Peroxisome proliferator-activated receptor $\gamma$ ligands inhibit development of atherosclerosis in LDL receptor-deficient mice

Andrew C. Li,<sup>1</sup> Kathleen K. Brown,<sup>2</sup> Mercedes J. Silvestre,<sup>3</sup>  
Timothy M. Willson,<sup>4</sup> Wulf Palinski,<sup>3</sup> and Christopher K. Glass<sup>1,3</sup>

<sup>1</sup>Department of Cellular and Molecular Medicine, University of California, San Diego, La Jolla, California, USA

<sup>2</sup>Department of Metabolic Diseases, Glaxo Wellcome Research and Development, Research Triangle Park, North Carolina, USA

<sup>3</sup>Department of Medicine, University of California, San Diego, La Jolla, California, USA

<sup>4</sup>Department of Medicinal Chemistry, Glaxo Wellcome Research and Development, Research Triangle Park, North Carolina, USA

Address correspondence to: Andrew C. Li, Department of Cellular and Molecular Medicine, University of California, San Diego, 9500 Gilman Drive, La Jolla, California 92093-0651, USA.  
Phone: (858) 534-7559; Fax: (858) 534-8549; E-mail: acl@ucsd.edu.

The Palinski and Glass laboratories contributed equally to this work.

Received for publication May 18, 2000, and accepted in revised form July 5, 2000.

The peroxisome proliferator-activated receptor  $\gamma$  (PPAR $\gamma$ ) is a nuclear receptor that regulates fat-cell development and glucose homeostasis and is the molecular target of a class of insulin-sensitizing agents used for the management of type 2 diabetes mellitus. PPAR $\gamma$  is highly expressed in macrophage foam cells of atherosclerotic lesions and has been demonstrated in cultured macrophages to both positively and negatively regulate genes implicated in the development of atherosclerosis. We report here that the PPAR $\gamma$ -specific agonists rosiglitazone and GW7845 strongly inhibited the development of atherosclerosis in LDL receptor-deficient male mice, despite increased expression of the CD36 scavenger receptor in the arterial wall. The antiatherogenic effect in male mice was correlated with improved insulin sensitivity and decreased tissue expression of TNF- $\alpha$  and gelatinase B, indicating both systemic and local actions of PPAR $\gamma$ . These findings suggest that PPAR $\gamma$  agonists may exert antiatherogenic effects in diabetic patients and provide impetus for efforts to develop PPAR $\gamma$  ligands that separate proatherogenic activities from antidiabetic and antiatherogenic activities.

*J. Clin. Invest.* 106:523–531 (2000).

## Introduction

Complications of atherosclerosis are the leading cause of death in Western societies and have an extremely high incidence in individuals with type 2 diabetes mellitus (1, 2). Atherosclerosis is initiated by the accumulation of plasma LDL in the arterial wall, its oxidation, and the recruitment of circulating monocytes (3, 4). Once monocytes in the arterial intima have undergone phenotypic transformation to macrophages, they take up oxidized LDL (oxLDL) via several scavenger receptors that include scavenger receptor A (SR-A), CD36, and macrophage mannose receptor (5–7). This results in massive cholesterol accumulation and formation of foam cells. Interactions between oxLDL, macrophages, smooth muscle cells infiltrated from the arterial media, and T cells recruited from the circulation result in a chronic inflammatory condition that is thought to influence the further evolution of early atherosclerotic lesions toward more advanced, clinically relevant lesions (8). Interactions between arterial cells are mediated by an array of cytokines and adhesion molecules (9), and increasing experimental evidence suggests that many of these factors promote atherogenesis. For example, hypercholesterolemic mice in which the gene encoding

macrophage chemotactic protein 1 (MCP-1) has been disrupted are resistant to the development of atherosclerosis (10, 11). In analogy, disruption of the SR-A and CD36 genes results in a significant reduction of hypercholesterolemia-induced atherosclerosis in mice (12, 13). These observations suggest that interventions directed at altering the genetic responses of vascular cells to proatherogenic stimuli, such as hypercholesterolemia, may be beneficial.

Several regulatory pathways have been identified that control the expression of potentially atherogenic genes. These include NF- $\kappa$ B, a transcription factor involved in the regulation of many proinflammatory factors and adhesion molecules, such as TNF- $\alpha$  and gelatinase B (14, 15). Recent studies have also documented the expression of the peroxisome proliferator-activated receptor  $\gamma$  (PPAR $\gamma$ ) in macrophage foam cells, endothelial cells, and smooth muscle cells of human and murine atherosclerotic lesions (16–20). PPAR $\gamma$  is a member of the nuclear receptor superfamily of ligand-dependent transcription factors that both positively and negatively regulate gene expression in response to the binding of a number of fatty acid metabolites, including oxidized linoleic acid (9- and 13-HODE) and

15 deoxy  $\Delta^{2,14}$  prostaglandin  $J_2$  (21–23). PPAR $\gamma$  is expressed in many other tissues and is particularly highly expressed in fat. PPAR $\gamma$  promotes adipocyte differentiation in vitro and has recently been shown to be essential for the development of adipose tissue in vivo (24–26). PPAR $\gamma$  also appears to play a critical role in glucose homeostasis, because it is the molecular target of a class of insulin-sensitizing drugs referred to as thiazolidinediones (TZDs) (27).

The biological roles of PPAR $\gamma$  in the macrophage and its effects on atherosclerosis are uncertain. PPAR $\gamma$ -specific ligands have been shown to inhibit the expression of a number of proinflammatory genes, including TNF- $\alpha$ , IL-1 $\beta$ , iNOS, and *gelatinase B* (28, 29). These findings suggested that PPAR $\gamma$  functions as a negative regulator of macrophage activation and that synthetic PPAR $\gamma$  ligands might exert anti-inflammatory and antiatherogenic effects. Consistent with this, PPAR $\gamma$  ligands have recently been shown to inhibit inflammatory bowel disease in a rodent model (30). However, PPAR $\gamma$  has also been shown to stimulate transcription of the CD36 gene (19, 21). In conjunction with the finding that PPAR $\gamma$  can be activated by 9- and 13-HODE present in oxLDL, a “PPAR $\gamma$  cycle” has been proposed in which oxLDL lipids would induce the activity of PPAR $\gamma$ , leading to increased expression of CD36, which in turn would increase the uptake of oxLDL. This cycle would thus promote foam-cell formation and atherosclerosis.

Resolving the question of whether PPAR $\gamma$  agonists promote or inhibit atherosclerosis is of clinical importance because many patients with type 2 diabetes, who are at high risk of developing atherosclerosis and its complications, are currently using PPAR $\gamma$  agonists for the control of hyperglycemia. To determine whether the activation of PPAR $\gamma$  promotes or inhibits the development of atherosclerosis in an animal model, we administered two structurally distinct PPAR $\gamma$ -specific ligands to LDL receptor-deficient (LDLR $^{-/-}$ ) mice fed a Western-style diet and measured their effects on lipid and glucose metabolism, extent of atherosclerosis, and expression of potential target genes in the artery wall. Both PPAR $\gamma$ -specific ligands exerted potent antiatherogenic effects in male mice despite upregulation of CD36 mRNA. Antiatherogenic effects correlated with improved insulin sensitivity and inhibition of TNF- $\alpha$  and *gelatinase B* expression.

## Methods

**Animals and diet.** A breeding colony was generated from the tenth-generation homozygous LDLR $^{-/-}$  mice in a C57BL/6 background (The Jackson Laboratories, Bar Harbor, Maine, USA). In three separate experiments, three groups of both males and females were matched for age (8 to 12 weeks), plasma cholesterol, and glucose levels before feeding. Four animals were housed per cage and in a facility with an 11-hour light cycle (light, 7 am to 6 pm). All three groups were fed a Western-style diet consisting of 0.01% added cholesterol and 21% milk fat

(TD98338; Harlan-Teklad, Madison, Wisconsin, USA), which induced extensive atherosclerosis in the aortic origin, but not in the descending aorta at 10 weeks. In addition to the diet, one group received rosiglitazone and another group received GW7845. The animals were fed 3–4 g food/mouse/day with a drug delivery of 20 mg/kg of body weight/day. New batches of food/drug were prepared weekly and stored at 4°C. The amount of food given and the food left remaining were weighed daily. The animals were weighed every 2 weeks, and the drug dosages were adjusted accordingly. To induce extensive atherosclerosis in the aorta, in a separate experiment male mice were fed a diet containing 1.25% cholesterol and 21% milk fat (TD96121; Harlan-Teklad) for 4 months. Two weeks before sacrifice, the animals were divided into three groups. A control group received the diet treated only with the solvent, the second group received the diet together with rosiglitazone (20 mg/kg/day), and the third group received the diet and GW7845 (20 mg/kg/day). All animals had ad libitum access to water. The animal experiments were performed according to NIH guidelines and were approved by UCSD's Animal Subjects Committee.

**Glucose, insulin, and lipid levels.** Retro-orbital bleeds were performed before the start of the studies and every 4 weeks thereafter until the animals were sacrificed at 10 weeks. The animals were bled, nonfasted, at 10 am and blood was drawn up in EDTA-coated microcapillary tubes. Plasma was isolated from whole blood and glucose levels were determined, using a Precision QID glucometer (MediSense Inc., Bedford, Massachusetts, USA). Insulin levels were determined using a competitive radioimmunoassay (Linco Research Inc., St. Charles, Missouri, USA). Plasma cholesterol and triglyceride levels were measured by enzymatic methods using an automated bichromatic analyzer (Abbot Diagnostics, Dallas, Texas, USA). To determine the lipoprotein profiles, remaining terminal plasma samples were pooled according to the animals' respective groups, and the cholesterol content of lipoprotein fractions in plasma was determined by FPLC. One hundred milliliters of the pooled plasma was loaded onto a Superose 6B column, and 250  $\mu$ L of sample fractions were collected and analyzed for cholesterol.

**Oral glucose tolerance test.** Two weeks before the mice were sacrificed, oral glucose tolerance tests were performed. Animals were fasted for 4 hours. Animals were gavaged with glucose (0.75 mg/g body weight) using 20% glucose. Blood samples (25  $\mu$ L) were taken at 0, 15, 30, 60, and 90 minutes. Glucose levels were determined in whole blood and insulin levels in plasma.

**Hemoglobin A<sub>1c</sub>, nonesterified fatty acid, HDL<sub>c</sub>, and drug levels.** Whole blood and plasma were sent to Glaxo Wellcome Research Institute (Research Triangle Park, North Carolina, USA) for analysis for HbA<sub>1c</sub>, HDL<sub>c</sub>, and nonesterified fatty acid (NEFA) levels. The plasma was isolated immediately and quickly frozen in liquid nitrogen to prevent the breakdown of NEFA. Drug levels were determined by mass spectrometry.

**Tissue preparation and morphometric analysis of atherosclerotic lesions.** The heart was perfused from its apex with cold PBS treated with diethylpyrocarbonate (DEPC). The heart, containing the aortic origin, was carefully dissected. The upper half of the heart was placed in a fixative containing 4% paraformaldehyde, 5% sucrose in PBS, pH 7.4, and fixed overnight, followed by alcohol dehydration and paraffin embedding. For morphometric determination of atherosclerosis, serial 9- $\mu$ m-thick sections were cut from the apex toward the base of the heart. Sections containing the aortic origin, totaling 180  $\mu$ m in length, were stained with a modified van Gieson's elastin stain to enhance the contrast between the atherosclerotic intima and the surrounding tissue (31). Analysis was performed on every other section ( $n = 8$ –10 per mouse). Thus, a total length of 180  $\mu$ m of the aortic origin was examined. Quantification of atherosclerosis was performed using computer-assisted image analysis, as described previously (32). All morphometry was performed by the same investigator blinded to the tissue identity.

**RNA isolation from aortic valves and aortas.** The upper half of the hearts, containing the aortic valves and the aortas, extending from the root to the second intercostal region and up to the carotids, were weighed and flash frozen in liquid nitrogen and stored at  $-80^{\circ}\text{C}$ . Isolation of total RNA was performed using RNeasy kit (QIAGEN Inc., Valencia, California, USA) according to the manufacturer's protocol. Total RNA was treated with deoxyribonuclease I (QIAGEN Inc.) for 20 minutes at room temperature to remove contaminating genomic DNA. The amount of RNA was determined by spectrophotometry, and 200 ng of RNA was loaded onto a 1.5% agarose gel to determine its quality before analysis.

**RT-PCR-based quantitative gene expression analysis.** Real-time detection of PCR was performed at the Center for Aids Research Genomics Core of the Veterans Medical Research Foundation in La Jolla, California, USA. Using the Perkin-Elmer ABI Prism 7700 and Sequence Detection System software (Perkin-Elmer, Foster City, California, USA), the differential displays of mRNAs for TNF- $\alpha$ , MCP-1, VCAM-1, gelatinase B, macrosialin, CD36, and SR-A were determined. Briefly, 1  $\mu$ g of total RNA was used to generate cDNA using an oligo dT oligodeoxynucleotide primer (T<sub>12-18</sub>) following the protocol for Omniscript (QIAGEN Inc.). The following primers and probes were made: TNF- $\alpha$ : 5'CGGAGTC-CGGGCAGGT 3' (forward), 5' GCTGGGTAGAGAATG-GATGAACA 3' (reverse), 5' ACTTTGGAGTCATTGCTCT-GTGAAGGG AATG 3' (probe); MCP-1: 5' CAGCCAGATGCAGTTAACGC 3' (forward), 5' GCC-TACTCATTGGGATCATCTTG 3' (reverse), 5' CCACT-CACCTGCTGCTACTCATTACCA 3' (probe); VCAM-1: 5' TGC GAGTCACCATTGTTCTCAT 3' (forward), 5' CATGGTCAGAACGGACTTGGGA 3' (reverse), 5' ACCCA-GATAGACAGCCCACTAAACGCGAA 3' (probe); gelatinase B: 5' TCACCTTACCCGCGTGTA 3' (forward), 5' GTGCTCCGCGACACCAA 3' (reverse), 5' ACCCGAAGCG-

GACATTGTCATCCAG 3' (probe); macrosialin: 5' CAAG-GTCCAGGGAGG TTGTG 3' (forward), 5' CCAAAG-GTAAGCTGTCCATAAGGA 3' (reverse), 5' CGGTACC-CATCCCCACCTGTCTCTCTC 3' (probe); CD36: 5' TCCAGCCCAATGCCTTTGC 3' (forward), 5' TGGAGAT-TACTTTTCAGTGCAGAA 3' (reverse), 5' TCACCCCTCCA-GAATCCAGACAACCA 3' (probe); SR-A: 5' CATGAACGA-GAGGATGCTGACT 3' (forward), 5' GGAAGGGATGCTGTCATTGAA 3' (reverse), 5' CAGTTCAGAATCCGTGAAATTTGACGCAC 3' (probe); and GAPDH: 5' CCACCCATGGCAAATTCC 3' (forward), 5' TGGGATTCCATTGATGACAAG 3' (reverse), 5' TGGCACCGTCAAGGCTGAGAACG 3' (probe). Equal amounts of cDNA were used in triplicate and amplified with the Taqman Master Mix provided by Perkin-Elmer. Amplification efficiencies were validated and normalized against GAPDH and nanograms of product were calculated using the standard curve method for quantitation against cDNA that was reverse transcribed from isolated aortas of LDLR<sup>-/-</sup> mice fed a 1.25% cholesterol and 21% milk-fat diet for 4 months. Total RNA that was not reverse transcribed was also analyzed to determine genomic DNA contamination.

**Statistical analysis.** Groups were compared by ANOVA and unpaired *t* tests using the StatView analysis program (SAS Institute Inc., Cary, North Carolina, USA). Data are expressed as the mean plus or minus SEM.

## Results

Intervention studies were performed in LDLR<sup>-/-</sup> mice fed a Western-style diet for 10 weeks, starting at age 8–12 weeks. To reduce the possibility that effects of a single PPAR $\gamma$  ligand on atherosclerosis resulted from PPAR $\gamma$ -independent mechanisms, two distinct PPAR $\gamma$  agonists were used: rosiglitazone and GW7845. Rosiglitazone is a member of the TDZ class of insulin sensitizers that was developed using rodent models of type 2 diabetes. It has an effective concentration of 50% (EC<sub>50</sub>) for murine PPAR $\gamma$  of 76 nM (33). GW7845 is a member of the tyrosine-based class of insulin sensitizers that was developed using human PPAR $\gamma$  as a molecular target. It has an EC<sub>50</sub> for murine PPAR $\gamma$  of 1.2 nM (33). Both drugs are highly specific for PPAR $\gamma$ , with EC<sub>50</sub> for PPAR $\alpha$  and PPAR $\delta$  in excess of 10  $\mu$ M (33). We initially performed a pilot study using a calculated dose of 20 mg rosiglitazone/kg/day to establish appropriate dietary cholesterol content and extent of atherosclerosis. Rosiglitazone exerted a significant antiatherogenic effect in male mice in this study, but not in female mice (data not shown). However, because the 1.25% added dietary cholesterol resulted in serum cholesterol levels in excess of 2,000 mg/dL, a potential protective effect in females could have been overwhelmed. Two subsequent intervention studies were therefore carried out in which the added cholesterol was reduced to 0.01%. Each experiment resulted in the same pattern of responses to dietary and drug treatments, and the data from the two studies were pooled to increase statistical power.

**Table 1**  
Average weights, cholesterol, triglyceride, and HDL<sub>c</sub> levels

	Weight g	Total Cholesterol mg/dL	Triglycerides mg/dL	HDL <sub>c</sub> mg/dL		Weight g	Total Cholesterol mg/dL	Triglycerides mg/dL	HDL <sub>c</sub> mg/dL
<b>Males</b>					<b>Females</b>				
<b>Control (n = 10)</b>					<b>Control (n = 10)</b>				
T = 0 weeks	24.4 ± 0.8	258 ± 11	128 ± 17		T = 0 weeks	19.0 ± 0.7	235 ± 12	37 ± 12	
T = 4 weeks	36.7 ± 1.2	1258 ± 143	1150 ± 195		T = 4 weeks	24.1 ± 1.9	1053 ± 97	576 ± 258	
T = 8 weeks	38.9 ± 1.3	1552 ± 83	1279 ± 170		T = 8 weeks	27.2 ± 1.3	1211 ± 68	621 ± 207	
T = 10 weeks	42.5 ± 1.4	1549 ± 89	1226 ± 153	127 ± 5	T = 10 weeks	28.4 ± 1.7	1240 ± 109	722 ± 241	115 ± 4
<b>Ro (n = 12)</b>					<b>Ro (n = 10)</b>				
T = 0 weeks	26.1 ± 0.9	245 ± 10	121 ± 20		T = 0 weeks	20.4 ± 0.5	242 ± 6	47 ± 11	
T = 4 weeks	36.7 ± 1.3	1258 ± 103	1150 ± 265		T = 4 weeks	23.7 ± 1.1	1027 ± 6	624 ± 24	
T = 8 weeks	38.6 ± 1.4	1371 ± 72	1366 ± 134		T = 8 weeks	27.6 ± 1.1	1395 ± 81	1000 ± 107	
T = 10 weeks	40.4 ± 1.3	1440 ± 69	1541 ± 126	115 ± 4 <sup>A</sup>	T = 10 weeks	29.7 ± 1.3	1513 ± 55 <sup>A</sup>	1251 ± 69 <sup>B</sup>	96 ± 3 <sup>B</sup>
<b>GW7845 (n = 10)</b>					<b>GW7845 (n = 7)</b>				
T = 0 weeks	26.3 ± 0.9	249 ± 9	116 ± 22		T = 0 weeks	20.0 ± 0.8	232 ± 11	48 ± 12	
T = 4 weeks	33.5 ± 3.5	1275 ± 168	1406 ± 276		T = 4 weeks	25.0 ± 1.1	1139 ± 82	927 ± 145	
T = 8 weeks	39.9 ± 1.0	1533 ± 81	1790 ± 184		T = 8 weeks	28.6 ± 1.2	1395 ± 90	1049 ± 131	
T = 10 weeks	41.7 ± 2.2	1626 ± 109	1507 ± 200	123 ± 3	T = 10 weeks	28.5 ± 1.4	1449 ± 136	1228 ± 157 <sup>B</sup>	104 ± 4 <sup>A</sup>

Data are expressed as the mean ± SEM; n represents the number of mice per group. Values were determined in plasma samples from nonfasting animals. Ro, rosiglitazone. <sup>A</sup>P < 0.05 and <sup>B</sup>P < 0.005, drug treatment group vs. control group.

At a dose of 20 mg/kg/day, rosiglitazone plasma levels averaged 6.4 plus or minus 0.06 µg/mL in male mice and 5.1 plus or minus 0.69 µg/mL in female mice at 10 weeks. GW7845 levels averaged 3.2 plus or minus 0.39 µg/mL in male mice and 3.2 plus or minus 0.46 µg/mL in female mice after 10 weeks of treatment. These serum levels are sufficient to exert inhibitory effects on proinflammatory gene expression in vitro (29). All animals appeared healthy throughout the study. Serum aspartate aminotransferase and alkaline phosphatase levels were used to assess potential liver toxicity and were not altered at the end of the study (data not shown). Histologic analysis of the bone marrow indi-

cated a significant increase in percentage of marrow fat, and marked extramedullary hematopoiesis was observed in both male and female mice (data not shown). There were no significant changes in complete blood counts or hemoglobin. Data for body weight, total cholesterol, triglycerides, and HDL<sub>c</sub> at specific time points are presented in Table 1. The body weights in all groups increased during the intervention period, but the relative weight gain in males was greater than that in females. The Western diet resulted in a marked increase in total cholesterol within 1 month; the total cholesterol then remained constant at approximately 1,500 mg/dL in males. There was a slight increase in

**Table 2**  
Average glucose, insulin, HbA<sub>1c</sub>, NEFA levels

	Glucose mg/dL	Insulin ng/mL	Hb A <sub>1c</sub> %	NEFA mEq/L		Glucose mg/dL	Insulin ng/mL	Hb A <sub>1c</sub> %	NEFA mEq/L
<b>Males</b>					<b>Females</b>				
<b>Control (n = 10)</b>					<b>Control (n = 10)</b>				
T = 0 weeks	307 ± 20	1.12 ± 0.17	5.50 ± 0.16		T = 0 weeks	267 ± 11	0.55 ± 0.04	5.57 ± 0.15	
T = 4 weeks	211 ± 24	1.38 ± 0.25	5.62 ± 0.11		T = 4 weeks	299 ± 14	1.48 ± 0.18	5.39 ± 0.05	
T = 8 weeks	245 ± 14	4.18 ± 0.41	5.29 ± 0.07		T = 8 weeks	273 ± 21	1.95 ± 0.49	4.96 ± 0.10	
T = 10 weeks	344 ± 22	4.24 ± 0.30	5.31 ± 0.13	0.60 ± 0.06	T = 10 weeks	347 ± 16	1.44 ± 0.30	5.11 ± 0.16	0.64 ± 0.06
<b>Ro (n = 12)</b>					<b>Ro (n = 10)</b>				
T = 0 weeks	282 ± 13	0.95 ± 0.08	5.46 ± 0.11		T = 0 weeks	250 ± 8	0.63 ± 0.13	5.39 ± 0.15	
T = 4 weeks	211 ± 11	1.38 ± 0.11	5.62 ± 0.11		T = 4 weeks	210 ± 10	0.75 ± 0.05	5.78 ± 0.03	
T = 8 weeks	207 ± 8	2.03 ± 0.44	5.08 ± 0.13		T = 8 weeks	216 ± 10	1.91 ± 0.53	4.94 ± 0.09	
T = 10 weeks	315 ± 10	1.45 ± 0.33 <sup>B</sup>	4.91 ± 0.12 <sup>A</sup>	0.65 ± 0.04	T = 10 weeks	312 ± 11	0.93 ± 0.33	4.87 ± 0.07	0.85 ± 0.11
<b>GW7845 (n = 10)</b>					<b>GW7845 (n = 7)</b>				
T = 0 weeks	317 ± 8	1.01 ± 0.18	5.78 ± 0.06		T = 0 weeks	261 ± 14	0.94 ± 0.13	5.20 ± 0.16	
T = 4 weeks	211 ± 13	1.54 ± 0.49	5.76 ± 0.11		T = 4 weeks	225 ± 16	1.07 ± 0.15	5.47 ± 0.12	
T = 8 weeks	204 ± 14	2.01 ± 0.32	5.32 ± 0.09		T = 8 weeks	190 ± 6	1.75 ± 0.59	4.75 ± 0.07	
T = 10 weeks	311 ± 13	1.65 ± 0.36 <sup>B</sup>	4.81 ± 0.16 <sup>A</sup>	0.63 ± 0.05	T = 10 weeks	311 ± 13	1.29 ± 0.37	4.80 ± 0.16	0.81 ± 0.08

Data are expressed as the mean ± SEM; n represents the number of mice per group. Values were determined in plasma samples from nonfasting animals. Ro, rosiglitazone. <sup>A</sup>P < 0.05 and <sup>B</sup>P < 0.005, drug treatment group vs. control group.

cholesterol levels of treated females, but this effect only reached statistical significance ( $P = 0.05$ ) in the rosiglitazone treatment group after 10 weeks. Triglycerides were significantly increased and HDL<sub>c</sub> levels were decreased in female mice treated with rosiglitazone or GW7845. A decrease in HDL<sub>c</sub> levels was seen in male mice treated with rosiglitazone only.

*PPAR $\gamma$  ligands inhibit the development of atherosclerosis in male mice.* Atherosclerosis at the aortic origin was determined by computer-assisted image analysis as described previously (32). Male and female control animals exhibited similar levels of atherosclerosis. Lesions were observed underneath most of the valve leaflets, with some lesions exhibiting areas of central necrosis (Figure 1a). Macroscopically detectable lesions were generally absent from the thoracic or abdominal aorta (data not shown). Markedly fewer and smaller lesions were found in male mice that were treated with either rosiglitazone or GW7845, with quantitative analysis indicating a 60 to 80% reduction in lesion area (Figure 1b). In contrast, the extent of atherosclerosis in female mice treated with either rosiglitazone or GW7845 was not statistically different from that in control mice, confirming the findings of the initial pilot study.

*Metabolic effects of PPAR $\gamma$  ligands.* To investigate possible mechanisms accounting for antiatherogenic effects of PPAR $\gamma$  ligands in male mice and lack of these effects in female mice, lipoprotein levels were evaluated in control and treatment groups. Fast-performance liquid chromatography (FPLC) analysis of pooled terminal serum samples indicated that GW7845 and rosiglitazone had no effect on the lipoprotein profile in male mice (Figure 2a). In contrast, in female mice the VLDL, IDL, and LDL fractions were increased and the HDL fraction decreased in both the rosiglitazone and GW7845 treatment groups (Figure 2b).

Effects of PPAR $\gamma$  ligands on serum glucose, insulin, HbA<sub>1c</sub>, and NEFA levels are presented in Table 2. The Western diet itself did not significantly alter glucose, HbA<sub>1c</sub>, or NEFA levels, but insulin levels rose in both male and female mice. Rosiglitazone and GW7845 treatment resulted in a significant decrease in insulin levels in male mice but had no significant effect on insulin levels in female mice (Table 2). HbA<sub>1c</sub> decreased in males treated with rosiglitazone and GW7845.

To further investigate the effects of rosiglitazone and GW7845 on glucose homeostasis, the response to an oral glucose challenge was assessed in LDLR<sup>-/-</sup> mice fed the Western diet for 8 weeks. LDLR<sup>-/-</sup> mice fed a nor-

mal chow diet were used as additional control groups. Mice were fasted for 4 hours before being given an oral glucose load of 0.75 mg/g. Blood samples were taken at 0, 15, 30, 60, and 90 minutes for measurement of glucose and insulin levels. In male mice, the Western diet had relatively little effect on glucose levels in response to the oral glucose challenge (Figure 3a). In female mice, after glucose administration, the Western diet resulted in modest elevations in glucose that were normalized by treatment with either rosiglitazone or GW7845 (Figure 3b). Striking differences in the insulin responses to oral glucose challenge were noted between

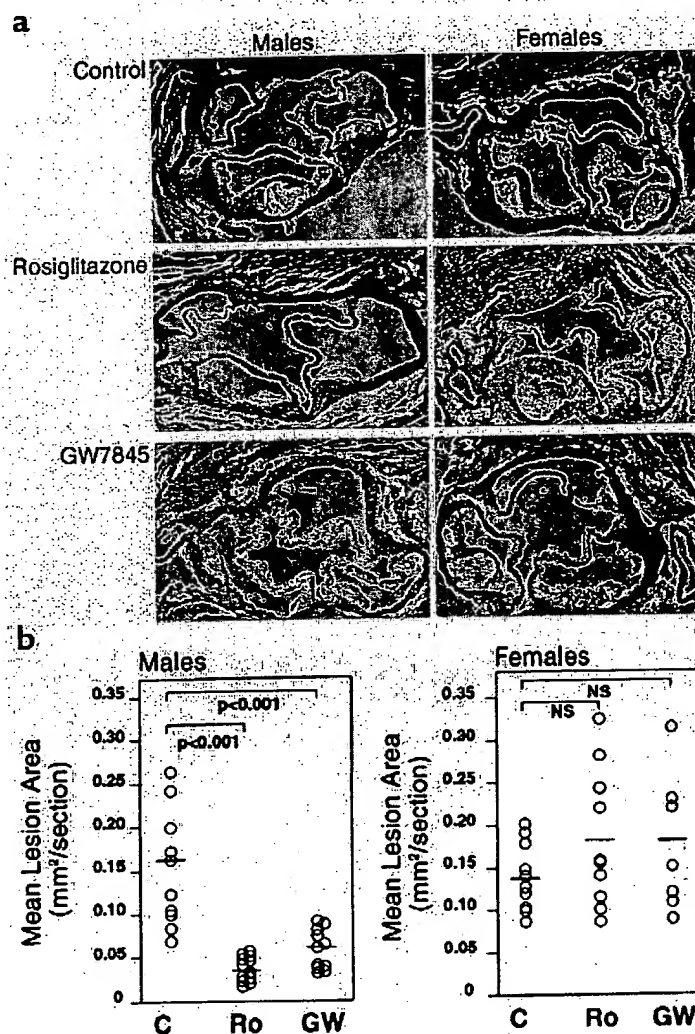


**Figure 1**

Atherosclerosis in LDLR<sup>-/-</sup> mice fed a high-fat, cholesterol-enriched Western diet for 10 weeks. (a) Sections through the aortic root at the levels of the aortic valves were stained for elastin to highlight the medial boundaries of atherosclerotic lesions. (b) Quantitative analysis of lesion areas in control mice (C), mice treated with rosiglitazone (Ro), and mice treated with GW7845 (GW). For male mice, means  $\pm$  SEM were: C,  $0.161 \pm 0.067$  mm<sup>2</sup>/section ( $n = 10$ ); Ro,  $0.037 \pm 0.014$  mm<sup>2</sup>/section ( $n = 12$ ); GW,  $0.063 \pm 0.027$  mm<sup>2</sup>/section ( $n = 10$ ). For female mice, means  $\pm$  SEM were: C,  $0.131 \pm 0.035$  mm<sup>2</sup>/section ( $n = 10$ ); Ro,  $0.183 \pm 0.088$  mm<sup>2</sup>/section ( $n = 10$ ); GW,  $0.181 \pm 0.0091$  mm<sup>2</sup>/section ( $n = 10$ ). NS, not statistically significant.

male and female mice treated with rosiglitazone and GW7845. The Western diet resulted in increased fasting insulin levels in both male and female mice (Figure 3, c and d), compared with the chow-fed controls. Treatment with rosiglitazone or GW7845 resulted in normalization of the fasting insulin levels and the insulin response to glucose challenge in male mice, but not in female mice (Figure 3, c and d), consistent with changes in insulin levels observed in the intervention studies (Table 2).

**Effects of PPAR $\gamma$  ligands on gene expression.** To investigate potential effects of PPAR $\gamma$  ligands on patterns of gene expression within the arterial wall, RNA analysis was performed in LDLR $^{-/-}$  mice fed a Western diet for 10 weeks in the absence or presence of rosiglitazone or GW7845 as described for the intervention studies. RNA was isolated from the base of the heart containing the aortic origin affected by atherosclerosis and analyzed for TNF- $\alpha$ , MCP-1, VCAM-1, and gelatinase B mRNA levels, using quantitative real-time PCR. TNF- $\alpha$  and

gelatinase B mRNA levels were significantly lower in male mice treated with rosiglitazone or GW7845 (Figure 4). Decreases in TNF- $\alpha$  and gelatinase B were smaller in female mice and did not reach statistical significance in the case of gelatinase B. Levels of VCAM-1 and MCP-1, which are thought to be involved in monocyte adhesion to the vessel wall and migration into the lesion, respectively (34), did not change significantly among the groups (Figure 4). Reductions in TNF- $\alpha$  and gelatinase B mRNA levels were also observed in RNA prepared from the apex of the heart, suggesting general effects of the PPAR $\gamma$  ligands (data not shown). Differences in the responses of TNF- $\alpha$  and gelatinase B genes to PPAR $\gamma$  ligand between male and female mice were not likely due to differences in PPAR $\gamma$  expression, because PPAR $\gamma$  mRNA levels were approximately two times higher in female tissues (data not shown).

Because there were significant differences in lesion size in male controls and animals treated with solvent, rosiglitazone, or GW7845, we also investigated whether PPAR $\gamma$  ligands altered levels of gene expression in the artery wall under conditions of equivalent degrees of atherosclerosis. LDLR $^{-/-}$  male mice were fed a 1.25% cholesterol and 21% milk-fat diet for 16 weeks to induce significant atherosclerosis in the aortic arch. Mice were then treated with rosiglitazone, GW7845, or control solvent for 2 weeks while maintaining the high-fat, high-cholesterol diet. Aortas were dissected and weighed to confirm comparable levels of atherosclerosis (35). As an additional control group, mRNA was isolated from aortas of normocholesterolemic animals. The aortas from each group were pooled, and mRNA was isolated for analysis of macrophage-specific membrane glycoprotein that serves as a marker of tissue macrophages (36). Macrophage expression was low in normal aortas and markedly increased in atherosclerotic aortas, as expected. Macrophage levels were not significantly altered by 2 weeks of treatment with rosiglitazone or GW7845, consistent with our observation that PPAR $\gamma$  ligands do not alter macrophage expression in peritoneal macrophages (data not shown) and reflecting comparable levels of atherosclerosis in these three groups. SR-A and MCP-1 mRNA levels were also elevated in atherosclerotic aortas, as expected. Surprisingly, the mRNA levels for VCAM-1 remained unchanged. In contrast to previous findings in cell-culture models (29, 37), mRNA levels for these genes were not decreased by treatment with PPAR $\gamma$  ligands. However, treatment with rosiglitazone or GW7845 significantly increased CD36 expression and inhibited TNF- $\alpha$  expression, indicating actions of PPAR $\gamma$  on gene expression in the artery wall. The effects on CD36 expression were tissue specific, because no increase in CD36 expression was observed in cardiac tissue of mice treated with rosiglitazone or GW7845 (data not shown).

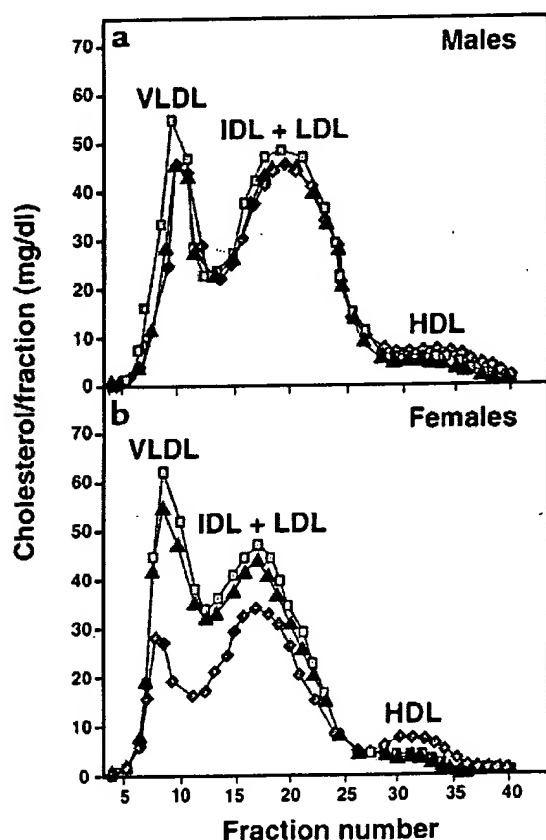
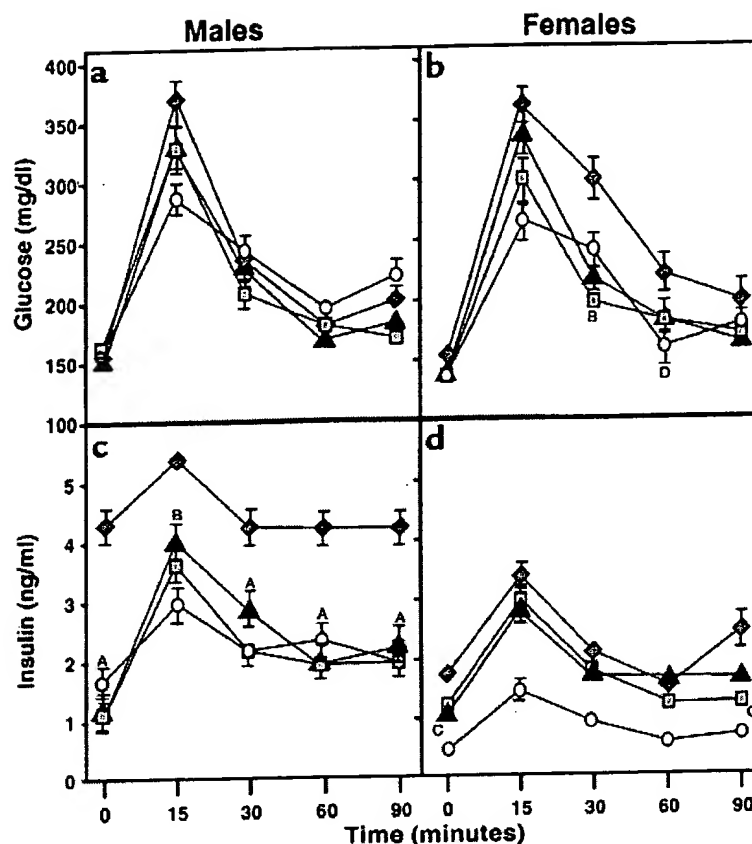


**Figure 2**  
Size distribution of lipoprotein particles in LDLR $^{-/-}$  mice fed a high-fat, cholesterol-enriched diet and treated with solvent (control; diamonds), rosiglitazone (squares), or GW7845 (triangles) for 10 weeks. Plasma was pooled from four mice from each treatment group and fractionated by FPLC. Mean cholesterol content in each fraction was determined in duplicate.



**Figure 3**

Glucose and insulin responses to an oral glucose challenge in LDLR<sup>-/-</sup> mice fed the normal chow (circles); high-fat, cholesterol-enriched diet and solvent (control; diamonds); rosiglitazone (squares); or GW7845 (triangles). Blood glucose and plasma insulin levels were determined at base line (after a 4-hour fast) and 15, 30, 60, and 90 minutes after oral administration of 0.75 mg glucose/g body weight. Samples were taken from eight animals per group. Data are expressed as the mean  $\pm$  SEM. <sup>A</sup>*P* < 0.0001, <sup>B</sup>*P* < 0.002, <sup>C</sup>*P* < 0.015, and <sup>D</sup>*P* < 0.04, drug treatment group vs. control group.



## Discussion

The present studies demonstrate that PPAR $\gamma$  ligands significantly inhibit the development of atherosclerosis in LDLR<sup>-/-</sup> male mice fed a Western-style diet. These mice, in addition to being hypercholesterolemic, were obese, hypertriglyceridemic, and insulin resistant. They thus exhibit clinical features of many human diabetic patients who are candidates for treatment with PPAR $\gamma$  ligands. Rosiglitazone and GW7845 reduced the extent of atherosclerosis despite a significant increase in the expression of CD36 in the vessel wall. These observations suggest that the potential of PPAR $\gamma$  ligands to promote the development of foam cells by upregulation of CD36 is overcome by other systemic and local actions. Several mechanisms could potentially account for the net antiatherosclerotic effects of rosiglitazone and GW7845. A number of proinflammatory cytokines, including TNF- $\alpha$ , IL-1 $\alpha$ , and IL-1 $\beta$ , have been suggested to promote the development of atherosclerosis (38). Systemic reductions in the circulating levels of these cytokines or reductions in their expression within cells of the artery wall could potentially underlie at least some of the antiatherosclerotic effects of rosiglitazone and GW7845. Although previous studies have suggested effects of PPAR $\gamma$  ligands on MCP-1 expression in macrophages and smooth muscle cells and VCAM-1 expression in endothelial cells (18, 39–41), we did not observe significant alter-

ations in VCAM-1 or MCP-1 expression in mice treated with PPAR $\gamma$  agonists. This may reflect the cellular heterogeneity of the aortic origin and vessel wall from which RNA was isolated for analysis. The antiatherogenic effects of rosiglitazone and GW7845 in male mice also correlated with improved insulin sensitivity. However, to date, no experimental evidence for a direct influence of insulin resistance on atherosclerosis has been provided in humans or murine models (42). Further investigation will be required to establish the major mechanisms underlying the therapeutic effects of PPAR $\gamma$  ligands in this model system.

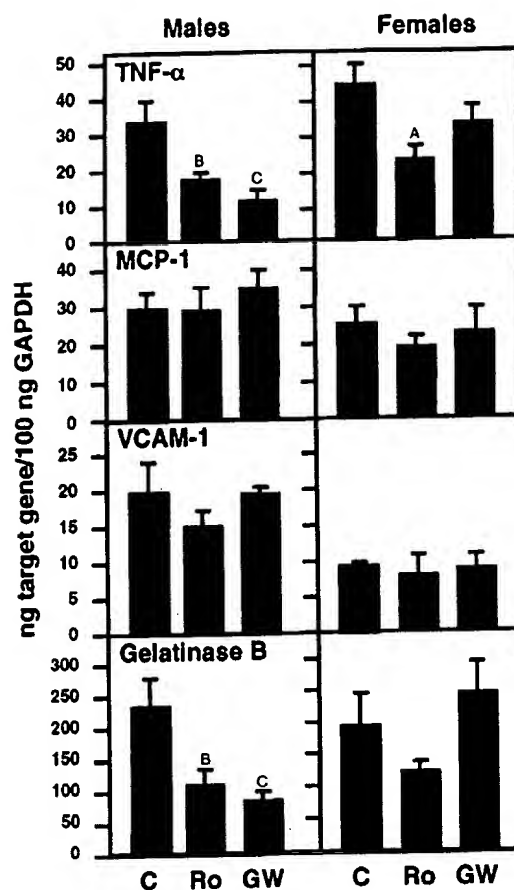
Intriguingly, female mice did not exhibit a reduction in atherosclerosis in response to PPAR $\gamma$ -specific ligands. This lack of a response was not due to altered drug levels or differences in levels of PPAR $\gamma$  expression in the artery wall. Rosiglitazone and GW7845 were less effective in correcting hyperinsulinemia in female mice and did not influence the expression of gelatinase B or TNF- $\alpha$  in tissues. In contrast to male mice, PPAR $\gamma$  ligands altered the lipoprotein size distribution in female mice, reducing HDL levels and skewing the profile to larger particles. Reductions in HDL levels could potentially account for lack of effect of rosiglitazone and GW7845 on the extent of atherosclerosis, but the lack of effect on gelatinase B and TNF- $\alpha$  levels suggest gender-specific differences in the responses to

**Figure 4**

Expression of TNF- $\alpha$ , MCP-1, VCAM-1, and gelatinase B mRNA in the aortic root. The mRNA levels were quantitated using real-time RT-PCR. Six to seven samples per group were analyzed. C, control; Ro, rosiglitazone; GW, GW7845. Data are expressed as mean  $\pm$  SEM. <sup>A</sup> $P < 0.05$ , <sup>B</sup> $P < 0.01$ , and <sup>C</sup> $P < 0.001$ , drug treatment groups vs. cholesterol group.

PPAR $\gamma$  ligands. The basis for these differences is unclear, but they are likely to relate to influences of estrogens and progestins. Consistent with this, preliminary studies of ovariectomized female mice indicate metabolic responses to rosiglitazone and GW7845 that are much more similar to male mice. Studies of the efficacy of TZDs as insulin sensitizers in human diabetic patients have not revealed any significant gender-specific differences, but most female patients enrolled in these studies are postmenopausal.

In concert, these studies provide clear evidence that activation of PPAR $\gamma$  inhibits the development of atherosclerosis in a murine model. These effects were observed using relatively high doses of PPAR $\gamma$  ligands that also induced adipogenesis in bone marrow and secondary extramedullary hematopoiesis. Extending this proof of principle to human populations will require clinical investigation in diabetic and nondiabetic patients. Because the PPAR $\gamma$  agonists used in these studies exerted both potentially antiatherogenic (e.g., down-regulation of TNF- $\alpha$ ) and potentially proatherogenic (e.g., upregulation of CD36) effects on patterns of gene expression in the artery wall, the development of novel PPAR $\gamma$  ligands that dissociate proatherogenic activities from antidiabetic and antiatherogenic activities would be highly desirable. Recent successes in the development of selective estrogen receptor modulators (43) suggest that such goals are attainable.

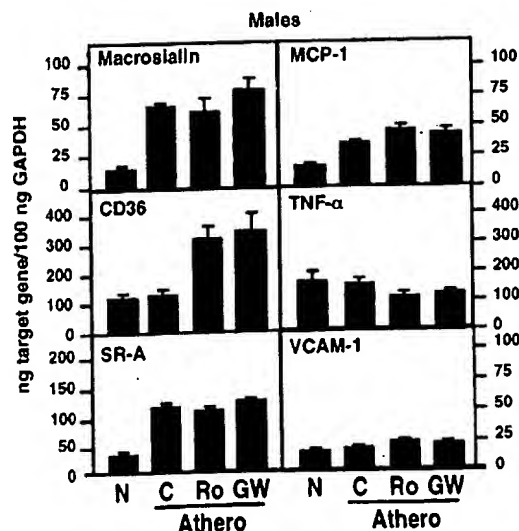


#### Acknowledgments

We wish to thank Florencia Casanada, Jennifer Patterson, and Joseph Juliano for isolating the aortas and determining the plasma cholesterol and triglycerides; Jane Binz and Jennifer Becker for HbA<sub>1c</sub>, NEFA, and HDL<sub>c</sub> analysis; Harry Marr for drug level determination; Jacques Corbeil and Christine Plotkin at the

**Figure 5**

Expression of macrosialin, CD36, SR-A, MCP-1, TNF- $\alpha$ , and VCAM-1 mRNA in the aorta. Male LDLR<sup>-/-</sup> mice were fed either a normal chow diet (N) or a high-cholesterol diet for 4 months to induce the development of atherosclerosis (Athero). Animals fed the high-cholesterol diet were then treated with either solvent control, rosiglitazone, or GW7845 for 2 weeks. The mRNA levels were quantitated using real-time RT-PCR. Data represent pooled aortas with an average weight of  $3.86 \pm 0.16$  mg/aorta for normal chow (N) ( $n = 11$ );  $5.75 \pm 0.67$  mg/aorta for high cholesterol (C) ( $n = 6$ );  $5.67 \pm 0.56$  mg/aorta for high cholesterol/rosiglitazone (Ro) ( $n = 6$ ); and  $5.80 \pm 0.70$  mg/aorta for high cholesterol/GW7845 (GW) ( $n = 6$ ). Data are in triplicates and expressed as mean  $\pm$  SEM.



Center for AIDS Research Genomics Core, Veterans Medical Research Foundation for advice and performing the RT-PCR quantification analysis; and Tanya Schneiderman and Amy Johnson for their assistance in preparing the manuscript. This work was supported by NIH Specialized Center of Research (SCOR) on Molecular Medicine and Atherosclerosis grant (HL-56989) and a grant from the Glaxo Wellcome Research Institute. A.C. Li is supported by a Mentored-Clinical Scientist Development Award (HL-03625). C.K. Glass is an Established Investigator of the American Heart Association.

- Kannel, W., and McGee, D. 1979. Diabetes and cardiovascular disease: the Framingham study. *JAMA*. 241:2035-2038.
- Uusitupa, M., Niskanen, L., and Siitonen, O. 1990. 5-year incidence of atherosclerotic vascular disease in relation to general risk factors, insulin levels, and abnormalities in lipoprotein composition in non-insulin-dependent diabetic and nondiabetic subjects. *Circulation*. 82:27-36.
- Steinberg, D., Parthasarathy, S., Carew, T.E., Khoo, J.C., and Witztum, J.L. 1989. Beyond cholesterol. Modifications of low-density lipoprotein that increase its atherogenicity. *N. Engl. J. Med.* 320:915-924.
- Napoli, C., et al. 1997. Fatty streak formation occurs in human fetal aorta and is greatly enhanced by maternal hypercholesterolemia. Intimal accumulation of low density lipoprotein and its oxidation precede monocyte recruitment into early atherosclerotic lesions. *J. Clin. Invest.* 100:2680-2690.
- Kodama, T., Reddy, P., Kishimoto, C., and Krieger, M. 1988. Purification and characterization of a bovine acetyl low density lipoprotein receptor. *Proc. Natl. Acad. Sci. USA*. 85:9238-9242.
- Endemann, G., et al. 1993. CD36 is a receptor for oxidized low density lipoprotein. *J. Biol. Chem.* 268:11811-11816.
- Ramprasad, M.P., Terpstra, V., Kondratenko, N., Quehenberger, O., and Steinberg, D. 1996. Cell surface expression of mouse macrophage and human CD68 and their role as macrophage receptors for oxidized low density lipoprotein. *Proc. Natl. Acad. Sci. USA*. 93:14833-14838.
- Ross, R. 1986. The pathogenesis of atherosclerosis. *N. Engl. J. Med.* 314:488-500.
- Ross, R. 1999. Atherosclerosis: an inflammatory disease. *N. Engl. J. Med.* 340:115-126.
- Boring, L., Gosling, J., Cleary, M., and Charo, I.F. 1998. Decreased lesion formation in CCR2<sup>-/-</sup> mice reveals a role for chemokines in the initiation of atherosclerosis. *Nature*. 394:894-897.
- Gosling, J., et al. 1999. MCP-1 deficiency reduces susceptibility to atherosclerosis in mice that overexpress human apolipoprotein B. *J. Clin. Invest.* 103:773-778.
- Suzuki, H., et al. 1997. A role for macrophage scavenger receptors in atherosclerosis and susceptibility to infection. *Nature*. 386:292-296.
- Febbraio, M., et al. 2000. Targeted disruption of the class B scavenger receptor CD36 protects against atherosclerotic lesion development in mice. *J. Clin. Invest.* 105:1049-1056.
- Barnes, P.J., and Karin, M. 1997. Nuclear factor-kappaB: a pivotal transcription factor in chronic inflammatory diseases. *N. Engl. J. Med.* 336:1066-1071.
- Sato, H., Kita, M., and Seiki, M. 1993. v-Src activates the expression of 92-kDa type IV collagenase gene through the AP-1 site and the GT box homologous to retinoblastoma control elements. A mechanism regulating gene expression independent of that by inflammatory cytokines. *J. Biol. Chem.* 268:23460-23468.
- Ricote, M., et al. 1998. Expression of the peroxisome proliferator-activated receptor  $\gamma$  (PPAR $\gamma$ ) in human atherosclerosis and regulation in macrophages by colony stimulating factors and oxidized low density lipoprotein. *Proc. Natl. Acad. Sci. USA*. 95:7614-7619.
- Marx, N., Sukhova, G., Murphy, C., Libby, P., and Plutsky, J. 1998. Macrophages in human atheroma contain PPAR $\gamma$ : differentiation-dependent peroxisomal proliferator-activated receptor gamma expression and reduction of MMP-9 activity through PPAR $\gamma$  activation in mononuclear phagocytes *in vitro*. *Am. J. Pathol.* 153:17-23.
- Jackson, S.M., et al. 1999. Peroxisome proliferator-activated receptor activators target human endothelial cells to inhibit leukocyte-endothelial cell interaction. *Arterioscler. Thromb. Vasc. Biol.* 19:2094-2104.
- Tontonoz, P., Nagy, L., Alvarez, J.G.A., Thomazy, V.A., and Evans, R.M. 1998. PPAR $\gamma$  promotes monocyte/macrophage differentiation and uptake of oxidized LDL. *Cell*. 93:241-252.
- Pasceri, V., Wu, H.D., Willerson, J.T., and Yeh, E.T. 2000. Modulation of vascular inflammation *in vitro* and *in vivo* by peroxisome proliferator-activated receptor-gamma activators. *Circulation*. 101:235-238.
- Nagy, L., Tontonoz, P., Alvarez, J.G.A., Chen, H., and Evans, R.M. 1998. Oxidized LDL regulates macrophage gene expression through ligand activation of PPAR-gamma. *Cell*. 93:229-240.
- Forman, B.M., et al. 1995. 15-Deoxy- $\Delta^{12,14}$ -prostaglandin J<sub>2</sub> is a ligand for the adipocyte determination factor PPAR $\gamma$ . *Cell*. 83:803-812.
- Kliwer, S.A., et al. 1997. Fatty acids and eicosanoids regulate gene expression through direct interactions with peroxisome proliferator-activated receptors  $\alpha$  and  $\gamma$ . *Proc. Natl. Acad. Sci. USA*. 94:4318-4323.
- Barak, Y., et al. 1999. PPAR $\gamma$  is required for placental, cardiac, and adipose tissue development. *Mol. Cell*. 4:585-595.
- Kubota, N., et al. 1999. PPAR $\gamma$  mediates high-fat diet-induced adipocyte hypertrophy and insulin resistance. *Mol. Cell*. 4:597-609.
- Rosen, E.D., et al. 1999. PPAR $\gamma$  is required for the differentiation of adipose tissue *in vivo* and *in vitro*. *Mol. Cell*. 4:611-617.
- Nolan, J.J., Ludvik, B., Beardsden, P., Joyce, M., and Olefsky, J. 1994. Improvement in glucose tolerance and insulin resistance in obese subjects treated with troglitazone. *N. Engl. J. Med.* 331:1188-1193.
- Jiang, C., Ting, A.T., and Seed, B. 1998. PPAR-gamma agonists inhibit production of monocyte inflammatory cytokines. *Nature*. 391:82-86.
- Ricote, M., Li, A.C., Willson, T.M., Kelly, C.J., and Glass, C.K. 1998. The peroxisome proliferator-activated receptor- $\gamma$  is a negative regulator of macrophage activation. *Nature*. 391:79-82.
- Su, C.G., et al. 1999. A novel therapy for colitis utilizing PPAR- $\gamma$  ligands to inhibit the epithelial inflammatory response. *J. Clin. Invest.* 104:383-389.
- Sheehan, D.C., and Hrapchak, B.B. 1980. *Theory and practice of histotechnology*. C.V. Mosby Co., St. Louis, Missouri, USA. 481 pp.
- Tangirala, R.K., Rubin, E.M., and Palinski, W. 1995. Quantitation of atherosclerosis in murine models: correlation between lesions in the aortic origin and in the entire aorta, and differences in the extent of lesions between sexes in LDL receptor-deficient and apolipoprotein E-deficient mice. *J. Lipid Res.* 36:1-9.
- Willson, T., Brown, P., Sternbach, D., and Henke, B. 2000. The PPARs: from orphan receptors to drug discovery. *J. Med. Chem.* 43:527-550.
- Fruebis, J., Gonzales, V., Silvestre, M., and Palinski, W. 1997. Effect of probucol treatment on gene expression of VCAM-1, MCP-1 and M-CSF in the aortic wall of LDL receptor-deficient rabbits during early atherosclerosis. *Arterioscler. Thromb. Vasc. Biol.* 17:1289-1302.
- Tsimikas, S., Shortal, B.P., Witztum, J.L., and Palinski, W. 2000. *In vivo* uptake of radiolabeled MDA2, an oxidation-specific monoclonal antibody, provides an accurate measure of atherosclerotic lesions rich in oxidized LDL and is highly sensitive to their regression. *Arterioscler. Thromb. Vasc. Biol.* 20:689-697.
- Holness, C.L., and Simmons, D.L. 1993. Molecular cloning of CD68, a human macrophage marker related to lysosomal glycoproteins. *Blood*. 81:1607-1613.
- Goetze, S., et al. 1999. PPAR gamma-ligands inhibit migration mediated by multiple chemoattractants in vascular smooth muscle cells. *J. Cardiovasc. Pharmacol.* 33:798-806.
- Libby, P., Sukhova, G., Lee, R.T., and Galis, Z.S. 1995. Cytokines regulate vascular functions related to stability of the atherosclerotic plaque. *J. Cardiovasc. Pharmacol.* 25(Suppl. 2):S9-S12.
- Murao, K., et al. 1999. Thiazolidinedione inhibits the production of monocyte chemoattractant protein-1 in cytokine-treated human vascular endothelial cells. *FEBS Lett.* 454:27-30.
- Law, R.E., et al. 1996. Troglitazone inhibits vascular smooth muscle cell growth and intimal hyperplasia. *J. Clin. Invest.* 98:1897-1905.
- Staels, B., et al. 1998. Activation of human aortic smooth-muscle cells is inhibited by PPAR $\alpha$  but not by PPAR $\gamma$  activators. *Nature*. 393:790-793.
- Merat, S., Casanada, F., Surphin, M., Palinski, W., and Reaven, P.D. 1999. Western-type diets induce insulin resistance and hyperinsulinemia in LDL receptor-deficient mice but do not increase aortic atherosclerosis compared with normoinsulinemic mice in which similar plasma cholesterol levels are achieved by a fructose-rich diet. *Arterioscler. Thromb. Vasc. Biol.* 19:1223-1230.
- Roe, E.B., Chiu, K.M., and Arnaud, C.D. 2000. Selective estrogen receptor modulators and postmenopausal health. *Adv. Intern. Med.* 45:257-278.

# Hyperlipidemia and Atherosclerotic Lesion Development in LDL Receptor-Deficient Mice Fed Defined Semipurified Diets With and Without Cholate

Andrew H. Lichtman, Steven K. Clinton, Kaeko Iiyama, Philip W. Connelly,  
Peter Libby, Myron I. Cybulsky

**Abstract**—Past studies of atherosclerosis in mice have used chow-based diets supplemented with cholesterol, lipid, and sodium cholate to overcome species resistance to lesion formation. Similar diets have been routinely used in studies with LDL receptor-deficient ( $LDLR^{-/-}$ ) mice. The nonphysiological nature and potential toxicity of cholate-containing diets have led to speculation that atherogenesis in these mice may not accurately reflect the human disease process. We have designed a semipurified AIN-76A-based diet that can be fed in powdered, pelleted, or liquid form and manipulated for the precise evaluation of diet-genetic interactions in murine atherosclerosis.  $LDLR^{-/-}$  mice were randomly assigned among 4 diets ( $n=6$ /diet) as follows: 1, control, 10% kcal lipid; 2, high fat (40% kcal), moderate cholesterol (0.5% by weight); 3, high fat, high cholesterol (1.25% by weight); and 4, high fat, high cholesterol, and 0.5% (wt/wt) sodium cholate. Fasting serum cholesterol was increased in all cholesterol-supplemented mice compared with controls after 6 or 12 weeks of feeding ( $P<0.01$ ). The total area of oil red O-stained atherosclerotic lesions was determined from digitally scanned photographs. In contrast to the control group, all mice in cholesterol-supplemented dietary groups 2 to 4 had lesions involving 7.01% to 12.79% area of the thoracic and abdominal aorta at 12 weeks ( $P<0.002$ , for each group versus control). The distribution pattern of atherosclerotic lesions was highly reproducible and comparable. The histological features of lesions in mice fed cholate-free or cholate-containing diets were similar. This study shows that sodium cholate is not necessary for the formation of atherosclerosis in  $LDLR^{-/-}$  mice and that precisely defined semipurified diets are a valuable tool for the examination of diet-gene interactions. (*Arterioscler Thromb Vasc Biol.* 1999;19:1938-1944.)

**Key Words:** atherosclerosis ■ LDL receptor ■ dietary lipids ■ cholesterol ■ mice

The development of murine models defective in genes controlling lipid metabolism and lipoprotein expression provides an opportunity to understand better the complex interactions between diet and genetics in atherosclerosis. In the last several years, embryonic stem cell and transgenic technologies have been used to alter the expression levels of various genes affecting lipoprotein metabolism and have led to the development of murine knockout and transgenic models of atherogenesis. The ApoE knockout ( $ApoE^{-/-}$ ),<sup>1,2</sup> LDL receptor knockout ( $LDLR^{-/-}$ ),<sup>3</sup> and human ApoB transgenic mice<sup>4,5</sup> develop lesions throughout the arterial tree. Their distribution pattern and morphological features share many similarities with human atherosclerosis, suggesting that similar pathogenic mechanisms may be involved.<sup>6,7</sup>  $ApoE^{-/-}$  mice develop hypercholesterolemia and atherosclerotic lesions spontaneously, and this can be accelerated by feeding a

Western-type diet.<sup>1,6</sup> In contrast,  $LDLR^{-/-}$  mice fed a chow diet have only a 2-fold elevation in plasma cholesterol compared with control mice and do not develop significant lesions in the first 6 months of life.<sup>3</sup> When fed a diet consisting of 1.25% cholesterol, 7.5% cocoa butter, 7.5% casein, and 0.5% cholic acid, these mice develop marked hypercholesterolemia and lesions throughout the aorta within 3 to 4 months.<sup>8</sup> Because hypercholesterolemia and lesion formation in  $LDLR^{-/-}$  mice are readily enhanced by a diet supplemented with fat, cholesterol, and cholate, these mice provide a unique opportunity for evaluation of early events in atherogenesis.

Before the development of atherosclerosis-prone gene-targeted mutant mice, many studies were performed with normal mice fed chow-based diets supplemented with varying amounts of saturated fats, cholesterol, and cholate to

Received September 22, 1998; revision accepted January 11, 1999.

From the Vascular Research Division (A.H.L.), Department of Pathology, and the Vascular Medicine and Atherosclerosis Unit (P.L.), Cardiovascular Division, Department of Medicine, Brigham and Women's Hospital, Harvard Medical School, Boston, Mass; the Arthur G. James Cancer Hospital and Research Institute (S.K.C.), Ohio State University, Columbus, Ohio; and the Department of Laboratory Medicine and Pathobiology (K.I., M.I.C.), University of Toronto, Toronto Hospital Research Centre, and the Departments of Laboratory Medicine and Pathobiology, Medicine, and Biochemistry (P.W.C.), University of Toronto, St Michael's Hospital, Toronto, Ontario, Canada.

Correspondence to Andrew H. Lichtman, MD, PhD, Department of Pathology, Brigham and Women's Hospital, 221 Longwood Avenue, Boston, MA 02115. E-mail alichtman@rics.bwh.harvard.edu

© 1999 American Heart Association, Inc.

*Arterioscler Thromb Vasc Biol.* is available at <http://www.atvbaha.org>

induce atheromatous lesions. In particular, C57BL/6 mice are susceptible to dietary intervention and develop foam cell-rich lesions in the aortic root, but not advanced atheromas.<sup>9-13</sup> Dietary cholate was required to achieve significant hypercholesterolemia, presumably by interfering with hepatobiliary excretion of cholesterol. Most published studies of atherosclerosis in the LDLR<sup>-/-</sup> mice have relied on similar diets supplemented with cholate, cholesterol, and lipid that were used in the earlier C57BL/6 mouse studies. This has led to criticisms of the LDLR<sup>-/-</sup> mouse model based on the speculation that toxic metabolic effects of cholate may modify the pathogenesis of vascular disease in ways not relevant to human atherosclerosis. For example, cholate may cause hepatic steatosis that can progress to cirrhosis accompanied by several host metabolic, physiological, and hormonal changes that can potentially interfere with the interpretation of studies focusing on the histopathological and molecular events during atherogenesis. Recent data from our group and others indicate that cholate is not necessary and that a diet supplemented with cholesterol and saturated fat is sufficient for aortic lesion development in LDLR<sup>-/-</sup> mice.<sup>14,15</sup>

From a nutritional perspective, the dilution of a chow diet with purified lipids, such as hydrogenated coconut oil, increases the caloric density of the diet and reduces the ratio of essential nutrients to dietary energy, thereby potentially contributing to marginal nutrient intake in mice consuming the atherogenic diet. Chow diets do not take advantage of the accumulated knowledge concerning nutritional requirements of mice and the experience of many investigators using precisely controlled semipurified or purified diets for studies of chronic disease processes in rodents.<sup>16-19</sup> Chow diets are formulated from natural ingredients to satisfy the minimal nutrient requirements for growth and reproduction but they differ individual nutrients over time, seasonally, in different geographic locations and between companies in the sources of ingredients included in the final product.<sup>20</sup> Furthermore, many man-made and natural toxins are detected in chow diets, such as aflatoxins, nitrosamines, pesticides, herbicides, and heavy metals.<sup>20-22</sup> Chow diets contain a variety of natural substances from grains, fruits, and vegetables that may modify lipid metabolism and atherogenesis, including a diverse array of soluble and insoluble fiber sources and a multitude of biologically active phytochemicals such as carotenoids and flavonoids. For example, the latter constituents may exert antioxidant actions that could influence atherogenesis and confound experiments.

We propose that investigators of atherogenesis using the many new transgenic and gene knockout models should consider using precisely defined semipurified diets in their studies. This approach adds very little to the overall costs of *in vivo* investigations and can help improve the quality of data obtained and the comparison of results among laboratories over time. Furthermore, the use of semipurified diets in murine studies provides a method for precise control of dietary and nutritional factors, allowing for a meaningful evaluation of specific nutritional interventions that may be relevant to human disease processes. We therefore designed and tested several semipurified diet formulations in a study of atherogenesis in LDLR<sup>-/-</sup> mice.

## Methods

### Mice

Male LDLR<sup>-/-</sup> mice (homozygous) from a mixed C57BL/6J × 129Sv background (50% C57BL/6J:50% 129Sv) were purchased from Jackson Laboratories and maintained in the Longwood Medical Research Center facility in accordance with guidelines of the Committee on Animals of the Harvard Medical School and those prepared by the Committee on Care and Use of Laboratory Animals of the Institute of Laboratory Resources, National Research Council [DHEW publication No. (NIH) FS-23]. At 8 to 12 weeks of age, mice that reached a weight of 21 to 22 g were randomly assigned to 1 of 4 diets (see below) fed *ad libitum* for 12 weeks. For experiments that included analyses of body weight, total plasma cholesterol and triglycerides, and atherosclerotic lesion formation in the aorta, groups consisted of 6 mice. Additional male LDLR<sup>-/-</sup> mice were fed identical diets and killed to obtain plasma for lipoprotein analysis, liver function tests, and tissues for histology.

### Diets

Four diets were used in this study. Each diet was a modification of the AIN-76A semipurified diet for mice and rats<sup>18,19</sup> and prepared by Dr Edward A. Ulman at Research Diets, Inc, according to our formulations (Table 1). The diets provide adequate concentrations of all known essential nutrients for the mouse. The carbohydrate component was altered from the original AIN-76A formulation by including expanded maltose dextrin, which allows the lipid concentration to vary from the range of 10% to 40% of total energy ( $\approx 5\%$  to 20% by weight) without a problem of "settling out." Furthermore, the carbohydrate modifications allow a diet to be fed as a powder, a liquid formulation, or processed into pellets (used in this study). The 4 experimental diet groups include diet 1 group (Research Diet D12102), control (10% kcal lipid); diet 2 group (Research Diet D12107), high fat (40% kcal lipid), moderate cholesterol (0.5% by weight); diet 3 group (Research Diet D12108), high fat, high cholesterol (1.25% by weight); and diet 4 group (Research Diet D12109), high fat, high cholesterol, and sodium cholate (0.5% by weight). The addition of lipid to the baseline diet formulation is achieved by substituting fat (9 kcal/g of metabolizable energy) for carbohydrate (4 kcal/g of metabolizable energy) based on an equal amount of energy (kcal) rather than an equal weight (g). This approach is necessary to maintain a constant ratio of all other nutrients in the diet to energy. This technique of diet formulation avoids the problem of reduced nutrient content of the high-fat diets prepared by the dilution technique (ie, chow diluted with fat) or when fat is substituted for carbohydrate on the basis of weight.

### Cholesterol Measurements and Liver Function Tests

Serum samples were collected for lipid analysis after overnight fasting. At 0 (initiation of the study), 6 and 12 weeks, blood was obtained from individual mice by tail-vein nicking and total serum cholesterol and triglyceride levels were determined by colorimetric assays (Sigma Chemical Co). Blood was obtained from the retro-orbital plexus for analysis of plasma lipoproteins by fast protein liquid chromatography gel-filtration chromatography after 12 weeks of diet. Samples were anticoagulated with EDTA (3 mmol/L or 0.1% final) and sodium azide 0.02% was added as a preservative. To obtain a plasma volume of at least 250  $\mu$ L, plasma was pooled from several mice within each group. Erythrocytes and leukocytes were removed by low-speed (400g, 10 minutes, 4°C) and platelets by high-speed (3000g, 5 minutes, 4°C) centrifugations. Plasma was stored at 4°C for <2 days. Plasma was subjected to fast protein liquid chromatography gel-filtration chromatography by using a Superose 6HR 10/30 column (Pharmacia Biotech) as was previously described.<sup>23</sup> Filtered plasma (200  $\mu$ L) was loaded on the column and was eluted with 2 mmol/L sodium phosphate, 0.14 mol/L NaCl, 5 mmol/L Na<sub>2</sub>EDTA, 0.02% NaN<sub>3</sub>, pH 7.4, at a constant flow rate of 0.5 mL/min. Fractions (0.5 mL) were collected and total cholesterol, triglycerides, free cholesterol, and choline-containing phospholipids were measured on a Technicon RA1000 (Bayer Corp). Triglycerides were corrected for free glycerol by using a triglyceride blank reagent (Bayer Corp). The cholesterol and triglyceride assays were standard-

TABLE 1. Formulation for the Diets Used in This Study and Their Macronutrient Contents as Percentages of Total Energy

Ingredient	Diet 1 (10% kcal fat, 0% cholesterol§§, 0% cholate§§)		Diet 2 (40% kcal fat, 0.5% cholesterol, 0% cholate)		Diet 3 (40% kcal fat, 1.25% cholesterol, 0% cholate)		Diet 4 (40% kcal fat, 1.25% cholesterol, 0.5% cholate)	
	Grams	kcal	Grams	kcal	Grams	kcal	Grams	kcal
Formulation								
Casein†	200.0	800	200.0	800	200.0	800	200.0	800
Cystine	3.0	12	3.0	12	3.0	12	3.0	12
Soy oil‡	25.0	225	25.0	225	25.0	225	25.0	225
Cocoa butter§	20.0	180	155.0	1395	155.0	1395	155.0	1395
Corn Starch	375.0	1500	212.0	848	212.0	848	212.0	848
Malto-dextrin	125.0	500	71.0	284	71.0	284	71.0	284
Sucrose	200.0	800	113.0	452	113.0	452	113.0	452
Cellulose¶	50.0	0	50.0	0	50.0	0	50.0	0
Mineral Mix#	10.0	0	10.0	0	10.0	0	10.0	0
Dicalcium phosphate#	13.0	0	13.0	0	13.0	0	13.0	0
Calcium carbonate#	5.5	0	5.5	0	5.5	0	5.5	0
Potassium citrate, monohydrate#	16.5	0	16.5	0	16.5	0	16.5	0
Vitamin mix**	10.0	40	10.0	40	10.0	40	10.0	40
Choline††	2.0	0	2.0	0	2.0	0	2.0	0
Cholesterol	0	0	4.5	0	11.25	0	11.25	0
Cholate	0	0	0	0	0	0	4.5	0
Total grams or kcal*	1055.0	4057	890.6	4056	897.35	4056	901.85	4056
	% kcal		% kcal		% kcal		% kcal	
Macronutrient content								
Protein	20		20		20		20	
Carbohydrate	70		40		40		40	
Lipid	10		40		40		40	
kcal/g in diet*	3.8		4.5		4.5		4.5	

\*Calculations based on estimated metabolizable energy of 4 kcal/g (16.7 kJ/g) of protein and carbohydrate and 9 kcal/g (37.7 kJ/g) of lipid. The concentrations of minerals, vitamins, and fiber were adjusted to maintain a constant ratio to energy.

†Alcohol extracted casein, 99% protein.

‡Soy oil provides a minimal supply of essential fatty acids.

§We have selected cocoa butter for this study, because it is a saturated fat but has no cholesterol.

||Malto-dextrin 10 is a component of the carbohydrate fraction that assists in maintaining the lipid fraction equally dispersed throughout the diet during shipping, storage, and feeding.

¶BW200 cellulose.

#AIN-76A mineral mixtures with the calcium and phosphate removed. Dicalcium phosphate, calcium carbonate, and potassium citrate, monohydrate are replaced, to increase phosphate and potassium relative to the original formulation.

\*\*AIN-76A vitamin mixture.

††Choline provided as choline bitartrate.

§§Cholesterol and cholate (which do not contribute to total energy) are expressed as percent w/w.

ized with the National Heart Lung and Blood Institutes—Center for Disease Control Lipid Standardization program. Reagents for free cholesterol and choline-containing phospholipid measurements were purchased from Boehringer Mannheim (Germany) and external standards were not available for these assays.

Liver function tests were performed on serum samples by the Tufts Veterinary Diagnostic Laboratory, using an automated analyzer. These tests included serum lactate dehydrogenase (LDH), serum glutamic-oxaloacetic transaminase (SGOT), serum glutamic-pyruvate transaminase (SGPT), and serum bilirubin.

### Tissue Sampling and Analyses

The surface area of aorta occupied by atherosclerotic lesions was quantified by en face oil red O staining, using an approach modified from Palinski et al.<sup>24</sup> Mice were killed, after 12 weeks of diet, by ether inhalation. A catheter was inserted into the left ventricle and

the arterial tree was perfused with PBS (25 mL), then 10% buffered formaldehyde (40 mL, pH 7.4) at a pressure of 100 mm Hg. The entire aorta attached to the heart was dissected and placed overnight in formaldehyde. Using a stereomicroscope, the adventitial fat was dissected and the aorta was stained with oil red O as described by Nunnari et al.<sup>25</sup> After staining, the remaining adventitial fat was easily detected and was removed. The aorta was opened longitudinally, pinned en face on a black silicone-covered dish, and photographed while immersed in PBS. Slides were scanned into a Macintosh computer and the percent surface area occupied by oil red O-stained lesions was determined by using image analysis software (NIH Image). The aortic arch (1 mm above the aortic valve cusps to 2 mm below the ostium of the right subclavian artery), the descending thoracic aorta (extending to 1 mm above the ostium of the celiac artery), the abdominal aorta (including the bifurcation and 0.5 mm of the iliac arteries), and the total aorta were evaluated. After photography, portions of aorta that contained lesions were cross-sectioned

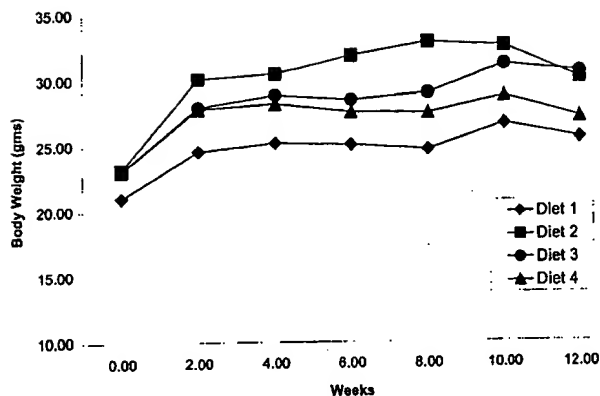


**Figure 1.** Body weights of LDLR<sup>-/-</sup> mice fed diets varying in fat, cholesterol, and cholate content. Mice were fed the diets described in Table 1 and were weighed every 2 weeks for 12 weeks. The data represent the mean weights for the 6 mice in each group at each time point.

and embedded in paraffin. Histological sections were prepared and stained with hematoxylin and eosin.

Liver slices, obtained from each animal at the time it was killed, were fixed in formalin, paraffin-embedded, and histological sections were stained with hematoxylin and eosin.

### Statistical Analysis

Food intake, body weight, and serum lipids were initially analyzed by ANOVA<sup>26</sup> followed by Fisher's PLSD<sup>26</sup> to calculate pairwise comparisons among treatment groups by using Statview 4.5 (Abacus Concepts, Inc).

## Results

### Body Weight

The mean body weight of mice fed each of the 4 diets for 12 weeks is shown in Figure 1. Mice fed the high-fat+0.5% cholesterol diet (diet 2) showed increased body weight ( $P<0.02$ ) compared with controls (diet 1) during weeks 2 through 10. This is a common observation in studies where rodents are provided a high-fat diet, which is more palatable, resulting in a slightly greater intake of diet (kcal). However, we did not attempt to measure food intake in this study, because mice were not individually housed and they typically waste significant amounts of food when provided ad libitum. Additional effort is necessary to accurately quantitate the amount of food consumed in murine studies. Those fed a high-fat diet with higher concentrations of cholesterol or supplemented with cholate did not exhibit a weight gain that was significantly different from controls.

### Lipid Analyses

The analyses of total serum cholesterol and triglyceride levels at 0, 6, and 12 weeks are shown in Table 2. A significant effect of diet on serum cholesterol was observed at 6 weeks ( $P<0.0009$ , ANOVA). Pairwise comparisons show that mice fed diet 1 (control diet) have significantly lower serum cholesterol than those fed the high-fat diets supplemented with 0.5% cholesterol (diet 2;  $P<0.02$ , PLSD), 1.25% cholesterol (diet 3;  $P<0.02$ , PLSD), or 1.25% cholesterol and cholate (diet 4;  $P<0.0001$ , PLSD). A statistically significant difference was not found between diet groups 2 and 3. However, the addition of cholate (diet 4) increased serum cholesterol compared with diets 1, 2, and 3 ( $P<0.009$ , for all comparisons; PLSD).

**TABLE 2.** Plasma Cholesterol and Triglycerides at Different Time Points

Diet	Cholesterol (mg/dL)		
	Week 0 (Baseline)	Week 6	Week 12
1 (10% fat)	104±18	97±21	124±49
2 (40% fat; 0.5% cholesterol)	133±51	327±56*	328±111
3 (40% fat; 1.25% cholesterol)	130±37	331±46*	597±131*
4 (40% fat; 1.25% cholesterol; 0.5% cholate)	129±59	598±71*†‡	761±208*†

Diet	Triglycerides (mg/dL)		
	Week 0 (Baseline)	Week 6	Week 12
1 (10% fat)	52±7	50±6	63±19
2 (40% fat; 0.5% cholesterol)	40±10	85±14	110±37
3 (40% fat; 1.25% cholesterol)	50±11	58±8	141±34
4 (40% fat; 1.25% cholesterol; 0.5% cholate)	41±10	74±10	80±37

Data represent mean±SEM values for nonfasting plasma cholesterol and triglycerides.

\* $P<0.02$  compared with diet group 1.

† $P<0.02$  compared with diet group 2.

‡ $P<0.02$  compared with diet group 3.

Similar results were observed at 12 weeks, although variation in serum cholesterol was greater ( $P<0.005$ , ANOVA). Pairwise comparisons at 12 weeks show that mice fed diet 1 (control diet) have lower serum cholesterol than those fed the high-fat diets supplemented with 0.5% cholesterol (diet 2;  $P<0.15$ , PLSD), 1.25% cholesterol (diet 3;  $P<0.007$ , PLSD), or 1.25% cholesterol and cholate (diet 4;  $P<0.001$ , PLSD). The addition of cholate (diet 4) increased serum cholesterol compared with those fed supplemental cholesterol without cholate ( $P<0.007$  versus diet 2 and  $P=0.31$  versus diet 3, both PLSD). Diets did not have any significant effect on serum triglyceride levels at 6 or 12 weeks.

The analysis of plasma lipoproteins by fast protein liquid chromatography gel-filtration chromatography after 12 weeks of diet is summarized in Figure 2. The extent of lipids recovered in Superose fractions was relatively uniform and comparable in all dietary groups. Percent recovery ranged from 83% to 87% for total cholesterol, 90% to 94% for choline-containing phospholipids, and 68% to 120% for triglycerides. The data revealed that elevated total cholesterol in dietary groups 2 through 4 was the result of increased VLDL and IDL/LDL lipoproteins (Figure 2). Levels of HDL lipoproteins varied inversely with VLDL and IDL/LDL. For each lipoprotein class, levels of free cholesterol and choline-containing phospholipids were as expected, and in different dietary groups their ratios were comparable. These ratios typically were between 1 and 2 for VLDL and IDL/LDL and  $<0.6$  for HDL (data not shown). There was no evidence for significant levels of lipoprotein X and HDL-E particles.

### Development of Atherosclerotic Lesions in the Aorta

En face oil red O staining revealed minimal atherosclerotic lesion formation in mice fed diet 1 (control diet) for 12 weeks. In contrast, lesions were readily detected in each of the groups fed cholesterol-containing diets (Figure 3 and



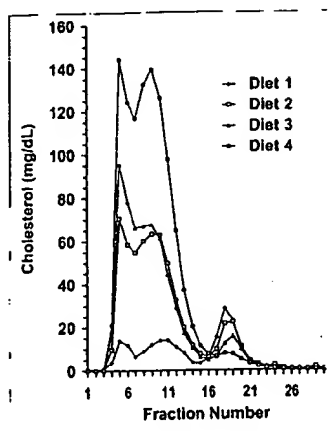


**Figure 2.** Plasma cholesterol profiles of LDLR<sup>-/-</sup> mice fed diets varying in fat, cholesterol, and cholate content. Mice were fed the diets described in Table 1 for 12 weeks, when blood samples were obtained from each dietary group and plasma was pooled. Plasma was subjected to fast protein liquid chromatography gel-filtration chromatography as described in Methods. Lipoproteins were measured in each fraction and the total cholesterol levels are plotted.

Table 3). The percent surface area of the entire aorta involved by lesions was significantly greater in mice fed diets 2, 3, and 4, compared with controls (diet 1), as well as in mice fed diet 4 compared with group 2. The interpretation was similar

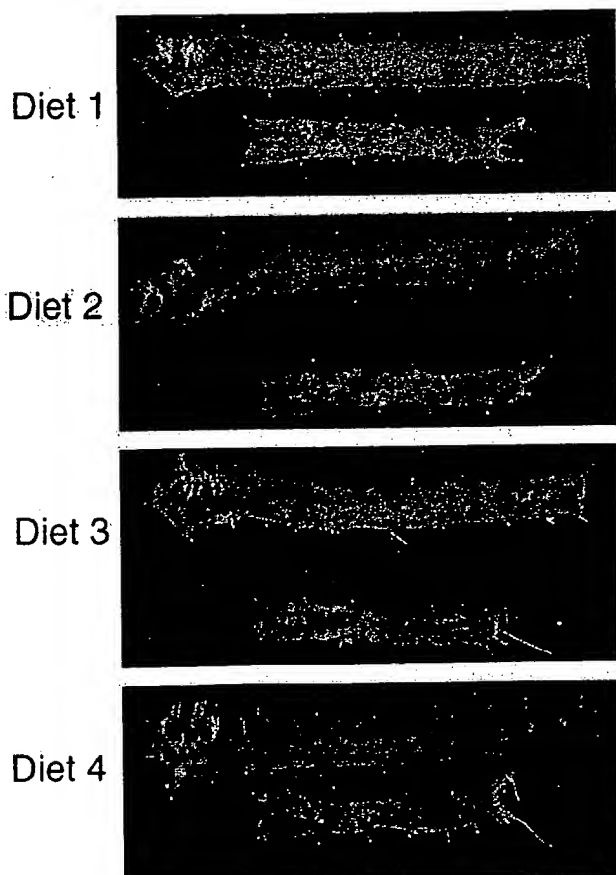


**Figure 3.** Oil red O-stained atherosclerotic lesions in aortas of LDLR<sup>-/-</sup> mice fed diets varying in fat, cholesterol, and cholate content. Mice were killed after being fed defined diets described in Table 1 for 12 weeks. Aortas were prepared and stained with oil red O as described in Methods. One representative aorta from a total of 6 in each of the 4 dietary groups is shown.

when the arch, thoracic, and abdominal regions were evaluated individually (Table 3). The anatomic distribution of atherosclerotic lesions was identical in dietary groups 2, 3, and 4 (Figure 3). Lesion-predisposed sites included the aortic root, the lesser curvature of the arch, and near the orifice of the brachiocephalic, intercostal, celiac, superior mesenteric, and renal arteries.

Histological examination revealed a similar morphology and cellularity in atheromas from each of the groups fed cholesterol-containing diets (Figure 4). The lesions had characteristic intimal thickening with foam cells, and apparent smooth muscle cell infiltration.

### Liver Function Tests and Histology

To determine if consumption of a cholate-containing diet for 12 weeks led to liver damage, serum liver enzyme levels and liver-derived products were measured and histological sections of liver were evaluated. The liver function test results were comparable between all dietary groups, suggesting that the liver parenchyma and biliary system were not seriously damaged after 12 weeks of feeding. Of particular interest, mice in group 4 (fed 1.25% cholesterol with cholate) did not have a significant elevation in serum bilirubin, alkaline phosphatase,  $\gamma$ -glutamyltransferase (GGT), alanine aminotransferase (ALT), or aspartate aminotransferase (AST), or decrease in albumin when compared with group 3 (also fed 1.25% cholesterol, but without cholate) (data not shown). Hematoxylin and eosin sections of liver revealed substantial steatosis in dietary groups 3 and 4, with greater fatty changes observed in the cholate-supplemented group. There was no histological evidence of hepatocyte necrosis, apoptosis, inflammation, fibrosis, or cirrhosis at the time point examined. However, all cholate-fed mice had stones in the gallbladder, whereas none were observed in mice fed cholate-free diets.

### Discussion

This study demonstrates that nutritionally defined semipurified diets are appropriate for the study of diet-genetic interactions in murine atherosclerosis. They offer several advantages compared with the commonly used chow-based diets, including reproducibility and uniformity of content, and the ability to precisely alter composition. Dietary lipid saturation and concentration are frequently the focus of hypotheses in experimental atherogenesis as a consequence of the enormous body of clinical and epidemiological data suggesting their importance in vascular disease. A semipurified diet allows the investigator to alter lipid concentration by substitution for an equivalent amount of energy from carbohydrate, to maintain a constant ratio of all other nutrients to energy in the control and high-fat diets. This is impossible to achieve when adding fat by dilution to a chow diet. The dilution technique confuses the interpretation of results. Indeed many investigators using diets prepared by dilution of chow with fat are seemingly unaware of the fact that mice consuming an identical amount of energy from the high-fat diet are also exposed to a significantly lower amount of all components of the chow, such as protein, all vitamins and minerals, and biologically active but nonnutrient factors such as fiber and phytochemicals, including those with antioxidant properties. The role of specific vitamin and mineral deficiencies or excess can be precisely examined by using semipurified diets

**TABLE 3. Atherosclerotic Lesion Formation in Mouse Aortas After 12 Weeks of Diet**

Dietary Group (n=6)	Percentages of Aortic Surface Area Involved by Oil Red O-Stained Lesions			
	Total	Arch	Thoracic	Abdominal
1 (control)	0.16±0.32	0.10±0.19	0.08±0.17	0.67±0.94
2 (0.5% cholesterol)	7.02±3.97‡	24.96±12.09§	2.80±2.35*	5.45±4.17*
3 (1.25% cholesterol)	8.27±3.59§	31.66±11.93§	3.57±3.50*	4.10±2.90*
4 (1.25% cholesterol+cholate)	12.79±4.80§	34.62±15.24§	10.30±3.63§	5.69±5.15*

\**P*<0.05; ‡*P*<0.003; §*P*<0.001, compared with group 1.||*P*<0.05, compared with group 2.

because their contents can be individually manipulated in the AIN vitamin and mineral formulations.<sup>18,19</sup> The use of standardized formulations will allow investigators to compare data derived from different laboratories without the concern that unquantifiable differences in the chow diets used contributed to the reported results.

The semipurified formulation can be provided as a liquid or in powdered form. The liquid diet allows the investigator to obtain more precise estimates of intake because mice typically disperse much of a solid diet in a cage. Liquid diets also facilitate studies of the effects of alcohol intake and are ideal for macrophage colony-stimulating factor-deficient mice, which exhibit osteopetrosis and have no teeth, making it impossible to consume a pelleted diet.<sup>27-29</sup>

The effects of dietary cholate on atherosclerosis susceptibility in genetically engineered mice should be reevaluated based on our results. Mice are very resistant to the development of atheromatous lesions in the arterial tree. Historically, investigators interested in genetic differences between murine strains in susceptibility to fatty streak formation devised diets

composed of chow diluted with saturated fat and supplemented with cholesterol and cholate.<sup>10</sup> This diet led to the discovery that the C57BL/6 strain was more susceptible to the formation of fatty streaks in the aortic root.<sup>9</sup> Although this dietary approach lacks many characteristics desired by experimental nutritionists, many investigators have subsequently used it in newer models of atherosclerosis developed with transgenic and gene-deletion technology. However, the potential hepatotoxic effects of cholate<sup>11,30,31</sup> have raised concerns that LDLR<sup>-/-</sup> mice fed such diets are not useful for modeling human disease.<sup>32</sup> Our study clearly shows that cholate is not required for the development of atherosclerotic lesions throughout the aorta in the LDLR<sup>-/-</sup> strain, and therefore cholate is unnecessary as a dietary additive in studies of atherogenesis in these mice. Subsequent experiments demonstrated a rapid onset of lesion formation, in that most mice fed diet 3 for 4 weeks had early lesions in the lesser curvature of the aortic arch (data not shown). Compared with mice fed diet 3 (high fat, 1.25% cholesterol), the inclusion of cholate (0.5%, wt/wt) in diet 4 caused a further increase in plasma lipids and a trend toward a greater area of the aortic surface involved by atheromatous lesions. This trend was not statistically significant because of high inter-animal variability. Cholate-fed mice also developed gallstones over the 12 weeks of investigation. It is our opinion that dietary cholate is unnecessary and perhaps a liability in studies of atherogenesis in the LDLR<sup>-/-</sup> mouse.

Traditionally, cholesterol supplements of ≥1% have been used in murine and rabbit studies to enhance hyperlipidemia and the rate of lesion formation, thereby shortening the duration of studies. Diets high in cholesterol and fat may cause time- and dose-dependent hepatotoxicity, therefore lowering cholesterol concentration, may be advantageous. Our study begins to address this issue. We demonstrated that the lesion area after 12 weeks of consuming 0.5% cholesterol (diet 2) was essentially indistinguishable from mice fed cholesterol at 1.25% (diet 3). At 12 weeks of feeding, there was a trend toward higher serum cholesterol and triglycerides in diet group 3. Perhaps this would lead to accelerated lesion progression and differences in lesion area would become significant in studies of longer duration. Cholesterol levels <0.5% can induce lesions in LDLR<sup>-/-</sup> mice. Palinski et al<sup>14</sup> fed LDLR<sup>-/-</sup> mice for 6 months with a diet containing 21% fat and 0.15% cholesterol (without cholate) and observed extensive atherosclerotic lesion formation throughout the aorta. In evaluating aortas of retired LDLR<sup>-/-</sup> breeders >1 year of age, we observed lesions in the aortic arch in most (unpublished data, 1998). This indicates that LDLR<sup>-/-</sup>

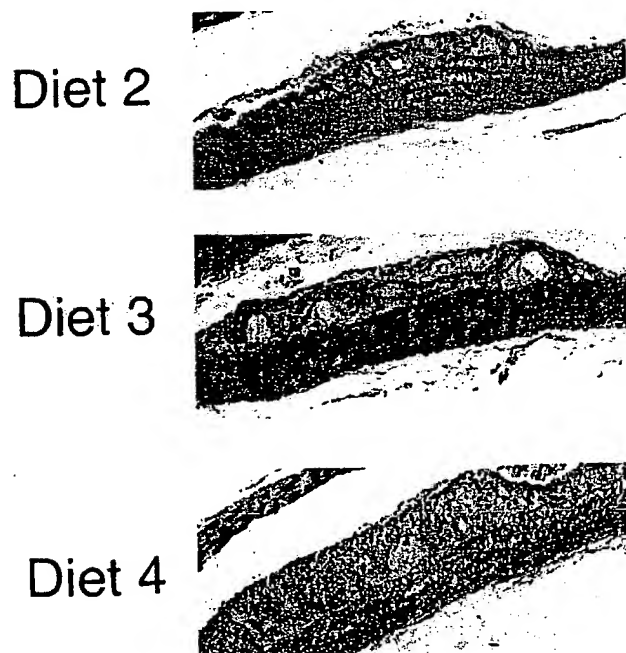


**Figure 4.** Histological appearance of aortic atherosclerotic lesions in LDLR<sup>-/-</sup> mice fed diets varying in fat, cholesterol, and cholate content. Hematoxylin and eosin-stained sections of formalin-fixed lesions from the aortas described in Figure 3 are shown.

mice can develop lesions spontaneously even when fed a regular laboratory chow; however, their rate of formation is very slow, as lesions generally are not found in mice <6 months old.

The existing literature on newer models of murine atherogenesis does not allow investigators to evaluate the role of dietary lipid concentration or the source of the lipid on lesion formation. In our study, the lipid content of diet 1 (control diet) was 10% of total energy (4.3% by weight), whereas in diets 2, 3, and 4 it was 40% (20% by weight). We included soy oil at 5.5% of total energy to ensure that a supply of essential fatty acids was constant in all diets. We then manipulated cocoa butter as the variable lipid. We recommend that future investigators maintain a constant baseline supply of essential fatty acids in the diet unless they are particularly interested in this as a variable. It is possible that investigators manipulating the fat source could naively prepare or purchase a saturated fat-enriched diet deficient in essential fatty acids, which could complicate the interpretation of murine studies. Furthermore, essential fatty acid deficiency is not observed in humans except in situations of several metabolic or gastrointestinal diseases. Humans consuming diets rich in saturated fat and cholesterol easily achieve adequate intake of essential fatty acids. Therefore, murine models will more closely mimic human dietary patterns if essential fatty acid intake is adequate.

### Acknowledgments

This work was supported by NIH grant 1 P50 HL56985 (A.H.L., P.L.), NIH grant RO1 CA 72482-01A1 (S.K.C.), Heart and Stroke Foundation of Ontario grant T-3032 (P.W.C.), and Heart and Stroke Foundation of Ontario grant T-3588 and an Established Investigatorship from the American Heart Association (M.I.C.).

### References

- Plump AS, Smith JD, Hayek T, Aalto-Setälä K, Walsh A, Verstuyft JG, Rubin EM, Breslow JL. Severe hypercholesterolemia and atherosclerosis in apolipoprotein E-deficient mice created by homologous recombination in ES cells. *Cell*. 1992;71:343-353.
- Zhang SH, Reddick RL, Piedrahita JA, Maeda N. Spontaneous hypercholesterolemia and arterial lesions in mice lacking apolipoprotein E. *Science*. 1992;258:468-471.
- Ishibashi S, Brown MS, Goldstein JL, Gerard RD, Hammer RE, Herz J. Hypercholesterolemia in low density lipoprotein receptor knockout mice and its reversal by adenovirus-mediated gene delivery. *J Clin Invest*. 1993;92:883-893.
- Callow MJ, Stoltzfus LJ, Lawn RM, Rubin EM. Expression of human apolipoprotein B and assembly of lipoprotein(a) in transgenic mice. *Proc Natl Acad Sci U S A*. 1994;91:2130-2134.
- McCormick SP, Linton MF, Hobbs HH, Taylor S, Curtiss LK, Young SG. Expression of human apolipoprotein B90 in transgenic mice: demonstration that apolipoprotein B90 lacks the structural requirements to form lipoprotein. *J Biol Chem*. 1994;269:24284-24289.
- Nakashima Y, Plump AS, Raines EW, Breslow JL, Ross R. ApoE-deficient mice develop lesions of all phases of atherosclerosis throughout the arterial tree. *Arterioscler Thromb*. 1994;14:133-140.
- Reddick RL, Zhang SH, Maeda N. Atherosclerosis in mice lacking apo E: evaluation of lesion development and progression. *Arterioscler Thromb*. 1994;14:141-147.
- Ishibashi S, Goldstein JL, Brown MS, Herz J, Burns DK. Massive xanthomatosis and atherosclerosis in cholesterol-fed low density lipoprotein receptor-negative mice. *J Clin Invest*. 1994;93:1885-1893.
- Paigen B, Morrow A, Brandon C, Mitchell D, Holmes P. Variation in susceptibility to atherosclerosis among inbred strains of mice. *Atherosclerosis*. 1985;57:65-73.
- Paigen B, Morrow A, Holmes PA, Mitchell D, Williams RA. Quantitative assessment of atherosclerotic lesions in mice. *Atherosclerosis*. 1987;68:231-240.
- Nishina PM, Verstuyft J, Paigen B. Synthetic low and high fat diets for the study of atherosclerosis in the mouse. *J Lipid Res*. 1990;31:859-869.
- Vesselinovitch D, Wissler RW. Experimental production of atherosclerosis in mice. 2. Effects of atherogenic and high-fat diets on vascular changes in chronically and acutely irradiated mice. *J Atheroscler Res*. 1968;8:497-523.
- Vesselinovitch D, Wissler RW, Doull J. Experimental production of atherosclerosis in mice. 1. Effect of various synthetic diets and radiation on survival time, food consumption and body weight in mice. *J Atheroscler Res*. 1968;8:483-495.
- Palinski W, Tangirala RK, Miller E, Young SG, Witztum JL. Increased autoantibody titers against epitopes of oxidized LDL in LDL receptor-deficient mice with increased atherosclerosis. *Arterioscler Thromb Vasc Biol*. 1995;15:1569-1576.
- Lichtman AH, Clinton SK, Iiyama K, Henault L, Libby P, Cybulsky MI. Comparative effects of precisely defined semipurified diets supplemented with lipid, cholesterol, and sodium cholate on serum lipids and aortic atherosclerosis in LDL receptor-deficient (LDLR<sup>-/-</sup>) mice. *FASEB J*. 1997;11:A154. Abstract.
- Reeves PG, Nielsen FH, Fahey GC Jr. AIN-93 purified diets for laboratory rodents: final report of the American Institute of Nutrition ad hoc writing committee on the reformulation of the AIN-76A rodent diet. *J Nutr*. 1993;123:1939-1951.
- Rao GN. Rodent diets for carcinogenesis studies. *J Nutr*. 1988;118:929-931.
- American Institute of Nutrition. AIN report of the AIN ad hoc committee on standards for nutritional studies. *J Nutr*. 1977;107:1340-1348.
- American Institute of Nutrition. AIN second report of the ad hoc committee on standards for nutritional studies. *J Nutr*. 1980;110:1726.
- Rao GN, Knapka JJ. Contaminant and nutrient concentrations of natural ingredient rat and mouse diet used in chemical toxicology studies. *Fundam Appl Toxicol*. 1987;9:329-338.
- Oller WL, Kendall DC, Greenman DL. Variability of selected nutrients and contaminants monitored in rodent diets: a 6-year study. *J Toxicol Environ Health*. 1989;27:47-56.
- Fowler GG. Toxicology of nisin. *Food Cosmet Toxicol*. 1973;11:351-352.
- van Gent T, van Tol A. Automated gel permeation chromatography of plasma lipoproteins by preparative fast protein liquid chromatography. *J Chromatogr*. 1990;525:433-441.
- Palinski W, Ord VA, Plump AS, Breslow JL, Steinberg D, Witztum JL. ApoE-deficient mice are a model of lipoprotein oxidation in atherosclerosis: demonstration of oxidation-specific epitopes in lesions and high titers of autoantibodies to malondialdehyde-lysine in serum. *Arterioscler Thromb*. 1994;14:605-616.
- Nunnari JJ, Zand T, Joris I, Majno G. Quantitation of oil red O staining of the aorta in hypercholesterolemic rats. *Exp Mol Pathol*. 1989;51:1-8.
- Steel RGD, Torrie JH. *Principals and Procedures of Statistics*. New York, NY: McGraw-Hill Book Co, Inc; 1980.
- Clinton SK, Underwood R, Hayes L, Sherman ML, Kufe DW, Libby P. Macrophage colony-stimulating factor gene expression in vascular cells and in experimental and human atherosclerosis. *Am J Pathol*. 1992;140:301-316.
- Qiao JH, Tripathi J, Mishra NK, Cai Y, Tripathi S, Wang XP, Imes S, Fishbein MC, Clinton SK, Libby P, Lusis AJ, Rajavashisth TB. Role of macrophage colony-stimulating factor in atherosclerosis: studies of osteopetrotic mice. *Am J Pathol*. 1997;150:1687-1699.
- Kodama H, Yamasaki A, Nose M, Niida S, Ohgame Y, Abe M, Kumegawa M, Suda T. Congenital osteoclast deficiency in osteopetrotic (op/op) mice is cured by injections of macrophage colony-stimulating factor. *J Exp Med*. 1991;173:269-272.
- Nishina PM, Wang J, Toyofuku W, Kuypers FA, Ishida BY, Paigen B. Atherosclerosis and plasma and liver lipids in nine inbred strains of mice. *Lipids*. 1993;28:599-605.
- Delzenne NM, Calderon PB, Taper HS, Roberfroid MB. Comparative hepatotoxicity of cholic acid, deoxycholic acid and lithocholic acid in the rat: in vivo and in vitro studies. *Toxicol Lett*. 1992;61:291-304.
- Breslow JL. Mouse models of atherosclerosis. *Science*. 1996;272:685-688.

183.9

# **MUCOSAL ADMINISTRATION OF HSP 65 DECREASES ATHEROSCLEROSIS AND INFLAMMATION IN THE AORTIC ARCH OF LDL RECEPTOR DEFICIENT MICE**

R. Maron, G.K. Sukhova, A.M. Faria, E. Hoffman, F. Mach, P. Libby, and H.L. Weiner. Center for Neurologic Diseases and Vascular Medicine and Atherosclerosis Unit, Brigham and Women's Hospital, Harvard Medical School, Boston, MA.

Increasing evidence supports the involvement of inflammation and immunity in atherogenesis, as well as the role of autoimmunity to heat shock proteins in the progression of atherosclerosis. Mucosal administration of autoantigens decreases organ specific inflammation and disease in animal models (diabetes, arthritis and EAE) and is being tested in human clinical trials. We examined the effect of nasal or oral administration of HSP65 on atherosclerotic lesion formation in mice lacking the receptor for low-density lipoprotein maintained on a high cholesterol diet. Animals were nasally treated with 0.8ug HSP 65 three times every second day or orally treated with 8 ug HSP 65 on 5 consecutive days. A high cholesterol diet was started after the last treatment and mice were mucosally treated once/week for 8 weeks at which time pathologic analysis was performed. In nasally treated animals, we found a reduction in macrophage-positive area in the aortic arch (3.44% vs. 13.03% in controls,  $p = 0.006$ ) as well as a reduced number of T-cells ( $p = 0.02$ ). There was also a decrease in the size of atherosclerotic plaques. A similar trend was observed in orally treated animals but was not significant. Mice nasally treated with HSP also gained significantly less weight than fed or control treated mice. Our results suggest that nasal treatment with HSP reduces the inflammatory process associated with atherosclerosis and may provide a new treatment approach.

183.11

# **Phase I Clinical Trial of Orally Delivered Hepatitis B Surface Antigen Expressed in Potato Tubers.**

<sup>1</sup>Yasmin Thanavala, <sup>1</sup>Adrienne Scott, <sup>1</sup>Srabani Pal, <sup>1</sup>Martin Mahoney and <sup>2</sup>Charles Arntzen. <sup>1</sup>Roswell Park Cancer Institute, Buffalo, NY; <sup>2</sup>Boyce Thompson Institute for Plant Research, Ithaca, NY.

A randomized, doubleblind, placebo-controlled phase I clinical trial has been completed at Roswell Park Cancer Institute to evaluate the safety, tolerability and immunogenicity of orally delivered HBsAg expressed as a protein in transgenic potato tubers. Forty-five healthy healthcare workers with a history of known positive anti-HBc

183.7

**CHOLERA TOXIN B SUBUNIT AS MUCOSAL CARRIER-DELIVERY SYSTEM FOR SPECIFIC IMMUNOTHERAPY.**C. Czerkinsky<sup>1</sup>, P. Anjuere<sup>2</sup>, C. Rask<sup>2</sup>, J. Holmgren<sup>2</sup>. <sup>1</sup>INSERM Unit 364, Nice, France, <sup>2</sup>Dept of Medical Microbiology, University of Göteborg, Sweden.

Over the past few years attention has been devoted to the development of effective formulations that could prevent or halt untoward immune responses, such as those underlying autoimmune disorders, allergic reactions, and by and large chronic inflammation. Studies initiated in this laboratory have documented the efficiency of cholera B subunit as a powerful mucosal immunomodulating and carrier-delivery system agent for optimal induction of immune tolerance in various preclinical models of autoimmune diseases. More recently, this system has proven to be especially effective for suppressing type I allergic responses and also for suppressing Th2-driven immunopathological responses to persistent infectious microorganisms. The mechanisms of action of this system and in particular the role of mucosal dendritic cells in the induction of such form of suppression is currently under study. These studies will be presented and their implications will be discussed. (supported by INSERM, Swedish Medical Research Council, European Communities EC Biotech IV NovoNordisk, Triotol)

183.9

**MUCOSAL ADMINISTRATION OF HSP 65 DECREASES ATHEROSCLEROSIS AND INFLAMMATION IN THE AORTIC ARCH OF LDL RECEPTOR DEFICIENT MICE**

R. Maron, G.K. Sakthi, A.M. Faru, E. Hoffman, E. Mach, P. Libby, and H.L. Widmer. Center for Neurologic Diseases and Vascular Medicine and Atherosclerosis Unit, Brigham and Women's Hospital, Harvard Medical School, Boston, MA.

Increasing evidence supports the involvement of inflammation and immunity in atherogenesis, as well as the role of autoimmunity to heat shock proteins in the progression of atherosclerosis. Mucosal administration of autoantigens decreases organ specific inflammation and disease in animal models (diabetes, arthritis and EAE) and is being tested in human clinical trials. We examined the effect of nasal or oral administration of HSP65 on atherosclerotic lesion formation in mice lacking the receptor for low-density lipoprotein maintained on a high cholesterol diet. Animals were nasally treated with 0.5µg HSP 65 three times every second day or orally treated with 5 µg HSP 65 on 5 consecutive days. A high cholesterol diet was started after the last treatment and mice were mucosally treated once/week for 8 weeks at which time pathologic analysis was performed. In nasally treated animals, we found a reduction in macrophage-positive area in the aortic arch (3.44% vs. 13.05% in controls,  $p = 0.006$ ) as well as a reduced number of T-cells ( $p = 0.02$ ). There was also a decrease in the size of atherosclerotic plaques. A similar trend was observed in orally treated animals but was not significant. Mice nasally treated with HSP also gained significantly less weight than fed or control treated mice. Our results suggest that nasal treatment with HSP reduces the inflammatory process associated with atherosclerosis and may provide a new treatment approach.

183.11

**Phase I Clinical Trial of Orally Delivered Hepatitis B Surface Antigen Expressed in Potato Tubers.**Yasmin Thasrala, Adrienne Scott, Graham Pal, Martin Mahoney and Charles Arntson. Roswell Park Cancer Institute, Buffalo, NY; <sup>2</sup>Boyer Thompson Institute for Plant Research, Ithaca, NY.

A randomized, double-blind, placebo-controlled phase I clinical trial has been completed at Roswell Park Cancer Institute to evaluate the safety, tolerability and immunogenicity of orally delivered HBsAg expressed as a protein in transgenic potatoes. Forty-five healthy healthcare workers with a history of known positive response to a primary series of recombinant hepatitis B vaccine (meeting all inclusion criteria and none of the exclusion criteria) were recruited for the trial. The 45 volunteers were randomized into one of three groups. Each group ate either vaccinated or placebo potato at defined intervals. Study subjects were randomized by use of a centrally generated block randomization list. This list was provided to the study pharmacist who was unblinded to study group assignments. All other study personnel and the study subjects remained blinded through the completion of the study. Subjects had baseline chemistry, hematology and anti-HBs antibody determinations performed before their first dose of vaccine and at predetermined intervals throughout the trial. As a phase I study, this was primarily an assessment of the relative safety and immunogenicity of transgenic HBsAg expressing potatoes.

183.8

**MYELIN-SPECIFIC TOLERANCE ATTENUATES DISEASE SEVERITY IN A VIRALLY INDUCED MODEL OF MULTIPLE SCLEROSIS.** Katherine L. Nayak, Lou Matti, and Stephen D. Miller. Northwestern University Medical School, Chicago, IL, 60611, and <sup>2</sup>Alexion Pharmaceuticals, New Haven, CT, 06511.

Theiler's Murine Encephalomyelitis Virus-induced Demyelinating Disease (TMEV-IDO) is a relevant model for the autoimmune disease multiple sclerosis (MS). Approximately 30 days after intracerebral inoculation of SJL mice with TMEV, clinical disease signs arise, characterized by spastic paralysis, chronic disease progression, and mononuclear cell infiltrate into the CNS. While initial demyelination in TMEV-IDO is mediated by virus-specific CD4<sup>+</sup> T cells, reactivity to myelin epitopes can be detected in TMEV infected mice 55 days post infection, demonstrating autoimmune specificity in this virally induced disease. Administration of the fusion protein MP4, a fusion of myelin proteins MBP and PLP, to TMEV infected SJL mice 40 days post infection attenuates disease severity in MP4 treated animals compared to controls, and also decreases DTH reactivity to myelin peptides, indicating anti-myelin responses are centrally involved in the chronic progressive nature of TMEV-induced paralysis. Additionally, T cells isolated from the spinal cords of TMEV infected animals proliferate and secrete IFN $\gamma$  in response to PLP139-151 peptide stimulation *in vitro*. Both isolation of myelin specific cells from the CNS of TMEV infected animals, and myelin specific tolerance in TMEV-IDO indicate anti-myelin T cell responses contribute to disease severity in this virally induced model of MS, and support the idea of antigen specific tolerance as an effective treatment of ongoing autoimmune disease. (Supported by NIH grant NS23349)

183.10

**HIGH DOSE -ANTIGEN FEEDING INDUCES CD4 T CELLS WITH SUPPRESSOR ACTIVITY IN THE LIVER.**

T. WATANABE, Y. WAKATSUKI, M. YOSHIDA, T. ITOH, T. ISHII, T. CHIBA, and T. KITA. Dept. of Clinical and Bio-Regulatory Science, Kyoto Univ. Grad. Sch. of Med., Kyoto 606-8507, Japan.

Oral feeding of low or high dose-antigens (Ag) induces Ag-specific immuno-suppression in subsequent systemic challenge with the same Ag. Since a part of Ag fed at high dose should reach to the liver as an immunogenic form, we examined the possibility that Ag-specific T cells are activated by high dose-Ag feeding. OVA-TCR transgenic mice were fed 100 mg or 1 mg of OVA, or PBS every other day for five times and then CD4 T cells were purified from Peyer's patch, spleen, and liver. Only intrasplenic CD4 T cells (IHLs) from high dose Ag-fed mice suppressed both Ag-specific DTH and antibody responses when adoptively transferred to naive Balb/c mice. Upon Ag-stimulation *in vivo*, the secretion of IL-10, TGF- $\beta$ , and especially IL-4 by IHLs from Ag-fed mice were increased in an Ag-dose dependent manner. In contrast, IL-2 secretion and proliferative responses by these T cells were decreased. In addition, these IHLs from Ag-fed mice inhibited Ag-specific proliferation of naive splenic CD4 T cells. FACS analysis revealed decreases in the population of Ag-specific CD4 T cells in the liver by Ag-feeding, associated with the up-regulation of FasL expression, suggesting that clonal deletion was induced in the liver. Naive splenic CD4 T cells cultured with OVA presented by liver-derived APCs showed a similar profile of cytokine production to that of IHLs. Taken together, these data suggest that high dose-Ag feeding induces CD4 T cells with suppressor activity in the liver. Not only clonal deletion but also active suppression is considered to be induced in the liver after high dose-Ag feeding.

183.12

**ORAL IMMUNIZATION BY FOOD IS LESS EFFECTIVE THAN INTRAGASTRIC IMMUNIZATION**

T.G.M. Leuninger and L.A.Th. Hilgers. (SPON: W.J.A. Boorman). DLO-Institute for Animal Science and Health, P.O.Box 65, 8200 AB, Lelystad, The Netherlands

The feasibility of edible vaccines was studied by oral immunization of mice with chicken ovalbumin (OVA) mixed with standard food. Other mice were immunized with a similar dose of OVA via intragastric immunization. Intragastric immunization elicited 20-fold higher numbers of anti-OVA IgA and 34-fold higher numbers of anti-OVA IgG producing cells in the lamina propria of the gut than food immunization. Furthermore, intragastric immunization elicited a 20-fold higher anti-OVA IgG response in serum and a 2-fold higher anti-OVA IgA response in faeces than food immunization. The addition of the *Vibrio cholerae* toxin to food did not enhance the immune response. Possible explanations for the differences between these immunization routes will be discussed. We concluded that intragastric immunization is merely limited indicative for the effectiveness of edible vaccines.

# Chronic treatment with nitric oxide-releasing aspirin reduces plasma low-density lipoprotein oxidation and oxidative stress, arterial oxidation-specific epitopes, and atherogenesis in hypercholesterolemic mice

Claudio Napoli<sup>1,2</sup>, Eric Ackah<sup>3</sup>, Filomena de Nigris<sup>1,†</sup>, Piero Del Soldato<sup>1</sup>, Francesco P. D'Armiento<sup>4</sup>, Ettore Crimi<sup>1</sup>, Mario Condorelli<sup>1</sup>, and William C. Sessa<sup>5</sup>

<sup>1</sup>Departments of Medicine and Human Pathology, School of Medicine, Federico II University of Naples, 80131 Naples, Italy; <sup>2</sup>Department of Medicine-0682, University of California at San Diego, La Jolla, CA 92093; <sup>3</sup>Department of Pharmacology and Molecular Cardiology Program, Boyer Center for Molecular Medicine, Yale University School of Medicine, New Haven, CT 06536; <sup>4</sup>NicOx, 06906 Sophia Antipolis, France; and <sup>5</sup>Department of Anesthesiology, University of Novara, 28100 Novara, Italy

Edited by Louis J. Ignarro, University of California, Los Angeles School of Medicine, Los Angeles, CA, and approved July 8, 2002 (received for review April 23, 2002)

The effects of chronic treatment with nitric oxide-containing aspirin (NO-aspirin, NCX-4016) in comparison with regular aspirin or placebo on the development of a chronic disease such as atherosclerosis were investigated in hypercholesterolemic low-density lipoprotein (LDL)-receptor-deficient mice. Male mice were assigned randomly to receive in a volume of 10 ml/kg either placebo ( $n = 10$ ), 30 mg/kg/day NO-aspirin ( $n = 10$ ), or 18 mg/kg/day of regular aspirin ( $n = 10$ ). After 12 weeks of treatment, the computer-assisted imaging analysis revealed that NO-aspirin reduced the aortic cumulative lesion area by  $39.8 \pm 12.3\%$  compared with that of the placebo ( $P < 0.001$ ). Regular aspirin did not reduce significantly aortic lesions ( $-5.1 \pm 2.3\%$ ) compared with the placebo [ $P = 0.867$ , not significant (NS)]. Furthermore, NO-aspirin reduced significantly plasma LDL oxidation compared with aspirin and placebo, as shown by the significant reduction of malondialdehyde content ( $P < 0.001$ ) as well as by the prolongation of lag-time ( $P < 0.01$ ). Similarly, systemic oxidative stress, measured by plasma isoprostanes, was significantly reduced by treatment with NCX-4016 ( $P < 0.05$ ). More importantly, mice treated with NO-aspirin revealed by immunohistochemical analysis of aortic serial sections a significant decrease in the intimal presence of oxidation-specific epitopes of oxLDL (E06 monoclonal antibody,  $P < 0.01$ ), and macrophages-derived foam cells (F4/80 monoclonal antibody,  $P < 0.05$ ), compared with placebo or aspirin. These data indicate that enhanced NO release by chronic treatment with the NO-containing aspirin has antiatherosclerotic and antioxidant effects in the arterial wall of hypercholesterolemic mice.

atherosclerosis | LDL-receptor-deficient mice

Endothelial dysfunction has been shown in the presence of atherosclerosis (ref. 1 and reviewed in refs. 2–4). Several lines of evidence indicate that restoring nitric oxide (NO)-mediated signaling pathways in atherosclerotic arteries may decrease the disease (2–4). The essential findings are that the biochemical properties of NO allow its exploitation as both a cell signaling molecule through its interaction with redox centers in heme proteins and a rapid reaction with other biologically relevant radical species. The direct reaction of NO with radicals can have, at least in part, antioxidant effects. In arterial cells, the antioxidant properties of NO can be greatly amplified by the activation of signal transduction pathways that lead to the increased synthesis of endogenous antioxidants or down-regulate responses to pro-inflammatory stimuli. Studies in humans and in animal models have shown that low-density lipoprotein (LDL) oxidation may play a pivotal role in the pathogenesis of atherosclerosis (reviewed in refs. 5, 6). Recent data indicate that LDL oxidation may promote *per se* activation of several signaling

pathways and transcription factors in human coronary arteries (7–9). Several of these pathways are reduced by concomitant administration of vitamin E (7, 9). Thus, compounds with antioxidant properties may reduce downstream effects induced by LDL oxidation in the arterial wall, and this phenomenon could retard the progression of atherosclerosis.

In preliminary experiments, we evaluated the antioxidant properties *in vitro* of several nitro-compounds and found that some of these agents had antioxidant properties. In this study, we used male LDL-receptor-deficient mice (10, 11) to address the effects of a NO-containing aspirin derivative (NCX-4016) on the development of a chronic disease such as atherosclerosis and on plasma LDL oxidation and systemic oxidative stress. NO-releasing aspirin (NCX-4016) is a drug well characterized *in vitro* and *in vivo* (reviewed in ref. 12). Hypercholesterolemic mice develop hypercholesterolemia on a cholesterol mouse chow diet (10, 13) and extensive atherosclerosis, with lesions progressing from lipid-laden fatty streaks to advanced lesions (10, 11, 13–15). By using this model, we investigated the chronic effects of treatment with NO-aspirin or regular aspirin on aortic lesion development, plasma LDL oxidation, and oxidative stress, as well as oxidation-specific epitopes of LDL in the arterial wall.

## Materials and Methods

**Drugs and Experimental Protocol.** The experiments conformed to the Guide for the Care and Use of Laboratory Animals (National Institutes of Health Publication No. 85–23, revised 1996) and the Guidelines of the American Heart Association. The experiments described here were carried out on male LDL-receptor-deficient mice of 18 weeks on high-cholesterol and cholate-free diet (21% by weight fat, 0.15% by weight cholesterol, and 19.5% by weight casein; no. 8137, Teklad, Madison, WI). LDL-receptor-deficient mice crossed with C57BL/6J mice for 10 generations, develop only “moderately” elevated plasma cholesterol levels (250–300 mg/dl) when fed regular mouse chow (10, 11). However, high cholesterol levels are easily achieved by enriched-cholesterol diets that induce extensive atherosclerosis throughout the arterial tree (10, 11). We selected only male mice to avoid gender-related differences (10). Mice were assigned randomly to be treated for 12 weeks with 30 mg/kg day of NCX-4016 (a generous gift from NicOx;  $n = 10$ , 30-mg compound contains 18 mg of aspirin) or 18 mg/kg/day

This paper was submitted directly (Track II) to the PNAS office.

Abbreviation: LDL, low-density lipoprotein.

<sup>†</sup>To whom reprint requests should be addressed. E-mail: claudnap@tin.it or cnapoli@ucsd.edu.



of aspirin (Sigma;  $n = 10$ ), or placebo (saline vehicle) given by gavage. These drug doses were chosen on the basis of previous studies *in vivo* (12, 16, 17) and did not affect blood pressure in mice measured by tail cuff ( $P = \text{NS}$ , not shown). At the end of the study, mice were killed with a lethal dose of sodium pentobarbital and *in situ* fixation of the aorta at physiologic pressure [100 mmHg (1 mmHg = 33 Pa)] was performed with PBS/paraformaldehyde (4%, 0.1 mol/liter, pH 7.3) for histology and normal saline for immunohistochemistry (see below).

**Plasma Determination and LDL Oxidation.** Blood was collected at the time of killing into Eppendorf tubes with 1 mM  $\text{Na}_2\text{EDTA}$ . Plasma cholesterol was determined enzymatically (18, 19). LDL particles ( $d = 1.006 - 1.063 \text{ g/ml}$ ) were isolated from 2 ml of pooled plasma from two animals of each group by sequential-density ultracentrifugation (18, 19). The protein content of LDL was measured by the method of Lowry (20). Susceptibility of LDL to *in vitro* oxidation was induced by 1  $\mu\text{M}$  copper sulfate at 37°C for 12 h, as described (18, 19, 21). At the end of the incubation, the formation of thiobarbituric acid reactive substances was determined by the thiobarbituric acid method, as described (18, 19, 21). Lag-time was determined by monitoring the changes measured at 234 nm in the absorbance and observed at room temperature (23°C) every 10 min for a period of 4 h (19, 21). Measurement of the isoprostane 8-epi-PGF<sub>2</sub> purified from plasma samples was made by using a commercially available immunoassay (Cayman Chemical, Ann Arbor, MI) according to the manufacturer's instructions.

**Morphometric Assessment of Lesions and Immunohistochemistry of Lesion Components.** The aorta was dissected, cleaned of adherent fat and fascia, cut open, washed thoroughly with cold sterile PBS containing 2 mM EDTA, placed in ice-cold PBS containing 50  $\mu\text{M}$  butylated hydroxytoluene, 0.001% aprotinin, 50 mM EDTA, and 0.008% chloramphenicol, and equilibrated with nitrogen (10, 11, 22, 23). Each arterial segment then was divided into two parts. One of these was immersed in cysteine prodrug 2-oxothiazolidine-4-carboxylate (5 mM)-containing medium (Dako, Milan) and flash frozen in liquid nitrogen; 7- $\mu\text{m}$ -thick sections were taken and prepared with a cryotome for computer-assisted morphometric determination of lipid-rich lesions (30 cryosections from arteries were stained with oil red-O and counterstained with hematoxylin), as described in detail (10, 11, 16, 22, 23). The second part of each arterial segment was fixed in buffered 10% formalin and paraffin embedded; 12–15 serial sections (5- $\mu\text{m}$  thickness) were prepared for immunohistochemistry (10, 11, 16, 22, 23). Duplicate serial sections of the fixed and paraffin-embedded arterial segments were immunostained with E06, murine monoclonal antibody against oxidation-specific lysine and oxidized phospholipid epitopes of ox-LDL, and F4/80, a monoclonal antibody against mouse monocyte/macrophages-derived foam cells (10, 11, 16, 22, 23). Antibodies were used at a dilution of 1:500. Epitopes recognized by the primary antibody were detected by an avidin-biotin-peroxidase computer-assisted method (10, 11, 16, 22, 23).

**Statistical Analysis.** Results are expressed as mean  $\pm$  SEM. Evaluation of the atherogenesis and the immunohistochemistry were performed in a blinded way regarding the treatment given to mice. A Student's *t* test was used to compare differences among groups. Statistical significance was defined as  $P < 0.05$ .

## Results

**Lipid Profile.** Plasma cholesterol levels were similar among groups of LDL-receptor-deficient mice ( $724 \pm 68 \text{ mg/dl}$ ,  $746 \pm 72$  and  $738 \pm 57$  in placebo, NCX-4016 and aspirin-treated groups, respectively;  $P = \text{NS}$  for all comparisons). Similarly, plasma triglyceride levels were comparable in all three groups of mice

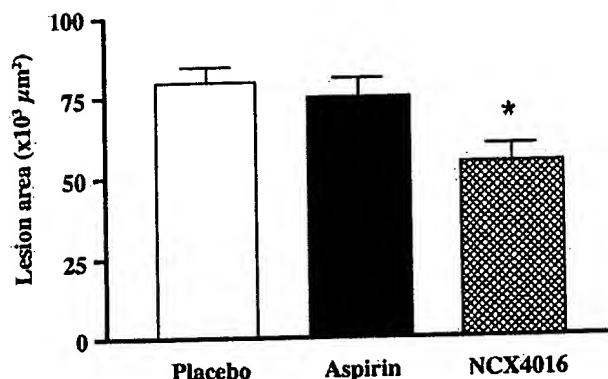


Fig. 1. Effects of various treatments on atherosclerotic lesion area in male LDL-receptor-deficient mice after 12 weeks of treatment with placebo, regular aspirin (18 mg/kg), or equimolar doses of nitric oxide-releasing aspirin (NCX-4016, 30 mg/kg). Mean lesion area of oil-red O-stained sections was calculated by computer-assisted imaging analysis. Results are expressed as the mean  $\pm$  SEM of the aortic lesions of 10 animals from each group. \*,  $P < 0.01$  vs. placebo-treated mice.

( $165 \pm 22 \text{ mg/dl}$ ,  $172 \pm 32$ , and  $170 \pm 28$  in placebo, NCX-4016, and aspirin-treated groups, respectively;  $P = \text{NS}$  for all comparisons).

**Evaluation of Atherogenesis.** Computer-assisted imaging analysis revealed that 30 mg/kg of NCX-4016 reduced the aortic cumulative lesion area by  $39.8 \pm 12.3\%$  compared with that of the placebo ( $P < 0.001$ ). In another set of experiments ( $n = 5$ ), 30 mg/kg of NCX-4016 reduced the aortic cumulative lesion area by  $24.1 \pm 10.8\%$  ( $P = 0.589$ , NS). The equimolar dose of aspirin (18 mg/kg) did not reduce significantly aortic lesions ( $-5.1 \pm 2.3\%$ ) compared with the placebo ( $P = 0.867$ , NS; Fig. 1). Fig. 2 shows some examples of high magnifications of oil-red O-stained aorta of a placebo-treated mouse (A) and NCX-4016-treated mouse (B). The reduction of the atherosclerotic lesions was coupled with a marked decrease in the thickness of lesions (oil-red O staining) of a NCX-4016-treated mouse in comparison to the placebo-treated mouse (C).

**Immunohistochemistry.** Mice treated with 30 mg/kg/day of NCX-4016 revealed a significant decrease of intimal macrophages-derived foam cells ( $-28.3 \pm 10.2\%$  of F4/80-positive arterial sections,  $P < 0.05$  vs. placebo-treated group) and oxidation-specific epitopes of oxidized LDL by ( $-35.8 \pm 11.9\%$  of E06-positive arterial section,  $P < 0.01$  vs. placebo-treated group; Fig. 3). Thus, NCX-4016 significantly reduced the expression of oxidation-specific epitopes and macrophage accumulation in the arterial wall compared with that of the placebo-treated group as well as aspirin-treated group.

**Effect of Different Treatments on Plasma LDL Oxidizability and Oxidative Stress.** Treatment with 30 mg/kg/day of NCX-4016 reduced significantly plasma LDL oxidation and systemic oxidative stress compared with both placebo and, to a lesser extent, aspirin (Table 1). This reduction of plasma LDL oxidation was shown by significant reduction of LDL malondialdehyde content of around 40% ( $P < 0.001$  vs. placebo;  $P < 0.04$  vs. aspirin), as well as by the prolongation of lag-time of oxidizability of around 20% ( $P < 0.01$  vs. placebo;  $P < 0.05$  vs. aspirin). In the same group of mice above ( $n = 5$ ) treated with 10 mg/kg of NCX-4016, the compound reduced LDL malondialdehyde content to  $19.3 \pm 4.0 \text{ nmol/mg}$  of protein ( $P < 0.05$  vs. placebo;  $P = \text{NS}$  vs. aspirin) and LDL lag-time reached  $120 \pm 33 \text{ min}$  ( $P = \text{NS}$  vs.



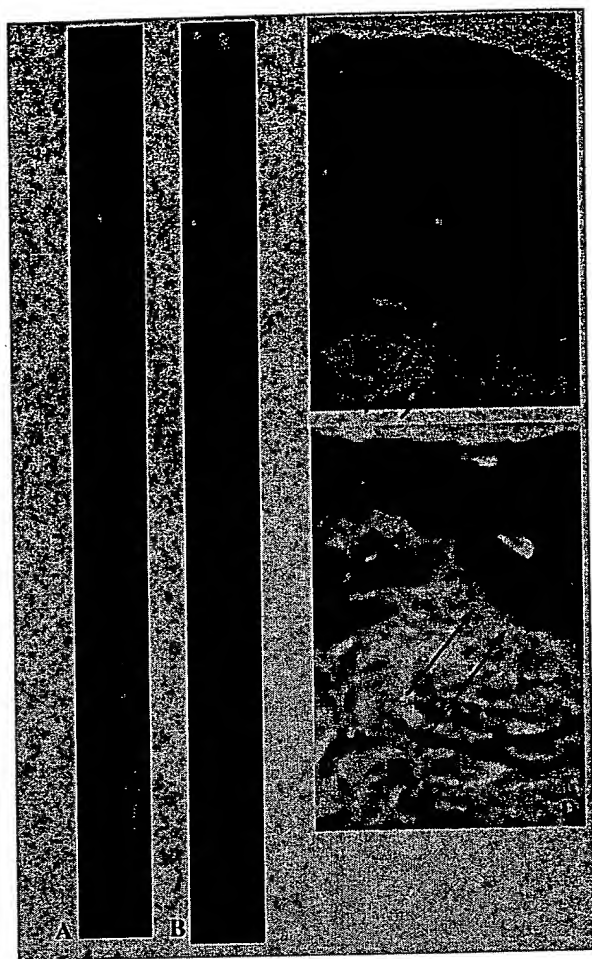


Fig. 2. High-magnifications ( $\times 25$ ) of oil-red O-stained thoracic aorta of placebo-treated mouse (A), placebo-treated mouse (B), and nitric oxide-releasing aspirin-treated mouse (30 mg/kg). Sustained reduction of the thickness of lesions of nitric oxide-releasing aspirin-treated mouse (D) in comparison to the placebo-treated mouse (C) (both  $\times 320$  magnification). Arrows indicate the degree of staining in relation to the intima.

placebo and aspirin). Similarly, plasma isoprostanes were reduced significantly by treatment with NCX-4016 (Table 1).

## Discussion

Our article demonstrates that chronic delivery of NO achieved with the NO-releasing aspirin significantly attenuates the devel-

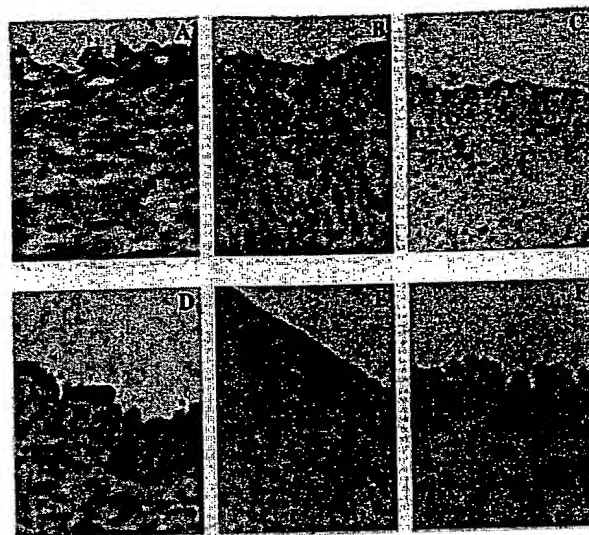


Fig. 3. Treatment with (C) 30 mg/kg nitric oxide-releasing aspirin (NCX-4016) was more effective than (B) 18 mg/kg of regular aspirin or (A) placebo in reducing oxidation-specific epitopes in E06-positive sections ( $\times 275$ ). Indeed, placebo-treated animals had a diffuse staining for oxidation-specific epitopes (A). This staining was partially reduced and increased in the sub-endothelial space in aspirin-treated mice (B). Nitric oxide-releasing aspirin reduced the overall immunostaining throughout the serial section (C). Similarly, macrophage accumulation was reduced in F4/80 positive sections in nitric oxide-releasing aspirin-treated animals (F) when compared with regular aspirin-treated (E) or placebo-treated (D) LDL-receptor-deficient mice ( $\times 275$ ). The negative immunostaining (brown) in C and F appears in blue.

opment of a chronic disease such as atherosclerosis in hypercholesterolemic LDL receptor-deficient mice without affecting plasma cholesterol levels. The enhancement of the NO pathway may play an important role in antiatherogenic effect of NO-releasing aspirin (reviewed in ref. 4). This study also demonstrates that in parallel to the attenuation of atherosclerosis, NO-aspirin reduced the susceptibility *ex vivo* of plasma LDL to oxidative modification and systemic oxidative stress measured by plasma isoprostanes. Isoprostane levels are a well recognized indicator of oxidative stress in animal models and in humans (24). Antioxidant protection could be related to the scavenging activity of free radicals by NO-containing aspirin both in plasma and in the arterial wall. Superoxide anion and NO are known to react rapidly to form the stable peroxynitrite anion, and peroxynitrite decomposition generates a strong oxidant with reactivity similar to hydroxyl radical (25). However, the causal role of peroxynitrite in atherogenesis is not established. Nevertheless, the properties of NO-releasing aspirin can also affect multiple

Table 1. Parameters of susceptibility to *ex vivo* peroxidation of LDL and systemic oxidative stress in LDL-receptor-deficient mice treated with nitric oxide-releasing aspirin (NCX-4016) or regular aspirin

	LDL lag-time, min	LDL MDA, nmol/mg prot	Plasma isoprostane 8-epi-PGF <sub>2</sub> , pg/ml
Placebo-treated LDL-receptor-deficient mice (n = 10)	112 $\pm$ 22	24.5 $\pm$ 4.2	143 $\pm$ 37 (n = 6)
NCX-4016-treated LDL-receptor-deficient mice (n = 10)	131 $\pm$ 18*	14.3 $\pm$ 2.4**	119 $\pm$ 21*** (n = 6)
Aspirin-treated LDL-receptor-deficient mice (n = 10)	115 $\pm$ 15	22.3 $\pm$ 4.7	128 $\pm$ 38 (n = 6)

LDL-receptor-deficient mice treated with NCX-4016 (30 mg/kg/day), and aspirin (18 mg/kg/day); MDA, malondialdehyde at 12 h after exposure of LDL to 1  $\mu$ M copper sulphate (n = 10 for each group). Lag-time represents an index of LDL oxidizability; increased values of lag-time reflect increased resistance of LDL to oxidative modification (n = 10 for each group, see also refs. 19 and 21). In a subset of animals (n = 6), plasma isoprostane levels (8-epi PGF<sub>2</sub>) were measured. \*,  $P < 0.05$  or \*\*,  $P < 0.01$  vs. placebo or aspirin-treated mice; \*\*\*,  $P < 0.05$  vs. placebo-treated mice by ANOVA followed by t test and Bonferroni's correction. See text for further details.



radical species generated in the arterial wall. An increasing number of compounds releasing NO or modulating the NO pathway are now available (reviewed in ref. 26). Further studies should evaluate whether these newly developed compounds, clinically used drugs, or other NO-donors could be helpful in retarding atherosclerotic lesion formation and its clinical sequelae.

Oxidative modification of LDL plays a crucial role in human early atherosclerotic lesions (22, 23, 27) leading to atherosclerosis-related diseases (5, 6). Some studies (28) also demonstrated the important role of inhibition of LDL oxidation on the attenuation of atherosclerosis in hypercholesterolemic mice. In the present study, we showed that NCX-4016 reduced formation in the arterial wall of oxidation-specific epitopes of oxidized LDL. Thus, NCX-4016 has a potent antioxidant effect also in the atherosclerotic lesions of mice probably by means of scavenging of the radical-induced oxidation of LDL also in the arterial wall. Oxidized LDL may induce apoptosis in human coronary cells (7, 8). This phenomenon may favor the development of unstable atherosclerotic lesions (7, 8). However, apoptosis in macrophages also may reduce a potential source of mediators which can contribute to destabilizing the plaque (e.g., metalloproteinases and MCP-1). Nevertheless, the reduction of oxidative stress *in vivo* could also attenuate the degree of unstable atheroma. In another experimental setting, we showed recently that NCX-4016 reduced restenosis after arterial injury and macrophage deposition in hypercholesterolemic mice (16) and in aged rats (17), perhaps, at least in part, through its antioxidant effects. These properties may be particularly useful when applied to hypercholesterolemic or elderly patients. Obviously, the chronic development of atherosclerosis is a completely different pathophysiological condition from restenosis after arterial injury. Indeed, restenotic inflammatory lesions already appear after 14 days from the arterial injury. In the present study, we have also shown that the antiatherogenic effect was coupled to

the reduction of macrophage-derived foam cells at the site of lesions. This beneficial effect may contribute to the reduction of lesion progression observed in hypercholesterolemic mice, and it is also consistent with the inhibition of macrophage-dependent LDL oxidation by *in vitro* NO donors (26, 29).

The findings of the present study are in agreement with an important role of NO in the development of atherosclerosis in hypercholesterolemic mice. Accordingly, the role of endogenous NO in the progression of atherosclerosis in apolipoprotein E-knockout mice was recently investigated by using N(omega)-nitro-L-arginine methyl ester (L-NAME), an inhibitor of nitric oxide synthase (NOS) or with the NOS substrate L-arginine for 8 weeks (30). L-NAME treatment resulted in a significant inhibition of NO-mediated vascular responses and a significant increase in the atherosclerotic plaque area in the aorta of these mice. In contrast, L-arginine treatment had no influence on endothelial function and did not alter lesion size. The acceleration in lesion size concomitant to the severely impaired NO-mediated responses indicates that lack of endogenous NO (4, 31) is an important progression factor of atherosclerosis in the apolipoprotein E-knockout mouse.

We conclude that enhanced NO release by chronic treatment with NO-containing aspirin attenuates the development of a chronic disease such as atherosclerosis in hypercholesterolemic mice. Although the natural history of the atherosclerotic disease is different between rodents and humans, these data should be considered a further piece of evidence supporting the key role of NO in atherogenesis. Inhibition of oxidation-sensitive mechanisms by NO-aspirin, and possible other NO-related anti-inflammatory effects (reviewed in ref. 32), both in plasma and in atherosclerotic lesions, together with reduced macrophage accumulation, may have an important role in contributing to this antiatherogenic effect.

This work was supported by National Institutes of Health Grants HL57665, HL41371, and HL64793, and by Italian Institutes of Health Grant ISNIH.99.56980.

- Ludmer, P. L., Selwyn, A. P., Shook, T. L., Wayne, R. R., Mudge, G. H., Alexander, R. W. & Ganz, P. (1986) *N. Engl. J. Med.* 315, 1046–1051.
- Ignarro, L. J., Cirino, G., Casini, A. & Napoli, C. (1999) *J. Cardiovasc. Pharmacol.* 34, 876–884.
- Drexler, H. (1999) *Cardiovasc. Res.* 43, 572–579.
- Napoli, C. & Ignarro, L. J. (2001) *Nitric Oxide* 5, 88–97.
- Witztum, J. L. & Steinberg, D. (1991) *J. Clin. Invest.* 88, 1785–1791.
- Steinberg, D. (1997) *J. Biol. Chem.* 272, 20963–20966.
- de Nigris, F., Maida, I., Palumbo, G., Anania, V. & Napoli, C. (2000) *Biochem. Pharmacol.* 59, 1477–1487.
- Napoli, C., Quehenberger, O., de Nigris, F., Abete, P., Glass, C. K. & Palinski, W. (2000) *FASEB J.* 14, 1996–2007.
- de Nigris, F., Youssef, T., Ciafrè, S., Franconi, F., Anania, V., Condorelli, G., Palinski, W. & Napoli, C. (2000) *Circulation* 102, 2111–2117.
- Palinski, W., Napoli, C. & Reaven, P. D. (2000) *Harvard Series*, eds Simon, D. I. & Rogers, C. (Humana, Totowa, NJ), pp. 149–174.
- Napoli, C., de Nigris, F., Welch, J. S., Calara, F. B., Stuart, R., Glass, C. K. & Palinski, W. (2002) *Circulation* 105, 1360–1367.
- Del Soldato, P., Sorrentino, R. & Pinto, A. (1999) *Trends Pharmacol. Sci.* 8, 319–323.
- Zhang, S. H., Reddick, R. L., Piedrahita, J. & Maeda, N. (1992) *Science* 258, 468–471.
- Nakashima, Y., Plump, A. S., Raines, E. W., Breslow, J. L. & Ross, R. (1994) *Arterioscler. Thromb.* 14, 133–139.
- Reddick, R. L., Zhang, S. H. & Maeda, N. (1994) *Arterioscler. Thromb.* 14, 141–148.
- Napoli, C., Cirino, G., Del Soldato, P., Sorrentino, R., Sica, V., Condorelli, M., Pinto, A. & Ignarro, L. J. (2001) *Proc. Natl. Acad. Sci. USA* 98, 2860–2864.
- Napoli, C., Aldini, G., Wallace, J. L., de Nigris, F., Maffei, R., Abete, P., Bonaduce, D., Condorelli, G., Rengo, F., Sica, V., et al. (2002) *Proc. Natl. Acad. Sci. USA* 99, 1689–1694.
- Napoli, C., Chiariello, M., Palumbo, G. & Ambrosio, G. (1996) *Cardiovasc. Drugs Ther.* 10, 417–424.
- Napoli, C., Mancini, F. P., Corso, G., Malorni, A., Crescenzi, E., Postiglione, A. & Palumbo, G. (1997) *J. Biochem.* 121, 1096–1101.
- Lowry, O. H., Rosebrough, N. J. & Farr, L. (1951) *J. Biol. Chem.* 193, 265–275.
- Napoli, C., Postiglione, A., Triggiani, M., Corso, G., Palumbo, G., Carbone, V., Rocco, A., Ambrosio, G., Montefusco, S., Malorni, A., et al. (1995) *Atherosclerosis* 11, 263–275.
- Napoli, C., D'Armiento, F. P., Mancini, F. P., Palumbo, G., Witztum, J. L. & Palinski, W. (1997) *J. Clin. Invest.* 100, 2680–2690.
- Napoli, C., Witztum, J. L., de Nigris, F., D'Armiento, F. P. & Palinski, W. (1999) *Circulation* 99, 2003–2010.
- Witztum, J. L. & Berliner, J. A. (1998) *Curr. Opin. Lipidol.* 9, 441–448.
- Beckman, J. S., Beckman, T. W., Chen, J., Marshall, P. A. & Freeman, B. A. (1990) *Proc. Natl. Acad. Sci. USA* 87, 1620–1624.
- Ignarro, L. J., Napoli, C. & Loscalzo, J. (2002) *Circ. Res.* 90, 21–28.
- Napoli, C., Glass, C. K., Witztum, J. L., D'Armiento, F. P., Deutch, R. & Palinski, W. (1999) *Lancet* 354, 1234–1241.
- Aviram, M., Maor, I., Keidar, S., Hayek, T., Oiknine, J., Bar-El, Y., Adler, Z., Kertzman, V. & Milo, S. (1995) *Biochem. Biophys. Res. Commun.* 216, 501–513.
- Hogg, N., Struck, A., Goss, S. P. A., Santanam, N., Joseph, J., Parthasarathy, S. & Kalyanaraman, B. (1995) *J. Lipid Res.* 36, 1756–1762.
- Kauser, K., da Cunha, V., Fitch, R., Mallari, C. & Rubanyi, G. M. (2000) *Am. J. Physiol.* 278, H1679–H1685.
- Rudic, R. D. & Sessa, W. C. (1999) *Am. J. Hum. Genet.* 64, 673–677.
- Wallace, J. L., Ignarro, L. J. & Fiorucci, S. (2002) *Nat. Rev. Drug Discovery* 1, 375–382.

Evidence Appendix

(*Arteriosclerosis, Thrombosis, and Vascular Biology*. 1996;16:1013.)  
© 1996 American Heart Association, Inc.

Articles

## Lymphocyte Populations in Atherosclerotic Lesions of ApoE -/- and LDL Receptor -/- Mice

### Decreasing Density With Disease Progression

Simon E. Roselaar; Paul X. Kakkanathu; Alan Daugherty

the Departments of Medicine (S.E.R., P.X.K., A.D.) and Biochemistry and Molecular Biophysics (A.D.), Washington University School of Medicine, St Louis, Mo.

Correspondence to Alan Daugherty, Box 8086, Cardiovascular Division, Washington University School of Medicine, St Louis, MO 63110. E-mail doco@imgate.wustl.edu.

### Abstract

Lymphocytes are prominent components of human atherosclerotic lesions, but their presence in murine models of disease has not been confirmed. Lymphocyte subpopulations have been identified in apoE -/- and LDL receptor -/- mice fed a cholesterol-enriched diet for up to 3 months. ApoE -/- mice had higher serum cholesterol concentrations than did LDL receptor -/- mice during most of the feeding period, primarily due to large increases in VLDL concentrations. Total area of atherosclerotic lesions was greater at all times in apoE -/- than LDL receptor -/- mice (lesion area after 3 months on cholesterol-enriched diet: apoE -/-,  $993 \pm 193$  and LDL receptor -/-,  $560 \pm 131 \mu\text{m}^2 \times 10^3$ , mean  $\pm$  SEM,  $n=6$  in each group). Lesions in apoE -/- mice contained larger macrophage-rich necrotic cores and more calcification than did those in LDL receptor -/- mice. Immunocytochemical analyses of tissue sections of ascending aortas performed with monoclonal antibodies to T and B lymphocytes and macrophages revealed that T lymphocytes immunoreactive for Thy 1.2, CD5, CD4, and CD8 were observed in lesions from both strains, but no B lymphocytes were detected. The density of Thy 1.2<sup>+</sup> T lymphocytes in lesions was greatest at 1 month (apoE -/-,  $98 \pm 23$  and LDL receptor -/-,  $201 \pm 40$  lymphocytes/mm<sup>2</sup>,  $n=6$  in each group), decreasing in apoE -/- mice to  $12 \pm 3$  and in LDL receptor -/- mice to  $51 \pm 20$  lymphocytes/mm<sup>2</sup> at 3 months. The presence of T lymphocytes in murine atherosclerotic lesions makes these animals potentially useful for studying the involvement of the immune system in atherogenesis.

**Key Words:** atherosclerosis • murine model • T lymphocytes • immunohistochemistry

Cellular processes that occur during human atherogenesis may be examined by using animal

### This Article

- ▶ [Abstract FREE](#)
- ▶ [Alert me when this article is cited](#)
- ▶ [Alert me if a correction is posted](#)
- ▶ [Citation Map](#)

### Services

- ▶ [Email this article to a friend](#)
- ▶ [Similar articles in this journal](#)
- ▶ [Similar articles in PubMed](#)
- ▶ [Alert me to new issues of the journal](#)
- ▶ [Download to citation manager](#)
- ▶ [Cited by other online articles](#)
- ▶ [Request Permissions](#)

### Google Scholar

- ▶ [Articles by Roselaar, S. E.](#)
- ▶ [Articles by Daugherty, A.](#)
- ▶ [Articles citing this Article](#)

### PubMed

- ▶ [PubMed Citation](#)
- ▶ [Articles by Roselaar, S. E.](#)
- ▶ [Articles by Daugherty, A.](#)

models of atherosclerosis that simulate human disease. The PDAY study<sup>1</sup> established similarities in the evolution of atherosclerotic disease in humans and Watanabe heritable hyperlipidemic rabbits, cholesterol-fed rabbits,<sup>2 3</sup> and rhesus monkeys.<sup>4 5</sup> In addition, initial studies with cholesterol-fed C57BL/6J mice have led to the increasing use of mice in the study of events in atherogenesis.<sup>6</sup> More recently, genetically modified mice deficient in either apoE<sup>7</sup> or LDL receptors<sup>8</sup> have become available. ApoE-deficient mice are grossly hypercholesterolemic and spontaneously develop atherosclerosis that has the morphological characteristics of human disease<sup>9 10 11</sup>; disease development is accelerated by feeding these mice cholesterol-enriched diets.<sup>12 13</sup> LDL receptor deficiency in mice produces only a mild increase in plasma cholesterol concentrations but imparts an increased responsiveness to cholesterol-enriched diets, leading to pronounced atherosclerotic lesion development.<sup>14</sup>

Atherosclerotic lesions are mostly made up of macrophages and smooth muscle cells, but there is increasing recognition of the presence of T lymphocytes.<sup>15 16 17 18</sup> Both CD4<sup>+</sup> and CD8<sup>+</sup> T lymphocytes are present at all stages of development of human lesions.<sup>19 20</sup> These T lymphocytes are activated, as judged from the presence of activation markers<sup>21</sup> and expression of MHC class II antigens on adjacent smooth muscle cells.<sup>22</sup> Expression of MHC class II is induced by the T lymphocyte-derived cytokine interferon gamma, which is detectable in lesions.<sup>23 24</sup> T lymphocytes in atherosclerotic lesions are polyclonal in origin.<sup>25</sup> The full spectrum of antigens against which T lymphocytes are directed has not been elucidated, but it is known that oxidized LDL activates a small subset.<sup>26</sup> B lymphocytes are also found in human atherosclerotic lesions.<sup>15 27</sup>

The role of the immune system in atherogenesis is controversial. Lesions that develop in cholesterol-fed rabbits contain T lymphocytes that may be active participants in lesion formation since immunosuppression results in enhancement of the atherogenic process.<sup>28</sup> The severity of atherosclerotic lesions is also increased in immune-suppressed<sup>29</sup> and MHC class I-deficient C57BL/6J mice<sup>30</sup> fed a cholesterol-enriched diet. However, in contrast to lesions in hypercholesterolemic rabbits, lymphocytes have not been detected in murine atherosclerotic lesions.<sup>31</sup> Studies to define the role of the immune system in atherogenesis require an animal model in which T lymphocytes are present in lesions, as they are in human disease. We therefore used monoclonal antibodies to evaluate whether lymphocytes are present in atherosclerotic lesions of cholesterol-fed apoE -/- and LDL receptor -/- mice. Immunostaining for Thy 1.2, CD5, CD4, and CD8 was positive in atherosclerotic lesions in both strains of mice, although the density of T lymphocytes in each strain differed markedly. The presence of lymphocytes in atherosclerotic lesions of these mice makes them valuable for the study of the role of the immune system in atherogenesis.

## Methods

### Animals

LDL receptor -/- and apoE -/- mice (8 female and 10 male in each group) were obtained from Jackson Laboratories. Both strains of mice were originally generated as C57BL/6JxC129 hybrids,

and mice used in this study were backcrossed six generations into a C57BL/6J background. Mice were housed in specific pathogen-free rooms and fed a normal mouse laboratory diet (Ralston Purina) until they were 6 weeks of age, after which they were fed a diet containing 1.25% cholesterol, 0.5% cholic acid, and 15% fat (Harlan Teklad, catalogue No. 88051) for up to 3 months. All procedures were approved by the Washington University Animal Studies Committee.

### **Removal of Aortas and Blood Samples**

Six mice of each strain were selected after 1, 2, and 3 months on a high-cholesterol diet. Nonfasting animals were anesthetized by metaphane inhalation (Pitman-Moore), bled retro-orbitally, and killed by cervical dislocation. Hearts were removed en bloc and placed in ice-cold Ringer's lactate, washed free of blood, and embedded and frozen in optimal cutting temperature compound (Tissue Tek). Sections of aorta (10  $\mu$ m) were cut on a cryostat<sup>6</sup> and placed on Probe-on-Plus microscope slides (Fisher Scientific). Serum was separated from whole blood by centrifugation and stored at 4°C.

### **Serum Cholesterol Concentrations and Lipoprotein Cholesterol Distribution**

Serum concentrations of total cholesterol were measured by using an enzyme-based colorimetric assay (Wako Chemical Co). Lipoprotein cholesterol distributions were determined by fast-performance liquid chromatography of pooled serum samples from all six mice in each group after 3 months of feeding.<sup>32</sup>

### **Histology and Immunocytochemistry**

Frozen sections were fixed in acetone for 5 minutes. Macrophages were detected with anti-mouse monoclonal antibody MOMA-2 (rat IgG<sub>2b</sub>, Serotec). All lymphocyte antibodies were initially screened for their ability to stain cells in splenic tissue (positive control). T lymphocytes were immunostained with monoclonal antibodies to murine CD5 (clone 57-7.3, rat IgG<sub>2a</sub>K, Life Technologies), Thy 1.2 (clone 30-H12, rat IgG<sub>2b</sub>, Collaborative Biomedical Products, and clone AT83A, rat IgM, Dr Osami Kanagawa, Washington University), CD8 (clone YTS 105.18, rat IgG<sub>2a</sub>, Serotec), and CD4 (clone GK1.5, rat IgG, Dr Osami Kanagawa). Tissue sections were blocked with nonimmune rabbit serum. The secondary antibody was an affinity-purified, mouse serum-adsorbed, biotinylated rabbit anti-rat IgG (BA 4001, Vector Laboratories).

Immunocytochemical analysis was performed by using a Fisher MicroProbe system and Vectastain Elite ABC kits (Vector). Negative controls were obtained with isotype-matched irrelevant antibodies or no primary antibody. Immunoreactivity was visualized by using 3-amino 9-ethyl carbazole (Biomedica Corp), which forms a red precipitate. Accumulation of neutral lipid in lesions was visualized by staining with oil red O. Tissue sections were counterstained with aqueous hematoxylin (Biomedica).

### **Quantification of Lesion Areas and Numbers of T Lymphocytes**

Consecutive 10- $\mu$ m-thick aortic cross sections were cut, beginning at the most proximal part of the aortic sinus.<sup>6</sup> Sections were placed consecutively on each of eight separate slides, after which

the ninth section was placed on the first slide, next to the first section, continuing for 48 sections. A single slide, upon which were six aortic cross sections from each mouse, was analyzed for lesion dimensions and for any given stain or immunostain. Total atherosclerotic lesion area and numbers of Thy 1.2<sup>+</sup> lymphocytes were quantified by using an image-analysis system consisting of a Nikon Optiphot-2 microscope attached to a Javelin JE3462 high-resolution camera and a personal computer equipped with a Coreco-Oculus OC-TCX frame grabber and high-resolution monitor. Computerized color-image analysis was performed by using Image-Pro Plus software (Media Cybernetics). The area of each lesion in all six cross sections in every mouse was recorded, as was the total number of T lymphocytes determined by immunostaining for Thy 1.2. For each mouse studied, total atherosclerotic lesion area was calculated as the sum of the areas of all lesions in all six aortic cross sections on one slide. Thy 1.2-immunopositive lymphocytes were counted per section, and T-lymphocyte density was expressed as the number of lymphocytes per square millimeter of atherosclerotic lesion area.

### Statistics

Differences in serum cholesterol concentrations, atherosclerotic lesion areas, and T-lymphocyte numbers were compared either by two-tailed Student's *t* test, or, if data failed to meet the requirements for use of this parametric test, by the Mann-Whitney rank-sum test. Data analyses were performed by using SigmaStat for Windows (Jandel Scientific).

### Results

All animals tolerated the cholesterol-enriched diet without overt adverse affects. Total serum cholesterol concentrations before commencing the diet and at 1 and 2 months were higher in apoE  $-/-$  than LDL receptor  $-/-$  mice, but they did not differ significantly at 3 months (Fig 1□). Analyses of lipoprotein cholesterol distribution by size-exclusion fast-performance liquid chromatography demonstrated that regardless of diet, apoE  $-/-$  mice carried the major fraction of cholesterol in VLDL, while LDL receptor  $-/-$  mice carried cholesterol predominantly in an LDL-sized fraction.<sup>8 9 10 11</sup>

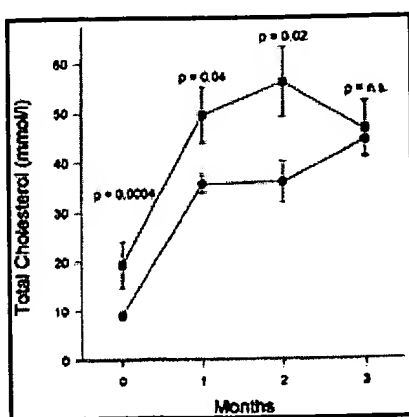


**Figure 1.** Line graph shows total serum cholesterol concentrations in apoE  $-/-$  and LDL receptor  $-/-$  mice. Cholesterol concentrations were measured by using enzymatic assays as described in "Methods." Points indicate means of six observations; bars, SEM; ■, apoE  $-/-$  mice; and •, LDL receptor  $-/-$  mice.

View larger version (16K):  
[in this window]

[\[in a new window\]](#)

Atherosclerotic lesions were characterized after 1, 2, and 3 months of cholesterol feeding for size, macrophage content, and lymphocyte number and distribution. The two strains of mice had atherosclerotic lesions with markedly different cellular architectures and areas. At all times, aortic atherosclerotic lesions of apoE  $-/-$  mice were larger than those in LDL receptor  $-/-$  mice (Fig 2). Lesions from the two types of mice were of similar cellular composition after 1 month of cholesterol feeding, composed predominantly of macrophages. By 3 months, lesions in apoE  $-/-$  mice had large cores of necrotic macrophages, a feature less abundant in LDL receptor  $-/-$  mice. Chondrocytes and early bone formation were readily discernible in all apoE  $-/-$  mice examined at 3 months, but in only one of six LDL receptor  $-/-$  mice. Bands of smooth muscle cells and extracellular matrix were present in apoE  $-/-$  but not LDL receptor  $-/-$  mice after 3 months (Fig 3).

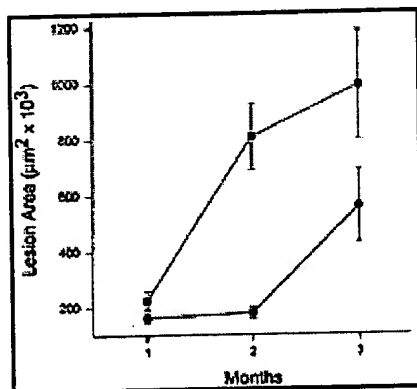
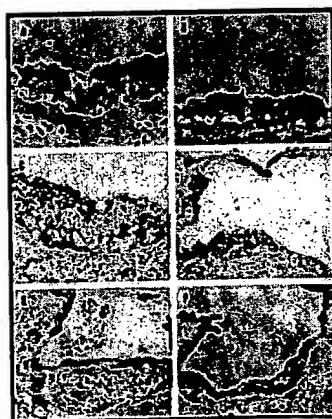


**Figure 2.** Line graph shows area of atherosclerotic lesions in apoE  $-/-$  and LDL receptor  $-/-$  mice after 1, 2, and 3 months on a cholesterol-enriched diet. Points indicate means of six observations; bars, SEM; ■, apoE  $-/-$  mice; and ●, LDL receptor  $-/-$  mice.

[View larger version \(13K\):](#)  
[\[in this window\]](#)  
[\[in a new window\]](#)



[View larger version](#)  
(115K):

**Figure 3.** Photomicrographs show presence of macrophages and lipid deposits in murine atherosclerotic lesions. Aortic sections were immunostained for macrophages as described in "Methods." Macrophages were immunostained with MOMA-2 after 1 month of cholesterol feeding in (A) apoE  $-/-$  and (B) LDL receptor  $-/-$  mice. At 1 month the two animal strains had lesions with similar morphological characteristics. After 3 months of cholesterol feeding, differences were observed in MOMA-2-immunostained macrophages: apoE  $-/-$  mice had necrotic macrophage core regions and macrophage accumulation under the endothelium separated by bands of nonstaining cells and matrix (C). In contrast, lesions from LDL receptor  $-/-$  mice immunostained uniformly for macrophages, and necrotic cores were uncommon (D).

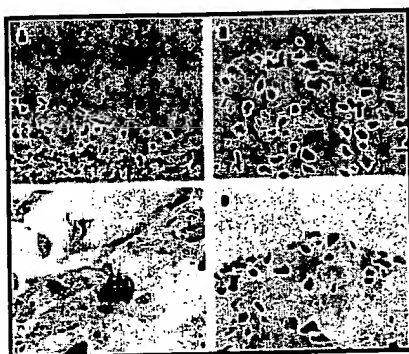


[\[in this window\]](#)  
[\[in a new window\]](#)

Staining for neutral lipids with oil red O was patchy in apoE  $-/-$  mice after 3 months of cholesterol feeding (E) but relatively uniform in LDL receptor  $-/-$  mice (F) (original magnification  $\times 100$  [A and B],  $\times 40$  [C through F]).

T lymphocytes were detected by using antibodies to Thy 1.2, CD5, CD4, and CD8 (Table 1). Thy 1.2 and CD5 antigens are pan-T-cell markers, although CD5 is also present on a subset of B lymphocytes in serosal cavities. Immunostaining for Thy 1.2 and CD5 was observed in lesions from both strains. Furthermore, the distribution and number of cells exhibiting positive immunostaining was similar with both Thy 1.2 antibodies (Fig 4A) and the CD5 antibody (Fig 4B). Several monoclonal antibodies directed against T-lymphocyte antigen CD4 and an antibody to the B-lymphocyte marker CD45R were used to identify the subsets of lymphocytes present in mouse atherosclerotic lesions (Table 1). No B lymphocytes were observed in lesions, although the CD45R antibody produced excellent immunostaining of splenic tissue that was used as a control. Because only one of the anti-CD4 antibodies (GK1.5) resulted in appreciable splenic immunostaining, it was used to demonstrate the presence of CD4 $^{+}$  cells in atherosclerotic lesions (Fig 4C). In splenic tissue, CD4 immunostaining was less intense on positive cells than was Thy 1.2, CD5, and CD8 immunostaining. CD8 $^{+}$  cells were detected in the lesions of both strains (Fig 4D). The relatively low intensity of CD4 $^{+}$  subset immunostaining indicated that formal quantification may result in a misleading underestimate of cell numbers. Therefore, because robust immunostaining of T-lymphocyte subsets was not as consistently achieved as for Thy 1.2 antigen, no quantitative assessment of these subtypes was performed.

**View this table:** [Table 1. Primary Antibodies Used to Detect Lymphocytes in Atherosclerotic Lesions](#)  
[\[in this window\]](#)  
[\[in a new window\]](#)



**View larger version (135K):**  
[\[in this window\]](#)  
[\[in a new window\]](#)

**Figure 4.** Photomicrographs. A, T lymphocytes positive for Thy 1.2 in shoulder region of a lesion from an LDL receptor  $-/-$  mouse fed a cholesterol-enriched diet for 1 month. B, T lymphocytes positive for CD5 in an apo E  $-/-$  mouse fed a cholesterol-enriched diet for 3 months. C, T lymphocytes positive for CD4 in a lesion from an LDL receptor  $-/-$  mouse after 1 month of cholesterol feeding. D, T lymphocytes positive for CD8 in an atherosclerotic lesion from an LDL receptor  $-/-$  mouse fed a cholesterol-enriched diet for 2 months (original magnification  $\times 200$  [A and B],  $\times 1000$  [C],  $\times 400$  [D]).

T lymphocytes, as determined by Thy 1.2 immunoreactivity, were present in atherosclerotic lesions at all intervals. The density of Thy 1.2<sup>+</sup> T lymphocytes was greatest after only 1 month of cholesterol feeding in both strains of mice (Fig 5). At the intervals studied beyond 1 month, there was a significant reduction in lesion T-lymphocyte density, which was particularly sparse after 3 months in apoE  $-/-$  mice. At all intervals, lesions of LDL receptor  $-/-$  mice contained a greater density of Thy 1.2<sup>+</sup> cells than did lesions of apoE  $-/-$  mice. In neither strain of mice was there a specific region in atherosclerotic lesions that preferentially accumulated T lymphocytes, as has been discerned in the human disease.<sup>15</sup> The distribution of lymphocytes was patchy, with small foci of cells generally located beneath the endothelium and few cells near the media or in the lipid core. No T lymphocytes were detected in the media.

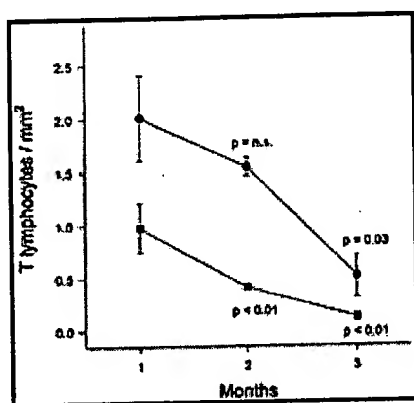


**Figure 5.** Line graph shows T-lymphocyte density of Thy 1.2<sup>+</sup> cells in both strains of mice at 1, 2, and 3 months. Points indicate means of six observations; bars, SEM; ■, apoE  $-/-$  mice; and ●, LDL receptor  $-/-$  mice. Statistical significance at 2 and 3 months (as determined by Mann-Whitney rank-sum test) is stated relative to the density at 1 month for each strain.

View larger version (13K):  
[\[in this window\]](#)  
[\[in a new window\]](#)

## Discussion

We observed striking differences in the dimensions and morphological characteristics of lesions in apoE  $-/-$  and LDL receptor  $-/-$  mice. Our observations of atherosclerotic lesions from apoE  $-/-$  mice are similar to earlier ones.<sup>10 11 12 13</sup> Compared with LDL receptor  $-/-$  mice, lesions in apoE  $-/-$  mice were larger at all intervals studied and had a markedly increased number of chondrocytes and bands of smooth muscle cells. ApoE  $-/-$  mice had significantly increased concentrations of total serum cholesterol at most intervals, with most being in a VLDL fraction. Cholesterol-enriched VLDL has been demonstrated to promote cholesterol esterification in macrophages,<sup>33 34 35</sup> which may be a factor in the formation of lesions of disparate morphology in apoE  $-/-$  and LDL receptor  $-/-$  mice, although this has not been proven.

The principal finding of this study is that Thy 1.2<sup>+</sup>, CD5<sup>+</sup>, CD4<sup>+</sup>, and CD8<sup>+</sup> T lymphocytes are present in atherosclerotic lesions in cholesterol-fed apoE  $-/-$  and LDL receptor  $-/-$  mice. Thy 1.2 is a 112-amino acid glycoprotein present in varying amounts on the surface of neural and lymphoid cells, with expression depending on the state of differentiation.<sup>36</sup> In mice, Thy 1.2 is found on

mature T lymphocytes. CD5 is a monomeric 67-kD glycoprotein on all mature T lymphocytes, with higher expression on CD4<sup>+</sup> than CD8<sup>+</sup> cells.<sup>37</sup> CD5 also occurs on the B1a subset of B lymphocytes found in serosal cavities. CD5 functions as a tyrosine kinase substrate in association with the T-cell receptor  $\zeta$  chain/CD3 and protein tyrosine kinases p56<sup>lck</sup> and p59<sup>fyn</sup> in T lymphocytes and may also act as an independent signaling molecule.<sup>38</sup>

Previous immunohistochemical analyses of atherosclerotic lesions in several strains of mice, including the apoE  $-/-$  strain, have shown an absence of T lymphocytes.<sup>31</sup> A possible explanation for this apparent contradiction is the interval at which lesions were studied. In the present study, lymphocyte density decreased with lesion maturity; particularly in apoE  $-/-$  mice, this cell type was sparse after 3 months of cholesterol feeding. The fact that Qiao et al<sup>31</sup> studied lesions after cholesterol feeding of a longer duration than in the present study may explain the lack of detectable lymphocytes. In addition, in our study, several of the anti-CD4 antibodies tested resulted in weak and diffuse immunostaining of splenic tissue (Table 2). Therefore, the difference between this and previous reports with regard to detection of lymphocytes might be partly attributed to differences in the affinity of antibodies used in immunohistochemical testing. However, while lymphocytes have not been reported in atherosclerotic lesions, CD4<sup>+</sup>, CD8<sup>+</sup>, and CD23<sup>+</sup> (B lymphocytes) have been demonstrated in aortic fatty streaks of vasculitis-prone MRL/lpr mice.<sup>39</sup>

In both apoE  $-/-$  and LDL receptor  $-/-$  mice, the density of T lymphocytes in lesions decreased as lesions matured. Signals responsible for recruitment of lymphocytes have not been defined, although one proposed mediator is the lysophospholipid formed by the oxidation of LDL.<sup>40 41</sup> Early lymphocytic recruitment to atherosclerotic lesions occurred, but further development of lesions ensued without a proportional increase in T lymphocytes. The early recruitment of lymphocytes to atherosclerotic lesions has also been observed in cholesterol-fed rabbits<sup>42 43</sup> and rats.<sup>44</sup> Lymphocyte residence time and trafficking within atherosclerotic lesions have not been defined but may be important parameters. Introduction of exogenous lymphocytes distinguishable on the basis of a genetically incorporated marker may assist in understanding the biology of lymphocytes within atherosclerotic lesions.

ApoE has been proposed as an endogenous regulator of the immune system, since it inhibits both monocyte<sup>45</sup> and T lymphocyte<sup>46</sup> proliferation. ApoE also inhibits interleukin-2-dependent T-cell proliferation, possibly by preventing transition from the G1<sub>A</sub> phase of the cell cycle.<sup>47</sup> ApoE synthesis by macrophages varies according to the state of cell differentiation<sup>48</sup> and may be inhibited by interferon gamma<sup>49</sup> and stimulated by increasing intracellular cholesterol concentrations.<sup>50</sup> However, since apoE  $-/-$  mice develop severe atherosclerosis and inhibition of T lymphocytes enhances development of atherosclerosis,<sup>28 29 30</sup> the physiological significance of the inhibitory effect of apoE on T lymphocytes in atherosclerotic lesions remains to be determined.

T lymphocytes are present in atherosclerotic lesions in apoE  $-/-$  and LDL receptor  $-/-$  mice,

making both strains useful for the study of immunologic factors affecting the development of atherosclerosis. In addition, we observed differences in morphological characteristics of lesions that could be due to altered lipoprotein metabolism or immunologic factors, both of which are likely to be targets of pharmacological intervention in the modulation of atherosclerotic disease.

## Acknowledgments

Simon E. Roselaar is a fellow of the American Heart Association, Missouri Affiliate. Alan Daugherty is an Established Investigator of the American Heart Association. We are grateful to Drs Jeffrey E. Saffitz and Osami Kanagawa for advice on histology and providing antibodies, to Dustie Delfel-Butteiger for technical assistance, to Beth Engeszer, Sandy Sendobry, and Debra Rateri for editorial assistance, and to Kelly Hall for secretarial assistance.

Received October 4, 1995; revision received February 22, 1996; **References**

1. Wissler RW and the PDAY Investigators. New insights into the pathogenesis of atherosclerosis as revealed by PDAY. *Atherosclerosis*. 1994;108(suppl):S3-S20.
2. Rosenfeld ME, Tsukada T, Gown AM, Ross R. Fatty streak initiation in Watanabe heritable hyperlipidemic and comparably hypercholesterolemic fat-fed rabbits. *Arteriosclerosis*. 1987;7:9-23. [\[Abstract\]](#)
3. Rosenfeld ME, Tsukada T, Chait A, Bierman EL, Gown AM, Ross R. Fatty streak expansion and maturation in Watanabe heritable hyperlipidemic and comparably hypercholesterolemic fat-fed rabbits. *Arteriosclerosis*. 1987;7:24-34. [\[Abstract\]](#)
4. Faggiotto A, Ross R, Harker L. Studies of hypercholesterolemia in the nonhuman primate, I: changes that lead to fatty streak formation. *Arteriosclerosis*. 1984;4:323-340. [\[Abstract\]](#)
5. Faggiotto A, Ross R. Studies of hypercholesterolemia in the nonhuman primate, II: fatty streak conversion to fibrous plaque. *Arteriosclerosis*. 1984;4:341-356. [\[Abstract\]](#)
6. Paigen B, Morrow A, Holmes PA, Mitchell D, Williams RA. Quantitative assessment of atherosclerotic lesions in mice. *Atherosclerosis*. 1987;68:231-240. [\[Medline\]](#) [\[Order article via Infotrieve\]](#)
7. Piedrahita JA, Zhang SH, Hagaman JR, Oliver PM, Maeda N. Generation of mice carrying a mutant apolipoprotein E gene inactivated by gene targeting in embryonic stem cells. *Proc Natl Acad Sci U S A*. 1992;89:4471-4475. [\[Abstract/Free Full Text\]](#)
8. Ishibashi S, Brown MS, Goldstein JL, Gerard RD, Hammer RE, Herz J. Hypercholesterolemia in low density lipoprotein receptor knockout mice and its reversal by adenovirus-mediated gene delivery. *J Clin Invest*. 1993;92:883-893. [\[Medline\]](#) [\[Order article via Infotrieve\]](#)
9. Zhang SH, Reddick RL, Piedrahita JA, Maeda N. Spontaneous hypercholesterolemia and arterial lesions in mice lacking apolipoprotein E. *Science*. 1992;258:468-471. [\[Medline\]](#) [\[Order article via Infotrieve\]](#)
10. Plump AS, Smith JD, Hayek T, Aalto-Setälä K, Walsh A, Verstuyft JG, Rubin EM, Breslow JL. Severe hypercholesterolemia and atherosclerosis in apolipoprotein-E-deficient mice created by homologous recombination in ES cells. *Cell*. 1992;71:343-353. [\[Medline\]](#) [\[Order article via Infotrieve\]](#)
11. Zhang SH, Reddick RL, Burke B, Maeda N. Diet-induced atherosclerosis in mice heterozygous and homozygous for apolipoprotein E gene disruption. *J Clin Invest*. 1994;94:937-945. [\[Medline\]](#) [\[Order article via Infotrieve\]](#)
12. Nakashima Y, Plump AS, Raines EW, Breslow JL, Ross R. ApoE-deficient mice develop lesions in all phases of atherosclerosis throughout the arterial tree. *Arterioscler Thromb*.

- 1994;14:133-140.[[Abstract](#)]
13. Reddick RL, Zhang SH, Maeda N. Atherosclerosis in mice lacking apo E. *Arterioscler Thromb.* 1994;14:141-147.[[Abstract](#)]
14. Ishibashi S, Goldstein JL, Brown MS, Herz J, Burns DK. Massive xanthomatosis and atherosclerosis in cholesterol-fed low density lipoprotein receptor-negative mice. *J Clin Invest.* 1994;93:1885-1893.[[Medline](#)] [[Order article via Infotrieve](#)]
15. Jonasson L, Holm J, Skalli OO, Bondjers B, Hansson GK. Regional accumulation of T cells, macrophages, and smooth muscle cells in human atherosclerotic plaques. *Arteriosclerosis.* 1986;6:131-138.[[Abstract](#)]
16. Emeson EE, Robertson AA. T lymphocytes in aortic and coronary intimas: their potential role in atherogenesis. *Am J Pathol.* 1988;130:369-376.[[Abstract](#)]
17. Hansson GK, Jonasson L, Lojsthe B, Stemme S, Kocher O, Gabbiani G. Localization of T lymphocytes and macrophages in fibrous and complicated human atherosclerotic plaques. *Atherosclerosis.* 1988;72:135-141.[[Medline](#)] [[Order article via Infotrieve](#)]
18. Katsuda S, Boyd HC, Fligner C, Ross R, Gown AM. Human atherosclerosis, III: immunocytochemical analysis of the cell composition of lesions of young adults. *Am J Pathol.* 1992;140:907-914.[[Abstract](#)]
19. Xu Q, Oberhuber G, Gruschwitz M, Wick G. Immunology of atherosclerosis: cellular composition and major histocompatibility complex class II antigen expression in aortic intima, fatty streaks and atherosclerotic plaques in young and aged human specimens. *Clin Immunol Immunopathol.* 1990;56:344-359.[[Medline](#)] [[Order article via Infotrieve](#)]
20. Munro JM, Van der Walt JD, Munro CS, Chalmers JAC, Cox EL. An immunohistochemical analysis of human aortic fatty streaks. *Hum Pathol.* 1987;18:375-380.[[Medline](#)] [[Order article via Infotrieve](#)]
21. Stemme S, Holm J, Hansson GK. T lymphocytes in human atherosclerotic plaques are memory cells expressing CD45RO and integrin VLA-1. *Arterioscler Thromb.* 1992;12:206-211.[[Abstract](#)]
22. Hansson GK, Jonasson L, Holm J, Claesson-Welsh L. Class II MHC antigen expression in the atherosclerotic plaque: smooth muscle cells express HLA-DR, HLA-DQ and the invariant gamma chain. *Clin Exp Immunol.* 1986;64:261-268.[[Medline](#)] [[Order article via Infotrieve](#)]
23. Hansson GK, Holm J, Jonasson L. Detection of activated T lymphocytes in the human atherosclerotic plaque. *Am J Pathol.* 1989;135:169-175.[[Abstract](#)]
24. Geng YJ, Holm J, Nygren S, Bruzelius M, Stemme S, Hansson GK. Expression of the macrophage scavenger receptor in atheroma: relationship to immune activation and the T-cell cytokine interferon- $\gamma$ . *Arterioscler Thromb Vasc Biol.* 1995;15:1995-2002. [[Abstract/Free Full Text](#)]
25. Stemme S, Rymo L, Hansson GK. Polyclonal origin of T lymphocytes in human atherosclerotic plaques. *Lab Invest.* 1991;65:654-660.[[Medline](#)] [[Order article via Infotrieve](#)]
26. Stemme S, Faber B, Holm J, Wiklund O, Witztum JL, Hansson GK. T lymphocytes from human atherosclerotic plaques recognize oxidized low density lipoprotein. *Proc Natl Acad Sci U S A.* 1995;92:3893-3897.[[Abstract/Free Full Text](#)]
27. Sohma Y, Sasano H, Shiga R, Saeki S, Suzuki T, Nagura H, Masato N, Yamamoto T. Accumulation of plasma cells in atherosclerotic lesions of Watanabe heritable hyperlipidemic rabbits. *Proc Natl Acad Sci U S A.* 1995;92:4937-4941. [[Abstract/Free Full Text](#)]
28. Roselaar SE, Schonfeld G, Daugherty A. Enhanced development of atherosclerosis in cholesterol-fed rabbits by suppression of cell-mediated immunity. *J Clin Invest.* 1995;96:1389-1394.[[Medline](#)] [[Order article via Infotrieve](#)]
29. Emeson EE, Shen ML. Accelerated atherosclerosis in hyperlipidemic C57BL/6 mice

- treated with cyclosporin A. *Am J Pathol.* 1993;142:1906-1915.[\[Abstract\]](#)
30. Fyfe AI, Qiao JH, Lusis AJ. Immune deficient mice develop typical atherosclerotic fatty streaks when fed an atherogenic diet. *J Clin Invest.* 1994;94:2516-2520.[\[Medline\]](#) [\[Order article via Infotrieve\]](#)
31. Qiao JH, Xie PZ, Fishbein MC, Kreuser J, Drake TA, Demer LL, Lusis AJ. Pathology of atheromatous lesions in inbred and genetically engineered mice. *Arterioscler Thromb.* 1994;14:1480-1487.[\[Abstract\]](#)
32. Daugherty A, Rateri DL. Heterogeneity of very low density lipoprotein fractions: factors influencing the ability of specific subfractions to modulate cholesterol metabolism in macrophages in vitro. *Coron Artery Dis.* 1991;2:775-787.
33. Goldstein JL, Ho YK, Brown MS. Cholesteryl ester accumulation in macrophages resulting from receptor-mediated uptake and degradation of hypercholesterolemic canine  $\beta$ -very low density lipoproteins. *J Biol Chem.* 1980;255:1839-1848.[\[Abstract/Free Full Text\]](#)
34. Mahley RW, Innerarity TL, Brown MS, Ho YK, Goldstein JL. Cholesteryl ester synthesis in macrophages: stimulation by  $\beta$ -very low density lipoproteins from cholesterol-fed animals of several species. *J Lipid Res.* 1980;21:970-980.[\[Abstract\]](#)
35. Daugherty A, Oida K, Sobel BE, Schonfeld G. Dependence of metabolic and structural heterogeneity of cholesterol ester-rich very low density lipoproteins on the duration of cholesterol feeding in rabbits. *J Clin Invest.* 1988;82:562-570.[\[Medline\]](#) [\[Order article via Infotrieve\]](#)
36. Giguère V, Isobe KI, Grosfeld F. Structure of the murine Thy-1 gene. *EMBO J.* 1985;4:2017-2024.[\[Abstract\]](#)
37. Ledbetter JA, Rouse RV, Micklem HS, Herzenberg LA. T cell subsets defined by expression of Lyt-1,2,3 and Thy-1 antigens: two-parameter immunofluorescence and cytotoxicity analysis with monoclonal antibodies modifies current views. *J Exp Med.* 1980;152:280-295.[\[Abstract/Free Full Text\]](#)
38. Tarakhovsky A, Müller W, Rajewsky K. Lymphocyte populations and immune responses in CD5-deficient mice. *Eur J Immunol.* 1994;24:1678-1684.[\[Medline\]](#) [\[Order article via Infotrieve\]](#)
39. Qiao JH, Castellani LW, Fishbein MC, Lusis AJ. Immune complex-mediated vasculitis increases coronary artery lipid accumulation in autoimmune-prone MRL mice. *Arterioscler Thromb.* 1993;13:932-943.[\[Abstract\]](#)
40. McMurray HF, Parthasarathy S, Steinberg D. Oxidatively modified low density lipoprotein is a chemoattractant for human T-lymphocytes. *J Clin Invest.* 1993;92:1004-1008.[\[Medline\]](#) [\[Order article via Infotrieve\]](#)
41. Daugherty A, Roselaar SE. Lipoprotein oxidation as a mediator of atherogenesis: insights from pharmacological studies. *Cardiovasc Res.* 1995;29:297-311.[\[Medline\]](#) [\[Order article via Infotrieve\]](#)
42. Hansson GK, Seifert PS, Olsson G, Bondjers G. Immunohistochemical detection of macrophages and T lymphocytes in atherosclerotic lesions of cholesterol-fed rabbits. *Arterioscler Thromb.* 1991;11:745-750.[\[Abstract\]](#)
43. Drew AF, Tipping PG. T helper cell infiltration and foam cell proliferation are early events in the development of atherosclerosis in cholesterol-fed rabbits. *Arterioscler Thromb Vasc Biol.* 1995;15:1563-1568.[\[Abstract/Free Full Text\]](#)
44. Haraoka S, Shimokama T, Watanabe T. Participation of T lymphocytes in atherogenesis: sequential and quantitative observation of aortic lesions of rats with diet-induced hypercholesterolaemia using en face double immunostaining. *Virchows Arch.* 1995;426:307-315.[\[Medline\]](#) [\[Order article via Infotrieve\]](#)
45. Okano Y, Macy M, Cardin AD, Harmony JAK. Suppression of lymphocyte activation by plasma lipoproteins: modulation by cell number and type. *Exp Cell Biol.* 1985;53:199-212.[\[Medline\]](#) [\[Order article via Infotrieve\]](#)

46. Pepe MG, Curtiss LK. Apolipoprotein E is a biologically active constituent of the normal immunoregulatory lipoprotein, LDL-In. *J Immunol.* 1986;136:3716-3723.  
[\[Abstract/Free Full Text\]](#)
47. Mistry MJ, Clay MA, Kelly ME, Steiner MA, Harmony JAK. Apolipoprotein E restricts interleukin-dependent T lymphocyte proliferation at the G1<sub>A</sub>/G1<sub>B</sub> boundary. *Cell Immunol.* 1995;160:14-23.  
[\[Medline\]](#) [\[Order article via Infotrieve\]](#)
48. Werb Z, Chin JR. Onset of apoprotein E secretion during differentiation of mouse bone marrow-derived mononuclear phagocytes. *J Cell Biol.* 1983;97:1113-1118.  
[\[Abstract\]](#)
49. Brand K, Mackman N, Curtiss LK. Interferon- $\gamma$  inhibits macrophage apolipoprotein E production by posttranslational mechanisms. *J Clin Invest.* 1993;91:2031-2039.  
[\[Medline\]](#) [\[Order article via Infotrieve\]](#)
50. Mazzone T, Gump H, Diller P, Getz GS. Macrophage free cholesterol content regulates apolipoprotein E synthesis. *J Biol Chem.* 1987;262:11657-11662.  
[\[Abstract/Free Full Text\]](#)



## Anti-atherosclerotic effect of simvastatin depends on the presence of apolipoprotein E

Yi-Xin (Jim) Wang <sup>a,\*</sup>, Baby Martin-McNulty <sup>a</sup>, Ling-Yuh Huw <sup>b</sup>, Valdeci da Cunha <sup>a</sup>, Joe Post <sup>a</sup>, Josephine Hinchman <sup>a</sup>, Ronald Vergona <sup>a</sup>, Mark E. Sullivan <sup>a</sup>, William Dole <sup>b</sup>, Katalin Kauser <sup>b</sup>

<sup>a</sup> Department of Pharmacology, Berlex Biosciences, P.O. Box 4099, 15049 San Pablo Avenue 15049 San Pablo Avenue, Richmond, CA 94804-0099, USA

<sup>b</sup> Department of Cardiovascular Research, Berlex Biosciences, PO Box Richmond, CA 94804, USA

Received 19 June 2001; received in revised form 19 July 2001; accepted 2 August 2001

### Abstract

Low density lipoprotein receptor deficient (LDLR-KO) and apolipoprotein E deficient (apo E-KO) mice both develop hyperlipidemia and atherosclerosis by different mechanisms. The aim of the present study was to compare the effects of simvastatin on cholesterol levels, endothelial dysfunction, and aortic lesions in these two models of experimental atherosclerosis. Male LDLR-KO mice fed a high cholesterol (HC; 1%) diet developed atherosclerosis at 8 months of age with hypercholesterolemia. The addition of simvastatin (300 mg/kg daily) to the HC diet for 2 more months lowered total cholesterol levels by ~57% and reduced aortic plaque area by ~15% compared with the LDLR-KO mice continued on HC diet alone,  $P < 0.05$ . Simvastatin treatment also improved acetylcholine (ACh)-induced endothelium-dependent vasorelaxation in isolated aortic rings, which was associated with an increase in NOS-3 expression by ~88% in the aorta measured by real time polymerase chain reaction (PCR),  $P < 0.05$ . In contrast, in age-matched male apo E-KO mice fed a normal diet, the same treatment of simvastatin elevated serum total cholesterol by ~35%, increased aortic plaque area by ~15%, and had no effect on endothelial function. These results suggest that the therapeutic effects of simvastatin may depend on the presence of a functional apolipoprotein E. © 2002 Elsevier Science Ireland Ltd. All rights reserved.

**Keywords:** HMG-CoA reductase inhibitor; Atherosclerotic plaque; Cholesterol; Endothelial dysfunction; NOS-3; Apo E-knockout; LDLR-knockout; Mouse

### 1. Introduction

Hypercholesterolemia is a major risk factor for development of atherosclerotic vascular disease [1]. Hydroxy-methylglutaryl-coenzyme A (HMG CoA) reductase inhibitors (statins) lower cholesterol and reduce cardiovascular morbidity and mortality in patients with atherosclerosis [2–4]. A growing data base suggests that the beneficial actions of statins may be due to direct effects on the vascular wall in addition to lipid lowering. Moreover, atherosclerosis is often

accompanied by endothelial dysfunction due to impaired endothelial nitric oxide (NO) production [5–8]. Statins have been shown to restore endothelial function by restoring NO-mediated vasodilation in hyperlipidemic rabbits [9] and in patients with coronary artery disease [10,11]. This improvement in endothelial function contributes to the cardiovascular benefits achieved by statin treatment.

Low density lipoprotein receptor deficient (LDLR-KO) and apolipoprotein E deficient (apo E-KO) mice have been used to study mechanisms of atherogenesis [12,13]. It has been shown that simvastatin lowers lipid levels in LDLR-KO [14], but not in apo E-KO [15] mice. The present study was to compare the effect of simvastatin on atherosclerosis development be-

\* Corresponding author. Tel.: +1-510-669-4489; fax: +1-510-669-4247.

E-mail address: jim\_wang@berlex.com (Y.-X.J. Wang).

tween the two animal models of atherosclerosis. In addition, the effects of simvastatin on endothelial function and endothelial nitric oxide synthase (NOS-3) were also examined.

## 2. Methods

### 2.1. Animals and experimental design

Two-month-old male LDLR-KO mice (Jackson Laboratories, Bar Harbor, ME) were fed a high cholesterol (HC; 1%) diet for 8 months. At 10 months of age the animals developed moderate atherosclerotic lesions in the aorta ( $35 \pm 3\%$ ) accompanied by hypercholesterolemia ( $591 \pm 75$  mg/dl). They were then randomly divided into three groups, control group; continued on a HC diet; simvastatin group; fed a HC diet supplemented with 0.15% simvastatin (HC + SIM); and regular diet (RD) group, withdrawn from the HC diet and fed a regular chow diet. The above treatments were continued for 2 months.

Apo E-KO mice spontaneously develop hypercholesterolemia and atherosclerosis without the need for a cholesterol supplementation. For the present studies, 10-month-old male apo E-KO mice (Jackson Laboratories, Bar Harbor, ME) were used. One group of mice were fed a grain-based rodent diet (Bio-Serv, NJ) as controls and the other was on the same diet supplemented with 0.15% simvastatin for 1–3 months. The daily dose of simvastatin in both LDLR-KO and apo E mice was approximately 300 mg/kg, which has been shown to effectively reduce cholesterol by 37% in LDLR-KO mice [14].

At the end of the treatment period, all animals were fasted overnight and euthanized. Blood samples were collected via cardiac puncture at the time of death. Total serum cholesterol, triglycerides and high density lipoprotein (HDL) levels were determined enzymatically (performed by IDEXX, West Sacramento, CA). LDL values were calculated from total cholesterol and HDL levels. The aortae were isolated for measurements of atherosclerotic lesion area, vascular reactivity, and NOS-3 mRNA expression.

### 2.2. Measurement of atherosclerotic plaque

The aortae were isolated, cleaned from the adherent connective tissue, fixed with 10% formalin, cut open longitudinally and pinned on black wax-coated petri dishes as previously described in detail [5]. Atherosclerotic plaque area is visible without staining. The images of the open luminal surface of the aortae were recorded at a resolution of  $512 \times 512$  using a

RGB 3-chip CCD digital camera (Sony) mounted on a dissecting microscope (Nikon SMZ-2T) attached to a computer in 24 bit true image format. The images were analyzed using C-Simple software (C. Imaging 1208, Compix, Mars, PA). Atherosclerotic plaque area was quantified and expressed as a percentage of total luminal surface area of the aorta.

### 2.3. Assessment of vascular reactivity

The thoracic aortae were dissected, cleaned from the adherent connective tissue, and placed in a HEPES-buffered solution containing (in mM), 140 NaCl; 4.5 KCl; 1.0  $\text{MgCl}_2$ ; 5.5 glucose; 1.5  $\text{CaCl}_2$ ; and 10 HEPES at pH 7.4 and 20 °C. The aortae were cut into four rings and were placed in organ-bath chambers containing 15 ml of Krebs solution with the following composition (in mM), 118 NaCl; 24.9  $\text{NaHCO}_3$ ; 4.7 KCl; 1.18  $\text{KH}_2\text{PO}_4$ ; 1.66  $\text{MgSO}_4$ ; 5.55 glucose; 2.0 Na-pyruvate; and 2.0  $\text{CaCl}_2$ . The solution was continually bubbled with a 5%  $\text{CO}_2$  and 95%  $\text{O}_2$  gas mixture and maintained at pH 7.4 and 37 °C. Vessels were pre-treated with indomethacin ( $10^{-5}$  M) for 30 min to inhibit cyclooxygenase mediated vascular effects and pre-contracted with KCl (40 mM), and washed with Krebs solution. Aortic rings were then stretched to 500 mg tension and allowed to equilibrate for 2 h prior to initiation of the experimental protocol. Tension measurements were recorded using Grass force-transducers connected to a data acquisition system (MP100 WS, Biopac, Goleta, CA). Data were digitized on-line at a rate of 1 sample per s and subsequently analyzed using Acknowledge software. Concentration response curves to U46619 (9,11-dideoxy-9 $\alpha$ , 11 $\alpha$ -methanoepoxy prostaglandin  $F_{2\alpha}$ ), a thromboxane receptor agonist, were then generated. The calculated concentration of U46619 that produced 80% of the maximal contractile response ( $\text{EC}_{80}$ ) was 20 nM. Endothelium-mediated relaxation was measured as the response to acetylcholine (ACh; 0.01 nM–10  $\mu\text{M}$ ) in rings pre-contracted with U-46619 (30 nM). In the LDLR-KO mice, endothelium-independent aortic ring relaxation was also measured as the response to sodium nitroprusside (SNP, 0.001–1  $\mu\text{M}$ ).

### 2.4. Measurement of NOS-3 mRNA

The isolated aortae were homogenized in 600  $\mu\text{l}$  RLT buffer (Qiagen) using disposable generator probes (Omni International). Total RNA was then isolated using a RNeasy kit with DNase I digestion (Qiagen). Relative abundance of NOS-3 and internal control GAPDH were measured by real-time quantitative polymerase chain reaction (PCR) performed on an ABI PRISM 7700 Sequence Detector (PE Biosys-

tems). One-step reverse transcriptase (RT)-PCR amplification of NOS-3 was carried out in a 50  $\mu$ l reaction mixture consisting of 1  $\times$  TaqMan buffer A with the following composition (mM), 5.5 MgCl<sub>2</sub>; 0.3 dATP; 0.3 dCTP; 0.3  $\mu$ M dGTP; 0.3 dUTP; 0.025 U/ $\mu$ l AmpliTaq Gold DNA polymerase, 0.025 U/ $\mu$ l RNase inhibitor, 0.025 U/ $\mu$ l multiscribe RT, 200 nM of each primer, and 100 nM probe. Thermal cycle conditions were 48 °C for 30 min and 95 °C for 10 min followed by 40 cycles at 95 °C for 15 s and 60 °C for 1 min. Primers and the probe for NOS-3 were, upper primer, 5'-CGTCATCGGCGTGCT-3' (nt 3436–3450), lower primer, 5'-ACCTCCTGGGTGCGC-3' (nt 3510–3496), and the probe, 5'-6FAM-CGGGATCAGCAACGCTACCA-TAMRA-3' (nt 3452–3471). Primers and TaqMan probe for rodent GAPDH were purchased from PE Biosystems (P/N 4308313). Hundred nanomol of each primer and 200 mM of the probe were used in the reaction. The expressions of NOS-3 and GAPDH were calculated against a standard curve with serial dilution of total RNA from murine hemangioendothelioma (EOMA) cells [16]. The experiment was repeated twice in triplicate for each sample. Values presented here are the ratio of NOS-3/GAPDH.

### 2.5. Statistics

All results are presented as the mean  $\pm$  S.E.M. for the number of animals (*n*) indicated. Multiple comparisons of mean values were performed by analysis of variance (ANOVA) followed by a subsequent Student–Newman–Keuls test for repeated measures. Differences were considered to be statistically significant when the *P* value was <0.05. The statistical analysis was performed using Statistica software (STATSOFT, Tulsa, OK).

## 3. Results

### 3.1. Effects of simvastatin in LDLR-KO mice

LDLR-KO mice fed a HC diet for 10 months had hypercholesterolemia and developed atherosclerotic lesions in the aorta (Fig. 1). Treatment with simvastatin (HC + SIM) decreased serum LDL cholesterol with no significant effects on HDL cholesterol or triglycerides levels (Table 1). As a result, the ratio of HDL/LDL was significantly higher in the HC + SIM compared with the HC group (Table 1). Simvastatin also reduced atherosclerotic lesion area by ~15%, compared with that in the HC group (Fig. 1). Mice given the regression diet for 2 months showed similar changes in lipid profiles and atherosclerotic lesions as were seen following simvastatin treatment (Table 1

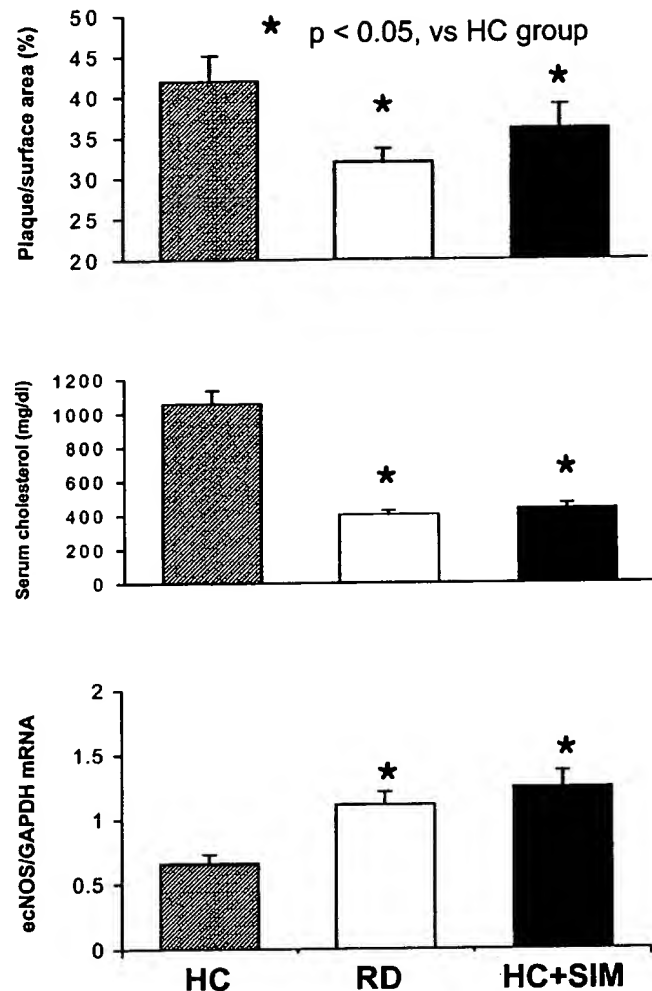


Fig. 1. Aortic atherosclerotic lesion area (top, *n* = 8 per group), total serum cholesterol levels (middle, *n* = 11 per group), and NOS-3 mRNA expression in the aorta (bottom, *n* = 3 per group) of the LDLR-KO mice fed a HC diet without or with (HC + SIM) the supplementation of simvastatin (300 mg/kg, daily), or withdrawn from a HC diet and fed a RD, for 2 months.

and Fig. 1). Combining the data from all three groups, aortic atherosclerotic lesion area was positively correlated to total serum cholesterol levels and negatively correlated to the ratio of HDL/LDL (Fig. 2).

Table 1  
Effects of simvastatin and diet on serum lipid profile (mg/dl) in LDLR-KO mice (*n* = 11 per group)

	HC	RD	HC+SIM
LDL	917 $\pm$ 80	256 $\pm$ 19**	322 $\pm$ 27**
HDL	98 $\pm$ 6	102 $\pm$ 8	77 $\pm$ 6
HDL/LDL	0.12 $\pm$ 0.01	0.38 $\pm$ 0.04**	0.24 $\pm$ 0.03**
Triglyceride	213 $\pm$ 16	226 $\pm$ 19	175 $\pm$ 21

\*, *P*, 0.05; \*\*, *P* < 0.01; vs. HC.

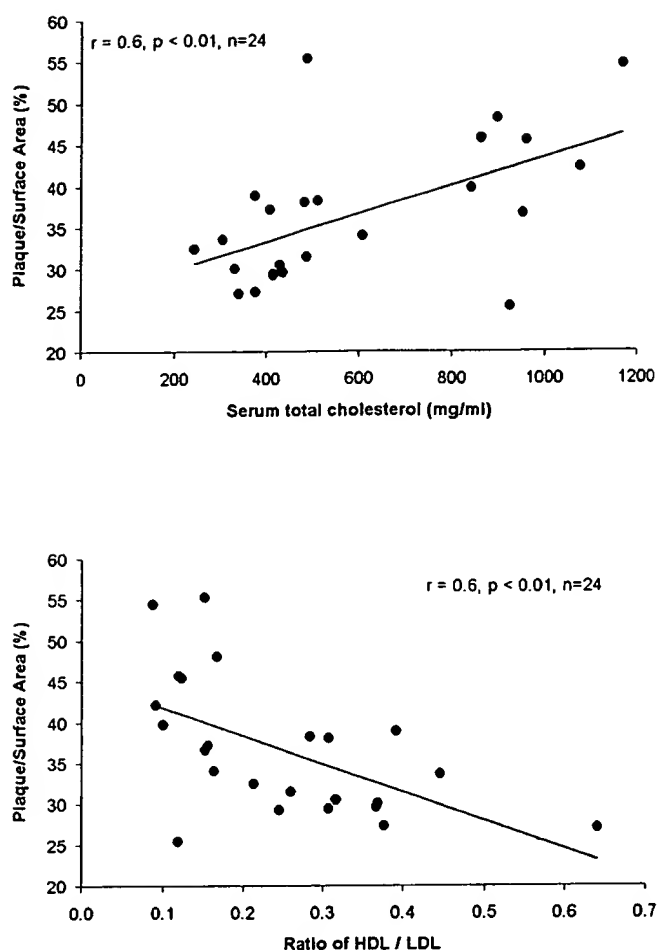


Fig. 2. The aortic atherosclerotic lesion area was positively correlated to the total circulating cholesterol levels (top) and negatively correlated to the ratio of HDL/LDL in the LDLR-KO mice. The data included all three groups of the mice fed a HC diet without or with (HC + SIM) the supplementation of simvastatin (300 mg/kg, daily), or withdrawn from a HC diet and fed a RD, for 2 months.

ACh-induced endothelial NO-mediated aortic relaxation was significantly greater in both the HC + SIM and RD groups than that in the HC group (Fig. 3A). Thus, the maximum responses were significantly greater in both the HC + SIM and RD groups than that in the HC group (Table 2). Endothelium-independent relaxation to SNP did not significantly differ among the three groups (Fig. 3B and Table 3). The expression of NOS-3 mRNA was significantly higher in both the HC + SIM and RD groups than the expression levels in the HC group (Fig. 1).

### 3.2. Effects of simvastatin in apo E-KO mice

Age-matched apo E-KO mice fed a RD had hypercholesterolemia and developed atherosclerotic lesions in the aorta, which tended to increase over time (Fig. 4). Serum total and LDL cholesterol levels were higher and HDL cholesterol levels lower in the simvastatin than in the control group (Fig. 4 and Table 3). As a result of these changes, the ratio of HDL/LDL was significantly lower in the simvastatin than the control group. Triglyceride levels were not significantly different between the two groups. Aortic lesion area was greater in the simvastatin than control group (Fig. 4). Combining the data from both groups at all time points, aortic atherosclerotic lesion area was positively correlated to total serum cholesterol levels and negatively correlated to the ratio of HDL/LDL (Fig. 5).

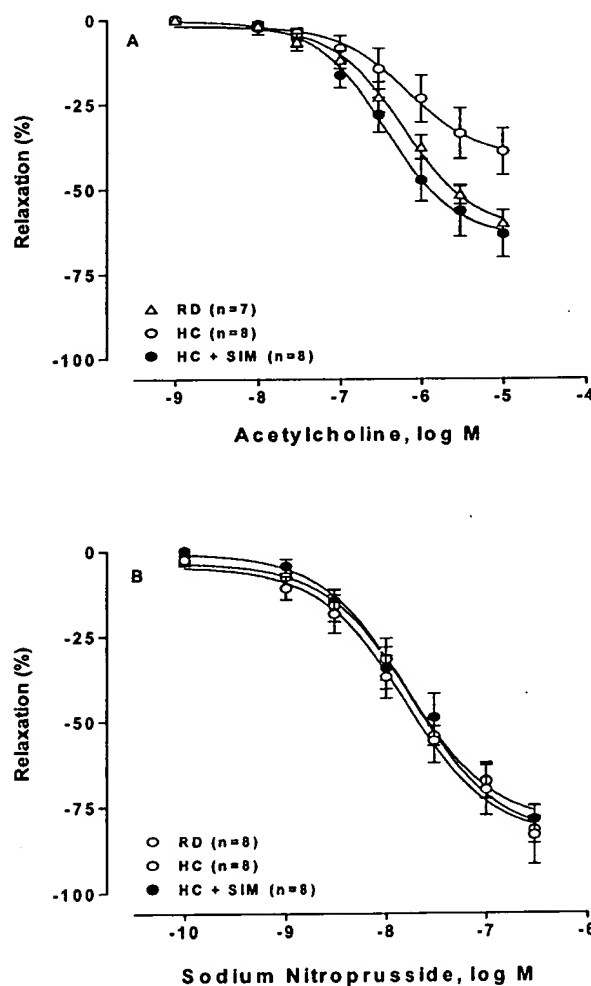


Fig. 3. Concentration-response curves of ACh (A) or SNP (B) induced relaxation in the aortic rings isolated from LDLR-KO mice fed a HC diet without or with (HC + SIM) the supplementation of simvastatin (300 mg/kg, daily), or withdrawn from a HC diet and fed a RD, for 2 months.

Table 2

Sensitivity ( $\log EC_{50}$ ,  $pD_2$ ) and maximal response ( $E_{max}$ ) to ACh and SNP in isolated aortae from LDLR-KO mice fed a RD, HC diet without or with simvastatin (HC+SIM)

Groups	N	ACh		SNP	
		$pD_2$	$E_{max}$ (%)	$pD_2$	$E_{max}$ (%)
HC	8	$6.17 \pm 0.20$	$39.2 \pm 6.8^a$	$7.74 \pm 0.18$	$81.8 \pm 3.8$
RD	7	$6.2 \pm 0.16$	$60.2 \pm 3.6$	$7.8 \pm 0.21$	$83.3 \pm 8.5$
HC+SIM	8	$6.45 \pm 0.11$	$63.4 \pm 6.9$	$7.79 \pm 0.22$	$78.8 \pm 4.2$

<sup>a</sup>  $P < 0.05$  vs. RD group.

ACh-induced relaxation of the aortae isolated from apo E-KO mice were not significantly different between the simvastatin and control groups at both the 2 and 3 months time points (Fig. 6 and Table 4).

#### 4. Discussion

The major findings of the present study are that simvastatin has opposite effects on serum lipids and atherosclerosis in two different genetic mouse model of atherosclerosis. In the LDLR-KO mice, simvastatin decreased serum cholesterol levels and aortic lesion area. These changes were associated with an improvement in endothelial NO-dependent vasorelaxation and an increased NOS-3 mRNA expression. In contrast, in the apo E-KO mice, the same treatment with simvastatin increased serum cholesterol levels and aortic lesion area, with no changes in endothelial NO-mediated vasorelaxation.

Table 3

Effects of simvastatin on serum lipid profiles (mg/dl) in apo E-KO mice ( $n = 7$ –12 per group)

Treatment (month)	Vehicle	Simvastatin
<b>LDL**</b>		
1	$463 \pm 55$	$630 \pm 41$
2	$474 \pm 42$	$727 \pm 39$
3	$462 \pm 46$	$605 \pm 42$
<b>HDL*</b>		
1	$70 \pm 6$	$59 \pm 4$
2	$88 \pm 10$	$51 \pm 6$
3	$100 \pm 5$	$48 \pm 6$
<b>HDL/LDL*</b>		
1	$0.16 \pm 0.01$	$0.10 \pm 0.01$
2	$0.19 \pm 0.02$	$0.07 \pm 0.01$
3	$0.26 \pm 0.05$	$0.08 \pm 0.01$
<b>Triglycerides</b>		
1	$193 \pm 32$	$198 \pm 48$
2	$173 \pm 19$	$141 \pm 7$
3	$158 \pm 21$	$109 \pm 8$

\*,  $P < 0.05$ ; \*\*,  $P < 0.01$  between two groups.

These data indicate that an intact functional apolipoprotein E may be essential for the lipid lowering, anti-atherosclerosis and other therapeutic benefits of simvastatin.

#### 4.1. Effects of simvastatin on hypercholesterolemia

In the present study, simvastatin at a daily dose of 300 mg/kg significantly reduced total cholesterol by

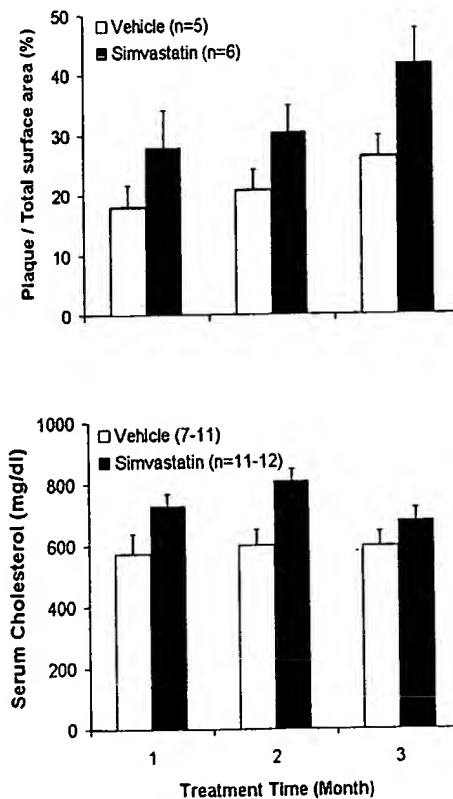


Fig. 4. Atherosclerotic lesion area in the aorta (top) and total serum cholesterol levels (bottom) of the apo E-KO mice treated with simvastatin (300 mg/kg, daily) or vehicle for 1–3 months.  $P < 0.05$  between the simvastatin and vehicle treatment group for both the plaque area and total serum cholesterol levels.

57% in LDLR-KO mice fed a HC diet. This result is consistent with a previous report by Bisgaier et al., who reported that at the same daily dose, simvastatin reduced total circulating cholesterol by 37% in LDLR-KO mice [14]. The magnitude of cholesterol lowering by simvastatin was also similar to that observed in untreated LDLR-KO mice fed a regression diet for 2 months. In contrast, the same dose of simvastatin resulted in a 27% increase in serum cholesterol in apo E-KO mice. This finding is consistent with that of Quarfordt et al., who also reported that lovastatin (50 mg/kg daily) increased circulating cholesterol by 70% in apo E-KO mice, but not in wild-type controls [15]. These results suggest that the lipid lowering effect of statins may depend on the presence of intact apolipoprotein E, which functions to transport circulating cholesterol into cells, particularly hepatocytes and acts as an important mediator

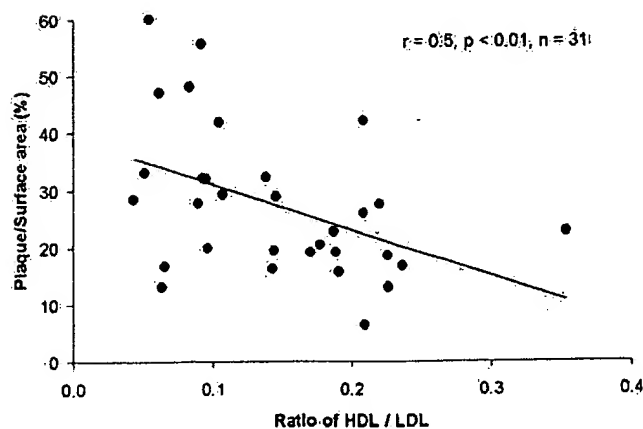
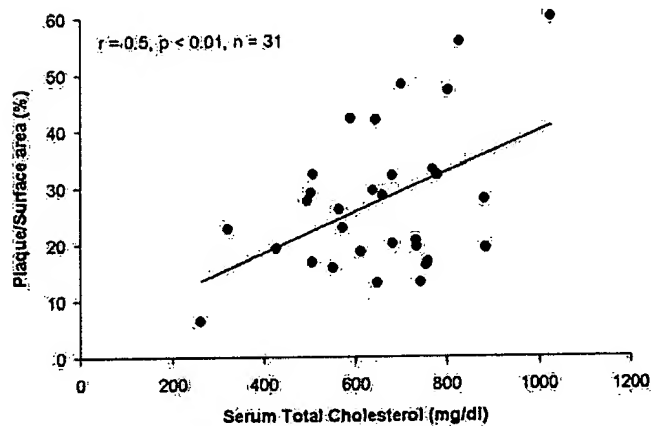


Fig. 5. The aortic atherosclerotic lesion area was positively correlated to the total circulating cholesterol levels (top) and negatively correlated to the ratio of HDL/LDL in the apo E-KO mice. The data included all groups of mice treated with simvastatin (300 mg/kg, daily) or vehicle for 1–3 months.

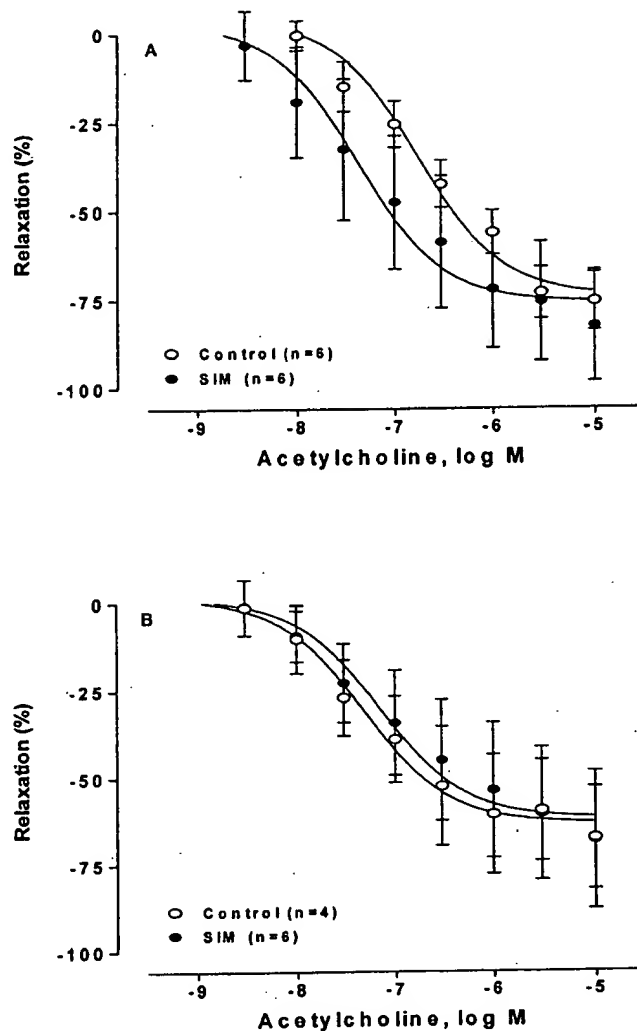


Fig. 6. Concentration–response curves of ACh-induced relaxation of the aortic rings isolated from apo E-KO mice treated with simvastatin (300 mg/kg per day) or vehicle for 2 (top) and 3 (bottom) months.

for hepatic metabolic clearance of circulating cholesterol [12]. In the absence of the apolipoprotein E, hepatic clearance and metabolism of cholesterol are reduced, resulting in hypercholesterolemia [12,13,17]. Impairment of hepatic cholesterol transport may also result in up-regulation of cholesterol synthesis [18]. Indeed, lovastatin has been reported to increase the expression of HMG CoA reductase mRNA [19] and protein [20], thereby increasing cholesterol synthesis [15] in apo E-KO mice, but not in wild-type controls. This may explain the paradoxical elevation of cholesterol in simvastatin-treated apo E-KO mice.

#### 4.2. Effects of simvastatin on atherosclerosis

Accompanied by its lipid lowering effect, simvastatin significantly reduced aortic atherosclerotic

Table 4  
Sensitivity ( $\log EC_{50}$ ,  $pD_2$ ) and maximal response ( $E_{max}$ ) to ACh and SNP in isolated aortae from apo E-KO mice treated without (control) or with simvastatin for 2 or 3 months

Groups	Duration					
	Two months			Three months		
	<i>N</i>	$pD_2$	$E_{max}$ (%)	<i>N</i>	$pD_2$	$E_{max}$ (%)
Control	6	$6.75 \pm 0.27$	$75.8 \pm 8.2$	4	$7.31 \pm 0.20$	$67.5 \pm 14.7$
Simvastatin	6	$7.37 \pm 0.34$	$82.6 \pm 15.7$	6	$7.15 \pm 0.32$	$68.0 \pm 19.8$

plaque area in LDLR-KO mice. In contrast, simvastatin accelerated atherosclerosis that accompanied an elevation of serum cholesterol levels in apo E-KO mice. Hypercholesterolemia is an important risk factor leading to atherosclerosis. Animals with hypercholesterolemia, resulting from either a HC diet [21–23] or from inherited defects in lipid metabolism [5–7], develop atherosclerotic plaques in the vascular wall. Therefore, the reduction in atherosclerotic lesions by simvastatin in LDLR-KO mice can be explained by its lipid lowering effect, since similar reduction in serum cholesterol and aortic lesion area were observed in untreated mice fed a RD. On the other hand, the increase in atherosclerosis by simvastatin in apo E-KO mice could be explained by elevated serum lipids. This is consistent with a previous report that feeding a HC diet to apo E-KO mice further exacerbated hypercholesterolemia and accelerated lesion development [24]. HDL is known to be involved in reversing cholesterol transport from the vascular wall [25,26]. Therefore, elevation of HDL/LDL ratio by simvastatin in LDLR-KO mice could also contribute to its anti-atherosclerotic effect. Likewise, reduction of HDL/LDL ratio by simvastatin in apo E-KO mice could contribute to acceleration of atherosclerosis. The fact that aortic lesions correlated positively to the total serum cholesterol levels and negatively to the HDL/LDL ratio in both the LDLR-KO and apo E-KO mice support the above view.

#### 4.3. Effect of simvastatin on endothelial function

Endothelial dysfunction, characterized by reduced NO-dependent vascular relaxation, is an early marker of atherosclerosis [27]. Endothelial function is impaired in a number of experimental models of atherosclerosis, including hyperlipidemic rabbits [9] and apo E-KO mice [5], as well as in patients with atherosclerosis [8]. Statins have been shown to reverse endothelial dysfunction in hyperlipidemic rabbits [9] and in humans [10,11]. This effect of statins has been attributed to stabilization of NOS-3 mRNA leading

to the increase in NOS-3 expression [28,29]. Indeed, in the present study, simvastatin treatment significantly increased the expression of NOS-3 mRNA in the aorta of LDLR-KO mice. This was associated with enhanced ACh-induced endothelial NO dependent vasorelaxation. Although there is strong evidence that direct effect on NOS-3 expression is the underlying mechanism for the improvement in endothelial function, the present study was not designed to determine the mechanism of action of simvastatin on NOS-3 and can not differentiate direct effects on the vascular wall from secondary effects due to changes in serum lipids. In apo E-KO mice, on the other hand, the potential direct beneficial effect of simvastatin on endothelial function could be masked or compromised by increased cholesterol levels and atherosclerosis. This may explain the lack of significant effect of simvastatin treatment on ACh-induced NO-dependent aortic ring relaxation in the apo E-KO mice.

During the preparation of this manuscript, Sparrow et al. published a paper demonstrating both anti-inflammatory and anti-atherosclerotic activities of simvastatin in apo E-KO mice [30]. In that study, simvastatin had no significant effect on circulating cholesterol levels. The apo E-KO mice were fed a HC diet, which resulted in a very high circulating cholesterol levels ( $\sim 1000$  mg/dl) and severe atherosclerosis in the aorta. The apo E-KO mice in the present study were fed a RD, resulting in moderate hyperlipidemia with serum cholesterol levels at  $\sim 500$  mg/dl and a less severe atherosclerosis. These differences in the diet and circulating lipid levels, as well as the severity of atherosclerosis, may contribute, at least in part, to the different results.

In summary, the present study demonstrates that in LDLR-KO mice, treatment with simvastatin for 2 months significantly decreased serum cholesterol levels, improved endothelial function, and reduced atherosclerosis. In contrast, in apo E-KO mice, the same treatment of simvastatin elevated serum cholesterol levels and increased atherosclerosis with no effect on endothelial function. Thus, the beneficial



effects of statins may depend on the presence of functional apolipoprotein E. It has to be pointed out that the mechanisms involved in atherosclerosis induction in these animal models are different. In LDLR-KO mice, it is diet-induced, while in apo E-KO mice, it is primarily due to 'genetics'. This difference may also explain the different effects observed regarding endothelial function. Thus, whether the current findings can be applied to human, as they are less dependent on apo E for the catabolism of LDL, is a new pharmacogenetic topic that needs to be further studied.

### Acknowledgements

The authors would like to thank the Animal Care Group under the direction of William Lillis for proper care and feeding the animals over the duration of these studies. We also would like to thank Merck & Co., Inc. for kindly providing simvastatin. During the period of these experiments, Valdeci da Cunha, as a visiting scientist at Berlex Biosciences from Federal University of Espirito Santo, Brazil, was supported by CAPES (0680/98-2).

### References

- [1] Anderson KM, Castelli WP, Levy D. Cholesterol and mortality. Thirty years of follow-up from the Framingham study. *J Am Med Assoc* 1987;257:2176–80.
- [2] Jones P, Kafonek S, Laurora I, Hunninghake D. Comparative dose efficacy study of atorvastatin versus simvastatin, pravastatin, lovastatin, and fluvastatin in patients with hypercholesterolemia (the CURVES study; see comments). *Am J Cardiol* 1998;81:582–7 [published erratum appears in *Am J Cardiol* 1998;82(1):128].
- [3] Dart A, Jerums G, Nicholson G, d'Emden M, Hamilton-Craig I, Tallis G, Best J, West M, Sullivan D, Bracs P, Black D. A multicenter, double-blind, 1-year study comparing safety and efficacy of atorvastatin versus simvastatin in patients with hypercholesterolemia (see comments). *Am J Cardiol* 1997;80:39–44.
- [4] Bertolini S, Bon GB, Campbell LM, Farnier M, Langan J, Mahla G, Pauciullo P, Sirtori C, Egros F, Fayyad R, Nawrocki JW. Efficacy and safety of atorvastatin compared to pravastatin in patients with hypercholesterolemia. *Atherosclerosis* 1997;130:191–7.
- [5] Wang YX, Halks-Miller M, Vergona R, Sullivan ME, Fitch R, Mallari C, Martin-McNulty B, da Cunha V, Freay A, Rubanyi GM, Kauser K. Increased aortic stiffness assessed by pulse wave velocity in apolipoprotein E-deficient mice. *Am J Physiol Heart Circ Physiol* 2000;278:H428–34.
- [6] Rosenfeld ME, Tsukada T, Gown AM, Ross R. Fatty streak initiation in Watanabe Heritable Hyperlipemic and comparably hypercholesterolemic fat-fed rabbits. *Arteriosclerosis* 1987;7:9–23.
- [7] Rosenfeld ME, Tsukada T, Chait A, Bierman EL, Gown AM, Ross R. Fatty streak expansion and maturation in Watanabe Heritable Hyperlipemic and comparably hypercholesterolemic fat-fed rabbits. *Arteriosclerosis* 1987;7:24–34.
- [8] Anderson TJ, Gerhard MD, Meredith IT, Charbonneau F, Delagrangé D, Creager MA, Selwyn AP, Ganz P. Systemic nature of endothelial dysfunction in atherosclerosis. *Am J Cardiol* 1995;75:71B–4B.
- [9] Senaratne MP, Thomson AB, Kappagoda CT. Lovastatin prevents the impairment of endothelium dependent relaxation and inhibits accumulation of cholesterol in the aorta in experimental atherosclerosis in rabbits. *Cardiovasc Res* 1991;25:568–78.
- [10] Anderson TJ, Meredith IT, Yeung AC, Frei B, Selwyn AP, Ganz P. The effect of cholesterol-lowering and antioxidant therapy on endothelium-dependent coronary vasomotion (see comments). *New Engl J Med* 1995;332:488–93.
- [11] Treasure CB, Klein JL, Weintraub WS, Talley JD, Stillabower ME, Kosinski AS, Zhang J, Boccuzzi SJ, Cedarholm JC, Alexander RW. Beneficial effects of cholesterol-lowering therapy on the coronary endothelium in patients with coronary artery disease (see comments). *New Engl J Med* 1995;332:481–7.
- [12] Breslow JL. Mouse models of atherosclerosis. *Science* 1996;272:685–8.
- [13] Zhang SH, Reddick RL, Piedrahita JA, Maeda N. Spontaneous hypercholesterolemia and arterial lesions in mice lacking apolipoprotein E. *Science* 1992;258:468–71.
- [14] Bisgaier CL, Essenburg AD, Auerbach BJ, Pape ME, Sekerke CS, Gee A, Wolle S, Newton RS. Attenuation of plasma low density lipoprotein cholesterol by select 3-hydroxy-3-methylglutaryl coenzyme A reductase inhibitors in mice devoid of low density lipoprotein receptors. *J Lipid Res* 1997;38:2502–15.
- [15] Quarfordt SH, Oswald B, Landis B, Xu HS, Zhang SH, Maeda N. In vivo cholesterol kinetics in apolipoprotein E-deficient and control mice. *J Lipid Res* 1995;36:1227–35.
- [16] Obeso J, Weber J, Auerbach R. A hemangioendothelioma-derived cell line: its use as a model for the study of endothelial cell biology. *Lab Invest* 1990;63:259–69.
- [17] Ghiselli G, Schaefer EJ, Gascon P, Breser HB Jr. Type III hyperlipoproteinemia associated with apolipoprotein E deficiency. *Science* 1981;214:1239–41.
- [18] Siperstein MD, Guest JM. Studies on the homeostatic control of cholesterol synthesis. *J Clin Invest* 1959;38:1043–4.
- [19] Pitman WA, Osgood DP, Smith D, Schaefer EJ, Ordovas JM. The effects of diet and lovastatin on regression of fatty streak lesions and on hepatic and intestinal mRNA levels for the LDL receptor and HMG CoA reductase in F1B hamsters. *Atherosclerosis* 1998;138:43–52.
- [20] Bilhartz LE, Spady DK, Dietschy JM. Inappropriate hepatic cholesterol synthesis expands the cellular pool of sterol available for recruitment by bile acids in the rat. *J Clin Invest* 1989;84:1181–7.
- [21] Nascimento CA, Kauser K, Rubanyi GM. Effect of 17 $\beta$ -estradiol in hypercholesterolemic rabbits with severe endothelial dysfunction. *Am J Physiol* 1999;276:H1788–94.
- [22] Masuda J, Ross R. Atherogenesis during low level hypercholesterolemia in the nonhuman primate. II. Fatty streak conversion to fibrous plaque. *Arteriosclerosis* 1990;10:178–87.
- [23] Masuda J, Ross R. Atherogenesis during low level hypercholesterolemia in the nonhuman primate. I. Fatty streak formation. *Arteriosclerosis* 1990;10:164–77.
- [24] van Ree JH, van den Broek WJ, Dahlmans VE, Groot PH, Vidgeon-Hart M, Frants RR, Wieringa B, Havekes LM, Hofker MH. Diet-induced hypercholesterolemia and atherosclerosis in heterozygous apolipoprotein E-deficient mice. *Atherosclerosis* 1994;111:25–37.
- [25] Kannel WB, Wilson PW. Efficacy of lipid profiles in prediction of coronary disease. *Am Heart J* 1992;124:768–74.
- [26] Badimon JJ, Badimon L, Fuster V. Regression of atherosclerotic lesions by high density lipoprotein plasma fraction in the cholesterol-fed rabbit. *J Clin Invest* 1990;85:1234–41.

- [27] Harrison DG. From isolated vessels to the catheterization laboratory. Studies of endothelial function in the coronary circulation of humans. *Circulation* 1989;80:703–6.
- [28] Laufs U, La Fata V, Plutzky J, Liao JK. Upregulation of endothelial nitric oxide synthase by HMG CoA reductase inhibitors. *Circulation* 1998;97:1129–35.
- [29] Laufs U, Liao JK. Post-transcriptional regulation of endothelial nitric oxide synthase mRNA stability by Rho GTPase. *J Biol Chem* 1998;273:24266–71.
- [30] Sparrow CP, Burton CA, Hernandez M, Mundt S, Hassing H, Patel S, Rosa R, Hermanowski-Vosatka A, Wang PR, Zhang D, Peterson L, Detmers PA, Chao YS, Wright SD. Simvastatin has anti-inflammatory and anti-atherosclerotic activities independent of plasma cholesterol lowering. *Arterioscler Thromb Vasc Biol* 2001;21:115–21.



# Blockade of endothelin receptors markedly reduces atherosclerosis in LDL receptor deficient mice: role of endothelin in macrophage foam cell formation

Saeid Babaei<sup>a,b</sup>, Pierre Picard, Amir Ravandi<sup>a</sup>, Juan Carlos Monge<sup>a</sup>, Tony C. Lee<sup>a</sup>,  
Peter Cernacek<sup>c</sup>, Duncan J. Stewart<sup>a,b,\*</sup>

<sup>a</sup>Division of Cardiology, Terrence Donnelly Heart Center, St. Michael's Hospital, 30 Bond Street, Toronto, Ontario, Canada, M5B 1W8

<sup>b</sup>Departments of Medicine and of Laboratory Medicine and Pathobiology, University of Toronto, Toronto, Ontario, Canada

<sup>c</sup>Montreal Heart Institute, Department of Laboratory Medicine, Montreal, Quebec, Canada

Received 19 January 2000; accepted 7 June 2000

## Abstract

**Objective:** We evaluated the direct effects of long-term blockade of ET<sub>A</sub> and ET<sub>B</sub> receptors using a mixed endothelin (ET) receptor antagonist, LU224332, in the low density lipoprotein receptor (LDL-R) knockout mouse model of atherosclerosis. **Methods:** Four groups of LDL-R deficient mice were studied: control mice fed normal chow (group I); mice fed a high cholesterol (HC, 1.25%) diet alone (group II), HC fed animals treated with LU224332 (group III); and mice fed normal chow treated with the LU compound (group IV). All treatments were continued for 8 weeks at which time the animals were sacrificed and the aortae were removed and stained with oil red O. Atherosclerotic area (AA) was determined by quantitative morphometry and normalized relative to total aortic area (TA). **Results:** Cholesterol feeding resulted in a marked increase in total plasma cholesterol (~15 fold) and widespread aortic atherosclerosis (AA/TA: group I: 0.013±0.007; group II: 0.33±0.11;  $P<0.001$ ). Atherosclerotic lesions were characterized by immunohistochemistry as consisting mainly of macrophages which also showed high levels of ET-1 expression. Treatment with ET antagonist significantly reduced the development of atherosclerosis (AA/TA: group III: 0.19±0.07,  $P<0.01$  vs. group II), without altering plasma cholesterol levels and blood pressure. The direct effect of LU224332 on macrophage activation and foam-cell formation was determined in vitro using a human macrophage cell line, THP-1. Treatment of the THP-1 cells with LU224332 significantly reduced cholesterol ester and triacylglycerol accumulation and foam-cell formation on exposure to oxidized LDL ( $P<0.01$  and  $P<0.05$ , respectively). **Conclusion:** We conclude that a nonselective ET receptor antagonist substantially inhibited the development of atherosclerosis in a genetic model of hyperlipidemia, possibly by inhibiting macrophage foam-cell formation, suggesting a role for these agents in the treatment and prevention of atherosclerotic vascular disease. © 2000 Elsevier Science B.V. All rights reserved.

**Keywords:** Atherosclerosis; Cholesterol; Endothelins; Macrophages; Receptors

## 1. Introduction

Spontaneous mutations in the low-density lipoprotein receptor (LDL-R) gene result in severe hypercholesterolemia and atherosclerosis in Watanabe rabbits and rhesus monkeys [1], and represents the genetic basis of familial hypercholesterolemia in humans [2]. Ishibashi et al. [3] have

produced LDL-R deficient mice by targeted disruption of this gene. On high cholesterol feeding these animals exhibited marked elevations in serum cholesterol-rich lipoprotein particles including very low density lipoprotein (VLDL), intermediate density lipoprotein (IDL) and LDL, associated with massive xanthomatosis and atherosclerosis in a manner similar to patients with familial hypercholesterolemia [3].

Endothelial cells normally protect against many of the

\*Corresponding author. Tel.: +1-416-864-5724; fax: +1-416-864-5419.

E-mail address: stewartd@smh.toronto.on.ca (D.J. Stewart).

Time for primary review 22 days.

initiating events in atherosclerosis by the production of vasodilator, antithrombotic and antiproliferative factors [4] such as nitric oxide (NO), which prevents adhesion of blood elements to the endothelium including platelets and monocytes, and inhibits migration and proliferation of medial smooth muscle cells (SMCs) [5,6]. Indeed, reduced endothelium-dependent dilation and decreased bioavailability of NO is an early feature of hyperlipidemia both in experimental models [4,7] and patients [8,9], which can be improved by administration of exogenous L-arginine, the substrate for NO generation by NO synthase (NOS) [10]. Endothelial dysfunction is characterized not only by reduced release of vasodilator autacoids such as NO, but also by increased production of vasoconstrictor factors including endothelin-1 (ET-1) [11]. ET-1 is a 21-amino-acid peptide which, in addition to its powerful vasoconstrictor and hypertensive actions [12], has a number of other biological activities which are likely important in chronic vascular disorders. These include stimulation of cellular proliferation [13], synthesis of matrix proteins [14], and chemotactic effects on monocytes [15,16]. Several indirect lines of evidence support a role for ET-1 in the development of atherosclerosis [17]. OxLDL results in increased ET-1 expression in cultured endothelial cells [18] and circulating ET-1 levels are elevated in patients with atherosclerosis [19]. More relevant, perhaps, are the observations of increased ET-1 expression in human atherosclerotic lesions [20,21], associated with complications of atherosclerosis [22].

ET-1 transduces its biological effects through an interaction with two specific receptors. ET<sub>A</sub> is selective for ET-1 and is found predominantly on target cells, such as vascular SMCs [23], and mediates the vasoconstrictor [24] and pro-proliferative actions of ET-1 [25]. In contrast, in the vessel wall ET<sub>B</sub> is found mostly on the endothelial cell, and mediates the release of NO and prostacyclin [26], which serves to counteract the direct effects of ET-1 on the underlying SMCs. However, ET<sub>B</sub> can also be found to a variable degree on SMCs [27,28] and has been described as the predominant receptor of a human monocyte/macrophage cell line [29,30].

The use of selective ET<sub>A</sub> receptor blockers has been recently shown to reduce atherosclerosis [31,32] and improve endothelium-dependent vasodilation [32,33], possibly by unmasking ET<sub>B</sub>-mediated NO production in response to endogenous ET-1. Whether the use of a mixed ET<sub>A</sub> and ET<sub>B</sub> antagonist, which would not be expected to increase vascular endothelial cell NO release, would produce a similar benefit is not certain. We hypothesized that a non-selective ET receptor blocker would reduce atherosclerosis in the LDL-R deficient mouse model by direct actions on SMCs and/or macrophages, inhibiting the proatherogenic response to increased endogenous vascular ET-1 production. We now report that LU224332, a mixed ET<sub>A</sub> and ET<sub>B</sub> antagonist, substantially reduced atherosclerosis in cholesterol-fed LDL-R deficient mice, and also

inhibited the uptake of OxLDL by macrophages *in vitro*. These data provide strong evidence for a direct role of ET-1 in atherogenesis.

## 2. Methods

### 2.1. Experimental protocol

LDL-R deficient mice in the C57BL/6J background were purchased from Jackson Laboratory. Sixty male LDL-R deficient mice were entered into the study at 22 weeks of age and were maintained on a 12-h-dark–12-h-light cycle with unrestricted access to food and water for the entire length of the experimental protocol. The use and care of LDL-R deficient mice was in accordance with the Canadian Council of Animal Care guidelines and was approved by the Animal Care and Ethics Committee of St. Michael's Hospital. Animals were assigned to four experimental groups (15 mice/group) as follows: (I) control (normal diet, no treatment); (II) high cholesterol (HC) diet without pharmacological intervention; (III) HC diet with ET antagonist treatment and (IV) ET antagonist treatment in mice receiving normal diet. All mice received their specific treatment for a period of 8 weeks before being sacrificed. The ET antagonist treatment groups received LU224332 (10 mg/kg/day) in their drinking water. This compound (a generous gift of Dr. M. Kirchengast from Knoll, Ludwigshafen, Germany) has previously been shown to exhibit equal affinity for the ET<sub>A</sub> and ET<sub>B</sub> receptors (ET<sub>A</sub>: 3.5 and ET<sub>B</sub>: 7.2 nmol/l; ratio: 2.1) [34]. To insure appropriate dosage of the ET antagonist, water intake was monitored at regular intervals and the drug dilution was adjusted accordingly. No difference in food intake, drinking patterns, or body weight was noted between animals from each group (Table 1). The HC diet consisted of 1.25% cholesterol, 7.5% (w/w) cocoa butter, 7.5% casein and 0.5% (w/w) sodium cholate. This chow preparation was shown in previous reports to promote atherogenesis [3]. After 8 weeks of treatment, mice were sacrificed and perfusion fixed with 10% formalin. The aorta were then dissected from the aortic valve to the iliac bifurcation and further fixed in 10% formalin overnight at 4°C.

Table 1  
Feeding behavior and body weight variations\*

	Group I	Group II	Group III	Group IV
Food intake (g/day)	2.4±0.3	2.0±0.5	2.1±0.6	2.4±0.6
Water intake (ml/day)	3.3±1.5	3.8±2.1	3.5±1.8	3.2±1.6
Body weight (g)	28.7±2.7	29.6±3.1	30.1±2.0	27.5±1.9

\* Values shown are mean±S.D. No difference was noted between any experimental groups for food intake, water intake or body weight measurements by the end of the experimental protocol when subjected to one-way ANOVA with post hoc student *t*-test.

## 2.2. Quantification of xanthomatosis

The degree of xanthomatosis was graded according to the following scale: facial lesions: 0=none; 1=mild (snout only); 2=moderate (snout and eye lids); 3=severe (marked lesions); and limb swelling: 0=none; 1=mild/moderate (front paws only); and 2=severe (all four limbs). Addition of facial lesion and limb swelling grades represented the semiquantitative score.

## 2.3. Morphometry and immunohistochemistry

Aortae from each experimental group were opened longitudinally and stained with oil red O and a computer-assisted video imaging system was used to assess the extent of the atherosclerosis area (C-imaging analysis). For immunohistochemistry, the aortae of four animals from each group were divided into three regions: aortic arch, thoracic and abdominal aorta. Paraffin sections (5  $\mu\text{m}$ ) were cut from each region and endogenous peroxidase activity was quenched by 3%  $\text{H}_2\text{O}_2$  in methanol for 20 min; nonspecific antibody binding was blocked with 10% goat serum in PBS for 30 min, and adjacent sections from each group were immunostained using the following antibodies: a polyclonal rabbit ET-1 antibody (Peninsula Labs., Belmont, CA, USA) at 1:150 dilution overnight at 4°C, and secondary reaction with goat anti-rabbit biotinylated antibody (1:250 dilution, Vector Labs. Burlingame, USA) for 45 min at room temperature (RT); a polyclonal rat antibody to the mouse monocyte/macrophage marker MOMA-2 (Serotec, Kidlington, Oxford, UK) at 1:100 dilution overnight at 4°C, and secondary reaction with biotinylated rabbit anti-rat IgG (1:250 dilution, Vector Laboratories) for 45 min at RT; a monoclonal mouse antibody to smooth muscle  $\alpha$ -actin (Boehringer Mannheim) at 1:100 dilution for 60 min at RT and secondary reaction with biotinylated anti-mouse IgG (1:150 dilution, Vector Laboratories) for 30 min at RT. Following incubation with the secondary antibodies, the sections were treated with streptavidin–biotin–peroxidase complexes (Vectastain ABC kit, Vector Labs.) for 30 min at RT. Diaminobenzadine was used as the peroxidase substrate and hematoxylin as the nuclear counterstain. Negative control slides were prepared by substituting preimmune serums for the primary antibody.

## 2.4. Cholesterol measurements

Blood was extracted by cardiac ventricular puncture in five animals in groups I, II and IV, and six for group III at the time of sacrifice and centrifuged at 1500 rpm for 10 min for plasma separation and collection. Total cholesterol was measured with an enzymatic cholesterol assay in a colorimetric procedure on a Technicon RA1000 (Bayer, Tarrytown, NY, USA).

## 2.5. Blood pressure measurements

In a separate experimental series, fifteen animals (five control; five HC-fed and five treated with the LU compound) were anaesthetized with an intraperitoneal injection of a mixture of xylazine (5 mg/kg, Bayer) and ketamine (50 mg/kg, Wyeth-Ayerst Canada) after 2 weeks of the representative treatments. A catheter constructed of stretched PE200 tubing (Becton Dickinson) was filled with 50 U/ml heparin in saline and was inserted into the right common carotid artery. Pulsatile blood pressure was measured using a CDXIII pressure transducer (COBE Canada) and recorded on the Biopac MP100 data acquisition system with ACKNOWLEDGE software (Biopac Systems). Animals were allowed to stabilize for 20 min after the onset of anesthesia, and then mean arterial pressure was registered continuously for 10 min and mean values were determined.

## 2.6. LU224332 concentrations in mouse plasma

Plasma levels of LU224332 were measured with a radioreceptor assay as previously described [35]. Briefly, 0.1 ml of plasma obtained from cardiac puncture-blood samples from animals receiving ( $n=7$ ) or not receiving ( $n=6$ ) the LU compound was mixed with 1 ml of methanol, thoroughly vortexed, and centrifuged for 15 min at 2800 g. The supernatant was evaporated under a stream of air. The dry residue was reconstituted in 150  $\mu\text{l}$  of the binding buffer. The reaction was carried out at RT in a total volume of 200  $\mu\text{l}$ ; 50  $\mu\text{l}$  of the radioligand ( $^{125}\text{I}$ -ET1,  $\approx 10\,000$  cpm per tube) was mixed with 50  $\mu\text{l}$  of the sample. The reaction was started by addition of 100  $\mu\text{l}$  of porcine aortic membranes (5–7  $\mu\text{g}$  protein/tube). It was terminated after 3 h by addition of 1 ml of ice-cold 5 g/l BSA in PBS, pH 7.4, followed immediately by a rapid centrifugation (3 min at 13 000 g). The supernatant was carefully aspirated, and the radioactivity of pellets was counted in an automated gamma-counter. The standard curves, constructed with 18.75 to 1200 nM of LU224332 added to normal rat plasma were linear within this range.

## 2.7. Cell culture

THP-1 monocyte/macrophage cell line was obtained from the American Type Tissue Culture Collection (TIB 202) and were propagated in RPMI 1640 with 10% FCS, penicillin/streptomycin (100 U/ml) at 37°C, 5%  $\text{CO}_2$ . Cells were plated at a density of  $1 \times 10^6$  cells/ml in 10% FCS medium containing phorbol myristate acetate ( $10^{-7}$  M) for 72 h to induce differentiation into macrophages, and washed extensively with serum-free RPMI medium prior to incubation with or without lipoproteins as indicated for each experiment. In all experiments, cell viability exceeded 90% as determined by trypan blue exclusion.

## 2.8. Lipoprotein isolation and oxidation

LDL (1.019–1.069 g/ml) was obtained by density gradient ultracentrifugation [36] from plasma of fasted normolipidemic individuals. LDL (2 mg protein/ml) was subsequently dialyzed against 0.1 M phosphate buffer, pH 7.4, containing 0.1 mM EDTA for 24 h (three buffer changes). LDL samples were sterilized by passing through an 0.22- $\mu$ m filter (Millipore, Milford, MA, USA), kept at 4°C, and used within 1 week. Lipoprotein concentration was determined by the method of Lowry et al. [37] and expressed as mg/ml. Oxidation of LDL (5 mg protein/5 ml) was performed by dialysis against 5  $\mu$ M  $\text{CuSO}_4 \cdot 5\text{H}_2\text{O}$  in 0.1 M phosphate buffer, pH 7.4, for 12 h at 37°C in the dark.

## 2.9. Cellular cholesterol and triacylglycerol accumulation

THP-1 cells were incubated for 24 h with 100  $\mu$ g/ml native or oxidized LDL (OxLDL) in the presence or absence of  $10^{-7}$  M LU224332. After incubation the cells were washed once with ice cold PBS containing 0.4% BSA and twice with PBS alone. Cells were scraped from the culture flask into PBS and sonicated. The cellular lipids were extracted with chloroform–methanol (2:1, v/v). The lipid extract was digested with phospholipase C (*Clostridium welchii*; Sigma) as previously described [38]. The reaction mixture was extracted with chloroform–methanol (2:1, v/v) containing 100  $\mu$ g tridecanoylglycerol as internal standard. The lipid extracts were then reacted for 30 min at 20°C with Sylon BFT (Sigma) plus one part dry pyridine. This procedure converts the free fatty acids into silyl esters and the free sterols, diacylglycerols and ceramides into silyl ethers, leaving the cholesteryl esters and triacylglycerols unmodified. The free cholesterol, cholesterol esters and triacylglycerols were quantified using a non-polar capillary column as previously described [39].

## 2.10. Data analysis

Statistical differences between groups were evaluated using the one-way ANOVA test with post hoc student *t*-test where appropriate. For semiquantitative scoring of xanthoma, the statistical difference between groups was evaluated using the Mann–Whitney test. Data are presented as mean  $\pm$  S.D. unless otherwise indicated. A value of  $P < 0.05$  was considered significant.

## 3. Results

Cholesterol-fed animals accumulated foam-cells along the inner curvature of the aortic arch and throughout the descending aortae, leading to the formation of fibro-fatty plaques at 8 weeks of treatment (Fig. 1b, d and f).

Histological examination revealed that the atherosclerotic plaques contained a necrotic core with cholesterol crystals covered by a thin fibrous cap. Occasional SMCs could be identified in the plaque area and fibrous cap by immunostaining with an antibody against  $\alpha$ -actin (Fig. 1b), however,  $\alpha$ -actin positive cells were mostly restricted to the medial layer of the aortae (Fig. 1a and b). Immunostaining with monocyte/macrophage specific antibody (MOMA-2) showed little or no staining in animals receiving normal chow (Fig. 1c), whereas the majority of cells within the intimal lesion of HC fed animals were MOMA-2 positive (Fig. 1d). In animals receiving normal chow, ET-1 staining was restricted to endothelial cells (Fig. 1e), whereas ET-1 was predominantly located to macrophage rich intimal aortic lesions of HC treated animals, consistent with previous reports [15,21] (Fig. 1f).

The degree of xanthomatosis, derived using a semiquantitative grading system, is presented in Fig. 2A. In LDL-R knockout mice fed a normal chow for 8 weeks (Fig. 2, group I), no xanthomatous lesions were observed. In contrast, in the cholesterol-fed LDL-R deficient mice (group II) xanthomatous lesions of the face, ventral surface of the trunk and swelling of the extremities began to appear at 6 weeks and were present in all animals by 8 weeks [xanthomatosis score (XS) of  $4.0 \pm 0.6$  (median  $\pm$  S.D.) Fig. 2]. In the cholesterol-fed LDL-R deficient mice treated with ET antagonist (group III), significantly fewer xanthomatous lesions were apparent in at 8 weeks [XS:  $1.5 \pm 0.5$  (median  $\pm$  S.D.) Fig. 2]. LDL-R deficient mice fed 1.25% cholesterol were severely hyperlipidemic with mean plasma cholesterol levels 15-fold higher than normal chow-fed animals (group I:  $4.8 \pm 0.6$  mM vs. group II:  $65.6 \pm 6.5$  mM;  $P < 0.001$ ). Treatment of cholesterol-fed LDL-R deficient mice with the ET antagonist did not alter plasma lipid levels (group III:  $66.6 \pm 5.1$  mM) (Fig. 2B). As well, arterial blood pressure was not significantly different in animals fed normal or HC diets ( $78 \pm 7$  and  $78 \pm 3$  mmHg, respectively), either with or without treatment with the ET antagonist for 15 days ( $74 \pm 7$  and  $78 \pm 3$  mmHg, respectively) (five animals in each group). These results are consistent with previous reports using endothelin antagonist in mice [32] and other normotensive animal models [40]. Treatment with LU224332 (10 mg/kg/day for 2 weeks) resulted in measurable plasma levels of the ET antagonist ( $708 \pm 357$  nmol/l), which was well in excess of the  $K_i$  for both ET receptors (see Methods).

The extent of aortic lipid deposition was visualised by oil red O staining (Fig. 3A) and quantified by computer assisted morphometry (Fig. 3B). Extensive atherosclerosis was seen in the HC diet group (group II), whereas only minimal lipid deposition was found in animals receiving normal mouse chow mainly at the bifurcations of great vessels (group I). LU224332 treatment (group III) significantly reduced the extent of atherosclerotic involvement in the aortae by almost 45% (Fig. 3B,  $P < 0.01$ ).



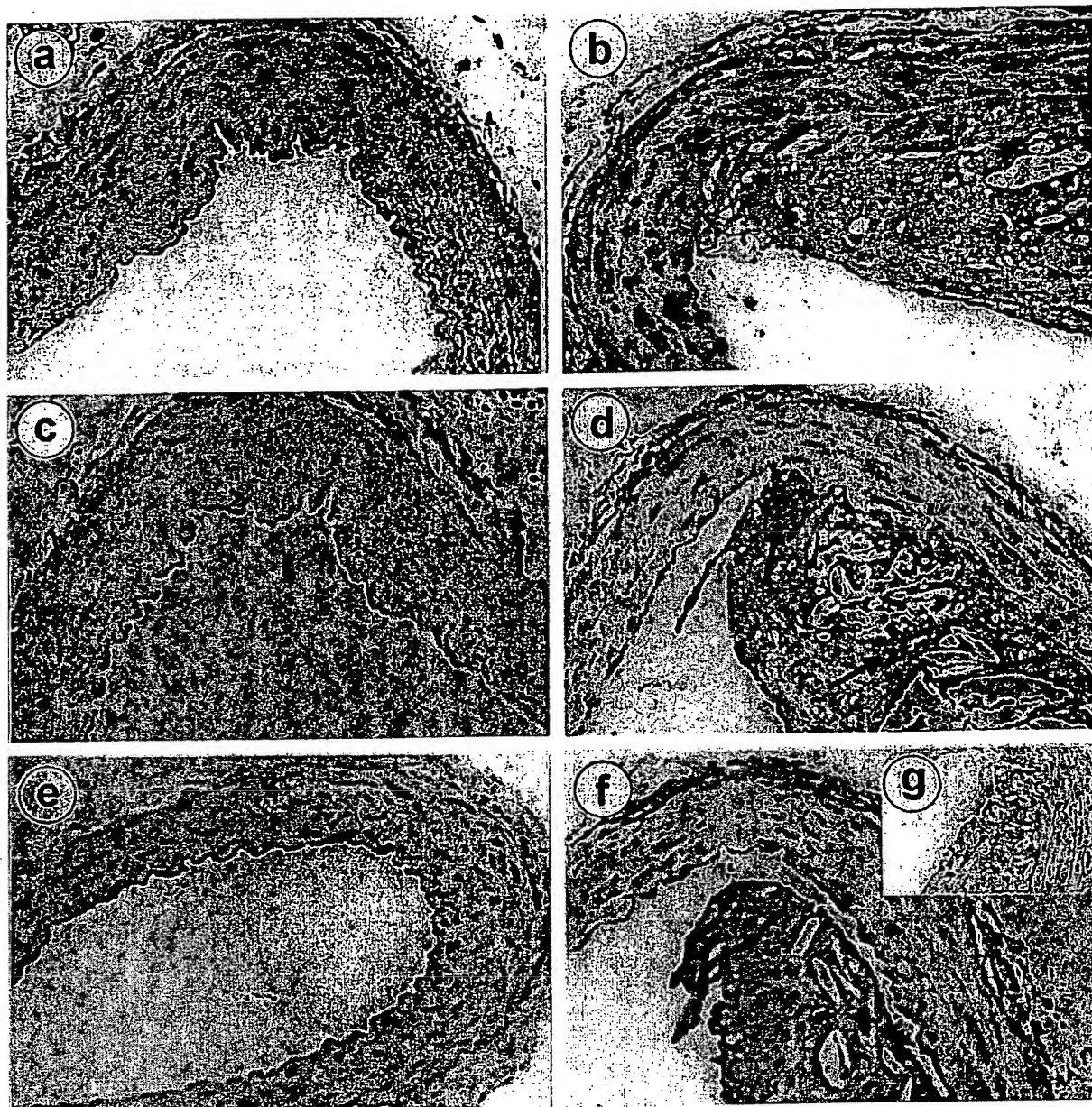


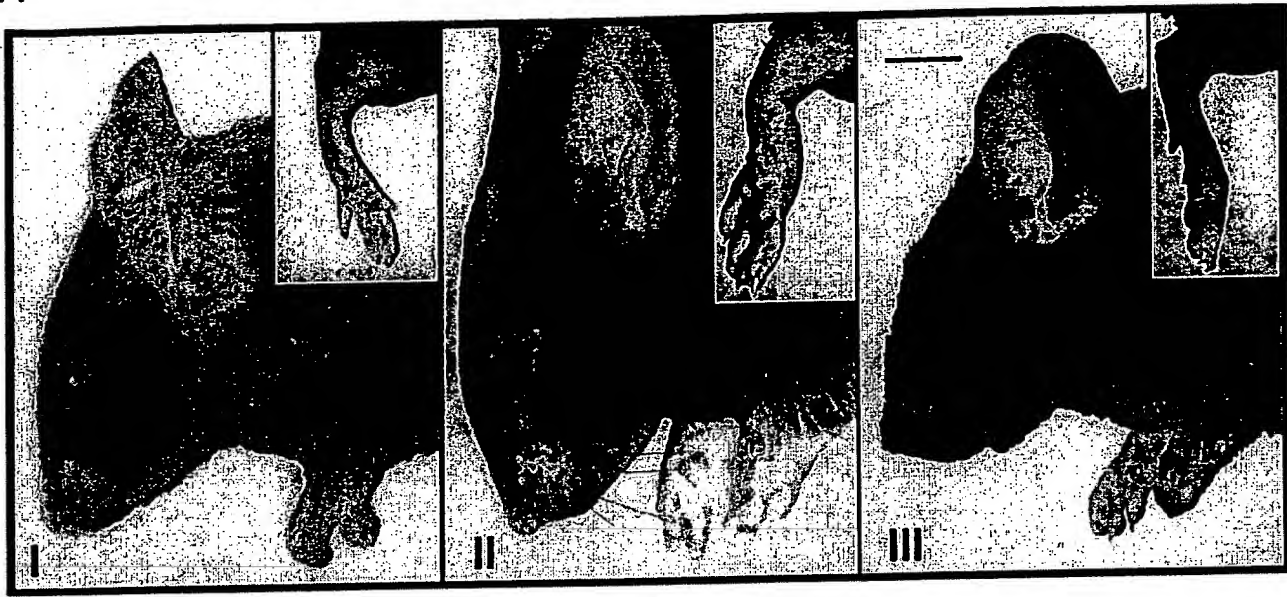
Fig. 1. Photomicrographs show representative sections of thoracic aorta from LDL-R deficient mice fed normal chow (groups I: a, c and e) or a high cholesterol diet (group II: b, d, f and g). Immunostaining for SMCs using an  $\alpha$ -actin antibody revealed a similar pattern of staining in both normal chow (a) and high cholesterol (b) fed animals, largely restricted to the medial layer of the vessels with only partial staining in the atherosclerotic lesion. In contrast, immunostaining with MOMA-2 revealed an absence of macrophages in normal chow fed animals (c) with a very dense accumulation of macrophages in the lesions of high cholesterol fed animals (d). Immunostaining for ET-1 on sequential sections revealed expression of this peptide limited to endothelial cells of normal chow-fed animals (e), with marked ET-1 staining in the HC animals (f) predominantly located to the intimal macrophage rich lesions. Negative control slides were prepared by substituting preimmune rabbit serum for the primary antibody in a section from group II (g).

In order to study the direct effect of endothelin receptor blockade on macrophage lipid accumulation, THP-1 human macrophages were incubated with 100  $\mu$ g/ml of native LDL (nLDL) or Ox LDL, in the presence or absence of LU224332 ( $10^{-7}$  M). After 24 h, cellular cholesteryl ester (CE) and triacylglycerol (TG) were quantified as described in Methods. Treatment of cells with Ox LDL

resulted in 3-fold increase in CE and TG levels compared to nLDL alone ( $P < 0.01$  and  $P < 0.05$ , respectively; Fig. 4A). The addition of LU224332 completely prevented macrophage CE and reduced TG deposition induced by Ox LDL ( $P < 0.01$  and  $P < 0.05$ , respectively; Fig. 4B), reducing macrophage lipid accumulation to levels not different from nLDL alone.



A



B

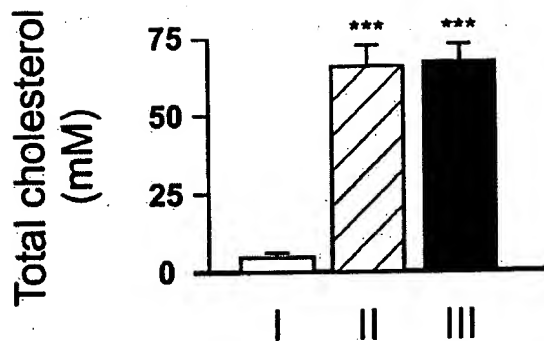


Fig. 2. Animals on regular chow diet, (group I), did not develop xanthomas. In contrast, mice fed high cholesterol (HC) diet alone, group II, developed facial xanthomatous lesions and marked swelling of the paws by the end of the experimental protocol. The LDL-R deficient mice receiving supplemental endothelin antagonist (LU224332) together with HC diet, (group III), showed much reduced facial xanthomatous and minimal swelling of the extremities (A). The mean xanthomatosis score for experimental groups II and III are presented in the results section. Average total plasma cholesterol values (mM) in groups I, II and III are shown in (B).

#### 4. Discussion

The results of the present study demonstrate an important anti-atherosclerotic effect of a non-selective ET receptor antagonist in a model of homozygous familial hypercholesterolemia, the LDL receptor (LDL-R) deficient mouse. In addition to preventing atherosclerosis, treatment with the ET antagonist significantly reduced xanthoma formation without affecting total cholesterol levels or arterial pressure. These results support the hypothesis that the ET system contributes directly to the pathogenesis of atherosclerosis and that ET blockers may have therapeutic utility in the treatment of this vascular disorder.

In the vessel wall, the  $ET_A$  receptor is located primarily on SMCs, whereas the  $ET_B$  subtype is found mainly on the endothelial layer, infiltrating macrophages [29] and to a variable extent SMCs [28]. Although  $ET_A$  may mediate many of the effects of ET-1 that are likely relevant to atherosclerosis, the presence of the  $ET_B$  receptors on macrophages and its up regulation on SMCs of vascular lesions [27], suggest that this receptor subtype may contribute importantly to the pathogenesis of atherosclerosis as well. In fact, a recent report has suggested that accumulation of foamy macrophages and T lymphocytes in the fibrous plaque may modulate the switching of ET receptor subtypes from  $ET_A$  to  $ET_B$  in SMCs [41].

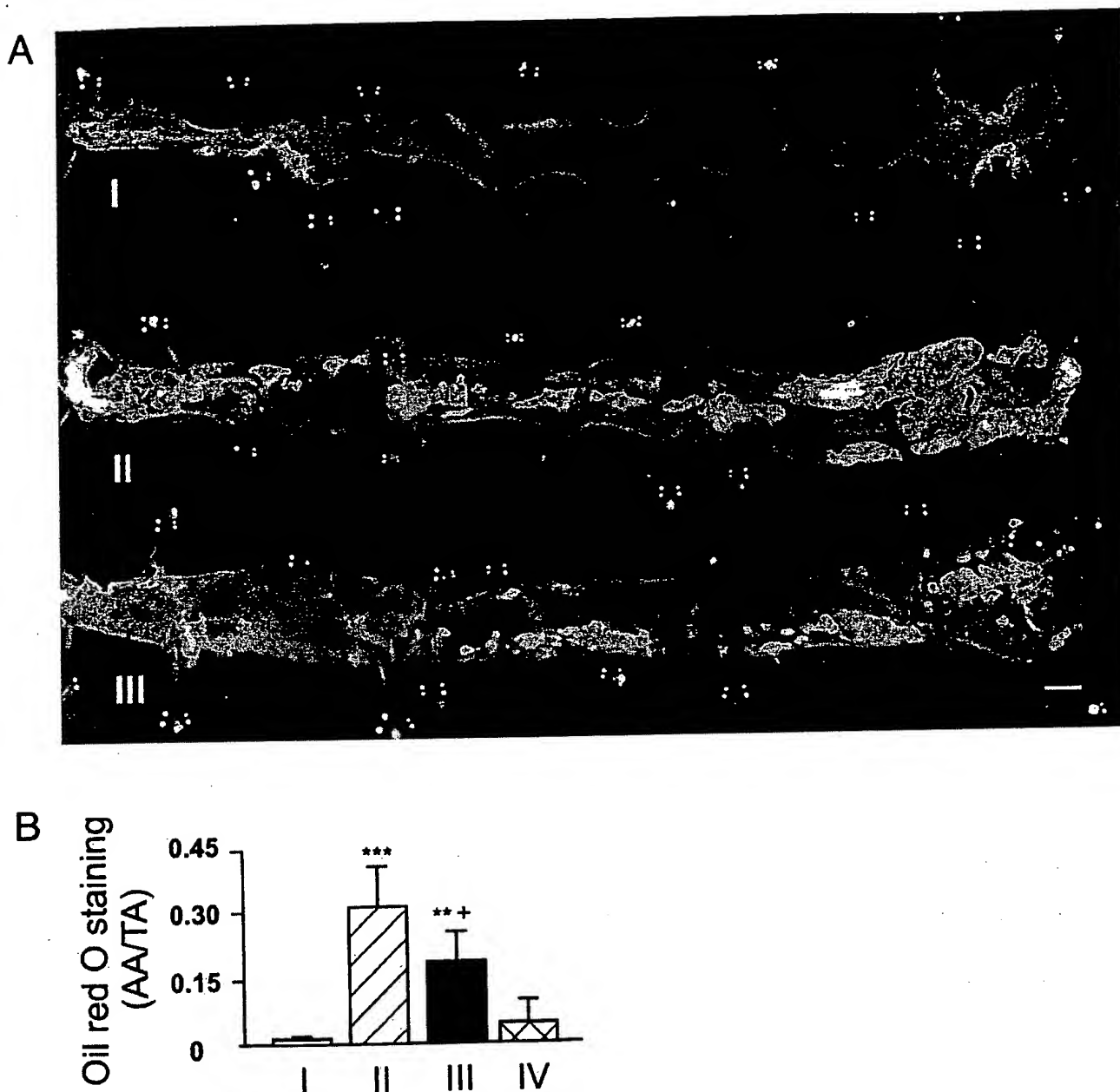


Fig. 3. Representative oil red O staining on the full length luminal surface of aortas from LDL-R deficient mice. Extensive lipid deposition could be seen in the HC diet group (group II), while only minimal lipid deposition was found in animals receiving normal mouse chow (group I). Aortas from LU224332 treated animals (group III) showed reduced aortic atherosclerosis (A). Mean values for atherosclerotic area relative to total aortic luminal surface are shown in panel B ( $n=6$ , group I;  $n=9$ , group II and III;  $n=5$ , group IV). Asterisks indicate statistical difference versus group I using the one-way ANOVA with post-hoc Student *t*-test (\*\*,  $P<0.01$ ; \*\*\*,  $P<0.001$ ). The plus sign indicates a statistical difference versus group II using the one-way ANOVA with post-hoc Student *t*-test (+,  $P<0.01$ ).

Cultured rat peritoneal macrophages have been described to express nearly exclusively  $ET_B$  receptors [42] whereas both  $ET_A$  and  $ET_B$  receptors have been demonstrated by in situ hybridization on macrophages in the early inflammatory intimal lesion of hyperlipidemic hamsters [31].

In contrast, stimulation of  $ET_B$  receptors on the endothelial cells releases vasodilators, such as NO, which may protect against atherosclerosis [43]. Kowala et al. [31] previously reported that an  $ET_A$  selective antagonist re-

duced fatty-streak formation in a hamster model of early atherosclerosis. However, to some extent this effect might have been due to a lipid lowering action of certain ET antagonists [31,44]. Recently, Barton et al. [32] reported that another  $ET_A$  selective antagonist reduced atherosclerosis in the apoE-deficient mouse model of atherosclerosis, further supporting an important role for ET-1 in this disease. This was associated with a marked improvement in endothelium-dependent dilation and increased nitrate/

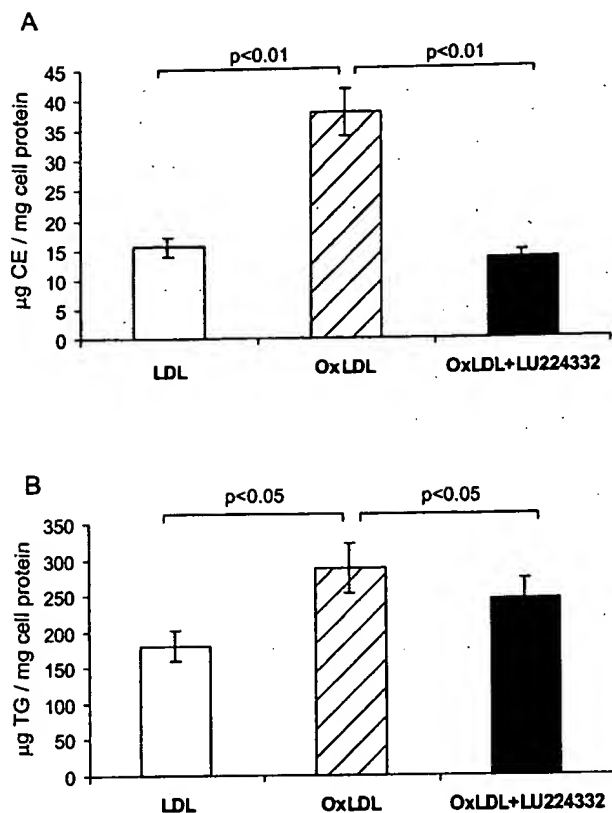


Fig. 4. Mean values  $\pm$  S.D. ( $n=4$ ) for cellular cholesterol ester (CE; A) and triacylglycerol (TG; B) accumulation in THP-1 cell line in presence of nLDL or OxLDL with or without LU224332 for 24 h. LU224332 prevented CE and TG uptake induced by OxLDL ( $P<0.01$  and  $P<0.05$ , respectively).

nitrite levels in the blood [32], likely as a result of selective  $ET_A$  blockade which spares the endothelial  $ET_B$  receptor. Therefore, it is possible that an increase in endothelial NO production may have contributed indirectly to the anti-atherogenic effects of  $ET_A$  blockade in these studies. It is well established that other strategies to increase endothelial NO release, i.e. L-arginine supplementation [45,46], and angiotensin converting enzyme inhibition [47,48] reduce atherosclerosis in a variety of animal models. In the present study a balanced  $ET_A$  and  $ET_B$  receptor antagonist was used, which would not be expected to favorably alter the balance of endothelial versus smooth muscle ET receptor activation. Indeed, it could be argued that blockade of endothelial  $ET_B$  receptor with this compound would be counterproductive and could reduce the overall beneficial effect of the ET antagonist in atherosclerotic models. Nonetheless, a marked reduction in atherosclerosis and xanthomatosis was seen with LU224332 in the absence of any changes in plasma lipids, which may be ascribed to direct effects of ET-1 on the cellular events leading to the initiating and/or progression of atherosclerosis. However, we cannot exclude the possibility that mixed ET blockade may have resulted in

improvement in endothelial function by an indirect mechanism. Increased NO production has been previously reported with both selective and non-selective ET antagonists in the rat Langerdorff heart model [49], possibly due to increased coronary flow and therefore intimal shear forces [49].

In addition to its potent vasoconstrictor effects, ET-1 has a number of biological activities, which might contribute directly to the morphological changes characteristic of atherosclerosis. Endothelin-1 is a co-mitogen for vascular SMCs [13], and can act in concert with other well-characterized growth factors, such as PDGF, which are believed to initiate and maintain cell proliferation in the atheromatous [17]. ET-1 is also a powerful stimulus for secretion of collagen [14] and other matrix components which represent a major constituent of the atherosclerotic lesion. Therefore the inhibition of ET-1 action on atheromatous SMCs may be critical in the anti-atherosclerotic effects of LU224332. As well, ET-1 may also contribute to the recruitment of monocytes into the developing intimal lesion either directly [15] or indirectly by increasing MCP-1 [16]. Macrophages play a key role in the pathogenesis of atherosclerosis [30]. The marked up-regulation of expression of ET-1 in macrophages seen in this and other studies also suggest that this peptide may contribute to chronic inflammatory changes in this disease.

ET-1 has been shown to increase the release of inflammatory cytokines from macrophages [50,51]. In turn, cytokines such as  $TNF\alpha$ , IL-1 and IL-6 have been shown to increase ET-1 production by macrophages [52]. Thus ET-1 may serve to amplify and sustain macrophage activation in the developing atheromatous [51]. Interruption of this positive feedback pathway is a potential mechanism by which ET receptor antagonists may reduce the progression of atherosclerosis in addition to its effects on SMC proliferation and matrix secretion. In support of this, a marked decrease in xanthomas formation, a non-vascular lesion which is dependent on macrophage activation [3] was also observed in LDL-R deficient mice treated with the ET antagonist. Further evidence in favor of a direct effect of ET-1 on macrophage foam-cell formation was provided by in vitro studies using the human THP-1 monocyte-macrophage cell line. These cells differentiate into macrophages on exposure to phorbol ester, in which state they have previously been characterized to express predominantly the  $ET_B$  receptor [29]. The ability of the LU224332 compound to largely prevent cholesterol ester and triacylglycerol accumulation in these cells on exposure to Ox LDL is consistent with a crucial role for endogenous ET-1 in macrophage activation and foam-cell formation.

In summary, nonselective inhibition of ET receptors with LU224332 reduced atherosclerosis and xanthomatosis independently of any change in lipid levels. Prominent ET-1 expression in macrophage-rich atherosclerotic lesions observed in vivo, together with the ability of the ET receptor antagonist to directly reduce macrophage lipid

accumulation in vitro, point to a role for ET-1 in foam-cell formation. Thus, antagonism of the ET system may provide a new pharmacological approach to reduce the vessel wall response to chronic injury induced by hyperlipidemia, and thereby inhibit intimal lesion formation and progression of atherosclerosis.

## Acknowledgements

This work was supported by the Medical Research Council of Canada (MRC MT11620). DJS is the Dexter H.C. Man Chair of Cardiology of the University of Toronto. SB is supported by a Fellowship from the KM Hunter/Medical Research Council of Canada. TCL is supported by a studentship from the Canadian Hypertension Society/Pfizer Canada Inc./MRC. We are grateful to Dr. Phil Connelly for assisting us in the measurements of plasma cholesterol levels and for his helpful comments and advice. Also we would like to thank Dr. M. Kirchengast from Knoll company for his generous gift of the LU224332 compound.

## References

- [1] Brown MS, Goldstein JL. Lipoprotein receptors in the liver. Control signals for plasma cholesterol traffic. *J Clin Invest* 1983;72(3):743–747.
- [2] Goldstein JL, Dana SE, Brunschede GY, Brown MS. Genetic heterogeneity in familial hypercholesterolemia: evidence for two different mutations affecting functions of low-density lipoprotein receptor. *Proc Natl Acad Sci USA* 1975;72(3):1092–1096.
- [3] Ishibashi S, Goldstein JL, Brown MS, Herz J, Burns DK. Massive xanthomatosis and atherosclerosis in cholesterol-fed low density lipoprotein receptor-negative mice. *J Clin Invest* 1994;93(5):1885–1893.
- [4] Dusting GJ, Fennessy P, Yin ZL, Gurevich V. Nitric oxide in atherosclerosis: vascular protector or villain? *Clin Exp Pharmacol Physiol Suppl* 1998;25:S34–S41.
- [5] Wever RM, Luscher TF, Cosentino F, Rabelink TJ. Atherosclerosis and the two faces of endothelial nitric oxide synthase. *Circulation* 1998;97(1):108–112.
- [6] Toutouzas PC, Tousoulis D, Davies GJ. Nitric oxide synthesis in atherosclerosis. *Eur Heart J* 1998;19(10):1504–1511.
- [7] Maxwell AJ, Tsao PS, Cooke JP. Modulation of the nitric oxide synthase pathway in atherosclerosis. *Exp Physiol* 1998;83(5):573–584.
- [8] Bult H. Nitric oxide and atherosclerosis: possible implications for therapy. *Mol Med Today* 1996;2(12):510–518.
- [9] John S, Schlaich M, Langenfeld M et al. Increased bioavailability of nitric oxide after lipid-lowering therapy in hypercholesterolemic patients: a randomized, placebo-controlled, double-blind study. *Circulation* 1998;98(3):211–216.
- [10] Thorne S, Mullen MJ, Clarkson P, Donald AE, Deanfield JE. Early endothelial dysfunction in adults at risk from atherosclerosis: different responses to L-arginine. *J Am Coll Cardiol* 1998;32(1):110–116.
- [11] Yanagisawa M, Kurihara H, Kimura S et al. A novel potent vasoconstrictor peptide produced by vascular endothelial cells. *Nature* 1988;332(6163):411–415.
- [12] Eglen RM, Michel AD, Sharif NA, Swank SR, Whiting RL. The pharmacological properties of the peptide, endothelin. *Br J Pharmacol* 1989;97(4):1297–1307.
- [13] Assender JW, Irenius E, Fredholm BB. Endothelin-1 causes a prolonged protein kinase C activation and acts as a co-mitogen in vascular smooth muscle cells. *Acta Physiol Scand* 1996;157(4):451–460.
- [14] Rizvi MA, Katwa L, Spadone DP, Myers PR. The effects of endothelin-1 on collagen type I and type III synthesis in cultured porcine coronary artery vascular smooth muscle cells. *J Mol Cell Cardiol* 1996;28(2):243–252.
- [15] Achmad TH, Rao GS. Chemotaxis of human blood monocytes toward endothelin-1 and the influence of calcium channel blockers. *Biochem Biophys Res Commun* 1992;189(2):994–1000.
- [16] Helset E, Sildnes T, Konopski ZS. Endothelin-1 stimulates monocytes in vitro to release chemotactic activity identified as interleukin-8 and monocyte chemotactic protein-1. *Mediators Inflamm* 1994;3:155–160.
- [17] Kowala MC. The role of endothelin in the pathogenesis of atherosclerosis. *Adv Pharmacol* 1997;37:299–318.
- [18] He Y, Kwan WC, Steinbrecher UP. Effects of oxidized low density lipoprotein on endothelin secretion by cultured endothelial cells and macrophages. *Atherosclerosis* 1996;119(1):107–118.
- [19] Lerman A, Edwards BS, Hallett JW, Heublein DM, Sandberg SM, Burnett Jr. JC. Circulating and tissue endothelin immunoreactivity in advanced atherosclerosis. *New Engl J Med* 1991;325(14):997–1001.
- [20] Jones GT, van Rij AM, Solomon C, Thomson IA, Packer SG. Endothelin-1 is increased overlying atherosclerotic plaques in human arteries. *Atherosclerosis* 1996;124(1):25–35.
- [21] Zeiher AM, Goebel H, Schachinger V, Ihling C. Tissue endothelin-1 immunoreactivity in the active coronary atherosclerotic plaque. A clue to the mechanism of increased vasoreactivity of the culprit lesion in unstable angina. *Circulation* 1995;91(4):941–947.
- [22] Lerman A, Webster MW, Chesebro JH et al. Circulating and tissue endothelin immunoreactivity in hypercholesterolemic pigs. *Circulation* 1993;88(6):2923–2928.
- [23] Bacon CR, Davenport AP. Endothelin receptors in human coronary artery and aorta. *Br J Pharmacol* 1996;117(5):986–992.
- [24] Kohan DE. Endothelins in the normal and diseased kidney. *Am J Kidney Dis* 1997;29(1):2–26.
- [25] Kanse SM, Wijelath E, Kanthou C, Newman P, Kakkar VV. The proliferative responsiveness of human vascular smooth muscle cells to endothelin correlates with endothelin receptor density. *Lab Invest* 1995;72(3):376–382.
- [26] Vane JR, Anggard EE, Botting RM. Regulatory functions of the vascular endothelium. *New Engl J Med* 1990;323(1):27–36.
- [27] Azuma H, Hamasaki H, Sato J, Isotani E, Obayashi S, Matsubara O. Different localization of ET<sub>A</sub> and ET<sub>B</sub> receptors in the hyperplastic vascular wall. *J Cardiovasc Pharmacol* 1995;25(5):802–809.
- [28] Sumner MJ, Cannon TR, Mundin JW, White DG, Watts IS. Endothelin ET<sub>A</sub> and ET<sub>B</sub> receptors mediate vascular smooth muscle contraction. *Br J Pharmacol* 1992;107(3):858–860.
- [29] Magazine HI, Andersen TT, Bruner CA, Malik AB. Vascular contractile potency of endothelin-1 is increased in the presence of monocytes or macrophages. *Am J Physiol* 1994;266(4 Pt 2):H1620–H1625.
- [30] Murakami T, Yamada N. Modification of macrophage function and effects on atherosclerosis. *Curr Opin Lipidol* 1996;7(5):320–323.
- [31] Kowala MC, Rose PM, Stein PD et al. Selective blockade of the endothelin subtype A receptor decreases early atherosclerosis in hamsters fed cholesterol. *Am J Pathol* 1995;146(4):819–826.
- [32] Barton M, Haudenschild CC, d'Uscio LV, Shaw S, Munter K, Luscher TF. Endothelin E.T.A. receptor blockade restores NO-mediated endothelial function and inhibits atherosclerosis in apolipoprotein E-deficient mice. *Proc Natl Acad Sci USA* 1998;95(24):14367–14372.
- [33] Best PJ, McKenna CJ, Hasdai D, Holmes Jr. DR, Lerman A.

- Chronic endothelin receptor antagonism preserves coronary endothelial function in experimental hypercholesterolemia. *Circulation* 1999;99(13):1747–1752.
- [34] Raschack M, Gock S, Unger L et al. LU302 872 and its racemate (LU224332) show balanced endothelin-A/B receptor affinity, high oral activity, and inhibit human prostate tissue contractions. *J Cardiovasc Pharmacol* 1998;31(Suppl 1):S241–S244.
- [35] Cernacek P, Franchi L, Dupuis J, Rouleau JL, Levy M. Radioreceptor assay of an endothelin A receptor antagonist in plasma and urine. *Clin Chem* 1998;44(8 Pt 1):1666–1673.
- [36] Havel RJ, Eder HA, Bragdon JH. The distribution and chemical composition of ultracentrifugally separated lipoproteins in human serum. *J Clin Invest* 1955;34:1345–1353.
- [37] Lowry OH, Rosebrough NJ, Farr AL, Randall RJ. Protein measurement with the Folin phenol reagent. *J Biol Chem* 1951;193:265–275.
- [38] Kuksis A, Myher JJ, Geher K et al. Comparative determination of plasma phospholipids by automated gas–liquid chromatographic and manual colorimetric phosphorus methods. *J Chromatogr* 1980;182(1):1–26.
- [39] Ravandi A, Kuksis A, Shaikh NA. Glycated phosphatidylethanolamine promotes macrophage uptake of low density lipoprotein and accumulation of cholesteryl esters and triacylglycerols. *J Biol Chem* 1999;274(23):16494–16500.
- [40] Moreau P. Endothelin in hypertension: a role for receptor antagonists? *Cardiovasc Res* 1998;39(3):534–542.
- [41] Iwasa S, Fan J, Shimokama T, Nagata M, Watanabe T. Increased immunoreactivity of endothelin-1 and endothelin B receptor in human atherosclerotic lesions. A possible role in atherogenesis. *Atherosclerosis* 1999;146(1):93–100.
- [42] Sakurai-Yamashita Y, Yamashita K, Yoshida A et al. Rat peritoneal macrophages express endothelin ET(B) but not endothelin ET(A) receptors. *Eur J Pharmacol* 1997;338(2):199–203.
- [43] Aji W, Ravalli S, Szabolcs M et al. L-Arginine prevents xanthoma development and inhibits atherosclerosis in LDL receptor knockout mice. *Circulation* 1997;95(2):430–437.
- [44] Iwasa S, Fan J, Miyauchi T, Watanabe T. Non-selective endothelin receptor antagonist, SB209670, reduces diet-induced hypercholesterolemia and atherosclerosis in apolipoprotein E-deficient mice. *Circulation* 1999;100(18):I–474, Abstract.
- [45] Jeremy RW, McCarron H, Sullivan D. Effects of dietary L-arginine on atherosclerosis and endothelium-dependent vasodilatation in the hypercholesterolemic rabbit. Response according to treatment duration, anatomic site, and sex. *Circulation* 1996;94(3):498–506.
- [46] Cooke JP, Andon NA, Gierd XJ, Hirsch AT, Creager MA. Arginine restores cholinergic relaxation of hypercholesterolemic rabbit thoracic aorta. *Circulation* 1991;83(3):1057–1062.
- [47] Dusting GJ, Hyland R, Hickey H, Makdissi M. Angiotensin-converting enzyme inhibitors reduce neointimal thickening and maintain endothelial nitric oxide function in rabbit carotid arteries. *Am J Cardiol* 1995;76(15):24E–27E.
- [48] Luscher TF, Wenzel RR, Moreau P, Takase H. Vascular protective effects of ACE inhibitors and calcium antagonists: theoretical basis for a combination therapy in hypertension and other cardiovascular diseases. *Cardiovasc Drugs Ther* 1995;9(3):509–523.
- [49] Goodwin AT, Amrani M, Gray CC, Jayakumar J, Yacoub MH. Role of endogenous endothelin in the regulation of basal coronary tone in the rat. *J Physiol* 1998;511(2):549–557.
- [50] Ruetten H, Thiemeermann C. Endothelin-1 stimulates the biosynthesis of tumour necrosis factor in macrophages: ET-receptors, signal transduction and inhibition by dexamethasone. *J Physiol Pharmacol* 1997;48(4):675–688.
- [51] Speciale L, Roda K, Saresella M, Taramelli D, Ferrante P. Different endothelins stimulate cytokine production by peritoneal macrophages and microglial cell line. *Immunology* 1998;93(1):109–114.
- [52] Kahaleh MB, Fan PS. Effect of cytokines on the production of endothelin by endothelial cells. *Clin Exp Rheumatol* 1997;15(2):163–167.

# Animal Models of Atherosclerosis and Interpretation of Drug Intervention Studies

Thomas M.A. Bocan

Department of Vascular and Cardiac Diseases, Parke-Davis Pharmaceutical Research, Division of Warner Lambert Company, 2800 Plymouth Road, Ann Arbor, MI 48105, USA

**Abstract:** Atherosclerosis has often been defined as a multifactorial disease; however, a common risk factor associated with accelerated vascular disease in man or animals is an elevated plasma cholesterol level. Even though there is no one perfect animal model that completely replicates the stages of human atherosclerosis, cholesterol feeding and mechanical endothelial injury are two common features shared by most models of atherosclerosis. The models may differ with respect to degree of dietary cholesterol supplementation, length of hypercholesterolemia, dietary regimen and type, duration and degree of mechanical endothelial injury. With the advent of genetic engineering, transgenic mouse models have supplemented the classical dietary cholesterol induced disease models such as the cholesterol-fed hamster, rabbit, pig and monkey. The desire to limit the progression of atherosclerosis has spawned numerous drug intervention studies. Biochemical as well as morphologic and morphometric changes in the extent, structure and composition of atherosclerotic lesions following drug intervention have become major endpoints of in vivo drug intervention studies. Interpretations of alterations in vascular pathology following drug administration are often confounded by associated changes in plasma lipids and lipoproteins; limitation of the animal models and additional properties of compounds unrelated to their primary mode of action. Thus, the current review will summarize the pathology of atherosclerosis, describe various animal models of vascular disease and provide a critical review of the methods utilized and conclusions drawn when evaluating pharmacologic agents in animals.



## Introduction

Atherosclerosis has often been defined as a multifactorial disease. In addition, hypercholesterolemia has become a widely accepted risk factor for premature development of coronary artery disease. Classical thinking argued that development of clinically significant atherosclerotic lesions was associated with two major processes. One is fibrocellular proliferation, which adds to intimal bulk and eventually leads to chronic ischemic syndromes via gradual constriction of the arterial lumen. The second process involves the combination of cellular necrosis and lipid deposition within the arterial intima. Enlargement of a lipid-rich core tends to erode the fibrous cap [1], eventuating in plaque rupture, exposure of circulating blood to highly thrombogenic material and sudden ischemic episodes such as myocardial infarction [2,3]. Considering our classical understanding of atherosclerosis progression, the current article will review the histologic landmarks of the various stages of atherosclerosis and also provide a dynamic understanding of how the stages might be interrelated. A comparison of various hypercholesterolemia-induced animal models of atherosclerosis will be made with a focus on their advantages and limitations when used to evaluate novel antiatherosclerotic drugs. Finally, the antiatherosclerotic activity of inhibitors of acyl-coenzyme A:cholesterol O-acyltransferase (ACAT) Fig. (1) (1-14), 3-hydroxy-3-methylglutaryl coenzyme A (HMG-CoA reductase) Fig. (2) (15-18), 15-lipoxygenase (15-LO) and lipoprotein oxidation (anti-oxidants) Fig. (3) (19-22) will be discussed; however, an emphasis will be on describing how the models can discern the compound's *direct* from *indirect* antiatherosclerotic activity.

## Pathology of Atherosclerosis

Atherosclerosis is a focal disease that has been shown to develop in a distinct pattern in both man and animals [4,5]. As depicted in Fig. (4), atherosclerotic lesion development can be divided into six histologically distinct stages or lesion types and five dynamic phases [6,7]. The formation of an intimal cushion at distinct sites within the arterial tree appears to precede the development of atherosclerosis and may be considered a normal aging process. Smooth muscle cells (SMC) migrate from the media, proliferate in the intima and secrete extracellular matrix. Extracellular lipid accumulation that is primarily of lipoprotein origin [8] decorates the secreted collagen, elastin and proteoglycans of the developing intima. Oxidation of the insudant lipoproteins [9] appears to set up a chemotactic gradient and stimulate endothelial cells to upregulate adhesion molecules, i.e., vascular cell adhesion molecule-1 (VCAM-1) [10], responsible for the recruitment of monocyte-macrophages. Monocyte-macrophages are a hallmark of Type I to III lesions and are both a culprit cell responsible for promoting lesion development and a potential point of therapeutic intervention. The major difference in Type I to III lesions lies in the relative amounts of monocyte-macrophage foam cells, SMC, extracellular matrix and lipid and the gross extent of these lesions on the arterial surface. These lesions have classically been termed fatty dots, fatty streaks or fibrolipid lesions to denote their relative extent and degree of fibrosis. Therefore, progression from the innocuous intimal cushion to the Type III lesion that may occur over the first 20 to 30 years of life can be characterized as Phase I.

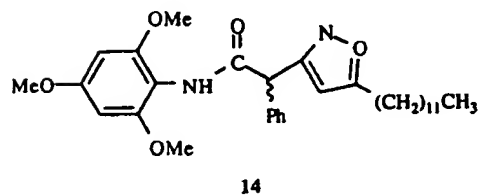
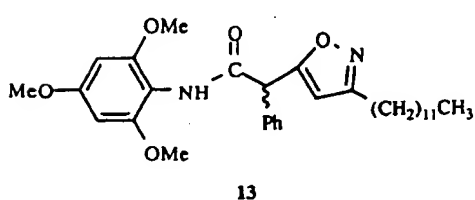
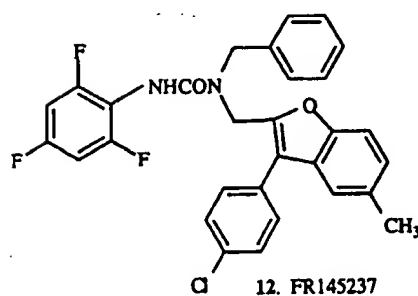
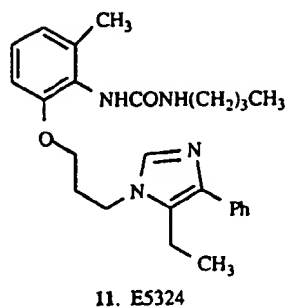
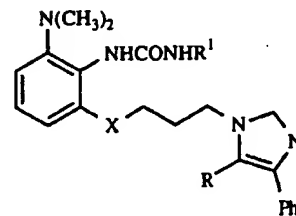
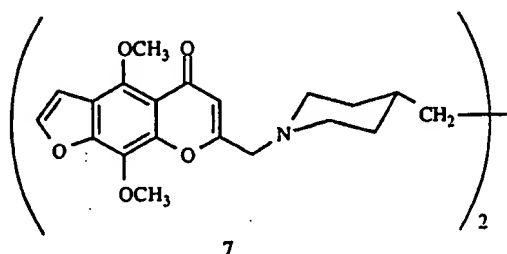
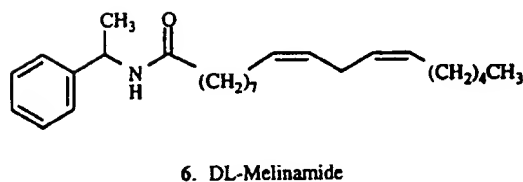
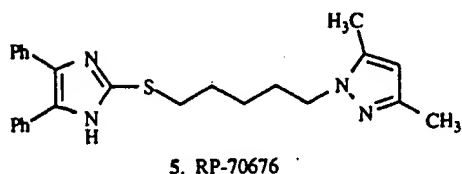
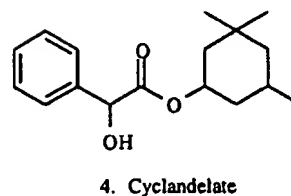
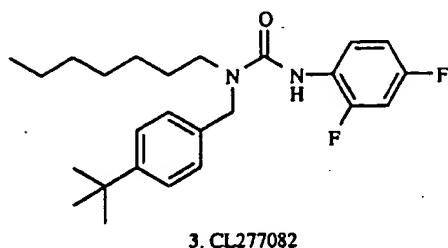
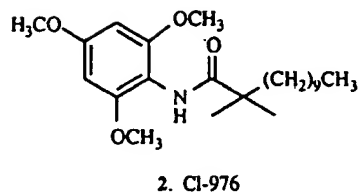
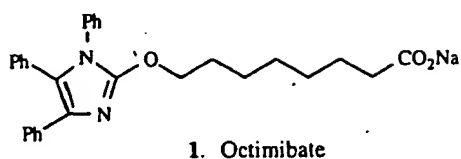


Fig. (1). ACAT inhibitors.

Enlargement of the extracellular lipid pool and formation of a deep intimal lipid-rich necrotic core is a distinguishing characteristic of the Type IV lesion. Type IV lesions can be described as a transitional lesion with many potential fates.

Episodic plaque fissures, microthrombi formation and expansion of the fibrous cap overlying the necrotic core can lead to the formation of the potentially more stable Type V lesions. (Phase 2). Type V lesions that are often referred to as fibrous plaques



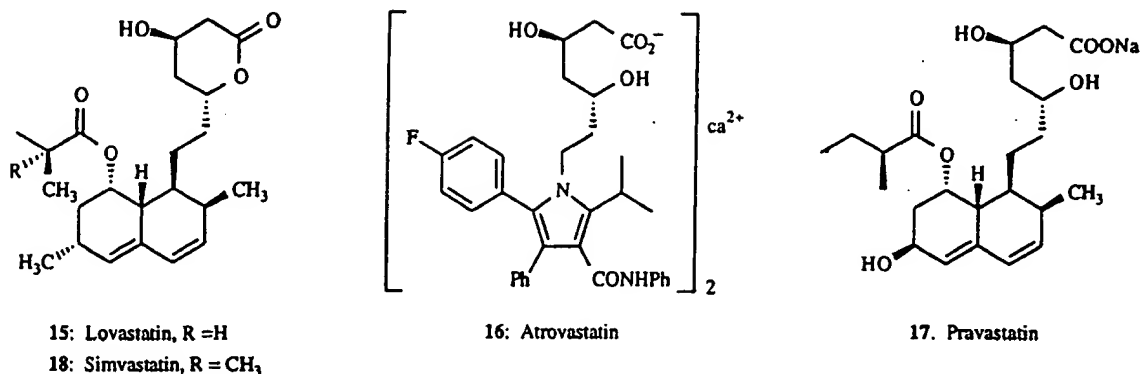


Fig. (2). HMG-CoA reductase inhibitors.

have a developed fibrous cap, deep-intimal necrosis and a lipid-rich necrotic core composed of cholesterol clefts, calcium deposits and evidence of neovascularization. Continued fibrosis of a Type V lesion could silently occlude the arterial lumen (Phase 5). Rupture of the fibrous cap of a Type IV lesion can also generate a mural thrombus that is rapidly recanalized and retracted into the arterial wall to form a Type V lesion (Phase 3). A marked rupture (Phase 4) of the fibrous cap, generation of an occlusive thrombus, myocardial infarction and sudden death is a final fate of the Type IV lesion and for the purpose of classification has been denoted as a Type VI complicated plaque.

In summary, atherosclerotic lesion progression in man involves episodes of SMC proliferation, extracellular matrix deposition and remodeling, lipid infiltration, endothelial cell-monocyte interactions, monocyte migration into the intima, monocyte-macrophage foam cell formation, necrotic lipid-rich core formation, calcium deposition, neovascularization, mural microthrombi and occlusive acute thrombosis. Some of the cell-derived factors that may contribute to atherosclerotic lesion development have previously been reviewed [11].

### Animal Models of Atherosclerosis

Given the complexity of atherosclerotic lesion development in man, the challenge exists to develop animal models that closely mimic the human disease. One must accept, however, that there is no one perfect animal model that completely replicates the stages of human atherosclerosis but that the models are useful in studying specific pathologic processes

associated with the disease. Irrespective of species, there are several common features shared by most models of atherosclerosis. Firstly, induction of vascular lesions in most animal models is dependent upon development of a plasma hypercholesterolemia. Plasma cholesterol elevations can either be induced by dietary supplementation with cholesterol, hepatic overproduction of lipoproteins or genetic mutation of receptors and/or receptor ligands responsible for lipoprotein clearance. Secondly, to accelerate development of atherosclerotic lesions in hypercholesterolemic animals various forms of acute or chronic endothelial damage have been employed. The animal models differ with respect to degree of dietary cholesterol supplementation, length of hypercholesterolemia, dietary regimen and type, duration and degree of mechanical endothelial injury. Thus, this section will describe the various rabbit, hamster, pig, monkey and transgenic mouse models of atherosclerosis with respect to the different experimental protocols utilized to induce atherosclerotic lesions, the stage of atherosclerotic lesion development being replicated and advantages or disadvantages of the model for drug intervention studies.

### Rabbits

The cholesterol-fed rabbit has been extensively used as a model of atherosclerosis since the identification by Anitschkow [12] in 1913 that short-term cholesterol feeding results in formation of foamy lesions within the aorta. Historically, supplementation of commercial rabbit chow with 1 to 3%

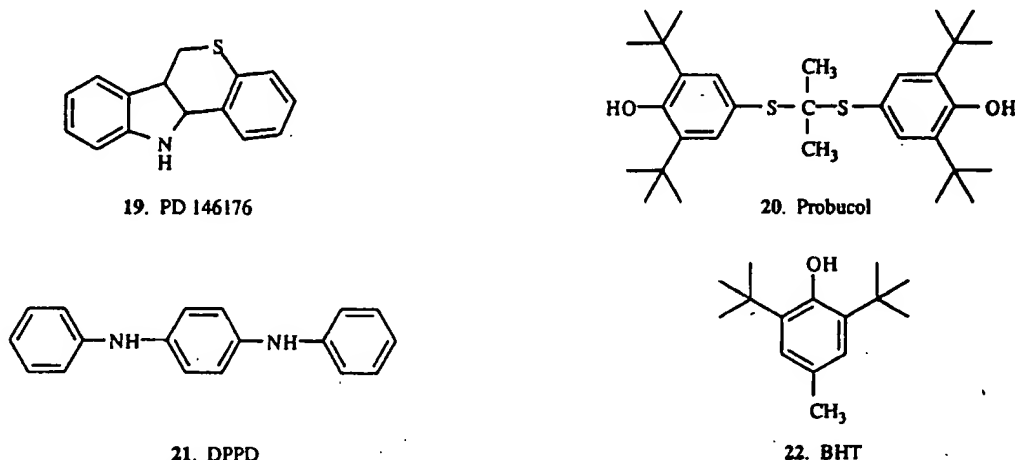


Fig. (3). Antioxidants and 15-LO inhibitors.

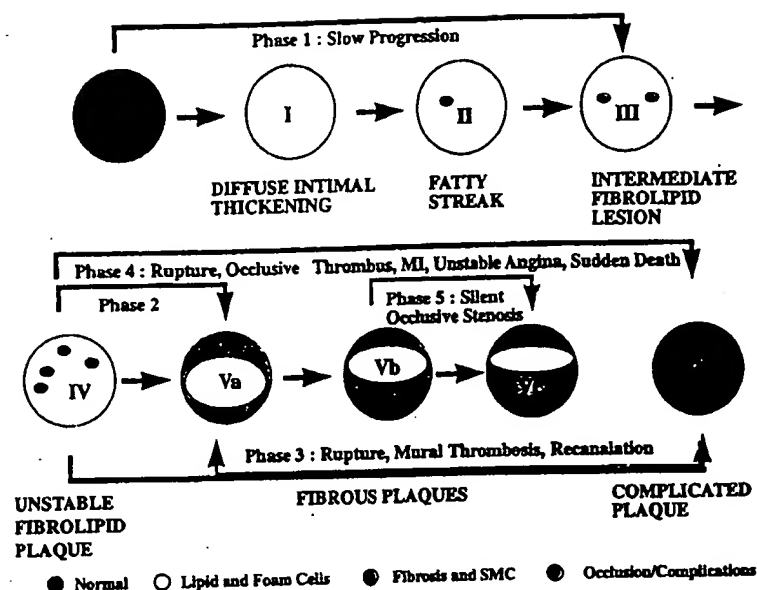


Fig. (4). Schematic representation of atherosclerotic lesion progression (adapted from references [6, 7]).

cholesterol and 4 to 8% fat [13] for 6 to 8 weeks has resulted in marked elevations in plasma cholesterol, i.e., 1000 to 3000 mg/dl, cholesteryl ester accumulation in hepatic and peripheral tissues [14,15] and development of aortic macrophage foam cell enriched lesions. Development of atherosclerosis in the coronaries is limited to the small intramyocardial vessels and not the larger epicardial vessels as has been found in man [16]. The rabbit atherosclerotic lesions were reminiscent in cellular composition to Type I to III human lesions. Kritchevsky and colleagues have performed numerous cholesterol feeding experiments in which they maintained the cholesterol supplementation constant, i.e., 2%, and altered the type of dietary fat to further refine the role of cholesterol metabolism in atherosclerosis progression. A notable finding was that upon addition of 6% peanut oil or 6% coconut oil to a 2% cholesterol diet two histologically distinct atherosclerotic lesions developed [17,18]. Peanut oil supplementation produced aortic lesions that contained relatively little lipid but abundant smooth muscle cell proliferation and collagen deposition. In contrast, addition of 6% coconut oil to the diet resulted in lesions with demonstrable intracellular lipid and intimal proliferation; however, less collagen and elastin were evident. Although elevated plasma cholesterol levels induce atherosclerotic lesions and dietary fat composition may affect the cellular composition of the lesion, in rabbits, prolonged hypercholesterolemia results in exponential cholesterol enrichment of many peripheral organs [19].

The marked cholesteryl ester enrichment of peripheral organs such as the liver and spleen may be problematic when evaluating pharmacologic agents. Liver metabolism of compounds may be compromised or enhanced in animals fed a high cholesterol diet and the resulting plasma levels may be either an underestimate or overestimate of the actual efficacious drug levels. Feeding a 2% cholesterol diet results in marked plasma total cholesterol levels and cholesteryl ester enriched beta-VLDL as the primary plasma lipoprotein [20]. Given the pro-atherogenic nature of beta-VLDL [21], the direct antiatherosclerotic activity of compounds with mechanisms

unrelated to cholesterol lowering may be masked due to the profound effect of beta-VLDL on monocyte-macrophage cholesteryl ester enrichment. We have noted that while compounds like ACAT inhibitors Fig. (1) (1-14) which prevent the accumulation of cholesteryl esters are antiatherosclerotic under such conditions, the 15-LO inhibitor, PD146176 Fig (3) (19), lacks activity because its mechanism of action may be related to oxidation of lipoproteins or pre-macrophage events such as monocyte adherence and transmigration.

Rabbit models of atherosclerosis have been developed which limit the amount of dietary cholesterol supplementation [22]; however, such models are time consuming and for that reason may have limited utility for screening antiatherosclerotic agents. Wilson and colleagues [22] fed rabbits an agar-gel diet containing 19% butter and 1% corn oil for up to 5 years. Plasma total cholesterol levels were approximately 300 mg/dl and over the course of 5 years atherosclerotic lesions representing Type I to V lesions were noted. Advanced atherosclerosis can also be induced in a shorter time frame by intermittent feeding of a 1% cholesterol, 5% cottonseed oil diet for 2 months followed by 6 months of a chow diet and 2 additional months of the cholesterol diet [23,24]. While plasma cholesterol levels fluctuated with dietary cholesterol supplementation, the five stages of atherosclerosis were present in both aorta and coronary arteries. Protracted feeding of a low cholesterol diet or intermittent feeding of high and low cholesterol diets produced histologically similar atherosclerotic lesions. Given the disparate plasma total cholesterol levels, these data suggest that the lipoprotein profile may play an important role in the rate at which atherosclerotic lesions develop. Feeding studies have indicated that beta-VLDL was the primary lipoprotein in rabbits fed a cholesterol diet while LDL-like particles predominated in animals fed a semisynthetic casein-enriched diet [25]. Morphologic and morphometric analysis of rabbits fed either a 0.125% to 0.5% cholesterol or casein-enriched diet for 6 months revealed that atherosclerotic lesions developed in both models; however, the nature and extent of lesions varied [25, 26]. At comparable plasma cholesterol levels, the cholesterol-fed

rabbits had approximately twice the extent of aortic atherosclerosis relative to the casein-fed animals and Type IV-V lesions predominated. In the casein-fed rabbits, 30% of the aorta contained atherosclerotic lesions that ranged in appearance from fatty dots to fibrous plaques with a necrotic lipid-rich core [25,26]. These data indicate that under a similar time frame and plasma cholesterol level the type of dietary supplementation can affect the quantity and type of atherosclerotic lesion that develops primarily by altering the major cholesterol carrying lipoprotein, i.e., beta-VLDL or LDL.

Genetic models of atherosclerosis, namely, the homozygote Watanabe Heritable Hyperlipidemic rabbit (WHHL) which lacks functional LDL receptors, have also been compared to cholesterol-fed rabbit models [27,28]. Like the casein-fed rabbits, plasma cholesterol was primarily distributed in LDL. In WHHL rabbits, leukocyte margination, subendothelial accumulation of isolated lipid-filled macrophages, accumulation of SMC and formation of fatty streaks occurred over the first 4 weeks of life [27]. A similar sequence of lesion formation was noted in New Zealand White rabbits fed a 0.1% to 0.2% cholesterol diet. Expansion of the lipid-filled monocyte-macrophage rich lesions, i.e., Type I-III fatty streaks, occurred during the first 6 months in both types of rabbits while complex Type V fibrous plaque lesions were noted in the WHHL and cholesterol-fed rabbits by 13 months of age [28-30]. An enrichment of cholesteryl ester, primarily cholesteryl oleate, was noted in the aorta of both animals over the course of 13 months and such a finding was consistent with the morphologic data noted above [31]. Despite the different lipoprotein distribution, one must conclude that the development of atherosclerosis in WHHL and cholesterol-fed rabbit is very similar and occurs within a similar time frame. One might propose that the WHHL rabbits may be useful to assess agents which lower plasma cholesterol by altering lipoprotein production since these animals lack functional LDL receptors. Cholesterol-fed models are less expensive and time consuming and may be manipulated by altering the level of cholesterol intake to assess the significance of graded degrees of hypercholesterolemia on cellular processes associated with lesion formation, e.g., monocyte adherence, margination and foam cell formation.

Thus far in the discussion of rabbits as models of atherosclerosis it is apparent that human-like atherosclerotic lesions can be induced by elevating plasma cholesterol levels through continuous or intermittent feeding of a cholesterol diet, a casein-enriched diet or by deleting functional LDL receptors as in the WHHL rabbit. It is also quite obvious that in such models a great deal of time is required to induce atherosclerotic lesions comparable to man, i.e., 6 months to 5 years.

Hypercholesterolemia and mechanical denudation of the endothelium in various vascular regions of the rabbit have been utilized to develop shorter-term models of atherosclerosis with a high degree of predictability as to the location and type of atherosclerotic lesion. Acute mechanical injury of the arterial vessel wall can be achieved using a variety of methods. A balloon embolectomy catheter [32] can denude the vessel and distend the media while gentle denudation can be achieved by drawing a nylon filament over the surface of the vessel [33, 34]. Moderate injury and denudation occur following cutting of the internal elastic lamina with a metal or diamond tipped catheter [35]. Chronic endothelial damage has been shown to promote

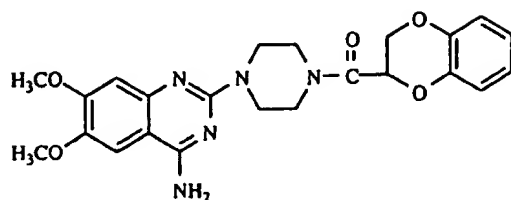
thrombosis at the catheter tip and formation of fibrous lesions [36, 37]. We have used a combination of chronic endothelial injury using a surgically implanted sterile nylon monofilament and dietary cholesterol supplementation [38, 39]. Combination of hypercholesterolemia and endothelial injury has allowed one to develop a model of atherosclerosis that is reproducible, has a high incidence of lesion formation and a predictable lesion site and type. The character of the atherosclerotic lesion is dependent upon the degree, length and type of hypercholesterolemia induced.

In summary, hypercholesterolemic rabbits are valuable models and the most widely used model for the evaluation of pharmacologic agents. Five types of human-like atherosclerotic lesions can be induced in the rabbit; however, the model is limited in that evidence of the complicated ruptured fibrous plaques cannot be found. Rabbits are also valuable for atherosclerosis research because unlike other models, atherosclerotic lesions progress even after removal of dietary cholesterol supplementation [23,40]. Evaluation of the direct antiatherosclerotic properties of hypocholesterolemic agents requires normalization of plasma cholesterol levels by diet prior to drug administration. Since rabbit atherosclerotic lesions will become more complex following cholesterol removal, agents which act by directly altering cellular processes such as ACAT inhibitors that limit macrophage accumulation can be discerned and their effect on lesion progression/regression can be monitored.

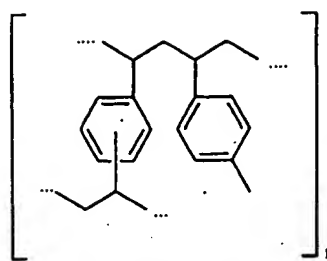
## Hamster

Another model of atherosclerosis that has received recent attention is the hypercholesterolemic hamster. Male hamsters fed a 3% cholesterol, 15% butterfat diet for up to a month had elevated plasma cholesterol levels and the presence of Type I fatty dots and fatty streaks within the aortic arch [41]. Within 3 to 4 months of the very high cholesterol/fat diet, expansion of the fatty streaks into the thoracic aorta around sites of intercostal ostia was noted [41]. By 10 months of cholesterol supplementation when plasma cholesterol levels were 17-times normal, advanced Type V lesions were observed in the aortic arch of the hamster but their extent was quite limited, i.e., 30% of the cross-sectional vessel surface. Feeding hamsters a 0.2% cholesterol, 10% coconut oil for 10 weeks [42] or 0.05% cholesterol, 10% coconut oil for 8 weeks [43] resulted in the accumulation of monocyte-macrophages within the aorta arch. Thus, short-term feeding of a cholesterol and either coconut oil or butterfat diet to hamsters is a model of subendothelial monocyte-macrophage foam cell formation. Atherosclerotic lesions can be found predictably within the inner curvature of the aortic arch and can be identified by staining with the lipid dye, Oil Red O. Such a model is useful due to its size for the acute evaluation of agents that may interfere with the early stages of lesion formation, e.g., monocyte adherence, transmigration and foam cell formation.

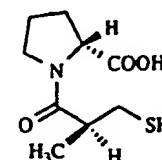
The hypercholesterolemic hamster has been used for the evaluation of numerous pharmacologic agents with varying mechanisms of action. Doxazosin Fig. (5) (23), an alpha-1 adrenergic inhibitor, and cholestyramine Fig. (5) (24) decreased the extent of Oil Red O-positive macrophage foam cells; however, one could not discern that this was a direct effect on the arterial wall because plasma cholesterol levels were



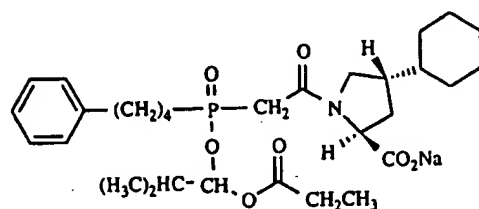
23. Doxazosin



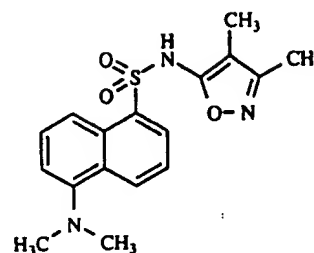
24. Cholestyramine



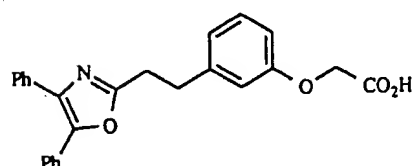
25. Captopril



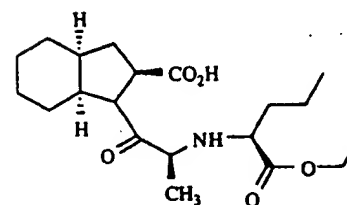
26. Fosinopril



27. BMS-182874



28. BMY-42393



29. Perindopril

Fig. (5). Broad group of compounds reported to possess antiatherosclerotic activities.

reduced by both groups and doxazosin (23) lowered blood pressure [43]. Higher doses of doxazosin (23) did not have any greater lipid lowering effect but a more marked reduction in macrophage foam cell area was noted and such data is suggestive that the compound may have a direct effect on monocyte-macrophage accumulation [42]. The HMG-CoA reductase inhibitor, lovastatin Fig. (2) (15), also was shown to reduce macrophage accumulation but again the changes were associated with a decrease in plasma cholesterol levels [44]. Inhibitors of angiotensin converting enzyme such as captopril Fig. (5) (25) without lowering plasma cholesterol and fosinopril Fig. (5) (26) by lowering LDL cholesterol, reduced aortic arch macrophage accumulation [45]. An additional study with captopril (25) and fosinopril (26) aimed at assessing the ability of these compounds to regress hamster atherosclerotic lesions was performed [46]. Both compounds were reported to reduce macrophage accumulation and thereby induce regression; however, while a group of animals was necropsied at 4 weeks to establish the degree of atherosclerosis prior to intervention only the drug treated animals were followed for an additional 6 weeks. A control designed to assess the effect of plasma cholesterol lowering or continued cholesterol feeding without intervention was not included. The ACAT inhibitor, octimibate [47] Fig. (1) (1), and endothelial subtype A receptor antagonist, BMS-182874 [48] Fig. (5) (27), both of which lowered plasma cholesterol, and the prostacyclin agonist, BMY42393 [47] Fig. (5) (28) in the absence of cholesterol lowering, have been

shown to limit macrophage accumulation in the hypercholesterolemic hamster. Thus, the hypercholesterolemic hamster has proven to be a useful model for the assessment of compounds; however, the changes in plasma cholesterol and blood pressure confound the interpretation of the antiatherosclerotic data and limit one's ability to ascribe the activity to a direct effect of the compounds.

## Swine

Swine are a non-rodent model of atherosclerosis in which atherosclerotic lesions have been found to develop spontaneously [49]. The pathogenesis of lesion development in pigs has been shown to closely parallel the stages of lesion formation as seen in man [50-52]. In addition, atherosclerotic lesion development can be exacerbated by combination of hypercholesterolemia and endothelial injury [53-56]. A strain of pigs with mutant apolipoprotein B alleles has been identified and these animals have been shown to be hypercholesterolemic due to defective lipoprotein clearance and prone to premature development of atherosclerosis [57-60]. Unlike the rabbit and hamster where lesions predominate in the aorta, atherosclerotic lesions have been observed in cerebral [61] and coronary [62] vessels of the pig. Thus, swine are a useful model for the evaluation of atherosclerosis from the perspective that lesions develop spontaneously, their circulatory system and localization of lesions are similar to man and the lesions are

responsive to dietary intervention by exhibiting regression after prolonged periods [63,64].

Despite their similarity to man with respect to atherosclerosis development, swine are not widely used for the evaluation of antiatherosclerotic agents. We have reported that the ACAT inhibitor, CI-976 Fig. (1) (2), blunted the progression of diet- and injury-induced atherosclerotic lesions in Yucatan miniature pigs potentially by inhibiting arterial ACAT and by lowering plasma VLDL-cholesterol levels [65]. The ACE inhibitor, perindopril Fig. (5) (29), was evaluated in hypercholesterolemic miniature pigs and noted to limit the development and monocyte-macrophage enrichment of aortic lesion; however, mean arterial blood pressure (MABP) was reduced in the animals [66]. Such reductions in MABP like the decrease in VLDL-cholesterol levels confound the interpretation of the data and limit one's ability to ascertain whether the compounds had a direct effect on lesion development. The limited a priori knowledge of a compound's effect on plasma cholesterol or blood pressure and the animal's inherent size are major disadvantages of using pigs for assessment of a compound's direct antiatherosclerotic potential. Miniature swine weigh approximately 12 kg at 4 months of age and in our studies feeding pigs a 2% cholesterol, 16% fat diet resulted in a doubling of their body weight within 4 months of diet initiation. Therefore, although swine are excellent models of atherosclerosis that mimic the human disease from the perspective of lesion pathology, such a model may be limited to evaluation of the antiatherosclerotic potential of compounds during their drug development stages rather than discovery phases.

## Monkeys

Non-human primates have often been portrayed as ideal models of human atherosclerosis due to their close phylogenetic association to man. The morphologic characterization of atherosclerotic lesion progression and regression has been performed in cynomolgous (*Macaca fascicularis*) [67-69], rhesus (*Macaca mulatta*) [70], cebus (*Cebus albifrons*) [71], squirrel (*Saimiri sciureus*) [71] and pigtail (*Macaca nemestrina*) [72-75] monkeys. The pathology of atherosclerotic lesion development in various monkey species has been shown to be quite similar to man. Spontaneous development of atherosclerotic lesions is rare in non-human primates; however, like in the animals noted above cholesterol feeding has been shown to promote the development of atherosclerosis in the monkey. Experimentally induced advanced atherosclerosis in monkeys requires approximately 3 years and addition of dietary cholesterol supplementation to produce plasma cholesterol levels of between 350 and 500 mg/dl. The localization of atherosclerotic lesions was similar to man in that lesions were present in the coronary arteries, abdominal aorta and iliac arteries. Plasma cholesterol levels of 200-400 mg/dl have been noted to produce advanced Type V fibrous plaques in *Macaca nemestrina* after 3.5 years of diet [72,73]. A retrospective evaluation of cebus and squirrel monkeys administered a normal diet without cholesterol supplementation and ranging in age from 12 to 20 years highlighted the difference in susceptibility to atherosclerosis and lesion character [71]. The older squirrel monkeys were found to have advanced Type IV-V atherosclerotic lesions containing lipid enrichment and a necrotic lipid core in the abdominal aorta

while lesions from older cebus monkeys were characterized as

diffuse intimal thickening without lipid accumulation [71]. Thus, it is apparent from evaluation of monkey models of atherosclerosis that lesions of comparable character to man, swine and in some cases rabbits can be achieved; however, a combination of a lower plasma cholesterol level and a longer period of time is required for lesion progression.

Few studies have been performed in monkeys using either dietary or pharmacologic intervention to promote lesion regression. After a 30 month lesion induction phase, switching cynomolgous monkeys to a chow diet initially, i.e., 6 months, results in a reduction in monocyte-macrophages and cholesteryl esters; however, intimal necrosis and free cholesterol monohydrate remain [67]. Within 12 months, the atherosclerotic lesions tended to resolve to an intimal scar with a lipid composition similar to normal vessels except for the presence of cholesterol crystals [67]. The bile acid sequestrant, cholestyramine Fig. (5) (24), the antioxidant, probucol Fig. (3) (20), either alone or upon coadministration was shown to promote atherosclerosis lesion regression in the rhesus monkeys [76] presumably due to lowering plasma cholesterol levels. Therefore, although atherosclerotic lesion development appears to mimic human disease progression, the utility of using these animals for drug discovery is limited by their availability and potential variability due to their underlying differences in age and degree of atherosclerosis progression. In addition, given the time frames required for lesion development in the monkey, rabbits fed a low cholesterol diet may be a viable substitute as shown by Wilson and colleagues [22].

## Transgenic Mice

Due to advances in molecular biology and the realization that mice, in general, are normally resistant to the development of atherosclerosis [77], genetically engineered mice have been developed which are predisposed to hypercholesterolemia-induced disease. Two well-characterized transgenic mouse models of atherosclerosis are the apolipoprotein E (apoE)-deficient mouse [78-80] and the low density lipoprotein (LDL) receptor-negative mouse [81,82]. ApoE is a major component of plasma lipoproteins that has a high affinity for LDL receptors and chylomicron remnant receptors [83,84] and may be important in facilitating reverse-cholesterol transport from peripheral tissues. The apoE-deficient mice have been shown to be hypercholesterolemic, i.e., 400 to 700 mg/dl at 5 to 55 weeks of age, while maintained on a chow diet [79]. Atherosclerotic lesions develop naturally over the time frame of 11 to 64 weeks within the aortic sinus and exhibit a similar histologic appearance as Type I to V lesions. Monocyte-macrophage foam cells predominate either as individual cells or clusters in the early stages of lesion development, i.e., less than 28 weeks, while fibrosis, intimal necrosis, acellular, necrotic lipid-rich cores with evidence of cholesterol clefts can be found after 32 weeks of age [79]. A similar histologic pattern can be seen in apoE-deficient mice fed a Western-type diet, i.e., 0.15% cholesterol; however, the timecourse of lesion development is shorter and the extent of atherosclerosis is greater [80]. Cholesterol-fed apoE-deficient mice have plasma cholesterol levels of 1000 to 4400 mg/dl over 6 to 40 weeks of age. Evidence of Type IV-V complex fibrous plaques can be seen as

early as 15 weeks and the lesions are not only present in the aortic sinus but also associated with the bifurcations of such major branch vessels as the common carotids, celiac, mesenteric, renal and iliac arteries [80].

The LDL receptor-negative transgenic mouse has also been developed [81,82]. Unlike the apoE-deficient mice, atherosclerotic lesions do not occur naturally during the timeframes currently studied, i.e., 6 months [82]. Dietary supplementation with 0.15% cholesterol results in plasma cholesterol levels of 900 to 1000 mg/dl over 6 months and the development of atherosclerotic lesions within the aortic sinus. The morphologic appearance and extent of atherosclerosis in the LDL receptor-negative mouse is similar to comparably fed apoE-deficient mice; however, plasma cholesterol levels are half that noted for the apoE-deficient mice and there is greater variability in the latter mouse model [82]. Thus, both the apoE and LDL receptor-deficient mice are viable small animal models for the evaluation of atherosclerotic lesion progression.

The utility of apoE and LDL receptor-deficient mice for the evaluation of antiatherosclerotic agents has yet to be determined. Few studies have been reported which utilize these mice in drug intervention studies. The antioxidant, N,N'-diphenyl 1,4-phenylenediamine (DPPD) Fig. (3) (21) has been evaluated in apoE-deficient mice fed along with a 0.15% cholesterol diet for 6 months and was found to reduce the extent of aortic atherosclerosis by 36%, i.e., control - 22%; DPPD (21) - 14% lesion coverage [85]. In contrast, probucol Fig. (3) (20), another antioxidant with hypolipidemic properties, accelerated the development of atherosclerosis in apoE-deficient mice irrespective of whether the compound was administered in a chow or cholesterol containing diet and despite lowering plasma cholesterol level [86]. Such paradoxical observations raise an important issue relating to interpretation of the results of drug intervention studies in genetically derived mouse models. One must question the appropriateness of the model for testing the specific compound of interest. For instance, unlike the LDL receptor-negative mouse that is a model of a naturally occurring abnormality, i.e., familial hypercholesterolemia, apoE-deficient mice possess a specific genetic deletion of an apolipoprotein that may be necessary for reverse-cholesterol transport. One can argue that if a compound's antiatherosclerotic activity is mediated through apoE metabolism such a mouse model would be inappropriate for assessing the compound's activity.

Numerous other transgenic mouse models have been developed. A few transgenic mouse models of potential relevance to atherosclerosis from the perspective of lipoprotein metabolism are the human apolipoprotein B [87], apolipoprotein (a) [88], Lp(a) [89,90] and cholesteryl ester transfer protein (CETP) [91] transgenic models. In addition, one might predict that site specific deletions or overexpression of pro-atherosclerotic molecules such as adhesion molecules, growth factors, cytokines or integrins, for example, would be useful models for the assessment of direct acting antiatherosclerotic agents. A caveat to such an approach is exemplified by the comparison of the apoE- and LDL receptor-deficient mice. Both genetic defects resulted in a similar atherosclerotic lesion pathology and required some degree of hypercholesterolemia. Therefore, temporal evaluations of lesion development in the presence and absence of pharmacologic agents may be more informative in assessing whether the specific gene product/defect exacerbates disease progression and

whether pathologic redundancies limit the efficacy of the specific pharmacologic entity.

## Pharmacologic Intervention Studies

### ACAT

Acyl-CoA:cholesterol O-acyltransferase (ACAT) is the primary enzyme responsible for the esterification of cholesterol in all mammalian cells, but under conditions of excessive cholesterol accumulation in the vascular wall, ACAT may be responsible for the generation of the hallmark of atherosclerosis, namely, the monocyte-macrophage foam cell. Since ACAT and cholesterol esterification may be considered a pro-atherogenic event, we and others have hypothesized that inhibition of arterial wall ACAT may prevent the formation of the macrophage-enriched fatty streak and the development of the clinically significant fibrous plaque. In addition, given the observations that monocyte-macrophages are localized to the potentially friable shoulder regions of atherosclerotic lesions and in association with matrix degrading enzymes, one might speculate that by limiting the accumulation of monocyte-macrophages through inhibition of ACAT one would promote the development of a stable plaque morphology.

Several inhibitors of ACAT have been evaluated in animals and they have been found to be antiatherosclerotic by measuring changes in lesion extent and/or cholesteryl ester enrichment. Schaffer and coworkers [92] reported that administration of CL277082 Fig. (1) (3) to rabbits for 16 weeks after a 10-week lesion induction phase resulted in a 49% reduction in aortic cholesteryl ester content. Cyclandalate Fig. (1) (4), a relatively weak inhibitor ( $IC_{50} = 80$  (M) with an unknown mechanism of inhibition [93] was shown to blunt the increase in aortic total cholesterol content when given to rabbits in a low-cholesterol chow diet after a lesion induction phase [94]. A more specific and potent inhibitor of ACAT, namely, RP-70676 Fig. (1) (5), administered in a similar manner as cyclandalate (4), was reported to decrease aortic free and esterified cholesterol content by 27 to 42% [95]. In addition, melinamide [96,97] Fig. (1) (6) and the furobenzochromene Fig. (1) (7) reported by Gammill et al. [98] were shown to prevent lesion formation in cholesterol-fed rabbits. Kimura and colleagues have also reported that a series of phenylureas Fig. (1) (8, 9, 10) limited the progression of aortic atherosclerotic lesions in the rabbit [99,100]. Other potent and systemically bioavailable inhibitors of ACAT, namely, E5324 [101] Fig. (1) (11) and FR145237 [102] Fig. (1) (12), significantly inhibited the progression and cholesterol enrichment of aortic atherosclerosis in rabbits. CI-976 Fig. (1) (2), a potent, systemically bioavailable inhibitor of ACAT was evaluated in hypercholesterolemic Yucatan micropigs and was noted to prevent the formation of atherosclerotic lesions [65]. Despite achieving plasma CI-976 (2) levels of 9 to 52 times the  $IC_{50}$  for inhibition of ACAT in mouse peritoneal macrophages, an accepted *in vitro* model of foam cell formation, one was left to conclude in this model that the antiatherosclerotic activity of the compound may be related to reductions in plasma VLDL-cholesterol since the antiatherosclerotic activity was highly correlated with plasma VLDL-cholesterol levels. Therefore, given the fact that in each of the studies cited above plasma total cholesterol levels were reduced in the animal models to the same extent or greater than



animals switched to a chow, low cholesterol diet, classification of these compounds as direct acting antiatherosclerotic agents is difficult.

Direct inhibition of arterial wall ACAT with a potent, systemically bioavailable agent although much harder to discern both preclinically and clinically may provide a greater vascular benefit than can be achieved by plasma cholesterol lowering alone. The ACAT inhibitor, CI-976 Fig. (1)(2), a fatty acid amide, was evaluated in a cholesterol-fed rabbit model of atherosclerosis at a dose that was bioavailable but did not lower plasma total cholesterol [39]. CI-976 (2) prevented the accumulation of monocyte-macrophages within a preestablished fibrofoamy lesion, attenuated the development of thoracic aortic fatty streak-like lesions and decreased the cholesteryl ester enrichment of the developed lesions. We have also reported that two isoxazoles Fig. (1)(13, 14) which were bioavailable based on a bioassay designed to assess plasma ACAT inhibitory bioequivalents limited the development of thoracic aortic foamy lesions but were inactive in the more fibroproliferative femoral lesions of the rabbit [103]. Others have also reported that in Watanabe heritable hyperlipidemic (WHHL) rabbits, a model of familial hypercholesterolemia lacking the LDL receptor, E5324 [104] Fig. (1)(11) and FR145237 [102] Fig. (1)(12) can limit the development of atherosclerotic lesions in the thoracic and coronary arteries in the absence of plasma cholesterol lowering. Kogushi et al. [104] have also shown that E5324 (11) markedly reduced aortic ACAT activity; however, such a decrease may be related to the reduction in lesion and macrophage extent and not a representation of direct arterial wall ACAT inhibition. Considering the data with CI-976 (2), E5324 (11) and FR145237 (12), one can conclude that ACAT inhibition has the potential to limit atherosclerosis progression by specifically affecting vascular monocyte-macrophage accumulation. However, it is also quite apparent from the various studies cited above that the experimental protocols can be quite varied.

The animal experimental protocols can be classified into several major categories. Firstly, compounds were administered either at the initiation of dietary cholesterol supplementation and the animals were necropsied after 2 to 4 months of treatment. These studies are often termed progression studies in that the effect of the compound on monocyte-macrophage accumulation or generation of Type I to Type III lesions is being studied. However, the hypocholesterolemic activity of the compounds limits the assessment of direct antiatherosclerotic activity. Secondly, compounds were given after a degree of hypercholesterolemia and atherosclerotic lesion development has been established. In most cases, animals were fed a cholesterol diet for 8 to 10 weeks and administered the various compounds either in the same cholesterol diet or a chow diet for an additional 6 to 8 weeks. Such studies can assess whether compounds can limit the further progression of a preestablished lesion and/or promote lesion regression. The ability to study lesion regression is often lost because few studies randomize animals based on their plasma total cholesterol and necropsy a group prior to drug intervention in order to assess the type, extent and composition of the lesions. Under these regression paradigms the antiatherosclerotic activity of the compound is best assessed when compared to either a group of animals switched to a chow diet or administered a cholesterol absorption inhibitor such as cholestyramine Fig. (5)(24) in order to match the degree of cholesterol lowering. Despite the extended period

of hypercholesterolemia such rabbit models are still representative of early fibrofoamy lesions (Type I-III) and not a reflection of the more advanced Type IV-V fibrous plaques. Thirdly, WHHL rabbits that appear refractory to plasma cholesterol lowering caused by ACAT inhibition can be used to assess a compound's antiatherosclerotic activity. The WHHL may be a very good model for the assessment of ACAT inhibitors in that plasma total and lipoprotein cholesterol levels remain relatively constant following treatment and more advanced atherosclerotic fibrous plaque lesions may develop in the long-term. Fourthly, as reported for CI-976 (2), a combination of chronic endothelial injury and cholesterol feeding in either a progression or regression paradigm can allow one to not only assess the development and regression of atherosclerotic lesions but also determine whether the compounds have an effect on the cellular composition of a defined, well-characterized lesion with a greater than 99% incidence of occurrence. Finally, models of more advanced atherosclerosis can also be developed and used to assess whether ACAT inhibitors can limit the formation or promote the more rapid development of advanced fibrous plaques. Rabbits exposed to chronic endothelial injury within one week of study initiation and sequentially fed a cholesterol, fat diet for 9 weeks, a fat only diet for 6 weeks and various compounds for 8 additional weeks has allowed us to develop advanced fibrous plaques in the rabbit within 23 weeks and to further address the benefit of ACAT inhibitors. Therefore, numerous models have been developed specifically for testing the direct antiatherosclerotic activity of ACAT inhibitors; however, our conclusions ascribing the activity of the compound to direct inhibition of arterial ACAT is still based on circumstantial evidence.

Numerous in vitro, biochemical and pharmacokinetic studies have been performed in order to relate plasma drug levels with the compound's  $IC_{50}$  for macrophage ACAT inhibition. The basis for claiming that an ACAT inhibitor is directly antiatherosclerotic appears to be rooted in the concept that if plasma drug levels are maintained above the  $IC_{50}$  for inhibition of macrophage ACAT and plasma total and lipoprotein cholesterol levels are unchanged then the compound has direct antiatherosclerotic properties. One assumes that the compound at steady state will partition into the various atherosclerotic lesions and inhibit macrophage ACAT. Direct measurement of arterial wall ACAT and vessel drug levels have been performed [104]. Given the observations that ACAT inhibitors limit arterial wall macrophage enrichment, i.e., a source of arterial ACAT, one must be cautious in interpreting a reduction in arterial wall ACAT activity as evidence for direct ACAT inhibition. A more plausible explanation is that there is a decrease in the amount of ACAT enzyme due to a reduction in macrophage accumulation. Standardization of atherosclerotic lesion size and cellular composition prior to acute administration of the ACAT inhibitor and assessment of ACAT activity may provide more definitive proof of direct arterial wall ACAT inhibition. However, an absence of ACAT inhibition may be misleading in that during the microsome isolation procedures compounds may be diluted out of the sample. Quantification of vessel drug levels is not only problematic and their accuracy can be questioned for the same reasons as noted above for the measurement of ACAT activity but also drug extraction efficiency and metabolism become an issue. Although still circumstantial another marker of arterial ACAT inhibition is the cholesteryl ester content of the vessel wall under comparable



levels of plasma total cholesterol exposure and atherosclerotic lesion/macrophage extents.

### HMG-CoA Reductase Inhibitors

3-hydroxy-3-methylglutaryl coenzyme A reductase (HMG-CoA reductase), in addition to being the rate limiting enzyme in the cholesterol biosynthetic pathway, is involved in the regulation of receptors for LDL-cholesterol [105]. In experimental animals [106], and patients with heterozygous familial hypercholesterolemia [107] inhibition of hepatic HMG-CoA reductase leads to an increased number of LDL receptors on the cell surface, which ultimately results in an enhanced clearance of plasma LDL and a reduction in plasma total cholesterol levels. However, in nonfamilial hypercholesterolemic and familial combined hyperlipidemic patients, HMG-CoA reductase inhibitors lower plasma cholesterol by inhibiting lipoprotein production [108]. Reductions in plasma total cholesterol of over 30% and in LDL-cholesterol of 40% have been observed in clinical trials with various doses of atorvastatin [109] Fig. (2)(16), lovastatin [110] Fig. (2)(15), pravastatin [111] Fig. (2)(17), and simvastatin [112] Fig. (2)(18). In addition, the recent Scandinavian Simvastatin Survival Study (4S) [113] has shown that lowering plasma cholesterol by 35% with diet and simvastatin (18) significantly reduces the risk of mortality by 30%, coronary heart disease mortality by 42%, and incidence of nonfatal myocardial infarction by 37%. The West of Scotland Study (WOSCOPS) has demonstrated that lowering plasma LDL-cholesterol by 26% with diet and pravastatin (17) significantly reduced the risk of mortality from definite coronary events by 31% [114]. Thus, the data in man indicate that inhibitors of HMG-CoA reductase by reducing plasma cholesterol may limit the development of atherosclerosis and reduce the risk of mortality.

Several animal studies have also shown that lovastatin (15) and pravastatin (17) can attenuate atherosclerotic lesion development when plasma total and LDL-cholesterol are reduced [115-118], and that atorvastatin (16) can limit lesion development independent of changes in plasma cholesterol [119]. Due to the potent hypolipidemic activity of HMG-CoA reductase inhibitors, the assessment of these compound's direct antiatherosclerotic potential in preclinical models of atherosclerosis is difficult. However, comparison of compounds with a similar plasma total cholesterol exposure may allow one to assess whether an agent has any inherent antiatherosclerotic properties. For instance, we reported that in a cholesterol-fed rabbit model of lesion progression, lovastatin (15), pravastatin (17) and atorvastatin (16) reduced plasma total cholesterol exposure over the course of the experiment by 37% to 43% [119]. Given the linear relationship between plasma cholesterol and atherosclerosis extent noted previously [120], one might expect that the degree and composition of the atherosclerotic lesions would be similar amongst the three treatment groups. Despite equal plasma cholesterol levels, pravastatin (17) and lovastatin (15) had no effect on thoracic aortic lesion extent or iliac-femoral cross-sectional lesion area. In contrast, atorvastatin (16) reduced the thoracic aortic lesion extent from 44% to 19% and iliac-femoral lesion area by 67%. Thus, we concluded that atorvastatin can directly limit atherosclerosis lesion progression.

Evaluation of the various HMG-CoA reductase inhibitors in a rabbit model of atherosclerosis lesion progression highlights the power of the experimental design in formulating an interpretation of the data. Given the fact that plasma cholesterol levels were reduced, an analysis of a subset of compounds with the same cholesterol exposure allowed one to assess their relative antiatherosclerotic activity and also ascribe the activity to a direct effect on the lesion. Establishment of the effect of lipid-lowering on atherosclerosis development is an important factor when assessing compound efficacy. Addition of control treatments such as cholestyramine Fig. (5)(24), a non-absorbable resin, or diets containing graded cholesterol contents are methods for assessing the antiatherosclerotic activity of a compound at defined plasma cholesterol levels. Reductions in lesion size, extent or composition above that predicted for a given plasma cholesterol level may indicate that the compound is directly altering a pro-atherogenic event.

Comparison of biochemical, morphologic and morphometric results may allow one to establish the consistency of the effect and to identify potential mechanisms for the observed antiatherosclerotic activity. For instance [119], not only did atorvastatin Fig. (2)(16) decrease the extent of thoracic aortic atherosclerosis but also reduced the cholesteryl ester content of the thoracic aorta, a secondary marker that is reflective of the lesion extent and composition, i.e., lipid, monocyte-macrophage enrichment. Examination of the histopathology of the atherosclerotic lesions and morphometric changes following treatment allowed one to discern potential mechanisms responsible for the observed antiatherosclerotic activity. For example, pravastatin Fig. (2)(17) had no effect on lesion or monocyte-macrophage area while atorvastatin Fig. (2)(16) reduced both parameters. One might conclude from these data that pravastatin (17) lacked sufficient plasma drug levels or did not penetrate the arterial wall and that atorvastatin (16) by directly limiting lesion size through inhibition of smooth muscle cell migration and proliferation indirectly reduced macrophage accumulation. The later hypothesis is consistent with observations made by others which indicate that HMG-CoA reductase inhibitors in tissue culture limit SMC proliferation [121-123] and migration [124] by interfering with isoprenoid synthesis [125].

Therefore, by controlling for the degree of plasma cholesterol lowering and combining multiple efficacy parameters, one might not only be able to discriminate the direct antiatherosclerotic activity of a compound from that due to plasma cholesterol lowering but also by evaluating the structure of the atherosclerotic lesions identify potential mechanisms which can be tested in vitro or in appropriate animal models.

### Anti-Oxidants and 15-Lipoxygenase Inhibitors

Steinberg and colleagues [126] have reported that oxidatively modified LDL may be important in the progression of atherosclerosis due to the observations that oxidized LDL is cytotoxic, chemotactic and chemostatic. Oxidative modification of insudant plasma lipoproteins is presumably an extracellular event [126] and the resulting oxidized lipoproteins have been implicated in the regulation of chemokines [127] and pro-atherogenic adhesion molecules [128]. Both apolipoprotein B [129-132], the major protein in LDL, and lipid peroxides have been localized to atherosclerotic lesions [133]. Oxidatively

modified LDL or such oxidation products as malondialdehyde-conjugated LDL or 4-hydroxynonenal-conjugated LDL have been localized to WHHL rabbits [134-136]. Thus, one can conclude that oxidation of lipoproteins may be important in the development of atherosclerosis and that general antioxidants may be antiatherosclerotic in both man and models of atherosclerosis.

Several studies investigating the antiatherosclerotic activity of general antioxidants have been performed in New Zealand white rabbits [137-140], WHHL rabbits [141,142], pigs [143] and monkeys [76] under a variety of experimental conditions. In cholesterol-fed rabbits, butylated hydroxytoluene (BHT) Fig. (3)(22), vitamins E plus C, vitamins E plus A and probucol Fig. (3)(20) limited the development of thoracic aortic lesions [137-140, 144-146]. Probuco (20) has been shown by numerous individuals to reduce the extent, cholesterol enrichment and cross-sectional lesion size of atherosclerotic lesions in WHHL rabbits [141,142], balloon-injured normocholesterolemic pigs [143] and hypercholesterolemic monkeys [76]. Close examination of the lesion histopathology revealed that probucol (20) reduced the extent of atherosclerosis by decreasing the abundance of monocyte-macrophages within the lesion [146]. Mechanistic studies in rabbits fed cholesterol for a short time period, i.e., 5 wks, indicated that probucol (20) can limit the adhesion of monocytes to the endothelial cell surface. The single study in coronary artery balloon-injured pigs also indicated that probucol (20) can limit the development of primarily fibroproliferative lesions through presumably affecting SMC migration and proliferation [143]. Thus, one can conclude that antioxidants and specifically, probucol (20), can limit the development and cellular composition of atherosclerotic lesions in various animal models of atherosclerosis irrespective of whether the compound was administered to animals with or without pre-established lesions.

In most of the studies noted above, plasma cholesterol lowering was minimal so attempts to identify surrogate markers of vascular efficacy of the various antioxidants were made. Resistance of lipoproteins to oxidation was a major surrogate marker used by most investigators [141,142]. Measurements of vascular reactivity were also made [147,148]. In hypercholesterolemic rabbits, probucol (20) treatment preserved endothelial function and vascular rings upon exposure to acetylcholine in organ culture were shown to relax normally [147]. The improved vascular responsiveness is quite remarkable and one can conclude that antioxidants may improve vascular function; however, while in both studies plasma total cholesterol levels were relatively constant among the control and probucol-treated (20) groups, one study [148] reported that the cholesterol content of vessels from the drug-treated group was reduced. Since atherosclerosis is comprised of multiple stages and drugs such as probucol (20) can alter the type as well as cellular and lipid composition of the atherosclerotic lesions, correlation of pathology with functional changes is important in the assessment of drug efficacy. Experimental protocols can be designed to assess the inherent activity of compounds to promote vasorelaxation. Given the observation that some agents lower plasma or vascular cholesterol levels, administration of agents to normocholesterolemic animals or atherosclerotic animals where plasma cholesterol levels are normalized by diet may allow one to assess whether the compound has a direct effect on vascular relaxation either in the presence or absence of underlying disease.

Based on the pathology data and the localization of epitopes of oxidized LDL within the arterial wall, one can suggest that general antioxidants may be useful antiatherosclerotic agents. However, specific inhibitors of the oxidation process may allow one to target a specific pro-atherogenic process and to better characterize the compound's activity in models of atherosclerosis. A new enzyme specific target, namely arachidonate 15-lipoxygenase (15-LO), has emerged [149]. Arachidonate 15-lipoxygenase is a lipid-peroxidizing enzyme that is also present in atherosclerotic lesions. Investigators have found the 15-LO gene [150], stereospecific products of the 15-LO enzyme [151] and coincident localization of 15-LO mRNA, protein and epitopes of oxidized LDL within macrophage-rich areas of atherosclerotic lesions [149]. We have identified a specific inhibitor of 15-LO, namely, PD146176 Fig. (3)(19), and have evaluated the compound in several models of atherosclerosis [152,153].

Evaluation of PD146176 (19) in the hypercholesterolemic rabbit under three specific experimental paradigms has allowed us to conclude that in the absence of lowering plasma total and lipoprotein cholesterol levels PD146176 (19) can attenuate the development of diet induced atherosclerotic lesions through specific inhibition of monocyte-macrophage accumulation. In addition, PD146176 (19) can limit the development and macrophage enrichment of pre-established atherosclerotic lesions. PD146176 (19) administered to rabbits coincident with a cholesterol diet reduced the gross extent of foamy lesions (Type I-III lesions) within and cholesterol enrichment of the thoracic and abdominal aorta [152]. PD146176 (19) administered to rabbits coincident with a cholesterol diet and induction of a chronic endothelial injury not only reduced the progression of foamy thoracic lesions but also specifically limited the accumulation of monocyte-macrophages within a fibrofoamy iliac-femoral lesion without affecting the overall lesion size [153]. PD146176 (19) administered after establishment of fibrofoamy Type IV lesions through a combination of chronic endothelial injury and dietary cholesterol supplementation reduced the extent, cross-sectional area and monocyte-macrophage content of the more advanced Type V fibrous plaque [153]. In all three studies, assessment of plasma total and lipoprotein levels, vascular lipid content and histologic evidence for the presence of 15-LO in the lesions were necessary to corroborate the findings and maintain the implication that 15-LO was involved. Thus, these data highlight the antiatherosclerotic potential of a specific 15-LO inhibitor.

The brief summary of the antiatherosclerotic effects of PD146176 (19) can also be used to exemplify the power of the animal models of atherosclerosis. The simplest model, a rabbit fed a 0.25% cholesterol, 3% peanut, 3% coconut oil diet illustrated that the compound can prevent the formation of cholesteryl ester enriched Type III foamy atherosclerotic lesions. One might propose that evaluation of rabbits fed cholesterol for shorter periods of time would allow one to assess whether the observed antiatherosclerotic activity was due to reduced monocyte adherence. In the second rabbit model, induction of a fibrofoamy lesion by chronic endothelial injury allowed one to build upon the first observation and suggest that the compound specifically limited monocyte-macrophage accumulation because the absolute lesion cross-sectional area was unchanged. In the most complex model, one was able to assess whether PD146176 (19) could limit the progression of the disease to a fibrous plaque or promote regression of a

preestablished fibrofoamy lesion. In addition, one can obtain such mechanistic information as to the involvement of 15-LO in advanced atherosclerosis and whether further monocyte-macrophage enrichment can be blunted.

## Conclusions

Atherosclerotic lesion development can be divided into six histologically distinct stages and five dynamic phases. Specifically, atherosclerotic lesion progression in man involves episodes of SMC proliferation, extracellular matrix deposition and remodeling, lipid infiltration, endothelial cell-monocyte interactions, monocyte migration into the intima, monocyte-macrophage foam cell formation, necrotic lipid-rich core formation, calcium deposition, neovascularization, mural microthrombi and occlusive acute thrombosis. Given the complexity of atherosclerotic lesion development in man, the challenge exists to develop animal models that closely mimic the human disease. One must accept, however, that there is no one perfect animal model that completely replicates the stages of human atherosclerosis but that the models are useful in studying specific pathologic processes associated with the disease. Hypercholesterolemic rabbits either with or without endothelial injury are valuable models and the most widely used model for the evaluation of pharmacologic agents. Five types of human-like atherosclerotic lesions can be induced in the rabbit; however, the model is limited in that evidence of the plaque rupture cannot be found. Hypercholesterolemic hamsters are a model of an early pro-atherogenic event, namely, subendothelial monocyte-macrophage foam cell formation. Swine are a useful model for the evaluation of atherosclerosis from the perspective that lesions develop spontaneously, their circulatory system and localization of lesions are similar to man and the lesions are responsive to dietary intervention by exhibiting regression after prolonged periods. Non-human primates have often been portrayed as ideal models of human atherosclerosis due to their close phylogenetic association to man; however, lesions of comparable character to man can be induced more efficiently and over shorter time periods in swine and in some cases rabbits through a combination of hypercholesterolemia and endothelial injury. Numerous transgenic mouse models have been developed in recent years. A common finding among the various mouse models of atherosclerosis is that a similar atherosclerotic lesion pathology develops and all require some degree of hypercholesterolemia. Therefore, temporal evaluations of lesion development in the presence and absence of pharmacologic agents may be more informative in assessing whether the specific gene product/defect exacerbates disease progression and whether pathologic redundancies limit the efficacy of the specific pharmacologic entity. Based on evaluation of the various animal models and pharmacologic agents, one can conclude that: (1) each animal model provides insight into specific aspects of the disease process; (2) a hypercholesterolemic state is required in all models for the development of atherosclerosis; (3) discrimination of the *direct* antiatherosclerotic activity of a compound from its *indirect* activity requires one to limit the number of confounding factors, e.g., hypocholesterolemic and antihypertensive effect; (4) combination of biochemical, morphologic and morphometric measures allows one to both validate the antiatherosclerotic effect and define potential mechanisms; (5) reducing monocyte-macrophage involvement irrespective of mechanism or animal

model effectively limits the development of atherosclerotic lesions.

## Abbreviations

ACAT	=	Acyl-coenzyme A:cholesterol O-acyltransferase
HMG-CoA reductase	=	3-Hydroxy-3-methylglutaryl coenzyme A
15-LO	=	15-Lipoxygenase
SMC	=	Smooth muscle cells
VCAM-1	=	Vascular cell adhesion molecule-1
VLDL	=	Very low density lipoproteins
LDL	=	Low density lipoproteins
WHHL	=	Watanabe heritable hyperlipidemic rabbit
ACE	=	Angiotensin converting enzyme
MABP	=	Mean arterial blood pressure
ApoE	=	Apolipoprotein E
CETP	=	Cholesteryl ester transfer protein
4S	=	Scandinavian Simvastatin Survival Study
WOSCOP	=	The West of Scotland Study

## Acknowledgement

I would like to thank Dr. D. Robert Sliskovic for his kind invitation to write this article and for his help in preparation of the figures depicting chemical structures of the compounds cited in the manuscript.

## References

- [1] Tracy, R.E. *Lab. Invest.*, 1979, 41, 546.
- [2] Constantinides, P. J. *Ultrastruct. Res.*, 1966, 6, 1.
- [3] Ridolfi, R.L.; Hutchins, G.M. *Am. Heart J.*, 1977, 93, 468.
- [4] Cornhill, J.F.; Herderick, E.E.; Stary, H.C. *Monogr. Atheroscler.*, 1990, 15, 13.
- [5] Cornhill, J.F.; Barrett, W.A.; Herderick, E.E.; Mahley, R.W.; Fry, D.L. *Arterioscler.*, 1985, 5, 415.
- [6] Stary, H.C.; Chandler, A.B.; Glagov, S.; Guyton, J.R.; Insull, W. Jr.; Rosenfeld, M.E.; Schaffer, S.A.; Schwartz, C.J.; Wagner, W.D.; Wissler, R.W. *Circ.*, 1994, 89, 2462.
- [7] Fuster, V. *Circ.*, 1994, 90, 2126.
- [8] Smith, E.B.; Evans, P.H.; Downham, M.D. *J. Atheroscler. Res.*, 1967, 7, 171.
- [9] Kume, N.; Cybulsky, M.I.; Gimbrone, M.A. *J. Clin. Invest.*, 1992, 90, 1138.
- [10] Cybulsky, M.I.; Gimbrone, M.A. *Science*, 1991, 252, 788.

- [11] Krause, B.R.; Sliskovic, D.R.; Bocan, T.M.A. *Exp. Opin. Invest. Drugs*, 1995, 4, 353.
- [12] Anitschkow, N. *Beitr. Pathol. Anat. Allgem. Pathol.*, 1913, 56, 379.
- [13] Jokinen, M.P.; Clarkson, T.B.; Prichard, R.W. *Exp. Mol. Pathol.*, 1985, 42, 1.
- [14] Prior, J.T.; Kurtz, D.M.; Ziegler, D.D. *Arch. Pathol.*, 1961, 71, 672.
- [15] Kroon, P.A.; Thompson; Chao, Y. *Atherosclerosis*, 1985, 56, 323.
- [16] Prior, J.T.; Kurtz, D.M.; Ziegler, D.D. *Arch. Pathol.*, 1961, 71, 82.
- [17] Kritchevsky, D.; Tepper, S.A.; Vesselinovitch, D.; Wissler, R.W. *Atherosclerosis*, 1971, 14, 53.
- [18] Kritchevsky, D.; Tepper, S.A.; Kim, H.K.; Story, J.A.; Vesselinovitch, D.; Wissler, R.W. *Exp. Molec. Pathol.*, 1976, 24, 375.
- [19] Ho, K.J.; Pang, L.C.; Taylor, C.B. *Atherosclerosis*, 1974, 19, 561.
- [20] Ross, A.C.; Minick, C.R.; Zilversmit, D.B. *Atherosclerosis*, 1978, 29, 301.
- [21] Mahley, R.W.; Innerarity, T.L.; Rall, S.C. Jr; Weisgraber, K.H. *Ann. NY Acad. Sci.*, 1985, 454, 209.
- [22] Wilson, R.B.; Miller, R.A.; Middleton, C.C.; Kinden, D. *Arterioscler.*, 1982, 2, 228.
- [23] Constantinides, P.; Booth, J.; Carlson, G. *Arch. Pathol.*, 1960, 70, 712.
- [24] Constantinides, P. *J. Atherosclerosis Res.*, 1961, 1, 374.
- [25] Daley, S.J.; Herderick, E.E.; Cornhill, F.; Rogers, K.A. *Arterioscler. Thromb.*, 1994, 14, 95.
- [26] Daley, S.J.; Klemp, K.F.; Guyton, J.R.; Rogers, K.A. *Arterioscler. Thromb.*, 1994, 14, 105.
- [27] Rosenfeld, M.E.; Tsukada, T.; Gown, A.M.; Ross, R. *Arterioscler.*, 1987, 7, 9.
- [28] Rosenfeld, M.E.; Tsukada, T.; Chait, A.; Bierman, E.L.; Gown, A.M.; Ross, R. *Arterioscler.*, 1987, 7, 24.
- [29] Tsukada, T.; Rosenfeld, M.; Ross, R.; Gown, A.M. *Arterioscler.*, 1986, 6, 601.
- [30] Shiomi, M.; Ito, T.; Tsukada, T.; Yata, T.; Ueda, M. *Arterioscler. Thromb.*, 1994, 14, 931.
- [31] Rosenfeld, M.E.; Chait, A.; Bierman, E.L.; King, W.; Goodwin, P.; Walden, C.E.; Ross, R. *Arterioscler.*, 1988, 8, 338.
- [32] Stadius, M.L.; Rowan, R.; Fleishhauer, J.F.; Kernoff, R.; Billingham, M.; Gown, A.M. *Arterioscler. Thromb.*, 1992, 12, 1267.
- [33] Reidy, M.A.; Harker, L.A.; Schwartz, S. *Fed. Proc.*, 1983, 42, 771.
- [34] Reidy, M.A.; Yoshida, K.; Harker, L.A.; Schwartz, S.M. *Arterioscler.*, 1986, 6, 305.
- [35] Bjorkerud, S.; Bondjers, G. *Atherosclerosis*, 1971, 13, 355.
- [36] Moore, S. *Lab. Invest.*, 1973, 29, 478.
- [37] Moore, S.; Friedman, R.J.; Singal, D.P.; Gaudie, J.; Blajchman, M.A.; Roberts, R.S. *Thrombos. Haemostasis (Stuttgart)*, 1976, 35, 70.
- [38] Bocan, T.M.A.; Bak Mueller, S.; Uhlendorf, P.D.; Ferguson, E.; Newton, R.S. *Exp. Molec. Pathol.*, 1991, 54, 201.
- [39] Bocan, T.M.A.; Bak Mueller, S.; Uhlendorf, P.D.; Newton, R.S.; Krause, B.R. *Arterioscler. Thromb.*, 1991, 11, 1830.
- [40] Friedman, M.; Byers, S.O. *Am. J. Pathol.*, 1963, 43, 349.
- [41] Nistor, A.; Bulla, A.; Filip, D.A.; Radu, A. *Atherosclerosis*, 1987, 68, 159.
- [42] Foxall, T.L.; Shwaery, G.T.; Stucchi, A.F.; Nicolosi, R.J.; Wong, S.S. *Am. J. Pathol.*, 1992, 140, 1357.
- [43] Kowala, M.C.; Nunnari, J.J.; Durham, S.K.; Nicolosi, R.J. *Atherosclerosis*, 1991, 91, 35.
- [44] Otto, J.; Ordovas, J.M.; Smith, D.; van Dongen, D.; Nicolosi, R.J.; Schaefer, E.J. *Atherosclerosis*, 1995, 114, 19.
- [45] Kowala, M.C.; Grove, R.I.; Aberg, G. *Atherosclerosis*, 1994, 108, 61.
- [46] Kowala, M.C.; Recce, R.; Beyer, S.; Aberg, G. *J. Cardiovascular Pharm.*, 1995, 25, 179.
- [47] Kowala, M.C.; Mazzucco, C.E.; Hartl, K.S.; Seiler, S.M.; Warr, G.A.; Abid, S.; Grove, R.I. *Arterioscler. Thromb.*, 1993, 13, 435.
- [48] Kowala, M.C.; Rose, P.M.; Stein, P.D.; Goller, N.; Recce, R.; Beyer, S.; Valentine, M.; Barton, D.; Durham, S.K. *Am. J. Pathol.*, 1995, 146, 819.
- [49] Gottlieb, H.; Lalich, J.J. *Am. J. Pathol.*, 1954, 30, 851.
- [50] Moreland, A.F.; Clarkson, T.B.; Lofland, H.B. *Arch. Pathol.*, 1963, 76, 99.
- [51] French, J.E.; Jennings, M.A.; Florey, H.W. *Ann. NY Acad. Sci.*, 1965, 127, 780.
- [52] Reitman, J.S.; Mahley, R.W.; Fry, D.L. *Atherosclerosis*, 1982, 43, 119.
- [53] Nam, S.C.; Lee, W.M.; Jarmolych, J.; Lee, K.T.; Thomas, W.A. *Exp. Molec. Pathol.*, 1973, 18, 369.
- [54] Lee, W.M.; Lee K.T. *Exp. Molec. Pathol.*, 1975, 23, 491.
- [55] Fritz, K.E.; Daoud, A.S.; Augustyn, J.M.; Jarmolych, J. *Exp. Molec. Pathol.*, 1980, 32, 61.
- [56] Dov Gal, D.V.M.; Rongione, A.J.; Slovenkai, G.A.; DeJesus, S.T.; Lucas, A.; Fields, C.D.; Isner, J.M. *Am. Heart J.*, 1990, 119, 291.
- [57] Rapacz, J.; Hasler-Rapacz, J.; Taylor, K.M.; Checovich, W.J.; Attie, A.D. *Science*, 1986, 234, 1573.
- [58] Lowe, S.W.; Checovich, W.J.; Rapacz, J.; Attie, A.D. *J. Biol. Chem.*, 1988, 263, 15467.
- [59] Checovich, W.J.; Fitch, W.L.; Krauss, R.M.; Smith, M.P.; Rapacz, J.; Smith, C.L.; Attie, A.D. *Biochem.*, 1988, 27, 1934.
- [60] Prescott, M.F.; McBride, C.H.; Hasler-Rapacz, L.; Von-Linden, J.; Rapacz, J. *Am. J. Pathol.*, 1991, 139.

- [61] Detweiler, D.K.; Ratcliffe, H.L.; Luginbuhl, H. *Ann. N. Y. Acad. Sci.*, 1968, 149, 868.
- [62] Reddick, R.L.; Read, M.S.; Brinkhous, K.M.; Bellinger, D.; Nichols, T.; Griggs, T.R. *Arterioscler.*, 1990, 10, 541.
- [63] Daoud, A.S.; Jarmolych, J.; Augustyn J.M.; Fritz, K.E.; Singh, J.K.; Lee, K.T. *Arch. Pathol. Lab. Med.*, 1976, 100, 372.
- [64] Fritz, K.E.; Augustyn, J.M.; Jarmolych, J.; Daoud, A.S.; Lee, K.T. *Arch. Pathol. Lab. Med.*, 1976, 100, 380.
- [65] Bocan, T.M.A.; Bak Mueller, S.; Uhlendorf, P.D.; QuenbyBrown, E.; Mazur, M.J.; Black, A.E. *Atherosclerosis*, 1993, 99, 175.
- [66] Charpiot, P.; Rolland, P.H.; Friggi, A.; Piquet, P.; Scalbert, E.; Bodard, H.; Barlatier, A.; Latrille, V.; Tranier, P.; Mercier, C.; Luccioni, R.; Calaf, R.; Garcon, D. *Arterioscler. Thromb.*, 1993, 13, 1125.
- [67] Small, D.M.; Bond, M.G.; Waugh, D.; Prack, M.; Sawyer, J.K. *J. Clin. Invest.*, 1984, 73, 1590.
- [68] Stary, H.C.; Malinow, M.R. *Atherosclerosis*, 1982, 43, 151.
- [69] Kramsch, D.M.; Hollander, W. *Expt. Molec. Pathol.*, 1968, 9, 1.
- [70] DePalma, R.G.; Klein, L.; Bellon, E.M.; Koletsky, S. *Arch. Surg.*, 1980, 115, 1268.
- [71] Hoover, G.A.; Nicolosi, R.J.; Camp, R.R.; Hayes, K.C. *Arterioscler.*, 1982, 2, 252.
- [72] Masuda, J.; Ross, R. *Arterioscler.*, 1990, 10, 164.
- [73] Masuda, J.; Ross, R. *Arterioscler.*, 1990, 10, 178.
- [74] Faggiotto, A.; Ross, R.; Harker, L. *Arterioscler.*, 1984, 4, 323.
- [75] Faggiotto, A.; Ross, R. *Arterioscler.*, 1984, 4, 341.
- [76] Wissler, R.W.; Vesselinovitch, D. *Appl. Pathol.*, 1983, 1, 89.
- [77] Paigen, B.; Ishida, B.Y.; Verstuyft, J.; Winters, R.B.; Albee, D. *Arterioscler.*, 1990, 10, 316.
- [78] Plump, A.S.; Smith, J.D.; Hayek, T.; Aalto-Setälä, K.; Walsh, A.; Verstuyft, J.G.; Rubin, E.M.; Breslow, J.L. *Cell*, 1992, 71, 343.
- [79] Reddick, R.L.; Zhang, S.H.; Maeda, N. *Arterioscler. Thromb.*, 1994, 14, 141.
- [80] Nakashima, Y.; Plump, A.S.; Raines, E.W.; Breslow, J.L.; Ross, R. *Arterioscler. Thromb.*, 1994, 14, 133.
- [81] Ishibashi, S.; Goldstein, J.L.; Brown, M.S.; Herz, J.; Burns, D.K. *J. Clin. Invest.*, 1994, 93, 1885.
- [82] Tangirala, R.K.; Rubin, E.M.; Palinski, W. *J. Lipid Res.*, 1995, 36, 2320.
- [83] Mahley, R.W. *Science*, 1988, 240, 622.
- [84] Brown, M.S.; Goldstein, J.L. *Science*, 1986, 232, 4.
- [85] Tangirala, R.K.; Casanada, F.; Miller, E.; Witzum, J.L.; Steinberg, D.; Palinski, W. *Arterioscler. Thromb. Vasc. Biol.*, 1995, 15, 1625.
- [86] Zhang, S.H.; Reddick, R.L.; Avdievich, E.; Surles, L.K.; Jones, R.G.; Reynolds, J.B.; Quarfordt, S.H.; Maeda, N. *J. Clin. Invest.*, 1997, 99, 2858.
- [87] Purcell-Huynh, D.A.; Farese, R.V., Jr.; Johnson, D.F.; Flynn, L.M.; Pierotti, V.; Newland, D.L.; Linton, M.F.; Sanan, D.A.; Young, S.G. *J. Clin. Invest.*, 1995, 95, 2246.
- [88] Lawn, R.M.; Wade, D.P.; Hammer, R.E.; Chiesa, G.; Verstuyft, J.G.; Rubin, E.M. *Nature*, 1992, 360, 670.
- [89] Mancini, F.P.; Newland, D.L.; Mooser, V.; Murata, J.; Marcovina, S.; Young, S.G.; Hammer, R.E.; Sanan, D.A.; Hobbs, H.H. *Arterioscler. Thromb. Vasc. Biol.*, 1995, 15, 1911.
- [90] Callow, M.J.; Verstuyft, J.; Tangirala, R.; Palinski, W.; Rubin, E.M. *J. Clin. Invest.*, 1995, 96, 1639.
- [91] Marotti, K.R.; Castle, C.K.; Boyle, T.P.; Lin, A.H.; Murray, R.W.; Melchior, G.W. *Nature*, 1993, 364, 73.
- [92] Schaffer, S.A.; Bloom, J.D.; DeVries, V.G.; Dutia, M.; Katocs, A.S. Jr.; Largis, E. In *Atherosclerosis VII*; Fidge, N.H.; Nestel, P.J., Eds; Elsevier Science Publishers B.V.: Amsterdam, 1986, pp 633-636.
- [93] Heffron, F.; Middleton, B.; White, D.A. *Biochem. Pharm.*, 1990, 39, 575.
- [94] Middleton, B.; Middleton, A.; White, D.A.; Bell, G.D. *Atherosclerosis*, 1984, 171, 171.
- [95] Ashton, M.J.; Bridge, A.W.; Bush, R.C.; Dron, D.I.; Harris, N.V.; Jones, G.D.; Lythgoe, D.J.; Riddell, D.; Smith, C. *Bioorg. Med. Chem. Lett.* 1992, 2, 375.
- [96] Fukushima, H.; Aono, S.; Nakamura, Y.; Endo, M.; Imai, T. *J. Atheroscler. Res.*, 1969, 10, 403.
- [97] Fukushima, H.; Toki, K.; Nakatani, H. *J. Atheroscler. Res.*, 1969, 9, 57.
- [98] Gammill, R.B.; Bell, F.P.; Bell, L.T.; Bisaha, S.N.; Wilson, G.J. *J. Med. Chem.* 1990, 33, 2686.
- [99] Kimura, T.; Takase, Y.; Hayashi, K.; Tanaka, H.; Ohtsuka, I.; Saeki, T.; Kogushi, M.; Yamada, T.; Fujimori, T.; Saitou, I.; Akasaka, K. *J. Med. Chem.*, 1993, 36, 1630.
- [100] Kimura, T.; Watanabe, N.; Matsui, M.; Hayashi, K.; Tanaka, H.; Ohtsuka, I.; Saeki, T.; Kogushi, M.; Kabayashi, H.; Akasaka, K.; Yamagishi, Y.; Saitou, I.; Yamatsu, I. *J. Med. Chem.*, 1993, 36, 1641.
- [101] Tanaka, H.; Ohtsuka, I.; Kogushi, M.; Kimura, T.; Fujimori, T.; Saeki, T.; Hayashi, K.; Kobayashi, H.; Yamada, T.; Hiyoshi, H.; Saito, I. *Atherosclerosis*, 1994, 107, 187.
- [102] Matsuo, M.; Ito, F.; Kondo, A.; Aketa, M.; Tomoi, M.; Shimomura, K. *Biochim. Biophys. Acta*, 1995, 1259, 254.
- [103] White, A.D.; Purchase II, C.F.; Picard, J.A.; Anderson, M.K.; Bak Mueller, S.; Bocan, T.M.A.; Bousley, R.F.; Hamelehle, K.L.; Krause, B.R.; Lee, P.; Stanfield, R.L.; Reindel, J.F. *J. Med. Chem.*, 1996, 39, 3908.
- [104] Kogushi, M.; Tanaka, H.; Ohtsuka, I.; Yamada, T.; Kobayashi, H.; Saeki, T.; Takada, M.; Hiyoshi, H.; Yanagimachi, M.; Kimura, T.; Yoshitake, S.; Saito, I. *Atherosclerosis*, 1996, 124, 203.
- [105] Brown, M.S.; Goldstein, J.L. *Science*, 1986, 232, 34.

- [106] Kovanen, P.T.; Bilheimer, D.W.; Goldstein, J.L.; Jaramillo, J.J.; Brown, M.S. *Proc. Natl. Acad. Sci. USA*, 1981, 78, 1194.
- [107] Bilheimer, D.W.; Grundy, S.M.; Brown, M.S.; Goldstein, J.L. *Proc. Natl. Acad. Sci. USA*, 1983, 80, 4124.
- [108] Arad, Y.; Ramakrishnan, R.; Ginsberg, H.N. *Metabolism*, 1992, 41, 487.
- [109] Nawrocki, J.W.; Weiss, S.R.; Davidson, M.H.; Sprecher, D.L.; Schwartz, S.S.; Lupien, P.J.; Jones, P.H.; Haber, H.E.; Black, D.M. *Arterioscl. Thromb. Vasc. Biol.*, 1995, 15, 678.
- [110] Walker, J.F. *Drugs*, 1988, 36, 83.
- [111] McTavish, D.; Sorkin, E.M. *Drugs*, 1991, 42, 65.
- [112] Todd, P.A.; Goa, K.L. *Drugs*, 1990, 40, 583.
- [113] *Lancet*, 1994, 344, 1383.
- [114] Shepherd, J.; Cobbe, S.M.; Ford, I.; Isles, C.G.; Lorimer, A.R.; MacFarlane, P.W.; McKillop, J.H.; Packard, C.J. *N. Engl. J. Med.*, 1995, 333, 1301.
- [115] Kritchevsky, D.; Tepper, S.A.; Klurfeld, D.M. *Pharm. Res. Comm.*, 1981, 13, 921.
- [116] Kobayashi, M.; Ishida, F.; Takahashi, T.; Taguchi, K.; Watanabe, K.; Ohmura, I.; Kamei, T. *Jpn. J. Pharmacol.* 1989, 49, 125.
- [117] Zhu, B.Q.; Sievers, R.E.; Sun, Y.P.; Isenberg, W.M.; Parmley, W.W. *J. Cardiovas. Pharm.*, 1992, 19, 246.
- [118] Shiomi, M.; Ito, T.; Watanabe, Y.; Tsujita, Y.; Kuroda, M.; Arai, M.; Fukami, M.; Fukushima, J.; Tamura, A. *Atherosclerosis* 1990, 83, 69.
- [119] Bocan, T.M.A.; Mazur, M.J.; BakMueller, S.; QuenbyBrown, E.; Sliskovic, D.R.; O'Brien, P.M.; Creswell, M.W.; Lee, H.; Uhlendorf, P.D.; Roth, B.D.; Newton, R.S. *Atherosclerosis*, 1994, 111, 127.
- [120] Bocan, T.M.A.; BakMueller, S.; Mazur, M.J.; Uhlendorf, P.D.; QuenbyBrown, E.; Kieft, K.A. *Atherosclerosis*, 1993, 102, 9.
- [121] Corsini, A.; Mazzotti, M.; Raiteri, M.; Soma, M.; Fumagalli, R.; Paoletti, R. *XI Intl. Symp. Drugs Affecting Lipid Metabolism*, 1992, 7.
- [122] Corsini, A.; Raiteri, M.; Soma, M.; Fumagalli, R.; Paoletti, R. *Pharmacol. Res.*, 1991, 23, 173.
- [123] Falke, P.; Mattiasson, I.; Stavenow, L.; Hood, B. *Pharm. Toxicol.*, 1989, 64, 173.
- [124] Hidaka, Y.; Tomoyo, E.; Yonemoto, M.; Kamei, T. *Atherosclerosis*, 1992, 95, 87.
- [125] Corsini, A.; Bernini, F.; Quarato, P.; Donetti, E.; Bellosa, S.; Fumagalli, R.; Paoletti, R.; Soma, V.M. *Cardiology*, 1996, 87, 458.
- [126] Steinberg, D.; Parthasarathy, S.; Carew, T.E.; Khoo, J.C.; Witztum, J.L. *New Engl. J. Med.*, 1989, 320, 915.
- [127] Rajavashisth, T.B.; Andalibi, A.A.; Territo, M.C.; Berliner, J.A.; Navab, M.; Fogelman, A.M.; Lusis, A.J. *Nature*, 1990, 344, 254.
- [128] Kume, N.; Cybulsky, M.I.; Gimbrone, M.A. *J. Clin. Invest.*, 1992, 90, 1138.
- [129] Kao, C.Y.; Wissler, R.W. *Exp. Molec. Pathol.*, 1965, 4, 465.
- [130] Knieriem, H.J.; Kao, C.Y.; Wissler, R.W. *Arch. Pathol. Lab. Med.*, 1967, 84, 118.
- [131] Yomantas, S.; Elner, V.M.; Schaffner, T.; Wissler, R.W. *Arch. Pathol. Lab. Med.*, 1984, 108, 374.
- [132] Bocan, T.M.A.; Brown, S.A.; Guyton, J.R. *Arterioscler.*, 1988, 8, 499.
- [133] Glavind, J.; Hartmann, S.; Clemmeson, J.; Jessen, K.E.; Dam, H. *Acta Pathol. Microbiol. Scand.*, 1952, 3-, 1.
- [134] Boyd, H.C.; Gown, A.M.; Wolfbauer, G.; Chait, A. *Am. J. Pathol.*, 1989, 135, 815.
- [135] Haberland, M.E.; Fong, D.; Cheng, L. *Science*, 1988, 241, 215.
- [136] Palinski, W.; Rosenfeld, M.E.; Yla-Herttuala, S.; Gurtner, G.C.; Socher, S.S.; Butler, S.W.; Parthasarathy, S.; Carew, T.E.; Steinberg, D.; Witztum, J.L. *Proc. Natl. Acad. Sci. USA*, 1989, 86, 1372.
- [137] Daugherty, A.; Zweifel, B.S.; Schonfeld, G. *Br. J. Pharmacol.*, 1989, 98, 612.
- [138] Tawara, K.; Ishihara, M.; Ogawa, H.; Tomikawa, M. *Jpn. J. Pharmacol.*, 1986, 41, 211.
- [139] Stein, Y.; Stein, O.; Delplanque, B.; Fesmire, J.D.; Lee, D.M.; Alaupovic, P. *Atherosclerosis*, 1989, 75, 145.
- [140] Carew, T.E.; Schwenke, D.C.; Steinberg, D. *Proc. Natl. Acad. Sci. USA*, 1987, 84, 7725.
- [141] Daugherty, A.; Zweifel, B.S.; Schonfeld, G. *Br. J. Pharmacol.*, 1991, 103, 1013.
- [142] Kita, T.; Nagano, Y.; Yokode, M.; Ishii, K.; Kume, N.; Ooshima, A.; Kawai, C. *Proc. Natl. Acad. Sci. USA*, 1987, 84, 5928.
- [143] Schneider, J.E.; Berk, B.C.; Gravanis, M.B.; Santoian, E.C.; Cipolla, G.D.; Tarazona, N.; Lassegue, B.; King, S.B., 3<sup>rd</sup> *Circ.*, 1993, 88, 628.
- [144] Bjorkhem, I.; Henriksson-Freyschuss, A.; Breuer, O.; Diczfalusy, U.; Berglund, L.; Henriksson, P. *Arterioscler. Thromb.*, 1991, 11, 15.
- [145] Brattsand, R. *Atherosclerosis*, 1975, 22, 47.
- [146] Bocan, T.M.A.; BakMueller, S.; QuenbyBrown, E.; Uhlendorf, P.D.; Mazur, M.J.; Newton, R.S. *Expt. Molec. Pathol.*, 1992, 57, 70.
- [147] Keaney, J.F., Jr.; Xu, A.; Cunningham, D.; Jackson, T.; Frei, B.; Vita, J.A. *J. Clin. Invest.*, 1995, 95, 2520.
- [148] Del Rio, M.; Chulia, T.; Ruiz, E.; Tejerina, T. *Br. J. Pharmacol.*, 1996, 118, 1639.
- [149] Ylahtertuala, S.; Rosenfeld, M.E.; Parthasarathy, S.; Glass, C.K.; Sigal, E.; Witztum, J.L.; Steinberg, D. *Proc. Natl. Acad. Sci. USA*, 1990, 87, 6959.
- [150] Ylahtertuala, S. *Herz*, 1992, 17, 270.
- [151] Kuhn, H.; Belkner, J.; Zalaa, S.; Fahrenklemper, T.; Wohlfeil, S. *J. Exp. Med.*, 1994, 179, 1903.

- [152] Sendobry, S.M.; Cornicelli, J.A.; Welch, K.; Bocan, T.; Tait, B.; Trivedi, B.K.; Colbry, N.; Dyer, R.D.; Feinmark, S.J.; Daugherty, A. *Br. J. Pharmacol.*, 1997, 120, 1199.
- [153] Bocan, T.M.A.; Rosebury, W.S.; BakMueller, S.; Kuchera, S.; Welch, K.; Daugherty, A.; Cornicelli, J.A. *Atherosclerosis*, 1997, in press.





## Inhibition of cyclooxygenase with indomethacin phenethylamide reduces atherosclerosis in apoE-null mice

Michael E. Burleigh<sup>a,1</sup>, Vladimir R. Babaev<sup>a,1</sup>, Mayur B. Patel<sup>b</sup>, Brenda C. Crews<sup>b</sup>,  
Rory P. Remmel<sup>c</sup>, Jason D. Morrow<sup>a,d</sup>, John A. Oates<sup>a,d</sup>, Lawrence J. Marnett<sup>b</sup>,  
Sergio Fazio<sup>a,c</sup>, MacRae F. Linton<sup>a,d,\*</sup>

<sup>a</sup> Department of Medicine, Division Cardiovascular Medicine, Vanderbilt University School of Medicine,  
383 Preston Research Building, Nashville, TN 37232-6300, USA

<sup>b</sup> Department of Biochemistry, Vanderbilt University Medical Center, Nashville, TN 37232-6300, USA

<sup>c</sup> Department of Pathology, Vanderbilt University Medical Center, Nashville, TN 37232-6300, USA

<sup>d</sup> Department of Pharmacology, Vanderbilt University Medical Center, Nashville, TN 37232-6300, USA

<sup>e</sup> Department of Medicinal Chemistry, College of Pharmacy, University of Minnesota, Minneapolis, MN 55455, USA

Received 7 December 2004; accepted 14 April 2005

### Abstract

Non-selective inhibition of cyclooxygenase (COX) has been reported to reduce atherosclerosis in both rabbit and murine models. In contrast, selective inhibition of COX-2 has been shown to suppress early atherosclerosis in LDL-receptor null mice but not more advanced lesions in apoE deficient (apoE<sup>-/-</sup>) mice. We investigated the efficacy of the novel COX inhibitor indomethacin phenethylamide (INDO-PA) on the development of different stages of atherosclerotic lesion formation in female apoE<sup>-/-</sup> mice. INDO-PA, which is highly selective for COX-2 in vitro, reduced platelet thromboxane production by 61% in vivo, indicating partial inhibition of COX-1 in vivo. Treatment of female apoE<sup>-/-</sup> mice with 5 mg/kg INDO-PA significantly reduced early to intermediate aortic atherosclerotic lesion formation (44 and 53%, respectively) in both the aortic sinus and aorta en face compared to controls. Interestingly, there was no difference in the extent of atherosclerosis in the proximal aorta in apoE<sup>-/-</sup> mice treated from 11 to 21 weeks of age with INDO-PA, yet there was a striking (76%) reduction in lesion size by en face analysis in these mice. These studies demonstrate the ability of non-selective COX inhibition with INDO-PA to reduce early to intermediate atherosclerotic lesion formation in apoE<sup>-/-</sup> mice, supporting a role for anti-inflammatory approaches in the prevention of atherosclerosis.

© 2005 Elsevier Inc. All rights reserved.

**Keywords:** Atherosclerosis; Prostaglandins; Cyclooxygenase; COX inhibition; ApoE<sup>-/-</sup> mice; Aorta

### 1. Introduction

Atherosclerosis has features of an inflammatory disease and is the leading cause of death in industrialized nations [1]. Cyclooxygenase (COX) plays a key role as an inflammatory mediator in virtually all diseases involving inflammation [2]. COX exists as two isoforms, which are coded for by two separate genes [2,3]. COX-1 is found in most tissues and mediates normal physiology requiring prostaglandin production. COX-2 is induced rapidly at sites of inflammation and is expressed in atherosclerotic lesions of

humans [4,5], and mice [6] by macrophages, smooth muscle cells and endothelial cells.

Eicosanoids produced by COX-1 and COX-2 have been ascribed a variety of functions in the promotion of cardiovascular health and disease. The beneficial effect of low dose aspirin in reducing cardiovascular events has been largely attributed to inhibition of platelet thromboxane production, a COX-1 mediated process [7]. In contrast, COX-2 has been proposed to play both beneficial and deleterious roles in cardiovascular health [8–11]. Recent evidence from the Adenomatous Polyp Prevention on Vioxx (APPROVe) trial indicating that selective COX-2 inhibition with rofecoxib results in increased cardiovascular events after 18 months compared to placebo has resulted in removal of rofecoxib from the market ([www.vioxx.com](http://www.vioxx.com)). Yet studies in animal

\* Corresponding author. Tel.: +1 615 936 1656; fax: +1 615 936 1872.

E-mail address: [macrae.linton@vanderbilt.edu](mailto:macrae.linton@vanderbilt.edu) (M.F. Linton).

<sup>1</sup> These authors have contributed equally to this work.

models and humans support roles for COX-2 in promoting endothelial dysfunction [12], early atherosclerotic lesion formation [6] and plaque instability [13,14]. The dramatic removal of rofecoxib from the market highlights our need for a better understanding of the roles of COX-1 and COX-2 in atherosclerosis, plaque rupture, and cardiovascular events.

Non-selective inhibition of COX has been reported to reduce atherosclerosis both in cholesterol fed rabbit models [15] and genetically altered murine models of atherosclerosis [6,16]. Belton et al. have reported that selective inhibition of COX-1 attenuates atherosclerosis in apoE deficient mice [9]. However, reports on the impact of selective COX-2 inhibition on the development of atherosclerosis in murine models have been mixed with decreased, increased or unchanged atherosclerotic lesion area [6,16–19]. The divergence in the results may be the consequence of differences in experimental design, including efficacy and selectivity of the inhibitors, gender of the mice and stage of atherosclerotic lesions.

A new class of COX-2 selective inhibitors has been developed by derivatization of the conventional non-steroidal anti-inflammatory drugs (NSAIDs) indomethacin, resulting in >1100 times more selectivity for COX-2 than COX-1 when tested *in vitro* [20]. In the current studies, we examined the impact of this novel amide derivative of indomethacin, designated INDO-PA, on the development of different stages of atherosclerosis in apoE<sup>-/-</sup> mice. Interestingly, INDO-PA was found to produce a 61% reduction in platelet thromboxane, indicating partial inhibition of COX-1 *in vivo*. Treatment of apoE<sup>-/-</sup> mice with INDO-PA dramatically reduced aortic prostaglandin levels and early and intermediate aortic atherosclerotic lesion formation. These studies demonstrate the ability of non-selective COX inhibition with INDO-PA to reduce early and intermediate atherosclerotic lesion formation in apoE<sup>-/-</sup> mice, supporting the efficacy of anti-inflammatory approaches in the prevention of atherosclerosis.

## 2. Methods

### 2.1. Animal procedures

Female apoE<sup>-/-</sup> mice were at the 10th backcross into the C57BL/6 background and originally purchased from Jackson Laboratories (Bar Harbor, ME). Mice were maintained on a rodent chow diet containing 4.5% fat (PMI No. 5010, St. Louis, MO) and autoclaved acidified (pH 2.8) water. Animal care and experimental procedures were carried out in accordance with the regulations and under the approval of Vanderbilt University's Animal Care Committee.

### 2.2. COX inhibition

The dose of INDO-PA used in our study was chosen based on oral dosing in acute studies of carageenan-

induced footpad edema plethysmometry in rats in which the oral ED<sub>50</sub> for this assay in rats is 1.5 mg/kg [20]. Treatment of apoE<sup>-/-</sup> mice with 5 mg/kg INDO-PA intraperitoneal (IP; 3.33-fold over ED<sub>50</sub> in rats) was well-tolerated and did not produce any gastric ulceration and toxicity even at a dose of 30 mg/kg of INDO-PA (data not shown). In contrast, apoE<sup>-/-</sup> mice were able to tolerate daily doses of 2.5-mg/kg indomethacin by the IP route but higher doses (3 mg/kg) of it resulted in gastrointestinal hemorrhage with 100% mortality by 1 week (data not shown). Drugs were administered daily based on the body weight by IP injection (100  $\mu$ l) in a sterile mixture of 1% DMSO, 5% ethanol, 5% Tween-80 and 89% PBS.

### 2.3. Serum cholesterol and triglyceride analysis

Mice were fasted for 4 h and blood was collected under isoflurane anesthesia. Serum was separated by centrifugation and lipoprotein integrity was preserved by using 1 mM phenylmethylsulfonyl fluoride (Sigma). The concentration of total cholesterol and triglycerides was determined using Sigma kits adapted for 96-well plate assay as described [21].

### 2.4. Platelet thromboxane level measurement

Nine-week-old apoE<sup>-/-</sup> mice were given vehicle ( $n = 10$ ) or 5 mg/kg INDO-PA ( $n = 9$ ) for 1 week. Ninety minutes after the final injection, blood samples were collected in the presence of 25 units of heparin sodium (Sigma) and 1.25  $\mu$ l 10  $\mu$ M A23187 Ca<sup>++</sup> ionophore (Calbiochem). Blood was placed in a 37 °C water bath for 30 min. Plasma was isolated by centrifugation at 1100 rpm for 10 min at 4 °C. Platelet thromboxane A<sub>2</sub> metabolite, thromboxane B<sub>2</sub> (TxB<sub>2</sub>) was quantified by gas chromatography/mass spectrometry (GC/MS) as described [22].

### 2.5. Aortic prostaglandin levels analysis

Seven-week-old apoE<sup>-/-</sup> mice were given daily vehicle ( $n = 4$ ) or 5 mg/kg INDO-PA ( $n = 5$ ) for 9 weeks. Ninety minutes after the last dose administration, mice were sacrificed by cervical dislocation. Aortas were dissected free of adjacent adventitial tissue and snap-frozen in liquid nitrogen. Prostacyclin metabolite 6-keto PGF<sub>1 $\alpha$</sub>  and PGE<sub>2</sub> were purified as described and quantified by GC/MS by the Eicosanoid Analysis Core at Vanderbilt University [23].

### 2.6. Analysis of Aortic Lesions

ApoE<sup>-/-</sup> mice were sacrificed and flushed with PBS through the left ventricle. The aorta was dissected and pinned out in an *en face* preparation as described previously [24]. In the first experiment, a subset of the distal aortas ( $n = 3$ ) in each group were snap-frozen in liquid nitrogen for prostaglandin determinations. The heart with

the proximal aorta was embedded in OCT and snap-frozen in liquid nitrogen. Fifteen alternate cryosections of 10- $\mu$ m thickness were collected from the proximal aorta starting from the beginning of the aortic sinus and extending 300  $\mu$ m distally as described [25]. The sections were stained with Oil-Red-O and lesion area was quantified using a Kontron computer system [24].

### 2.7. Data analysis

Data are expressed as mean  $\pm$  S.E.M. Total serum cholesterol, triglycerides, PGE<sub>2</sub>, 6-keto PGF<sub>1 $\alpha$</sub> , TxB<sub>2</sub> and aortic lesion areas between the groups were determined using the SigmaStat V.2 Software (SPSS Inc., Chicago, IL) by Student's *t*-test and the Mann–Whitney rank sum test, respectively.

## 3. Results

### 3.1. INDO-PA inhibits platelet thromboxane production in apoE<sup>-/-</sup> mice

INDO-PA has been reported to be a highly selective COX-2 inhibitor in vitro [20]. The structures of indomethacin and the amide derivative used in the treatments, INDO-PA, are shown in panels A and B of Fig. 1.

To test the COX-2 selectivity of INDO-PA, we measured platelet thromboxane production in apoE<sup>-/-</sup> deficient mice (Fig. 1C). Surprisingly, INDO-PA inhibited platelet thromboxane A<sub>2</sub> metabolite TxB<sub>2</sub> production by 61% compared to vehicle (25.7  $\pm$  3.0 ng/ml versus 65.9  $\pm$  2.4 ng/ml, respectively; *p* = 0.001). Thus, in contrast to its behavior in vitro, INDO-PA significantly inhibited COX-1 expression in apoE<sup>-/-</sup> mice in vivo.

### 3.2. INDO-PA does not affect plasma lipid levels in apoE<sup>-/-</sup> mice

To examine the impact of treatment with INDO-PA on lipid metabolism and atherosclerosis, three independent studies were designed to allow the development of fatty streak, intermediate and advanced atherosclerotic lesions in female apoE<sup>-/-</sup> mice. These mice were treated for different periods: from ages 7 to 16 weeks, from 9 to 18 weeks and from 11 to 21 weeks. However, serum lipids remained unchanged throughout the course of treatment in all three studies (Tables 1–3).

Table 1

Serum lipid levels in apoE<sup>-/-</sup> mice treated with vehicle or INDO-PA from 7 to 16 weeks of age

Animal group	Baseline		6 weeks		10 weeks	
	Chol.	Trigl.	Chol.	Trig.	Chol.	Trig.
Vehicle ( <i>n</i> = 10)	320 $\pm$ 13	55 $\pm$ 3	276 $\pm$ 10	62 $\pm$ 2	311 $\pm$ 9	69 $\pm$ 5
INDO-PA ( <i>n</i> = 10)	333 $\pm$ 16	54 $\pm$ 6	260 $\pm$ 6	69 $\pm$ 3	322 $\pm$ 6	72 $\pm$ 4

Values are in mg/dl (mean  $\pm$  S.E.M.). The number of animals in each group is indicated by *n*.

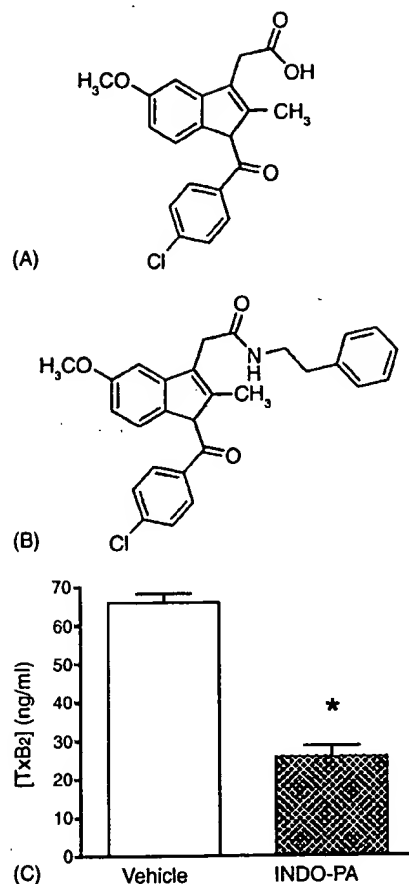


Fig. 1. Inhibition of Ca<sup>2+</sup> ionophore stimulated platelet thromboxane production: (A) chemical structure of indomethacin, (B) chemical structure of indomethacin amide derivative INDO-PA and (C) ApoE<sup>-/-</sup> mice were given vehicle (clear bar) or INDO-PA (hatched bar) for a week. Blood was collected and stimulated using A23187 Ca<sup>2+</sup> ionophore. Platelet production of the thromboxane metabolite TxB<sub>2</sub> was analyzed by GC/MS.

### 3.3. INDO-PA reduces atherosclerosis in apoE<sup>-/-</sup> mice

Treatment of 7-week-old apoE<sup>-/-</sup> mice with INDO-PA for 16 weeks significantly reduced atherosclerotic lesion formation in the proximal aorta by 44% (29620  $\pm$  4148  $\mu$ m<sup>2</sup> versus 52525  $\pm$  6007  $\mu$ m<sup>2</sup>; *p* = 0.013) and by 47% in the en face analysis of the aortas (0.43  $\pm$  0.04% versus 0.81  $\pm$  0.08%; *p* = 0.033) compared to mice treated with vehicle, respectively (Fig. 2A and B). Representative Oil-Red-O stained sections from the proximal aorta of mice treated with vehicle (Fig. 3A) or INDO-PA (Fig. 3B) indicate fatty streak lesions consisting predominantly of foam cells.

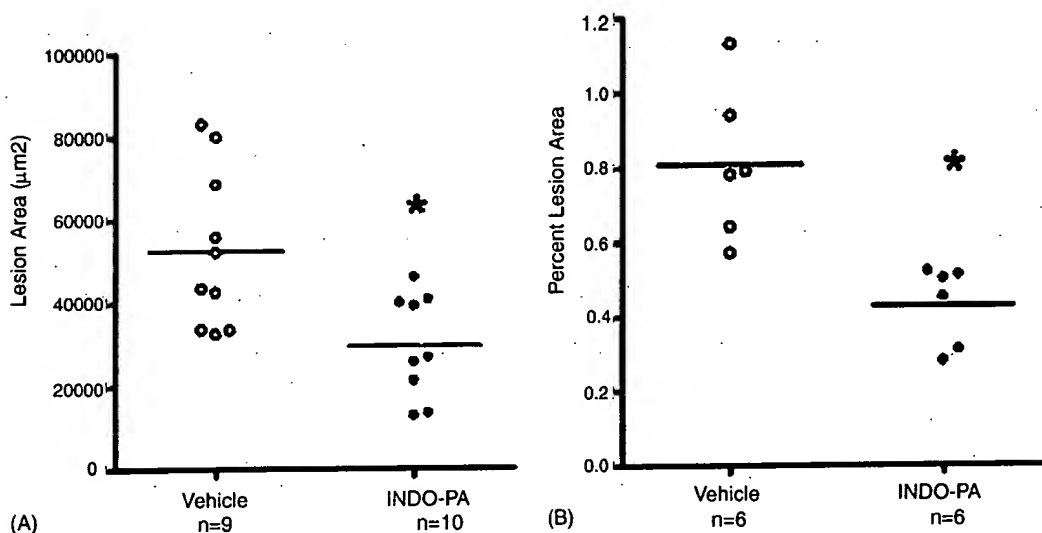


Fig. 2. Reduced atherosclerosis in apoE<sup>-/-</sup> mice treated with INDO-PA from 7 to 16 weeks of age. (A) The extent of atherosclerotic lesions in female apoE<sup>-/-</sup> after treatment with vehicle (open circles) or INDO-PA (filled circles) was quantified using Oil-Red-O stained sections. Values are in µm<sup>2</sup> with horizontal bar representing the mean of each group. (B) En face preparation of whole aortas were stained with Sudan IV and analyzed by a video imaging system. Data are represented as the percent of lesion area for each mouse and the horizontal bar represents the mean for each group.

Table 2

Serum lipid levels in apoE<sup>-/-</sup> mice treated with vehicle or INDO-PA from 9 to 19 weeks of age

Animal group	2 weeks		9 weeks	
	Chol.	Trig.	Chol.	Trig.
Vehicle (n = 13)	352 ± 24	101 ± 8	396 ± 30	72 ± 5
INDO-PA (n = 10)	343 ± 9	110 ± 5	408 ± 27	89 ± 6

Values are in mg/dl (mean ± S.E.M.). The number of animals in each group is indicated by n.

To examine the impact of INDO-PA on the production of two aortic prostaglandins, PGE<sub>2</sub> and PGI<sub>2</sub>, apoE<sup>-/-</sup> mice were treated with INDO-PA or vehicle for 9 weeks. As shown in Fig. 4, INDO-PA inhibited production of PGE<sub>2</sub> by 88% compared to vehicle (5.13 ± 1.01 ng/mg versus 43.79 ± 14.31 ng/mg tissue, respectively; *p* = 0.001). INDO-PA also inhibited production of the PGI<sub>2</sub> metabolite by 87% compared to vehicle (29.13 ± 9.21 ng/mg versus 229.22 ± 61.98 ng/mg tissue, respectively; *p* = 0.002).

In the next study, INDO-PA treatment of 9-week-old apoE<sup>-/-</sup> mice for 9 weeks significantly reduced atherosclerosis by 53% in the proximal aorta (60997 ± 12280 µm<sup>2</sup> versus 129808 ± 18926 µm<sup>2</sup>; *p* = 0.023; Fig. 5A) and by 64% in the en face analysis of the aorta (0.40 ± 0.05% versus 1.12 ± 0.22%; *p* = 0.021; Fig. 5B) compared to the vehicle treatment group. The atherosclerotic lesions in these mice consisted of both fatty streaks and intermediate

lesions in the proximal aorta in the vehicle group (Fig. 3C) and INDO-PA treated group (Fig. 3D).

In contrast, treatment of 11-week-old apoE<sup>-/-</sup> mice with INDO-PA for 10 weeks produced only a trend for a 19% (*p* = 0.38) reduction in the extent of atherosclerosis in the proximal aorta that did not achieve statistical significance compared to mice treated with vehicle (Fig. 6A). The atherosclerotic lesions in the proximal aortas of these mice were intermediate to advanced in stage both in the vehicle-treated (Fig. 3E) and INDO-PA-treated mice (Fig. 3F) with evidence of connective tissue. Interestingly, there was a dramatic 76% reduction (Fig. 6B) in the en face analysis of the extent of aortic atherosclerosis in the apoE<sup>-/-</sup> mice treated with INDO-PA compared to the vehicle-treated group (0.61 ± 0.18% versus 2.5 ± 0.39%, respectively; *p* = 0.022).

#### 4. Discussion

We examined the impact of a novel amide derivative of indomethacin, INDO-PA, on the development of atherosclerosis in female apoE<sup>-/-</sup> mice. Although INDO-PA is highly selective for COX-2 enzyme in vitro [20], we have found that INDO-PA inhibits platelet thromboxane in vivo. Treatment of apoE<sup>-/-</sup> mice with INDO-PA dramatically reduced early to intermediate atherosclerotic

Table 3

Serum lipid levels in apoE<sup>-/-</sup> mice treated with vehicle or INDO-PA from 11 to 21 weeks of age

Animal group	Baseline		2 weeks		9 weeks	
	Chol.	Trig.	Chol.	Trig.	Chol.	Trig.
Vehicle (n = 9)	292 ± 9	64 ± 3	242 ± 15	98 ± 6	271 ± 18	89 ± 3
INDO-PA (n = 9)	282 ± 16	58 ± 5	257 ± 23	99 ± 9	306 ± 29	96 ± 4

Values are in mg/dl (mean ± S.E.M.). The number of animals in each group is indicated by n.

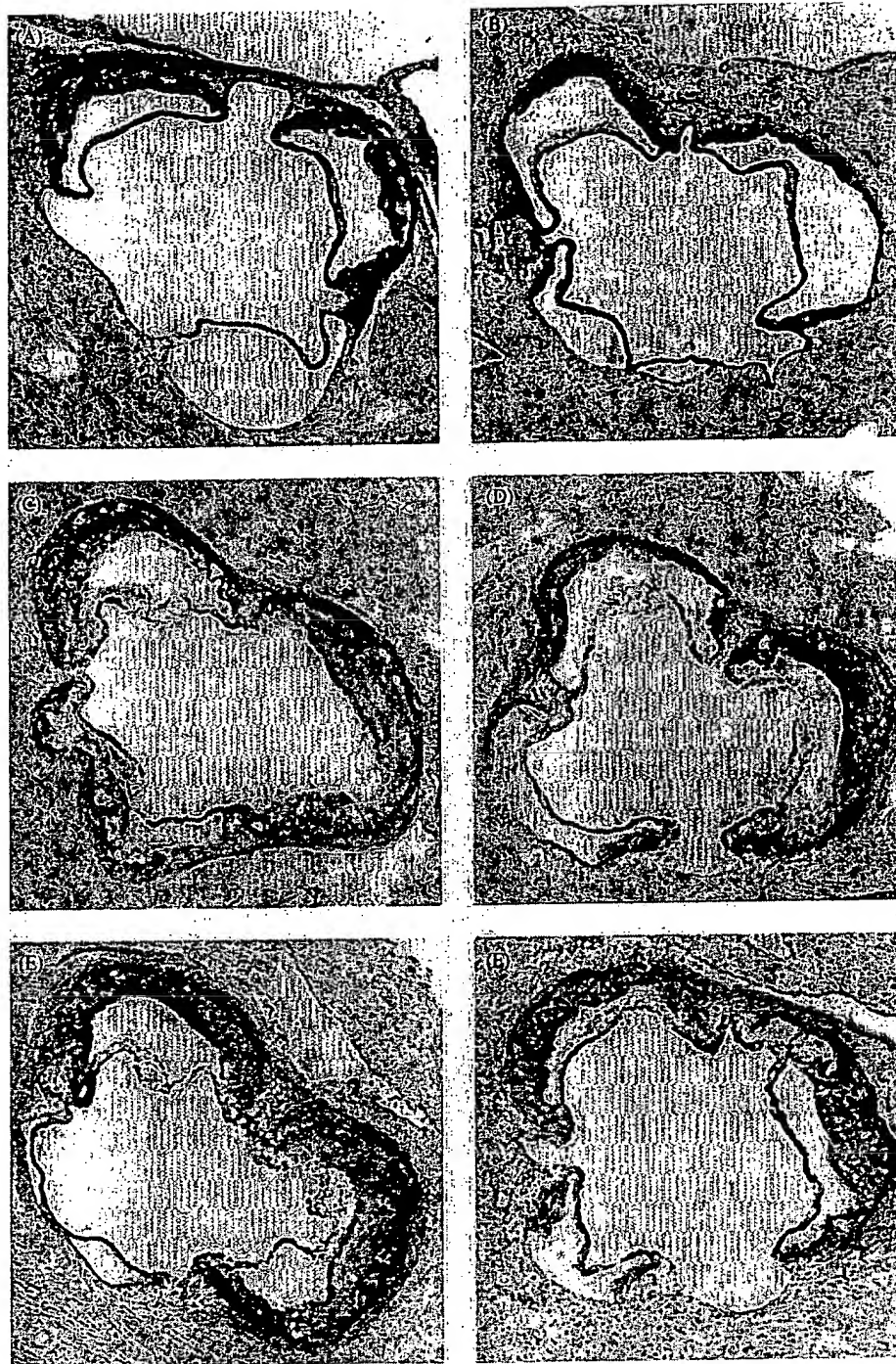


Fig. 3. Representative Oil-Red-O stained aortic root sections from groups treated with vehicle and INDO-PA. (A and B) Early stage atherosclerotic lesions in apoE<sup>-/-</sup> mice treated with vehicle (A) and INDO-PA (B) from 7 to 16 weeks of age. (C and D). Intermediate stage atherosclerotic lesions in apoE<sup>-/-</sup> mice treated with vehicle (C) and INDO-PA (D) from 9 to 18 weeks of age. (E and F) Advanced stage atherosclerotic lesions in apoE<sup>-/-</sup> mice treated with vehicle (E) and INDO-PA (F) from 7 to 16 weeks of age.

lesion formation. In addition, INDO-PA inhibited PGE<sub>2</sub> and PGI<sub>2</sub> metabolite production in the aorta by 88 and 87%, respectively, demonstrating efficacy of the INDO-PA in inhibiting prostaglandins in the artery wall *in vivo*. Thus, non-selective inhibition of COX with INDO-PA reduces the development of atherosclerosis in apoE<sup>-/-</sup> mice, supporting the potential for COX inhibition and

anti-inflammatory approaches in the prevention of atherosclerosis.

Treatment with 5 mg/kg INDO-PA (3.33-fold over ED<sub>50</sub> for oral dosing in rats [20]) was well-tolerated and did not produce gastric ulceration in apoE<sup>-/-</sup> mice. In these mice at steady state of INDO-PA, we observed a significant but incomplete (61%) inhibition of platelet thromboxane pro-

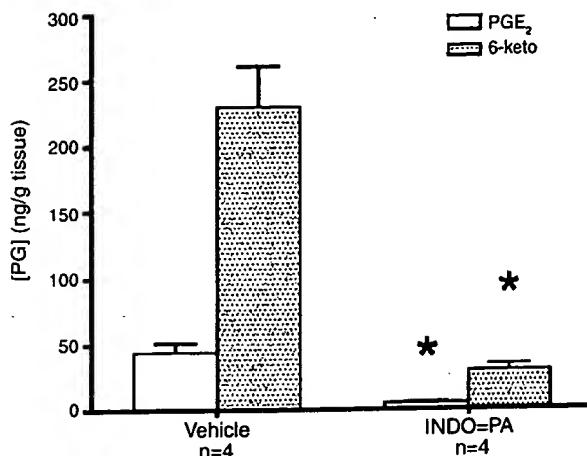


Fig. 4. Inhibition of prostaglandin production in aortic tissue of apoE<sup>-/-</sup> mice. ApoE<sup>-/-</sup> mice were given vehicle or INDO-PA beginning at 7 weeks of age for 9 weeks. Aortas were analyzed by GC/MS for PGE<sub>2</sub> and PGI<sub>2</sub> metabolite 6-keto-PGF<sub>1α</sub>.

duction indicating partial inhibition of platelet COX-1. Further studies in rats have verified that a small percentage of INDO-PA (5–10%) is converted into indomethacin in vivo (R.P. Remmel and L.J. Marnett, unpublished results). Although these data indicate that INDO-PA is only partially selective, previous data demonstrating that >90% inhibition of platelet thromboxane is required to inhibit platelet aggregation [26,27] suggests that inhibition of thromboxane-mediated-platelet aggregation is unlikely to have contributed significantly to the reduction in atherosclerosis. Three decades ago, non-selective inhibition of COX was reported to reduce atherosclerosis in cholesterol fed rabbits. [15]. We and others have shown that non-selective inhibition of COX with indomethacin associated with 90–95% reductions in platelet thromboxane reduces

early and intermediate atherosclerotic lesions in LDLR<sup>-/-</sup> mice fed a western diet [6,16]. In contrast, Egan et al. have recently reported that treatment of 6-week-old western diet fed apoBec-1/LDLR DKO mice with indomethacin for 13 weeks was associated with only a 70% reduction in platelet thromboxane and caused a 12.9% reduction in complex atherosclerotic lesions [28]. Thus, differences in these studies include the mouse model used, the extent of atherosclerosis and the efficacy of the indomethacin. Data with regard to the impact of aspirin on murine models have been conflicting, with a study by Cayatte et al. showing no effect [29] and studies in high-fat diet fed apoE<sup>-/-</sup> [30] and LDLR<sup>-/-</sup> mice [31] demonstrating significant reductions in lesion formation. However, Cayatte et al. reported that a thromboxane receptor antagonist, which inhibited serum thromboxane activity by only 39%, reduced atherosclerosis in apoE<sup>-/-</sup> mice [29]. The authors interpreted these results as indicating that eicosanoids other than thromboxane are involved in promoting atherosclerosis. Recently, Belton et al. have reported that selective inhibition of COX-1, which reduced urinary 2,3-dinor-TxB<sub>2</sub>, by around 50% reduced atherosclerotic lesion formation in apoE deficient mice [9]. Thus, it is possible that inhibition of thromboxane may have contributed to the reduction in atherosclerosis seen with INDO-PA by partially offsetting potentially negative effects of reducing prostacyclin. However, it is also possible that reductions of other eicosanoids due to inhibition of COX-1 and/or COX-2 may have contributed to the reduction in atherosclerosis.

Reports on the impact of selective COX-2 inhibition on the development of atherosclerosis in murine models have been mixed indicating decreased, increased or unchanged atherosclerotic lesion area [6,16–19]. The differences in results of these studies may be explained by variability in

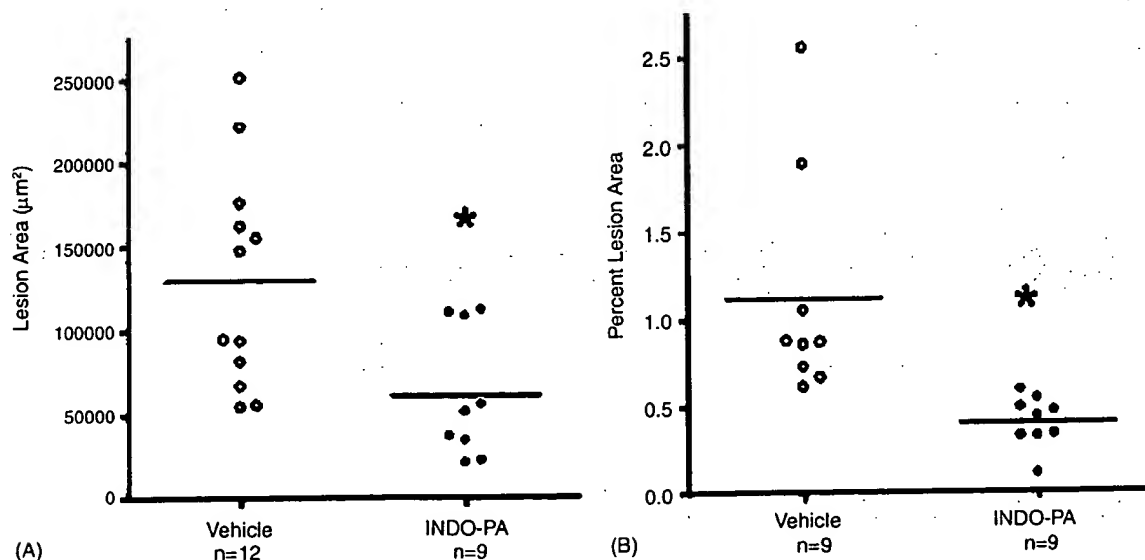


Fig. 5. Reduced atherosclerosis in apoE<sup>-/-</sup> mice treated with INDO-PA from 9 to 18 weeks of age. (A) The extent of atherosclerotic lesions in the proximal aorta of apoE<sup>-/-</sup> mice after treatment with vehicle (open circles) or INDO-PA (filled circles) was quantified using Oil-Red-O stained sections. (B) En face preparation of whole aortas were stained with Sudan IV and analyzed by a video imaging system. Data are represented as the percent of lesion area for each mouse and the horizontal bar represents the mean for each group.

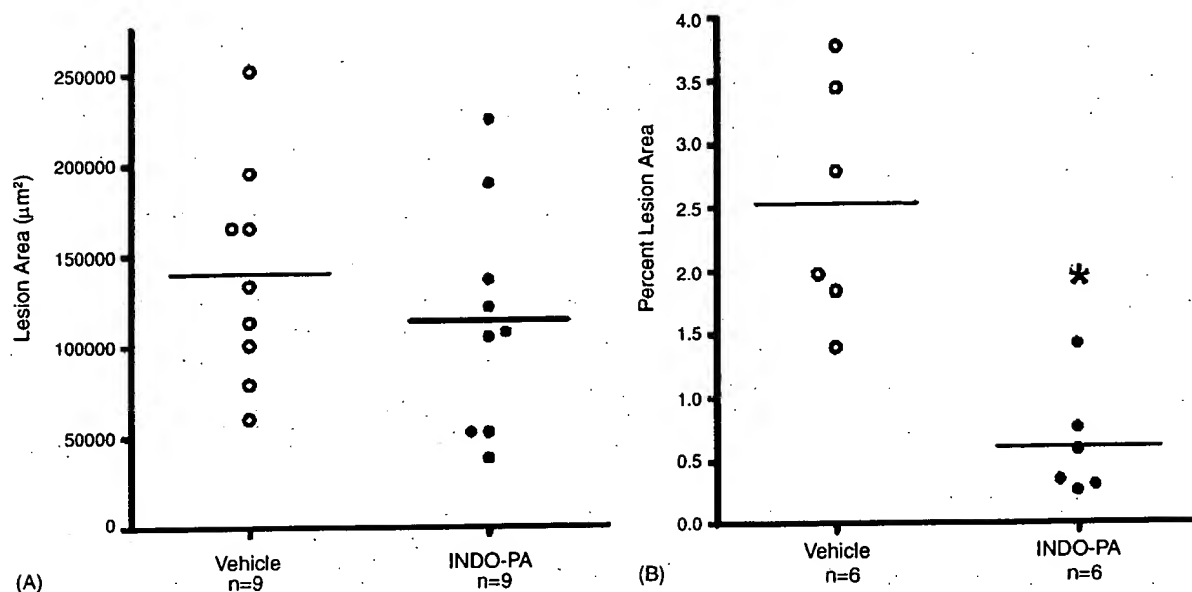


Fig. 6. Impact of INDO-PA treatment on atherosclerosis in apoE<sup>-/-</sup> mice from 11 to 21 weeks of age. (A) The extent of atherosclerotic lesions in the proximal aorta of apoE<sup>-/-</sup> after treatment with vehicle (open circles) or INDO-PA (filled circles) was quantified using Oil-Red-O stained sections from 300 µm of the proximal aorta. (B) En face preparation of whole aortas were stained with Sudan IV and analyzed by a video imaging system.

experimental design, including efficacy and selectivity of the inhibitors, gender of the mice and atherosclerotic lesion stage. We have previously reported that rofecoxib reduces early atherosclerotic lesion formation in LDLR<sup>-/-</sup> mice [6]. Consistent with our results, Krul et al. have presented data that treatment of apoE<sup>-/-</sup> mice with a selective COX-2 inhibitor, celecoxib, results in a significant reduction in aortic atherosclerosis [32]. Using bone marrow transplantation studies, we have demonstrated that macrophage COX-2 expression promotes early atherosclerotic lesion formation in LDLR<sup>-/-</sup> mice [6], providing genetic evidence consistent with COX-2 inhibition reducing early atherosclerotic lesion formation. In contrast, the ability of selective inhibition of COX-2 to impact atherogenesis appears to be limited in the setting of advanced atherosclerotic lesions [9,17,18], perhaps due to LXR-mediated downregulation of COX-2 in macrophage-derived foam cells [33] and the inhibition of anti-proliferative effects of COX-2 expression in smooth muscle cells [34]. Thus, the impact of COX-2 on atherosclerosis is complex and may vary according to the cell type and lesion stage.

Our current results demonstrate that non-selective inhibition of COX with INDO-PA reduces the formation of early and intermediate atherosclerotic lesions in female apoE<sup>-/-</sup> mice. Interestingly, we saw a non-significant trend for a reduction of atherosclerosis in the proximal aortas of apoE<sup>-/-</sup> mice with advanced stage lesions, whereas the extent of atherosclerosis in the en face aortas was dramatically reduced by 76%. In murine models, atherosclerosis develops first in the proximal aorta and then progresses distally [24,25]. These results are reminiscent of the findings that treatment with the selective COX-2 inhibitor, nimesulide, produced a non-significant trend for a reduction in atherosclerosis in

LDLR<sup>-/-</sup> mice with intermediate stage lesions, whereas treatment with indomethacin produced a significant reduction in atherosclerosis [16]. Although INDO-PA partially inhibits COX-1, we believe that it is acting largely as a COX-2 inhibitor, given the relatively low rate of conversion to indomethacin in vivo, the incomplete inhibition of platelet COX-1, and the much improved safety profile of INDO-PA compared to indomethacin. These results suggest that as the disease progresses from intermediate to advanced lesion stage, COX-2 inhibition appears to have less of an effect on modulating progression of atherosclerosis. Interestingly, INDO-PA virtually eliminated the progression of atherosclerosis in the en face aortas, as can be seen by the similar lesion burdens in all three treatment groups.

Although atherosclerosis is the pathological substrate underlying heart attack and stroke, plaque rupture and thrombosis are responsible for precipitating acute cardiovascular events. Mounting evidence supports the critical involvement of eicosanoids in the processes of plaque rupture and thrombosis. Inhibition of COX-1 mediated production of platelet thromboxane by aspirin reduces the risk for myocardial infarction and stroke [7]. In contrast, rofecoxib, a highly selective COX-2 inhibitor, has recently been taken off the market due to evidence from the APPROVe trial demonstrating increased cardiovascular events after 18 months ([www.viox.com](http://www.viox.com)). The mechanism responsible for the increased cardiovascular events in patients on rofecoxib remains to be elucidated. Concerns have been raised that COX-2 inhibition may promote cardiovascular events by inhibiting prostacyclin and promoting a prothrombotic state [11]. However, the impact of a prothrombotic state might be expected to cause an increase in cardiovascular events sooner than the



18 months seen in the APPROVe trial, suggesting that other mechanisms may be responsible.

Although three published studies have reported an increase in cardiovascular events in patients taking rofecoxib, principally at doses >25 mg a day [10,35,36], other studies found no evidence for increased risk of cardiovascular events with rofecoxib [37,38] or celecoxib [39]. Several important questions remain to be answered. Is the increase in cardiovascular events seen with rofecoxib a class effect that pertains to all other COX-2 inhibitors? Does the presence of COX-1 inhibition in addition to COX-2 inhibition, as seen with non-selective COX inhibitors, eliminate this risk of increased cardiovascular events due to chronic COX-2 inhibition alone? Recently, Pfizer has announced an increase in cardiovascular events associated with valdecoxib in patients in two small studies of patients undergoing coronary artery bypass grafting [19], and no increase in cardiovascular events based on clinical trial database of nearly 8000 patients treated with valdecoxib for durations ranging from 6 to 52 weeks ([http://www.pfizer.com/are/news\\_releases/2004pr/mn\\_2004\\_1015.html](http://www.pfizer.com/are/news_releases/2004pr/mn_2004_1015.html)). Although our current studies do not address the issues of plaque rupture and thrombosis, our results support the ability of non-selective COX inhibition to reduce atherosclerosis. Thus, non-selective inhibition of COX has the potential to favorably impact atherosclerosis, plaque rupture and thrombosis. A better understanding of the complex roles of COX-1 and COX-2 in atherogenesis and plaque stability may lead to new therapeutic approaches to the prevention of cardiovascular disease.

## Acknowledgements

The authors are thankful to Lei Ding and Youmin Zhang for excellent technical expertise. This work was supported by National Institutes of Health grants HL65405, HL53989, HL 57986, DK59637 (Lipid, Lipoprotein and Atherosclerosis Core of the Vanderbilt Mouse Metabolic Phenotyping Centers). M.E.B. is supported by American Heart Association grant (0215110B). V.R.B. is supported by American Heart Association grant (0160160B).

## References

- [1] Ross R. Atherosclerosis—an inflammatory disease. *New Eng J Med* 1999;340:115–26.
- [2] DuBois R, Abramson S, Crofford L, Gupta RA, Simon L, Van De Putte L, et al. Cyclooxygenase in biology and disease. *FASEB J* 1998;12:1063–73.
- [3] Vane JR, Bakhle YS, Botting RM. Cyclooxygenase 1 and 2. *Ann Rev Pharmacol Toxicol* 1998;38:97–120.
- [4] Baker CS, Hall RJ, Evans TJ, Pomerance A, Maclof J, Creminon C, et al. Cyclooxygenase-2 is widely expressed in atherosclerotic lesions affecting native and transplanted human coronary arteries and colocalizes with inducible nitric oxide synthase and nitrotyrosine particularly in macrophages. *Arterioscler Thromb Vasc Biol* 1999;19(3):646–55.
- [5] Schonbeck U, Sukhova GK, Graber P, Coulter S, Libby P. Augmented expression of cyclooxygenase-2 in human atherosclerotic lesions. *Am J Pathol* 1999;155:1281–91.
- [6] Burleigh ME, Babaev VR, Oates JA, Harris RC, Gautam S, Riendeau D, et al. Cyclooxygenase-2 promotes early atherosclerotic lesion formation in LDL receptor-deficient mice. *Circulation* 2002;105: 1816–23.
- [7] Hennekens CH, Dyken ML, Fuster V. Aspirin as a therapeutic agent in cardiovascular disease: a statement for healthcare professionals from the American Heart Association. *Circulation* 1997;96:2751–3.
- [8] Cheng Y, Austin SC, Rocca B, Koller BH, Coffman TM, Gresser T, et al. Role of prostacyclin in the cardiovascular response to thromboxane A<sub>2</sub>. *Science* 2002;296(5567):539–41.
- [9] Belton OA, Duffy A, Toomey S, Fitzgerald DJ. Cyclooxygenase isoforms and platelet vessel wall interactions in the apolipoprotein E knockout mouse model of atherosclerosis. *Circulation* 2003;108: 3017–23.
- [10] Bombardier C, Laine L, Reicin A, Shapiro D, Burgos-Vargas R, Davis B, et al. VIGOR Study Group. Comparison of upper gastrointestinal toxicity of rofecoxib and naproxen in patients with rheumatoid arthritis. *New Eng J Med* 2000;343:1520–8.
- [11] Mukherjee D, Nissen SE, Topol EJ. Risk of cardiovascular events associated with selective COX-2 inhibitors. *J Am Med Assoc* 2001;286:954–9.
- [12] Chenevard R, Hurlimann D, Bechir M, Enseleit F, Spicker L, Hermann M, et al. Selective COX-2 inhibition improves endothelial function in coronary artery disease. *Circulation* 2003;107(3):405–9.
- [13] Cipollone F, Prontera C, Pini B, Marini M, Fazio M, De Cesare D, et al. Overexpression of functionally coupled cyclooxygenase-2 and prostaglandin E synthase in symptomatic atherosclerotic plaques as a basis of prostaglandin E<sub>2</sub>-dependent plaque instability. *Circulation* 2001;104(8):921–7.
- [14] Cipollone F, Toniato E, Martinotti S, Fazio M, Lezzi A, Cuccurullo C, et al. Identification of new elements of plaque stability study G, a polymorphism in the cyclooxygenase 2 gene as an inherited protective factor against myocardial infarction and stroke. *J Am Med Assoc* 2004;291:2221–8.
- [15] Bailey JM, Butler J. Anti-inflammatory drugs in experimental atherosclerosis. I. Relative potencies for inhibiting plaque formation. *Atherosclerosis* 1973;17(3):515–22.
- [16] Pratico D, Tillmann C, Zhang ZB, Li H, FitzGerald GA. Acceleration of atherogenesis by COX-1-dependent prostanooid formation in low density lipoprotein receptor knockout mice. *Proc Natl Acad Sci USA* 2001;98:3358–63.
- [17] Olesen M, Kwong E, Mezili A, Kontny F, Seljeflot I, Arnesen H, et al. No effect of cyclooxygenase inhibition on plaque size in atherosclerosis-prone mice. *Scand Cardiovasc J* 2002;36:362–7.
- [18] Bea F, Blessing E, Bennett BJ, Kuo CC, Campbell LA, Kreuzer J, et al. Chronic inhibition of cyclooxygenase-2 does not alter plaque composition in a mouse model of advanced unstable atherosclerosis. *Cardiovasc Res* 2003;60:198–204.
- [19] Rott D, Zhu J, Burnett MS, Zhou YF, Zalles-Ganley A, Ogunmakinwa J, et al. Effects of MF-tricyclic, a selective cyclooxygenase-2 inhibitor, on atherosclerosis progression and susceptibility to cytomegalovirus replication in apolipoprotein-E knockout mice. *J Am Coll Cardiol* 2003;41:1812–9.
- [20] Kalgutkar AS, Crews BC, Rowlinson SW, Marnett AB, Kozak KR, Remmel RP, et al. Biochemically based design of cyclooxygenase-2 (COX-2) inhibitors: facile conversion of nonsteroidal antiinflammatory drugs to potent and highly selective COX-2 inhibitors. *Proc Natl Acad Sci USA* 2000;97(2):925–30.
- [21] Linton MF, Atkinson JB, Fazio S. Prevention of atherosclerosis in apoE deficient mice by bone marrow transplantation. *Science* 1995;267:1034–7.

- [22] Marnett LJ, Wright TL, Crews BC, Tannenbaum SR, Morrow JD. Regulation of prostaglandin biosynthesis by nitric oxide is revealed by targeted deletion of inducible nitric-oxide synthase. *J Biol Chem* 2000;275:13427–30.
- [23] Reese J, Paria BC, Brown N, Zhao X, Morrow JD, Dey SK. Coordinated regulation of fetal and maternal prostaglandins directs successful birth and postnatal adaptation in the mouse. *Proc Natl Acad Sci USA* 2000;97(17):9759–64.
- [24] Babaev VR, Patel MB, Semenkovich CF, Fazio S, Linton MF. Macrophage lipoprotein lipase promotes foam cell formation and atherosclerosis in low density lipoprotein receptor-deficient mice. *J Biol Chem* 2000;275:26293–9.
- [25] Paigen B, Holmes P, Mitchell D, Albee D. Comparison of atherosclerotic lesions and HDL-lipid levels in male, females, and testosterone-treated female mice from strains C57BL/6, BALB/c and C3H. *Atherosclerosis* 1987;68:215–21.
- [26] Czervionke RL, Hoak JC, Fry GL. Effect of aspirin on thrombin-induced adherence of platelets to cultured cells from the blood vessel wall. *J Clin Invest* 1978;62(4):847–56.
- [27] FitzGerald GA, Oates JA, Hawiger J, Maas RL, Roberts 2nd LJ, Lawson JA, et al. Endogenous biosynthesis of prostacyclin and thromboxane and platelet function during chronic administration of aspirin in man. *J Clin Invest* 1983;71(3):676–88.
- [28] Egan KM, Wang M, Lucitt MB, Zukas AM, Pure E, Lawson JA, et al. Cyclooxygenases, thromboxane, and atherosclerosis: plaque destabilization by cyclooxygenase-2 inhibition combined with thromboxane receptor antagonism. *Circulation* 2005;111(3):334–42.
- [29] Cayatte AJ, Du Y, Oliver-Krasinski J, Lavielle G, Verbeuren TJ, Cohen RA. The thromboxane receptor antagonist S18886 but not aspirin inhibits atherogenesis in apo E-deficient mice: evidence that eicosanoids other than thromboxane contribute to atherosclerosis. *Arterioscler Thromb Vasc Biol* 2000;20:1724–8.
- [30] Paul A, Calleja L, Camps J, Osada J, Vilella E, Ferre N, et al. The continuous administration of aspirin attenuates atherosclerosis in apolipoprotein E-deficient mice. *Life Sci* 2000;68(4):457–65.
- [31] Cyrus T, Sung S, Zhao L, Funk CD, Tang S, Pratico D. Effect of low-dose aspirin on vascular inflammation, plaque stability, and atherogenesis in low-density lipoprotein receptor-deficient mice. *Circulation* 2002;106(10):1282–7.
- [32] Krul ES, Napawan N, Butteiger DT, Hayes K, Krause L, Freidrich GE, et al. Atherosclerosis is reduced in cholesterol-fed apoE<sup>-/-</sup> mice administered an ASBT inhibitor or a selective COX-2 inhibitor. *Arterioscler Thromb Vasc Biol* 2002;22:P409.
- [33] Joseph SB, Castrillo A, Laffitte BA, Mangelsdorf DJ, Tontonoz P. Reciprocal regulation of inflammation and lipid metabolism by liver X receptors. *Nat Med* 2003;9:213–9.
- [34] Kothapalli D, Fuki I, Ali K, Stewart S, Zhao L, Yahil R, et al. Antimitogenic effects of HDL and APOE mediated by Cox-2-dependent IP activation. *J Clin Invest* 2004;113(4):609–18.
- [35] Ray WA, Stein CM, Daugherty JR, Hall K, Arbogast PG, Griffin MR. COX-2 selective non-steroidal anti-inflammatory drugs and risk of serious coronary heart disease. *Lancet* 2002;360:1071–3.
- [36] Solomon D, Schneeweiss S, Glynn R, Kiyota Y, Levin R, Mogun H, et al. Relationship between selective cyclooxygenase-2 inhibitors and acute myocardial infarction in older adults. *Circulation* 2004;109:2068–73.
- [37] Konstam MA, Weir MR, Reicin A, Shapiro D, Sperling RS, Barr E, et al. Cardiovascular thrombotic events in controlled, clinical trials of rofecoxib. *Circulation* 2001;104:2280–8.
- [38] Reicin AS, Shapiro D, Sperling RS, Barr E, Yu Q. Comparison of cardiovascular thrombotic events in patients with osteoarthritis treated with rofecoxib versus nonselective nonsteroidal anti-inflammatory drugs (ibuprofen, diclofenac, and nabumetone). *Am J Cardiol* 2002;89:204–9.
- [39] Silverstein F, Faich G, Goldstein J, Simon L, Pincus T, Whelton A, et al. Gastrointestinal toxicity with celecoxib vs nonsteroidal anti-inflammatory drugs for osteoarthritis and rheumatoid arthritis: the CLASS study. A randomized controlled trial. Celecoxib Long-term Arthritis Safety Study. *J Am Med Assoc* 2000;284:1247–55.

# Simvastatin Reduces Neointimal Thickening in Low-Density Lipoprotein Receptor–Deficient Mice After Experimental Angioplasty Without Changing Plasma Lipids

Zhiping Chen, MS; Tatsuya Fukutomi, MD; Alexandre C. Zago, MD; Raila Ehlers, MD; Patricia A. Detmers, PhD; Samuel D. Wright, PhD; Campbell Rogers, MD; Daniel I. Simon, MD

**Background**—Statins exert antiinflammatory and antiproliferative actions independent of cholesterol lowering. To determine whether these actions might affect neointimal formation, we investigated the effect of simvastatin on the response to experimental angioplasty in LDL receptor–deficient (LDLR<sup>−/−</sup>) mice, a model of hypercholesterolemia in which changes in plasma lipids are not observed in response to simvastatin.

**Methods and Results**—Carotid artery dilation (2.5 atm) and complete endothelial denudation were performed in male C57BL/6J LDLR<sup>−/−</sup> mice treated with low-dose (2 mg/kg) or high-dose (20 mg/kg) simvastatin or vehicle subcutaneously 72 hours before and then daily after injury. After 7 and 28 days, intimal and medial sizes were measured and the intima to media area ratio (I:M) was calculated. Total plasma cholesterol and triglyceride levels were similar in simvastatin- and vehicle-treated mice. Intimal thickening and I:M were reduced significantly by low- and high-dose simvastatin compared with vehicle alone. Simvastatin treatment was associated with reduced cellular proliferation (BrdU), leukocyte accumulation (CD45), and platelet-derived growth factor–induced phosphorylation of the survival factor Akt and increased apoptosis after injury.

**Conclusions**—Simvastatin modulates vascular repair after injury in the absence of lipid-lowering effects. Although the mechanisms are not yet established, additional research may lead to new understanding of the actions of statins and novel therapeutic interventions for preventing restenosis. (*Circulation*. 2002;106:20-23.)

**Key Words:** restenosis ■ statins ■ inflammation ■ apoptosis

Statins inhibit the enzyme 3-hydroxy-3-methylglutaryl coenzyme A (HMG-CoA) reductase, the first committed step of sterol synthesis, and lower plasma cholesterol levels. In large clinical trials, statins have been shown to reduce coronary events in primary or secondary prevention settings.<sup>1</sup> Effects on clinical and angiographic restenosis after coronary intervention, however, have not been conclusively demonstrated. Several clinical studies have failed to demonstrate a link between statin therapy and the risk of restenosis after balloon angioplasty,<sup>2</sup> whereas more recent studies suggest that statins may reduce restenosis after stenting.<sup>3</sup>

Statins are known to have broad effects in addition to lowering plasma cholesterol. The product of HMG-CoA reductase, mevalonate, is an important precursor for many isoprenoids, thereby endowing statins with the ability to directly alter cellular events other than cholesterol synthesis. For example, the isoprenoids farnesylpyrophosphate and geranylgeranylpyrophosphate play important roles in signal transduction in cellular migration, proliferation, and survival via their attachment to critical signaling proteins, such as Ras and Rho.<sup>4</sup>

We used a hyperlipidemic model, the LDLR<sup>−/−</sup> mouse, to test the antiinflammatory and antiproliferative actions of simvastatin on neointimal thickening after experimental angioplasty in an atherosclerotic background. An essential feature of the chosen model is that simvastatin does not affect plasma lipid levels in mice, allowing the study of effects of simvastatin distinct from cholesterol lowering.

## Methods

### Carotid Injury

Male LDLR<sup>−/−</sup> C57BL/6J mice (Jackson Laboratories, Bar Harbor, Me), maintained on a high-fat (20.1%) diet containing 1.25% cholesterol for 12 weeks after weaning, underwent unilateral carotid artery dilation (2.5 atm) and complete endothelial denudation.<sup>5</sup> Animal care and procedures were reviewed and approved by Harvard Medical School Standing Committee on Animals and performed in accordance with the guidelines of the American Association for Accreditation of Laboratory Animal Care and the National Institutes of Health.

### Simvastatin Treatment

Treatments were via subcutaneous injection 72 hours before and daily after injury. LDLR<sup>−/−</sup> mice were divided into 3 treatment

Received March 29, 2002; revision received May 8, 2002; accepted May 9, 2002.  
From the Cardiovascular Division (Z.C., T.F., A.C.Z., R.E., C.R., D.I.S.), Brigham and Women's Hospital, Boston, Mass; Harvard-MIT Division of Health Sciences and Technology (C.R.), Cambridge, Mass; and Merck Research Laboratories (P.A.D., S.D.W.), Rahway, NJ.  
Correspondence to Daniel I. Simon, MD, Cardiovascular Division, Brigham and Women's Hospital, 75 Francis St, Tower 3, Boston, MA 02115. E-mail dsimon@rics.bwh.harvard.edu

© 2002 American Heart Association, Inc.

*Circulation* is available at <http://www.circulationaha.org>

DOI: 10.1161/01.CIR.0000022843.76104.01

### Quantitative Morphometry and Immunohistochemical Analysis of Mouse Carotid Arteries After Injury

	Simvastatin			ANOVA	P	
	Vehicle	Low	High		Vehicle vs Low	Vehicle vs High
Cholesterol, 21 d, mg/dL	856±89	922±167	1130±279	0.074	NS	NS
Triglyceride, 21 d, mg/dL	216±36	234±43	223±44	0.751	NS	NS
Intimal area, mm <sup>2</sup>						
7 d	0.010±0.004	0.006±0.004	0.006±0.004	0.320	NS	NS
28 d	0.047±0.023	0.021±0.013	0.019±0.015	0.004	0.011	0.012
Medial area, mm <sup>2</sup>						
28 d	0.078±0.015	0.063±0.014	0.074±0.031	0.299	NS	NS
I:M, 28 d	0.64±0.37	0.32±0.17	0.24±0.15	0.008	0.036	0.012
EEL, mm <sup>2</sup>						
7 d	0.104±0.013	0.113±0.035	0.103±0.014	0.778	NS	NS
28 d	0.223±0.032	0.191±0.040	0.192±0.053	0.184	NS	NS
BrdU+ cells, %						
Media, 7 d	19.2±2.8	12.0±5.8	11.0±4.5	0.299	NS	NS
Intima, 28 d	4.6±1.8	1.7±0.5	1.9±0.8	0.0184	0.042	0.050
CD45+ cells, %						
Intima, 7 d	59.2±11.9	44.2±5.2	39.1±12.8	0.0429	0.047	0.049
Intima, 28 d	34.4±3.6	24.3±2.2	20.9±8.0	0.0120	0.026	0.025
TUNEL+ cells, %						
Intima, 7 d	3.5±1.1	6.9±3.3	9.2±4.2	0.0872	0.193	0.039
Media, 7 d	2.5±0.4	4.2±0.3	5.8±1.0	0.0002	0.002	0.001

groups: PBS vehicle (control group) or 2 mg/kg (low-dose) or 20 mg/kg (high-dose) alkaline-hydrolyzed simvastatin.<sup>6</sup>

#### Lipid Analysis

Blood was collected via retro-orbital puncture into heparin-coated capillary tubes. Plasma cholesterol and triglyceride measurements were performed as reported.<sup>7</sup>

#### Tissue Harvesting and Analysis

Carotid arteries were harvested and processed for quantitative morphometry 7 days (control, n=5; low-dose, n=5; high-dose, n=4) or 28 days (control, n=9; low-dose, n=10; high-dose, n=7) after vascular injury.<sup>5</sup> Standard avidin-biotin procedures for mouse leukocytes (CD45) and macrophages (Mac-3) (PharMingen, San Diego, Calif), BrdU (DAKO, Carpinteria, Calif), and smooth muscle cell (SMC)  $\alpha$ -actin (DAKO) were used for immunohistochemistry. Apoptotic cells were detected by the TUNEL method using Apo Tag (Intergen). Immunostained sections were quantified as the number of immunostained-positive cells per total number of nuclei.

#### Ex Vivo Akt Signaling Assay

Aortas were harvested from all animals, opened longitudinally, and incubated with 30 ng/mL platelet-derived growth factor (PDGF)-BB (R&D Systems, Minneapolis, Minn) for 15 minutes at 37°C. Aortic lysates were prepared<sup>8</sup> and then subjected to Western analysis using antibodies to Akt and Phospho-Akt (Ser473) (Cell Signaling Technology, Beverly, Mass).

#### Data Analysis

All data are presented as mean±SD. Statistical comparisons of the principal end points were performed using one-way ANOVA to determine a difference in mean values between the 3 groups, followed by *t* tests for the 3 pair-wise comparisons when the ANOVA false-positive rate was <5%. For ANOVA with a false-

positive rate of >5%, the pair-wise comparisons were reported to be statistically nonsignificant (NS). For the primary study end point of intimal area 28 days after injury, a Bonferroni corrective for 3 pair-wise comparisons was applied, in which the *t* test  $P<0.0167$  was used to signify a false-positive rate of 5%.

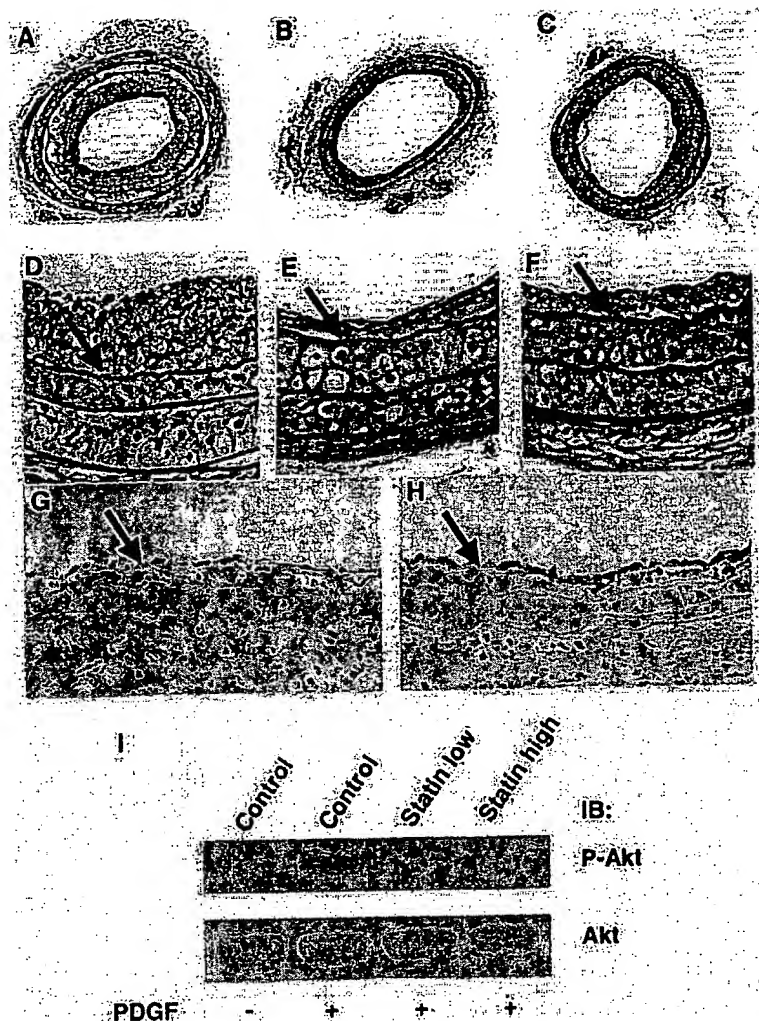
### Results

#### Simvastatin Does Not Alter Plasma Lipids in LDLR<sup>-/-</sup> Mice

We sought evidence that simvastatin modulates vascular repair independent of cholesterol lowering. To determine whether plasma cholesterol is unresponsive to simvastatin in LDLR<sup>-/-</sup> mice, as it is in normal<sup>9</sup> and apoE-deficient<sup>7</sup> mice, we dosed LDLR<sup>-/-</sup> animals with 2 mg/kg simvastatin, 20 mg/kg simvastatin, or vehicle control and measured plasma lipid levels. Simvastatin did not alter plasma cholesterol or triglyceride levels in LDLR<sup>-/-</sup> mice at either of the 2 doses tested (Table).

#### Simvastatin Decreases Neointimal Thickening, Cellular Proliferation, and Leukocyte Accumulation After Carotid Injury

Carotid artery dilation and complete endothelial denudation were performed in LDLR<sup>-/-</sup> mice treated with 2 or 20 mg/kg simvastatin or vehicle subcutaneously 72 hours before and then daily after injury until euthanasia. In mice receiving vehicle, intimal thickening began by 7 days after injury and progressed significantly between 7 days (0.010±0.004 mm<sup>2</sup>) and 28 days (0.047±0.023 mm<sup>2</sup>). Low- and high-dose simvastatin reduced intimal thickening at 28 days by 55%



Photomicrographs of mouse carotid arteries after injury (A through H). VerHoeff elastin stain 28 days after injury: vehicle (A); low-dose simvastatin (B); high-dose simvastatin (original magnification  $\times 38$ ) (C); vehicle (D); low-dose simvastatin (E); and high-dose simvastatin ( $\times 150$ ) (F). Neointima separates the internal elastic lamina (arrows) from the lumen. Apoptotic (TUNEL-positive) cells 7 days after injury: vehicle (G); high-dose simvastatin ( $\times 150$ ) (H). Simvastatin and Akt signaling (I). Aortae were harvested from mice treated with simvastatin or vehicle and incubated with PDGF-BB. Aortic lysates were immunoblotted sequentially using antibodies to Akt and Phospho-Akt (Ser473).

( $P=0.012$ ) and 60% ( $P=0.011$ ), respectively (Figure, panels A through F, Table). Medial area was unaffected by simvastatin treatment. I:M at 28 days in control mice was  $0.64 \pm 0.37$  and was reduced 50% by low-dose ( $P=0.036$ ) and 62% by high-dose ( $P=0.012$ ) simvastatin. Intimal and medial thickening were accompanied by progressive vessel enlargement (ie, positive remodeling), as determined by external elastic lamina area measurements over time, which was comparable in vehicle- and simvastatin-treated mice.

We assessed cellular proliferation by quantifying incorporation of BrdU. Substantial proliferation was observed 7 days after injury in control vessels (19.2% of medial cells), and proliferation was still evident at 28 days (4.6% of intimal cells). Low- and high-dose simvastatin reduced medial proliferation at 7 days by 38% and 43%, respectively, and intimal proliferation at 28 days by 63% ( $P=0.042$ ) and 59% ( $P=0.050$ ) (Table).

Immunohistochemistry was performed to identify the cellular components of the neointima 28 days after injury. In vehicle-treated animals, 48% of cells were SMCs ( $\alpha$ -actin-positive) and 34% were monocytes or macrophages (CD45- and Mac3-positive). Altered leukocyte accumulation within vessels was observed in simvastatin-treated mice. Inflammatory cells (CD45-positive) invading the intima were reduced

by 25% to 34% ( $P<0.05$ ) at 7 days and 29% to 39% ( $P<0.03$ ) at 28 days in simvastatin-treated compared with control mice.

### Simvastatin Increases Apoptosis

Because statins prevent isoprenylation of Rho proteins and their translocation to the membrane fraction, and because there is increasing evidence that Rho activates signals that regulate apoptosis,<sup>10</sup> we investigated the effects of simvastatin on apoptosis after injury. Low- and high-dose simvastatin significantly increased the number of apoptotic (TUNEL-positive) cells in the intima (by 197% and 263%, respectively) and media (168% and 232%, respectively) at 7 days compared with control (Table, Figure, panels G and H).

To identify a biochemical correlate of simvastatin action promoting apoptosis, we examined signaling of the survival factor, Akt, in arteries from mice treated with simvastatin. Injured carotid arteries are completely devoid of endothelium and lined with a platelet monolayer.<sup>5</sup> Therefore, we examined PDGF-induced phosphorylation and activation of Akt by Western blot analysis of aortic samples from mice treated with low- and high-dose simvastatin or vehicle for 7 days. PDGF-induced phosphorylation of Akt was impaired in the aortae of simvastatin-treated mice (Figure, panel I).

## Discussion

Our study provides definitive in vivo evidence that simvastatin inhibits neointimal thickening in a cholesterol-independent manner accompanied by reduced vascular inflammation and proliferation and increased apoptosis. These results establish a role for statins in inhibiting neointimal formation after experimental angioplasty in a setting in which simvastatin did not alter plasma lipids.

Restenosis is a complex cascade of wound-healing responses to vascular injury, characterized by thrombosis, inflammation, cellular proliferation/migration, and extracellular matrix deposition. Increasing evidence suggests that antiinflammatory<sup>7</sup> and antiproliferative<sup>11</sup> effects of statins play important roles in attenuating atherosclerosis,<sup>1,7</sup> transplant vasculopathy,<sup>12</sup> and restenosis.<sup>3</sup> Statins inhibit the synthesis of isoprenoid intermediates that are important lipid attachments for signaling proteins, including Ras and the Rho family of small GTP-binding proteins (eg, Rho, Rac, and Cdc42).<sup>4</sup> Rho is implicated in various biological functions relevant to vascular injury, including cellular migration, proliferation, and survival.<sup>10,13</sup> Statins attenuate vascular SMC proliferation in vitro by decreasing Rho geranylgeranylation and membrane localization and inhibiting Cdk activity.<sup>11</sup>

We provide biochemical evidence that PDGF-induced phosphorylation of Akt is inhibited in aortic tissue from simvastatin-treated mice. Akt functions as an antiapoptotic protein, protecting against cell death induced by growth factor withdrawal or ischemia-reperfusion injury.<sup>14</sup> The effects of statins on Akt signaling seem to be tissue-specific. Statins rapidly activate Akt signaling in endothelial cells, enhance phosphorylation of endothelial NO synthase, and inhibit apoptosis.<sup>15</sup> In contrast, statins impair Akt activation in SMCs,<sup>16</sup> leading to diminished SMC proliferation and induction of apoptosis via effects on phosphatidylinositol-3 kinase or Rho.<sup>11</sup> These divergent actions of statins on Akt activation in endothelial cells and SMCs may act in synchrony to diminish neointimal thickening after denuding injury.

Prior clinical trials of statins after balloon angioplasty have failed to show a reduction in restenosis,<sup>2</sup> likely because of the predominant role of vascular remodeling rather than neointimal thickening in this setting.<sup>17</sup> However, recent studies of statin use after stenting, with minimal remodeling and profound neointimal thickening,<sup>17</sup> have suggested benefit.<sup>3</sup>

Our results support the hypothesis that simvastatin has antiinflammatory, antiproliferative, and proapoptotic actions relevant to preventing restenosis. Although mechanisms are not yet established, additional research may lead to new

understanding of the actions of statins, additional impetus for broad statin use after vascular intervention independent of lipid profile, and novel therapies for preventing restenosis.

## Acknowledgments

This research was supported by National Institutes of Health Grants R01 HL57506 (to Dr Simon), R01 DK55656 (to Dr Simon), and K08 HL03104 (to Dr Rogers) and a Merck Medical School Grant (to Dr Simon).

## References

1. Bucher HC, Griffith LE, Guyatt GH. Systematic review on the risk and benefit of different cholesterol-lowering interventions. *Arterioscler Thromb Vasc Biol.* 1999;19:187-195.
2. Weintraub WS, Bocuzzi SJ, Klein JL, et al. Lack of effect of lovastatin on restenosis after coronary angioplasty: Lovastatin Restenosis Trial Study Group. *N Engl J Med.* 1994;331:1331-1337.
3. Walter DH, Schachinger V, Elsner M, et al. Effect of statin therapy on restenosis after coronary stent implantation. *Am J Cardiol.* 2000;85:962-968.
4. Casey PJ. Protein lipidation in cell signaling. *Science.* 1995;268:221-225.
5. Simon DI, Chen Z, Seifert P, et al. Decreased neointimal formation in Mac-1<sup>-/-</sup> mice reveals a role for inflammation in vascular repair after angioplasty. *J Clin Invest.* 2000;105:293-300.
6. Endres M, Laufs U, Huang Z, et al. Stroke protection by 3-hydroxy-3-methylglutaryl (HMG)-CoA reductase inhibitors mediated by endothelial nitric oxide synthase. *Proc Natl Acad Sci USA.* 1998;95:8880-8885.
7. Sparrow CP, Burton CA, Hernandez MA Jr, et al. Simvastatin has anti-inflammatory and antiatherosclerotic activities independent of plasma cholesterol lowering. *Arterioscler Thromb Vasc Biol.* 2001;21:115-121.
8. DiChiara MR, Kiely JM, Gimbrone MA Jr, et al. Inhibition of E-selectin gene expression by transforming growth factor  $\beta$  in endothelial cells involves coactivator integration of Smad and nuclear factor  $\kappa$ B-mediated signals. *J Exp Med.* 2000;192:695-704.
9. Endo A, Tsujita Y, Kuroda M, et al. Effects of ML-236B on cholesterol metabolism in mice and rats: lack of hypocholesterolemic activity in normal animals. *Biochim Biophys Acta.* 1979;575:266-276.
10. van Nieuw Amerongen GP, van Hinsbergh VW. Cytoskeletal effects of rho-like small guanine nucleotide-binding proteins in the vascular system. *Arterioscler Thromb Vasc Biol.* 2001;21:300-311.
11. Laufs U, Marra D, Node K, et al. 3-Hydroxy-3-methylglutaryl-CoA reductase inhibitors attenuate vascular smooth muscle cell proliferation by preventing rho GTPase-induced down-regulation of p27Kip1. *J Biol Chem.* 1999;274:21926-21931.
12. Kobashigawa JA, Katznelson S, Laks H, et al. Effect of pravastatin on outcomes after cardiac transplantation. *N Engl J Med.* 1995;333:621-627.
13. Shibata R, Kai H, Seki Y, et al. Role of Rho-Associated kinase in neointima formation after vascular injury. *Circulation.* 2001;103:284-289.
14. Fujio Y, Nguyen T, Wencker D, et al. Akt promotes survival of cardiomyocytes in vitro and protects against ischemia-reperfusion injury in mouse heart. *Circulation.* 2000;101:660-667.
15. Kureishi Y, Luo Z, Shiojima I, et al. The HMG-CoA reductase inhibitor simvastatin activates the protein kinase Akt and promotes angiogenesis in normocholesterolemic animals. *Nat Med.* 2000;6:1004-1010.
16. Weiss RH, Ramirez A, Joo A. Short-term pravastatin mediates growth inhibition and apoptosis, independently of Ras, via the signaling proteins p27Kip1 and p13 kinase. *J Am Soc Nephrol.* 1999;10:1880-1890.
17. Hoffmann R, Mintz GS, Dussaillant GR, et al. Patterns and mechanisms of in-stent restenosis: a serial intravascular ultrasound study. *Circulation.* 1996;94:1247-1254.

# Atherosclerosis and Lipoproteins

## Troglitazone Inhibits Formation of Early Atherosclerotic Lesions in Diabetic and Nondiabetic Low Density Lipoprotein Receptor-Deficient Mice

Alan R. Collins, Woerner P. Meehan, Ulrich Kintscher, Simon Jackson, Shu Wakino, Grace Noh, Wulf Palinski, Willa A. Hsueh, Ronald E. Law

**Abstract**—Peroxisome proliferator-activated receptor- $\gamma$  (PPAR $\gamma$ ) is a ligand-activated nuclear receptor expressed in all of the major cell types found in atherosclerotic lesions: monocytes/macrophages, endothelial cells, and smooth muscle cells. In vitro, PPAR $\gamma$  ligands inhibit cell proliferation and migration, 2 processes critical for vascular lesion formation. In contrast to these putative antiatherogenic activities, PPAR $\gamma$  has been shown in vitro to upregulate the CD36 scavenger receptor, which could promote foam cell formation. Thus, it is unclear what impact PPAR $\gamma$  activation will have on the development and progression of atherosclerosis. This issue is important because thiazolidinediones, which are ligands for PPAR $\gamma$ , have recently been approved for the treatment of type 2 diabetes, a state of accelerated atherosclerosis. We report herein that the PPAR $\gamma$  ligand, troglitazone, inhibited lesion formation in male low density lipoprotein receptor-deficient mice fed either a high-fat diet, which also induces type 2 diabetes, or a high-fructose diet. Troglitazone decreased the accumulation of macrophages in intimal xanthomas, consistent with our in vitro observation that troglitazone and another thiazolidinedione, rosiglitazone, inhibited monocyte chemoattractant protein-1-directed transendothelial migration of monocytes. Although troglitazone had some beneficial effects on metabolic risk factors (in particular, a reduction of insulin levels in the diabetic model), none of the systemic cardiovascular risk factors was consistently improved in either model. These observations suggest that the inhibition of early atherosclerotic lesion formation by troglitazone may result, at least in part, from direct effects of PPAR $\gamma$  activation in the artery wall. (*Arterioscler Thromb Vasc Biol.* 2001;21:365-371.)

**Key Words:** atherosclerosis ■ diabetes mellitus ■ pharmacology

Peroxisome proliferator-activated receptor- $\gamma$  (PPAR $\gamma$ ), a nuclear receptor, is expressed in all major cell types participating in vascular injury: endothelial cells (ECs), macrophages, and vascular smooth muscle cells (VSMCs).<sup>1-6</sup> Activation of this receptor in vitro inhibits inflammatory processes, including cytokine production and expression of NO synthase.<sup>2</sup> In early clinical investigations, ligands of PPAR $\gamma$ , such as thiazolidinediones (TZDs), have also been reported to improve endothelium-dependent vasodilation, suggesting that PPAR $\gamma$  activation enhances NO production and protects against vascular injury.<sup>7,8</sup> Activation of PPAR $\gamma$  also inhibits 2 other processes critical for vascular lesion formation, cell proliferation, and migration.<sup>3,5,6,9,10</sup> In vivo, 2 TZDs, troglitazone (TRO) and pioglitazone, significantly reduced arterial neointimal hyperplasia after endothelial injury in rats.<sup>11-13</sup> In such balloon-catheterized arteries, neointima formation essentially reflects increased migration and proliferation of VSMCs, a major contributor to the growth of

See page 295

atherosclerotic lesions. TRO also inhibited neointima formation in stents placed in the coronary arteries of patients with type 2 diabetes.<sup>14</sup>

We and others have recently demonstrated that PPAR $\gamma$  activation by TZDs and 15-deoxy- $\Delta^{12,14}$ -prostaglandin J<sub>2</sub> inhibits EC expression of vascular cell adhesion molecule-1, which mediates monocyte adherence to the endothelial surface.<sup>4,15</sup> Because inflammation, dysregulated growth, and migration of monocytes and VSMCs play an important role in the development of atherosclerosis, we hypothesized that PPAR $\gamma$  activation in cells of the vasculature would inhibit the atherosclerotic process. On the other hand, TZDs also stimulate conversion of macrophages into foam cells; therefore, ligand-dependent activation of PPAR $\gamma$  has been postulated to promote atherosclerosis.<sup>16</sup>

Received August 10, 2000; revision accepted December 1, 2000.

From the Division of Endocrinology, Diabetes, and Hypertension (A.R.C., W.P.M., U.K., S.J., S.W., G.N., W.A.H., R.E.L.), Department of Medicine, UCLA School of Medicine, Los Angeles, Calif; the Molecular Biology Institute (W.A.H., R.E.L.), Los Angeles, Calif; the Department of Medicine/Cardiology (U.K.), Virchow-Klinikum, Humboldt University, and the German Heart Institute (U.K.), Berlin, Germany; and the Department of Medicine (W.P.), UCSD, La Jolla, Calif.

Correspondence to Ronald E. Law, PhD, University of California, Los Angeles, Division of Endocrinology, Diabetes, and Hypertension, 900 Veteran Ave, Suite 24-130, Box 957073, Los Angeles, CA 90095. E-mail rlaw@mednet.ucla.edu

© 2001 American Heart Association, Inc.

*Arterioscler Thromb Vasc Biol.* is available at <http://www.atvbaha.org>



The impact of TZDs on atherosclerosis is a critical issue. TZDs improve insulin-mediated glucose uptake and are used extensively in the treatment of insulin resistance and type 2 diabetes mellitus.<sup>17</sup> Coronary artery disease mortality is increased 2- to 4-fold in type 2 diabetes.<sup>18</sup> Atherosclerosis is the major cause of demise in people with diabetes; therefore, it is important to determine the action of any antidiabetic drug on the atherosclerotic process.

To determine whether PPAR $\gamma$  activation has proatherogenic or antiatherogenic effects, we administered TRO to male LDL receptor-deficient (LDLR<sup>-/-</sup>) mice fed either a high-fat or a high-fructose atherogenic diet. Both models develop substantial hypercholesterolemia and macrophage-laden lesions, designated intimal xanthomata, which do not normally progress to mature atherosclerotic plaques.<sup>19</sup> In addition, the high-fat diet induces hyperglycemia and hyperinsulinemia in the LDLR<sup>-/-</sup> mouse, making it also a model of type 2 diabetes.<sup>20,21</sup> In contrast, fructose does not increase glucose or insulin in this model<sup>21</sup> and, therefore, was useful because the effects of TZDs on atherosclerosis could be studied in the absence of improvements in insulin action.

## Methods

### Transendothelial Monocyte Migration

THP-1 cells ( $5 \times 10^4$ ), a human monocytic leukemia cell line, were added to a human aortic EC monolayer covering a gelatin-coated 8- $\mu$ m porous membrane and incubated for 30 minutes at 37°C to facilitate their attachment. Cells were then pretreated with the indicated ligands or vehicle (dimethyl sulfoxide) for 30 minutes at 37°C. Migration was induced by the addition of monocyte chemoattractant protein-1 (MCP-1, 50 ng/mL) to the lower compartment. After 90 minutes, nonmigrating THP-1 cells and human aortic ECs were removed with a cotton tip, and the membranes were fixed and stained with the Quik-Diff Stain Set (DADE, Miami, Fla) to identify migrated cells. The number of migrated cells was determined per  $\times 320$  high-power field. Experiments were performed in duplicate and were repeated at least 3 times.

### Western Blots

Western immunoblots were performed as previously described.<sup>10</sup> Membranes were incubated with rabbit polyclonal antibodies (1:1000 dilution, New England Biolabs) that recognize either (1) total extracellular signal-regulated kinase (ERK) or (2) ERK phosphorylated on threonine 202 and tyrosine 204.

### Animals and Diets

Male LDLR<sup>-/-</sup> mice were obtained (C57BL/6J-Ldlr<sup>tm11er</sup>, stock No. 002207, Jackson Laboratory, Bar Harbor, Me) and were group-housed under a 12-hour light and 12-hour dark regimen. All animal protocols were approved by the UCLA Animal Research Committee and complied with all federal, state, and institutional regulations. At 3 months of age, the mice were randomly assigned to 1 of 5 dietary regimens: (1) chow (Harlan Teklad 8604), (2) high-fat complex carbohydrate (Research Diets), (3) high-fat complex carbohydrate with 4 g TRO/kg of food, (4) high fructose (Research Diets), or (5) high fructose with 4 g TRO/kg of food. The high-fat diet consisted of 21% fat, 20% protein, 50% carbohydrate, and 0.15% cholesterol. Our high-fat diet differed from those commonly used to study atherogenesis in LDLR<sup>-/-</sup> mice in that the majority of the nonfat energy came from complex carbohydrate sources instead of sucrose. The high-fructose diet contained 4% fat, 16% protein, 71% fructose, and 0.15% cholesterol. Sources of fat in the diets were corn oil (1% in all diets) and anhydrous milk fat (3% in the fructose diets and 20% in the high fat diets). Mice and feed were weighed weekly, and the rate of consumption of drug was computed. The mice were fed for a period of 12 weeks.

### Metabolic Measurements

Blood samples from the retro-orbital sinus were obtained from the mice before the beginning of treatment and every month thereafter and from the abdominal vena cava at euthanasia. Mice were fasted overnight before the collection of the blood samples. Plasma glucose was measured by glucose oxidase reaction (Beckman Glucose Analyzer 2, Beckman Instruments). Plasma lipids were measured by the UCLA Lipid Analysis Laboratory. Plasma insulin was determined by ELISA. Blood pressures were obtained by using an indirect tail-cuff method with a controlled temperature chamber (IITC, Inc) by a technician blinded to the treatment groups.

### Vessel Preparation and Image Analysis

Mice were euthanized and perfused with 7.5% sucrose in 4% paraformaldehyde. Aortas were dissected out, split longitudinally, pinned flat in a dissection pan, and stained with Sudan IV to detect lipids and determine lesion area. Images were captured by use of a Sony 3-CCD video camera and analyzed by a single technician who was blinded to the study protocol and used ImagePro image analysis software. The extent of lesion formation is expressed as the percentage of the total aortic surface area covered by lesions.

### Cross Sections: Determination of Intimal Macrophage Content

The largest lesions from the aortic arch were excised and embedded in paraffin. The avidin-biotin-peroxidase complex technique for immunostaining was used. Macrophages were stained by using monoclonal antibody to CD68 (titer 1:100, KP1 clone, M0814, Dako Corp). Nonimmune serum was used as a control. Primary antibody incubations were performed in 1% BSA/2% goat serum containing PBS for 60 minutes. Biotinylated rabbit anti-mouse (Dako) was applied; incubation with a streptavidin-peroxidase complex followed. Peroxidase activity was detected with the use of diaminobenzidine tetrahydrochloride as a chromogen. Slides were then counterstained with hematoxylin. Images of the stained sections were analyzed by using the software described above. After tracing the intimal area to be measured with a cursor, 5 pixels of color, which defined the anti-CD68 stain, were sampled by the operator. The area encompassed by the pixels, which was not contiguous, in the color range for anti-CD68 was then computed automatically by the software. This approach has been successfully used by Shi et al<sup>22</sup> to quantify lesional macrophages in a mouse model of transplant arteriosclerosis.

### Statistical Analysis

Statistical analysis was performed by using 2-factorial ANOVA with Student-Newman-Keuls to determine the differences between individual group means.

## Results

### TRO Inhibits Monocyte Migration

VSMC migration and proliferation play an important atherogenic role in the progression of fatty streaks toward more advanced atherosclerotic lesions, such as transitional lesions and classical atheromas. We have previously shown that PPAR $\gamma$  ligands inhibit ERK mitogen-activated protein kinase (MAPK)-dependent migration of VSMCs.<sup>10,11</sup> However, in the earliest stages of atherosclerotic lesions, recruitment of adherent monocytes through their migration into the subendothelium and their phenotypic transformation to macrophages and foam cells play a far greater role than VSMCs in humans and in murine models.<sup>23</sup>

To investigate whether TRO-mediated PPAR $\gamma$  activation affects monocyte recruitment and to further explore its mechanism, we carried out a series of in vitro experiments before our in vivo studies. MCP-1 is an important in vivo migration factor promoting the subendothelial accumulation of monocytes. TRO inhibited MCP-1-directed transmigration

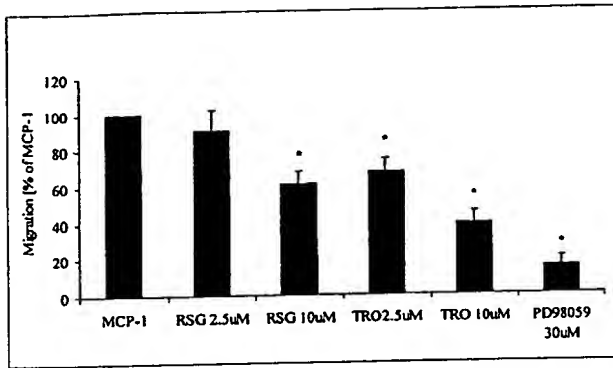


**Figure 1.** PPAR $\gamma$  ligands inhibit MCP-1-directed transendothelial migration of monocytes. Migration of THP-1 monocytes through ECs was determined by using a modified Boyden chamber assay as described in Methods. The number of migrating cells was quantified by microscopy with the use of high-power fields. Results represent 3 independent experiments performed in duplicate. \* $P < 0.05$  vs MCP-1 alone.

tion of THP-1 monocytes by  $32.7 \pm 6.5\%$  at  $2.5 \mu\text{mol/L}$  and by  $61.4 \pm 6.7\%$  at  $10 \mu\text{mol/L}$  (Figure 1). TRO contains a vitamin E moiety that may confer an antioxidant activity that can inhibit monocyte recruitment and endothelial expression of adhesion molecules. However, rosiglitazone (RSG), another PPAR $\gamma$  ligand that lacks antioxidant activity, also inhibited monocyte transmigration, albeit with a lesser potency than TRO (Figure 1). Inhibition of monocyte transmigration by TRO, therefore, is likely to be mediated at least in part through PPAR $\gamma$ .

MCP-1 rapidly induced ERK activation, reaching a peak at 5 minutes, which was blocked by PD98059, an inhibitor of MAPK ERK kinase (MEK, an upstream kinase), which phosphorylates and activates ERK (Figure 2). PD98059 attenuated MCP-1-directed transmigration by  $84.8 \pm 4.8\%$ . In combination, these data suggest that activation of PPAR $\gamma$  in monocytes may inhibit their migration by interfering with ERK-MAPK signaling, although the precise mechanism remains to be determined.

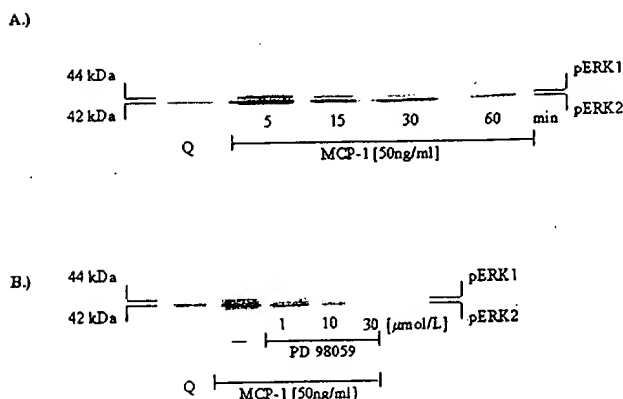


**Figure 2.** MCP-1 activates the ERK-MAPK pathway in THP-1 human monocytes. A, Quiescent (Q) THP-1 cells were stimulated with MCP-1 (50 ng/mL) for 5 minutes. Whole-cell protein extracts were immunoblotted with a phosphospecific ERK1 (pERK1)/ERK2 (pERK2) MAPK antibody. A representative blot of 3 different experiments is shown. B, Conditions were the same as in panel A except that cells were treated with MEK inhibitor PD98059 (1 to  $30 \mu\text{mol/L}$ ) or vehicle (dimethyl sulfoxide, -) before and during stimulation with MCP-1 (50 ng/mL). A representative blot of 3 different experiments is shown.

### TRO Inhibits Intimal Macrophage Accumulation and Lesion Formation in Male LDLR $^{-/-}$ Mice

LDLR $^{-/-}$  mice that were fed a regular chow diet develop few lesions across the surface of the aorta. Male 3-month-old LDLR $^{-/-}$  mice were placed on either a high-fat or high-fructose diet to induce atherosclerosis. LDLR $^{-/-}$  males were used in the present study because they develop hyperglycemia and become diabetic on a high-fat diet but remain normoglycemic when fed a high-fructose diet. Moreover, males develop twice the level of surface lesions as do females,<sup>24</sup> and their use obviates the potentially confounding influence of the vascular protection in females afforded by estrogen. Comparison of the impact of TRO on atherogenesis in these 2 dietary models was undertaken to distinguish any activity of PPAR $\gamma$  to normalize metabolic abnormalities accompanying diabetes that contribute to high-fat-induced xanthomata formation from any direct effects on the vasculature. To assess the impact of TRO on aortic lesions, 1 high-fat diet group and 1 high-fructose diet group received TRO at 400 mg/kg body wt per day from drugs pelleted into the atherogenic diets. This dose of TRO was chosen because we previously demonstrated its efficacy in inhibiting intimal hyperplasia in rats after balloon injury.<sup>11</sup>

The en face method, which makes use of computer-assisted analysis of color images of Sudan IV-stained lipid-containing material in the entire aorta, was used to determine the percentage of surface area affected by lesions.<sup>24</sup> Male LDLR $^{-/-}$  mice on normal chow for 3 months had  $<0.20\%$  lesions (Figure 3A). The high-fat diet increased the amount of surface lesions after 3 months to  $3.90 \pm 0.16\%$  ( $n=8$ , Figure 3B). TRO inhibited the high-fat-induced lesions by 30% ( $2.76 \pm 0.36\%$  of the aortic surface,  $n=8$ ,  $P < 0.02$ ; Figure 3C). Similar to Merat et al,<sup>21</sup> we noted that the high-fructose diet was more atherogenic than the high-fat diet, causing  $8.42 \pm 0.94\%$  lesions ( $n=17$ , Figure 3D). TRO reduced lesions in fructose-fed LDLR $^{-/-}$  males by 42% ( $4.90 \pm 0.65\%$ ,  $n=14$ ,  $P < 0.01$ ; Figure 3E). Quantitative results are summarized in Figure 4.

TRO-treated male LDLR $^{-/-}$  mice fed either the high-fat or high-fructose diet for 3 months developed lesions that contained substantially fewer CD68-staining macrophages (Figure 5A through 5D). Lesions induced by a high-fat diet contained  $39.1 \pm 6.8\%$  macrophages (percent of cross-sectional intimal area) compared with  $13.3 \pm 4.9\%$  ( $P < 0.01$ ) in mice administered TRO (Figure 5E). Similar results were obtained for males fed the high-fructose diet, where TRO decreased macrophage accumulation from  $40.4 \pm 3.5\%$  to  $17.1 \pm 1.7\%$  ( $P < 0.01$ , Figure 5E). The lesions in the TRO-fed animals tended to be smaller in volume than those in males not fed TRO. The relative macrophage content in the larger lesions (not treated with TRO) exceeded the content in the smaller lesions (treated with TRO) by 140% to 200%. The reduction in macrophage accumulation in the lesions of TRO-treated animals is unlikely to be the result of their being an earlier lesion stage, because the relative macrophage content is known to be greatest in the smaller (ie, early-stage) lesions.

### Effect of TRO on Metabolic Parameters

All metabolic measurements determined on blood samples drawn before treatment were similar in all groups (Tables 1

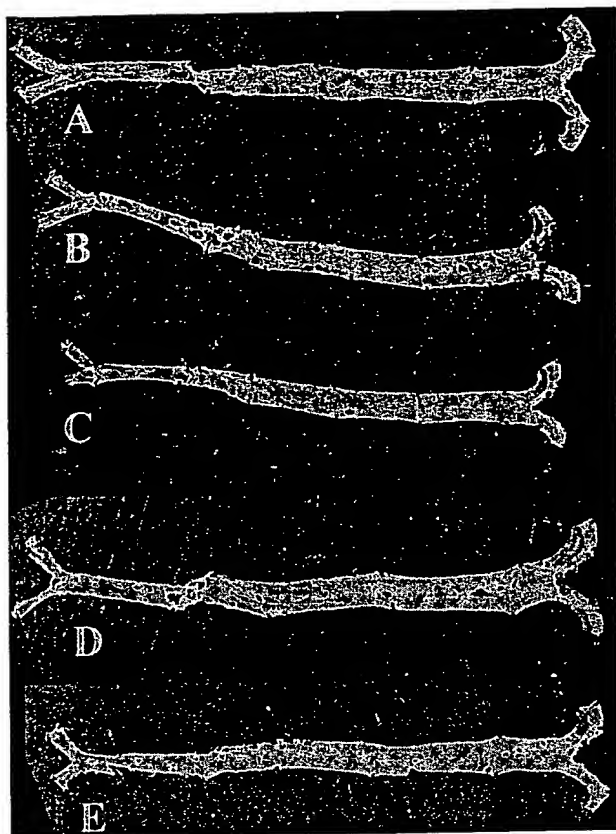


**Figure 3.** TRO attenuates atherosclerosis in male  $LDLR^{-/-}$  mice. The aorta is stained by Sudan IV to detect the lipids present in lesions. A, Chow diet. B, High-fat diet. C, High-fat diet and TRO. D, High-fructose diet. E, High-fructose diet and TRO.

and 2). In accordance with previous studies on male  $LDLR^{-/-}$  mice, we found that a high-fat diet induced diabetes<sup>20,21</sup> (Table 1). Glucose levels progressively increased throughout

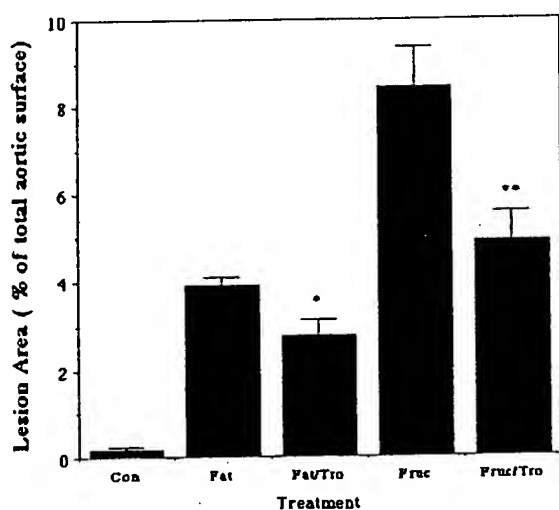


**Figure 4.** Quantification of the antiatherogenic activity of TRO in male  $LDLR^{-/-}$  mice. Mean atherosclerotic surface lesion areas were determined in mice fed a normal chow, high-fat, or high-fructose diet in the absence or presence of TRO for 3 months. Image analysis and quantification of the percentage of the total aortic area staining for Sudan IV were performed by using computer-assisted image analysis. TRO produced a significant decrease in mice fed a high-fat (30% decrease,  $*P<0.05$ ) and high-fructose (42% decrease,  $**P<0.05$ ) diet.

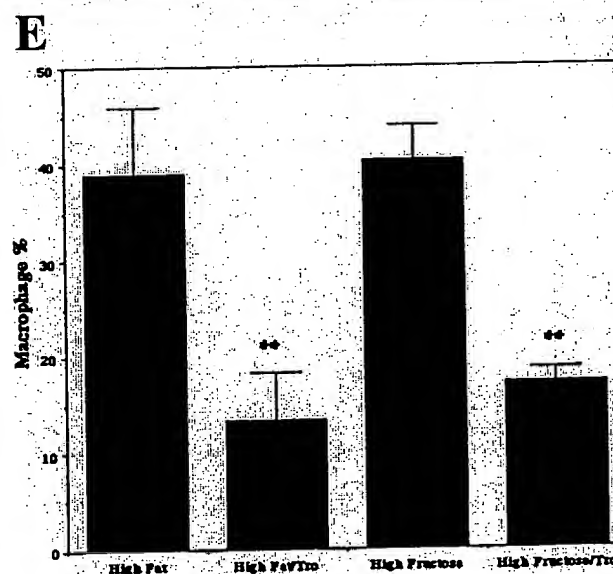
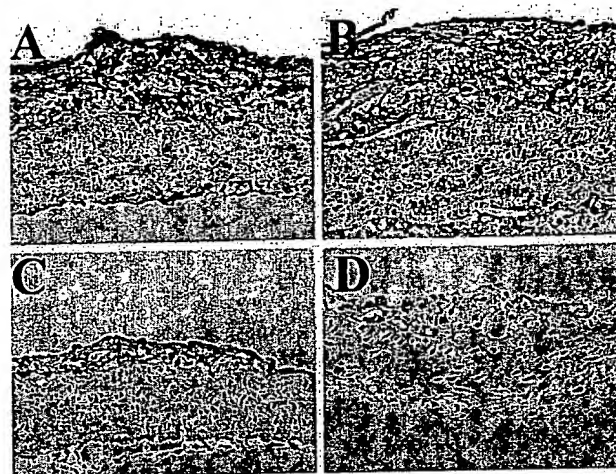


**Figure 5.** TRO inhibits accumulation of lesional macrophages. Sections from the aortic arch were immunostained by using antibody against CD68 to detect macrophages. Quantification of the percentage of the intimal area staining ( $**P<0.05$ ) for CD68 was performed by computer-assisted image analysis. A, High-fat diet ( $n=6$ ). B, High-fat diet and TRO ( $n=6$ ). C, High-fructose diet ( $n=6$ ). D, High-fructose diet and TRO ( $n=6$ ). E, Quantification of the macrophage content.

the study, reaching a maximum of 285 mg/dL at 3 months compared with 148 mg/dL for mice on normal chow. The fat-fed males were also hyperinsulinemic ( $1198 \pm 149$  versus  $664 \pm 113$  pg/mL on normal chow), consistent with the development of early-stage type II diabetes. Although TRO did not decrease hyperglycemia in high-fat-fed male mice, TRO administration completely normalized their plasma insulin levels. In marked contrast, mice on a high-fructose diet had normal fasting plasma glucose and insulin levels, which were not altered by TRO.

$LDLR^{-/-}$  males developed severe hypercholesterolemia on either the high-fat or high-fructose diet, achieving levels 3- to 4-fold greater than those in animals maintained on regular chow (Table 2). TRO lowered total plasma cholesterol by 27% in males on the high-fructose diet but had no effect on the high-fat-fed mice. Triglycerides were elevated in the high-fat-fed males but not in the high-fructose group; TRO

TABLE 1. Plasma Glucose and Insulin Levels and Final Body Weights

	Chow Diet	High-Fat Diet	High-Fat Diet/TRO	High-Fructose Diet	High-Fructose Diet/TRO
Glucose, mg/dL					
Start	158.7±14.63	173.2±12.12	169.4±7.98	137.8±11.53	148.5±27.67
1 mo	148.9±6.60	190.5±10.92	155.1±9.13*	121.2±6.44	114.8±4.55
2 mo	144.8±10.96	201.1±9.09	189.6±27.37	128.6±13.09	121.89±17.32
3 mo	148.5±14.87	284.8±25.00	268.9±13.90	152.3±15.80	181.9±23.47
Insulin, pg/mL					
3 mo	664.7±113.62	1198.7±149.81	691.2±109.14†	304.4±47.49	278.7±37.9
Body weight, g	27.3±0.56	42.5±0.66	37.0±0.89†	25.9±0.37	24.2±0.34

Values are mean±SEM.

\* $P<0.05$  vs high-fat; † $P<0.01$  vs high-fat diet.

did not alter triglycerides in either model. HDL cholesterol (HDL-C) decreased with both of the diets, compared with normal chow, as frequently reported.<sup>3</sup> TRO further lowered the HDL-C in the high-fat-fed males but increased it in the high-fructose-fed group. Plasma free fatty acid levels increased in males on the high-fat diet but not in those on the high-fructose diet; TRO decreased free fatty acid levels in both models.

### Discussion

The most significant finding of the present study is that TRO inhibited lesion formation in a type 2 diabetic mouse model and a nondiabetic LDLR<sup>-/-</sup> mouse model of intimal xanthomata. Mice fed the high-fat diet developed extensive hypercholesterolemia that was not affected by TRO. These mice also gained substantial weight and showed an

increase in circulating free fatty acid levels, which probably contributed to their insulin resistance, hyperinsulinemia, and fasting hyperglycemia.<sup>25</sup> The increase in triglycerides and decrease in HDL-C are consistent with insulin resistance. TRO decreased circulating insulin but did not affect glucose in this model. The same has been reported in humans with type 2 diabetes, of whom 20% treated with TRO showed no improvement in glucose control, but all demonstrated improved insulin sensitivity.<sup>26</sup> In contrast to the response in humans, TRO did not alter triglycerides and further decreased HDL-C. Mice fed the high-fructose diet also developed severe hypercholesterolemia but did not gain weight or develop hyperinsulinemia or elevations in free fatty acids or triglycerides. In this model, TRO decreased the free fatty acids, increased HDL-C, and decreased total cholesterol.

TABLE 2. Plasma Lipid Levels

	Chow Diet	High-Fat Diet	High-Fat Diet/TRO	High-Fructose Diet	High-Fructose Diet/TRO
Total Cholesterol, mg/dL					
Start	292.2±14.63	277.7±5.77	278.8±9.24	321.8±20.87	328.0±18.32
1 mo	316.0±11.51	583.3±72.18	541.9±62.22	489.1±24.58	360.8±21.37†
2 mo	315.8±10.26	1307.0±110.11	1173.0±122.11	1052.3±33.78	816.7±25.02‡
3 mo/final	317.9±17.79	1341.9±52.14	1313.63±28.83	1167.7±46.17	862.1±23.70‡
HDL-C, mg/dL					
Start	110.6±4.51	111.2±1.87	109.9±3.07	121.2±2.59	113.5±8.39
1 mo	111.2±3.19	108.2±1.93	108.9±2.65	104.2±3.08	106.6±4.58
2 mo	112.1±4.06	94.4±3.52	98.2±12.66	100.4±3.56	105.3±4.76
3 mo	112.4±5.00	104.8±7.84	81.8±6.86*	90.1±4.48	108.4±5.10†
Free fatty acids, mg/dL					
Start	67.1±2.82	63.5±1.82	58.2±2.67	91.0±6.96	82.5±4.38
1 mo	69.4±2.97	70.4±2.11	66.6±2.67	66.9±4.90	71.2±3.75
2 mo	65.7±2.87	88.6±7.32	74.2±4.19	68.7±3.67	65.8±3.57
3 mo	61.7±3.68	72.5±2.42	57.1±2.07*	61.7±1.52	53.1±2.81†
Triglycerides, mg/dL					
Start	122.0±4.43	109.1±5.32	101.1±5.72	84.8±5.09	111.83±16.00
1 mo	126.0±11.1	124.3±7.00	113.6±7.48	85.8±4.98	94.0±6.47
2 mo	86.9±4.98	156.6±30.55	191.8±64.47	81.2±5.98	79.8±6.47
3 mo	71.6±6.92	141.8±7.84	159.1±19.79	75.3±6.89	69.0±4.85

Values are mean±SEM.

\* $P<0.01$  vs high-fat diet; † $P<0.05$  vs high-fructose diet, and ‡ $P<0.001$  vs high-fructose diet.

Despite the difference in metabolic responses between the diabetic and nondiabetic animals, both hypercholesterolemic models responded to TRO with decreased lesion formation. These results suggest that TRO has direct vascular effects, separate from its metabolic effects, that decrease the atherosclerotic process. Alternatively, the antiatherogenic effects of TRO in the 2 different models might involve the collection of distinct metabolic processes. For example, hemodynamic effects of TRO related to its reported activity to lower blood pressure in animal models and in humans could also impact pathophysiological processes in high-fat- and high-fructose-fed LDLR<sup>-/-</sup> mice.<sup>27-30</sup> All major cell types contributing to this vascular lesion formation express PPAR $\gamma$ , which provides a mechanism for the direct effect of thiazolidinedione ligands in the vessel wall.<sup>3,5,6,9</sup> Data from *in vitro* experiments had suggested mechanisms by which activation of PPAR $\gamma$  could either accelerate or attenuate the atherosclerotic process.<sup>2-6,9,10,16</sup> The present study provides conclusive evidence that ligand-induced PPAR $\gamma$  activation by TRO reduces intimal xanthomata in murine models.

TRO had several systemic effects that may have contributed to its attenuation of intimal xanthomata. In the diabetic high-fat-fed mouse, TRO lowered insulin and glucose levels and decreased HDLC (which is thought to promote atherogenesis). In the fructose-fed model, TRO decreased total cholesterol and increased HDLC. Our finding that TRO was more potent in suppressing lesion formation in the fructose-fed model compared with the high-fat-fed mice could be due to the observed 27% reduction in total cholesterol. A common effect of TRO in the high-fat-fed and high-fructose-fed LDLR<sup>-/-</sup> models is its suppression of circulating free fatty acid levels. However, increased circulating free fatty acids have not been shown to be an independent risk factor for atherosclerosis.

Inflammation in the vascular wall has clearly emerged as a major culprit in the development of atherosclerosis.<sup>31</sup> Damage to the endothelium and the subsequent recruitment and transendothelial migration of monocytes constitute critical early cellular responses during atherogenesis.<sup>31</sup> Transmigration of monocytes into the subendothelial space is strongly stimulated by the chemokine MCP-1, which is expressed and secreted by ECs and VSMCs. The essential role of MCP-1 in atherogenesis is underscored by a recent study demonstrating that crossing MCP-1-deficient mice into LDLR<sup>-/-</sup> mice attenuated lesion formation by >80%.<sup>32</sup> Our group and others have shown that TRO and other PPAR $\gamma$  ligands inhibit growth factor-directed ERK-MAPK-dependent VSMC migration.<sup>5,10,11</sup> Cell migration requires *de novo* gene transcription that is consistent with PPAR $\gamma$  acting in the nucleus to inhibit this process.<sup>10</sup> In particular, activation of PPAR $\gamma$  can inhibit ERK-MAPK signaling to the nucleus.<sup>11,33</sup> Because MCP-1-directed migration of monocytes is ERK-MAPK dependent, interference with this pathway by TRO could contribute to the observed reduction in intimal xanthomata and lesional macrophages in treated LDLR<sup>-/-</sup> mice.

TRO and another PPAR $\gamma$  ligand, RSG, which does not contain an  $\alpha$ -tocopherol moiety, inhibited MCP-1-directed migration of human monocytes *in vitro*. TRO also consistently decreased intimal macrophage accumulation in the diabetic and nondiabetic mice. These findings support the concept that inhibition of monocyte attachment and migration

in the vessel by TRO may be one of the mechanisms contributing to the reduction of atherogenesis. Although it cannot be ruled out that the reduction of intimal monocytes in part reflected the reduced lesion size induced by TRO treatment, this is unlikely to be the sole explanation, because the relative intimal monocyte/macrophage content is known to be greatest in the early stages (smaller lesions) of atherosclerosis. In any case, the antiatherosclerotic activity of TRO-induced PPAR $\gamma$  activation clearly prevailed over its hypothesized promotion of foam cell formation via increased expression of the scavenger receptor CD36.<sup>16</sup>

Unlike other PPAR $\gamma$  ligands, TRO has an  $\alpha$ -tocopherol (vitamin E) moiety that theoretically could contribute to its antiatherogenic activity through antioxidant effects.<sup>34</sup> Vitamin E has been shown to suppress atherosclerosis in the apoE knockout model, which develops advanced atherosclerotic lesions.<sup>35,36</sup> Whether the dose of vitamin E provided by TRO in the present study is enough to impact lesion formation is doubtful. At 400 mg/kg TRO per day, LDLR<sup>-/-</sup> mice received the equivalent of 8 IU of vitamin E, a dose much lower than that reported to affect atherosclerosis or to significantly protect LDL against oxidation.<sup>35-38</sup> Another line of evidence for the assumption that the effect of TRO on lesion formation was not, to a significant degree, dependent on antioxidant effects is provided by a parallel study demonstrating that 2 other PPAR $\gamma$  ligands, RSG and GW7845, which do not contain the  $\alpha$ -tocopherol moiety, inhibited atherogenesis in the aortic root of male LDLR<sup>-/-</sup> mice fed a high-fat, cholesterol-enriched diet.<sup>39</sup> In addition, the recent Heart Outcomes Prevention Evaluation (HOPE) clinical trial in humans did not show an effect of vitamin E on coronary artery disease events or mortality.<sup>40</sup>

In summary, given the absence of consistent major metabolic changes present in diabetic and nondiabetic mice, it is likely that TRO at least in part decreases early atherosclerotic lesion formation through direct vascular effects. In human subjects with diabetes, who have a high risk for coronary disease, TRO improves insulin resistance and other proatherogenic metabolic parameters, which may improve cardiovascular risk. It is possible that some of the vascular effects observed in our murine models may also be present in humans. Although Li et al<sup>39</sup> and our data demonstrate that PPAR $\gamma$  ligands suppress early atherosclerotic lesions, intimal xanthomata do not inexorably progress to more advanced atherosclerotic plaques; in fact, they often regress.<sup>19</sup> Therefore, determining the effects of PPAR $\gamma$  ligands on more advanced atherosclerotic lesions may prove to be a stronger predictor of their potential clinical benefit. Nonetheless, the present results indicate that an investigation of potential antiatherogenic effects of PPAR $\gamma$  ligands is strongly warranted.

### Acknowledgments

This work was supported by National Institutes of Health grant HL-58328 to Willa A. Hsueh. Shu Wakino was supported by a Mary K. Iacocca Fellowship in Diabetes. Ulrich Kintscher was supported by a Gonda (Goldschneid) Fellowship in Diabetes.

### References

1. Ricote M, Huang J, Fajas L, Li A, Welch J, Najib J, Witztum JL, Auwerx J, Palinski W, Glass CK. Expression of the peroxisome proliferator-activated receptor gamma (PPARgamma) in human atherosclerosis and

- regulation in macrophages by colony stimulating factors and oxidized low density lipoprotein. *Proc Natl Acad Sci U S A*. 1998;95:7614-7619.
2. Ricote M, Li AC, Willson TM, Kelly CJ, Glass CK. The peroxisome proliferator-activated receptor- $\gamma$  is a negative regulator of macrophage activation. *Nature*. 1998;391:79-82.
  3. Xin X, Yang S, Kowalski J, Gerritsen ME. Peroxisome proliferator-activated receptor  $\gamma$  ligands are potent inhibitors of angiogenesis in vitro and in vivo. *J Biol Chem*. 1999;274:9116-9121.
  4. Jackson SM, Parhami F, Xi XP, Berliner JA, Hsueh WA, Law RE, Demer LL. Peroxisome proliferator-activated receptor activators target human endothelial cells to inhibit leukocyte-endothelial cell interaction. *Arterioscler Thromb Vasc Biol*. 1999;19:2094-2104.
  5. Marx N, Schonbeck U, Lazar MA, Libby P, Plutzky J. Peroxisome proliferator-activated receptor  $\gamma$  activators inhibit gene expression and migration in human vascular smooth muscle cells. *Circ Res*. 1998;83:1097-1103.
  6. Law RE, Goetze S, Xi XP, Jackson S, Kawano Y, Demer L, Fishbein MC, Meehan WP, Hsueh WA. Expression and function of PPAR $\gamma$  in rat and human vascular smooth muscle cells. *Circulation*. 2000;101:1311-1318.
  7. Tack CJ, Ong MK, Lutterman JA, Smits P. Insulin-induced vasodilatation and endothelial function in obesity/insulin resistance: effects of troglitazone. *Diabetologia*. 1998;41:569-576.
  8. Murakami T, Mizuno S, Ohsato K, Moriuchi I, Arai Y, Nio Y, Kaku B, Takahashi Y, Ohnaka M. Effects of troglitazone on frequency of coronary vasospastic-induced angina pectoris in patients with diabetes mellitus. *Am J Cardiol*. 1999;84:92-94. A8. Abstract.
  9. Tanaka T, Itoh H, Do KK, Fukunaga Y, Arai H, Hosoda K. Activation of PPAR $\gamma$  inhibits macrophage proliferation and migration: possible therapeutic effectiveness of thiazolidinediones on diabetic vascular complications. *Diabetes*. 1999;48(suppl 1):A30. Abstract.
  10. Goetze S, Xi XP, Kawano H, Gotlibowski T, Fleck E, Hsueh WA, Law RE. PPAR  $\gamma$ -ligands inhibit migration mediated by multiple chemoattractants in vascular smooth muscle cells. *J Cardiovasc Pharmacol*. 1999;33:798-806.
  11. Law RE, Meehan WP, Xi XP, Graf K, Wuthrich DA, Coats W, Faxon D, Hsueh WA. Troglitazone inhibits vascular smooth muscle cell growth and intimal hyperplasia. *J Clin Invest*. 1996;98:1897-1905.
  12. Igarashi M, Takeda Y, Ishibashi N, Takahashi K, Mori S, Tominaga M, Saito Y. Pioglitazone reduces smooth muscle cell density of rat carotid arterial intima induced by balloon catheterization. *Horm Metab Res*. 1997;29:444-449.
  13. Yoshimoto T, Naruse M, Shizume H, Naruse K, Tanabe A, Tanaka M, Tago K, Irie K, Muraki T, Demura H, et al. Vascular-protective effects of insulin sensitizing agent pioglitazone in neointimal thickening and hypertensive vascular hypertrophy. *Atherosclerosis*. 1999;145:333-340.
  14. Takagi T, Akasaka T, Yamamuro A, Honda Y, Hozumi T, Morioka S, Yoshida K. Troglitazone reduces neointimal tissue proliferation after coronary stent implantation in patients with non-insulin dependent diabetes mellitus: a serial intravascular ultrasound study. *J Am Coll Cardiol*. 2000;36:1529-1535.
  15. Pasceri V, Wu HD, Willerson JT, Yeh ET. Modulation of vascular inflammation in vitro and in vivo by peroxisome proliferator-activated receptor- $\gamma$  activators. *Circulation*. 2000;101:235-238.
  16. Tontonoz P, Nagy L, Alvarez JG, Thomazy VA, Evans RM. PPAR $\gamma$  promotes monocyte/macrophage differentiation and uptake of oxidized LDL. *Cell*. 1998;93:241-252.
  17. Saltiel AR, Olefsky JM. Thiazolidinediones in the treatment of insulin resistance and type II diabetes. *Diabetes*. 1996;45:1661-1669.
  18. Savage PJ. Cardiovascular complications of diabetes mellitus: what we know and what we need to know about their prevention. *Ann Intern Med*. 1996;124:123-126.
  19. Virmani R, Kolodgie FD, Burke AP, Farb A, Schwartz SM. Lessons from sudden coronary death: a comprehensive morphological classification scheme for atherosclerotic lesions. *Arterioscler Thromb Vasc Biol*. 2000;20:1262-1275.
  20. Towler DA, Bidder M, Latifi T, Coleman T, Semenkovich CF. Diet-induced diabetes activates an osteogenic gene regulatory program in the aortas of low density lipoprotein receptor-deficient mice. *J Biol Chem*. 1998;273:30427-30434.
  21. Merat S, Casanada F, Sutphin M, Palinski W, Reaven PD. Western-type diets induce insulin resistance and hyperinsulinemia in LDL receptor-deficient mice but do not increase aortic atherosclerosis compared with normoinsulinemic mice in which similar plasma cholesterol levels are achieved by a fructose-rich diet. *Arterioscler Thromb Vasc Biol*. 1999;19:1223-1230.
  22. Shi C, Lee WS, Russell ME, Zhang D, Fletcher DL, Newell JB, Haber E. Hypercholesterolemia exacerbates transplant arteriosclerosis via increased neointimal smooth muscle cell accumulation: studies in apolipoprotein E knockout mice. *Circulation*. 1997;96:2722-2728.
  23. Nakashima Y, Plump AS, Raines EW, Breslow JL, Ross R. ApoE-deficient mice develop lesions of all phases of atherosclerosis throughout the arterial tree. *Arterioscler Thromb*. 1994;14:133-140.
  24. Tangirala RK, Rubin EM, Palinski W. Quantitation of atherosclerosis in murine models: correlation between lesions in the aortic origin and in the entire aorta, and differences in the extent of lesions between sexes in LDL receptor-deficient and apolipoprotein E-deficient mice. *J Lipid Res*. 1995;36:2320-2328.
  25. Kelley DE, Goodpaster B, Wing RR, Simoneau JA. Skeletal muscle fatty acid metabolism in association with insulin resistance, obesity, and weight loss. *Am J Physiol*. 1999;277:E1130-E1141.
  26. Suter SL, Nolan JJ, Wallace P, Gumbiner B, Olefsky JM. Metabolic effects of new oral hypoglycemic agent CS-045 in NIDDM subjects. *Diabetes Care*. 1992;15:193-203.
  27. Fujiwara K, Hayashi K, Matsuda H, Kubota E, Honda M, Ozawa Y, Saruta T. Altered pressure-natriuresis in obese Zucker rats. *Hypertension*. 1999;33:1470-1475.
  28. Sung BH, Izzo JL Jr, Dandona P, Wilson MF. Vasodilatory effects of troglitazone improve blood pressure at rest and during mental stress in type 2 diabetes mellitus. *Hypertension*. 1999;34:83-88.
  29. Kawai T, Takei I, Oguma Y, Ohashi N, Tokui M, Oguchi S, Katsukawa F, Hirose H, Shimada A, Watanabe K, et al. Effects of troglitazone on fat distribution in the treatment of male type 2 diabetes. *Metabolism*. 1999;48:1102-1107.
  30. Chen S, Noguchi Y, Izumida T, Tatebe J, Katayama S. A comparison of the hypotensive and hypoglycaemic actions of an angiotensin converting enzyme inhibitor, an AT1a antagonist and troglitazone. *J Hypertens*. 1996;14:1325-1330.
  31. Ross R. Atherosclerosis is an inflammatory disease. *Am Heart J*. 1999;138:S419-S420.
  32. Gu L, Okada Y, Clinton SK, Gerard C, Sukhova GK, Libby P, Rollins BJ. Absence of monocyte chemoattractant protein-1 reduces atherosclerosis in low density lipoprotein receptor-deficient mice. *Mol Cell*. 1998;2:275-281.
  33. Goetze S, Xi XP, Graf K, Fleck E, Hsueh WA, Law RE. Troglitazone inhibits angiotensin II-induced extracellular signal-regulated kinase 1/2 nuclear translocation and activation in vascular smooth muscle cells. *FEBS Lett*. 1999;452:277-282.
  34. Inoue I, Katayama S, Takahashi K, Negishi K, Miyazaki T, Sonoda M, Komoda T. Troglitazone has a scavenging effect on reactive oxygen species. *Biochem Biophys Res Commun*. 1997;235:113-116.
  35. Shaish A, George J, Gilburd B, Keren P, Levkovitz H, Harats D. Dietary beta-carotene and alpha-tocopherol combination does not inhibit atherogenesis in an apoE-deficient mouse model. *Arterioscler Thromb Vasc Biol*. 1999;19:1470-1475.
  36. Pratico D, Tangirala RK, Rader DJ, Rokach J, FitzGerald GA. Vitamin E suppresses isoprostane generation in vivo and reduces atherosclerosis in apoE-deficient mice. *Nat Med*. 1998;4:1189-1192.
  37. Crawford RS, Kirk EA, Rosenfeld ME, LeBoeuf RC, Chait A. Dietary antioxidants inhibit development of fatty streak lesions in the LDL receptor-deficient mouse. *Arterioscler Thromb Vasc Biol*. 1998;18:1506-1513.
  38. Bird DA, Tangirala RK, Fruebis J, Steinberg D, Witztum JL, Palinski W. Effect of probucol on LDL oxidation and atherosclerosis in LDL receptor-deficient mice. *J Lipid Res*. 1998;39:1079-1090.
  39. Li AC, Brown KK, Silvestre MJ, Willson TM, Palinski W, Glass CK. Peroxisome proliferator-activated receptor  $\gamma$  ligands inhibit development of atherosclerosis in LDL receptor-deficient mice. *J Clin Invest*. 2000;106:523-531.
  40. Yusuf S, Dagenais G, Pogue J, Bosch J, Sleight P. Vitamin E supplementation and cardiovascular events in high-risk patients: the Heart Outcomes Prevention Evaluation Study Investigators. *N Engl J Med*. 2000;342:154-160.



## Vitamin E Reduces Progression of Atherosclerosis in Low-Density Lipoprotein Receptor-Deficient Mice With Established Vascular Lesions

Tillmann Cyrus, MD; Yuemang Yao, BSc; Joshua Rokach, PhD;  
Lina X. Tang, MD; Domenico Praticò, MD

**Background**—A growing body of evidence from animal studies supports the hypothesis that oxidative stress-mediated mechanisms play a central role in early atherogenesis. In contrast, clinical trials with antioxidant vitamins have not produced consistent results in humans with established atherosclerosis.

**Methods and Results**—Low-density lipoprotein receptor-deficient mice (LDLR KO) were fed a high-fat diet for 3 months to induce atheroma. At this time, 1 group of mice was euthanized for examination of atherosclerosis, and 2 other groups were randomized to receive high-fat diet either alone or supplemented with vitamin E for 3 additional months. At the end of the study, LDLR KO on a vitamin E-supplemented fat diet had decreased 8,12-*iso*-isoprostane (iP)F<sub>2a</sub>-VI and monocyte chemoattractant protein-1 levels, but increased nitric oxide levels compared with mice on placebo. No difference in lipid levels was observed between the 2 groups. Compared with baseline, placebo group had progression of atherosclerosis. In contrast, vitamin E-treated animals showed a significant reduction in progression of atherosclerosis.

**Conclusions**—These results demonstrate that in LDLR KO, vitamin E supplementation reduces progression of established atherosclerosis by suppressing oxidative and inflammatory reactions and increasing nitric oxide levels. (*Circulation*. 2003;107:521-523.)

**Key Words:** atherosclerosis ■ antioxidants ■ lipids ■ inflammation ■ nitric oxide

Atherogenesis is a chronic disease influenced by multiple genetic and environmental factors that involves a complex interplay between blood components and the artery wall and is characterized by oxidative and inflammatory reactions.<sup>1</sup> Consistent data indicate that oxidative processes are of functional importance in animal models of atherogenesis.<sup>2</sup> Epidemiological studies support these findings, indicating an inverse relationship between antioxidant vitamin intake and cardiovascular disease.<sup>3</sup> Several clinical trials, however, have shown conflicting results as to whether or not antioxidant vitamins reduce atherosclerosis progression and cardiovascular events.<sup>4</sup> Furthermore, in healthy subjects, vitamin E supplementation did not reduce the progression of the carotid artery intima-media thickness over a 3-year period.<sup>5</sup>

Several considerations can be made to explain these conflicting results, among them the endogenous antioxidant status of the study participants before enrollment and the timing of the intervention relative to the atherosclerotic process. It is plausible that in mice, vitamin E is effective because it is typically given at an early stage of the disease. In contrast, in humans, it has little or no effect because it is

administered when atherosclerotic lesions are already established.

Most animal studies have focused their attention on the effect of antioxidants on the formation of fatty streaks, the earliest cellular lesion of atherosclerosis. In contrast, the possible contribution of oxidative stress to the progression of atherosclerosis has been poorly investigated. Previously, we have shown that vitamin E suppresses *in vivo* lipid peroxidation and induces a significant reduction of early atherogenesis in different mouse models of atherosclerosis.<sup>6,7</sup> The present study was designed to test the hypothesis that chronic attenuation of oxidative stress by vitamin E would have an impact on established atherosclerosis in low-density lipoprotein-receptor deficient (LDLR KO) mice.

### Methods

#### Animal Experimental Protocol

All procedures were approved by the Institutional Committee. LDLR KO mice (n=42, Jackson Laboratories, Bar Harbor, Me) were allowed to age to 12 months and were then fed a high-fat diet (normal chow supplemented with 0.15% cholesterol and 20% butter fat) for a total of 12 weeks prior baseline analysis. At this time-point blood was drawn, plasma cholesterol was quantitated, and mice were

Received November 8, 2002; revision received December 11, 2002; accepted December 12, 2002.

From the Center for Experimental Therapeutics and Department of Pharmacology, University of Pennsylvania, School of Medicine, Philadelphia, Pa; and The Claude Pepper Institute and Department of Chemistry (J.R.), Florida Institute of Technology, Melbourne, Fla.

Correspondence to Domenico Praticò, MD, University of Pennsylvania, Biomedical Research Building 2/3, Room 812, 421, Curie Blvd, Philadelphia, PA 19104. E-mail domenico@spirit.gcrp.upenn.edu

© 2003 American Heart Association, Inc.

*Circulation* is available at <http://www.circulationaha.org>

DOI: 10.1161/01.CIR.0000055186.40785.C4



divided in 3 groups of 14 animals each, with mean cholesterol levels that were not significantly different. One group of animals was killed immediately for analysis of atherosclerosis (baseline group). The remaining mice were randomized to receive high-fat diet alone or supplemented with vitamin E (2 IU/g diet) for 3 additional months. Blood samples were obtained from mice at baseline and then at monthly intervals until the end of the study.

### Biochemical Analyses

Plasma cholesterol and triglyceride levels were measured enzymatically and vitamin E levels were assayed by high-performance liquid chromatography as previously described.<sup>6,7</sup> Total plasma NO metabolites were evaluated with measurements of nitrite+nitrate by a colorimetric assay (Assay Design). Plasma 8,12-iso-iPF<sub>2a</sub>-VI levels were measured by gas chromatography/mass spectrometry, as previously described.<sup>7,8</sup> Levels of soluble intercellular adhesion molecules-1 (s-ICAM1) and monocyte chemoattractant protein-1 (MCP-1) were measured by ELISA kits (Endogen, Inc and R&D System).<sup>7,9</sup>

### Preparation of Mouse Aortas and Quantitation of Atherosclerosis

After the final blood collection, mice were euthanized and the aortic tree was perfused for 10 minutes with ice-cold PBS containing 20  $\mu$ mol/L BHT and 2 mmol/L EDTA (pH 7.4) as previously described.<sup>7,9</sup> After removal of the surrounding adventitial fat tissue, the aorta was opened longitudinally, fixed in formal-sucrose, and stained with Sudan IV. The extent of atherosclerosis was determined using the en face method, in a blinded fashion as previously described.<sup>6,7</sup>

### Histology and Immunohistochemistry

Briefly, serial frozen sections of the aortic root of the proximal aorta, starting at the sinus, were examined. Immunostaining for macrophage content was performed as previously described.<sup>7,9</sup> Briefly, a Mab to mouse macrophages (MOMA-2; Accurate Chemicals), and a Mab anti-human smooth muscle  $\alpha$ -actin (Sigma Chemical Co) for smooth muscle cells were used. Antibody reactivity was detected using a Nova red substrate kit (SK-4800, Vector Laboratory). Cross sections were counterstained with hematoxylin. As control, no primary antibody was added to the same sections. Images of immunostained sections were captured and analyzed in a blinded fashion as previously described.<sup>7,9</sup>

### Statistical Analysis

Results were expressed as mean $\pm$ SEM. Data were analyzed by ANOVA and subsequently by Student's unpaired 2-tailed *t* test, as indicated. Probability values less than 0.05 were considered as significant.

## Results

### Vitamin E Effects on Plasma Lipids

Compared with baseline group, mice from the placebo group showed a further significant increase in both plasma cholesterol and triglycerides. This increase was also evident in LDLR KO mice receiving the high-fat diet supplemented with vitamin E (Table). No significant difference in lipid levels was found between mice on vitamin E or high-fat diet alone. Compliance with vitamin E dietary regimen was demonstrated by a significant increase in its circulating levels in mice on vitamin E-enriched diet (Table). Elevation of plasma vitamin E levels was also evident when the values were normalized for cholesterol (data not shown).

### Vitamin E Effects on Oxidative and Inflammatory Processes

Plasma levels of 8,12-iso-iPF<sub>2a</sub>-VI, a major F<sub>2</sub>-isoprostane and a specific marker of lipid peroxidation,<sup>8</sup> were further

### Characteristics of the 3 Groups of Mice

	Baseline	High-Fat Diet	
		Placebo	Vitamin E
Cholesterol, mg/dL	800 $\pm$ 50	1150 $\pm$ 100†	1115 $\pm$ 85
Triglycerides, mg/dL	450 $\pm$ 45	710 $\pm$ 60†	680 $\pm$ 70
Vitamin E, $\mu$ M	20 $\pm$ 2	16 $\pm$ 1.8†	52 $\pm$ 2.2*
8,12-iso-iPF <sub>2a</sub> -VI, pg/mL	750 $\pm$ 60	1100 $\pm$ 55†	630 $\pm$ 50
sICAM-1, ng/ml	11 $\pm$ 1.5	14 $\pm$ 2	10 $\pm$ 2*
MCP-1, ng/ml	200 $\pm$ 15	245 $\pm$ 21	180 $\pm$ 16*
Nox, $\mu$ M	30 $\pm$ 3.2	18 $\pm$ 2.6†	48 $\pm$ 2.4*

Each group includes 14 mice. Results are expressed as mean $\pm$ SEM.

\**P*<0.05 vs placebo; †*P*<0.05 vs baseline.

elevated in LDLR KO mice kept on a high-fat diet alone when compared with the baseline group. In contrast, vitamin E significantly reduced these levels to values that were similar to the ones observed in mice at baseline (Table). At the end of the study, mice on the high-fat diet alone had a further increase in s-ICAM-1 and MCP-1 circulating levels, whereas vitamin E significantly reduced them (Table). Because impaired NO synthesis has been described in hypercholesterolemia,<sup>10</sup> we examined the effect of vitamin E supplementation on NO metabolite (NOx) levels. Compared with baseline, plasma NOx levels were further reduced in mice on a high-fat diet alone. In contrast, vitamin E supplementation preserved higher plasma NOx levels compared with both baseline and the placebo group (Table).

### Vitamin E Effects on Preexisting Atherosclerotic Lesions

The Sudan IV-stained aorta preparations of the LDLR KO mice on the high-fat diet for 3 months showed atherosclerotic lesions mainly localized in the sinus and arch portions, covering 11.2 $\pm$ 1.4% of the entire vessel (Figure 1). The aortas from mice receiving a high-fat diet for 3 additional months demonstrated further progression of atherosclerosis, which involved the thoracic and abdominal portions of the aorta. In contrast, this area was significantly reduced in LDLR KO mice on high-fat diet supplemented with vitamin E (Figure 1). No significant difference was observed with the baseline group (Figure 1).

Immunohistochemical analyses of aortic root sections showed no difference in the percentage area occupied by

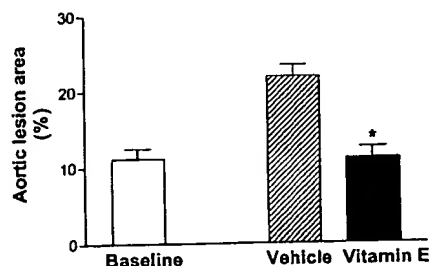
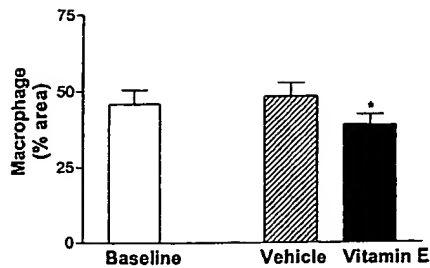


Figure 1. Percentage of total aortic atherosclerotic lesion areas in LDLR KO mice fed a high-fat diet for 3 months (baseline), and those fed a high-fat diet alone or with vitamin E for 12 additional weeks (n=14 per group). \**P*<0.01 versus placebo.



**Figure 2.** Percentage area of aortic root atherosclerotic lesions occupied by macrophages in LDLR KO mice fed high-fat diet for 3 months (baseline), and those fed a high-fat diet alone or with vitamin E for 12 additional weeks (n=8 per group). \* $P<0.01$  versus placebo.

macrophages between baseline and placebo group after normalized to total lesion area. However, this area was significantly reduced in mice receiving vitamin E compared with placebo (Figure 2). Finally, no difference in smooth muscle cell content was observed among the 3 groups (data not shown).

### Discussion

In the current study, we demonstrated for the first time that chronic supplementation of vitamin E retards the progression of established atherosclerotic lesions in LDLR KO mice on a high-fat diet by decreasing oxidative and inflammatory reactions and increasing NO levels.

Lipid peroxidation, in particular oxidative modification of LDL in vivo, is thought to play a functional role in atherogenesis.<sup>2</sup> Evidence consistent with this hypothesis includes the presence of oxidized lipids in atherosclerotic lesions and the reduction of murine atherosclerosis by structurally distinct antioxidants.<sup>11–13</sup> Several trials have shown, however, that antioxidants do not reduce the risk of fatal or non-fatal infarction in an unselected population with established atherosclerosis.<sup>4</sup> These conflicting results do not necessarily mean that the oxidative hypothesis of atherosclerosis is incorrect. It is possible that the animal intervention studies deal primarily with early lesions, whereas clinical trials deal with established ones. We have previously shown that in vivo lipid peroxidation is increased in the apolipoprotein E-deficient mice and LDLR KO mice, and that its inhibition by vitamin E coincides with a reduction in atherosclerosis.<sup>6,7</sup> It is plausible that in humans antioxidants have little or no effect because they are given when lesions are already established. To test this hypothesis, LDLR KO mice initially kept on a high-fat diet for 3 months were subsequently randomized to either receive a high-fat diet supplemented with vitamin E or stay on the high-fat diet alone for 12 additional weeks. We found that vitamin E reduced progression of atherosclerosis without affecting lipid levels by suppressing oxidative stress. These results support the concept that vitamin E is effective in LDLR KO mice whether it is given at the early phase of atherogenesis or after the disease is established.

Atherosclerosis is associated with oxidative stress, which is characterized by a reduction of endogenous antioxidants and NO levels.<sup>14,15</sup> We confirmed these data by showing that vitamin E restores and increases these levels. Reactive oxygen species can interact with NO and produce peroxynitrate, which in turn can further sustain oxidative injury to the endothelium. By restoring the endogenous antioxidant status, vitamin E increases NO levels and limits peroxynitrate formation, which could then act as additional antiatherogenic mechanisms by reducing vascular inflammation. Indeed, our present findings demonstrate that by reducing oxidative stress, vitamin E improves indices of inflammation and endothelial function, which are critically involved in the progression of atherosclerosis.

In interpreting our results, we must consider an important limitation of this study; no animal model mimics perfectly human atherosclerosis. Despite this fact, our study supports the hypothesis that the discrepancies between animal studies and clinical trials with vitamin E cannot be explained by the timing of the intervention, ie, early versus established lesions.

### Acknowledgments

This work was supported by a grant from the American Heart Association (030211N) to Dr Praticò.

### References

- Glass CK, Witztum JL. Atherosclerosis: the road ahead. *Cell*. 2001;104:503–516.
- Witztum JL, Steinberg D. The oxidative modification hypothesis of atherosclerosis: does it hold for humans. *Trends Cardiovasc Med*. 2001;11:93–102.
- Rimm EB, Stampfer MJ, Ascherio A, et al. Vitamin E consumption and the risk of coronary heart disease in men. *N Engl J Med*. 1993;328:1450–1456.
- Praticò D. Vitamin E: murine studies versus clinical trials. *Ital Heart J*. 2001;2:878–881.
- Hodis HN, Mack WJ, LaBree L, et al. Alpha-tocopherol supplementation in healthy individuals reduces low-density lipoprotein oxidation but not atherosclerosis. *Circulation*. 2002;106:1453–1459.
- Praticò D, Tangirala RK, Rader DJ, et al. Vitamin E suppresses isoprostane generation in vivo and reduces atherosclerosis in Apo-E-deficient mice. *Nat Med*. 1998;4:1189–1192.
- Cyrus T, Tang LX, Rokach J, et al. Lipid peroxidation and platelet activation in murine atherosclerosis. *Circulation*. 2001;104:1940–1945.
- Praticò D, Lawson JA, Rokach J, et al. The isoprostanes in biology and medicine. *Trends Endocr Metab*. 2001;12:243–247.
- Praticò D, Cyrus T, Zhang Z, et al. Acceleration of atherogenesis by COX-1-dependent prostanoid formation in low-density lipoprotein receptor deficient mice. *Proc Natl Acad Sci U S A*. 2001;98:3358–3363.
- Ishikawa I, Sugawara D, Wang X, et al. Heme oxygenase-1 inhibits atherosclerotic lesion formation in LDL-receptor knockout mice. *Circ Res*. 2001;88:506–512.
- Witztum JL, Berliner JA. Oxidized phospholipids and isoprostanes in atherosclerosis. *Curr Opin Lipidol*. 1998;9:441–448.
- Tangirala RK, Casanada F, Miller E, et al. Effect of the anti-oxidant N,N'-diphenyl 1,4-phenylenediamine (DPPD) on atherosclerosis in apoE-deficient mice. *Arterioscler Thromb Vasc Biol*. 1994;15:1625–1630.
- Cynshi O, Kawabe Y, Suzuki T, et al. Antiatherogenic effects of the antioxidant BO-653 in three different animal models. *Proc Natl Acad Sci U S A*. 1998;95:10123–10128.
- Praticò D. Lipid peroxidation in mouse models of atherosclerosis. *Trends Cardiovasc Med*. 2001;11:112–116.
- Oemar B, Tschudi MR, Godoy N, et al. Reduced endothelial synthase expression and production in human atherosclerosis. *Circulation*. 1998;97:2494–2498.

Vascular Biology, Atherosclerosis and Endothelium Biology

# The Atheroprotective Effect of 17 $\beta$ -Estradiol Depends on Complex Interactions in Adaptive Immunity

Rima Elhage,\* Pierre Gourdy,\* Jacek Jawien,<sup>†</sup>  
Laurent Bouchet,\* Caroline Castano,\*  
Catherine Fievet,<sup>‡</sup> Göran K. Hansson,<sup>†</sup>  
Jean-François Arnal,\* and Francis Bayard\*

From INSERM U589,\* IFR31, Institut L. Bugnard, Toulouse, France; INSERM U545 Institut Pasteur,<sup>‡</sup> Lille, France; and the Center for Molecular Medicine and Department of Medicine,<sup>†</sup> Karolinska Institute, Stockholm, Sweden

**Estradiol prevents fatty streak formation in chow-fed atherosclerosis-prone apolipoprotein E (ApoE)-deficient mice. We previously reported that fatty streak development of immunodeficient ApoE<sup>-/-</sup>/recombination activating gene 2 (RAG-2<sup>-/-</sup>) double-deficient mice was insensitive to estradiol. In the present work, we demonstrate that the reconstitution of ApoE<sup>-/-</sup>/RAG-2<sup>-/-</sup> with bone marrow from immunocompetent ApoE<sup>-/-</sup>/RAG-2<sup>+/+</sup> mice restores the protective effect of estradiol on fatty streak constitution. We extended this demonstration to the model of low-density lipoprotein receptor-deficient mice, establishing the obligatory role of mature lymphocytes in this process. We then investigated whether the protective effect of estradiol was mediated by a specific lymphocyte subpopulation by studying the hormonal effect on fatty streak constitution in recently developed models of ApoE<sup>-/-</sup> mice deficient in selective T-lymphocyte subsets (either TCR $\alpha\beta$ <sup>+</sup>, CD4<sup>+</sup>, CD8<sup>+</sup>, or TCR $\gamma\delta$ <sup>+</sup> lymphocytes) or B lymphocytes. In all these specifically immunodeficient mice, estradiol administration to ovariectomized mice conferred protection as in immunocompetent ApoE<sup>-/-</sup> mice, clearly demonstrating that no single lymphocyte subpopulation was specifically required for this effect. These results point to additional lymphocyte-dependent mechanisms such as modulating the interactions among lymphocytes and between lymphocytes and endothelial and/or antigen-presenting cells. (*Am J Pathol* 2005, 167:267–274)**

Fuller understanding of the mechanism of atherosclerosis prevention by estrogens is urgently needed.<sup>1</sup> Two controlled prospective and randomized studies did not demonstrate a beneficial effect of hormone replacement therapy whether in secondary<sup>2</sup> or in primary prevention.<sup>3</sup> In contrast to these clinical data, estrogen hormones have been shown to decrease macrophage-derived foam-cell infiltration in different animal species including atherosclerosis-prone apolipoprotein E-deficient (ApoE<sup>-/-</sup>) mice<sup>4,5</sup> although the mechanisms of this effect have remained obscure.

Recent cumulative evidence have suggested that both innate and adaptive immune responses modulate the rate of lesion progression.<sup>6–8</sup> Indeed, several studies have confirmed the importance of T lymphocytes present in early lesions of atherosclerosis.<sup>9–12</sup> Furthermore, previous observations have demonstrated the particular role for specific T-lymphocyte subsets. For example, Zhou and colleagues<sup>13</sup> showed that CD4<sup>+</sup> T cells aggravate the atherosclerotic process.

In this context, we previously reported that ApoE<sup>-/-</sup> mice with homozygous disruption at the recombination activating gene 2 (RAG-2<sup>-/-</sup>) loci presented a reduced level of atherosclerotic lesions that were insensitive to estradiol (E2).<sup>14</sup> In the present studies, we first demonstrated that the reconstitution of ApoE<sup>-/-</sup>/RAG-2<sup>-/-</sup> with bone marrow from immunocompetent ApoE<sup>-/-</sup>/RAG-

Supported in part by INSERM, the Ministère de la Recherche et de la Technologie (Université Paul Sabatier), Action Concertée Incitative 2001 and 2003, Association pour la Recherche contre le Cancer, MSD, Theramex Laboratories, European Vascular Genomics Network (grant no.503254), Fondation de France, the Conseil Régional Midi-Pyrénées, and the French Society of Atherosclerosis (to R.E.).

Accepted for publication February 10, 2005.

Supplemental material for this article appears on <http://ajp.amj-pathol.org>.

Present address of J.J.: Department of Pharmacology, Jagiellonian University School of Medicine, Grzegorzeczka 16, PL 31-531 Krakow, Poland.

Address reprint requests to F. Bayard, INSERM U589, IFR31, Institut L. Bugnard, BP 84225, 31432 Toulouse Cédex 4, France. E-mail: bayard@toulouse.inserm.fr.

2<sup>+/+</sup> mice restores the protective effect of E2 on fatty streak constitution and extended this demonstration to the model of low-density lipoprotein receptor (LDLR)-deficient mice. We then hypothesized that E2 could target a specific lymphocyte subset to exert its protective effect on fatty streak constitution. To solve this question, we compared the effect of E2 in immunocompetent ApoE<sup>-/-</sup> mice and in models of ApoE<sup>-/-</sup> mice deficient in specific lymphocyte subsets developed in our laboratory. We observed that no T- or B-lymphocyte subpopulation specifically mediated the protective effect of E2, pointing to additional lymphocyte-dependent mechanisms.

## Materials and Methods

### Animals

The specific pathogen-free conditions of animal care and regular chow diet feeding as well as the production of ApoE- and RAG-2-deficient mice (ApoE<sup>-/-</sup>/RAG-2<sup>-/-</sup>) have been described previously.<sup>14,15</sup> The ApoE<sup>-/-</sup>/RAG-2<sup>-/-</sup> mice had been backcrossed into a C57BL/6 background for six generations.

Low-density lipoprotein receptor-deficient (LDLR<sup>-/-</sup>) mice were purchased from Charles River (L'Arbresle, France). RAG-2-deficient (RAG-2<sup>-/-</sup>) mice were purchased from CDTA (Orléans, France). Both strains had been backcrossed into a C57BL/6 background for more than 10 generations. Female LDLR<sup>-/-</sup> mice were crossed with male RAG-2<sup>-/-</sup> mice in our animal facility to obtain LDLR and RAG-2 double-deficient mice (LDLR<sup>-/-</sup>/RAG-2<sup>-/-</sup>). RAG-2 and LDLR gene disruptions were assessed by polymerase chain reaction genotyping as previously described.<sup>16,17</sup> The production of the double-deficient models is reported elsewhere.<sup>12</sup> Briefly, TCRβ-deficient (TCRβ<sup>-/-</sup>), CD4-deficient (CD4<sup>-/-</sup>), CD8-deficient (CD8<sup>-/-</sup>), TCRδ-deficient (TCRδ<sup>-/-</sup>) male mice were crossed with female ApoE<sup>-/-</sup> mice. B-lymphocyte-deficient mice were obtained similarly by crossing μmt-deficient<sup>18</sup> B<sup>-/-</sup> male mice with female ApoE<sup>-/-</sup> mice. Heterozygous ApoE<sup>-/-</sup>/TCRβ<sup>+/-</sup>, ApoE<sup>-/-</sup>/CD4<sup>+/-</sup>, ApoE<sup>-/-</sup>/CD8<sup>+/-</sup>, ApoE<sup>-/-</sup>/TCRδ<sup>+/-</sup>, ApoE<sup>-/-</sup>/B<sup>+/-</sup> populations were generated and used as the parental genotypes. The offspring of these heterozygous strains, TCRβ<sup>+/+</sup>, CD4<sup>+/+</sup>, CD8<sup>+/+</sup>, TCRδ<sup>+/+</sup>, B<sup>+/+</sup> and TCRβ<sup>-/-</sup>, CD4<sup>-/-</sup>, CD8<sup>-/-</sup>, TCRδ<sup>-/-</sup>, B<sup>-/-</sup> served as the subjects of our studies. Confirmation of gene disruption was screened by polymerase chain reaction genotyping and phenotyping of blood lymphocytes or splenocytes by flow cytometry.<sup>12</sup> All strains had been backcrossed into a C57BL/6 background for more than 10 generations.

Only female animals were used in the present studies. As shown in Figure 1, mice were ovariectomized at 5 weeks of age and, 1 week later, were administered with either 60-day time-release placebo or 0.1 mg of estradiol-17β pellets (Innovative Research of America, Sarasota, FL) implanted subcutaneously into the back of the animals, using a sterile trochar and forceps. New pellets were reimplanted 7 weeks later. The dose of 0.1 mg of E2, releasing 80 μg/kg/day, had previously been defined

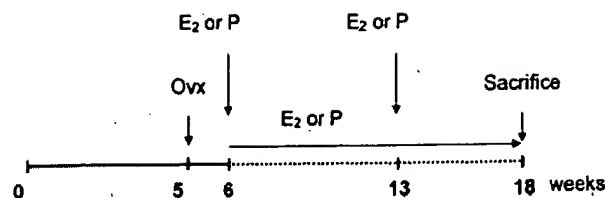


**Figure 1.** Protocol to study fatty streak formation in immunocompetent or immunodeficient ApoE-deficient mice. OvX, ovariectomy; E2, estradiol-17β pellet; P, placebo pellet.

as adequate for a maximal effect on fatty streak constitution in female mice.<sup>15</sup> ApoE<sup>-/-</sup> mice were maintained under chow diet throughout the experiments, whereas LDLR<sup>-/-</sup> mice were switched to a high-fat diet (15% fat, 1.25% cholesterol, no cholate, TD96335; Harlan Teklad, WI) at 5 weeks of age. After E2 or placebo treatment for 12 weeks, all mice were sacrificed with an overdose of ketalar after a 16-hour fast. Blood was collected by orbital puncture for serum lipid analysis.<sup>15</sup> Uterus was weighted to assess the efficacy of E2 treatment. All experimental procedures were performed in accordance with the recommendations of the European Accreditation of Laboratory Animal Care Institute.

### Bone Marrow Transplantation

As shown in Figure 2, ApoE<sup>-/-</sup>/RAG-2<sup>-/-</sup> and LDLR<sup>-/-</sup>/RAG-2<sup>-/-</sup> mice were ovariectomized at 5 weeks of age and received a sublethal dose of whole-body irradiation (400 rads) 1 week later. The day after irradiation, donor ApoE<sup>-/-</sup> or ApoE<sup>-/-</sup>/RAG-2<sup>-/-</sup>, C57BL/6 or RAG-2<sup>-/-</sup> mice were killed, and their femurs and tibias removed aseptically. Marrow cavities were flushed, and single-cell

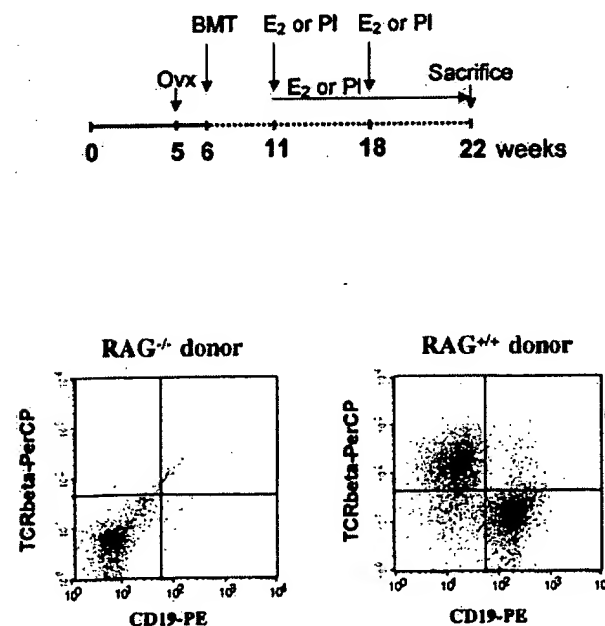


**Figure 2.** Protocol of bone marrow transplantation (BMT) and flow cytometry analysis of spleen lymphocyte repopulation of ApoE<sup>-/-</sup>/RAG-2<sup>-/-</sup> mice transplanted using bone marrow from ApoE<sup>-/-</sup>/RAG-2<sup>-/-</sup> or ApoE<sup>-/-</sup>/RAG-2<sup>+/+</sup> donor mice. Splenocytes were co-labeled with anti-TCRβ-PerCP/anti-CD19-PE-conjugated antibodies.

**Table 1.** Body Weight, Total Cholesterol, and Aortic Root Lesion Area in Placebo (PI)- or Estradiol-17 $\beta$  (E<sub>2</sub>)-Treated Ovariectomized ApoE<sup>-/-</sup>/RAG<sup>-/-</sup> Female Mice after Bone Marrow Transplantation from ApoE<sup>-/-</sup>/RAG<sup>-/-</sup> or ApoE<sup>-/-</sup>/RAG<sup>+/+</sup> Donors

Donor genotype	Treatment	Body weight (g)	Total cholesterol (g/L)	Lesion area ( $\mu\text{m}^2$ )
ApoE <sup>-/-</sup> /RAG <sup>+/+</sup>	PI	25.3 $\pm$ 0.7	5.9 $\pm$ 0.4	66662 $\pm$ 5838
	E <sub>2</sub>	23.5 $\pm$ 0.6	4.8 $\pm$ 0.4	34919 $\pm$ 6532*
ApoE <sup>-/-</sup> /RAG <sup>-/-</sup>	PI	26.8 $\pm$ 1.7	5.4 $\pm$ 0.4	33451 $\pm$ 5816†
	E <sub>2</sub>	24.3 $\pm$ 0.3	4.4 $\pm$ 0.7	41844 $\pm$ 5294

Results are means  $\pm$  SEM (n = 7).

\*P < 0.05 versus the corresponding PI-treated mice.

†P < 0.05 versus ApoE<sup>-/-</sup>/RAG<sup>+/+</sup>-transplanted PI-treated mice.

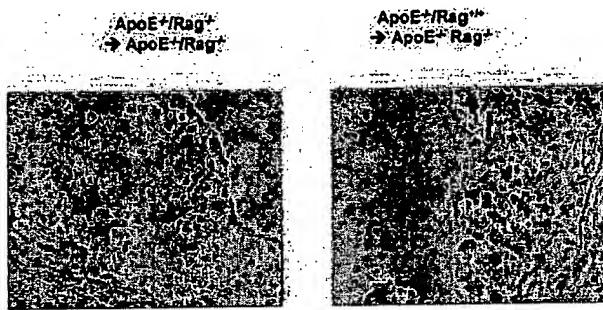


**Figure 3.** Immunohistochemical analysis of representative lesions from individual ApoE<sup>-/-</sup>/RAG<sup>-/-</sup> transplanted using bone marrow from ApoE<sup>-/-</sup>/RAG<sup>-/-</sup> or ApoE<sup>-/-</sup>/RAG<sup>+/+</sup> donor mice using anti-CD3 antibodies.

suspensions were prepared. The irradiated recipients received  $15 \times 10^6$  bone marrow cells in 0.2 ml of phosphate-buffered saline by tail vein injection. One week before and 4 weeks after the bone marrow transplantation, Bactrim (sulfamethoxazole 200 mg/ml, trimethoprim 48 mg/ml) was added to drinking water. After 5 additional weeks, all transplanted mice were implanted subcutaneously with placebo or E<sub>2</sub> pellets and LDLr<sup>-/-</sup>/RAG<sup>-/-</sup> mice were switched to the high-fat diet to induce atherosclerotic lesion formation. Mice were sacrificed 11 weeks later (at 22 weeks of age). Blood and tissues were collected as described above.

### Tissue Preparation and Lesion Analysis

The circulatory system was perfused with 0.9% NaCl by cardiac intraventricular canalization. The heart and ascending aorta were removed and kept frozen. Surface lesion area was measured by computer-assisted image quantification in the aortic root, by a trained observer blinded to the genotype and treatment of the mice, as previously described<sup>15</sup> but using a Leica image analyzer.

The rest of the entire aortic tree was removed and cleaned of adventitia, split longitudinally to the iliac bifurcation, and pinned flat on a dissection pan for analysis by *en face* preparation. Images were captured using a Sony-3CCD video camera and fraction covered by lesions evaluated as a percentage of the total aortic area.

### Immunohistochemistry

Cryostat sections from the proximal aorta were fixed in acetone, air-dried, and reacted with a primary rat monoclonal anti-mouse macrophage (clone MOMA-2 from Serotec, Oxford, UK) used at a 1:50 dilution or a primary goat polyclonal anti-CD3 (clone M-20 from Santa Cruz Biotechnology, Santa Cruz, CA) used at a 1:100 dilution. Then, sections were incubated with corresponding preadsorbed secondary biotinylated antibodies (Vector Laboratories, Burlingame, CA): binding of rat monoclonal anti-macrophage was revealed using biotinylated rabbit anti-rat IgG and binding of goat polyclonal anti-CD3 was revealed using biotinylated horse anti-goat IgG. The binding of the biotinylated antibodies was visualized with an avidin DH-biotinylated peroxidase complex (Vectastain ABC kit, Vector Laboratories) and AEC peroxidase substrate kit (Vector Laboratories). Counterstaining was performed using Mayer's hemalun. Macrophage and T-cell quantification was determined by scoring samples from at least four sections per animal. A minimum of three animals was analyzed per group. Two investigators who were blinded to the sample identity performed analysis.

### Analysis of Plasma Lipids and Lipoproteins

Serum cholesterol concentrations were determined by an enzymatic assay adapted to microtiter plates using com-

**Table 2.** Body Weight, Total Cholesterol, and Aortic Root Lesion Area in Placebo (PI)- or Estradiol-17 $\beta$  (E<sub>2</sub>)-Treated Ovariectomized LDLr<sup>-/-</sup>/RAG<sup>-/-</sup> Female Mice after Bone Marrow Transplantation from RAG<sup>-/-</sup> or C57BL/6 Mice

Donor genotype	Treatment	Body weight (g)	Total cholesterol (g/L)	Lesion area ( $\mu\text{m}^2$ /section)
C57BL/6	PI	28.1 $\pm$ 1.2	9.3 $\pm$ 0.8	84480 $\pm$ 9185
	E <sub>2</sub>	24.9 $\pm$ 0.7*	6.4 $\pm$ 0.7*	35333 $\pm$ 8317*
RAG <sup>-/-</sup>	PI	27.1 $\pm$ 0.6	11.1 $\pm$ 0.6	35900 $\pm$ 5600†
	E <sub>2</sub>	24.0 $\pm$ 0.5*	9.9 $\pm$ 0.5	42800 $\pm$ 6600

The animals had been on HFD for 12 weeks. Results are means  $\pm$  SEM (n  $\geq$  7).

\*P < 0.05 versus C57BL/6-transplanted PI-treated mice.

†P < 0.05 versus the corresponding PI-treated mice.

**Table 3.** Body Weight, Total Cholesterol, and Lesion Area of Ovariectomized Placebo (PI)- or Estradiol-17 $\beta$  (E<sub>2</sub>)-Treated Immunocompetent ApoE<sup>-/-</sup> Control and Immunodeficient ApoE<sup>-/-</sup>/TCR $\delta$ <sup>-/-</sup>, CD4<sup>-/-</sup>, CD8<sup>-/-</sup>, TCR $\delta$ <sup>-/-</sup> or B<sup>-/-</sup> Female Mice

Genotype	Body weight (g)			Total cholesterol (g/L)
	NC	PI	E2	NC
ApoE <sup>-/-</sup>	22.0 $\pm$ 0.5	28.7 $\pm$ 1.5	22.9 $\pm$ 0.5*	3.4 $\pm$ 0.1
ApoE <sup>-/-</sup> /TCR $\delta$ <sup>-/-</sup>	21.0 $\pm$ 0.5	20.9 $\pm$ 0.6†	21.5 $\pm$ 0.5	3.0 $\pm$ 0.2
ApoE <sup>-/-</sup> /CD4 <sup>-/-</sup>	19.5 $\pm$ 0.4	21.9 $\pm$ 1.2†	21.9 $\pm$ 0.6	3.0 $\pm$ 0.2
ApoE <sup>-/-</sup> /CD8 <sup>-/-</sup>	21.5 $\pm$ 0.5	23.5 $\pm$ 0.8†	22.9 $\pm$ 0.5	3.1 $\pm$ 0.2
ApoE <sup>-/-</sup> /TCR $\delta$ <sup>-/-</sup>	20.1 $\pm$ 0.4	27.6 $\pm$ 1.4	21.9 $\pm$ 0.1*	2.9 $\pm$ 0.1
ApoE <sup>-/-</sup> /B <sup>-/-</sup>	—	26.8 $\pm$ 0.9	24.3 $\pm$ 0.4*	—

Data of intact corresponding mice (NC) have been published previously<sup>12</sup> and are indicated in italics for comparison. Results are means  $\pm$  SEM ( $n \geq 8$ ).

\* $P < 0.05$  versus corresponding C (placebo-treated) mice.

† $P < 0.05$  versus corresponding immunocompetent mice.

(table continues)

mercially available reagents (Roche Molecular Biochemicals, Germany). Lipoprotein cholesterol profiles were obtained by Fast Protein liquid chromatography as previously described.<sup>19</sup>

### Statistical Analysis

The results are expressed as means  $\pm$  SEM. For each parameter (body weight, total cholesterol, lesion area), the effects of genotype were studied by comparing each immunodeficient group with its corresponding immunocompetent group of mice. The effect of E2 treatment was studied comparing placebo- and E2-treated mice in selective immunodeficient or in immunocompetent mice. A one-factor analysis of variance was used (Bonferroni/Dunn's test);  $P < 0.05$  was considered as significant. Statistical analyses were performed using the Statview statistical software (Abacus Concepts, Inc., Berkeley, CA). When appropriate, an unpaired t-test was also performed.

## Results

### Immunocompetent Bone Marrow Transplantation Restored Both the Level of Lesions and E2 Sensitivity in ApoE<sup>-/-</sup>/RAG-2<sup>-/-</sup> and LDLr<sup>-/-</sup>/RAG-2<sup>-/-</sup> Mice

To explore the role of lymphocytes in fatty streak constitution and E2 prevention, ApoE<sup>-/-</sup>/RAG-2<sup>-/-</sup> ovariectomized female mice received bone marrow transplantation from ApoE<sup>-/-</sup>/RAG-2<sup>-/-</sup> (ApoE<sup>-/-</sup>/RAG-2<sup>-/-</sup>  $\rightarrow$  ApoE<sup>-/-</sup>/RAG-2<sup>-/-</sup>) or from ApoE<sup>-/-</sup>/RAG-2<sup>+/+</sup> (ApoE<sup>-/-</sup>/RAG-2<sup>+/+</sup>  $\rightarrow$  ApoE<sup>-/-</sup>/RAG-2<sup>-/-</sup>) mice (Figure 2), and then were treated with placebo or E2 pellets. Sixteen weeks after bone marrow transplantation, ApoE<sup>-/-</sup>/RAG-2<sup>+/+</sup>  $\rightarrow$  ApoE<sup>-/-</sup>/RAG-2<sup>-/-</sup> placebo-treated mice presented a significantly higher level of fatty streaks when compared with ApoE<sup>-/-</sup>/RAG-2<sup>-/-</sup>  $\rightarrow$  ApoE<sup>-/-</sup>/RAG-2<sup>-/-</sup> placebo-treated mice (Table 1). Immunohistochemical analysis showed the presence of CD3-reactive cells in lesions obtained from ApoE<sup>-/-</sup>/RAG-2<sup>+/+</sup>  $\rightarrow$  ApoE<sup>-/-</sup>/RAG-2<sup>-/-</sup> mice but not in lesions obtained from ApoE<sup>-/-</sup>/RAG-2<sup>-/-</sup>  $\rightarrow$  ApoE<sup>-/-</sup>/

RAG-2<sup>-/-</sup> mice, irrespective of placebo or E2 treatment (Figure 3 and data not shown). Importantly, although E2 was still ineffective in ApoE<sup>-/-</sup>/RAG-2<sup>-/-</sup>  $\rightarrow$  ApoE<sup>-/-</sup>/RAG-2<sup>-/-</sup> mice, the protective effect of the hormone was restored in ApoE<sup>-/-</sup>/RAG-2<sup>+/+</sup>  $\rightarrow$  ApoE<sup>-/-</sup>/RAG-2<sup>-/-</sup> mice (Table 1).

Because ApoE-deficiency could be involved in these observations and because the RAG-2-deficient mice used were not fully backcrossed into the C57/BL6 background, similar experiments were performed in the LDLr-deficient mice. We first confirmed that E2 significantly decreased body weight (26.1  $\pm$  0.6 g versus 23.6  $\pm$  0.5 g,  $P < 0.05$ ), serum cholesterol (11.1  $\pm$  0.4 g/L versus 7.9  $\pm$  0.7 g/L,  $P < 0.01$ ), and fatty streak deposit (119,400  $\pm$  7400  $\mu$ m<sup>2</sup>/section versus 41,400  $\pm$  5400  $\mu$ m<sup>2</sup>/section for placebo- and E2-treated mice, respectively;  $n = 9$ ,  $P < 0.01$ ) in immunocompetent LDLr<sup>-/-</sup> mice on a 12-week high-fat diet in agreement with a previous report.<sup>20</sup> The effect on fatty streak was abolished in LDLr<sup>-/-</sup>/RAG-2<sup>-/-</sup> mice (42,000  $\pm$  13,100  $\mu$ m<sup>2</sup>/section versus 40,300  $\pm$  11,300  $\mu$ m<sup>2</sup>/section, respectively;  $n = 8$ ) whereas the effect on body weight (24.4  $\pm$  1.3 g/L versus 22.9  $\pm$  0.9 g/L,  $P < 0.05$ ) and serum cholesterol (9.9  $\pm$  0.4 g/L versus 7.4  $\pm$  0.7 g/L,  $P < 0.01$ ) persisted. Bone marrow graft experiments were also performed in this last model of ovariectomized female LDLr<sup>-/-</sup>/RAG-2<sup>-/-</sup> mice. As shown in Table 2, Placebo-treated LDLr<sup>-/-</sup>/RAG-2<sup>-/-</sup> mice that had received C57BL/6 bone marrow, presented a significantly higher level of fatty streaks when compared with those that had received RAG-2<sup>-/-</sup> bone marrow. Again, although E2 remained ineffective in RAG-2<sup>-/-</sup>  $\rightarrow$  LDLr<sup>-/-</sup>/RAG-2<sup>-/-</sup> mice, the protective effect of the hormone was restored in C57BL/6  $\rightarrow$  LDLr<sup>-/-</sup>/RAG-2<sup>-/-</sup> mice (Table 2).

### Effect of E2 Treatment on Body Weight and Serum Lipids in Immunocompetent and Selectively Immunodeficient ApoE<sup>-/-</sup> Mice

We then asked whether the protective effect of E2 could be mediated by a specific T-lymphocyte subset or B lymphocytes, considering the hormonal effect in selec-

Table 3. Continued

Total cholesterol (g/L)		Lesion area ( $\mu\text{m}^2/\text{section}$ )		
PI	E2	NC	PI	E2
5.6 $\pm$ 0.3	3.1 $\pm$ 0.2*	73,214 $\pm$ 2963	113,465 $\pm$ 5288	36,299 $\pm$ 1979*
4.4 $\pm$ 0.2†	3.1 $\pm$ 0.2*	37,048 $\pm$ 4749	65,053 $\pm$ 7753†	37,104 $\pm$ 4418*
5.8 $\pm$ 0.5	2.7 $\pm$ 0.2*	77,745 $\pm$ 12,629	114,835 $\pm$ 21,656	42,541 $\pm$ 5431*
5.6 $\pm$ 0.4	3.2 $\pm$ 0.1*	76,909 $\pm$ 4722	110,537 $\pm$ 16,142	47,782 $\pm$ 11,285*
5.6 $\pm$ 0.3	2.8 $\pm$ 0.2*	57,589 $\pm$ 3737	101,557 $\pm$ 8125	27,730 $\pm$ 3637*
4.6 $\pm$ 0.2†	2.6 $\pm$ 0.3*	—	93,432 $\pm$ 11,183	38,348 $\pm$ 5752*

tively immunodeficient ApoE<sup>-/-</sup> female mice. The statistical analysis presented in Table 3 refers to comparisons of each group of immunodeficient mice with its corresponding immunocompetent group. Data from a group of 10 ApoE<sup>-/-</sup> female mice are given for comparison (Table 3, line 1).

Uterine weight was <20 mg in ovariectomized mice and increased to 172  $\pm$  13 mg on average with E2 treatment, showing that the level of E2 stimulation was similar in all genotypes. Body weight decreased, reflecting mainly adipose tissue reduction, in immunocompetent ApoE<sup>-/-</sup> control and in immunodeficient ApoE<sup>-/-</sup>/TCR $\delta$ <sup>-/-</sup> and ApoE<sup>-/-</sup>/B<sup>-/-</sup> mice under E2 treatment. In the immunodeficient ApoE<sup>-/-</sup>/TCR $\beta$ <sup>-/-</sup>, ApoE<sup>-/-</sup>/CD4<sup>-/-</sup>, and ApoE<sup>-/-</sup>/CD8<sup>-/-</sup> mice, body weight was lower in placebo-treated mice when compared to their immunocompetent littermates and was not influenced by E2, suggesting a role for TCR $\alpha\beta$ <sup>+</sup> T lymphocytes in weight regulation. Total serum cholesterol was lower in ovariectomized ApoE<sup>-/-</sup>/TCR $\beta$ <sup>-/-</sup> and ApoE<sup>-/-</sup>/B<sup>-/-</sup> when compared with their respective immunocompetent littermates and decreased under E2 treatment in all strains. Fast performance liquid chromatography showed that the E2-induced decrease concerned the very low-density lipoprotein, intermediary/low-density lipoprotein, and high-density lipoprotein fractions (see Supplemental Figure A at <http://ajp.amjpathol.org>) in agreement with our previous report.<sup>15</sup>

#### Effect of E2 Treatment on Lesion Area in Immunocompetent and Selectively Immunodeficient ApoE<sup>-/-</sup> Mice

At the level of the aortic root, the lesion area of ovariectomized immunodeficient mice given placebo did not differ significantly from the corresponding immunocompetent mice except for the ApoE<sup>-/-</sup>/TCR $\beta$ <sup>-/-</sup> mice, which presented a decreased level of lesions (Table 3). E2 treatment induced a significant decrease of fatty streak development in all groups of mice, including the ApoE<sup>-/-</sup>/TCR $\beta$ <sup>-/-</sup> strain. To further analyze the influence of serum cholesterol on the lesion formation, we sought to analyze subgroups of mice with comparable serum cholesterol levels. Such subgroups could be selected among

the whole series of immunocompetent mice that serve as control for the immunodeficient groups (ie, a total of 50 PI-treated and 50 E2-treated mice) with cholesterolemia arbitrarily encompassed between 4 and 6 g/L. In these subgroups of ovariectomized placebo ( $n = 19$ )- and E2 ( $n = 12$ )-treated mice, with similar serum cholesterol (5.0  $\pm$  0.1 g/L and 4.9  $\pm$  0.1 g/L, respectively;  $P = 0.67$ ), lesion area still dramatically differed (109,824  $\pm$  4304  $\mu\text{m}^2/\text{section}$  and 35,722  $\pm$  4206  $\mu\text{m}^2/\text{section}$ ,  $P < 0.001$ ), strongly suggesting that the E2-induced decrease of serum cholesterol is not the main factor preventing fatty streak formation.

Histo- as well as immunohistochemical analysis showed that, under E2 treatment, residual lesions were essentially fatty streaks containing lipid-laden macrophages, with few characteristics of advanced lesions such as fibrous caps and were substantially less complex than lesions in ovariectomized ApoE<sup>-/-</sup> control mice (not shown). Remarkably, T lymphocytes were still detectable at a comparable density (2  $\pm$  1%) in these residual lesions (Figure 4). Similar observations were made in all of the series of specifically immunodeficient mice including the ApoE<sup>-/-</sup>/TCR $\beta$ <sup>-/-</sup> (Figure 4).

In the rest of the aorta, lesions were identifiable by *en face* analysis at predilection sites including the aortic arch and the orifices of the brachiocephalic, left subclavian, common carotid, and intercostal arteries. However, the level was low (<3.0% of the total aortic area) except in the ApoE<sup>-/-</sup>/CD4<sup>-/-</sup> group of mice (13.5  $\pm$  3.0%,  $n = 3$ ). In this last group, lesions were observed at the predilection sites and also at the orifice of the large abdominal arteries, in particular the celiac trunk and renal arteries. E2 induced a spectacular (more than fivefold)



Figure 4. Anti-CD3 immunolabeling of representative lesions from ovariectomized ApoE<sup>-/-</sup>, ApoE<sup>-/-</sup>/TCR $\beta$ <sup>-/-</sup>, and ApoE<sup>-/-</sup>/TCR $\delta$ <sup>-/-</sup> mice after 3 months of treatment with E2 pellets.



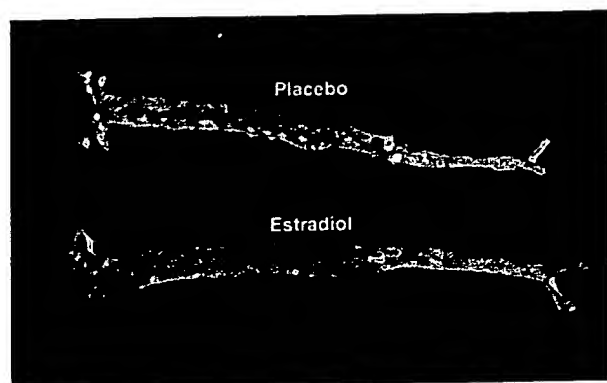


**Figure 5.** Representative *en face* aorta preparations from placebo- and E2-treated ovariectomized ApoE<sup>-/-</sup>/CD4<sup>-/-</sup> mice.

protective effect at these different sites, especially in the ApoE<sup>-/-</sup>/CD4<sup>-/-</sup> group (<3.0%, *n* = 3; Figure 5).

## Discussion

The present results definitely demonstrate that, in the C57BL/6 mouse strain, mature lymphocytes are required for the preventive effect of E2 on the atheromatous process irrespective of the model of genetically-induced hypercholesterolemia, namely ApoE<sup>-/-</sup> and LDLr<sup>-/-</sup> mice. Indeed, after bone marrow transplantation from immunocompetent donors into immunodeficient mice, lymphocytes were recovered in the lesions and a significant increase in the level of these lesions could be demonstrated. Most importantly, E2 activity was restored after bone marrow transplantation from immunocompetent donors, while E2 was still inactive after bone marrow transplantation from immunodeficient donors to the immunodeficient recipients.

Like our data obtained in intact nonovariectomized mice,<sup>12</sup> the measurement of lesion area in placebo-treated ovariectomized mice show a similar level of lesions in immunocompetent and immunodeficient mice, except in the ApoE<sup>-/-</sup>/TCRβ<sup>-/-</sup> mice, supporting the deleterious role of αβ T lymphocytes in the atheromatous process. Noteworthy, considering our previous<sup>12</sup> and present data, a protective effect of endogenous ovarian estrogens could be demonstrated in all strains because ovariectomized mice developed a higher level of lesions than intact mice. This observation is in accordance with a previous report.<sup>21</sup> Moreover, E2 treatment, administered at a dose previously defined as adequate for a maximal effect,<sup>15</sup> induced a significant decrease in lesion size in all groups of mice (Table 3). Except in ApoE<sup>-/-</sup>/TCRβ<sup>-/-</sup> mice, the residual lesion level was lower than that measured in intact female mice.<sup>12</sup> In addition, *en face* analysis showed that the effect of E2 was not restricted to the aortic sinus. Interestingly, E2 exerted a stronger preventive effect of lesion development in the thoracic and abdominal sites than at the level of the aortic sinus, particularly in ApoE<sup>-/-</sup>/CD4<sup>-/-</sup> mice (Figure 5). Although the selective immune deficiency may generate compensatory expansion of other lymphocyte subsets, such as ApoE<sup>-/-</sup>/CD4<sup>-/-</sup> mice presenting with a greater number

of CD8<sup>+</sup> and double-negative CD4-CD8 cells than ApoE<sup>-/-</sup> mice,<sup>12,22</sup> we demonstrate here that E2 was active in all strains, suggesting that no single T-lymphocyte subpopulation directly mediated the protective effect. This included the populations of regulatory T cells able to control the expansion and differentiation of activated T cells<sup>23,24</sup> and the TCRγδ<sup>+</sup> T cells. E2 has been recently claimed to induce one of these regulatory T-lymphocyte subpopulations<sup>25,26</sup> suggesting that it could play a key role in the suppression of harmful immune responses. Our data do not support such a hypothesis in the atherosclerotic process. Finally, the protective effect was also maintained in B-lymphocyte-deficient mice. This excluded a protective role mediated by immunoglobulins that are known to increase under E2 stimulation<sup>27</sup> and have been suggested to prevent atherosclerosis.<sup>27-30</sup>

Interestingly, E2 administration significantly decreased serum cholesterol levels in nearly all conditions analyzed in the present work. However, although serum cholesterol level remains a key determinant of atherosclerosis, several lines of evidence support the fact that the protective effect of E2 occurs mainly at the level of the arterial wall. First, although E2 decreased serum cholesterol levels in immunodeficient LDLr<sup>-/-</sup>/RAG-2<sup>-/-</sup> mice (the present work) as well as ApoE<sup>-/-</sup>/RAG-2<sup>-/-</sup> mice<sup>14</sup> to a similar extent than in immunocompetent mice, it was completely inactive on lesion area. Second, although the maximal decrease of serum cholesterol was obtained with endogenous E2 (Table 3), the maximal decrease in lesion area required higher E2 doses, in line with previous reports.<sup>15,21</sup> Third, in subgroups of ovariectomized placebo- or E2-treated ApoE<sup>-/-</sup> mice arbitrarily selected for similar serum cholesterol levels, fatty streak area was threefold lower in the latter group. Indeed, using cholesterol-clamped rabbits, Holm and colleagues<sup>31</sup> had previously demonstrated a plasma lipid-independent anti-atherogenic effect of estrogen, in line with Adams and co-workers,<sup>32</sup> who suggested, as early as 1990, a similar conclusion in surgically postmenopausal monkeys.

Altogether, these series of observation points to one (or more) additional lymphocyte-dependent mechanism(s) involved in the protective effect of E2. E2 is a negative regulator of lymphopoiesis, that selectively depletes functional precursors of B and T cells.<sup>33</sup> It also inactivates the intrathymic T-cell differentiation pathway and induces thymocyte apoptosis.<sup>34</sup> Indeed, we observed a remarkable 80% thymic atrophy (85.2 ± 7.5 mg versus 14.1 ± 1.8 mg) and 50% decrease of circulating lymphocytes in our E2-treated ApoE<sup>-/-</sup> mice (6804 ± 568 per μl versus 3520 ± 215 per μl; *P* < 0.001). However, in agreement with Hodgkin and colleagues,<sup>35</sup> T lymphocytes were still detectable in the residual lesions (Figure 3), showing that, despite their decrease in blood, lymphocytes could still reach and infiltrate the remaining lesions.

The protective effect could also be mediated through the modulation of the interactions between lymphocytes and other cell populations, such as endothelial and/or antigen-presenting cells, leading to a local control of the intimal immune process. First, Shi and colleagues<sup>36,37</sup> recently provided strong evidence for the crucial role of

endothelial cells rather than hematopoietic cells as determinants of atherosclerosis susceptibility in C57BL/6 mice. Second, decreased proinflammatory<sup>38–40</sup> or increased anti-inflammatory cytokine<sup>41,42</sup> production resulting from the local interaction between lymphocytes and antigen-presenting cells could explain the protective effect of E2. Indeed, it has recently been reported that estrogens repress Th1 activity and T-cell production of the key inflammatory cytokine tumor necrosis factor- $\alpha$  in bone<sup>43</sup> but we reported the opposite effect in antigen-specific CD4<sup>+</sup> or NKT cell response.<sup>44,45</sup> Further work will be necessary to precisely define the mechanisms of these interactions.

In conclusion, we have demonstrated that lymphocytes are instrumental in the protective effect of E2 but that no single lymphocyte subpopulation is specifically required for this effect. These data point to additional lymphocyte-dependent mechanisms such as modulating the interactions among lymphocytes and between lymphocytes and endothelial and/or antigen-presenting cells.

## Acknowledgments

We thank Mrs. M.J. Fouque, P. Guillou, and M. Larribe for technical and secretarial assistance.

## References

- Waters DD, Gordon D, Rossouw JE, Cannon III RO, Collins P, Herrington DM, Hsia J, Langer R, Mosca L, Ouyang P, Sopko G, Stefanick ML: Women's ischemic syndrome evaluation: current status and future research directions: report of the National Heart, Lung and Blood Institute Workshop: October 2–4, 2002: section 4: lessons from hormone replacement trials. *Circulation* 2004, 109:e53–e55
- Hulley S, Grady D, Bush T, Furberg C, Herrington D, Riggs B, Vittinghoff E: Randomized trial of estrogen plus progestin for secondary prevention of coronary heart disease in postmenopausal women. Heart and Estrogen/Progestin Replacement Study (HERS) Research Group. *JAMA* 1998, 280:605–613
- Rossouw JE, Anderson GL, Prentice RL, LaCroix AZ, Kooperberg C, Stefanick ML, Jackson RD, Beresford SA, Howard BV, Johnson KC, Kotchen JM, Ockene J: Risks and benefits of estrogen plus progestin in healthy postmenopausal women: principal results from the Women's Health Initiative randomized controlled trial. *JAMA* 2002, 288:321–333
- Arnal JF, Gourdy P, Elhage R, Garmy-Susini B, Delmas E, Bouchet L, Castano C, Barreira Y, Couloumiers JC, Prats H, Prats AC, Bayard F: Estrogens and atherosclerosis. *Eur J Endocrinol* 2004, 150:113–117
- Hodgin JB, Maeda N: Minireview: estrogen and mouse models of atherosclerosis. *Endocrinology* 2002, 143:4495–4501
- Ross R: Atherosclerosis—an inflammatory disease. *N Engl J Med* 1999, 340:115–125
- Hansson GK, Libby P, Schonbeck U, Yan ZQ: Innate and adaptive immunity in the pathogenesis of atherosclerosis. *Circ Res* 2002, 91:281–291
- Binder CJ, Chang MK, Shaw PX, Miller YI, Hartvigsen K, Dewan A, Witztum JL: Innate and acquired immunity in atherogenesis. *Nat Med* 2002, 8:1218–1226
- Roselaar SE, Kakkanathu PX, Daugherty A: Lymphocyte populations in atherosclerotic lesions of apoE<sup>−/−</sup> and LDL receptor<sup>−/−</sup> mice. Decreasing density with disease progression. *Arterioscler Thromb Vasc Biol* 1996, 16:1013–1018
- Song L, Leung C, Schindler C: Lymphocytes are important in early atherosclerosis. *J Clin Invest* 2001, 108:251–259
- Reardon CA, Blachowicz L, White T, Cabana V, Wang Y, Lukens J, Bluestone J, Getz GS: Effect of immune deficiency on lipoproteins and atherosclerosis in male apolipoprotein E-deficient mice. *Arterioscler Thromb Vasc Biol* 2001, 21:1011–1016
- Elhage R, Gourdy P, Bouchet L, Jawien J, Fouque M-J, Fiévet C, Huc X, Barreira Y, Couloumiers J-C, Arnal J-F, Bayard F: Deleting TCR $\alpha$  or CD4+ T lymphocytes leads to opposite effects on site-specific atherosclerosis in female apolipoprotein E-deficient mice. *Am J Pathol* 2004, 165:2013–2019
- Zhou X, Nicoletti A, Elhage R, Hansson GK: Transfer of CD4(+) T cells aggravates atherosclerosis in immunodeficient apolipoprotein E knockout mice. *Circulation* 2000, 102:2919–2922
- Elhage R, Clamens S, Reardon-Alulius C, Getz GS, Fievet C, Maret A, Arnal JF, Bayard F: Loss of atheroprotective effect of estradiol in immunodeficient mice. *Endocrinology* 2000, 141:462–465
- Elhage R, Arnal JF, Pierragi M-T, Duverger N, Fiévet C, Faye JC, Bayard F: Estradiol-17 $\beta$  prevents fatty streak formation in apolipoprotein E-deficient mice. *Arterioscl Thromb Vasc Biol* 1997, 17:2679–2684
- Ishibashi S, Goldstein JL, Brown MS, Herz J, Burns DK: Massive xanthomatosis and atherosclerosis in cholesterol-fed low density lipoprotein receptor-negative mice. *J Clin Invest* 1994, 93:1885–1893
- Shinkai Y, Rathbun G, Lam KP, Oltz EM, Stewart V, Mendelsohn M, Charron J, Datta M, Young F, Stall AM, Alt FW: RAG-2-deficient mice lack mature lymphocytes owing to inability to initiate V(D)J rearrangement. *Cell* 1992, 68:855–867
- Kitamura D, Roes J, Kuhn R, Rajewsky K: A B cell-deficient mouse by targeted disruption of the membrane exon of the immunoglobulin mu chain gene. *Nature* 1991, 350:423–426
- Duez H, Chao YS, Hernandez M, Torpier G, Poulain P, Mundt S, Mallat Z, Teissier E, Burton CA, Tedgui A, Fruchart JC, Fievet C, Wright SD, Staels B: Reduction of atherosclerosis by the peroxisome proliferator-activated receptor alpha agonist fenofibrate in mice. *J Biol Chem* 2002, 277:48051–48057
- Marsh MM, Walker VR, Curtiss LK, Banka CL: Protection against atherosclerosis by estrogen is independent of plasma cholesterol levels in LDL receptor-deficient mice. *J Lipid Res* 1999, 40:893–900
- Bourassa P-A, Milos PM, Gaynor BJ, Breslow JL, Aiello RJ: Estrogen reduces atherosclerotic lesion development in apolipoprotein E-deficient mice. *Proc Natl Acad Sci USA* 1996, 93:10022–10027
- Shedlock DJ, Whitmire JK, Tan J, MacDonald AS, Ahmed R, Shen H: Role of CD4 T cell help and costimulation in CD8 T cell responses during *Listeria monocytogenes* infection. *J Immunol* 2003, 170:2053–2063
- Shevach EM, McHugh RS, Piccirillo CA, Thornton AM: Control of T-cell activation by CD4+ CD25+ suppressor T cells. *Immunol Rev* 2001, 182:58–67
- Roncarolo MG, Bacchetta R, Bordignon C, Narula S, Levings MK: Type 1 T regulatory cells. *Immunol Rev* 2001, 182:68–79
- Matejuk A, Bakke AC, Hopke C, Dwyer J, Vandenbark AA, Offner H: Estrogen treatment induces a novel population of regulatory cells, which suppresses experimental autoimmune encephalomyelitis. *J Neurosci Res* 2004, 77:119–126
- Polanczyk MJ, Carson BD, Subramanian S, Afentoulis M, Vandenbark AA, Ziegler SF, Offner H: Cutting edge: estrogen drives expansion of the CD4+CD25+ regulatory T cell compartment. *J Immunol* 2004, 173:2227–2230
- Caligiuri G, Nicoletti A, Poirier B, Hansson GK: Protective immunity against atherosclerosis carried by B cells of hypercholesterolemic mice. *J Clin Invest* 2002, 109:745–753
- Verthelyi DI, Ahmed SA: Estrogen increases the number of plasma cells and enhances their autoantibody production in nonautoimmune C57BL/6 mice. *Cell Immunol* 1998, 189:125–134
- Horkko S, Bird DA, Miller E, Itabe H, Leitinger N, Subbanagounder G, Berliner JA, Friedman P, Dennis EA, Curtiss LK, Palinski W, Witztum JL: Monoclonal autoantibodies specific for oxidized phospholipids or oxidized phospholipid-protein adducts inhibit macrophage uptake of oxidized low-density lipoproteins. *J Clin Invest* 1999, 103:117–128
- Major AS, Fazio S, Linton MF: B-lymphocyte deficiency increases atherosclerosis in LDL receptor-null mice. *Arterioscler Thromb Vasc Biol* 2002, 22:1892–1898
- Holm P, Korsgaard N, Shalmi M, Andersen HL, Hougaard P, Skouby SO, Stender S: Significant reduction of the antiatherogenic effect of estrogen by long-term inhibition of nitric oxide synthesis in cholesterol-clamped rabbits. *J Clin Invest* 1997, 100:821–828

32. Adams MR, Kaplan JR, Manuck SB, Koritnik DR, Parks JS, Wolfe MS, Clarkson TB: Inhibition of coronary artery atherosclerosis by 17-beta estradiol in ovariectomized monkeys. Lack of an effect of added progesterone. *Arteriosclerosis* 1990, 10:1051-1057
33. Medina KL, Garrett KP, Thompson LF, Rossi MI, Payne KJ, Kincade PW: Identification of very early lymphoid precursors in bone marrow and their regulation by estrogen. *Nat Immunol* 2001, 2:718-724
34. Okasha SA, Ryu S, Do Y, McKallip RJ, Nagarkatti M, Nagarkatti PS: Evidence for estradiol-induced apoptosis and dysregulated T cell maturation in the thymus. *Toxicology* 2001, 163:49-62
35. Hodgins JB, Kregel JH, Reddick RL, Korach KS, Smithies O, Maeda N: Estrogen receptor alpha is a major mediator of 17beta-estradiol's atheroprotective effects on lesion size in ApoE<sup>-/-</sup> mice. *J Clin Invest* 2001, 107:333-340
36. Shi W, Haberland ME, Jien ML, Shih DM, Lusis AJ: Endothelial responses to oxidized lipoproteins determine genetic susceptibility to atherosclerosis in mice. *Circulation* 2000, 102:75-81
37. Shi W, Wang NJ, Shih DM, Sun VZ, Wang X, Lusis AJ: Determinants of atherosclerosis susceptibility in the C3H and C57BL/6 mouse model: evidence for involvement of endothelial cells but not blood cells or cholesterol metabolism. *Circ Res* 2000, 86:1078-1084
38. Gupta S, Pablo AM, Jiang X, Wang N, Tall AR, Schindler C: IFN-gamma potentiates atherosclerosis in ApoE knock-out mice. *J Clin Invest* 1997, 99:2752-2761
39. Lee TS, Yen HC, Pan CC, Chau LY: The role of interleukin 12 in the development of atherosclerosis in ApoE-deficient mice. *Arterioscler Thromb Vasc Biol* 1999, 19:734-742
40. Elhage R, Jawien J, Rudling M, Ljunggren HG, Takeda K, Akira S, Bayard F, Hansson GK: Reduced atherosclerosis in interleukin-18 deficient apolipoprotein E-knockout mice. *Cardiovasc Res* 2003, 59:234-240
41. Mallat Z, Besnard S, Duriez M, Deleuze V, Emmanuel F, Bureau MF, Soubrier F, Esposito B, Duez H, Fievet C, Staels B, Duverger N, Scherman D, Tedgui A: Protective role of interleukin-10 in atherosclerosis. *Circ Res* 1999, 85:e17-e24
42. Robertson AKL, Rudling M, Zhou X, Gorelik L, Flavell RA, Hansson GK: Disruption of TGF-(beta) signaling in T cells accelerates atherosclerosis. *J Clin Invest* 2003, 112:1342-1350
43. Cenci S, Toraldo G, Weitzmann MN, Roggia C, Gao Y, Qian WP, Sierra O, Pacifici R: Estrogen deficiency induces bone loss by increasing T cell proliferation and lifespan through IFN-gamma-induced class II transactivator. *Proc Natl Acad Sci USA* 2003, 100:10405-10410
44. Maret A, Coudert JD, Garidou L, Foucras G, Gourdy P, Krust A, Dupont S, Chambon P, Druet P, Bayard F, Guery JC: Estradiol enhances primary antigen-specific CD4 T cell responses and Th1 development in vivo. Essential role of estrogen receptor alpha expression in hematopoietic cells. *Eur J Immunol* 2003, 33:512-521
45. Gourdy P, Araujo LM, Zhu R, Garmy-Susini B, Diem S, Laurell H, Leite-De-Moraes M, Dy M, Arnal JF, Bayard F, Herbelin A: Relevance of sexual dimorphism to regulatory T cells: estradiol promotes IFN-gamma production by invariant natural killer T cells. *Blood* 2005, 105:2415-2420

## Hypercholesterolemia in Low Density Lipoprotein Receptor Knockout Mice and its Reversal by Adenovirus-mediated Gene Delivery

Shun Ishibashi,\* Michael S. Brown,\* Joseph L. Goldstein,\* Robert D. Gerard,† Robert E. Hammer,\*\* and Joachim Herz\*  
Departments of \*Molecular Genetics and ‡Biochemistry and †Howard Hughes Medical Institute, University of Texas Southwestern Medical Center at Dallas, Dallas, Texas 75235

### Abstract

We employed homologous recombination in embryonic stem cells to produce mice lacking functional LDL receptor genes. Homozygous male and female mice lacking LDL receptors (*LDLR*<sup>-/-</sup> mice) were viable and fertile. Total plasma cholesterol levels were twofold higher than those of wild-type littermates, owing to a seven- to ninefold increase in intermediate density lipoproteins (IDL) and LDL without a significant change in HDL. Plasma triglyceride levels were normal. The half-lives for intravenously administered <sup>125</sup>I-VLDL and <sup>125</sup>I-LDL were prolonged by 30-fold and 2.5-fold, respectively, but the clearance of <sup>125</sup>I-HDL was normal in the *LDLR*<sup>-/-</sup> mice. Unlike wild-type mice, *LDLR*<sup>-/-</sup> mice responded to moderate amounts of dietary cholesterol (0.2% cholesterol/10% coconut oil) with a major increase in the cholesterol content of IDL and LDL particles. The elevated IDL/LDL level of *LDLR*<sup>-/-</sup> mice was reduced to normal 4 d after the intravenous injection of a recombinant replication-defective adenovirus encoding the human LDL receptor driven by the cytomegalovirus promoter. The virus restored expression of LDL receptor protein in the liver and increased the clearance of <sup>125</sup>I-VLDL. We conclude that the LDL receptor is responsible in part for the low levels of VLDL, IDL, and LDL in wild-type mice and that adenovirus-encoded LDL receptors can acutely reverse the hypercholesterolemic effects of LDL receptor deficiency. (*J. Clin. Invest.* 1993. 92:883-893.) Key words: homologous recombination • lipoprotein metabolism • very low density lipoprotein • gene therapy • liver receptors

### Introduction

The LDL receptor removes cholesterol-rich intermediate density lipoproteins (IDL)<sup>1</sup> and LDL from plasma and thereby regulates the plasma cholesterol level (1). The lipoproteins that

bind to the LDL receptor are derived from triglyceride-rich VLDL, which are secreted by the liver. In the circulation some of the triglycerides of VLDL are removed by lipoprotein lipase, and the resultant IDL particle is cleared rapidly into the liver, owing to its content of apolipoprotein E (apo E), a high affinity ligand for the LDL receptor. Some IDL particles escape hepatic uptake and are converted to LDL in a reaction that leads to the loss of apo E. The sole remaining protein, apo B-100, binds to LDL receptors with relatively low affinity, thus causing LDL particles to circulate for relatively prolonged periods (2).

Triglyceride-depleted, cholesterol-rich remnants of intestinal chylomicrons are taken into the liver by the LDL receptor and by a genetically distinct molecule designated the chylomicron remnant receptor (3, 4). The latter receptor recognizes apo E when it is present on chylomicron remnant particles together with apo B-48, a truncated version of apo B-100 that is produced in the intestine (3). Circumstantial evidence suggests that the chylomicron remnant receptor is the same as the LDL receptor-related protein/ $\alpha_2$ -macroglobulin receptor (LRP) (4). The action of this receptor may be facilitated by the preliminary binding of the chylomicron remnants to cell-associated glycosaminoglycans in hepatic sinusoids (5).

Genetic defects in the LDL receptor produce hypercholesterolemia in humans with familial hypercholesterolemia (FH) (6), Watanabe-heritable hyperlipidemic (WHHL) rabbits (7), and rhesus monkeys (8). Humans and rabbits with two defective LDL receptor genes (FH and WHHL homozygotes) have massively elevated levels of IDL and LDL, and they develop fulminant atherosclerosis at an early age. Tracer studies with <sup>125</sup>I-labeled lipoproteins revealed a retarded clearance of IDL and LDL, and an increased conversion of IDL to LDL in humans (9) and rabbits (10) with LDL receptor deficiency.

Evidence from one human pedigree (11) and from monozygotic/dizygotic twin pair correlations (12) indicates that other genes can influence the degree of hypercholesterolemia in subjects with LDL receptor deficiency. These genes are likely to influence cholesterol levels even in people with normal LDL receptors. Identification of these genes has not been possible in human linkage studies, nor in breeding experiments with WHHL rabbits. Linkage studies would be facilitated by the availability of an inbred mouse strain with LDL receptor deficiency. The consequences of LDL receptor deficiency in mice are difficult to predict because mice, like rats, have a fundamental difference in LDL metabolism when compared with other species that have been studied (13). In mice and rats a substantial fraction of the VLDL secreted from liver contains apo B-48 instead of apo B-100 (14-16). Remnants derived from the apo B-48 containing particles are cleared into the liver and are not converted to LDL (17). Some of this clearance may be mediated by the chylomicron remnant receptor. For this reason, LDL receptor deficiency in mice would not be predicted to raise the plasma LDL level as profoundly as it does in WHHL rabbits.

Received for publication 1 April 1993.

1. Abbreviations used in this paper: AdCMV-Luc, recombinant adenovirus containing luciferase cDNA; AdCMV-LDLR, recombinant adenovirus containing human LDL receptor cDNA; CMV, cytomegalovirus; ES, embryonic stem cells; FH, familial hypercholesterolemia; FPLC, fast performance liquid chromatography; IDL, intermediate density lipoproteins; LRP, LDL receptor-related protein/ $\alpha_2$ -macroglobulin receptor; *LDLR*<sup>-/-</sup> and *LDLR*<sup>+/-</sup>, mice homozygous and heterozygous, respectively, for LDL receptor gene disruption; pfu, plaque-forming units; WHHL, Watanabe-heritable hyperlipidemic rabbits.

*J. Clin. Invest.*

© The American Society for Clinical Investigation, Inc.

0021-9738/93/08/0883/11 \$2.00

Volume 92, August 1993, 883-893

Mice deficient in LDL receptors might also aid in the development of gene therapy techniques designed to enhance the expression of hepatic LDL receptors. Using homozygous WHHL rabbits as a model, Chowdhury et al. (18) infected autologous hepatocytes *ex vivo* with a recombinant retrovirus carrying an expressible cDNA copy of the rabbit LDL receptor under control of the chicken  $\beta$ -actin promoter. After infusion of these transduced hepatocytes into the spleen, LDL receptor expression was visualized in 2–4% of liver cells. Although functional studies of  $^{125}\text{I}$ -LDL turnover were not performed, these workers observed a fall of  $\sim 30\%$  in the level of total plasma cholesterol, which did not occur in animals injected with hepatocytes transduced with a control retrovirus encoding an irrelevant protein. With this technique the expression of LDL receptors persisted for 2–4 mo. Although the 30% reduction in plasma cholesterol was statistically significant, the level remained quite elevated (above 500 mg/dl) when compared with normal rabbits, ( $< 100$  mg/dl), presumably owing to the expression of LDL receptors in only a small percentage of hepatocytes. Similar results were obtained in transient experiments following the intravenous injection of a plasmid containing the LDL receptor cDNA complexed to an asialo-orosomucoid/poly-L-lysine conjugate (19).

In mice, gene manipulation has produced significant effects on LDL receptor expression. Several years ago Hofmann et al. (20) and Yokode et al. (21) produced transgenic mice that overexpressed hepatic LDL receptors encoded by the human LDL receptor gene driven by the metallothionein or transferrin promoter. They showed that these receptors enhanced the clearance of radiolabeled LDL from plasma of normal mice. Yokode et al. (22) then demonstrated that these mice were resistant to the cholesterol-elevating effects of a high cholesterol diet.

Recently, Herz and Gerard (23) developed a recombinant replication-defective adenovirus vector containing an expressible cDNA copy of the human LDL receptor driven by the cytomegalovirus (CMV) promoter. 4 d after its intravenous injection, this virus elicited the expression of high levels of human LDL receptors in more than 90% of mouse hepatocytes, and this enhanced markedly the uptake of  $^{125}\text{I}$ -LDL by the liver. The use of adenovirus vectors was based on the observations of Stratford-Perricaudet et al. (24), who injected recombinant adenoviruses encoding ornithine transcarbamylase into neonatal mice homozygous for a defect in this gene. The recombinant adenovirus produced a level of enzyme activity in liver sufficient to eliminate the pathologic manifestations of the disease, and expression apparently persisted for 1 yr.

The current studies were conducted in order to learn the consequences of LDL receptor deficiency in mice and to learn whether adenovirus vectors will acutely reverse these consequences. For these purposes, we have used the techniques of homologous recombination in cultured embryonic stem (ES) cells (25–27) to produce mice that lack functional LDL receptors. We show that these mice develop a marked elevation in plasma IDL and LDL levels when compared with control mice and that this elevation can be eliminated acutely by the intravenous administration of a recombinant adenovirus encoding the human LDL receptor.

## Methods

**General methods.** Unless otherwise indicated, DNA manipulations were performed by standard techniques (28). Immunoblot (29) and

ligand blot analyses (30) were performed as described in the indicated references. Cholesterol and triglycerides were determined enzymatically with assay kits obtained from Boehringer Mannheim (Biochemicals, Indianapolis, IN) and Sigma Chemical Co. (St. Louis, MO), respectively. The normal mouse diet (Teklad 4% Mouse/Rat Diet 7001 from Harlan Teklad Premier Laboratory Diets, Madison, WI) contained 4% (wt/wt) animal fat with  $< 0.04\%$  (wt/wt) cholesterol. Mouse VLDL ( $d < 1.006$  g/ml), LDL ( $d 1.025$ – $1.50$  g/ml), and HDL ( $d 1.063$ – $1.215$  g/ml) were isolated by sequential ultracentrifugation (31) from pooled plasma obtained from *LDLR*<sup>-/-</sup> mice that had been fasted overnight. Rabbit VLDL ( $d < 1.006$  g/ml) was isolated by the same procedure from plasma obtained from fasted WHHL rabbits. Lipoproteins were radiolabeled with  $^{125}\text{I}$  by the iodine monochloride method (31). A 0.2% cholesterol/10% coconut oil diet was prepared by supplementing the normal mouse diet with 0.2% (wt/wt) cholesterol dissolved in a final concentration of 10% (vol/vol) coconut oil.

**Cloning of mouse LDL receptor cDNA.** Mouse LDL receptor cDNA was amplified by PCR from mouse liver first strand cDNA using poly(A)<sup>+</sup> RNA and the following primers:

Primer A, 5'-ATTCTAGAGGGTGAAGTGGTGTGAG-3' (exon 14);  
Primer B, 5'-ATAATTCACCTGACCATCTGTCTCGAGGGGTAG-3' (exon 18);  
Primer C, 5'-AAATG(T/C)ATC(T/G)(T/C)C(T/A)GCAAG-TGGGTCTG(C/T)GA(T/C)GGCAG-3' (exon 2);  
Primer D 5'-CTGCTCCTCATTCCTCTGCCAGCCA-3' (exon 16).

Amplification with primers A and B yielded a cDNA fragment corresponding to exons 14–18. cDNA spanning exons 2–16 was amplified with primers C and D. Primers A, B, and C were designed and based on the conservation of the LDL receptor coding sequence between human, rabbit, hamster, rat, and cow (32, 33). Primer D was designed and based on the mouse exon 16 cDNA sequence contained in the amplification product obtained with primers A and B. Amplification products were blunt-end cloned into pGEM3Zf(+) (Promega Corp., Madison, WI) and sequenced.

**Construction of gene replacement vector.** Southern blot analysis of mouse C57B1/6 genomic DNA with an exon 2–16 cDNA probe revealed a 16-kb BamHI fragment. This fragment was enriched by sucrose density ultracentrifugation and cloned into the  $\lambda$ Dash II vector (Stratagene Corp., La Jolla, CA), and recombinant phages containing the fragment were isolated by plaque screening. After subcloning into pGEM3Zf(+), the *Pol2sneobpA* expression cassette (34) was inserted into a unique *Sal*I site in exon 4 (Fig. 1). This *neo* expression cassette was flanked by 12 kb of LDL receptor genomic sequences including exons 1 to 4. The short arm of the targeting vector contained a 1.2-kb *Sal*I-*Sac*I fragment with sequences of exon 4 and intron 4. The *Sal*I sites were destroyed during the cloning. Two copies of the herpes simplex thymidine kinase gene (35) were inserted in tandem at the 3' end of the short arm of the targeting vector (Fig. 1).

**ES cell culture.** Mouse ES cells (AB-1, kindly provided by A. Bradley, Baylor College of Medicine, Houston) were cultured on leukemia inhibitory factor-producing STO feeder cells as described (36). Approximately  $2 \times 10^7$  cells were electroporated with linearized targeting vector (25  $\mu\text{g}/\text{ml}$ , 275 V, 330  $\mu\text{F}$ ) in an electroporator (GIBCO Bethesda Research Laboratories) and seeded onto irradiated feeder layers (10,000 rad). After selection with 190  $\mu\text{g}/\text{ml}$  G418 and 0.25  $\mu\text{M}$  1-[2-deoxy, 2-fluoro- $\beta$ -D-arabinofuranosyl]-5-iodouracil (FIAU; Bristol-Myers Co., New York, NY) recombinant clones were identified by PCR as described (34) using Primers E and F (Primer E, located in 3'-untranslated region of *neo* cassette, 5'-GATTGGGAAGACAAT-AGCAGGCATGC-3'; Primer F, located in intron 4, 5'-GGCAAG-ATGGCTCAGCAAGCAAAGGC-3'). Homologous recombination was verified by Southern blot analysis after *Bam*HI digestion and probing with a genomic DNA fragment located 3' of the targeting construct (Fig. 1). Nine independent stem cell clones containing a disrupted LDL receptor allele were injected into C57B1/6 blastocysts (27), yielding a total of 17 chimeric males whose coat color (agouti) indi-

cated a contribution of stem cells ranging from 30 to 100%. Of the 17 chimeric males, 15 were fertile, and 13 gave offspring that carried the disrupted LDL receptor allele. Five of these males exclusively transmitted the stem cell-derived genome through the germline. All experiments were performed with the F2 or F3 generation descendants, which were hybrids between the C57Bl/6J and 129Sv strains.

**Plasma lipoprotein analysis.** Blood was sampled from the retro-orbital plexus into tubes containing EDTA (Microvette CB 1000 capillary tubes; Sarstedt, Inc., Newton, NC). Pooled mouse plasma (0.6 ml from 3 to 5 mice) was ultracentrifuged at  $d = 1.215$  g/ml, and the resulting lipoprotein fraction ( $d < 1.215$  g/ml) was subjected to fast performance liquid chromatography (FPLC) gel filtration on a Superose 6 (Sigma Chemical Co.) column as previously described (22). For apoprotein analysis, peak fractions were pooled, precipitated with trichloroacetic acid, washed with acetone, and subjected to electrophoresis on 3–15% SDS polyacrylamide gels as described (22). Gels were calibrated with Rainbow high molecular weight markers (Amersham Corp., Arlington Heights, IL) and stained with Coomassie blue.

**Preparation of recombinant adenoviruses.** Recombinant replication-deficient adenoviruses containing the firefly luciferase cDNA (AdCMV-Luc) and the human LDL receptor cDNA (AdCMV-LDLR) driven by the cytomegalovirus promoter/enhancer were prepared as previously described (23). Briefly, virus particles for injection into animals were grown on human embryonic kidney 293 cells and purified by cesium chloride density gradient centrifugation. Particles were further purified by gel filtration on a Sepharose CL-4B (Pharmacia LKB Biotechnology, Piscataway, NJ) column equilibrated with 10 mM Tris-HCl, 137 mM NaCl, 5 mM KCl, 1 mM MgCl<sub>2</sub> at pH 7.4. BSA was added at a final concentration of 1 mg/ml, after which each virus preparation was stored in multiple aliquots at  $-70^{\circ}\text{C}$ . Viruses were titered on 293 cells; the titer ranged between  $10^{10}$  and  $10^{11}$  plaque-forming units (pfu) per ml.

For administration to mice, each recombinant adenovirus was injected as a single dose ( $2 \times 10^9$  pfu in 200  $\mu\text{l}$ ) into the external jugular vein of a nonfasted animal that had been anesthetized with sodium pentobarbital as previously described (23).

**Immunohistochemistry.** Mice were killed 4 d after injection of recombinant virus, the liver was removed, and a sector extending from the surface of the liver to the portal area was immediately frozen (without fixation) in OCT Compound 4583 (Miles Laboratories, Inc., Elkhart, IN) at  $-196^{\circ}\text{C}$  and stored at  $-70^{\circ}\text{C}$  until cutting. For immunohistochemistry, sections of 6  $\mu\text{m}$  were cut on a Leitz Cryostat (E. Leitz, Inc., Rockleigh, NJ) at  $-20^{\circ}\text{C}$  and mounted onto polylysine-coated slides. Before immunostaining, tissue sections were fixed in 100% (vol/vol) methanol at  $-20^{\circ}\text{C}$  for 30 s followed by two washes in PBS. All incubations were performed at  $20^{\circ}\text{C}$ . Samples were blocked by incubation for 20 min with 50 mM Tris-HCl, 80 mM NaCl, 2 mM CaCl<sub>2</sub> at pH 8 containing 10% (vol/vol) fetal calf serum. Sections were then incubated for 1 h with 20  $\mu\text{g}/\text{ml}$  of polyclonal rabbit IgG directed against the bovine LDL receptor (37) followed by three 5-min washes with PBS. Bound primary antibody was detected by incubation for 45 min with the indicated concentrations of FITC-labeled goat anti-rabbit IgG (GIBCO Bethesda Research Laboratories, Gaithersburg, MD). Slides were washed again three times in PBS, rinsed once briefly in water, and mounted under a coverslip with DABCO (90% vol/vol glycerol, 50 mM Tris-HCl at pH 9, 25% (wt/vol) 1,4-diazabicyclo-[2.2.2]-octane).

## Results

To disrupt the LDL receptor gene in murine ES cells, we constructed a gene targeting vector of the replacement type (35) as described in Methods. The targeting vector and the expected genomic structure of the disrupted locus are shown in Fig. 1. The *neo* cassette was inserted into exon 4 of the LDL receptor gene. The disrupted locus is predicted to encode a nonfunctional protein that is truncated within the ligand binding do-

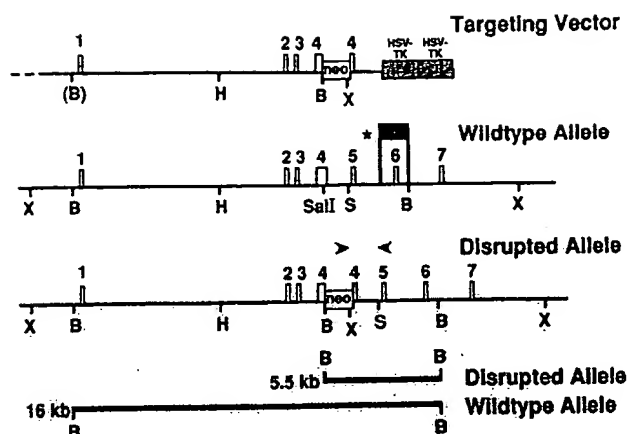


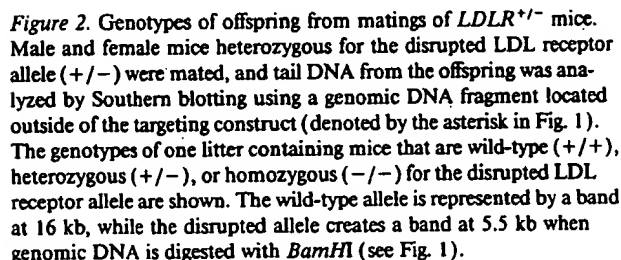
**Figure 1.** Strategy for targeted disruption of the LDL receptor locus in the mouse genome. A targeting vector of the replacement type was constructed as described in Methods. The *neo* gene is driven by the murine RNA polymerase II promoter and followed by the 3'-untranslated region of the bovine growth hormone gene containing the polyadenylation signal (34). The transcriptional direction of the *neo* gene is parallel to that of the LDL receptor. Two copies of the herpes simplex virus thymidine kinase gene (HSV-TK) (reference 35) flank the 3' homology segment. In the event of homologous recombination, the disrupted allele will have acquired additional sites for the restriction endonucleases *Bam*HI (B) and *Xba*I (X). The expected *Bam*HI digestion pattern resulting from a targeting event is shown at the bottom. The DNA probe used for Southern blotting (denoted by the asterisk and the heavy bracket) is a 1.7-kb *Bgl*II-*Bam*HI genomic fragment containing exon 6 and flanking intron sequences. The positions of the two oligonucleotides used for PCR diagnosis of homologous recombination are indicated by the arrows (oligo 1: 3' end of *neo* cassette; oligo 2: downstream of *Sac*I site in intron 4). B, *Bam*HI; H, *Hind*III; X, *Xba*I; S, *Sac*I.

main of the receptor. This receptor fragment should not bind LDL, and it should not remain associated with the cell membrane since it lacks the membrane spanning segment.

ES cells were electroporated with the linearized targeting vector and subjected to positive and negative selection using standard procedures (36). Homologous recombination events were detected by PCR and verified by digestion of genomic ES cell DNA with *Bam*HI. The presence of a diagnostic 5.5-kb *Bam*HI fragment in addition to the wild-type 16-kb fragment is indicative of gene targeting when the Southern blot is probed with a genomic DNA fragment located outside of the targeting vector (indicated by the asterisk in Fig. 1). The frequency of homologous recombination was very high. Approximately 50% of clones that were resistant to both G418 and FIAU exhibited homologous recombination.

Recombinant stem cell clones injected into C57Bl/6 blastocysts (27) gave rise to chimeric animals with a stem cell-derived coat color contribution that ranged from 30 to 100%. Several male chimeras derived from independently targeted stem cell clones efficiently transmitted the stem cell-derived genome through the germ line. Offspring heterozygous for the disrupted LDL receptor allele were diagnosed by Southern blotting. When heterozygous animals were mated to each other, their offspring included animals that were wild-type (+/+), heterozygous (+/-), and homozygous (-/-) for the disrupted LDL receptor allele. Fig. 2 shows a representative

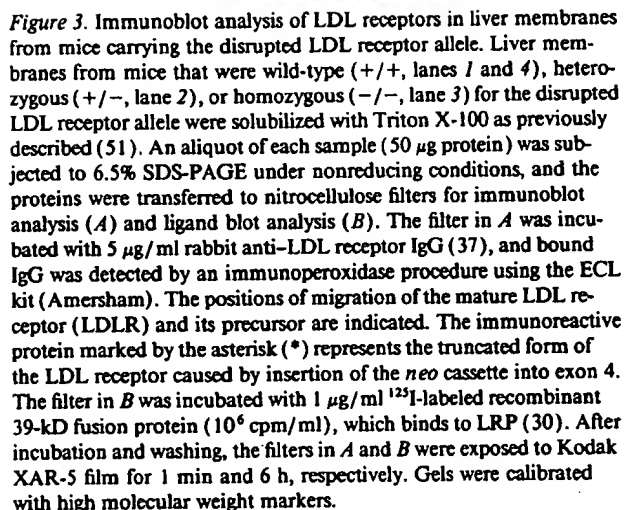




To confirm the inability of the disrupted gene to produce full-length LDL receptors, we prepared liver membranes from wild-type, heterozygous, and homozygous animals. Proteins were solubilized with detergent, and 50  $\mu$ g of each sample were analyzed by SDS gel electrophoresis and immunoblotting with a polyclonal antibody that detects the mouse LDL receptor. As shown in Fig. 3A, normal LDL receptor protein was readily detected by the antibody in wild-type (+/+), lanes 1 and 4) and in heterozygous animals (+/-, lane 2), but was undetectable in animals that were homozygous for the LDL receptor defect (-/-, lane 3). An abnormal band (marked by an asterisk) was present in liver membranes prepared from heterozygous (lane

Sex	Total Plasma Cholesterol Level (mg/dl)		
	+/+	+/-	-/-
Male	119±4 (n = 19)	158±4 (n = 39)	228±9 (n = 16)
Female	100±4* (n = 28)	138±4* (n = 54)	239±8 (n = 21)

\* Sex difference,  $P = 0.01$  (unpaired  $t$  test).



Mice heterozygous or homozygous for the disrupted LDL receptor allele have elevated plasma cholesterol levels when compared with their wild-type litter mates. Table I shows total plasma cholesterol levels of mice from 28 litters derived from the mating of heterozygous animals and fed a normal chow diet. The mean age of the animals at the time of measurement was 52 d. Total (nonfasting) plasma cholesterol values are ~ 35% elevated in heterozygotes and about two times higher in *LDLR*<sup>-/-</sup> mice when compared to wild-type litter mates. In animals of wild-type or heterozygous genotype, females had a lower total plasma cholesterol level than males. This difference was absent in the *LDLR*<sup>-/-</sup> mice. There was no significant



difference in plasma triglyceride concentration among animals of the three genotypes (8–10 animals per group) whose average nonfasting values on a normal chow diet ranged from 119 to 133 mg/dl (data not shown).

To learn which lipoprotein fraction was affected by the loss of functional LDL receptors in the mouse, we used FPLC to determine the lipoprotein cholesterol profiles of male and female mice of the three different genotypes fed a normal chow diet (Fig. 4 A–C). Plasma of wild-type mice contained very little cholesterol in the IDL/LDL fraction. A small but definite increase in this fraction was observed in heterozygous mice of either sex. Animals homozygous for the LDL receptor defect showed a marked increase almost exclusively in the IDL/LDL fraction with a small increase in VLDL. For all genotypes, the HDL-cholesterol level was slightly higher in male mice as compared with female mice, but there was no dramatic effect of LDL receptor gene disruption.

To estimate the relative elevation of IDL/LDL from the data of Fig. 4 A–C, we added up the total cholesterol content of each column fraction within the IDL/LDL peak and then expressed the data relative to the levels observed in wild-type mice of the same sex. These data revealed that the IDL/LDL cholesterol was elevated about twofold in *LDLR*<sup>+/-</sup> mice of either sex and 7.4- to 9-fold in male and female *LDLR*<sup>-/-</sup> mice, respectively. The HDL-cholesterol was elevated only modestly (~1.3-fold) in the *LDLR*<sup>-/-</sup> mice.

Fig. 4 D–F shows comparisons of the lipoprotein cholesterol profiles of male mice of the different genotypes fed either a normal chow diet with or without 0.2% cholesterol/10% coconut oil. Wild-type mice showed only a small difference in lipoprotein profile in response to the cholesterol-enriched diet. Heterozygous mice responded with a small, but distinct elevation in IDL/LDL cholesterol. In the *LDLR*<sup>-/-</sup> mice the cholesterol content of the IDL/LDL fraction rose about threefold. The mean total plasma cholesterol levels for the three genotypes before (fasted) and after (nonfasted) cholesterol feeding were as follows: +/+, 146 and 149 mg/dl; +/-, 188 and 196 mg/dl; and -/-, 293 and 425 mg/dl, respectively.

The apoproteins of the various fractions in Fig. 4 D–F were analyzed by SDS polyacrylamide gel electrophoresis and Coomassie blue staining (Fig. 5). On the normal chow diet, the heterozygous mice showed a distinct elevation in apo B-100 and apo E in the IDL/LDL fraction. The IDL/LDL fraction from *LDLR*<sup>-/-</sup> mice had a much more marked increase of these two apoproteins as well as of apo B-48. The 0.2% cholesterol/10% coconut oil diet elicited a pronounced increase in apo B-100, apo B-48, and apo E in the IDL/LDL fraction of the *LDLR*<sup>-/-</sup> mice. A small increase in the apo E of VLDL and HDL was also apparent in the cholesterol-fed mice (homozygotes > heterozygotes > wild-type).

To evaluate the functional effect of the LDL receptor deficiency, we compared the ability of *LDLR*<sup>-/-</sup> mice and wild-

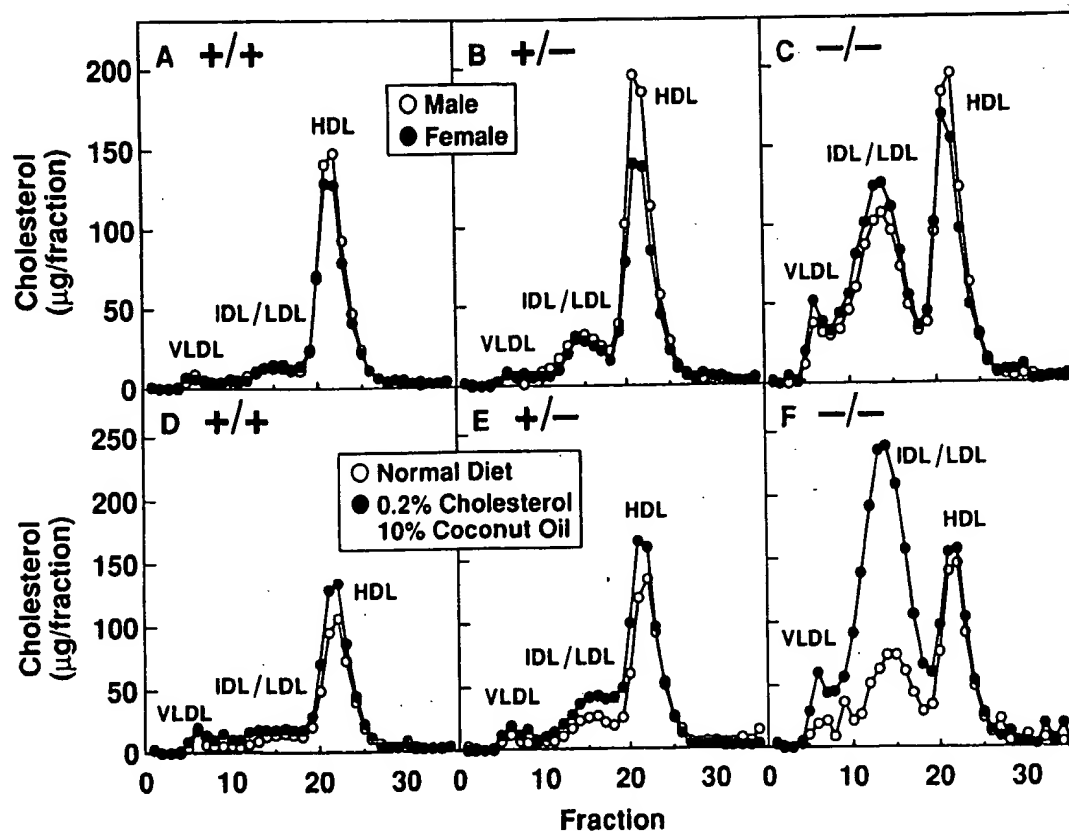


Figure 4. FPLC profiles of mouse plasma lipoproteins from wild-type (+/+) and mutant mice carrying the disrupted LDL receptor allele in heterozygous (+/-) and homozygous (-/-) forms. Mice with the indicated genotype ( $n = 10$  for each sex in A–C and  $n = 5$  males in D–F) were fed a normal diet in A–C or the indicated diet in D–F for 7 wk. The pooled plasma from each group (collected from 12-h fasted animals in A–C and from nonfasted animals in D–F) was subjected to gel filtration on FPLC, and the cholesterol content of each fraction was measured as described in Methods. The mice were 8–9 wk of age in A–C and 16–17 wk in D–F.

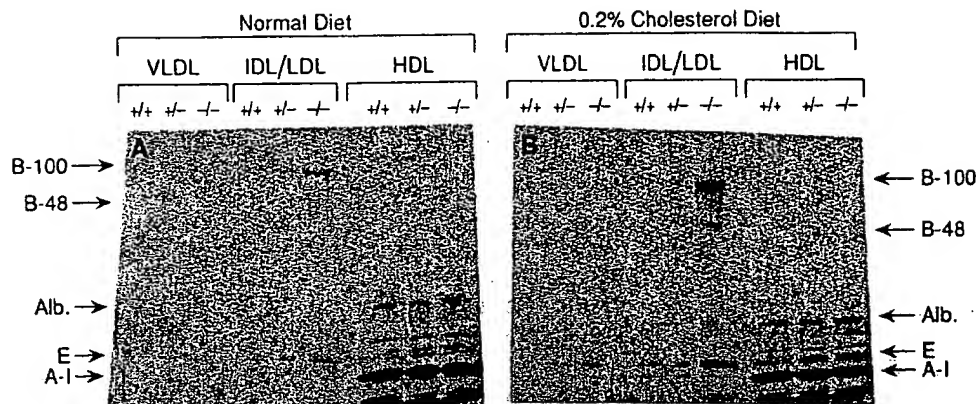


Figure 5. SDS-gel electrophoresis of lipoprotein fractions from wild-type and mutant mice fed different diets. Male mice ( $n = 5$  per group) that were wild-type (+/+), heterozygous (+/-) or homozygous (-/-) for the disrupted LDL receptor allele were fed either a normal diet (A) or a diet containing 0.2% cholesterol and 10% coconut oil (B) as described in the legend to Fig. 4. The apoproteins from the VLDL, IDL/LDL, and HDL containing fractions in Fig.

4 (equivalent to 70  $\mu$ l of plasma) were subjected to electrophoresis on 3–15% SDS gradient gels. Proteins were stained with Coomassie blue. The positions of migration of apo B-100, apo B-48, albumin (Alb.), apo E, and apo A-I are indicated.

type mice to clear  $^{125}$ I-labeled lipoproteins from the circulation (Fig. 6). For this purpose, we isolated three lipoprotein fractions (VLDL, LDL, and HDL) by ultracentrifugation of pooled plasma of 50  $LDLR^{-/-}$  mice. After radiolabeling with  $^{125}$ I, each lipoprotein was injected into the external jugular vein of three wild-type (+/+) and three homozygous (-/-) animals. Blood was obtained at the indicated intervals, and the radioactivity was expressed relative to the radioactivity at 2 min after injection of the label. As shown in Fig. 6A, wild-type mice (open circles) clear  $^{125}$ I-VLDL much more efficiently than  $LDLR^{-/-}$  animals (closed circles). In the wild-type ani-

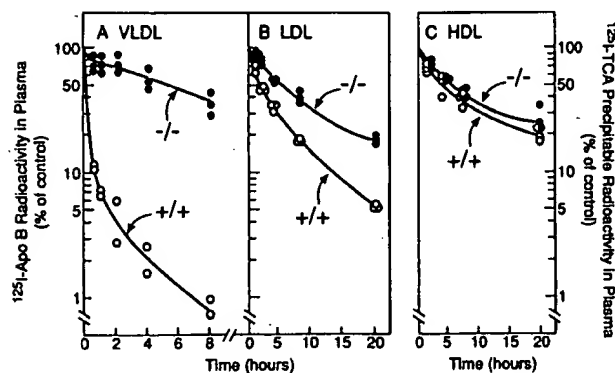


Figure 6. Disappearance of  $^{125}$ I-labeled lipoproteins from the circulation in wild-type (o) and  $LDLR^{-/-}$  (●) mice. For each graph, 3 wild-type and 3  $LDLR^{-/-}$  male mice, 20–24 wk of age that had been fasted for 12 h, were anesthetized with sodium pentobarbital (60 mg/kg). Each mouse received an intravenous bolus via the external jugular vein of 0.25 ml of 0.15 M NaCl containing bovine serum albumin (2 mg/ml) and one of the following  $^{125}$ I-labeled mouse lipoproteins: 15  $\mu$ g protein of  $^{125}$ I-VLDL (2,500 cpm/ng protein), 15  $\mu$ g protein of  $^{125}$ I-LDL (1,110 cpm/ng protein), or 15  $\mu$ g protein of  $^{125}$ I-HDL (491 cpm/ng protein). Blood was collected at the indicated time by retro-orbital puncture. In A and B, the plasma content of  $^{125}$ I-labeled apo B was measured by isopropanol precipitation followed by gamma counting (10, 52). In C, the plasma content of trichloroacetic acid-precipitable  $^{125}$ I-radioactivity was measured. The "100% of control" represents the average value for plasma  $^{125}$ I-radioactivity in the wild-type and mutant mice at 2 min after injection. One wild-type animal in A died ~ 30 min after the intravenous injection.

mals 50% of the radioactivity had been eliminated within 10 min, and this was prolonged to 5 h in the  $LDLR^{-/-}$  mice. The clearance of  $^{125}$ I-LDL was also retarded in the  $LDLR^{-/-}$  animals (half-time for disappearance, 5 h in the  $LDLR^{-/-}$  mice vs. 2 h in the wild-type animals) (Fig. 6B). The clearance of  $^{125}$ I-HDL (half-time of 5.5 h) was not affected by the receptor deficiency (Fig. 6C).

In order to determine whether adenovirus-mediated gene transfer of the human LDL receptor can reverse the abnormalities caused by the knockout of the LDL receptor, we injected  $2 \times 10^9$  pfu of recombinant virus containing either the luciferase cDNA (AdCMV-Luc) or the LDL receptor cDNA (AdCMV-LDLR) into  $LDLR^{-/-}$  mice. This dose has been found previously to cause expression of the foreign gene in the majority of hepatocytes (23). 4 d after administration of the recombinant viruses, liver membrane proteins were prepared from the individual animals and separated by SDS gel electrophoresis (Fig. 7). Lane 1 shows an immunoblot of a wild-type mouse liver,

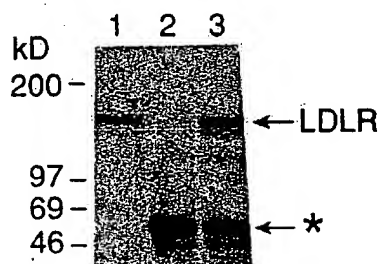


Figure 7. Immunoblot analysis of LDL receptors in liver membranes from  $LDLR^{-/-}$  mice 4 d after injection of recombinant adenovirus expressing the human LDL receptor cDNA. Male mice homozygous for the disrupted LDL receptor allele, 17 wk of age, were injected intra-

venously with  $2 \times 10^9$  pfu of adenovirus containing either the luciferase cDNA (lane 2) or the human LDL receptor cDNA (lane 3) as described in Methods. 4 d after administration of the virus, the animals were killed, and liver membranes were prepared from single mice, subjected to SDS gel electrophoresis under reducing conditions (5% [vol/vol] 2-mercaptoethanol), and transferred to filters for immunoblot analysis with a rabbit anti-LDL receptor IgG as described in the legend to Fig. 3. Lane 1 contains liver membrane proteins from a wild-type mouse not injected with recombinant adenovirus. The position of migration of the mature LDL receptor (LDLR) is indicated by the arrow. The immunoreactive protein marked by the asterisk (\*) represents the truncated form of the LDL receptor caused by insertion of the *neo* cassette into exon 4.

revealing the normal mouse LDL receptor. As expected, no intact LDL receptor protein is detectable by immunoblotting in the liver of an *LDLR*<sup>-/-</sup> mouse injected with the luciferase-containing control virus (lane 2). In contrast, injection of AdCMV-LDLR led to high-level expression of the intact receptor in the liver of an *LDLR*<sup>-/-</sup> mouse (lane 3).

Fig. 8 shows an immunohistochemical analysis of LDL receptor expression in the livers of *LDLR*<sup>-/-</sup> mice 4 d after injection of AdCMV-Luc (A) or AdCMV-LDLR (B). In animals injected with the luciferase-containing virus, there were no detectable LDL receptors (A). In the mice injected with AdCMV-LDLR the majority of cells showed positive immunofluorescence (B). The enhanced magnification in C shows that the virally encoded receptor was expressed in a polarized fashion on the blood-sinusoidal surface of the hepatocyte, as is the human LDL receptor in transgenic mice (21).

To test the function of the adenovirus-encoded receptor, we measured the clearance of <sup>125</sup>I-labeled VLDL (Fig. 9). For this experiment we used VLDL isolated from WHHL rabbits, which are deficient in functional LDL receptors. In preliminary experiments we found that <sup>125</sup>I-labeled VLDL from WHHL rabbits is cleared from the circulation of normal mice approximately as rapidly as <sup>125</sup>I-labeled mouse VLDL, and the rabbit lipoprotein is much easier to obtain. *LDLR*<sup>-/-</sup> mice that received recombinant adenovirus encoding the human LDL receptor cleared the <sup>125</sup>I-labeled rabbit VLDL from their plasma at a rapid rate (Fig. 9). In contrast, mice that had received the luciferase-containing virus cleared the <sup>125</sup>I-VLDL at a rate that was similar to that of uninjected animals (compare with Fig. 6A).

We next sought to determine whether the adenovirus-encoded receptors could normalize the lipoprotein profile of *LDLR*<sup>-/-</sup> mice. For this purpose we injected the control virus (AdCMV-Luc) or the LDL receptor-containing virus (AdCMV-LDLR) into *LDLR*<sup>-/-</sup> male mice (3 animals per group). 4 d after injection the animals were exsanguinated, the pooled plasma of each group was subjected to FPLC gel filtration, and the cholesterol content of the fractions was plotted (Fig. 10). The lipoprotein profile of the mice that had been injected with the luciferase-containing virus closely resembled the profile of uninjected animals (compare with Fig. 4). In the group that had received the LDL receptor-containing virus, the IDL/LDL peak disappeared, and there was a slight increase in VLDL-cholesterol.

## Discussion

The current results demonstrate that elimination of functional LDL receptor genes by homologous recombination profoundly elevates IDL and LDL levels in mice and that these abnormalities can be reversed postnatally by adenovirus-mediated transfer of a gene encoding the LDL receptor. The experiments establish a new animal model by which to explore genetic and environmental factors that interact with LDL receptors to control cholesterol levels. They also provide a new model system in which to study somatic cell gene therapy targeted at the liver.

The most profound functional change observed in the current study was the marked reduction in the clearance rate of <sup>125</sup>I-labeled VLDL from plasma in the homozygous *LDLR*<sup>-/-</sup> mice. The time required for clearance of 50% of the injected lipoprotein rose from 10 min to 300 min, a 30-fold change. These data indicate that the LDL receptor is responsible for

most of the rapid clearance of VLDL remnants and IDL from plasma of mice. The exact proportion cleared by the LDL receptor may be overestimated in these studies because the labeled VLDL was prepared from LDL receptor-deficient animals, i.e., *LDLR*<sup>-/-</sup> mice or homozygous WHHL rabbits. Although these particles float in the VLDL density range ( $d < 1.006$  g/ml), they are likely to represent partially metabolized VLDL particles that have overaccumulated in the donor animals because of the LDL receptor deficiency. Any VLDL particle that is rapidly cleared from plasma in the receptor-deficient animals would be underrepresented in the sample that is used for labeling. This would include large apo E-rich VLDL particles containing either apo B-48 or apo B-100, which may be cleared in part by the chylomicron remnant receptor (38). This problem of underrepresentation of rapidly cleared particles is a problem with all lipoprotein clearance studies (see Discussion in reference 38). Despite these limitations, the data indicate clearly that the VLDL fraction of mice contains a substantial number of particles that are normally cleared by the LDL receptor, presumably owing to their content of apo E. In LDL receptor deficiency states, these particles remain in plasma for long periods and are presumably converted to LDL. Although such conversion was not studied in the current study, it was previously demonstrated in WHHL rabbits (10, 39).

Striking parallels exist between the findings in the current study of *LDLR*<sup>-/-</sup> mice and previous studies of lipoprotein clearance in homozygous WHHL rabbits (10, 39) and FH homozygotes (9). In all three species the most profound abnormality involves the clearance of VLDL remnants and IDL. In WHHL rabbits, the half-time for VLDL clearance was extended from 12 to 480 min (10), a result that parallels the 10 to 300 min change in the current study. In a study of <sup>125</sup>I-VLDL turnover in FH homozygotes, Soutar et al. (9) observed a sevenfold decrease in the clearance of <sup>125</sup>I-IDL derived from <sup>125</sup>I-VLDL (fractional turnover rate 0.48/h in normal subjects vs. 0.064/h in FH homozygotes). Using a more complex kinetic analysis, James et al. (43) also found a decreased clearance of VLDL remnants and IDL. This indicates that a major function of the LDL receptor in all three species is the clearance of remnant particles derived from VLDL, thereby preventing their conversion into LDL.

The relative decline in LDL clearance observed in LDL receptor-deficient mice (2.5-fold) also correlates well with observations in WHHL rabbits. Yamada et al. (39) observed a reduction of 2-fold, Pittman et al. (40) 2.6-fold, and Spady et al. (41) 3.5-fold. In FH homozygotes the reduction in LDL clearance is also about threefold (42, 43). These data indicate that about 60% of LDL particles are normally cleared by the LDL receptor in mice. The residual clearance of LDL observed in the absence of LDL receptors is likely to be mediated by another receptor with a lower affinity for LDL. Like the LDL receptor, this alternate receptor functions primarily in the liver (40).

The absolute level of plasma LDL-cholesterol in the *LDLR*<sup>-/-</sup> mice is much lower than that observed in WHHL rabbits or FH homozygotes. Although we did not measure LDL-cholesterol quantitatively, it is apparent from the FPLC profiles that the IDL/LDL peak contains ~ 50% of the total cholesterol in the plasma of the *LDLR*<sup>-/-</sup> mice, which would indicate an IDL/LDL-cholesterol level of ~ 130 mg/dl. This contrasts with LDL-cholesterol levels above 450 mg/dl in WHHL rabbits (10, 44) and FH homozygotes (2). This differ-

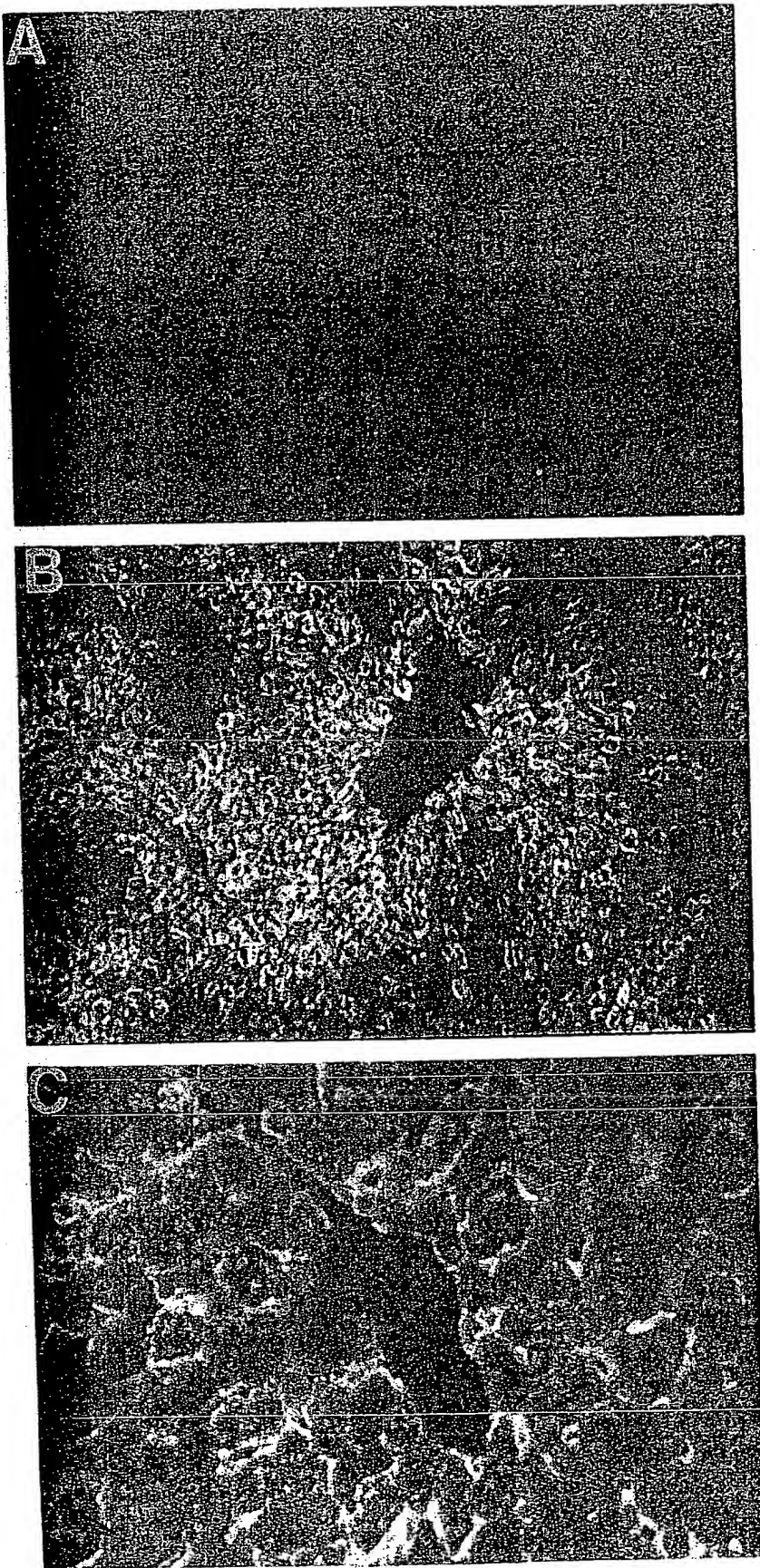


**Figure 8.** Immunohistochemical staining of LDL receptors in the liver of an *LDLR*<sup>-/-</sup> mouse after treatment with recombinant adenovirus expressing the human LDL receptor cDNA. Male mice homozygous for the disrupted LDL receptor allele, 18 wk of age, were injected intravenously with  $2 \times 10^9$  pfu of either AdCMV-Luciferase (*A*) or AdCMV-LDLR (*B* and *C*) as described in Methods. Four days after administration of the virus, the livers were removed for immunohistochemistry. Frozen sections were incubated with 20  $\mu$ g/ml of rabbit polyclonal anti-LDL receptor antibody, and bound IgG was detected with 5  $\mu$ g/ml FITC-labeled goat anti-rabbit IgG as described in Methods. Magnification, *A* and *B*,  $\times 25$ ; *C*,  $\times 100$ .

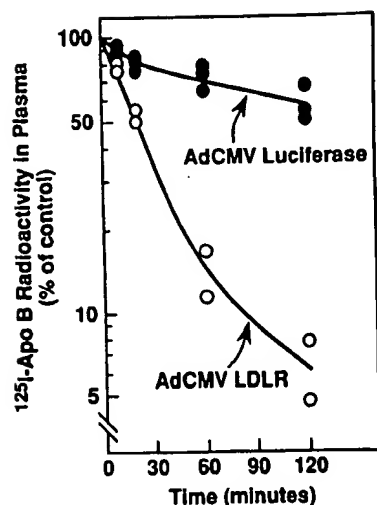


Figure 9. Disappearance of  $^{125}\text{I}$ -VLDL from the circulation of  $\text{LDLR}^{-/-}$  mice after treatment with recombinant adenovirus expressing the human LDL receptor cDNA. Three male mice homozygous for the disrupted LDL receptor allele, 19 wk of age, were injected intravenously with  $2 \times 10^9$  pfu of either AdCMV-LDLR (○) or AdCMV-Luciferase (●). 4 d after administration of the virus, the animals (nonfasted) were injected with 15

$\mu\text{g}$  protein of  $^{125}\text{I}$ -labeled VLDL (308 cpm/ng protein) isolated from WHHL rabbits. Blood was collected at the indicated time by retro-orbital puncture, and the plasma content of  $^{125}\text{I}$ -labeled apo B was measured by isopropanol precipitation (10, 52). The "100% of control" represents the average value for plasma  $^{125}\text{I}$ -radioactivity 1 min after injection. One animal injected with AdCMV-LDLR died  $\sim 10$  min after injection of the  $^{125}\text{I}$ -VLDL.

ence might be explained by the production of VLDL containing apo B-48 in livers of mice, but not rabbits or humans. About 70% of the apo B mRNA in the livers of adult mice encodes the apo B-48 isoform (14). Remnants derived from apo B-48 containing VLDL might be cleared relatively rapidly by the livers of the  $\text{LDLR}^{-/-}$  mice, owing to the ability of the

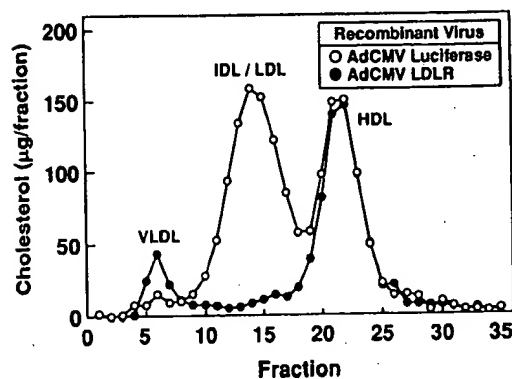


Figure 10. FPLC profiles of plasma lipoproteins from  $\text{LDLR}^{-/-}$  mice after treatment with recombinant adenovirus expressing the human LDL receptor cDNA. Three male mice homozygous for the LDL receptor disrupted allele, 17 wk of age, were injected with  $2 \times 10^9$  pfu of adenovirus containing either the luciferase cDNA (○) or the human LDL receptor cDNA (●). 4 d after administration of the virus, blood was collected from the animals (nonfasted), and the plasma from the three animals in each group was pooled and subjected to gel filtration on FPLC. The cholesterol content of each fraction was determined as described in Methods. The mean total plasma cholesterol levels in the two groups of mice were 279 mg/dl (○) and 139 mg/dl (●).

apo E/apo B-48 particles to bind to chylomicron remnant receptors, thereby leading to lower levels of LDL.

The hypothesized role of apo E/apo B-48 particles is supported by a comparison of the current data with those of Zhang et al. (45) and Plump et al. (46), who eliminated the gene for apo E in mice using a similar homologous recombination technique. Apo E $^{-/-}$  mice had total plasma cholesterol levels of 400–500 mg/dl, nearly all of which was contained in particles with the size of VLDL and VLDL remnants. The level of apo B-48 in plasma was also markedly elevated (45). The severity of this abnormality in comparison with the effects of LDL receptor deficiency supports the notion that apo E binds to two receptors, the LDL receptor and the chylomicron remnant receptor. Knockout of apo E therefore has a more profound effect on lipoprotein clearance than knockout of the LDL receptor in mice.

In humans the opposite is true, i.e., LDL receptor deficiency raises the total plasma cholesterol more than does apo E deficiency. Receptor-negative FH homozygotes have total plasma cholesterol levels of 700–1,000 mg/dl (2), whereas individuals with an absence of apo E have plasma cholesterol levels of 443 to 614 mg/dl (47). This is likely due, in part, to the fact that human livers do not produce apo B-48 and that apo E accelerates the removal of apo B-100 containing VLDL remnants primarily by binding to only one receptor, namely, the LDL receptor.

LDL receptors are believed to constitute an important defense against the cholesterol-elevating effect of dietary cholesterol (1). In rabbits (48) and hamsters (49), dietary cholesterol elevates plasma LDL-cholesterol levels in part by suppressing LDL receptors. In the current study, LDL receptor-deficient mice responded to the 0.2% cholesterol/10% coconut oil diet with a rise in plasma LDL-cholesterol that was much greater than was observed in wild-type mice. There was also a definite increase in the amounts of apo B-100 and apo E in plasma, particularly in the IDL/LDL fraction (Fig. 5). Thus, when LDL receptors are already absent as a result of genetic elimination, mice become hyperresponsive to dietary cholesterol.

The current experiments with recombinant adenovirus demonstrate that this vector can restore LDL receptor expression within 4 d in an LDL receptor-deficient mouse. However, many technical problems would have to be overcome before such therapy could be considered for humans. First, it is unknown whether or not the expression of adenovirus-encoded genes in liver will persist for long periods. The genome of the defective virus does not replicate, nor does it integrate into the genome at any appreciable frequency. On the other hand, Stratford-Perricaudet et al. (24) did note persistent expression for a year after injection of the virus into neonatal animals lacking ornithine transcarbamylase activity. Second, adenovirus-encoded proteins are likely to be the targets of immune reactions. Mice are known to develop an immune response to adenoviral proteins (50), which might hamper its use for long periods in these animals. Nearly all humans are expected to possess antibodies against adenovirus, and these might prevent use of this vector in people. Despite these reservations about human applicability, the adenovirus vector is a useful experimental tool to change the expression of genes acutely in the liver. In the current studies, we used it to reveal the type of result to be expected when more applicable long-term gene delivery methods have been developed.



## Acknowledgments

We thank Phil Soriano for expert advice and help. Scott Clark, Lucy Lundquist, Wen-Ling Niu, and Sadeq Hassan provided excellent technical assistance.

This work was supported by National Institutes of Health grants HL-20948 and HL-17669, and by grants from the Moss Heart Foundation and the Perot Family Foundation. S. Ishibashi is the recipient of a postdoctoral fellowship from the Sasakawa Health Science Foundation, Tokyo, Japan. R. D. Gerard is an Established Investigator of the American Heart Association. J. Herz is supported by the Syntex Scholar Program and is a Lucille P. Markey Scholar.

*Note added in proof.* The LDL receptor-deficient mice described in this paper will become available in September 1993 from Jackson Laboratories, 600 Main Street, Bar Harbor, ME 04609.

## References

1. Brown, M. S., and J. L. Goldstein. 1986. A receptor-mediated pathway for cholesterol homeostasis. *Science (Wash. DC)*. 232:34-47.
2. Goldstein, J. L., and M. S. Brown. 1989. Familial hypercholesterolemia. In *The Metabolic Basis of Inherited Disease*. C. R. Scriver, A. L. Beaudet, W. S. Sly, and D. Valle, editors. McGraw-Hill Publishing Co., New York, 1215-1250.
3. Mahley, R. W. 1988. Apolipoprotein E: Cholesterol transport protein with expanding role in cell biology. *Science (Wash. DC)*. 240:622-630.
4. Brown, M. S., J. Herz, R. C. Kowal, and J. L. Goldstein. 1991. The low-density lipoprotein receptor-related protein: double agent or decoy? *Curr. Opin. in Lipidol.* 2:65-72.
5. Ji, Z.-S., W. J. Brecht, D. Miranda, M. M. Hussain, T. L. Innerarity, and R. W. Mahley. 1993. Role of heparan sulfate proteoglycans in the binding and uptake of apolipoprotein E-enriched remnant lipoproteins by cultured cells. *J. Biol. Chem.* 268:10160-10167.
6. Hobbs, H. H., M. S. Brown, and J. L. Goldstein. 1992. Molecular genetics of the LDL receptor gene in familial hypercholesterolemia. *Hum. Mutat.* 1:445-466.
7. Watanabe, Y., T. Ito, and M. Shioimi. 1985. The effect of selective breeding on the development of coronary atherosclerosis in WHHL rabbits. An animal model for familial hypercholesterolemia. *Atherosclerosis*. 56:71-97.
8. Scanu, A. M., A. Khalil, L. Neven, M. Tidore, G. Dawson, D. Pfaffinger, E. Jackson, K. D. Carey, H. C. McGill, and G. M. Fless. 1988. Genetically determined hypercholesterolemia in a rhesus monkey family due to a deficiency of the LDL receptor. *J. Lipid Res.* 29:1671-1681.
9. Soutar, A. K., N. B. Myant, and G. R. Thompson. 1982. The metabolism of very low density and intermediate density lipoproteins in patients with familial hypercholesterolemia. *Atherosclerosis*. 43:217-231.
10. Kita, T., M. S. Brown, D. W. Bilheimer, and J. L. Goldstein. 1982. Delayed clearance of very low density and intermediate density lipoproteins with enhanced conversion to low density lipoprotein in WHHL rabbits. *Proc. Natl. Acad. Sci. USA*. 79:5693-5697.
11. Hobbs, H. H., E. Leitersdorf, C. C. Leffert, D. R. Cryer, M. S. Brown, and J. L. Goldstein. 1989. Evidence for a dominant gene that suppresses hypercholesterolemia in a family with defective low density lipoprotein receptors. *J. Clin. Invest.* 84:656-664.
12. Lamon-Fava, S., D. Jimenez, J. C. Christian, R. R. Fabsitz, T. Reed, D. Carmelli, W. P. Castelli, J. M. Ordovas, P. W. F. Wilson, and E. J. Schaefer. 1991. The NHLBI twin study: heritability of apolipoprotein A-I, B, and low density lipoprotein subclasses and concordance for lipoprotein(a). *Atherosclerosis*. 91:97-106.
13. Spady, D. K., L. A. Woollett, and J. M. Dietschy. 1993. Regulation of plasma LDL-cholesterol levels by dietary cholesterol and fatty acids. *Annu. Rev. Nutr.* 13:355-381.
14. Higuchi, K., K. Kitagawa, K. Kogishi, and T. Takeda. 1992. Developmental and age-related changes in apolipoprotein B mRNA editing in mice. *J. Lipid Res.* 33:1753-1764.
15. Scott, J. 1989. The molecular and cell biology of apolipoprotein-B. *Mol. Biol. Med.* 6:65-80.
16. Chan, L. 1992. Apolipoprotein B, the major protein component of triglyceride-rich and low density lipoproteins. *J. Biol. Chem.* 267:25621-25624.
17. Van't Hooft, F. M., D. A. Hardman, J. P. Kane, and R. J. Havel. 1982. Apolipoprotein B (B-48) of rat chylomicrons is not a precursor of the apolipoprotein of low density lipoproteins. *Proc. Natl. Acad. Sci. USA*. 79:179-182.
18. Chowdhury, J. R., M. Grossman, S. Gupta, N. R. Chowdhury, J. R. Baker, Jr., and J. M. Wilson. 1991. Long-term improvement of hypercholesterolemia after *ex vivo* gene therapy in LDLR-deficient rabbits. *Science (Wash. DC)*. 254:1802-1805.
19. Wilson, J. M., M. Grossman, C. H. Wu, N. R. Chowdhury, G. Y. Wu, and J. R. Chowdhury. 1992. Hepatocyte-directed gene transfer *in vivo* leads to transient improvement of hypercholesterolemia in low density lipoprotein receptor-deficient rabbits. *J. Biol. Chem.* 267:963-967.
20. Hofmann, S. L., D. W. Russell, M. S. Brown, J. L. Goldstein, and R. E. Hammer. 1988. Overexpression of low density lipoprotein (LDL) receptor eliminates LDL from plasma in transgenic mice. *Science (Wash. DC)*. 239:1277-1281.
21. Pathak, R. K., M. Yokode, R. E. Hammer, S. L. Hofmann, M. S. Brown, J. L. Goldstein, and R. G. W. Anderson. 1990. Tissue-specific sorting of the human LDL receptor in polarized epithelia of transgenic mice. *J. Cell Biol.* 111:347-359.
22. Yokode, M., R. E. Hammer, S. Ishibashi, M. S. Brown, and J. L. Goldstein. 1990. Diet-induced hypercholesterolemia in mice: Prevention by overexpression of LDL receptors. *Science (Wash. DC)*. 250:1273-1275.
23. Herz, J., and R. D. Gerard. 1993. Adenovirus-mediated low density lipoprotein receptor gene transfer accelerates cholesterol clearance in normal mice. *Proc. Natl. Acad. Sci. USA*. 90:2812-2816.
24. Stratford-Perricaudet, L. D., M. Levrero, J.-F. Chasse, M. Perricaudet, and P. Briand. 1990. Evaluation of the transfer and expression in mice of an enzyme-encoding gene using a human adenovirus vector. *Hum. Gene Ther.* 1:241-256.
25. Capecchi, M. R. 1989. Altering the genome by homologous recombination. *Science (Wash. DC)*. 244:1288-1292.
26. Smithies, O. 1991. Altering genes in animals and humans. In *Etiology of Human Disease at the DNA Level*. J. Lindsten and U. Pettersson, editors. Raven Press, New York. 221-259.
27. Bradley, A. 1987. Production and analysis of chimeric mice. In *Teratocarcinomas and Embryonic Stem Cells: A Practical Approach*. E. J. Robertson, editor. IRL Press, Oxford, UK/Washington, DC. 113-151.
28. Sambrook, J., E. F. Fritsch, and T. Maniatis. 1989. *Molecular cloning: A Laboratory Manual*. Cold Spring Harbor Laboratory Press, Cold Spring Harbor, New York.
29. Yokode, M., R. K. Pathak, R. E. Hammer, M. S. Brown, J. L. Goldstein, and R. G. W. Anderson. 1992. Cytoplasmic sequence required for basolateral targeting of LDL receptor in livers of transgenic mice. *J. Cell Biol.* 117:39-46.
30. Willnow, T. F., J. L. Goldstein, K. Orth, M. S. Brown, and J. Herz. 1992. Low density lipoprotein receptor-related protein (LRP) and gp330 bind similar ligands, including plasminogen activator-inhibitor complexes and lactoferrin, an inhibitor of chylomicron remnant clearance. *J. Biol. Chem.* 267:26172-26180.
31. Goldstein, J. L., S. K. Basu, and M. S. Brown. 1983. Receptor-mediated endocytosis of LDL in cultured cells. *Methods Enzymol.* 98:241-260.
32. Yamamoto, T., C. G. Davis, M. S. Brown, W. J. Schneider, M. L. Casey, J. L. Goldstein, and D. W. Russell. 1984. The human LDL receptor: A cysteine-rich protein with multiple Alu sequences in its mRNA. *Cell*. 39:27-38.
33. Mehta, K. D., W.-J. Chen, J. L. Goldstein, and M. S. Brown. 1991. The low density lipoprotein receptor in *Xenopus laevis*. I. Five domains that resemble the human receptor. *J. Biol. Chem.* 266:10406-10414.
34. Soriano, P., C. Montgomery, R. Geske, and A. Bradley. 1991. Targeted disruption of the *c-src* proto-oncogene leads to osteopetrosis in mice. *Cell*. 64:693-702.
35. Mansour, S. L., K. R. Thomas, and M. R. Capecchi. 1988. Disruption of the proto-oncogene *int-2* in mouse embryo-derived stem cells: a general strategy for targeting mutations to non-selectable genes. *Nature (Lond.)*. 336:348-352.
36. McMahon, A. P., and A. Bradley. 1990. The *Wnt-1* (*int-1*) proto-oncogene is required for development of a large region of the mouse brain. *Cell*. 62:1073-1085.
37. Russell, D. W., W. J. Schneider, T. Yamamoto, K. L. Luskey, M. S. Brown, and J. L. Goldstein. 1984. Domain map of the LDL receptor: sequence homology with the epidermal growth factor precursor. *Cell*. 37:577-585.
38. Yamada, N., D. M. Shames, K. Takahashi, and R. J. Havel. 1988. Metabolism of apolipoprotein B-100 in large very low density lipoproteins of blood plasma. *J. Clin. Invest.* 82:2106-2113.
39. Yamada, N., D. M. Shames, and R. J. Havel. 1987. Effect of LDL receptor deficiency on the metabolism of apolipoprotein B-100 in blood plasma: kinetic studies in normal and Watanabe heritable hyperlipidemic rabbits. *J. Clin. Invest.* 80:507-515.
40. Pittman, R. C., T. E. Carew, A. D. Attie, J. L. Witztum, Y. Watanabe, and D. Steinberg. 1982. Receptor-dependent and receptor-independent degradation of low density lipoprotein in normal rabbits and in receptor-deficient mutant rabbits. *J. Biol. Chem.* 257:7994-8000.
41. Spady, D. K., M. Huettinger, D. W. Bilheimer, and J. M. Dietschy. 1987. Role of receptor-independent low density lipoprotein transport in the maintenance of tissue cholesterol balance in the normal and WHHL rabbit. *J. Lipid Res.* 28:32-41.
42. Bilheimer, D. W., N. J. Stone, and S. M. Grundy. 1979. Metabolic studies in familial hypercholesterolemia: evidence for a gene-dosage effect *in vivo*. *J. Clin. Invest.* 64:524-533.
43. James, R. W., B. Martin, D. Pometta, J. C. Fruchart, P. Duriez, P. Fuchois, J. P. Farriaux, A. Tacquet, T. Demant, R. J. Clegg, A. Munro, M. F. Oliver

et al. 1989. Apolipoprotein B metabolism in homozygous familial hypercholesterolemia. *J. Lipid Res.* 30:159-169.

44. Havel, R. J., T. Kita, L. Kotite, J. P. Kane, R. L. Hamilton, J. L. Goldstein, and M. S. Brown. 1982. Concentration and composition of lipoproteins in blood plasma of WHHL rabbits. *Arteriosclerosis*. 3:467-474.

45. Zhang, S. H., R. L. Reddick, J. A. Piedrahita, and N. Maeda. 1992. Spontaneous hypercholesterolemia and arterial lesions in mice lacking apolipoprotein E. *Science (Wash. DC)*. 258:468-471.

46. Plump, A. S., J. D. Smith, T. Hayek, K. Aalto-Setälä, A. Walsh, J. G. Verstuyft, E. M. Rubin, and J. L. Breslow. 1992. Severe hypercholesterolemia and atherosclerosis in apolipoprotein E deficient mice created by homologous recombination in ES cells. *Cell*. 71:343-353.

47. Schaefer, E. J., R. E. Gregg, G. Ghiselli, T. M. Forte, J. M. Ordovas, L. A. Zech, and H. B. Brewer, Jr. 1986. Familial apolipoprotein E deficiency. *J. Clin. Invest.* 78:1206-1219.

48. Kovanen, P. T., M. S. Brown, S. K. Basu, D. W. Bilheimer, and J. L. Goldstein. 1981. Saturation and suppression of hepatic lipoprotein receptors: a

mechanism for the hypercholesterolemia of cholesterol-fed rabbits. *Proc. Natl. Acad. Sci. USA*. 78:1396-1400.

49. Spady, D. K., and J. M. Dietschy. 1988. Interaction of dietary cholesterol and triglycerides in the regulation of hepatic low density lipoprotein transport in the hamster. *J. Clin. Invest.* 81:300-309.

50. Ginsberg, H. S., L. L. Moldawer, P. B. Sehgal, M. Redington, P. L. Kilian, R. M. Chanock, and G. A. Prince. 1991. A mouse model for investigating the molecular pathogenesis of adenovirus pneumonia. *Proc. Natl. Acad. Sci. USA*. 88:1651-1655.

51. Kowal, R. C., J. Herz, J. L. Goldstein, V. Esser, and M. S. Brown. 1989. Low density lipoprotein receptor-related protein mediates uptake of cholesteryl esters derived from apoprotein E-enriched lipoproteins. *Proc. Natl. Acad. Sci. USA*. 86:5810-5814.

52. Holmquist, L., K. Carlson, and L. A. Carlson. 1978. Comparison between the use of isopropanol and tetramethylurea for the solubilisation and quantitation of human serum very low density apolipoproteins. *Anal. Biochem.* 88:457-460.



# Peroxisome proliferator-activated receptor $\gamma$ ligands inhibit development of atherosclerosis in LDL receptor-deficient mice

Andrew C. Li,<sup>1</sup> Kathleen K. Brown,<sup>2</sup> Mercedes J. Silvestre,<sup>3</sup>  
Timothy M. Willson,<sup>4</sup> Wulf Palinski,<sup>3</sup> and Christopher K. Glass<sup>1,3</sup>

<sup>1</sup>Department of Cellular and Molecular Medicine, University of California, San Diego, La Jolla, California, USA

<sup>2</sup>Department of Metabolic Diseases, Glaxo Wellcome Research and Development, Research Triangle Park, North Carolina, USA

<sup>3</sup>Department of Medicine, University of California, San Diego, La Jolla, California, USA

<sup>4</sup>Department of Medicinal Chemistry, Glaxo Wellcome Research and Development, Research Triangle Park, North Carolina, USA

Address correspondence to: Andrew C. Li, Department of Cellular and Molecular Medicine, University of California, San Diego, 9500 Gilman Drive, La Jolla, California 92093-0651, USA.  
Phone: (858) 534-7559; Fax: (858) 534-8549; E-mail: acl@ucsd.edu.

The Palinski and Glass laboratories contributed equally to this work.

Received for publication May 18, 2000, and accepted in revised form July 5, 2000.

The peroxisome proliferator-activated receptor  $\gamma$  (PPAR $\gamma$ ) is a nuclear receptor that regulates fat-cell development and glucose homeostasis and is the molecular target of a class of insulin-sensitizing agents used for the management of type 2 diabetes mellitus. PPAR $\gamma$  is highly expressed in macrophage foam cells of atherosclerotic lesions and has been demonstrated in cultured macrophages to both positively and negatively regulate genes implicated in the development of atherosclerosis. We report here that the PPAR $\gamma$ -specific agonists rosiglitazone and GW7845 strongly inhibited the development of atherosclerosis in LDL receptor-deficient male mice, despite increased expression of the CD36 scavenger receptor in the arterial wall. The antiatherogenic effect in male mice was correlated with improved insulin sensitivity and decreased tissue expression of TNF- $\alpha$  and gelatinase B, indicating both systemic and local actions of PPAR $\gamma$ . These findings suggest that PPAR $\gamma$  agonists may exert antiatherogenic effects in diabetic patients and provide impetus for efforts to develop PPAR $\gamma$  ligands that separate proatherogenic activities from antidiabetic and antiatherogenic activities.

*J. Clin. Invest.* 106:523-531 (2000).

## Introduction

Complications of atherosclerosis are the leading cause of death in Western societies and have an extremely high incidence in individuals with type 2 diabetes mellitus (1, 2). Atherosclerosis is initiated by the accumulation of plasma LDL in the arterial wall, its oxidation, and the recruitment of circulating monocytes (3, 4). Once monocytes in the arterial intima have undergone phenotypic transformation to macrophages, they take up oxidized LDL (oxLDL) via several scavenger receptors that include scavenger receptor A (SR-A), CD36, and macrophage mannose receptor (5-7). This results in massive cholesterol accumulation and formation of foam cells. Interactions between oxLDL, macrophages, smooth muscle cells infiltrated from the arterial media, and T cells recruited from the circulation result in a chronic inflammatory condition that is thought to influence the further evolution of early atherosclerotic lesions toward more advanced, clinically relevant lesions (8). Interactions between arterial cells are mediated by an array of cytokines and adhesion molecules (9), and increasing experimental evidence suggests that many of these factors promote atherogenesis. For example, hypercholesterolemic mice in which the gene encoding

macrophage chemotactic protein 1 (MCP-1) has been disrupted are resistant to the development of atherosclerosis (10, 11). In analogy, disruption of the SR-A and CD36 genes results in a significant reduction of hypercholesterolemia-induced atherosclerosis in mice (12, 13). These observations suggest that interventions directed at altering the genetic responses of vascular cells to proatherogenic stimuli, such as hypercholesterolemia, may be beneficial.

Several regulatory pathways have been identified that control the expression of potentially atherogenic genes. These include NF- $\kappa$ B, a transcription factor involved in the regulation of many proinflammatory factors and adhesion molecules, such as TNF- $\alpha$  and gelatinase B (14, 15). Recent studies have also documented the expression of the peroxisome proliferator-activated receptor  $\gamma$  (PPAR $\gamma$ ) in macrophage foam cells, endothelial cells, and smooth muscle cells of human and murine atherosclerotic lesions (16-20). PPAR $\gamma$  is a member of the nuclear receptor superfamily of ligand-dependent transcription factors that both positively and negatively regulate gene expression in response to the binding of a number of fatty acid metabolites, including oxidized linoleic acid (9- and 13-HODE) and

15 deoxy  $\Delta^{2,14}$  prostaglandin  $J_2$  (21–23). PPAR $\gamma$  is expressed in many other tissues and is particularly highly expressed in fat. PPAR $\gamma$  promotes adipocyte differentiation in vitro and has recently been shown to be essential for the development of adipose tissue in vivo (24–26). PPAR $\gamma$  also appears to play a critical role in glucose homeostasis, because it is the molecular target of a class of insulin-sensitizing drugs referred to as thiazolidinediones (TZDs) (27).

The biological roles of PPAR $\gamma$  in the macrophage and its effects on atherosclerosis are uncertain. PPAR $\gamma$ -specific ligands have been shown to inhibit the expression of a number of proinflammatory genes, including TNF- $\alpha$ , IL-1 $\beta$ , iNOS, and *gelatinase B* (28, 29). These findings suggested that PPAR $\gamma$  functions as a negative regulator of macrophage activation and that synthetic PPAR $\gamma$  ligands might exert anti-inflammatory and antiatherogenic effects. Consistent with this, PPAR $\gamma$  ligands have recently been shown to inhibit inflammatory bowel disease in a rodent model (30). However, PPAR $\gamma$  has also been shown to stimulate transcription of the *CD36* gene (19, 21). In conjunction with the finding that PPAR $\gamma$  can be activated by 9- and 13-HODE present in oxLDL, a “PPAR $\gamma$  cycle” has been proposed in which oxLDL lipids would induce the activity of PPAR $\gamma$ , leading to increased expression of *CD36*, which in turn would increase the uptake of oxLDL. This cycle would thus promote foam-cell formation and atherosclerosis.

Resolving the question of whether PPAR $\gamma$  agonists promote or inhibit atherosclerosis is of clinical importance because many patients with type 2 diabetes, who are at high risk of developing atherosclerosis and its complications, are currently using PPAR $\gamma$  agonists for the control of hyperglycemia. To determine whether the activation of PPAR $\gamma$  promotes or inhibits the development of atherosclerosis in an animal model, we administered two structurally distinct PPAR $\gamma$ -specific ligands to LDL receptor-deficient (LDLR $^{-/-}$ ) mice fed a Western-style diet and measured their effects on lipid and glucose metabolism, extent of atherosclerosis, and expression of potential target genes in the artery wall. Both PPAR $\gamma$ -specific ligands exerted potent antiatherogenic effects in male mice despite upregulation of *CD36* mRNA. Antiatherogenic effects correlated with improved insulin sensitivity and inhibition of TNF- $\alpha$  and *gelatinase B* expression.

## Methods

**Animals and diet.** A breeding colony was generated from the tenth-generation homozygous LDLR $^{-/-}$  mice in a C57BL/6 background (The Jackson Laboratories, Bar Harbor, Maine, USA). In three separate experiments, three groups of both males and females were matched for age (8 to 12 weeks), plasma cholesterol, and glucose levels before feeding. Four animals were housed per cage and in a facility with an 11-hour light cycle (light, 7 am to 6 pm). All three groups were fed a Western-style diet consisting of 0.01% added cholesterol and 21% milk fat

(TD98338; Harlan-Teklad, Madison, Wisconsin, USA), which induced extensive atherosclerosis in the aortic origin, but not in the descending aorta at 10 weeks. In addition to the diet, one group received rosiglitazone and another group received GW7845. The animals were fed 3–4 g food/mouse/day with a drug delivery of 20 mg/kg of body weight/day. New batches of food/drug were prepared weekly and stored at 4°C. The amount of food given and the food left remaining were weighed daily. The animals were weighed every 2 weeks, and the drug dosages were adjusted accordingly. To induce extensive atherosclerosis in the aorta, in a separate experiment male mice were fed a diet containing 1.25% cholesterol and 21% milk fat (TD96121; Harlan-Teklad) for 4 months. Two weeks before sacrifice, the animals were divided into three groups. A control group received the diet treated only with the solvent, the second group received the diet together with rosiglitazone (20 mg/kg/day), and the third group received the diet and GW7845 (20 mg/kg/day). All animals had ad libitum access to water. The animal experiments were performed according to NIH guidelines and were approved by UCSD's Animal Subjects Committee.

**Glucose, insulin, and lipid levels.** Retro-orbital bleeds were performed before the start of the studies and every 4 weeks thereafter until the animals were sacrificed at 10 weeks. The animals were bled, nonfasted, at 10 am and blood was drawn up in EDTA-coated microcapillary tubes. Plasma was isolated from whole blood and glucose levels were determined, using a Precision QID glucometer (MediSense Inc., Bedford, Massachusetts, USA). Insulin levels were determined using a competitive radioimmunoassay (Linco Research Inc., St. Charles, Missouri, USA). Plasma cholesterol and triglyceride levels were measured by enzymatic methods using an automated bichromatic analyzer (Abbot Diagnostics, Dallas, Texas, USA). To determine the lipoprotein profiles, remaining terminal plasma samples were pooled according to the animals' respective groups, and the cholesterol content of lipoprotein fractions in plasma was determined by FPLC. One hundred milliliters of the pooled plasma was loaded onto a Superose 6B column, and 250  $\mu$ L of sample fractions were collected and analyzed for cholesterol.

**Oral glucose tolerance test.** Two weeks before the mice were sacrificed, oral glucose tolerance tests were performed. Animals were fasted for 4 hours. Animals were gavaged with glucose (0.75 mg/g body weight) using 20% glucose. Blood samples (25  $\mu$ L) were taken at 0, 15, 30, 60, and 90 minutes. Glucose levels were determined in whole blood and insulin levels in plasma.

**Hemoglobin A $_{1c}$ , nonesterified fatty acid, HDL $_c$ , and drug levels.** Whole blood and plasma were sent to Glaxo Wellcome Research Institute (Research Triangle Park, North Carolina, USA) for analysis for HbA $_{1c}$ , HDL $_c$ , and nonesterified fatty acid (NEFA) levels. The plasma was isolated immediately and quickly frozen in liquid nitrogen to prevent the breakdown of NEFA. Drug levels were determined by mass spectrometry.

**Tissue preparation and morphometric analysis of atherosclerotic lesions.** The heart was perfused from its apex with cold PBS treated with diethylpyrocarbonate (DEPC). The heart, containing the aortic origin, was carefully dissected. The upper half of the heart was placed in a fixative containing 4% paraformaldehyde, 5% sucrose in PBS, pH 7.4, and fixed overnight, followed by alcohol dehydration and paraffin embedding. For morphometric determination of atherosclerosis, serial 9- $\mu$ m-thick sections were cut from the apex toward the base of the heart. Sections containing the aortic origin, totaling 180  $\mu$ m in length, were stained with a modified van Gieson's elastin stain to enhance the contrast between the atherosclerotic intima and the surrounding tissue (31). Analysis was performed on every other section ( $n = 8-10$  per mouse). Thus, a total length of 180  $\mu$ m of the aortic origin was examined. Quantification of atherosclerosis was performed using computer-assisted image analysis, as described previously (32). All morphometry was performed by the same investigator blinded to the tissue identity.

**RNA isolation from aortic valves and aortas.** The upper half of the hearts, containing the aortic valves and the aortas, extending from the root to the second intercostal region and up to the carotids, were weighed and flash frozen in liquid nitrogen and stored at  $-80^{\circ}\text{C}$ . Isolation of total RNA was performed using RNeasy kit (QIAGEN Inc., Valencia, California, USA) according to the manufacturer's protocol. Total RNA was treated with deoxyribonuclease I (QIAGEN Inc.) for 20 minutes at room temperature to remove contaminating genomic DNA. The amount of RNA was determined by spectrophotometry, and 200 ng of RNA was loaded onto a 1.5% agarose gel to determine its quality before analysis.

**RT-PCR-based quantitative gene expression analysis.** Real-time detection of PCR was performed at the Center for Aids Research Genomics Core of the Veterans Medical Research Foundation in La Jolla, California, USA. Using the Perkin-Elmer ABI Prism 7700 and Sequence Detection System software (Perkin-Elmer, Foster City, California, USA), the differential displays of mRNAs for TNF- $\alpha$ , MCP-1, VCAM-1, gelatinase B, macrosialin, CD36, and SR-A were determined. Briefly, 1  $\mu$ g of total RNA was used to generate cDNA using an oligo dT oligodeoxynucleotide primer (T<sub>12-18</sub>) following the protocol for Omniscript (QIAGEN Inc.). The following primers and probes were made: TNF- $\alpha$ : 5'CGGAGTC-CGGGCAGGT 3' (forward), 5' GCTGGGTAGAGAATG-GATGAACA 3' (reverse), 5' ACTTTGGAGTCATTGCTCT-GTGAAGGG AATG 3' (probe); MCP-1: 5' CAGCCAGATGCAGTTAACGC 3' (forward), 5' GCC-TACTCATTGGGATCATCTTG 3' (reverse), 5' CCACT-CACCTGCTGCTACTCATTACCA 3' (probe); VCAM-1: 5' TGC GAGTCACCATTTGTTCTCAT 3' (forward), 5' CATGGTCAGAACGGACTTGGGA 3' (reverse), 5' ACCCA-GATAGACAGCCCACTAAACGCGAA 3' (probe); gelatinase B: 5' TCACCTTACCCGCGTGTA 3' (forward), 5' GTGCTCCGCGACACCAA 3' (reverse), 5' ACCGAAGCG-

GACATTGTCATCCAG 3' (probe); macrosialin: 5' CAAG-GTCCAGGGAGG TTGTG 3' (forward), 5' CCAAAG-GTAAGCTGTCCATAAGGA 3' (reverse), 5' CGGTACC-CATCCCCACCTGTCTCTCTC 3' (probe); CD36: 5' TCCAGCCCAATGCCTTTGC 3' (forward), 5' TGGAGAT-TACTTTTCAGTGCAGAA 3' (reverse), 5' TCACCCCTCCA-GAATCCAGACAACCA 3' (probe); SR-A: 5' CATGAACGA-GAGGATGCTGACT 3' (forward), 5' GGAAGGGATGCTGTCATTGAA 3' (reverse), 5' CAGTTCAGAATCCGTGAAATTTGACGCAC 3' (probe); and GAPDH: 5' CCACCCATGGCAAATTC 3' (forward), 5' TGGGATTTCATTGATGACAAG 3' (reverse), 5' TGGCACCGTCAAGGCTGAGAACG 3' (probe). Equal amounts of cDNA were used in triplicate and amplified with the Taqman Master Mix provided by Perkin-Elmer. Amplification efficiencies were validated and normalized against GAPDH and nanograms of product were calculated using the standard curve method for quantitation against cDNA that was reverse transcribed from isolated aortas of LDLR $^{-/-}$  mice fed a 1.25% cholesterol and 21% milk-fat diet for 4 months. Total RNA that was not reverse transcribed was also analyzed to determine genomic DNA contamination.

**Statistical analysis.** Groups were compared by ANOVA and unpaired  $t$  tests using the StatView analysis program (SAS Institute Inc., Cary, North Carolina, USA). Data are expressed as the mean plus or minus SEM.

## Results

Intervention studies were performed in LDLR $^{-/-}$  mice fed a Western-style diet for 10 weeks, starting at age 8–12 weeks. To reduce the possibility that effects of a single PPAR $\gamma$  ligand on atherosclerosis resulted from PPAR $\gamma$ -independent mechanisms, two distinct PPAR $\gamma$  agonists were used: rosiglitazone and GW7845. Rosiglitazone is a member of the TDZ class of insulin sensitizers that was developed using rodent models of type 2 diabetes. It has an effective concentration of 50% (EC<sub>50</sub>) for murine PPAR $\gamma$  of 76 nM (33). GW7845 is a member of the tyrosine-based class of insulin sensitizers that was developed using human PPAR $\gamma$  as a molecular target. It has an EC<sub>50</sub> for murine PPAR $\gamma$  of 1.2 nM (33). Both drugs are highly specific for PPAR $\gamma$ , with EC<sub>50</sub> for PPAR $\alpha$  and PPAR $\delta$  in excess of 10  $\mu$ M (33). We initially performed a pilot study using a calculated dose of 20 mg rosiglitazone/kg/day to establish appropriate dietary cholesterol content and extent of atherosclerosis. Rosiglitazone exerted a significant antiatherogenic effect in male mice in this study, but not in female mice (data not shown). However, because the 1.25% added dietary cholesterol resulted in serum cholesterol levels in excess of 2,000 mg/dL, a potential protective effect in females could have been overwhelmed. Two subsequent intervention studies were therefore carried out in which the added cholesterol was reduced to 0.01%. Each experiment resulted in the same pattern of responses to dietary and drug treatments, and the data from the two studies were pooled to increase statistical power.

**Table 1**  
Average weights, cholesterol, triglyceride, and HDL<sub>c</sub> levels

	Weight g	Total Cholesterol mg/dL	Triglycerides mg/dL	HDL <sub>c</sub> mg/dL		Weight g	Total Cholesterol mg/dL	Triglycerides mg/dL	HDL <sub>c</sub> mg/dL
<b>Males</b>					<b>Females</b>				
<b>Control (n = 10)</b>					<b>Control (n = 10)</b>				
T = 0 weeks	24.4 ± 0.8	258 ± 11	128 ± 17		T = 0 weeks	19.0 ± 0.7	235 ± 12	37 ± 12	
T = 4 weeks	36.7 ± 1.2	1258 ± 143	1150 ± 195		T = 4 weeks	24.1 ± 1.9	1053 ± 97	576 ± 258	
T = 8 weeks	38.9 ± 1.3	1552 ± 83	1279 ± 170		T = 8 weeks	27.2 ± 1.3	1211 ± 68	621 ± 207	
T = 10 weeks	42.5 ± 1.4	1549 ± 89	1226 ± 153	127 ± 5	T = 10 weeks	28.4 ± 1.7	1240 ± 109	722 ± 241	115 ± 4
<b>Ro (n = 12)</b>					<b>Ro (n = 10)</b>				
T = 0 weeks	26.1 ± 0.9	245 ± 10	121 ± 20		T = 0 weeks	20.4 ± 0.5	242 ± 6	47 ± 11	
T = 4 weeks	36.7 ± 1.3	1258 ± 103	1150 ± 265		T = 4 weeks	23.7 ± 1.1	1027 ± 6	624 ± 24	
T = 8 weeks	38.6 ± 1.4	1371 ± 72	1366 ± 134		T = 8 weeks	27.6 ± 1.1	1395 ± 81	1000 ± 107	
T = 10 weeks	40.4 ± 1.3	1440 ± 69	1541 ± 126	115 ± 4 <sup>A</sup>	T = 10 weeks	29.7 ± 1.3	1513 ± 55 <sup>A</sup>	1251 ± 69 <sup>B</sup>	96 ± 3 <sup>B</sup>
<b>GW7845 (n = 10)</b>					<b>GW7845 (n = 7)</b>				
T = 0 weeks	26.3 ± 0.9	249 ± 9	116 ± 22		T = 0 weeks	20.0 ± 0.8	232 ± 11	48 ± 12	
T = 4 weeks	33.5 ± 3.5	1275 ± 168	1406 ± 276		T = 4 weeks	25.0 ± 1.1	1139 ± 82	927 ± 145	
T = 8 weeks	39.9 ± 1.0	1533 ± 81	1790 ± 184		T = 8 weeks	28.6 ± 1.2	1395 ± 90	1049 ± 131	
T = 10 weeks	41.7 ± 2.2	1626 ± 109	1507 ± 200	123 ± 3	T = 10 weeks	28.5 ± 1.4	1449 ± 136	1228 ± 157 <sup>B</sup>	104 ± 4 <sup>A</sup>

Data are expressed as the mean ± SEM; n represents the number of mice per group. Values were determined in plasma samples from nonfasting animals. Ro, rosiglitazone. <sup>A</sup>P < 0.05 and <sup>B</sup>P < 0.005, drug treatment group vs. control group.

At a dose of 20 mg/kg/day, rosiglitazone plasma levels averaged 6.4 plus or minus 0.06 µg/mL in male mice and 5.1 plus or minus 0.69 µg/mL in female mice at 10 weeks. GW7845 levels averaged 3.2 plus or minus 0.39 µg/mL in male mice and 3.2 plus or minus 0.46 µg/mL in female mice after 10 weeks of treatment. These serum levels are sufficient to exert inhibitory effects on proinflammatory gene expression *in vitro* (29). All animals appeared healthy throughout the study. Serum aspartate aminotransferase and alkaline phosphatase levels were used to assess potential liver toxicity and were not altered at the end of the study (data not shown). Histologic analysis of the bone marrow indi-

cated a significant increase in percentage of marrow fat, and marked extramedullary hematopoiesis was observed in both male and female mice (data not shown). There were no significant changes in complete blood counts or hemoglobin. Data for body weight, total cholesterol, triglycerides, and HDL<sub>c</sub> at specific time points are presented in Table 1. The body weights in all groups increased during the intervention period, but the relative weight gain in males was greater than that in females. The Western diet resulted in a marked increase in total cholesterol within 1 month; the total cholesterol then remained constant at approximately 1,500 mg/dL in males. There was a slight increase in

**Table 2**  
Average glucose, insulin, HbA<sub>1c</sub>, NEFA levels

	Glucose mg/dL	Insulin ng/mL	Hb A <sub>1c</sub> %	NEFA mEq/L		Glucose mg/dL	Insulin ng/mL	Hb A <sub>1c</sub> %	NEFA mEq/L
<b>Males</b>					<b>Females</b>				
<b>Control (n = 10)</b>					<b>Control (n = 10)</b>				
T = 0 weeks	307 ± 20	1.12 ± 0.17	5.50 ± 0.16		T = 0 weeks	267 ± 11	0.55 ± 0.04	5.57 ± 0.15	
T = 4 weeks	211 ± 24	1.38 ± 0.25	5.62 ± 0.11		T = 4 weeks	299 ± 14	1.48 ± 0.18	5.39 ± 0.05	
T = 8 weeks	245 ± 14	4.18 ± 0.41	5.29 ± 0.07		T = 8 weeks	273 ± 21	1.95 ± 0.49	4.96 ± 0.10	
T = 10 weeks	344 ± 22	4.24 ± 0.30	5.31 ± 0.13	0.60 ± 0.06	T = 10 weeks	347 ± 16	1.44 ± 0.30	5.11 ± 0.16	0.64 ± 0.06
<b>Ro (n = 12)</b>					<b>Ro (n = 10)</b>				
T = 0 weeks	282 ± 13	0.95 ± 0.08	5.46 ± 0.11		T = 0 weeks	250 ± 8	0.63 ± 0.13	5.39 ± 0.15	
T = 4 weeks	211 ± 11	1.38 ± 0.11	5.62 ± 0.11		T = 4 weeks	210 ± 10	0.75 ± 0.05	5.78 ± 0.03	
T = 8 weeks	207 ± 8	2.03 ± 0.44	5.08 ± 0.13		T = 8 weeks	216 ± 10	1.91 ± 0.53	4.94 ± 0.09	
T = 10 weeks	315 ± 10	1.45 ± 0.33 <sup>B</sup>	4.91 ± 0.12 <sup>A</sup>	0.65 ± 0.04	T = 10 weeks	312 ± 11	0.93 ± 0.33	4.87 ± 0.07	0.85 ± 0.11
<b>GW7845 (n = 10)</b>					<b>GW7845 (n = 7)</b>				
T = 0 weeks	317 ± 8	1.01 ± 0.18	5.78 ± 0.06		T = 0 weeks	261 ± 14	0.94 ± 0.13	5.20 ± 0.16	
T = 4 weeks	211 ± 13	1.54 ± 0.49	5.76 ± 0.11		T = 4 weeks	225 ± 16	1.07 ± 0.15	5.47 ± 0.12	
T = 8 weeks	204 ± 14	2.01 ± 0.32	5.32 ± 0.09		T = 8 weeks	190 ± 6	1.75 ± 0.59	4.75 ± 0.07	
T = 10 weeks	311 ± 13	1.65 ± 0.36 <sup>B</sup>	4.81 ± 0.16 <sup>A</sup>	0.63 ± 0.05	T = 10 weeks	311 ± 13	1.29 ± 0.37	4.80 ± 0.16	0.81 ± 0.08

Data are expressed as the mean ± SEM; n represents the number of mice per group. Values were determined in plasma samples from nonfasting animals. Ro, rosiglitazone. <sup>A</sup>P < 0.05 and <sup>B</sup>P < 0.005, drug treatment group vs. control group.

cholesterol levels of treated females, but this effect only reached statistical significance ( $P = 0.05$ ) in the rosiglitazone treatment group after 10 weeks. Triglycerides were significantly increased and HDL<sub>c</sub> levels were decreased in female mice treated with rosiglitazone or GW7845. A decrease in HDL<sub>c</sub> levels was seen in male mice treated with rosiglitazone only.

**PPAR $\gamma$  ligands inhibit the development of atherosclerosis in male mice.** Atherosclerosis at the aortic origin was determined by computer-assisted image analysis as described previously (32). Male and female control animals exhibited similar levels of atherosclerosis. Lesions were observed underneath most of the valve leaflets, with some lesions exhibiting areas of central necrosis (Figure 1a). Macroscopically detectable lesions were generally absent from the thoracic or abdominal aorta (data not shown). Markedly fewer and smaller lesions were found in male mice that were treated with either rosiglitazone or GW7845, with quantitative analysis indicating a 60 to 80% reduction in lesion area (Figure 1b). In contrast, the extent of atherosclerosis in female mice treated with either rosiglitazone or GW7845 was not statistically different from that in control mice, confirming the findings of the initial pilot study.

**Metabolic effects of PPAR $\gamma$  ligands.** To investigate possible mechanisms accounting for antiatherogenic effects of PPAR $\gamma$  ligands in male mice and lack of these effects in female mice, lipoprotein levels were evaluated in control and treatment groups. Fast-performance liquid chromatography (FPLC) analysis of pooled terminal serum samples indicated that GW7845 and rosiglitazone had no effect on the lipoprotein profile in male mice (Figure 2a). In contrast, in female mice the VLDL, IDL, and LDL fractions were increased and the HDL fraction decreased in both the rosiglitazone and GW7845 treatment groups (Figure 2b).

Effects of PPAR $\gamma$  ligands on serum glucose, insulin, HbA<sub>1c</sub>, and NEFA levels are presented in Table 2. The Western diet itself did not significantly alter glucose, HbA<sub>1c</sub>, or NEFA levels, but insulin levels rose in both male and female mice. Rosiglitazone and GW7845 treatment resulted in a significant decrease in insulin levels in male mice but had no significant effect on insulin levels in female mice (Table 2). HbA<sub>1c</sub> decreased in males treated with rosiglitazone and GW7845.

To further investigate the effects of rosiglitazone and GW7845 on glucose homeostasis, the response to an oral glucose challenge was assessed in LDLR<sup>-/-</sup> mice fed the Western diet for 8 weeks. LDLR<sup>-/-</sup> mice fed a nor-

mal chow diet were used as additional control groups. Mice were fasted for 4 hours before being given an oral glucose load of 0.75 mg/g. Blood samples were taken at 0, 15, 30, 60, and 90 minutes for measurement of glucose and insulin levels. In male mice, the Western diet had relatively little effect on glucose levels in response to the oral glucose challenge (Figure 3a). In female mice, after glucose administration, the Western diet resulted in modest elevations in glucose that were normalized by treatment with either rosiglitazone or GW7845 (Figure 3b). Striking differences in the insulin responses to oral glucose challenge were noted between

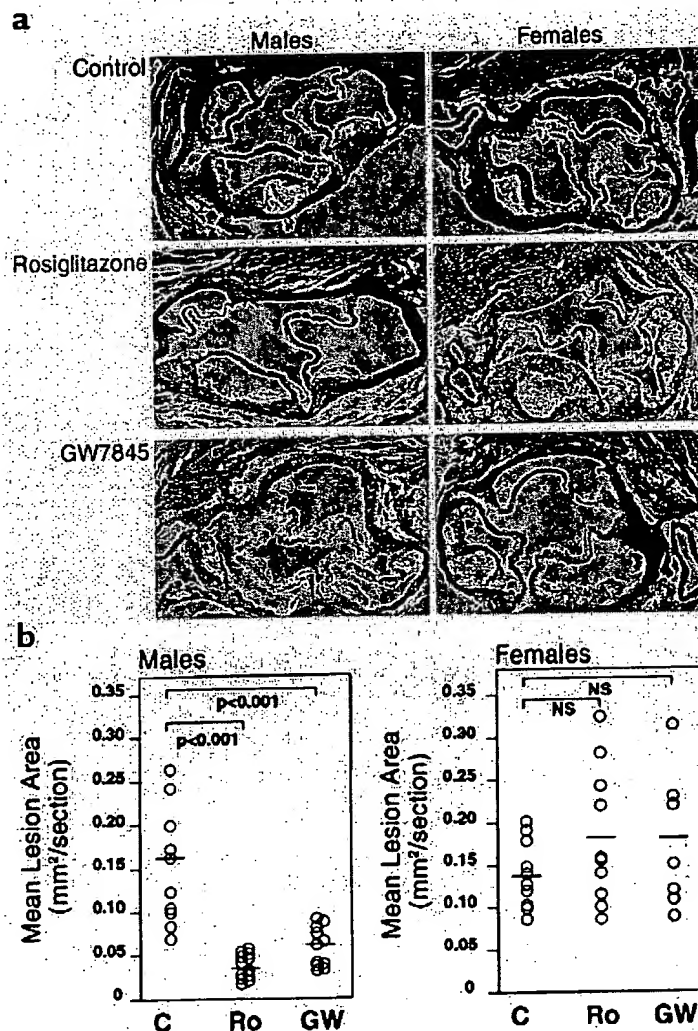


**Figure 1**

Atherosclerosis in LDLR<sup>-/-</sup> mice fed a high-fat, cholesterol-enriched Western diet for 10 weeks. (a) Sections through the aortic root at the levels of the aortic valves were stained for elastin to highlight the medial boundaries of atherosclerotic lesions. (b) Quantitative analysis of lesion areas in control mice (C), mice treated with rosiglitazone (Ro), and mice treated with GW7845 (GW). For male mice, means  $\pm$  SEM were: C,  $0.161 \pm 0.067$  mm<sup>2</sup>/section ( $n = 10$ ); Ro,  $0.037 \pm 0.014$  mm<sup>2</sup>/section ( $n = 12$ ); GW,  $0.063 \pm 0.027$  mm<sup>2</sup>/section ( $n = 10$ ). For female mice, means  $\pm$  SEM were: C,  $0.131 \pm 0.035$  mm<sup>2</sup>/section ( $n = 10$ ); Ro,  $0.183 \pm 0.088$  mm<sup>2</sup>/section ( $n = 10$ ); GW,  $0.181 \pm 0.0091$  mm<sup>2</sup>/section ( $n = 10$ ). NS, not statistically significant.

male and female mice treated with rosiglitazone and GW7845. The Western diet resulted in increased fasting insulin levels in both male and female mice (Figure 3, c and d), compared with the chow-fed controls. Treatment with rosiglitazone or GW7845 resulted in normalization of the fasting insulin levels and the insulin response to glucose challenge in male mice, but not in female mice (Figure 3, c and d), consistent with changes in insulin levels observed in the intervention studies (Table 2).

**Effects of PPAR $\gamma$  ligands on gene expression.** To investigate potential effects of PPAR $\gamma$  ligands on patterns of gene expression within the arterial wall, RNA analysis was performed in LDLR $^{-/-}$  mice fed a Western diet for 10 weeks in the absence or presence of rosiglitazone or GW7845 as described for the intervention studies. RNA was isolated from the base of the heart containing the aortic origin affected by atherosclerosis and analyzed for TNF- $\alpha$ , MCP-1, VCAM-1, and gelatinase B mRNA levels, using quantitative real-time PCR. TNF- $\alpha$  and

gelatinase B mRNA levels were significantly lower in male mice treated with rosiglitazone or GW7845 (Figure 4). Decreases in TNF- $\alpha$  and gelatinase B were smaller in female mice and did not reach statistical significance in the case of gelatinase B. Levels of VCAM-1 and MCP-1, which are thought to be involved in monocyte adhesion to the vessel wall and migration into the lesion, respectively (34), did not change significantly among the groups (Figure 4). Reductions in TNF- $\alpha$  and gelatinase B mRNA levels were also observed in RNA prepared from the apex of the heart, suggesting general effects of the PPAR $\gamma$  ligands (data not shown). Differences in the responses of TNF- $\alpha$  and gelatinase B genes to PPAR $\gamma$  ligand between male and female mice were not likely due to differences in PPAR $\gamma$  expression, because PPAR $\gamma$  mRNA levels were approximately two times higher in female tissues (data not shown).

Because there were significant differences in lesion size in male controls and animals treated with solvent, rosiglitazone, or GW7845, we also investigated whether PPAR $\gamma$  ligands altered levels of gene expression in the artery wall under conditions of equivalent degrees of atherosclerosis. LDLR $^{-/-}$  male mice were fed a 1.25% cholesterol and 21% milk-fat diet for 16 weeks to induce significant atherosclerosis in the aortic arch. Mice were then treated with rosiglitazone, GW7845, or control solvent for 2 weeks while maintaining the high-fat, high-cholesterol diet. Aortas were dissected and weighed to confirm comparable levels of atherosclerosis (35). As an additional control group, mRNA was isolated from aortas of normocholesterolemic animals. The aortas from each group were pooled, and mRNA was isolated for analysis of macrophage-specific membrane glycoprotein that serves as a marker of tissue macrophages (36). Macrophage expression was low in normal aortas, as expected. Macrophage levels were not significantly altered by 2 weeks of treatment with rosiglitazone or GW7845, consistent with our observation that PPAR $\gamma$  ligands do not alter macrophage expression in peritoneal macrophages (data not shown) and reflecting comparable levels of atherosclerosis in these three groups. SR-A and MCP-1 mRNA levels were also elevated in atherosclerotic aortas, as expected. Surprisingly, the mRNA levels for VCAM-1 remained unchanged. In contrast to previous findings in cell-culture models (29, 37), mRNA levels for these genes were not decreased by treatment with PPAR $\gamma$  ligands. However, treatment with rosiglitazone or GW7845 significantly increased CD36 expression and inhibited TNF- $\alpha$  expression, indicating actions of PPAR $\gamma$  on gene expression in the artery wall. The effects on CD36 expression were tissue specific, because no increase in CD36 expression was observed in cardiac tissue of mice treated with rosiglitazone or GW7845 (data not shown).

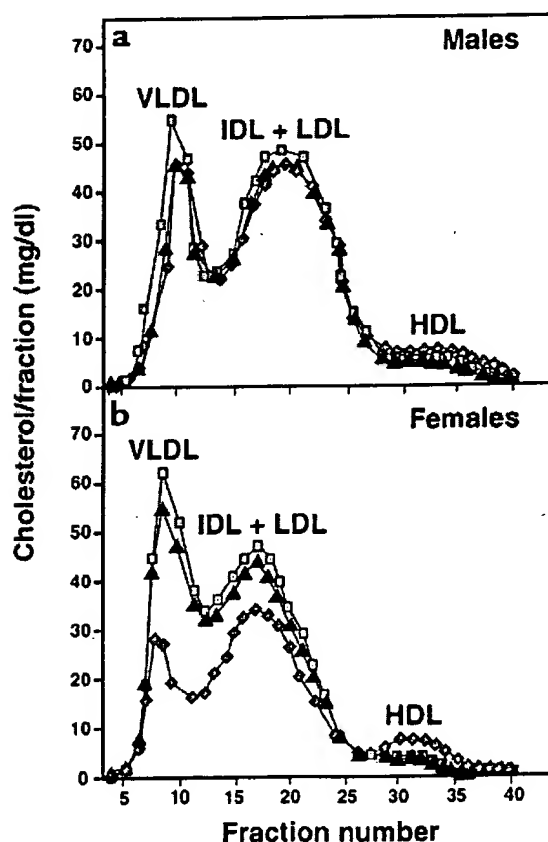
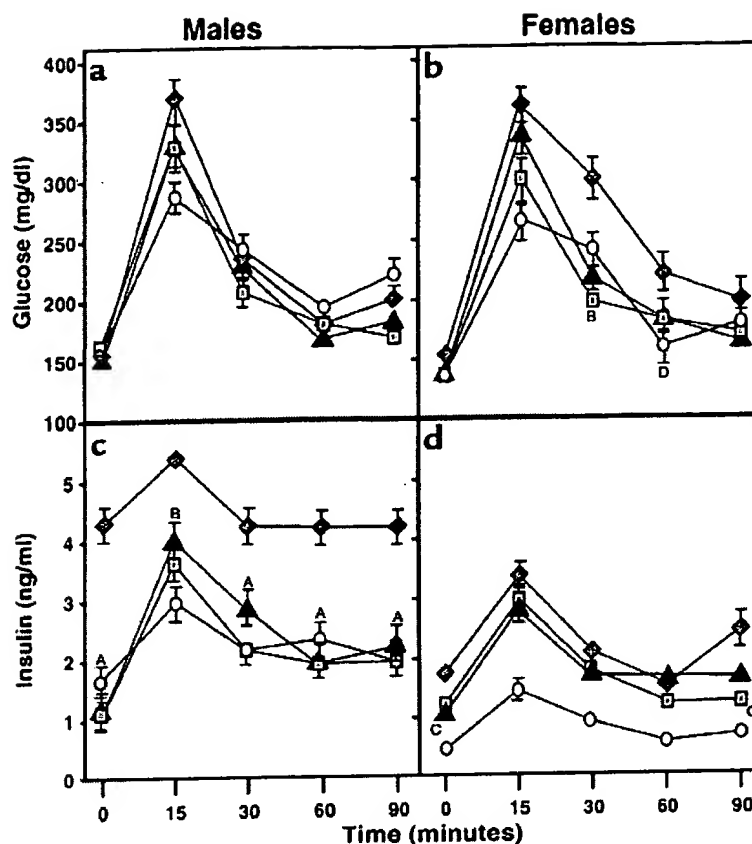


**Figure 2**  
Size distribution of lipoprotein particles in LDLR $^{-/-}$  mice fed a high-fat, cholesterol-enriched diet and treated with solvent (control; diamonds), rosiglitazone (squares), or GW7845 (triangles) for 10 weeks. Plasma was pooled from four mice from each treatment group and fractionated by FPLC. Mean cholesterol content in each fraction was determined in duplicate.

**Figure 3**

Glucose and insulin responses to an oral glucose challenge in LDLR<sup>-/-</sup> mice fed the normal chow (circles); high-fat, cholesterol-enriched diet and solvent (control; diamonds); rosiglitazone (squares); or GW7845 (triangles). Blood glucose and plasma insulin levels were determined at base line (after a 4-hour fast) and 15, 30, 60, and 90 minutes after oral administration of 0.75 mg glucose/g body weight. Samples were taken from eight animals per group. Data are expressed as the mean  $\pm$  SEM. <sup>A</sup>*P* < 0.0001, <sup>B</sup>*P* < 0.002, <sup>C</sup>*P* < 0.015, and <sup>D</sup>*P* < 0.04, drug treatment group vs. control group.



## Discussion

The present studies demonstrate that PPAR $\gamma$  ligands significantly inhibit the development of atherosclerosis in LDLR<sup>-/-</sup> male mice fed a Western-style diet. These mice, in addition to being hypercholesterolemic, were obese, hypertriglyceridemic, and insulin resistant. They thus exhibit clinical features of many human diabetic patients who are candidates for treatment with PPAR $\gamma$  ligands. Rosiglitazone and GW7845 reduced the extent of atherosclerosis despite a significant increase in the expression of CD36 in the vessel wall. These observations suggest that the potential of PPAR $\gamma$  ligands to promote the development of foam cells by upregulation of CD36 is overcome by other systemic and local actions. Several mechanisms could potentially account for the net antiatherosclerotic effects of rosiglitazone and GW7845. A number of proinflammatory cytokines, including TNF- $\alpha$ , IL-1 $\alpha$ , and IL-1 $\beta$ , have been suggested to promote the development of atherosclerosis (38). Systemic reductions in the circulating levels of these cytokines or reductions in their expression within cells of the artery wall could potentially underlie at least some of the antiatherosclerotic effects of rosiglitazone and GW7845. Although previous studies have suggested effects of PPAR $\gamma$  ligands on MCP-1 expression in macrophages and smooth muscle cells and VCAM-1 expression in endothelial cells (18, 39–41), we did not observe significant alter-

ations in VCAM-1 or MCP-1 expression in mice treated with PPAR $\gamma$  agonists. This may reflect the cellular heterogeneity of the aortic origin and vessel wall from which RNA was isolated for analysis. The antiatherogenic effects of rosiglitazone and GW7845 in male mice also correlated with improved insulin sensitivity. However, to date, no experimental evidence for a direct influence of insulin resistance on atherosclerosis has been provided in humans or murine models (42). Further investigation will be required to establish the major mechanisms underlying the therapeutic effects of PPAR $\gamma$  ligands in this model system.

Intriguingly, female mice did not exhibit a reduction in atherosclerosis in response to PPAR $\gamma$ -specific ligands. This lack of a response was not due to altered drug levels or differences in levels of PPAR $\gamma$  expression in the artery wall. Rosiglitazone and GW7845 were less effective in correcting hyperinsulinemia in female mice and did not influence the expression of gelatinase B or TNF- $\alpha$  in tissues. In contrast to male mice, PPAR $\gamma$  ligands altered the lipoprotein size distribution in female mice, reducing HDL levels and skewing the profile to larger particles. Reductions in HDL levels could potentially account for lack of effect of rosiglitazone and GW7845 on the extent of atherosclerosis, but the lack of effect on gelatinase B and TNF- $\alpha$  levels suggest gender-specific differences in the responses to

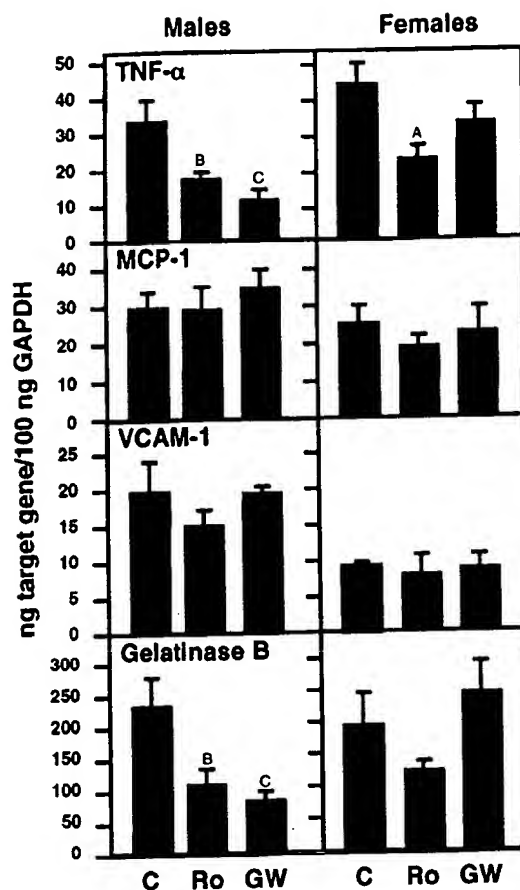


**Figure 4**

Expression of TNF- $\alpha$ , MCP-1, VCAM-1, and gelatinase B mRNA in the aortic root. The mRNA levels were quantitated using real-time RT-PCR. Six to seven samples per group were analyzed. C, control; Ro, rosiglitazone; GW, GW7845. Data are expressed as mean  $\pm$  SEM. <sup>A</sup> $P < 0.05$ , <sup>B</sup> $P < 0.01$ , and <sup>C</sup> $P < 0.001$ , drug treatment groups vs. cholesterol group.

PPAR $\gamma$  ligands. The basis for these differences is unclear, but they are likely to relate to influences of estrogens and progestins. Consistent with this, preliminary studies of ovariectomized female mice indicate metabolic responses to rosiglitazone and GW7845 that are much more similar to male mice. Studies of the efficacy of TZDs as insulin sensitizers in human diabetic patients have not revealed any significant gender-specific differences, but most female patients enrolled in these studies are postmenopausal.

In concert, these studies provide clear evidence that activation of PPAR $\gamma$  inhibits the development of atherosclerosis in a murine model. These effects were observed using relatively high doses of PPAR $\gamma$  ligands that also induced adipogenesis in bone marrow and secondary extramedullary hematopoiesis. Extending this proof of principle to human populations will require clinical investigation in diabetic and nondiabetic patients. Because the PPAR $\gamma$  agonists used in these studies exerted both potentially antiatherogenic (e.g., down-regulation of TNF- $\alpha$ ) and potentially proatherogenic (e.g., upregulation of CD36) effects on patterns of gene expression in the artery wall, the development of novel PPAR $\gamma$  ligands that dissociate proatherogenic activities from antidiabetic and antiatherogenic activities would be highly desirable. Recent successes in the development of selective estrogen receptor modulators (43) suggest that such goals are attainable.

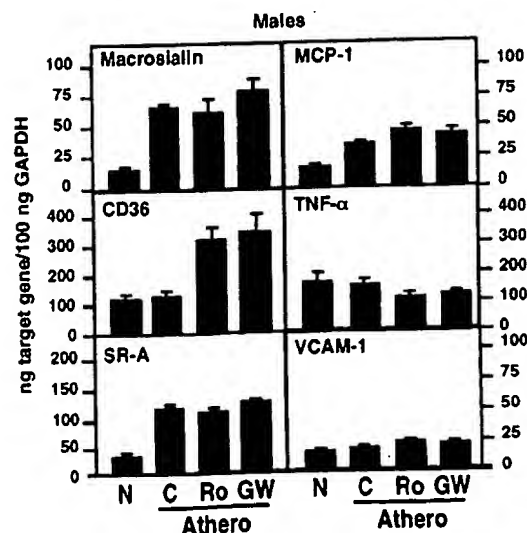


#### Acknowledgments

We wish to thank Florencia Casanada, Jennifer Patterson, and Joseph Juliano for isolating the aortas and determining the plasma cholesterol and triglycerides; Jane Binz and Jennifer Becker for HbA<sub>1c</sub>, NEFA, and HDL<sub>c</sub> analysis; Harry Marr for drug level determination; Jacques Corbeil and Christine Plotkin at the

**Figure 5**

Expression of macrophage markers, MCP-1, TNF- $\alpha$ , and VCAM-1 mRNA in the aorta. Male LDLR<sup>-/-</sup> mice were fed either a normal chow diet (N) or a high-cholesterol diet for 4 months to induce the development of atherosclerosis (Athero). Animals fed the high-cholesterol diet were then treated with either solvent control, rosiglitazone, or GW7845 for 2 weeks. The mRNA levels were quantitated using real-time RT-PCR. Data represent pooled aortas with an average weight of  $3.86 \pm 0.16$  mg/aorta for normal chow (N) ( $n = 11$ );  $5.75 \pm 0.67$  mg/aorta for high cholesterol (C) ( $n = 6$ );  $5.67 \pm 0.56$  mg/aorta for high cholesterol/rosiglitazone (Ro) ( $n = 6$ ); and  $5.80 \pm 0.70$  mg/aorta for high cholesterol/GW7845 (GW) ( $n = 6$ ). Data are in triplicates and expressed as mean  $\pm$  SEM.



Center for AIDS Research Genomics Core, Veterans Medical Research Foundation for advice and performing the RT-PCR quantification analysis; and Tanya Schneiderman and Amy Johnson for their assistance in preparing the manuscript. This work was supported by NIH Specialized Center of Research (SCOR) on Molecular Medicine and Atherosclerosis grant (HL-56989) and a grant from the Glaxo Wellcome Research Institute. A.C. Li is supported by a Mentored-Clinical Scientist Development Award (HL-03625). C.K. Glass is an Established Investigator of the American Heart Association.

- Kannel, W., and McGee, D. 1979. Diabetes and cardiovascular disease: the Framingham study. *JAMA*. 241:2035-2038.
- Uusitupa, M., Niskanen, L., and Siitonen, O. 1990. 5-year incidence of atherosclerotic vascular disease in relation to general risk factors, insulin levels, and abnormalities in lipoprotein composition in non-insulin-dependent diabetic and nondiabetic subjects. *Circulation*. 82:27-36.
- Steinberg, D., Parthasarathy, S., Carew, T.E., Khoo, J.C., and Witztum, J.L. 1989. Beyond cholesterol. Modifications of low-density lipoprotein that increase its atherogenicity. *N. Engl. J. Med.* 320:915-924.
- Napoli, C., et al. 1997. Fatty streak formation occurs in human fetal aortas and is greatly enhanced by maternal hypercholesterolemia. Intimal accumulation of low density lipoprotein and its oxidation precede monocyte recruitment into early atherosclerotic lesions. *J. Clin. Invest.* 100:2680-2690.
- Kodama, T., Reddy, P., Kishimoto, C., and Krieger, M. 1988. Purification and characterization of a bovine acetyl low density lipoprotein receptor. *Proc. Natl. Acad. Sci. USA*. 85:9238-9242.
- Endemann, G., et al. 1993. CD36 is a receptor for oxidized low density lipoprotein. *J. Biol. Chem.* 268:11811-11816.
- Ramprasad, M.P., Terpstra, V., Kondratenko, N., Quehenberger, O., and Steinberg, D. 1996. Cell surface expression of mouse macrophage and human CD68 and their role as macrophage receptors for oxidized low density lipoprotein. *Proc. Natl. Acad. Sci. USA*. 93:14833-14838.
- Ross, R. 1986. The pathogenesis of atherosclerosis. *N. Engl. J. Med.* 314:488-500.
- Ross, R. 1999. Atherosclerosis: an inflammatory disease. *N. Engl. J. Med.* 340:115-126.
- Boring, L., Gosling, J., Cleary, M., and Charo, I.F. 1998. Decreased lesion formation in CCR2<sup>-/-</sup> mice reveals a role for chemokines in the initiation of atherosclerosis. *Nature*. 394:894-897.
- Gosling, J., et al. 1999. MCP-1 deficiency reduces susceptibility to atherosclerosis in mice that overexpress human apolipoprotein B. *J. Clin. Invest.* 103:773-778.
- Suzuki, H., et al. 1997. A role for macrophage scavenger receptors in atherosclerosis and susceptibility to infection. *Nature*. 386:292-296.
- Febbraio, M., et al. 2000. Targeted disruption of the class B scavenger receptor CD36 protects against atherosclerotic lesion development in mice. *J. Clin. Invest.* 105:1049-1056.
- Barnes, P.J., and Karin, M. 1997. Nuclear factor-kappaB: a pivotal transcription factor in chronic inflammatory diseases. *N. Engl. J. Med.* 336:1066-1071.
- Sato, H., Kita, M., and Seiki, M. 1993. v-Src activates the expression of 92-kDa type IV collagenase gene through the AP-1 site and the GT box homologous to retinoblastoma control elements. A mechanism regulating gene expression independent of that by inflammatory cytokines. *J. Biol. Chem.* 268:23460-23468.
- Ricote, M., et al. 1998. Expression of the peroxisome proliferator-activated receptor  $\gamma$  (PPAR $\gamma$ ) in human atherosclerosis and regulation in macrophages by colony stimulating factors and oxidized low density lipoprotein. *Proc. Natl. Acad. Sci. USA*. 95:7614-7619.
- Marx, N., Sukhova, G., Murphy, C., Libby, P., and Plutsky, J. 1998. Macrophages in human atheroma contain PPAR $\gamma$ : differentiation-dependent peroxisomal proliferator-activated receptor gamma expression and reduction of MMP-9 activity through PPAR $\gamma$  activation in mononuclear phagocytes *in vitro*. *Am. J. Pathol.* 153:17-23.
- Jackson, S.M., et al. 1999. Peroxisome proliferator-activated receptor activators target human endothelial cells to inhibit leukocyte-endothelial cell interaction. *Arterioscler. Thromb. Vasc. Biol.* 19:2094-2104.
- Tontonoz, P., Nagy, L., Alvarez, J.G.A., Thomazy, V.A., and Evans, R.M. 1998. PPAR $\gamma$  promotes monocyte/macrophage differentiation and uptake of oxidized LDL. *Cell*. 93:241-252.
- Pasceri, V., Wu, H.D., Willerson, J.T., and Yeh, E.T. 2000. Modulation of vascular inflammation *in vitro* and *in vivo* by peroxisome proliferator-activated receptor-gamma activators. *Circulation*. 101:235-238.
- Nagy, L., Tontonoz, P., Alvarez, J.G.A., Chen, H., and Evans, R.M. 1998. Oxidized LDL regulates macrophage gene expression through ligand activation of PPAR-gamma. *Cell*. 93:229-240.
- Forman, B.M., et al. 1995. 15-Deoxy- $\Delta^{12,14}$ -prostaglandin J<sub>2</sub> is a ligand for the adipocyte determination factor PPAR $\gamma$ . *Cell*. 83:803-812.
- Kliwer, S.A., et al. 1997. Fatty acids and eicosanoids regulate gene expression through direct interactions with peroxisome proliferator-activated receptors  $\alpha$  and  $\gamma$ . *Proc. Natl. Acad. Sci. USA*. 94:4318-4323.
- Barak, Y., et al. 1999. PPAR $\gamma$  is required for placental, cardiac, and adipose tissue development. *Mol. Cell*. 4:585-595.
- Kubota, N., et al. 1999. PPAR $\gamma$  mediates high-fat diet-induced adipocyte hypertrophy and insulin resistance. *Mol. Cell*. 4:597-609.
- Rosen, E.D., et al. 1999. PPAR $\gamma$  is required for the differentiation of adipose tissue *in vivo* and *in vitro*. *Mol. Cell*. 4:611-617.
- Nolan, J.J., Ludvik, B., Beersden, P., Joyce, M., and Olefsky, J. 1994. Improvement in glucose tolerance and insulin resistance in obese subjects treated with troglitazone. *N. Engl. J. Med.* 331:1188-1193.
- Jiang, C., Ting, A.T., and Seed, B. 1998. PPAR-gamma agonists inhibit production of monocyte inflammatory cytokines. *Nature*. 391:82-86.
- Ricote, M., Li, A.C., Willson, T.M., Kelly, C.J., and Glass, C.K. 1998. The peroxisome proliferator-activated receptor- $\gamma$  is a negative regulator of macrophage activation. *Nature*. 391:79-82.
- Su, C.G., et al. 1999. A novel therapy for colitis utilizing PPAR- $\gamma$  ligands to inhibit the epithelial inflammatory response. *J. Clin. Invest.* 104:383-389.
- Sheehan, D.C., and Hrapchak, B.B. 1980. *Theory and practice of histotechnology*. C.V. Mosby Co., St. Louis, Missouri, USA. 481 pp.
- Tangirala, R.K., Rubin, E.M., and Palinski, W. 1995. Quantitation of atherosclerosis in murine models: correlation between lesions in the aortic origin and in the entire aorta, and differences in the extent of lesions between sexes in LDL receptor-deficient and apolipoprotein E-deficient mice. *J. Lipid Res.* 36:1-9.
- Willson, T., Brown, P., Sternbach, D., and Henke, B. 2000. The PPARs: from orphan receptors to drug discovery. *J. Med. Chem.* 43:527-550.
- Fruebis, J., Gonzalez, V., Silvestre, M., and Palinski, W. 1997. Effect of probucol treatment on gene expression of VCAM-1, MCP-1 and M-CSF in the aortic wall of LDL receptor-deficient rabbits during early atherosclerosis. *Arterioscler. Thromb. Vasc. Biol.* 17:1289-1302.
- Tsimikas, S., Shortal, B.P., Witztum, J.L., and Palinski, W. 2000. *In vivo* uptake of radiolabeled MDA2, an oxidation-specific monoclonal antibody, provides an accurate measure of atherosclerotic lesions rich in oxidized LDL and is highly sensitive to their regression. *Arterioscler. Thromb. Vasc. Biol.* 20:689-697.
- Holness, C.L., and Simmons, D.L. 1993. Molecular cloning of CD68, a human macrophage marker related to lysosomal glycoproteins. *Blood*. 81:1607-1613.
- Goetze, S., et al. 1999. PPAR gamma-ligands inhibit migration mediated by multiple chemoattractants in vascular smooth muscle cells. *J. Cardiovasc. Pharmacol.* 33:798-806.
- Libby, P., Sukhova, G., Lee, R.T., and Galis, Z.S. 1995. Cytokines regulate vascular functions related to stability of the atherosclerotic plaque. *J. Cardiovasc. Pharmacol.* 25(Suppl. 2):S9-S12.
- Murao, K., et al. 1999. Thiazolidinedione inhibits the production of monocyte chemoattractant protein-1 in cytokine-treated human vascular endothelial cells. *FEBS Lett.* 454:27-30.
- Law, R.E., et al. 1996. Troglitazone inhibits vascular smooth muscle cell growth and intimal hyperplasia. *J. Clin. Invest.* 98:1897-1905.
- Staels, B., et al. 1998. Activation of human aortic smooth-muscle cells is inhibited by PPAR $\alpha$  but not by PPAR $\gamma$  activators. *Nature*. 393:790-793.
- Merat, S., Casanada, F., Sutphin, M., Palinski, W., and Reaven, P.D. 1999. Western-type diets induce insulin resistance and hyperinsulinemia in LDL receptor-deficient mice but do not increase aortic atherosclerosis compared with normoinsulinemic mice in which similar plasma cholesterol levels are achieved by a fructose-rich diet. *Arterioscler. Thromb. Vasc. Biol.* 19:1223-1230.
- Roe, E.B., Chiu, K.M., and Arnaud, C.D. 2000. Selective estrogen receptor modulators and postmenopausal health. *Adv. Intern. Med.* 45:257-278.

# Hyperlipidemia and Atherosclerotic Lesion Development in LDL Receptor-Deficient Mice Fed Defined Semipurified Diets With and Without Cholate

Andrew H. Lichtman, Steven K. Clinton, Kaeko Iiyama, Philip W. Connelly,  
Peter Libby, Myron I. Cybulsky

**Abstract**—Past studies of atherosclerosis in mice have used chow-based diets supplemented with cholesterol, lipid, and sodium cholate to overcome species resistance to lesion formation. Similar diets have been routinely used in studies with LDL receptor-deficient (LDLR<sup>-/-</sup>) mice. The nonphysiological nature and potential toxicity of cholate-containing diets have led to speculation that atherogenesis in these mice may not accurately reflect the human disease process. We have designed a semipurified AIN-76A-based diet that can be fed in powdered, pelleted, or liquid form and manipulated for the precise evaluation of diet-genetic interactions in murine atherosclerosis. LDLR<sup>-/-</sup> mice were randomly assigned among 4 diets (n=6/diet) as follows: 1, control, 10% kcal lipid; 2, high fat (40% kcal), moderate cholesterol (0.5% by weight); 3, high fat, high cholesterol (1.25% by weight); and 4, high fat, high cholesterol, and 0.5% (wt/wt) sodium cholate. Fasting serum cholesterol was increased in all cholesterol-supplemented mice compared with controls after 6 or 12 weeks of feeding ( $P<0.01$ ). The total area of oil red O-stained atherosclerotic lesions was determined from digitally scanned photographs. In contrast to the control group, all mice in cholesterol-supplemented dietary groups 2 to 4 had lesions involving 7.01% to 12.79% area of the thoracic and abdominal aorta at 12 weeks ( $P<0.002$ , for each group versus control). The distribution pattern of atherosclerotic lesions was highly reproducible and comparable. The histological features of lesions in mice fed cholate-free or cholate-containing diets were similar. This study shows that sodium cholate is not necessary for the formation of atherosclerosis in LDLR<sup>-/-</sup> mice and that precisely defined semipurified diets are a valuable tool for the examination of diet-gene interactions. (*Arterioscler Thromb Vasc Biol.* 1999;19:1938-1944.)

**Key Words:** atherosclerosis ■ LDL receptor ■ dietary lipids ■ cholesterol ■ mice

The development of murine models defective in genes controlling lipid metabolism and lipoprotein expression provides an opportunity to understand better the complex interactions between diet and genetics in atherosclerosis. In the last several years, embryonic stem cell and transgenic technologies have been used to alter the expression levels of various genes affecting lipoprotein metabolism and have led to the development of murine knockout and transgenic models of atherogenesis. The ApoE knockout (ApoE<sup>-/-</sup>),<sup>1,2</sup> LDL receptor knockout (LDLR<sup>-/-</sup>),<sup>3</sup> and human ApoB transgenic mice<sup>4,5</sup> develop lesions throughout the arterial tree. Their distribution pattern and morphological features share many similarities with human atherosclerosis, suggesting that similar pathogenic mechanisms may be involved.<sup>6,7</sup> ApoE<sup>-/-</sup> mice develop hypercholesterolemia and atherosclerotic lesions spontaneously, and this can be accelerated by feeding a

Western-type diet.<sup>1,6</sup> In contrast, LDLR<sup>-/-</sup> mice fed a chow diet have only a 2-fold elevation in plasma cholesterol compared with control mice and do not develop significant lesions in the first 6 months of life.<sup>3</sup> When fed a diet consisting of 1.25% cholesterol, 7.5% cocoa butter, 7.5% casein, and 0.5% cholic acid, these mice develop marked hypercholesterolemia and lesions throughout the aorta within 3 to 4 months.<sup>8</sup> Because hypercholesterolemia and lesion formation in LDLR<sup>-/-</sup> mice are readily enhanced by a diet supplemented with fat, cholesterol, and cholate, these mice provide a unique opportunity for evaluation of early events in atherogenesis.

Before the development of atherosclerosis-prone gene-targeted mutant mice, many studies were performed with normal mice fed chow-based diets supplemented with varying amounts of saturated fats, cholesterol, and cholate to

Received September 22, 1998; revision accepted January 11, 1999.

From the Vascular Research Division (A.H.L.), Department of Pathology, and the Vascular Medicine and Atherosclerosis Unit (P.L.), Cardiovascular Division, Department of Medicine, Brigham and Women's Hospital, Harvard Medical School, Boston, Mass; the Arthur G. James Cancer Hospital and Research Institute (S.K.C.), Ohio State University, Columbus, Ohio; and the Department of Laboratory Medicine and Pathobiology (K.I., M.I.C.), University of Toronto, Toronto Hospital Research Centre, and the Departments of Laboratory Medicine and Pathobiology, Medicine, and Biochemistry (P.W.C.), University of Toronto, St Michael's Hospital, Toronto, Ontario, Canada.

Correspondence to Andrew H. Lichtman, MD, PhD, Department of Pathology, Brigham and Women's Hospital, 221 Longwood Avenue, Boston, MA 02115. E-mail alichtman@rics.bwh.harvard.edu

© 1999 American Heart Association, Inc.

*Arterioscler Thromb Vasc Biol.* is available at <http://www.atvbaha.org>

induce atheromatous lesions. In particular, C57BL/6 mice are susceptible to dietary intervention and develop foam cell-rich lesions in the aortic root, but not advanced atheromas.<sup>9-13</sup> Dietary cholate was required to achieve significant hypercholesterolemia, presumably by interfering with hepatobiliary excretion of cholesterol. Most published studies of atherosclerosis in the LDLR<sup>-/-</sup> mice have relied on similar diets supplemented with cholate, cholesterol, and lipid that were used in the earlier C57BL/6 mouse studies. This has led to criticisms of the LDLR<sup>-/-</sup> mouse model based on the speculation that toxic metabolic effects of cholate may modify the pathogenesis of vascular disease in ways not relevant to human atherosclerosis. For example, cholate may cause hepatic steatosis that can progress to cirrhosis accompanied by several host metabolic, physiological, and hormonal changes that can potentially interfere with the interpretation of studies focusing on the histopathological and molecular events during atherogenesis. Recent data from our group and others indicate that cholate is not necessary and that a diet supplemented with cholesterol and saturated fat is sufficient for aortic lesion development in LDLR<sup>-/-</sup> mice.<sup>14,15</sup>

From a nutritional perspective, the dilution of a chow diet with purified lipids, such as hydrogenated coconut oil, increases the caloric density of the diet and reduces the ratio of essential nutrients to dietary energy, thereby potentially contributing to marginal nutrient intake in mice consuming the atherogenic diet. Chow diets do not take advantage of the accumulated knowledge concerning nutritional requirements of mice and the experience of many investigators using precisely controlled semipurified or purified diets for studies of chronic disease processes in rodents.<sup>16-19</sup> Chow diets are formulated from natural ingredients to satisfy the minimal nutrient requirements for growth and reproduction but they differ individual nutrients over time, seasonally, in different geographic locations and between companies in the sources of ingredients included in the final product.<sup>20</sup> Furthermore, many man-made and natural toxins are detected in chow diets, such as aflatoxins, nitrosamines, pesticides, herbicides, and heavy metals.<sup>20-22</sup> Chow diets contain a variety of natural substances from grains, fruits, and vegetables that may modify lipid metabolism and atherogenesis, including a diverse array of soluble and insoluble fiber sources and a multitude of biologically active phytochemicals such as carotenoids and flavonoids. For example, the latter constituents may exert antioxidant actions that could influence atherogenesis and confound experiments.

We propose that investigators of atherogenesis using the many new transgenic and gene knockout models should consider using precisely defined semipurified diets in their studies. This approach adds very little to the overall costs of *in vivo* investigations and can help improve the quality of data obtained and the comparison of results among laboratories over time. Furthermore, the use of semipurified diets in murine studies provides a method for precise control of dietary and nutritional factors, allowing for a meaningful evaluation of specific nutritional interventions that may be relevant to human disease processes. We therefore designed and tested several semipurified diet formulations in a study of atherogenesis in LDLR<sup>-/-</sup> mice.

## Methods

### Mice

Male LDLR<sup>-/-</sup> mice (homozygous) from a mixed C57BL/6J×129Sv background (50% C57BL/6J:50% 129Sv) were purchased from Jackson Laboratories and maintained in the Longwood Medical Research Center facility in accordance with guidelines of the Committee on Animals of the Harvard Medical School and those prepared by the Committee on Care and Use of Laboratory Animals of the Institute of Laboratory Resources, National Research Council [DHEW publication No. (NIH) FS-23]. At 8 to 12 weeks of age, mice that reached a weight of 21 to 22 g were randomly assigned to 1 of 4 diets (see below) fed *ad libitum* for 12 weeks. For experiments that included analyses of body weight, total plasma cholesterol and triglycerides, and atherosclerotic lesion formation in the aorta, groups consisted of 6 mice. Additional male LDLR<sup>-/-</sup> mice were fed identical diets and killed to obtain plasma for lipoprotein analysis, liver function tests, and tissues for histology.

### Diets

Four diets were used in this study. Each diet was a modification of the AIN-76A semipurified diet for mice and rats<sup>18,19</sup> and prepared by Dr Edward A. Ulman at Research Diets, Inc, according to our formulations (Table 1). The diets provide adequate concentrations of all known essential nutrients for the mouse. The carbohydrate component was altered from the original AIN-76A formulation by including expanded maltose dextrin, which allows the lipid concentration to vary from the range of 10% to 40% of total energy (≈5% to 20% by weight) without a problem of "settling out." Furthermore, the carbohydrate modifications allow a diet to be fed as a powder, a liquid formulation, or processed into pellets (used in this study). The 4 experimental diet groups include diet 1 group (Research Diet D12102), control (10% kcal lipid); diet 2 group (Research Diet D12107), high fat (40% kcal lipid), moderate cholesterol (0.5% by weight); diet 3 group (Research Diet D12108), high fat, high cholesterol (1.25% by weight); and diet 4 group (Research Diet D12109), high fat, high cholesterol, and sodium cholate (0.5% by weight). The addition of lipid to the baseline diet formulation is achieved by substituting fat (9 kcal/g of metabolizable energy) for carbohydrate (4 kcal/g of metabolizable energy) based on an equal amount of energy (kcal) rather than an equal weight (g). This approach is necessary to maintain a constant ratio of all other nutrients in the diet to energy. This technique of diet formulation avoids the problem of reduced nutrient content of the high-fat diets prepared by the dilution technique (ie, chow diluted with fat) or when fat is substituted for carbohydrate on the basis of weight.

### Cholesterol Measurements and Liver Function Tests

Serum samples were collected for lipid analysis after overnight fasting. At 0 (initiation of the study), 6 and 12 weeks, blood was obtained from individual mice by tail-vein nicking and total serum cholesterol and triglyceride levels were determined by colorimetric assays (Sigma Chemical Co). Blood was obtained from the retro-orbital plexus for analysis of plasma lipoproteins by fast protein liquid chromatography gel-filtration chromatography after 12 weeks of diet. Samples were anticoagulated with EDTA (3 mmol/L or 0.1% final) and sodium azide 0.02% was added as a preservative. To obtain a plasma volume of at least 250  $\mu$ L, plasma was pooled from several mice within each group. Erythrocytes and leukocytes were removed by low-speed (400g, 10 minutes, 4°C) and platelets by high-speed (3000g, 5 minutes, 4°C) centrifugations. Plasma was stored at 4°C for <2 days. Plasma was subjected to fast protein liquid chromatography gel-filtration chromatography by using a Superose 6HR 10/30 column (Pharmacia Biotech) as was previously described.<sup>23</sup> Filtered plasma (200  $\mu$ L) was loaded on the column and was eluted with 2 mmol/L sodium phosphate, 0.14 mol/L NaCl, 5 mmol/L Na<sub>2</sub>EDTA, 0.02% NaN<sub>3</sub>, pH 7.4, at a constant flow rate of 0.5 mL/min. Fractions (0.5 mL) were collected and total cholesterol, triglycerides, free cholesterol, and choline-containing phospholipids were measured on a Technicon RA1000 (Bayer Corp). Triglycerides were corrected for free glycerol by using a triglyceride blank reagent (Bayer Corp). The cholesterol and triglyceride assays were standard-

TABLE 1. Formulation for the Diets Used in This Study and Their Macronutrient Contents as Percentages of Total Energy

Ingredient	Diet 1 (10% kcal fat, 0% cholesterol§§, 0% cholate§§)		Diet 2 (40% kcal fat, 0.5% cholesterol, 0% cholate)		Diet 3 (40% kcal fat, 1.25% cholesterol, 0% cholate)		Diet 4 (40% kcal fat, 1.25% cholesterol, 0.5% cholate)	
	Grams	kcal	Grams	kcal	Grams	kcal	Grams	kcal
Formulation								
Casein†	200.0	800	200.0	800	200.0	800	200.0	800
Cystine	3.0	12	3.0	12	3.0	12	3.0	12
Soy oil‡	25.0	225	25.0	225	25.0	225	25.0	225
Cocoa butter§	20.0	180	155.0	1395	155.0	1395	155.0	1395
Corn Starch	375.0	1500	212.0	848	212.0	848	212.0	848
Malto-dextrin	125.0	500	71.0	284	71.0	284	71.0	284
Sucrose	200.0	800	113.0	452	113.0	452	113.0	452
Cellulose¶	50.0	0	50.0	0	50.0	0	50.0	0
Mineral Mix#	10.0	0	10.0	0	10.0	0	10.0	0
Dicalcium phosphate#	13.0	0	13.0	0	13.0	0	13.0	0
Calcium carbonate#	5.5	0	5.5	0	5.5	0	5.5	0
Potassium citrate, monohydrate#	16.5	0	16.5	0	16.5	0	16.5	0
Vitamin mix**	10.0	40	10.0	40	10.0	40	10.0	40
Choline††	2.0	0	2.0	0	2.0	0	2.0	0
Cholesterol	0	0	4.5	0	11.25	0	11.25	0
Cholate	0	0	0	0	0	0	4.5	0
Total grams or kcal*	1055.0	4057	890.6	4056	897.35	4056	901.85	4056
	% kcal		% kcal		% kcal		% kcal	
Macronutrient content								
Protein	20		20		20		20	
Carbohydrate	70		40		40		40	
Lipid	10		40		40		40	
kcal/g in diet*	3.8		4.5		4.5		4.5	

\*Calculations based on estimated metabolizable energy of 4 kcal/g (16.7 kJ/g) of protein and carbohydrate and 9 kcal/g (37.7 kJ/g) of lipid. The concentrations of minerals, vitamins, and fiber were adjusted to maintain a constant ratio to energy.

†Alcohol extracted casein, 99% protein.

‡Soy oil provides a minimal supply of essential fatty acids.

§We have selected cocoa butter for this study, because it is a saturated fat but has no cholesterol.

||Malto-dextrin 10 is a component of the carbohydrate fraction that assists in maintaining the lipid fraction equally dispersed throughout the diet during shipping, storage, and feeding.

¶BW200 cellulose.

#AIN-76A mineral mixtures with the calcium and phosphate removed. Dicalcium phosphate, calcium carbonate, and potassium citrate, monohydrate are replaced, to increase phosphate and potassium relative to the original formulation.

\*\*AIN-76A vitamin mixture.

††Choline provided as choline bitartrate.

§§Cholesterol and cholate (which do not contribute to total energy) are expressed as percent w/w.

ized with the National Heart Lung and Blood Institutes—Center for Disease Control Lipid Standardization program. Reagents for free cholesterol and choline-containing phospholipid measurements were purchased from Boehringer Mannheim (Germany) and external standards were not available for these assays.

Liver function tests were performed on serum samples by the Tufts Veterinary Diagnostic Laboratory, using an automated analyzer. These tests included serum lactate dehydrogenase (LDH), serum glutamic-oxaloacetic transaminase (SGOT), serum glutamic-pyruvate transaminase (SGPT), and serum bilirubin.

### Tissue Sampling and Analyses

The surface area of aorta occupied by atherosclerotic lesions was quantified by en face oil red O staining, using an approach modified from Palinski et al.<sup>24</sup> Mice were killed, after 12 weeks of diet, by ether inhalation. A catheter was inserted into the left ventricle and

the arterial tree was perfused with PBS (25 mL), then 10% buffered formaldehyde (40 mL, pH 7.4) at a pressure of 100 mm Hg. The entire aorta attached to the heart was dissected and placed overnight in formaldehyde. Using a stereomicroscope, the adventitial fat was dissected and the aorta was stained with oil red O as described by Nunnari et al.<sup>25</sup> After staining, the remaining adventitial fat was easily detected and was removed. The aorta was opened longitudinally, pinned en face on a black silicone-covered dish, and photographed while immersed in PBS. Slides were scanned into a Macintosh computer and the percent surface area occupied by oil red O-stained lesions was determined by using image analysis software (NIH Image). The aortic arch (1 mm above the aortic valve cusps to 2 mm below the ostium of the right subclavian artery), the descending thoracic aorta (extending to 1 mm above the ostium of the celiac artery), the abdominal aorta (including the bifurcation and 0.5 mm of the iliac arteries), and the total aorta were evaluated. After photography, portions of aorta that contained lesions were cross-sectioned

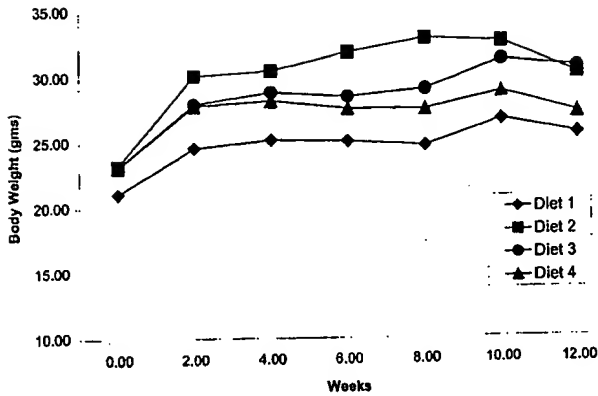


**Figure 1.** Body weights of LDLR<sup>-/-</sup> mice fed diets varying in fat, cholesterol, and cholate content. Mice were fed the diets described in Table 1 and were weighed every 2 weeks for 12 weeks. The data represent the mean weights for the 6 mice in each group at each time point.

and embedded in paraffin. Histological sections were prepared and stained with hematoxylin and eosin.

Liver slices, obtained from each animal at the time it was killed, were fixed in formalin, paraffin-embedded, and histological sections were stained with hematoxylin and eosin.

### Statistical Analysis

Food intake, body weight, and serum lipids were initially analyzed by ANOVA<sup>26</sup> followed by Fisher's PLSD<sup>26</sup> to calculate pairwise comparisons among treatment groups by using Statview 4.5 (Abacus Concepts, Inc).

## Results

### Body Weight

The mean body weight of mice fed each of the 4 diets for 12 weeks is shown in Figure 1. Mice fed the high-fat+0.5% cholesterol diet (diet 2) showed increased body weight ( $P<0.02$ ) compared with controls (diet 1) during weeks 2 through 10. This a common observation in studies where rodents are provided a high-fat diet, which is more palatable, resulting in a slightly greater intake of diet (kcal). However, we did not attempt to measure food intake in this study, because mice were not individually housed and they typically waste significant amounts of food when provided ad libitum. Additional effort is necessary to accurately quantitate the amount of food consumed in murine studies. Those fed a high-fat diet with higher concentrations of cholesterol or supplemented with cholate did not exhibit a weight gain that was significantly different from controls.

### Lipid Analyses

The analyses of total serum cholesterol and triglyceride levels at 0, 6, and 12 weeks are shown in Table 2. A significant effect of diet on serum cholesterol was observed at 6 weeks ( $P<0.0009$ , ANOVA). Pairwise comparisons show that mice fed diet 1 (control diet) have significantly lower serum cholesterol than those fed the high-fat diets supplemented with 0.5% cholesterol (diet 2;  $P<0.02$ , PLSD), 1.25% cholesterol (diet 3;  $P<0.02$ , PLSD), or 1.25% cholesterol and cholate (diet 4;  $P<0.0001$ , PLSD). A statistically significant difference was not found between diet groups 2 and 3. However, the addition of cholate (diet 4) increased serum cholesterol compared with diets 1, 2, and 3 ( $P<0.009$ , for all comparisons; PLSD).

**TABLE 2.** Plasma Cholesterol and Triglycerides at Different Time Points

Diet	Cholesterol (mg/dL)		
	Week 0 (Baseline)	Week 6	Week 12
1 (10% fat)	104±18	97±21	124±49
2 (40% fat; 0.5% cholesterol)	133±51	327±56*	328±111
3 (40% fat; 1.25% cholesterol)	130±37	331±46*	597±131*
4 (40% fat; 1.25% cholesterol; 0.5% cholate)	129±59	598±71*†‡	761±208*†
Diet	Triglycerides (mg/dL)		
	Week 0 (Baseline)	Week 6	Week 12
1 (10% fat)	52±7	50±6	63±19
2 (40% fat; 0.5% cholesterol)	40±10	85±14	110±37
3 (40% fat; 1.25% cholesterol)	50±11	58±8	141±34
4 (40% fat; 1.25% cholesterol; 0.5% cholate)	41±10	74±10	80±37

Data represent mean±SEM values for nonfasting plasma cholesterol and triglycerides.

\* $P<0.02$  compared with diet group 1.

† $P<0.02$  compared with diet group 2.

‡ $P<0.02$  compared with diet group 3.

Similar results were observed at 12 weeks, although variation in serum cholesterol was greater ( $P<0.005$ , ANOVA). Pairwise comparisons at 12 weeks show that mice fed diet 1 (control diet) have lower serum cholesterol than those fed the high-fat diets supplemented with 0.5% cholesterol (diet 2;  $P<0.15$ , PLSD), 1.25% cholesterol (diet 3;  $P<0.007$ , PLSD), or 1.25% cholesterol and cholate (diet 4;  $P<0.001$ , PLSD). The addition of cholate (diet 4) increased serum cholesterol compared with those fed supplemental cholesterol without cholate ( $P<0.007$  versus diet 2 and  $P=0.31$  versus diet 3, both PLSD). Diets did not have any significant effect on serum triglyceride levels at 6 or 12 weeks.

The analysis of plasma lipoproteins by fast protein liquid chromatography gel-filtration chromatography after 12 weeks of diet is summarized in Figure 2. The extent of lipids recovered in Superose fractions was relatively uniform and comparable in all dietary groups. Percent recovery ranged from 83% to 87% for total cholesterol, 90% to 94% for choline-containing phospholipids, and 68% to 120% for triglycerides. The data revealed that elevated total cholesterol in dietary groups 2 through 4 was the result of increased VLDL and IDL/LDL lipoproteins (Figure 2). Levels of HDL lipoproteins varied inversely with VLDL and IDL/LDL. For each lipoprotein class, levels of free cholesterol and choline-containing phospholipids were as expected, and in different dietary groups their ratios were comparable. These ratios typically were between 1 and 2 for VLDL and IDL/LDL and  $<0.6$  for HDL (data not shown). There was no evidence for significant levels of lipoprotein X and HDL-E particles.

### Development of Atherosclerotic Lesions in the Aorta

En face oil red O staining revealed minimal atherosclerotic lesion formation in mice fed diet 1 (control diet) for 12 weeks. In contrast, lesions were readily detected in each of the groups fed cholesterol-containing diets (Figure 3 and

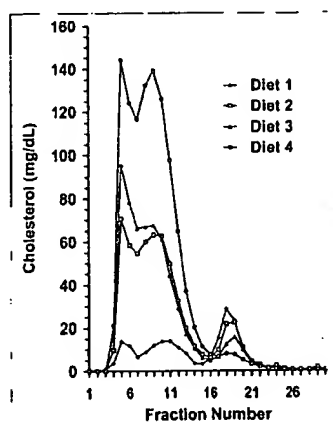


**Figure 2.** Plasma cholesterol profiles of LDLR<sup>-/-</sup> mice fed diets varying in fat, cholesterol, and cholate content. Mice were fed the diets described in Table 1 for 12 weeks, when blood samples were obtained from each dietary group and plasma was pooled. Plasma was subjected to fast protein liquid chromatography gel-filtration chromatography as described in Methods. Lipoproteins were measured in each fraction and the total cholesterol levels are plotted.

Table 3). The percent surface area of the entire aorta involved by lesions was significantly greater in mice fed diets 2, 3, and 4, compared with controls (diet 1), as well as in mice fed diet 4 compared with group 2. The interpretation was similar

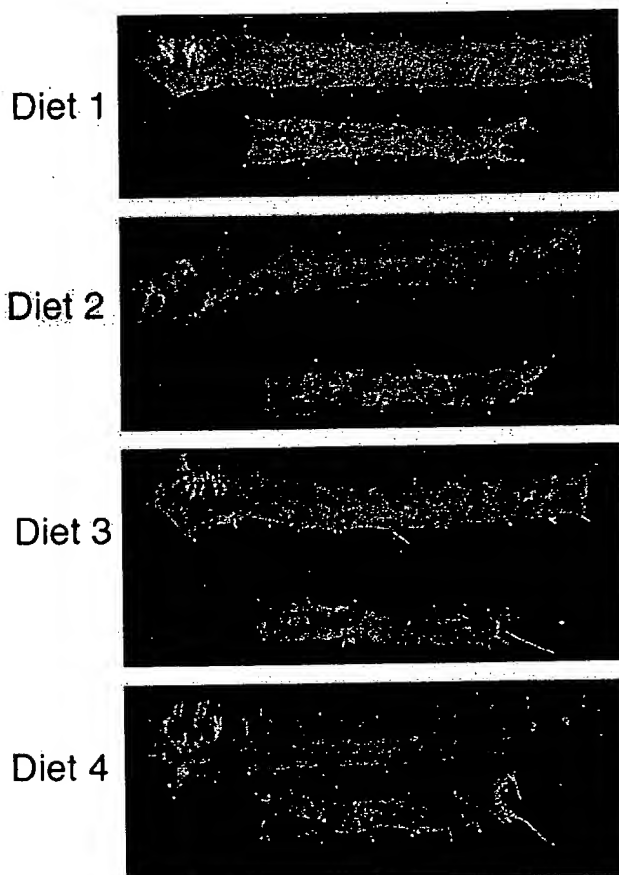


**Figure 3.** Oil red O-stained atherosclerotic lesions in aortas of LDLR<sup>-/-</sup> mice fed diets varying in fat, cholesterol, and cholate content. Mice were killed after being fed defined diets described in Table 1 for 12 weeks. Aortas were prepared and stained with oil red O as described in Methods. One representative aorta from a total of 6 in each of the 4 dietary groups is shown.

when the arch, thoracic, and abdominal regions were evaluated individually (Table 3). The anatomic distribution of atherosclerotic lesions was identical in dietary groups 2, 3, and 4 (Figure 3). Lesion-predisposed sites included the aortic root, the lesser curvature of the arch, and near the orifice of the brachiocephalic, intercostal, celiac, superior mesenteric, and renal arteries.

Histological examination revealed a similar morphology and cellularity in atheromas from each of the groups fed cholesterol-containing diets (Figure 4). The lesions had characteristic intimal thickening with foam cells, and apparent smooth muscle cell infiltration.

### Liver Function Tests and Histology

To determine if consumption of a cholate-containing diet for 12 weeks led to liver damage, serum liver enzyme levels and liver-derived products were measured and histological sections of liver were evaluated. The liver function test results were comparable between all dietary groups, suggesting that the liver parenchyma and biliary system were not seriously damaged after 12 weeks of feeding. Of particular interest, mice in group 4 (fed 1.25% cholesterol with cholate) did not have a significant elevation in serum bilirubin, alkaline phosphatase,  $\gamma$ -glutamyltransferase (GGT), alanine aminotransferase (ALT), or aspartate aminotransferase (AST), or decrease in albumin when compared with group 3 (also fed 1.25% cholesterol, but without cholate) (data not shown). Hematoxylin and eosin sections of liver revealed substantial steatosis in dietary groups 3 and 4, with greater fatty changes observed in the cholate-supplemented group. There was no histological evidence of hepatocyte necrosis, apoptosis, inflammation, fibrosis, or cirrhosis at the time point examined. However, all cholate-fed mice had stones in the gallbladder, whereas none were observed in mice fed cholate-free diets.

### Discussion

This study demonstrates that nutritionally defined semipurified diets are appropriate for the study of diet-genetic interactions in murine atherosclerosis. They offer several advantages compared with the commonly used chow-based diets, including reproducibility and uniformity of content, and the ability to precisely alter composition. Dietary lipid saturation and concentration are frequently the focus of hypotheses in experimental atherogenesis as a consequence of the enormous body of clinical and epidemiological data suggesting their importance in vascular disease. A semipurified diet allows the investigator to alter lipid concentration by substitution for an equivalent amount of energy from carbohydrate, to maintain a constant ratio of all other nutrients to energy in the control and high-fat diets. This is impossible to achieve when adding fat by dilution to a chow diet. The dilution technique confuses the interpretation of results. Indeed many investigators using diets prepared by dilution of chow with fat are seemingly unaware of the fact that mice consuming an identical amount of energy from the high-fat diet are also exposed to a significantly lower amount of all components of the chow, such as protein, all vitamins and minerals, and biologically active but nonnutrient factors such as fiber and phytochemicals, including those with antioxidant properties. The role of specific vitamin and mineral deficiencies or excess can be precisely examined by using semipurified diets



TABLE 3. Atherosclerotic Lesion Formation in Mouse Aortas After 12 Weeks of Diet

Dietary Group (n=6)	Percentages of Aortic Surface Area Involved by Oil Red O-Stained Lesions			
	Total	Arch	Thoracic	Abdominal
1 (control)	0.16±0.32	0.10±0.19	0.08±0.17	0.67±0.94
2 (0.5% cholesterol)	7.02±3.97†	24.96±12.09§	2.80±2.35*	5.45±4.17*
3 (1.25% cholesterol)	8.27±3.59§	31.66±11.93§	3.57±3.50*	4.10±2.90*
4 (1.25% cholesterol+cholate)	12.79±4.80§	34.62±15.24§	10.30±3.63§	5.69±5.15*

\**P*<0.05; †*P*<0.003; §*P*<0.001, compared with group 1.||*P*<0.05, compared with group 2.

because their contents can be individually manipulated in the AIN vitamin and mineral formulations.<sup>18,19</sup> The use of standardized formulations will allow investigators to compare data derived from different laboratories without the concern that unquantifiable differences in the chow diets used contributed to the reported results.

The semipurified formulation can be provided as a liquid or in powdered form. The liquid diet allows the investigator to obtain more precise estimates of intake because mice typically disperse much of a solid diet in a cage. Liquid diets also facilitate studies of the effects of alcohol intake and are ideal for macrophage colony-stimulating factor-deficient mice, which exhibit osteopetrosis and have no teeth, making it impossible to consume a pelleted diet.<sup>27-29</sup>

The effects of dietary cholate on atherosclerosis susceptibility in genetically engineered mice should be reevaluated based on our results. Mice are very resistant to the development of atheromatous lesions in the arterial tree. Historically, investigators interested in genetic differences between murine strains in susceptibility to fatty streak formation devised diets

composed of chow diluted with saturated fat and supplemented with cholesterol and cholate.<sup>10</sup> This diet led to the discovery that the C57BL/6 strain was more susceptible to the formation of fatty streaks in the aortic root.<sup>9</sup> Although this dietary approach lacks many characteristics desired by experimental nutritionists, many investigators have subsequently used it in newer models of atherosclerosis developed with transgenic and gene-deletion technology. However, the potential hepatotoxic effects of cholate<sup>11,30,31</sup> have raised concerns that LDLR<sup>-/-</sup> mice fed such diets are not useful for modeling human disease.<sup>32</sup> Our study clearly shows that cholate is not required for the development of atherosclerotic lesions throughout the aorta in the LDLR<sup>-/-</sup> strain, and therefore cholate is unnecessary as a dietary additive in studies of atherogenesis in these mice. Subsequent experiments demonstrated a rapid onset of lesion formation, in that most mice fed diet 3 for 4 weeks had early lesions in the lesser curvature of the aortic arch (data not shown). Compared with mice fed diet 3 (high fat, 1.25% cholesterol), the inclusion of cholate (0.5%, wt/wt) in diet 4 caused a further increase in plasma lipids and a trend toward a greater area of the aortic surface involved by atheromatous lesions. This trend was not statistically significant because of high inter-animal variability. Cholate-fed mice also developed gallstones over the 12 weeks of investigation. It is our opinion that dietary cholate is unnecessary and perhaps a liability in studies of atherogenesis in the LDLR<sup>-/-</sup> mouse.

Traditionally, cholesterol supplements of ≥1% have been used in murine and rabbit studies to enhance hyperlipidemia and the rate of lesion formation, thereby shortening the duration of studies. Diets high in cholesterol and fat may cause time- and dose-dependent hepatotoxicity, therefore lowering cholesterol concentration, may be advantageous. Our study begins to address this issue. We demonstrated that the lesion area after 12 weeks of consuming 0.5% cholesterol (diet 2) was essentially indistinguishable from mice fed cholesterol at 1.25% (diet 3). At 12 weeks of feeding, there was a trend toward higher serum cholesterol and triglycerides in diet group 3. Perhaps this would lead to accelerated lesion progression and differences in lesion area would become significant in studies of longer duration. Cholesterol levels <0.5% can induce lesions in LDLR<sup>-/-</sup> mice. Palinski et al<sup>14</sup> fed LDLR<sup>-/-</sup> mice for 6 months with a diet containing 21% fat and 0.15% cholesterol (without cholate) and observed extensive atherosclerotic lesion formation throughout the aorta. In evaluating aortas of retired LDLR<sup>-/-</sup> breeders >1 year of age, we observed lesions in the aortic arch in most (unpublished data, 1998). This indicates that LDLR<sup>-/-</sup>

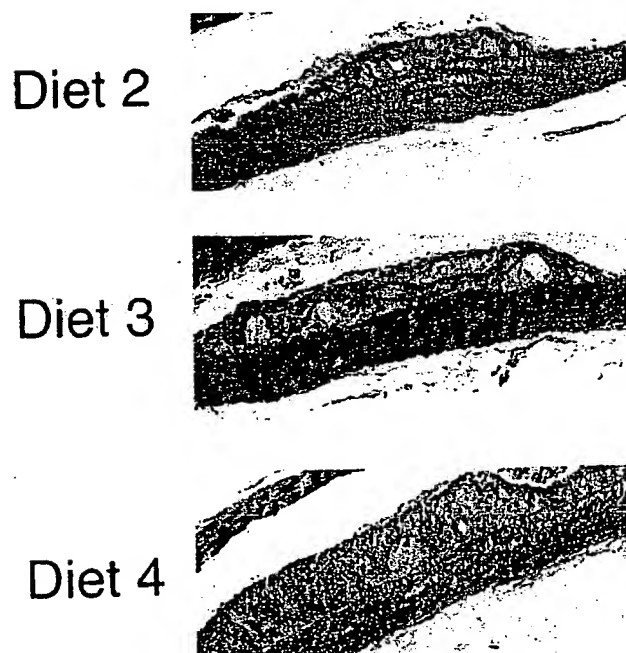


Figure 4. Histological appearance of aortic atherosclerotic lesions in LDLR<sup>-/-</sup> mice fed diets varying in fat, cholesterol, and cholate content. Hematoxylin and eosin-stained sections of formalin-fixed lesions from the aortas described in Figure 3 are shown.

mice can develop lesions spontaneously even when fed a regular laboratory chow; however, their rate of formation is very slow, as lesions generally are not found in mice <6 months old.

The existing literature on newer models of murine atherogenesis does not allow investigators to evaluate the role of dietary lipid concentration or the source of the lipid on lesion formation. In our study, the lipid content of diet 1 (control diet) was 10% of total energy (4.3% by weight), whereas in diets 2, 3, and 4 it was 40% (20% by weight). We included soy oil at 5.5% of total energy to ensure that a supply of essential fatty acids was constant in all diets. We then manipulated cocoa butter as the variable lipid. We recommend that future investigators maintain a constant baseline supply of essential fatty acids in the diet unless they are particularly interested in this as a variable. It is possible that investigators manipulating the fat source could naively prepare or purchase a saturated fat-enriched diet deficient in essential fatty acids, which could complicate the interpretation of murine studies. Furthermore, essential fatty acid deficiency is not observed in humans except in situations of several metabolic or gastrointestinal diseases. Humans consuming diets rich in saturated fat and cholesterol easily achieve adequate intake of essential fatty acids. Therefore, murine models will more closely mimic human dietary patterns if essential fatty acid intake is adequate.

### Acknowledgments

This work was supported by NIH grant 1 P50 HL56985 (A.H.L., P.L.), NIH grant RO1 CA 72482-01A1 (S.K.C.), Heart and Stroke Foundation of Ontario grant T-3032 (P.W.C.), and Heart and Stroke Foundation of Ontario grant T-3588 and an Established Investigatorship from the American Heart Association (M.I.C.).

### References

- Plump AS, Smith JD, Hayek T, Aalto-Setälä K, Walsh A, Verstuyft JG, Rubin EM, Breslow JL. Severe hypercholesterolemia and atherosclerosis in apolipoprotein E-deficient mice created by homologous recombination in ES cells. *Cell*. 1992;71:343-353.
- Zhang SH, Reddick RL, Piedrahit JA, Maeda N. Spontaneous hypercholesterolemia and arterial lesions in mice lacking apolipoprotein E. *Science*. 1992;258:468-471.
- Ishibashi S, Brown MS, Goldstein JL, Gerard RD, Hammer RE, Herz J. Hypercholesterolemia in low density lipoprotein receptor knockout mice and its reversal by adenovirus-mediated gene delivery. *J Clin Invest*. 1993;92:883-893.
- Callow MJ, Stoltzfus LJ, Lawn RM, Rubin EM. Expression of human apolipoprotein B and assembly of lipoprotein(a) in transgenic mice. *Proc Natl Acad Sci U S A*. 1994;91:2130-2134.
- McCormick SP, Linton MF, Hobbs HH, Taylor S, Curtiss LK, Young SG. Expression of human apolipoprotein B90 in transgenic mice: demonstration that apolipoprotein B90 lacks the structural requirements to form lipoprotein. *J Biol Chem*. 1994;269:24284-24289.
- Nakashima Y, Plump AS, Raines EW, Breslow JL, Ross R. ApoE-deficient mice develop lesions of all phases of atherosclerosis throughout the arterial tree. *Arterioscler Thromb*. 1994;14:133-140.
- Reddick RL, Zhang SH, Maeda N. Atherosclerosis in mice lacking apo E: evaluation of lesion development and progression. *Arterioscler Thromb*. 1994;14:141-147.
- Ishibashi S, Goldstein JL, Brown MS, Herz J, Burns DK. Massive xanthomatosis and atherosclerosis in cholesterol-fed low density lipoprotein receptor-negative mice. *J Clin Invest*. 1994;93:1885-1893.
- Paigen B, Morrow A, Brandon C, Mitchell D, Holmes P. Variation in susceptibility to atherosclerosis among inbred strains of mice. *Atherosclerosis*. 1985;57:65-73.
- Paigen B, Morrow A, Holmes PA, Mitchell D, Williams RA. Quantitative assessment of atherosclerotic lesions in mice. *Atherosclerosis*. 1987;68:231-240.
- Nishina PM, Verstuyft J, Paigen B. Synthetic low and high fat diets for the study of atherosclerosis in the mouse. *J Lipid Res*. 1990;31:859-869.
- Vesselinovitch D, Wissler RW. Experimental production of atherosclerosis in mice. 2. Effects of atherogenic and high-fat diets on vascular changes in chronically and acutely irradiated mice. *J Atheroscler Res*. 1968;8:497-523.
- Vesselinovitch D, Wissler RW, Doull J. Experimental production of atherosclerosis in mice. 1. Effect of various synthetic diets and radiation on survival time, food consumption and body weight in mice. *J Atheroscler Res*. 1968;8:483-495.
- Palinski W, Tangirala RK, Miller E, Young SG, Witztum JL. Increased autoantibody titers against epitopes of oxidized LDL in LDL receptor-deficient mice with increased atherosclerosis. *Arterioscler Thromb Vasc Biol*. 1995;15:1569-1576.
- Lichtman AH, Clinton SK, Iiyama K, Henault L, Libby P, Cybulsky MI. Comparative effects of precisely defined semipurified diets supplemented with lipid, cholesterol, and sodium cholate on serum lipids and aortic atherosclerosis in LDL receptor-deficient (LDLR<sup>-/-</sup>) mice. *FASEB J*. 1997;11:A154. Abstract.
- Reeves PG, Nielsen FH, Fahey GC Jr. AIN-93 purified diets for laboratory rodents: final report of the American Institute of Nutrition ad hoc writing committee on the reformulation of the AIN-76A rodent diet. *J Nutr*. 1993;123:1939-1951.
- Rao GN. Rodent diets for carcinogenesis studies. *J Nutr*. 1988;118:929-931.
- American Institute of Nutrition. AIN report of the AIN ad hoc committee on standards for nutritional studies. *J Nutr*. 1977;107:1340-1348.
- American Institute of Nutrition. AIN second report of the ad hoc committee on standards for nutritional studies. *J Nutr*. 1980;110:1726.
- Rao GN, Knapka JJ. Contaminant and nutrient concentrations of natural ingredient rat and mouse diet used in chemical toxicology studies. *Fundam Appl Toxicol*. 1987;9:329-338.
- Oller WL, Kendall DC, Greenman DL. Variability of selected nutrients and contaminants monitored in rodent diets: a 6-year study. *J Toxicol Environ Health*. 1989;27:47-56.
- Fowler GG. Toxicology of nisin. *Food Cosmet Toxicol*. 1973;11:351-352.
- van Gent T, van Tol A. Automated gel permeation chromatography of plasma lipoproteins by preparative fast protein liquid chromatography. *J Chromatogr*. 1990;525:433-441.
- Palinski W, Ord VA, Plump AS, Breslow JL, Steinberg D, Witztum JL. ApoE-deficient mice are a model of lipoprotein oxidation in atherosclerosis: demonstration of oxidation-specific epitopes in lesions and high titers of autoantibodies to malondialdehyde-lysine in serum. *Arterioscler Thromb*. 1994;14:605-616.
- Nunnari JJ, Zand T, Joris I, Majno G. Quantitation of oil red O staining of the aorta in hypercholesterolemic rats. *Exp Mol Pathol*. 1989;51:1-8.
- Steel RGD, Torrie JH. *Principals and Procedures of Statistics*. New York, NY: McGraw-Hill Book Co, Inc; 1980.
- Clinton SK, Underwood R, Hayes L, Sherman ML, Kufe DW, Libby P. Macrophage colony-stimulating factor gene expression in vascular cells and in experimental and human atherosclerosis. *Am J Pathol*. 1992;140:301-316.
- Qiao JH, Tripathi J, Mishra NK, Cai Y, Tripathi S, Wang XP, Imes S, Fishbein MC, Clinton SK, Libby P, Lusis AJ, Rajavashisth TB. Role of macrophage colony-stimulating factor in atherosclerosis: studies of osteopetrotic mice. *Am J Pathol*. 1997;150:1687-1699.
- Kodama H, Yamasaki A, Nose M, Niida S, Ohgame Y, Abe M, Kumegawa M, Suda T. Congenital osteoclast deficiency in osteopetrotic (op/op) mice is cured by injections of macrophage colony-stimulating factor. *J Exp Med*. 1991;173:269-272.
- Nishina PM, Wang J, Toyofuku W, Kuypers FA, Ishida BY, Paigen B. Atherosclerosis and plasma and liver lipids in nine inbred strains of mice. *Lipids*. 1993;28:599-605.
- Delzenne NM, Calderon PB, Taper HS, Roberfroid MB. Comparative hepatotoxicity of cholic acid, deoxycholic acid and lithocholic acid in the rat: in vivo and in vitro studies. *Toxicol Lett*. 1992;61:291-304.
- Breslow JL. Mouse models of atherosclerosis. *Science*. 1996;272:685-688.

183.9

# **MUCOSAL ADMINISTRATION OF HSP 65 DECREASES ATHEROSCLEROSIS AND INFLAMMATION IN THE AORTIC ARCH OF LDL RECEPTOR DEFICIENT MICE**

R. Maron, G.K. Sukhova, A.M. Faria, E. Hoffman, F. Mach, P. Libby, and H.L. Weiner. Center for Neurologic Diseases and Vascular Medicine and Atherosclerosis Unit, Brigham and Women's Hospital, Harvard Medical School, Boston, MA.

Increasing evidence supports the involvement of inflammation and immunity in atherogenesis, as well as the role of autoimmunity to heat shock proteins in the progression of atherosclerosis. Mucosal administration of autoantigens decreases organ specific inflammation and disease in animal models (diabetes, arthritis and EAE) and is being tested in human clinical trials. We examined the effect of nasal or oral administration of HSP65 on atherosclerotic lesion formation in mice lacking the receptor for low-density lipoprotein maintained on a high cholesterol diet. Animals were nasally treated with 0.8ug HSP 65 three times every second day or orally treated with 8 ug HSP 65 on 5 consecutive days. A high cholesterol diet was started after the last treatment and mice were mucosally treated once/week for 8 weeks at which time pathologic analysis was performed. In nasally treated animals, we found a reduction in macrophage-positive area in the aortic arch (3.44% vs. 13.03% in controls,  $p = 0.006$ ) as well as a reduced number of T-cells ( $p = 0.02$ ). There was also a decrease in the size of atherosclerotic plaques. A similar trend was observed in orally treated animals but was not significant. Mice nasally treated with HSP also gained significantly less weight than fed or control treated mice. Our results suggest that nasal treatment with HSP reduces the inflammatory process associated with atherosclerosis and may provide a new treatment approach.

183.11

# **Phase I Clinical Trial of Orally Delivered Hepatitis B Surface Antigen Expressed in Potato Tubers.**

<sup>1</sup>Yasmin Thanavala, <sup>1</sup>Adrienne Scott, <sup>1</sup>Srabani Pal, <sup>1</sup>Martin Mahoney and <sup>2</sup>Charles Arntzen. <sup>1</sup>Roswell Park Cancer Institute, Buffalo, NY; <sup>2</sup>Boyce Thompson Institute for Plant Research, Ithaca, NY.

A randomized, doubleblind, placebo-controlled phase I clinical trial has been completed at Roswell Park Cancer Institute to evaluate the safety, tolerability and immunogenicity of orally delivered HBsAg expressed as a protein in transgenic potato tubers. Forty-five healthy healthcare workers with a history of known positive anti-HBc

183.7

**CHOLERA TOXIN B SUBUNIT AS MUCOSAL CARRIER-DELIVERY SYSTEM FOR SPECIFIC IMMUNOTHERAPY.**C. Czernik<sup>1</sup>, P. Anjures<sup>2</sup>, C. Rank<sup>2</sup>, J. Holmgren<sup>2</sup>. <sup>1</sup>INSERM Unit 364, Nice, France, <sup>2</sup>Dept of Medical Microbiology, University of Göteborg, Sweden.

Over the past few years attention has been devoted to the development of effective formulations that could prevent or halt untoward immune responses, such as those underlying autoimmune disorders, allergic reactions, and by and large chronic inflammation. Studies initiated in this laboratory have documented the efficiency of cholera B subunit as a powerful mucosal immunomodulating and carrier-delivery system agent for optimal induction of immune tolerance in various preclinical models of autoimmune diseases. More recently, this system has proven to be especially effective for suppressing type I allergic responses and also for suppressing Th2-driven immunopathological responses to persistent infectious microorganisms. The mechanisms of action of this system and in particular the role of mucosal dendritic cells in the induction of such form of suppression is currently under study. These studies will be presented and their implications will be discussed. (supported by INSERM, Swedish Medical Research Council, European Communities EC Biotech IV NovoNordisk, Triotol)

183.9

**MUCOSAL ADMINISTRATION OF HSP 65 DECREASES ATHEROSCLEROSIS AND INFLAMMATION IN THE AORTIC ARCH OF LDL RECEPTOR DEFICIENT MICE**

R. Maron, G.K. Sathorn, A.M. Faruqi, E. Hoffman, E. Mach, P. Libby, and H.L. Weiss. Center for Neurologic Diseases and Vascular Medicine and Atherosclerosis Unit, Brigham and Women's Hospital, Harvard Medical School, Boston, MA.

Increasing evidence supports the involvement of inflammation and immunity in atherogenesis, as well as the role of autoimmunity to heat shock proteins in the progression of atherosclerosis. Mucosal administration of autoantigens decreases organ specific inflammation and disease in animal models (diabetes, arthritis and EAE) and is being tested in human clinical trials. We examined the effect of nasal or oral administration of HSP65 on atherosclerotic lesion formation in mice lacking the receptor for low-density lipoprotein maintained on a high cholesterol diet. Animals were nasally treated with 0.8ug HSP 65 three times every second day or orally treated with 8 ug HSP 65 on 5 consecutive days. A high cholesterol diet was started after the last treatment and mice were mucosally treated once/week for 8 weeks at which time pathologic analysis was performed. In nasally treated animals, we found a reduction in macrophage-positive area in the aortic arch (3.44% vs. 13.03% in controls,  $p = 0.008$ ) as well as a reduced number of T-cells ( $p = 0.02$ ). There was also a decrease in the size of atherosclerotic plaques. A similar trend was observed in orally treated animals but was not significant. Mice nasally treated with HSP also gained significantly less weight than fed or control treated mice. Our results suggest that nasal treatment with HSP reduces the inflammatory process associated with atherosclerosis and may provide a new treatment approach.

183.11

**Phase I Clinical Trial of Orally Delivered Hepatitis B Surface Antigen Expressed in Potato Tubers.**Yasmina Thanavala, <sup>1</sup>Adrienne Scott, <sup>2</sup>Srabani Pal, <sup>1</sup>Martin Mahoney and <sup>2</sup>Charles Arntson. <sup>1</sup>Roswell Park Cancer Institute, Buffalo, NY; <sup>2</sup>Boyer Thompson Institute for Plant Research, Ithaca, NY.

A randomized, double-blind, placebo-controlled phase I clinical trial has been completed at Roswell Park Cancer Institute to evaluate the safety, tolerability and immunogenicity of orally delivered HBsAg expressed as a protein in transgenic potatoes. Forty-five healthy healthcare workers with a history of known positive response to a primary series of recombinant hepatitis B vaccine (meeting all inclusion criteria and none of the exclusion criteria) were recruited for the trial. The 45 volunteers were randomized into one of three groups. Each group ate either vaccinated or placebo potato at defined intervals. Study subjects were randomized by use of a centrally generated block randomization list. This list was provided to the study pharmacist who was unblinded to study group assignments. All other study personnel and the study subjects remained blinded through the completion of the study. Subjects had baseline chemistry, hematology and anti-HBs antibody determinations performed before their first dose of vaccine and at predetermined intervals throughout the trial. As a phase I study, this was primarily an assessment of the relative safety and immunogenicity of transgenic HBsAg expressing potatoes.

183.8

**MYELIN-SPECIFIC TOLERANCE ATTENUATES DISEASE SEVERITY IN A VIRALLY INDUCED MODEL OF MULTIPLE SCLEROSIS.** Katherine L. Neville, Lou Mato, and Stephen D. Miller. Northwestern University Medical School, Chicago, IL, 60611, and \*Alexion Pharmaceuticals, New Haven, CT, 06511. Theiler's Murine Encephalomyelitis Virus-induced Demyelinating Disease (TMEV-IDO) is a relevant model for the autoimmune disease multiple sclerosis (MS). Approximately 30 days after intracerebral inoculation of SJL mice with TMEV, clinical disease signs arise, characterized by spastic paralysis, chronic disease progression, and mononuclear cell infiltrate into the CNS. While initial demyelination in TMEV-IDO is mediated by virus-specific CD4+ T cells, reactivity to myelin epitopes can be detected in TMEV infected mice 55 days post infection, demonstrating autoimmune specificity in this virally induced disease. Administration of the fusion protein MP4, a fusion of myelin proteins MBP and PLP, to TMEV infected SJL mice 40 days post infection attenuates disease severity in MP4 treated animals compared to controls, and also decreases DTH reactivity to myelin peptides, indicating anti-myelin responses are centrally involved in the chronic progressive nature of TMEV-induced paralysis. Additionally, T cells isolated from the spinal cords of TMEV infected animals proliferate and secrete IFN $\gamma$  in response to PLP139-151 peptide stimulation *in vitro*. Both isolation of myelin specific cells from the CNS of TMEV infected animals, and myelin specific tolerance in TMEV-IDO indicate anti-myelin T cell responses contribute to disease severity in this virally induced model of MS, and support the idea of antigen specific tolerance as an effective treatment of ongoing autoimmune disease. (Supported by NIH grant NS23349)

183.10

**HIGH DOSE -ANTIGEN FEEDING INDUCES CD4 T CELLS WITH SUPPRESSOR ACTIVITY IN THE LIVER.**

T. WATANABE, Y. WAKATSUKI, M. YOSHIDA, T. ITOH, T. UHUI, T. CHIBA, and T. KITA. Dept. of Clinical and Bio-Regulatory Science, Kyoto Univ. Grad. Sch. of Med., Kyoto 606-8507, Japan.

Oral feeding of low or high dose-antigens (Ag) induces Ag-specific immune-suppression in subsequent systemic challenge with the same Ag. Since a part of Ag fed at high dose should reach to the liver as an immunogenic form, we examined the possibility that Ag-specific T cells are activated by high dose-Ag feeding. OVA-TCR transgenic mice were fed 100 mg or 1 mg of OVA, or PBS every other day for five times and then CD4 T cells were purified from Peyer's patch, spleen, and liver. Only intrasplenic CD4 T cells (IHLs) from high dose Ag-fed mice suppressed both Ag-specific DTH and antibody responses when adoptively transferred to naive Balb/c mice. Upon Ag-stimulation *in vivo*, the secretion of IL-10, TGF- $\beta$ , and especially IL-4 by IHLs from Ag-fed mice were increased in an Ag-dose dependent manner. In contrast, IL-2 secretion and proliferative responses by these T cells were decreased. In addition, these IHLs from Ag-fed mice inhibited Ag-specific proliferation of naive splenic CD4 T cells. FACS analysis revealed decrease in the population of Ag-specific CD4 T cells in the liver by Ag-feeding, associated with the up-regulation of FasL expression, suggesting that clonal deletion was induced in the liver. Naive splenic CD4 T cells cultured with OVA presented by liver-derived APCs showed a similar profile of cytokine production to that of IHLs. Taken together, these data suggest that high dose-Ag feeding induces CD4 T cells with suppressor activity in the liver. Not only clonal deletion but also active suppression is considered to be induced in the liver after high dose-Ag feeding.

183.12

**ORAL IMMUNIZATION BY FOOD IS LESS EFFECTIVE THAN INTRAGASTRIC IMMUNIZATION**

T.G.M. Lasterdager and L.A.Th. Hilgers. (SPON: W.J.A. Boersma). DLO-Institute for Animal Science and Health, P.O. Box 65, 8200 AB, Lelystad, The Netherlands

The feasibility of edible vaccines was studied by oral immunization of mice with chicken ovalbumin (OVA) mixed with standard food. Other mice were immunized with a similar dose of OVA via intragastric immunization. Intragastric immunization elicited 20-fold higher numbers of anti-OVA IgA and 34-fold higher numbers of anti-OVA IgG producing cells in the lamina propria of the gut than food immunization. Furthermore, intragastric immunization elicited a 20-fold higher anti-OVA IgG response in serum and a 2-fold higher anti-OVA IgA response in faeces than food immunization. The addition of the *Vibrio cholerae* toxin to food did not enhance the immune response. Possible explanations for the differences between these immunization routes will be discussed. We concluded that intragastric immunization is merely limited indicative for the effectiveness of edible vaccines.

# Chronic treatment with nitric oxide-releasing aspirin reduces plasma low-density lipoprotein oxidation and oxidative stress, arterial oxidation-specific epitopes, and atherogenesis in hypercholesterolemic mice

Claudio Napoli<sup>\*,†</sup>, Eric Ackah<sup>‡</sup>, Filomena de Nigris<sup>\*,†</sup>, Piero Del Soldato<sup>§</sup>, Francesco P. D'Armiento<sup>\*</sup>, Ettore Crimi<sup>||</sup>, Mario Condorelli<sup>\*</sup>, and William C. Sessa<sup>‡</sup>

<sup>\*</sup>Departments of Medicine and Human Pathology, School of Medicine, Federico II University of Naples, 80131 Naples, Italy; <sup>†</sup>Department of Medicine-0682, University of California at San Diego, La Jolla, CA 92093; <sup>‡</sup>Department of Pharmacology and Molecular Cardiology Program, Boyer Center for Molecular Medicine, Yale University School of Medicine, New Haven, CT 06536; <sup>§</sup>NicOx, 06906 Sophia Antipolis, France; and <sup>||</sup>Department of Anesthesiology, University of Novara, 28100 Novara, Italy

Edited by Louis J. Ignarro, University of California, Los Angeles School of Medicine, Los Angeles, CA, and approved July 8, 2002 (received for review April 23, 2002)

The effects of chronic treatment with nitric oxide-containing aspirin (NO-aspirin, NCX-4016) in comparison with regular aspirin or placebo on the development of a chronic disease such as atherosclerosis were investigated in hypercholesterolemic low-density lipoprotein (LDL)-receptor-deficient mice. Male mice were assigned randomly to receive in a volume of 10 ml/kg either placebo ( $n = 10$ ), 30 mg/kg/day NO-aspirin ( $n = 10$ ), or 18 mg/kg/day of regular aspirin ( $n = 10$ ). After 12 weeks of treatment, the computer-assisted imaging analysis revealed that NO-aspirin reduced the aortic cumulative lesion area by  $39.8 \pm 12.3\%$  compared with that of the placebo ( $P < 0.001$ ). Regular aspirin did not reduce significantly aortic lesions ( $-5.1 \pm 2.3\%$ ) compared with the placebo ( $P = 0.867$ , not significant (NS)). Furthermore, NO-aspirin reduced significantly plasma LDL oxidation compared with aspirin and placebo, as shown by the significant reduction of malondialdehyde content ( $P < 0.001$ ) as well as by the prolongation of lag-time ( $P < 0.01$ ). Similarly, systemic oxidative stress, measured by plasma isoprostanes, was significantly reduced by treatment with NCX-4016 ( $P < 0.05$ ). More importantly, mice treated with NO-aspirin revealed by immunohistochemical analysis of aortic serial sections a significant decrease in the intimal presence of oxidation-specific epitopes of oxLDL (E06 monoclonal antibody,  $P < 0.01$ ), and macrophages-derived foam cells (F4/80 monoclonal antibody,  $P < 0.05$ ), compared with placebo or aspirin. These data indicate that enhanced NO release by chronic treatment with the NO-containing aspirin has antiatherosclerotic and antioxidant effects in the arterial wall of hypercholesterolemic mice.

atherosclerosis | LDL-receptor-deficient mice

Endothelial dysfunction has been shown in the presence of atherosclerosis (ref. 1 and reviewed in refs. 2–4). Several lines of evidence indicate that restoring nitric oxide (NO)-mediated signaling pathways in atherosclerotic arteries may decrease the disease (2–4). The essential findings are that the biochemical properties of NO allow its exploitation as both a cell signaling molecule through its interaction with redox centers in heme proteins and a rapid reaction with other biologically relevant radical species. The direct reaction of NO with radicals can have, at least in part, antioxidant effects. In arterial cells, the antioxidant properties of NO can be greatly amplified by the activation of signal transduction pathways that lead to the increased synthesis of endogenous antioxidants or down-regulate responses to pro-inflammatory stimuli. Studies in humans and in animal models have shown that low-density lipoprotein (LDL) oxidation may play a pivotal role in the pathogenesis of atherosclerosis (reviewed in refs. 5, 6). Recent data indicate that LDL oxidation may promote *per se* activation of several signaling

pathways and transcription factors in human coronary arteries (7–9). Several of these pathways are reduced by concomitant administration of vitamin E (7, 9). Thus, compounds with antioxidant properties may reduce downstream effects induced by LDL oxidation in the arterial wall, and this phenomenon could retard the progression of atherosclerosis.

In preliminary experiments, we evaluated the antioxidant properties *in vitro* of several nitro-compounds and found that some of these agents had antioxidant properties. In this study, we used male LDL-receptor-deficient mice (10, 11) to address the effects of a NO-containing aspirin derivative (NCX-4016) on the development of a chronic disease such as atherosclerosis and on plasma LDL oxidation and systemic oxidative stress. NO-releasing aspirin (NCX-4016) is a drug well characterized *in vitro* and *in vivo* (reviewed in ref. 12). Hypercholesterolemic mice develop hypercholesterolemia on a cholesterol mouse chow diet (10, 13) and extensive atherosclerosis, with lesions progressing from lipid-laden fatty streaks to advanced lesions (10, 11, 13–15). By using this model, we investigated the chronic effects of treatment with NO-aspirin or regular aspirin on aortic lesion development, plasma LDL oxidation, and oxidative stress, as well as oxidation-specific epitopes of LDL in the arterial wall.

## Materials and Methods

**Drugs and Experimental Protocol.** The experiments conformed to the Guide for the Care and Use of Laboratory Animals (National Institutes of Health Publication No. 85–23, revised 1996) and the Guidelines of the American Heart Association. The experiments described here were carried out on male LDL-receptor-deficient mice of 18 weeks on high-cholesterol and cholate-free diet (21% by weight fat, 0.15% by weight cholesterol, and 19.5% by weight casein; no. 8137, Teklad, Madison, WI). LDL-receptor-deficient mice crossed with C57BL/6J mice for 10 generations, develop only “moderately” elevated plasma cholesterol levels (250–300 mg/dl) when fed regular mouse chow (10, 11). However, high cholesterol levels are easily achieved by enriched-cholesterol diets that induce extensive atherosclerosis throughout the arterial tree (10, 11). We selected only male mice to avoid gender-related differences (10). Mice were assigned randomly to be treated for 12 weeks with 30 mg/kg day of NCX-4016 (a generous gift from NicOx;  $n = 10$ , 30-mg compound contains 18 mg of aspirin) or 18 mg/kg/day

This paper was submitted directly (Track II) to the PNAS office.

Abbreviation: LDL, low-density lipoprotein.

<sup>\*</sup>To whom reprint requests should be addressed. E-mail: claudnap@tin.it or cnapoli@ucsd.edu.

of aspirin (Sigma;  $n = 10$ ), or placebo (saline vehicle) given by gavage. These drug doses were chosen on the basis of previous studies *in vivo* (12, 16, 17) and did not affect blood pressure in mice measured by tail cuff ( $P = \text{NS}$ , not shown). At the end of the study, mice were killed with a lethal dose of sodium pentobarbital and *in situ* fixation of the aorta at physiologic pressure [100 mmHg (1 mmHg = 33 Pa)] was performed with PBS/paraformaldehyde (4%, 0.1 mol/liter, pH 7.3) for histology and normal saline for immunohistochemistry (see below).

**Plasma Determination and LDL Oxidation.** Blood was collected at the time of killing into Eppendorf tubes with 1 mM Na<sub>2</sub>EDTA. Plasma cholesterol was determined enzymatically (18, 19). LDL particles ( $d = 1.006 - 1.063$  g/ml) were isolated from 2 ml of pooled plasma from two animals of each group by sequential-density ultracentrifugation (18, 19). The protein content of LDL was measured by the method of Lowry (20). Susceptibility of LDL to *in vitro* oxidation was induced by 1  $\mu\text{M}$  copper sulfate at 37°C for 12 h, as described (18, 19, 21). At the end of the incubation, the formation of thiobarbituric acid reactive substances was determined by the thiobarbituric acid method, as described (18, 19, 21). Lag-time was determined by monitoring the changes measured at 234 nm in the absorbance and observed at room temperature (23°C) every 10 min for a period of 4 h (19, 21). Measurement of the isoprostane 8-epi-PGF<sub>2</sub> purified from plasma samples was made by using a commercially available immunoassay (Cayman Chemical, Ann Arbor, MI) according to the manufacturer's instructions.

**Morphometric Assessment of Lesions and Immunohistochemistry of Lesion Components.** The aorta was dissected, cleaned of adherent fat and fascia, cut open, washed thoroughly with cold sterile PBS containing 2 mM EDTA, placed in ice-cold PBS containing 50  $\mu\text{M}$  butylated hydroxytoluene, 0.001% aprotinin, 50 mM EDTA, and 0.008% chloramphenicol, and equilibrated with nitrogen (10, 11, 22, 23). Each arterial segment then was divided into two parts. One of these was immersed in cysteine prodrug 2-oxothiazolidine-4-carboxylate (5 mM)-containing medium (Dako, Milan) and flash frozen in liquid nitrogen; 7- $\mu\text{m}$ -thick sections were taken and prepared with a cryotome for computer-assisted morphometric determination of lipid-rich lesions (30 cryosections from arteries were stained with oil red-O and counterstained with hematoxylin), as described in detail (10, 11, 16, 22, 23). The second part of each arterial segment was fixed in buffered 10% formalin and paraffin embedded; 12–15 serial sections (5- $\mu\text{m}$  thickness) were prepared for immunohistochemistry (10, 11, 16, 22, 23). Duplicate serial sections of the fixed and paraffin-embedded arterial segments were immunostained with E06, murine monoclonal antibody against oxidation-specific-lysine and oxidized phospholipid epitopes of ox-LDL, and F4/80, a monoclonal antibody against mouse monocyte/macrophages-derived foam cells (10, 11, 16, 22, 23). Antibodies were used at a dilution of 1:500. Epitopes recognized by the primary antibody were detected by an avidin-biotin-peroxidase computer-assisted method (10, 11, 16, 22, 23).

**Statistical Analysis.** Results are expressed as mean  $\pm$  SEM. Evaluation of the atherogenesis and the immunohistochemistry were performed in a blinded way regarding the treatment given to mice. A Student's *t* test was used to compare differences among groups. Statistical significance was defined as  $P < 0.05$ .

## Results

**Lipid Profile.** Plasma cholesterol levels were similar among groups of LDL-receptor-deficient mice ( $724 \pm 68$  mg/dl,  $746 \pm 72$  and  $738 \pm 57$  in placebo, NCX-4016 and aspirin-treated groups, respectively;  $P = \text{NS}$  for all comparisons). Similarly, plasma triglyceride levels were comparable in all three groups of mice

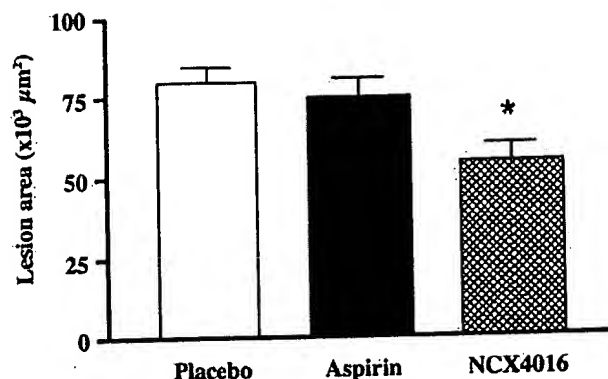


Fig. 1. Effects of various treatments on atherosclerotic lesion area in male LDL-receptor-deficient mice after 12 weeks of treatment with placebo, regular aspirin (18 mg/kg), or equimolar doses of nitric oxide-releasing aspirin (NCX-4016, 30 mg/kg). Mean lesion area of oil-red O-stained sections was calculated by computer-assisted imaging analysis. Results are expressed as the mean  $\pm$  SEM of the aortic lesions of 10 animals from each group. \*,  $P < 0.01$  vs. placebo-treated mice.

( $165 \pm 22$  mg/dl,  $172 \pm 32$ , and  $170 \pm 28$  in placebo, NCX-4016, and aspirin-treated groups, respectively;  $P = \text{NS}$  for all comparisons).

**Evaluation of Atherogenesis.** Computer-assisted imaging analysis revealed that 30 mg/kg of NCX-4016 reduced the aortic cumulative lesion area by  $39.8 \pm 12.3\%$  compared with that of the placebo ( $P < 0.001$ ). In another set of experiments ( $n = 5$ ), 30 mg/kg of NCX-4016 reduced the aortic cumulative lesion area by  $24.1 \pm 10.8\%$  ( $P = 0.589$ , NS). The equimolar dose of aspirin (18 mg/kg) did not reduce significantly aortic lesions ( $-5.1 \pm 2.3\%$ ) compared with the placebo ( $P = 0.867$ , NS; Fig. 1). Fig. 2 shows some examples of high magnifications of oil-red O-stained aorta of a placebo-treated mouse (A) and NCX-4016-treated mouse (B). The reduction of the atherosclerotic lesions was coupled with a marked decrease in the thickness of lesions (oil-red O staining) of a NCX-4016-treated mouse in comparison to the placebo-treated mouse (C).

**Immunohistochemistry.** Mice treated with 30 mg/kg/day of NCX-4016 revealed a significant decrease of intimal macrophages-derived foam cells ( $-28.3 \pm 10.2\%$  of F4/80-positive arterial sections,  $P < 0.05$  vs. placebo-treated group) and oxidation-specific epitopes of oxidized LDL by ( $-35.8 \pm 11.9\%$  of E06-positive arterial section,  $P < 0.01$  vs. placebo-treated group; Fig. 3). Thus, NCX-4016 significantly reduced the expression of oxidation-specific epitopes and macrophage accumulation in the arterial wall compared with that of the placebo-treated group as well as aspirin-treated group.

**Effect of Different Treatments on Plasma LDL Oxidizability and Oxidative Stress.** Treatment with 30 mg/kg/day of NCX-4016 reduced significantly plasma LDL oxidation and systemic oxidative stress compared with both placebo and, to a lesser extent, aspirin (Table 1). This reduction of plasma LDL oxidation was shown by significant reduction of LDL malondialdehyde content of around 40% ( $P < 0.001$  vs. placebo;  $P < 0.04$  vs. aspirin), as well as by the prolongation of lag-time of oxidizability of around 20% ( $P < 0.01$  vs. placebo;  $P < 0.05$  vs. aspirin). In the same group of mice above ( $n = 5$ ) treated with 10 mg/kg of NCX-4016, the compound reduced LDL malondialdehyde content to  $19.3 \pm 4.0$  nmol/mg of protein ( $P < 0.05$  vs. placebo;  $P = \text{NS}$  vs. aspirin) and LDL lag-time reached  $120 \pm 33$  min ( $P = \text{NS}$  vs.



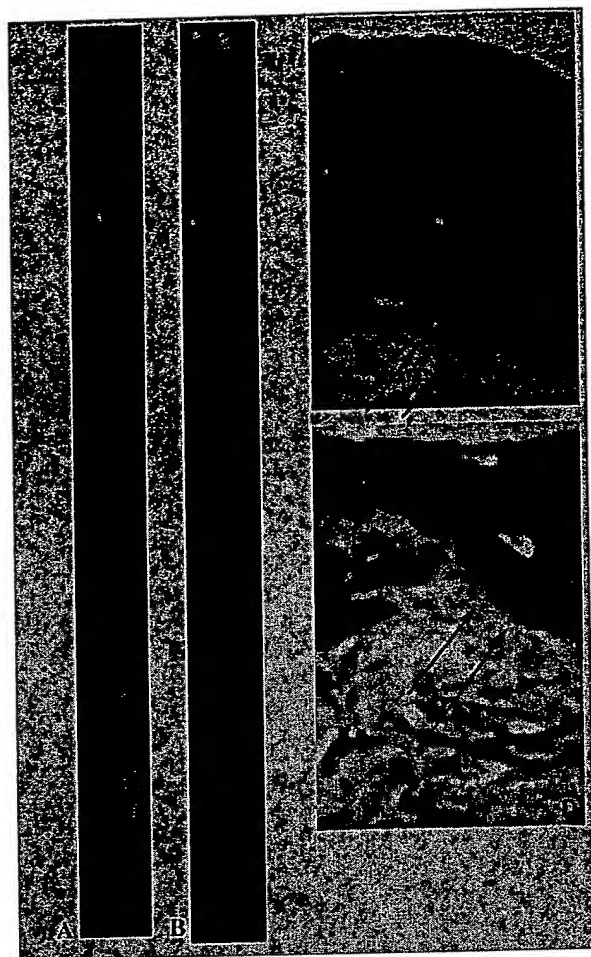


Fig. 2. High-magnifications ( $\times 25$ ) of oil-red O-stained thoracic aorta of placebo-treated mouse (A), placebo-treated mouse (B), and nitric oxide-releasing aspirin-treated mouse (30 mg/kg) (C). Sustained reduction of the thickness of lesions of nitric oxide-releasing aspirin-treated mouse (D) in comparison to the placebo-treated mouse (C) (both  $\times 320$  magnification). Arrows indicate the degree of staining in relation to the intima.

placebo and aspirin). Similarly, plasma isoprostanes were reduced significantly by treatment with NCX-4016 (Table 1).

## Discussion

Our article demonstrates that chronic delivery of NO achieved with the NO-releasing aspirin significantly attenuates the devel-

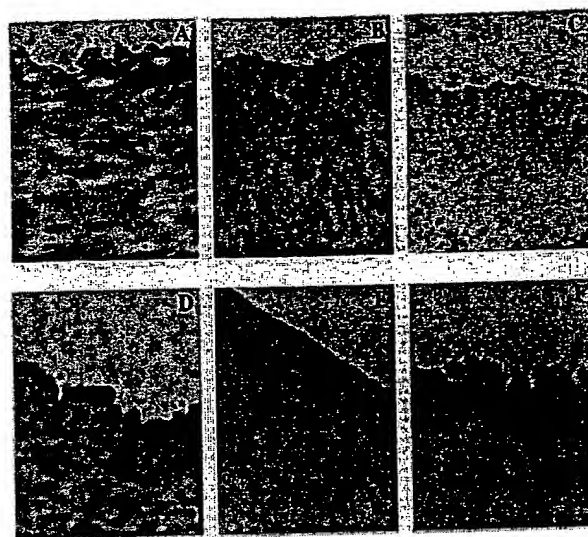


Fig. 3. Treatment with (C) 30 mg/kg nitric oxide-releasing aspirin (NCX-4016) was more effective than (B) 18 mg/kg of regular aspirin or (A) placebo in reducing oxidation-specific epitopes in E06-positive sections ( $\times 275$ ). Indeed, placebo-treated animals had a diffuse staining for oxidation-specific epitopes (A). This staining was partially reduced and increased in the sub-endothelial space in aspirin-treated mice (B). Nitric oxide-releasing aspirin reduced the overall immunostaining throughout the serial section (C). Similarly, macrophage accumulation was reduced in F4/80 positive sections in nitric oxide-releasing aspirin-treated animals (F) when compared with regular aspirin-treated (E) or placebo-treated (D) LDL-receptor-deficient mice ( $\times 275$ ). The negative immunostaining (brown) in C and F appears in blue.

opment of a chronic disease such as atherosclerosis in hypercholesterolemic LDL receptor-deficient mice without affecting plasma cholesterol levels. The enhancement of the NO pathway may play an important role in antiatherogenic effect of NO-releasing aspirin (reviewed in ref. 4). This study also demonstrates that in parallel to the attenuation of atherosclerosis, NO-aspirin reduced the susceptibility *ex vivo* of plasma LDL to oxidative modification and systemic oxidative stress measured by plasma isoprostanes. Isoprostane levels are a well recognized indicator of oxidative stress in animal models and in humans (24). Antioxidant protection could be related to the scavenging activity of free radicals by NO-containing aspirin both in plasma and in the arterial wall. Superoxide anion and NO are known to react rapidly to form the stable peroxynitrite anion, and peroxynitrite decomposition generates a strong oxidant with reactivity similar to hydroxyl radical (25). However, the causal role of peroxynitrite in atherogenesis is not established. Nevertheless, the properties of NO-releasing aspirin can also affect multiple

Table 1. Parameters of susceptibility to *ex vivo* peroxidation of LDL and systemic oxidative stress in LDL-receptor-deficient mice treated with nitric oxide-releasing aspirin (NCX-4016) or regular aspirin

	LDL lag-time, min	LDL MDA, nmol/mg prot	Plasma isoprostane 8-epi-PGF <sub>2</sub> , pg/ml
Placebo-treated LDL-receptor-deficient mice (n = 10)	112 $\pm$ 22	24.5 $\pm$ 4.2	143 $\pm$ 37 (n = 6)
NCX-4016-treated LDL-receptor-deficient mice (n = 10)	131 $\pm$ 18*	14.3 $\pm$ 2.4**	119 $\pm$ 21*** (n = 6)
Aspirin-treated LDL-receptor-deficient mice (n = 10)	115 $\pm$ 15	22.3 $\pm$ 4.7	128 $\pm$ 38 (n = 6)

LDL-receptor-deficient mice treated with NCX-4016 (30 mg/kg/day), and aspirin (18 mg/kg/day); MDA, malondialdehyde at 12 h after exposure of LDL to 1  $\mu$ M copper sulphate (n = 10 for each group). Lag-time represents an index of LDL oxidizability; increased values of lag-time reflect increased resistance of LDL to oxidative modification (n = 10 for each group, see also refs. 19 and 21). In a subset of animals (n = 6), plasma isoprostane levels (8-epi PGF<sub>2</sub>) were measured. \*, P < 0.05 or \*\*, P < 0.01 vs. placebo or aspirin-treated mice; \*\*\*, P < 0.05 vs. placebo-treated mice by ANOVA followed by t test and Bonferroni's correction. See text for further details.





radical species generated in the arterial wall. An increasing number of compounds releasing NO or modulating the NO pathway are now available (reviewed in ref. 26). Further studies should evaluate whether these newly developed compounds, clinically used drugs, or other NO-donors could be helpful in retarding atherosclerotic lesion formation and its clinical sequelae.

Oxidative modification of LDL plays a crucial role in human early atherosclerotic lesions (22, 23, 27) leading to atherosclerosis-related diseases (5, 6). Some studies (28) also demonstrated the important role of inhibition of LDL oxidation on the attenuation of atherosclerosis in hypercholesterolemic mice. In the present study, we showed that NCX-4016 reduced formation in the arterial wall of oxidation-specific epitopes of oxidized LDL. Thus, NCX-4016 has a potent antioxidant effect also in the atherosclerotic lesions of mice probably by means of scavenging of the radical-induced oxidation of LDL also in the arterial wall. Oxidized LDL may induce apoptosis in human coronary cells (7, 8). This phenomenon may favor the development of unstable atherosclerotic lesions (7, 8). However, apoptosis in macrophages also may reduce a potential source of mediators which can contribute to destabilizing the plaque (e.g., metalloproteinases and MCP-1). Nevertheless, the reduction of oxidative stress *in vivo* could also attenuate the degree of unstable atheroma. In another experimental setting, we showed recently that NCX-4016 reduced restenosis after arterial injury and macrophage deposition in hypercholesterolemic mice (16) and in aged rats (17), perhaps, at least in part, through its antioxidant effects. These properties may be particularly useful when applied to hypercholesterolemic or elderly patients. Obviously, the chronic development of atherosclerosis is a completely different pathophysiological condition from restenosis after arterial injury. Indeed, restenotic inflammatory lesions already appear after 14 days from the arterial injury. In the present study, we have also shown that the antiatherogenic effect was coupled to

the reduction of macrophage-derived foam cells at the site of lesions. This beneficial effect may contribute to the reduction of lesion progression observed in hypercholesterolemic mice, and it is also consistent with the inhibition of macrophage-dependent LDL oxidation by *in vitro* NO donors (26, 29).

The findings of the present study are in agreement with an important role of NO in the development of atherogenesis in hypercholesterolemic mice. Accordingly, the role of endogenous NO in the progression of atherosclerosis in apolipoprotein E-knockout mice was recently investigated by using N(omega)-nitro-L-arginine methyl ester (L-NAME), an inhibitor of nitric oxide synthase (NOS) or with the NOS substrate L-arginine for 8 weeks (30). L-NAME treatment resulted in a significant inhibition of NO-mediated vascular responses and a significant increase in the atherosclerotic plaque area in the aorta of these mice. In contrast, L-arginine treatment had no influence on endothelial function and did not alter lesion size. The acceleration in lesion size concomitant to the severely impaired NO-mediated responses indicates that lack of endogenous NO (4, 31) is an important progression factor of atherosclerosis in the apolipoprotein E-knockout mouse.

We conclude that enhanced NO release by chronic treatment with NO-containing aspirin attenuates the development of a chronic disease such as atherosclerosis in hypercholesterolemic mice. Although the natural history of the atherosclerotic disease is different between rodents and humans, these data should be considered a further piece of evidence supporting the key role of NO in atherogenesis. Inhibition of oxidation-sensitive mechanisms by NO-aspirin, and possible other NO-related anti-inflammatory effects (reviewed in ref. 32), both in plasma and in atherosclerotic lesions, together with reduced macrophage accumulation, may have an important role in contributing to this antiatherogenic effect.

This work was supported by National Institutes of Health Grants HL57665, HL41371, and HL64793, and by Italian Institutes of Health Grant ISNIH.99.56980.

- Ludmer, P. L., Selwyn, A. P., Shook, T. L., Wayne, R. R., Mudge, G. H., Alexander, R. W. & Ganz, P. (1986) *N. Engl. J. Med.* 315, 1046–1051.
- Ignarro, L. J., Cirino, G., Casini, A. & Napoli, C. (1999) *J. Cardiovasc. Pharmacol.* 34, 876–884.
- Drexler, H. (1999) *Cardiovasc. Res.* 43, 572–579.
- Napoli, C. & Ignarro, L. J. (2001) *Nitric Oxide* 5, 88–97.
- Witztum, J. L. & Steinberg, D. (1991) *J. Clin. Invest.* 88, 1785–1791.
- Steinberg, D. (1997) *J. Biol. Chem.* 272, 20963–20966.
- de Nigris, F., Maida, I., Palumbo, G., Anania, V. & Napoli, C. (2000) *Biochem. Pharmacol.* 59, 1477–1487.
- Napoli, C., Quehenberger, O., de Nigris, F., Abete, P., Glass, C. K. & Palinski, W. (2000) *FASEB J.* 14, 1996–2007.
- de Nigris, F., Youssef, T., Ciafrè, S., Franconi, F., Anania, V., Condorelli, G., Palinski, W. & Napoli, C. (2000) *Circulation* 102, 2111–2117.
- Palinski, W., Napoli, C. & Reaven, P. D. (2000) *Harvard Series*, eds Simon, D. I. & Rogers, C. (Humana, Totowa, NJ), pp. 149–174.
- Napoli, C., de Nigris, F., Welch, J. S., Calara, F. B., Stuart, R., Glass, C. K. & Palinski, W. (2002) *Circulation* 105, 1360–1367.
- Del Soldato, P., Sorrentino, R. & Pinto, A. (1999) *Trends Pharmacol. Sci.* 8, 319–323.
- Zhang, S. H., Reddick, R. L., Piedrahita, J. & Maeda, N. (1992) *Science* 258, 468–471.
- Nakashima, Y., Plump, A. S., Raines, E. W., Breslow, J. L. & Ross, R. (1994) *Arterioscler. Thromb.* 14, 133–139.
- Reddick, R. L., Zhang, S. H. & Maeda, N. (1994) *Arterioscler. Thromb.* 14, 141–148.
- Napoli, C., Cirino, G., Del Soldato, P., Sorrentino, R., Sica, V., Condorelli, M., Pinto, A. & Ignarro, L. J. (2001) *Proc. Natl. Acad. Sci. USA* 98, 2860–2864.
- Napoli, C., Aldini, G., Wallace, J. L., de Nigris, F., Maffei, R., Abete, P., Bonaduce, D., Condorelli, G., Rengo, F., Sica, V., et al. (2002) *Proc. Natl. Acad. Sci. USA* 99, 1689–1694.
- Napoli, C., Chiariello, M., Palumbo, G. & Ambrosio, G. (1996) *Cardiovasc. Drugs Ther.* 10, 417–424.
- Napoli, C., Mancini, F. P., Corso, G., Malorni, A., Crescenzi, E., Postiglione, A. & Palumbo, G. (1997) *J. Biochem.* 121, 1096–1101.
- Lowry, O. H., Rosebrough, N. J. & Farr, L. (1951) *J. Biol. Chem.* 193, 265–275.
- Napoli, C., Postiglione, A., Triggiani, M., Corso, G., Palumbo, G., Carbone, V., Rocco, A., Ambrosio, G., Montefusco, S., Malorni, A., et al. (1995) *Atherosclerosis* 11, 263–275.
- Napoli, C., D'Armiento, F. P., Mancini, F. P., Palumbo, G., Witztum, J. L. & Palinski, W. (1997) *J. Clin. Invest.* 100, 2680–2690.
- Napoli, C., Witztum, J. L., de Nigris, F., D'Armiento, F. P. & Palinski, W. (1999) *Circulation* 99, 2003–2010.
- Witztum, J. L. & Berliner, J. A. (1998) *Curr. Opin. Lipidol.* 9, 441–448.
- Beckman, J. S., Beckman, T. W., Chen, J., Marshall, P. A. & Freeman, B. A. (1990) *Proc. Natl. Acad. Sci. USA* 87, 1620–1624.
- Ignarro, L. J., Napoli, C. & Loscalzo, J. (2002) *Circ. Res.* 90, 21–28.
- Napoli, C., Glass, C. K., Witztum, J. L., D'Armiento, F. P., Deutch, R. & Palinski, W. (1999) *Lancet* 354, 1234–1241.
- Aviram, M., Maor, I., Keidar, S., Hayek, T., Oiknine, J., Bar-El, Y., Adler, Z., Kertzman, V. & Milo, S. (1995) *Biochem. Biophys. Res. Commun.* 216, 501–513.
- Hogg, N., Struck, A., Goss, S. P. A., Santanam, N., Joseph, J., Parthasarathy, S. & Kalyanaram, B. (1995) *J. Lipid Res.* 36, 1756–1762.
- Kauser, K., da Cunha, V., Fitch, R., Mallari, C. & Rubanyi, G. M. (2000) *Am. J. Physiol.* 278, H1679–H1685.
- Rudic, R. D. & Sessa, W. C. (1999) *Am. J. Hum. Genet.* 64, 673–677.
- Wallace, J. L., Ignarro, L. J. & Fiorucci, S. (2002) *Nat. Rev. Drug Discovery* 1, 375–382.

Evidence Appendix

(*Arteriosclerosis, Thrombosis, and Vascular Biology*. 1996;16:1013.)  
© 1996 American Heart Association, Inc.

Articles

## Lymphocyte Populations in Atherosclerotic Lesions of ApoE -/- and LDL Receptor -/- Mice

### Decreasing Density With Disease Progression

Simon E. Roselaar; Paul X. Kakkanathu; Alan Daugherty

the Departments of Medicine (S.E.R., P.X.K., A.D.) and Biochemistry and Molecular Biophysics (A.D.), Washington University School of Medicine, St Louis, Mo.

Correspondence to Alan Daugherty, Box 8086, Cardiovascular Division, Washington University School of Medicine, St Louis, MO 63110. E-mail doco@imgate.wustl.edu.

### Abstract

Lymphocytes are prominent components of human atherosclerotic lesions, but their presence in murine models of disease has not been confirmed. Lymphocyte subpopulations have been identified in apoE -/- and LDL receptor -/- mice fed a cholesterol-enriched diet for up to 3 months. ApoE -/- mice had higher serum cholesterol concentrations than did LDL receptor -/- mice during most of the feeding period, primarily due to large increases in VLDL concentrations. Total area of atherosclerotic lesions was greater at all times in apoE -/- than LDL receptor -/- mice (lesion area after 3 months on cholesterol-enriched diet: apoE -/-,  $993 \pm 193$  and LDL receptor -/-,  $560 \pm 131 \mu\text{m}^2 \times 10^3$ , mean  $\pm$  SEM,  $n=6$  in each group). Lesions in apoE -/- mice contained larger macrophage-rich necrotic cores and more calcification than did those in LDL receptor -/- mice. Immunocytochemical analyses of tissue sections of ascending aortas performed with monoclonal antibodies to T and B lymphocytes and macrophages revealed that T lymphocytes immunoreactive for Thy 1.2, CD5, CD4, and CD8 were observed in lesions from both strains, but no B lymphocytes were detected. The density of Thy 1.2<sup>+</sup> T lymphocytes in lesions was greatest at 1 month (apoE -/-,  $98 \pm 23$  and LDL receptor -/-,  $201 \pm 40$  lymphocytes/mm<sup>2</sup>,  $n=6$  in each group), decreasing in apoE -/- mice to  $12 \pm 3$  and in LDL receptor -/- mice to  $51 \pm 20$  lymphocytes/mm<sup>2</sup> at 3 months. The presence of T lymphocytes in murine atherosclerotic lesions makes these animals potentially useful for studying the involvement of the immune system in atherogenesis.

**Key Words:** atherosclerosis • murine model • T lymphocytes • immunohistochemistry

Cellular processes that occur during human atherogenesis may be examined by using animal

### This Article

- ▶ [Abstract FREE](#)
- ▶ [Alert me when this article is cited](#)
- ▶ [Alert me if a correction is posted](#)
- ▶ [Citation Map](#)

### Services

- ▶ [Email this article to a friend](#)
- ▶ [Similar articles in this journal](#)
- ▶ [Similar articles in PubMed](#)
- ▶ [Alert me to new issues of the journal](#)
- ▶ [Download to citation manager](#)
- ▶ [Cited by other online articles](#)
- ▶ [Request Permissions](#)

### Google Scholar

- ▶ [Articles by Roselaar, S. E.](#)
- ▶ [Articles by Daugherty, A.](#)
- ▶ [Articles citing this Article](#)

### PubMed

- ▶ [PubMed Citation](#)
- ▶ [Articles by Roselaar, S. E.](#)
- ▶ [Articles by Daugherty, A.](#)

models of atherosclerosis that simulate human disease. The PDAY study<sup>1</sup> established similarities in the evolution of atherosclerotic disease in humans and Watanabe heritable hyperlipidemic rabbits, cholesterol-fed rabbits,<sup>2 3</sup> and rhesus monkeys.<sup>4 5</sup> In addition, initial studies with cholesterol-fed C57BL/6J mice have led to the increasing use of mice in the study of events in atherogenesis.<sup>6</sup> More recently, genetically modified mice deficient in either apoE<sup>7</sup> or LDL receptors<sup>8</sup> have become available. ApoE-deficient mice are grossly hypercholesterolemic and spontaneously develop atherosclerosis that has the morphological characteristics of human disease<sup>9 10 11</sup>; disease development is accelerated by feeding these mice cholesterol-enriched diets.<sup>12 13</sup> LDL receptor deficiency in mice produces only a mild increase in plasma cholesterol concentrations but imparts an increased responsiveness to cholesterol-enriched diets, leading to pronounced atherosclerotic lesion development.<sup>14</sup>

Atherosclerotic lesions are mostly made up of macrophages and smooth muscle cells, but there is increasing recognition of the presence of T lymphocytes.<sup>15 16 17 18</sup> Both CD4<sup>+</sup> and CD8<sup>+</sup> T lymphocytes are present at all stages of development of human lesions.<sup>19 20</sup> These T lymphocytes are activated, as judged from the presence of activation markers<sup>21</sup> and expression of MHC class II antigens on adjacent smooth muscle cells.<sup>22</sup> Expression of MHC class II is induced by the T lymphocyte-derived cytokine interferon gamma, which is detectable in lesions.<sup>23 24</sup> T lymphocytes in atherosclerotic lesions are polyclonal in origin.<sup>25</sup> The full spectrum of antigens against which T lymphocytes are directed has not been elucidated, but it is known that oxidized LDL activates a small subset.<sup>26</sup> B lymphocytes are also found in human atherosclerotic lesions.<sup>15 27</sup>

The role of the immune system in atherogenesis is controversial. Lesions that develop in cholesterol-fed rabbits contain T lymphocytes that may be active participants in lesion formation since immunosuppression results in enhancement of the atherogenic process.<sup>28</sup> The severity of atherosclerotic lesions is also increased in immune-suppressed<sup>29</sup> and MHC class I-deficient C57BL/6J mice<sup>30</sup> fed a cholesterol-enriched diet. However, in contrast to lesions in hypercholesterolemic rabbits, lymphocytes have not been detected in murine atherosclerotic lesions.<sup>31</sup> Studies to define the role of the immune system in atherogenesis require an animal model in which T lymphocytes are present in lesions, as they are in human disease. We therefore used monoclonal antibodies to evaluate whether lymphocytes are present in atherosclerotic lesions of cholesterol-fed apoE  $-/-$  and LDL receptor  $-/-$  mice. Immunostaining for Thy 1.2, CD5, CD4, and CD8 was positive in atherosclerotic lesions in both strains of mice, although the density of T lymphocytes in each strain differed markedly. The presence of lymphocytes in atherosclerotic lesions of these mice makes them valuable for the study of the role of the immune system in atherogenesis.

## Methods

### Animals

LDL receptor  $-/-$  and apoE  $-/-$  mice (8 female and 10 male in each group) were obtained from Jackson Laboratories. Both strains of mice were originally generated as C57BL/6JxC129 hybrids,

and mice used in this study were backcrossed six generations into a C57BL/6J background. Mice were housed in specific pathogen-free rooms and fed a normal mouse laboratory diet (Ralston Purina) until they were 6 weeks of age, after which they were fed a diet containing 1.25% cholesterol, 0.5% cholic acid, and 15% fat (Harlan Teklad, catalogue No. 88051) for up to 3 months. All procedures were approved by the Washington University Animal Studies Committee.

### **Removal of Aortas and Blood Samples**

Six mice of each strain were selected after 1, 2, and 3 months on a high-cholesterol diet. Nonfasting animals were anesthetized by metaphane inhalation (Pitman-Moore), bled retro-orbitally, and killed by cervical dislocation. Hearts were removed en bloc and placed in ice-cold Ringer's lactate, washed free of blood, and embedded and frozen in optimal cutting temperature compound (Tissue Tek). Sections of aorta (10  $\mu$ m) were cut on a cryostat<sup>6</sup> and placed on Probe-on-Plus microscope slides (Fisher Scientific). Serum was separated from whole blood by centrifugation and stored at 4°C.

### **Serum Cholesterol Concentrations and Lipoprotein Cholesterol Distribution**

Serum concentrations of total cholesterol were measured by using an enzyme-based colorimetric assay (Wako Chemical Co). Lipoprotein cholesterol distributions were determined by fast-performance liquid chromatography of pooled serum samples from all six mice in each group after 3 months of feeding.<sup>32</sup>

### **Histology and Immunocytochemistry**

Frozen sections were fixed in acetone for 5 minutes. Macrophages were detected with anti-mouse monoclonal antibody MOMA-2 (rat IgG<sub>2b</sub>, Serotec). All lymphocyte antibodies were initially screened for their ability to stain cells in splenic tissue (positive control). T lymphocytes were immunostained with monoclonal antibodies to murine CD5 (clone 57-7.3, rat IgG<sub>2a</sub>K, Life Technologies), Thy 1.2 (clone 30-H12, rat IgG<sub>2b</sub>, Collaborative Biomedical Products, and clone AT83A, rat IgM, Dr Osami Kanagawa, Washington University), CD8 (clone YTS 105.18, rat IgG<sub>2a</sub>, Serotec), and CD4 (clone GK1.5, rat IgG, Dr Osami Kanagawa). Tissue sections were blocked with nonimmune rabbit serum. The secondary antibody was an affinity-purified, mouse serum-adsorbed, biotinylated rabbit anti-rat IgG (BA 4001, Vector Laboratories).

Immunocytochemical analysis was performed by using a Fisher MicroProbe system and Vectastain Elite ABC kits (Vector). Negative controls were obtained with isotype-matched irrelevant antibodies or no primary antibody. Immunoreactivity was visualized by using 3-amino 9-ethyl carbazole (Biomed Corp), which forms a red precipitate. Accumulation of neutral lipid in lesions was visualized by staining with oil red O. Tissue sections were counterstained with aqueous hematoxylin (Biomed).

### **Quantification of Lesion Areas and Numbers of T Lymphocytes**

Consecutive 10- $\mu$ m-thick aortic cross sections were cut, beginning at the most proximal part of the aortic sinus.<sup>6</sup> Sections were placed consecutively on each of eight separate slides, after which

the ninth section was placed on the first slide, next to the first section, continuing for 48 sections. A single slide, upon which were six aortic cross sections from each mouse, was analyzed for lesion dimensions and for any given stain or immunostain. Total atherosclerotic lesion area and numbers of Thy 1.2<sup>+</sup> lymphocytes were quantified by using an image-analysis system consisting of a Nikon Optiphot-2 microscope attached to a Javelin JE3462 high-resolution camera and a personal computer equipped with a Coreco-Oculus OC-TCX frame grabber and high-resolution monitor. Computerized color-image analysis was performed by using Image-Pro Plus software (Media Cybernetics). The area of each lesion in all six cross sections in every mouse was recorded, as was the total number of T lymphocytes determined by immunostaining for Thy 1.2. For each mouse studied, total atherosclerotic lesion area was calculated as the sum of the areas of all lesions in all six aortic cross sections on one slide. Thy 1.2-immunopositive lymphocytes were counted per section, and T-lymphocyte density was expressed as the number of lymphocytes per square millimeter of atherosclerotic lesion area.

### Statistics

Differences in serum cholesterol concentrations, atherosclerotic lesion areas, and T-lymphocyte numbers were compared either by two-tailed Student's *t* test, or, if data failed to meet the requirements for use of this parametric test, by the Mann-Whitney rank-sum test. Data analyses were performed by using SigmaStat for Windows (Jandel Scientific).

### Results

All animals tolerated the cholesterol-enriched diet without overt adverse affects. Total serum cholesterol concentrations before commencing the diet and at 1 and 2 months were higher in apoE  $-/-$  than LDL receptor  $-/-$  mice, but they did not differ significantly at 3 months (Fig 1). Analyses of lipoprotein cholesterol distribution by size-exclusion fast-performance liquid chromatography demonstrated that regardless of diet, apoE  $-/-$  mice carried the major fraction of cholesterol in VLDL, while LDL receptor  $-/-$  mice carried cholesterol predominantly in an LDL-sized fraction.<sup>8 9 10 11</sup>

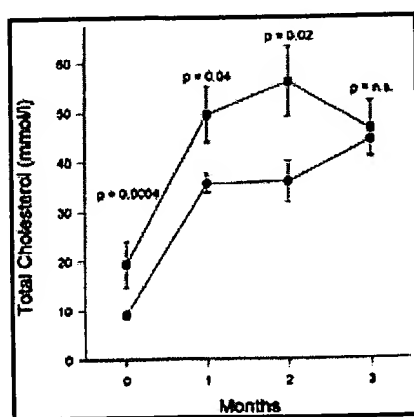


**Figure 1.** Line graph shows total serum cholesterol concentrations in apoE  $-/-$  and LDL receptor  $-/-$  mice. Cholesterol concentrations were measured by using enzymatic assays as described in "Methods." Points indicate means of six observations; bars, SEM; ■, apoE  $-/-$  mice; and •, LDL receptor  $-/-$  mice.

View larger version (16K):  
[in this window]

[\[in a new window\]](#)

Atherosclerotic lesions were characterized after 1, 2, and 3 months of cholesterol feeding for size, macrophage content, and lymphocyte number and distribution. The two strains of mice had atherosclerotic lesions with markedly different cellular architectures and areas. At all times, aortic atherosclerotic lesions of apoE  $-/-$  mice were larger than those in LDL receptor  $-/-$  mice (Fig 2). Lesions from the two types of mice were of similar cellular composition after 1 month of cholesterol feeding, composed predominantly of macrophages. By 3 months, lesions in apoE  $-/-$  mice had large cores of necrotic macrophages, a feature less abundant in LDL receptor  $-/-$  mice. Chondrocytes and early bone formation were readily discernible in all apoE  $-/-$  mice examined at 3 months, but in only one of six LDL receptor  $-/-$  mice. Bands of smooth muscle cells and extracellular matrix were present in apoE  $-/-$  but not LDL receptor  $-/-$  mice after 3 months (Fig 3).

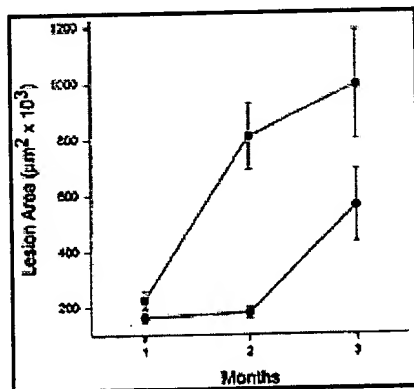
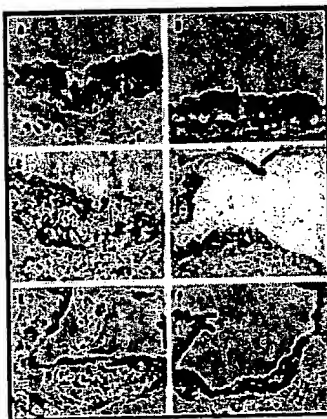


**Figure 2.** Line graph shows area of atherosclerotic lesions in apoE  $-/-$  and LDL receptor  $-/-$  mice after 1, 2, and 3 months on a cholesterol-enriched diet. Points indicate means of six observations; bars, SEM; ■, apoE  $-/-$  mice; and •, LDL receptor  $-/-$  mice.

[View larger version \(13K\):](#)  
[\[in this window\]](#)  
[\[in a new window\]](#)



[View larger version](#)  
 (115K):

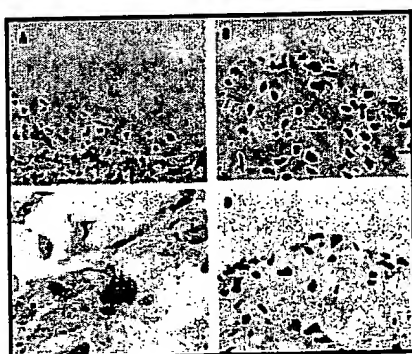
**Figure 3.** Photomicrographs show presence of macrophages and lipid deposits in murine atherosclerotic lesions. Aortic sections were immunostained for macrophages as described in "Methods." Macrophages were immunostained with MOMA-2 after 1 month of cholesterol feeding in (A) apoE  $-/-$  and (B) LDL receptor  $-/-$  mice. At 1 month the two animal strains had lesions with similar morphological characteristics. After 3 months of cholesterol feeding, differences were observed in MOMA-2-immunostained macrophages: apoE  $-/-$  mice had necrotic macrophage core regions and macrophage accumulation under the endothelium separated by bands of nonstaining cells and matrix (C). In contrast, lesions from LDL receptor  $-/-$  mice immunostained uniformly for macrophages, and necrotic cores were uncommon (D).

[\[in this window\]](#)  
[\[in a new window\]](#)

Staining for neutral lipids with oil red O was patchy in apoE -/- mice after 3 months of cholesterol feeding (E) but relatively uniform in LDL receptor -/- mice (F) (original magnification x100 [A and B], x40 [C through F]).

T lymphocytes were detected by using antibodies to Thy 1.2, CD5, CD4, and CD8 (Table 1). Thy 1.2 and CD5 antigens are pan-T-cell markers, although CD5 is also present on a subset of B lymphocytes in serosal cavities. Immunostaining for Thy 1.2 and CD5 was observed in lesions from both strains. Furthermore, the distribution and number of cells exhibiting positive immunostaining was similar with both Thy 1.2 antibodies (Fig 4A) and the CD5 antibody (Fig 4B). Several monoclonal antibodies directed against T-lymphocyte antigen CD4 and an antibody to the B-lymphocyte marker CD45R were used to identify the subsets of lymphocytes present in mouse atherosclerotic lesions (Table 1). No B lymphocytes were observed in lesions, although the CD45R antibody produced excellent immunostaining of splenic tissue that was used as a control. Because only one of the anti-CD4 antibodies (GK1.5) resulted in appreciable splenic immunostaining, it was used to demonstrate the presence of CD4<sup>+</sup> cells in atherosclerotic lesions (Fig 4C). In splenic tissue, CD4 immunostaining was less intense on positive cells than was Thy 1.2, CD5, and CD8 immunostaining. CD8<sup>+</sup> cells were detected in the lesions of both strains (Fig 4D). The relatively low intensity of CD4<sup>+</sup> subset immunostaining indicated that formal quantification may result in a misleading underestimate of cell numbers. Therefore, because robust immunostaining of T-lymphocyte subsets was not as consistently achieved as for Thy 1.2 antigen, no quantitative assessment of these subtypes was performed.

**View this table:** [Table 1. Primary Antibodies Used to Detect Lymphocytes in Atherosclerotic Lesions](#)  
[\[in this window\]](#)  
[\[in a new window\]](#)



**View larger version (135K):**  
[\[in this window\]](#)  
[\[in a new window\]](#)

**Figure 4.** Photomicrographs. A, T lymphocytes positive for Thy 1.2 in shoulder region of a lesion from an LDL receptor -/- mouse fed a cholesterol-enriched diet for 1 month. B, T lymphocytes positive for CD5 in an apo E -/- mouse fed a cholesterol-enriched diet for 3 months. C, T lymphocytes positive for CD4 in a lesion from an LDL receptor -/- mouse after 1 month of cholesterol feeding. D, T lymphocytes positive for CD8 in an atherosclerotic lesion from an LDL receptor -/- mouse fed a cholesterol-enriched diet for 2 months (original magnification x200 [A and B], x1000 [C], x400 [D]).



T lymphocytes, as determined by Thy 1.2 immunoreactivity, were present in atherosclerotic lesions at all intervals. The density of Thy 1.2<sup>+</sup> T lymphocytes was greatest after only 1 month of cholesterol feeding in both strains of mice (Fig 5). At the intervals studied beyond 1 month, there was a significant reduction in lesion T-lymphocyte density, which was particularly sparse after 3 months in apoE  $-/-$  mice. At all intervals, lesions of LDL receptor  $-/-$  mice contained a greater density of Thy 1.2<sup>+</sup> cells than did lesions of apoE  $-/-$  mice. In neither strain of mice was there a specific region in atherosclerotic lesions that preferentially accumulated T lymphocytes, as has been discerned in the human disease.<sup>15</sup> The distribution of lymphocytes was patchy, with small foci of cells generally located beneath the endothelium and few cells near the media or in the lipid core. No T lymphocytes were detected in the media.

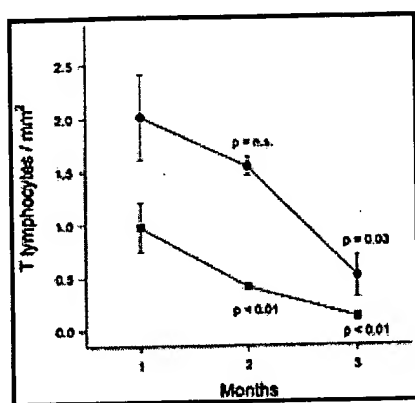


**Figure 5.** Line graph shows T-lymphocyte density of Thy 1.2<sup>+</sup> cells in both strains of mice at 1, 2, and 3 months. Points indicate means of six observations; bars, SEM; ■, apoE  $-/-$  mice; and ●, LDL receptor  $-/-$  mice. Statistical significance at 2 and 3 months (as determined by Mann-Whitney rank-sum test) is stated relative to the density at 1 month for each strain.

View larger version (13K):  
[\[in this window\]](#)  
[\[in a new window\]](#)

## Discussion

We observed striking differences in the dimensions and morphological characteristics of lesions in apoE  $-/-$  and LDL receptor  $-/-$  mice. Our observations of atherosclerotic lesions from apoE  $-/-$  mice are similar to earlier ones.<sup>10 11 12 13</sup> Compared with LDL receptor  $-/-$  mice, lesions in apoE  $-/-$  mice were larger at all intervals studied and had a markedly increased number of chondrocytes and bands of smooth muscle cells. ApoE  $-/-$  mice had significantly increased concentrations of total serum cholesterol at most intervals, with most being in a VLDL fraction. Cholesterol-enriched VLDL has been demonstrated to promote cholesterol esterification in macrophages,<sup>33 34 35</sup> which may be a factor in the formation of lesions of disparate morphology in apoE  $-/-$  and LDL receptor  $-/-$  mice, although this has not been proven.

The principal finding of this study is that Thy 1.2<sup>+</sup>, CD5<sup>+</sup>, CD4<sup>+</sup>, and CD8<sup>+</sup> T lymphocytes are present in atherosclerotic lesions in cholesterol-fed apoE  $-/-$  and LDL receptor  $-/-$  mice. Thy 1.2 is a 112-amino acid glycoprotein present in varying amounts on the surface of neural and lymphoid cells, with expression depending on the state of differentiation.<sup>36</sup> In mice, Thy 1.2 is found on

mature T lymphocytes. CD5 is a monomeric 67-kD glycoprotein on all mature T lymphocytes, with higher expression on CD4 $^{+}$  than CD8 $^{+}$  cells.<sup>37</sup> CD5 also occurs on the B1a subset of B lymphocytes found in serosal cavities. CD5 functions as a tyrosine kinase substrate in association with the T-cell receptor  $\zeta$  chain/CD3 and protein tyrosine kinases p56<sup>lck</sup> and p59<sup>fyn</sup> in T lymphocytes and may also act as an independent signaling molecule.<sup>38</sup>

Previous immunohistochemical analyses of atherosclerotic lesions in several strains of mice, including the apoE  $-/-$  strain, have shown an absence of T lymphocytes.<sup>31</sup> A possible explanation for this apparent contradiction is the interval at which lesions were studied. In the present study, lymphocyte density decreased with lesion maturity; particularly in apoE  $-/-$  mice, this cell type was sparse after 3 months of cholesterol feeding. The fact that Qiao et al<sup>31</sup> studied lesions after cholesterol feeding of a longer duration than in the present study may explain the lack of detectable lymphocytes. In addition, in our study, several of the anti-CD4 antibodies tested resulted in weak and diffuse immunostaining of splenic tissue (Table 2). Therefore, the difference between this and previous reports with regard to detection of lymphocytes might be partly attributed to differences in the affinity of antibodies used in immunohistochemical testing. However, while lymphocytes have not been reported in atherosclerotic lesions, CD4 $^{+}$ , CD8 $^{+}$ , and CD23 $^{+}$  (B lymphocytes) have been demonstrated in aortic fatty streaks of vasculitis-prone MRL/*lpr* mice.<sup>39</sup>

In both apoE  $-/-$  and LDL receptor  $-/-$  mice, the density of T lymphocytes in lesions decreased as lesions matured. Signals responsible for recruitment of lymphocytes have not been defined, although one proposed mediator is the lysophospholipid formed by the oxidation of LDL.<sup>40 41</sup> Early lymphocytic recruitment to atherosclerotic lesions occurred, but further development of lesions ensued without a proportional increase in T lymphocytes. The early recruitment of lymphocytes to atherosclerotic lesions has also been observed in cholesterol-fed rabbits<sup>42 43</sup> and rats.<sup>44</sup> Lymphocyte residence time and trafficking within atherosclerotic lesions have not been defined but may be important parameters. Introduction of exogenous lymphocytes distinguishable on the basis of a genetically incorporated marker may assist in understanding the biology of lymphocytes within atherosclerotic lesions.

ApoE has been proposed as an endogenous regulator of the immune system, since it inhibits both monocyte<sup>45</sup> and T lymphocyte<sup>46</sup> proliferation. ApoE also inhibits interleukin-2-dependent T-cell proliferation, possibly by preventing transition from the G1<sub>A</sub> phase of the cell cycle.<sup>47</sup> ApoE synthesis by macrophages varies according to the state of cell differentiation<sup>48</sup> and may be inhibited by interferon gamma<sup>49</sup> and stimulated by increasing intracellular cholesterol concentrations.<sup>50</sup> However, since apoE  $-/-$  mice develop severe atherosclerosis and inhibition of T lymphocytes enhances development of atherosclerosis,<sup>28 29 30</sup> the physiological significance of the inhibitory effect of apoE on T lymphocytes in atherosclerotic lesions remains to be determined.

T lymphocytes are present in atherosclerotic lesions in apoE  $-/-$  and LDL receptor  $-/-$  mice,

making both strains useful for the study of immunologic factors affecting the development of atherosclerosis. In addition, we observed differences in morphological characteristics of lesions that could be due to altered lipoprotein metabolism or immunologic factors, both of which are likely to be targets of pharmacological intervention in the modulation of atherosclerotic disease.

## Acknowledgments

Simon E. Roselaar is a fellow of the American Heart Association, Missouri Affiliate. Alan Daugherty is an Established Investigator of the American Heart Association. We are grateful to Drs Jeffrey E. Saffitz and Osami Kanagawa for advice on histology and providing antibodies, to Dustie Delfel-Butteiger for technical assistance, to Beth Engeszer, Sandy Sendobry, and Debra Rateri for editorial assistance, and to Kelly Hall for secretarial assistance.

Received October 4, 1995; revision received February 22, 1996; **References**

1. Wissler RW and the PDAY Investigators. New insights into the pathogenesis of atherosclerosis as revealed by PDAY. *Atherosclerosis*. 1994;108(suppl):S3-S20.
2. Rosenfeld ME, Tsukada T, Gown AM, Ross R. Fatty streak initiation in Watanabe heritable hyperlipidemic and comparably hypercholesterolemic fat-fed rabbits. *Arteriosclerosis*. 1987;7:9-23. [Abstract]
3. Rosenfeld ME, Tsukada T, Chait A, Bierman EL, Gown AM, Ross R. Fatty streak expansion and maturation in Watanabe heritable hyperlipidemic and comparably hypercholesterolemic fat-fed rabbits. *Arteriosclerosis*. 1987;7:24-34. [Abstract]
4. Faggiotto A, Ross R, Harker L. Studies of hypercholesterolemia in the nonhuman primate, I: changes that lead to fatty streak formation. *Arteriosclerosis*. 1984;4:323-340. [Abstract]
5. Faggiotto A, Ross R. Studies of hypercholesterolemia in the nonhuman primate, II: fatty streak conversion to fibrous plaque. *Arteriosclerosis*. 1984;4:341-356. [Abstract]
6. Paigen B, Morrow A, Holmes PA, Mitchell D, Williams RA. Quantitative assessment of atherosclerotic lesions in mice. *Atherosclerosis*. 1987;68:231-240. [Medline] [Order article via Infotrieve]
7. Piedrahita JA, Zhang SH, Hageman JR, Oliver PM, Maeda N. Generation of mice carrying a mutant apolipoprotein E gene inactivated by gene targeting in embryonic stem cells. *Proc Natl Acad Sci U S A*. 1992;89:4471-4475. [Abstract/Free Full Text]
8. Ishibashi S, Brown MS, Goldstein JL, Gerard RD, Hammer RE, Herz J. Hypercholesterolemia in low density lipoprotein receptor knockout mice and its reversal by adenovirus-mediated gene delivery. *J Clin Invest*. 1993;92:883-893. [Medline] [Order article via Infotrieve]
9. Zhang SH, Reddick RL, Piedrahita JA, Maeda N. Spontaneous hypercholesterolemia and arterial lesions in mice lacking apolipoprotein E. *Science*. 1992;258:468-471. [Medline] [Order article via Infotrieve]
10. Plump AS, Smith JD, Hayek T, Aalto-Setälä K, Walsh A, Verstuyft JG, Rubin EM, Breslow JL. Severe hypercholesterolemia and atherosclerosis in apolipoprotein-E-deficient mice created by homologous recombination in ES cells. *Cell*. 1992;71:343-353. [Medline] [Order article via Infotrieve]
11. Zhang SH, Reddick RL, Burkey B, Maeda N. Diet-induced atherosclerosis in mice heterozygous and homozygous for apolipoprotein E gene disruption. *J Clin Invest*. 1994;94:937-945. [Medline] [Order article via Infotrieve]
12. Nakashima Y, Plump AS, Raines EW, Breslow JL, Ross R. ApoE-deficient mice develop lesions in all phases of atherosclerosis throughout the arterial tree. *Arterioscler Thromb*.

- 1994;14:133-140.[[Abstract](#)]
13. Reddick RL, Zhang SH, Maeda N. Atherosclerosis in mice lacking apo E. *Arterioscler Thromb.* 1994;14:141-147.[[Abstract](#)]
14. Ishibashi S, Goldstein JL, Brown MS, Herz J, Burns DK. Massive xanthomatosis and atherosclerosis in cholesterol-fed low density lipoprotein receptor-negative mice. *J Clin Invest.* 1994;93:1885-1893.[[Medline](#)] [[Order article via Infotrieve](#)]
15. Jonasson L, Holm J, Skalli OO, Bondjers B, Hansson GK. Regional accumulation of T cells, macrophages, and smooth muscle cells in human atherosclerotic plaques. *Arteriosclerosis.* 1986;6:131-138.[[Abstract](#)]
16. Emeson EE, Robertson AA. T lymphocytes in aortic and coronary intimas: their potential role in atherogenesis. *Am J Pathol.* 1988;130:369-376.[[Abstract](#)]
17. Hansson GK, Jonasson L, Lojsthe B, Stemme S, Kocher O, Gabbiani G. Localization of T lymphocytes and macrophages in fibrous and complicated human atherosclerotic plaques. *Atherosclerosis.* 1988;72:135-141.[[Medline](#)] [[Order article via Infotrieve](#)]
18. Katsuda S, Boyd HC, Fligner C, Ross R, Gown AM. Human atherosclerosis, III: immunocytochemical analysis of the cell composition of lesions of young adults. *Am J Pathol.* 1992;140:907-914.[[Abstract](#)]
19. Xu Q, Oberhuber G, Gruschwitz M, Wick G. Immunology of atherosclerosis: cellular composition and major histocompatibility complex class II antigen expression in aortic intima, fatty streaks and atherosclerotic plaques in young and aged human specimens. *Clin Immunol Immunopathol.* 1990;56:344-359.[[Medline](#)] [[Order article via Infotrieve](#)]
20. Munro JM, Van der Walt JD, Munro CS, Chalmers JAC, Cox EL. An immunohistochemical analysis of human aortic fatty streaks. *Hum Pathol.* 1987;18:375-380.[[Medline](#)] [[Order article via Infotrieve](#)]
21. Stemme S, Holm J, Hansson GK. T lymphocytes in human atherosclerotic plaques are memory cells expressing CD45RO and integrin VLA-1. *Arterioscler Thromb.* 1992;12:206-211.[[Abstract](#)]
22. Hansson GK, Jonasson L, Holm J, Claesson-Welsh L. Class II MHC antigen expression in the atherosclerotic plaque: smooth muscle cells express HLA-DR, HLA-DQ and the invariant gamma chain. *Clin Exp Immunol.* 1986;64:261-268.[[Medline](#)] [[Order article via Infotrieve](#)]
23. Hansson GK, Holm J, Jonasson L. Detection of activated T lymphocytes in the human atherosclerotic plaque. *Am J Pathol.* 1989;135:169-175.[[Abstract](#)]
24. Geng YJ, Holm J, Nygren S, Bruzelius M, Stemme S, Hansson GK. Expression of the macrophage scavenger receptor in atheroma: relationship to immune activation and the T-cell cytokine interferon- $\gamma$ . *Arterioscler Thromb Vasc Biol.* 1995;15:1995-2002. [[Abstract/Free Full Text](#)]
25. Stemme S, Rymo L, Hansson GK. Polyclonal origin of T lymphocytes in human atherosclerotic plaques. *Lab Invest.* 1991;65:654-660.[[Medline](#)] [[Order article via Infotrieve](#)]
26. Stemme S, Faber B, Holm J, Wiklund O, Witztum JL, Hansson GK. T lymphocytes from human atherosclerotic plaques recognize oxidized low density lipoprotein. *Proc Natl Acad Sci U S A.* 1995;92:3893-3897.[[Abstract/Free Full Text](#)]
27. Sohma Y, Sasano H, Shiga R, Saeki S, Suzuki T, Nagura H, Masato N, Yamamoto T. Accumulation of plasma cells in atherosclerotic lesions of Watanabe heritable hyperlipidemic rabbits. *Proc Natl Acad Sci U S A.* 1995;92:4937-4941. [[Abstract/Free Full Text](#)]
28. Roselaar SE, Schonfeld G, Daugherty A. Enhanced development of atherosclerosis in cholesterol-fed rabbits by suppression of cell-mediated immunity. *J Clin Invest.* 1995;96:1389-1394.[[Medline](#)] [[Order article via Infotrieve](#)]
29. Emeson EE, Shen ML. Accelerated atherosclerosis in hyperlipidemic C57BL/6 mice

- treated with cyclosporin A. *Am J Pathol.* 1993;142:1906-1915.[[Abstract](#)]
30. Fyfe AI, Qiao JH, Lusis AJ. Immune deficient mice develop typical atherosclerotic fatty streaks when fed an atherogenic diet. *J Clin Invest.* 1994;94:2516-2520.[[Medline](#)] [[Order article via Infotrieve](#)]
31. Qiao JH, Xie PZ, Fishbein MC, Kreuser J, Drake TA, Demer LL, Lusis AJ. Pathology of atheromatous lesions in inbred and genetically engineered mice. *Arterioscler Thromb.* 1994;14:1480-1487.[[Abstract](#)]
32. Daugherty A, Rateri DL. Heterogeneity of very low density lipoprotein fractions: factors influencing the ability of specific subfractions to modulate cholesterol metabolism in macrophages in vitro. *Coron Artery Dis.* 1991;2:775-787.
33. Goldstein JL, Ho YK, Brown MS. Cholesteryl ester accumulation in macrophages resulting from receptor-mediated uptake and degradation of hypercholesterolemic canine  $\beta$ -very low density lipoproteins. *J Biol Chem.* 1980;255:1839-1848.[[Abstract/Free Full Text](#)]
34. Mahley RW, Innerarity TL, Brown MS, Ho YK, Goldstein JL. Cholesteryl ester synthesis in macrophages: stimulation by  $\beta$ -very low density lipoproteins from cholesterol-fed animals of several species. *J Lipid Res.* 1980;21:970-980.[[Abstract](#)]
35. Daugherty A, Oida K, Sobel BE, Schonfeld G. Dependence of metabolic and structural heterogeneity of cholesterol ester-rich very low density lipoproteins on the duration of cholesterol feeding in rabbits. *J Clin Invest.* 1988;82:562-570.[[Medline](#)] [[Order article via Infotrieve](#)]
36. Giguère V, Isobe KI, Grosfeld F. Structure of the murine Thy-1 gene. *EMBO J.* 1985;4:2017-2024.[[Abstract](#)]
37. Ledbetter JA, Rouse RV, Micklem HS, Herzenberg LA. T cell subsets defined by expression of Lyt-1,2,3 and Thy-1 antigens: two-parameter immunofluorescence and cytotoxicity analysis with monoclonal antibodies modifies current views. *J Exp Med.* 1980;152:280-295.[[Abstract/Free Full Text](#)]
38. Tarakhovsky A, Müller W, Rajewsky K. Lymphocyte populations and immune responses in CD5-deficient mice. *Eur J Immunol.* 1994;24:1678-1684.[[Medline](#)] [[Order article via Infotrieve](#)]
39. Qiao JH, Castellani LW, Fishbein MC, Lusis AJ. Immune complex-mediated vasculitis increases coronary artery lipid accumulation in autoimmune-prone MRL mice. *Arterioscler Thromb.* 1993;13:932-943.[[Abstract](#)]
40. McMurray HF, Parthasarathy S, Steinberg D. Oxidatively modified low density lipoprotein is a chemoattractant for human T-lymphocytes. *J Clin Invest.* 1993;92:1004-1008.[[Medline](#)] [[Order article via Infotrieve](#)]
41. Daugherty A, Roselaar SE. Lipoprotein oxidation as a mediator of atherogenesis: insights from pharmacological studies. *Cardiovasc Res.* 1995;29:297-311.[[Medline](#)] [[Order article via Infotrieve](#)]
42. Hansson GK, Seifert PS, Olsson G, Bondjers G. Immunohistochemical detection of macrophages and T lymphocytes in atherosclerotic lesions of cholesterol-fed rabbits. *Arterioscler Thromb.* 1991;11:745-750.[[Abstract](#)]
43. Drew AF, Tipping PG. T helper cell infiltration and foam cell proliferation are early events in the development of atherosclerosis in cholesterol-fed rabbits. *Arterioscler Thromb Vasc Biol.* 1995;15:1563-1568.[[Abstract/Free Full Text](#)]
44. Haraoka S, Shimokama T, Watanabe T. Participation of T lymphocytes in atherogenesis: sequential and quantitative observation of aortic lesions of rats with diet-induced hypercholesterolaemia using en face double immunostaining. *Virchows Arch.* 1995;426:307-315.[[Medline](#)] [[Order article via Infotrieve](#)]
45. Okano Y, Macy M, Cardin AD, Harmony JAK. Suppression of lymphocyte activation by plasma lipoproteins: modulation by cell number and type. *Exp Cell Biol.* 1985;53:199-212.[[Medline](#)] [[Order article via Infotrieve](#)]

46. Pepe MG, Curtiss LK. Apolipoprotein E is a biologically active constituent of the normal immunoregulatory lipoprotein, LDL-In. *J Immunol.* 1986;136:3716-3723.  
[\[Abstract/Free Full Text\]](#)
47. Mistry MJ, Clay MA, Kelly ME, Steiner MA, Harmony JAK. Apolipoprotein E restricts interleukin-dependent T lymphocyte proliferation at the G1<sub>A</sub>/G1<sub>B</sub> boundary. *Cell Immunol.* 1995;160:14-23.[\[Medline\]](#) [\[Order article via Infotrieve\]](#)
48. Werb Z, Chin JR. Onset of apoprotein E secretion during differentiation of mouse bone marrow-derived mononuclear phagocytes. *J Cell Biol.* 1983;97:1113-1118.[\[Abstract\]](#)
49. Brand K, Mackman N, Curtiss LK. Interferon- $\gamma$  inhibits macrophage apolipoprotein E production by posttranslational mechanisms. *J Clin Invest.* 1993;91:2031-2039.[\[Medline\]](#) [\[Order article via Infotrieve\]](#)
50. Mazzone T, Gump H, Diller P, Getz GS. Macrophage free cholesterol content regulates apolipoprotein E synthesis. *J Biol Chem.* 1987;262:11657-11662.[\[Abstract/Free Full Text\]](#)

## Anti-atherosclerotic effect of simvastatin depends on the presence of apolipoprotein E

Yi-Xin (Jim) Wang <sup>a,\*</sup>, Baby Martin-McNulty <sup>a</sup>, Ling-Yuh Huw <sup>b</sup>, Valdeci da Cunha <sup>a</sup>,  
Joe Post <sup>a</sup>, Josephine Hinchman <sup>a</sup>, Ronald Vergona <sup>a</sup>, Mark E. Sullivan <sup>a</sup>,  
William Dole <sup>b</sup>, Katalin Kauser <sup>b</sup>

<sup>a</sup> Department of Pharmacology, Berlex Biosciences, P.O. Box 4099, 15049 San Pablo Avenue 15049 San Pablo Avenue, Richmond, CA 94804-0099, USA

<sup>b</sup> Department of Cardiovascular Research, Berlex Biosciences, PO Box Richmond, CA 94804, USA

Received 19 June 2001; received in revised form 19 July 2001; accepted 2 August 2001

### Abstract

Low density lipoprotein receptor deficient (LDLR-KO) and apolipoprotein E deficient (apo E-KO) mice both develop hyperlipidemia and atherosclerosis by different mechanisms. The aim of the present study was to compare the effects of simvastatin on cholesterol levels, endothelial dysfunction, and aortic lesions in these two models of experimental atherosclerosis. Male LDLR-KO mice fed a high cholesterol (HC; 1%) diet developed atherosclerosis at 8 months of age with hypercholesterolemia. The addition of simvastatin (300 mg/kg daily) to the HC diet for 2 more months lowered total cholesterol levels by ~57% and reduced aortic plaque area by ~15% compared with the LDLR-KO mice continued on HC diet alone,  $P < 0.05$ . Simvastatin treatment also improved acetylcholine (ACh)-induced endothelium-dependent vasorelaxation in isolated aortic rings, which was associated with an increase in NOS-3 expression by ~88% in the aorta measured by real time polymerase chain reaction (PCR),  $P < 0.05$ . In contrast, in age-matched male apo E-KO mice fed a normal diet, the same treatment of simvastatin elevated serum total cholesterol by ~35%, increased aortic plaque area by ~15%, and had no effect on endothelial function. These results suggest that the therapeutic effects of simvastatin may depend on the presence of a functional apolipoprotein E. © 2002 Elsevier Science Ireland Ltd. All rights reserved.

**Keywords:** HMG-CoA reductase inhibitor; Atherosclerotic plaque; Cholesterol; Endothelial dysfunction; NOS-3; Apo E-knockout; LDLR-knockout; Mouse

### 1. Introduction

Hypercholesterolemia is a major risk factor for development of atherosclerotic vascular disease [1]. Hydroxy-methylglutaryl-coenzyme A (HMG CoA) reductase inhibitors (statins) lower cholesterol and reduce cardiovascular morbidity and mortality in patients with atherosclerosis [2–4]. A growing data base suggests that the beneficial actions of statins may be due to direct effects on the vascular wall in addition to lipid lowering. Moreover, atherosclerosis is often

accompanied by endothelial dysfunction due to impaired endothelial nitric oxide (NO) production [5–8]. Statins have been shown to restore endothelial function by restoring NO-mediated vasodilation in hyperlipidemic rabbits [9] and in patients with coronary artery disease [10,11]. This improvement in endothelial function contributes to the cardiovascular benefits achieved by statin treatment.

Low density lipoprotein receptor deficient (LDLR-KO) and apolipoprotein E deficient (apo E-KO) mice have been used to study mechanisms of atherogenesis [12,13]. It has been shown that simvastatin lowers lipid levels in LDLR-KO [14], but not in apo E-KO [15] mice. The present study was to compare the effect of simvastatin on atherosclerosis development be-

\* Corresponding author. Tel.: +1-510-669-4489; fax: +1-510-669-4247.

E-mail address: jim\_wang@berlex.com (Y.-X.J. Wang).



tween the two animal models of atherosclerosis. In addition, the effects of simvastatin on endothelial function and endothelial nitric oxide synthase (NOS-3) were also examined.

## 2. Methods

### 2.1. Animals and experimental design

Two-month-old male LDLR-KO mice (Jackson Laboratories, Bar Harbor, ME) were fed a high cholesterol (HC; 1%) diet for 8 months. At 10 months of age the animals developed moderate atherosclerotic lesions in the aorta ( $35 \pm 3\%$ ) accompanied by hypercholesterolemia ( $591 \pm 75$  mg/dl). They were then randomly divided into three groups, control group; continued on a HC diet; simvastatin group; fed a HC diet supplemented with 0.15% simvastatin (HC + SIM); and regular diet (RD) group, withdrawn from the HC diet and fed a regular chow diet. The above treatments were continued for 2 months.

Apo E-KO mice spontaneously develop hypercholesterolemia and atherosclerosis without the need for a cholesterol supplementation. For the present studies, 10-month-old male apo E-KO mice (Jackson Laboratories, Bar Harbor, ME) were used. One group of mice were fed a grain-based rodent diet (Bio-Serv, NJ) as controls and the other was on the same diet supplemented with 0.15% simvastatin for 1–3 months. The daily dose of simvastatin in both LDLR-KO and apo E mice was approximately 300 mg/kg, which has been shown to effectively reduce cholesterol by 37% in LDLR-KO mice [14].

At the end of the treatment period, all animals were fasted overnight and euthanized. Blood samples were collected via cardiac puncture at the time of death. Total serum cholesterol, triglycerides and high density lipoprotein (HDL) levels were determined enzymatically (performed by IDEXX, West Sacramento, CA). LDL values were calculated from total cholesterol and HDL levels. The aortae were isolated for measurements of atherosclerotic lesion area, vascular reactivity, and NOS-3 mRNA expression.

### 2.2. Measurement of atherosclerotic plaque

The aortae were isolated, cleaned from the adherent connective tissue, fixed with 10% formalin, cut open longitudinally and pinned on black wax-coated petri dishes as previously described in detail [5]. Atherosclerotic plaque area is visible without staining. The images of the open luminal surface of the aortae were recorded at a resolution of  $512 \times 512$  using a

RGB 3-chip CCD digital camera (Sony) mounted on a dissecting microscope (Nikon SMZ-2T) attached to a computer in 24 bit true image format. The images were analyzed using C-Simple software (C. Imaging 1208, Compix, Mars, PA). Atherosclerotic plaque area was quantified and expressed as a percentage of total luminal surface area of the aorta.

### 2.3. Assessment of vascular reactivity

The thoracic aortae were dissected, cleaned from the adherent connective tissue, and placed in a HEPES-buffered solution containing (in mM), 140 NaCl; 4.5 KCl; 1.0  $\text{MgCl}_2$ ; 5.5 glucose; 1.5  $\text{CaCl}_2$ ; and 10 HEPES at pH 7.4 and 20 °C. The aortae were cut into four rings and were placed in organ-bath chambers containing 15 ml of Krebs solution with the following composition (in mM), 118 NaCl; 24.9  $\text{NaHCO}_3$ ; 4.7 KCl; 1.18  $\text{KH}_2\text{PO}_4$ ; 1.66  $\text{MgSO}_4$ ; 5.55 glucose; 2.0 Na-pyruvate; and 2.0  $\text{CaCl}_2$ . The solution was continually bubbled with a 5%  $\text{CO}_2$  and 95%  $\text{O}_2$  gas mixture and maintained at pH 7.4 and 37 °C. Vessels were pre-treated with indomethacin ( $10^{-5}$  M) for 30 min to inhibit cyclooxygenase mediated vascular effects and pre-contracted with KCl (40 mM), and washed with Krebs solution. Aortic rings were then stretched to 500 mg tension and allowed to equilibrate for 2 h prior to initiation of the experimental protocol. Tension measurements were recorded using Grass force-transducers connected to a data acquisition system (MP100 WS, Biopac, Goleta, CA). Data were digitized on-line at a rate of 1 sample per s and subsequently analyzed using Acknowledge software. Concentration response curves to U46619 (9,11-dideoxy-9 $\alpha$ , 11 $\alpha$ -methanoepoxy prostaglandin  $F_{2\alpha}$ ), a thromboxane receptor agonist, were then generated. The calculated concentration of U46619 that produced 80% of the maximal contractile response ( $\text{EC}_{80}$ ) was 20 nM. Endothelium-mediated relaxation was measured as the response to acetylcholine (ACh; 0.01 nM–10  $\mu\text{M}$ ) in rings pre-contracted with U-46619 (30 nM). In the LDLR-KO mice, endothelium-independent aortic ring relaxation was also measured as the response to sodium nitroprusside (SNP, 0.001–1  $\mu\text{M}$ ).

### 2.4. Measurement of NOS-3 mRNA

The isolated aortae were homogenized in 600  $\mu\text{l}$  RLT buffer (Qiagen) using disposable generator probes (Omni International). Total RNA was then isolated using a RNeasy kit with DNase I digestion (Qiagen). Relative abundance of NOS-3 and internal control GAPDH were measured by real-time quantitative polymerase chain reaction (PCR) performed on an ABI PRISM 7700 Sequence Detector (PE Biosys-

tems). One-step reverse transcriptase (RT)-PCR amplification of NOS-3 was carried out in a 50  $\mu$ l reaction mixture consisting of 1  $\times$  TaqMan buffer A with the following composition (mM), 5.5 MgCl<sub>2</sub>; 0.3 dATP; 0.3 dCTP; 0.3  $\mu$ M dGTP; 0.3 dUTP; 0.025 U/ $\mu$ l AmpliTaq Gold DNA polymerase, 0.025 U/ $\mu$ l RNase inhibitor, 0.025 U/ $\mu$ l multiscribe RT, 200 nM of each primer, and 100 nM probe. Thermal cycle conditions were 48 °C for 30 min and 95 °C for 10 min followed by 40 cycles at 95 °C for 15 s and 60 °C for 1 min. Primers and the probe for NOS-3 were, upper primer, 5'-CGTCATCGGCGTGCT-3' (nt 3436–3450), lower primer, 5'-ACCTCCTGGGT-GCGC-3' (nt 3510–3496), and the probe, 5'-6FAM-CGGGATCAGCAACGCTACCA-TAMRA-3' (nt 3452–3471). Primers and TaqMan probe for rodent GAPDH were purchased from PE Biosystems (P/N 4308313). Hundred nanomol of each primer and 200 mM of the probe were used in the reaction. The expressions of NOS-3 and GAPDH were calculated against a standard curve with serial dilution of total RNA from murine hemangioendothelioma (EOMA) cells [16]. The experiment was repeated twice in triplicate for each sample. Values presented here are the ratio of NOS-3/GAPDH.

### 2.5. Statistics

All results are presented as the mean  $\pm$  S.E.M. for the number of animals ( $n$ ) indicated. Multiple comparisons of mean values were performed by analysis of variance (ANOVA) followed by a subsequent Student–Newman–Keuls test for repeated measures. Differences were considered to be statistically significant when the  $P$  value was  $<0.05$ . The statistical analysis was performed using Statistica software (STATSOFT, Tulsa, OK).

## 3. Results

### 3.1. Effects of simvastatin in LDLR-KO mice

LDLR-KO mice fed a HC diet for 10 months had hypercholesterolemia and developed atherosclerotic lesions in the aorta (Fig. 1). Treatment with simvastatin (HC + SIM) decreased serum LDL cholesterol with no significant effects on HDL cholesterol or triglycerides levels (Table 1). As a result, the ratio of HDL/LDL was significantly higher in the HC + SIM compared with the HC group (Table 1). Simvastatin also reduced atherosclerotic lesion area by  $\sim 15\%$ , compared with that in the HC group (Fig. 1). Mice given the regression diet for 2 months showed similar changes in lipid profiles and atherosclerotic lesions as were seen following simvastatin treatment (Table 1

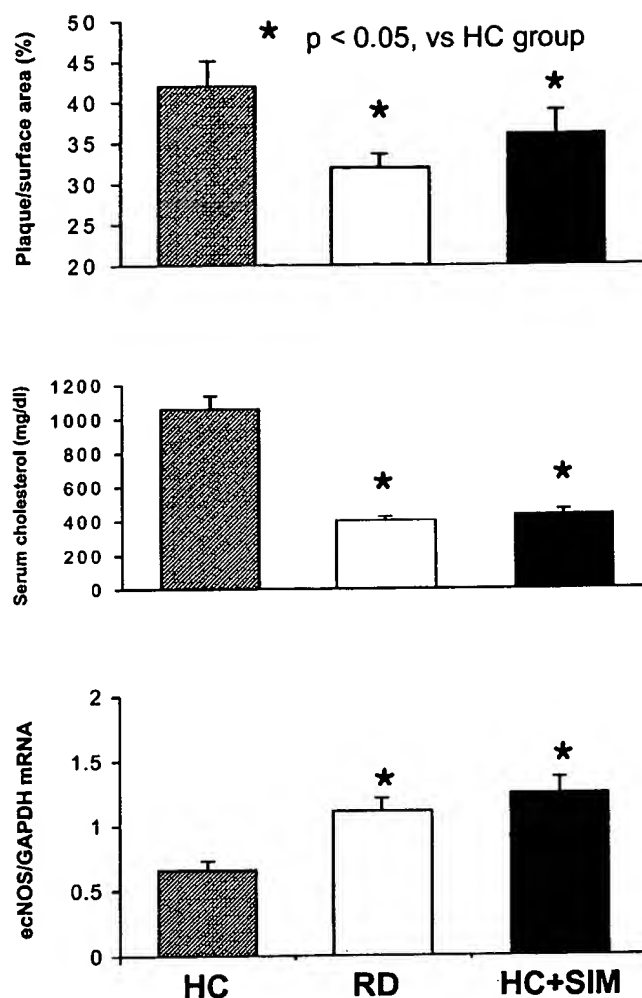


Fig. 1. Aortic atherosclerotic lesion area (top,  $n = 8$  per group), total serum cholesterol levels (middle,  $n = 11$  per group), and NOS-3 mRNA expression in the aorta (bottom,  $n = 3$  per group) of the LDLR-KO mice fed a HC diet without or with (HC + SIM) the supplementation of simvastatin (300 mg/kg, daily), or withdrawn from a HC diet and fed a RD, for 2 months.

and Fig. 1). Combining the data from all three groups, aortic atherosclerotic lesion area was positively correlated to total serum cholesterol levels and negatively correlated to the ratio of HDL/LDL (Fig. 2).

Table 1  
Effects of simvastatin and diet on serum lipid profile (mg/dl) in LDLR-KO mice ( $n = 11$  per group)

	HC	RD	HC+SIM
LDL	917 $\pm$ 80	256 $\pm$ 19**	322 $\pm$ 27**
HDL	98 $\pm$ 6	102 $\pm$ 8	77 $\pm$ 6
HDL/LDL	0.12 $\pm$ 0.01	0.38 $\pm$ 0.04**	0.24 $\pm$ 0.03**
Triglyceride	213 $\pm$ 16	226 $\pm$ 19	175 $\pm$ 21

\*,  $P, 0.05$ ; \*\*,  $P < 0.01$ ; vs. HC.

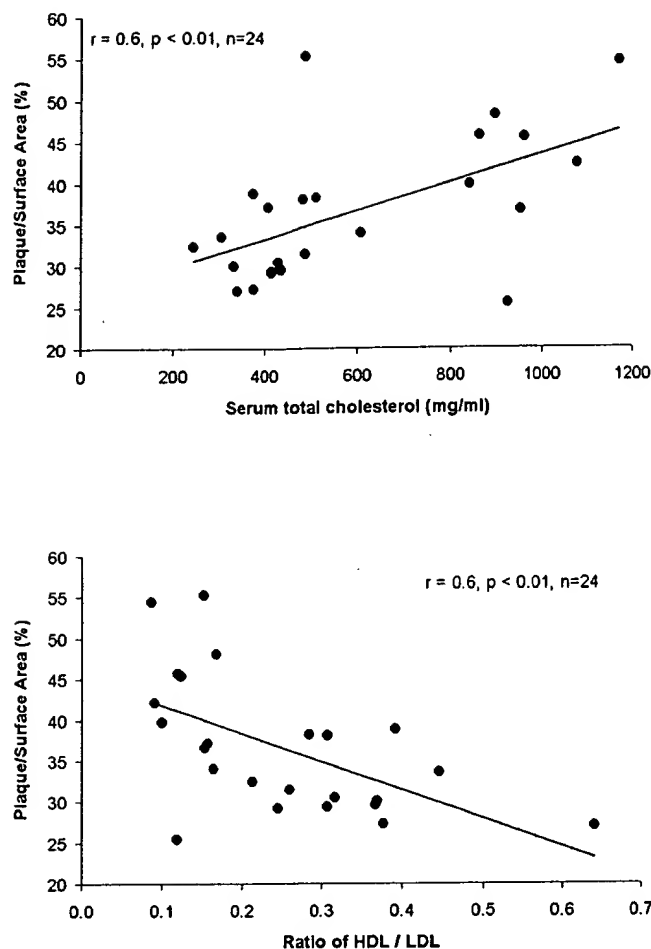


Fig. 2. The aortic atherosclerotic lesion area was positively correlated to the total circulating cholesterol levels (top) and negatively correlated to the ratio of HDL/LDL in the LDLR-KO mice. The data included all three groups of the mice fed a HC diet without or with (HC + SIM) the supplementation of simvastatin (300 mg/kg, daily), or withdrawn from a HC diet and fed a RD, for 2 months.

ACh-induced endothelial NO-mediated aortic relaxation was significantly greater in both the HC + SIM and RD groups than that in the HC group (Fig. 3A). Thus, the maximum responses were significantly greater in both the HC + SIM and RD groups than that in the HC group (Table 2). Endothelium-independent relaxation to SNP did not significantly differ among the three groups (Fig. 3B and Table 3). The expression of NOS-3 mRNA was significantly higher in both the HC + SIM and RD groups than the expression levels in the HC group (Fig. 1).

### 3.2. Effects of simvastatin in apo E-KO mice

Age-matched apo E-KO mice fed a RD had hypercholesterolemia and developed atherosclerotic lesions in the aorta, which tended to increase over time (Fig. 4). Serum total and LDL cholesterol levels were higher and HDL cholesterol levels lower in the simvastatin than in the control group (Fig. 4 and Table 3). As a result of these changes, the ratio of HDL/LDL was significantly lower in the simvastatin than the control group. Triglyceride levels were not significantly different between the two groups. Aortic lesion area was greater in the simvastatin than control group (Fig. 4). Combining the data from both groups at all time points, aortic atherosclerotic lesion area was positively correlated to total serum cholesterol levels and negatively correlated to the ratio of HDL/LDL (Fig. 5).

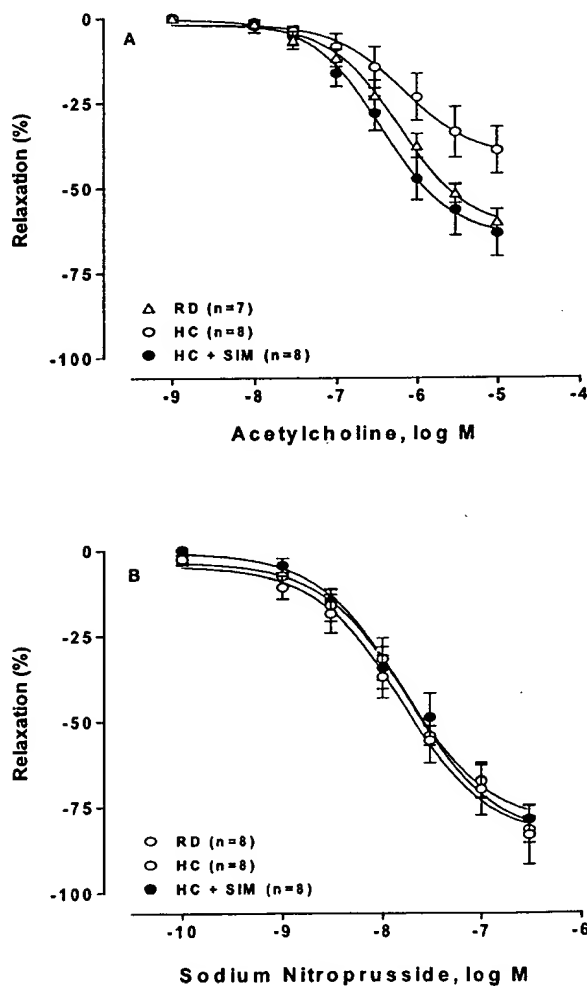


Fig. 3. Concentration-response curves of ACh (A) or SNP (B) induced relaxation in the aortic rings isolated from LDLR-KO mice fed a HC diet without or with (HC + SIM) the supplementation of simvastatin (300 mg/kg, daily), or withdrawn from a HC diet and fed a RD, for 2 months.

Table 2

Sensitivity (log EC<sub>50</sub>, pD<sub>2</sub>) and maximal response (*E*<sub>max</sub>) to ACh and SNP in isolated aortae from LDLR-KO mice fed a RD, HC diet without or with simvastatin (HC+SIM)

Groups	N	ACh		SNP	
		pD <sub>2</sub>	<i>E</i> <sub>max</sub> (%)	pD <sub>2</sub>	<i>E</i> <sub>max</sub> (%)
HC	8	6.17 ± 0.20	39.2 ± 6.8 <sup>a</sup>	7.74 ± 0.18	81.8 ± 3.8
RD	7	6.2 ± 0.16	60.2 ± 3.6	7.8 ± 0.21	83.3 ± 8.5
HC+SIM	8	6.45 ± 0.11	63.4 ± 6.9	7.79 ± 0.22	78.8 ± 4.2

<sup>a</sup> *P* < 0.05 vs. RD group.

ACh-induced relaxation of the aortae isolated from apo E-KO mice were not significantly different between the simvastatin and control groups at both the 2 and 3 months time points (Fig. 6 and Table 4).

#### 4. Discussion

The major findings of the present study are that simvastatin has opposite effects on serum lipids and atherosclerosis in two different genetic mouse model of atherosclerosis. In the LDLR-KO mice, simvastatin decreased serum cholesterol levels and aortic lesion area. These changes were associated with an improvement in endothelial NO-dependent vasorelaxation and an increased NOS-3 mRNA expression. In contrast, in the apo E-KO mice, the same treatment with simvastatin increased serum cholesterol levels and aortic lesion area, with no changes in endothelial NO-mediated vasorelaxation.

Table 3

Effects of simvastatin on serum lipid profiles (mg/dl) in apo E-KO mice (*n* = 7–12 per group)

Treatment (month)	Vehicle	Simvastatin
<b>LDL**</b>		
1	463 ± 55	630 ± 41
2	474 ± 42	727 ± 39
3	462 ± 46	605 ± 42
<b>HDL*</b>		
1	70 ± 6	59 ± 4
2	88 ± 10	51 ± 6
3	100 ± 5	48 ± 6
<b>HDL/LDL*</b>		
1	0.16 ± 0.01	0.10 ± 0.01
2	0.19 ± 0.02	0.07 ± 0.01
3	0.26 ± 0.05	0.08 ± 0.01
<b>Triglycerides</b>		
1	193 ± 32	198 ± 48
2	173 ± 19	141 ± 7
3	158 ± 21	109 ± 8

\*, *P* < 0.05; \*\*, *P* < 0.01 between two groups.

These data indicate that an intact functional apolipoprotein E may be essential for the lipid lowering, anti-atherosclerosis and other therapeutic benefits of simvastatin.

#### 4.1. Effects of simvastatin on hypercholesterolemia

In the present study, simvastatin at a daily dose of 300 mg/kg significantly reduced total cholesterol by

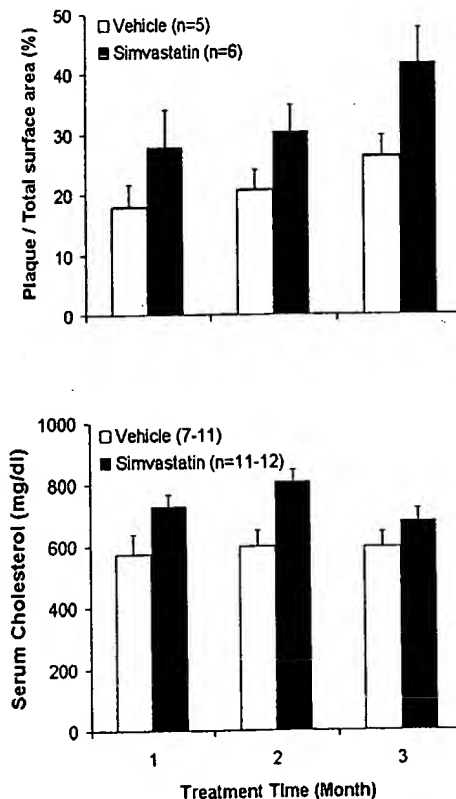


Fig. 4. Atherosclerotic lesion area in the aorta (top) and total serum cholesterol levels (bottom) of the apo E-KO mice treated with simvastatin (300 mg/kg, daily) or vehicle for 1–3 months. *P* < 0.05 between the simvastatin and vehicle treatment group for both the plaque area and total serum cholesterol levels.

57% in LDLR-KO mice fed a HC diet. This result is consistent with a previous report by Bisgaier et al., who reported that at the same daily dose, simvastatin reduced total circulating cholesterol by 37% in LDLR-KO mice [14]. The magnitude of cholesterol lowering by simvastatin was also similar to that observed in untreated LDLR-KO mice fed a regression diet for 2 months. In contrast, the same dose of simvastatin resulted in a 27% increase in serum cholesterol in apo E-KO mice. This finding is consistent with that of Quarfordt et al., who also reported that lovastatin (50 mg/kg daily) increased circulating cholesterol by 70% in apo E-KO mice, but not in wild-type controls [15]. These results suggest that the lipid lowering effect of statins may depend on the presence of intact apolipoprotein E, which functions to transport circulating cholesterol into cells, particularly hepatocytes and acts as an important mediator

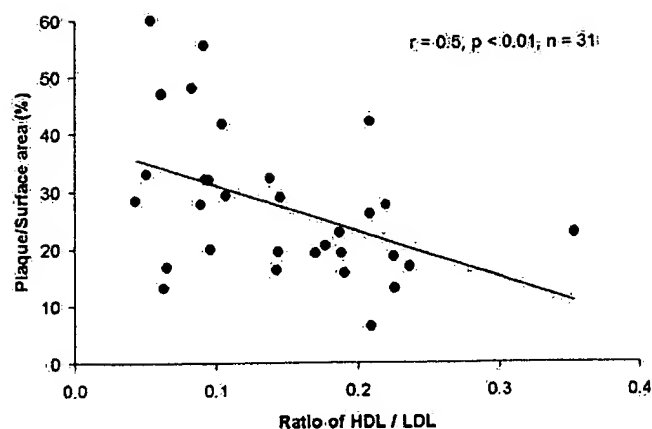
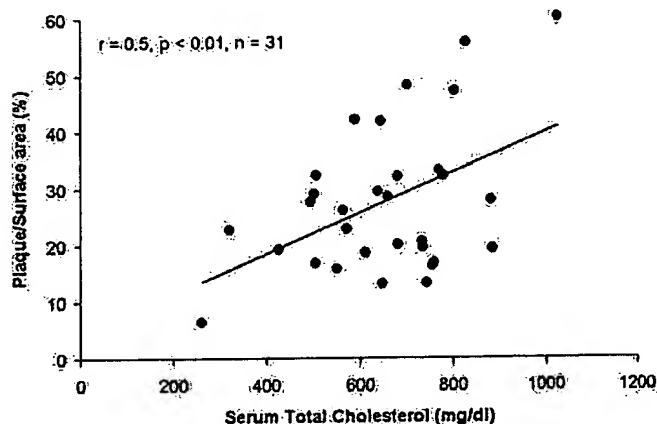


Fig. 5. The aortic atherosclerotic lesion area was positively correlated to the total circulating cholesterol levels (top) and negatively correlated to the ratio of HDL/LDL in the apo E-KO mice. The data included all groups of mice treated with simvastatin (300 mg/kg, daily) or vehicle for 1–3 months.

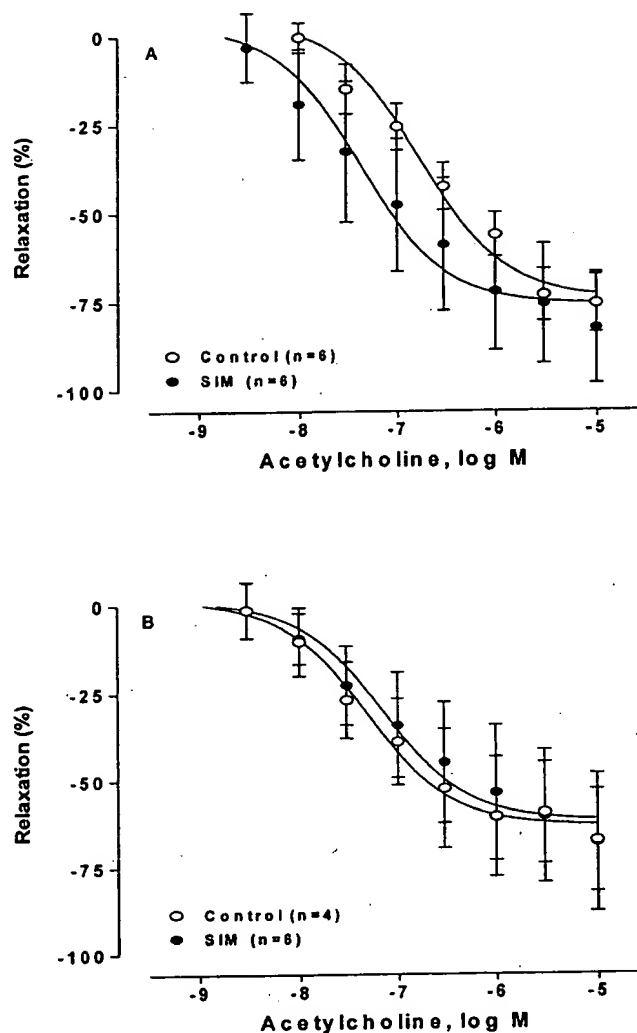


Fig. 6. Concentration–response curves of ACh-induced relaxation of the aortic rings isolated from apo E-KO mice treated with simvastatin (300 mg/kg per day) or vehicle for 2 (top) and 3 (bottom) months.

for hepatic metabolic clearance of circulating cholesterol [12]. In the absence of the apolipoprotein E, hepatic clearance and metabolism of cholesterol are reduced, resulting in hypercholesterolemia [12,13,17]. Impairment of hepatic cholesterol transport may also result in up-regulation of cholesterol synthesis [18]. Indeed, lovastatin has been reported to increase the expression of HMG CoA reductase mRNA [19] and protein [20], thereby increasing cholesterol synthesis [15] in apo E-KO mice, but not in wild-type controls. This may explain the paradoxical elevation of cholesterol in simvastatin-treated apo E-KO mice.

#### 4.2. Effects of simvastatin on atherosclerosis

Accompanied by its lipid lowering effect, simvastatin significantly reduced aortic atherosclerotic

Table 4  
Sensitivity ( $\log EC_{50}$ ,  $pD_2$ ) and maximal response ( $E_{max}$ ) to ACh and SNP in isolated aortae from apo E-KO mice treated without (control) or with simvastatin for 2 or 3 months

Groups	Duration					
	Two months			Three months		
	<i>N</i>	$pD_2$	$E_{max}$ (%)	<i>N</i>	$pD_2$	$E_{max}$ (%)
Control	6	$6.75 \pm 0.27$	$75.8 \pm 8.2$	4	$7.31 \pm 0.20$	$67.5 \pm 14.7$
Simvastatin	6	$7.37 \pm 0.34$	$82.6 \pm 15.7$	6	$7.15 \pm 0.32$	$68.0 \pm 19.8$

plaque area in LDLR-KO mice. In contrast, simvastatin accelerated atherosclerosis that accompanied an elevation of serum cholesterol levels in apo E-KO mice. Hypercholesterolemia is an important risk factor leading to atherosclerosis. Animals with hypercholesterolemia, resulting from either a HC diet [21–23] or from inherited defects in lipid metabolism [5–7], develop atherosclerotic plaques in the vascular wall. Therefore, the reduction in atherosclerotic lesions by simvastatin in LDLR-KO mice can be explained by its lipid lowering effect, since similar reduction in serum cholesterol and aortic lesion area were observed in untreated mice fed a RD. On the other hand, the increase in atherosclerosis by simvastatin in apo E-KO mice could be explained by elevated serum lipids. This is consistent with a previous report that feeding a HC diet to apo E-KO mice further exacerbated hypercholesterolemia and accelerated lesion development [24]. HDL is known to be involved in reversing cholesterol transport from the vascular wall [25,26]. Therefore, elevation of HDL/LDL ratio by simvastatin in LDLR-KO mice could also contribute to its anti-atherosclerotic effect. Likewise, reduction of HDL/LDL ratio by simvastatin in apo E-KO mice could contribute to acceleration of atherosclerosis. The fact that aortic lesions correlated positively to the total serum cholesterol levels and negatively to the HDL/LDL ratio in both the LDLR-KO and apo E-KO mice support the above view.

#### 4.3. Effect of simvastatin on endothelial function

Endothelial dysfunction, characterized by reduced NO-dependent vascular relaxation, is an early marker of atherosclerosis [27]. Endothelial function is impaired in a number of experimental models of atherosclerosis, including hyperlipidemic rabbits [9] and apo E-KO mice [5], as well as in patients with atherosclerosis [8]. Statins have been shown to reverse endothelial dysfunction in hyperlipidemic rabbits [9] and in humans [10,11]. This effect of statins has been attributed to stabilization of NOS-3 mRNA leading

to the increase in NOS-3 expression [28,29]. Indeed, in the present study, simvastatin treatment significantly increased the expression of NOS-3 mRNA in the aorta of LDLR-KO mice. This was associated with enhanced ACh-induced endothelial NO dependent vasorelaxation. Although there is strong evidence that direct effect on NOS-3 expression is the underlying mechanism for the improvement in endothelial function, the present study was not designed to determine the mechanism of action of simvastatin on NOS-3 and can not differentiate direct effects on the vascular wall from secondary effects due to changes in serum lipids. In apo E-KO mice, on the other hand, the potential direct beneficial effect of simvastatin on endothelial function could be masked or compromised by increased cholesterol levels and atherosclerosis. This may explain the lack of significant effect of simvastatin treatment on ACh-induced NO-dependent aortic ring relaxation in the apo E-KO mice.

During the preparation of this manuscript, Sparrow et al. published a paper demonstrating both anti-inflammatory and anti-atherosclerotic activities of simvastatin in apo E-KO mice [30]. In that study, simvastatin had no significant effect on circulating cholesterol levels. The apo E-KO mice were fed a HC diet, which resulted in a very high circulating cholesterol levels ( $\sim 1000$  mg/dl) and severe atherosclerosis in the aorta. The apo E-KO mice in the present study were fed a RD, resulting in moderate hyperlipidemia with serum cholesterol levels at  $\sim 500$  mg/dl and a less severe atherosclerosis. These differences in the diet and circulating lipid levels, as well as the severity of atherosclerosis, may contribute, at least in part, to the different results.

In summary, the present study demonstrates that in LDLR-KO mice, treatment with simvastatin for 2 months significantly decreased serum cholesterol levels, improved endothelial function, and reduced atherosclerosis. In contrast, in apo E-KO mice, the same treatment of simvastatin elevated serum cholesterol levels and increased atherosclerosis with no effect on endothelial function. Thus, the beneficial

effects of statins may depend on the presence of functional apolipoprotein E. It has to be pointed out that the mechanisms involved in atherosclerosis induction in these animal models are different. In LDLR-KO mice, it is diet-induced, while in apo E-KO mice, it is primarily due to 'genetics'. This difference may also explain the different effects observed regarding endothelial function. Thus, whether the current findings can be applied to human, as they are less dependent on apo E for the catabolism of LDL, is a new pharmacogenetic topic that needs to be further studied.

### Acknowledgements

The authors would like to thank the Animal Care Group under the direction of William Lillis for proper care and feeding the animals over the duration of these studies. We also would like to thank Merck & Co., Inc. for kindly providing simvastatin. During the period of these experiments, Valdeci da Cunha, as a visiting scientist at Berlex Biosciences from Federal University of Espirito Santo, Brazil, was supported by CAPES (0680/98-2).

### References

- [1] Anderson KM, Castelli WP, Levy D. Cholesterol and mortality. Thirty years of follow-up from the Framingham study. *J Am Med Assoc* 1987;257:2176–80.
- [2] Jones P, Kafonek S, Laurora I, Hunninghake D. Comparative dose efficacy study of atorvastatin versus simvastatin, pravastatin, lovastatin, and fluvastatin in patients with hypercholesterolemia (the CURVES study; see comments). *Am J Cardiol* 1998;81:582–7 [published erratum appears in *Am J Cardiol* 1998;82(1):128].
- [3] Dart A, Jerums G, Nicholson G, d'Emden M, Hamilton-Craig I, Tallis G, Best J, West M, Sullivan D, Bracs P, Black D. A multicenter, double-blind, 1-year study comparing safety and efficacy of atorvastatin versus simvastatin in patients with hypercholesterolemia (see comments). *Am J Cardiol* 1997;80:39–44.
- [4] Bertolini S, Bon GB, Campbell LM, Farnier M, Langan J, Mahla G, Pauciullo P, Sirtori C, Egros F, Fayyad R, Nawrocki JW. Efficacy and safety of atorvastatin compared to pravastatin in patients with hypercholesterolemia. *Atherosclerosis* 1997;130:191–7.
- [5] Wang YX, Halks-Miller M, Vergona R, Sullivan ME, Fitch R, Mallari C, Martin-McNulty B, da Cunha V, Freay A, Rubanyi GM, Kauser K. Increased aortic stiffness assessed by pulse wave velocity in apolipoprotein E-deficient mice. *Am J Physiol Heart Circ Physiol* 2000;278:H428–34.
- [6] Rosenfeld ME, Tsukada T, Gown AM, Ross R. Fatty streak initiation in Watanabe Heritable Hyperlipemic and comparably hypercholesterolemic fat-fed rabbits. *Arteriosclerosis* 1987;7:9–23.
- [7] Rosenfeld ME, Tsukada T, Chait A, Bierman EL, Gown AM, Ross R. Fatty streak expansion and maturation in Watanabe Heritable Hyperlipemic and comparably hypercholesterolemic fat-fed rabbits. *Arteriosclerosis* 1987;7:24–34.
- [8] Anderson TJ, Gerhard MD, Meredith IT, Charbonneau F, Delagrangé D, Creager MA, Selwyn AP, Ganz P. Systemic nature of endothelial dysfunction in atherosclerosis. *Am J Cardiol* 1995;75:71B–4B.
- [9] Senaratne MP, Thomson AB, Kappagoda CT. Lovastatin prevents the impairment of endothelium dependent relaxation and inhibits accumulation of cholesterol in the aorta in experimental atherosclerosis in rabbits. *Cardiovasc Res* 1991;25:568–78.
- [10] Anderson TJ, Meredith IT, Yeung AC, Frei B, Selwyn AP, Ganz P. The effect of cholesterol-lowering and antioxidant therapy on endothelium-dependent coronary vasomotion (see comments). *New Engl J Med* 1995;332:488–93.
- [11] Treasure CB, Klein JL, Weintraub WS, Talley JD, Stillabower ME, Kosinski AS, Zhang J, Boccuzzi SJ, Cedarholm JC, Alexander RW. Beneficial effects of cholesterol-lowering therapy on the coronary endothelium in patients with coronary artery disease (see comments). *New Engl J Med* 1995;332:481–7.
- [12] Breslow JL. Mouse models of atherosclerosis. *Science* 1996;272:685–8.
- [13] Zhang SH, Reddick RL, Piedrahita JA, Maeda N. Spontaneous hypercholesterolemia and arterial lesions in mice lacking apolipoprotein E. *Science* 1992;258:468–71.
- [14] Bisgaier CL, Essenburg AD, Auerbach BJ, Pape ME, Sekerke CS, Gee A, Wolle S, Newton RS. Attenuation of plasma low density lipoprotein cholesterol by select 3-hydroxy-3-methylglutaryl coenzyme A reductase inhibitors in mice devoid of low density lipoprotein receptors. *J Lipid Res* 1997;38:2502–15.
- [15] Quarfordt SH, Oswald B, Landis B, Xu HS, Zhang SH, Maeda N. In vivo cholesterol kinetics in apolipoprotein E-deficient and control mice. *J Lipid Res* 1995;36:1227–35.
- [16] Obeso J, Weber J, Auerbach R. A hemangioendothelioma-derived cell line: its use as a model for the study of endothelial cell biology. *Lab Invest* 1990;63:259–69.
- [17] Ghiselli G, Schaefer EJ, Gascon P, Breser HB Jr. Type III hyperlipoproteinemia associated with apolipoprotein E deficiency. *Science* 1981;214:1239–41.
- [18] Siperstein MD, Guest JM. Studies on the homeostatic control of cholesterol synthesis. *J Clin Invest* 1959;38:1043–4.
- [19] Pitman WA, Osgood DP, Smith D, Schaefer EJ, Ordovas JM. The effects of diet and lovastatin on regression of fatty streak lesions and on hepatic and intestinal mRNA levels for the LDL receptor and HMG CoA reductase in F1B hamsters. *Atherosclerosis* 1998;138:43–52.
- [20] Bilhartz LE, Spady DK, Dietschy JM. Inappropriate hepatic cholesterol synthesis expands the cellular pool of sterol available for recruitment by bile acids in the rat. *J Clin Invest* 1989;84:1181–7.
- [21] Nascimento CA, Kauser K, Rubanyi GM. Effect of 17 $\beta$ -estradiol in hypercholesterolemic rabbits with severe endothelial dysfunction. *Am J Physiol* 1999;276:H1788–94.
- [22] Masuda J, Ross R. Atherogenesis during low level hypercholesterolemia in the nonhuman primate. II. Fatty streak conversion to fibrous plaque. *Arteriosclerosis* 1990;10:178–87.
- [23] Masuda J, Ross R. Atherogenesis during low level hypercholesterolemia in the nonhuman primate. I. Fatty streak formation. *Arteriosclerosis* 1990;10:164–77.
- [24] van Ree JH, van den Broek WJ, Dahlmans VE, Groot PH, Vidgeon-Hart M, Frants RR, Wieringa B, Havekes LM, Hofker MH. Diet-induced hypercholesterolemia and atherosclerosis in heterozygous apolipoprotein E-deficient mice. *Atherosclerosis* 1994;111:25–37.
- [25] Kannel WB, Wilson PW. Efficacy of lipid profiles in prediction of coronary disease. *Am Heart J* 1992;124:768–74.
- [26] Badimon JJ, Badimon L, Fuster V. Regression of atherosclerotic lesions by high density lipoprotein plasma fraction in the cholesterol-fed rabbit. *J Clin Invest* 1990;85:1234–41.



- [27] Harrison DG. From isolated vessels to the catheterization laboratory. Studies of endothelial function in the coronary circulation of humans. *Circulation* 1989;80:703–6.
- [28] Laufs U, La Fata V, Plutzky J, Liao JK. Upregulation of endothelial nitric oxide synthase by HMG CoA reductase inhibitors. *Circulation* 1998;97:1129–35.
- [29] Laufs U, Liao JK. Post-transcriptional regulation of endothelial nitric oxide synthase mRNA stability by Rho GTPase. *J Biol Chem* 1998;273:24266–71.
- [30] Sparrow CP, Burton CA, Hernandez M, Mundt S, Hassing H, Patel S, Rosa R, Hermanowski-Vosatka A, Wang PR, Zhang D, Peterson L, Detmers PA, Chao YS, Wright SD. Simvastatin has anti-inflammatory and anti-atherosclerotic activities independent of plasma cholesterol lowering. *Arterioscler Thromb Vasc Biol* 2001;21:115–21.